European Commission

JRC TECHNICAL REPORT

ESARDA 37th Annual Meeting Proceedings

2015 Symposium
19-21 May 2015
Midland Hotel, Manchester (UK)

Filippo Sevini
Editor: Andrea De Luca

2015

Report EUR 27342

Joint Research Centre

European Commission
Joint Research Centre
Institute for Transuranium Elements

Contact information
Filippo Sevini
Address: Joint Research Centre, ITU Nuclear Security unit, T.P. 800, Via E Fermi 2749, 21027 Ispra, Italy
E-mail: filippo.sevini@jrc.ec.europa.eu
Tel.: +39 0332 78 6793

JRC Science Hub
https://ec.europa.eu/jrc

JRC96321

EUR 27342

ISBN 978-92-79-49495-6 (PDF)

ISSN 1831-9424 (online)

doi: 10.2789/099293

Luxembourg: Publications Office of the European Union, 2015

Abstract

The 37th ESARDA symposium on Safeguards and Nuclear Non-Proliferation was held in Manchester, United Kingdom from 19-21 May, 2015. The Symposium has been preceded by meetings of the ESARDA Working Groups on 18 May 2015. The event has once again been an opportunity for research organisations, safeguards authorities and nuclear plant operators to exchange information on new aspects of international safeguards and non-proliferation, as well as recent developments in nuclear safeguards and non-proliferation related research activities and their implications for the safeguards community.
The Proceedings contains the papers (118) submitted according to deadlines.

Programme

Monday 18 May

Working Group Meetings (and Friday 22 May)……	*See agenda*
Building Capability in Safeguards R&D ……..	*09:30 – 16:00, Derby Room*
INMM International Safeguards Division…….	*17:00 – 19:00, Derby Room*
Reception at Midland Hotel……..	*19:00, Trafford Room*

Tuesday 19 May

Plenary……	*09:00 – 12:40, Alexandra Suite*
01 Implementation of Safeguards……..	*14:00 – 15:40, Alexandra Suite*
02 He-3 Alternatives for Neutron Detection……..	*14:00 – 15:40, Trafford Room*
03 International Collaboration……...	*16:00 – 17:40, Alexandra Suite*
04 Uncertainties in NDA Measurements……...	*16:00 – 17:40, Trafford Room*

Wednesday 20 May

05 Spent Fuel Verification…….	*08:40 – 10:40, Alexandra Suite*
06 Integrated Measurement and Monitoring……..	*08:40 – 10:40, Derby Room*
07 Safeguards Concepts…….	*08:40 – 10:40, Trafford Room*
08 Neutron Measurements…….	*11:00 – 12:40, Alexandra Suite*
09 Training and Knowledge Management…….	*11:00 – 12:40, Derby Room*
10 Quality Control in Destructive Analysis……..	*11:00 – 12:40, Trafford Room*
Poster Session……	*14:00 – 15:20, Alexandra Suite*
11 Gamma Measurements…….	*15:20 – 17:00, Alexandra Suite*
12 Export Control……..	*15:20 – 17:00, Derby Room*
13 Geospatial Information…….	*15:20 – 17:00, Trafford Room*
Conference Dinner……	*18:00 Transport from Midland*

Thursday 21 May

14 Combined Analytical Techniques…….	*08:40 – 10:40, Alexandra Suite*
15 Novel Technologies and Forensics……...	*08:40 – 10:40, Derby Room*
16 Containment and Surveillance……..	*08:40 – 10:40, Trafford Room*
17 Inhomogeneous Material Verification……..	*11:00 – 12:40, Alexandra Suite*
18 Destructive Analysis Measurements…….	*11:00 – 12:40, Derby Room*
19 Geological Repositories……	*11:00 – 12:40, Trafford Room*
20 Tomography for Spent Fuel Verification…….	*14:00 – 15:20, Alexandra Suite*
21 Non-Proliferation and Arms Control……	*14:00 – 15:20, Derby Room*
22 Nuclear Material Accountancy…….	*14:00 – 15:20, Trafford Room*
Closing Plenary……..	*15:20 Alexandra Suite*

Friday 22 May

Working Group Meetings…….	*See agenda*
Site Visit……	*Urenco Capenhurst*

Tuesday Morning, 09:00-12:40

Plenary 1 – *Alexandra Suite*
Chair – Jim Tushingham

09:00 Welcome and opening remarks
J. Tushingham, ESARDA President, and F. Sevini, ESARDA Secretary

Keynotes:

09:20 ONR Deputy Chief Nuclear Inspector and Programme Director, *Mr G. Sallit*

09:40 EC ENER E Director, *Dr P. Szymanski*

10:00 IAEA Dir SGCP, *Ms T. Renis*

10:20 EC JRC DG, *Professor V. Sucha*

10:40 Coffee break – *Alexandra Suite*

Plenary 2 – *Alexandra Suite*
Chair – Jim Tushingham

11:00 INMM President, *Dr L. Satkowiak*

11:20 Nuclear safeguards activities of the European Commission Joint Research Centre (80)
S. Abousahl and Z. Palajova

11:40 Recent Developments in IAEA Safeguards Guidance and Outreach (128)
C. Mathews, A. Braunegger-Guelich, and I. Suseanu

12:00 Overview of JAEA-ISCN's NDA Development Programs (100)
M. Seya, M. Koizumi, H. Tomikawa, Y. Naoi, M. Kureta, H. Harada, R. Hajima and H. Nakamura

12:20 Experience implementing the UK Additional Protocol (127)
L. Johnson, M. Beaman and W. McCarthy

12:40 **Lunch** – *Alexandra Suite*

Tuesday Afternoon, 14:00-15:40

	01 Implementation of Safeguards – *Alexandra Suite* *Chair – Mike Beaman*	**02 He-3 Alternatives for Neutron Detection** – *Trafford Room* *Chair – Anne-Laure Weber*
14:00	United States of America Nuclear Regulatory Commission's Approach to Inspections and Quality Control of Data (2) *D. Hanks and E. Freeman*	Workshop on He-3 alternatives for safeguards applications (17) *P. Peerani, C. Carrapico, B. Pedersen, V. Forcina, F. Rosas, A. Rozite, H. Tagziria and A. Tomanin*
14:20	French Additional Protocol: technical implementation (51) *G. Daniel*	Demonstration Result of Sample Assay System equipped Alternative He-3 Detectors (101) *H. Nakamura, Y. Mukai, H. Tobita, H. Nakamichi, A. Ohzu, M. Kureta, T. Kurita and M. Seya*
14:40	Safeguards-relevant information collection from small holders – experiences and challenges (49) *E. Sundén, M. Dufva and J. Dahlberg*	Real-time, fast neutron detection for stimulated safeguards assay (106) *M. Joyce, M. Aspinall, F. Cave and R. Plenteda*
15:00	Implementation of the SNRI concept in the FBFC Romans Fuel Fabrication Plant and the installation of unattended measurement stations for fuel assemblies (30) *A. Terrasi, W. Koehne and P. Beuseling*	Experimental Assessment of a 6LiF:ZnS(Ag) Prototype Neutron Coincidence Counter for Safeguards (111) *H. Tagziria, M. Foster, M. Schear, D. Ramsden, G. Dermody, B. Pedersen, P. Peerani and P. Schwalbach*
15:20	Safeguards Indexing Method for the Regulatory Assessment of Safeguards Culture at Nuclear Facilities (83) *Z. Stefanka, É. Hedvig Nagy and Á. Vincze*	A prototype BF3 based neutron multiplicity counter for nuclear safeguards (114) *B. Pedersen, J-M. Crochemore, M. Mosconi, V. Mayorov, H. Tagziria, A. Ocherashvili, E. Roesgen and P. Schwalbach*
15:40	Coffee break – *Alexandra Suite*	

Tuesday Afternoon, 16:00-17:40

	03 International Collaboration – *Alexandra Suite* *Chair – Said Abousahl*	**04 Uncertainties in NDA Measurements** – *Trafford Room* *Chair – Patrick Chard*
16:00	EU - ABACC Cooperation: Strengthening Safeguards Capabilities (63) *J. Goncalves, F. Littmann, V. Sequeira, M. Sironi, O. Peixoto, S. de Almeida and S. Fernandez Moreno*	Emerging Applications of Bottom-Up Uncertainty Quantification in Nondestructive Assay (78) *B. Weaver, A. Favalli, B. Williams, S. Croft, D. Dale and T. Burr*
16:20	Overview of Activities and Outcomes at Integrated Support Center for Nuclear Nonproliferation and Nuclear Security Related to Japanese Commitment at Nuclear Security Summit Process (99) *Y. Naoi, N. Kobayashi, T. Mochiji and M. Senzaki*	TRIPOLI-4® and FREYA for Stochastic Analog Neutron Transport. Application to Neutron Multiplicity Counting (55) *J. Verbeke and O. Petit*
16:40	JAEA − JRC Collaboration on the Development of Active Neutron NDA Techniques (109) *M. Kureta, M. Koizumi, A. Ohzu, K. Furutaka, M. Seya and H. Harada*	Use of a Plutonium Piece Monitor and Improved Offline Plutonium Assay Algorithms in Support of a Residues Retrieval Programme (74) *E. Waterhouse, J. Rackham, J. Sharpe, N. Clarke and M. Wilson*
17:00	Integrated NDA User Laboratories at the JRC in Ispra for Nuclear Safeguards and Nuclear Security (112) *W. Janssens, K. Abbas, R. Berndt, V. Berthou, C. De Almeida Carrapico, J. Crochemore, G. Eklund, V. Forcina, M. Marin-Ferrer, V. Mayorov, P. Mortreau, M. Mosconi, B. Pedersen, P. Peerani, F. Rosas, A. Rozite, E. Roesgen, H. Tagziria and A. Tomanin*	Particle Swarm Imaging (PSIM) – A swarming algorithm for the reporting of robust, optimal measurement uncertainties (88) *D. Parvin and S. Clarke*
17:20	Assessing 'Gold Standard' Status: Is the United Arab Emirates nuclear energy program suited to fit the bill? (61) *M. Fisher*	Monte Carlo modelling of EURATOM neutron detectors for operational purposes (19) *D. Ancius, P. De Baere and P. Schwalbach*

Wednesday Morning, 08:40-10:40

	05 Spent Fuel Verification – *Alexandra Suite* *Chair – Kåre Axell*	**06 Integrated Measurement and Monitoring** – *Derby Room, Chair – Joao Gonçalves*	**07 Safeguards Concepts** – *Trafford Room* *Chair – Elina Martikka*
08:40	Extension of the SCK•CEN spent fuel inventory library (5) *A. Borella, R. Rossa, K. van der Meer, M. Cometto and R. Remetti*	Progress and Status of Remote Data Transmission in EURATOM Safeguards (23) *K. Schoop, J. Stronkhorst, J-F. Levert, C. Demartini, J. Pekkarinen, M. Garrisi, S. Kurek and K. Ruuska.*	Exploring Operational Safeguards, Safety, and Security by Design to Address Real Time Threats in Nuclear Facilities (76) *M. Schanfein and S. Mladineo*
09:00	Influence of fuel composition on the spent fuel verification by Self-Interrogation Neutron Resonance Densitometry (35) *R. Rossa, A. Borella, P-E. Labeau, N. Pauly and K. van der Meer*	An update on the implementation of remote data transmission (RDT) in the dry interim storage facilities in Germany (28) *A. Jussofie, K. van Bevern, W. Geißler, I. Niemeyer, A. Rezniczek, W. Trautwein and K. Schoop*	Safeguards by Design for Pyroprocessing Facilities in the ROK (6) *H. Kim, E-H. Kwon and S-H. Park*
09:20	Development of Differential Die-Away Instrument for Characterization of Swedish Spent Nuclear Fuel (24) - *T. Martinik, V. Henzl, M. Swinhoe, A. Goodsell, S. Grape, S. Jacobsson Svärd, P. Jansson and S. Tobin.*	Verification of Spent Fuel Transfers in Germany (129) *I. Tsvetkov, G. Morris, D. Parise, B. Pudjanto, W. Kahnmeyer and W.Trautwein*	An Operators' Experience of Applying Safeguards by Design (113) *A. Homer, V. Ferguson and C. Frears*
09:40	Improving the prediction model for Cherenkov light generation by irradiated nuclear fuel assemblies in wet storage for enhanced partial-defect verification capability (31) *E. Branger, S. Jacobsson Svärd and S. Grape*	Automated processing of safeguards data: Perspectives on software requirements for a future "All in One Review Platform" based on iRAP (27) *A. Smejkal, P. Schwalbach and R. Linnebach*	Clandestine Proliferation: A Stochastic Process Model (65) *N. Kyriakopoulos*
10:00	Underwater Testing of Detectors and Electronics Hardware for Spent Fuel Measurements (68) *K. Ianakeiv, M. Swinhoe, M. Iliev, S. Tobin, A. Sjöland, H. Liljenfeldt and P. Jansson*	The role of the VARO inspection software for the implementation of an Integrated Management System (IMS) at the EURATOM Safeguards Office (29) *P. Dossogne, W. Koehne, J. Lupo P. Kaypaghian, M. Vlietinck, M. Vassart, F. Rowie C. Cosmo, A. Terrasi, P. Schwalbach, O. Alique*	Formalizing Acquisition Path Analysis for the IAEA's State-Level Concept (67) *C. Listner, M. Canty, G. Stein, A. Rezniczek and I. Niemeyer*
10:20	In-field Performance Testing of the Fork Detector for Quantitative Spent Fuel Verification (90) *I. Gauld, S. Vaccaro, P. Schwalbach, J. Hu, P. de Baere, H. Liljenfeldt and S. Tobin*	Applying the Data Analysis and Interpretation Software to Analyze Feed and Withdrawal Operations (87) *J. Garner and M. Whitaker*	Methodological aspects on the IAEA State Level Concept and related Acquisition Path Analysis (91) *G. Renda, L-K. Kim and G. Cojazzi*
10:40	**Coffee break** – *Alexandra Suite*		

Wednesday Morning, 11:00-12:40

	08 Neutron Measurements - *Alexandra Suite Chair – Alessandro Borella*	**09 Training and Knowledge Management** *– Derby Room, Chair – Paolo Peerani*	**10 Quality Control in Destructive Analysis** *– Trafford Room, Chair – Guy Granier*
11:00	Comparison of Fresh Fuel Experimental Measurements to MCNPX Results using the Differential Die-Away Instrument for Nuclear Safeguards Applications (16) *A. Goodsell, V. Henzl, M. Swinhoe, C. Rael, D. Desimone and W. Charlton*	Canada's Standardized Program for Training Safeguards Inspection Staff (44) *P. Creary and K. Owen-Whitred*	Quality control tools for age dating in nuclear safeguards and forensics (122) *Y. Aregbe, C. Venchiarutti, A. Fankhauser, Z. Varga, R. Jakopic, S. Richter, K. Mayer, C. Rivier and D. Roudil*
11:20	Detection of fission signatures induced by a low-energy neutron source (104) *A. Ocherashvili, V. Mayorov, A. Beck, E. Roesgen, G. Heger, J-M. Crochemore and B. Pedersen*	The Belgian approach in education and training in nuclear safeguards (81) *K. van der Meer, A. Borella, R. Rossa, M. Coeck, R. Jakopic, Y. Aregbe, P. Schillebeeckx and B. Pedersen*	Experimental estimation of the uncertainties associated to low-background alpha-spectrometry measurements (45) *N. Cherubini, A. Dodaro, R. Iacovacci and G. Marzo*
11:40	Preliminary Results of the 2014 Field Trial of the Advanced Experimental Fuel Counter (AEFC) for Verification of Research Reactor Spent Fuel at the Institute of Nuclear Physics (INP) (115) *K. Miller and H. Menlove*	The UK's Long Term Commitment to Training and Development in the International Safeguards Community (110) *S. Francis*	Preparation of Uranium Micro-Particles as Reference Material for Nuclear Safeguards (66) *R. Middendorp, A. Knott and M. Duerr*
12:00	A theoretical and experimental investigation of using Feynman-Y functions for the total and gamma detections in a nuclear and radioactive material assay (38) *D. Chernikova, K. Axell and A. Nordlund*	Nuclear knowledge management in higher education. Case of Tomsk Polytechnic University (11) *M. Perminova and D. Demyanyuk*	The Preparation of a Uranium-235 Solid Reference Material (107) *S. Jerome, C. Larijani, S. Judge and S. Woods*
12:20	Improved Holdup Blender Assay System (IBAS) Slope Validation Measurements to Improve Nuclear Material Accountancy of High Alpha Holdup (72) *A. Lafleur, H. Nakamura, H. Menlove, Y. Mukai, M. Swinhoe, J. Marlow and T. Kuroita*	Building a Strategy for ESARDA - Education, Training and Knowledge Management (139) *S. Grape, K. Persson and E. Andersson Sundén*	Stabilisation of uranium/plutonium dried spikes with a cellulose matrix (42) *R. Buda, R. Carlos- Marquez, K. Lützenkirchen, P. van Belle*
12:40	**Lunch** – *Alexandra Suite*		

Wednesday Afternoon, 14:00-15:20

Poster Session – *Alexandra Suite*
Chair – Irmgard Niemeyer

Each author will be invited to give a 2 minutes' presentation of their poster, according to the order indicated below. The short presentation may be just oral, or may be supported by one or two electronic slides, which should be provided before the start of the session. Time keeping will be very strict. After the short presentations, the session will continue in the poster area. Coffee will be served during the poster session.

Chromatographic separation and on-line detection of long life alkali, alkaline earth and transition metal radionuclides by ICP-MS (73)
A. Budreika, D. Plausinaitis, E. Naujalis, B. Knašienė, A. Prokopchik and A. Karaliūnas

An efficient and sensitive optical sensor based on Furosemide as a new fluoroionophore for determination of uranyl ion (105)
O. Elhefnawy and A. Elabd

Image analysis methods for partial defect detection using tomographic images on nuclear fuel assemblies (48)
A. Davour, S. Jacobsson Svärd and S. Grape

Shielded Neutron Source Detection Option (22) *A. Rozite*

Conceptual Model of Security Threat Detection System of Intermediate Level Radioactive Waste at Banda Sea (9)
D. Kurniawan, S. Putero and H. Santosa

Nuclear Instrumentation & Control (1)
M. Koshti and K. Modi

Nuclear fuel cycle (enrichment and reprocessing) (57)
R. Vyas and K. Modi

Software Development for Radionuclide Analysis Applications (121)
M. Kaiser, S. Kim, V. Danilenko and K. Eugene

Method and validation for the preparation of a plutonium age dating reference material (123)
Z. Varga, J. Zsigrai, A. Nicholl, M. Wallenius and K. Mayer

Potential Causes of Inventory Differences at Bulk Handling Facilities and the Importance of Inventory Difference Action Levels (26)
A. Homer and B. O'Hagan

Wednesday Afternoon, 15:20-17:00

	11 Gamma Measurements – *Alexandra Suite* *Chair – to be confirmed*	**12 Export Control** – *Derby Room* *Chair – Christoph Treppmann*	**13 Geospatial Information** – *Trafford Room* *Chair – Bhupendra Jasani*
15:20	Best practices for determining uranium isotopic composition by MGAU and FRAM (21) *T. Ruther and J. Zsigrai*	Nuclear suppliers' enhanced export control compliance and communication with authorities (82) *F. Sevini, A. Viski, R. Chatelus, C. Charatsis, Q. Michel and S. Zero*	Nuclear Verification from Space - Satellite Imagery within Nuclear Non- proliferation and Arms Control Verification Regimes (56) *I. Niemeyer*
15:40	Determination of Uranium enrichment with FRAM - Comparison of electrically cooled Germanium detector Detective200 and U-Pu detector (15) *T. Köble, W. Berky, H. Friedrich, E. Lieder, M. Risse, O. Schumann, J. Glabian and W. Rosenstock*	SSM Research in Export Control (43) *J. Peterson, H. Moberg, E. Koblet and L. Hildingsson*	Remote Sensing Technique in Support to Nuclear Non-Proliferation Monitoring (59) *M. Lafitte and J-P. Robin*
16:00	Analytical estimate of high energy gamma-ray emissions from neutron induced reactions in U-235, U-238, Pu-239 and Pu-240 (32) *F. Postelt and G. Kirchner*	Comparison between Additional Protocol Annex II and current NSG trigger list through semantic representation (47) *L. Falconi, G. Marzo, G. Giorgiantoni and M. Sepielli*	Monitoring uranium mining and milling using commercial observation satellites (94) *L. Sundaresan, C. Srinivasan and B. Jasani*
16:20	An investigation of impurities and associated neutron signatures of strong orphan source of alpha (α) particles (40) *D. Chernikova, K. Axell, A. Vesterlund and H. Ramebäck*	International Secure Platform for Export-controlled Computing Tools (60) *T. Valentine*	Integrated Analysis of Satellite Imagery for Nuclear Monitoring - G-SEXTANT Findings (117) *I. Niemeyer, M. Canty, J-M. Lagrange, C. Listner, D. Schwartz, S. Uruñuela Hernández and E. Wolfart*
16:40	A rapid sample digestion procedure to aid initial nuclear forensics investigations for uranium-bearing ores and concentrates prior to gamma spectrometry (124) *D. Reading, I. Croudace, P. Warwick and R. Britton*	3D Printing: Implications for Non-Proliferation (102) *G. Christopher*	Mobile 3D Laser Scanning for Nuclear Safeguards (34) *E. Wolfart, V. Sequeira, M. Murtezi, A. Zein, P. Turzak, S. Rocchi and L. Enkhjin*

18:00 Transport departs for Conference Dinner

Thursday Morning, 08:40-10:40

	14 Combined Analytical Techniques – *Alexandra Suite, Chair – Jozsef Zsigrai*	**15 Novel Technologies and Forensics** *– Derby Room, Chair – Harri Toivonen*	**16 Containment and Surveillance** *– Trafford Room, Chair – Pierre Funk*
08:40			EURATOM experiences on NGSS field implementation preparation (25) *J. Pekkarinen, K. Schoop and J-M. Mazur*
09:00	A user-friendly tool for easy and fast in-field Monte Carlo simulation of neutron collars (18) *P. Peerani, H. Tagziria and M. Vescovi*	Nuclear Forensics Technologies in Japan (96) *N. Shinohara, Y. Kimura, A. Okubo and H. Tomikawa*	New Ultrasonic Optical Sealing Bolts for Dry Storage Containers (13) *F. Littmann, M. Sironi, V. Kravtchenko, B. Wishard, P. Schwalbach and L. Matloch*
09:20	Non-destructive measurement of the plutonium content of high-active liquid waste (33) *J. Zsigrai, A. Leterrier, G. Duhamel, A. Maddison, J-G. Decaillon and A. Bosko*	Gamma spectrometric age dating of uranium samples (10) *A. Kocsonya, Z. Kovacs, T. Nguyen and L. Lakosi*	Activities towards Ceramic Seal Operational Readiness (75) *H. Smartt and D. Krementz*
09:40	Relative Actinide K-Shell Vacancy Production Rates in Hybrid K-Edge Densitometry (120) *R. McElroy, S. Cleveland, S. Croft, G. Mickum and A. Nicholson*	Standoff LIBS and Raman for security and safeguards applications (89) *N. Smith, L. Li, D. Whitehead, C. Lennon, O. Horsfall and D. Trivedi*	Enhanced Containment and Surveillance System: Active Container Tracking System (SACTS) (85) – *C. Britton, E. Farquhar, S. Frank, M. Kuhn, C. Pickett, B. Stinson, J. Younkin, D. Krementz, Y. Liu and J. Shuler*
10:00	Mass Attenuation Coefficient Data for Hybrid K-Edge Densitometry (119) *S. Croft, R. McElroy, and A. Nicholson*	Determining the origins of Uranium Ore Concentrates using laboratory characterisation techniques (118) *J. Caborn, C. Holmes and J. Edwards*	Enhancement of Safeguards Efficiency for Spent Fuel in Canada (46) *H. Gao and K. Owen-Whitred*
10:20	Validation of the new software for in-field uranium concentration and enrichment measurements by "COMPUCEA" (39) *H. Schorle, J. Zsigrai, M. Vargas-Zuniga, M. Toma and A. Berlizov*	A Safeguards Friendly Device for Monitoring Reactor Anti-Neutrinos (71) *M. Murdoch*	Development of structural materials identification approach based on iris recognition algorithms (12) *S. Sharavina and D. Sednev*
10:40	**Coffee break** – *Alexandra Suite*		

Thursday Morning, 11:00-12:40

	17 Inhomogeneous Material Verification – *Alexandra Suite, Chair – to be confirmed*	**18 Destructive Analysis Measurements** – *Derby Room, Chair – Eva Szeles*	**19 Geological Repositories** – *Trafford Room Chair – Joakim Dahlberg*
11:00	Utilizing Delayed Gamma Rays for Fissionable Material Measurement in NDA (92) *D. Rodriguez, J. Takamine, M. Koizumi and M. Seya*	Semi-Automatic Separation Unit for Actinides at JRC-ITU and IAEA (41) *R. Buda, L. Emblico, A. Schachinger, E. Zuleger*	"Cigéo" – The French Industrial Project of Deep Geological Repository Developed by Andra - Future Safeguards Considerations (50) *F. Poidevin, P. Leverd and S. Farin*
11:20	R&D Status of Nondestructive Assay System Based on Nuclear Resonance Fluorescence (93) *T. Shizuma, R. Hajima, T. Hayakawa, C. Angell and M. Seya*	Implementation of Large Geometry SIMS for Safeguards: 4 Years Later (77) *L. Sangely, J. Poths, T. Tanpraphan, O. Bildstein and H. Siegmund*	Encapsulation and final disposal of spent nuclear fuel in Sweden (37) *J-O. Stål*
11:40	Technique of Neutron Resonance Transmission Analysis for Active Neutron NDA (97) *H. Tsuchiya, M. Koizumi, F. Kitatani, M. Kureta, H. Harada, M. Seya, J. Heyse, S. Kopecky, W. Mondelaers, C. Paradela and P. Schillebeeckx*	Validation of a Cameca 1280 High Resolution SIMS Instrument for Analysis of Nuclear Safeguards Environmental Swipes (126) *A. Simons, N. Montgomery, T. Nicholls, A. Pidduck, S. Crooks and J. Collins*	Safeguards instrumentation to the final disposal facility in Finland (62) *O. Okko*
12:00	Techniques of Neutron Resonance Capture Analysis and Prompt Gamma-ray Analysis for Active Neutron NDA (98) *M. Koizumi, H. Tsuchiya, F. Kitatani, M. Kureta, M. Seya, H. Harada, J. Heyse, S. Kopecky, W. Mondelaers, , C. Paradela and P. Schillebeeckx*	Precise and Accurate U Isotope Analysis using 1E13 Ohm Resistor Amplifiers on a Thermo Scientific ™ TRITON Plus™ MC-TIMS (7) *A. Trinquier, H. Isnard, M. Aubert, P. Komander, P. Huelstede, H. Bars, R. Heming, C. Bouman, J. Schwieters and H. Lerche*	Modelling Seismic-Signal Propagation at a Salt Dome for Safeguards Monitoring (58) *J. Altmann*
12:20	Characterization of special nuclear material by neutron resonance spectroscopy (103) *C. Paradela Dobarro, B. Becker, J. Heyse, S. Kopecky and P. Schillebeeckx*	Retaining a global resource of Plutonium-244 (108) *S. Jerome and J. Morrison*	Application of safeguards in the geological disposal of spent nuclear fuel: safeguards data requirements and contribution to very long lasting records and knowledge retention (20) *M. Murtezi, C. Koutsoyannopoulos, A. Zein, W. Kahnmeyer, P. Turzak, P. Schwalbach, A. Smejkal, V. Sequeira and E. Wolfart*
12:40	**Lunch** – *Alexandra Suite*		

Thursday Afternoon, 14:00-16:00

	20 Tomography for Spent Fuel Verification *– Alexandra Suite, Chair – Peter Schwalbach*	**21 Non-proliferation and Arms Control** *– Derby Room, Chair – Hamid Tagziria*	**22 Nuclear Material Accountancy** *– Trafford Room, Chair – Arnold Rezniczek*
14:00	Gamma-ray Emission Tomography for Partial Defect Verification: Response Modeling Methodology and Benchmarking (86) *V. Mozin, T. White, E. Smith, H. Trellue, N. Deshmukh, R. Wittman, S. Jacobsson Svärd, P. Jansson, A. Davour, S. Grape, T. Honkamaa, S. Vaccaro and J. Ely*	Systems Approach to Arms Control Verification (116) *K. Allen, C. Chen, M. Dreicer, I. Niemeyer, C. Listner and G. Stein*	The Use of Measurement Uncertainty in Nuclear Materials Accountancy and Verification (36) *O. Alique, S. Vaccaro and J. Svedkauskaite*
14:20	Monte Carlo simulations of a Universal Gamma-Ray Emission Tomography Device (64) *P. Jansson, T. White and V. Mozin*	Neutron Multiplicity Counting for Warhead Authentication: Bias Quantification and Reduction (8) *M. Göttsche and G. Kirchner*	Nuclear material management system PATI (125) *J. Sorjonen and T. Henttonen*
14:40	Passive Tomography for Spent Fuel Verification: Analysis Framework and Instrument Design Study (95) *T. White, S. Jacobsson Svärd, E. Smith, V. Mozin, P. Jansson, A. Davour, S. Grape, H. Trellue, N. Deshmukh, R. Wittman, T. Honkamaa, S. Vaccaro and J. Ely*	Disposition of Certain U.S. Exports of High Enriched Uranium (HEU) (3) *D. Hanks and P. Habighorst*	Implementing a model for a Computerised Nuclear Materials Accounting System (84) *R. Last and J. Kirkman*
15:00	Tomographic determination of spent fuel assembly pin-wise burnup and cooling time for detection of anomalies (52) *S. Jacobsson Svärd, A. Davour, S. Grape, S. Holcombe and P. Jansson*	Addressing proliferation concerns within the existing NRC regulatory framework (4) *D. Hanks and T. Grice*	Potential Causes of Inventory Differences at Bulk Handling Facilities and the Importance of Inventory Difference Action Levels (26) *A. Homer and B. O'Hagan*
15:20	**Closing Plenary** *Irmgard Niemeyer*		
	Coffee – *Alexandra Suite*		

Session 1

Implementation of Safeguards

United States of America Nuclear Regulatory Commission's Approach to Inspections and Quality Control of Data

David H. Hanks, Eric Freeman

U.S. Nuclear Regulatory Commission
Washington, D.C.
David.Hanks@nrc.gov
Eric.Freeman@nrc.gov

Abstract

In recent years, the International Atomic Energy Agency (IAEA) has benefited greatly from an increased number of data sources along with enhanced capabilities to assist safeguards inspectors who analyze this new data. However, the quality and reliability of State declared information used by the IAEA to draw safeguards conclusions remains critically important. Each State or Regional Authority has the responsibility to ensure reports provided to the IAEA are accurate and complete. This paper describes the United States Nuclear Regulatory Commission's (US NRC) approach to quality control of safeguards declarations provided to the IAEA and how this process supports fulfillment of the United States' international obligations. The US NRC's audit-based approach to domestic inspections will be reviewed along with the advantages and challenges of such an approach to the quality control of information. Furthermore, examples of quality control of safeguards-relevant information at facilities, the national nuclear materials database, and the NRC will be cited and used to show how each step helps build confidence in the final declaration provided to the IAEA.

Introduction

At the end of World War II and beginning of the world's awareness of atomic weapons, the United States of America (U.S.) Congress established a system intended to protect the world from uncontrolled use of atomic energy for peaceful or non-peaceful uses. Congress passed the Atomic Energy Act of 1946 which resulted in creation of an Atomic Energy Commission (AEC) and the transfer of ownership and responsibility of special nuclear material (SNM) in the U.S. from the Manhattan Project to the AEC. The Act authorized the AEC to produce nuclear materials and nuclear weapons, but only to the extent authorized by the U.S. President. It also authorized research and development activities, but only at AEC facilities or facilities under an AEC contract. As a direct result, nuclear material controls were first conceived and introduced by the Special and Fissionable Material Accountability Branch of the AEC in 1947[1 2].

Slow progress was made between 1946 and 1954 in developing reliable accountancy measures for SNM because of the limited understanding of what was needed in this area and lack of appropriate verification technology. It became clear by 1954 that large scale peaceful uses of nuclear energy were possible, but could not be developed commercially under the strict rules of the original Atomic Energy Act of 1946. The U.S. Congress passed a completely revised Act in 1954 that included the ability for private individuals to possess (but not own) SNM for peaceful purposes. In addition, the AEC was authorized to issue licenses to qualified applicants requesting the possession/use of materials and performed inspections at all facilities working with special nuclear material. The philosophy of why there should be nuclear material control and accounting (MC&A) changed markedly during the late 1950's. The former Special and Fissionable Accountability Branch was renamed the Division of Nuclear Materials Management at the AEC, eliminating a perceived stigma that accountability was a synonym for bookkeeping. By 1964, the U.S. Congress passed the Private Ownership Act which authorized individuals or corporations to own SNM requiring the AEC to grow its material control and accounting program to meet the new challenge.

Evolving Safeguards in the United States

Nuclear material safeguards objectives and principles were introduced in the Atoms for Peace speech given in 1953 by U.S. President Dwight D. Eisenhower to the United Nations General Assembly, ending an era based solely on nuclear material management and beginning an era of international safeguards. A strong safeguards article was introduced into the newly established International Atomic Energy Agency charter in 1957. Some changes were made in the AEC beginning in 1963, which included its material control and accounting system employing an increased emphasis on safeguards. The U.S. offered to share much of its non-weapons nuclear materials and equipment with other nations that would agree to bilateral U.S. safeguards, including inspections, to ensure continued peaceful use of the materials furnished. Later, the Private Ownership Act of 1964 determined that the AEC had the ability to safeguard nuclear material as a function of who had physical possession, rather than who had legal title to the material.

In 1967 and 1968 the AEC began to focus its efforts more on nuclear material safeguards instead of financially motivated nuclear material management. Where, in the case of precious metals monetary value was more important than strategic value of a material that might be used in an atomic bomb. Of particular importance was the addition of a series of license conditions designed to ensure SNM was safeguarded by its licensees. The AEC's inspection responsibility of U.S. licensed nuclear facilities was moved into the Division of Nuclear Materials Safeguards under the Director of Regulation. Routine inspections were performed by the AEC at these facilities to ensure compliance with Federal Regulations.

As part of the Atoms for Peace program, bilateral agreements for cooperation were concluded with a few Non-nuclear Weapons States. Assurances were given by the recipient governments that U.S. assistance would be used only for peaceful purposes. The State also agreed to maintain adequate records, submit periodic reports to the U.S., and allow U.S. inspections for safeguards purposes. Additionally, the U.S. began discussions with the IAEA on the potential for the U.S. to accept IAEA safeguards on US-supplied nuclear materials and facilities, while retaining a right to resume bilateral safeguards and inspections in the event of IAEA inability to carry out its safeguards responsibilities on US-origin SNM and facilities. It was a first step in providing safeguards declarations of nuclear material inventories to an autonomous international organization.

The IAEA worked on safeguards approaches for facilities beginning in 1961, publishing IAEA information circular (INFCIRC) 26 which outlined a safeguard system for research reactors. To demonstrate a willingness to be safeguarded and to provide a proving ground for new concepts, the U.S. offered to place four research reactors under IAEA safeguards. INFCIRC/26 was extended in 1964 to include power reactors. INFCIRC/26 was then replaced by INFCIRC/66 in 1965 which allowed for safeguards on specific principle nuclear facilities, nuclear material, and nonnuclear material to be safeguarded and prohibited their use for military purposes. A model comprehensive safeguards agreement was then described in INFCIRC/153 and in 1977 the U.S. signed the *Agreement between the U.S. and the IAEA for the Application of Safeguards in the U.S. (and Initial Protocol thereto) (INFCIRC/288).* The United States brought its US-IAEA Safeguards Agreement into force in 1980.

The Energy Reorganization Act of 1974 divided the AEC into two distinct organizations. The Nuclear Regulatory Commission (NRC) to license and regulate civilian uses of nuclear materials and facilities, along with the Energy Research and Development Administration (Department of Energy (DOE) precursor) to direct development and production of nuclear weapons, promotion of nuclear power and other energy-related work, and regulation of defense nuclear facilities. Acting as the U.S. National Regulatory Authority (NRA) for its commercial nuclear industry, the NRC was charged with providing oversight for implementation of procedures and practices necessary to facilitate information gathering, timely reporting, and in-field verification of all commercial nuclear activities.

Components of the NRC designed to prevent proliferation of nuclear weapons or make them available to terrorists were exercised by the newly formed agency. By far the leading supplier of nuclear fuel and other materials for the production of nuclear power abroad, the U.S. had a responsibility to ensure exports did not encourage proliferation. Global increase in terrorist activities, transfers of reprocessing and enrichment technologies, as well as India's nuclear explosion, which occurred during the decade of the 1970's triggered U.S. policy makers to reevaluate domestic and international safeguards. The U.S. Congress passed legislation during that period, called the Export Reorganization Act of 1975, which gave the NRC responsibility for determining whether an importing

State's imposed safeguards were "at least substantially comparable" to those required by the United States. Determining suitability of safeguards, including material accountability, in these States was an enormous task. The NRC lacked the resources and expertise to make these broad foreign policy assessments. It was ultimately determined that implementation of IAEA safeguards under a comprehensive safeguards agreement in those States fulfilled this obligation.[3].

In 1980, under the US-IAEA Safeguards Agreement (INFCIRC/288), "Voluntary Offer," the U.S. allowed the IAEA to begin applying international safeguards on all special nuclear material (SNM) within the U.S., *only* excluding facilities associated with direct national security significance activities, with a view to enabling the IAEA to verify that such material is not withdrawn, except as provided for in the Agreement, from activities in facilities while such material is being safeguarded. The U.S. continues to periodically provide the IAEA with a list of facilities eligible for the application of safeguards; adding or removing facilities from that list as necessary. Revisions to this eligible facilities list (EFL) by the NRC and DOE are submitted for a 60-day Congressional review before they are submitted to the IAEA. As a result, the U.S. submits a completed IAEA Design Information Questionnaire (DIQ) and negotiates a Subsidiary Arrangement for those facilities formally selected by the IAEA from this list under the US-IAEA Safeguards Agreement or its Initial Protocol.

The US-IAEA Safeguards Agreement and its associated EFL stems from discussions held between Nuclear Weapon States (NWS)[1] and major industrial Non-Nuclear Weapon States (NNWS), who were concerned that acceptance of safeguards under the NPT would place them at a commercial and industrial disadvantage in developing nuclear energy for peaceful uses. Interferences of IAEA safeguards inspections could affect the efficient operation of their commercial activities and possibly compromise their industrial secrets through IAEA personnel's access to their facilities and records. In recognition of this concern, President Lyndon B. Johnson stated on December 2, 1967 that the United States would not ask any country to accept safeguards that the U.S. was unwilling to accept for its own nuclear activities—excluding those with direct national security significance[4].

The Initial Protocol to the US-IAEA Safeguards Agreement was brought into force at the same time as the Agreement in 1980. The Initial Protocol allows for a secondary type of selection of facilities on the US EFL that only submit design information, permit IAEA inspectors to verify such information in the facility, maintain accounting records, and provide accounting reports to the IAEA without inspections. The technical provisions in the protocol follow closely the comparable provisions in the Agreement itself. Providing an initial protocol to the US-IAEA Safeguards Agreement creates a succinct distinction between facilities selected for full safeguards and those required to only submit information and perform maintenance of records.

In order to minimize costs to the IAEA, it was decided that safeguards would only be applied to a select number of facilities in the U.S., based on advanced designs or sensitivity in terms of international competition. Historically, the IAEA implemented and subsequently withdrew traditional safeguards at several NRC and DOE facilities under the US-IAEA Safeguards Agreement. The list of NRC licensed facilities inspected by the IAEA intermittently between 1980 and 2005 includes: 6 commercial power reactors, 5 LEU fuel fabrication facilities, and two HEU down-blending projects.

Nuclear Material Control and Accounting (MC&A)

Safeguarding licensed facilities, for domestic safeguards purposes, by the NRC continued to evolve from the routine inspections established by the AEC in the late 1940s and throughout the 1950s, becoming more comprehensive over time. Inspector practices were further enhanced in the 1960s-1970s by the need to meet domestic legislative requirements. As in the early years, nuclear material accountancy was always the key element of ensuring that no diversion of SNM was taking place and the prevention of diversion by threat of early detection.

In the commercial nuclear industry, quantitative control of SNM began as a philosophy that was first aimed at balancing cost of the nuclear material with effectiveness of its use to produce energy. However, in theory, as control and accounting of SNM became commensurate with the U.S. dollar,

[1] Article IX.3 of the NPT defines a nuclear-weapon State as one which manufactured and exploded a nuclear weapon or other nuclear explosive device prior to January 1, 1967. Those States are: China, France, the Russian Federation, the United Kingdom, and the United States of America.

SNM worth also became proportional to its strategic value for possible weapons production. The outdated philosophy for safeguarding purposes in the commercial industry was corrected by 1968, when the concept of a material balance area (MBA) and its importance to material control was introduced as a safeguards license condition by the AEC. Periodic physical inventories and adjustment of records accordingly helped to force licensees to prepare closed material balances at the end of each material balance period. Rules for how licensees were to construct, operate, decommission and report were codified in Title 10 of the Code of Federal Regulations (10CFR).

After 1974, nuclear material control and accounting procedures once performed under the AEC were improved by the U.S. Government through cooperation and financing of both the NRC and DOE. In time, a centralized national database for tracking and accounting for source and SNM in the U.S. was established using a computerized system under a DOE contract. The Nuclear Materials Management and Safeguards System (NMMSS) database now supports all the U.S. Government source and SNM accountancy programs. All facility identifier codes, nuclear material transactions, material balances and inventories are documented by NMMSS and used as a centralized reporting system that provides information to the IAEA under the US-IAEA Safeguards Agreement. Additionally, some facilities use a facility-specific NMMSS software program called Safeguards Management Software (SAMS) which enables the user to resolve problems and make corrections prior to sending data to NMMSS. Quality assurance is incorporated into the software as described in DOE Order O 413.1b.

Licensed facility operators in the U.S. are required to prepare nuclear material inventory and material flow report(s) and send them to the NRC for review. Normally, under domestic regulations (10CFR), data is transmitted electronically in the U.S. from the facility operator to the national accounting program managed by NMMSS utilizing proper domestic codes. When selected by the IAEA for safeguards, the facility operator generally performs the same procedure with the addition of key measurement points (KMPs), IAEA material description codes and measurement basis to their reports. Once this essential data is received by NMMSS, the information is structured into the proper IAEA reporting format outlined in the Facility Attachment (or Transitional Facility Attachment) and routed to the NRC, which then finalizes and submits the report(s) to the IAEA. Impact of this additional reporting to the IAEA is primarily absorbed by selected facilities from the U.S. EFL. However, the NRC and NMMSS bear the added responsibility of ensuring all reports from facilities under IAEA safeguards are accurate and complete.

It is important to note that accurate and complete information recorded in facility records and reported to the IAEA be identifiable to inspectors and consistent with international standards. Information as it relates to certain items and batches of material should be recorded and referenced in the accounting records, inventory change documents and general ledger, so that data can be traced to its origin. Although the act of maintaining the accurate and complete information isn't an additional impact, providing feedback to inquiries from the IAEA inspector could present some amount of burden to the NRC and facility operators.

Performance-Based Domestic Safeguards

US NRC inspectors have performed routine and unannounced inspections at licensed facilities constantly since the AEC was abolished. Techniques used by the NRC inspectors at reactors, spent fuel storage and nuclear fuel cycle facilities (fuel fabrication, enrichment and conversion) during the late 1970s included several methods of verification for inventory and nuclear material flow. Instrumentation for measuring unique items, scales for weighing, destructive analysis of bulk material and human surveillance were all part of the domestic safeguards approach.

After the 1979 Three Mile Island event, the NRC focused more resources on nuclear safety and began to utilize an oversight program that included audit-based inspections for safeguards. The current material control and accounting process by the licensee is designed to use control and monitoring measures to prevent or detect loss when it occurs or soon thereafter. Additionally, statistical and accounting measures are used to maintain knowledge of the quantities of special nuclear material present in each area of a facility. Physical inventories and material balances are used to verify the presence of licensed material or to detect the loss of such material after it occurs, in particular, through theft by an insider.[5]

Oversight of the licensee's MC&A recordkeeping system by NRC inspections ensures accountability of nuclear material and demonstrates that performance objectives and facility system capabilities are met. Facility records used to provide complete and accurate information to the IAEA can also be used to trace source material and SNM declared inventory and flow in monthly inventory change reports (ICRs), physical inventory listings (PILs) and material balance reports (MBRs). Inspectors also review facility MC&A procedures associated with the receipt and shipment of imports and exports as described in a facility import or export license. Quality control of the US Government reports to the IAEA begins with the assurance of proper MC&A recordkeeping accuracy and completeness by the facility as outlined in the 10CFR 50.9 and 70.5. Facility quality assurance programs provide for the adequate review, approval, and use of those material control and accounting procedures that are identified in the approved NRC Fundamental Nuclear Material Control Plan as being critical to the effectiveness of the described system.

Fuel Cycle Facilities

The framework for oversight includes gathering and processing performance information from a facility, evaluating risk by using a significance determination process based on results from risk assessments that licensees prepare under 10CFR Part 70. The NRC uses licensee provided performance indicator data to complement its core inspection, allowing the NRC to reduce the scope of these inspections, thereby enhancing efficiency for both the NRC and licensees.

The fuel cycle facility oversight program employs a predictable, graded process to focus NRC oversight and is based on risk and acceptability of performance. The NRC inspection program carries out a base level oversight program for all licensed facilities, focusing on the most safety and safeguards significant plant activities being performed.

Inspections at fuel cycle facilities occur several times a year and typically cover activities such as nuclear criticality control, chemical process, emergency preparedness, fire safety, and radiation safety. The facility Fundamental Nuclear Material Control Plan is required for each fuel cycle facility and is used as the framework for MC&A inspections. Resident inspectors are assigned to operating Category I Fuel Facilities and perform daily inspections at those sites. Periodic specialized inspections are conducted using personnel from NRC headquarters in Rockville, Maryland and the Region II office in Atlanta, Georgia. The NRC Inspection Manual provides guidance for inspectors on the objectives for each type of inspection and procedures to be used.

The Office of Nuclear Material Safety and Safeguards (NMSS) has overall responsibility for the NRC's regulation of fuel cycle facilities. NMSS personnel review all ICR, PIL and MBR reports prior to their transmission to IAEA Headquarters in Vienna, Austria. Currently there are three NRC licensed low enriched uranium (LEU) fuel fabrication facilities and one gas centrifuge enrichment plant reporting to the IAEA under the U.S. Initial Protocol, utilizing a Transitional Facility Attachment (TFA) for guidance and a completed IAEA DIQ describing essential equipment and routine operations of the plant.

U.S. Additional Protocol

When the U.S. Additional Protocol (AP) entered into force on January 6, 2009, the U.S. Government began providing data to the IAEA that differed from previous data sets and required a new approach to quality control. In particular, the AP does not focus on accountancy reports from nuclear facilities but instead requires the U.S. to provide information on fuel cycle research and development activities not involving nuclear material, uranium recovery, site layout and building descriptions, export information, and other Article 2 activities. In order to ensure the overall quality of the U.S. declaration to the IAEA, the NRC recognized that two different approaches were required. First, the industry needed to be educated about the U.S. AP and its associated requirements to help ensure quality data is reported to the U.S. Government. Second, the NRC needed to perform continuous quality control reviews of the data that was submitted in order to catch any mistakes or negative trends.

The NRC began providing outreach on the U.S. AP and its associated requirements in 2008. It was recognized early in the process that one critical component of ensuring the quality of data provided to the IAEA was an adequate understanding of the U.S. AP by the domestic nuclear industry. Through tradeshows, conferences, and meetings, the NRC and Department of Commerce provided information to a variety of different licensees, and non-licensed advocacy groups (e.g., Nuclear Energy Institute).

The focus of this outreach effort was on the various reporting requirements under the U.S. AP and the U.S. Government process and deadlines for submitting data.

Beginning with its initial declaration, the U.S. Government instituted a review process for the quality control of data. Multiple U.S. Government agencies reviewed the data to ensure it is consistent with requirements under the U.S. AP. While this was a fairly straightforward change, there is a fundamental difference between how data under the VOA and AP is treated within the U.S.

The Department of Commerce is used as the central repository for the entire U.S. Government data submitted pursuant to the AP. This means that NMMSS is not involved in the processing of data for the annual declaration, or the quarterly import/export requirements. By removing the traditional role of NMMSS, one critical quality control step is also removed from the process. Therefore, over time, the NRC adopted an internal review process that helps to augment the U.S. Government-wide process. As an example, beginning between late 2012 and early 2013, the NRC incorporated a review of AP documentation and source data into the domestic inspection program at uranium recovery facilities. Approximately once a year while on-site for an inspection, NRC inspectors will ask for the facility to produce the declared AP reports and any source data used to produce the final report. This process helps to ensure that licensees reporting under articles 2.a.v and 2.a.vi are correctly interpreting the requirements in 10 CFR Part 75, and that there are no typographical errors in what is sent to the Department of Commerce.

Summary

Accurate and complete reports provided to the International Atomic Energy Agency by the U.S. Government from selected US NRC licensed facilities is ensured by a series of measures established over nearly 70 years of experience in nuclear material control and accounting. After the U.S. Congress passed the Energy Reorganization Act of 1974 and the Export Reorganization Act of 1975, the NRC was made responsible for ensuring importing States of U.S. supplied SNM and equipment were under suitable safeguards. States with a comprehensive safeguards agreement in place fulfilled this obligation. Nuclear material accountancy has always been the key element to verify that no diversion of SNM has taken place and prevent diversion by threat of early detection. The U.S. Government utilizes a national database to track all source and SNM in the U.S., and provide reports to the IAEA. Quality control is incorporated into the nuclear material management and safeguards system software that provides reports for IAEA selected licensed facilities. The ICRs, PILs and MBRs are reviewed by the NRC prior to being sent to the IAEA. The Additional Protocol declaration review process is different than the nuclear material accountancy review process, in that it has an additional U.S. Government-wide review for initial declaration, annual updates and changes that takes place after the lead agencies review the declarations from those entities for which they are responsible.

---

1 J.S. Walker and T.R. Wellock, A Short History of the Nuclear Regulation, 1949-2009, US Nuclear Regulatory Commission, October 2010

2 J.E. Lovett, Nuclear Materials Accountability Management Safeguards, American Nuclear Society, Nov. 1974

3J.S. Walker, Nuclear Power and Nonproliferation: The Controversy over Nuclear Exports, 1974-1980

4 http://www.State.gov/t/isn/5209.htm, 2012

5 US NRC Regulatory Guide 5.29 (Rev 2) Special Nuclear material Control and Accounting Systems for Nuclear Power Plants, June 2013

French Additional Protocol: technical implementation

Guillaume DANIEL

Institute for Radioprotection and Nuclear Safety (IRSN)
International Safeguards and CWC Implementation Department
International Safeguards Implementation Unit
B.P. 17 – 92262 Fontenay-aux-roses Cedex France
E-mail: guillaume.daniel@irsn.fr

Abstract:

This paper will describe the technical organization implemented since 2004 and the different steps required to achieve an exhaustive and compliant Additional Protocol declaration (identification of concerned entities, data collection, processing and cross-matching, analysis).
It will include appropriate information about content of the declaration. The feedback concerning the challenges associated to the collection of information to ensure correctness and completeness will be addressed. One of them is the understanding of the Additional Protocol by the industrials when contacted about their activities, particularly when they are not focused on the nuclear sector and therefore not used to its vocabulary. Analysis of the consistency of the gathered information is also a big issue. Some examples will be given for a better understanding.

Additionally, the future of the French Additional Protocol data collection and compilation process will be addressed, especially using the IT to improve the quality of the declaration thanks to a new web portal. The aim of the recently developed software is to facilitate the work of entities submitted to declarations on one hand and of IRSN analysts, in terms of data input and control on the other hand.
This tool will also take into account the feedback given by the Agency and the resulting evolution requests to support its role within the international non-proliferation regime.

Keywords: Additional Protocol; France; Information technology; Safeguards

1. Introduction

On the 22nd of September 1998, in order to participate in the strengthening of IAEA safeguards, France signed an additional protocol (INFCIRC/290/add.1) to its safeguards agreement (INFCIRC/290). The protocol entered into force at the same time as those of the other Member States of the European Union, on the 30th of April 2004. Under that protocol, France supplies additional information to the IAEA on activities carried out in cooperation with non-nuclear-weapon States (NNWS):

- Nuclear fuel cycle related public and private research and development activities,
- Manufacturing of Annex I equipment,
- Imports and exports from and to a NNWS outside of the Community of intermediate or high-level waste containing plutonium, high enriched uranium or uranium-233,
- Exports out of France to a NNWS outside of the Community of Annex I and II equipment and material,
- Planned co-operation activities with a NNWS for the succeeding ten-year period relevant to the development of the nuclear fuel cycle.

The objective of the Additional Protocol is to provide relevant information to help the Secretariat to detect clandestine activities conducted by NNWS, for example by the identification of mistakes or lack in statements. It is important to note that the scope of relevant French stakeholders involved in the declarations under the Additional Protocol is pretty wider than the holders of nuclear materials or nuclear operators.

As the purpose of this commitment by the French authorities is to facilitate the detection of undeclared nuclear activities in a NNWS, IAEA may also request complementary accesses (CA) to declared locations or anywhere upon the French territory.

2. Technical organization and feedback

The Euratom Technical Committee (CTE) is the French authority responsible for safeguards. The CTE relies on the technical support provided by the IRSN's (Radiation protection and Nuclear Safety Institute) International Safeguards Implementation Unit. IRSN is the French national expert for nuclear risk assessment including safety, security, safeguards.
As the AP covers activities which may not involve nuclear materials, the first challenge was to identify the French entities potentially concerned, as they were not limited to those usually monitored either by the French authorities, the European Commission or the IAEA. At the end of 2003, no specific data base of these companies existed. For this reason, IRSN had to use different information sources to define a list of entities potentially concerned. Almost 4000 entities were primarily preselected, but only 1741 were contacted for the initial statement after reviewing each one in depth. The list has been rendered more selective with 202 entities in 2013.

An annual partial review of the entities is made, with, for example, the analysis of export licences granted and European Framework Programs. In 2014, ten years after the submission of the French AP initial declaration, a new global evaluation of all potentially concerned entities has been carried carried out, to ensure that the list is up-to-date, using open source information and national firms directories.

In parallel, CTE and IRSN organised several meetings with the main actors of the French nuclear sector (EDF, AREVA…) and nuclear public research organisations (CEA, CNRS…). The aim of these meetings was to introduce the French organisation for the implementation of the AP, to explain the various types of declarations and to identify contact points inside these entities.
During the last 10 years, the interest of involving stakeholders was demonstrated in several occasions as it ensures that they are able to provide the right elements. It implied to develop an appropriate language, easily understandable but also sufficiently accurate to ensure the suitability of the answers.

Data collection and processing is divided in several steps:

(a) Contact the entire list of entities. In 2004, this preliminary step was completed at the end of April with the sending of the declaration files containing a letter explaining the aims of the AP, the national declaration forms and the French declaration handbook (See figure 1 below). The following years, specific information for each entity, extracted from previous declarations, was also sent. This habit proved to be very useful to maximise the general consistency of the declaration.
To answer to entities questions. IRSN implemented dedicated hot line and email address to assist the operators who needed help to analyse their situation regarding the declaration criteria or to fill the declaration forms. These specifics means of communication are commonly used by the operators. Especially the first time, a lot of questions arose concerning the kind of cooperation that should be declared.

(b) Analyse the data collected. The collection of information from different entities has many advantages:
(i) Cross matching when more than one French entity work on a subject is a good way to ensure correctness of the declaration.
(ii) Contacted entities may as well give information on other companies working in the same domain of activity and potentially cooperating in a relevant field of the Additional Protocol.

In the French statement for 2013, 694 lines were declared in annual or quarterly declarations. From the beginning of its AP, 205 declarations were realized, representing more than 5000 lines.

Figure 1: National declaration handbook.

3. Future of the declaration

In 2012, French authorities expressed their willingness to improve the format and content of its declarations to assist the IAEA in fulfilling its mandate. Thus, the Agency suggested some adjustments in order to facilitate the review process and make it more efficient in assessing the correctness and completeness of French and NNWS partners declarations.

Considering the possibilities given by the democratization of Internet, IRSN decided to implement a web portal called PASTEL (Additional Protocol: Electronic Input and Processing). This evolution has the following interests:

(a) Take into account some of the suggestions from the Agency in terms of format by using more detailed forms.

(b) Facilitate the work done by the contacted entities by guiding them more accurately and by allowing them to reuse previously registered information (e.g. lists of address).

(c) Reduce drastically the rewriting work done by IRSN analysts to focus on the content assessment

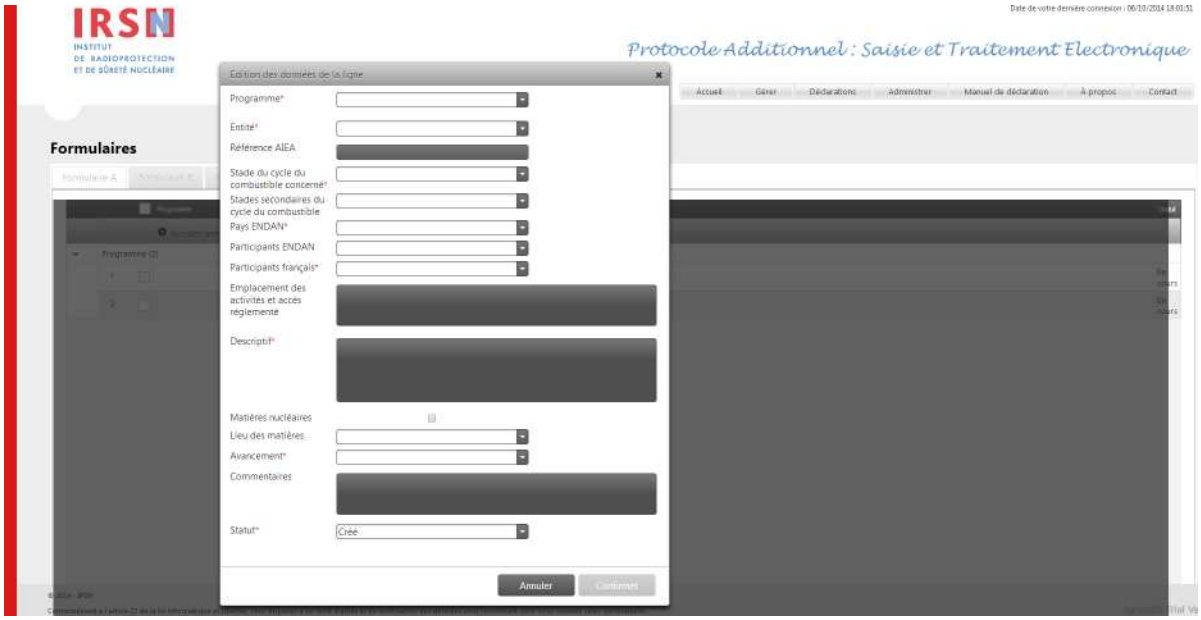

Figure 2: Article 2.a.i) declaration form in PASTEL.

This portal is now being tested internally. Access will be given to a small batch of entities during the second semester of 2015 and full access next year.

Safeguards-relevant information collection from small holders – experiences and challenges

Erika Sundén, Martina Dufva, Joakim Dahlberg

Nuclear Non-proliferation and Transport
Swedish Radiation Safety Authority
Solna Strandväg 96, SE-171 16 Stockholm, Sweden
E-mail: erika.sunden@ssm.se

Abstract:

A number of universities, research institutions, hospitals, and other businesses are in possession of relatively small amounts of nuclear material. In some cases the material is in activities related to the nuclear fuel cycle, but there are also a wide variety of other applications. Regardless of application, material accountancy must be reported to the European Commission (EC) and, in Sweden, to the Swedish Radiation Safety Authority (SSM). However, checking the completeness and correctness of the reports from operators with very small amounts of nuclear material can easily be forgotten or viewed as being less important. In the beginning of 2013 SSM started to prioritize this area and began working on more actively gathering information and checking its correctness. Informing the operators in possession of nuclear material of the rules and regulations are a major part of this work, as we have found that the knowledge level of safeguarding nuclear material in many locations is very low.

This paper will give a description of the work being performed by SSM to ensure that information related to the possession of nuclear material are gathered and correctly declared. It will give an overview of the different procedures that are applied to different categories of small holders in Sweden (where the differences are mostly due to historical reasons). It will also entail some of the challenges we have met along the way; such as explaining to radiographers that for nuclear non-proliferation purposes we are interested in the shielding uranium container, not in the isotope emitting the radiation. What we have experienced being the major differences between collecting information from small holders as compared to larger nuclear facilities will also be outlined. We will end with some plans for the future.

Keywords: small holders, information collection, LOF

1. Introduction

Sweden is a country with a long tradition of nuclear related activities. Already in the 1940s both a civil and a military nuclear programme were developing. However, signing and ratifying the Treaty on the Non-Proliferation of Nuclear Weapons (NPT) in 1970 officially set an end to the military dimension of the Swedish nuclear programme. In the 1970s and 80s the civil program grew and industry related to the civil nuclear fuel cycle expanded. Currently Sweden has ten light water reactors in operation and two permanently shut down. There is also a fuel fabrication factory and a research facility that up until 2005 contained a research reactor in operation. For the back-end of the fuel cycle a central interim storage facility for spent nuclear fuel was built and started operation in 1985. A final geological repository is planned and a first round of applications from the Swedish Nuclear Fuel and Waste Management Co (SKB) are currently under review by SSM and the Land and Environmental Court.

In addition to the large fuel cycle related facilities in Sweden there are also a number of small holders of nuclear material. Some of the nuclear material, especially at schools and universities, was purchased a long time ago and predates the Swedish signing of the NPT. The amounts of material and applications vary and the holders can be anywhere from a small company with a handful of employees to large research institutions with thousands of people within the organization. The number

of small holders is not static over time, as a contrast to the very long-term operations of larger nuclear fuel cycle facilities, and new holders can emerge quickly and others disappear by selling or transferring their material elsewhere. These small holders are subjected to requirements for safeguarding their material and should follow basically the same rules and regulations in this area as the power plants and the other large facilities. This paper will describe the work being done by the Swedish Radiation Safety Authority (SSM) for ensuring the completeness and correctness of the declarations submitted from this section of nuclear material holders.

2. Overview of holders of small amounts of nuclear material in Sweden

As of April 2015 there are in total 21 registered holders of small amounts of nuclear material in Sweden. All together they are in possession of approximately 0.6 kg low enriched uranium, 1,000 kg natural uranium, 1,300 kg depleted uranium and 11 kg of thorium. The bulk part of the depleted uranium is in the form of radiation shielding devices. The sum of the holders combined amount of highly enriched uranium and plutonium is of the order of 50 g in each category. Their approximate locations can be viewed in figure 1. “WSWE” is the Material Balance Area (MBA)-code for the Swedish national Location Outside Facility (LOF). “CAM” refers to the holders which are organized within the European “Catch-all” MBA. “Own MBA” refers to holders which have their own MBA-code. More on the differences between these three categories of nuclear material holders will be explained in section 3.2.

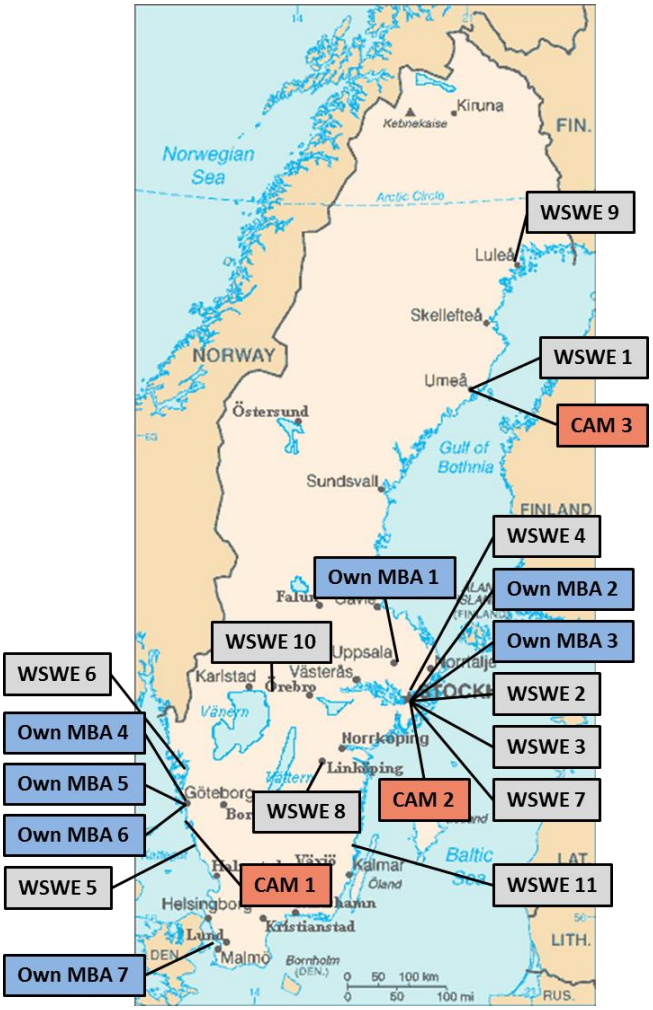

Figure 1: A map of Sweden with the general location of registered holders of small amounts of nuclear material. The labels refer to the three categories of holders. “WSWE” is the national LOF, “Own MBA” means holders which have separate MBA-codes, and “CAM” refers to the holders included in the European Catch-All MBA. The categories are more thoroughly explained in section 3.2. The map reflects the situation as of April 2015 (map adapted from WikiMedia Commons).

The registered holders of small amounts of nuclear material include radiographers, scrap metal yards, recycling facilities, universities, laboratories, research institutions and hospitals. They use different types of nuclear material for different applications. We suspect that there are more installations in possession of nuclear material than presently registered and work is on-going to investigate this. As of yet, a structured approach to such an investigation have not been employed, but there have been some activities to this end. One out-reach activity aimed at radiation experts at universities have been conducted and plans exists for similar out-reach activities to other professional groups, such as radiographers. Information about unregistered holders can come from the installation itself or through an already registered holder, from open sources, or from other parts of SSM. When information about unregistered holders reaches us we include the installation in WSWE and reports the material to the EU Commission.

Every time we encounter an installation with nuclear material which has not yet been reported, the reason given is lack of knowledge. Once information about the rules and regulations a holder of nuclear material must abide by is provided, the holder tries to provide the correct information to the Authority. This process is sometimes quite slow because there is often a need to search for documentation and/or make measurements on the material to determine its properties.

The Authority keeps a national registry over all known nuclear material in Sweden. This registry includes both the nuclear fuel cycle material as well as the nuclear material at each small installation. When nuclear material is discovered and registered, the national registry is updated.

3. The legal framework for Swedish nuclear non-proliferation

Sweden is a party to the NPT and a member of the European Union (EU). Following that, Sweden has accepted safeguards by the International Atomic Energy Agency (IAEA) to control that all nuclear material declared by the state is not misused. The control is based on a safeguards agreement concluded with the state. Before entering the EU a Comprehensive Safeguards Agreement (CSA, INFCIRC/234) according to the model agreement INFCIRC/153 was in force in Sweden. By joining the EU the agreement was replaced with INFCIRC/193 where the major difference lies in that the European Commission (through Euratom) is the contact for all Swedish facilities. In 2000 Sweden ratified the Additional Protocol (AP) and in 2004 the AP entered into force. Sweden decided to be a so called ‘non-side-letter state’, i.e. Sweden is responsible for Articles 2a(i), 2a(iv), 2a(ix), 2a(x), and 2b(i), which entails declaring nuclear fuel cycle-related research, the manufacturing of certain products, the export of other products, and general plans for the succeeding ten-year period relevant to the development of the nuclear fuel cycle. For Articles 2a(iii) and 2a(viii), which entail providing the IAEA with a general description of each site and information about processing of intermediate of high-level waste, there is a shared responsibility between Sweden and the EU Commission. Sweden decided to nominate its Competent Authority, the Swedish Radiation Safety Authority, as the site responsible for each site in Sweden. For articles 2a(v), 2a(vi) and 2a(vii), which entail declaring information about mines and source material, and quantities of material exempted from safeguards under article 36 or 37 under INFCIRC/193, the EU Commission is the responsible party.

As a member of the European Union, the Commission Regulation (Euratom) no 302/2005 has the same legal standing as a national law in Sweden. To fulfil the articles in the Additional Protocol the sentiment of the articles have been incorporated into Swedish national law. This was done by updating the Act and Ordinance on Nuclear Activities (*Lag (1984:3) och Förordning (1984:14) om kärnteknisk verksamhet*), the Act and Ordinance on Inspections according to International Agreements on the Non-proliferation of Nuclear Weapons (*Lag (2000:140) och Förordning (2005:275) om inspektioner enligt internationella avtal om förhindrande av spridning av kärnvapen*), and in regulations prescribed by the Authority (mainly *SSMFS 2008:3; Strålsäkerhetsmyndighetens föreskrifter om kontroll av kärnämne m.m.*).

There are thus EU-regulations and national laws and regulations that implement the international agreements on safeguards (such as the AP). In addition to this there are also national laws and regulations. In the Act on Nuclear Activities it is specified that nuclear activities requires a licence, either from the Government or from SSM. The Ordinance on Nuclear Activities specifies the limits of the amount of nuclear material an entity can hold before it needs a licence from the Government or from SSM, and what amounts only need to be reported but does not require licences. The Act on

Nuclear Activities gives SSM the right to issue the regulations necessary to ensure compliance with obligations in agreements aimed at preventing the proliferation of nuclear weapons and unauthorised dealings with nuclear material and such nuclear waste that comprises spent nuclear fuel.

3.1. National rules and regulations for small holders

As mentioned in the introduction, the holders of small amounts of nuclear material must follow basically the same rules and regulations for safeguarding their material as the large nuclear fuel cycle related facilities. Of course, not all articles are applicable to all types of activities or businesses, but the same basic rules apply. In particular, all holders must have control over their stock of nuclear material. This entails keeping a current list over all nuclear material and up-date it as needed.

Most of the additional rules regarding nuclear non-proliferation for holders of nuclear material are specified in regulations prescribed by the Authority, where the majority can be found in SSMFS 2008:3 (The Swedish Radiation Safety Authority's Regulations on the Control of Nuclear Material etc.). The national rules on nuclear non-proliferation most applicable to the holders of small amounts of nuclear material are summarized here:

All holders must have control over their stock of nuclear material. All changes to the inventory must be reported to SSM within three business days. The nuclear material must be stored so identification and verification can be made, and at an inspection there must be personnel with enough competence present so that international inspectors can fulfil their inspection tasks. After a request by the Authority, the holder must establish a site description over the buildings or parts of buildings where nuclear material is used or stored. All holders must also appoint a person responsible for safeguards within their organisation and report a point of contact for communications with the Authorities (the State Authority, the EU Commission, and the IAEA). All holders must have a system and an organization with enough financial and personnel resources to ensure these tasks are fulfilled.

In addition to the rules and regulations aimed at ensuring nuclear non-proliferation summarized above there is also several other rules a holder of nuclear material must abide by. For example, they must have a system for physical protection of the material, a waste management system, financial means to take responsibility for the material until it is placed in a final repository, and handle the material correctly to limit the radiation exposure to those coming in contact with the nuclear material. Some of these additional rules derive from the Radiation Protection Act (*Strålskyddslagen (1988:220)*) which aims at protecting humans, animals, and the environment from harmful exposure to radiation. An amount of nuclear material can be exempted from license according to the Ordinance on Nuclear Activities but require a license according to the Radiation Protection Act.

3.2. Different categories of small holders and international regulations

In Sweden the holders of small amounts of nuclear material are divided into three categories. With different combinations of exemptions and derogations in these categories the set of international rules they must abide by will vary between them, in addition to the national rules and regulations described in the previous section. In this paper we label the three categories "Own MBA", "National LOF", and "Catch-All MBA".

"Own MBA" refers to the holders which have their own separate Material Balance Area (MBA) code. In general, they report their inventory and changes to it directly to the EU Commission using the reporting tool ENMAS. They are also obligated to provide annual activity reports, Basic Technical Characteristics (BTC), and site descriptions, and keep them updated. However, several of these holders hold nuclear material in amounts low enough to ask the EU Commission to apply for exemption from safeguards under Article 37 in INFCIRC/193, or use nuclear material in such applications that it can be exempted under Article 36 in INFCIRC/193. If granted, they will not have to provide a site declaration or be subjected to inspections by the IAEA. By applying for derogations under Article 19 in the Commission Regulation (Euratom) no 302/2005 the reporting format and frequency can be simplified. If granted derogation the holder need only report when a change has occurred, instead of monthly, and they can do so using a special form instead of using ENMAS. They do however need to provide a report annually of their entire stock of nuclear material. Exemptions and derogations are not connected, i.e. being granted one of them does not mean being granted the other one. This means that there is in total four possible combinations here, where each combination comes

with different rules and obligations (i.e. exemption + derogation, no exemption + derogation, exemption + no derogation, and no exemption + no derogation). All four combinations are or have been represented in the group "Own MBA" in Sweden.

The "National LOF" in Sweden is a single Material Balance Area with the code WSWE. The members within this MBA are located all over Sweden. When a business or research institution acquires nuclear material (or as in most cases, discover that they already are in possession of nuclear material but had not reported it to the Authority) the first step the SSM does is to include them in this MBA. Changes within an MBA should not be reported to the EU Commission; however SSM keeps track of the individual stock of nuclear material for all members of this MBA and records changes also within the MBA. When a change in inventory in or out of WSWE is reported to SSM we report it to the EU Commission using ENMAS. Exemptions and derogations can only be granted for an entire MBA, and since the inventory quite frequently changes for some of the members within WSWE no exemptions or derogations can be granted for any individual entity within this MBA. Therefore site descriptions are needed for all members. The first site declaration for this MBA was created and submitted in 2014 and the process leading up to this is described in section 5.

The "Catch-All MBA" is a common European Material Balance Area which gathers holders of small amounts of nuclear material in the Non-Nuclear Weapons States in the EU. There is a strict limit of how much material a member is allowed to have (specified in Annex I-G in the Commission regulation (Euratom) no 302/2005), and the total amount of nuclear material in the whole MBA must not exceed one effective kg (as stated in the Commission Recommendation of 15 December 2005, p. 35). The holders in this group are automatically granted derogation according to the Commission Regulation (Euratom) no 302/2005 and need only report to the EU Commission when there are changes in the inventory. They are also exempted from IAEA safeguards and thus not subjected to inspections from the IAEA or under the obligation of providing a site declaration[4].

Table 1 shows a summary of some of the tasks and reports the holders in the different categories must do and submit.

	Own MBA	**National LOF**	**Catch-All MBA**
Keep inventory list	yes	Yes	yes
Report changes in NM stock to SSM	yes	Yes	yes
Report changes in NM stock to EU Commission	yes	no (SSM reports)	yes
Report changes in NM stock using ENMAS	yes[1]	no (SSM reports)	no[2]
Report NM stock monthly	yes[1]	no (SSM reports)	no[2]
Site description (AP 2a(iii))	yes[3]	Yes	no
Programme of activities	yes	no (SSM reports)	no[4]

Table 1: The table shows a summary of some of the obligations holders of small amounts of nuclear material have. For more information, see text in section 3.2.

[1] If derogation has been granted by the EU Commission under Article 19 in the Commission Regulation (Euratom) no 302/2005, the frequency and format of the inventory reports can be modified from the standard way of reporting.
[2] Members of the Catch all MBA are automatically granted derogation from the Commission Regulation (Euratom) no 302/2005.
[3] If exemption has been granted by the IAEA under Article 37 or 36 in INFCIRC/193, the NM is no longer under IAEA Safeguards and therefor no site description is required.
[4] The requirements for Catch-All MBA members are further specified in the Facility Attachment "Safeguards agreement in connection with NPT, Subsidiary arrangements" from 1985.

4. Inspections of small holders

To ensure that requirements set up by the international organisations and the national Authority is met there is a need for communication, visits, and inspections. In the beginning of 2013 SSM started to put more resources into the work with holders of small amounts of nuclear material. The EU Commission had previously announced that they would start to prioritize inspections of small holders and during 2013 they carried out a round of inspections of most holders in the category “Own MBA” in Sweden. The national work regarding small holders was further fuelled by a request from the IAEA to SSM to provide site descriptions according to the AP for all the members within the National LOF WSWE.

4.2. National inspections

An inspection carried out at a holder of small amounts of nuclear material must be prepared well in advance. Because of the vast differences between such companies and organizations that hold small amounts of nuclear material, the approach to ensure compliance with national and international regulations works best if it is tailor-made to fit the type of business. It has been a learning curve for the national inspectors on how to best get the message across; on the one hand avoiding the use of too many abbreviations or technical jargon that unnecessary complicated things and on the other hand not simplifying too much or being too specific in instructing the installations.

Usually an inspection at a holder of small amounts of nuclear material that has not been visited in a long time (or has not been visited at all) starts with a phone call where the purpose of the inspection is explained. After that we send an email summarizing the call and giving explicit instructions on what kind of preparations we expect from the holder before our visit. This can entail up-dating (or in some cases, creating) an inventory list (we supply specifications on what information such a list should contain), prepare to show shipping- or transport-documentation, and to make sure all nuclear material is available for id-checks and verification at the time of the visit. References to paragraphs in legal documents are also enclosed in the letter.

During the inspection we discuss the inventory of nuclear material and frequently we find that it differs from the inventory previously reported to SSM. Together we try to straighten out where material has been moved if it no longer can be found on the site, and update the registry at SSM with material that has either been found at the site or purchased without being reported. Often there is a need for a longer discussion and explanation of what should be reported and what type of information should be included. Then SSM verifies all material by number identification and sometimes by measurement by the use of an identiFINDER^{TM} (HM5-type detector of gamma and neutrons). Depending on the category of the installation (see section 3.2) we also discuss what other information the installation need to provide or update, such as the basic technical characteristic (BTC) and/or a description of the site.

After the inspection there are usually a number of follow-up activities that need to be carried out and these are specified in a report written by SSM and distributed to the holder. The holders often need to further up-date their list of inventory items (LII), sometimes work harder in trying to locate different types of documents supporting transfers of materials, or perform additional measurements on certain items to be able to declare them correctly. SSM often needs to update its registry of nuclear material as well as the registry on types of activities carried out by the holder and their contact information. The updated information is also reported to the EU Commission.

In summary, an inspection of an installation with very small amounts of nuclear material, as compared to a larger fuel cycle related facility is much more time-consuming in large part due to the preparations and the follow-up activities. To ensure the best result follow-up inspections should be made, but so far only a few such inspections have been carried out.

4.3. Inspections with international organizations

The Swedish Government has appointed SSM to accompany IAEA inspectors during international inspections in Sweden. (In the case of inspections initiated by the EU Commission and where the IAEA chose not to participate, SSM makes a case by case decision to participate or not. The inspections at small facilities are prioritized.) These inspections follow basically the same format as for inspections in larger facilities. The books are audited and the internal book-keeping compared to the

reported stock of nuclear material. The material is itemidentified and parts of it verified by non-destructive analysis (NDA) measurements. Because of the inadequacies we have encountered in many places we try to prepare the holders before the inspection as much as possible. If possible, we make a separate visit before the international inspection is scheduled. At the international inspections there is often less time to discuss matters of book-keeping, inventory lists, and reporting obligations. This is why visits made without international inspectors are a very important complement in ensuring compliance to regulations.

5. Site descriptions for the National LOF WSWE

The IAEA requested that Sweden (through the EU Commission) would either ask for an exemption or provide a site description for the “National LOF” WSWE. The task sounds simple but was in reality not so simple, especially when contacts with and inspections of the members within this MBA had been few and far apart in time. Even finding out valid contact-information for some members proved difficult.

It was quite quickly determined that an exemption from IAEA Safeguards was not a suitable option. The MBA fulfils the requirements on amounts of nuclear material (Article 37 of INFCIRC/193) but because of frequent material movements in and out of the MBA an exemption would be very impractical. Once this was determined discussions started with the EU Commission and to some extent also with the IAEA on how such a site declaration should be made and what information it should contain. As is shown in figure 1, the members of WSWE are scattered across the country. There was also the question of how unified the declaration should be, because the nature of the businesses for the members within WSWE can be quite different. It was decided that the level of details provided for the different members did not have to be unified, but instead depends on the activities within the specific installation. I.e. for metal scrap yards we included an overview map of the area and a brief explanation of the major activities performed on the site. For research institutions the site description need to be more detailed with floor-plans and description of rooms and activities performed therein.

To simplify for the members of WSWE a template of a site declaration was made by SSM for each installation where as much information as possible was already filled in. The members only had to check and correct or in some instances provide us with some additional information. The ideal would have been to visit all installations before submitting the site declaration, to ensure its correctness and completeness, but unfortunately there was no time for that. It is instead an on-going task and we hope to have visited most of the installations within a couple of years.

After all the templates were checked and completed the site declaration could finally be submitted to the EU Commission in December 2014, and the first update to it was submitted in March 2015.

6. Experiences from working with small holders of nuclear material

In the past two years of working with holders of small amounts of nuclear material we have gained a lot of experience and learned a lot about different applications of nuclear material. The challenges we have encountered can be divided up into two main parts; communicating and explaining to the holders what their responsibilities as owners of nuclear material are, and interpreting the national and international regulations and determining where the bar should be set.

The first set of challenges relates to communication of the rules and regulations to the holders. One of the surprises is that it is not always beneficial for the purpose of reporting if the holder has a great knowledge of nuclear physics. Every gram of nuclear material should be reported, when used in nuclear activities as well as for other purposes. A person with knowledge in the field might think that a couple of grams (or kilograms) of depleted or natural uranium cannot be used for anything illegal, and therefor does not need to be reported.

Other types of holders, such as radiographers, are used to contacts with other departments of the Authority in applying for licenses to hold, use and transport radioactive isotopes. When we contact them demanding information regarding the depleted uranium container in which the isotope is placed, it can lead to many misunderstandings. Another common misconception is that natural or depleted

uranium or thorium in the form of compounds such as nitrates or acetates are automatically exempted from safeguards and safeguard reporting.

Even though the rules and regulations for all holders of nuclear material are basically the same, the prerequisites for fulfilling the obligations can be very different. At e.g. a nuclear power plant there are usually one or several people that have the dedicated task of keeping the inventory updated and managing the reporting duties of the plant. For a smaller installation responsibilities are often not formalized and the task of maintaining control of the nuclear material is not given enough time. When communicating with these holders one must bear that in mind. One must also understand that some words and abbreviations commonly used when communicating with larger facilities should be avoided or at least thoroughly explained.

There is a need for a graded approach in applying regulations initially intended for facilities such as nuclear power plants on installations with small amounts of nuclear material. Often, a graded approach to requirements is not formalized, but employed nonetheless. SSM has the mandate to set terms or grant exceptions from national regulations, but the Commission Regulation (Euratom) no 302/2005 must be followed by all holders and the organization with a mandate to determine compliance is the EU Commission. Without guidance documents on how to interpret rules and regulations from the viewpoint of a small holder makes it difficult for SSM to help the installations on where to set the bar in trying to fulfil their obligations. Particular Safeguard Provisions (PSPs) or Facility Attachments (FAs) are not in place for the individual small holders in Sweden (with the exception of the ”Safeguards agreement in connection with NPT, Subsidiary arrangements” from 1985 which is valid for all members within the European “Catch All MBA”). When the holders ask questions such as “Is the reply to this question in the BTC specific enough?” or “Can we collect information about our experiments for a year and only report a re-batch at one time?” we can give advice based on previous experiences but we cannot give definitive answers.

6.1. On-going work

In order to ensure correctness and completeness of the reports provided by the small holders themselves, or declarations that pass through the Authority such as site declarations, inspections are needed. Since the start of 2013 the Authority has increased its presence at these locations, and so far 13 of the 21 registered holders of small amounts of nuclear material have been visited at least once. Some have required several visits. We have increased our contact with all 21 of them in order to get updated information for e.g. BTC:s and site descriptions.

After a visit to a location and a meeting face-to-face where both we at the Authority and the representatives from the installations have the opportunity to ask questions, the rest of the communication runs much more smoothly. This is one reason why, even if the amounts of nuclear material is extremely small, a physical visit to such an installation is prioritized over some other tasks. The ambition is thus to perform inspections of as many of the small holders as possible, and to do it as soon as possible. But, since the follow-up tasks after an inspection in some cases is a lengthy process, we try not to initiate more contacts at one time than can be properly followed up.

Prioritizing what installation to inspect is based on a number of factors; amount and type of nuclear material, application of nuclear material, perceived control by the installation of the nuclear material, and its physical location and closeness to other installations.

An inspection can be triggered by the holder itself. With new staff at positions such as radiation safety experts we have sometimes been invited to talk about procedures for reporting and discussions on how to apply the rules and regulations to their specific businesses. These visits are of course given high priority.

6.2. Plans for future work

To maintain correct and updated information on nuclear material inventory and information provided in BTC:s and site descriptions we believe there is a need for regular follow-up activities. After this initial round of inspections has been completed we anticipate some sort of more scheduled plan of activities, e.g. a rolling schedule of approximately 4-5 inspections annually and follow-up letters or phone calls biannually to all installations. Even though the regulations states that changes should be reported

without reminders we believe that to ensure complete and correct information some legwork is required from the Authority's side.

For most of the installations the nuclear material remains static for longer periods of time. However, a couple of installations use their material for experiments where the material form changes and material is relatively often sent and received, e.g. to and from collaborators. For these installations we plan to focus our inspections on their system for ensuring that their declarations of both nuclear inventory and technical capacity are complete and correct. This is especially important when there are several people involved and where there is a large turnover of personnel, e.g. at universities.

We also plan to, in a more structured way, find installations which are in possession of nuclear material but are unaware of their reporting duties. This can be achieved by better co-operation and exchanging of information within the Authority, by various out-reach activities such as participating in meetings at relevant trade associations, and by using the knowledge we have gained over the past two years of what types of installations most likely to possess nuclear material.

To make it easy to understand and to follow the rules and regulations applicable to holders of nuclear material we have plans to compose some sort of guide documents. These documents can either be tailored to a specific type of installation, or be more general. Because of the three categories we have in Sweden (described in section 3.2) there might be a need to compose at least differentiated documents for these three.

As mentioned in section 3.1, installations which are in possession of nuclear material are also subjected to rules and regulations outside the area of nuclear non-proliferation and safeguards. To reduce the number of inspections at a specific installation and make better use of both theirs and the Authority's time we are thinking about performing joint inspections, where e.g. nuclear non-proliferation, physical protection, and radiation protection is combined. In that way we have expertise from more areas and can provide the installations with a collected view on what works well and where improvements can be made. The national inspectors can also learn from each other and after a couple of joint inspections cover an area which is usually not covered by that inspector.

7. Conclusions

Working to ensure nuclear non-proliferation with holders of small amounts of nuclear material, often not part of the nuclear fuel cycle business is both challenging and time-consuming work, but also varying and fun. It demands a solid understanding of both national and international regulations, and the ability to transfer and translate it so that parties not familiar with non-proliferation still can abide by them. When we find installations not compliant with rules and regulations, the reason seems almost always to be a lack of knowledge. Keeping contact by telephone calls and emails and making regular physical visits enables for easier communication and better compliance to rules.

A formalized graded approach to rules and regulations, made in collaboration with the international organizations, would simplify working with small holders of nuclear material. This could be in the form of PSP:s of FA:s, or perhaps as a guide document similar to the "Guidance for States Implementing Comprehensive Safeguards Agreements and Additional Protocols" in the IAEA Service Series 21.

8. Acknowledgements

The authors would like to acknowledge those at the unit Nuclear Non-proliferation and Transport at the Swedish Radiation Safety Authority who have reviewed and made valuable contributions to both this paper and to the work described herein.

The authors would also like to acknowledge the co-operation with the EU Commission, with special thanks to Ali Zein, Timo Lindberg, Jean Schreiner and Christelle Charpentier, who have given good and speedy advice and help in interpreting regulations and providing reports.

9. Legal matters

9.1. Privacy regulations and protection of personal data

I agree that ESARDA may print my name/contact data/photograph/article in the ESARDA Bulletin/Symposium proceedings or any other ESARDA publications and when necessary for any other purposes connected with ESARDA activities.

9.2. Copyright

The authors agree that submission of an article automatically authorises ESARDA to publish the work/article in whole or in part in all ESARDA publications – the bulletin, meeting proceedings, and on the website.

The authors declare that their work/article is original and not a violation or infringement of any existing copyright.

Implementation of the SNRI concept in the FBFC Romans Fuel Fabrication Plant and the installation of unattended measurement stations for fuel assemblies

A. Terrasi, W. Köhne, P. Beuseling,

P. De Baere, M. Maggi, P. Schwalbach, K. Schoop

European Commission, Directorate General for Energy,
Directorate E Nuclear Safeguards, Luxembourg

Email: antonio.terrasi@ec.europa.eu

Abstract:
Inspection schemes in large Fuel Fabrication Plants require - due to limited inspection resources - concepts that allow for a flexible resource allocation but still ensure that all nuclear material under Safeguards in the European Union has a probability to be selected for physical verifications.

Having started from regular, sometimes dense, inspection schemes to cover all relevant material flows, EURATOM is moving towards more randomised inspections, which allow for a more flexible inspection planning and execution. In this respect, EURATOM has implemented the SNRI (Short Notice Random Inspection) concept at the FBFC LEU Fuel Fabrication Plant (FFP), located in Romans, France, which is the FFP with the highest throughput in Europe.

The randomisation of the inspections gives the EURATOM inspectorate more flexibility in their planning and allows the verification coverage of the complete flow of nuclear material going into and out of the facility during a Material Balance Period (MBP), while consuming a reasonable level of inspectorate resources. The operators are asked to inform the inspectorate about their operational planning on a regular basis, to allow inspectors to plan and prepare their inspection activities in advance.

However, with the given throughput of the plant, in order to avoid production delays and minimise dose uptake for inspectors when performing measurements in the fuel assembly stores, it was decided to combine the SNRI concept in the near future with an unattended measurement and surveillance system to ensure that all fuel assemblies produced can be verified without any requirement on inspectors to be present but still achieving the EURATOM verification goals.

The Remote Data Transmission (RDT) of instrument and camera signals via a VPN channel to the EURATOM HQ in Luxembourg, together with the transmission of operating data by the operator in electronic format, would be a further step to use the available inspection resources in the most efficient way.

Keywords: Short Notice Random Inspection, Material Balance Period, unattended measurements, Remote Data Transmission

1. Introduction

In large Fuel Fabrication Plants, the quantities of nuclear materials going into and out of the facilities during a Material Balance Period (MBP) are much higher than the inventory and contribute significantly to the MUF (Material Unaccounted For) and its uncertainty, the Sigma MUF (σMUF). Therefore, information on the input and output flows and their verification are essential to draw a

safeguards conclusion at the end of the MBP. In order to optimise inspection resources and ensure that all the nuclear material under safeguards, going into and out of the facility during a MBP, is eligible to be selected for physical safeguards verifications, concepts that allow a flexible resource allocation are needed. A new approach based on the SNRI (Short Notice Random Inspection) concept has been implemented by EURATOM at the biggest LEU FFP in Europe, FBFC Romans (France).

2. SNRI Objectives

The main objective of this new approach is to allow a random verification of the complete flow of material going into and out of the facility during a Material Balance Period (MBP). Before the SNRI concept was implemented at the LEU FFP of Romans, five scheduled bi-monthly interim inspections were performed during a MBP and the verifications were limited to the population of items present at the time of inspections. However, with the given plant throughput, a significant increase in the number of interim inspections and resources, together with some retention time arrangements, would have been required to achieve the verification coverage of the complete flow of nuclear material going in and out of the facility over a MBP.

With the introduction of the randomisation factor, the SNRI concept makes the coverage of the complete flow of nuclear material going into and out of the facility possible without increasing the inspection frequencies and resources. The short notice aspect provides also additional assurance that the facility is being operated as declared.

3. Plant operation forecast

In order to achieve the SNRI objective and allow the inspectorate to optimise the inspection planning, the operator provides the inspectors on a monthly basis with a detailed forecast on the plant operations for the next two months. The forecast includes weekly information about receipts and shipments of nuclear material in the different forms (UF6, powder, scrap, rods, and assemblies), as well as production information. However, the mandatory annual activity programme and advanced notifications required by Commission Regulation 302/2005 for receipts and shipments of nuclear material remain applicable.

The data to be provided in the forecast are:

For shipments and receipts

- The week number
- The type of activity (shipment/receipt)
- The type of items (UF6 cylinders, powder, scrap, rods, assemblies)
- The number of items
- The shipper/receiver
- The estimated quantities of U_{total} and U_{235}
- The date of unpacking / packing of material.

For the fuel production

- The week number
- The type and number of assemblies produced
- The country of delivery.

4. SNRI inspection process

Three to five SNRI inspections will be normally performed during each MBP. The inspections are performed by 2 inspectors and over 3 days. The timing of the inspections is random and unknown to the operator. However, in order to allow the inspectorate to achieve the SNRI objective, the selection of the date for SNRI inspections can also be driven by pragmatic factors such as the known operational programme of the facility. Dedicated regular inspections might also be carried out as appropriate in order to verify and seal exports of nuclear material to countries outside of European Union. These inspections are scheduled according to the advance notifications received from the operator.

The SNRI inspections are notified by e-mail between 9:00 am and 10:00 am to the State Authority and the operator 48 hours in advance of the start of the inspection. Upon arrival of the inspectors on site, an inspection opening meeting is held at which the operator provides the inspectors with information on the latest operational status of the plant, the List of Inventory Items (LII) for the UF6 cylinders and the fuel assembly stores and an update of the accountancy to 0:00 o'clock of the inspection start date. Then the inspection team proceeds into the facility and starts with the verification activities. The scope of the verification activities performed on-site during inspection is twofold: to confirm operator declarations and to make sure that the operator's physical follow-up system is working effectively and is up-to-date. The verification activities performed include physical verifications and accountancy verifications.

4.1 Accountancy verifications

The accountancy verifications include nuclear material declarations check and records verifications and is performed covering the period from the starting date of the previous inspection to 0:00 o'clock of the first day of the actual inspection. To do so, the operator is asked to provide in electronic format an update of the inventory change reports (ICR). These ICRs are then loaded into the EURATOM VARO software (Validation of Accountancy Records of Operators) and checked for syntax, consistency and errors. The ICRs are then merged with the HQ data to compute the books ending at the start date of the inspection and to produce the Working Paper Accountancy (WPA).

EURA - RESTRICTED

Working Paper Accountancy: WPA

Accountancy ( )
Updating ( )

		EURATOM	IAEA	Year: 2014
MBA Code: [illegible]3	Inspection no.	MA-100[illegible]		Week: 11
	Names	[illegible]		Sheet:1

Book values as of : 31/12/2013	U tot (g) : 127000991	U235 & U233 (g) : 400147										7589514.887	11	9398043	116721690
Rep \ Line num	Transac id	Accounting date	IC code	MBA from \ to	Batch	Mat Form /Cont /Stat	Measurement	Correction	Original date	Prev Rep \ Line	#Item	P (g)	H (g)	L (g)	D (g)
80 \ 83	12604	02/01/2014	NL		[illegible]2	PH / O / F	M			- \ -	1	-253.531			
80 \ 84	12604	02/01/2014	NL		[illegible]I	PH / O / F	M			- \ -	1	-90.608			
80 \ 85	12604	02/01/2014	NL		[illegible]6	PH / O / F	M			- \ -	1	-100.955			
80 \ 86	12603	02/01/2014	RD	[illegible]1	[illegible]2	PH / O / F	N			- \ -	1	13984			
80 \ 87	12603	02/01/2014	RD	[illegible]1	[illegible]I	PH / O / F	N			- \ -	1	13727			
80 \ 88	12603	02/01/2014	RD	[illegible]1	[illegible]6	PH / O / F	N			- \ -	1	13194			
80 \ 89	12606	05/01/2014	NL		[illegible]2	PH / O / F	M			- \ -	1	-104.929			
80 \ 90	12606	05/01/2014	NL		[illegible]I	PH / O / F	M			- \ -	1	-254.186			
80 \ 91	12606	05/01/2014	NL		[illegible]I	PH / O / F	M			- \ -	1	-96.601			
80 \ 92	12606	05/01/2014	NL		[illegible]2	PH / O / F	M			- \ -	1	-89.436			
80 \ 93	12606	05/01/2014	NL		[illegible]I	PH / O / F	M			- \ -	1	-82.093			
80 \ 94	12606	05/01/2014	NL		[illegible]I	PH / O / F	M			- \ -	1	-105.638			
80 \ 95	12606	05/01/2014	NL		[illegible]I	PH / O / F	M			- \ -	1	-199.969			
80 \ 96	12606	05/01/2014	NL		[illegible]2	PH / O / F	M			- \ -	1	-97.364			
80 \ 97	12605	05/01/2014	RD	[illegible]1	[illegible]2	PH / O / F	N			- \ -	1	14165			
80 \ 98	12605	05/01/2014	RD	[illegible]1	[illegible]I	PH / O / F	N			- \ -	1	14011			
80 \ 99	12605	05/01/2014	RD	[illegible]1	[illegible]I	PH / O / F	N			- \ -	1	14616			
80 \ 100	12605	05/01/2014	RD	[illegible]1	[illegible]2	PH / O / F	N			- \ -	1	12882			
80 \ 101	12605	05/01/2014	RD	[illegible]1	[illegible]I	PH / O / F	N			- \ -	1	12786			
80 \ 102	12605	05/01/2014	RD	[illegible]1	[illegible]I	PH / O / F	N			- \ -	1	14244			
80 \ 103	12605	05/01/2014	RD	[illegible]1	[illegible]I	PH / O / F	N			- \ -	1	14140			
80 \ 104	12605	05/01/2014	RD	[illegible]1	[illegible]2	PH / O / F	N			- \ -	1	12663			
80 \ 105	12608	06/01/2014	NL		[illegible]I	PH / O / F	M			- \ -	1	-89.382			
80 \ 106	12608	06/01/2014	NL		[illegible]I	PH / O / F	M			- \ -	1	-142.982			
80 \ 107	12607	06/01/2014	RD	[illegible]1	[illegible]I	PH / O / F	N			- \ -	1	12803			
80 \ 108	12607	06/01/2014	RD	[illegible]1	[illegible]I	PH / O / F	N			- \ -	1	14916			
80 \ 1	12609	07/01/2014	SD	[illegible]T	[illegible]20C	MA / D / F	M			- \ -	-1				-10530
80 \ 2	12610	07/01/2014	SD	[illegible]R	[illegible]KD	EA / S / F	M			- \ -	0				-415221
80 \ 3	12610	07/01/2014	SD	[illegible]R	[illegible]KZ	EA / S / F	M			- \ -	0				-415570
80 \ 4	12610	07/01/2014	SD	[illegible]R	[illegible]LF	EA / S / F	M			- \ -	0				-415076
80 \ 5	12610	07/01/2014	SD	[illegible]R	[illegible]LK	EA / S / F	M			- \ -	0				-415114
80 \ 6	12610	07/01/2014	SD	[illegible]R	[illegible]LL	EA / S / F	M			- \ -	0				-415782
80 \ 7	12610	07/01/2014	SD	[illegible]R	[illegible]M4	EA / S / F	M			- \ -	0				-413970
80 \ 8	12610	07/01/2014	SD	[illegible]R	[illegible]MA	EA / S / F	M			- \ -	0				-414801
80 \ 9	12610	07/01/2014	SD	[illegible]R	[illegible]MJ	EA / S / F	M			- \ -	0				-416519
80 \ 109	12285	07/01/2014	NL		[illegible]6	CP / O / F	M	D	06/09/2013	76 \ 77	-1	1.928			
												7765940.141	11	9398043	113389107
Sub total :	U tot (g) : 123668408	U235 & U233 (g) : 400147													

Generated with VARO by [illegible] on 15/04/2014 - 16:07

Based on the WPA produced with VARO, the inspectors perform a book audit consisting of:

- Comparison of accountancy records against operating records (source documents)
- Comparison of the book stocks calculated with VARO with the book stock values declared by the operator
- Follow-up of accountancy remarks (if applicable)
- Comparison of all shipments and receipts declared since the last inspection with the weekly flow information provided by operator in the operational forecast.

4.2 Physical verifications

During the SNRI inspections, the physical verifications activities are performed on items of the input and output flows of the process, present in the facility at the time of performing the inspection. They consist of quantitative testing including various methods of non-destructive assay (NDA), destructive analysis (DA) and associated item counting and tag checking.

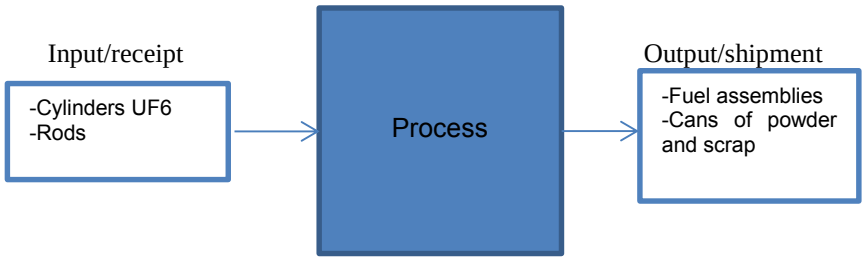

4.2.1 Non Destructive assay

The number of items to be verified by NDA for gross and partial defect detection is calculated for each process flow using the Jaech and Russell sampling algorithm with the required detection probability (e.g. medium for low enriched and low for natural and depleted Uranium), taking into account the throughput since the last inspection. The table below gives an indication for the number of UF6 cylinders to be measured for gross and partial defect (GD/PD) at different throughputs to cover the EURATOM detection goals.

UF6 Cylinders	Minimum number of items to be measured during SNRI inspections with different detection probability (DP)	
	40% DP GD/PD	60% DP GD/PD
100	12/11	19/18
75	9/8	14/14
50	7/5	10/9
25	3/3	5/5

The sum of items verified for each flow during the SNRI inspections must however be equal or superior to the number of items which would be calculated to cover the complete annual input/output flow of the facility with the appropriate detection probability. Due to the high throughput of the plant,

the number of fuel assemblies to be measured for gross and partial defect (GD/PD) to cover the EURATOM detection goals at different throughputs can however result in a quite significant number of items to be measured at each SNRI inspection. As an example, the table below gives an indication of the number of fuel assemblies to be measured for gross and partial defect (GD/PD) at different throughputs to cover the EURATOM detection goals.

No. of Fuel assemblies produced	Minimum number of items to be measured during SNRI inspections with different detection probabilities (DP)	
	40% DP GD/PD	60% DP GD/PD
400	36/12	61/21
300	27/9	46/16
200	18/6	30/11
100	9/3	16/5

Therefore, in order to avoid production delays while still achieving the EURATOM verification goals and minimise the inspection's effort, as well as dose uptake for inspectors when measuring in the fuel assembly stores, it was decided to install an unattended Neutron Coincidence Counter (NCC) located in the normal production flow in each of the two fuel assembly stores. All fuel assemblies transferred into the stores will be measured and identified through a video surveillance system. After the measurement, the fuel assemblies will remain under C&S until they are packed for shipment. The signals of the instruments and cameras will be directly transmitted to the EURATOM office on-site for central storage. During SNRI inspections, the inspectors will evaluate and review these data directly transmitted to their office on site and compare the results with the operator's declarations using the RADAR/iRAP software.

C&S system Fuel Assembly Stores

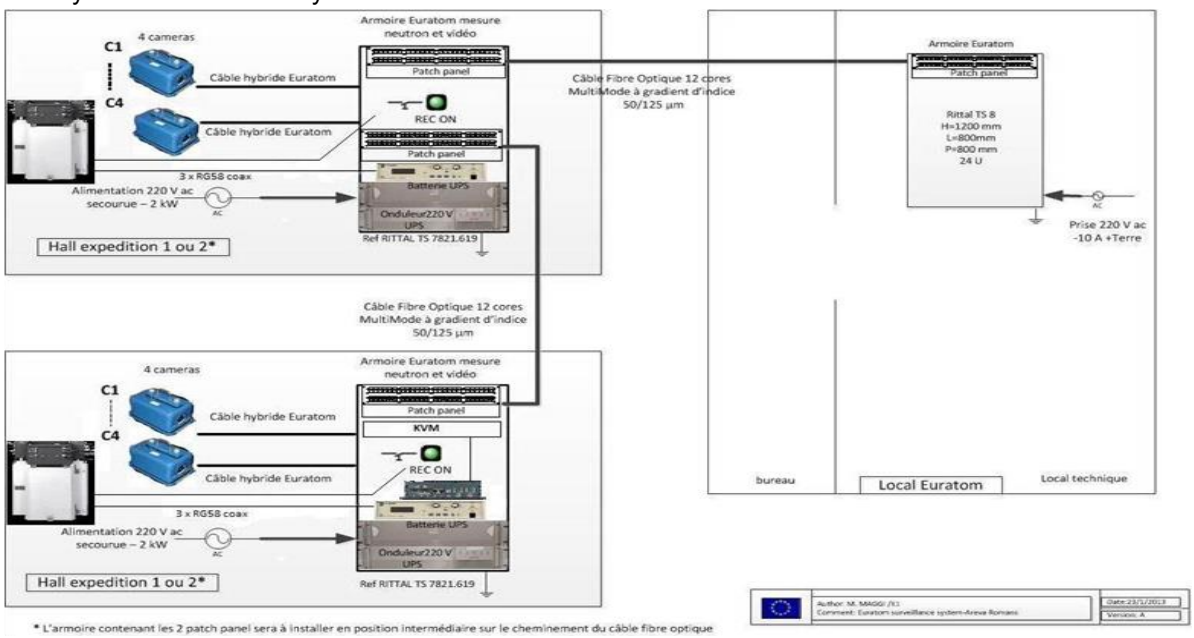

Moreover, to avoid inspectors' presence during the fuel assemblies export packing operations, electronic seals placed by the operator under camera surveillance will be used to maintain continuity of knowledge until the transport containers are finally sealed by inspectors. The implementation of this

unattended C&S system will reduce the inspection effort, minimise dose uptake by the inspectors, and enable EURATOM to achieve the required level of assurance on the complete throughput while offering more flexibility to the operator at the same time.

4.2.2 Destructive Analysis

A pellet sample is also taken at each SNRI inspection from the process line or the pellet store for the detection of bias defects and it is left under seal at the facility. All samples collected during SNRI inspections and at the PIV are sent to the EURATOM laboratory of ITU Karlsruhe to be analysed. The results are compared with the operator's analysis results to evaluate the precision and accuracy of his measurement system. In order to draw conclusions about the quality and effectiveness of the overall operator's NMAC system in relation to his statutory obligations according to EURATOM Regulation 302/2005, it might also be necessary for EURATOM to perform audits. These audits will be planned in consultation with the operator and the State Authority.

5. Further development in the SNRI approach

Currently, operating data are handed over in electronic format to the inspectors during the monthly interim inspection performed at CERCA Romans and loaded into inspectors' computer at the EURATOM on-site office. The operator, the national Authorities and EURATOM are looking for ways to improve this data transmission. The transfer of these data to EURATOM headquarter is under examination.

Remote Data Transmission (RDT) of instrument and camera signals via a VPN channel to EURATOM's HQ in Luxembourg, together with the transmission of operating data by the operator in electronic format, would be a further step towards using the available inspection resources in the most efficient way.

6. Conclusion

The SNRI concept has become an effective method to perform the verification coverage of the complete flow of nuclear materials into and out of the Romans facility without increasing the number of inspections or personnel resources. The significant investment in the safeguards instrument infrastructure in the fuel assembly store will pay off in terms of reduction of inspection effort on site and intrusiveness of safeguards verifications.

The network transmission of safeguards data in electronic format directly to EURATOM's Headquarter will be a further step to maintain high detection probabilities and use the available inspection resources in the most efficient way.

7. References:

[1] P. Schwalbach et al; Data acquisition systems in large nuclear facilities - challenges, experiences, solutions; IAEA Safeguards Symposium 2010, Vienna

[2] A Smejkal et al; Automated processing of safeguards data: Perspectives on software requirements for a future "All in One Review Platform" based on iRAP; ESARDA Symposium 2015, Manchester, UK

[3] W. Köhne et al; The role of the VARO inspection software for the implementation of an Integrated Management System (IMS) at the EURATOM Safeguards Office; ESARDA Symposium 2015, Manchester, UK

[4] EURATOM Regulation 302/2005

[5] IAEA-Tecdoc-261, IAEA Safeguards Technical Manual, Part F: Statistical Concepts and Techniques

[6] IAEA STR – 261, Algorithms to calculate sample sizes for inspection sampling plans

[7] IAEA STR-368, International Target Values 2010 for Measurement Uncertainties in Safeguarding Nuclear Materials

Safeguards Indexing Method for the Regulatory Assessment of Safeguards Culture at Nuclear Facilities

Zsolt Stefánka, Hedvig Éva Nagy, Árpád Vincze

Hungarian Atomic Energy Authority
P.O.B.: 676, H-1539, Budapest, Hungary

E-mail: stefanka@haea.gov.hu

Abstract
The Hungarian Atomic Energy Authority (HAEA) has just introduced a safeguards indexing method for evaluation the safeguards culture at Hungarian nuclear facilities. The main goal of indexing method is to provide a useful tool for the regulatory body to evaluate the safeguards culture at nuclear facilities. The evaluated parameters are e.g. educational requirement for safeguards staff, quality of safeguards report for IAEA and EC, results of safeguards inspections etc. Input of the method is for the one hand the outcome of the comprehensive domestic safeguards verification system consisting of regular comprehensive SSAC verifications of the facilities. The main goals of the comprehensive verification system is: (i) to assess the facility's safeguards system compliance with the relevant national legislation and recommendations, (ii) to assess the activities of the facility aimed at maintaining and further developing its safeguards system and (iii) to revise validity of data and information previously provided by the facility subject to safeguards licensing procedures. On the other hand the annual report of the nuclear facilities also supports the safeguards indexing method, which is a good indicator of the present and future effectiveness of the facility level safeguards system and the level of safeguards culture.

Keywords: safeguards culture assessment, safeguards indexing method, national safeguards system, comprehensive domestic safeguards verification system, SSAC

1. Introduction

The effectiveness and efficiency of an SSAC greatly depends on how the management in the nuclear facilities is committed to the non-proliferation objectives of the country.

In Hungary safeguards licensing procedures are obligatory to possess nuclear material, launch any activity related thereto, launch any modification important to safeguards, transport nuclear materials, as well as to terminate safeguards requirements in case of terminating nuclear activities. In addition to it, facilities are obliged to maintain a facility level nuclear material accountancy system and create the required conditions for international, regional and national verification activities. It is, however, essential that the above obligations be integral parts of a coherent facility management policy.

Based on very promising experiences in the field of nuclear safety, the Hungarian SSAC has introduced a comprehensive domestic safeguards verification system consisting of regular comprehensive SSAC verifications in the whole lifetime of the facilities.

The structure, preparation, conduction, documentation and initial experiences of the comprehensive safeguards verification system is introduced below.

Additionally, HAEA has just introduced a safeguards indexing method for evaluation the safeguards culture at Hungarian nuclear facilities. The main goal of indexing method and the evaluated parameters are also shown in the paper.

2. The comprehensive domestic safeguards verification system (CDSVS)

The introduction of the comprehensive domestic safeguards verification system (CDSVS) by the Hungarian SSAC started with laying down the procedure of the CDSVS in the Hungarian Atomic

Energy Authority's (HAEA) Quality Assurance System. The QA procedure for the CDSVS was approved by the General Deputy Director General of the HAEA. Carrying out CDSV falls into the competence of the Department of Nuclear Security, Non-proliferation and Emergency Management of the HAEA (hereinafter referred to as the Safeguards Department).

2.1. Goal of the CDSVS

The main goal for the CDSVS was defined as follows: to review whether the facility level safeguards system of the organization is run in compliance with the relevant legal instruments and recommendations in force. To reach this goal two tools are to be applied:

a.) to review all the safeguards relevant procedures of the organization. In this review the focus is to check whether procedures for fulfilling the obligations are regulated by internal documentations (e.g. instructions, procedures) and to find practical examples for the procedures by the competent staff.

b.) to assess the activities of the organization in view whether it ensures sustainability and improvement of the safeguards system in all levels of organisation, with special regards to the commitment on management level.

During the last four years the Safeguards Department of the HAEA conducted comprehensive verification inspection in every Hungarian nuclear facility on annual basis, e.g. in 2011 at the Modular Vault Dry Storage (MVDS) of the Spent Fuel Assemblies, in 2012 at the Paks Nuclear Power Plant, in 2013 at the Training Reactor at the Budapest University of Technology and Economics and in 2014 at the Budapest Research Reactor. Verification of the management systems (highest management and safeguards division management) as well as safeguards relevant areas as operation and maintenance, accountancy and data provision were selected for verification.

2.2. Verification levels

2.2.1. 'Level – A' verification

As the primary goal of the verification is to assess the commitment of the highest management, verification 'Level A' was assigned to the top management of the organisation. 'Level – A' verification was planned to assess the commitments of the managers in the field of safeguards and the guarantees provided by the management to enable the organization to meet its safeguards obligations.

A list of issues in 6 themes was provided in advance for the management to help preparation for the on site inspection. Issues were grouped in 10 themes. Short description of the issues:

1) External influence (e.g. dependence of meeting their safeguards obligation on political changes, TSOs; public acceptance of their mission, safeguards in their external communication; possible responds of the organization in case of negative effects.)
2) Objectives and strategies (objectives of non-proliferation relevance, consultation process in drafting strategies, possible future plans on any changes in this field)
3) Management functions and their review (selection criteria in the management, evaluation of proper and improper safeguards related decisions, competences, etc.)
4) Allocation of resources (corporate procurement and/or restructuring with non-proliferation and safeguards aspects)
5) Human resource management (reduction of staff - giving priority to safeguards staff; vacancy and fluctuation in safeguards staff; promotion, reward system for safeguards staff, etc.)
6) Training (professional training possibilities for the safeguards staff, safeguards for the staff in general, etc.)
7) Knowledge management (ensuring continuity of safeguards staff, communication channels for safeguards knowledge, etc.)
8) Regulation (regulation work processes in view with safeguards obligations, inclusion of safeguards aspects in revision of documents, etc.)

9) Organization culture (evaluation of the performance safeguards related tasks on individuals' appraisal or on organization's level, who performs the appraisal of the individual in the safeguards unit, etc.)
10) Communication (channels of information from external source to the safeguards staff and vice-versa.)

2.2.2. 'Level – B verification'

'Level - B' was assigned to different safeguards related fields with the following subdivision:

B1 – Safeguards division (analyses of the safeguards division structure, its relation with the highest managements, scope of competences; educational background and professional training of the safeguards staff; adequate human resource for the related tasks, etc.)

B2 – Operation and maintenance (availability, authentication and maintenance of the measurement equipment to support the accountancy, measures to ensure safe and secure operation of the safeguards containment and surveillance systems, utilization of the organization's own operational experience as well as safeguards experience and research and development activities of other organizations; procedures established to enable national and international inspections, e.g. ground pass systems, safeguards duty system with telephone contact availability, etc.

B3 – Accountancy and data provision (internal procedures regulating the nuclear material accountancy and safeguards related data provision system, operation and reliability of the computer based accountancy system, etc.)

2.3. Schedule of the verification

The CDSV is carried out along the following schedule:

1.) Preparatory phase (review and process of the related internal documents of the organization)
2.) On site inspection
3.) Assessment

2.3.1. The preparatory phase

The preparatory phase is very important part of the verification. The Safeguards Department held an initial meeting to prepare the verification. On this meeting goals of the CDSVS and levels of verification were explained to the representatives of the facilities. Participants of the meeting agreed on collecting the internal documents regulating the tasks of the organization and allocating the responsibilities within the units of the organization. It was agreed that these documents would be provided for the HAEA well in advance of the meeting to enable the staff's preparation for the verification. Potential participants on the on-site inspection both from the HAEA and the facilities were discussed but not finalized.

In the preparatory phase representatives of HAEA on the on-site inspections will study the internal documents of the facilities and finalize the list of issues on the areas assigned to them.

2.3.2. The on-site inspection phase

The on-site inspection is planned to be conducted according to the following agenda:

- Kick-off meeting – information on the goal and areas of inspection, and the methods to be applied
- Inspections to be conducted
    - with participants identified in advance
    - based on list of issues for revision (While level – A list of issues were handed over in advance, list of issues for the level – B areas will be used on the on-site inspection only)

    - detailed records on answers and other observations will be prepared by the inspectors
- Closing meeting – preliminary evaluation will be given. There will be possibility given for the licensee to argue the preliminary evaluation results.

2.3.3. Assessment phase and corrective actions

After the on-site inspection, HAEA has finalized the report on the inspection and send it to the facilities for comments. The report focused on identifying best practices and deficiencies, if any, and clearly state the authority's positions how to make corrective actions. The facilities shall comment on the main findings and formulate its position on the HAEA's conclusions and recommendations. Moreover, facilities shall identify the means and timeframe of the corrective actions to be performed. Taking the response and proposal from facilities full into account, the HAEA will issue a regulatory resolution on the corrective actions to be taken and determine deadlines for each. In addition the HAEA will establish the next review program of the CDSVS focusing on those areas where corrective actions were identified.

3. The Safeguards Performance Assessment Index for evaluation the safeguards culture

The Safeguards Performance Assessment Index (SPAI) for nuclear facilities has been developed by the Hungarian Atomic Energy Authority for the facilitation of the periodical comprehensive regulatory review of the performance of the operators' safeguards system. The parameters included into SPAI were selected on the basis of objectivity, availability and operability.

The SPAI is designed to be compatible with the system that was developed for the safety performance assessment of the facilities, therefore the comprehensive assessment of the facilities including safety, security and safeguards will be possible in the future.

Definitions:
• Safeguards Assessment Index (Index): a particular value determined by one or several characteristics of the performance of the facility's safeguards system.
• Safeguards Characteristics (Characteristics): A classification value based on quantitative data determined by the individual rule of assessment.

For the assessment of safeguards characteristic four rates are defined, as follows:

• **acceptable:** A safeguards characteristic is acceptable if the authority finds the level of performance such that no corrective actions are required. A safeguards characteristic marked with green colour indicates compliance with all of the relevant regulatory requirements. This rating may show a good practice as well where the facility is proactive and shares a good practice leading to efficient performance without any regulatory requirements.

• **alarming:** A safeguards characteristic is alarming if there is a slight deviation from the desired value within the regulatory permissible set of values. Though only minor mistakes but no serious issues exist yet, characteristics falling into the yellow zone may need improvement. The licensee shall be instructed to set up a plan of actions to make the necessary improvements. As a respond to the plan of actions the regulatory body sends a written notice to the licensee calling for the implementation of the plan of actions. Execution of the required actions are to be checked in course of regulatory inspections.

• **not acceptable:** It means that the safeguards characteristic is not acceptable. Rating in the red zone refers to a non-compliance, however, only characteristics covered by regulations may be qualified as red. If a safeguards characteristic has been assessed as red, an explanation is required on what occurred, exact time and date when the non-compliance occurred, its consequences and measures taken by the regulatory authority. The licensee is obliged to set up a plan of actions which will be then sent back by the regulatory body in the form of a regulatory notice, including additional measures considered to be important by the regulatory body. Execution of the required actions shall be checked in course of regulatory inspection.

• **not known:** The system of safeguards index is the same for all nuclear facilities. It may occur, however, that certain characteristics of the index are not relevant for every licensee. In this case characteristics not relevant for the facility are marked white.

Margins for a four-grade zone will be individually determined for the different characteristics. In case of several characteristics determined for a Safeguards assessment index, the index gets the same rating as its characteristic with the worst assessment among all.

3.1. Areas of the assessment

The areas assessed by SPAI for nuclear facilities covers the three major parts of the facility safeguards system, such as (i) safeguards organisation; (ii) operation of the safeguards system; (iii) safeguards licensing procedures. In the following section the assessment indexes, characteristics and evaluation criteria for the above mentioned three assessment areas are introduced.

3.1.1. Safeguards organisation

Assessment indexes

a) Number of staff
b) Training

Characteristics

a) Number of staff, Substitution
   Quantitative characteristic of the safeguards organization (number of staff, order of substitution within the safeguards organization, ensuring preparedness outside working hours)
b) Requirements for competence of safeguards officer
   Qualitative characteristic of safeguards organization (Quality of training for the new staff and to maintain the safeguards knowledge, its frequency, education background, etc.)

Evaluation

a) Quantitative characteristic of the safeguards organization

Rule of quantification: Ratio of the number of safeguards relevant tasks and the available number of qualified staff. Quantitative assessment of the safeguards organization is made based on the number of the tasks performed by the safeguards staff. Safeguards tasks performed within the given period of time are summed and the number of safeguards relevant tasks (inspections, reports, licensing procedures) incumbent for one person within the given period of time is checked.

Comments: The value is based on good practice. The preceding four years (2009-2012) were evaluated for acceptable level of operation of safeguards organizations and the average results of the four years were considered as appropriate. Classification values were defined accordingly.

b) Qualitative characteristic of the safeguards organisation

Rule of quantification: Relative percentage of compliance of the staff with the required trainings.
Comments: The required qualification and trainings should always be satisfied.

3.1.2. Operation of the safeguards system

Assessment indexes:

a) Nuclear material accountancy system (reports)
b) Information provision system (BTC, Additional Protocol)
c) Conclusions of the inspections

Characteristics

a) Nuclear material accountancy system
   i. Correctness of reports sent (error lines, correction lines)
   ii. On time delivery of reports (late lines)
b) Information provision system (R&D, site description, waste)

i. Correctness and completeness of information submitted (requirements for additional data, corrections, etc.)
ii. On time delivery of information, declaration

c) Experience of inspections
   i. Conditions provided for inspections (ground pass, access to nuclear material, clear spent fuel pond water, etc)
   ii. Non-compliance discovered in course of inspections (discrepancies, anomalies)

Evaluation:

a) Nuclear material accountancy system
   i. Correctness of accountancy data transmitted
   Rule of quantification: Relative percentage correct and inadequate reports
   Comments:

   ii. On time delivery of reports
   Rule of quantification: Relative percentage of accountancy reports sent on time and those sent beyond the time limit
   Comments: The index is marked with the colour of the characteristic assessed as the worst. If a report is not transmitted on time, time-limit of the accountancy report is be marked as yellow, and in this case the indicator of the accountancy system cannot be better than yellow.

b) Information provision system (R&D, site description, waste)

   i. Correctness and completeness of information submitted (Provision of information)
   Rule of quantification: Relative percentage of information submitted in compliance and those in non-compliance
   Comment s: Provision of information subject to Additional Protocol are analysed

   ii. On time delivery of information, declaration
   Rule of quantification: Relative percentage of declarations sent on time and those sent beyond the time limit
   Comments: Provision of information subject to Additional Protocol is checked. The index is marked with the colour of the character assessed as the worst. If any of the information is not transmitted on time, time-limit of the information provision is be marked as yellow, and in this case the indicator of the information provision system cannot be better than yellow.

c) Experience of inspections

   i. Facilitating inspections
   Rule of quantification: Relative percentage of inspections where all the conditions necessary for an inspection were provided for and of those that lacked one or some of the conditions.
   Comment: Conclusions of the inspections are drawn based on the evaluation of the inspection reports

   ii. Non-compliance found in course of the inspections
   Rule of quantification: Relative percentage of inspections where no anomaly was found and inspections where anomalies were experienced by the inspector.
   Comments: Conclusions of the inspections are drawn on the evaluation of the inspection reports

3.3.3. Safeguards licensing procedures

Assessment indexes:

a) Regulatory measures/resolutions
b) Meeting regulatory deadlines

Characteristics

a) Regulatory measures
   Execution of regulatory measures, requests for additional information by the regulatory authority to make the licensing documentation complete, licensing applications refused by the regulatory authority
b) Deadlines
   Meeting the regulatory time-limits

Evaluation

a) Execution of measures requested by the regulatory body

Rule of quantification: Content and administrative compliance of safeguards relevant applications with legal requirements. Ratio of applications in compliance and those in no-compliance with the requirements.
Comments: The value is based on good practice. The preceding four years (2009-2012) were evaluated for acceptable level of operation of safeguards organizations and the average results of the four years were considered as appropriate. Classification values were defined accordingly.

b) Deadlines

Rule of quantification: Meeting the time limits defined by relevant regulations or the regulatory authority for the safeguards licensing applications (e.g. first safeguards licence, requests to complete licensing documentation, etc.) Ratio of documents submitted within and beyond the required time-limits.
Comments: The value is based on good practice. The preceding four years (2009-2012) were evaluated for acceptable level of operation of safeguards organizations and the average results of the four years were considered as appropriate. Classification values were defined accordingly.

4. Conclusion

The new comprehensive domestic safeguards verification system has been introduced in 2011. Based on the experiences collected during the 4 years period it can be concluded that the new program has reached the following objectives:

- The management became more aware on its safeguards obligation. ‘Level – A’ list of issues helps the management to analyse the set of documents of the facility, from the organization’s strategy documents to the low level internal documents. Safeguards related scope of competence needs to be assessed from the top management level to the safeguards officers’ level.

- Review all the safeguards relevant procedures of the organization helps to disclose the possible gaps in the regulation of the procedures or in the scope of competence.

- The need for sustainability of the safeguards system and improve in performance at all levels within the organization will clearly be highlighted through the whole verification process.

The nuclear safeguards indexing method was designed using the experience collected from the nuclear safety indexing method, therefore using both methods an integrated assessment can be carried out. Moreover, the developed nuclear safeguards indexing method helps the authority to assess the safeguards culture at the specific site. [1,2]

In this way improving the nuclear safeguards culture in the organization is expected to get the same importance as nuclear safety and security culture.

5. REFERENCES

[1] E. SZÖLLÖSI, G. RÁCZ, Zs. STEFANKA, Á. VINCZE, K. HORVÁTH
Assessing and Promoting the Level of Safeguards Culture in Hungarian Nuclear Facilities, 2011 33rd ESARDA Annual Meeting, Budapest
[2] Assessing and Promoting the Level of Safeguards Culture in Hungarian Nuclear Facilities
Zsolt Stefánka, Árpád Vincze. IAEA Safeguards Symposium 2014, Vienna

Session 2

He-3 Alternatives for Neutron Detection

Workshop on He-3 alternatives for safeguards applications

Carlos Carrapico, Bent Pedersen, Vittorio Forcina, Paolo Peerani, Francesca Rosas, Arturs Rozite, Hamid Tagziria, Georgios Takoudis, Alice Tomanin

European Commission, Joint Research Centre (JRC), Institute for Transuranium Elements (ITU), Nuclear Security Unit, Via Enrico Fermi 2749, 21027 Ispra (VA), Italy

E-mail: paolo.peerani@jrc.ec.europa.eu

Abstract:

On 13-17 October 2014, the Joint Research Centre (JRC) hosted the second of two workshops on helium-3 (He-3) alternative materials and technologies for safeguards applications, under the U.S. Department of Energy/National Nuclear Security Administration (DOE/NNSA)-Euratom Action Sheet 47, at the JRC Ispra Site.
The recent Ispra workshop served as a direct follow-up to the Los Alamos workshop. Participants provided updates on several of the technologies discussed in 2013. In particular, workshop participants evaluated the applicability of the He-3 alternative technologies to a pre-established list of use cases and identify any capability gaps. In addition, the workshop included discussions of implementation strategies for advancing the prototype technologies to commercially deployable systems. The workshop included a demonstration of some of these technologies. Moreover, a field trial has been held on the margins of this workshop to provide a head-to-head comparison of various He-3 alternative prototypes for nuclear fuel verification.

Keywords: NDA; neutron counting; He3 shortage; neutron detection

1. Introduction

On 13-17 October 2014, the Joint Research Centre (JRC) hosted the second of two workshops on helium-3 (He-3) alternative materials and technologies for safeguards applications, under the U.S. Department of Energy/National Nuclear Security Administration (DOE/NNSA)-Euratom Action Sheet 47, at the JRC Ispra Site.

The International Atomic Energy Agency (IAEA) and regional safeguards inspectorates rely heavily on neutron assay techniques, and in particular, on coincidence counters for the verification of declared nuclear materials under safeguards and for monitoring purposes. The reliability, safety, ease of use, gamma-ray insensitivity, and high intrinsic detection efficiency of He-3 based detectors made it an ideal detector material. However, an anticipated shortage of He-3 led to efforts to develop and field neutron detectors that make use of alternative materials.

From 22-24 March 2011, the IAEA held an international meeting to address the question of possible replacement technologies for He-3 based neutron detectors. This was followed by a workshop at Los Alamos National Laboratory in June 2013, which provided an in-depth review of selected international efforts to develop and deploy technologies designed to serve as viable, near-term alternatives to He-3 based systems for international safeguards applications. Participants included experts from U.S. national laboratories and Universities, Euratom, JRC, Japan Atomic Energy Agency (JAEA), and the IAEA.

The recent Ispra workshop served as a direct follow-up to the Los Alamos workshop. Participants provided updates on several of the technologies discussed in 2013. In particular, workshop participants evaluated the applicability of the He-3 alternative technologies to a pre-established list of use cases and identify any capability gaps. In addition, the workshop included discussions of implementation strategies for advancing the prototype technologies to commercially deployable

systems. The workshop included a demonstration of some of these technologies. Moreover, a field trial has been held on the margins of this workshop to provide a head-to-head comparison of various He-3 alternative prototypes for nuclear fuel verification.

2. Inter-comparison benchmark

In the margins of the "Workshop on He-3 alternatives for Safeguards applications", JRC hosted an inter-comparison benchmark that took place in the PERLA laboratory at the JRC facilities of Ispra on the two days before the workshop (October 13th-14th, 2014).

The scope of the benchmark was to compare the performances of few prototypes of neutron counters based on alternative technologies among them and compared to those of ordinary He-3 devices ordinarily used by IAEA and Euratom for safeguards inspections.

Six prototypes were tested and compared to three reference He-3 instruments corresponding to three different usage cases, as described in table 1. During the benchmark each developer operated his own instrument, whereas JRC staff operated the reference instruments.

Usage cases	**Reference ^{3}He instrument**	**Alternative prototypes**	**Developer**
Passive coincidence counting in Pu-bearing cans	HLNCC	ABUNCL with B-coated tubes	GERS
		HLNCC with straw Boron tubes	PTI
		Well counter with Li6-ZnS blades	Symetrica
Active coincidence counting for fresh fuel elements	UNCL	Liquid scintillator neutron coincidence collar	IAEA
Neutron monitors	UNCL slab	Parallel plate B slab counter	LANL
		Stilbene scintillator	UMICH

Table 1: Prototypes tested in the benchmark

2.1. Short description of the prototypes

2.1.1. ABUNCL with B-coated tubes

The ABUNCL was initially developed by General Electric Reuter Stokes as a collar for active measurement of fuel elements and as such had been demonstrated at the Los Alamos workshop in 2013. The prototype tested in Ispra was a modification of the original collar that transformed the ABUNCL into a well counter by adding a fourth detecting side (see figure 1). The counter is equipped with 72 10B-lined proportional tubes.

2.1.2. HLNCC with straw Boron tubes

The straw HLNCC has been developed by PTI. It consists of 804 straws (narrow diameter ^{10}B-lined proportional tubes) embedded in a structure have roughly the same dimensions (cavity, height and footprint) of a standard HLNCC (figure 2).

2.1.3. Well counter with Li6-ZnS blades

This prototype was developed by Symetrica in collaboration with JRC. It was only a partial prototype equipped with 8 blades out of the 32 foreseen in the final instrument (see figure 3). Each blade consists in a sandwich of PVT wavelength shifter coated with ZnS scintillator for charged particles doped with ^{6}Li acting as neutron converter.

2.1.4. Liquid scintillator neutron coincidence collar

This collar was developed by IAEA in collaboration with JRC and Hybrid Instruments and consists in 3 slabs, each containing 4 cubic liquid scintillators; the fourth slab can host the interrogation AmLi source like in a common UNCL.

2.1.5. Parallel plate slab counter

This is a neutron slab based on boron-lined parallel plate technology; the same as in the HLNB prototype demonstrated in Los Alamos in 2013. This slab prototype has been particularly targeted for challenging conditions like high count rates and gamma fields. The demo was particularly intended to show the fast signal processing electronics.

2.1.6. Stilbene scintillator

The University of Michigan provided a couple of stilbene detectors with pulse shape discrimination capability.

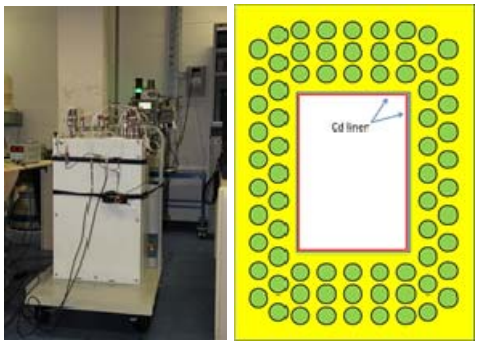

Figure 1: ABUNCL with B-coated tubes (picture and cross section)

Figure 2: Straw HLNCC

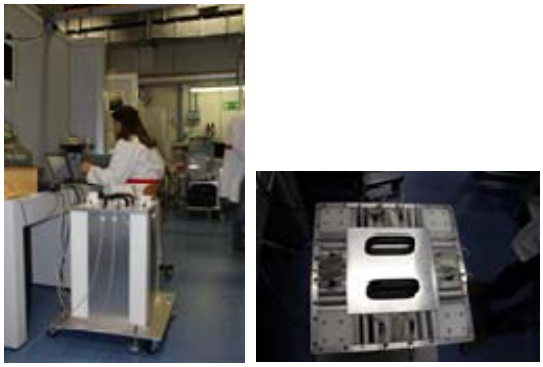

Figure 3: Well counter with Li6-ZnS blades (side and top views)

Figure 4: Liquid Scintillator NCC

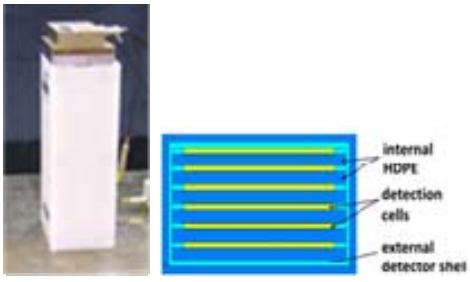

Figure 5: Parallel plate slab (picture and cross section)

Figure 6: Stilbene scintillator

2.2. Testing procedures

The purpose of the benchmark was to demonstrate the performance of alternative ^{3}He systems against safeguards relevant parameters and perform benchmarking of these systems against available reference ^{3}He-based systems. The key component of this activity involved side-by-side comparative measurements of a range of available SNM samples in the ^{3}He-based systems and their proposed alternatives. The actual procedures have been slightly different for the three usage cases.

2.2.1. HLNCC-types

The main benchmarking parameters were:
- HV plateau and gamma sensitivity: the plateau was measured in the presence of a ^{252}Cf and gamma-ray sources (with dose rates of operational interest) to establish the optimum HV setting for benchmarking measurements and efficiency evaluation.
- Efficiency: using available well-characterized ^{252}Cf source and the optimum HV setting determined in step 1 the neutron detection efficiency was measured and compared with the reference 3He-based system.
- Figure of Merit: the die-away was measured and then the FOM was computed as FOM = ε / sqrt(τ) and compared to the reference ^{3}He-based system.
- Gamma sensitivity: the gamma influence was assessed by measuring a strong gamma source in absence and presence of a reference ^{252}Cf source.
- Statistical uncertainty: side-by-side measurements were performed using the available SNM samples in the alternative and reference ^{3}He-based system and the statistical uncertainty was compared.

2.2.2. UNCL-types

The main benchmarking parameters were:
- Efficiency: using available well-characterized ^{252}Cf source the neutron detection efficiency was measured and compared with the reference ^{3}He-based system.
- GARR: the gamma rejection was estimated by adding a strong gamma source to the reference 252Cf source.
- Statistical uncertainty: side-by-side measurements were performed mimicking passive and active fuel measurements in the alternative and reference ^{3}He-based system and the statistical uncertainty was compared.

Due to the unavailability of a real fuel element the operating conditions were simulated by placing a 252Cf source in the cavity providing a fission rate comparable to that expected in presence of a fuel element. Three types of measurements have been simulated:
- Passive measurement (with weak ^{252}Cf source in the cavity reproducing the spontaneous fission rate from U-238)
- Active measurement in thermal mode (with AmLi in the lateral slab and a strong ^{252}Cf source in the cavity reproducing the induced fission rate in U-235 in thermal mode: ratio AmLi/Cf = 10:1)
- Active measurement in fast mode (with AmLi in the lateral slab and a weak ^{252}Cf source in the cavity reproducing the induced fission rate in U-235 in fast mode: ratio AmLi/Cf = 100:1)

2.2.3. Monitor-types

The main benchmarking parameters were:
- Efficiency: using available well-characterized ^{252}Cf source the neutron detection efficiency was measured and compared with the reference ^{3}He-based system.
- Gamma sensitivity: the gamma influence was assessed by measuring a strong gamma source in absence and presence of a reference ^{252}Cf source.

In addition for the parallel plate using list-mode data acquisition, the performance of the parallel-plate detector with fast amplifier was demonstrated and compared with standard PDT amplifier.

2.3. Benchmark results

We report hereby the main results obtained during the benchmark.

2.3.1. HLNCC-types

The major detection characteristics are reported in table 2, whereas table 3 gives the performance with respect to gamma sensitivity and table 4 the statistical uncertainty for measurements of MOX samples.

The results can be quickly summarized as follows:

- The PTI system has a slightly lower efficiency than the ^{3}He HLNCC, but compensated by a much shorter die-away. As a combination of the two it gives a slightly better FOM, whose effect is confirmed by the lower statistical uncertainty in the Pu sample measurement. Moreover it has better gamma rejection.
- The partial Symetrica system has half of the efficiency of the HLNCC and a longer die away, but we should recall that the prototype contains only one quarter of the expected blades (8 out of 32); Monte Carlo extrapolations have estimated that a full system would have and efficiency of 25%, a die away of 31 μs and a FOM of 4.6 (60% better than HLNCC). Gamma sensitivity is comparable with HLNCC.
- The GERS system has inferior performances than HLNCC both in term of efficiency and die-away. Also in this case it has to be reminded that the demonstrator was a modification of the collar prototype, so it was not optimized in terms of geometry.

Parameters	^{3}He-based HLNCC	GERS-NCC	^{6}Li/ZnS based HLNCC	B-straw HLNCC
Efficiency [%]	16.50	10.20	8.90	13.56
Die-away time [μs]	43.30	65.40	55.90	26.00
FOM (ε/√τ)	2.51	1.26	1.19	2.66

Table 2: Detection characteristics of HLNCC prototypes

Source type	^{3}He-based HLNCC		GERS-NCC		^{6}Li/ZnS based HLNCC		B-straw HLNCC	
	Singles [s^{-1}]	Doubles [s^{-1}]	Singles [s^{-1}]	Doubles [s^{-1}]	Singles [s^{-1}]	Doubles [s^{-1}]	Singles [s^{-1}]	Doubles [s^{-1}]
^{137}Cs (3.7 MBq)	40.3	0.008	11.4	0.013	0.7	0.000	4.9	0.003
^{137}Cs + ^{252}Cf	1196.6	218.003	1888.6	178.779	-	93.830	-	-
^{252}Cf (7000 n/s)	1194.1	215.991	1893.9	183.927	-	92.610	-	-

Table 3: Gamma sensitivity results of HLNCC prototypes

	^{3}He-based HLNCC	GERS-NCC	^{6}Li/ZnS based HLNCC	B-straw HLNCC
MOX1 (168 g Pu)				
Measurement time [s]	600	600	600	600
Doubles [s^{-1}]	1088.95	315.81	165.33	770.76
σ	8.71	3.74	4.39	4.19
Relative precision [%]	0.80	1.18	2.66	0.54
MOX2 (191 g Pu)				
Measurement time [s]	600	600	NA	NA
Doubles [s^{-1}]	1242.54	357.43		
σ	9.94	4.99		
Relative precision [%]	0.80	1.40		

Table 4: Statistical uncertainty on Pu sample measurements of HLNCC prototypes

2.3.2. UNCL-types

The results are reported in table 5. From the data we can conclude that the LS-NCC has the potential to provide better performances of UNCL, especially for measurements in fast mode (used mostly for Gd-loaded fuel elements).

Safeguards parameters	**^{3}He-based HLNCC**	**LS-NCC**
Efficiency - singles (S) [%]	10.01	9.54
Efficiency - doubles (D) [%]	3.23	3.43
GARR = S/(S+γ)	< 1.0e-8	8.4e-4
D - passive mode (^{252}Cf only)	61.55±0.87%	67.30±0.50%
D – active thermal mode (AmLi+^{252}Cf 10:1)	64.78±2.05%	68.98±0.49%
D – active fast mode (AmLi+^{252}Cf 100:1)	4.07±9.77%	4.77±1.87%

Table 5: Comparison of results for UNCL and LS-NCC

2.3.3. Monitor-types

By nature slab monitors are scalable, so the efficiency has to be compared either as intrinsic efficiency (neutron detected per neutron hitting the surface of the detector) or the absolute efficiencies should be normalized per unit surface or covered solid angle. In the case of the systems demonstrated during the benchmark, the main purpose was not necessarily to provide a direct comparison of performance with He-3 detectors.

For the University of Michigan the goal was to demonstrate the capabilities of novel plastic scintillators (in particular stilbene) as dual-particle detector with satisfactory gamma/neutron distinction by pulse shape discrimination. Figure 8 shows for instance the gamma sensitivity result: the neutron detection in presence of a strong gamma source was unaffected up to a dose rate of 30 μSv/h.

For the parallel plate slab the main purpose was to demonstrate the high-count rate performances. Unfortunately the response of the Boron module was affected by noise on one of the amplifiers that has somehow degraded the performance of the detector during the benchmark.

3. Conclusions from the workshop

The workshop was attended by 45 participants coming from several research centres in Europe, United States and Japan, industry and inspectorates (IAEA and Euratom). 25 presentations were delivered in the three technical sessions (general concepts / Li- and B-based alternatives / scintillation technologies), followed by a demonstration of the prototypes and concluded by a round table discussion table to which all participants contributed. The discussion was structured in four consecutive topics; for each topic an expert was invited to present a short statement that was supposed to trigger the discussion involving the entire audience. The four topics were:

- Technical challenges
- Standardized best practices for testing instruments
- Use cases and technology gap
- Implementation and path forward

a) Technical challenges (facilitator S. Croft)

In the introductory statement the facilitator has evidenced three major areas for research:

- the need to further develop the fundamental theory of coincidence and multiplicity counting,
- simulation tools for the alternative technologies
- availability of experimental facilities and round robin exercises

Concerning Monte Carlo simulation, the current tools work very well for He-3 counters, but require improvements to properly model the physics of the novel technologies. Modelling of boron or lithium based detectors would require a complete charged particle transport, whereas organic scintillators need modelling of a complex process including light emission/transport/collection and computation of pulse shape/height distributions.

The use of spectroscopy could bring some advantages, but this needs to be first investigated and assessed.

There would not probably be a fit-all-purposes solution, but we should seek for matching technologies to specific applications.

In some cases a change from the classical way of working could be needed; the traditional way of measuring coincidences through the shift register logics could be replaced by other way of processing raw data, in particular for fast neutron detectors. In this view list mode data collection and analysis can open to a wider spectrum of possibilities in data processing.

The use of fast neutron detectors (organic scintillators) would get a remarkable boost from developments in the data acquisition electronics: for instance, the capability to perform pulse shape analysis in real time and/or wave form digitalization.

The lifetime of the new technologies has still to be demonstrated.

Finally it was identified the need of bringing the appropriate competence from different disciplines to the NDA field.

b) Standardized Best Practices for Testing (facilitator R. Kouzes)

The first fundamental question is: there are no standards for safeguards: do we need them? The safeguards “market” is relatively small and restricted and maybe do not justify the effort of developing standards.

Then, as a consequence, the next question follows: can best practices replace standards and how? The answer is probably yes, but this would in any case require an intensive review of testing campaigns and the publication of agreed testing methods/protocols.

The organization of benchmarks can be challenging, mostly from a logistic point of view. Benchmarks can be performed both as inter-comparisons (among different technologies) and versus real material and have to be targeted to end-user goals.

The expected performance should be driven by the end-user needs; for instance the International Target Values (ITV) of IAEA are useful for some applications, but are not fully comprehensive and are in any case determined by experience on past performances.

c) Use Cases and Technology Gaps (facilitator B. McElroy)

A provoking statement: since He-3 solves everything and it is not going to disappear totally in the short term, new technologies might find a place to only specific applications. Developers should aim to identify and target where their technology fits and where it can provide viable solution for replacement or even for improving the current situation. For instance attended/unattended applications might be tackled with different perspectives.

Use cases where current equipment is not fully satisfactory and where R&D should be focused can include:

- fresh fuel with poisons
- fresh fuel with heterogeneity
- partial defect in spent fuel
- encapsulation/final repository safeguards

d) Implementation and path forward (facilitator T.H. Lee)

Here the facilitator has listed some of the issues considered of main relevance:
- Optimize the use of He-3 (e.g. deploying hybrid B10+ tubes and modular detector assemblies)
- Replacement of He-3 by B-10 or other alternatives for less challenging applications and where efficiency is not an issue (e.g. gross counting)
- Still relying on He-3 for demanding applications (e.g. multiplicity counting)
- active interrogation applications: fast neutron systems (organic or noble gas scintillators)
- additional information from gamma/neutron detectors (multi-particle coincidences)

Other properties of replacement technologies according to IAEA requirements are:
- modeling possibility (required)
- simple physical swap (desired)
- compatibility with existing electronics (strongly desired)

Finally the requirements for future systems should take into account:
- field deployable (weight, cost, stability,…)
- user friendliness
- authorization process through evaluation vs existing systems

Demonstration Result of Sample Assay System equipped Alternative He-3 Detectors

Hironobu Nakamura, Yasunobu Mukai, Hiroshi Tobita, Hideo Nakamichi, Akira Ohzu, Masatoshi Kureta, Tsutomu Kurita, Michio Seya

Japan Atomic Energy Agency (JAEA),
4-33 Muramatsu Tokai-mura, Ibaraki-ken, Japan

E-mail: nakamura.hironobu@jaea.go.jp; mukai.yasunobu@jaea.go.jp; tobita.hiroshi@jaea.go.jp; nakamichi.hideo@jaea.go.jp; ohzu.akira@jaea.go.jp; kureta.masatoshi@jaea.go.jp; kurita.tsutomu@jaea.go.jp; seya.michio@jaea.go.jp

Abstract:

JAEA has been conducting an R&D project (for past 4 years) to develop a new type of neutron detector using ZnS/$^{10}B_2O_3$ ceramic scintillator (as an alternative neutron detector to He-3) with a support of Japanese government. The design of the JAEA's alternative system (ASAS: Alternative Sample Assay System using ceramic scintillator tubes) refers basically to the INVS (INVentory Sample assay system) which is the passive type of neutron assay system equipped with total 18 He-3 tubes and capable of measuring the small amount of Pu in MOX powder or Pu nitrate solution in a vial for nuclear material accountancy and safeguards verification. In order to prove the alternative technology and the performance instead of He-3 detector, and to establish Pu measurement capability, JAEA developed and fabricated ASAS equipped with 24 alternative ceramic scintillator tubes and demonstrated. The demonstration activity implemented the confirmation of reproducibility about sample positioning, optimization of detector parameters, obtaining counting statistical uncertainty and figure of merit (FOM) using Cf check source and actual MOX powder in PCDF (Plutonium Conversion Development Facility). In addition, performance comparison between the current INVS and the ASAS was also implemented.

In this paper, we present demonstration results with design information by Monte-Carlo simulation code (MCNP). It is thought that these results give us the beneficial alternative technology with Pu measurement capability and help to hedge risks of He-3 shortage.

Keywords: He-3 alternative, ceramic scintillator, neutron assay, figure of merit

1. Introduction

Existing neutron based NDA systems used for the detection of nuclear material in safeguards application are typically based on He-3 proportional counters which require relatively large volume of rare gas. Owing to the severe ^{3}He shortage, an alternative technology for neutron detection is required. In Japan Atomic Energy Agency (JAEA), the alternative technologies to detect neutrons for nuclear security and safeguards systems are being developed. With the support of Japanese government (MEXT; Ministry of Education, Culture, Sports & Technology), the Integrated Support Centre for Nuclear Non-proliferation and Nuclear Security ("ISCN", hereafter) of JAEA had started an R&D project of ZnS scintillation neutron detectors for non-destructive assay of Pu in clean MOX since 2011.

To solve the international issue about He-3 shortage, many types of potential alternative He-3 neutron detectors such as BF_3 gas detector, Li or B based inorganic solid state scintillator, plastic or liquid scintillator, B-10 lined detector [1] and others were reported. In comparison with those detectors, however all types of He-3 alternative detectors which are being developed could not achieved the He-3 performance (efficiency) in a detection tube, we started to develop alternative He-3 detector using ceramic scintillator to achieve the efficiency as well as He-3. JAEA has been developing an alternative

neutron detection technology using ZnS/$^{10}B_2O_3$ ceramic scintillator, since 2011 JFY [2] [3] [4]. On the basis of the current specifications and performance characteristics of the ceramic scintillator detector, one novel type of safeguards type of NDA detector equipped with the ceramic scintillator detectors could have been designed and fabricated. It is a small size NDA system with references of HLNCC type of detector called INVS (INVentory Sample verification system). In this report, we introduce a development and demonstration result of a new Pu NDA system called ASAS (Alternative Sample Assay System) which is equipped with ZnS/$^{10}B_2O_3$ ceramic scintillator as an alternative He-3 system. The demonstration activities including calibration by actual MOX powder was implemented at PCDF (Plutonium Conversion Development Facility) in Japan.

2. Specification of Current INVS system (He-3 type)

The INVS was developed to quantify the Pu amount in a sample vial. The measurement target of the INVS is pellets, Pu solution and MOX powder in a sample vial containing a few grams of plutonium. The INVS is normally used for the inventory verification (attended mode) at the timing of Fixed-day RII (Fixed-day Random Interim Inspection) in PCDF. Since DA (Destructive Analysis) takes a few days to get Pu mass in the item, INVS system which can determine Pu mass in the item quickly is very useful in order to get the result of inspection. With the HRGS (High resolution gamma spectroscopy) measurement resulting in the Pu isotopic compositions, our results are verified quickly (during one day). Since the total measurement uncertainty in the current INVS is expected about less than 6%, the verification type by using INVS is categorized as a partial defect detection equipment (Method F).

As shown in the Figure 1, the INVS (HLNCC type of detector) in PCDF has 16 He-3 tubes that surround sample chamber. The height of the detector is about 42cm, the external diameter of the detector is about 28cm, and the weight of the detector is about 20kg. To make flatness response and improve die-away time, cadmium liner is attached in the internal surface of sample chamber. Figure 1 also shows the image of sample vial. The vial can store maximum 50gMOX (about 20gPu). Since the size of sample vial is small, the sample chamber is made small (ϕ55mm x 157mm) to set a vial to the just center of sample chamber and it helps to increase relatively high counting efficiency (~31%).

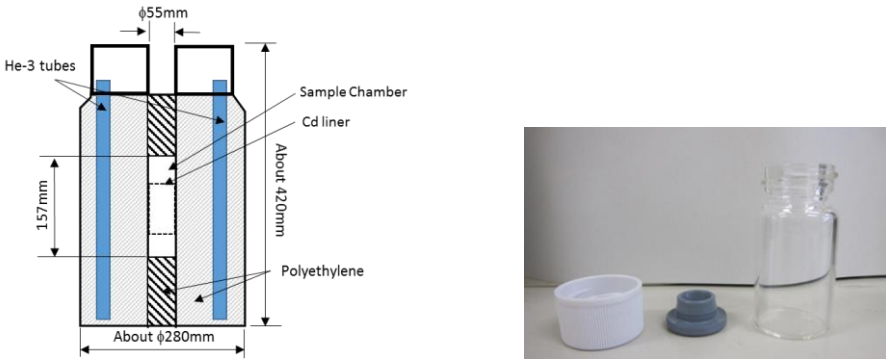

Figure 1: Axial sectional view of INVS and picture of a sample vial (ϕ24mm x 50mm (H))

It is estimated that the historical difference between measured (INVS) and declared in the current INVS is about +/- 6%. And the recent measured doubles counting statistical uncertainty for 10-minutes measurement is about +/-1.2% for MOX powder and about +/-1.2% for Pu nitrate solution. Since the INVS is one of representative coincidence assay type of verification system, in order to prove and present the ASAS performance, we would select it for the target of development and comparison.

3. Development of alternative He-3 system (ASAS)

To establish an alternative technique of He-3 neutron detector that is used for nuclear material accountancy and safeguards, we developed a new type of neutron detector (Pu NDA system) using ZnS/$^{10}B_2O_3$ ceramic scintillator. The design of the alternative system (ASAS: Alternative Sample Assay System) refers basically to the INVS, and the small amount of Pu in the MOX powder or Pu nitrate solution in a vial can be measured. The basic design of ASAS is shown in the Figure 2.

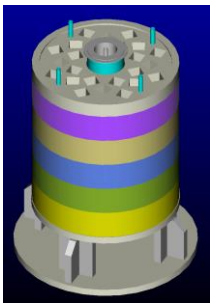

Overall view

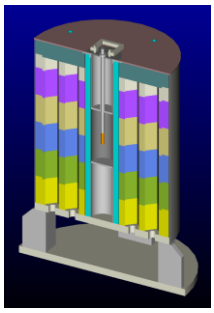

Axial sectional view.

Figure 2: Schematic views of Alternative Sample Assay System (ASAS)

We developed the ZnS/$^{10}B_2O_3$ ceramic scintillator detector module for safeguards and security use. The photomultiplier tubes (PMTs) for scintillation light counting has been selected, and new electronic circuitry has been developed. Figure 3 shows a photograph of the exterior view of the unit module built on an experimental basis. The detector module is composed mainly of three components: an aluminum regular square tube, a scintillator with a rectangular ZnS/$^{10}B_2O_3$ ceramic sheet and two PMTs. The sheet is fit on the diagonal inside the square tube, while the two PMTs are installed at both ends of the tube. Nuclear reactions, between the neutrons that enter the scintillator from outside the tube and the B-10 atoms in the scintillator, induce the emission of scintillation light from the surface of the scintillator. The light photons are divided into two directions, towards both ends of the tube, and are detected individually by the two PMTs as two pulse signals. Figure 4 shows the electronics circuit that enables the alternative detector to detect neutron signals. The light signals detected with the PMTs are amplified with pre-amplifiers. Then, the amplified signals are discriminated with certain levels. The neutron signal is finally detected according to the coincidence of the two light signals from the two PMTs, to eliminate the electrical noise signal which arises from various causes.

For the neutron detection efficiency of the ZnS/$^{10}B_2O_3$ ceramic scintillator detector module of which size is shown in Figure 3, we aimed at achievement of 70-80% of that of the conventional He-3 gas (1in. diameter, 0.4MPa) detector with the same effective length (250 mm). For the gamma-ray sensitivity of the ZnS/$^{10}B_2O_3$ ceramic scintillator detector, we already achieved a sensitivity of less than 10^{-6}.

Figure 3: Square-type neutron detector module (32mm x 32mm x 330mm) with ceramic scintillator and 2 PMTs.

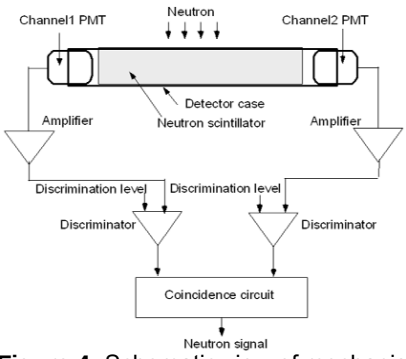

Figure 4: Schematic view of mechanism of alternative neutron detector

In order to prove the alternative system including alternative He-3 tubes, JAEA fabricated an ASAS detector as a Pu measurement system. The system used ZnS/$^{10}B_2O_3$ solid ceramic scintillator as alternative He-3 tubes. Figure 5 shows cross-sectional views of ASAS detector design drawn by the MCNP5. In the current design of ASAS, 24 neutron detection modules with PMT and sample chamber (ϕ67mm x 158mm) for a sample vial are equipped. In the tube, 4mm thickness of glass plate and 2mm thickness of ZnS/$^{10}B_2O_3$ ceramic scintillator are placed diagonally, and the all plates are faced to the sample chamber to detect neutrons effectively. As shown in the Figure 6, the ASAS is composed of a detector unit using the ZnS/$^{10}B_2O_3$ solid scintillator module, HV power supply and digital signal processer box, AMSR (Advanced Multiplicity Shift Register) and data acquisition PC. Compatibility with the current safeguards equipment is very important to use safeguards purposes. Therefore, the ASAS detector transfers TTL pulse signals to the conventional shift register.

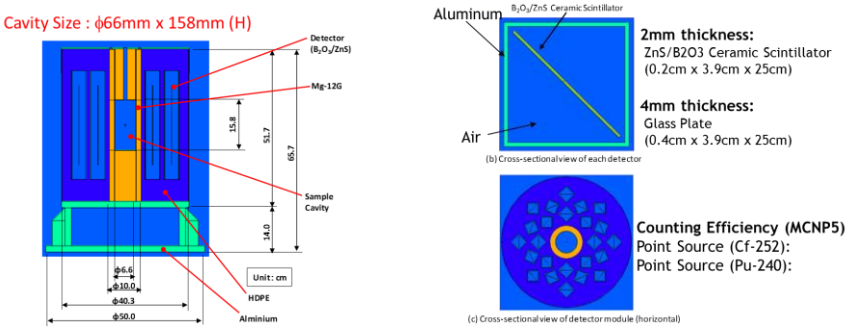

(a)

Figure 5: (a) Cross-sectional view of ASAS detector (X-Z plane (Vertical))
(b) Cross-sectional view of each tube equipped ZnS/$^{10}B_2O_3$ Ceramic Scintillator (X-Y plane).
(c) Cross-sectional view of ASAS detector (X-Y plane (horizontal))

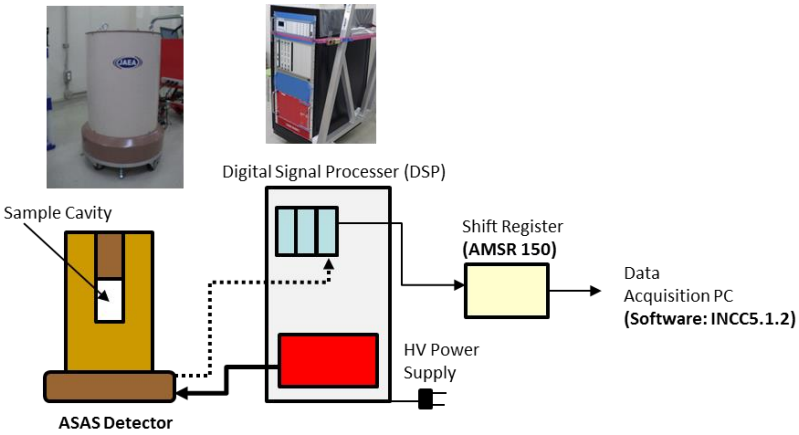

Figure 6: System Configuration of ASAS system

4. Performance Demonstration

In order to prove progress of the technology and performance after the fabrication of the new detector, fundamental performance check and calibration exercise for ASAS detector were conducted from the end of February 2015 to March 2015 in PCDF in accordance with the demonstration plan [5]. To evaluate the performance of alternative He-3 detector, side-by-side test by INVS was conducted to compare the performance of ASAS. The fundamental performance check and the calibration for each system were implemented using Cf check source and MOX powder in a sample vial in March 2015 at PCDF. During the demonstration activity, JAEA showed their performances to relevant organizations that are neutron based NDA specialists, safeguards regulation organizations and He-3 workshop members on 17th and 18th March, 2015.

4.1 Fundamental Performance Check between INVS and ASAS

In order to confirm the possibility that ASAS can be used for the verification system as well as INVS, JAEA conducted fundamental performance check which is focused on the detector performance of itself. For the check, counting efficiency (ε), die-away time (τ) and vertical response profile check in a sample chamber were determined by using Cf-check source and a “figure of merit” that is one of index to compare the neutron detector performance was calculated for ASAS and INVS. Table 1 shows a background measurement results. To minimize the counting statistical uncertainty, the 60min (30 seconds x 120 cycles) measurement was conducted. Table 2 shows Cf check source measurement results to determine the counting efficiency for INVS and ASAS for 10 minutes measurement (30 seconds x 20 cycles). In the singles rate shown in the Table 2, the background measurement results shown in the Table 1 were subtracted. As a result, 30.82% of counting efficiency for INVS and 15.97% of counting efficiency for ASAS were calculated respectively.

Table 1: Background Measurement Results for ASAS and INVS

Date	Description	Condition	Singles (cps)	σ(S)	Doubles (cps)	σ(D)	Note
16th Mar.	INVS Background	30s x 120c	19.143	0.082	0.008	0.004	
	ASAS Background	30s x 120c	10.212	0.057	0.031	0.003	

Table 2: Counting Efficiency Measurement Results for ASAS and INVS

Date	Description	Condition	Cf Rate** (cps) (1)	Singles (cps) (2)	σ(S)	**Efficiency (2)/(1)x100 (%)**	Note
17th Mar.	INVS Efficiency Check	30s x 20c	88020	27127.673	8.729	**30.82**	RSD: 0.032%
	ASAS Efficiency Check			14058.778	6.433	**15.97**	RSD: 0.046%

*** Neutron Emission Rate with decay correction at 17th Mar. 2015*

In case of die-away time (averaged neutron lifetime in the detector) determination, the comparison method between 32μs of gate width and 64μs of gate width to change gate width setting in AMSR was applied. The die-away time measurement results for ASAS and INVS are shown in the Table 3. The measurement time was 5 minutes (30 seconds x 10 cycles). As a result, 45.4μs of die-away time for INVS and 77.7μs of die-away time for ASAS was calculated by using formulas shown below Table 3. In the demonstration, 4.5μs of pre-delay which is default value of INVS was applied for both systems.

Table 4 shows the vertical response profile of ASAS in the sample chamber (see Figure 5). Since the height of sample vial is about 5cm in PCDF, if we set the sample vial into the centre, the position bias is expected about +/- 1% (see +/- 3cm of RSD (%) from centre). To apply known-α method for the calibration and sample setting reproducibility viewpoint, it is very important to establish flatness response profile. It is thought that +/-1% deference in ASAS is very interesting and significant point by comparing with the INVS detector (+/- 2%).

Table 3: Die-away Time Measurement Results of ASAS and INVS

Date	Description	Condition	Doubles (cps)	σ(D)	R+A	A	**Die-away (τ)**	σ(τ)
17th Mar	INVS Die-away Time (GW:32μs)	30s x 10c	5542.088	13.485	28496	23137	**45.359**	0.056
	INVS Die-away Time (GW:64μs)		8279.149	17.700	54336	46330		
	ASAS Die-away Time (GW:32μs)		1137.364	4.879	7008	6002	**77.668**	2.321
	ASAS Die-away Time (GW:64μs)		1890.662	8.598	13660	11987		

Detector Parameter: Pre-delay (4υs),

$$\sigma(R_p) = 100\frac{\sqrt{(R+A)+A}}{(R+A)-A} \qquad \tau = \frac{-32}{ln\left(\frac{R_{p2}}{R_{p1}}-1\right)} \qquad \sigma(\tau) = \frac{32}{\left[ln\left(\frac{R_{p2}}{R_{p1}}-1\right)\right]^2}\frac{\left[R_{p1}\sigma(R_{p2}) - R_{p2}\sigma(R_{p1})\right]}{R_{p1}(R_{p2}-R_{p1})}$$

where, R_p is measured Reals.R_{p1} is measured Reals of gate length 32. R_{p2} is measured Reals of gate length 64, $\sigma(R_p)$ is standard deviation of R_p.

Table 4: Vertical Response Profile Measurement Results for ASAS

Date	Description	Condition	Singles (cps)	σ(S)	RSD (%) from Center	Note
17th Mar.	Vertical Profile (+6cm)	20s x 5c	13404.277	7.453	-5.089	
	Vertical Profile (+3cm)	20s x 5c	13928.914	11.423	-1.374	
	Vertical Profile (Center)	20s x 5c	14122.927	9.678	0	
	Vertical Profile (-3cm)	20s x 5c	13977.829	15.763	-1.027	
	Vertical Profile (-6cm)	20s x 5c	13519.287	17.507	-4.274	

As a summary of fundamental performance check, the counting efficiency, die-away time and the calculated figure or merit (FOM; 2 cases) are shown in the Table 5. Due to the lower counting efficiency and higher die-away time, ASAS FOM (ε^2/τ) was 1/7 of INVS one. So, it is concluded that fundamental performance of ASAS detector could not achieved the conventional He-3 type of sample assay system (INVS). In order to achieve the ASAS performance as well as INVS, it is thought that following 3 improvement points are necessary based on our investigation result by MCNP simulation and electronics viewpoint.

1) Improvement for structure of detector module (ZnS/$^{10}B_2O_3$)
2) Optimization of detector module arrangement in the detector.

3) Improvement of electronics (for instance, optimization of discrimination level and Installation of de-randomizer board).

Table 5: Summary of Fundamental Performance Check for ASAS and INVS

	ASAS	INVS
Counting Efficiency (e)	**15.97%**	**30.82%**
Die-away Time (μs)	**77.67**	**45.36**
Dead-time (μs)	8.9	1.2
Figure of Merit (FOM) $<\varepsilon^2/\tau>$	**328.4**	**2094.1**
Figure of Merit (FOM) $<\varepsilon/\tau^{1/2}>$	**1.81**	**4.58**

4.2 Calibration

To prove the detector performance, the measurement uncertainty is the one of important evaluation point. In the demonstration, the calibration exercise using MOX powder and blind sample measurement by comparing PSMC (Plutonium Scrap Multiplicity Counter) were conducted.

4.2.1 Sample Preparation

Table 6 shows the MOX standard list for ASAS and INVS calibration. In the periodical verification activity by INVS (Method F), MOX and Pu solution containing 1gPu of sample are normally being sub-sampled and used. Therefore, from 0.1gPu (0.24gMOX) to 10gPu (23.97gMOX) of MOX standards were prepared in order to obtain appropriate calibration curve. In the sample preparation, well-calibrated balance and analysis method (IDMS) were applied, and the uncertainty of Pu mass determination of each standard is expected about less than 0.5%. To obtain the calibration slopes, Pu-240 effective mass highlighted in red is used to compare with doubles count rate. Picture 1 shows the picture of MOX standard which is wrapped by double plastic bags (0.3mm x 2) to maintain safety, and the height of the vial is about 5cm.

Table 6: MOX standard list for the ASAS and INVS calibration

Sample ID	**Expected Standard Pu (gPu)**	Sampled MOX (gMOX)	Pu Cont. (wt%)	**Pu Amount by DA (gPu)**	Pu-240 Eff. @3/6/2015	**Pu-240 Eff. Mass (gPu-eff)**
1	**0.1**	0.24	41.72	**0.100**	33.042	**0.033**
2	**0.25**	0.6	41.72	**0.250**	33.042	**0.083**
3	**0.5**	1.2	41.72	**0.501**	33.042	**0.166**
4	**1**	2.4	41.72	**1.001**	33.042	**0.331**
5	**2.5**	5.99	41.72	**2.499**	33.042	**0.826**
6	**5**	11.98	41.72	**4.998**	33.042	**1.651**
7	**10**	23.97	41.72	**10.000**	33.042	**3.304**

Picture 1: MOX Standard (10gPu)

4.2.2 Calibration

In the calibration exercise for ASAS and INVS using standard MOX powder, “passive calibration curve method” and “known-α method” were applied. Prior to start the calibration measurement, detector parameters shown in the Table 7 were determined and calculated. In the case of ASAS gate setting, although 64μs which is considered from die-away time is closer than 128μs, since it was found that minimum of RSD (%) in doubles was 128μs, the 128μs was selected. On the other hand, ρ0 factors to correct multiplication for known-α method were also calculated and applied as appropriate.

Table 8 shows the ASAS measurement results for calibration to obtain passive calibration curve. The measurement time for each standard was 30minutes (30 seconds x 60 cycles). Due to the low Pu mass, less than 1.0gPu of sample could not achieve 1% of statistical uncertainty in Doubles. In the range of standards, 3.16% of statistical uncertainty in Doubles was maximum. To obtain the correlation between Pu-240 effective mass and Doubles count rate, as shown in Figure 7, we could obtain a calibration curve as quadratic formula (Doubles=$0.45x^2$+15.38x (X: Pu-240 eff. mass)). It was confirmed that the quadratic formula was better correlation than liner formula. Table 8 also shows the calibration check. To evaluate the actual difference from the formula, relative difference between Pu-240 effective mass calculated by quadratic formula (slope) using measured double and actual Pu-240 effective mass was calculated. As a result, about -2% difference in 0.5gPu was observed.

Table 7: Detector Parameter Setting for Calibration Exercise

	Efficiency (%)	Predelay (μs)	Die-away Time (μs)	Gate Setting (μs)	HV Setting (V)	Deadtime (μs)	Doubles Gate Fraction (-)	ρ0 (known-α)
INVS	30.82	4.5	45.36	64	1780	1.2	0.6866	0.1518
ASAS	15.97	4.5	77.67	128*	**	8.9	0.5259	0.094

* 128μs was selected because minimum of RSD in doubles was 128μs.
** Due to ceramic scintillator, individual HV is provided with each PMT

Table 8: ASAS Measurement Results for Calibration and Calibration Check for Passive Calibration Curve

ID	Standard Pu mass (gPu)	Pu-240 eff. Mass (g) (1)	Measurement		Measurement				
			Singles (cps)	σ (cps)	Doubles (cps)	σ (cps)	σ (%)	Pu-240 eff. Mass from Qudratic Formula (g) (2)	Difference (%) (1) and (2)
1	0.1	0.033	9.355	0.109	0.538	0.017	3.16	0.033	0.550
2	0.25	0.083	26.172	0.171	1.374	0.030	2.18	0.084	-0.837
3	0.5	0.166	51.337	0.207	2.676	0.042	1.57	0.163	**2.052**
4	1	0.331	98.353	0.278	5.451	0.068	1.25	0.330	0.353
5	2.5	0.826	243.223	0.41	13.901	0.121	0.87	0.830	-0.463
6	5	1.651	484.245	0.523	28.236	0.204	0.72	1.649	0.104
7	10	3.304	975.623	0.688	59.031	0.334	0.57	3.304	-0.009

Table 9 shows the ASAS measurement results for calibration to obtain known-α calibration curve. Though the measurement results from 0.25gPu to 5gPu were same as the result of Table 8, the other 2 standards were measured for a long time (2 hours) in order to reduce statistical uncertainty. To obtain the correlation Pu-240 effective mass and multiplication corrected doubles count rate (MCD), as shown in Figure 7, we could obtain a calibration curve as liner formula (MCD= 16.3x (X: Pu-240 eff. Mass). Table 9 also shows the calibration check. To evaluate actual difference from the formula, relative difference between standard Pu-240 effective mass and measured Pu mass using calibration formula was calculated. As a result about -2.4% difference in 0.1gPu was observed.

Table 9: ASAS Measurement Results for Calibration and Calibration Check for Known-α Method

ID	Standard Pu mass (gPu)	Pu-240 eff. Mass (g) (1)	Measurement		Measurement			Calibration Check (known-α)		
			Singles (cps)	σ (cps)	Doubles (cps)	σ (cps)	σ (%)	Multiplication Corrected Doubles (MCD) (cps)	Pu-240 eff. mass from MCD (g) (2)	Difference (%) (1) and (2)
1	0.1*	0.033	11.264	0.073	0.538	0.007	1.30	0.525	0.032	**-2.418**
2	0.25	0.083	26.172	0.171	1.374	0.030	2.18	1.374	0.084	1.539
3	0.5	0.166	51.337	0.207	2.676	0.042	1.57	2.676	0.164	-1.121
4	1.0	0.331	98.353	0.278	5.451	0.068	1.25	5.451	0.334	1.012
5	2.5	0.826	243.223	0.410	13.901	0.121	0.87	13.586	0.833	0.888
6	5.0	1.651	484.245	0.523	28.236	0.204	0.72	26.93	1.652	0.050
7	10*	3.304	977.663	0.315	59.031	0.182	0.31	53.825	3.301	-0.076

* Longer measurements (2 hours) were conducted for 0.1gPu and 10gPu

In case of INVS, same calibration approaches were conducted, and we could obtain calibration curves for passive calibration and known-α method, respectively.

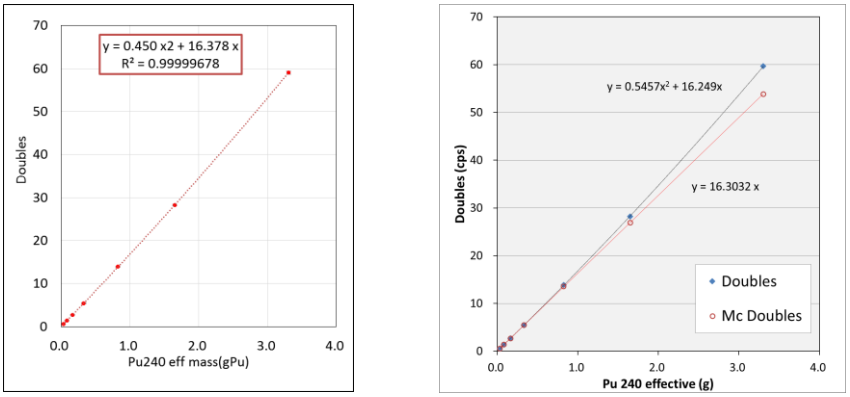

(a) (b)

Figure 7: ASAS Calibration Results for Passive Calibration Curve (a) and Known-α Method (b)

Additionally, to prove the ASAS performance easily, blind MOX sample which is different Pu isotopic composition and unknown Pu mass were measured for 20 minutes and compared between ASAS and INVS. Once we determined Pu mass in the sample by PSMC measurement, the value was compared with the Pu mass measured by INVS and ASAS in passive calibration curve and known-α method. As a result, those differences are very consistent within 1.5% of uncertainty. It is also concluded that ASAS had almost same Pu measurement capability with INVS.

Table 10: Performance check by measuring blind sample (different Pu isotopic of MOX powder)

Description	Pu mass by PSMC (gPu)	Pu mass (gPu) (Passive Calib.)	Pu mass (σ) (Passive Calib.)	Diff (%) from Standard	Pu mass (gPu) (known α)	Pu mass (σ) (known α)	Diff (%) from Standard
Blind Sample by INVS	1.353	1.343	0.012	0.586	1.367	0.005	-1.156
Blind Sample by ASAS	1.353	1.331	0.016	1.48	1.354	0.017	-0.174

Through the series of measurements using Cf-check source and MOX powder, it was confirmed that neutron measurement raw data including coincidence data could be acquired and processed in the AMSR (safeguards shift-register) and INCC (IAEA Neutron Coincidence Counting software).

4.3 Uncertainty Evaluation

For a comprehensive evaluation for safeguards neutron detector, JAEA conducted an uncertainty evaluation obtained from the calibration exercise that is shown in the Table 11. The total measurement uncertainty of ASAS was 3.91% for passive calibration curve and 4.14% for known-α method. On the other hand, the total measurement uncertainty of INVS was 3.66% for passive calibration curve and 5.74% for known-α method. Due to the different efficiency between ASAS and INVS, statistical uncertainty of ASAS is about 1.5 times higher than the INVS. And the dominant reason against relative big systematic and random uncertainties for each detector is the low mass (less than 1.0gPu) measurement. In addition to the uncertainty evaluation, the low detection limits (LDL) were also calculated. As a result, LDL for ASAS and INVS was 0.029gPu, 0.013gPu, respectively.

Table 11: Measurement Uncertainty Evaluation Table

	ASAS		INVS @ PCDF	
	Passive Cal.	Known-α	Passive Cal.	Known-α
Position Bias (s)	1% within sample vial		2% within sample vial	
Statistical Uncertainty (30min Meas.(r))	3.2%		2.2%	
MOX Standard Uncertainty (DA (r, s))	0.35% (s), 0.35%(r)		0.35% (s), 0.35%(r)	
Calibration Curve (s)	+2.0%	-2.4%*	-2.1	+4.9%
Random Uncertainty	**3.2%**	**3.2%**	**2.2%**	**2.2%**
Systematic Uncertainty	**2.25%**	**2.62%**	**2.92%**	**5.3%**
Total Measurement Uncertainty (TMU)	**3.91%**	**4.14%**	**3.66%**	**5.74%**

* To reduce statistical uncertainty, 0.1gPu and 10gPu standards are not measured “30min”, but “120”min.

The fundamental performance of ASAS, for instance, counting efficiency and die-away time, could not achieve the INVS one, we could confirm that quantitative performance of ASAS in the total measurement uncertainty was almost same as INVS. We think that these result of ASAS was satisfied with the requirement of partial defect detection equipment of safeguards (less than 6% as total measurement uncertainty). In normal, the detector performance should be compared with the international target value (ITV2010 [6]) as HLNC detector (>10%MOX). The ITV shows the uncertainty 2.1% in 5 minutes measurement. Assuming that more than 2.5gPu of standards are used for the ASAS calibration measurements and more than 1gPu of standards are used for the INVS calibration measurements, it was confirmed that 2.1% of uncertainty shown in the ITV2010 can be achieved.

5. Summary and Conclusion

JAEA achieved in the 4th year the demonstration of ASAS using ZnS/$^{10}B_2O_3$ instead of He-3 for small sample as an alternative of INVS. Though the FOM of ASAS could not achieve the one of INVS due to lower counting efficiency and higher die-away time, we could confirm that the measurement uncertainty related to the Pu measurement capability was achieved to the same level. And it is thought that ASAS can be applied to the partial verification system of uncertainty (~6%) as well as INVS detector. It has a possibility to be applied as an alternative technology for future safeguards. It is also confirmed that Pu mass by alternative He-3 detector can be measured quantitatively. This proves the measurement capability for nuclear materials.

Since we think that ASAS is very innovative and interesting technology for assay plutonium although fundamental performance of ASAS could not yet achieve the one of INVS, we would like to continue improving the ASAS performance.

6. Acknowledgements

We would like to acknowledge the Japanese government (MEXT; Ministry of Education, Culture, Sports & Technology), the International Atomic Energy Agency (IAEA) and the Integrated Support Centre for Nuclear Non-proliferation and Nuclear Security (ISCN in JAEA) for supporting this work.

7. References

[1] K. Mckinny, et al., “Validation of a ^{10}B Lined Proportional Counter Technology for Replacing ^{3}He in Radiation Portal Monitors”, 52nd INMM annual meeting proceedings, July 2011.

[2] M. Kureta, K. Soyama, M. Seya, A. Ohzu, M. Haruyama, M. Takase, K. Sakasai, T. Nakamura, and K, Toh “Development Plan of Pu NDA System using ZnS Ceramic Scintillator,” Proceedings INMM 53rd Annual Meeting, Orlando, FL, USA, July 2012.

[3] K.Sakasai et al., “Development of a ZnS/$^{10}B_2O_3$ Ceramic Scintillator Neutron Detector for Safeguards NDA Systems”, Proceedings INMM 54th Annual Meeting, Palm Desert, CA, USA, July 2013.

[4] M. Kureta et al., “Design of an Advanced Plutonium Canister Assay system (APCA) using Ceramic Scintillator Neutron Detectors for the Safeguards NDA”, Proceedings INMM 54th Annual Meeting, Palm Desert, CA, USA, July 2013.

[5] H. Nakamura et al., “Development and Demonstration of a Pu NDA System using ZnS/10B2O3 Ceramic Scintillator Detectors”, Proceedings INMM 55th Annual Meeting, Atlanta, GA, USA, July 2014.

[6] International Atomic Energy Agency, “International Target Value 2010 for Measurement Uncertainties in Safeguards Nuclear Materials”, STR-368, Vienna, November 2010: Page33

Real-time, fast neutron detection for stimulated safeguards assay

Malcolm J. Joyce[1], Justyna Adamczyk[2], Michael D. Aspinall[3], Francis D. Cave[3], and Romano Plenteda[2],

[1]Department of Engineering, Lancaster University, United Kingdom
E-mail: m.joyce@lancaster.ac.uk
[2]Department of Safeguards, International Atomic Energy Agency, Vienna, Austria
[3]Hybrid Instruments Ltd., Birmingham Research Park, United Kingdom

Abstract:

The advent of low-hazard organic liquid scintillation detectors and real-time pulse-shape discrimination (PSD) processing has suggested a variety of modalities by which fast neutrons, as opposed to neutrons moderated prior to detection, can be used directly to benefit safeguards needs. In this paper we describe a development of a fast-neutron based safeguards assay system designed for the assessment of ^{235}U content in fresh fuel. The system benefits from real-time pulse-shape discrimination processing and auto-calibration of the detector system parameters to ensure a rapid and effective set-up protocol. These requirements are essential in optimising the speed and limit of detection of the fast neutron technique, whilst minimising the intervention needed to perform the assay.

Keywords: neutron; assay; scintillator; fast

1. Introduction

Neutrons constitute the main route by which nuclear material might be assayed, non-destructively and remotely. Generally they can be considered to exist in two groups in terms of their energy: *fast* and *thermal*, wherein the former can be considered for most purposes to be limited to a maximum of ~5 MeV whilst the latter is usually defined by the ambient conditions at 0.0253 eV. Thermal neutrons are often considered easier to detect because of the significant capture cross sections on materials containing ^{10}B and ^{3}He compared to higher energies. Fission neutrons emitted by isotopes that might provide useful signatures of nuclear materials are almost always emitted in the fast domain. Hence, if a thermal neutron detection modality is to be used, this requires that the neutrons are thermalized by hydrogenous materials (usually polyethylene) prior to detection. Such materials are bulky and can restrict the flexibility of such measurements. Thermal detection media, such as boron trifluoride and ^{3}He gas, are often considered either hazardous in use or supply limited, respectively; although these limitations have not prevented many forms of apparatus based on them being developed and used for nuclear materials assay over the last 50 years or so.

However, as the world seeks alternative sources of energy (and especially electricity) in light of depleted oil stocks and the desire to decarbonise electricity supplies, the nuclear industry is under renewed focus in terms of novel reactor design i.e. small modular reactors, Generation IV systems and alternative fuels. The latter includes revised thinking about such matters as fuel reuse, recycling, mixed-oxide variants and thorium. Whilst nuclear fission remains the only proven technology for massive production of carbon-free electricity, it is also being considered as an energy source for desalination, hydrogen production and bulk chemical synthesis. This multi-faceted nuclear renaissance heralds an era in which there is likely to be an escalation in international nuclear fuel trading and transportation, and all of these matters present challenges for the nuclear safeguards analyst. Such challenges go beyond the need to ensure that new capabilities are grasped to ensure the continuous improvement of safeguards assay and to encompass the need to replace and seek alternatives to established methods, particularly those based on thermal neutron detection.

Neutron detection is often preferred for fissile materials assay because it enables those neutrons emitted simultaneously in fission to be detected providing, in some cases, an *a priori* measurement of quantity of nuclear material present. The detection of neutrons in coincidence enables these neutrons to be discriminated from *single* neutrons that originate from a variety of other, competing contaminant sources and processes. An important example in this context are the isotopes that are susceptible to fission, such as ^{235}U, ^{238}U, ^{239}Pu, ^{240}Pu etc. which constitute sources that emit neutrons that are emitted simultaneously, whilst neutrons that result from the interaction of α particles (usually arising from α decay in actinide species) on light isotopes are emitted independently of each other.

To a thermal neutron detector, neutrons arising from α,n reactions or from fission are identical since the moderation process wipes out any information available associated with their initial energy. The discrimination is done instead by the processing electronics using the time correlation information associated with the fission neutrons. To isolate the coincident signature of fission neutrons from those not correlated in time, a time window is usually applied, either electronically or in subsequent analysis; this time window is usually referred to as the coincidence gate. The uncorrelated neutron fluence constitutes a random, accidental contribution to the total number of coincident neutron events that fall within this gate. While the coincident events are distributed very close to the first event (depending on the detector characteristic) exhibiting the so-called "Rossi-Alpha distribution", the accidental events have a constant probability at whatever distance in time they occur. Hence, the larger the gate, the larger the probability of a random accidental contribution. In order to account for these random accidental events, a delayed gate with the same width as the coincident gate is opened far from the first event. This technique is usually carried out within hardware or firmware referred to as a shift register and is a well-established means for identifying the accidental contribution. In certain conditions in which the amount of real coincidences is very small in comparison to the accidental contribution, the statistical uncertainty in the mass estimate required will be too large for a practical acquisition time to be achieved.

It is hence very clear that a significant factor that governs the uncertainty in coincidence measurements is the gate width. In thermal neutron detection systems the average delay between two coincident detections is due mainly to the time necessary for the thermalisation prior to detection. In sharp contrast, in the case of fast neutron detection, the delay between two coincident events is not driven by the time needed for thermalisation but only by the difference in time of flight of the two fission neutrons. This can be three orders of magnitude lower in comparison with a thermal detector.

This can be depicted by comparing the Rossi-Alpha distributions for a thermal system that requires moderation prior to detection, and a fast system that does not. These are shown in Figure 1, and illustrate the basis on which it is possible to move from an unavoidably wide time window for thermal systems to a much shorter, ~ 100 ns window for fast systems; the latter inferring significantly-reduced accidentals rates relative to the former.

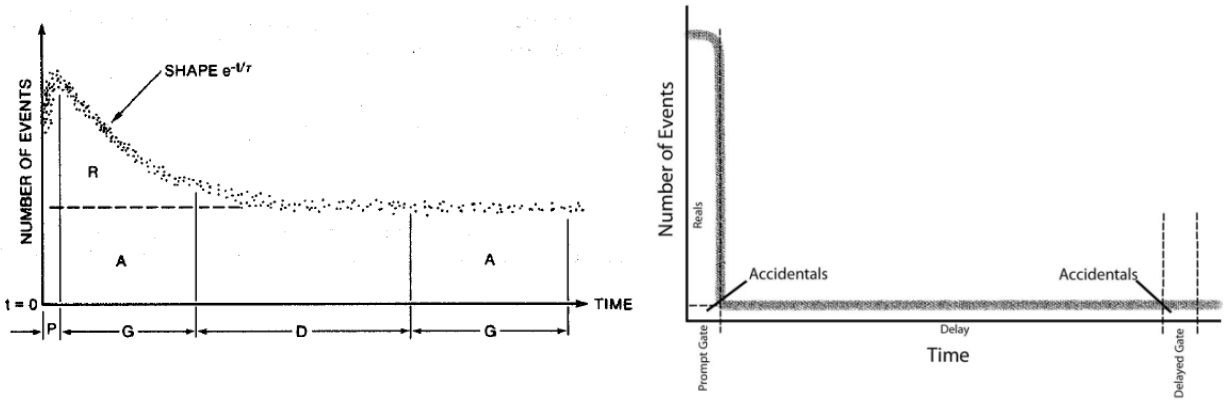

Figure 1: Rossi-alpha distribution for thermal systems (left) [1] and for fast systems (right).

This paper concerns the use of fast neutrons for neutron coincidence assay in contrast to long-established thermal neutron assays, the latter reliant predominantly on the use of ^{3}He. It describes measurements made in collaboration with the International Atomic Energy Agency (IAEA). This paper is focussed on development of the electronics that has been necessary to promote the use of long-

established liquid scintillator detectors into a field-deployable active interrogation assay of uranium materials.

2. Concept outline and system architecture

Nuclear safeguards assay based on fast neutrons has been made possible by two developments: i) the availability of low-hazard, organic scintillation detectors and ii) electronic hardware and firmware that is sufficiently fast to enable real-time discrimination of neutrons from γ-ray contamination.

A single neutron detector cannot detect two coincident neutrons due to the dead time (100-300 ns) in the detector and electronics. Therefore a number of distinct, single detection cells is necessary for coincidence assays. On the other hand, it is proven that a large single liquid scintillator cell would distort the pulse too much to apply pulse shape discrimination between neutron and γ effectively [2]. Detector systems comprising a limited number of detectors i.e. a pair of detectors are, by definition, no use for multiplicity measurements but they serve as a useful basis with which to introduce the system architecture for fast-neutron safeguards assay. A twin-detector arrangement is shown in Figure 2. This comprises two high-flashpoint, low-hazard EJ309 detectors (Scionix, Netherlands) connected through to two single-channel mixed-field analysers (Hybrid Instruments Ltd.). The analyser comprises the high-voltage supply to drive the photomultiplier tube of a given detector and the firmware to discriminate the long-tailed neutron pulses from the shorter γ ray events; it is a single-unit alternative to laboratory-based rack modules. The discriminated signals from these analysers are fed into a shift register configured on a field-programmable gate array on an embedded controller (National Instruments Ltd.).

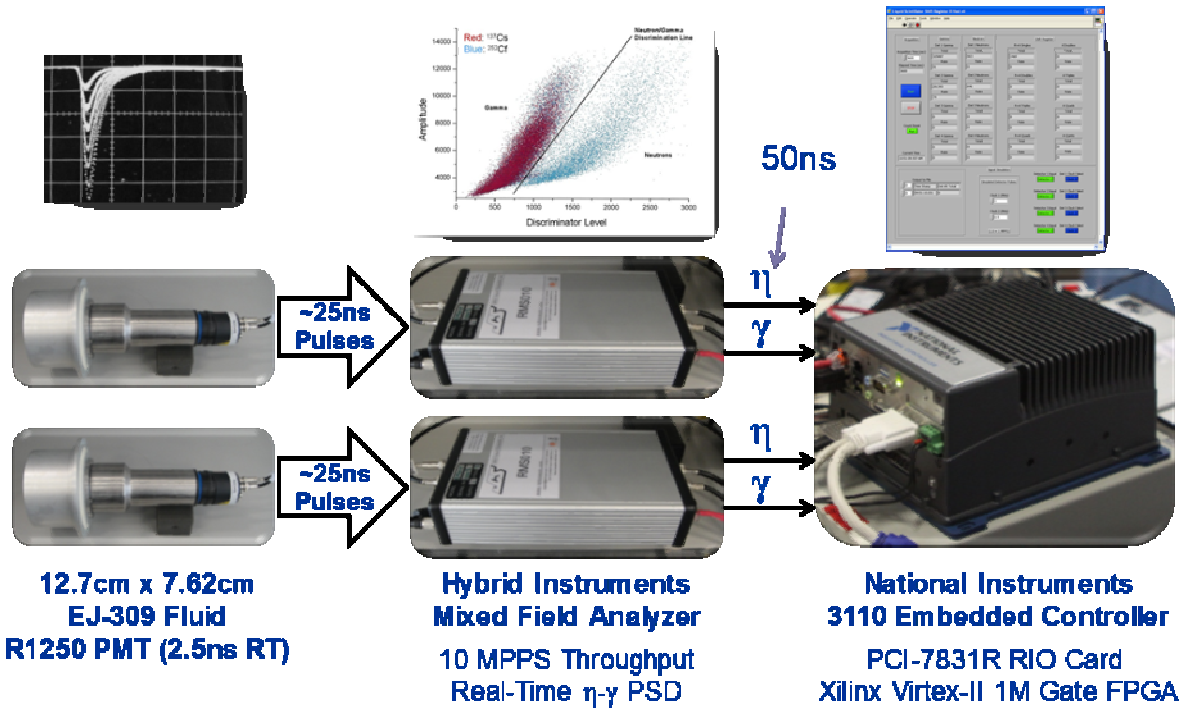

Figure 2: The fundamental system architecture for fast-neutron assay.

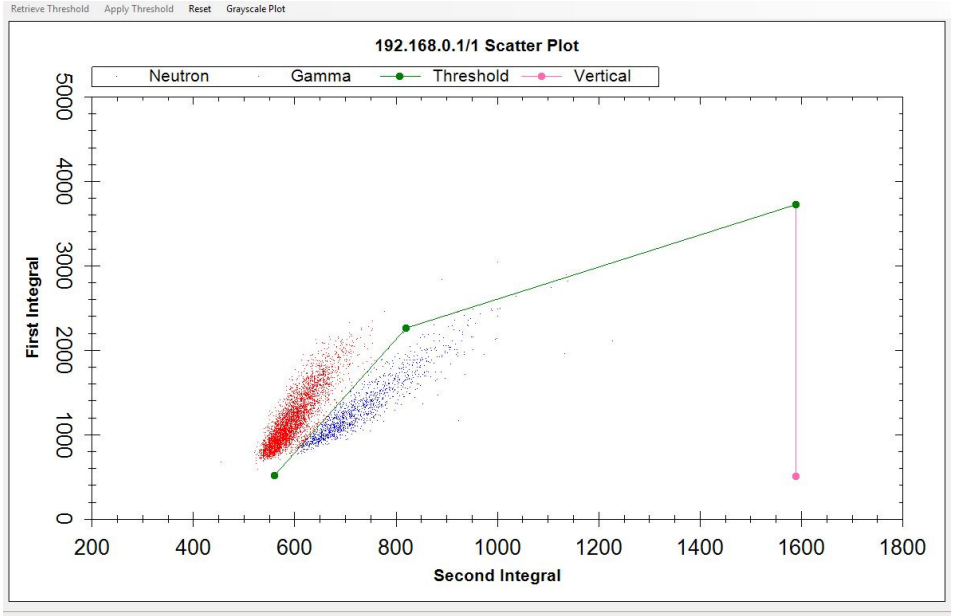

Figure 3: An exemplar scatter plot for one detector showing γ rays in red and neutrons in blue, with a threshold separation line in green.

Neutrons and γ rays interact with the organic scintillant differently; the former lose their energy predominantly via proton recoil whilst the latter interact with the electron structure of the scintillant molecules. This distinction in interaction processes results in a well-known albeit subtle difference in profile of the light pulse that results, with the neutron pulses exhibiting a longer falling edge than that of the γ-ray events. When the data are plotted in terms of a long- and short integral of the area under the pulse the data separate into two clear loci which can then be used as a basis for separating the neutrons from the total field detected. An exemplar depiction of the separation of events or *scatter plot* is given in Figure 3.

The distinction of this arrangement from long-established, laboratory-based methods of pulse-shape discrimination (PSD) is that it enables *real-time* PSD i.e. radiation incident on the detector is processed immediately, without the need for post-processing but retaining the synchronisation with pulse arrival time to enable the essential coincidence function. This is an important requirement for the application to be used autonomously in commercial fuel production facilities because post-processing would introduce a delay, thus interfering with the manufacturing process which is highly undesirable. Also the availability of a digital signal corresponding to each neutron event synchronised in time with the detection of the incident event renders the system compatible with existing acquisition systems at the IAEA. The mixed-field analyser also offers very high levels of throughput to enable the requisite levels of sensitivity to be reached with a practical number of detectors and within a reasonable period of acquisition. A more comprehensive description of the approach is available in [3].

In support of the research reported here, three significant developments have been made to the electronics and firmware:

- The high-voltage supply systems have been upgraded to provide for much greater stabilisation in use, to optimise the consistency of the gains across a significant number of detector cells, as necessary in this application.
- Very large events, that can become saturated in processing and thus in the past have contributed to an extensive and erroneous source of high-amplitude noise in the scatter plot data have been identified in firmware and removed. This leaves behind much better localised plumes that enables the better separation of neutrons and γ rays, and has the potential for simpler PSD thresholding.
- The matching of gains across a significant number of detector cells i.e. >10 has been enabled by the real-time acquisition of pulse-height spectra for each cell. The auto-calibration of these

spectra is enabled via the graphical user interface, providing a quick and effective approach to setting up arrays of detector systems of this type.

3. System design for fuel assembly assay

3.1. Detector system design: the IAEA Liquid Scintillator Uranium Neutron Collar (LS-UNCL)

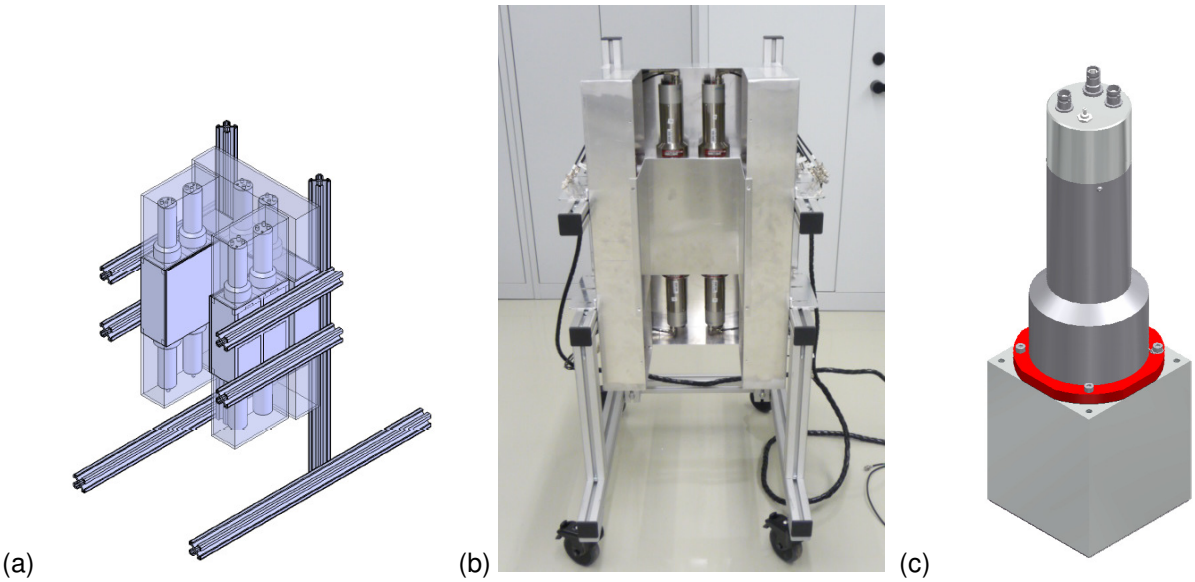

Figure 4: The detector system used in this research. Schematic design (a), physical embodiment (b) and a single detector (c).

The detector system used for this research is shown in Figure 4. It comprises 12 individual VS-1105-21 EJ309 detectors (Scionix, Netherlands). Each of these detectors is a cube of dimensions of 100 mm × 100 mm × 120 mm with a photomultiplier tube of type 9821 FLB (ADIT Electron Tubes, Sweetwater, TX). The detectors are positioned in three gangs of four, with the detector cells facing one another and the PMTs aligned vertically, opposite one another. The pulse-shape discrimination is provided by three, 4-channel mixed-field analysers (Hybrid Instruments, UK) and the acquisition system to perform the shift register processing is as described in Section 2. The design of the system was influenced by simulations that were performed by the Joint Research Centre, Ispra, Italy.

Figure 5: A bank of MFAX4.3 4-channel analysers used in this research.

3.2. Multiple-channel real-time pulse-shape discrimination

An extended number of single-channel units is clearly not a satisfactory practical arrangement to process the pulses from a significant number of detectors. Therefore for this application three 4-channel analysers from a bank of four were

configured, as shown in Figure 5.

This unit provides processing capability for 16 detectors ensuring that there is redundancy for 4 extra detectors if they are needed. As in the case of the system architecture discussed in Section 2, these analysers provide for 500 MHz processing per channel, 6 ns jitter between events and a processing period of 333 ns per event from detection through to output. They output discriminated 50 ns TTL pulses for each neutron and γ ray, with the former being fed to the shift register firmware. A comprehensive description of the analyser is available in [4,5].

3.3. System control

The MFAX4.3 systems are controlled via a graphical user interface, and the system can operate in two modes. The first of these is as a multi-channel analyser (MCA) in order to match the gain of all detection cells through the control of the high-voltage settings for each of the detectors; the user interface displays plots of counts versus channel for each of the channels in use and these are integrated in real time to enable quick and simple configuration on the fly. Two examples of these plots are given in Figure 6 below; one for ^{137}Cs (the usual choice of calibration source due to its single, 662 keV γ ray), and ^{252}Cf, the latter a popular choice for configuring PSD thresholds. The other mode is as a PSD analyser, the unit's main role, in which it provides scatter plots for diagnostic purposes which are once again updated in real-time, as depicted in Figure 3. The user interface, as shown in Figure 7, allows high-voltage levels, trigger thresholds, pre-amplifier gains and pulse-shape discrimination thresholds to be adjusted. Once configured, these settings are written to the FPGA on the MFAX4.3 analyser so that after powering off, the settings for each channel are set in firmware, allowing for autonomous operation independent of the user interface.

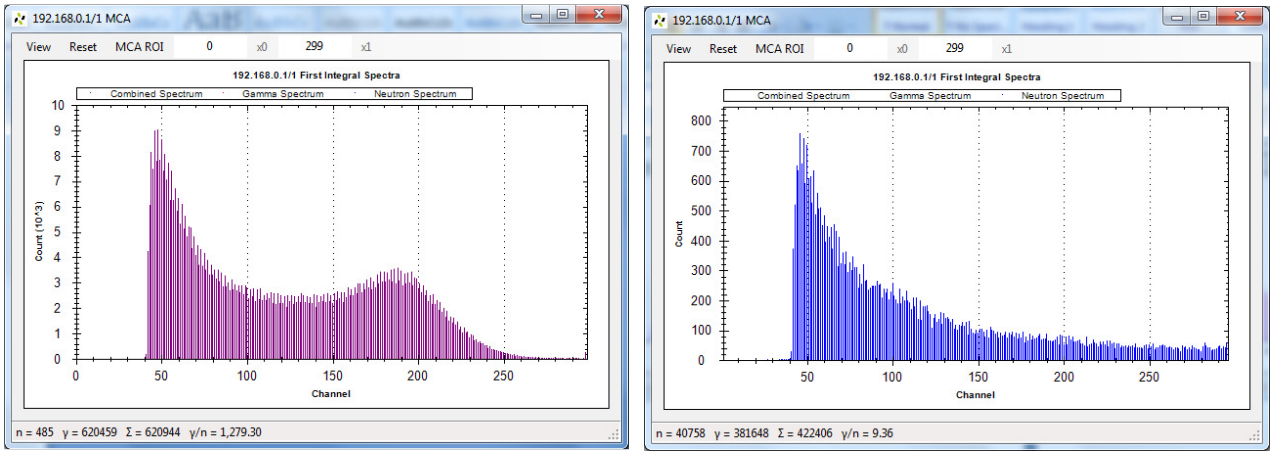

Figure 6: MCA plots for ^{137}Cs (left) and ^{252}Cf (right) provided in real-time by the MFAX4.3.

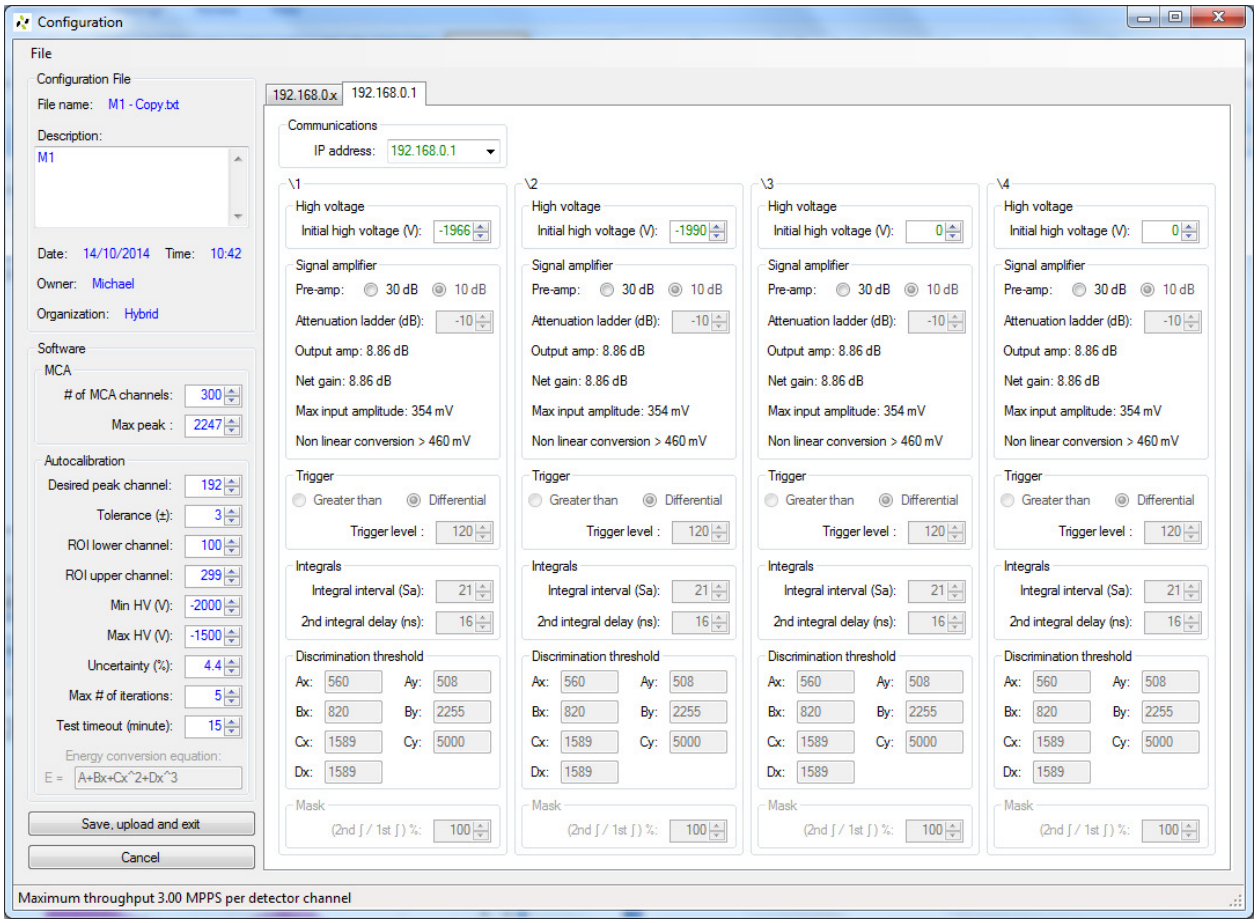

Figure 7: A screen shot from the control laptop of one of the control environments on the MFAX4.3.

The FPGA-based shift register is configured via a separate user interface, and an example screen shot of this is shown in Figure 8. This provides information for each pod (i.e. collection of four detectors), detection rates for each detector including GARRN estimates and doubles detection rates as a function of position in terms of time bins which is also displayed in terms of events versus bin number for each pod.

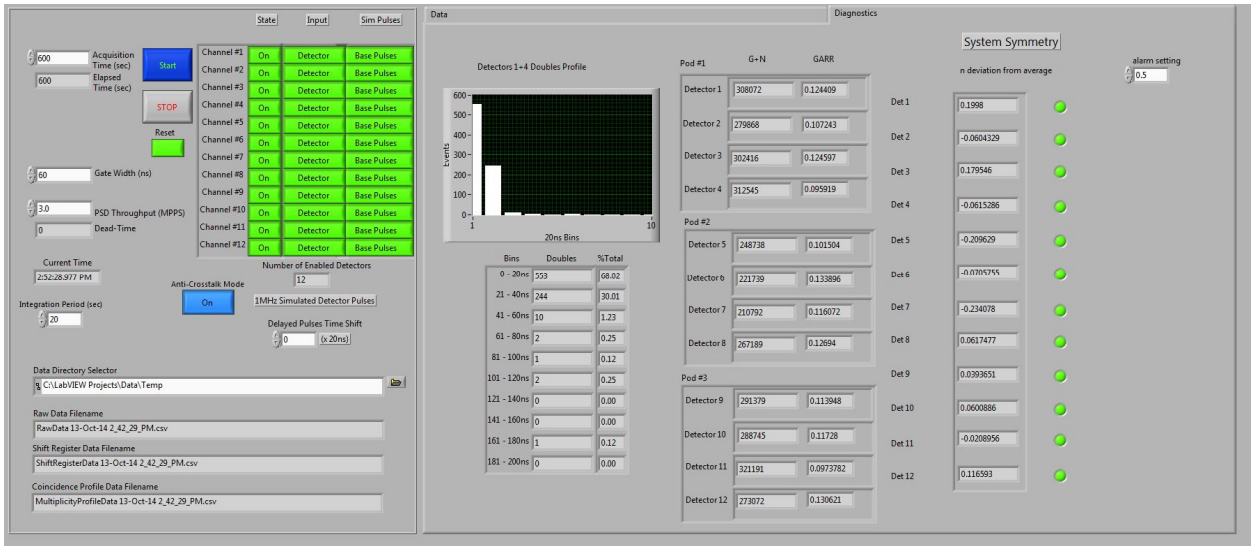

Figure 8: A screen shot from the control laptop of LabView ® environment configured to control the shift register.

3.4. Combatting cross-talk

One consequence of using an array of fast neutron detectors is that to ensure satisfactory levels of detection efficiency the detectors are best positioned near to the sample under scrutiny. However, this exacerbates the possibility that neutrons might scatter from one detector to another. This is shown schematically in Figure 9.

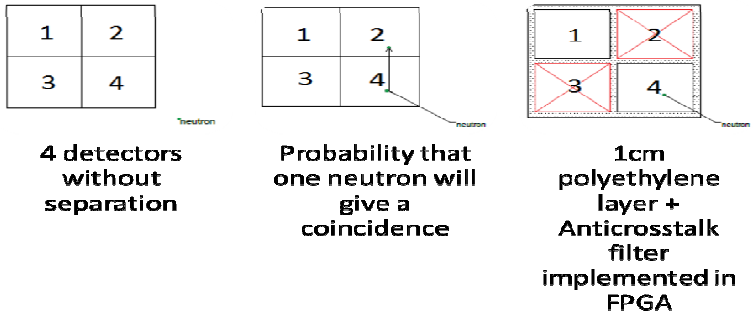

Figure 9: A schematic depicting the cross-talk phenomena between four detectors arranged adjacent to one another.

The significance of a cross-talk event is that it results in a single neutron stimulating two counts in neighbouring detectors and, in the case of a single scatter from one detector to another, a coincident event despite in reality there only being one neutron, not two. If left uncorrected this contribution to the dataset would lead to an overestimate in the reals and a corresponding overestimate in the amount of material under assay.

In the system used in this work a filter has been constructed to reduce this possibility, which comprises a 1 cm polyethylene layer separating the detectors from one another, and a software function which discounts coincident events in neighbouring detectors.

4. Experimental details

4.1. Premise for the measurement

We have previously reported the assay of plutonium with a real-time fast neutron system, comprising 4 detectors and based on the detection of coincident events [5]. In this paper we describe an application for enriched uranium fresh fuel. Nuclear fuel of this type that has yet to be irradiated is a challenge to safeguards because the ^{235}U (for which the level of enrichment is of safeguards concern) emits a very weak radiation signature that does not provide for a quick and accurate measurement of the quantity of material present. Hence, for this aspect of the fuel cycle active methods are often employed in which a neutron source is used to stimulate ^{235}U fission in the fuel. The radiation that arises as a result is measured to infer fuel quantity and, ideally, enrichment (usually the neutron component of the stimulated field is the focus of the measurement). In certain conditions, when the stimulating neutrons are above the absorption energy for gadolinium (to be independent of the presence of this component), the neutron fluence from stimulated fission is very small compared with the interrogating source (i.e. 1:1000) and design challenges can arise in the context of the use of thermal detectors. The premise for this measurement is described in more detail in [6].

In this work we have adopted a similar rationale, with a ^{241}Am-Li source as the stimulus but with the combination of the liquid scintillator UNCL detector system, the MFAX4.3 analyser and the FPGA-based shift register instead of a thermal neutron detection system. This approach has two significant advantages in principle. Firstly, the coincidence counting approach with a shorter coincidence gate allows for data corresponding to the true coincident neutrons detected with significantly-reduced accidentals rates. Secondly, the system can also discriminate the stimulating source from the fission source on the basis of energy since it still preserves the original emission energy. In order to reduce the cross-talk contribution from the ^{241}Am-Li to negligible levels, the low-energy cut-off of the organic

liquid scintillation materials (EJ309) in neutron energy is raised to approximately 500 keV. This ensures that the same neutron surviving the first detection is very unlikely to have enough have energy to be detected again.

4.2. Experimental set-up

Figure 10: LS-UNCL system in use in Vienna.

The experiments central to the research described in this paper were carried out at the Atominstitut, TU-Wien, Vienna, Austria. The LS-UNCL was positioned near to the MFAX4.3 units and the associated HV, signal-input, and signal-output (neutron and γ-ray) cables were connected to the MFAX4.3. The gains of the detectors were matched over Ethernet using a ^{137}Cs source and the signal output cables were connected to the National Instruments ® industrial controller for the multiplicity data collection. The ^{241}Am-Li source (neutron emission rate 5×10^{4} per second) was placed in the vacant face of the LS-UNCL detector system i.e. the face void of any detectors. The source was removed to allow for passive measurements to be made of the material under test (predominantly of the ^{238}U content present in the sample) and then active measurements were made (stimulating neutrons from the ^{235}U content).

The sample was a WWER-440 fuel assembly, of 3.6% enrichment as shown with the LS-UNCL system and MFAX4.3 in Figure 10. Data were acquired for 15 minutes, both passive and active, and the threshold was set to 400 keV neutron-equivalent energy.

4.3. Results

Duration of measurement	Neutron detection rates (totals) per second			Uncertainty
	Passive reals	Active reals	Net reals	
15 minutes	1.28	5.57	4.28	2%

Table 1: Data recorded for the passive and active measurement of a 3.6%-enriched WWER-440 fuel assembly.

The results from a 15-minute measurement of the WWER-440 fuel assembly are given in Table 1. These include the passive-real neutron rates (without the source) and the active-reals neutron rates (with the source). The net reals rate is obtained via subtraction, giving a 2% uncertainty in the measurement.

5. Conclusions

The research described in this paper demonstrates that liquid organic scintillators can be used effectively for the analysis of enrichment levels in a nuclear fuel assembly, in this case a 3.6%-enriched WWER-440 assembly. In particular, three advancements made to the electronics in terms of high-voltage stabilisation, removal of saturated pulse profiles and auto-calibration of detector gains have yielded significant advantages in operation. The use of liquid scintillators, coupled with real-time digital pulse-shape discrimination, results in extremely low accidentals rates offering the potential for the assay of a wider range of nuclear materials than previously considered possible. The approach offers the benefits of faster assay of fresh fuel than was previously considered possible as a result of the very low accidentals rates or conversely, measurements with smaller stimulating sources where this presents benefits in terms of radiation protection and ease of use.

5. References

[1] N. Ensslin, *Principles of neutron coincidence counting, chapter 16, Passive non-destructive assay manual,* pp. 457-492, http://www.lanl.gov/orgs/n/n1/panda/00326411.pdf

[2] Private communication, A. Lavietes, Interational Atomic Energy Agency, Vienna, Austria, June 2011.

[3] Malcolm Joyce, 'Fast neutron multiplicity assay', Nuclear Future 9 (6) 43-46 Nov./Dec. 2013.

[4] M.J. Joyce, M.D. Aspinall, F.D. Cave, A. Lavietes, *A 16-channel real-time digital processor for pulse-shape discrimination in multiplicity assay*, IEEE Trans. Nuc. Sci. 61 (4) pp. 2222-2227 (2014).

[5] M.J. Joyce, K.A.A. Gamage, M.D. Aspinall, F.D. Cave, A. Lavietes, *Fast Neutron Coincidence Assay of Plutonium with a 4-Channel Multiplexed Analyzer and Organic Scintillators*, IEEE Trans. Nuc. Sci. 61 (3) pt. 2 pp. 1340-1348 (2014).

[6] 'Development of a liquid scintillator–based active interrogation system for LEU fuel assemblies', A. Lavietes, R. Plenteda, N. Mascarenhas, M. Cronholm. M. Aspinall, F. Cave, M.J. Joyce, oral paper for the IEEE Advancements in Nuclear Instrumentation, Measurement Methods and Analysis (ANIMMA), Marseille (June 2013), paper #1257, DoI: 10.1109/ANIMMA.2013.6728037.

6. Acknowledgments

This work was funded by the UK Department of Energy and Climate Change through the UK Safeguards Technical Support Programme in support of IAEA safeguards. We acknowledge the support of P. Peerani and A. Tomanin at the JRC ISPRA, Italy, for supporting calculations.

Experimental Assessment of a ^{6}LiF:ZnS(Ag) Prototype Neutron Coincidence Counter for Safeguards

H. Tagziria[a1], M. Foster[b], M. Schear[c], D. Ramsden[b], G. Dermody[b], B. Pedersen[a], P. Peerani [a] and P. Schwalbach [d]

[a]European Commission, Joint Research Center, ITU-Nuclear Security Unit, I-21027 Ispra, Italy

[b]Symetrica Security Ltd., Roman House, 39 Botley Road, Southampton, SO52 9AB, UK

[c]Symetrica Inc., 63 Great Road, Maynard MA 01754

[d]European Commission, DG-ENER, Nuclear Safeguards - Unit E1, Section Measurement Systems, On Site Laboratories, Cooperation Programmes, EUFO 3477, L-2557 Luxemburg

Abstract

A prototype ^{3}He-free neutron coincidence counter for safeguards applications has been developed and built following comprehensive Monte Carlo modeling. It consists of eight compact ^{6}LiF:ZnS(Ag) thermal neutron absorbers (or blades) dispersed in four moderating slabs surrounding the sample chamber.

This paper describes the results of an extensive campaign of measurements carried out at the JRC in Ispra to validate the Monte Carlo models, characterize and calibrate the counter in order to assess the suitability of the technology as an alternative to ^{3}He based ones. Its compliance with safeguards requirements regarding a number of important parameters such as neutron efficiency, die-away time, gamma rejection, dead-time amongst others is also evaluated.

The counter successfully took part in an inter-comparison measurement campaign at the JRC in Ispra (Italy) within the International Safeguards Workshop on ^{3}He alternatives in October 2014 attended by a number of laboratories and research institutes from Europe, IAEA and USA with Japan as observers

The performance of the counter is compared to that of a commonly deployed HLNCC-II-II counter which makes use of now scarcely available ^{3}He gas.

Keywords: NDA; Nuclear Safeguards; Neutron Coincidence Counting

1. Introduction

Over the past few decades, non-destructive assay (NDA) in the field of nuclear safeguards has relied on the neutron coincidence counter (NCC), using the time-correlation of fission neutrons to produce measurements of fission rate from which plutonium mass can be calculated. Such systems consist of a sample cavity surrounded by He^{3} proportional counters embedded in high density polyethylene (HDPE), with attached electronics to carry out the time-delayed coincidence measurement. The “classic” design is represented by the HLNCC-II in service around the world [1].

However, in recent years the supply of ^{3}He has been outstripped by demand [2], leading to a perceived shortage in many fields, including nuclear safeguards. To mitigate this problem extensive research has been carried out worldwide into alternatives, focussing mostly on ^{10}B and ^{6}Li thermal neutron detectors or fast neutron detection using organic scintillators.

[1]**Contact**: hamid.tagziria@jrc.ec.europa.eu

This paper describes research by JRC and Symetrica into a ^{6}Li-based system, utilising the safeguards and NDA expertise of JRC and the detector development expertise of Symetrica. The latter has demonstrated excellent performance in terms of gamma-ray rejection and sensitivity when applying ^{6}Li-loaded scintillators in systems ranging from roadside portals to handheld neutron detectors [3]. It was then a natural step to apply Symetrica compact thermal neutron detectors to the neutron coincidence counting problem.

It was decided that the development effort would be staged. The first stage consisted of two parts: designing an NCC capable of outperforming the HLNCC-II using simulations in MCNPx; and developing and testing the thermal neutron detectors that would populate it. Since the thermal neutron detectors are a new design, this stage only involved making a small number sufficient for testing the NCC in a partially populated mode. That testing was used to validate models and provide an improved estimate of the performance of the fully populated NCC.

In order to judge the success of this effort, a detailed characterisation and calibration campaign of the partly populated NCC was carried out at JRC, culminating in a comparison of plutonium mass estimates against a benchmark set by an HLNCC-II.

The planned second stage will consist of using the results presented here to further develop the thermal neutron detectors and to improve the design of the NCC. A larger set of thermal neutron detectors including improvements will be manufactured and used to test the full NCC, again against the HLNCC-II benchmark.

2. Thermal Neutron Detector Design

2.1 Neutron Detector "Blade" Description

The neutron coincidence counter under test relies on a number of thin thermal neutron detectors utilising ^{6}LiF/ZnS scintillators and silicon photomultiplier (SiPM) readout, dubbed "blades" for their form factor. Figure 1 shows images and the physical parameters of the thermal neutron detector "blades" developed for this project.

Each blade consists of a sensitive element and processing electronics. The sensitive element is made up of two ^{6}LiF/ZnS screens (EJ-426) sandwiching a wavelength shifting PVT plate of 500 x 60 x 3mm (EJ-280), both sourced from Eljen Technologies. The screens cover the whole face area of the wavelength shifter and have an average thickness of 0.75mm. Scintillation light from the screens is transmitted by the wavelength shifter to a row of silicon photomultipliers (S10931-050P) supplied by Hamamatsu Photonics optically bonded to one end.

The processing electronics is a single-board solution that includes the following functions:

- Preamplifier to provide current to voltage conversion and signal conditioning.
- Temperature stabilized SiPM bias supply in the range 66V to 76V using a linear function of 56mV/°C. A temperature sensor is placed near the SiPMs for this purpose.
- Neutron/gamma/SiPM noise pulse shape discrimination (PSD). An internal 20MHz clock gives a 50ns time resolution.
- Simple internal fault detection and reporting via a "device ready line" that can be picked up by attached electronics.
- Communication over SPI to set parameters such as SiPM bias and neutron/gamma discrimination thresholds. Internal memory holds these settings following calibration.
- A TTL output signal to indicate detection of neutrons. The pulse is +5V and 120ns in duration.

The electronics are placed at the end of the sensitive element. An aluminium enclosure fits over the electronics and is electrically connected to a thin aluminum case over the sensitive element to provide RFI and EMI shielding. A layer of black heat-shrink plastic then shrouds the aluminum case to provide a protective layer.

Discrimination between neutrons, gamma-rays and SiPM noise is based on the measured length of pulses against a programmable threshold. A paralysable dead time of 10μs follows each neutron detection TTL. Each blade is self-contained and requires only a power line to operate. In return it provides a ready line to indicate that it is operating, and a TTL pulse for each neutron detected.

- **Mass** = 430g
- **Dimensions** = 560 x 68 x 12 mm
- **Power requirement** = 9mA at 12V
- **Temperature range** = 10 to 30°C
- **Neutron detection signal =** +5V, 120ns TTL pulse

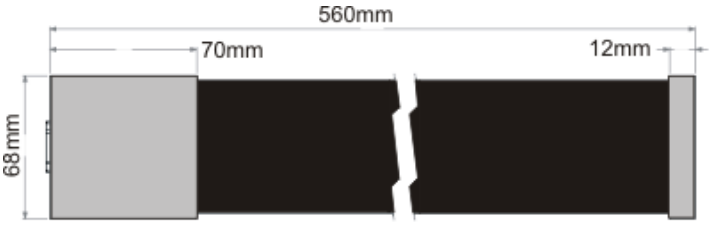

Figure 1: Clockwise from top left: An image of two blades, physical parameters of a blade, three blades showing their processing electronics, the dimension of a blade.

2.2 Aggregation of Blade Detectors

To facilitate testing of systems containing multiple blades, an Aggregator Unit was developed. It serves to distribute power to up to 32 blades and contains a 32-input logical OR function with a single BNC output. This BNC can then be connected to counting circuits or pulse train analyzers for data collection. Blades are connected to the Aggregator Unit by 32 cables of 1.5m length that carry 12V power, TTL signals and ready lines.

Figure 2: The Aggregator Unit (left) connected to eight blades in a moderator slab (right). Only eight cables have been fitted to the Aggregator for convenience.

2.3 Neutron Detector Testing

For this project a total of eight blades were assembled and tested for their thermal neutron detection efficiency and gamma-ray rejection. One of the set was also subjected to thermal tests to measure its variation in detection efficiency as a function of temperature.

2.3.1 Thermal Neutron Detection Efficiency and Gamma-Ray Rejection

The detectors used in the test module were calibrated to achieve the best thermal neutron detection efficiency whilst still meeting a gamma-ray rejection limit of 10^{-7} or better, which means the probability of an incident gamma-ray being mistaken for a neutron was less than 10^{-7}.

The efficiency of each blade relative to the rest of the set was determined by irradiation with a 5.21ng ^{252}Cf source moderated in a 5cm thick HDPE cylinder (10cm Ø x 10cm L), as shown in Figure 3. Measurements were taken indoors since environmental scatter was not relevant for relative measurements.

For gamma sensitivity measurements, a 17.7mCi ^{137}Cs source was illuminating the largest face of the detector at a dose rate of 100μSv/hr. Results are shown in Table 1. Since there exists a tradeoff between these two measurements depending on pulse shape discrimination thresholds, the two measurements were carried out simultaneously.

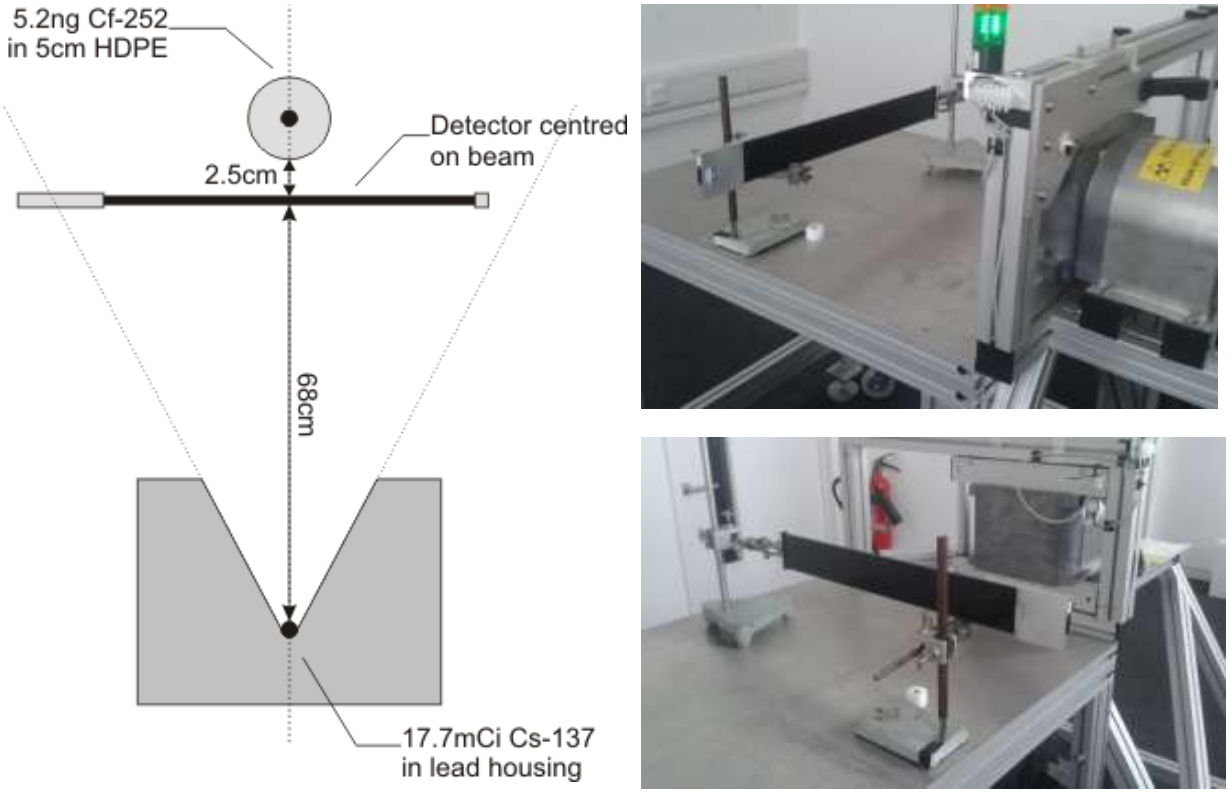

Figure 3: Left: a sketch of the detector in front of the gamma-ray source, with the neutron source in place, and the detector sensitive element centred on the gamma beam. Right: photographs of a blade in the test position.

Detector Serial Number	Relative Sensitivity (n/s)	Relative Sensitivity (% of average)	Gamma-ray Rejection (x 10^{-7})
140001	45.01 ± 0.39	101.3%	0.26 ± 0.11
140002	46.57 ± 0.40	104.8%	0.55 ± 0.12
140003	44.29 ± 0.39	99.7%	0.70 ± 0.14
140004	44.63 ± 0.39	100.5%	0.18 ± 0.10
140005	45.18 ± 0.39	101.7%	0.47 ± 0.11
140006	45.30 ± 0.39	102.0%	0.60 ± 0.13
140007	41.06 ± 0.37	92.4%	0.82 ± 0.14
140008	43.30 ±0.40	97.5%	0.50 ± 0.10

Table 1: Summarised results from the individual blade tests for relative thermal neutron detection efficiency and gamma-ray rejection.

The distribution of sensitivity is very tight, showing a standard deviation of only 3.7%. During this work it was found that the relative efficiency correlated strongly with the ^{6}LiF/ZnS screen thickness indicating that this sets the limit on uniformity, since each blade was tuned for the best sensitivity. If this distribution is later found to be too broad, then the highest performing blades can then be de-tuned slightly to narrow it.

Gamma-ray rejection is very good in all blades, so gamma-ray rejection in the whole system is expected to be good.

2.3.2 Temperature Tests

In this test, blade S/N 140002 was placed in an environmental chamber and cycled in the range 10°C to 30°C multiple times. A neutron source in a 5cm HDPE moderator was also placed to provide a high count rate. During the cycle, the count rate was monitored. Figure 4 shows the results indicating a high degree of consistency over the range with no apparent hysteresis between cycles.

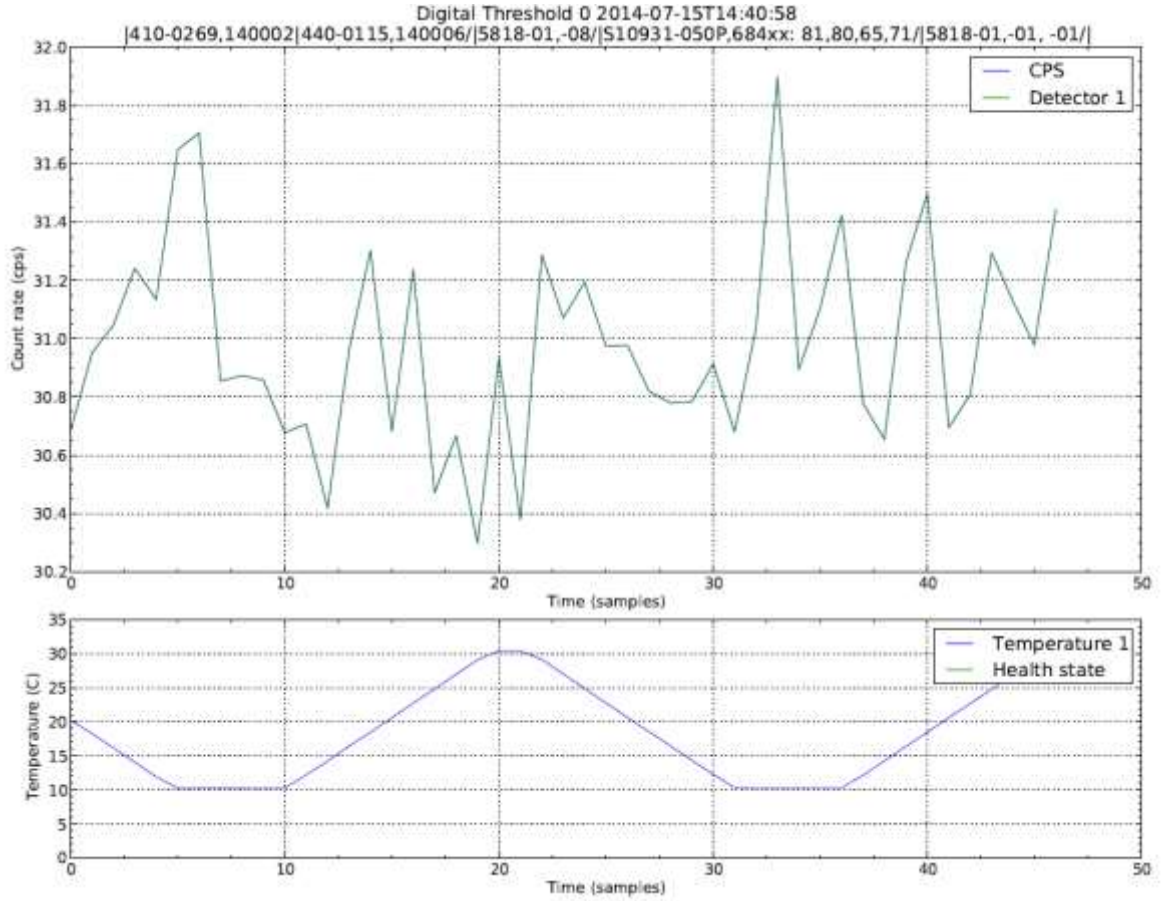

Figure 4: Data showing the consistency of neutron sensitivity as a function of temperature in the range 10°C to 30°C.

2.3.3 Readout Efficiency Measurement

The blades rely on a wavelength shifting process and pulse-shape discrimination to detect the capture of thermal neutrons in the ^{6}LiF/ZnS screens. These processes are not simulated in Monte Carlo models and so must be accounted for as the “readout efficiency” of the thermal neutron detectors to prevent the model overestimating the absolute efficiency of the NCC. Readout efficiency represents the probability of a neutron captured in the ^{6}Li producing sufficient signal to pass the discrimination threshold and result in a TTL pulse being counted.

The simplest way to estimate readout efficiency in the absence of a well-characterised thermal neutron flux is to place a detector in a low scatter environment and compare a measured absolute efficiency with a simulated one. That is,

$$E_R = \frac{\varepsilon_{abs,meas}}{\varepsilon_{abs,sim}}$$

Where ε_{abs} is the absolute efficiency of the detector when exposed to a known neutron source.

This technique was used to measure the readout efficiency of the blades by placing all eight into a HDPE moderator that represented one quarter of the NCC (see Section 3). A sketch of the moderator is shown in Figure 5, along with a depiction of the model used. The blades were connected to the Aggregator Unit and the whole detector placed in an outdoor low-scatter environment. A ^{252}Cf neutron source of 5.21ng (± 0.9%) was placed at 8 cm from the centre of the largest face of the detector, as shown in Figure 5.

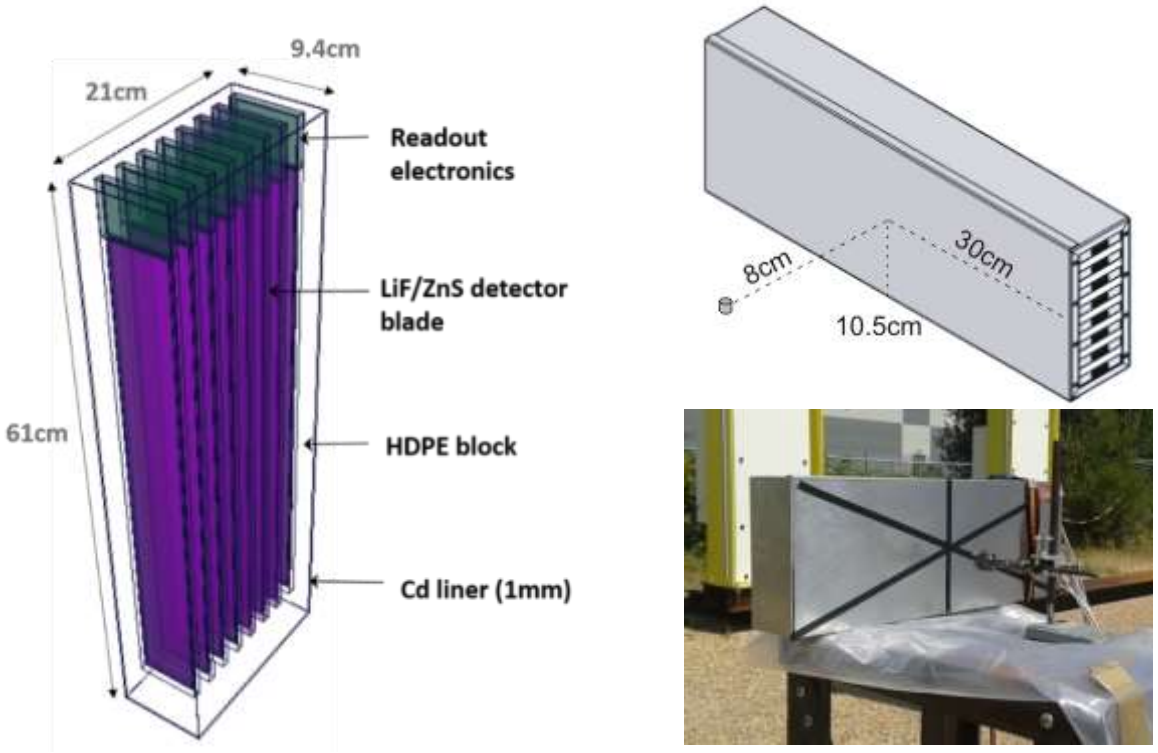

Figure 5: Left: A depiction of the modelled moderator with blades. Right: A sketch of the ^{252}Cf source placement, and a photograph of the measurement configuration.

	Simulated	Measured
Absolute efficiency, ε_{abs}	6.07% ±.09%	5.17% ± 0.17%
Intrinsic efficiency, ε_{int}	21.4%±.09%	18.5%
Readout Efficiency, *RE*	**85.1%±2.9%**	

Table 2: Results of the readout efficiency measurement.

These results show a high readout efficiency of 85.1%, indicating a good optical path between the screens and SiPMs and that the pulse-shape discrimination algorithm performs well at finding neutron events amongst the SiPM noise.

3. Coincidence Counter Design

After having established the functionality of the blade detectors individually and within a slab module (see Figure 5), the next stage in the development consisted of designing and optimizing a full-scale coincidence counter build primarily consisting of four slab modules surrounding an assay chamber of square cross-section, as shown in Figure 6 (left). The modular design will also allow us to configure three modules as a collar for active measurements.

Monte Carlo N-Particle extended (MCNPX) simulations were performed to estimate the detection efficiency and the die-away time of the counter in order to compare to the HLNCC-II. Figure 6 (center) shows the MCNPX model of the counter showing the distribution of up to 32 blades in the HDPE moderating wall of the counter.

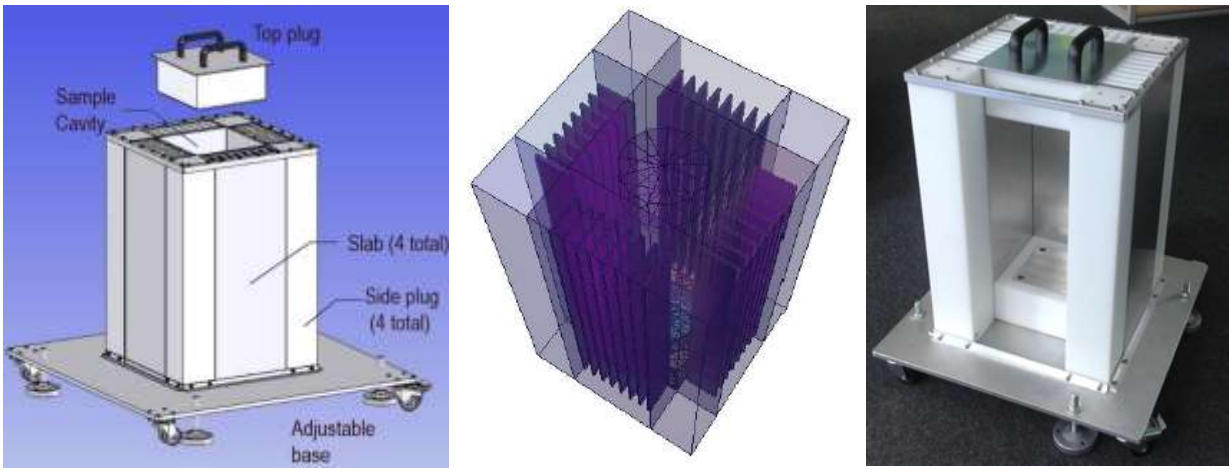

Figure 6: Full-scale NCC build illustration (L), MCNPX model (centre), and built with one slab removed (right)

Each slab module is enveloped in a cadmium sleeve to maintain a low die-away time by minimizing the thermal neutron albedo to the sample chamber. Top and bottom plugs were added comprising HDPE and aluminium neutron reflectors to give a good vertical profile. The design was completed by adding four corner posts of HDPE to increase absolute efficiency, without unduly increasing the die-away time since they are outside of the cadmium liners. The top and bottom plugs as well as the corner posts are visible in the right-hand panel of Figure 6.

The neutron source was simulated as a point isotropic ^{252}Cf in the center of the chamber. The simulated ^{6}Li capture probabilities were multiplied by the measured 85.1% readout efficiency. The die-away time of the counter was obtained using the built-in coincidence capture feature of MCNPX and the sequential gate width method, as well as fitting to the time distribution of the neutron population in the counter. A Figure-of-Merit, FoM, for comparison purposes was quantified as:

$$FoM = \frac{\varepsilon}{\sqrt{\tau}}$$

Where ε is the absolute efficiency and τ is the die-away time.

Figure 7 shows an iso-plot of FoM values for the blade counter design, normalized to the FoM of the HLNCC-II. The efficiency for a fully populated neutron blade coincidence counter (25.4%) is predicted to exceed that of the HLNCC (16.5%), and yet have a lower die-away time of 31μs, resulting in a coincidence counting figure-of-merit (FoM) of 4.56 compared to the 2.54 of the HLNCC-II.

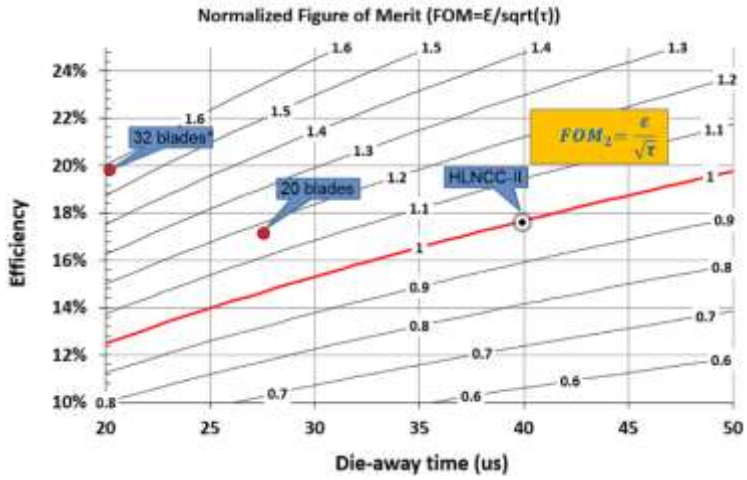

Figure 7: Simulated Figure-of-Merit for NCC compared to FOM of HNLCC-II

4. Experimental Verification

4.1 Counting and Analysis Electronics

During the measurement campaign, the blades were used with the Aggregator Unit which provided power and a logical OR of their output TTLs. As a consequence, the output of the system was a single BNC connector with output pulses of 150ns. The BNC output was connected to a PTR-32 from EK which was used to perform coincidence analysis. The PTR-32 provides the following functions using accompanying software:

- Recording of time interval data for replay and reanalysis
- Plotting of time interval histograms
- Calculation of Rossi-Alpha distributions
- Measurement of coincidence rates using the two-gate R and R+A method

Figure 8 shows a block diagram of the blades, Aggregator Unit and PTR-32.

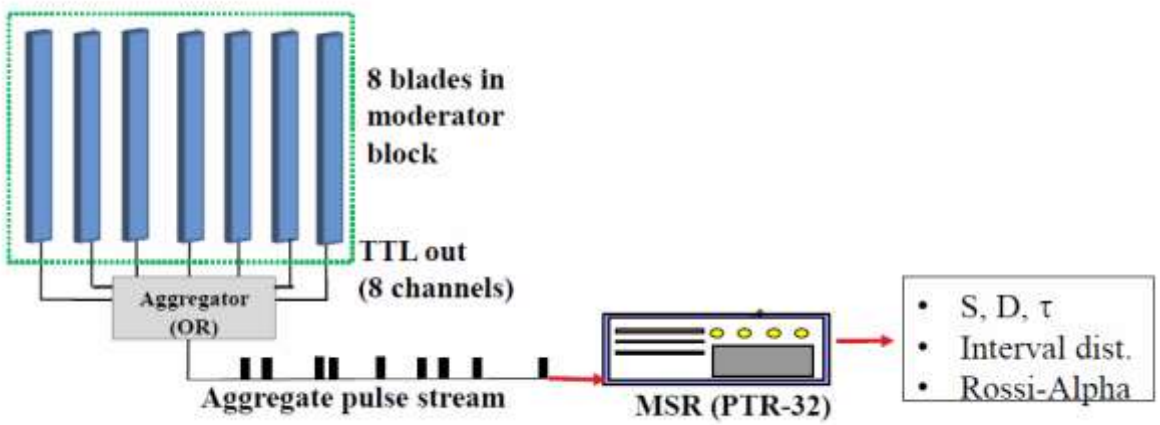

Figure 8: A block diagram showing the signal path used in this study.

4.2 Measurement of Basic Parameters

The NCC with eight blades was assembled in the PERLA laboratory at JRC in Ispra for testing. A number of HDPE “blanks” were manufactured that could be fitted into the spare blade slots to allow for reconfiguration of the NCC. **Error! Reference source not found.** shows the NCC in place with the Aggregator Unit connected to the blades. The blades were inserted with their electronics at the top of the NCC.

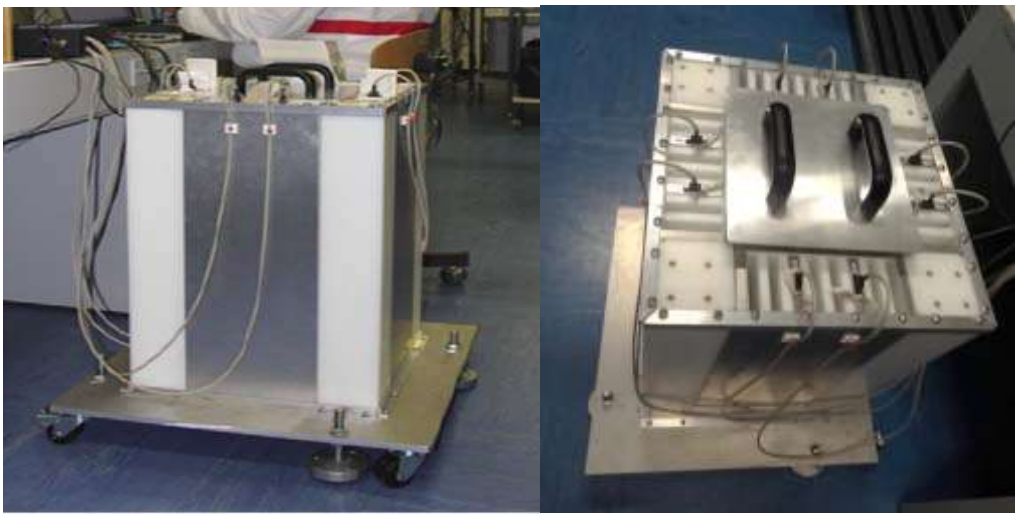

Figure 9: The NCC installed at JRC with eight blades and Aggregator Unit showing.

The basic performance parameters of the partially-populated NCC were measured, namely absolute efficiency and die-away time with ^{252}Cf. This was done with the blades and HDPE blanks in a number of different configurations. Results with these configurations are shown below in Figure 10.

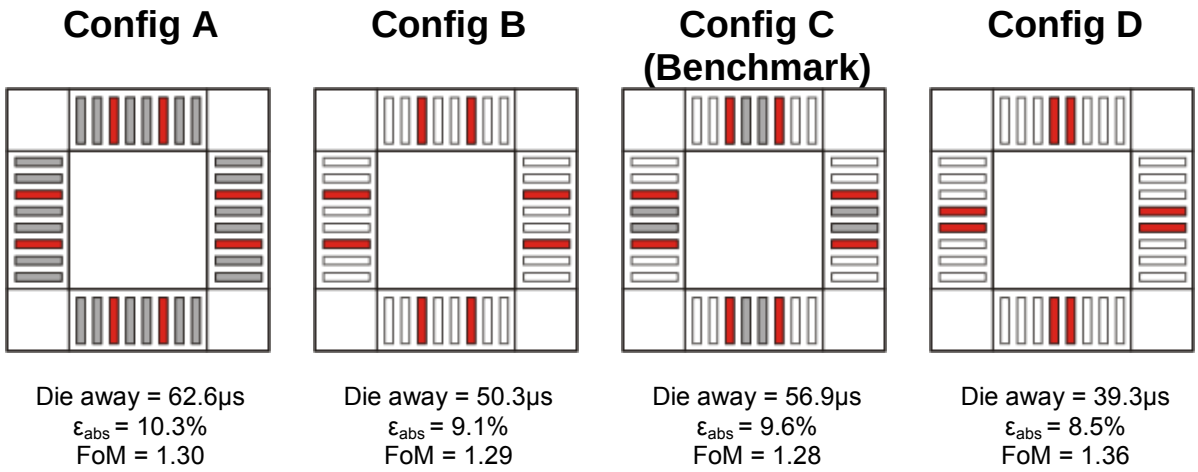

Figure 10: The basic parameters of the NCC as measured with the blades in various configurations. Absolute efficiency and die-away time were measured using ^{252}Cf.

The efficiency achieved here is about half of what is expected of a fully-populated NCC, and varies only slightly with configuration. Clearly with a partially populated system, it is possible to trade off efficiency against die-away time using the HDPE blanks in the unpopulated slots. The presence of blanks has a greater effect on die-away time than on absolute efficiency and the best FoM is achieved by a configuration with the lowest die-away (Configuration D).

The efficiency of the NCC was measured for different neutron sources to understand the effect of neutron energy. Measurements were taken with blades in Configuration D.

Neutron Source and mean energy	Absolute Efficiency
Am-Li (alpha,n), 0.3 MeV	11.1%
Am-Be (alpha,n), 5.0 MeV	5.3%
Cf^{252} (fission), 1 MeV	8.5%
Pu^{240} (fission), 1MeV	9.9%

Table 3: Measured absolute efficiency for a range of neutron sources.

Am-Li clearly gives a very good efficiency due to its low average neutron energy. We can also see that Pu has a significantly higher absolute efficiency than ^{252}Cf. Am-Be has a very low absolute efficiency due to its high energy and the under-moderated nature of the NCC design, intended to keep die-away times to a minimum.

4.2.1 Comparison with Other He^3 Free Systems

The NCC was benchmarked alongside a number of other ^{3}He free systems in October 2014 at JRC [4,5]. Sample results as published are shown below.

	HLNCC-II	PTI	Symetrica (8 blades)	Symetrica (32 blades) (simulated)	GE Reuter Stokes
Technology	^{3}He tubes	Numerous ^{10}B lined straws	^{6}Li loaded blades	^{6}Li loaded blades	Combined ^{10}B and ^{3}He proportional counter
Abs. Eff (%)	16.5	13.6	9.6	25.4	10.2
Die away time (s)	43.3	26	56.9	31.6	65.4
FoM	2.51	2.66	1.28	4.56	1.26

Table 4: Comparative results of three ^{3}He-free technologies and the HLNCC-II taken at JRC in October 2014

The predicted FoM of the fully-populated NCC is very high, exceeding the HLNCC-II by ~80%, driven by a very high absolute efficiency. The results with the partially populated system are encouraging. However, FoM is a limited expression of the quality of a neutron coincidence counter, so further investigation is required to obtain a complete picture of how useful the NCC will be.

5. Characterization of Safeguards Relevant Parameters

5.1 Bias and Timing Characteristics

Bias is a key property of a neutron coincidence counter which is quantifies any processes that produce false coincidences amongst otherwise Poissonian neutron events. For this study, bias was measured for each blade individually and for the NCC as a whole. Am-Li sources were used for their Poissonian neutron output. The individual blade tests were conducted with all eight blades in the NCC with only one connected to the Aggregator Unit at a time. Results were analysed by taking Rossi-Alpha distributions of the recorded pulse trains using the PTR-32 software, and by calculating bias with the equation:

$$Bias\ (\%) = \frac{(R+A)-A}{A} \times 100.$$

Bias measurements were also taken at two count rates separated by an order of magnitude to assess variation with count rate.

5.1.1 Individual Blades

The measured bias differed considerably between blades, with six displaying an average negative bias of -3.5%. The remaining two had an average positive bias of 3.7%. Sample Rossi-Alpha plots shown in Figure 11 and Table 5 shows the results. Pre-delay was set to 15μs and gate width was set to 64μs.

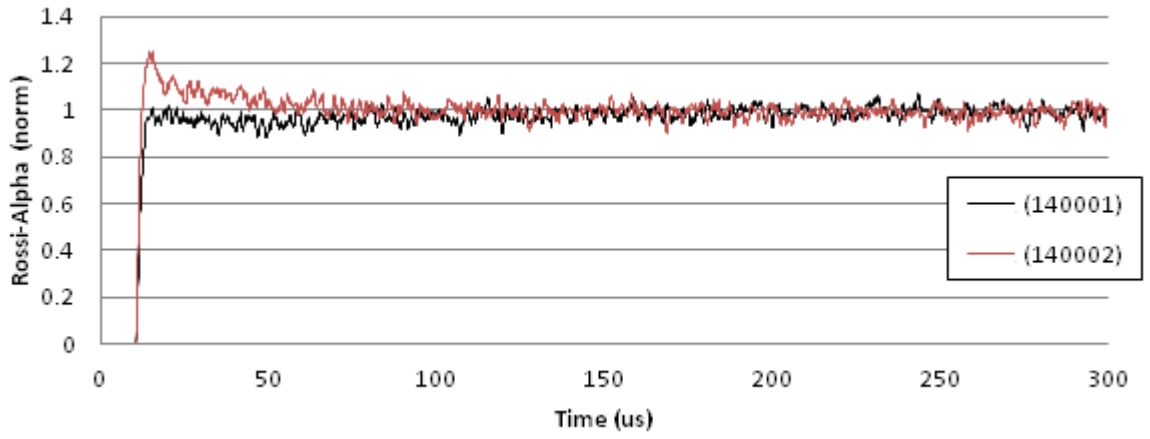

Figure 11: Sample Rossi-Alpha plots with two blades demonstrating the negative bias and positive bias cases. Both are normalised to the average value they settle at beyond 300µs.

The plot above shows the dead time of a blade as being 10µs. This is the processing time of a neutron event, meaning that no two events closer than 10µs can be reported with TTL pulses. Note that this is internal to the blade, so another blade could detect a second neutron immediately after the first.

This sets a limit on pre-delay and therefore forces a lower gate fraction than for a system with a shorter dead time. For the following measurements, pre-delay is set to 15µs to exclude this region.

S/N	140001	140002	140003	140004	140005	140006	140007	140008
Bias (1800cps)	-4.2%	4.9%	-3.4%	-3.7%	-4.8%	2.6%	-2.5%	-2.6%
Bias (13000cps)	-4.0%	1.9%	-2.4%	-3.3%	-3.4%	2.1%	-1.8%	-2.2%

Table 5: Measured bias for each blade using pre-delay = 15µs and gate width = 64µs.

A count rate of 13000cps in a single blade is equivalent to a 58.5ng ^{252}Cf source in the sample chamber.

The range of biases observed is due to two effects: Undershoot in the analogue electronics within the blade, and the long decay components present in ZnS(Ag). The former induces a negative bias due to a negative undershoot in the pre-amplified signal prior to processing. This undershoot follows every neutron event and lasts for up to 150µs, so any subsequent neutron event arriving during that time will appear to the processing electronics to be weaker than it is. This manifests as a temporary reduction in neutron sensitivity following a neutron event, and a negative bias. The extent of the overshoot depends on specific component values in the analogue electronics and variations between blades are due to tolerances.

The effect of the long decay components of ZnS(Ag) is that each neutron event has a long tail that is visible above SiPM noise up to ~100µs after the onset. Subsequent neutron events occurring within that time will be stood on a “pedestal” set by the tail of the first, which increases its signal strength when processed, increasing its chance of passing the discrimination threshold. This manifests as a temporary increase in readout efficiency and thus a positive bias but this effect competes with the negative undershoot. The resultant bias in any given blade is therefore determined by one of these effects dominating the other.

The data appears to show a reduction in bias as count rate increases, whether positive or negative. The mechanism of this requires further study.

5.1.2 Partially Populated NCC

The bias of the NCC with all eight blades was measured with Am-Li sources again at multiple count rates. Blades and HDPE blanks were arranged in Configuration A. Two rates were tested with Am-Li sources to determine whether the total bias changed with count rate. Three different configurations were tested: all blades connected, two positive-bias blades disconnected, two negative-bias blades disconnected.

	All blades	Without positive blades 140002 & 140006	Without negative blades 140004 & 140008
5,000 cps	0.00%	-0.37%	0.00%
14,000 cps	-0.33%	-0.46%	-0.31%
100,000 cps	-0.19%	-0.45%	-0.19%

Table 6: The measured bias of the whole system in three different blade configurations.

We can see that when the whole set of blades is present that the bias is slightly negative and that there is no clear relationship with count rate. Figure 12 shows the normalised Rossi-Alpha plots for the all blades case at the three different count rates. Note how in the region below 10μs the neutron response does not fall to zero, instead falling to 7/8. This is because during that time only the one blade that detected the first neutron is in its dead state and subsequent neutrons can be detected by the other seven blades.

A bias of -0.3% is not considered to be a serious problem since it does not vary with count rate, so it will be accounted for in any plutonium mass measurement calibration (see Section 6).

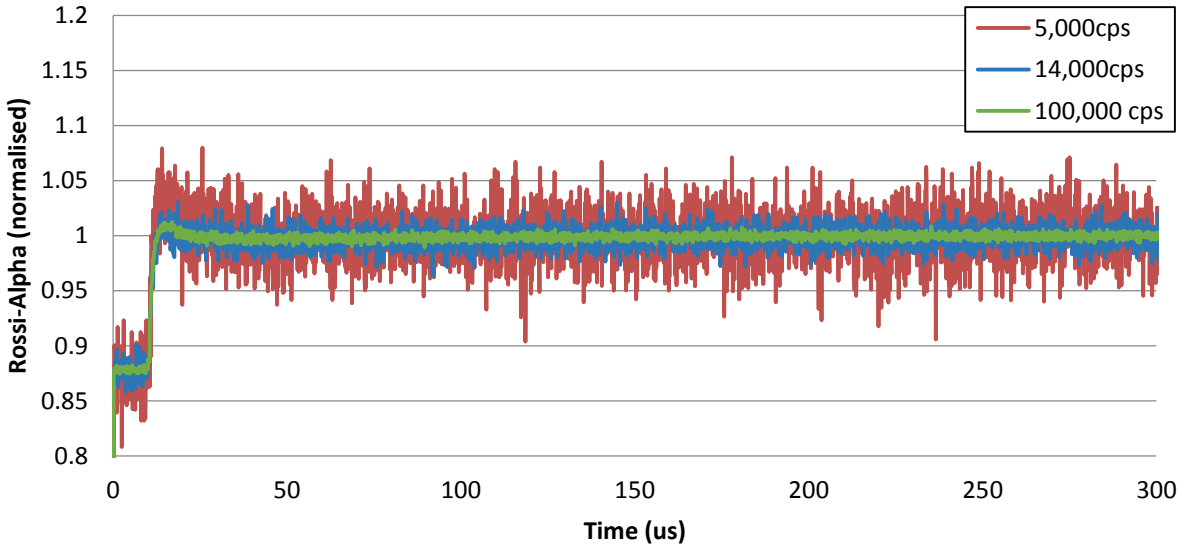

Figure 12: Rossi-Alpha plots taken using all eight blades at three different count rates.

Attempting to achieve zero bias will be a challenge, since whilst the analogue electronics can be changed to remove the overshoot, that will leave a significant positive bias. This is driven by the long decay time of the ZnS(Ag) which presents a fundamental limit unless the scintillator is changed. This is an area of active research, with some focus on so-called “nickel” killed ZnS which suppresses the long pulses. Other effort is focussed on changing the PSD algorithm to better reject the effect of neutron pile-up described above.

5.2 Selection of Operating Parameters

The pre-delay and gate width parameters are important coincidence settings since they determine the measurement performance of the counter, such as the doubles rate counting efficiency, as well as the relative uncertainty and measurement bias in the doubles rates. Post-processing of stored timed interval distributions was done for varying combinations of pre-delay (4.5, 8, 10, 15, 20, 30 μs) and gate width (16, 32, 64, 128μs) to determine the optimal combination that would minimize the measurement bias and the relative uncertainty in doubles rates, while achieving a gate fraction (fraction of coincidence signal measured) comparable to typical ^{3}He systems. For an uncorrelated source such as Am-Li the counting rates in the R+A gate should be equal to that in the A gate. If they are not equal, then there is a measurement bias in the counter, likely due to dead time effects and as well as electronics.

Due to the 10μs processing time in each blade, there is a stronger negative bias in doubles for PD<10μs due to the loss of a fraction of the coincidence signal from same-channel correlations. Figure 13 shows the negative bias as a function of pre-delay and gate width for an intense Am-Be source (singles rate of 81,877 cps). Beyond the dead-time effect (i.e. for PD >10us), the observed bias reduces to and stabilizes to negative 0.2%-0.3%, for all three gate width settings. A pre-delay of at least 10us is recommended in this case to minimize bias effects.

The minimum uncertainty is a shallow, flat response between 64μs and 80μs. This corroborates the standard rule-of-thumb for optimal gate width of 1.257 times the , die-away time (τ)(for an accidentals-dominated thermal system), where, in our case, is τ=56.9μs for the 8-blade system, resulting in an optimal gate width of 71.1μs. The fully-instrumented system is expected to have a shorter die-away time of 31.6μs, so the gate width may be shortened, keeping in mind the effect of the gate width on the gate fraction of the counter. A typical HLNCC-II has a typical gate fraction of 0.696.

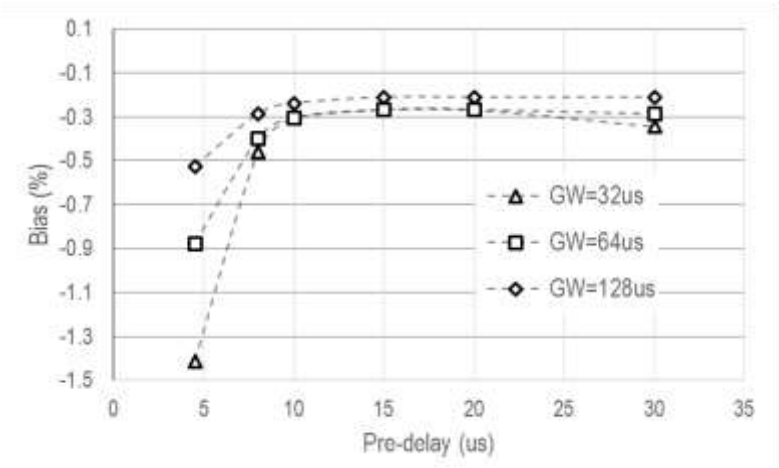

Figure 13: Bias vs pre-delay for fixed gate width values. Am-Li was used in this case.

Figure 14 shows the relative uncertainty in the doubles rate from a ^{252}Cf source vs. gate width for various pre-delay settings.

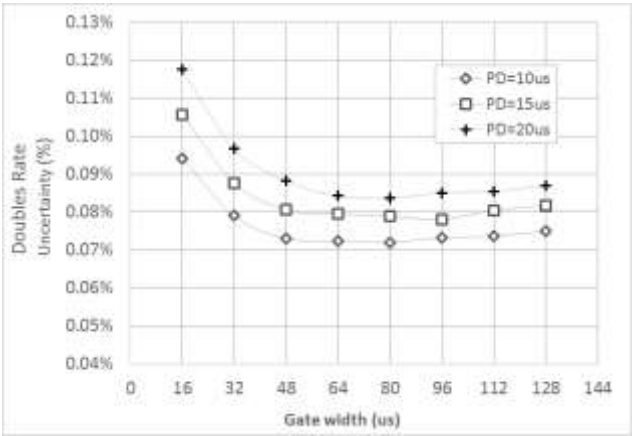

Figure 14: Relative uncertainty in doubles rate vs. gate width

The values in Table 7 show several choices highlighted in blue from our system that meet or exceed this gate fraction for various pre-delay and gate width combinations. There is no optimum single pair of pre-delay and gate width; rather the choice will ultimately depend on sample type and the precision required for the sample type measurement. For high-alpha samples, it is more important to limit the gate width so as to the limit the accidental contributions at the expense of the gate factor. For the purposes of this work, a 10 μs pre-delay and a gate width of 80μs may be used in the analysis, and results in a gate fraction of 0.633. spite the larger pre-delay setting of the ^{6}Li-based counter, gate fractions comparable to the HLNCC-II are achievable.

		8-blades	32-blades
PD	GW	τ=58.9	τ=31.6
10	48	0.478	0.569
10	64	0.566	0.633
10	80	0.633	0.671
10	96	0.684	0.694
8	80	0.656	0.715
8	96	0.708	0.739
7	64	0.597	0.696

Table 7: Gate fractions for pre-delay and gate width combinations. Values with 32 blades are predicted based on the performance measured in Section 4).

5.3 Gamma-Ray Rejection

Gamma-ray rejection tests of the whole system were carried out using ^{137}Cs and ^{241}Am, two isotopes that the NCC will encounter in service. The objective was to quantify whether the calibration of individual blades to a GRR [6] of better than 10^{-7} was sufficient and whether the blades had a response to the low energy gamma-rays from ^{241}Am.

5.3.1 ^{137}Cs Response

The ^{137}Cs response was tested by placing combinations of ^{137}Cs sources and ^{252}Cf sources into the sample chamber and measuring the total count rate and the doubles count rate. The background-subtracted total count rate when exposed to just ^{137}Cs gives the gamma-ray rejection of the system. Comparing the measured total count rate and doubles rate with ^{252}Cf with and without ^{137}Cs exposure gives the practical effect of that GRR on coincidence measurements.

GRR is calculated as: $$GRR = \frac{CR - Background}{A \cdot BR \cdot \Omega / 4\pi}$$

Where CR is the measured total rate with ^{137}Cs, A is the source activity in Bq, BR is the branching ratio of the 662keV line (0.85) and Ω is the solid angle subtended by the detector. In this case Ω = 4π.

We have also measured GARRn (gamma absolute rejection ration (neutrons)) which quantifies any change in neutron efficiency due to gamma-ray exposure. It is calculated as:

$$GARRn = \frac{\varepsilon_{abs\ neutron}}{\varepsilon_{abs\ neutron+gamma}}.$$

In this system, it quantifies the effect of gamma-rays piling up with weaker neutron events in a blade to increase the readout efficiency. In all cases, the sources were placed in the centre of the cavity and the eight blades were distributed evenly about the counter in Configuration D. Pre-delay was set to 15μs and gate width was set to 128μs. Table 8 shows the results of these measurements.

Gamma-ray source	Neutron Source	Excess counts due to Cs above background	Change in total rate due to Cs (GARRn)	Doubles rate (Cf only)	Doubles rate (Cf + Cs)
^{137}Cs (3.7MBq)	^{252}Cf	Not measured	+0.28%	105.25 ± 1.25 cps	105.06 ± 1.25 cps (-0.2%)
^{137}Cs (7.4MBq)	^{252}Cf	0.21 cps GRR = 3.3 x 10^{-8}	+0.48%	105.25 ± 1.25 cps	107.7 ± 1.26 cps (+2.3%)
^{137}Cs (370MBq)	^{252}Cf	0.37 cps GRR = 2.1 x 10^{-9}	+0.83%	125.52 ± 1.38 cps	129.07 ± 1.39 cps (+2.8%)

Table 8: Results of measurements with ^{137}Cs and ^{252}Cf. Quoted uncertainties are at the 1σ level.

We can see that the GRR of the whole system is very low over a broad range of ^{137}Cs activities, never exceeding 10^{-7}. This implies that there is no significant pile-up of gamma-rays in the neutron detector blades.

We can also see that GARRn reaches up to 0.83% when ^{137}Cs during high doses, which is still quite low. It is believed that gamma-rays are adding to the signal of weaker neutron events, causing them to meet the detection threshold. Therefore, this GARRn would quantify an increase in readout efficiency due to neutron-gamma pile-up. More significantly to coincidence counting, we can see that the doubles count rate increases by up to +2.8% against a 1σ uncertainty of ±1.7%. This means that very strong gamma-ray exposure can induce a positive bias in the NCC. Further characterisation of the system is needed to quantify this relationship so that a correction factor with dose can be calculated. Otherwise, the gamma-ray rejection can be improved further by adjusting the neutron detection threshold at the expense of absolute efficiency.

5.3.2 ^{241}Am Response

The response to ^{241}Am was measured using an Am-Li source and an Am-Be source. In both cases, the source was placed at the centre of the cavity, and the total count rate, doubles rate and bias recorded. This was done both with and without a 3mm lead shield. Comparing results gives the response of the system to ^{241}Am gamma-rays. Pre-delay was set to 15μs and gate width was set to 128μs.

		Am-Li (S/N 252)	Am-Be (S/N 307)
Total count rate	Shield on	12343.1 ± 4.5 cps	81877.2 ± 11.7 cps
	Shield off	12457.3 ± 8.0 cps	81843.4 ± 11.7 cps
Change due to Am exposure =		+1.65%	-0.48%
Doubles rate	Shield on	-58.7 ± 7.9 cps	-1794.7 ± 48.3 cps
	Shield off	-59.7 ± 8.0 cps	-1881.4 ± 48.0 cps
Change due to Am exposure =		+1.62%	+4.83%
Bias	Shield on	-0.32%	-0.21%
	Shield off	-0.31%	-0.22%

Table 9: Results of measurements with Am-Li and Am-Be

Table 9 show that ultimately the bias in the detector does not vary with ^{241}Am gamma-ray exposure, even though there are variations in the measured total count rate and doubles rate.

In the case of Am-Li removing the shield causes a slight increase in totals rate, which is reflected in the slight reduction in negative bias. There is no statistically significant change in the doubles rate. This implies that the blades are sensitive to Am^{241} gamma-rays and that there is a need to either recalibrate the blades to improve gamma-ray rejection or to add a liner to the sample cavity. The Am-Be case is different in that the singles rate does not change much when ^{241}Am gamma-rays are introduced. We also observe a noticeable decrease in the negative doubles rate when the shield is introduced. This is to be investigated further.

5.4 Absolute Efficiency Profile

The absolute efficiency of the NCC was profiled in two sets of measurements. The first was a vertical line up the centre of the cavity, and the second was a grid of points in a horizontal plane at the mid-height of the cavity. In all positions a pre-delay of 15μs and a gate width of 64μs. The blades and HDPE blanks were arranged in Configuration C. In all cases, a bare ^{252}Cf source of 25.5ng (59000 n/s) was used.

5.4.1 Vertical Profile

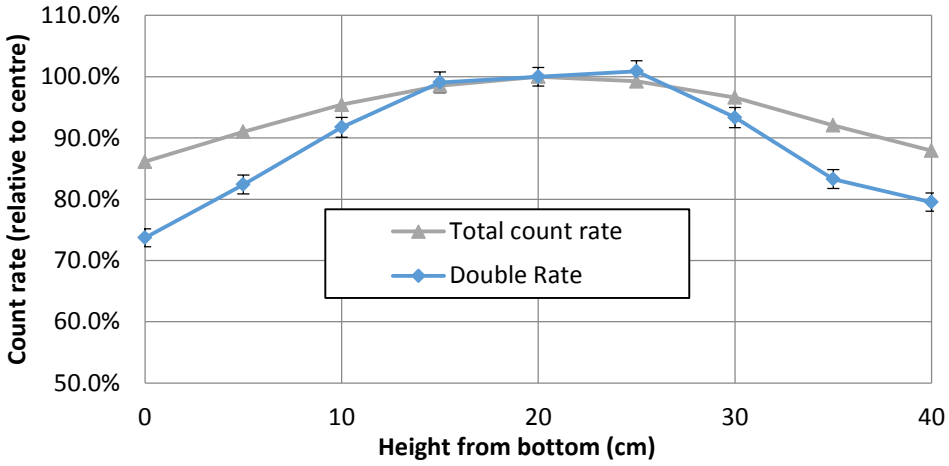

Figure 15: Plots of how the total count rate and doubles rate vary with vertical position.

The vertical profile plot shows that the absolute efficiency varies quite strongly with vertical position and that the doubles rate drops to as much as 73% that at the centre. This is consistent with the square of the drop in absolute efficiency indicating that the absolute efficiency profile dominates the doubles rate profile and there are no significant effects due to gate fraction. This can be confirmed by Figure 16 which shows the measured die-away time as a function of vertical position. It is quite consistent and appears to be slightly lower at the extremes, so the gate fraction would not reduce at those points.

Absolute efficiency is lower at the bottom of the chamber indicating that perhaps the blades have lower sensitivity at their ends, warranting further investigation. Until this problem is resolved, testing will be limited to the centre of the sample cavity, and as it stands, the NCC is unsuitable for measuring extended sources.

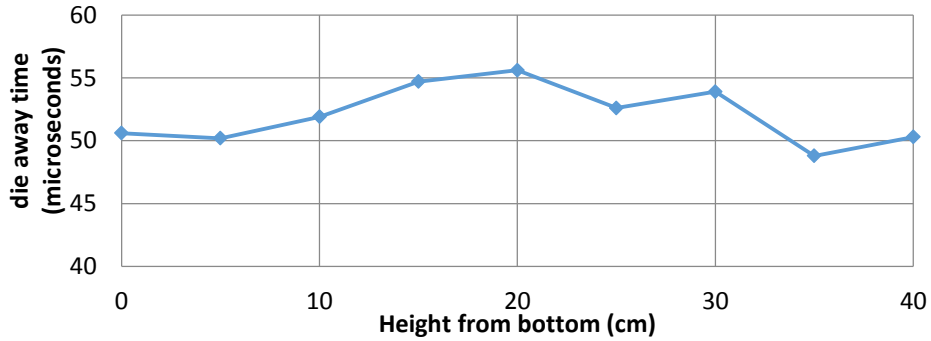

Figure 16: Die-away time as a function of vertical position. 20cm represents the centre of the sample cavity.

5.4.2 Horizontal Profile

Measurements of absolute efficiency, doubles rate and die-away time were taken over a horizontal plane at the mid-height of the sample cavity. Results are shown in Figure 17 and Figure 18, expressed as values relative to the centre position.

It is clear that with the blades and HDPE blanks in Configuration C, the NCC exhibits poor horizontal uniformity, with clear peaks at the sides and nadirs and the corners. This is explained by the concentration of blades and extra HDPE in the middle of the slabs, and away from the corners of the NCC.

The doubles rate shows a great non-uniformity that follows the same pattern as the total count rate, as expected. As in the vertical profile case, the measured non-uniformity of the doubles rate agrees well with the square of the non-uniformity in totals count rate. This implies that the gate fraction does not significantly vary over the horizontal plane, which would otherwise cause the doubles rate to vary independently of the total count rate.

Totals rate	X = -8.0	-7.5	-5.7	-4.0	-2.8	0.0	2.8	4.0	5.7	7.5	X = 8.0
Y = -8.0						105%					
-7.5		96%								97%	
-5.7			100%						101%		
-4.0						100%					
-2.8					100%		101%				
0.0	107%			101%		100%		102%			108%
2.8					101%		101%				
4.0						102%					
5.7			101%						102%		
7.5		98%								98%	
Y = 8.0						108%					

Figure 17: A plot of how the total count rate varies over the horizontal plane relative to the central position.

Doubles rate	X = -8.0	-7.5	-5.7	-4.0	-2.8	0.0	2.8	4.0	5.7	7.5	X = 8.0
Y = -8.0						114%					
-7.5		91%								96%	
-5.7			100%						101%		
-4.0						105%					
-2.8					101%		102%				
0.0	113%			99%		100%		103%			118%
2.8					103%		105%				
4.0						103%					
5.7			104%						104%		
7.5		96%								99%	
Y = 8.0						120%					

Figure 18: A plot of how the measured doubles rate varied over the horizontal plane. All values are given relative to the central position. Pre-delay was set to 15μs and gate width was set to 64μs.

There appears to be a bias towards higher total count rate and doubles rate in the +X and +Y directions. Such observations can be explained by the fact that the measurements were not taken in a low-scatter environment. In both the +X and +Y directions scattering material was present which would return partially moderated neutrons above the cadmium cut-off energy which would then thermalise inside the NCC.

6. Assay of Pu samples - give comparative results with known samples compared to HLNCC-II-II.

The final performance parameter of interest, and one that relies on those explored above, is the linearity of the NCC plutonium mass calibration function. To measure this, a number of plutonium-gallium (Pu-Ga) samples were tested at JRC. They were all taken from the same series and this have the same isotopic composition, shown in Table 10. The samples were thin disks and were placed at the centre of the sample cavity on aluminium stands.

Isotope	Iso.Compo. wt %	rsd %	Specific Power mW/g (error)	Half Life (y)
Pu-238	0.1336	0.04	567.57 (0.26)	87.74
Pu-239	75.6606	0.03	1.9288 (0.0003)	24119
Pu-240	21.4898	0.07	7.0824 (0.002	6564
Pu-241	1.9510	0.93	3.412 (0.002)	14.348
Pu-242	0.7651	0.38	0.1159 (0.0003)	376300
Am-241	1.86	0.02	114.2 (0.42)	433.6

Table 10: The isotopic composition of the Pu-Ga samples tested here.

Analysis was carried out using the PTR-32 and INCC software to extract the effective plutonium mass. As according to the analysis in Section 5.2, the pre-delay was set to 10μs and the gate width was set to 80μs. Figure 19 shows the results in terms of doubles rate as a function of known plutonium mass.

The NCC was set up in Configuration C with two blades and two blanks per module. For comparison, the same plutonium samples were measure by an HLNCC-II also at JRC Ispra.

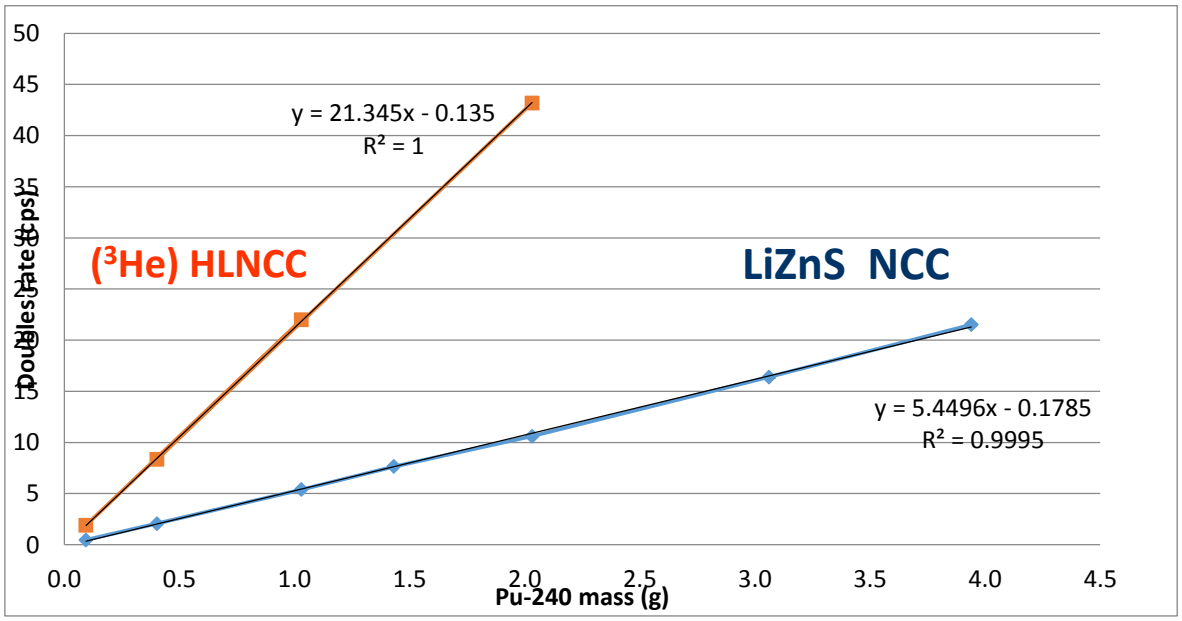

Figure 19: A plot of doubles rate as a function of Pu mass for the partially populated NCC and an HLNCC-II.

We can see a linear relationship between plutonium mass and measured doubles rate. The linear fit shows a negative intercept, which reflects the negative bias measured in this NCC. The HLNCC-II shows a far greater gradient due to its higher efficiency (16.5% vs 9%), and a much smaller negative intercept since it has nearly zero bias.

7. Conclusion

A prototype NCC was designed and tested in a partially populated configuration against a benchmark set by a JCC-31. The results of that testing were then used to predict the performance of a fully-populated NCC with encouraging results. In summary, our findings were:

- The readout efficiency of the blades is high at 85.1% and their gamma-ray rejection is excellent.
- The FoM of the partially-populated NCC is lower than the JCC-31 at ~1.3 depending on configuration, but this is sufficient to obtain good data.
- The gamma-ray rejection of the whole NCC is good but it shows a slight sensitivity to very high gamma-ray fluxes due to neutron-gamma pile-up
- The NCC shows a negative bias of -0.3% due to the analogue electronics in the blade. This can be developed further but achieving zero bias is limited by the length of the ZnS(Ag) scintillation pulse.
- The profile of the partially-populated NCC is poor. Whilst this is expected in the horizontal plane, it was not in the vertical plane. This restricts plutonium mass measurements to point sources at the centre f the cavity.
- Plutonium mass measurements show a very linear relationship.

This performance is deemed to be very good in a prototype though some work remains to solve the problems that have been highlighted.

8. Future Work

Now that a reduced version of a neutron coincidence counter has been characterized and calibrated, further work can be considered.

Firstly, the counter will be fully instrumented with 32 blades and then characterized and calibrated in the same way. Furthermore, recent improvements in SiPM technology will be incorporated in those blades to improve dead time and thermal neutron detection efficiency further. The optical design of the blades will be investigated to quantify any loss of readout efficiency along their length.

Other coincidence counter geometries can be explored which are predicted to offer better absolute efficiency profiles, especially in the vertical plane. Another improvement to the coincidence counter will be the addition of a low-Z liner to aid in rejection of low energy gamma-rays.

The positive bias induced by the long decay time of the ZnS(Ag) scintillator will be addressed by investigating alternative scintillators such as ZnS(Ag,Ni) or “nickel killed” ZnS which shows suppression of the long components. Another avenue of research is changing the PSD algorithm to better detect the strength of the tail and remove it from the measurement of neutron event strength, to remove this effect.

A range of high-rate samples will be tested to provide empirical data of the systems dead time behavior. This data will be used to compute a correction matrix.

On the broader scale, the modules developed for this counter can be used in an active system as an UNCL. The blades are also suitable for development of a module for multiplicity counters such as the ENMC, especially if their dead time can be reduced to exploit the low die-away times of such systems. If not, then any ENMC can be expected to contain a very high number of blades (~200) so the step due to dead time will only introduce a bias of -0.5%.

9. Acknowledgements

The authors would like to thank DG-ENER for supporting the project. We also thank the staff at JRC Ispra for their ready assistance in taking measurements, and the engineers at Symetrica Security for their excellent work in producing the system itself.

10. Legal matters

10.1 Privacy regulations and protection of personal data

The authors agree that ESARDA may print their names/contact data/photograph/article in the ESARDA Bulletin/Symposium proceedings or any other ESARDA publications and when necessary for any other purposes connected with ESARDA activities.

10.2 Copyright

The authors agree that submission of an article automatically authorise ESARDA to publish the work/article in whole or in part in all ESARDA publications – the bulletin, meeting proceedings, and on the website.

The authors declare that their work/article is original and not a violation or infringement of any existing copyright.

11. References

[1] Menlove HO, Krick, M. (1979). The High-Level Neutron Coincidence Counter (HLNCC): User's Manual. Report LA-7779-M. Los Alamos, NM: Los Alamos National Laboratory.

[2] Kouzes RT. 2009. The ^{3}He Supply Problem. Technical Report PNNL-18388, Pacific Northwest National Laboratory, Richland, WA.

[3] G. Dermody, A Scalable 3He---free neutron detector for multiple applications. Presentation at the ESARDA Novel Approaches/Novel Technologies Working Group workshop held in Oxford in March 2014

[4] Current Status of ^{3}He Alternative Technologies for Nuclear Safeguards, international measurement campaign and workshop on He3 alternatives for safeguards, at the JRC in Ispra October 2014, within a DOE-Euratom Action Sheet 47. Report LA-UR-15-21201 Ver. 2 , 2015

[5] P. Peerani, C. Carrapico, B. Pedersen, V. Forcina, F. Rosas, A. Rosite, H. Tagziria, A. Tomanin, Workshop on He-3 alternatives for safeguards applications, presented at the 37th ESARDA symposium in Manchester May 2015

[6] Kouzes RT, JH Ely, AT Lintereur, EK Mace, DL Stephens, ML Woodring. 2011. Neutron detection gamma ray sensitivity criteria. NIM A 654 (2011) 412–416.

A prototype BF3 based neutron multiplicity counter for nuclear safeguards

Bent Pedersen[1], Jean-Michel Crochemore[1], Marita Mosconi[1], Valeriy Mayorov[1], Hamid T agziria[1], Aharon Ocherashvili[2], Eric Roesgen[1], Peter Schwalbach[3]

[1]Institute for Transuranium Elements (ITU)
Joint Research Centre, European Commission
Via E. Fermi 2749, Ispra 21027 (VA), Italy
bent.pedersen@jrc.ec.europa.eu

[2]Physics Department
Nuclear Research Center Negev
P.O. Box 9001, 84190 Beer-Sheva, Israel

[3]European Commission, DG-ENER, Nuclear Safeguards - Unit E1, Section Measurement Systems, On Site Laboratories, Cooperation Programmes, EUFO 3477, L-2557 Luxemburg

Abstract:
Neutron coincidence counting and neutron multiplicity counting are standard techniques for mass determination of fissile materials in nuclear safeguards applications. Traditionally the preferred neutron detector design incorporates ^{3}He gas proportional counters in a cylindrical polyethylene moderator block with a central sample cavity. The detector tubes are embedded in the polyethylene in a ring shape approximating a 4π geometry. This standard layout has been adopted in several detector designs such as the High Level Neutron Coincidence Counter (HLNCC-II).

The recent worldwide shortage of ^{3}He gas has prompted research into alternative detection technologies for neutrons. An obvious candidate from a physics point of view is ^{10}B due to the high thermal neutron cross section and the inexpensive enrichment process of the ^{10}B isotope. An important advantage includes the fact that when in form of boron trifluoride gas this neutron detector the can replace ^{3}He gas tubes while maintaining other standard counter materials, the well counter design, and even the detector electronics. The toxicity of the BF_3 gas however has been mentioned as a potential problem for using this neutron detector is large size neutron coincidence or multiplicity counters in nuclear facilities.

The paper describes design elements the newly developed prototype well counter based on BF_3 detector tubes including a discussion of results of test bed experiments and Monte Carlo simulations carried out to reach the final design. A prototype detector based on this design is currently under construction. This detector will have same cavity dimensions as the standard HLNCC but with neutron detection efficiency high enough to allow neutron multiplicity counting in practical applications. The paper also discusses how the issue of the toxicity of the gas has been addressed in the design of the new counter.

Keywords: nuclear safeguards, neutron multiplicity counter, alternative to 3He, boron trifluoride

1 Introduction

Neutron coincidence counting and neutron multiplicity counting are standard techniques for mass determination of fissile materials in nuclear safeguards applications. The preferred neutron detector layout incorporates ^{3}He gas proportional counters in a cylindrical polyethylene moderator block with a central sample cavity. The detector tubes are embedded in the polyethylene approximating a 4π geometry. This standard layout has been adopted in several detector designs such as the High Level Neutron Coincidence Counter (HLNCC-II) [1].

The recent worldwide shortage of ^{3}He gas has prompted research into alternative detection technologies for neutrons. An obvious candidate from a physics point of view is ^{10}B due to the high thermal neutron cross section and the inexpensive enrichment process of the ^{10}B isotope. Gas proportional counters based on boron trifluoride gas (BF_3) enriched in the ^{10}B component have been used as over the last fifty years as thermal neutron detectors. Applications are wide ranging from reactor instrumentation to survey meters. In relation to well counters as used in nuclear safeguards, an important advantage includes the fact that boron trifluoride gas as a neutron detector the can replace ^{3}He gas tubes while maintaining other standard counter materials, the well counter design, and even the detector electronics.

The obvious advantages of BF_3 gas proportional counters include the high capture cross section for ^{10}B, the high Q value for the (n, α) reaction in ^{10}B, and consequently the good γ/n discrimination capabilities, the uniformity of detection efficiency in extended detectors . Finally the relatively low price of BF_3 gas, even when enrich in ^{10}B to 99%, is an important factor. Disadvantages include the loss of pulse linearity at higher gas pressures, and perhaps most importantly the toxicity of BF_3 gas. The toxicity of the BF_3 gas has been mentioned as a potential problem for using this neutron detector in large size neutron coincidence or multiplicity counters in nuclear facilities.

2 Experimental comparison of boron based proportional counters

Due to the potential advantages (mentioned above) of using boron based detectors as alternative to ^{3}He, we decided to investigate the feasibility of building a complete HLNCC type instrument based on such counters. The premise was to design and build a prototype well type neutron counter with sample cavity of same size as the HLNCC-II, neutron detection efficiency sufficiently high to allow neutron multiplicity counting. The prototype detector was named Boron Based Neutron Correlation Counter (BBNCC).

The design process included experimental comparison of single boron based detectors in polyethylene in our detector test bed, and comparison of measured and Monte Carlo calculated neutron efficiency and die-away parameters of the test bed detector configurations. All Monte Carlo calculations were performed with MCNP [2].

Based on the simulations of the simple test bed configurations, the various detector configurations of the prototype BBNCC detector were compared in MCNP simulations. The test bed experiments included both BF_3 gas detectors and ^{10}B lined proportional counters. The BF_3 gas detectors were both one-inch and two-inch diameter types, and of various gas pressures. The ^{10}B lined detectors were of 2 and 2½ inch diameter. In principle the ^{10}B lined detectors can achieve a higher neutron detection probability due to a potentially higher loading of boron when in solid form.

The detector modules of the test bed can accommodate a single neutron detector in a central channel. The width of the modules is 300 mm which is sufficient for making the detector comparison independent of the module width. The thickness of the modules was variable to allow for optimization of moderator thickness for the various detector diameters. The thickness of the HDPE modules was variable in steps of 10 mm. All module surfaces were covered in a cadmium liner. When possible, same pre-amplifier and amplifier settings were applied.

For comparison neutron detection efficiency of detectors, the distance from the ^{252}Cf source to the centre of the detector was kept constant irrespective of the thickness of the moderator. All measurements were compared to a module with a standard 4 bar, one-inch diameter ^{3}He proportional counter.

Parameters such as γ/n discrimination, die-away time, detection efficiency were compared for all detectors at certain moderator thicknesses. A full report of these measurements is currently in elaboration [3]. Figure 1 shows the test bed including four vertical one-metre long moderator modules at same distance to the central source holder.

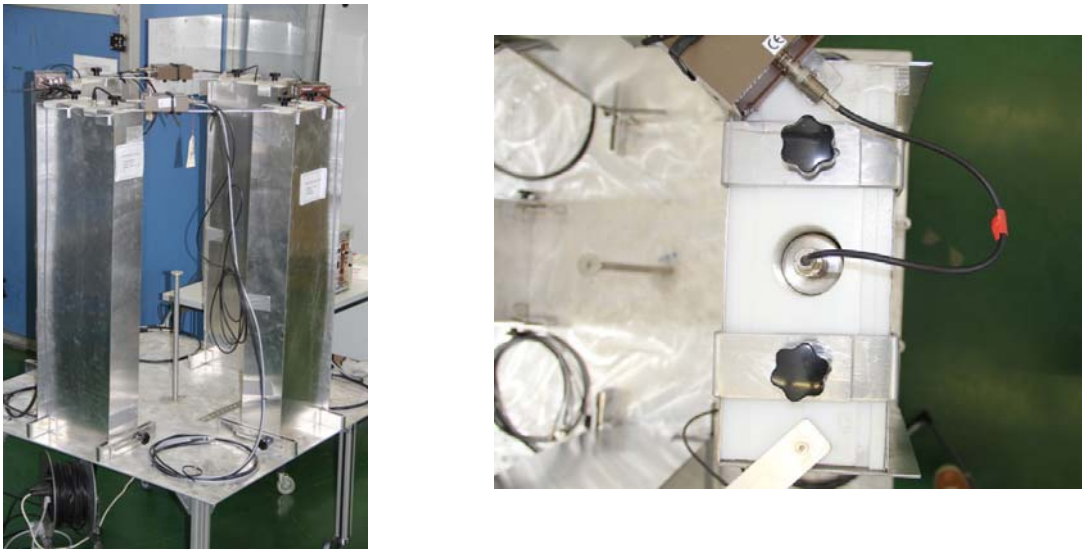

Figure 1. JRC test bed (side and top view) for gas proportional counters with variable poly thickness, various detector diameters, ^{3}He, BF_3 of various pressures, ^{10}B-lined detectors.

The outcome of the test bed measurements favoured BF_3 gas over the ^{10}B lined detectors mainly due to the superior γ/n discrimination, and two-inch detectors rather than one-inch to achieve a sufficiently high neutron detection efficiency. The gas pressure of the BF_3 detectors was found to be not critical for the γ/n discrimination as along as the pressure remained below one bar. The higher pressure however meant a high voltage well above 2 kV.

One encouraging observation from the measurements of one-inch tubes of BF_3 gas was that at optimal thickness (with respect to neutron detection efficiency) of the polyethylene moderator, the tube of 0.92 bar BF_3 had detection efficiency of 0.42 relative to the 4 bar ^{3}He tube. This ratio is far better than expected when considering only the pressure ratios and the reaction cross section ratios of the two tubes. The result indicates that the gas volume is better utilized for the "thinner" ^{10}B gas compared the "denser" ^{3}He gas for thermal neutrons.

Figure 2 gives a summary of test bed measurements of die-away time and relative efficiency of some of the detectors at the moderator thickness of 80 mm and at the "efficiency optimized" thickness for the given detector.

Detector	^{3}He, 1 inch 4 bar (3He) +1 bar (Ar)	BF_3 gas 1 inch 700 mmHg	BF_3 gas 2 inch 700 mmHg	^{10}B-lined 2 inch 9 tubelets	^{10}B-lined 2½ inch 14 tubelets
Die away time	35.8 ± 1.8 μs @ 80mm	99.0 ± 6.8 μs @ 80mm	74.1 ± 0.4 μs @ 80mm	76.2 ± 2.9 μs @ 80mm	86.2 ± 2.0 μs @ 80mm
Die away time	85.7 ± 0.5 μs @ 120mm	122.8 ± 2.2 μs @ 120mm	76.0 ± 0.4 μs @ 120mm	89.6 ± 2.8 μs @ 120mm	102.4 ± 1.8 μs @ 120mm
Max relative efficiency	1 @ 120mm	0.419 @ 120mm	1.026 @ 120mm	0.349 @ 140mm	0.527 @ 160mm

Figure 2. Measurement of single detectors in the test bed using a small ^{252}Cf neutron source, "@ xx" indicates the thickness of the polyethylene module, Cd liner applied on all external surfaces.

Changing to boron based gas detectors has an adverse effect on the die away time. Compared to ^{3}He the boron based detectors show longer die away time either because of the thinner absorber (one-inch tubes) or because of the larger detector volume (two-inch tubes).

Generally speaking when using polyethylene moderated low pressure BF_3 gas in two-inch tubes rather than high pressure ^{3}He gas in one-inch tubes, the value of the die away time will increase both because of the lower absorption per gas volume and because of the larger detector volume. This

means that a BF_3 based system of comparable detection efficiency will always have a larger die away time compared to a ^3He based system.

Both experiments and Monte Carlo calculations confirmed that when using two-inch detectors the benefits in efficiency however outweigh the disadvantage in the increased die away time. The BF_3 gas detector of two-inch diameter in Figure 2 was selected in the final design of the BBNCC counter.

2.1 BF_3 Based Neutron Correlation Counter (BBNCC)

The initial design calculations using MCNP included a variety of detector configurations of both one-inch and two-inch configurations. For example a sandwich type of configuration where the polyethylene moderator was arranged inner and outer ring surrounding the dense array of detectors was tried in the attempt to bring down the die away time by means of reducing the volume of moderator. This however had the consequence of low detection efficiency due to poor utilization of the detector volume. This kind of simulations confirmed that indeed the best usage of the detector volume is in a two-ring configuration with equal number of detectors in each ring (for the cases where the detector volume is so large that a single ring configuration cannot be achieved). Design parameters such as inner ring radius, outer ring radius, external radius, top/bottom plug design were optimized using the standard FOM ($\varepsilon/\sqrt{\tau}$) in the Monte Carlo calculations. Figure 3 shows some of the calculated efficiencies as function of the inner and outer ring radius.

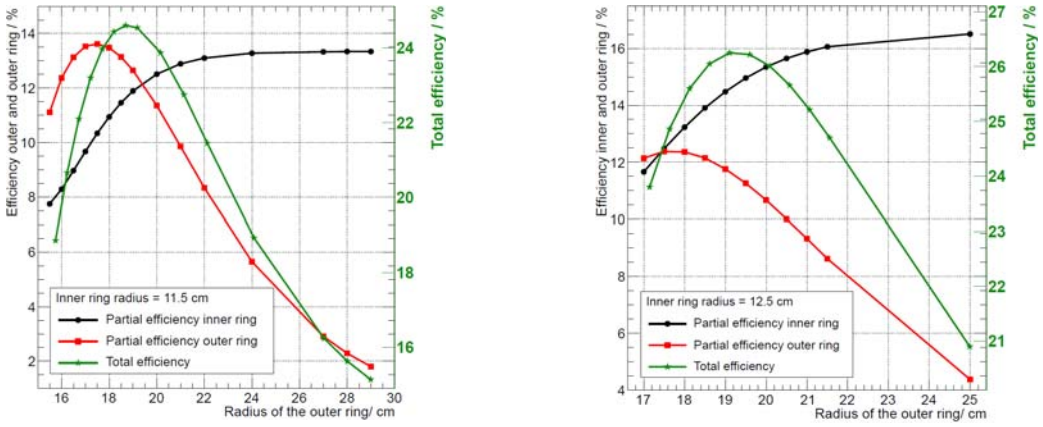

Figure 3. Example of data from the MCNP optimization of inner and outer ring positions, 12 BF_3 two-inch tubes in each ring.

2.2 Final design of BF_3 Based Neutron Correlation Counter (BBNCC)

The final configuration of the BBNCC counter based on the Monte Carlo calculations is shown in Figure 4 from the MCNP input file. The active length of the detector tubes is 50% more than in the HLNCC-II. The number of detectors is 24 compared to 18 in the HLNCC-II. The greater detector length combined with the top and bottom plug makes the axial efficiently profile slightly better than the HLNCC-II over the same sample volume.

The MCNP calculations for a neutron source produced in a bulk Pu sample in a stainless steel containment resulted in the following values for the detection efficiency and die away time: about 25.0 % and 73.70 μs, respectively.

The BBNCC detector is both wider and taller than the standard HLNCC-II. A sealed junction box is included, as well as a base plate with four wheels. The total height of the instrument is 1150 mm.

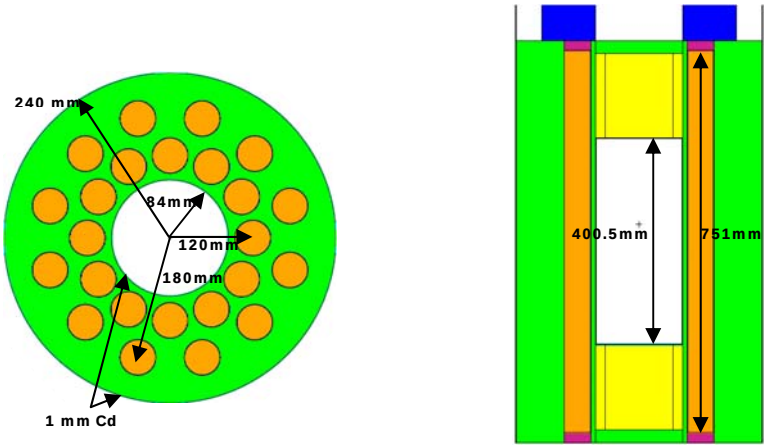

Figure 4. Final configuration of the BBNCC well counter based on MCNP calculations and measurements of single detectors in the test bed.

3 Toxicity of BF3 gas

Boron trifluoride, with the unique shipping identification number UN1008, has a Hazard Class Number of 2.3 indicating the substance to be a toxic gas. In earlier yeas transportation of the gas by public means was prohibited. Since 1 January 2013 however the International Aviation Transport Association (IATA) has relaxed transportation regulations of BF_3 gas. The standing IATA Special Provision A190 applies to BF_3 neutron detectors containing less then 12.8 grams of BF_3 and filled to a pressure of no more than 105 kPa at 20 degrees C. In addition, radiation detection systems, such as radiation portal monitors, containing up to 51.2 grams of BF_3 may be shipped under the special provision.

The BBNCC counter as in the design described above uses detectors containing approximately 2.1 grams of BF_3 gas at a pressure below one bar. The number of detectors is 24 bringing the total amount of gas to about 50.4 grams. As such the BBNCC detection system falls within the scope of the IATA special provision allowing transportation by public means such as world-wide cargo aircrafts, but also by ocean vessels, rail and road shipment.

In a recent reply to a report on alternatives to ^{3}He for neutron detectors [4], the NNSA suggested that perhaps the boron trifluoride gas has not been accurately valuated as an alternative to ^{3}He, considering, among other facts, that less than atmospheric pressure in the detectors has a mitigating effect of a leak.

In the design of the BBNCC the issue of toxicity has been addressed by incorporating an additional air tight barrier towards the environment. This is done by sealing the channels for the detectors tubes and the electronics junction box. In this way the detector channels and the (sealed) junction box constitutes an intercommunicating secondary containment for the detector gas. The concept includes implementing a reservoir inside the junction box for a chemical reactant such as soda lime (mainly calcium hydroxide and water) or activated alumina (Al_2O_3). Both of theses substances are known as defluoridation agents due to their ability to neutralize fluoride gas. If activated alumina is implemented in the ratio 6:1 all fluoride gas can be absorbed. E.g. if 12 grams is deposited in the junction box, all BF_3 gas from one leaking detector will eventually be absorbed.

Whether this approach will be acceptable to the plant management in a nuclear installation remains to be seen. Certainly, the approach of isolating the BF_3 gas from the environment by means of air tight barriers and implementing defluoridation agents inside the containment, as is the preferred safety measure for transportation of bulk BF_3 gas, is a reasonable way of securing the toxic gas.

4 Conclusions

We have designed a helium free prototype neutron multiplicity counter for safeguards verification measurements of bulk plutonium samples. The counter named Boron Based Neutron Correlation Counter (BBNCC) is currently under construction in our laboratory. The counter incorporates 24 proportional detectors based on boron trifluoride gas enriched to above 99% in ^{10}B. The instrument will have a neutron detection efficiency above 25% which should make multiplicity measurement possible. Using a thermal neutron absorber such as ^{10}B in a polyethylene moderator means that the instrument can operate using standard safeguards assay parameters (pre-delay, gate width, die away time, updating dead-time parameters etc.). This has the advantage that the safeguards inspector can directly apply the well-tested analysis algorithms, software packages, and signal analyzers, used in neutron measurements for safeguards purposes today.

Although a high detection efficiency is achieved, a technical drawback of using BF_3 detectors is the relatively long die away time which may call for longer measurement times in high count rate applications. From an operational point of view the toxicity of the BF_3 gas is an issue. The BBNCC counter contains roughly 50 grams of BF_3 gas. The design includes the technical solution of an additional air tight barrier combined with a fluoride gas absorber against a possible release of the toxic BF_3 gas to the environment. Similar solutions are adopted for transportation of bulk quantities of fluoride gas. A recent review of transport regulations has let to a relaxation with respect to the quantities that can be transported without special precautions. The simple (passive) technical solution to significantly reduce the risk of an accidental release of the toxic gas, and the recent easing of public transportation restrictions, should have a positive effect on the assessment of whether such counter systems can be permitted in nuclear installations.

As soon as the prototype BBNCC becomes operational work will start to confirm the calculated assay parameters. Also the performance in multiplicity mode and in high count rate applications will be investigated.

References

[1] M. S. Krick and H. O. Menlove, “The High-Level Neutron Coincidence Counter (HLNCC): Users’ Manual,” Los Alamos Scientific Laboratory report LA-7779-M
(1978).

[2] J. F. Briesmeister (Ed); *MCNP—A General Monte Carlo N-Particle Transport Code, Version 4C*; LA-13709-M; Los Alamos National Laboratory; 2000.

[3] E. Pirovano, V. Mayorov, J.-M. Crochemore, M. Mosconi, E. Roesgen, B. Pedersen, “Performance testing of ^{10}B based neutron detectors as alternatives to ^{3}He” JRC Technical Report, in publication (2015).

[4] Letter of 13 September 2011 from National Nuclear Security Administration (NNSA, DoE) to Director of Natural Resources and Environment, Government Accountability Office (GAO) regarding review of report: “Technology Assessment: Alternatives to using Helium-3 for Neutron Detectors” GAO-11-753.

Session 3

International Collaboration

EU - ABACC Cooperation: Strengthening Safeguards Capabilities

João G.M. Gonçalves[1], François Littmann[1], Vítor Sequeira[1], Marco Sironi[1], Martin Andersen[2], Luís Machado[3], Orpet Peixoto[3], Silvio de Almeida[3], Sónia Fernandez Moreno[3]

[1] European Commission – Joint Research Centre (JRC), Ispra, Italy, [2] European Commission – Directorate General for International Cooperation and Development (DEVCO), Brussels, Belgium, [3] ABACC – Brazilian-Argentine Agency for Accounting and Control of Nuclear Materials, Rio de Janeiro, Brazil

Corresponding author: joao.goncalves@jrc.ec.europa.eu

Abstract

Following initial discussions in 2006 within the framework of the EURATOM – ABACC R&D Cooperation Agreement, in 2012 the European Union engaged into a cooperation project to strengthen Safeguards Capabilities at ABACC (the Brazilian-Argentinean Agency for Accountancy and Control). ABACC expressed interest in having access to two new Safeguards capabilities based on two JRC technologies approved for Safeguards use by both EURATOM and IAEA. This four-year cooperation project is funded by the European Commission Directorate General for Development and Cooperation – EuropeAid (DEVCO), under the Instrument for Nuclear Safety Cooperation (INSC). The new capabilities to be created at ABACC are: (i) Verification of complex plant design and lay-out ("as-is") and (ii) Containment of Spent Fuel in a complex Storage Environment. This is to be achieved by transferring to ABACC two JRC-owned technologies: (a) 3D Laser Verification System and (b) Ultrasonic Seals. The development of the two technologies to be transferred were funded by JRC's internal work-programme and targeted to Safeguards under the framework of the European Commission Support Programme to the IAEA (tasks EC-E-1425 and EC-E-1559). The transfer of technologies includes a set of comprehensive training actions and field support activities. Close coordination with the International Atomic Energy Agency (IAEA) takes place during the whole project's lifetime. The European Commission Directorate General for Energy (EURATOM Safeguards) is also informed on the project progress and achievements. Given the technologies to be transferred have been approved and are used by the IAEA, it could be possible at the end of the project to have the Safeguards equipment being jointly used by ABACC and the IAEA. This paper details all aspects of this cooperation project.

Keywords: Nuclear Safeguards, International Cooperation, ABACC, 3D Laser Verification System, Ultrasonic Seals

1. Introduction

The Brazilian-Argentine Agency for Accounting and Control of Nuclear Materials (ABACC) is a regional Safeguards organisation created by the Bilateral Agreement signed in December 1991 between Argentina and Brazil[1]. ABACC is mandated to apply a full scope Nuclear Safeguards system in Brazil and Argentina.

In March 1994, the Quadripartite Agreement between the International Atomic Energy Agency (IAEA), ABACC, Argentina and Brazil entered into force [1]. For more than 20 years, the IAEA and ABACC jointly coordinate Safeguards activities avoiding unnecessary duplication of efforts, while maintaining the principle that both organisations shall be able to reach independent conclusions.

[1] Agreement between the Republic of Argentina and the Federative Republic of Brazil for the Exclusively Peaceful Use of Nuclear Energy.

The selection of Safeguards tools to be used by ABACC is guided by the goal of implementing effective and efficient safeguards while reducing intrusiveness and protecting sensitive information, when so required.

ABACC and EURATOM – the European Atomic Energy Community, signed in February 1999 a long standing cooperation agreement focussing on Safeguards related Research and Development and Training. Within the framework of this agreement, and as precursors of the current project, (a) a training course to ABACC staff on "3D Laser based Verification" was held at the JRC in Nov. 2007 (together with IAEA inspectors); (b) technology demonstrations took place at ABACC premises of 3D Laser based Verification (Nov. 2008) and Ultrasonic Sealing Bolt (Containment and Surveillance Workshop, Oct. 2010).

The European Commission approved in 2012 the project "*Strengthening the Safeguards Capabilities of ABACC*". The project is implemented by the European Commission's Joint Research Centre (JRC) and aims at creating at ABACC new technical, human and know-how capabilities addressing two major safeguards challenges:

A. Verification of Complex Plant Design and Layout

B. Containment of Spent Fuel in Complex Storage Environments

JRC will provide two specific Containment and Surveillance technologies: (a) 3D Laser Verification and (b) Ultrasonic Sealing. Both technologies were developed at the JRC's Institute for Transuranium Elements, Ispra, Italy, and are approved for Safeguards use by the IAEA and EURATOM Safeguards.

The following sections detail this cooperation project with ABACC, the technologies and the proposed implementation, including training and transfer of know-how.

2. Instrument for Nuclear Safety Cooperation

The EURATOM Community's *Instrument for Nuclear Safety Cooperation* (INSC) [2] promotes the application of efficient and effective safeguards of nuclear material in third countries. While pursuing a close cooperation with the IAEA, the Community finances measures supporting the application of effective safeguards of nuclear material in third countries, building on its own safeguard activities within the European Union.

In 2012, and following a specific request from ABACC, the project "*Strengthening the Safeguards Capabilities of ABACC*" was approved by the European Commission Directorate General for Development and Cooperation (DEVCO). The project is funded by the European Commission *Instrument for Nuclear Safety Cooperation* (INSC). The four year project is implemented by the European Commission's Joint Research Centre (JRC) in cooperation with ABACC.

Following the appointment of the Commission of the ABACC[2], the ABACC Secretariat became the Beneficiary of the project.

[2] The Commission of ABACC is ABACC's policy planning organ and is constituted by diplomatic and technical representatives of Argentina and Brazil. The Commission is responsible for the approval of the decisions, resolutions and regulations applied to the performance of the ABACC's Safeguards. Among other responsibilities, the Commission of ABACC approves the General Procedures and the Manuals for Application of nuclear safeguards in Brazil and Argentina.

3. Project Structure

The project aims at creating new Safeguards capabilities, ie, technical, human and know-how, at ABACC. To achieve this objective the project includes the following actions:

i) Transfer of two Safeguards technologies: (a) 3D Verification System and (b) Ultrasonic Seals;

ii) Prototype and field demonstrations of the two above technologies at selected facilities (to be agreed with national authorities and operators);

iii) Training courses for ABACC staff and inspectors, including:

(a) Train-the-Trainers: train a selected group of ABACC officers on how to teach the two new technological capabilities

(b) Inspectors' Training: train a first group of inspectors on the use of the above mentioned technologies for safeguards verification and inspection purposes.

iv) Cooperation and technical support on the practical use of the two above technologies

In terms of implementation, the project is divided in three tasks:

Task A. Verification of Plant Design and Layout

Task B. Containment of Spent Fuel in Complex Storage Environments

Task C: Project Management

4. Technologies

The technologies to be transferred to ABACC were selected and requested by ABACC as they fit ABACC's mandate to strengthen and implement nuclear safeguards in Brazil and Argentina. The project involves two technical tasks, each one addressing the use of a specific Containment and Surveillance technology as follows:

A) 3D Laser Verification for detecting spatial changes in a nuclear site (indoor application)

B) Ultrasonic Sealing to safeguard irradiated fuel in interim or permanent storage (Figure 1).

Figure 1: Examples of JRC Ultrasonic Seals.

Both technologies were initially developed at the JRC's Institute for Transuranium Elements, Ispra site, Italy, as an internal research activity and then applied to EURATOM and IAEA safeguards. In what concerns the IAEA, the application of both technologies was done under the framework of the European Commission Support Programme (EC-SP) [3] to the IAEA, namely:

i) EC-SP Task: EC-E-01425 – "*3D Laser Range Finder for Design Verification at the Rokkasho Reprocessing Plant (RRP)"* and EC-E-01993 – "*3DLR Support"*

ii) EC-SP Task: EC-E-01559 – "*Update of the Ultrasonic Sealing Bolt*"

Both technologies are approved for safeguards use by both the IAEA (responsible for the implementation of the Nuclear Non-Proliferation Treaty – NPT) and by the European Commission's DG-Energy (responsible for the implementation of the EURATOM Treaty).

4.1 Task A: Verification of Plant Design and Layout

The verification of minute details over large areas in complex environments represents a difficult task. Covering these scenarios, the application of safeguards has to verify if changes or new elements relevant to safeguards are introduced into the facility operating conditions and/or its layout.

The application of laser technology for the verification of plant layout and configuration relies on the capability of the system to measure accurate distances of objects, and between objects, in a given scene [4, 5]. It is thus possible to detect minor changes in three dimensions (as opposed to normal video surveillance projecting the 3D world onto an image plane) – 3D scene change detection. Furthermore, 3D visualization tools help an inspector to interpret the spatial changes, their origins, safeguards relevance and impact (see Figure 2). The system is able to remount a 3D model independent from the capture point of the system.

Characteristics of the 3DLR[3] system such as self-illumination, independence of ambient lighting, high spatial resolution, high accuracy, fast speed acquisition, well defined measurement parameters (such as: distance, size, speed, motion orientation and easy interfacing) make this type of system suitable for the detection of changes in complex environments.

4.2 Task A: Results to be achieved

The specific objective to be achieved during this project is "to create within the regional authority ABACC a new Safeguards capability enabling the verification of complex plant design and lay-out ('as-is')". The results to be achieved include:

i) **Provision of two 3DLR (Laser based Verification) systems.** Each system integrates commercial equipment (3D laser scanner, associated computers and accessories, e.g., tripod, carrying equipment, …) with JRC's proprietary dedicated software, i.e., JRC 3D Reconstructor© and JRC 3D Verificator©;

[3] 3DLR is the code name for JRC's laser based system for Design Information Verification – DIV - used by the IAEA. A similar system (code name: 3DLVS) is used by the European Commission's DG-Energy for inventory verification purposes (in quasi-static storage areas). The 3DLR system (3DLVS also) includes two JRC's proprietary software packages: JRC 3D Reconstructor© and JRC 3D Verificator©.

(a)

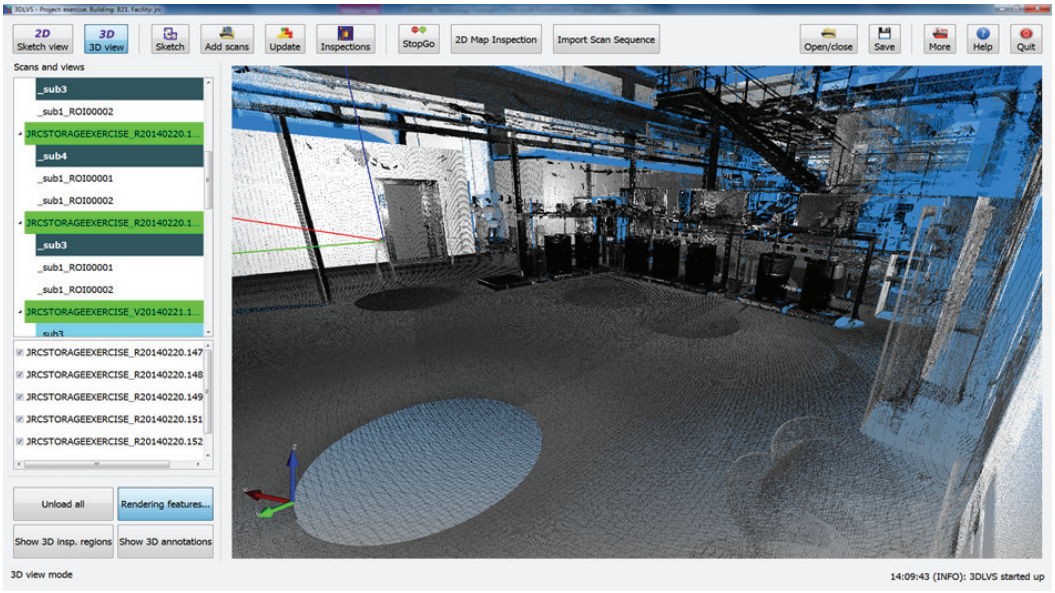

(b)

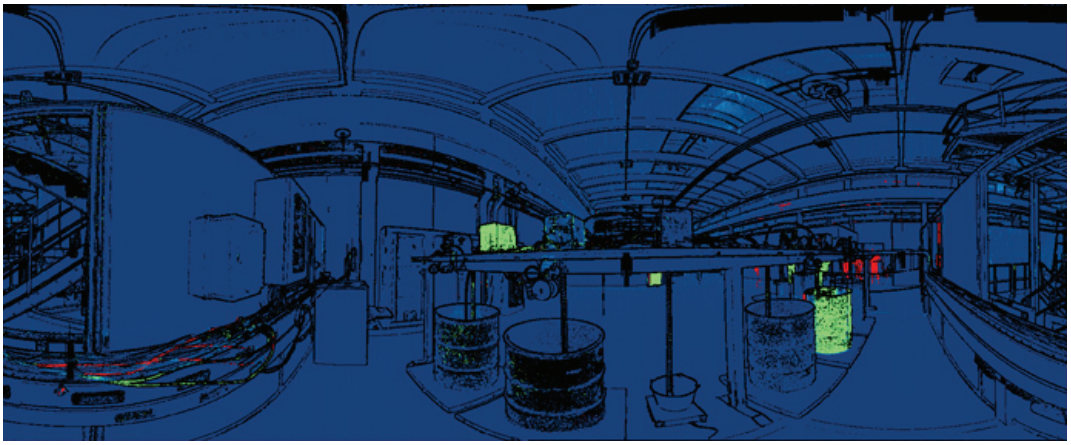

Figure 2. (a) 3D model of a facility as shown by JRC's 3DLVS software; (b) Map of changes derived from two 3D models acquired at different points of time. Changes are highlighted in red and green.

ii) **Field Test of a Laser based 3D Verification System**, for Design Information Verification purposes, at a nuclear facility in Brazil.

iii) **Train-the-Trainers**: train two ABACC officers on how to teach the new technological capability – 3D Laser Verification, to ABACC inspectors.

iv) **Inspectors' Training**: train a first group of 16-20 inspectors on the use of the 3D Laser Verification technology for safeguards verification and inspection purposes.

v) **Cooperation and technical support** on the practical use of the 3D Laser Verification System.

vi) **Maintenance activities**, including two further releases of the application specific software and yearly calibration of the laser range finders.

vii) **Delivery of support documentation** (operation guide and maintenance manuals)

4.3 Task B. Containment of Spent Fuel in a Complex Storage Environment

The second challenging goal is applying efficient and effective safeguards for on load reactors, based on the verification of the irradiated fuels that leave the core and keep the knowledge of such items during interim or permanent storage. For doing that, tools such Core Discharge Monitor and Fuel Bundle Counter are used together with containment and surveillance. Besides, the verification of the inventory of the spent fuel stored at the reactor's pools is periodically performed.

One way to maintain the knowledge on the nuclear material at a spent fuel pond is to apply containment measures at flasks or racks where these fuels are stored. It is important to guarantee that ABACC and IAEA maintain the knowledge over multiple layers of the spent fuel storage through the application of seals on fuel elements, racks or hangers.

For this application, ultrasonic seals[4] [6] have the necessary characteristics since they are designed to be attached underwater, are very resistant to harsh environments like storage pools, are easy to apply and can be regularly verified. The verification of ultrasonic seals does not involve the replacement of cables or substitution of the seal, nor does it require the movement of spent fuel. This improves inspectors' productivity, takes due care of radiation safety considerations and decreases the disturbance to the plant operator.

4.4 Task B: Results to be achieved

The specific objective to be achieved during this project is "to create within the regional authority ABACC a new Safeguards capability based on JRC ultrasonic sealing technology, and have a demonstration prototype adapted to specific PHWR underwater storage deeper ponds and particular spent fuel storage configuration". The results to be achieved include:

i) **Design of a complete and specific sealing system** based on real conditions of an underwater spent fuel storage pond;

ii) **Field Test and demonstration of Ultrasonic Seals**, for maintaining the continuity of knowledge of verified irradiated fuel. For this test, It will be assumed that spent fuel is stored in a closed packed way, in two layers at the storage pool (see Figure 3). For verification of this particular configuration, the accessibility of nuclear instrumentation to the lower layer of spent fuel is very complex and time consuming. Ultrasonic seals should make verification much more easy and straightforward. This test will be also useful to consider the technology for other types of nuclear reactors with different spent fuel storage configurations.

iii) **Improvement of the control software**, including tele-operation assistance requested by the high water depth;

iv) **Equipment** to be supplied: 150 ultrasonic seals and three reading systems. Handling tool interfaces and specific sealing accessories will be also supplied.

v) **Associated computers, accessories and JRC's dedicated software** for identifying and reading the seals;

vi) **Train-the-Trainers**: train two ABACC officers on how to teach the new technological capability – Ultrasonic Sealing, to ABACC inspectors.

[4] Ultrasonic seals developed by the JRC are patented and currently used in Canada, France, Pakistan, Romania and UK by both EURATOM Safeguards and IAEA.

vii) **Inspectors' Training**: train a first group of 16-20 inspectors on the use of Ultrasonic Sealing for safeguards verification and inspection purposes.

viii) **Cooperation and technical support** on the practical use of Ultrasonic Sealing.

ix) **Delivery of support documentation** (operation guide and maintenance manuals);

x) **Preventive maintenance** (2 years).

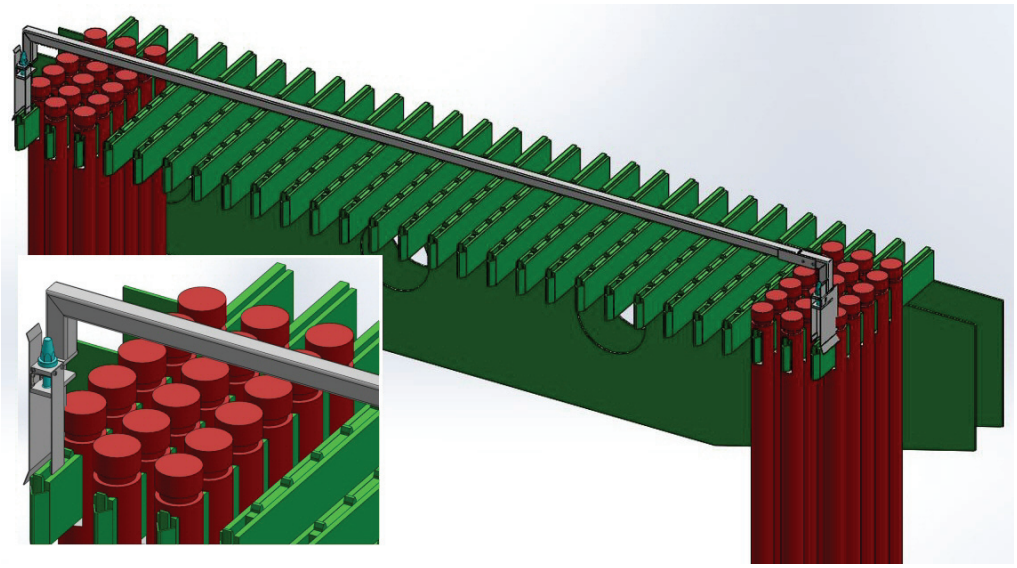

Figure 3. Proposed solution to seal a spent fuel pond

5. Safeguards and Coordination with the IAEA

The project foresees close interaction with the International Atomic Energy Agency (IAEA). Indeed, the IAEA has been, and will be, invited for major project events, including:

i) Kick-off meeting,

ii) Technical meetings,

iii) Demonstration of the technologies,

iv) Distribution of specific documentation issued during the project

v) Training sessions, both in Europe (Train-the-Trainers) and in South America (inspectors' training)

It should be noted that by creating new safeguards capabilities at ABACC, it will be possible (and desirable) that the instrumentation provided can be jointly used with the IAEA. To this effect, the IAEA will be contacted for relevant technical decisions. This will ensure that IAEA expectations in terms of the equipment to be supplied will be met in view of future joint-use.

More specifically, the IAEA met ABACC and EC/JRC representatives in the following occasions:

- September 2013: the European Commission and ABACC organised a presentation of the project to the IAEA Deputy Director General for Safeguards (see Figure);
- February 2014: JRC and ABACC met the IAEA to discuss in detail how EC funded equipment and systems, namely 3D laser scanners, can be made available later for Joint

Safeguards Use by both ABACC and the IAEA. This led to the agreement on the technical specifications of the 3D laser scanners to be procured.

- September 2014: short presentation of the status of the project was made by ABACC and JRC to IAEA staff.

6. Status of the Project

The following activities have already taken place or are programmed shortly:

- Technical specifications for the laser based equipment to be procured, 2014;
- Technical specifications for the ultrasonic sealing equipment to be procured, 2014;
- Specification of the demonstration and field test of the 3DLR system at a nuclear facility in Brazil, November 2014;
- Train-the-Trainers course for the Ultrasonic Seals, May 2015;
- Train-the-Trainers course for the 3DLR verification system, June 2015;
- Technical proposals for sealing a multiple layer spent fuel storage pond, considering Atucha I spent fuel storage configuration, March 2015
- Specification of the demonstration and field test of the Ultrasonic Seals at a storage configuration type of Atucha I, Argentina, June 2015

7. Discussion and Conclusions

Looking for the best practices in the safeguards application, ABACC and EURATOM – the European Atomic Energy Community – signed in February 1999 a cooperation agreement based on mutually agreed Research and Development topics and the training of nuclear safeguards inspectors in the field of nuclear safeguards. Cooperation between the parties to this Agreement shall be on the basis of mutual benefit, equality and reciprocity.

ABACC and the European Commission engaged into a collaborative project on Strengthening the Safeguards Capabilities. This project involves two technologies – 3D Laser Verification and Ultrasonic Sealing, the benefits of which are to be evaluated for possible Safeguards application at facilities in Argentina and Brazil.

3D laser-based techniques continue to improve and cover a large range of activities including Design Information Verification (DIV), containment verification and UF6 cylinders tracking. The ABACC expectation is that the use of 3D laser-based instrumentation will increase over the coming years and a direct benefit to the effectiveness and efficiency of its safeguards implementation can be provided in a near future.

The main purpose of sealing using ultrasonic technique is to maintain the continuity of knowledge and avoid re-measurement of nuclear material inventories. This is particularly important when applied to spent fuel storages. The historical application of this technique has been analysed by ABACC since the development of the underwater seal based on ultrasound in conjunction with a randomly produced wire coil which create the seal signature. The new bolt for underwater sealing is derived from the design of the sealing bolts already used in the La Hague reprocessing plant. On-going developments of various

Ultrasonic Sealing Systems for both underwater and dry spent fuel storages applications, in particular for dry storages using cask with concrete biological shielding have been tested.

Within the framework of the Quadripartite Agreement [1], ABACC, together with national authorities and operators in Brazil and Argentina, is analysing the application of 3D laser and/or ultrasonic seals technologies. In particular, the analysis will focus on how the use of the new technologies improves safeguards without affecting operational tasks and turning activities less intrusive and more efficient.

The use of new technologies is key to enhancing Safeguards effectiveness and efficiency. In this particular case, any future application of these technologies should be developed and implemented such that it allows Joint Use between ABACC and IAEA when the application on safeguards is discussed and approved. Results from the containment provided by the ultrasonic seals and verification of design by 3D laser-based techniques shall permit that ABACC and IAEA draw independent conclusions.

8. References

[1] IAEA INFCIRC 435, http://www.abacc.org.br/wp-content/uploads/2015/02/infcirc435-ing.pdf, 1994.

[2] COUNCIL REGULATION (EURATOM) No 300/2007 of 19 February 2007 establishing an Instrument for Nuclear Safety Cooperation, Official Journal of the European Union L 81/1, of 22 March 2007.

[3] Gonçalves, J.G.M., Abousahl S., Aregbe Y., Janssens W., Lützenkirchen K., Meylemans P., Schwalbach P. – "The European Commission Cooperative Support Programme: Activities and Cooperation", 12th IAEA Symposium on International Safeguards, Vienna, 19-24 October 2014.

[4] Agboraw E., Johnson S., Creusot C., Poirier S., Saukkonen H., Chesnay B., Sequeira V. – "IAEA experience using the 3-Dimensional Laser Range Finder (3DLRF) for Design Information Verification at the Rokkasho Reprocessing Plant", IAEA-CN-148/200, Proc. IAEA Safeguards Symposium: Addressing Verification Challenges, Vienna (2006).

[5] Chare P., Lahogue Y., Schwalbach P., Smejkal A., Patel B.. – "Safeguards By Design – As applied to the Sellafield Product and Residue Store (SPRS)". ESARDA Bulletin (46); 2011. p. 72-78.

[6] Chiaramello M., Sironi M., Littmann F., Schwalbach P., Kravtchenko V. – "JRC CANDU Sealing Systems for Cernavoda (Romania) and Upcoming Developments", ESARDA Bulletin n°44 June 2010.

Overview of Activities and Outcomes at ISCN Related to Japanese Commitment at Nuclear Security Summit Process

Yosuke NAOI, Naoki KOBAYASHI, Toshiro Mochiji, Masao SENZAKI, Michio SEYA

Integrated Support Center for Nuclear Nonproliferation and Nuclear Security (ISCN),
Japan Atomic Energy Agency
765-1 Funaishikawa, Tokai-mura, Ibaraki-ken, 319-1184, Japan
E-mail: naoi.yosuke@jaea.go.jp

Abstract:
In April 2010 at the Nuclear Security Summit in Washington, D.C., Japan made a commitment to establish a center of excellence on nuclear nonproliferation and security. This center would support capacity building for strengthening nuclear nonproliferation and security mainly in the Asian region and also would engage in development of technology related measurement and detection of nuclear material including nuclear forensics based on international cooperation.
According to this statement, Integrated Support Center for Nuclear Nonproliferation and Nuclear Security (ISCN) was established under Japan Atomic Energy Agency (JAEA) in December 2010. Since its establishment four and a half years ago, ISCN has developed its activities, having already conducted 79 training courses for the nuclear nonproliferation and security fields and having trained 2,217 participants from 49 countries (including Japan) and three international organizations. As for technical development on detection and measurement of nuclear material, ISCN has carried out substantial outcome with the international cooperation of U.S. and EU/JRC. It can be said that it is a significant achievement of the Nuclear Security Summit process. This paper will overview the outcome of ISCN's activities over the past four years.

1. Introduction

How the preparations were advanced toward the establishment of ISCN, with cooperation from domestic relevant organizations and how cooperation was promoted with the United States (US) and the European Union (EU) have been described in a previous paper[i]. This paper will present concrete results mainly in the ISCN's capacity-building activities over the past four and a half years.

2. Overview and achievement of capacity-building assistance activities of ISCN

For capacity-building assistance activities of ISCN[ii], JAEA offers training courses in three categories: (1) International Nonproliferation Framework Courses, (2) Nuclear Security Courses, and (3) State Systems of Accounting for and Control of Nuclear Material (SSAC) and Safeguards (SG) Courses. Target countries for ISCN's training activities are those that are part of the Association of Southeast Asian Nations (ASEAN), that participate in the Forum for Nuclear Cooperation in Asia (FNCA), that have the possibility of extended nuclear cooperation with Japan or that have requested cooperation at the government level. ISCN has conducted its support activities in close collaboration with the Japanese government and has determined target countries. As a general rule, those target countries are re-examined every year. Some training courses are hosted by ISCN in Tokai-mura, Japan, and other courses are organized by target countries with the lecturers dispatched from ISCN. International Nonproliferation Framework Courses are based on bilateral cooperation, and the courses are basically hosted by the target countries. The achievements of each category of training courses since the establishment of ISCN are as described below.

2.1 International Nonproliferation Framework Courses

ISCN conducts seminars on "Peaceful Uses of Nuclear Energy and Nuclear Nonproliferation" to fulfill the purposes to convey to the target country the importance of nuclear nonproliferation and security activities, to broadly understand the target country's current state of nuclear energy development and corresponding need for training in nuclear nonproliferation and security, and to lay a foundation of understanding for future cooperation between related organizations in Japan and in the target country. The duration of the seminar is usually one or two days. The participants come from a wide range of organizations related to nuclear nonproliferation and security in the partner country, such as the ministries of foreign affairs and energy, nuclear regulatory authorities, security authorities, operators, and research and development institutions. A typical seminar consists of presentations about the partner country's plans for the peaceful use of nuclear energy and the measures that they have taken for nuclear nonproliferation and security, Japan's experiences in these areas, and keynote speeches on the status and framework of international nuclear nonproliferation and security. As a result, while the seminar itself fosters a general awareness of nuclear nonproliferation and nuclear security, ISCN's goal is that, after the seminar, the interaction with the partner country advances and shifts to specific support based on the partner country's needs, such as the development of domestic legislation and SSAC, the

ratification and implementation of an Additional Protocol (AP), or the improvement of nuclear security. This kind of cooperation actually started in 2007, even before the creation of ISCN, so that JAEA/ISCN has already organized seminars in eleven countries, as shown in Table 1. Not only bilateral cooperation, but also cooperation with a multi-country framework such as the ASEAN Center for Energy (ACE) has been promoted, and ISCN and ACE have jointly organized a seminar. At the seminars, simultaneous interpretation service to and from the local language is sometimes arranged, in order to accommodate a wider range of participants.

Table-1 Results of International Nonproliferation Framework Courses

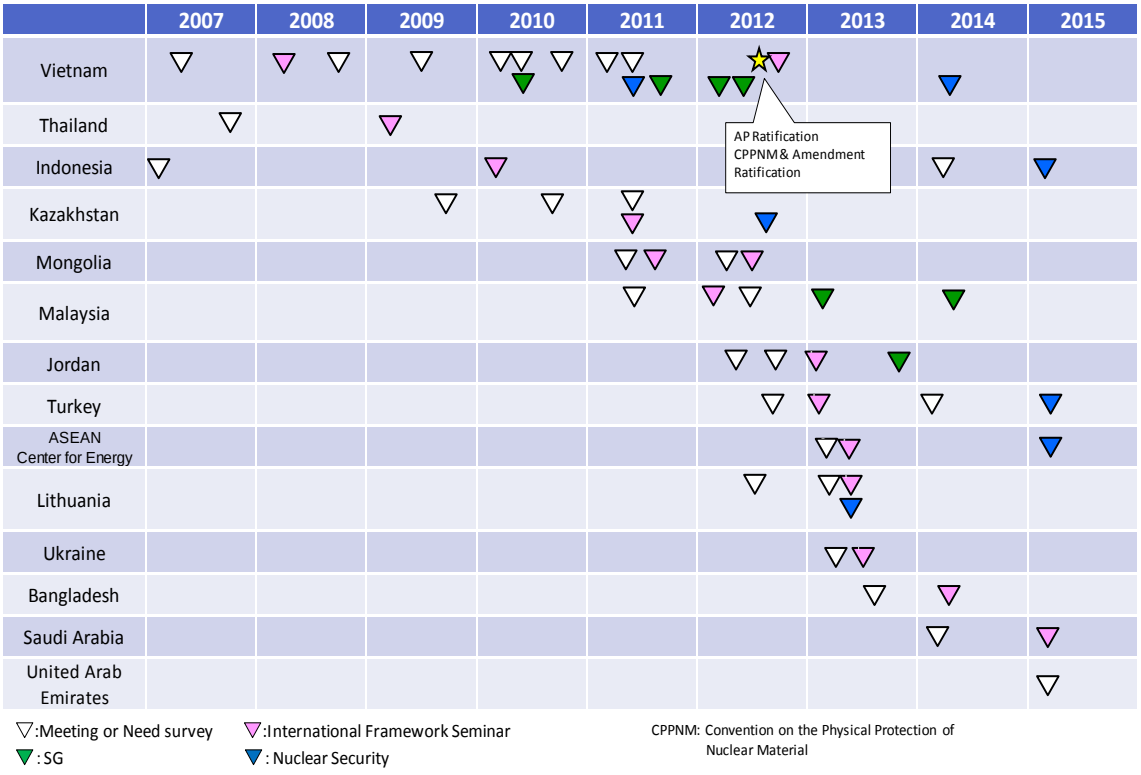

2.2 Nuclear Security Courses

As shown in Table 2, in Japan fiscal year (JFY) 2011, ISCN started its capacity-building in nuclear security support activities with offering two training courses: a basic training course on physical protection of nuclear material (PP-RTC) and a workshop on the IAEA's recommendations on physical protection of nuclear material (INFCIRC225/Rev.5). Since then, ISCN has extended the scope of its training courses as well as the total number of courses to meet increasing needs.

In JFY 2014, besides the PP-RTC, which has been conducted yearly since JFY 2011, ISCN is

planning to organize many training courses including new ones, such as training courses on measures against insider threats and security of radioactive sources and a regional workshop on nuclear security culture.

In addition to these international and regional training courses that are held in Japan, ISCN provides assistance based on bilateral cooperation and organizes seminars or workshops abroad in the field of nuclear security. A seminar on border security conducted in Lithuania and a basic seminar on physical protection of nuclear material conducted in Vietnam are examples. Recently, the National Nuclear Energy Agency (BATAN) of Indonesia requested ISCN cooperation in connection with the establishment of their training center. The areas of requested cooperation include training of trainers and development of training curriculums.

Table-2 Provision of Nuclear Security Courses

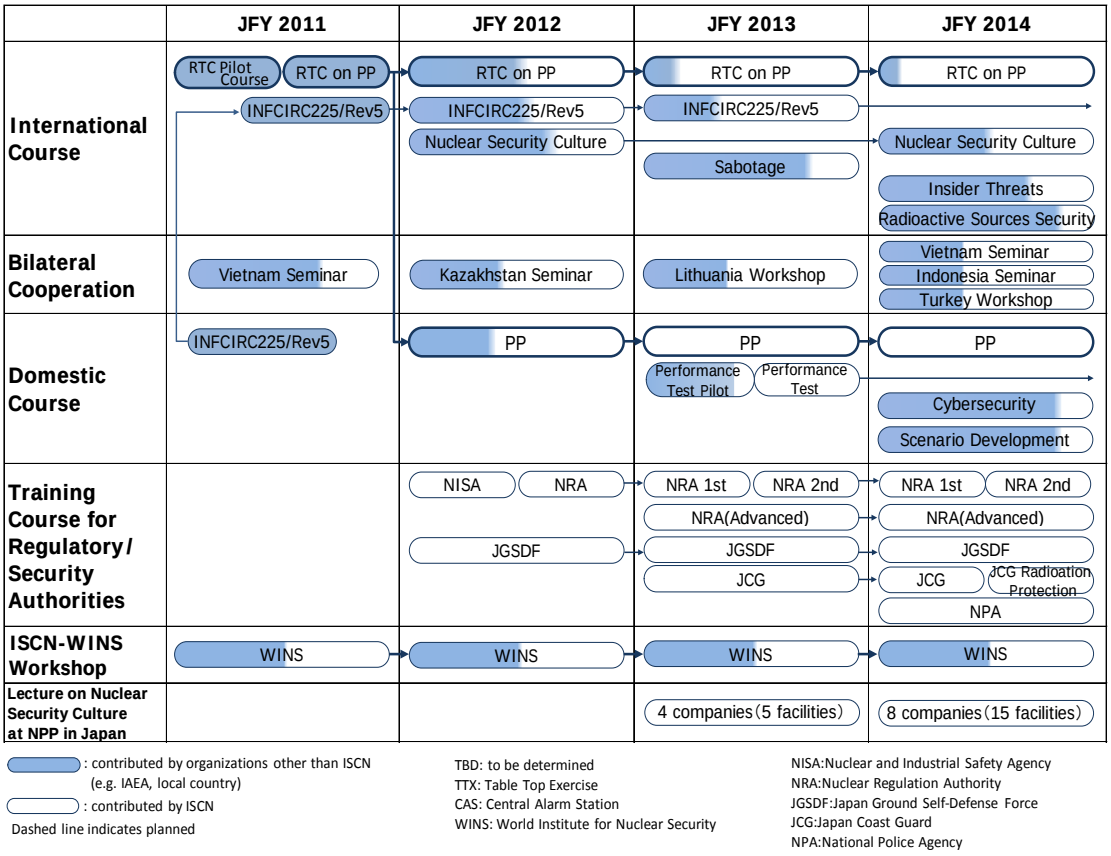

In regard to training the ISCN's own lecture staff, ISCN has conducted the PP-RTC every year with cooperation from the US Department of Energy (DOE) and Sandia National Laboratories (SNL), striving for the goal of conducting international training courses all by itself. In JFY 2011, ISCN held a train-the-trainer course to train its own staff, with cooperation from SNL. Since then,

the proportion of ISCN training staff has increased and almost 80% of the training course lectures are now taught by the ISCN staff. Acquiring the knowledge and ability to deliver training courses by itself provides ISCN flexibility in scheduling training courses at the appropriate time. By doing so, ISCN will have a foundation of providing intensive courses. When developing a new training course, ISCN lecturers receive training at SNL and utilize the experience for the development of curriculum and training materials. Especially, ISCN developed and established the Virtual Reality System[iii] (Cave system), one of the virtual space experience system where the participants can walk in and around a virtual nuclear plant, and the Physical Protection (PP) Training Field where participants can learn and practice the performance and the features of nuclear protection equipment (protective fences, invasion detection sensor, surveillance camera, access management system and so on). These facilities are incorporated into the training curriculums and make the training original and unique. There is also increased demand from domestic government organizations. For example, ISCN organized a training course for inspectors of the regulatory authority (Nuclear Regulation Authority) in the field of regulation of physical protection. After that, ISCN has been making an effort to make courses more effective by improving the curriculums. This has been done through consultations with the regulatory authority. In JFY 2013, ISCN offered two basic courses and one specialized course. Upon request, ISCN continues to offer those courses in this JFY. This is evidence that ISCN's training courses are highly regarded. ISCN's training activities have extended not only to training courses for Japan Ground Self-Defense Force Chemical School (started in JFY2012), for Japan Coast Guard (started in JFY2013) or National Police Agency (started in JFY 2014), but also training courses on performance testing of physical protection detection system or on cybersecurity. This is a great achievement of ISCN.

2.3 State Systems of Accounting for and Control of Nuclear Material (SSAC) and Safeguards (SG) Courses

JAEA has been providing an international training course on SSAC in Japan every year since 1996, before the establishment of ISCN, and has contributed to the capacity building of key persons for safeguards activities in other countries. Some examples are noted below. A participant in JAEA's SSAC course in 2006 has become the director of the nuclear safeguards division in the Vietnamese regulatory authority. She has been working to promote nuclear security and safeguards in Vietnam and contributing to strengthening safeguards systems in Asia at multilateral forums, such as the Asia-Pacific Safeguards Network (APSN) and FNCA. A Czech SSAC course participant in 2002 served as an IAEA lecturer in the SSAC course in 2013. A Korean participant in 2006 is now a vice-president of the safeguards and physical protection

regulatory authority in Korea. These clearly illustrate that participants in the JAEA's capacity-building activities are playing an important role in their countries or in the IAEA. Also, a 2012 SSAC course participant from Jordan Nuclear Regulatory Commission took initiative and explained in Arabic to other participants during exercise sessions at the ISCN's workshop on safeguards in Jordan in 2013, to increase understanding. These show the good practice of ISCN's capacity-building activities.

The good practice shown above cannot be achieved in a short space of time, however, this is evidence that the knowledge and human network acquired through the ISCN's capacity-building activities is instrumental in achieving these concrete results. It is also evidence that the ISCN's activities contributed to fostering persons who work for the implementation of safeguards both at home and abroad.

In addition, ISCN has conducted not only multilateral training courses but also training courses based on bilateral cooperation. These bilateral cooperation activities include training courses held in the partner countries, such as the ones conducted in Vietnam, Malaysia and Jordan to promote ratification of an Additional Protocol (AP) or to help participants learn basic safeguards. In Vietnam, ISCN has organized three training courses on SG, and Vietnam ratified an AP in September 2012. This is a good example of a visible result of ISCN's capacity-building assistance activities.

In response to a request from the IAEA, the SSAC course that is to be held in 2014 will be an international course. The invitation will not be limited to the Asian region, but participants will be invited from 88 countries in the world. This can be considered to be the result of the appreciation of trust that has been built over nearly 20 years of achievement and cooperation, even before the establishment of ISCN, through conducting SSAC training courses with cooperation from the IAEA. Table 3 presents the achievement of SSAC and SG courses after the establishment of ISCN.

Table-3 Progress in Provision of SSAC and SG Courses

	JFY 2011	JFY 2012	JFY 2013	JFY 2014
International Training (conducted in Japan annually from JPY 1996 to 2010)	ITC on SSAC	ITC on SSAC	ITC on SSAC	ITC on SSAC
Training Course for IAEA Inspector	Reprocessing	Reprocessing DCVD	Reprocessing IS for JNC-1	Reprocessing
Dispatching Training Course	Vietnam AP Vietnam SSAC	Vietnam AP Malaysia AP	Jordan SG	Malaysia AP

: contributed by organizations other than ISCN (e.g. IAEA, local country) : contributed by JAEA, ISCN

3. Technical development on detection and measurement of nuclear material

ISCN/JAEA has been implementing development of basic technologies of the following advanced NDA (Non-Destructive Assay) of nuclear material that could be used as tools not only for safeguards (measurement of nuclear material) application but also for nuclear security one (detection of nuclear material). We have been involved in the following 5 programs with state of the art technologies of Japan, in collaboration with the international counterparts. The outcomes of the programs 2), 3), 4) and 5) will be reported in detail at “The ESARDA Symposium 2015”. In this paper we roughly introduce our development of each NDA technology.

(1) Demonstration tests for a spent fuel Pu-NDA (Non-Destructive Assay) system
(2) NRF (nuclear resonance fluorescence)-NDA using laser Compton scattered (LCS) gamma-rays (intense mono-energetic gamma-rays)
(3) Alternative to He-3 neutron detection using ZnS/B O ceramic scintillator
(4) NRD (Neutron Resonance Densitometry) using NRTA (Neutron Resonance Transmission Analysis) and NRCA (Neutron Resonance Capture Analysis)
(5) Nuclear forensics technology development project

3.1 Demonstration tests for a spent fuel Pu-NDA (Non-Destructive Assay) system

ISCN/JAEA and the United States Department of Energy (USDOE)/Los Alamos National Laboratory (LANL) have been collaborating on spent fuel measurements. We have conducted several important NRF and NRD experiments with a PNAR (Passive Neutron Albedo Reactivity) and SINRD (Self-Interrogation Neutron Resonance Densitometry)

NDA instrument (Figure 1 NDA apparatus) at Fugen nuclear power station[iv].

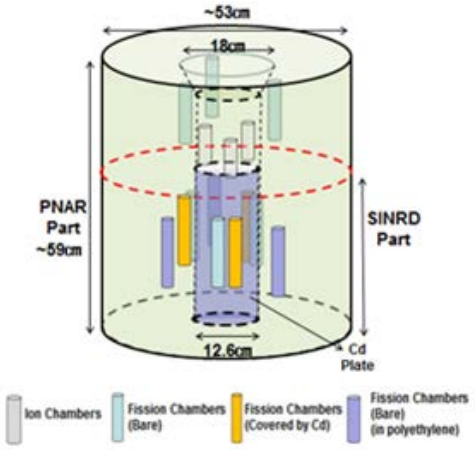

Figure 1 NDA apparatus of PNAR and SINRD

3.2 NRF (Nuclear Resonance Fluorescence)-NDA using Laser Compton Scattered (LCS) gamma-rays (intense mono-energetic gamma-rays)[v]

ISCN/JAEA has developed a non-destructive detection system for measurement and detection of nuclear materials, such as measurement of nuclear material hidden in heavy shields in cargo containers, quantitative measurement of nuclear material in spent fuel, and non-destructive quantification of nuclear material in targets such as particle-like melted fuel debris. We have considered this technology difficult to be developed since long before. This system is able to detect and identify isotopes of nuclear material by employing Nuclear Resonance Fluorescence (NRF) with Laser Compton Scattering (LCS) gamma-rays, which are generated by the collision of laser quanta with high energy electrons.

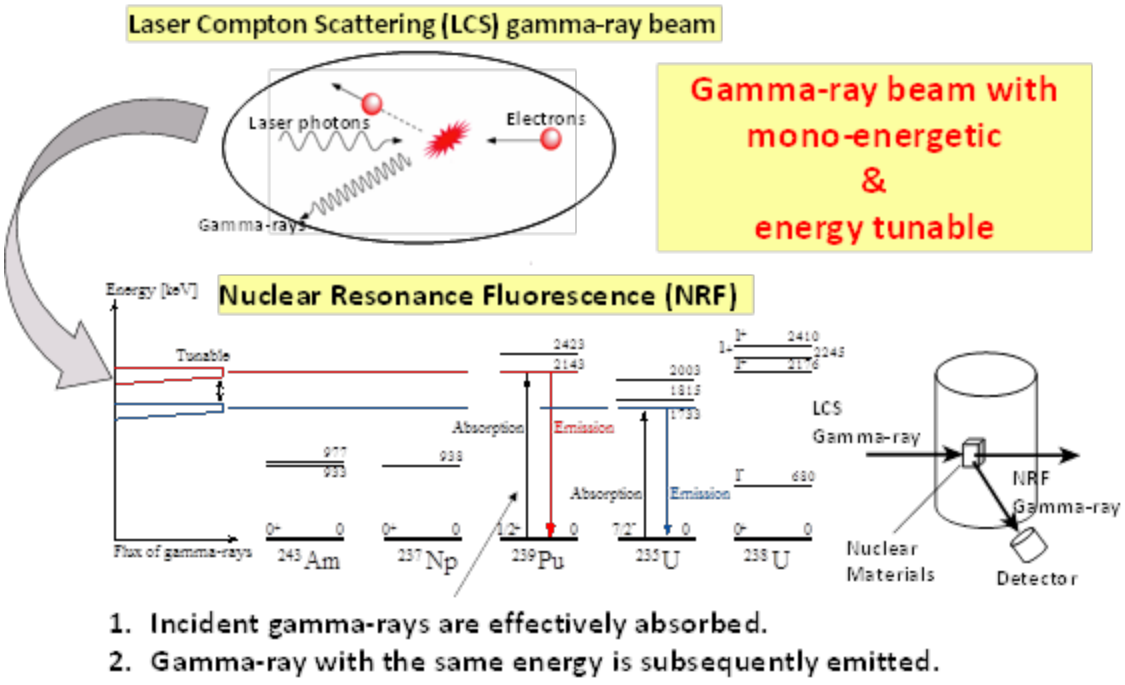

Figure 2 Nuclear Resonance Fluorescence (NRF) with Laser Compton Scattering (LCS) gamma-rays

3.3 Alternative to He-3 neutron detection using ZnS/B2O3 ceramic scintillator[vi]

Against the background of the serious shortage of He-3 gas, the neutron-sensitive ZnS/10B2O3 ceramic scintillator detectors have been developed by JAEA for a safeguards-specific alternative to He-3 for neutron detection. He-3 for neutron detection has been in critical short supply since the simultaneous terrorist attacks in the United States on September 11, 2001. The US Department of Homeland Security used a great number of neutron detectors for detecting nuclear materials along the national borders and the port facilities in the United States. The United States, as a major supplier, established its policy to decrease their supply of He-3 gas in the area of safeguards which alternative to He-3 neutron detection can be applied. In the end of March, 2011, the IAEA held a workshop for the experts of neutron and neutron detector development, and asked the States participated in the workshop to cooperate and develop the technology of alternative to He-3 neutron detection. While we have improved neutron detection units based on a neutron-sensitive ZnS/10B2O3 ceramic scintillator detector technology developed by JAEA (J-PARC Center) and digital processing circuits, we have involved in development and demonstration of NDA apparatus for nuclear safeguards with those neutron detector units.

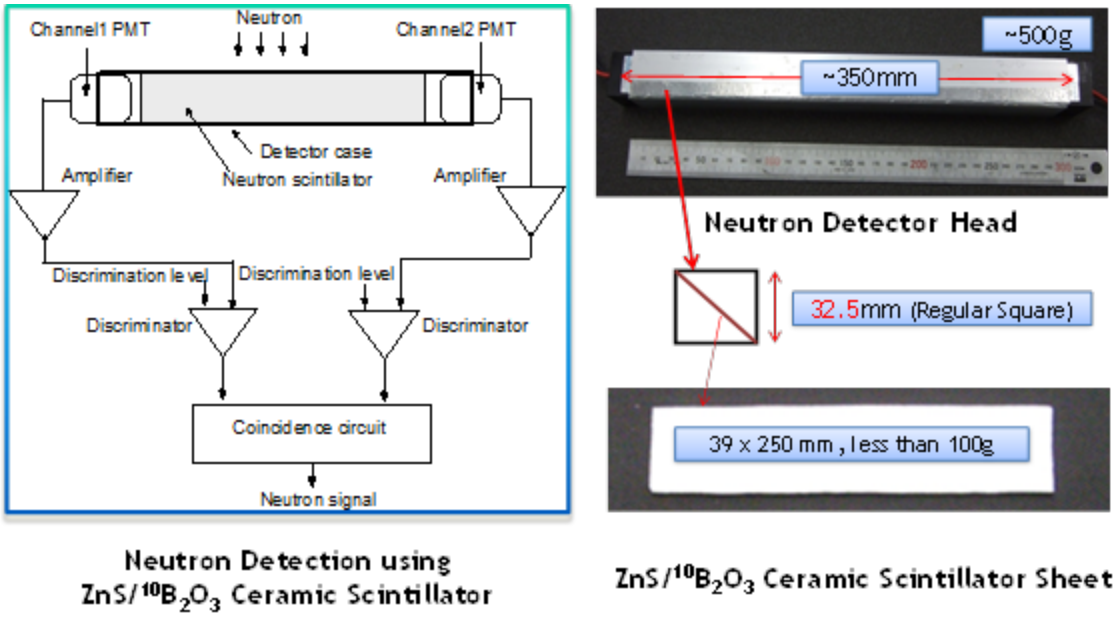

Figure 3 Overview of a ZnS/10B2O3 Ceramic Scintillator Neutron Detector

3.4 Neutron Resonance Densitometry (NRD)[vii]

ISCN/JAEA has been undertaking to develop fundamental part of advanced Non-Destructive Assay (NDA) technologies for nuclear materials, under the collaboration with EC-JRC-IRMM. Neutron Resonance Densitometry (NRD) has been proposed to quantify nuclear materials in particle-like debris of melted fuel (a molten mixture of nuclear fuel and structural material) by the types of isotopes formed in severe accidents of nuclear reactors. NRD is a method combining NRTA (Neutron Resonance Transmission Analysis; quantification of nuclear fuel nuclei) and NRCA (Neutron Resonance Capture Analysis; quantification of mixed nuclei). It relies on neutron technique using a pulsed white neutron source. (Figure 4)

3.5 Nuclear forensics technology development[viii]

ISCN/JAEA has started a nuclear forensics technology development project since 2011. Nuclear forensics is the analysis of intercepted illicit nuclear or radioactive material and any associated material to provide evidence for nuclear attribution by determining origin, history, transit routes and purpose involving such material. This project includes the developments of analytical technologies such as isotope and impurity measurements, morphology analysis, age determination technique, and the prototype of National Nuclear Forensics Library (NNFL).

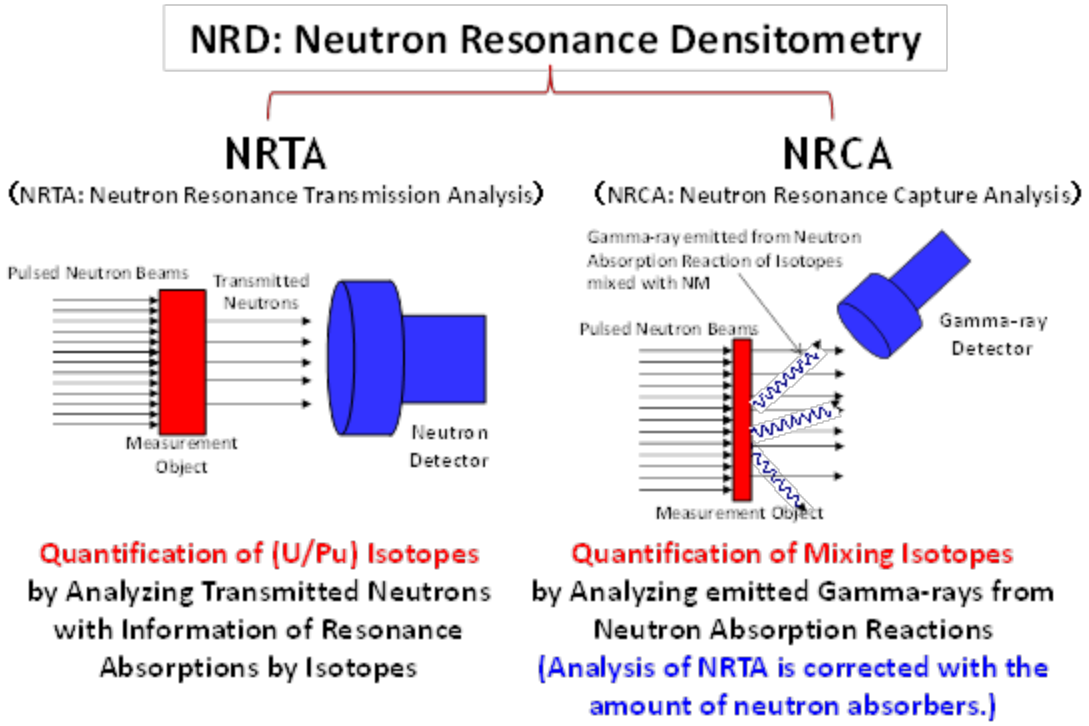

Figure 4 Neutron Resonance Densitometry

[i] Yosuke Naoi, et al.," Development of Centers of Excellence Play Major Role in International Capacity Building" INMM 54th Annual meeting, July 2013
[ii] http://www.jaea.go.jp/04/iscn/index_en.html
[iii] Tasuku Hanai, et al.," Development of a Virtual Reality System for Training Use on the Nuclear Security" INMM 54th Annual meeting, July 2013
[iv] J. Eigenbrodt, S. J. Tobin, W. S. Charlton, A. M. Bolind, H. O. Menlove, M. Seya and H. R. Trellue, "PNAR Measurement of Fugen Fuel, INMM 55th Annual meeting, July 2014
[v] R. Nagai, R. Hajima, et al., "Overview of laser Compton-scattered photon source at the cERL, Proc. Of Nuclear Physics and Gamma-ray sources for nuclear secutity and nonproliferation, Tokai-mura, Japan, January 2014
[vi] H. Nakamura, M. Kureta, A. Ohzu, K. Soyama, et al., "Demonstration plan of Pu NDA system using ZnS Ceramic scintillator", 53rd INMM annual meeting, Orland U.S.A., July 2012
[vii] H. Harada, P. Schillabeeckx, et al., "Development of Neutron Resonance Densitometry" 55th INMM annual meeting, Atlanta U.S.A., July 2014
[viii] A. Okubo, Y. Kimura, N. Shinohara, et al., "Report on research and development of nuclear forensics technologies" JAEA-Technology 2015-001 (in Japanese)

JAEA – JRC Collaboration on the Development of Active Neutron NDA Techniques

Masatoshi Kureta[1], Mitsuo Koizumi[1], Akira Ohzu[1], Kazuyoshi Furutaka[1], Harufumi Tsuchiya[1], Michio Seya[1], Hideo Harada[1], and Said Abousahl[2], Jan Heyse[3], Stefan Kopecky[3], Willy Mondelaers[3], Bent Pedersen[4], Peter Schillebeeckx[3]

[1] Japan Atomic Energy Agency (JAEA)
Tokai-mura, Naka-gun, Ibaraki 319-1195, Japan
E-mail: kureta.masatoshi@jaea.go.jp
[2] Joint Research Centre – Brussels
Marsveldstraat 21, B - 1050 Brussels, Belgium
[3] Joint Research Centre – Geel
Retieseweg 111, B - 2440 Geel, Belgium
[4] Joint Research Centre – Ispra
Via E. Fermi, 2749, 1-21027 Ispra (VA), Italy

Abstract:

The Japan Atomic Energy Agency in collaboration with the Joint Research Centre of the European Commission started a program titled "Development of active neutron NDA techniques". The program aims at developing an innovative non-destructive analysis (NDA) system for various applications in the field of nuclear safety, security and safeguards.

A Non Destructive Analysis (NDA) system is proposed that is based on a combination of different active neutron interrogation techniques, i.e. DDA (Differential Die-Away Analysis), PGA (Prompt Gamma-ray Analysis) combined with NRCA (Neutron Resonance Capture Analysis), NRTA (Neutron Resonance Transmission Analysis) and DGS (Delayed Gamma Spectroscopy). The activities include the development of simulation tools and of improved data processing and analysis procedures. In addition, validation experiments will be carried out at the nuclear facilities of the JRC. The objective is to construct a prototype instrument at JAEA based on a 14 MeV pulsed neutron source for testing and demonstration experiments.

At present no adequate NDA technique exists that can determine the amount of Special Nuclear Materials (SNM) and Minor Actinides (MA) in high radioactive nuclear materials, including fresh and spent fuel, debris of melted fuel, transuranic (TRU) waste and next generation nuclear fuel (e.g. fuel for nuclear transmutation). A system based on a combination of the above mentioned techniques is proposed to assess the quantity of SNM and MA for a wide variety of applications, i.e. nuclear safeguards and proliferation, decommissioning and waste management. In addition, the use of the system for the detection of explosives and nuclear forensics will be investigated.

In this paper, the background and motivation of the program, the selected active neutron techniques and the master plan are described.

Keywords: NDA; measurement; active neutron technique

1. Introduction

In the field of nuclear material accountancy and safeguards, several material types are difficult to characterize for the content of SNM, i.e. the amount of ^{235}U and Pu, and MA, especially in the presence of a high radioactive nuclides. Material composition and difficulties vary strongly according to the specific application.

The development of nuclear transmutation technology using a fast reactor or an accelerator-driven system is strongly promoted in Japan. By transmuting MA, the burden for conditioning and disposal of high-level radioactive waste will be significantly reduced. The fuel for a nuclear transmutation scheme results from reprocessing of LWR fuel. It contains large quantities of MA (Np, Am, Cm) mixed with Pu [1] and can be categorized as next generation fuel. Characterization of such material by conventional passive neutron techniques will be strongly hampered by the presence of ^{244}Cm due to its high specific spontaneous fission rate. Hence, for conventional passive neutron techniques also the ^{244}Cm/^{240}Pu ratio is required. Unfortunately, due to high neutron emission rate γ-ray, spectroscopic measurements using HP-Ge detectors are excluded to determine this ratio. Hence, an alternative NDA technique is required for the nuclear material accountancy of this next generation fuel related to nuclear transmutation programmes.

In the field of nuclear security and safeguards, there is a strong emphasis on the control of spent fuel assemblies. Therefore, the US-DOE has promoted the “Next generation safeguards initiative’s (NGSI) spent fuel non-destructive assay project” with national laboratories and universities since 2009 [2]. Within this project various R&D projects are carried out. They mainly concentrate on verification of spent fuel assemblies of the present fuel cycle. Techniques to verify spent fuel from reprocessing activities, which is obviously more complicated, are not considered.

Decommissioning of nuclear power plants becomes an important activity. The characterisation of materials resulting from decommissioning activities in terms of the U and Pu content is required for material accountancy, classification of waste and clearance declarations. TRU waste is mostly contained in a 200 litter drum with a great variety in matrix material. In case of metal-based waste, resulting from fuel conversion and reprocessing facilities, conventional passive γ-ray techniques cannot be applied. In addition, results of passive neutron counting techniques might be biased due to the sensitivity of the results to the specific matrix materials.

To prevent the risk of a “dirty bomb” or “Radiological Dispersal Device (RDD)” as a radiological weapon, dedicated detection techniques are required. Since explosives always contain a substantial amount of nitrate, the presence of ^{14}N can be used as a signature. Hence, the development of techniques for the detection of ^{14}N is important for nuclear security. Such techniques can also be applied for the detection of plutonium-nitrate solutions.

Characterisation of debris of melted fuel resulting from the damaged reactors at the Fukushima Daiichi nuclear power plants is extremely challenging. This is due to the high yield of fission neutrons from spontaneous fission of ^{244}Cm and the high γ-ray dose from the decay of fission products. In addition, it is expected that the melted fuel will contain water, boron, concrete and structural materials. Unfortunately, the elemental (and isotopic) composition of such material cannot be predicted. Hence, conventional methods which rely on information about the elemental and isotopic composition cannot be applied. Although characterization of such debris for safeguards material accountancy will be required at the time of removal of the melted fuel, at the moment no official strategy exists for these materials. Possible scenarios have been investigated by the Japan Atomic Energy Agency (JAEA) and U.S. Department of Energy [3,4,5]. A more concrete solution resulted from a collaboration between Japan Atomic Energy Agency (JAEA) and the Joint Research Centre of the European Commission (JRC) [6,7]. A method referred to as Neutron Resonance Densitometry (NRD) was proposed. The method relies on Neutron Resonance Transmission Analysis (NRTA) combined with Neutron Resonance Capture Analysis (NRCA) and Prompt Gamma-ray Analysis (PGA). The results of this collaboration are very promising [8]. It is expected that the amount of ^{235}U and ^{239}Pu present in particle like debris samples from melted fuel can be determined within 2% [9]. It should be noted that NRTA is an absolute method which does not require any calibration by representative samples.

One can conclude that the development of innovative NDA techniques for nuclear material accountancy, safeguards, nuclear security and decommissioning is required. Based on the success of the JAEA/JRC NRD project [6,7,8] a new joint JAEA/JRC R&D project has been defined and its programme is discussed in this paper.

2. R&D programme and activities

The R&D programme is schematically summarised in Figure 1. The aim is to combine different active neutron interrogation techniques, i.e. DDA (Differential Die-Away Analysis), PGA (Prompt Gamma-ray Analysis) / NRCA (Neutron Resonance Capture Analysis), NRTA (Neutron Resonance Transmission Analysis) and DGS (Delayed Gamma Spectroscopy). Each of these techniques has its limitations and advantages. The main objective is to make optimum use of the complementarity between them.

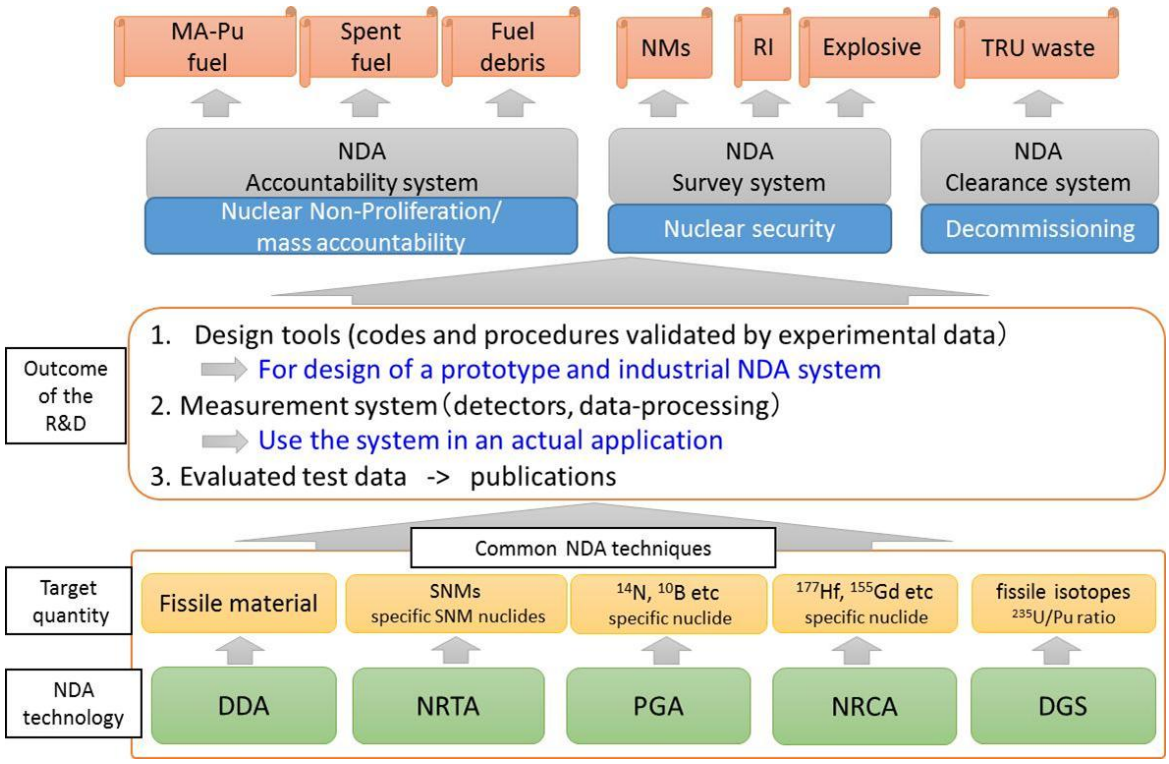

Figure 1: Schematic outline of the "Development of active neutron NDA techniques" programme

The project consists of three phases:

1. Development and experimental validation of simulation tools that are used to optimise the design of the system. In addition, the quality of the nuclear data and models that are needed for data processing and analysis, is verified.
2. Modelling, design and construction of a prototype system for measurements in a MA-Pu fuel conversion facility as part of nuclear transmutation activities.
3. Development and construction of an industrial NDA system to be installed in a MA-Pu fuel conversion facility.

In phase 1 Monte Carlo codes for neutron and γ-ray transport simulations, e.g. PHITS [10] and MVP [11] that have been developed by JAEA, will be validated together with the resonance analysis code REFIT [12]. The latter is used at JRC and JAEA for the analysis of cross section data. The prototype system will be used to demonstrate and optimize the performance of the techniques and the data processing and analysis procedures. In addition, dedicated measurements will be carried out at the nuclear facilities of the JRC, i.e. the neutron facilities at the Geel site and the PUNITA facility at the Ispra site. The results of these measurements are used to verify the nuclear data and will be part of the validation procedures.

To develop a full NDA system that can be used for a variety of applications and that fulfils the requirements of different authorities, a more extended international programme is required. The activities within such a programme should concentrate on:

- Standardization of methods for the performance assessment of active neutron interrogation NDA techniques
- Exchange of information and experience and pooling of resources

- Execution of common R&D projects

Instrument performances and measurement uncertainties are often evaluated based on experiments using working standards and procedures, which are both produced by the user of the instrument. Improved evaluation procedures could be part of a more international research framework. Such a framework should result in recommendations for the specifications, production and characterization of working reference materials which are traceable to primary standards or certified reference materials. Evidently, these requirements strongly depend on both the applied NDA technique and characteristics of the samples of interest. Ideally such a programme involves dissemination of good practice, exchange of staff and access to facilities. Experimental activities are foreseen at the following facilities:

- JAEA-NUCEF(NUclear fuel Cycle safety Engineering research Facility)-BECKY(Back-End Cycle Key element research facilitY)
- JAEA-PCDF(Plutonium Conversion Development Facility)
- GELINA (Geel Electron LINear Accelerator) at the JRC Geel site
- PUNITA(Pulsed Neutron Interrogation Test Assembly) at the JRC Ispra site

Such a pooling of resources and infrastructures will also result in a cost effective execution of R&D projects, e.g. the project will definitely benefit from combining JRC's experience in DDA measurements with JAEA's experience in Fast Neutron Direct Interrogation (FNDI) (see Appendix).

3. Basic principles

The basic principles of the active neutron interrogation techniques that will be integrated in the NDA system are summarised in Table 1. A final industrial system for DDA, PGA and DGS applications will be based on a 14 MeV D-T pulsed neutron source with a neutron intensity of at least 10^8 n/s. For neutron resonance analysis applications, in particular NRTA, the focus is on a pulsed electron linear accelerator with a pulse-width < 500 ns and a neutron intensity of at least 10^{10} n/s.

Table 1: Brief description of the studied active neutron interrogation techniques.

Technique	Principle	Quantity of interest
DDA	– Interrogation by a moderated pulsed neutron beam – Detection of neutron induced prompt fission neutrons – Make use of die-away time difference	Total fissile content
DGS (DGSI*)	– Interrogation by a moderated pulsed neutron beam – Detection of neutron induced prompt fission neutrons – Make use of die-away time difference	$^{235}U/^{239}Pu$ and $^{241}Pu/^{239}Pu$
NRTA	– Interrogation by (moderated) pulsed neutron beam – Detection of neutron transmission through a sample – Analysis of resonance transmission dips	Quantity of U and Pu isotopes (absolute measurement)
PGA/NRCA	– Interrogation by a (moderated) pulsed neutron beam – Detection of prompt γ-rays after (n,γ) reactions – Make use of prompt γ-ray energy combined with neutron resonance energy	Presence and quantity of specific nuclides

* delayed gamma-ray spectroscopy combined with self-interrogation

3.1. DDA

The DDA technique uses the detection of prompt fission neutrons, following neutron induced fission, as a means for quantifying the fissile mass. Normally small-sized D-T or D-D pulsed neutron generators are used as the interrogating external neutron source. The pulse width needs to be short (typically about 10 μs) compared to the interrogation time range and the neutron lifetime in the fission neutron detection system. The prompt fission neutrons are detected in thermal neutron detector modules, and can be separated from the interrogation neutrons and background signals. In this

context background signals include spontaneous neutrons, (α,n) neutrons, delayed neutrons, cosmic-ray induced events, random neutrons from the D-T generator and finally electronic noise.

The measured quantity in the DDA technique is the total fission rate of the sample. The key fissile nuclides are ^{235}U, ^{239}Pu and ^{241}Pu. If the ratios ^{235}U/^{239}Pu and ^{241}Pu/^{239}Pu can be evaluated by other means, the fission rate can be expressed as the mass of $^{239}Pu_{effective}$ ($=C_1{}^{235}U+{}^{239}Pu+C_2{}^{241}Pu$). In this way the DDA can be classified as a direct measurement technique for the fissile mass which is important for nuclear safeguards purposes.

The DDA technique has been investigated at many laboratories. For this reason several types of hardware and methodologies have been proposed. The method of thermal neutron interrogation is most common, the advantage being that fission cross-sections remain constant during the interrogation period. On the other hand, JAEA-DDA mainly uses fast and epi-thermal neutron interrogation (Fast Neutron Direct Interrogation method (FNDI)). FNDI has many difference points in methodology, hardware and software from thermal neutron DDA. An introduction to FNDI is given in the Appendix.

In the joint JAEA – JRC programme regarding the DDA technique various activities will be undertaken. This includes exchange of information of DDA methodology and hardware implementations, as well as experimental investigations. The experimental work includes investigation of important quantities such as the time and spatial distribution of the interrogating neutron flux inside relevant passive matrix materials, together with methods for estimating these variations through instrumentation placed outside the containers. For this purpose some standard containers and matrices will be produced. The standard matrices will be prepared with re-entrant tubes to allow insertion of small sealed Pu and U standards, as well as sensors for neutron flux measurements. Measurements will be carried out both at JAEA and JRC in parallel with Monte Carlo simulations of the experiments. The results of this collaboration will demonstrate the sensitivity of the method applied to the standard matrices, and propose the best suited measurement procedures for unknown samples of this kind.

3.2. NRTA

NRTA is an absolute NDA technique to determine the elemental and isotopic composition of materials, which have a thickness of a few cm. NRTA is based on the analysis of characteristic dips in a transmission spectrum resulting from a measurement of the attenuation of a pulsed neutron beam by the sample under investigation [8]. It relies on the time-of-flight technique, which is a standard technique for neutron resonance spectroscopy [12]. It is an absolute method and can be considered as one of the most accurate NDA techniques to quantify the amount of SNM and MA.

The experimental and analysis procedures for the analysis of homogeneous samples are well established [12]. The applicability of the technique for particle size debris samples of melted fuel resulting from severe nuclear accidents has been demonstrated by measurements at the GELINA facility of the JRC Geel site [8,13], as part of a previous JAEA/JRC collaboration project [7]. This project will be continued to define the optimum conditions, e.g. container dimensions, of the samples and the impact of the sample temperature by measurements at a 10m flight path of GELINA using an oven.

In this joint programme the applicability of NRTA for the characterization of fresh and spent nuclear fuel of the present and next generation fuel cycle and for nuclear decommissioning and waste management will be studied. This involves measurements with high radioactive material. Therefore, a radiation resistant neutron detector will be developed and tested.

In addition, reference samples will be produced to evaluate the performance of NRTA for a wide variety of applications e.g. characterization of fuel for transmutation applications, including powder samples and fresh and spent fuel pellets containing SNM and MA. Constraints of a NRTA system for these applications, i.e. minimum flight path length, pulse width and neutron intensity, will be defined.

A NRTA system will be designed and installed at the JAEA-NUCEF-BECKY facility. The system will be based on a D-T pulsed neutron source with a 10 μs pulse width. The implications of such a pulse width will be studied by predictions obtained from calculations with REFIT. These results will be validated by measurements at GELINA.

The REFIT code has been developed to determine resonance parameters from a resonance shape analysis of TOF cross section data. The code will be adapted and optimised for NRTA applications, i.e. for elemental and isotopic analysis starting from well-defined resonance parameters. A more user-friendly and full documented version will be produced.

3.3. PGA/NRCA

The PGA technique is a γ-ray spectroscopic NDA technique which is extensively used for elemental analysis. The technique relies on characteristic properties of prompt γ-rays emitted after a (n,γ) reaction. The applicability of PGA combined with Neutron Resonance Capture Analysis (NRCA) for nuclear material accountancy and nuclear security will be investigated. In particular the use of PGA/NRCA to determine the elemental and isotopic composition of fuel containing MA will be verified.

PGA can also be applied to detect the presence of SNM. For example, the detection of γ-rays following neutron capture in ^{14}N is a signature for nitride fuel. The detection of high-energy γ-rays from neutron capture in light elements like H, C, N and O can also be used for the detection of explosives.

For the majority of elements NRCA has a more favourable detection limit compared to NRTA. The difference is roughly one order of magnitude. For elements with resonances between 1 eV and 100 eV the detection limit is in the range of parts per million (ppm). Since NRCA is very sensitive when elements are present as impurities or trace elements, it can be a useful tool for nuclear forensics.

Reference samples will be produced and a performance assessment will be carried out using a D-T pulsed neutron generator installed at the JAEA-NUCEF-BECKY facility. High energy prompt γ-rays will be detected with a large $LaBr_3$ scintillator detector. The testing of such a detector and optimization of its shielding [17] were part of the previous JAEA/JRC collaboration project.

3.4. DGS

DGS has already been proposed as a NDA technique for the characterization of spent nuclear fuel [18]. The experimental observables are high energetic γ-rays which are emitted after the decay of fission products. Use is made of the difference in fission fragment yields of ^{235}U, ^{239}Pu and ^{241}Pu. The amount of ^{235}U and ^{241}Pu relative to ^{239}Pu is derived from the intensity of the emitted delayed γ-rays. Hence, these results combined with the total amount of fissile material resulting from DDA measurements are valuable input data for nuclear safeguards applications. It is intended to use the technique for the verification of Pu nitrate solutions in a MA-Pu conversion facility. It is planned to perform a pilot experiment at JAEA-PCDF.

4. Prototype system

JAEA intends to build a multipurpose active neutron interrogation system based on a D-T pulsed neutron source with a maximum neutron intensity of 10^9 s^{-1}, a 10 μs pulse width and a 100 Hz nominal frequency. A layout of the system, which combines DDA, NRTA and PGA/NRCA, is shown in Figure 2. The system will be optimised for measurements of low radioactive samples containing SNM. The design and construction of the device are scheduled for 2015 and 2016. The first measurements are planned in 2017.

The DDA part consists of a neutron reflector and moderator placed close to the neutron generator, a sample holder on a rotating table and a neutron detector bank. The NRTA part includes a moderator, a sample changer, a vacuum tube with collimators and a neutron detector placed at 5 m distance from the neutron producing target. The PGA part consists of a sample holder and γ-ray detector.

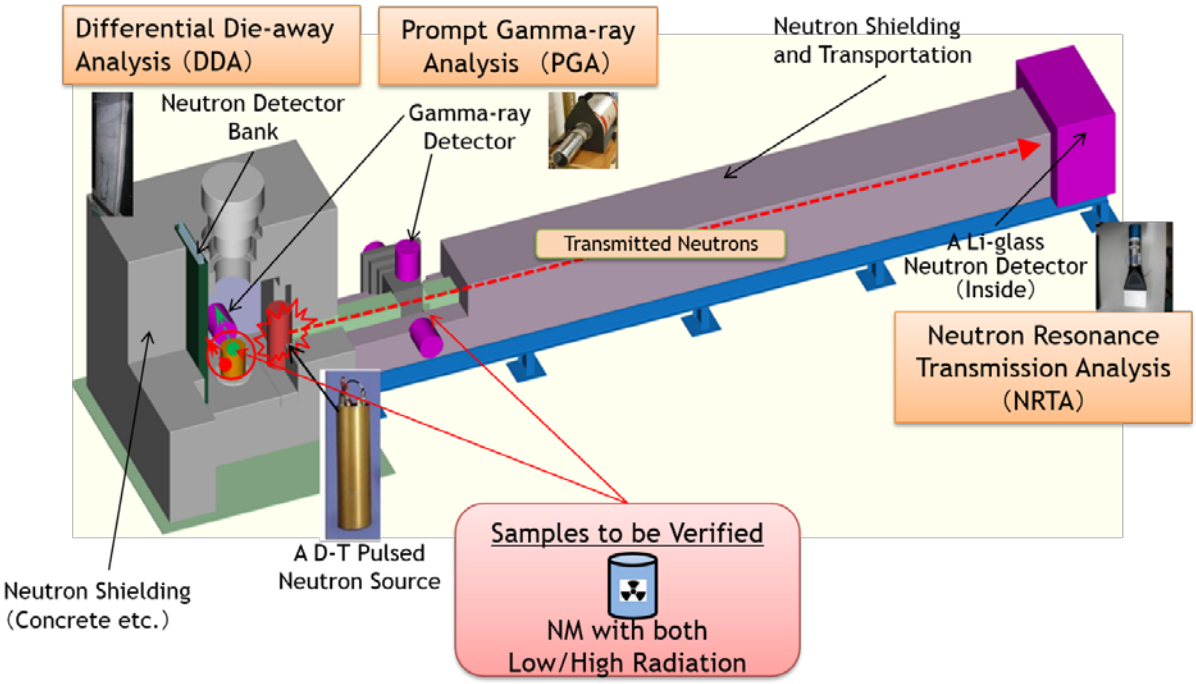

Figure 2: Layout of an active neutron NDA prototype system combining DDA, PGA and NRTA.

5. Summary

JAEA in collaboration with JRC launched a new R&D programme "Development of active neutron interrogation techniques". The programme concentrates on a method that combines complementary active neutron techniques, i.e. DDA, NRTA, PGA/NRCA and DGS. Such a combination of techniques should result in a more accurate determination of the amount of SNM and MA in low and high radioactive nuclear materials of the present and next generation fuel cycle. The method can be applied for nuclear safety, security and safeguards applications, e.g. characterization of nuclear fuel (including spent fuel, fuel for nuclear transmutation and melted fuel), nuclear decommissioning and detection of explosives. To demonstrate its potential a prototype facility using a high intensity D-T pulsed neutron generator will be constructed. The programme also includes a performance assessment of different NDA techniques using dedicated reference samples and procedures based on a more extended international collaborative effort.

6. Acknowledgements

We would like to acknowledge the Japanese government (MEXT; Ministry of Education, Culture, Sports & Technology).

7. Appendix

Fast Neutron Direct Interrogation (FNDI) is a DDA type of NDA technique [19]. The experimental observable is the total number of fission neutrons induced by interrogating the sample with a pulsed 14 MeV neutron source. The method can be used to verify the content of 200 l waste drums for the amount of SNM.

The interrogation with a non-thermalized neutron source has some fundamental difficulties such as variations in the source neutron spectrum as function of time, matrix materials, sample size, sample location etc. Some advantages however also exist which are worthwhile investigating.
One of the differences between thermal neutron DDA and FNDI is the spatial distribution of neutron induced fission events in the sample, as illustrated in Figure 3 for an ideal case. Due to this difference

results obtained with FNDI may in some cases prove to be less sensitive to the spatial distribution of the nuclear material in the sample as those derived from the more conventional thermal DDA systems.

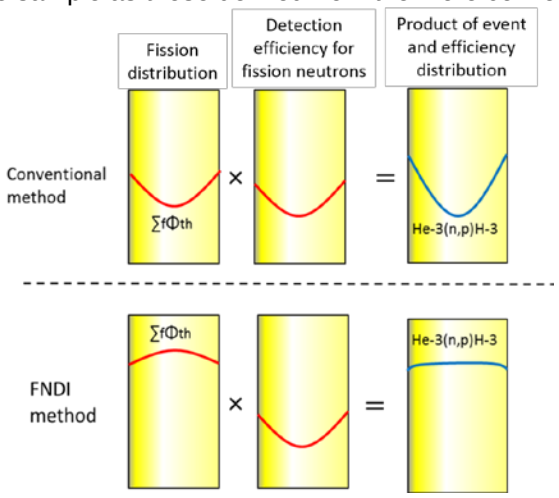

Figure 3: Illustration of the spatial distribution of neutron induced fission events and the detection probability for a conventional thermal neutron DDA and FNDI.

Typical die-away curves, i.e. counts as a function of time after the neutron pulse, are shown in Figure 4. The component due to the detection of induced fission neutrons can be clearly distinguished from the one caused by detection of interrogating neutrons. A least squares fit can be applied to derive the amplitude and die-away time of the two components. The total amount of fissile material present in the sample is estimated using quantities such as the amplitude and die-away time of the induced fission neutron component. The FNDI apparatus JAWAS-N installed at JAEA-Ningyo-toge is shown in Figure 5.a. Results from measurements at this facility with waste drums containing uranium are shown in Figure 5.b.

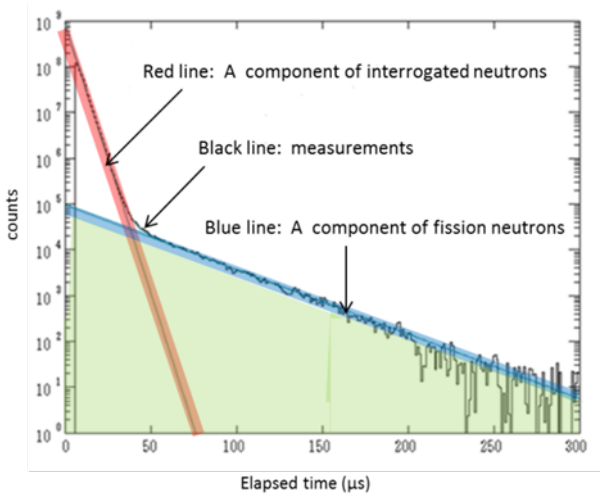

Figure 4: A typical die-away curve resulting from FNDI measurements at the JAWAS-N facility. The total number of detected neutrons is plotted as a function of time after the creation of the pulsed neutron beam.

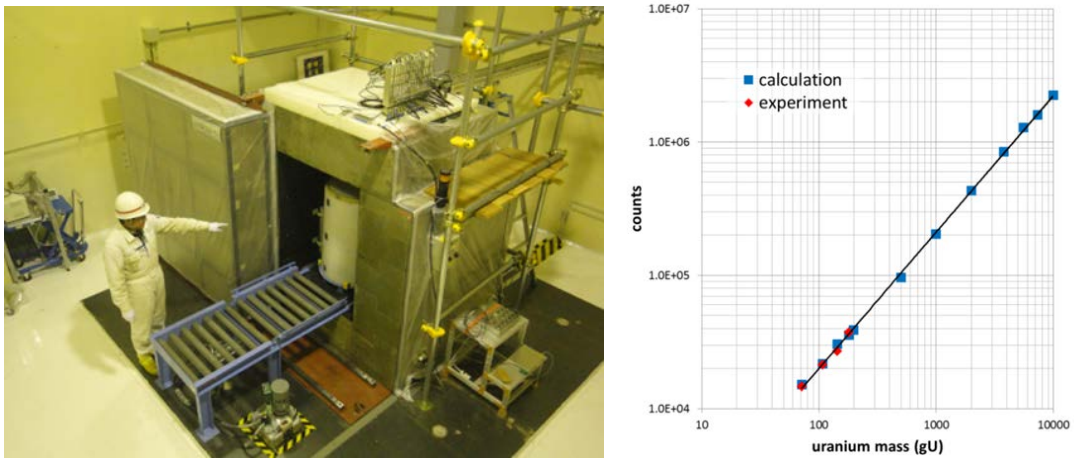

(a) FNDI apparatus "JAWAS-N" (b) verification result

Figure 5: A photograph of the JAWAS-N facility (a) and the results of measurements with different uranium samples at this facility (b). In the latter the amplitude of the induced prompt fission neutrons is plotted as a function the total uranium mass.

8. References

[1] Tsujimoto K et al.; *Neutronics Design for Lead-Bismuth Cooled Accelerator-Driven System for Transmutation of Minor Actinide*; Journal of Nuclear Science and Technology; 41[1]; 2004; p 21-36.

[2] Tobin S et al.; *Technical Cross-cutting Issues for the Next Generation Safeguards Initiative's Spent Fuel Nondestructive Assay Project*; Journal of Nuclear Materials Management, XL[3], 2012; p 18-24.

[3] Heinberg C et al.; *The Status of the Japanese Project on Material Accountancy of Fuel Debris and U.S.-Japan Cooperation on Survey of Technologies for Nuclear Material Accountancy at Fukushima Daiichi Nuclear Power Plant*; Proceedings of INMM 55th Annual Meeting; Atlanta, Georgia, USA; 2014; #535.

[4] Nagatani T et al.; *Recommendations for Measurement Systems for Nuclear Material Accountancy of Fukushima Daiichi Fuel Debris: Neutron Technologies*; Proceedings of INMM 55th Annual Meeting; Atlanta, Georgia, USA; 2014; #534.

[5] Tomikawa H et al.; *Recommendations for Measurement Systems for Nuclear Material Accountancy of Fukushima Daiichi Fuel Debris: Gamma Technologies*; Proceedings of INMM 55th Annual Meeting; Atlanta, Georgia, USA; 2014; #529.

[6] *The Hague Nuclear Security Summit Communique*; http://www.nss2014.com/en; 2014; #2.

[7] Harada H., Kitatani F., Koizumi M., Tsuchiya H., Takamine J., Kureta M., Iimura H., Seya M., Becker B., Kopecky S., Schillebeeckx P., ., Proceedings of the 35th ESARDA symposium on Safeguards and Nuclear Non-Proliferation, 28 – 30 May 2013, Brugge (Belgium)

[8] P. Schillebeeckx, S. Abousahl, B. Becker, A. Borella, H. Harada, K. Kauwenberghs, F. Kitatani, M. Koizumi, S. Kopecky, A. Moens, G. Sibbens and H. Tsuchiya, Development of Neutron Resonance Densitometry at the GELINA TOF Facility, ESARDA Bulletin 50, 9 – 17 (2013).

[9] P. Schillebeeckx, B. Becker, H. Harada and S. Kopecky. Neutron resonance Spectroscopy for the characterisation of materials and objects. JRC Science and Policy Reports. European Commission, Joint Research Centre Institute for Reference Materials and Methods, Report EUR 26848-EN (2014).

[10] Sato T et al.; *Particle and Heavy Ion Transport code System, PHITS, version 2.52;* Journal of Nuclear Science and Technology; 50[9]; 2013; p 913-923.

[11] Nagaya Y et al.; *MVP/GMVP II: General Purpose Monte Carlo Codes for Neutron and Photon Transport Calculations based on Continues Energy and Multigroup Methods;* JAERI 1348; 2004.

[12] Moxon M and Brisland J; *GEEL REFIT, "A least squares fitting program for resonance analysis of neutron transmission and capture data computer code"*; AEA-InTec-0630; AEA Technology; October 1991.

[13] P. Schillebeeckx, B. Becker, Y. Danon, K. Guber, H. Harada, J. Heyse, A.R. Junghans, S. Kopecky, C. Massimi, M.C. Moxon, N. Otuka, I. Sirakov and K. Volev, Determination of Resonance Parameters and their Covariances from Neutron Induced Reaction Cross Section Data, Nucl. Data Sheets 113, 3054 – 3100 (2012).

[14] B. Becker, S. Kopecky, H. Harada and P. Schillebeeckx, Measurement of the direct particle transport through stochastic media using neutron resonance transmission analysis, Eur. Phys. J. Plus 129, 58 – 59 (2014)

[15] Israelashvili I et al.; *Fissile mass estimation by pulsed neutron source interrogation*; Nuclear Instruments and Methods in Physics Research A; 785; 2015; p 14-20.

[16] Haruyama M et al.; *Improvement of Detection Limit in 14 MeV Neutron Direct Interrogation Method by Decreasing Background*; Journal of Nuclear Science and Technology; 45[5]; 2008; p 432-440.

[17] Segawa M et al.; *Development of three-dimensional prompt g-ray analysis system*; Nuclear Instruments and Methods in Physics Research A; 605; 2009; p 54-56.

[18] Koizumi M et al.; *Development of a $LaBr_3$ scintillation detector system for neutron resonance densitometry (NRD)*; Proceedings of INMM 55th Annual Meeting; Atlanta, Georgia, USA; 2014; #237.

[19] Rodriguez D et al.; *Utilization Delayed Gamma-Rays to Establish High-Precision Fission Yields*; Proceedings of INMM 55th Annual Meeting; Atlanta, Georgia, USA; 2014; #543.

[20] Komeda M et al.; *Analytical study on uranium measurement in uranium waste drums by the fast neutron direct interrogation method*; Proceedings of INMM 55th Annual Meeting; Atlanta, Georgia, USA; 2014; #250.

Integrated NDA User Laboratories at the JRC in Ispra for Nuclear Safeguards and Nuclear Security

W. A. M. Janssens, K. Abbas, R. Berndt, V. Berthou, C. Carrapico, J. M. Crochemore, G. Eklund, V. Forcina, M. Marin-Ferrer, P. Mortreau, B. Pedersen, P. Peerani, F. Rosas, A. Rozite, E. Roesgen, H. Tagziria[1] and A. Tomanin

Nuclear Security Unit, ITU, Joint Research Centre,
European Commission, Via Fermi 2749, I-21027 Ispra (Va), Italy

Abstract

For many decades, the JRC's Nuclear Security Unit in Ispra (Italy) has continued to play an important role in international nuclear safeguards and nuclear security based on sound R&D programmes in non-destructive analysis (NDA) methods and instrumentation, testing and benchmarking of detection systems, user accessibility to laboratories and reference material, together with a comprehensive training programme. Beneficiaries of these programmes have generally been the European Commission DG's (ENER, HOME, DEVCO, TAXUD, RTD), the IAEA, EU research institutions, EU member states and many international partners.

The need for a modern and integrated infrastructure to promote synergy and efficient operation of all activities has been recognised and a new laboratory named INS3L (**I**spra **N**uclear **S**afeguards, **S**ecurity and **S**tandardization **L**aboratory) which will house all activities and facilities under one roof has indeed been approved and is now in its planning phase with its completion expected within about three years.

This paper aims to describe the activities performed with reference to relevant publications and will present the conceptual design of the new INS3L as a user laboratory within an integrated approach that shall benefit all users and stakeholders, partners and EU member states in general.

Keywords: NDA, nuclear safeguards, nuclear security, R&D, training, international co-operation, INS3L

1. Introduction

Three decades ago Walter Hage working at the JRC's Nuclear Security Unit in Ispra (Italy) published his fundamental papers on the Point Model for neutron correlation counting. The legacy of Walter and his co-workers is the foundation on which the unit still today reinforces its important role in international nuclear safeguards and nuclear security built on a sound R&D programme in non-destructive analysis (NDA) methods and instrumentation, user accessibility to laboratories and reference material, and the various training programmes offered to end users and stakeholders.

In essence, the activities currently carried out within the unit can be subdivided as follows:

- R&D in NDA techniques for nuclear safeguards and nuclear security
- Scientific/Technical support to ENER, IAEA and EU member states
- Instrument testing, validation, benchmarking and standardization
- Monte Carlo simulation and modeling combined with measurements for validation
- Training of inspectors in nuclear safeguards
- Training of Front Line officers (FLO) and Train the Trainer of FLO in nuclear security and detection of nuclear and radioactive materials.

Laboratories and facilities such as PERLA, PUNITA, ITRAP Dynamic, ITRAP Static and EUSECTRA-Ispra combined with the availability of reference NDA samples of nuclear materials have been instrumental for all the above-mentioned work areas. Recent collaborative projects such as

[1] Corresponding author: E-mail: hamid.tagziria@jrc.ec.europa.eu

SCINTILLA, ITRAP+10, ^{3}He alternatives R&D and METRODECOM (in support to decommissioning) fundamentally depend and thrive on them.

International projects of this kind are anticipated for the foreseeable future, and the need of a modern and integrated infrastructure to promote synergy and efficient operation has been recognised. The construction of a new laboratory named INS3L (**I**spra **N**uclear **S**afeguards, **S**ecurity and **S**tandardization **L**aboratory), which will house all activities and facilities under one roof has indeed been approved and has entered the planning phase with its completion expected within 3 years.

This paper aims to describe the activities performed giving some of the most important results and publications as well as the conceptual design of the new INS3L as a user laboratory within an integrated approach for the benefit of all users, stakeholders, international collaborators and EU member states in general.

2. Facilities for R&D, Testing, Benchmarking and Standardization

2.1 PERLA Laboratory for R&D and Training in Nuclear Safeguards

A substantial part of the safeguards activities performed at ITU is carried out in the PERformance LAboratory (PERLA) at the Ispra site of JRC where Non-Destructive Analysis (NDA) methods are applied for the determination of the isotopic composition of Uranium and Plutonium by gamma spectrometry and their masses by passive and active neutron measurements or calorimetry, used either individually or in integrated systems. The main activities performed therein are generally related to the:

- Assessment and performance evaluation of non-destructive assay (NDA) techniques applied to nuclear safeguards and security.
- R&D, Testing, Calibration of safeguards instrumentation and associated Data acquisition systems and software
- Training of Inspectors (IAEA/Euratom)
- External user laboratories for partners, member states, DG-ENER and IAEA and universities etc. for both nuclear safeguards and nuclear security

2.1.1 Gamma measurements

Changes in the fuel cycle or new facilities continuously require new solutions for safeguards. Currently there a number being carried out in PERLA laboratory mostly on request from either DG-ENER or IAEA [5-11]. For instance the digital MCA-527 was studied in view of its use as a gamma and neutron spectrometry system thus replacing old electronics [5-6]. Important contributions were also made in PERLA for the development of a Prototype Tomographic Spent-Fuel Detector System [8, 9].

Support to customers represents an important part of PERLA activities whereby for instance the EURATOM measurement stations in the plutonium storages (units UP2 and UP3) in La Hague (France) [15] were replaced and an unattended monitoring system for plutonium storage in Magnox plant (United Kingdom) was developed.

2.1.2 Neutron Measurements

PERLA has been systematically used to train inspectors for the classical applications of active and passive neutron counting: HLNCC, AWCC, PSMC, UNCL. The availability of well characterized nuclear material standards (U, Pu, MOX, etc.) has also allowed performing here the calibration of most Euratom instrumentation prior to field deployment. In addition to the support activities described above an extensive programme of R&D has been carried out. A number of innovative neutron counters have been designed and built within the unit in order to overcome some inspection issues not solved by the commercial instruments. As examples one can mention the High Efficiency Passive Counter (HEPC) for large LEU containers in fabrication plants [17], the Scrap Neutron Multiplicity Counter (SNMC) for MOX fuel plants [18], the can monitor for Melox [19].

In recent years the neutron research has focused on finding suitable alternatives to He-3 and several replacement candidates have been investigated and tested in Ispra: boron-based (like BF3 or boron coated proportional tubes), lithium-based (like LiZnS blades [this symposium] and Li-coated Si pads [20]) and organic scintillators (liquid and plastic, like the LS-NCC collar developed in collaboration with IAEA [12, 21]).

The experimental work carried out within the laboratory is often extensively associated with numerical simulation activities using Monte Carlo methods. The nuclear security unit in Ispra has in particular developed the MCNP-PTA code specifically dedicated to modelling neutron coincidence and multiplicity counters [22]. This has allowed to pioneer and demonstrate the possibility to replace empirical by numerical calibration for applications where either standards are not readily available or detectors not easily accessible [22] for instance.

Within the unit, the performance of the various NDA counters and detectors are indeed routinely assessed and their models validated and optimised using Monte Carlo simulations codes such as MCNP and its extensions (MCNP-PTA, MCNP-Polimi) and GEANT in combination with good measurements using reference nuclear materials. Examples of such projects are characterization of a cubic EJ-309 liquid scintillator detector [12], the calibration and Monte Carlo Modelling (MCNP) of a fast-UNCL for the IAEA [13], and development, characterisation and Monte Carlo modelling (MCNP-Polimi) a liquid scintillator based neutron coincidence counter for the IAEA with the PhD thesis [28].

2.1.3 Calorimetry Measurements

Calorimetry remains one of the most accurate non-destructive assay (NDA) technique for materials containing plutonium, when combined with accurate isotopic analysis using high resolution gamma-ray spectrometry. This is mainly due to the fact that the technique is accurate, unbiased and unaffected by geometry and sample matrix effects due to the fact that the magnitude of the heat flux leaving the sample container at equilibrium is not affected by the matrix. Furthermore calorimetry requires no physical standards to represent the samples of interest. In late 90's the JRC's Performance Laboratory (PERLA) in Ispra (Italy) purchased a compact and transportable small sample calorimeter (SSCAL model 601C) shown in Figure 1, able to accurately measure samples of Pu bearing materials corresponding to powers of less than 20 mW with a precision better than 0.2% at 10 mW powers. Calorimetry technique can be used as an NDA measurement tool in order to reduce the number of samples subjected to costly destructive analysis.

Figure 1: Photo of the SSCAL

The SSCAL has since been extensively upgraded and tested and its performance evaluated as the first of a new generation of plutonium calorimeters based on thermopile technology. It was used for

instance at the Institute of Isotopes of the Hungarian Academy of Science in Budapest for the characterisation [23], as dictated by IAEA safeguards requirements, of about 250 Pu-Be and Am-Be sources that came into the country during the soviet union era mainly. More recently, seven Am sources produced by ITU to be used cross section measurements by the JRC-IRMM have been measured using calorimetry in conjunction to gamma and neutron spectrometry and these measurements were compared to declared masses measured at ITU using various means [24]. In conjunction with calorimetry measurements in stable and controllable humidity and temperature, the SSCAL is often used within a large (4 by 4 m) climatic chamber in our laboratory.

2.2 PUNITA for R&D in nuclear safeguards and Security

The **Pu**lsed **N**eutron **I**nterrogation **T**est **A**ssembly (PUNITA) at the Joint Research Centre in Ispra is designed for experimental studies in NDA methods and instrumentation for nuclear safeguards and security applications. The facility is composed of a large graphite liner surrounding the central sample cavity. The (D–T) pulsed neutron generator, the sample and the scintillation detector are located inside the sample cavity. Various permanently installed neutron detectors are located in and around the instrument. The dimensions of the sample cavity are 500 mm by 500 mm by 800 mm. This design yields a relatively high neutron flux in the cavity and provides flexibility with respect to detector configurations. As such PUNITA is a versatile tool for studying detection methods although not an instrument intended for practical applications [32].
The pulsing of the neutron generator (Model A-211 from Thermo Fisher Scientific Inc.) at 100 Hz is tailored to the exponential decay of the thermal neutron flux in the sample cavity with a decay time of about 1.0 ms. The interrogating thermal flux peaks at about 250 μs after the 14-MeV neutron burst. Due to the pulsing of both the Penning ion source and the acceleration voltage this generator model is able to produce a sharp burst of 14-MeV neutrons with absolutely no neutron emission between bursts. This fact together with the very short duty cycle of 0.001 of the generator allows separation of the neutron interrogation into a “fast period” (from zero to 100 μs) and a “thermal period” (from 250μs to 9 ms). Figure 2 shows a vertical cross section of PUNITA with the permanently installed neutron detectors visible.

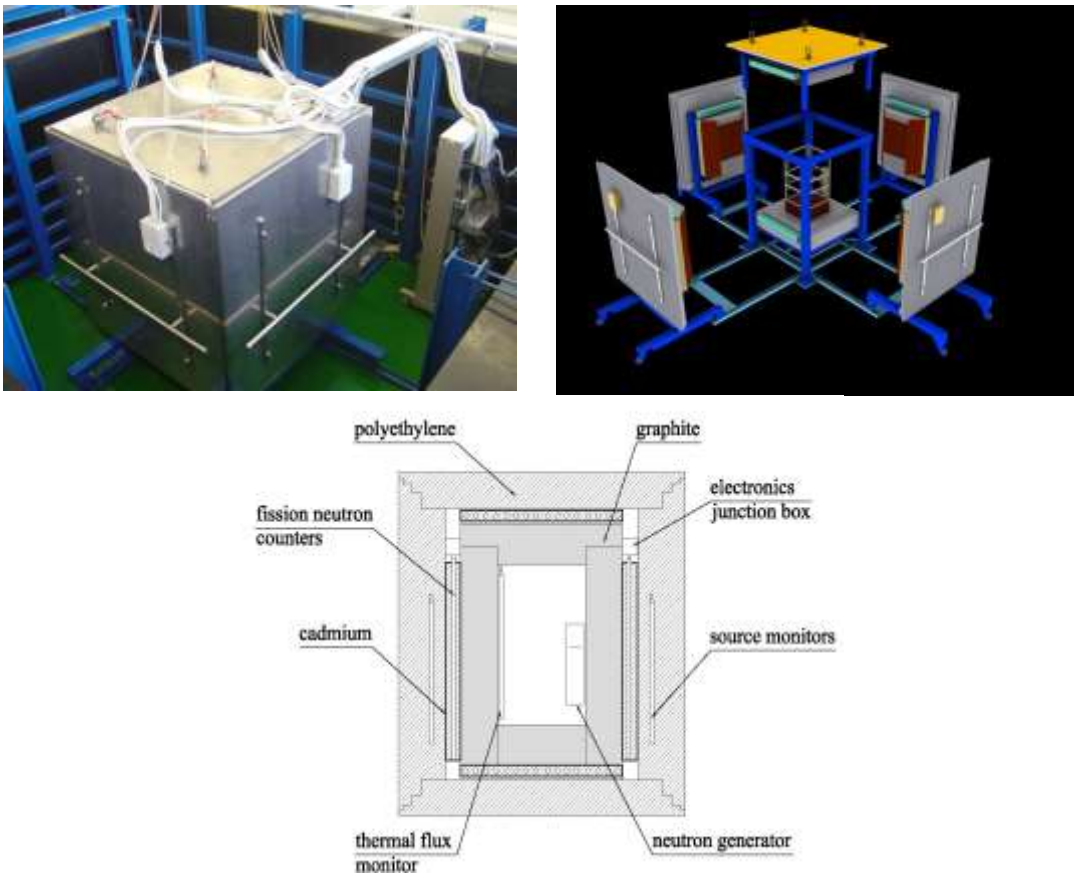

Figure 2: Pulsed Neutron Interrogation Test Assembly (PUNITA)

Various collaborative projects with external partners such as CEA of France and NRCN of Israel are carried out in the areas of nuclear safeguards and security. An example is the feasibility study of using a pulsed neutron generator in a graphite assembly together with liquid scintillation detectors for the detection of special nuclear materials (SNM). In this study epi-thermal and thermal source neutrons induce fission in fissile material present in the sample. By means of pulse shape discrimination (PSD) the detector signals from fast fission neutrons are easily identified among the signals from gamma rays and the interrogating thermal neutrons. The method was found to have potential in applications for detection of SNM in shielded containers such as air cargo containers (ULD) [33].

2.2 ITRAP for testing, benchmarking and standardisation

The ITRAP laboratories have been built in the frame of the ITRAP+10 project funded by DG HOME [1]. The purpose was to test detection equipment used in nuclear security to intercept illicit trafficking of nuclear and radiological material at borders and other nodal points. The laboratories have been explicitly designed in order to execute radiological performance tests of detectors and verify their compliance with international standards (IEC, ANSI, IAEA guidelines, etc.). They are constituted from two halls: the static and dynamic laboratory.

The ITRAP laboratory for static tests has been designed to host irradiation tests for small equipment, such as pagers, hand-held instruments and backpacks. Typical tests performed here cover the response to gamma/neutron sources (including single/multiple sources, bare/shielded sources, mixed photon/beta/neutron field, high over-range fields) and time-to-alarm measurement. The laboratory is equipped with two irradiators specifically designed by JRC for this purpose: the Gamma and Neutron Irradiators (GNIR and NNIR), see figure 3.

The ITRAP laboratory for dynamic tests has been designed to host irradiation tests with moving sources in order to reproduce transit situations at fixed portals or search with moving detectors. The laboratory is placed in a large hall hosting a conveyor system placed on 30-meter long rails, see figure 4. The conveyor can be programmed to perform multiple passages at predefined speed: typical testing speeds are 8 km/h (2.2 m/s) for vehicular portals and 1.2 m/s for pedestrian portals, and 0.2 m/s for handhelds (to simulate a manual scanning). A number of instruments can be placed beside the rails and exposed to sources mounted on the conveyor passing by the detectors. The conveyor has a vertical bar on which the source holder can be raised to the required height. In addition to the ITRAP+10 project (now extended to phase-II) where approximately 50 units of commercial detection instruments have been intensively tested, the laboratories have served as a basis for preliminary evaluation of innovative and prototypic solutions, like in the SCINTILLA and MODES (both FP7) projects and the FLASH project (collaboration with Arktis-AWE-US/DHS/DNDO).

Figure 3: ITRAP static laboratory with irradiators (gamma and neutron)

Figure 4: ITRAP dynamic laboratory with conveyor rail

2.4 EUSECTRA-Ispra for training in Nuclear Security

Over the last two decades, increasing security concerns with respect to illicit trafficking of nuclear and other radioactive materials were largely acknowledged by the international community. The Joint Research Centre was consequently tasked by the European Commission (DG HOME) to set up a dedicated European Nuclear Security Training Centre (EUSECTRA) as recommended by the EU CBRN Action plan adopted by the European Council in December 2009. The aim of such training centre is to train front line officers and their trainer on the radiation detection techniques and procedures at borders to detect and interdict illicit trafficking of radioactive and nuclear materials.

Based on the unique combination of scientific expertise, specific technical infrastructure and availability of a wide range of nuclear materials, long standing experience in training, the JRC Ispra established the first pilot training centre in 2009. It require the acquisition of various type of fixed and handheld equipment, some of them were donated by the US Department of Energy, and the establishment of dedicated classroom and Central Alarm Systems room. Further duplicated at the JRC Karlsruhe and designated as EUSECTRA, the training centres complement national training efforts by providing realistic scenarios with the availability of special nuclear material. The training program offers a unique opportunity for trainees to see and experience actual materials and commodities. This is one of the few places in the world where a wide range of samples of plutonium and uranium of different isotopic compositions can be used for training in detection, categorization and characterization of nuclear material. EUSECTRA-Ispra facility (Figures 5 and 6) provides different models and type of handheld equipment an indoor training area to simulate airport conditions, equipped with pedestrian portal monitors and outdoor facilities with different types of radiation portal monitors to simulate land border or port infrastructure.

The facility is used to carry training courses for various types of customers, US DoE, IAEA, DG DEVCO under the Instrument for Stability projects, DG TAXUD, and host participants from Europe, Africa, Asia, etc. It hosts about 15 to 20 participants per session, in English or in the participants' language with interpretation and syllabus translation. The EUSECTRA Ispra is hosting about 10 sessions per year since 2009.

In addition to providing training to many customers, the facility is also available to run R&D projects to improve the capability and performance of detection of illicit trafficking of radioactive and nuclear material. A scientific exploratory research on the effect of rainfall on the performance of radiation portal monitors, as well as a PhD research on the improvement of NORMs discrimination on radiation portal monitors have been conducted in this facility [27].

Figure 5: use of handheld device at EUSECTRA

Figure 6: use of RPM at EUSECTRA

3. Training and Education

The Nuclear Security Unit of the Joint Research Centre based on the Ispra site has a long standing experience in providing education and training (E&T) to a large variety of customers and audience in the following fields of expertise:

- Nuclear Safeguards (non-destructive analysis, containment, surveillance, sealing and advanced verification techniques, mass/volume measurements and innovative process monitoring): both training and academically recognized courses
- Nuclear Security (detection of and response to radioactive and nuclear material out of regulatory control)
- Non Proliferation and Strategic Trade Control

In recent years the unit started providing training in the field of Nuclear Decommissioning and Waste Management. This strong portfolio of E&T activities has been gradually developed and established to support the EU and international policies. It is based on long standing technical and scientific, unique infrastructure, laboratories and materials, and clearly identified customers' needs. This training support is complementary to the unit core's activities in Research and Development. The development of technical solutions and their deployment in field as well the development of new measurement techniques and safeguards approaches/methodologies necessitates an adequate training program that can only be performed by the experts.

The NDA safeguards training, the ESARDA education course, the nuclear security trainings and the nuclear decommissioning school are all performed on site making use of the unique set of facilities, infrastructures, instrumentations, nuclear materials and expertise presents at the nuclear security unit in Ispra. It is foreseen that these shall be further strengthened in the new INS3L laboratory. As an indication, the unit has trained 266 persons in 2013, and 201 persons in 2014, in the above mentioned fields of NDA for nuclear safeguards and nuclear security.

3.1. Nuclear Safeguards

For over thirty years, the Nuclear Security Unit has provided training to nuclear safeguards inspectors of DG ENER and the IAEA which is essential to the proper implementation of the international safeguards and in line with the JRC mandate to support DG ENER under the EURATOM treaty. It covers three of the four main categories of activities of nuclear safeguards: non-destructive analysis (gamma spectrometry and neutron counting), process monitoring and containment and surveillance. These activities belong to the core business of the unit, being driven by this R&D and its results, i.e. the development of new technical solutions and methodologies for the nuclear inspectors on their requests. These solutions and instrumentation are routinely used by the inspectorates and require continuous training. An average of 12 weeks of safeguards courses per year are held, mostly in the Ispra site and laboratories, and on demand also in an operational facilities abroad. All the training performed for the IAEA inspectors is done under the EC support programme to the IAEA. A complete description of these courses is given at: http://npns.jrc.ec.europa.eu/web_inspector_v2/01-courses.php

Figure 7: Training of nuclear inspectors

In addition to this broad spectrum of technical training courses, the Nuclear Security Unit has been for the last ten years providing the ESARDA education course for nuclear safeguards and non-proliferation, under the umbrella of ESARDA. This unique education course can complement nuclear engineering and other universities studies and is recognized for 3 ECTS (European Credit Transfer System). A syllabus was published and the course is yearly run with a panel of internationally recognized experts in the field. The course is now being duplicated outside Europe with funding from the European Commission, DG DEVCO, with two courses for South East Asian states hosted in Malaysia in 2013 and in Thailand in 2014 [2-4]. A complete description of the ESARDA course is given at: https://esarda.jrc.ec.europa.eu/

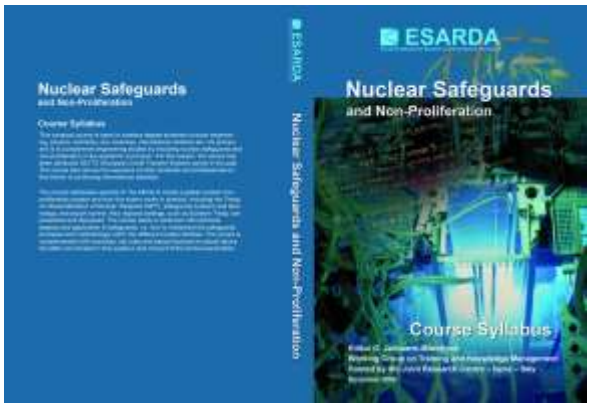

Figure 8 : ESARDA course syllabus

Figure 9: participants at ESARDA course

3.2. Nuclear Security

The unit has more than 5 years experience in Nuclear Security training, with a focus on detection and response to radioactive and nuclear material out of regulatory control. The EUSECTRA training centre pilot site has been established and inaugurated in 2009 on the Ispra site, in line with the DG HOME 2009 CBRN Action Plan recommendations. Specific infrastructures, a dedicated set of detection instruments and curriculum syllabus has been established and developed in order to provide specialised training to border guards, customs, advanced operators and their trainers in the field of radiation detection techniques and response procedures [31]. This one-week training course in Ispra is fundamentally based on hands-on exercises using genuine nuclear materials and a variety of nuclear detection tools. Occasionally those trainings are also held in the field in a relevant setting (e.g. border crossing points in partner country) under outreach projects funded by DG DEVCO and its Instrument contributing to Stability and Peace and implemented by JRC. The syllabus both for Front Line Officers training and train the trainer training has been developed and approved by the Border Monitoring Working Group in collaboration with the IAEA and the US DoE which are both customers of the training centre. Around 10 training courses per year are held in EUSECTRA-Ispra with about 15 participants per 5 days long session.

4. User Laboratories and International Collaborations

Many projects embarked on by the Nuclear Security Unit in Ispra provide valuable access to the laboratories, nuclear standards and expertise on site for the benefit of manufacturers of equipment, research laboratories, universities and generally member states in their developments and research work. We refer to this as user laboratory herein.

PERLA in particular has over the years offered to external users easy access to nuclear material and NDA expertise for their development work, and has welcome several workshops per year, the most recent of which are Scintilla [16] R&D, testing and benchmark campaigns described below, the testing and benchmarking of alternatives to ^{3}He based neutron coincidence counting (October 2014) within a

DOE-Euratom/JRC action sheet with the participation of IAEA and JAEA and finally the JRC-IAEA-EURATOM test campaigns for the development of MCA-527.

SCINTILLA (EC FP7 project- www.scintilla-project.eu) mentioned above is an example of a wide reaching project based on usage cases and customer demands and aims to a) build an innovative and comprehensive toolbox of devices and best-of-breed technologies for the enhanced detection and identification of difficult-to-detect radioactive and nuclear material and b) find a reliable alternative to ^{3}He based neutron detection systems c) offer test bed and benchmarking services at JRC laboratories in Ispra to its partners and beyond d) Establish the Scintilla Partnership Network to encourage collaborations and synergies in the related fields, bringing together manufacturers, scientists, other EC funded projects and thus building a strong network around nuclear security. EU partners within the consortium are: JRC, CEA, Symetrica, INFN, FraunhoferEuskirchen, SAPHYMO, ARTTIC, IKI,) Three benchmarking exercises and about five testing campaigns each lasting 1 to 2 intensive weeks of measurements have been carried out based on ITRAP+10 experience in Ispra. Another FP7 project MODES also benefited from the facilities thus cross fertilisation and sharing of experience and knowledge.

Below is a non-exhaustive list of partners, collaborators and institutions which have benefited from the JRC facilities in Ispra, its nuclear material, knowledge transfer and competences resulting in a number of publications.

- IAEA + EURATOM: Neutron counter tests (running, to grant IAEA Cat A license)
- IAEA + EURATOM: Gamma spectrometer test (to grant IAEA Cat A license)
- INFN, Italy: Security and Safeguards Instruments
- University of Michigan, regularly, also with a number of students
- Los Alamos National Laboratory – detector development, calibration and testing
- CEA (France) , security instrument testing
- SAPHYMO , Italy
- NRCN Israel: numerous lab campaigns in PUNITA and PERLA (scrap counter)
- Arktis-Detectors and Polytechnic of Zurich in collaboration with DOE and AWE
- Symetrica Ltd UK R&D detection systems in nuclear safeguards and security
- FraunhoferEuskirchen: detection devices, spectrometers
- GBS Elektronik / German support programme to IAEA: Spectrometer testing
- Swedish Defence Research Agency
- University of Hamburg
- Politecnico di Milano
- STUK (Finland) …

5. The New Integrated User Laboratory (INS3L) in Ispra

International projects and activities of the kind described above are anticipated for the foreseeable future, and the need of a modern and integrated infrastructure to promote synergy and efficient operation has been recognised. The construction of a new laboratory named INS3L (**I**spra **N**uclear **S**afeguards, **S**ecurity and **S**tandardization **L**aboratory; pronounced INSEL), which will house all activities and facilities under one roof has indeed been approved and has entered the planning phase

with its completion expected within three years. This section of the paper will present the conceptual design of the new INS3L as a user laboratory within an integrated approach that shall benefit all users and stakeholders, international partners and collaborators and EU member states in general.

The INS3L laboratory shall group the different existing nuclear facilities of the nuclear Security Unit, i.e.:

- PERLA
- ITRAP Dynamic (with a rail track for dynamic testing)
- ITRAP Static
- EUSECTRA-Ispra (with outdoor space for radiation portal monitors)
- PUNITA instrument room (with its sealed (D,T) neutron generator) adjacent to a control room
- Physics laboratory which includes a 4m by 4 m climatic chamber with temperature and humidity controls
- Offices, meeting rooms, storage areas ..

5.1 Infrastructure and capabilities

The INS3L laboratory now in its design phase (figures 8 and 9 for first draft) shall group in one experimental hall all the existing nuclear facilities, , on a footprint of 49 m by 20 m. Adjacent to it shall be the building which will house offices, meeting rooms and utility areas on two floors with a footprint of 20 m by 16 m . The total functional area shall be about 1300 m^2. EUSECTRA-Ispra shall have an outdoor training area viewable from the inside room through large glass windows.

The laboratory shall continue the activities presently carried out in the different nuclear areas the NUSEC unit, both for nuclear safeguards and nuclear security i.e.:

1. R&D in NDA techniques applied to nuclear safeguards and nuclear security
2. Scientific/Technical support to ENER/IAEA and member states
3. Instruments testing, validation and standardization
4. Monte Carlo simulation and modeling combined with measurements
5. Training of inspectors in nuclear safeguards
6. Training of Front Line officers (FLO) and Train the Trainer of FLO in nuclear security and detection

The laboratory INS3L will not only house activities currently carried out but will also reinforce itself as a “user laboratory” with easy access to nuclear material for guests and trainees, which in many way it has been. This will be further facilitated and ensured by the fact that only sealed sources with a low level of radiation emission and the low inventory of nuclear material, compared to other nuclear facilities which in addition usually host open radioactive and nuclear materials as well.

It is also intended to integrate new tasks and activities such as addressing the important standardization for detection instruments in nuclear security. The Integration of nuclear and non-nuclear laboratories e.g. PERLA and AS3ML (Advanced safeguards Measurements, Monitoring and Modelling Laboratory) of Figure 10 will be take an important place whilst the RADAR / iRAP/ iRAP evaluation course for DG ENER will go ahead. Integration of methods will also be sought as the laboratories may deliver integrated solutions e.g. for the supervision of the first final repository in the world at Onkalo in Finland. Furthermore, the staff experience shall be used beyond the laboratory work e.g. in outreach and training activities initiative and in addressing new policy requirements and needs.

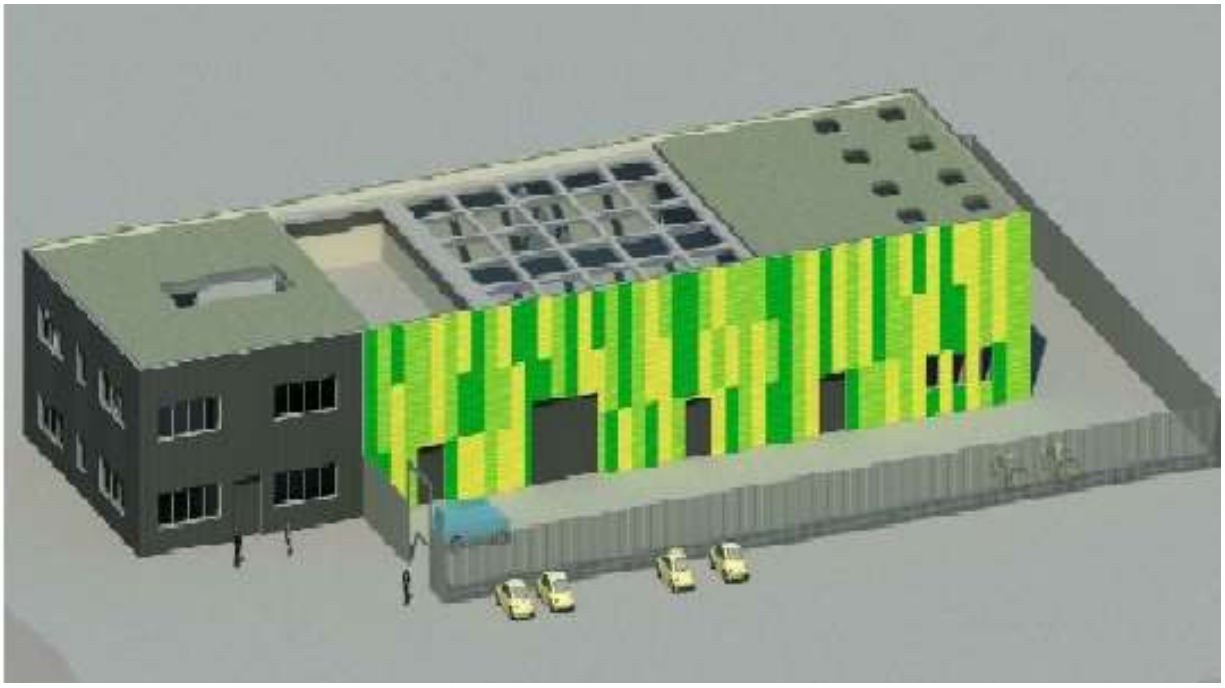

Figure 8: Perspective view of INS3L

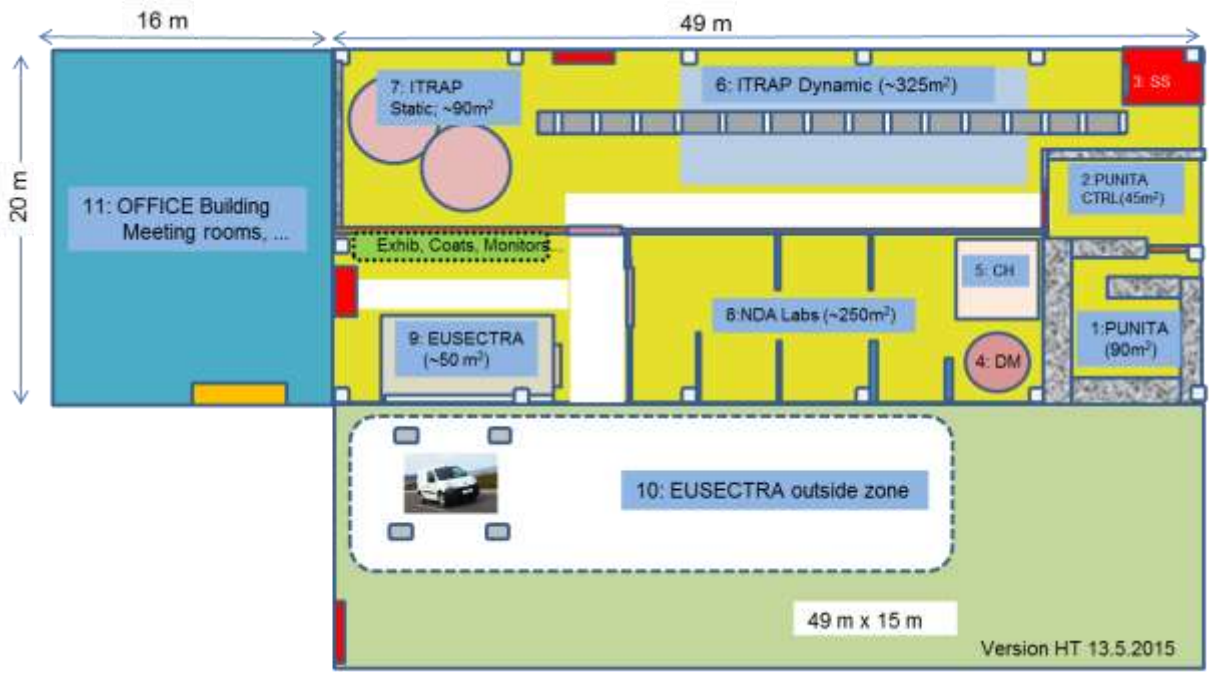

Figure 9: General schematic layout of the INS3L

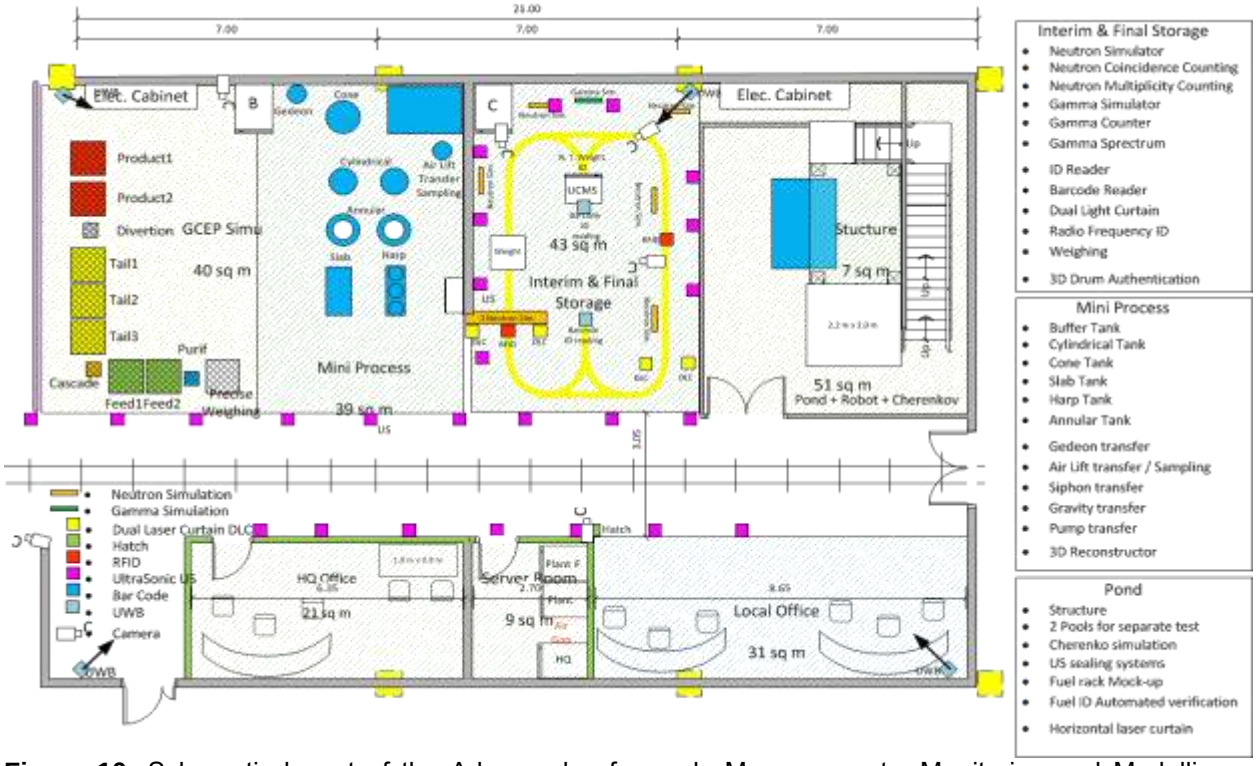

Figure 10: Schematic layout of the Advanced safeguards Measurements, Monitoring and Modelling Laboratory

6. Summary

It was shown that a large array of R&D programmes in non-destructive analysis (NDA) methods and instrumentation, testing and benchmarking of detection systems, user accessibility to laboratories and reference material, together with a comprehensive training programme exist at JRC's Nuclear Security Unit in Ispra (Italy) for the benefit European Commission DG's, the IAEA, EU research institutions, EU member states and many international partners. The unit shall continue to play its important role in international nuclear safeguards and nuclear security as demonstrated by the JRC's plan to build a new modern and integrated infrastructure on the Ispra Site, namely the INS3L laboratory building which will house all activities and facilities under one roof thus promoting synergy and efficient operation of all activities. The integration of INS3L with the newly setup AS3ML laboratory will be particularly beneficial.

Privacy regulations and protection of personal data

We agree that ESARDA may print our names/contacts data/photograph/article in the ESARDA Bulletin/Symposium proceedings or any other ESARDA publications and when necessary for any other purposes connected with ESARDA activities.

Copyright

The authors agree that submission of an article automatically authorises ESARDA to publish the work/article in whole or in part in all ESARDA publications – the bulletin, meeting proceedings, and on the website. The authors declare that their work/article is original and not a violation or infringement of any existing copyright.

7. References

[1] M. Marin Ferrer, S. Abousahl, W. Janssens , Illicit trafficking radiation assessment program (ITRAP+10), Future security 2013 conference organized by Fraunhofer

[2] P. Daures, P. Peerani, M. Marin-Ferrer, P. Richir, V. Berthou, A. Tomanin, J. Bagi, V. Forcina, S. Frison, Setting-up the Nuclear Security Training Centre ESARDA 33th Annual Meeting, Symposium on Safeguards and Nuclear Material Management, Budapest, 2011

[3] W. A. M. Janssens, Need for Strengthening Nuclear Non-Proliferation and Safeguards Education to Prepare the Next Generation of Experts, Symposium on International Safeguards, Vienna, 20-24 October 2014

[4] E. Hrnecek, V. Berthou, C. Carrapico, V. Forcina, J. Galy, L. Holzleitner, I. Krevica, K. Mayer, A. Nicholl, P. Peerani, F. Rosas, A. Rozite, H. Tagziria, M. Toma, A. Tomanin, Z. Varga, M. Wallenius, T. Wiss, J. Zsigrai , European Nuclear Security Training Centre (EUSECTRA) International Conference on Advances in Nuclear Forensics: Countering the Evolving Threat of Nuclear and Other Radioactive Material out of Regulatory Control

[5] R. Berndt, P. Mortreau, Performance test of the Multi-Channel Analyzer MCA-527 for Nuclear Safeguards Applications , Test in the PERLA Laboratory at JRC, Ispra, JRC83621, 2013

[6] R. Berndt, P. Mortreau ; ^{235}Uranium enrichment determination with the MCA-527- Test of spectrometric properties, Report JRC 79595, 2013

[7] R.Berndt, P. Mortreau, Experimental Determination of the Self-Absorption Factor for MTR Plates by Passive Gamma Spectrometric Measurement, NIMA 644 (2011) 27-32

[8] R. Berndt, F. Levai, C. Rovei, L. DiCesare, P. Timossi, R. Covini, T. Honkamaa, A. Turunen, Passive Gamma Emission Tomograph for Spent Nuclear Fuel Test in the ESSOR Spent Fuel Pond at JRC, Ispra, Interim Report EUR 25672 EN, 2012

[9] R. Berndt, T. Honkamaa, F. Levai , Pin-Level Verification Experiments with Gamma Tomography at Ispra in June 2012, Presentation ASTOR meeting, Vienna, 2012

[10] R. Berndt , E. Franke, P. Mortreau , ^{235}U enrichment or UF_6 mass determinationonUF_6 cylinders with non-destructive analysis methods, A 612 (2010) 309–319

[11] R. Berndt, P. Mortreau, Effect of Temperature on the performance of a CdZnTe Micro Spectrometer µSPEC , Report JRC 89701

[12] A. Tomanin, J. Paepen, P. Schillebeeckx, R. Wynants, R. Nolte, A. Lavietes ; Characterization of a cubic EJ-309 liquid scintillator detector , A7569 (2014) 45-54

[13] H. Tagziria, J. Bagi, P. Peerani, A. Belian , Calibration, characterisation and Monte Carlo Modelling of a fast-UNCL , NIMA 687 (2012) 82-91

[14] P. Mortreau, R. Berndt , Monte Carlo Modelling of a n-type coaxial high purity germanium detector , NIM A 694 (2012) 341-437

[15] D. Ancius, R. Berndt, P. Mortreau, J. Löschner, P. de Baere, J.F. Levert, W. Eestermans, P. Schwalbach, Modernization of EURATOM's unattended measurement stations at Melox MOX Fuel Fabrication and La Hague Reprocessing Plants, 35th ESARDA Annual Meeting, Bruges, Belgium, 2013

[16] G. Sannies, S. Normand, P. Peerani, H. Tagziria, H. Friedrich, S. Chmer, R. De Vita, M. Pavan, M. Grattarola, E. Botta, A. S. Kovacs, L. Lakoso, C. Baumhauer, M. Equios, G Petrossian, J. M. Picard, G. Dermody, G. Crossingham, Scintilla: A New International Platform for the Development, Evaluation and Benchmarking of Technologies to Detect Radioactive and Nuclear Material

International Conference on Advancements in Nuclear Instrumentation Measurements Methods and their Applications, 24-27 /06/2013 Marseille, France

[17] P. Peerani, V. Canadell, J. Garrijo, K. Jackson, R. Jaime, M. Looman, A. Ravazzani, P. Schwalbach, M. Swinhoe, Development of high-efficiency passive counters (HEPC) for the verification of large LEU samples , Nucl. Instr. Meth., 601 (2009) 326-332.

[18] M. Marin Ferrer, P. Peerani, M. Looman, L. Dechamp , Design and performances of the Scrap Neutron Multiplicity Counter , Nucl. Instr. Meth., 574 (2007) 297-314.

[19] H. Tagziria, P. Peerani, P. deBaere, P. Schwalbach, Neutron coincidence counter for the verification of PuO2 cans, Nucl. Instr. Meth., 580 (2007) 377-379.

[20] BARBAGALLO M.; COSENTINO Luigi; FORCINA Vittorio; MARCHETTA Carmelo; PAPPALARDO Alfio; PEERANI Paolo; SCIRE' Carlotta; SCIRE' Sergio; SCHILLACI Maria; VACCARO Stefano; VECCHIO Gianfranco; FINOCCHIARO Paolo, Thermal neutron detection using a silicon pad detector and 6LiF removable converters, Review of Scientific Instruments, 84 (2013)

[21] A. Lavietes, R. Plenteda, N. Mascarenhas, L.M. Cronholm, M. Aspinall, M. Joyce, A. Tomanin, P. Peerani, Liquid Scintillator-Based Neutron Detector Development, Proc. IEEE Nuclear Science Symposium (2012) 230-244.

[22] M. Looman, P. Peerani, H. Tagziria , Monte Carlo simulation of neutron counters for safeguards applications, Nucl. Instr. Meth., 598 (2009) 542-550.

[23] H. Tagziria, J. Bagi , B. Pedersen, P. Schillebeeckx , Absolute determination of small samples of Pu and Am by calorimetry, NIM A, Volume 691, 1 November 2012, Pages 90–96

[24] J. Bagi, C. Tam Nguyen, L. Lakosi, H. Tagziria, B.Pedersen, P. Schillebeeckx, Characterisation of PuBe sources by non-destructive analysis, in: Proceedings of the 27th ESARDA Annual Meeting: Safeguards and Nuclear Material

[25] W. Janssens, M. Scholtz, T. Jonter, M. Marin Ferrer, A. De Luca, Nuclear Safeguards and Non Proliferation Education and Training, initiatives by ESARDA, INMM and JRC, ESARDA Symposium 2012, JRC82002

[26] P. Mortreau, R. Berndt, Experience with Nuclear Inspector Training at JRC, Ispra, 2012, JRC67636

[27] Rosas, F., Peerani, P., Janssens-Maenhout, G., Richir, P., “Investigation on the exploitation of spectroscopic capabilities of Radiation Portal Monitors based on plastic scintillator detectors.” Proceedings of the International Conference on Nuclear Security, IAEA, 2013

[28] A. Tomanin “Development of a Liquid Scintillator-Based Neutron Coincidence Counter for Safeguards Applications” in Doctoral Thesis at Gent University Faculty of Engineering and Architecture Academic Year 2014 ISBN 978-90-8578-753-2

[29] R. Berndt, K. Abbas, V. Berthou, C. De Almeida Carrapico, G. Eklund, V. Forcina, V. Mayorov, P. Mortreau, M. Mosconi, B. Pedersen, P. Peerani, F. Rosas, H. Tagziria, A. Tomanin, A. Rozite, M. Marin-Ferrer, J. M. Crochemore, E. Roesgen, and W. A. M. Janssens, Evolution of the Nuclear Safeguards Performance Laboratory PERLA of the Ispra Site of the Institute for Transuranium Elements, IAEA Nuclear Safeguards Symposium 2014

[30] V. Berthou, E. Melamed, V. Rouillet-Chatelus, A. Church, S. Abousahl, W. Janssens “Complementarities and Synergies of EU, U.S. and IAEA Nuclear Security Outreach Projects”, , INMM conference 2013

[31] Abbas, K., Peerani, P., Janssens, W., Rosas, F., Rozite, A., Sevini, F., Viski, A., Mayer, K., Rosanelli, R., Vichot, L., Schrenk, M., Berthou, V., “Train the Trainers on Nuclear Security”, Syllabus of the T-t-T course in Radiation Detection Techniques for Tajikistan, European Commission - Joint Research Centre, 2013

[32] Favalli A, Mehner H-C, Crochemore J-M, Pedersen B; *Pulsed Neutron Facility for Research in Illicit Trafficking and Nuclear Safeguards*; IEEE Transactions on Nuclear Science; 56(3); 2009; p. 1292-1296.

[33] A. Ocherashvili, M. Mosconi, J-M. Crochemore, A. Beck, E. Roesgen, V. Mayorov, B. Pedersen, Fast neutron coincidences from induced fission as a method for detection of SNM, ESARDA Bulletin, Issue No 49, p42-51, July 2013.

[34] C. Dubi, T. Ridnik, I. Israelashvili, B. Pedersen ,
"A novel method for active fissile mass estimation with a pulsed neutron source", Nuclear Instruments and Methods in Physics Research Section A: Accelerators, Spectrometers, Detectors and Associated Equipment, Volume 715, 1 July 2013, Pages 62-69, ISSN 0168-9002,
http://dx.doi.org/10.1016/j.nima.2013.03.004

[35] Beck, I. Israelashvili, U. Wengrowicz, E.N. Caspi, I. Yaar, A. Osovizki, A. Ocherashvili, H. Rennhofer, B. Pedersen, J.-M. Crochemore, E. Roesgen, "Time Dependent Measurements of Induced Fission for SNM Interrogation", Journal of Instrumentation JINST_028P_0313, July 2013

Assessing 'Gold Standard' Status: Is the United Arab Emirates nuclear energy program suited to fit the bill?

Marianne Nari Fisher

Institut d'études politiques de Paris (Sciences Po)
Paris School of International Affairs
28 rue des Saints-Pères, 75007 Paris, France
E-mail: marianne.fisher@sciencespo.fr or mariannenari@gmail.com

Abstract:

The United Arab Emirates (UAE) is constructing four nuclear power reactors that are slated to become operational in 2017, expediting the first completely new nuclear energy program in over 25 years. Yet, before the reactors have even been connected to the grid, popular discourse already refers to the Emirati program as the 'Gold Standard' despite its checkered history on nonproliferation and export control issues. Indeed, construction of the UAE nuclear program may be outpacing its regulatory infrastructure in two regards:

First, despite signing the 123 Agreement with the United States, among numerous other accords, the UAE's continued reliance on an original Small Quantities Protocol (SQP) holds a number of Subsidiary Arrangements in abeyance and does not allow for IAEA inspections or oversight until it receives its first reactor fuel load or until a defined 'significant quantity' of nuclear material is imported.

Second, there are still concerns stemming from disjointed export control authorities operating within the Emirates. Although some progress has been made since the UAE first implemented trade controls in 2007, its ability to effectively regulate export controls is jeopardized by the lack of formalized coordination between its domestic regulatory authorities.

Indeed, these considerations do not suggest a lack of commitment on behalf of the Emirates. Certainly, the UAE has signed onto every major international treaty dealing with nonproliferation issues and continues to receive assistance from multinational entities such as the International Atomic Energy Agency and members of the European Union, setting a high precedent for completeness and verification of its program. Further, the UAE also maintains strong ties on technical cooperation with countries such as the United States and South Korea.

Above all, however, additional confidence-building measures could still be adopted to strengthen the Emirati legal and export control framework, therein bolstering international safeguards and ensuring that the UAE lives up to its 'gold standard' title before the 2017 deadline. In doing so, the Emirates would certainly serve as an example to other aspiring nuclear states and signal to the world that Abu Dhabi fits the bill of the model state.

Keywords: safeguards; export controls; United Arab Emirates; nonproliferation; gold standard

1. Introduction

The United Arab Emirates (UAE) is on a fast track to acquiring four nuclear power reactors, expediting a robust nuclear energy program that is slated to go live in 2017. When the four planned reactors are connected to the grid in 2020, the UAE will become the second state in the region to maintain nuclear

energy capabilities after Iran. It will also be the first new nuclear newcomer state in more than a quarter of a century. Though, years before the program has gone live, popular discourse already routinely refers to the Emirati nuclear energy program as a 'Gold Standard' or 'model state' for other aspiring newcomer nuclear energy states. In academic spheres, this special status is afforded to the UAE due to its strictly negotiated 123 Agreement, where the Emirates agreed to forgo domestic enrichment and reprocessing capabilities (ENR) in exchange for technical assistance. Yet, this widely held and popular view ignores a number of historical factors that have previously hindered the UAE's ability to effectively mitigate proliferation concerns within its own borders, a fear that is only furthered by an underdeveloped legal infrastructure and nascent export controls – these two concerns often remain underappreciated.

In 2008, nonproliferation expert George Perkovich noted "the effects of a Gulf Cooperation Council (GCC) 'nuclear program' will be ambiguous and muddled, at least for the 10-15 years it would take to develop basic capabilities." [1] In the same year, the Emirates declared its intentions to pursue its ambitious, yet peaceful nuclear energy program. Staying true to its word, the Emirates is pushing forward on its nuclear agenda with record speed and will achieve its program in just under a decade. To date, the Emirati program has remained on schedule and the international community remains assured that it will meet its 2017 deadline. Indeed, nuclear material could be shipped to the Emirates as early as next year for reactor test runs, though its nuclear regulatory framework is currently incomplete. Be that as it may, there appears to be a critical lack of legislative, technical, and political infrastructure that impedes the UAE's ability to effectively safeguard its nuclear program and could potentially open the door to proliferation if left unaddressed.

As the UAE is slated to become the first wholly new nuclear program in more than 27 years, more must be done to ensure that the Emirates is readily equipped to manage its program safely before its reactors go live. In this paper, the Emirati framework is predominantly explored from two perspectives. First, the soundness and completeness of safeguards are carefully evaluated alongside its legal code. Second, the UAE export control regime and its commerce control mechanisms to thwart potential diversion are assessed. Also examined to a lesser extent is the federal regulatory framework that oversees development of the nuclear program. Fundamentally, it is imperative for the UAE to secure a solid programmatic and regulatory foundation before the first reactor goes live in 2017.

In order to signal to the world that Abu Dhabi is ready to fit the bill of the 'model state,' additional confidence building measures could be adopted to strengthen its legal and export control framework, bolstering international safeguards in the process and ensuring that the UAE remains the 'gold standard':

First, the UAE could rescind its current unmodified, original Small Quantities Protocol (SQP) in favor of a modified SQP. Generally, an SQP is administered by the IAEA to countries with minimal to no nuclear activity and is a required addendum under any signed Comprehensive Safeguards Agreement, holding a significant number of safeguards measures in abeyance. As the Emirates looks to become a notable player in the nuclear energy field, rescinding its original SQP would force it to develop a robust state systems for accounting and control (SSACs), among other necessary measures. Indeed, few states still adhere an original SQP, and the exposure of loopholes within this accord has rattled the international community before. Of course, if the UAE were to move to the modified SQP, more strict measures would be implemented before introduction of nuclear material into the country, in addition to pushing the UAE to develop better reporting capabilities under the Additional Protocol (AP) and subsequent state system for accounting and control of nuclear materials.

Second, the Emirates should formalize and nationally implement a comprehensive export controls list to expand its strategic trade controls systems. This move would inform responders and allow professionals working on these issues to accurately manage materials moving in and out of ports. Further, developing 'Measures of Success' could be expanded to evaluate progress of its export controls measures, a system that would effectively monitor, protect, and report the movement of sensitive technologies. As of now, the country loosely adheres to the EU export control list, yet this has not been formally published nor uniformly implemented across the seven Emirates.

Third, there are a large number of non-indigenous experts currently working the UAE, though the Emirates intends to push its program to be fully indigenous in the future. The number of employees dedicated to the program is also expected to swell in coming years. Its latest internal International Advisory Board report suggested that the number of employees would double from its current levels to meet the gap. [2] However, until that goal is realized, the Emirates could improve its regulatory framework by training workers, more clearly defining roles of its numerous regulatory institutions, in addition to expanding its consultations with international experts and multinational export control regimes.

Finally, the most recent Safeguards Implementation Report for 2013 produced by the IAEA goes to show that a broader conclusion for the country has not yet been drawn and integrated safeguards have not been implemented. [3] While the two-year deadline before its four reactors are slated to go live is not an official date put forth by the UAE to have all of these measures in place, it would be wise for Abu Dhabi to secure a robust legal and export controls framework before nuclear material is introduced to the country or its reactors are connected to the grid sometime between late 2016 and 2017.

1.1 The Bid for Nuclear Power

By most standards, the UAE is an energy rich country, though its resources stem largely from two primary sources – upwards of 98% of Emirati energy consumption draws from oil and gas sources alone. While these two assets have secured the UAE a sizeable wallet and steadfast seat as a major energy player, its recent wealth and population growth has led the country to become not only a major energy producer, but also a large energy consumer. Further, its energy requirements will continue to expand rapidly over the coming years; while the country is rich with natural gas and produced 90.6 billion kWh of power in 2009, there is very little energy diversity to accommodate future needs. Further, nearly all its domestic electrical generation currently stems from natural gas resources, an increasing amount of which must be imported from neighboring countries. As it turns out, “projected escalating electricity demand [in the UAE will grow] from 15.5GWe in 2008 to over 40GWe in 2020, with natural gas supplies sufficient for only half of this.” [4] While its current consumption rests at about 19GWe, UAE electrical demand is slated to grow by 9% annually. With needs rapidly growing, the move will shift the Emirates away from a baseload of fossil fuels and towards a more low-carbon future as nuclear and renewables are added in the fold.

In 2008, the UAE decided to pursue an ambitious nuclear program to diversify its energy mix to combat these rising needs. Primarily, nuclear power would serve as a source of baseload power generation, or minimum power requirements, allowing the Emirates to rely less on imported gas and the use of its own reserves, which could be exported at a much higher price. In the region, burning conventional fossil fuels such as gas and oil is still the primary way to produce electricity. Yet, burning conventional fossil fuels is inefficient, expensive, and releases high amounts of CO2 emissions. On the other hand, nuclear power plants harness the power of the atom by converting heat into steam that then drives a turbine, which is also typically hooked up to a generator to create an output of electricity. Though, the UAE was not the only power in the region to openly declare the move towards nuclear in recent years – alongside the Emirati decision followed public calls for the pursuit of nuclear power by the following regional countries: Bahrain, Egypt, Israel, Jordan, Kuwait, Oman, Qatar, Saudi Arabia, Syria, Turkey, and Yemen. [5]

Initially, the Emirates had hoped to use nuclear power as a baseload electricity source, allowing the country to export more of its domestic resources and sell oil and gas commodities for a higher price to maximize potential profits of its natural resources. In short, the pursuit of nuclear power was initially done to fill the energy gap between the UAE’s rising levels of gas and oil consumption, while also increasing renewables investments alongside nuclear as its domestic demand continue to grow. As of now, the Emirates celebrate nuclear power as a reliable and clean source of energy with a long-term guaranteed supply of electricity in addition to much needed water desalination for its inhabitants.

The UAE is looking to diversify its domestic energy supply and is the first country to break ground on a new nuclear energy program since the 1986 Chernobyl disaster. Though, the playing field between nuclear weapon states and non-nuclear weapon states has changed dramatically since that time. Surely, the UAE would have to secure support from the United States, and the initial push for the bilateral 123

Agreement was mired in Washington politics, though several public campaigns allowed the Emirates to leverage key stakeholders in the US. Some of the largest players in the US nonproliferation realm, including William Cohen, the former US Secretary of Defense, and Sam Nunn, former US Senator and Co-Chairman & Chief Executive Officer of the Nuclear Threat Initiative (NTI), pushed for the US to sign the deal through a piece titled 'Nuclear cooperation with UAE in our interest,' also showcasing support for the strict conditions of 123. [6] As such, the agreement looked to restrict the sensitive nature of the full nuclear fuel cycle from mining to reprocessing – several steps of which can be repurposed to produce potentially dangerous fissile materials used in nuclear weapons – and pushed the UAE to forfeit any right to domestic uranium enrichment and reprocessing through the hailed '123 Agreement' or 'Gold Standard' nuclear cooperation agreement between the two countries. The agreement was signed in 2009.

While the 123 Agreement set a high precedent for the US Congress and potential future agreements with other aspiring nuclear energy countries, other newcomer countries are not necessarily required to adhere to such hard-and-fast measures, rendering the Emirati accord inherently discriminatory. Yet, the UAE program is also distinguished for its negotiated 'Agreed Minute,' where conditions of the bilateral US-UAE 123 agreement was set as a precedent for any future nuclear agreements in the Middle East region. Indeed, the UAE maintains the right to renegotiate the terms of its 123 Agreement should any *regional* power be granted the ability to engage in processes that handle or convert uranium to be used as a reactor fuel. To this end, the United States has negotiated other 123 agreements with a number of other countries including Vietnam and India that did not have to sign onto such stringent preconditions, but the US has yet to settle similar accords with others in the region.

Through the 123 Agreement, the UAE agreed to a number of concessions on its program and remains a strong champion of nuclear power to meet its domestic energy needs. And while refocusing efforts to export its own gas resources for profit, the Emirates should ensure that its upcoming atomic energy program is able to meet international nuclear regulation standards before its first reactor goes live. It goes without saying that its emerging program should be regulated with the highest level of safeguards and export controls to mitigate any legal or verification challenges that may arise. All this rings especially true for a newcomer state, as other states aspire to join the nuclear energy ranks have typically built up programs over the course of several decades to establish an adequate framework in support of a nuclear energy program – in contrast, the entirety of the UAE program will likely be completed in the timeframe of a decade or less.

Table 1: Timeline of the projected UAE nuclear program.

In 2009, France, the United States, and Russia were all eager to sell nuclear technologies to the UAE following its initial nuclear bid, with France and the South Korea ascending to the final round for the tender. In January 2010, the Korea Electric Power Corporation (KEPCO) consortium was selected by the UAE to construct the first four commercial nuclear reactors and will provide construction, commissioning, and fuel security in addition to near full oversight of regulation of the program that will be located at Barakah. The site is situated on the coast of the Gulf, about 300 miles west of Abu Dhabi and near the border of Saudi Arabia. The reactor site would operate at a capacity of over 90% to provide baseload power to the UAE with a lifespan of a projected 60 years. [7] The initial bid for the four reactors was set at $20 billion, a move largely welcomed by the nuclear community and especially for the South Koreans, as KEPCO seeks to make an example of this site as the first export of Korean reactor technology abroad. The move will certainly leverage a foot in the door of the nuclear power industry, leading the Republic Of Korea (ROK) to become an exporter of nuclear technologies for the first time. [8]

Similarly, in 2010, the US based Lightbridge Corporation entered the stage to assist aspiring nuclear newcomer countries by manufacturing programmatic roadmaps that would outline the steps to securing a peaceful nuclear energy future, primarily with aspirations to cater to members of the Gulf Cooperation Council (GCC) market. In particular, the United Arab Emirates gladly moved forward with the deal, allowing Lightbridge Corporation to develop a comprehensive nuclear roadmap for the Emirati program. Lightbridge pulled together experts and consultants to aid these countries to develop strategies from planning to implementation stages of the Emirati framework. The company agreed to provide guidance on issues ranging from site assessment to fuel security, among other stipulations to help develop the emerging nuclear power to become the 'Gold Standard.' Lightbridge currently assists with capacity building and regulatory affairs. [9]

It should be noted however, that selecting the bidders and signing deals is the first series of events that must take place before construction is even allowed to begin. Following any initial bid, there are a number of site selection processes that are necessary for new projects looking to build up nuclear power. Summarized, the process is as follows:

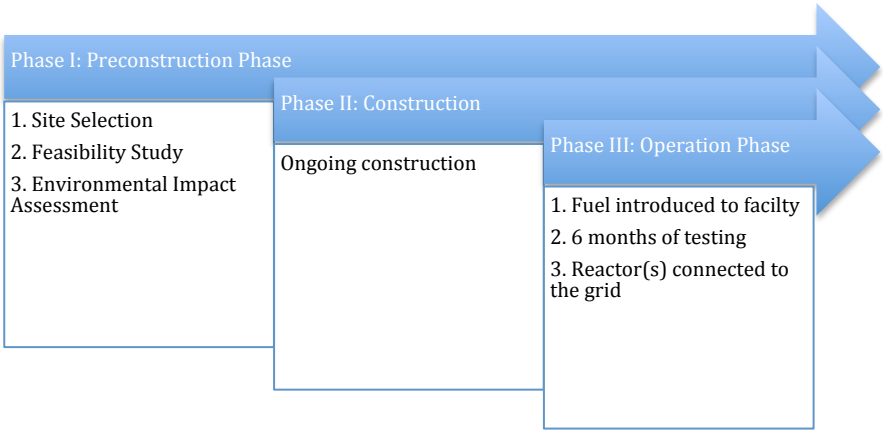

Table 2: Necessary steps for nuclear power program.

For any aspiring nuclear state, first, there is an economic feasibility study to gauge rough estimates of the cost of a reactor. Further, contractors often perform full economic and feasibility assessments at this time. This incudes a thorough breakdown of payback periods, internal rate of return, levelized cost of energy, debts, equity, among other calculations. Following this, the environmental impact assessment is characterized by two aspects, the first being financial which typically includes impact assessments over the complete lifecycle of the reactors and evaluates the payback period, emissions, energy expenditure, and more. Further, the Greenhouse Gas Emissions lifecycle, calculated in tonnes of CO2 equivalent per MW, is also factored. It is only after all this extensive, preliminary work that construction is able to commence.

Construction on the first commercial reactor in the Emirates began in July 2012, with work beginning on the second reactor in May 2013. [10] The Emirati Federal Authority granted approval for construction of the third and fourth reactors under the Federal Authority for Nuclear Regulation (FANR) in September 2014. [11] The first reactor upon completion will, however, need to be tested at full power before it is connected to the grid. Generally speaking, these test runs include power levels and criticality trials, which are conducted a full four to six months before the reactor is live. First, completely fresh fuel is introduced to the core to ensure that the reactor is safe to run before the reactor is hooked to the power supply grid and to ensure that there are no malfunctions. The process includes running the reactors at different power levels and different criticalities, allowing potential poisons in the fuel such as Xe-135 to be bred out and set the baseline behavior for the reactor. Starting up the nuclear reactor for this type would typically take about two weeks, or potentially require more time in the case of initial startup. In essence, these pilot runs are done to test the power grid and ensure that the power generation is grid-compatible. Not conducting such tests would run huge risks that could have an enormous detrimental effect on the grid, resulting in a power surge that would likely lead to an outage or potential damage to the grid as a whole. [12] Tests of

this nature are carried out in order to evaluate the reactor stresses in terms of its ability to handle thermal and structural strains with the introduction of immense amounts of heat stemming from the reactors.

Tying all this to the timeline of the UAE nuclear program, there are implications that nuclear material could be introduced to the Barakah facility as early as late 2016 before its first reactor is officially declared as 'live' or connected to the grid in 2017. The tests are not exclusive to any particular nuclear reactor technology, but are applicable to the most common of reactors. In this case, it refers to Pressurized Water Reactors, including the APR1400 to be used in the Emirati program. While tests are inherently a time consuming process the time to import or transport these materials and prepare the reactors are likely already being factored into the Emirati timeline.

The first 1400-MWe plant is expected to go live in 2017, with electricity being sold and distributed by the Abu Dhabi Water and Electricity Authority. Additional reactors are expected to join the grid one-by-one annually in subsequent years, with all four reactors becoming operational by 2020 to provide electricity and meet domestic and regional needs. Furthermore, initial fuel and fuel reload commitments are supposedly guaranteed for a number of years through its prime contract negotiated with the South Korean contingency. Regulation authorities will largely be delegated to KEPCO in conjunction with the Emirates Nuclear Energy Corporation (ENEC).

1.2 Potential for 'Nuclear Diversion'

Since 2009, when the United Arab Emirates made the decision to pursue nuclear power, a great deal of effort has gone into developing the necessary regulatory bodies and export control authorities alongside construction of the reactors. And while the UAE has done much to counter proliferation risks to date, construction is moving along quickly. The program remains in relatively early stages, yet it appears construction may be outpacing regulation. In the past, Dubai, the largest trading port in the UAE has proliferated sensitive technologies as far reaching as Iran, Pakistan, and other states.

The notorious A.Q. Khan (Abdul Qadeer Khan) – also known as the father of the Pakistani bomb – was one of the most prominent agents of proliferation in the late twentieth century. His personal network manipulated the export regimes network to pass along sensitive materials to a number of outside actors with ease. Khan serves as the most prominent example of both the UAE and international community's failure to oversee and control a swelling transshipment network. In this particular case, Khan had used Free Trade Zones (FTZs) across the Emirates to transfer illicit materials, while all activities were conducted through a legitimate front company based in the Emirate of Dubai. For years, the company operated as a hub of illicit transactions and was a primary shipping point for a number of sensitive materials. In the wake of the Khan episode, the UAE was pressured by the international community to ramp up its export controls and create a comprehensive framework to regulate these issues. Yet even as recently as 2013, a US citizen "allegedly made a variety of false statements on shipper's export declaration forms" and used "his New York company to illegally export carbon fiber (which has nuclear applications in uranium enrichment as well as applications in missiles) from the United States" to other countries such as China, demonstrating that all transfers of sensitive materials are impossible to circumvent entirely, but additional steps could still be taken to thwart such activities. [13]

The UAE's checkered track record on export controls was brought up before congress during the negotiations of the 123 Agreement. And in order to push through the legislation, strict measures regulating the nuclear program were placed on the Emirates in order to win the favor and support of those in office involved on the matter. [14] Though, following the passing of the 123 in 2009, there has been little follow-up in the adoption and implementation of the clear stipulations made in the agreement. Most of the pressure placed on Abu Dhabi simply disappeared after 2010.

Meanwhile, South Korea's KEPCO is slated to bear a large brunt of the responsibility for export controls under its negotiated exporter "conditions of supply," yet these informal codes do not remove greater UAE responsibility to regulate sensitive technologies that move through its borders. Further, language within the 123 document notes that the United Arab Emirates would be held solely responsible for any diversion of goods and technology moving through its borders and moreover, is expected to uphold due diligence of

any nuclear related programmatic endeavor. Also, according to the UAE's negotiated INFCIRC//622 safeguards agreement with the IAEA, it is stipulated in Article 15 that "the United Arab Emirates and the Agency will bear the expenses incurred by them in implementing their respective responsibilities under this Agreement." [15] Under its International Transfers Article 90, it quotes that "nuclear material subject or required to be subject to safeguards under this Agreement which is transferred internationally shall, for purposes of this Agreement, be regarded as being the responsibility of the United Arab Emirates." At the very least, this agreement dictates that it is the responsibility of the "contractual nation" to safeguard technology and circumvent potential leakage of technical know-how. In this case, responsibility falls on the United Arab Emirates. [16] Yet, it is also the responsibility of the international community as well to thwart potential challenges and refocus resources to overcome challenges posed by shadow networks.

With ongoing development on its nuclear energy program, the UAE is now afforded a full-fledged legal and legitimate capacity in which to operate with sensitive materials, granting the country certain privileges in the arenas of nuclear sales and transshipments. Certainly, Abu Dhabi will have to do everything in its power to thwart diversion. It must be clearly stated, however, that there is no insinuation that the United Arab Emirates is pursuing anything aside from a peaceful program. When dealing with proliferation risks in any new nuclear program, there are usually two types of perils to be aware of in the traditional school of non-proliferation thought. Yet, the UAE program presents a different type of proliferation that is discussed further below.

In nonproliferation literature, the possibilities of vertical and horizontal proliferation are often examined. Yet, vertical proliferation refers to states that already possess nuclear weapons or delivery capacities and are actively looking to increase the domestic stockpile or improve existing technical capabilities, growing upwards and onwards internally. The UAE case deviates from this vertical proliferation definition insofar that the Emirates has no preexisting technical know-how or nuclear capability, but instead are looking to acquire an entirely new program for energy purposes only. Horizontal proliferation refers to governments that make an active decision to proliferate already developed nuclear capabilities to other states, expanding the greater nuclear regime whether for peaceful or non-peaceful purposes. The threat of diversion or illicit activities is worrisome for the United Arab Emirates, as it has historically served as a massive transit hub for regional nuclear ambitions in the past where dangerous materials were diverted to notorious programs in Syria, Iran, and more. [17] While the Emirates continue to make moves and hedge against proliferation or illicit transfers within its borders, much more must be done to mitigate this challenge.

Ultimately, the UAE remains separated from these two schools of thought. Instead, it would be more useful to explore the uniqueness of the United Arab Emirates case, which departs from traditional discourse concerning vertical and horizontal proliferation, especially as the program is intended to be entirely peaceful by nature. Instead, the United Arab Emirates houses a third, arguably new type of risk in the nonproliferation community where a 'nuclear cover' could potentially support detrimental activities without the bidding of the government. In this case, the program is moving beyond the dichotomy of vertical and horizontal risks posed by states, whereas in the UAE, illegal transshipments can now take place without government involvement due to potential loopholes in regulation and infrastructure. While the UAE is more of a special case, where its government does not necessarily seek to proliferate, weak export controls could still facilitate the transfer of sensitive materials including dual-use components without the consent or knowledge of the Emirati government. This type of risk instead deals with the likelihood of diversion of materials and ongoing, transshipment issues that could aid external proliferation on an international level. Further, this type of proliferation addresses its domestic legal mechanisms that are currently insufficient to effectively deal with illicit diversion and could potentially serve as a cover for unintended proliferation activities. The greater fear lays in the fact that a legitimate UAE nuclear 'cover' may lead to other unexpected and illicit activities by nongovernmental actors that could undermine the effectiveness of the nonproliferation regime. In short, loopholes in the legal framework could serve as a cover for proliferation activities.

Certainly, Emirati leaders have taken strides to deter proliferation within its borders over the last decade. However, ongoing loopholes in its legal codes and export controls can be leveraged to facilitate the transfer of sensitive materials or technical know-how, presenting a new type of proliferation that falls

outside the realms of vertical and horizontal proliferation. It instead poses a risk insofar as it is a newcomer program that could provide legitimate 'nuclear cover' under which diversion or proliferation may be leveraged, yet not necessarily by the will or consent of the state. This emerging hazard presents a fresh issue for the nonproliferation community, particularly those who still look to preserve the nonproliferation regime and combat nuclear mishandling. In order to hedge against these risks, the UAE will need to develop its ability to follow-up on potential abuses through rigid export controls and expansive safeguards in order to be hailed as a success story. This is especially so if it looks to serve as an example to other nuclear energy bids and upstarting programs.

Indeed, its acquisition of nuclear capabilities and technical know-how is coupled with significant responsibility to hedge against potential avenues of vertical and horizontal proliferation that may arise within its program. It is important to note that while the UAE program does not appear to pose immediate threats, programs of this nature are inherently risky. The following points will examine if the current legal and export control framework is strong enough to mitigate these concerns. In the past, the UAE has failed to successfully combat sensitive materials transit through its borders – and so, can the international community accept UAE's rhetoric to translate to commitment and this commitment to action in order to narrow any possibility of a 'commitment-compliance gap,' as first described by Dr. Bryan Early at the Harvard Belfer Center. [18] As of now, while the UAE has made strides to combat proliferation, its domestic legislation is still lacking and could be exploited to transfer or divert sensitive technologies. With that, before the nuclear program is set to go live, the UAE and broader international community must further develop its ability to thwart potential diversion of materials by bolstering legislation and training. Working against this type of diversion would be in the favor of the Emirates – there is nothing to gain by allowing these materials to find their way into the hands of actors that should not have them, as issues regarding non-state actors, terrorists, among other entities still present very real concerns.

1.3. Overcoming Adversary

The Emirates has numerous hurdles to overcome in order to quell safety and security concerns in order to push it to model state status. Controlling international trade and access to strategic items is certainly no easy feat. Proliferators are constantly working to get around official measures in order to carry out illicit activities. Such actors seek access to controlled items using alternative suppliers or shipping routes and multiple transshipment points, going as far as to falsify papers or use front companies to facilitate diversion of sensitive items. The UAE and international community must continue to be ahead of proliferators. Dual-use items are of particular concern, as production of these weapons is much harder to follow whether used legitimately or for indigenous production of weapons.

According to the IAEA, the official definition of safeguards applied in the field is described as a mechanism to deter proliferation. The goal is to first help states build up assurances that the application of nuclear power programs is credible and honors international obligations. To take this a step further, states should be able to detect potential misuse of nuclear technologies, including the use of inspections, verifications, and other physical mechanisms to deter tampering. [19] Export controls (or commerce control), on the other hand, looks to constrain and manage sensitive materials through an efficient and streamlined service. Commonly, export controls refer to regulation of sensitive or dual-use technologies through extensive licensing procedures and limiting use of these technologies. The goals are to strengthen collective security, limit access to potentially dangerous materials, ensure compliance with international standards, and prevent such materials ending up in the hands of potentially harmful end-users. In the UAE, the challenge of both safeguards and export controls rest in the ability to effectively identify, follow, and subsequently prosecute violations of strategic trade controls.

In the field, the Treaty on the Non-Proliferation of Nuclear Weapons (more commonly referred to as the Nonproliferation Treaty or NPT), is often championed as the 'central or grand bargain' where "non-nuclear-weapon states agree never to acquire nuclear weapons and the NPT nuclear-weapon states in exchange agree to share the benefits of peaceful nuclear technology and to pursue nuclear disarmament aimed at the ultimate elimination of their nuclear arsenals." [20] On another note, the UAE became party to the NPT in 1995, the last country in the region to sign onto the accord just 25 years after its inception. While it had

signed onto the non-aligned movement in 1970, it is not clear why there was such a disparity in signing onto the NPT.

Internationally, all states party to the Nonproliferation Treaty (NPT) are guaranteed the right to peaceful uses of nuclear technologies. In particular, aspiring nuclear energy states such as the Emirates is guaranteed the right to develop and produce nuclear energy for peaceful purposes. The specific language under the text of the NPT includes:

> *Article IV*: 1. Nothing in this Treaty shall be interpreted as affecting the inalienable right of all the Parties to the Treaty to develop research, production and use of nuclear energy for peaceful purposes without discrimination.
>
> 2. All the Parties to the Treaty undertake to facilitate, and have the right to participate in, the fullest possible exchange of equipment, materials and scientific and technological information for the peaceful uses of nuclear energy…

According to the above text, the Emirates is guaranteed the right to develop a nuclear energy program for peaceful purposes. And yet, also stipulated by the NPT is the obligation of the Emirates to conclude and apply all relevant safeguards measures in order to ensure rightful operation of its nuclear energy framework.

> *Article III*: Each non-NWS party undertakes to conclude an agreement with the IAEA for the application of its safeguards to all nuclear material in all of the state's peaceful nuclear activities and to prevent diversion of such material to nuclear weapons or other nuclear explosive devices. [21]

And so, conversely, the UAE is required to adhere to all concluded agreements with the IAEA. In recent years, the Emirates is certainly on track to developing comprehensive safeguards and a framework to combat potential diversion. Through the 123 Agreement and other accords, the UAE has already signaled good faith to the international community by foregoing both front end and back end processing abilities that could be repurposed or diverted for obtaining weapons grade uranium and plutonium. These two sides of the fuel cycle pose significant dangers and proliferation challenges. Yet, even stronger countermeasures on strategic trade fronts will be necessary to secure the proper legal foundation and export controls processes that will be necessary to regulating materials of its emerging nuclear energy program before 2017.

1.4. Current Regulatory Mechanisms in Place – Is it Enough?

There is much ground to cover on the Emirati program, though an analysis of projected proliferation risks within the Emirati nuclear energy program would be incomplete without a thorough examination of the many institutions at play and greater legal framework. A closer look at the UAE's current legal capabilities will be surveyed, in addition to examining the Emirates' historical role as a procurement transit point for clandestine nuclear programs.

International institutions that interact with Emirati regulators and key domestic players are the two groups that are building up the nuclear framework. Beyond this, a number of global institutions and several governments work in tandem with Abu Dhabi to tackle potential illicit trafficking, diversions of materials and other hindrances to the nonproliferation agenda. In the UAE specifically, the main players include the following:

a. Relationships with International Institutions

Since the decision to pursue nuclear power, the United Arab Emirates continues to work with a number of countries and international organizations to build up its domestic capacity. Along these lines, it would be wise for the UAE to leverage its many bilateral and multilateral relationships to bolster domestic Emirati

regulatory mechanisms. Engagements with the United States government alone are plentiful. The Emirates holds partnerships with the Department of Energy (DOE), including the National Nuclear Security Administration (NNSA) & International Nuclear Safeguards and Engagement Program (INSEP), Department Of State (DOS) including the Proliferation Security Initiative (PSI) & Cooperative Threat Reduction (CTR) & Export Control & Related Border Security (EXBS) & Partnership for Nuclear Security (PNS), Nuclear Regulatory Commission (NRC), among other organizations, all have a hand in engaging and training UAE personnel through a number of channels. [22] Yet, many of these engagements remain largely ceremonial in nature.

Institution	Description	Status of Organization
International Atomic Energy Agency	Primary contact of engagement for developing safeguards, adopting comprehensive regulations, heading verification efforts and providing technical assistance	Active, mostly after sufficient nuclear material is introduced into the country
International Nuclear Safeguards and Engagement Program (INSEP)	Primary US contact as a basis institution of engagement, advancing safeguards, ensuring effective implementation of SSACs	Active, intermittent annual updates
United Nations Security Council (UNSC)	International regulator, offers legal structure to track sensitive materials and implement effective export controls	Active, largely removed from direct UAE engagement
International Framework for Nuclear Energy Cooperation	Partnership to expand nuclear energy "for peaceful purposes proceeds in a manner that is efficient, safe, secure, and supports non-proliferation and safeguards" [23]	Active, largely ceremonial

Table 3: International engagements on UAE nuclear program, (not to be ignored are partnerships with EU and other countries).

b. Domestic Regulators

Within the UAE, there are a number of domestic institutions that oversee law making, regulation and implementation of the Emirati nuclear program. In parallel with international standards, countries typically establish one law-making institution and one technical agency to oversee the program. In particular, there are two primary federal authorities working with these issues, FANR and ENEC. These two continue to be the major regulatory players in regards to building up and enforcing effective laws governing the nuclear energy program, though a number of other partnerships and implementation organizations remain in operation across the country and are more opaque in nature. Further, the absence of a clearly defined agenda or role for these numerous 'secondary organizations' housed in country may eventually become distractive and ultimately counterproductive to regulation of the program and the overall nonproliferation agenda.

Following the release of Policy of the United Arab Emirates on the Evaluation and Potential Development of Peaceful Nuclear Energy, the Federal Authority for Nuclear Regulation (FANR) was established largely as a nuclear regulatory and lawmaking body. Its operations include departments dealing with Nuclear Safety, Security, Radiation Safety, Safeguards and Education & Training. By most milestones FANR is the most established institution working on nuclear issues in the Emirates, as it writes the legislation and clarifies rules on regulatory matters concerning the nuclear energy program. Its legislation is broken down into two facets: regulations and regulatory guides, regulations that govern safeguards and legal matters while regulatory guides are pertinent to operators or regulation of respective nuclear facilities. Though, most all safeguards and relevant legal measures are currently encompassed in Regulation on the Export and Import Control of Nuclear Material, Nuclear Related Items and Nuclear Related Dual-Use Items (FANR-REG-09) and the Regulation for the System of Accounting for and Control of Nuclear Material and Application of Additional Protocol (FANR-REG-10), both produced by FANR. [24] These two accords put forth the necessary steps for licensing and providing the scope for the proper paperwork to work with

sensitive materials – on the greater FANR website, there is an FAQ section that allows the public to access information on potentially hazardous nuclear materials, even those relating to medical or research purposes via a series of official, published Regulations and Regulatory Guides. In operation, FANR will require import permits at the initial phase through the executive office. Yet, because FANR serves primarily as a lawmaking institution, its counterpart, the Emirates Nuclear Energy Corporation, was created in tandem to implement the legal code into practice.

In 2009, the Emirates Nuclear Energy Corporation (ENEC) was also founded in Abu Dhabi after signing of the UAE Federal Law Regarding the Peaceful Uses of Nuclear Energy (Federal Law by Decree No 6 of 2009). ENEC oversees deployment and technical operation of the nuclear power plants in conjunction with the primary contractor, KEPCO. It operates on the federal level and works on strategic partnerships and engagements both domestically and abroad work to develop and ensure the civilian Emirati nuclear program aligns with the projected infrastructural scheme and nuclear framework of the UAE. The duties of ENEC ranges across many spectrums: communication with the public, developing the educational strategy and planning for the energy needs, decisions on investments related to the program, among other needs. [25] Its official and stated corporate values include; Safety, Integrity, Transparency and Efficiency, which, interestingly are also the same vision and core values that are reflected in FANR – yet, changes could be on the horizon as the UAE President recently reshuffled the board of directors. [26] Looking to exact safety and security standards in line with the IAEA and national authorities, ENEC is at the forefront of implementing the national vision of nuclear power, and deals directly with operational readiness, capacity development and delivery of the power plant projects. [27]

Institution	Description	Status of Organization
Federal Authority for Nuclear Regulation (FANR)	Primary head of safeguards, lawmaking, drafting federal regulations and ensuring effective implementation of legal codes, providing nuclear oversight writ large. Requires and issues permits on nuclear related items.	Active
Emirates Nuclear Energy Corporation (ENEC)	Oversees implementation of law and codes set forth by FANR, heads efforts on the ground such as environmental radiological monitoring	Active
Export Control Executive Office (ECEO)	In conjunction with FANR, ECEO has the ability to work across all seven Emirates. Any item that falls under international accords must obtain proper import permits. Facilitates commerce control from initial to final stages and at cabinet level	Active
Nuclear Energy Programme Implementing Organization (NEPIO)	Status confidential with no open source trail, may have been brought under ENEC supervision	Unknown
International Advisory Board (IAB)	Headed by Dr. Hans Blix, includes exclusive panel of experts that closely monitors status and progress of program and offers recommendations	Active, meets bi-annually
Critical National Infrastructure Authority (CNIA)	Absorbed by Critical Infrastructure & Coastal Protection Authority (CICPA), handles internal security by securing critical land and sea infrastructure	Inactive, now under CICPA
UAE Counterproliferation Task Force/Executive Committee on Commodity Control Procedures	Based within the Ministry of Foreign Affairs, this task force coordinates with FANR on export controls, licensing, and authorizations for the legal transit of sensitive or dual-use materials	Active
Gulf Nuclear Energy Infrastructure Institute (GNEII)	Housed at Khalifa University, works with INSEP to facilitate specialized training, providing “educational and professional development capabilities on nuclear energy safety, safeguards, and security topics” [28]	Active, ongoing development

Table 4: List of internal regulators and organizations involved in the nuclear program.[1]

On the ground, the Committee for Goods and Materials Subject to Import and Export Controls was established under Emirati Decree Number 299/3 of 2009 in order to control strategic commodities. While based in the Ministry of Foreign Affairs, this committee coordinates with the UAE Ministry of Interior, Ministry of Economy, Federal Customs Authority, Preventive Security Department within the Ministry of Interior, and the Armed Forces including Chemical Defense, Civil Defense factions within Ministry of Interior. Under the international legal framework, the Emirati legal code is largely based on Law No. (40) of 2006 regarding the Prohibition of Innovating, Producing, Storing, and Using Chemical Weapons Law No (13) of 2007 regarding commodities that are subject to import, in addition to export control Law No (6) of 2009 regarding the Peaceful Uses of Nuclear Energy. This committee permits goods and commodities, issuing Import, Export, Re-export, Transit, Transshipment and Brokering licenses to numerous federal agencies such as FANR, the Ministry of Industry, the Ministry of Health, among others. This is, of course, before coordination is done with customs and port security.

The Abu Dhabi Ports Company (ADPC), established in 2006, also plays a role to govern industrial zones and regulate commercial ports. It oversees commercial, community, fishing, and private logistics ports across Abu Dhabi. Its Imports & Exports Controls Customs process includes: pre-arrival manifest, risk management system, scanning facilities, radiation facilities, and manual inspection. It coordinates with the Ministry of the Interior and the UAE Ministry of Environment and Water to "provide intelligence in cooperation with local and international security agencies" to oversee multiple clearance levels and ensure the integrity of commodities that are being moved. Its primary Khalifa Port, which was inaugurated in 2012, commands a very impressive and technologically complex means of operation with connections to road, rail, and air transportation hubs.

1.4.1. Beware of Overlap of Regulatory Institutions

The governance of the seven federations within the United Arab Emirates is unique and has historically been subject to political qualms of the United Kingdom alongside several other regional powers in the Gulf. After it gained its independence from a British protectorate in 1971, Abu Dhabi, Dubai, Ajman, Fujairah, Sharjah and Umm al Qaiwain launched separate spheres of influence that were joined by Ras al

[1] *Other Known Major Partnerships (with no particular ranking or order)*

Institutions/Memberships:
Nuclear Regulatory Commission (NRC) Office of International Programs; Department of State (DOS)/Partnership for Nuclear Security (PNS); DOE/Nuclear Energy International Framework for Nuclear Energy Cooperation (IFNEC); DOE/National Nuclear Security Administration (NNSA)/International Nuclear Safeguards and Engagement Program (INSEP)/International Nonproliferation Export Control Program (INECP); Gulf Nuclear Energy Infrastructure Institute (GNEII); Co-operative Agreement for Arab States in Asia for Research, Development, and Training Related to Nuclear Sciences and Technology (ARASIA); World Association of Nuclear Operators (WANO); Gulf Cooperation Council (GCC); Proliferation Security Initiative (PSI).

Existing Bi-lateral Arrangements: [29]
Republic of Korea (ROK), primary consortium contract (2009); United Kingdom (UK), Agreement for Co-operation in the Peaceful Uses of Nuclear Energy (2010); France (2008), Canada, Argentina, Nuclear Cooperation Agreement (2013); Russia, Nuclear Cooperation Agreement (2012); Japan, bilateral Nuclear Cooperation/technical transfer agreements (2009); Australia Nuclear Cooperation Agreement (2012), safeguards agreement; Canada, Nuclear Cooperation Agreement, safeguards agreement (2012). FANR itself, however, has signed agreements with the following international bodies: FANR-Republic of Korea Institute of Nuclear Safety, Implementing Arrangement (2010); FANR-US Nuclear Regulatory Commission, Cooperation Arrangement (2010); FANR-Korea Institute of Nuclear Safety, Special Agreement (2011); FANR-Korea Institute of Nuclear Non-proliferation and Control sign Implementing Arrangement (2011); FANR-Finnish Radiation and Nuclear Safety Authority, bilateral arrangement (2011); FANR-French Nuclear Safety Authority (ASN), Cooperation Arrangement (2012); FANR-The French Institute for Radiological Protection and Nuclear Safety, Cooperation Arrangement (2013); FANR-The Norwegian Institute for Energy Technology, Associated Party Agreement (2013); FANR-Australian Radiation Protection and Nuclear Safety Agency, Cooperation Arrangement (2013); . On the domestic side, the following has been done: FANR-Critical National Infrastructure Authority, Cooperation Agreement (2011); FANR-Khalifa University of Science, Technology and Research (2011); FANR-National Transport Authority, Memorandum of Understanding (2012); FANR-National Emergency, Crisis and Disasters Management Authority (NCEMA), Memorandum of Understanding (2012); FANR-Abu Dhabi National Oil Company (ADNOC), Memorandum of Understanding (2012); FANR –The Telecommunications Regulatory Authority (TRA) sign Memorandum of Understanding (2013); FANR –The Environment Agency - Abu Dhabi (EAD), Memorandum of Understanding (2014); FANR –The Department of Civil of Aviation – Sharjah Emirates (DCA) sign Memorandum of Understanding (2014). [30]

Khaimah only a year later. Each Emirate, therefore, has an Emir who is appointed to the Federal Supreme Council, which is tasked to designate members of the cabinet and the Prime Minister (who also serves as the Vice President). This political process in practice ensures harmony among the seven absolute monarchs presiding over each respective Emirate. Electoral processes for public office, however, only began after December 2006. [31] Abu Dhabi, which maintains about 86% of total UAE land, remains the primary governmental capital and is politically authoritarian. [32] Historically, Abu Dhabi takes lead of the Presidency while Dubai serves as the vice presidency.

Aside from the few federal regulations in place, there is little overarching federal law that governs the seven Emirates generally. As it stands, each emirate offers its own independent export controls process and governance. This current Emirati structure implies that certain emirates may have stronger or weaker controls than others, leaving vulnerabilities open at the greater state-level. While interactions between FANR and ENEC head law-making and implementation of federal nuclear regulation, the realms of responsibility for other existing regulatory institutions are unclear, remain ceremonial, or are phasing out. As the regulatory framework matures, there should be caution of the numerous domestic institutions carrying out redundant activities by mirroring other organizations while federal institutions simultaneously assert more influence that harmonizes the Emirates.

Additionally, United Arab Emirates continues to work extensively with the United States, closely collaborating on technical exchanges, programmatic monitoring and capacity-building assistance. Second to this is its extensive joint effort in collaboration with the South Korean consortium. Other contractors are involved in the project, including numerous domestic entities that provide construction and other aid in addition to carrying out provisions put forth by the numerous contracts and agreements that have been negotiated bilaterally or multilaterally. While the UAE should strengthen its growing number of protocols, agreements, and conventions that are signed, it should also be careful that redundancy may occur if not coordinated carefully.

Further, some have argued there is an even larger issue of coordinating the training of the Emirati workforce by outsider partner or ‘donor countries’ that continue to offer a number of services and training for the UAE. [33] As the UAE remains on the fast track towards a robust nuclear energy program, it continues to accept enormous amounts of external assistance to bolster capacity building, leading to overlap in training modules and professional development. Further, numerous ‘Emirati’ delegations that are set to engage in training often send their non-indigenous colleagues, leading to further redundancy. Yet, it is without a doubt that such training modules are necessary, and it is important to note that redundancy or overlap in training is not an experience limited to the United Arab Emirates.

1.4.2. Indigenous Capability Not Yet Fully Realized

Prior to the signing of the 2008 US-UAE MOU on Nuclear Energy Cooperation, the United Arab Emirates had virtually no indigenous nuclear capacity or technical know-how on development or maintenance of a robust nuclear energy agenda. Typically, this implies that large amounts of support and reliance on the international community and foreign expertise would be required in order to move forward with such a program. As of now, there is a high reliance on foreign workers and expertise – the majority of workers at FANR alone are foreign nationals, drawing from more than 21 countries as of December 2010. [34] Certainly, that number has grown in the last five years. And while FANR is comprised of mostly foreigners, it is expected to make a full transition to an Emirati workforce over the next few decades when the reins of responsibility to fully govern the nuclear program are passed from South Korea to the UAE. Yet, the UAE goal for a fully indigenous program cannot be fully realized until much later when proper, effective legislation is adopted and a substantial, capable workforce is fully trained.

The Emirates is currently attempting to tackle its lack of specialized workers in the field, and efforts to bolster effective training mechanisms include the inauguration of the Institute for Applied Technology (IAT) in Abu Dhabi and Simulator Training Center (STC) just a stone’s throw away from the Barakah site. [35] In October 2014, ENEC announced that forty Emirati students have graduated from the ENEC human capital development program, appropriately named Energy Pioneers, which divides about eighteen months of

time of its participants between specialized training sessions at the IAT in Abu Dhabi and in South Korean facilities. [36]

Further, there are numerous countries currently involved in the enrichment and fabrication processes, handling the front of the fuel cycle of the program. Abu Dhabi is currently working with a number of international nuclear contractors that will be serving specific roles, including but not limited to involvement of; Canada's Uranium One, Rio Tinto in the United Kingdom, France's Areva, Tenex in Russia, URENCO based in the European Union, and the US' Converdyn. [37] It appears these entities will coordinate with KEPCO on the front-end of the fuel cycle to convert, enrich and fabricate reactor fuel, which will then supply the UAE with the nuclear fuel assemblies and fuel to power the four reactors.

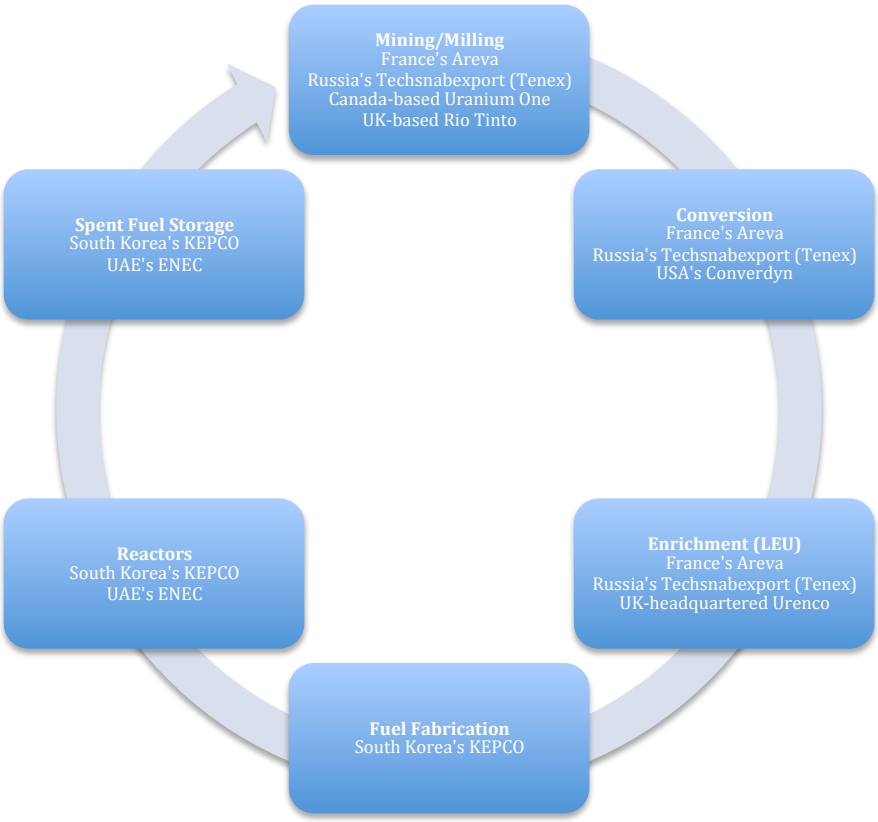

Table 5: Projected supply chain of the UAE.

Indeed, there are many players that have a hand in the fuel cycle and program of the UAE, as displayed in the chart above. This chart also evenly divides up the rights of the UAE to certain elements of the fuel cycle. It is made clear that the 'front end' of the cycle, meaning the processes between mining and milling to fuel fabrication will be completed outside of the UAE, and these are the capabilities that the UAE forfeit through the negotiated 123 agreement. The 'front end' cycle is often viewed as a proliferation concern due to the fact that enrichment can be diverted for non-peaceful purposes and used to enrich uranium for a bomb. However, the above chart goes to show that the Emirates really only deals with the operation of reactors and power generation (and to be determined, spent fuel storage may also potentially end up in the bill). Safeguards should be administered at every stage in which sensitive materials can be diverted for non-peaceful purposes. In the UAE, this is especially true for energy production and fuel storage stages. Yet, the UAE has also given up its reprocessing capabilities and so will not have the ability to filter out plutonium from its spent fuel stocks on the back end of the cycle, eliminating potential for the Emirates to ability to effectively weaponize a plutonium bomb.

At the very least, the Emirati example demonstrates that states with little former indigenous nuclear fluency compels governments to 'import' the technical know-how and workers with the appropriate skill-set until its own citizens are trained properly. Though, in the case of the UAE, the number of players involved in the fuel cycle itself should not change dramatically so long as the UAE is obligated to forgo domestic enrichment and reprocessing. With that, the many international players in the UAE program will make it increasingly difficult to gauge the role of each state and its contributions – positive or detrimental – to the UAE's peaceful nuclear energy program until much later. [38]

Above, we see that there are numerous regulators and institutions both domestically and abroad that are hard at work to promote security, build out regulation, and grow the program exponentially in a short amount of time. With that, there is significant demand placed on the limited number of bureaucrats working on these issues in the Emirates. The Emirates should seek to strike the balance between international and domestic players to effectively govern its program and continue to develop its nuclear framework.

2. Shortcoming One: Underdeveloped Legal Infrastructure

In October 2008, the "Federal Law Regarding the Peaceful Uses of Nuclear Energy" was signed, putting the UAE on a path towards utilizing the power of the atom for peaceful purposes. At first glance, the UAE has set a high precedent for commitment and compliance to international accords and treaties that hedge against the threat of illicit activities related to nuclear programs and detrimental transshipments. Under closer examination, however, there are a number of 'legal loopholes' that exist and could be exploited or leveraged to facilitate illicit activities. The Emirates should close potential gaps in its legal infrastructure and ensure that its legal framework will effectively combat illicit smuggling before its program goes live in 2017.

The United Arab Emirates has ratified the historic Additional Protocol and a number of other accords to strengthen its safeguards framework, despite the fact that much of this rhetoric has been limited to measures of intent and not necessarily been translated into action or legislation on the ground. While the UAE has signed onto a number of International Atomic Energy Agency (IAEA) and international safeguards that allow it a façade of a solid framework, each individually negotiated accord should be carefully scanned for potential shortcomings.

Current IAEA Safeguards and other relevant international accords negotiated with the UAE include:

Title	Description	Entry Into Force (EIF)
Non-Proliferation Treaty (NPT)	The NPT aims to prevent the spread of nuclear weapons, promote peaceful nuclear energy programs & pursue global disarmament	1995
Comprehensive Safeguards Agreement (CSA), INFCIRC/622	Based on standardized model INFCIRC/153, an adapted version was negotiated to apply safeguards "on all sources of source and special fissionable material" in cooperation with the IAEA	2003
Original, Unmodified Small Quantities Protocol (SQP)	In place for states without significant quantities of nuclear materials to bypass most requirements for detailed nuclear material accountancy reports and IAEA inspections	2003
UNSC Resolution 1540	Binding agreement, complementary to multilateral treaties that require states to prevent development, acquisition, transfer or	2004

	use of CBRN-related materials and associated delivery systems to address threats posed by non-state actors [39]	
INFCIRC/254/Part1 & INFCIRC/254/Part2	NSG Guidelines for conditions of transfer on the export or transit of sensitive nuclear and nuclear-related materials, equipment, and technology	2007
U.S.–UAE Section 123 Agreement for Peaceful Civilian Nuclear Energy Cooperation (123 Agreement)	Agreement signed between the US and UAE for cooperation on peaceful uses of nuclear energy, where UAE forgoes domestic uranium enrichment & reprocessing and signs AP – often referred to as 'Gold Standard'	2009
Additional Protocol (AP/INFCIRC540)	Model Protocol Additional to CSAs between states and IAEA for application of Safeguards, requiring states to collect, declare and report to IAEA, complementary access to ensure verification and comprehensiveness and completeness of information provided.	2010

Table 6: List of current international regulatory treaties.

It is important to note that this list is not exhaustive. The UAE has also signed onto the Convention on the Physical Protection of Nuclear Material (2003), Convention for the Suppression of Acts of Nuclear Terrorism (2005), Convention on Nuclear Safety (2009), Joint Convention on the Safety of Spent Fuel and Radiological Waste (2009), among other agreements not listed here.

On the international level, the UAE follows a number of protocols set forth by the IAEA and UN, including the hailed Additional Protocol that expands IAEA ability to provide reasonable assurance against the existence of undeclared nuclear activities. [40] To date, the 123 Agreement and AP provide the fundamental basis of safeguards and offer the most restrictive regulatory legal codes to date. As such, the AP alone requires one random IAEA headed inspection annually in addition to quarterly verification of each light water reactor. Another heavy hitting piece of legislation includes the Comprehensive Safeguards Agreements (INFCIRC/622) and the call to develop Systems of Accounting for and Control (SSAC) within the UAE. The basic obligations of any CSAs (whether under the model 153 agreement or negotiated 622 with the UAE) is to establish SSACs in order to facilitate cooperation, provide access, and declare information to the IAEA of its nuclear materials and facilities. With that, the need to develop bookkeeping, verification of nuclear material inventory, containment and surveillance, among other measures remains to be done in the case of the UAE. [41] On the domestic front, aside from the need to solidify SSAC regulations, the UAE's Federal Authority for Nuclear Regulation (FANR) continues to take the lead in drafting nuclear regulatory code, yet much ground remains to be covered before 2017.

2.1. Reliance on Original SQP

Perhaps the most unsettling aspect of the UAE legal code is its reliance on the original SQP I, granting the Emirates greater flexibility to handle sensitive nuclear materials without obligation to declare such materials to the IAEA until it receives its first reactor fuel load. Initially, this agreement was negotiated to reduce the burden on countries with little or no nuclear materials from inspections and other obligations such as to declare materials to the IAEA. According to Matthew Cottee of the International Institute for Strategic Studies (IISS) in London, the original SQP is "designed to reduce pressure on resources, both at the IAEA and in SQP states, many of the reporting and access requirements under the CSA are held in abeyance." [42] However, these protections have now reversed on the Emirates, as the IAEA now carries little to no authority over the Emirati program until the original SQP is rescinded, as called for under the 123 Agreement negotiated in 2009.

As a greater part of Comprehensive Safeguards Agreements negotiated with states, certain countries are eligible for the original SQP if there is no significant amount of nuclear material statewide and there is no nuclear material in any given facility. The original 1974 SQP does not require these states to declare their activities and holds in abeyance most all safeguards measures in Part II of the model protocol INFCIRC/153. [43] The motivations of the IAEA to exempt certain states were prompted in efforts to reduce redundancy, as many states during the early nuclear age did not have any facilities or materials to

declare. In order to remove the burden of declaratory or invasive activities by the IAEA in states where such measures carried little relevancy, the SQP also acted as an incentive for states to join onto otherwise cumbersome agreements. [44] This is due to the fact that under the original SQP I code, there is no requirement to provide the IAEA an inventory of nuclear materials, nor allow inspection of those materials, as long as the total quantity of nuclear materials in the state is small and no nuclear material yet has been introduced into a nuclear facility.

Initial reporting and record keeping is also required for aspiring and established nuclear states, yet this first piece is missing. Without required declarations, there is no ability for the IAEA to conduct inspections, ensure that proper measures are being met, nor request additional data from the Emirates regarding the materials that may be imported or exported. It appears the most recent evaluation carried out by the IAEA in the UAE was done by its Site and External Events Design (SEED) Review Mission between 21-24 November, 2011 or the Emergency Preparedness Review Service with the IAEA on March 31, 2015. This mission gauged site characterization and reviewed sections of the greater Emirati nuclear framework, but much has changed since 2011. On the other hand, the 2015 visit was a safety exercise that did not include verification of construction nor official inspections. [45] Moreover, the latest Safeguards Implementation Report for 2013 by the IAEA reports that the Emirates has offered numerous additional protocol declarations and declares one facility under safeguards, though zero declarations have been made in several other areas, including: number of inspections, number of design information verification, number of complementary accesses, among others. [46]

The UAE signed onto the original SQP in 2003, and although the implementation of the US-UAE 123 Agreement requires that the original SQP be rescinded before the US agrees to license any nuclear exports to the UAE, Abu Dhabi will not go back on its SQP I. That is, not until nuclear material is introduced into a nuclear reactor or a threshold amount of nuclear materials is present the country, which would nullify the original SQP anyway – so likely no earlier than late 2016 or 2017.

While the SQP may be sufficient to ensure safeguards are being met in the meantime, there are numerous shortcomings to the original SQP as the program continues to develop. At the time of its signing (for original SQPs), many states were required to report the import or export of nuclear materials, design information questionnaires and plans to introduce nuclear material into a facility. Yet, for many countries, these reports are decades old and the IAEA has no mechanisms to follow-up on initial declarations. Further, the IAEA also no longer has the right to conduct inspections or formally request further information on these updates. In part, the original SQP left numerous gaps that were leveraged by numerous states for clandestine nuclear programs, such as the 1991 discovery of an illicit Iraqi program. Rising up to the challenge and realizing the need for a strengthened safeguards regime, the IAEA modified and updated the SQP in 2005, also formally known as the Modified Small Quantities Protocol (GOV/INF/276/Mod.1).

The revamped Small Quantities Protocol II is much more comprehensive in the areas it covers. It requires initial nuclear materials declaration, annual reports, design information questionnaires and declaration to the IAEA upon the decision to build up a nuclear program. This last point is indispensible, as this notification happens as soon as a *decision* is made to build a nuclear facility, rendering the updated SQP null and void and all previous articles held in abeyance become required. Now, while the updated 2005 SQP (SQP II) is much more comprehensive in terms of requiring declaration and verification of initial inventory of nuclear materials, many states have still not updated their original, negotiated small quantities protocol. The UAE falls into this category.

Simply, the UAE explicitly opted to not make the transition to the modified, updated SQP II. All reporting to the IAEA (other than imports and exports) until the original SQP is rescinded remains voluntary, and without the obligation of inspections. Without inspections, the time between now and the 2017 deadline creates a phase where the program is suspended in the grey areas of legality of required declarations and what is actually moving through Emirati borders until the 2017 deadline is met. It is without a doubt that UAE adherence to the original SQP remains a large sore point for the IAEA and the nonproliferation regime. [47] It is important to note, however, this shortcoming will likely become irrelevant after 2017 after large quantities of ROK-supplied nuclear fuel arrives in country, well in excess of the limits for continued

SQP eligibility. The SQP will be automatically rescinded at that point, as specified in its original negotiated SQP text, subjecting the UAE to relevant IAEA protocols set forth in its comprehensive safeguards agreement.

2.1.1. Subsidiary Arrangements Held in Abeyance

When Comprehensive Safeguards Agreements are signed, as the UAE did in 2003, subsidiary arrangements are typically negotiated within 90 days of CSA entry into force. And while Article 39 of the negotiated CSA (INFCIRC622) calls for implementation of subsidiary arrangements that expand safeguards activities, this statute – along with a number of other commitments – is held in abeyance while the SQP remains in effect. In essence, this shortcoming allows the UAE to be exempt from implementing Subsidiary Arrangement Codes 1-9, legal codes which typically complement comprehensive safeguards agreements and strengthen safeguards until the original SQP is rescinded.

2.1.2. Inability to Conduct Design Information Verification Before 2016 or 2017

While the topic remains sensitive to the Abu Dhabi government, it is likely that the UAE has already submitted facility design information on the Barakah nuclear reactors in the form of design information questionnaires (DIQ), providing some early transparency to the program. Though, the CSA article (INFCIRC/622, Article 47) that allows for inspectors to conduct on-site verification of the submitted design information is also held in abeyance so long as the SQP is in effect. [48] Typically, declarations of this nature include “the facility description; the form, quantity, location and flow of nuclear material being used; facility layout and containment features; and procedures for nuclear material accountancy and control.” [49]

Under current conditions of the original SQP, no IAEA inspector has the right to step foot in a UAE facility to conduct design information verifications or safeguards inspections until the SQP is rescinded or declared no longer in effect. Once a DIQ has been submitted (6 months before fuel is introduced to the facility, if not before then), Barakah officially becomes a nuclear “site,” only then subjecting it to a number safeguards and allowing the IAEA to act under AP Article 5.a(i) facilitating complementary access rights anywhere within the boundaries of the site to verify absence of undeclared nuclear materials and activities. Before that time (if an updated DIQ has not yet been submitted), the IAEA would in principle only be allowed to act under AP Article 5.c, allowing complementary access rights to conduct environmental sampling anywhere in the UAE to “resolve a question or inconsistency” about the correctness and completeness of the UAE’s AP declarations – in practice, IAEA follow-up of 5.c access is far more rare than 5.a(i) access. [50]

More specifically, with the supply of APR-1400s, the design dictates that one third of the allotted fuel assemblies are switched out of the reactor core with each refueling, indicating that three fuel cycles take place before the entirety of the fuel cycle is completed. Characteristics of light water reactors poses several areas of interest for those who may be looking to divert or misuse nuclear materials, including materials found in fresh fuel or storage, core fuel in reactor vessel and spent fuel in ponds. There is also potential of diversion of fresh LEU or spent fuel or manipulation of shipments of spent fuel. [51] With that, fuel pins can also be inserted or removed causing a proliferation risk, but in theory these risks would be verified by IAEA safeguard routines after the program goes live. Though, the largest proliferation risk may fall under the switch-outs and verification of materials that are swapped out during the refueling process. Also, it may be important to note that no decisions have yet been made on accommodating future nuclear waste and spent reactor fuel, which could pose an additional layer of risk should the UAE not develop an effective nuclear waste strategy. While the APR-1400 reactor may accommodate mixed-oxide fuel (MOX), its use should be discouraged from a safeguards perspective, as there is a sizeable risk of reconversion of fresh MOX fuel to extract weapons usable plutonium.

To the credit of the Emirates, Safeguards Plans (SP) and Design Information Questionnaires (DIQ) are carried out as required by the IAEA, at least internally, but it is not clear that this information is made public or shared. These practices include drafting definitions, information protection, designating roles and responsibility, reporting and recording, compliance and more. The Emirates also models its practices

directly off IAEA templates to cover data collections, nuclear material handling, nuclear material accountancy and control, general reactor data, and more. As of September 2014, the licensing process is as follows: Construction License Application Review, including a Preliminary Safety Analysis & Summary Report, Quality Assurance Manual, Management System Manual, Preliminary Safeguards Plan, Physical Protection Plan, Aircraft Impact Assessment Report, and Regulatory Commitments. And while the UAE claims DIQs were done for reactor sites 3 & 4, it was quoted that DIQs were "submitted as part of a routine annual safeguards update." [52] Though, is not entirely clear who the Emirates provided this information to or whether or not there were any official containment or surveillance verification activities. Simply put, the IAEA may only conduct environmental sampling to gauge suspected inconsistency under the AP as of now, but would still need more valid reason or explicit invitation for such an inspection.

With that, there are still two ways potential threats could arise: internal nonproliferation and external transshipment. Any interdictions at the front end would have to be foreign based, though any issues dealing with reactors or the back end of the fuel cycle is likely to fall under UAE authority insofar as storage and potential shipments of spent fuel to be processed could be manipulated on Emirati soil. In order to verify soundness and completeness of safeguards implementation and a robust framework to support the safety of the nuclear energy program, the IAEA will need complimentary access to facilities to gauge the integrity of safeguards implementation. Though, once fuel is introduced to the reactor, the SQP would automatically be rescinded and the IAEA would be able to begin the process to conduct ad hoc inspections as it saw fit.

2.2. Potential Maintained Ability to Sell/Transfer Sensitive Technologies Under '123 Agreement'

The US-Emirati 123 Agreement and the Agreed Minute is now regularly hailed as a 'gold standard' for newcomer nuclear programs and mitigates a number of proliferation concerns, yet does not close all loopholes that may allow for internal or external proliferation. While the 123 Agreement has been required for nuclear cooperation with the US since the early nuclear age as a standard enabling agreement, the ENR clause in the agreed minute is more specifically what is referred to as the Gold Standard in the Emirati case. It goes without saying the UAE demonstrated huge nonproliferation commitments by signing onto the 123 Agreement, but there is still currently no language in the agreement that actively prevents the exchange of sensitive components that could be readily repurposed, exposing yet another proliferation concern.

With that, the hailed 123 Agreement between the US and UAE contains one significant shortfall: the UAE retains the right to transfer sensitive components, technologies, and materials that could have dual-use or proliferation worthy applications even with its forgoing of ENR capabilities; a right that could be considered an inherent shortcoming of design of the 123 'Gold Standard.' While Abu Dhabi has given up the right to enrich domestically, there is no detailed statute in the brokered agreement that would hinder its ability to become a nuclear supplier at some point in the future or transfer point of nuclear materials, which is increasingly a very real prospective with the bolstering of its own domestic technical capabilities and know-how.

This is not to say that there are no hurdles for the UAE to become a nuclear broker, indeed, there are several. There are numerous obstacles placed before the UAE through other safeguards agreements and negotiated bilateral contracts. In the language of Article VI of the 123 Agreement – *Reprocessing, Other Alteration in Form or Content, and Enrichment* – it is stipulated that the UAE is not restricted in its development or transfer of sensitive components or materials for purposes aside from official use. It goes onto to also state, however, that "material transferred pursuant to this agreement and material used in or produced through the use of material or equipment so transferred shall not be reprocessed unless the Parties agree." Yet under this rhetoric, the 123 still does not address the development, sale, or transfer of related technologies so long as such materials are not being purposed for reprocessing and enrichment capabilities domestically on Emirati soil. In effect, it permits the transfers and sales of nuclear-related material and major components of other sensitive nuclear technologies, certainly undercutting the US' and international community's ability to hinder the ability of the UAE in moving these types of products in the future, should it make such moves in the future.

While this language may currently be considered an unaddressed loophole, the Emirates still has its hands tied due to clauses with a number of other states and would likely never pursue this option. It is, however, discussed here to go to show that improvements could be made in the language of negotiated 123 Agreements in the future, particularly for other aspiring nuclear energy states.

3. Shortcoming Two: Unsettled Export Control Concerns

Despite a spotty history with illicit trade and strategic trade control issues (STC), the United Arab Emirates works to effectively deal with the threat of illicit transfers taking place within its borders, though uniform or standardized export controls remain underdeveloped to date. Given the historical and ongoing role of the UAE as a major commercial establishment, proliferation risks remain due to large traffic moving through ports primarily based in the emirates of Dubai, Abu Dhabi, and Sharjah. Before 2007, the United Arab Emirates had virtually zero export controls in place – both in terms of relevant legal codes and the ability to follow up on abuses of transshipments through its borders. Due to this, its many free trade zones were previously exploited into serving illicit channels that provided sensitive technologies to nuclear programs in Iran, Syria, North Korea, among others. This issue, among developing effective STCs, remain to be a hurdle even today. Yet, it is imperative to effectively regulate authorizations, control dual-use items, and bolster other restrictive measures. [53]

Following the A.Q. Khan episode, among other concerns to the export control regime, the UAE was pressured by the international community to comply with the stipulations of the United Nations Security Council Resolution (UNSCR) 1540 in 2004, a legally binding document that seeks to push member states to “have and enforce appropriate and effective measures against the proliferation of nuclear, chemical, and biological weapons (WMD), their delivery systems, including by establishing controls.” Further, in the case of potentially hazardous or dual-use materials, UNSCR 1540 “closes gaps in nonproliferation treaties and conventions to help prevent terrorists and criminal organizations from obtaining the world’s most dangerous weapons.” [54] And although 1540 outlines the stipulations states must make to achieve its basic obligations over controls, it does not put forth measures on how states will carry it out in practice. Without a doubt, the trade control regime within the Emirates is still largely in its infancy, yet looks to serve as an example for its neighbors in the GCC even in matters concerning safeguards and export controls infrastructure. Undoubtedly, measures of enforcement have improved and there have been huge efforts to crack down on general trading companies and money flow, especially to Iran. The UAE took steps to combat this beginning in 2007 by instituting new export control laws that shut down a number of money laundering and dual-use trafficking activities with Iran. [55] Undoubtedly, the UAE pursued these measures in step with joining the ranks of export control regimes.

While entities such as the Nuclear Suppliers Group (NSG), Wassenaar Agreement, and the Australia group are in place to deal with dual-use issues, state level export controls are not under the purview of nuclear cooperation agreements in general nor are the Emirates party to these relevant institutions. In the UAE, it is only recently that legal and prosecutorial export controls mechanisms been implemented, but remain relatively new and untested. Often, the UAE tackles internal governances issues through multilateral efforts and by working with a number of international services or governments that ensure a baseline level of legal obligations. For the most part, the UAE acknowledges its former position as a transit hub and aims to change this reputation, though Abu Dhabi must endeavor to further enable its legal infrastructure to mitigate such concerns to ensure its export controls infrastructure does not facilitate smuggling or transit of sensitive materials. In March 2014, the Emirates hosted the International Export Controls Conference, bringing together experts from around the world to discuss effective trade control measures in addition to being an opportunity for the UAE to showcase its port security and beyond.

At first glance, the export controls process in the United Arab Emirates is relatively simple. Initially, the Federal Authority for Nuclear Regulation conjures law on the matter, requiring importers and exporters to apply for and obtain permits for sensitive items. [56] On the ground, however, the United Arab Emirates’ Export Control Executive Office (ECEO) takes over and ensures that all measures are being met. Carriers or shippers of radioactive material must first receive authorization from FANR, in addition to fulfilling compliance for all laws and regulations within the emirates, identifying the end user, and ensuring the

proper authorities also have the appropriate clearance. Typical movement of any sensitive cargo relating to the UAE nuclear program first requires KEPCO to notify the IAEA of upcoming shipments and verification of such items before the material is moved, as the Korean consortium heads management of the front-end of the fuel cycle. On the other hand, the UAE is required to notify the IAEA of any upcoming imports, and to verify the materials upon arrival in addition to when the materials are introduced to the fresh fuel storage site. All the while, the UAE, ROK, and IAEA must agree on effective safeguards approach, including cameras, seals, and other measures of safeguards verification. [57] Within the Emirates, The UAE Committee on Commodities Subject to Import and Export Controls, evidently now housed within the Ministry of Foreign Affairs, remains to be another primary export and import control agency for the Emirati nuclear program. Typically, any company or agency dealing with sensitive materials for import or export purposes must acquire a license to handle controlled items. Only then does each import or export through Abu Dhabi subsequently receive a permit, differing from typical conventions and procedure elsewhere. [58]

According to the US Bureau of Industry and Security, exporters should:

> "know whether foreign customers are obligated to obtain import or other authorizations prior to receiving controlled items. As a best practice, prior to shipment, BIS recommends U.S. exporters provide foreign customers with the Export Control Classification Number (ECCN) of items to be exported and request a copy of any required foreign authorizations. Failure of a foreign customer to honor a request to provide a copy of any required foreign import or export authorizations would present a 'red flag' that indicates an export may be destined for an inappropriate end use, end user or destination." [59]

These authorizations are universally applied within the EU to manage items from import countries to the end user, and an Emirati royal decree made in 2014 effectively set the EU Export controls list to be considered as national law to be carried out in the same fashion across the seven Emirates. Hence, an export controls list within the Emirates is to be modeled off of the EU Export controls list. Surely, there will be a greater effort by the international export control regime to push for such comprehensive rules that will guide importers and exporters to harmonize best practices in order to regulate control and dual-use items. [60] And while this is an applaudable effort on paper, there are still no clear stipulations on how the law was to be carried out.

From the perspective of proper governance, the two major players appear for trade control to be the ECEO committee and FANR. First, FANR will establish the rule of law on export controls and the transit of dual-use items. ECEO is the secondary step to actually issue permits and follow up on abuses.

3.1. No Formal Export Controls List

A large number of sensitive nuclear technologies and material are slated for import to the UAE, yet no formal export controls list has been adopted to Emirati law. The Export Control Law No. 13 was enacted in 2007, the first code to deal with commodities that are subject to import and export control through Emirati borders, but remains limited in its capacity to effectively head all export controls endeavors. [61] While the UAE currently follows the guidelines set forth by the Nuclear Suppliers Group, adopting INFCIRC/254/Part1 & INFCIRC/254/Part2 that sets guidelines for "nuclear transfers" and "guidelines for transfers of nuclear-related dual-use equipment, materials, software, and related technology" respectively, more could be done on this front in the form of a formalized export control list. [62] FANR and the UAE Committee on Commodities Subject to Import and Export Controls continue to loosely adhere to the EU dual-use list, NSG guidelines, and operative paragraphs of their 123 and safeguards agreements, but has yet to formalize adoption of any such lists to law. No formal list currently exists nor plans to develop a comprehensive export controls list. [63]

Unlike the EU, which is included in numerous multilateral regimes and has adopted measures to strengthen international cooperation to counter threats posed by misuse or diversion of materials, the UAE still has much work to do. [64] Engagement of already present enforcement communities will be key to securing the Emirates' ability to effectively enforce export controls. Leveraging numerous authorities and

agencies would help the Emirates bolster their exports control regime. This includes engagement of customs authorities, law enforcement, regulatory and licensing agencies, scientific and academic communities, among others to reach this goal.

The UAE is not totally in the dark on the issue, however, as FANR proposed federal code to address export controls issues and combat proliferation in 2014, a move which was promptly adopted into law and neatly outlined in Code 9. This code looks to "establish licensing and reporting requirements for the Transfer of Regulated Items," laying out the responsibilities of FANR and the UAE Imports Exports Control Committee to regulate licensing and authorizing movement of sensitive technologies that adhere to INFCIRC/254 and INFCIRC/622. [65] However, the division of labor between FANR and the Committee remains opaque, informal, and largely ad hoc. And still, none of the seven Emirates nor the federal government of the UAE currently sustains a formal exports list, going to show that effective and consistent export controls will be hard to achieve without one – Emirati rhetoric remains to be translated into action through a detailed list adopted into law. [66] While materials continue to move through numerous UAE ports, there is simply no ability to equally regulate all imports and exports moving through its borders with the status quo.

3.2. Disjointed Emirati Law

An additional layer of complication that may affect effective governance of export controls includes the relatively new federal government structure within the United Arab Emirates. Until recent years, the seven Emirates enjoyed a fair amount of independence and flexibility to draft their own laws with limited federal oversight. For the most part, each Emirate enjoyed a great degree of self-governance until larger, coordinated federal efforts were implemented in recent decades, such as with the Abu Dhabi National Oil Company, FANR, and other entities. The nuclear energy program effort in particular, however, looks to force the hands of each independent Emirate to shift from an individual state mentality towards strengthening federal-level law and institutions (albeit in the nuclear case a large discretion is granted to Abu Dhabi, where the Barakah site is based). [67]

The UAE is diligent in maintaining its status as the leading country in the region on nonproliferation issues. In 2010, it even went as far as to freeze 41 Iran-linked accounts and thwart other questionable activities. It was reported that the UAE has also cracked down on more than 40 firms engaged in dual-use materials or money laundering. However, when this took place and which businesses were involved have yet to be seen. [68] In many instances of this nature, the cooperation between the UAE and the international community has been mostly positive despite publicity of these successful interdictions being limited or hardly hailed. Indeed, it appears the international community is fast to respond to failures rather than successes.

To ensure the rate of success in the Emirates to interdict potential hazards, there is a need for more coordinated investigations, improved efficiency of resources, easing public sector bureaucracy (including foreign customs regimes), improving information sharing and reducing potential overlaps. There must have a primary point of contact between the licensing FANR and enforcement on the ground. The Federal Authority for Nuclear Regulation already published a number of regulatory guides and licensing controls to regulate the nuclear program and build out the framework so that its nuclear ambitions may be realized, yet more remains to be done to bridge the gap between policymakers and federal institutions that are seeing these policies through. A number of unaddressed issues remain, including nuclear waste regulation and the development of state system for accounting and control of nuclear materials.

A number of regulatory measures have been in place for years, namely, UNSCR 1540 that seeks to address Weapons of Mass Destruction (WMD), which should have led to the development of a number of other domestic measures and obligations placed on stakeholders in the program. Further, regulations set forth by FANR and ENEC have been set to manage incoming exports to support and strengthen measures that would address with potential gaps in legislation. However, the implementation of these laws has taken much longer, and still there is not concrete means on how to follow-up on abuses. The big question remains on how the UAE intends to follow up on abuses. For the most part, the Emirates is an authoritarian state and by default is at liberty to shut down any suspect company or importers or exporters

without notice. Yet, there is a fine line to walk between dealing with official legalities and overstepping of power on related issues. The Emirates should ensure that it has sound mechanisms to keep its legislation up to date, with the principal purpose to change behavior of actors that may not be using the law as intended.

3.3. Other Considerations

The UAE has made strides to develop the most comprehensive nuclear energy program to date, but other concerns may hinder its ability to effectively regulate its borders and export concerns before the reactors start going live in 2017. To date, it has received wide praise from top international experts and governments alike, and is increasingly being considered a steward in the field as it goes onto aid other programs such as the one currently under development in Jordan. Certainly, the Emirates continues to rely on outside assistance, namely from the United States, who would be able to aid national stakeholders develop a detailed framework to operate, regulate and oversee protection of its materials. Further, the question of implementation remains to be the biggest question: how will the program look in practice once it goes live? There are a few other outstanding considerations that should be assessed.

First, the Emirates should seek to maximize the potential of its citizens working on nuclear issues and minimize bureaucracy. Indeed, the Emirates has set up work programs and centers to train and equip its indigenous population with the necessary skills to run such a program, yet these institutes are still in their infancy and their activities should be expanded. Other facilities have been built near the site to train its modest numbers of students and employees, but many of these individuals have yet to accumulate the required experience necessary to take the lead on a nuclear program. Although the workforce issue is certainly not limited to the Emirates, the region and beyond deals with extreme bureaucratic issues and may not be fully equipped to deal with concerns that may arise in regards to legal shortcomings or implementing federal regulation in a timely manner. Indeed, the Emirates will be shuffling its top management in the future, forcing it to reassess the phase out foreign workers over time if they are to achieve the goal of a 100% Emirati workforce to head the nuclear power project.

Second, while the UAE continues to work with its Korean and American counterparts to further develop the framework agenda, cultural factors that may affect the growth of the program must also be considered, as each party often bring divergent strengths and weaknesses to the table. Naturally, this all stems from the very diverse and robust network involved in the project. For instance, the constitution of the UAE under Article 14 speaks to “equality, social justice, and providing safety, security, and equal opportunities to all the citizens are pillars on which the community is grounded. Solidarity and shared sympathies are close links that tie the Emirates together.” In practice, while its citizens (which constitute the minority) routinely receive favorable treatment, the situation for others working on the program is much different.

It would also be wise to take into consideration cultural aspects and potential misunderstandings that may arise between the many hired hands working on the project. Through conducted interviews on the ground in Abu Dhabi, it was clear that the Koreans and the Emiratis have had disagreements on ways forward in developing the program. To be sure, this is normal when cultures come together to tackle tough issues, yet the large number of different nationalities working on the program may actually create more uncertainty and distrust among the ranks rather than promote fraternalism. However, the many parties involved in the development and deployment of this program can conversely push for common understanding and encourage stronger controls.

The primary contractor for the four reactors is South Korea, which runs about a third of its electricity from nuclear power, also has a spotty record of nonproliferation within its own borders. As recently as mid-2013, the ROK suspended operation in two reactors and shutdown a third amid reports of falsified safety reports. [69] This scandal follows a similar incident in 2012 where operation of 23 reactors were stopped due to the use of industrial supplies that had been exchanged and implemented with fake certificates, a reported up to 10,000 components over the course of a decade were installed under the pretenses of false paperwork. [70] Another scandal of the firing of the vice president of KEPCO and chief executive at its subsidiary Korea Hydro and Nuclear Power certainly does not provide comfort to the Emiratis, particularly

as some of those directly involved in the scandal had worked with the UAE to develop its nuclear program. [71]

Third, criticism of the government is near illegal and media within the Emirates is heavily restricted, which may hinder transparency and fair dialogue on development of the nuclear program. For example, Article 30 of the UAE constitution stipulates: “Freedom of opinion and of expressing that opinion verbally, in writing, or by any other medium of expression is guaranteed as provided in law.” [72] In theory, this would guarantee freedom of speech and the right of the press. However, in practice, the UAE is still heavily reliant on perpetrating official news and government releases that go through heavy edits. Most Emirati media networks are subsidized by the government, and it is illegal to criticize the King, the Royal Family, or decisions of government. Hence, the system actively works against criticism of the government or of the ruling family. It is also sensitive to issues pertaining to radicalism or pornography. As of 2014, according to the World Press Freedom Index produced by Reporters Without Borders, places the United Arab Emirates at a ranking of 118. [73] All in all, such censorship and lack of freedom of press could be detrimental for the transparency of its program in the long run.

Fourth, there are other political considerations to take into account. Numerous others wonder if its acquisition of nuclear power is a hedging strategy against the Iran nuclear deal and ongoing program. While much debate surrounds the question of prestige and the role of nuclear energy programs in the region to hedge against Iran, it does not, at least overtly, appear to be a hedging strategy.

Undoubtedly, there are layers of concerns to take into consideration when assessing the UAE program, and while not all these presented considerations are dangerous or detrimental to a developing nuclear energy program, it is wise to keep these cultural and technical factors in mind.

4. The UAE’s ‘Gold Opportunity’

As of now, it appears illicit transshipment or diversion of sensitive technologies and materials tied to the United Arab Emirates’ nuclear energy program is possible under the status quo. Surely, there is an immediate need to strengthen the legal infrastructure, export controls, and regulatory capacity before the program goes live in 2017 to effectively mitigate these challenges if it is to live up to its model state status. This is especially so if the UAE is looking to avoid a ‘commitment-compliance gap’ as it continues on a fast track towards acquiring nuclear power capabilities. [74]

Although the Emirates has continued to work closely with the International Atomic Energy Agency, among numerous countries, further assistance will be required in order to help the UAE “graduate” from its newcomer status into a full-fledged and thriving nuclear program. Clarified and more rigorous criteria to develop the regulatory framework and export controls could help its endeavor to crack down on potential abuses.

4.1. Policy Counsel l – Augment the Legal Infrastructure

The Emirates must further develop its legal and federal codes to work against misuse and expand its ability to prosecute abuses – there must be a strong and robust legal code to support a framework combatting vertical proliferation or potential loopholes that may be exploited or leveraged for non-peaceful or non-official uses. Further, the UAE should work alongside other nations to increase outreach concurrent with development and provide training to inform companies and transshipment companies in the business community; this would also include bolstering exercises in the country and training of indigenous personnel. The Emirates should seek to:

i. Integrate the legal systems of the seven emirates, at the very least between customs administrations and export declaration systems. This would include furthering an effective federal agenda, and bolstering an effective and cooperative framework to ease the process for international and domestic players to coordinate on safety or prosecutory issues.
ii. Rescind the unmodified, original SQP in favor of the modified SQP before nuclear materials are introduced to the country or Barakah site. While this may not be a popular option for the

UAE, it is absolutely essential to securing the ability to develop and implement subsidiary arrangements as required under comprehensive safeguards agreements. Further, to conduct inspections and receive more information on the transiting nuclear materials and technology before 2017.

iii. Develop a better reporting capability for requirements under the Additional Protocol and mature SSACs upon finalization, including a means to gauge safeguards measurements. Moreover, the Emirates should seek to initiate a national strategy to thoroughly implement SSAC requirements.

4.2. Policy Counsel II – Expand Comprehensive Export Controls

Currently, there is adequate opportunity for illicit materials to slip through the cracks of the current commerce controls system in the UAE, demonstrating the need for strengthening its exports control regime before 2017. Given its strategic geographical location, the many ports and Free Trade Zones housed by the UAE make it an attractive hub for illicit transshipments. One of the first steps the UAE should take would be to bolster its commitment to nonproliferation and ensure compliance through stricter export controls. The UAE is not currently part of a multinational export controls regime, though it intends to model its own guidelines after suggestions put forth by other multinational agendas. It should draft more guidelines and publish a formal control list, such as the EU list, in addition to tightening controls on strategic dual-use equipment and import licenses to optimize risk management capacity in order to establish a robust legal foundation that bolsters export controls and ability to respond to future incidents.
Certainly, the UAE should actively work to fully develop and publish its export control list that is set to mirror the EU in order to meet international standards and obligations. This is particularly so as some private sectors working with sensitive materials are still not totally clear about what is controlled material, and the government should look to bridge the public-private gap to facilitate greater understanding of export controls. Also, definitions should be further refined while technical and scientific expertise is further developed. [75]

As it turns out, there is a new shipping port being built at Barakah to accommodate transfers of sensitive materials into the UAE, and so will fall under Abu Dhabi governance. Whether or not the legal or illicit transfer of technologies through the UAE to third parties is deliberate by its leaders in the future, this new nuclear player should be able to clearly identify its end users. It would be wise for the Emirates to consider:

i. Formalizing a comprehensive export controls list that tightens controls on strategic dual-use equipment and import licenses, explicitly outlining sensitive technologies and regulations on how to address noncompliance at the federal level – or, at least develop strict guidelines within Abu Dhabi where most of the transfers concerning nuclear technology will take place.

ii. Adopting and publishing a formal export controls list that makes controlled items clear to importers and exports. The UAE's primary concern should be to coordinate this and promote transparency of its requirements, as a number of industries are still not clear on what constitutes a sensitive object and the proper channels to obtain licensing. This issue is furthered by the free trade zones in operation that may facilitate loose exchange of goods and materials within Emirati borders.

iii. Building measures of success to gauge effectiveness of institutions and regulations administering export controls.

iv. Establish clear sentencing guidelines and fines, which would also bolster the legal infrastructure to be more equipped to deal with potential abuses that may arise. As it currently stands, the UAE is free to conduct raids and shut down companies without notice. While this may be fine to do in the short-term in order to deal with abuses, a wider framework should be established to strengthen both the rule of law and export control matters simultaneously.

v. Bolstering responsiveness, hence building levels of trust and confidence in the ability of the UAE to effectively hedge against actors looking to proliferate and transit materials through deepening partnerships with institutions, such as through the Security Freight Initiative and Proliferation Security initiative.

vi. Clarifying roles of the different export control regimes, committees, and task forces at play, which all appears to be operating in tandem towards the creation a single authority to head all

work related to licensing and enforcement. Currently, this appears to be split between FANR and the ECNO, among others, yet it would be more effective to place responsibility in the hands of just one institution to ease the burden on importers and exporters of their obligations and to have a strengthened liaising department to work with regard export control related topics.

4.3. Policy Counsel III – Bolster Regulatory Framework

The UAE would have much to gain from more clearly defining the roles of FANR and ENEC, which continue to be the two largest regulatory institutions of the nuclear program. It could bolster these two firms and deepen its ability to leverage federal oversight and develop the regulatory framework of the Emirati nuclear power program. Further, the UAE could:

i. Build the bridge between the federal level, Emirate level, and municipalities to further synthesize regulation, in line with the National Programme launched in December 2005, which would closely correlate with the unveiled 2007 UAE government strategy. Sheikh Mohammed had noted, “creating synergy between the federal and the local governments is one of the most important and vital elements of development underlined in this strategy.” [76]
ii. Join or further consult with multinational export control regimes such as the Nuclear Suppliers Group (NSG), Australia Group (AG), Wassenaar Arrangement (WA), or coordinate with the regional EU CBRN Centre of Excellence based in Amman to guide best practices in the UAE.
iii. Bolster its internal human capacity. Without former, formal expertise on nuclear matters, it would be wise for the UAE to continue to build capacity of port security but also provide training to inform companies and within the transshipment business communities. Capacity building could include tabletop exercises, in addition to social assessments. Yet, it is important to keep in mind to avoid redundancies and overlaps with training.
iv. Finally, the Emirates should look to establish metrics of success to gauge their progress and conclude more agreements with other nations to receive technical assistance.

5. Conclusion

The United Arab Emirates already maintains a prestigious chair on the Board of Governors at the IAEA through 2015, affirming its position as a technologically advanced country on nuclear affairs within the Middle East. Yet, it is still a wholly newcomer nuclear energy state, and goes to show there is a certain degree of responsibility that falls on the international community to aid its efforts to hedge against clandestine, misuse or diversion of nuclear materials. While the UAE has already signed onto a number of treaties and committees that demonstrate its commitment to nonproliferation ideals, the international community must ensure that Emirati rhetoric matches the reality on the ground. Furthermore, the Emirates should seek to avoid a potential disconnection between construction and operation that may arise before the import of nuclear materials before 2017 and general ‘commitment-compliance gap’ of its nuclear infrastructure by taking on additional layers of transparency and relevant legislation. [77] Plant construction of the first reactor was more than halfway completed by September 2014. [78]

Acquisition of nuclear capabilities in the Emirates and subsequent expansion of technical know-how is coupled with significant responsibility to hedge against potential avenues of proliferation that may arise within its program. In the past, the UAE has failed to successfully mitigate sensitive materials transit through its borders – and so, can the international community accept Emirati rhetoric and aid the program to translate its commitment to action? Though the UAE has agreed to abstain from most all ‘sensitive processes’ of the fuel cycle in order to reaffirm its commitments to international nonproliferation efforts, Abu Dhabi must do more overcome its historical position as a major transshipment point for sensitive nuclear technologies. As it stands, near-term risks could become very real without sufficient safeguards and export control provisions. As of now, while the UAE has made strides to combat proliferation, domestic legislation is lacking and could be exploited to transfer or divert sensitive technologies. Further, transshipment remains to be a large challenge that has led to horizontal proliferation in the past. With that, before the nuclear program is set to go live, the UAE and broader international community must look to do

more to secure its nuclear framework through avenues such as developing adequate legislation and training.

In order to ensure success of the nuclear energy program in the United Arab Emirates, there is a strong need for foreign assistance and ample time to follow through on its pledges. Some steps that the UAE may take could include: first, further its legal infrastructure by rescinding the original SQP for the modified version and developing a better reporting capability, and second to expand export controls, all in addition to improving its internal regulatory framework. These notes of policy advice, among others, should be considered and adopted in order to facilitate additional transparency and build confidence of the international community in its program before the UAE model or its 123 agreement can serve as a normative standard for other aspiring nuclear powers in the future. Certainly, as other countries look to acquire nuclear technologies in the upcoming years, the UAE can serve as an example to these aspiring states, though there are still areas to improve. South Africa, Turkey and Vietnam are well on their way to developing respective nuclear energy programs, yet these countries will likely not do so at the speed of which the Emirates has expanded its program. This highlights the need for increased international collaboration with the Emiratis to aid them in their pursuit of peaceful nuclear energy, particularly as the UAE looks to collaborate with others in the regional and beyond.

Fundamentally, the UAE does set a precedent for future 123 agreements negotiated with the United States government, but perhaps model state status cannot be applied to the Emirati framework until more is done on multiple fronts. The ‘gold standard’ status in particular refers to the Agreed Minute that forfeits enrichment and reprocessing capabilities. Certainly, this move alone sends a huge signal for future agreements, yet other countries have not signed onto such hard-and-fast preconditions before breaking ground on equally ambitious nuclear programs. And so while it was intended by the US Congress to have the Emirati example set a precedent for future 123 agreements, the UAE agreement is much more restrictive in nature compared to other agreements. Nevertheless, more could still be done to meet international accords in order to promote transparency of the program and push it to global ‘model state’ status.

Certainly, the UAE is hard at work to thwart potential abuses and build up its best practices in order to be considered the Gold Standard for both the region and indeed the world. Yet, much of this is still held at face value and it should go above and beyond what it has already done to demonstrate that the highest standards of reactor and nuclear safety are being upheld. While the Emirates continues to meet its milestones for completion and maintain a good track record, it should also demonstrate that it is meeting all its safeguards obligations as nuclear material is introduced to the facility in late 2016 or 2017. [79]

The United Arab Emirates is only several years away from having its full nuclear program go live that will in turn supply nuclear power to the grid, eventually slated to provide the country with a quarter of its electricity, yet several obstacles remain. [80] The UAE should continue to bolster its internal measures so that the international community will not one day have to carry to burden of proof for presumed illicit or potentially detrimental activities that may arise in the future. If the Emirates truly seeks to set the ‘Gold Standard’ model for upcoming nuclear programs, the UAE must translate its intent to action before 2017.

6. Acknowledgements

I would like to thank the Kuwait Programme at the Institut d'études politiques de Paris (Sciences Po) for their support of this project. In addition, I want to extend my heartfelt appreciation to the James Martin Center for Nonproliferation Studies and the Lawrence Livermore National Laboratories for providing me with the resources and working space that enabled me to carry out this research.

I would also like to thank J. and G. at the Department of Energy for their mentorship and feedback during the initial months of this project, in addition to my friends and family who were supportive throughout the research and writing process. Further, I would like to extend my highest regards and thanks to the many individuals who were kind enough to take the time to be interviewed for this project.

7. References

[1] Perkovich, G. *Nuclear Developments in the GCC: Risks and Trends*. Carnegie Endowment for International Peace; 2008.

[2] *NINTH SEMI-ANNUAL REPORT 2014*. International Advisory Board; Abu Dhabi; 2014.

[3] *The Safeguards Implementation Report for 2013*. IAEA Board of Governors; Vienna; 2013.

[4] *Nuclear Power in the United Arab Emirates. Country Profiles*. World Nuclear Association; 2014.

[5] Early, B. *ACQUIRING FOREIGN NUCLEAR ASSISTANCE IN THE MIDDLE EAST - Strategic Lessons from the United Arab Emirates;* vol. 17, no. 2. Nonproliferation Review; 2010. 259-80.

[6] Cohen, W, and Nunn, S. *Nuclear Cooperation with U.A.E. in Our Interest.* The Hill; 2006.

[7] Katzman, K. *The United Arab Emirates (UAE): Issues for U.S. Policy.* Congressional Research Service; Washington; 2014.

[8] *UAE NATIONAL REPORT For the 6th Review Meeting of the CONVENTION ON NUCLEAR SAFETY.* April/May 2014.

[9] *Our Company History.* Lightbridge Corporation.

[10] *United Arab Emirates' Nuclear Power Plant Project.* Permanent Mission of the United Arab Emirates to the International Atomic Energy Agency; Vienna; 2013.

[11] *Two Nuclear Reactors to Be Built in UAE.* Gulf News; 2014.

[12] A., D. *"Reactor Types and Nuclear Energy in the Middle East."* Interview by author. 2014.

[13] *SUMMARY OF MAJOR U.S. EXPORT ENFORCEMENT, ECONOMIC ESPIONAGE, TRADE SECRET AND EMBARGO-RELATED CRIMINAL CASES.* US Department of Justice; 2014.

[14] Early, B. *UAE 'Commitment-Compliance Gap' Question.* E-mail interview by author. 2015.

[15] *INFCIRC/622 Agreement between the United Arab Emirates and the International Atomic Energy Agency for the Application of Safeguards in Connection with the Treaty on the Non-proliferation of Nuclear Weapons*. International Atomic Energy Agency; Vienna; 2003.

[16] USA, Obama, B. *Agreement for Cooperation between the Government of the United States and the Government of the United Arab Emirates Message from the President of the United States Transmitting the Text of a Proposed Agreement for Cooperation between the Government of the United States of America and the Government of the United Arab Emirates concerning Peaceful Uses of Nuclear Energy, Pursuant to 42 U.S.C. 2153(b), (d)*. Washington; 2009.

[17] *SUMMARY OF MAJOR U.S. EXPORT ENFORCEMENT, ECONOMIC ESPIONAGE, TRADE SECRET AND EMBARGO-RELATED CRIMINAL CASES.* Department of Justice; 2014.

[18] Early, B. *Export Control Development in the United Arab Emirates: From Commitments to Compliance.* Belfer Center; 2009.

[19] *Safeguards.* International Atomic Energy Agency; 2015.

[20] Graham Jr., T. *Avoiding the Tipping Point.* Arms Control Today; 2004.

[21] *Treaty on the Non-Proliferation of Nuclear Weapons (NPT).* UN News Center; 2000.

[22] Stein, A. *U.S. - UAE Nuclear Cooperation.* Nuclear Threat Initiative (NTI); 2009.

[23] *History.* International Framework for Nuclear Energy Cooperation (IFNEC).

[24] Federal Authority for Nuclear Regulation (FANR). *Regulation for the System of Accounting for and Control of Nuclear Material and Application of Additional Protocol (FANR-REG-10).*

[25] *Our Vision, Mission & Core Values.* Federal Authority for Nuclear Regulation (FANR).

[26] *Mohamed Bin Zayed Reshuffles ENEC*. UAE Interact; 2014.

[27] *Mission & Vision.* Emirates Nuclear Energy Corporation (ENEC).

[28] *Gulf Nuclear Energy Infrastructure Institute.* Khalifa University.

[29] *International & Domestic Cooperation.* Federal Authority for Nuclear Regulation. 2014.

[30] Ibid.

[31] *Arab Political Systems - United Arab Emirates.* Carnegie Endowment for International Peace.

[32] *United Arab Emirates Profile - Overview*. BBC News; 2015.

[33] O, G. *Emirati Export Controls*. Interview by author. 2014. #6

[34] Kaufer, B. *Development of Nuclear Regulations and Guides in the United Arab Emirates*. Lecture.

[35] *Emirates Nuclear Energy Corporation Inaugurates New Simulator Training Center In Barakah.* Emirates Nuclear Energy Corporation (ENEC); 2014.

[36] *First Emirati Nuclear Engineers Graduate*. Gulf News; 2014.

[37] *Nuclear Power in the United Arab Emirates. Country Profiles*, World Nuclear Association; 2014.

[38] *UAE Awards Nuclear Fuel Contracts*. World Nuclear News; 2012.

[39] *United Nations Security Council Resolution 1540.* United Nations; 2004.

[40] *The 1997 IAEA Additional Protocol At a Glance*. Arms Control Association; 2014.

[41] O, G. *Emirati Export Controls.* Interview by author. 2014. #2

[42] Cottee, M. *The Additional Protocol and the Modified Small Quantities Protocol.* Lecture, Myanmar-US/UK Dialogue from International Institute for Strategic Studies; London; 2014.

[43] Kerr, P. *IAEA Board Closes Safeguards Loophole*. Arms Control Today; 2005.

[44] Moore, B. *Safeguards Case Study - Myanmar.* Lecture, Safeguards Policy Course from Monterey Institute of International Studies; Monetrey; 2014.

[45] *SAFETY EVALUATION REPORT OF AN APPLICATION FOR A LICENCE TO CONSTRUCT BARAKAH UNITS 3 AND 4.* Federal Authority for Nuclear Regulation; 2014.

[46] *The Safeguards Implementation Report for 2013.* International Atomic Energy Agency; Vienna; 2014.

[47] *Limits to the Safeguards System. Against the Spread of Nuclear Weapons*. IAEA.

[48] *Design Information.* Nuclear Safeguards Education Portal. Nuclear Security Science and Policy Institute.

[49] *Development of IAEA High Level Guidelines for Designers and Operators: Safeguards-By-Design*. JRC - European Commission; IAEA Safeguards Symposium; 2010.

[50] O, G. *Emirati Export Controls.* Interview by author. 2014. #3

[51] Ibid.

[52] *SAFETY EVALUATION REPORT OF AN APPLICATION FOR A LICENCE TO CONSTRUCT BARAKAH UNITS 3 AND 4.* Federal Authority for Nuclear Regulation; 2014.

[53] Dunne, A. *Strategic Trade Controls in the United Arab Emirates: Key Considerations for the European Union.* EU Non-Proliferation Consortium; 2012.

[54] *UN Security Council Resolution 1540.* U.S. Department of State.

[55] *ABRAMS: An Arab Counterexample.* Washington Times; 2009.

[56] *United Arab Emirates Import Rules and 'Red Flag' Indicators.* US Bureau of Industry and Security.

[57] O, G. *Emirati Export Controls*. Interview by author. 2014. #3

[58] O, G. *Emirati Export Controls*. Interview by author. 2014. #4

[59] *United Arab Emirates Import Rules and "Red Flag" Indicators.* US Bureau of Industry and Security.

[60] O, G. *Emirati Export Controls.* Interview by author. 2014. #7

[61] *Executive Office: Committee for Goods and Materials Subject to Import and Export Control, United Arab Emirates.*

[62] *Guidelines.* Nuclear Suppliers Group.

[63] O, G. *Emirati Export Controls.* Interview by author. 2014. #5

[64] *EU Export Controls.* Visual Compliance.

[65] *Regulation on the Export and Import Control of Nuclear Material, Nuclear Related Items and Nuclear Related Dual-Use Items, § REG-09 (Federal Authority for Nuclear Regulation 2014).* Federal Authority for Nuclear Regulation. 2014.

[66] O, G. *Emirati Export Controls.* Interview by author. 2014. #4

[67] *United Arab Emirates. Independent Statistics and Analysis.* U.S. Energy Information Administration.

[68] *UAE Freezes 41 Iran-linked Bank Accounts-report.* Reuters; 2010.

[69] Cho, M. *South Korea Shuts More Nuclear Reactors over Fake Certificates*. Reuters; 2013.

[70] Sang-hun, C. *Scandal in South Korea Over Nuclear Revelations*. The New York Times; 2013.

[71] *Indictments for South Korea Forgery Scandal.* World Nuclear News; 2010.

[72] *United Arab Emirates Constitution By-Law of The Federal National Council.* Federal National Council; 2011.

[73] *World Press Freedom Index 2014.* Reporters Without Borders.

[74] Early, B. *Export Control Development in the United Arab Emirates: From Commitments to Compliance.* Belfer Center; 2009.

[75] Almehrezi, S. *The U.A.E. Export Control System.* Lecture, Ministry of Foreign Affairs U.A.E. from Committee for Goods and Materials Subject to Import and Export Controls; 2014.

[76] *Shaikh Mohammed Unveils Federal Government Strategy.* Khaleej Times; 2007.

[77] Early, B. *Export Control Development in the United Arab Emirates: From Commitments to Compliance.* Belfer Center; 2009.

[78] *Barakah: Putting the UAE on the Nuclear Map.* Power Engineering International; 2014.12-14.

[79] *ENEC Completes Concrete Dome for Unit 1 Reactor Containment Building.* UAE Interact; 2015.

[80] *Lightbridge, Lloyd's Register Energy to Support Nuclear Industry in UAE.* Energy Business Review; 2014.

*Please note that all ‘O, G.’ references refer to interviews with officials who requested not to be named in this paper.

Disclaimer: All views expressed here are explicitly those of the author alone and do not in any way represent the views of her employer, affiliated institution or any entity of the US Government.

Session 4

Uncertainties in NDA Measurements

Emerging Applications of Bottom-Up Uncertainty Quantification in Nondestructive Assay

[1]Burr, T., [2]Croft, S., [3]Dale, D.,[3]Favalli, A., [3]Weaver, B., [3]Williams, B.

[1]International Atomic Energy Agency
[2] Oak Ridge National Laboratory
[3] Los Alamos National Laboratory
E-mail: tburr@iaea.org, crofts@ornl.gov
djdale@lanl.gov,afavalli@lanl.gov,theguz@lanl.gov, briaw@lanl.gov

Abstract

The Guide to the Expression of Uncertainty in Measurement (GUM) provides guidance on expressing measurement uncertainty for calibration, laboratory accreditation, and metrology services. Nondestructive assay (NDA) of items containing nuclear material uses calibration and modelling to infer item characteristics on the basis of detected radiation such as neutron and gamma emissions. Uncertainty quantification (UQ) can be approached from a bottom-up or top-down analysis.. Top-down UQ compares measurements of the same item(s) from multiple assay techniques and/or laboratories. Bottom-up UQ quantifies sources of input uncertainty to a process and the resulting output uncertainty. Bottom up UQ is the focus of this paper. UQ for NDA has always been important, but there is a need for application of better statistical techniques and for UQ to play more of a role in assay development and assessment. This paper describes NDA applications (the enrichment meter, distributed-source term analysis, Cf shuffler, Uranium neutron collar) that have emerging UQ topics that are not specifically addressed by the GUM, including: item-specific biases, errors in predictors, model error effects, and quantification of uncertainty in computer model errors and parameters. This paper also includes an initial UQ case study using the Uranium neutron collar assay method.

Keywords: Bottom-up uncertainty quantification (UQ); emerging UQ topics; errors in predictors; item-specific biases

1. Introduction

Uncertainty quantification (UQ) for non-destructive assay (NDA) in nuclear safeguards applications has always been important. But, currently it is recognized that greater rigor is needed and achievable using modern statistical methods and by letting UQ have a more prominent role in assay development and assessment [1-3]. UQ is often difficult, but if done well, can lead to improving the assay procedure itself. Therefore, we describe the extent to which the guideline for expression of uncertainty in measurements (GUM) [4] can be used for UQ in NDA [1-3]. This paper also takes steps toward better UQ for NDA by illustrating UQ challenges that are not addressed by the GUM. These challenges include item-specific biases, calibration with errors in predictors, and model error, especially when the model is a key step in the assay. We briefly describe a specific NDA application, the enrichment meter principle, for which a variation of the GUM approach can be applied, and other NDA applications for which the GUM approach must be extended. Then, a case study of the Uranium neutron collar is presented. The paper is organized as follows. Section 2 gives additional background on NDA and UQ for NDA. Section 3 describes the GUM and a few example NDA applications for which the GUM is applicable. Section 4 is the Uranium neutron collar (UNCL) case study. Section 5 is a discussion and summary.

2. UQ for NDA

The GUM [4] indirectly addresses top-down methods, but is most known for illustrating a bottom-up option that applies uncertainty propagation of uncertainty in each assay step to estimate the uncertainty in the assay. For bottom-up UQ, the GUM's measurement equation is

$$Y = f(X_1, X_2, ..., X_p) \quad (1),$$

where Y is the estimate of the measurand, and the Xs are p inputs. The p inputs can be measurement or adjustment factors, and can be regarded as having a joint probability distribution that can include covariances among some or all of the inputs. For example, some of the inputs can be estimated calibration parameters, others can be measured values, and others can be adjustment factors. The GUM distinguishes two types of evaluations to describe how to estimate the probability distribution of one or more inputs. "Type A" evaluations uses statistical methods applied to measured data. "Type B" evaluations use judgments, models, or other non-statistical methods. The inputs Xs in Eq. (1) can be obtained using Type A and/or Type B evaluations.

There is recent interest in revising and extending the GUM for reasons described in Bich [5]. However, there are many applications for which Eq. (1) is adequate for defensible UQ for Y. One needs to know the functional form $f()$, and know how to quantify the error magnitudes in each of the Xs. Because the GUM does not focus on top-down UQ, there is no attempt to describe sources of uncertainty such as omitted physical effects or model uncertainty.

In NDA applications, items emit neutrons and/or gamma-rays that provide information about the source material, such as isotopic content. However, item properties such as density, or the distribution of radiation-absorbing isotopes, which relate to neutron and/or gamma absorption behaviour of the item, can partially obscure the relation between detected radiation and the source material; this adds a source of uncertainty to the estimated amount of SNM in the item. One can express item-specific impacts on uncertainty using a model such as

$$CR/M = g(X_1, X_2, ..., X_p), \quad (2)$$

where CR is the item's neutron or gamma count rate, M is the item SNM mass, g is a known function, and $X_1, X_2, ..., X_p$ are p auxiliary predictor variables such as item density, source SNM heterogeneity within the item, and container thickness, which will generally be estimated or measured with error and so are regarded as random variables [6,7].

To map Eq. (2), to GUM's Eq. (1), write

$$M = CR / g(X_1, X_2, ..., X_p) = h(X_1, X_2, ..., X_{p+1}) \quad (3),$$

where the measured CR is now among the p+1 inputs. Because p is generic notation for the number of inputs, and f, g, and h simply depict three distinct functional forms, we can rewrite Eq. (3) as Eq. (1), and interpret Y as the SNM mass M, so Eq. (1) is alternatively expressed as

$$M = f(X_1, X_2, ..., X_p). \quad (4).$$

Eq. (4) is intended for bottom-up UQ. But top-down UQ often suggests the need for a measurement error model that allows for both systematic and random errors, such as

$$M = T + S + R \quad (5),$$

where T is the true SNM mass, R is random error, and S is systematic error that accounts for all unmodeled or incorrectly modelled effects for each item. The systematic error could scale with the true value or not (that is, the error model could be multiplicative or additive or something else), and could vary across items or not, depending on the context [6-11]. If S

varies across items, then it is item-specific bias [9,10]. Item-specific bias is nearly always present to some extent, because test items differ to some extent from calibration items. Many NDA examples adjust test items (as do the three examples in Section 3 and example in Section 4) to calibration items using some type of modelling. Model uncertainty must therefore be addressed.

Top-down UQ estimates the *R* and *S* error magnitudes, typically quantified by their standard deviations σ_R and σ_S, which are estimated from data sets that have measurements of some or all items from each of two or more assay methods. We use the hat notation to denote estimated quantities; for example, $\hat{\sigma}_R$ and $\hat{\sigma}_S$ denote estimates of σ_R and σ_S, respectively. We use capital letters to denote random variables. The random error term *R* can include variation in background that cannot be perfectly adjusted for, Poisson counting statistics effects, and other random effects. In principle, the $X_1, X_2, ..., X_p$ could be estimated for each item as part of the assay protocol. However, there would still be modelling error because the function *f* must be chosen or somehow inferred, possibly using purely empirical data mining applied to calibration data [6,8,11], or physics-based radiation transport codes such as Monte-Carlo-n-particle (MCNP, [12]). Typically, only some of $X_1, X_2, ..., X_p$ will be measured as part of the assay protocol, as we illustrate in the uranium neutron collar case study.

3. The GUM and UQ for NDA

Recall that Eq. (4) is aimed primarily at bottom-up UQ, using either steps in the assay method and uncertainties in $X_1, X_2, ..., X_p$, or using calibration data (see the UNCL case study in Section 4). However, supplements to the GUM describe analysis of variance in the context of top-down UQ using measurement results from multiple laboratories and/or assay methods to measure the same measurand.

The purpose of a measurement is to provide information about the measurand, such as the SNM mass. Both frequentist and Bayesian viewpoints are used in estimating the measurand and in characterizing the estimate's uncertainty. Elster [13] and Willink [14] point out that the GUM invokes both Bayesian and frequentist approaches in a manner that is potentially confusing. To modify the GUM so that a consistent approach is taken for all types of uncertainty, [14] suggests an entirely frequentist approach while others suggest an entirely Bayesian approach. Bich [5] also points out confusion between frequentist and Bayesian terminology and approaches in the GUM, which is one reason it would be useful to revise the GUM. No matter which approach is used, making it clear which quantities are viewed as random and which are viewed as unknown constants will avoid needless confusion. However, the real challenges involve choosing a likelihood for the data, a model to express how the measurand is estimated, and a model to describe the measurement process. These challenges are present in both frequentist and Bayesian approaches.

Ambiguities in the GUM arise for at least three reasons [3,14,16]: (**1**) The GUM divides the treatment of errors into those evaluated by type A evaluation (traditional data-based empirical assessment), and those addressed by type B evaluation (expert opinion, experience with other similar measurements). However, type B evaluations are primarily Bayesian (degree of belief) without explicitly stating so (and need not be), while type A evaluations are primarily frequentist (and need not be). The jargon used in describing type B evaluations implies that the true value *T* has a variance (a Bayesian view based on quantification of our state of knowledge). The jargon used in describing type A evaluations is frequentist, with statements such as $P(X - T > k_1\sigma) = 0.05$, with the interpretation that *X* varies randomly around the fitted quantity *T*, where σ is the known measurement error standard deviation. We

endorse either view, when clearly explained, but typically write $P(X - T > k_2\hat{\sigma}) = 0.05$ where the hat notation conveys that the standard deviation is an unknown parameter that must be estimated, so $k_2 > k_1$. (**2**) The GUM uses the same symbol X for a measurement result and for a true value, which also confuses the frequentist and Bayesian views. (**3**) There is vague use of the term "quantity." And, although the GUM attempted to clarify confusion between "error" and "uncertainty," it did not clearly use the term "error" when measurement error (which has a sign, positive or negative) was meant. Willink [14] aims to resolve these ambiguities by paying attention to notation and jargon, being careful to separate Bayesian from frequentist views, and pointing out a confusion of true values with measurements of true values. Also, the GUM does not explicitly address calibration; however, because calibration is almost never a completely straight-forward application of ordinary regression, we agree with [13] that UQ for calibration deserves attention, as we illustrate with the UNCL example in Section 4.

Elster [13] points out that Eq. (4) is Bayesian because it implies a probability distribution for the SNM mass *M*, and [13] shows that for a particular form of noninformative (large variance) prior probability distribution for *M*, there is Bayesian approach that exactly agrees with that implied by placing a joint probability distribution on the inputs. We point out here that historically, Bayesians have regarded the posterior probability distribution as the central feature of a Bayesian analysis. Frequentists interpret probability as the frequency of occurrence of an event. In metrology (for NDA or more generally), there is opportunity to merge some of the best Bayesian and frequentist practices. Prior probabilities can encode constraints, such as true quantities being nonnegative; then, the actual frequency within which a 95% Bayesian probability interval actually includes the true value can be observed; thus, metrology provides a practical application for the notion of being a "calibrated Bayesian." A calibrated Bayesian borrows Bayesian and frequentist ideas.

3.1 Example application of GUM to NDA

Nearly all assay methods, including all NDA methods rely on calibration. However, NDA methods are sometimes applied to test items that have different physical properties than calibration items. Elster [13] shows why GUM's measurement Eq. (1) is not directly set up for calibration. However, with some creativity, one could map calibration problems to Eq. (1), which we now illustrate using a simple version of the enrichment meter principle (EMP).

Suppose we fit the known enrichment in each of several standards to observed counts in a few energy channels near the 185.7 keV energy as the "peak" region and to the counts in a few energy channels just below and just above the 185.7 keV energy to estimate background, expressed as

$$Y = \beta_1 X_1 + \beta_2 X_2 + R, \qquad (6)$$

where Y is the enrichment, $X1$ is the observed peak count rate, $X2$ is the observed background count rate, and R is random error. The calibration data is used to estimate $\beta 1$, and $\beta 2$. One could constrain the estimates $\hat{\beta}_1$ of β_1 and $\hat{\beta}_2$ of β_2 to be equal in magnitude in the case where the same number of energy channels is used for both the peak and background. That would correspond to assuming a constant (non-sloping) background throughout the peak region, which is sometimes, but not always, appropriate. Therefore, in practice, we do not force the constraint $\hat{\beta}_1 = -\hat{\beta}_2$. Also, note that the true enrichment is never known exactly, not even in standards; however, the uncertainty in standards can be accounted for, and for convenience here will be assumed to be negligible.

Because $X1$ and $X2$ are the measured count rates, they have measurement error. However, as we show numerically in the UNCL case study, there is no need to use the errors in predictors literature [7,17]. There is the need to estimate the 2-by-2 covariance matrix of $(\hat{\beta}_1, \hat{\beta}_2)$, which is best done by simulation unless one can safely assume that the errors in $X1$ and $X2$ can be neglected in this context. Some will argue that using simulation to estimate cov(($\hat{\beta}_1, \hat{\beta}_2$) is beyond application of GUM's Eq. (1). However, if we adopt a general interpretation of Eq. (1), allowing type A and/or type B analyses to inform on the probability distribution of the inputs, then we can compute the estimated Y using $\hat{Y}_{\text{test}} = \hat{\beta}_1 X_{1,\text{test}} + \hat{\beta}_2 X_{2,\text{test}}$, which can be thought of as being an example of $Y = f(X_1, X_2, X_3, X_4) = f(\hat{\beta}_1, \hat{\beta}_2, X_{1,\text{test}}, X_{2,\text{test}}) = \hat{\beta}_1 X_{1,\text{test}} + \hat{\beta}_2 X_{2,\text{test}}$, which has a probability distribution that can be inferred from simulation applied to the calibration data. If the count times in training differ from the count times in testing, then modifications are necessary. Also, see [13], who points out that there is not a unique functional form analogous to GUM's Eq. (1), $Y = f(X_1, X_2, ..., X_p)$. Instead, there is a collection of (Y, $X_{1,\text{train}}$, $X_{2,\text{train}}$) triples from which $(\hat{\beta}_1, \hat{\beta}_2)$ is estimated, using, for example, errors in predictors methods or not. So, even relatively simple calibration applications such as the EMP without complications (next paragraph) are not fully treated by GUMs measurement Eq. (1). Nevertheless, one could defend regarding $\hat{\beta}_1 X_{1,\text{test}} + \hat{\beta}_2 X_{2,\text{test}}$ as a deterministic function of random quantities, and so it has a probability distribution, paving the way for a Bayesian treatment if desired.

Several departures from calibration items can occur in test items; one common departure from calibration items is that test items could have meaningfully different container thicknesses, which must be measured and then the count rates $X1$ and $X2$ are adjusted accordingly, using the factor exp(μρx), where x is container thickness, μρ is the gamma linear absorption coefficient that adjusts for test items and calibration items having different container thicknesses. Reference [2] gives more detail about calibration and analyses of EMP data. If such departures occur, then a model is used to adjust to calibration conditions, which might still be amenable to a GUM-type UQ analysis, depending on the complexity of the model and the methods needed to validate the model for the NDA application.

3.2 Example NDA applications that require extensions to the GUM

This subsection describes two NDA applications (the Cf shuffler, and the distributed source term analysis) that have emerging UQ topics that are not specifically addressed by the GUM, including: item-specific biases, errors in predictors, and quantification of uncertainty in computer models. Many NDA applications are like the extended version of the EMP where model-based adjustments are needed to adjust physical attributes of test items to those in the calibration items.

3.2.1 Cf Shuffler

Shufflers measure fissile masses nondestructively by counting neutrons released as a result of fissions that are induced by successive irradiations from a source consisting of ^{252}Cf neutrons. As the hydrogen density from the non-SNM material increases, the shuffler accuracy can degrade because the detected count rate varies with the SNM positions within the item. In some cases, hardware additions to reduce the average energy of the irradiating neutrons reduces this problem, but increase item self-shielding, leading to other bias sources.

Alternate strategies, including imaging, have been pursued, but none have been completely acceptable.

Certified standards exist for only a few material categories (categories are defined on the basis of material type and packaging), while measurements are needed for a wide variety of categories. The standards are used in a calibration step to estimate the pseudo-source strength of the ^{252}Cf neutrons. The procedure is to determine the source strength that minimizes the difference between the measured and MCNP-calculated count rates (CR) for the standards. The calculated count rate is the product of three numbers, F1 *x* F2 *x* F3, where F1 is a MCNP-based estimate of the expected total number of counts (over all shuffle cycles) per source ^{252}Cf neutron per gram of SNM, F2 is a known constant that is determined by cycle time parameters such as count times with and without the ^{252}Cf source neutrons, and F3 is a calibration parameter to be estimated [18]. The equation M = CR/(F1 *x* F2 *x* F3) + error can be fit to the measured data for calibration standards, leading to a least squares estimate of F3. Because of nonnegligible error in F1 due to MCNPX-based model uncertainty, this is another "errors in predictors" problem. However, in this case, there is no direct interest in the estimate of F1, F2,or F3. The main goal is to use the estimated F1 *x* F2 *x* F3 to convert CRs on test items to estimates of SNM mass.

If there were no model error (and all the relevant properties of the standards such as density and material form were known exactly), then F3 would estimate the actual ^{252}Cf neutron source strength. Following calibration on standards to estimate F3, we convert measured CR on a test item to estimated SNM mass using M = CR/(F1 *x* F2 *x* F3) + error. There will be errors in the predictor CR due to having a modest total count time, and there will be errors in the product F1 *x* F2 *x* F3 arising from errors in F1 *x* F3 due to modelling imperfections.

An unusual aspect of the calibration procedure is the partitioning into measurement categories. From the procedure described above, we recognize that if a new material category is to be assayed, using the F3 associated with calibration on the standards, then model errors arise from: (1) unmodeled effects that impact the new material category in a different manner than they impact the standards, and/or (2) improperly specified material properties in either the standards or the new category. Either of these effects leads to errors in F1 *x* F3 that could be different for the new category than for the standards and also different than errors in other measurement categories.

Examples of unmodeled or inaccurately modeled effects include some of the following: (1) the Cadmium liners on the detector banks have holes that are not currently modeled; (2) The detector is not technically modeled exactly as built. It would take a great deal of effort to include all the details, for examples there are certainly air gaps in the assembly of polyethlene blocks, yet the blocks are assumed to be one solid mass;(3) The ^{252}Cf neutrons are inside of a small metal capsule, yet this capsule is not included in the model for cost/benefit reasons. (4) There is a motor below the rotating turntable in the floor of the shuffler; it was not put in the model for cost/benefit reasons. This example list is current but subject to change; however, for any implementation there will be unmodeled effects, some of which could be important in UQ, although it is usually assumed that biases due to such modelling imperfections largely cancel out in relative calculations.

We regard the Cf shuffler with computational adjustments (F1 *x* F3 is estimated from imperfect application of MCNP) as having uncertainty that, while in principle, might be amenable to a type B evaluation, regulators will not yet accept the computational adjustments without further study. In short, the "propagate uncertainty in inputs to uncertainty in the output" guidance as implied by GUMs Eq. (1), is useful, but still leaves most of the work to understanding uncertainty in the inputs (which include computational adjustments) to those performing bottom-up UQ. Also, fundamental nuclear data, which is used, for example, by

MCNP in the Cf shuffler example, and in many other examples, has uncertainties whose impact depends on how calibration data and models are used.

3.2.2 Distributed Source Term Analysis

The distributed source-term analysis (DSTA) is a measurement technique that has been applied to a variety of safeguards and verification situations where the amount of neutron-producing material contained within a large area needs to be measured in a timely fashion. The technique was originally developed to assay material present in uranium enrichment cascade halls [19] using neutron counting. It has also been applied to the assay of low-activity waste storage areas, and static material storage areas. Current development of the DSTA technique is focused on material accountancy in plutonium glovebox process lines. In these cases, tools are being developed to assist the operator to localize materials to improve cleanout operations.

The DSTA is applied in situations where a neutron assay of a large area is required. In these cases, the sampled area is too large to be placed inside a counter as is done in a traditional neutron assay measurement. Instead, the detector is positioned at a variety of known positions within the sample volume and the neutron count rate is measured at each position. The sample area is then divided into a number of discrete source voxel locations. A room-response matrix is determined using MCNP to estimate the source-to-detector coupling for each voxel-measurement position pair. The MCNP-based estimate of the room response and measurement data are then used to estimate the neutron activity in each source voxel in the assay area.

The DSTA analysis consists of three basic activities: sampling, simulation, and fitting. During sampling, measurement positions are selected throughout the assay area to insure that the entire sample volume is adequately measured, where adequacy is determined by the particular application. The measured counts for positions 1, 2, …, P, are placed in a vector M_P ([counts/sec]) and the location of each measurement position is recorded for use in the simulation phase.

In the simulation phase, the sample itself (large storage area, process hall, etc.) is modeled using MCNP. The sample can be divided into V discrete source voxels, the activity of which (A_V [neutrons/sec]) can be estimated from the DSTA method, provided the number of measurement positions P > V. The MCNP code is used to determine the source-to-detector coupling between each of the V source voxels and each of the P measurement positions. The MCNP efficiency results are used to populate a response matrix, R_{VP} ([counts/neutron]). The resulting system of linear equations is used to estimate the neutron production activity of each source voxel in units of neutrons/second.

The DSTA data model is then $M_p \sim \text{Poisson}(t\sum_V R_{VP}A_V)\Big/t$, and the main goal is to estimate the total activity, $\sum_V A_V$ (or total SNM mass). This is another errors-in-predictors problem, where the predictors R_{VP} are estimated using MCNP and the estimates are partially validated using real (and corresponding MCNP-modeled) Cf sources at known source locations and recording their measured source strength at known detector locations. Because the error structure in the R_{VP} matrix is currently not well known, [20] could only perform a "what if" sensitivity study, simply evaluating the error in the estimated total activity, $\sum_V A_V$ under various assumptions about the error structure in the MCNP-based estimate of R_{VP}, and using various options for dealing with errors in predictors. None of the errors in predictors

literature deals with the types of error structure that is possibly present in $R_{VP,}$ such as having both random and systematic components. As in the EMP example, one could map the data model $M_p \sim \text{Poisson}(t\sum_V R_{VP}A_V)\Big/t$ to one that expresses the estimate for total activity, $\sum_V A_V$ as a function of several inputs, including MCNP-based estimates of $R_{VP.}$ However, this again still leaves most of the work to understanding uncertainty in the inputs (which include MCNP-based estimates of R_{VP}) to those performing bottom-up UQ.

4. UNCL case study

The UNCL uses an active neutron source (AmLi) to induce fission in the ^{235}U in fresh fuel assemblies [21-23]. Figure 1 is a simple overhead view produced by MCNP [12, 21-23]. Neutron coincidence counting is used to measure the "reals", i.e. neutron coincident rate R attributable to fission events, which can then be used to determine the linear density of ^{235}U in a fuel assembly (g-^{235}U/cm) from calibration parameters, a_1 and a_2. The equation used to convert the measured R to Y (gms ^{235}U per cm) is

$$Y = \frac{kX}{a_1 - a_2 kX} \qquad (7),$$

are calibration parameters, and k = $k_0k_1k_2k_3k_4k_5$ is a product of correction factors that adjust R ($R = X$ in Eq. (7)) to item-, detector-, and source-specific conditions in the calibration [21-23]. Therefore, Eq. (7) is a special case of GUM's Eq. (1), where the two calibration parameters a_1 and a_2 and the 6 correction factors k_0 ,$k_{1,}$ $k_{2,}$ $k_{3,}$ k_4 , and k_5 are among the X's in Eq. (1). We caution readers that GUM does not fully treat multi-parameter calibration uncertainties, so there are open issues in applying GUM's Eq. (1) even to this relatively straightforward calibration problem. Also, there is much current research on options ot improve the UNCL method for new types of fuels, which will be reported elsewhere. Nevertheless, it provides a practical basis to support discussion of the current practice for NDA and to describe a roadmap for more comprehensive UQ for NDA.

4.1 Description of UNCL Calibration and the 6 Correction Factors k_0, k_1, k_2, k_3, k_4, and k_5

Menlove et al. [22] introduced correction factors to adjust the measured reals count rate to the corresponding reals count rates observed in the calibration condition for a particular a_1, a_2 coefficient pair. Coefficient-pairs were defined for standard PWR and BWR fuel types by [16]. Since that original reporting coefficient pairs have been determined for WWER-440 and WWER-1000 fuel types [21-23].

The term k_0 accounts for uncertainty in the true Am/Li source strength (approximately historically 3.7% relative error standard deviation (RSD) if use recent IAEA estimates). The term k_1 accounts for uncertainty due to electronic drift (considered negligible with modern electronics, so k_1=1). The term k_2 accounts for uncertainty due to differences in detector efficiencies (approximately 1.5% RSD). The term k_3 accounts for the effects of burnable poison (burnable poison absorbs neutrons). The term k_4 accounts for differences in the total uranium loading (U-total/cm) between the calibration case and the measurement case. The term k_5 accounts for all other effects (eg spacers, bagged assemblies).

The *k*-factors were introduced to allow for the use of the same a_1 and a_2 values over a wide range of measurement cases and different UNCL detector systems. In the present consideration the calibration factors, a_1 and a_2, and the *k*-factors help to identify error sources in the UNCL measurement and calibration.

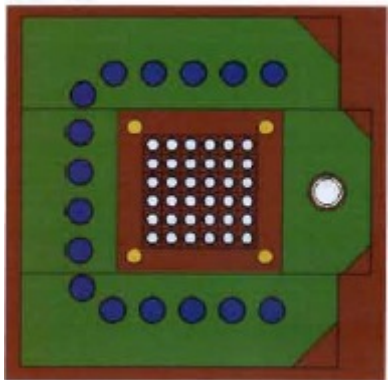

Figure 1. Simple overhead view of an UNCL, produced from MCNP. The 6*x*6 fuel pins of the assembly are in the center of the detector cavity in white. The 16 blue circles forming a "collar" around the sample are the ^{3}He neutron proportional counters. The green is the detector body; the red areas are air. The source is the large white circle towards the right.

4.2 Example analyses

We reanalysed 9 pairs of (R, ^{235}U) from Table VII for PWR from [22], fitting Eq. (7) with approximately 2% RSD. Figure 2 plots the 9 (R, ^{235}U) pairs. We then applied a single noise factor and $k = k_0\, k_1\, k_2\, k_3\, k_4\, k_5$ to introduce noise due to departure from calibration conditions as described in Section 4.1.

Figure 3 gives example RSD values for the 9 (R,^{235}U) pairs in 10^5 simulations in R [24]. In each simulation, 6 of the 9 (R,^{235}U) pairs were randomly selected to calibrate, and the other 3 (R,^{235}U) pairs were used to test. Dividing into training and testing helps to account for model uncertainty in Eq. (7). Varying amount of random error in *k* was applied, ranging from approximately 1 to 5% RSD, which represents the aggregate effect of errors in each of k_0-k_5. The plot in Figure 3 assumed that the same RSD values in *k* were present in the 6 training pairs as in the 3 testing pairs. If there are different error magnitudes in testing than in training, then bias can be introduced in the estimated ^{235}U [3,7]. Also, if there is an adjustment for errors in predictors [7,17], then the RSD is higher (option 2 in Figure 3) compared to not adjusting for errors in predictor (option 1 in Figure 3). And, there is a very large bias component contributing to the large RSD in the option 2 results in Figure 3. Interestingly, there is sometimes a large bias being observed in top-down evaluations of the UNCL [3]. The adjustment for errors in predictors is to choose values of $x_{i,true}$ and a_1, a_2 to minimize

$RSS_1 = \sum_{i=1}^{n_{train}} \frac{(x_i - \hat{x}_i)^2}{\sigma_{x_i}^2} + \frac{(y_i - \hat{y}_i)^2}{\sigma_{y_i}^2}$, where $\hat{x}_i$ is the estimate of $x_{i,true}$ is the first term, and

$Y = \frac{kX}{a_1 - a_2 kX}$ is used to calculate $\hat{y}_i$ in the second term (using $\hat{x}_i$, the estimate of $x_{i,true}$ in the expression $\hat{y}_i = \frac{k\hat{x}_i}{a_1 - a_2 k\hat{x}_i}$). The weights $\sigma_{x_i}^2$ and $\sigma_{y_i}^2$ are assumed here to be known; we used a range of possible values (approximately 1 to 5% RSD) for $\sigma_{x_i}^2$ (which includes the effect of errors in *R* and in *k*) and we used the residual variance from the fit of ^{235}U to R (with *k* set equal to 1) using all 9 (R, ^{235}U) pairs for $\sigma_{y_i}^2$. If there is no adjustment for errors in predictors,

then a_1, a_2 are chosen to minimize $RSS_2 = \sum_{i=1}^{n_{train}} \frac{(y_i - \hat{y}_i)^2}{\sigma_{y_i}^2}$, which is the appropriate and familiar criterion if the goal is to predict y.

GUM's key measurement equation (our Eq. (1) and (4)), $M = f(X_1, X_2, ..., X_p)$ could be modified to allow for both "computational calibration" in which one uses modelling to adjust test items to calibration items (via the k factor in the UNCL example) and errors in predictors. However, one would need to allow for bias in the adjustment to calibration items by having different probability distributions for some of the inputs $X_1, X_2, ..., X_p$ in training and testing. This moves the analysis toward Monte Carlo simulation assessments, without concern for whether the probability distribution for the item SNM mass can be expressed as a known function, $M = f(X_1, X_2, ..., X_p)$. Because we do not yet have a defensible estimate of the probability distribution of the k factor, this example is for illustration only, not for a defensible bottom-up UQ for the UNCL. Also, choices in how to perform the calibration (with or without adjusting for errors in predictors for example) are best assessed using simulation, as we did in Figure 3.

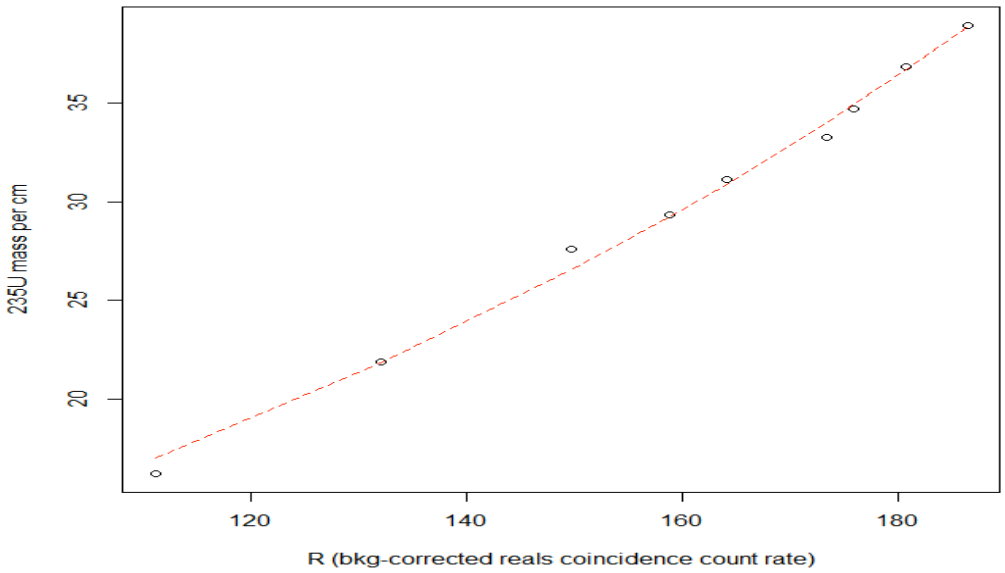

Figure 2. The ^{235}U mass per cm (linear density) versus the background-corrected reals coincidence rate R. The fit to Eq. (7) from the data is also shown. The 9 R values are 111.1, 132.0, 149.7, 158.8, 164.1, 173.4, 176.0, 180.8, 186.5 [/s]. The corresponding 9 ^{235}U values are 16.20, 21.89, 27.59, 29.37, 31.15, 33.28, 34.71, 36.84, 38.98 [g/cm].

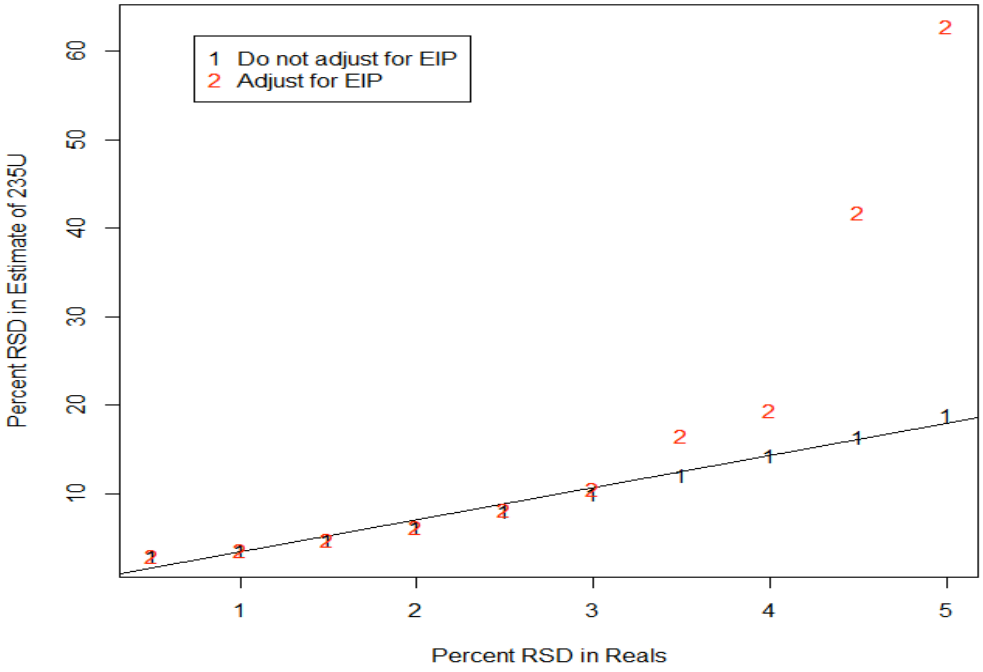

Figure 3. The RSD in UNCL prediction versus RSD in *k*R on the basis of 10^5 simulations. The data are the 9 data pairs from [22]. A large bias component is contributing to the large RSD in the option 2 results, due to adjusting for EIP by using the RSS_1 criterion rather than the RSS_2 criterion to estimate a_1, a_2.

5. Discussion and Summary

This article has illustrated several challenges in UQ for NDA (EMP, Cf shuffler, DSTA, and UNCL). As the need for better UQ for NDA is becoming recognized, the GUM [4] is being revised [5]. It is possible that the NDA community will need a modified GUM, or that NDA UQ needs can influence the in-progress GUM revision. For example, the UNCL case study illustrates that there is a need for attention to errors in predictors in the GUM supplement that deals with calibration. The UNCL case study is also an example of "computational calibration," in which one uses modelling to adjust test items to calibration items. Other examples of computational calibration include the Cf shuffler [18], and possibly, in new applications of NDA to spent fuel assay [8]. In the case of spent fuel assay, it is currently unclear to what extent MCNP modelling will be used as part of the assay procedure once working standards become available.

6. Acknowledgements

The authors acknowledge the IAEA, and US Nuclear Nonproliferation Agency NA-22

7. References

[1] McElroy, R., Croft, S., Nakazawa, D., Kirkpatrick, J., Venkataramin, R., Burr, T., The need and opportunity for improved uncertainty quantification and reporting for nondestructive assay, Proceedings Institute of Nuclear Materials Management, 2012.

[2] Burr, T., Trellue, H., Tobin, S., Croft, S., Uncertainty quantification challenges in nondestructive assay of nuclear material, Conference on Data Analysis, 2014.
[3] Bonner, E., Burr, T., Guzzardo, T., Norman, C., Zhao, K., Beddingfield, D., Geist, W., Laughter, M., Lee, T., Improving the effectiveness of safeguards through comprehensive uncertainty quantification, to appear, Journal of the Institute of Nuclear Materials Management, 2015.
[4] Guide to the expression of uncertainty in measurement, JCGM 100: 2008, www.bipm.org
[5] Bich, W., Revision of the guide to the expression of uncertainty in measurement. Why and How, Metrologia 51, S155-S158, 2014.
[6] Burr, T., Pickrell, M., Rinard, P., Wenz, T, Data mining: applications to nondestructive assay data, Journal of Nuclear Materials Management 27(2), 40-47, 1999.
[7] Burr ,T., Knepper, P., A study of the effect of measurement error in predictor variables in nondestructive assay, Applied Radiation and Isotopes 53 (4-5), 547-555, 2000.
[8] Burr, T., Trellue, H., Tobin, S., Favalli, A., Dowell, J., Henzl, V., Mozin, V., Integrated nondestructive assay systems to estimate plutonium in spent fuel assemblies Nuclear Science and Engineering 179(3), 321-332, 2015.
[9] Burr, T., Sampson, T, Vo, D., Statistical evaluation of FRAM γ-ray isotopic analysis data, Applied Radiation and Isotopes 62, 931-940, 2005.
[10] Burr, T., Hemphill, G., Multi-component radiation measurement error models, Applied Radiation and Isotopes 64(3), 379-385, 2006.
[11] Burr, T., Dowell, J., Trellue, T., Tobin, S., Measuring the effects of data mining on inference, Encyclopedia of Information Science and Technology, Third Edition, 2015.
[12] Monte Carlo N- Particle code, see mcnp.lanl.gov at Los Alamos National Laboratory.
[13] Elster, C., Bayesian Uncertainty analysis compared to the application of the GUM and its supplements, Metrologia 51, S159-S166, 2014.
[14] Willink, R., Measurement uncertainty and probability, Cambridge University Press, Cambridge, 2013.
[15] Standard test method for measurement of 235U fraction using the enrichment meter principle, C 1514-08, ASTM.
[16] Elster, C., Toman, Bayesian uncertainty analysis for a regression model versus application of GUM supplement 1 to the least-squares estimate, Metrologia 48, 233-240, 2011.
[17]Fuller, W. (1987). Measurement Error Models, Wiley, New York.
[18] Tobin, S., Swinhoe, M., and MacArthur, D., Monte Carlo Study of Replacing Cf in a Shuffler with a Neutron Generator, LA-UR-04-4354. Institute of Nuclear Materials Management Annual Proceedings, 2004.
[19] Beddingfield, D.H., and Menlove, H.O., Distributed source term analysis, a new approach to nuclear material inventory verification, Nuclear Instruments and Methods-A, 485, 797-804, 2002.
[20] Beddingfield, D., Burr, T., Longo, C., Error evaluation in distributed source-term analysis, LAUR10-01947, 2010.
[21] Favalli, A., Croft, S., Swinhoe, M., Perturbation and burnable poison rod corrections for bwr uranium neutron collar, Proceedings ESARDA, 2011.
[22] Menlove, H., et al, Neutron collar calibration and evaluation for assay of LWR fuel assemblies containing burnable neutron absorbers, Los Alamos National Laboratory Report, LA-11965-MS (also ISPO-323), 1990.
[23] Peerani, P., Computational calibration of UNCL neutron collars for fresh fuel elements, Technical Note I.04.142, European Commission Joint Research Center, 2004.

[24] R Core Team (2012). R: A language and environment for statistical computing. R Foundation for Statistical Computing, Vienna, Austria. ISBN 3-900051-07-0, www.R-project.org

TRIPOLI-4® and FREYA for Stochastic Analog Neutron Transport. Application to Neutron Multiplicity Counting.

Jérôme M. Verbeke[1], Odile Petit[2]

[1] Lawrence Livermore National Laboratory
P.O Box 808, Livermore, California 94551, USA.
[2] Commissariat à l'Energie Atomique et aux Energies Alternatives
CEA-Saclay, DEN, DM2S, SERMA, LTSD
F-91191 Gif-sur-Yvette Cedex, France.
E-mail: verbeke2@llnl.gov, odile.petit@cea.fr

Abstract:

From nuclear safeguards to homeland security applications, the need for better modeling of nuclear interactions has grown over the past decades. Current Monte Carlo radiation transport codes compute average quantities with great accuracy and performance, but performance and averaging come at the price of limited interaction-by-interaction modeling. These codes often lack the capability of modeling interactions exactly: for a given collision, energy is not conserved, energies of emitted particles are uncorrelated, multiplicities of prompt fission neutrons and photons are uncorrelated. Many modern applications require more exclusive quantities than averages, such as the fluctuations in certain observables (e.g. the neutron multiplicity) and correlations between neutrons and photons. In an effort to meet this need, the radiation transport Monte Carlo code TRIPOLI-4® was modified to provide a specific mode modeling nuclear interactions in a full analog way, replicating as much as possible the underlying physical process. Furthermore, the computational model FREYA (Fission Reaction Event Yield Algorithm) was coupled with TRIPOLI-4® to model complete fission events. FREYA automatically includes fluctuations as well as correlations resulting from conservation of energy and momentum.

Neutron Multiplicity Counting (NMC) exploits the correlated nature of fission chains, and thus requires analog neutron transport. With the latest analog neutron transport developments in TRIPOLI-4®, we will show that NMC can now be properly simulated, by reconstructing the mass and multiplication of an object by analyzing the measured signal from ^{3}He tubes in a well counter.

Keywords: Monte Carlo radiation transport code; Neutron Multiplicity Counting; TRIPOLI-4®; FREYA; analog transport

1. Introduction

Methods based on time-correlated signals have been developed over many years to characterize fissile materials. For NMC, sequences of thermal neutron captures are recorded in ^{3}He tubes. To determine features of the measured objects, the sequences are split into time windows, and the numbers of neutrons arriving in each window are recorded to build statistical count distributions. These distributions are in turn analyzed to authenticate or characterize fissile materials. Some materials such as ^{252}Cf emit several neutrons simultaneously, whereas others such as uranium and plutonium multiply the number of neutrons to form bursts. This translates into unmistakable time-correlated signatures.

General Monte Carlo codes that are used for criticality safety evaluations are typically meant for calculation of an integral reactor parameter such as k_{eff} and for estimation of neutron fluxes and derived quantities of interest. They make use of well established variation reduction techniques leading to more efficient calculations. These techniques are meant to speed up calculations and are sufficient for the calculation of average quantities such as flux, energy deposition and multiplication.

However, they suffer from approximations of the underlying physical interactions, and are thus unsuitable for studying detailed correlations between neutrons and/or photons on an interaction-by-interaction basis, and in particular for NMC which relies on the correlated nature of fission chains.

The first part of this paper will focus on the latest TRIPOLI-4® [1][2] developments that were necessary to simulate NMC experiments: analog neutron transport, coupling with the LLNL Fission Library/FREYA [3]-[5] package for fission interactions, development of a spontaneous fission source, and new options to reduce memory footprint of ROOT [6] track files. The second part will focus on the use of these new capabilities for NMC. We will show that the mass and multiplication of a PuO_2 ball in a well counter (see Fig. 1) can be determined from measurements of the neutron captures in the ^{3}He tubes.

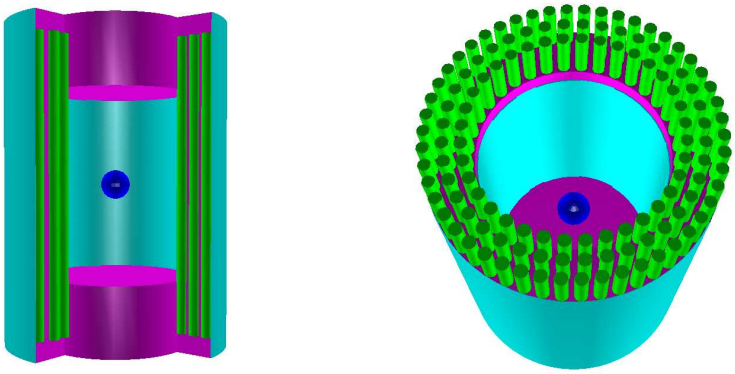

Figure 1: (color online) Cutouts to show the inside of a well counter. Polyethylene (magenta), Cadmium (cyan), ^{3}He tubes (green), representation of a generic neutron source to be characterized (blue). Left: multiple ^{3}He tubes removed for clarity. Right: upper polyethylene plug removed.

2. Developments in TRIPOLI-4® for NMC

TRIPOLI-4® solves the linear Boltzmann equation for neutrons, photons, electrons and positrons with the Monte Carlo method, in any 3-D geometry. The code uses ENDF format continuous-energy cross sections from various international evaluations. It has advanced variance reduction methods to address deep penetration issues and can be run in parallel. TRIPOLI-4® is used as a reference code for industrial purposes (fission/fusion) for CEA[1], EDF[2] and branches of AREVA, as well as an R&D and teaching tool, for radiation protection and shielding, core physics, nuclear criticality safety and nuclear instrumentation.

This section presents the list of the most important TRIPOLI-4® developments that were required for the NMC application, starting from version 9 of the code. These developments were made using a recent version of TRIPOLI-4® with analog mode capabilities [7]. While simulating the well counter was the objective of this study, these developments would also apply to multiplicity counting with liquid scintillators for fast neutrons and photons.

2.1. Coupling of FREYA and TRIPOLI-4® for fission modeling

To model fission, general-purpose Monte Carlo codes TRIPOLI-4®, MCNP6/X [8], TART [9], COG [10], Geant [11], etc.) employ the “average fission model” which is characterized by outgoing projectiles (fission neutrons and photons) that are uncorrelated, and sampled from the same probability density functions.

During the past decade several code extensions have been developed that allow the modeling of correlations in fission. MCNP-DSP [12] and MCNPX-PoliMi [13] added limited angular correlations of

[1] Commissariat à l’Energie Atomique et aux Energies Alternatives
[2] Electricité de France

fission neutrons. The LLNL Fission Library [14], introduced in MCNPX2.7.0 [15], Geant 4.9 [11] and MCNP6 featured time-correlated sampling of photons from neutron-induced fission, photofission and spontaneous fission. The capabilities for correlations are, however, limited, as they sample outgoing particles from average fission distributions instead of sampling them from individual realizations of a fission process.

In recent years, various simulation treatments addressed fluctuations of and correlations between fission observables. In particular, a Monte Carlo approach was developed [16] for the sequential emission of neutrons and photons from individual fission fragments in binary fission. The more recent event-by-event fission model, FREYA, has been specifically designed for producing large numbers of fission events in a fast simulation [17]. Employing nuclear data for fragment mass and kinetic energy distributions, using statistical evaporation models for neutron and photon emission, and conserving energy, momentum, and angular momentum throughout, FREYA is able to predict a host of correlation observables, including correlations in neutron multiplicity, energy, and angles, and the energy sharing between neutrons and photons. For modeling of fission on an interaction-by-interaction basis, the new LLNL Fission Library/FREYA package was coupled with TRIPOLI-4®.

2.2. Development of a spontaneous fission source

A spontaneous fission source was developed to sample time-correlated neutrons and photons from fission. This source emits bursts of time-correlated prompt neutrons and photons from individual fission events, whose multiplicities and energies are sampled from the LLNL Fission Library/FREYA package. TRIPOLI-4® accesses this source as an *external source* (see User Manual [1]). The times of spontaneous fissions are sampled randomly and uniformly within a given time interval ΔT [3]. The rate of spontaneous fissions has to match the rate F_s of spontaneous fissions of the object to be measured experimentally. It is therefore essential to set the correct number of particles accordingly.

2.3. Reduction in tracks memory footprint

To model NMC for the well counter shown in Fig. 1, it is necessary to store the time tags of all the neutron capture reactions in the ^{3}He tubes. It was quickly realized that the ROOT tracks stored by TRIPOLI-4® became bloated for large simulations, leading to files that were close to terabytes in size for seconds of experimental data. Most of the tracks did not result in ^{3}He(n,p) reactions and were thus cluttering the disk. When filtering out tracks failing to traverse detector cells, we were able to substantially decrease the memory footprint, but not enough. Two new options were therefore introduced to further reduce the size of the track files. The first option enables us to store full tracks containing one or several events of interest, whereas the second option enables storage of only specific events with those tracks. With these two additional filters, we could keep the footprint of the ROOT track files in check.

3. PuO_2 ball

Let's consider a PuO_2 object spherical in shape, of weight equal to 5.5366 kg, density 3 g/cc, and of outer radius 7.62 cm [4]. Knowing the neutron yields of the different isotopes composing the object, we calculated the rate of spontaneous fissions to be 140170 spontaneous fissions/s. The spontaneous fission source is uniformly distributed across the sphere. A simulation of the PuO_2 source in the well counter shown in Fig. 1 was performed. While the intensity of the (α,n) source could be calculated, we will neglect this contribution for the purpose of this study.

3.1. Fitting count distributions to determine system parameters

The arrival times of the neutrons in each of the ^{3}He tubes were recorded in the simulation. Randomly splitting the sequence of time tags into N segments of width T (where T is of the order of microseconds to hundreds of microseconds) one can count how many neutrons arrive in the first

[3] The time tags of the ^{3}He(n,p) reactions in the ^{3}He tubes are re-ordered chronologically in post-processing.
[4] The isotopics of the plutonium are 0.014% ^{238}Pu, 93.5% ^{239}Pu, 6% ^{240}Pu, 0.5% ^{241}Pu, 0.03% ^{242}Pu, and traces of other isotopes.

segment, how many in the second segment, in the third one, etc. to build a distribution $B_n(T)$ of the number *n* of neutrons arriving in the segments of width *T*. The blue dots labelled “simulated data” in the left-hand graph of Fig. 4 show a typical count distribution.

The probability distributions $b_n(T)$ (where $b_n(T)$ is the probability of recording *n* counts in a time gate *T*, which is equivalent to $B_n(T)$ normalized by the number of segments of width *T*) can be reconstructed theoretically [18] using different sets of the three free parameters (*M*, ε, $\bar{\nu}_{sp} F_s$), where *M* is the multiplication of the object, ε the efficiency of the detector array, $\bar{\nu}_{sp}$ the average number of neutrons emitted per spontaneous fission and F_s the intensity in units of spontaneous fissions per second of the spontaneous fission sources in the object. Using a likelihood function, one can determine which parameters (*M*, ε, $\bar{\nu}_{sp} F_s$) generate the theoretical count distribution $b_n^{theory}(T)$ closest to the measured data points $b_n(T)$. This method is best described in Ref. [19].

Each set of parameters (*M*, ε, $\bar{\nu}_{sp} F_s$) has an associated likelihood that the reconstructed $b_n^{theory}(T)$ will be a good match to the measured $b_n(T)$. Using Bayes' theorem, we calculate the posterior probability of each such set. To determine the region of the (*M*, ε, $\bar{\nu}_{sp} F_s$) space that contains the solution with a credibility of 68.27%, we have to accumulate high posterior probability sets until the cumulative probability reaches 68.27%. Fig. 2 shows the credible regions in the (*M*, ε) and (*M*, $\bar{\nu}_{sp} F_s$) parameter spaces for credibilities of 68.27% (red), 95.45% (yellow) and 99.73% (blue). The top two graphs are computed with FREYA. The bottom two graphs are computed without FREYA. Without FREYA, $\bar{\nu}$ is statistically rounded up or down at each fission site to get a number of neutrons. Fig. 3 shows the same credible regions for 2530 seconds.

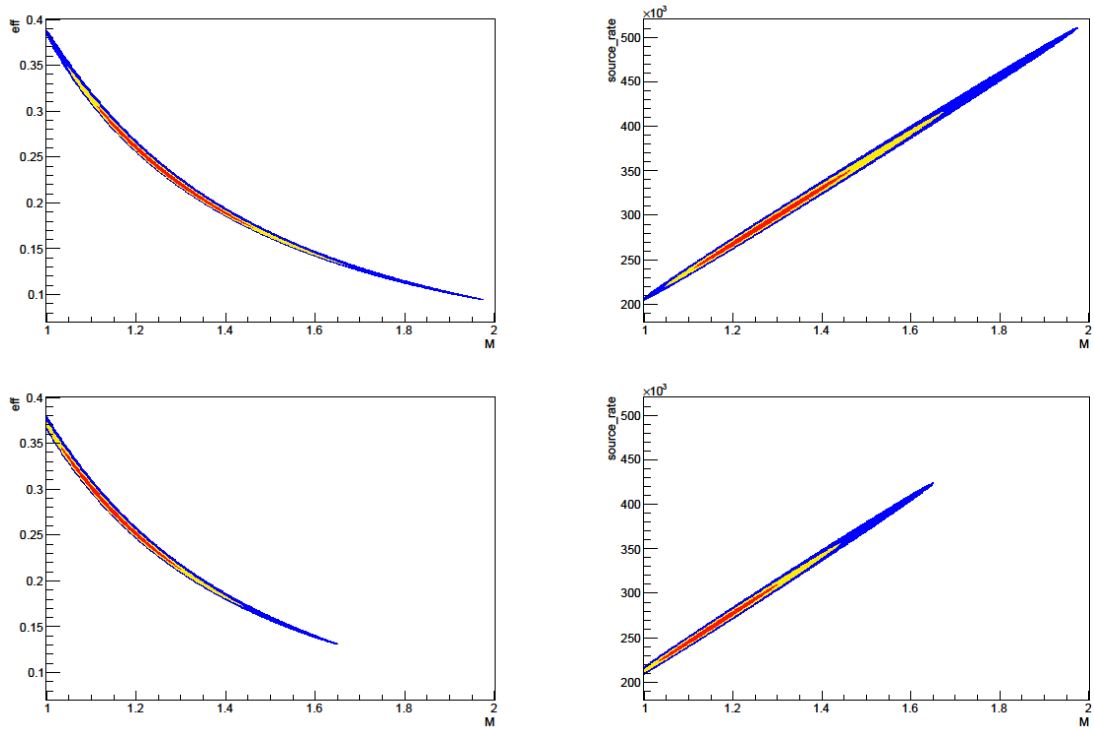

Figure 2: (color online) Credible regions for theoretical reconstructions of PuO_2 ball:
68.27% (red), 95.45% (yellow), 99.73% (blue).
Nuclear data for induced fission of ^{239}Pu at 1 MeV. The measurement time is equivalent to 350 seconds.
Top left: (*M*, ε) with FREYA. Top right: (*M*, $\bar{\nu}_{sp} F_s$) with FREYA.
Bottom left: (*M*, ε) without FREYA. Bottom right: (*M*, $\bar{\nu}_{sp} F_s$) without FREYA.

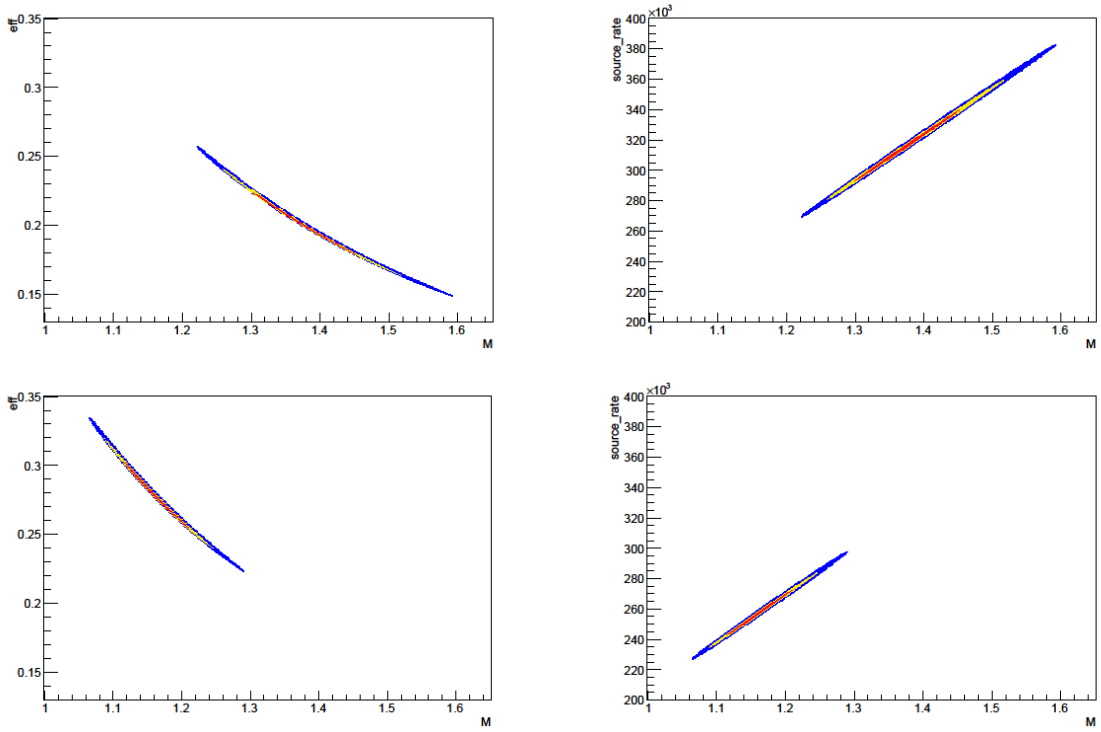

Figure 3: (color online) Credible regions for theoretical reconstructions of PuO_2 ball:
68.27% (red), 95.45% (yellow), 99.73% (blue).
Nuclear data for induced fission of ^{239}Pu at 1 MeV. The measurement time equivalent to 2530 seconds.
Top left: (M, ε) with FREYA. Top right: (M, $\bar{\nu}_{sp} F_s$) with FREYA.
Bottom left: (M, ε) without FREYA. Bottom right: (M, $\bar{\nu}_{sp} F_s$) without FREYA.

3.2. Discussions

Table 1 shows the multiplication calculated by TRIPOLI-4® in different modes: either a criticality calculation including a convergence process of the fission source, or a fixed source criticality calculation where the same neutron source is kept during the whole simulation and fission neutrons are sampled but not used for the source convergence (see TRIPOLI-4® User Manual [1]).

TRIPOLI-4® simulation mode	LLNL Fission Library/FREYA	$M \pm \sigma$
CRITICALITY	no	1.3312 ± 0.0012 [5]
FIXED_SOURCES_CRITICALITY	no	1.3140 ± 0.0007
FIXED_SOURCES_CRITICALITY	yes	1.3124 ± 0.0008

Table 1: Neutron multiplication for PuO_2 ball in the well counter calculated with TRIPOLI-4®.

With TRIPOLI-4® running in analog mode, the multiplication of the PuO_2 ball within the well counter was calculated to be 1.3124 ± 0.0008 with FREYA, and 1.3140 ± 0.0007 without FREYA. These multiplications are very close and show that average quantities are not affected by the choice of the fission model, whether it statistically samples $\bar{\nu}$ rounded up or down, or a full neutron multiplicity distribution.

[5] This multiplication was calculated using $M = 1/(1-k_{eff})$ and the k-eigenvalue method of TRIPOLI-4® for k_{eff}. Since this method does not solve the same problem as the FIXED_SOURCES_CRITICALITY method [20], it is not expected to produce the same multiplication. It is only shown for the sake of completeness.

For the reconstruction with FREYA, the best solution is (M, ε, $\overline{\nu}_{sp} F_s$) = (1.35, 20.9%, 308368 n/s).

One may wonder whether the credible regions shown in the top two graphs of Fig. 3 contain the true solution, which is the one with the source intensity used for the simulation and the multiplication computed by TRIPOLI-4®. The solution (1.33, 21.5%, 303041 n/s) in these two graphs is within the 68.27% credible region and gives the correct source intensity of 302799 n/s. The small discrepancies are likely to be attributed to systematic errors, and to inadequacies in the theory to model the experiment. This is discussed at length in Ref. [19].

It is interesting to compare the count distributions reconstructed from the different solutions within the 68.27% credible region. A set of three such distributions is shown in the left-hand graph of Fig. 4. All the solutions within the credible region are essentially indistinguishable, which explains the size of the uncertainty in that region, and illustrates the highly degenerate nature of the model.

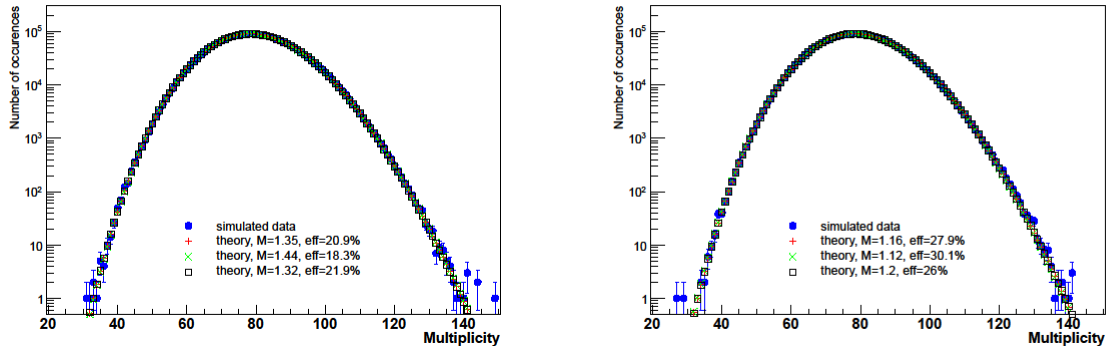

Figure 4: (color online) Comparison between theoretically reconstructed count distributions within the 68.27% credible region in Fig. 3. Random time gate count distribution. Time gate width = 1 ms. Simulation result in blue. Nuclear data for induced fission of ^{239}Pu at 1 MeV. The measurement time is equivalent to 2530 seconds. Left: with FREYA. Right: without FREYA.

Without FREYA, the best solution for the reconstruction is (M, ε, $\overline{\nu}_{sp} F_s$) = (1.16, 27.9%, 257174 n/s). Within the 68.27% credible region, the solution that gives the closest source intensity is (M, ε, $\overline{\nu}_{sp} F_s$) = (1.2, 26.0%, 269471 n/s). The model still gives very good count distribution reconstructions, as the right-hand graph of Fig. 4 illustrates, but unfortunately, these reconstructions are for the incorrect parameters. For correlated quantities and low multiplication, sampling the full distribution for the fission neutron multiplicity is important. The correct solution could be found with FREYA, whereas without FREYA the default neutron multiplicity sampling gave incorrect solutions.

4. Conclusion

FREYA was coupled to TRIPOLI-4® for the purpose of using the latter for NMC. With the addition of a few modifications such as analog transport, spontaneous fission sources and improved tracking capabilities, we demonstrated by way of a PuO_2 ball simulation that TRIPOLI-4® when coupled with FREYA can simulate physical correlations sufficiently well to reproduce predicted count distributions measured by a well counter.

Average quantities like neutron flux, reaction rate, multiplication are not affected by the choice of the fission model. Whether the fission model statistically samples $\overline{\nu}$ rounded up or down, or a full fission neutron multiplicity distribution, to emit a number of secondary neutrons, has little to no impact on the result.

For methods using correlated quantities, sampling the full distribution for the fission neutron multiplicity is paramount. The correct solution to the PuO_2 ball problem could be found with the fission model

FREYA, whereas the default neutron multiplicity sampling gave incorrect solutions[6]. Thus, including such capabilities in Monte Carlo transport codes is important.

5. Acknowledgments

This work was performed under the auspices of the U.S. Department of Energy by Lawrence Livermore National Laboratory under Contract DE-AC52-07NA27344.

TRIPOLI-4® is a registered trademark of CEA. We gratefully acknowledge EDF for their long term partnership and AREVA for their support.

J.M. Verbeke wishes to acknowledge the Office of Defense Nuclear Nonproliferation Research and Development in DOE/NNSA for their support, and to thank the stochastic team (LTSD) of the Service d'Etudes de Réacteurs et de Mathématiques Appliquées (SERMA) in the CEA at Saclay, France for hosting him while this paper was being written and while FREYA was being coupled with TRIPOLI-4®.

6. References

[1] TRIPOLI-4® Project Team; *TRIPOLI-4 version 8 User Guide*; CEA-R-6316; 2013; see also http://www.nea.fr/abs/html/nea-1716.html.

[2] TRIPOLI-4® Project Team; *TRIPOLI-4, CEA, EDF and AREVA Reference Monte Carlo Code*; Joint Int. Conf. on SNA and MC 2013 (SNA+MC 2013), Paris, France; 2013; also accepted for publication in Annals of Nuclear Energy, 2015.

[3] Verbeke J.M, Randrup J, Vogt R; *Fission Reaction Event Yield Algorithm FREYA for Event-by-Event Simulation of Fission*; to be published in Computer Physics Communications.

[4] Hagmann C, Randrup J, Vogt R; *FREYA - A new Monte Carlo code for improved modeling of fission chains*; Trans. Nucl. Sci. **60**, p 545-549; 2013.

[5] Verbeke J.M, Hagmann C.A, Randrup J, Vogt R; *Integration of FREYA into MCNP6: An Improved Fission Chain Modeling Capability*; Lawrence Livermore National Laboratory; Livermore, CA; LLNL-PROC-638986; 2013.

[6] Brun R, Rademakers F; *ROOT - An Object Oriented Data Analysis Framework*; Proceedings AIHENP'96 Workshop, Lausanne; Sep. 1996; Nucl. Inst. Meth. Phys. Res. A **389**, p 81-86, 1997; see also http://root.cern.ch/.

[7] Petit O, Dumonteil E; *Analog neutron transport for nuclear instrumentation applications with the Monte-Carlo code TRIPOLI-4*; ANS RPSD 2014 - 18th Topical Meeting of the Radiation Protection & Shielding Division of ANS Knoxville, TN, Sep. 14 - 18, 2014; American Nuclear Society; LaGrange Park, IL; 2014.

[8] Goorley T et al.; *Initial MCNP6 Release Overview - MCNP6 version 1.0*; Los Alamos National Laboratory; Los Alamos, NM; LA-UR-13-22934; 2013.

[9] Cullen D.E; *TART2005: A Coupled Neutron-Photon 3-D, Combinatorial Geometry, Time Dependent Monte Carlo Transport Code*; Lawrence Livermore National Laboratory; Livermore, CA; UCRL-SM-218009; 2005.

[10] Buck R.M, Lent E.M; *COG User's Manual: A Multiparticle Monte Carlo Transport Code*; Lawrence Livermore National Laboratory; Livermore, CA; UCRL-TM-202590, 5th Edition; 2002.

[6] We could show that the choice of the fission multiplicity distribution becomes less important the higher the multiplication, but the theoretical developments required for this are beyond the scope of this paper.

[11] Available from the European Organization for Nuclear Research, http://geant4.cern.ch.

[12] Valentine T.E; *MCNP-DSP Users Manual*; Oak Ridge National Laboratory; Oak Ridge, TN; ORNL/TM-13334 R2; 2001.

[13] Padovani E, Pozzi S.A, Clarke S.D, Miller E.C; *MCNPX-PoliMi User's Manual*; C00791 MNYCP; Radiation Safety Information Computational Center; Oak Ridge National Laboratory; 2012.

[14] Verbeke J.M, Hagmann C, Wright D; *Simulation of Neutron and Gamma-Ray Emission from Fission and Photofission*; Lawrence Livermore National Laboratory; Livermore, CA; UCRL-AR-228518; 2010.

[15] Pelowitz D.B et al.; *MCNPX2.7.0 Extensions*; Los Alamos National Laboratory; Los Alamos, NM; LA-UR-11-02295; 2011.

[16] Lemaire S, Talou P, Kawano T, Chadwick M.B, Madland D.G; *Monte Carlo approach to sequential γ-ray emission from fission fragments*; Phys. Rev. C **73**; 014602; 2006.

[17] Vogt R, Randrup J; *Event-by-event study of photon observables in spontaneous and thermal fission*; Phys. Rev. C **87**; 044602; 2013.

[18] Prasad M.K, Snyderman N.J; *Statistical Theory of Fission Chains and Generalized Poisson Neutron Counting Distributions*; Nucl. Sci. Eng. **172**; p 300; 2012.

[19] Verbeke J.M; *Neutron Multiplicity Counting: Confidence Intervals for Reconstruction Parameters*; Lawrence Livermore National Laboratory; Livermore, CA; LLNL-JRNL-668401-DRAFT; submitted to Nuclear Science and Engineering; 2015.

[20] Cullen D.E, Clouse C.J, Procassini R, Little R.C; *Static and Dynamic Criticality: Are They Different*; Lawrence Livermore National Laboratory; Livermore, CA; UCRL-TR-201506; 2003.

Use of a Plutonium Piece Monitor and Improved Offline Plutonium Assay Algorithms in Support of a Residues Retrieval Programme

Mark Wilson[#], Jamie Rackham[#], Elizabeth Waterhouse[#], Jonathan Sharpe[#], Nicholas Clarke*

A joint paper between Cavendish Nuclear[#] and Sellafield Ltd*.
E-mail: mark.wilson@cavendishnuclear.com; nicholas.i.clarke@sellafieldsites.com

Abstract:

At Sellafield, a retrievals programme has recently been completed recovering a number of bottles containing residues from a legacy store. The material in these bottles originated from the cleanout of a range of different plutonium process gloveboxes, mixed-oxide (MOX) manufacturing processes and from sweepings collected following various decommissioning activities. The bottles fell into two categories; Residues (either plutonium or MOX) which were decanted into new containers, consolidated and exported to a purpose built store, and low fissile content 'Dross' bottles, which were consigned as plutonium contaminated material (PCM) waste.

The Dross bottles, which mainly consisted of floor sweepings and dusts arising from decommissioning operations, were assayed in a Plutonium Piece Assay Monitor (PPAM) and consigned as PCM waste using the standard assay process: Passive Neutron Coincidence Counting (PNCC) combined with High Resolution Gamma-ray Spectrometry (HRGS).

The PPAM was also used to assay consolidated Residue containers in order to provide Best Estimates of the plutonium and uranium content for Safeguards purposes. The majority of these residues contained high plutonium content and many also had a high proportion of plutonium fluoride (PuF_4) present, resulting in high neutron count rates leading to large statistical uncertainty on the coincident neutron count rate and also significant elevation of this count rate due to high rates of induced fission. The high statistical uncertainty meant the PNCC measurements could not meet the required precision, and offline analysis was required to accurately determine the plutonium and uranium content.

An innovative fluoride correction was successfully applied to the Residues with significant PuF_4 content, utilising the HRGS data to determine the relative amount of PuF_4 (with respect to total plutonium) in addition to the isotopic composition, thereby allowing computation of the plutonium content from the total neutron count rate. This analysis provided results that were broadly consistent with estimates of the plutonium and uranium content produced previously from sampling and process knowledge and significantly improved the accuracy and substantiation basis of the estimates that would otherwise have been used for Safeguards purposes (for example, derived from the net weight of the residue material).

Keywords: Non-Destructive Assay, Plutonium Fluoride, PPAM, MOX, Plutonium, Residues, HRGS, PNCC, SNM.

1. Introduction

An innovative solution was required to support the Residues Retrieval Programme (RRP) by characterising a large number of Special Nuclear Material (SNM) containers from several legacy SNM stores on the Sellafield site, prior to their export to long-term engineered SNM storage facilities. The SNM containers, which contained either "Dross" or "Residue" material, originated following the cleanout of a range of different plutonium process gloveboxes, mixed-oxide (MOX) fuel manufacturing processes and from sweepings collected following decommissioning activities. In order to comply with ALARP practices, and to follow the waste hierarchy, the Dross bottles, which were expected to have low masses of plutonium, were to be assayed for Nuclear Safety and Accountancy and consigned as

Plutonium Contaminated Material (PCM) if possible, whilst the Residue containers were to be assayed for accountancy (Safeguards) purposes only.

A desktop technical study had previously been carried out by Sellafield Ltd. in 2005 which used process knowledge to estimate the nature and SNM content of the majority of the containers in the stores for accountancy purposes. This study also assessed the feasibility of assaying such material and highlighted that the complexity of the measurements would challenge both the hardware of the existing assay system and the limitations of the Passive Neutron Coincidence Counting (PNCC) technique currently used at Sellafield to assay such materials. This complexity was compounded by the short timescales required of the project, which necessitated close collaboration between Cavendish Nuclear and Sellafield Ltd, together with prompt technical analysis of measurement data.

2. Technology

2.1. Decommissioning SNM Residue Containers

Prior to assay and export from the legacy stores, the Residue material, which had mainly been stored within poly-vinyl chloride (PVC) bottles, was decanted and consolidated into new decommissioning SNM residue containers (see Figure 1 below). Export limits constrained the net mass of the material in each container to a maximum of 1400 g, and for the Residue containers, this net mass value was used as a pessimistic (conservative) estimate of the Nuclear Safety fissile mass.

Figure 1: Pictures of Decommissioning SNM Residue Containers.

The Dross material was not decanted and was therefore measured in the original PVC bottles.

2.2. Plutonium Piece Assay Monitor

The consolidated Residue containers and Dross bottles were measured in a Plutonium Piece Assay Monitor (PPAM) (see Figure 2), using the PNCC technique combined with High Resolution Gamma ray Spectrometry (HRGS), in order to provide Best Estimate (Accountancy) and Nuclear Safety mass values (calculated from the Best Estimate mass by the addition of three standard deviations of total uncertainty). The PPAM was originally designed and commissioned for the measurement of PCM waste packages, which typically contain low plutonium masses (i.e. less than a few hundreds of grams total plutonium mass). In standard operation, it is used to ensure that a PCM package does not exceed the 230 g Nuclear Safety limit for total plutonium mass.

The PPAM instrument consists of a measurement chamber surrounded by four banks of three ^{3}He neutron detectors embedded in a moderating polyethene matrix (12 neutron detectors in total). The signal from each bank of detectors is fed into a separate amplifier and then to a rack of summing units and a coincidence counting card, which determines the total (Totals) and coincident (or Reals) neutron count rate. The system reports a plutonium mass determined from the Reals neutron count rate combined with a HRGS measurement of the plutonium isotopic composition.

Figure 2: (left) Picture of a Typical PPAM Prior to Installation. (right) Operator in Air Fed Suit Placing a PCM Piece in a PPAM Measurement Chamber for Assay.

Given the challenging time constraints, only minor modifications to improve the functionality of the system were considered possible. A Timestamper system was added in parallel to the PPAM's coincidence counting card to provide an independent measure of the Totals and Reals neutron count rates, providing a check of the correct function of the PPAM. Note that although the Timestamper card has the capability to measure higher orders of neutron multiplicity, the neutron emissions were such that the statistical precision on the Triples count rate was too poor to be used.

For the Dross bottles, which contained floor sweepings and dusts from decommissioning activities, the plutonium mass content was expected to be low and assay using the standard PPAM measurement was sufficient. Assuming the plutonium mass was below the 230 g Nuclear Safety limit, the Dross bottles were consigned as PCM. However, the Residue containers were known to have a higher plutonium content (of the order of one kilogram), with a more challenging chemical composition, such that the neutron emission would lie outside of the calibrated and tested range of the PPAM, leading to the requirement for additional testing and the use of alternative analysis techniques.

3. Technical Challenges

The measurement of Residue containers posed a challenge to the standard PNCC technique, requiring the measurement of kilogram quantities of plutonium in challenging chemical form, and a significant extension to the previously demonstrated working range of the instrument.

The plutonium composition of the majority of the Residue containers was expected to be in oxide form (i.e. PuO_2). However, the previous desktop technical study identified a number of the containers in which plutonium fluoride (i.e. PuF_4) was likely to be present in significant quantities. Measurement of PuF_4 is more challenging than other more typical plutonium compounds due to an (α, n) reaction in fluorine, which leads to a neutron emission that can be 100 times higher than that of PuO_2. This contribution to the neutron emission potentially leads to excessive neutron count rates which could exceed the capabilities of the PPAM hardware.

High neutron dose rates can lead to a loss of functionality of the PPAM; such as that due to system dead time, pile up in the neutron counting chain, or potentially an overflow of the counter card which ultimately could lead to an underestimation of the neutron coincidence count rate. High neutron emissions originating from PuF_4 also affect the magnitude of the uncertainty reported for standard PNCC measurements, leading to imprecise values for the Accountancy mass and high values for the Nuclear Safety mass. High count rate testing and additional testing of the PPAM hardware was carried out to ensure that the system could operate with the high neutron emission rates expected from the Residue containers. The correct performance of the neutron counting system was demonstrated up to dead time corrected Totals neutron count rate of ~400,000 $c.s^{-1}$ (contact neutron dose rate ~1.2 $mSv.hr^{-1}$) using the highest available neutron sources. Although the maximum Totals neutron count

rate and neutron dose rate from the Residues containers were significantly higher, at ~1,340,000 $c.s^{-1}$ and ~2.5 $mSv.hr^{-1}$ respectively, offline trend analysis of the measurement data confirmed that the PPAM hardware was not underestimating the dead time corrected count rates across the measured range.

The PPAM was designed to provide pessimistic measurement of low masses of plutonium. It does this by using worst case values for parameters (e.g. detection efficiency) and making basic assumptions (e.g. negligible self-multiplication), which produces safe but pessimistic results. However, these intrinsic pessimisms will result in substantial overestimations when measuring Residue containers, as they contain higher masses of plutonium for which the earlier assumptions made are no longer valid. Alternative analysis techniques were required if precise Accountancy masses were to be obtained for the Residue containers.

4. Method

Alongside the Timestamper, the PPAM was used to measure each Residue container and Dross bottle in turn. A phased offline assessment approach was then employed for the determination of the Accountancy mass and for Dross bottles, the Nuclear Safety mass. In total, the following six methods for plutonium mass measurement were compared:

(i) Result reported by the standard PPAM measurement

(ii) Offline recalculation of the PPAM result (see Section 4.1)

(iii) Offline recalculation of PPAM result with revised calibration (see Section 4.2)

(iv) Offline PuF_4 correction using the Totals count rate and a measured PuF_4 fraction (i.e. measured Alpha value) (see Section 4.3)

(v) Offline Krick-Ensslin correction for self-multiplication (M), using both the Totals and Reals count rates and using the Alpha value derived from the PuF_4 technique (see Section 4.4)

(vi) Offline PuF_4 correction using the Totals count rate and incorporating correction using Krick-Ensslin derived M value (see Section 4.5)

A uranium accountancy mass was also calculated offline as described in Section 4.6.

4.1. Offline Recalculation of PPAM Result

The first phase of the analysis was to replicate the functionality of the PPAM by reproducing the calculations as carried out by the instrument offline. This had the double advantage of independently verifying the result from the PPAM and confirming that the correct raw measurement data has been selected prior to applying the alternative analyses.

The PPAM uses a standard PNCC technique, calculating the Totals neutron count rate (singles, S) and the Reals neutron count rate (doubles, D). In PNCC, there are four unknown quantities:

- The ^{240}Pu effective mass determined from the sample spontaneous fission rate (F)
- The enhancement of the neutron signal due to self-multiplication (M)
- The spatial and energy dependent neutron detection efficiency of the measurement chamber (E)
- The effect on the total neutron emission of the chemical form and impurity content of the plutonium material, alpha (α), where:

$$\alpha = \frac{neutrons\ from\ (\alpha, n)\ reactions}{neutrons\ from\ spontaneous\ fission}$$

These values can be equated to the measured singles (S) and doubles (D) rate using the equations given below:

$$S = F\,E\,M\,\nu_{s1}(1+\alpha) \qquad \text{Eq. 4.1.1 [1]}$$

$$D = \frac{Ff_d\,E^2\,M^2}{2}\left[\nu_{s2} + \left(\frac{M-1}{V_{i1}-1}\right)\nu_{s1}(1+\alpha)\nu_{i2}\right] \qquad \text{Eq. 4.1.2 [1]}$$

Where ν_{s1}, ν_{s2}, ν_{i1}, ν_{i1} are the nuclear data terms describing the spontaneous and induced fission first and second order multiplicity coefficients and f_d is the coincidence gate timing correction factor.

For a coincidence counting system measuring PCM waste items, it can be assumed that the plutonium content will be low and therefore there will be little self-multiplication, and M =1. A conservative but therefore pessimistic value for the efficiency is also applied.

Using the Doubles rate, the ^{240}Pu effective mass, $^{240}Pu_{Eff}$, can then be expressed as:

$$^{240}Pu_{Eff} = \frac{D}{R_{SENS}} \qquad \text{Eq. 4.1.3 [1]}$$

Where R_{SENS} is the calibration factor accounting for the known efficiency, E, the timing gates and the nuclear data constants.

The HRGS spectrum was then analysed by the Banham algorithm [2] to determine the isotopic correction factor, $F_{Isotopic}$, which is used to convert the $^{240}Pu_{Eff}$ mass into the plutonium Nuclear Safety and Accountancy masses. (Note that previous work has confirmed the accuracy of the Banham isotopic analysis method for the Pu of Magnox origin known to be present in these containers).

$$Pu\_mass = {}^{240}Pu_{Eff} \times F_{isotopic} \qquad \text{Eq. 4.1.4 [1]}$$

4.2. Offline Recalculation of PPAM Result with Revised Calibration

To ensure the results were conservative, the Reals-to-Accidentals (R/A) Bias correction capability of the PPAM has been disabled. R/A bias becomes significant at high total neutron signals and leads to overestimation of the Reals rate. Hence to improve the accuracy of the results for the Residues, a R/A bias correction was applied during offline analysis to account for this effect.

The systematic error term to account for the spatial dependence of the neutron detection efficiency of the measurement chamber was also reduced in the Revised Calibration as the Residue container was known to be in the centre of the measurement chamber, hence reducing this uncertainty and further reducing the reported Nuclear Safety mass.

4.3. Offline PuF_4 Correction using the Totals Count Rate and a Measured PuF_4 Fraction (i.e. Measured Alpha Value)

For Residue containers with PuF_4 present, it was necessary to calculate an appropriate alpha value (α) because as detailed earlier, the standard PNCC technique is not suitable since the measured Doubles rate is highly influenced by the enhanced induced fission rate and by poor statistics. Hence, a PuF_4 technique which was previously developed by Cavendish Nuclear [3] was applied which used HRGS to determine the fraction of PuF_4 within a container.

An example HRGS gamma ray spectrum from a PuF_4 waste item is shown in Figure 3.

.

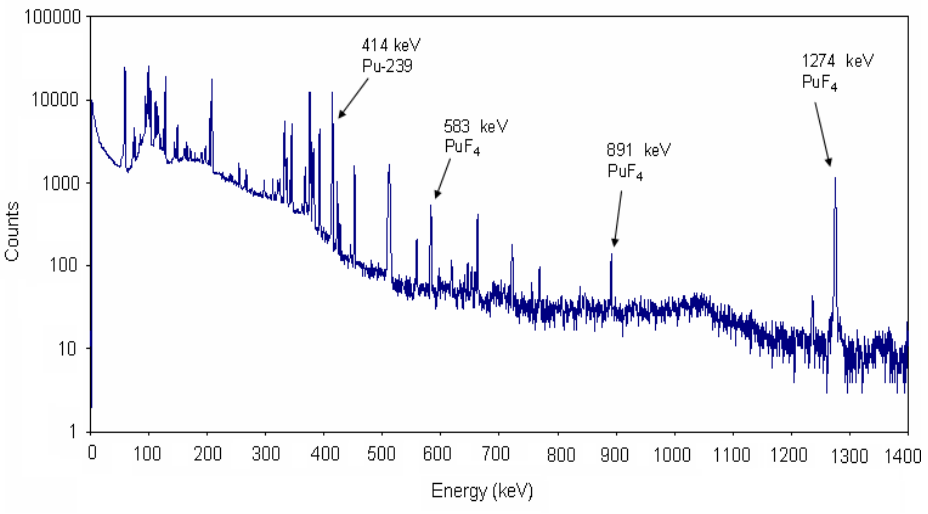

Figure 3: Example Gamma Ray Spectrum from a PuF_4 Waste Item. [3]

Figure 3 shows the prominent 414 keV gamma peak directly from ^{239}Pu and the 583, 891 and 1274 keV gamma ray peaks emitted from the decay chain associated with the (α,n) reaction on fluorine (see Figure 4).

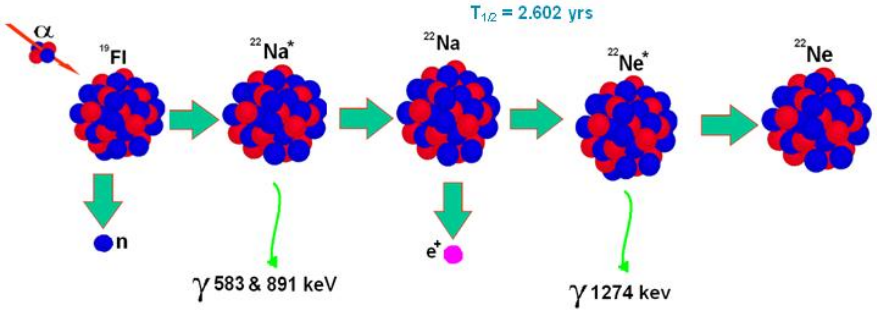

Figure 4: The (α,n) Reaction with Fluorine (* nucleus is formed in an excited state). [3]

The basic principle of the correction technique is to determine the fraction of the Pu in the sample which exists as PuF_4, R_{PuF4}, using the ratio of the ^{239}Pu 414 keV peak to the PuF_4 583 keV peak count rates (and knowledge of the measured Pu isotopic fractions), as shown in the simplified equation below:

$$R_{PuF4} = \frac{583keVCountRate}{414keVCountRate} \cdot NuclearData \cdot DetectionEfficiencyRatios \qquad \text{Eq. 4.3.1 [3]}$$

Where:

- *NuclearData* is a term to correct for the different emission probabilities of the gamma rays.
- *DetectionEfficiencyRatios* is a term to allow for the fact that gamma rays of different energies are detected by the gamma ray detector with different efficiencies and will be attenuated by different degrees when passing through the Residue container to the detector.

Several different gamma rays associated with PuF_4 were selected and used to calculate different measures of the fluoride content (e.g. using 891 keV or 1274 keV instead of 583 keV). Each measure accounts for the effect of attenuation within the plutonium residue material by using the observed effect on the ratios of the 345 keV and 414 keV ^{239}Pu peaks to adjust the detection efficiency ratios.

The most suitable assumed attenuating matrix material of either CaF_2, PuO_2, or Fe, was determined by analysis of the relative gamma peaks and alignment of the different fluoride fractions calculated using different characteristic gamma peaks. Assuming a consistent set of results could be obtained with a realistic assumption of the attenuating material, the most precise PuF_4 fraction was then selected and used to determine the total neutron emission per gram of the material, and hence the

alpha value, by combining the PuF_4 fraction with the isotopic composition determined from the standard gamma ray measurement analysis. Using this calculated alpha value, the Pu mass can be determined from the measured Totals neutron count rate using Eq. 4.1.1.

A further adaptation of this technique is to use the self-multiplication value in order to correct the totals rate for self-multiplication (M) as described in section 4.5.

4.4. Offline Krick-Ensslin Correction for Self-Multiplication (M) using both the Totals and Reals count rates and using the α value Derived from the PuF_4 Technique

For higher plutonium mass Residue containers, where the assumption of a low self-multiplication (M) value was unrealistic, the Krick-Ensslin technique was applied using the alpha value determined using the PuF_4 correction (see section 4.3). The correction for self-multiplication is important for the Residue containers, as typically for PuO_2 at these levels a self-multiplication of up to 1.06 might be expected which would lead to an approximately 40% overestimation of the plutonium mass [4]. The magnitude of the overestimate can become substantially larger than this (as can be seen from Eq. 4.1.2) if the sample also contains plutonium fluoride and therefore has a high (α,n) emission and hence a high α value.

With the Krick-Ensslin technique, M can be obtained by evaluating the roots of the quadratic formula:

$$0 = \left\lfloor \frac{\nu_{s1}\nu_{i2}}{(\nu_{i1}-1)\nu_{s2}} \right\rfloor (1+\alpha)\mathrm{M}^2 - \left(\left\lfloor \frac{\nu_{s1}\nu_{i2}}{(\nu_{i1}-1)\nu_{s2}} \right\rfloor (1+\alpha) - 1 \right) \mathrm{M} - \mathrm{r} \qquad \text{Eq. 4.4.1 [4]}$$

Where,

$$\mathrm{r} = \frac{\mathrm{D/S}}{\mathrm{D_0/S_0}} \frac{(1+\alpha)}{(1+\alpha_0)} \qquad \text{Eq. 4.4.2 [4]}$$

From here the ^{240}Pu effective mass is expressed as:

$$^{240}Pu_{Eff} = \frac{D \times C_f}{R_{SENS}} \qquad \text{Eq. 4.4.3 [4]}$$

Where,

$$\mathrm{C_f} = \frac{1}{\mathrm{M}r} \qquad \text{Eq. 4.4.4 [4]}$$

4.5. Offline PuF_4 Correction using the Totals Count Rate and also Incorporating Correction using the Krick-Ensslin Derived M Value

As the standard fluoride correction technique (described in Section 4.3) did not correct for self-multiplication the result was slightly overestimated for high Pu mass samples. An additional calculation was therefore added, which corrected the fluoride technique for the effect of self-multiplication using an estimate determined from the calculations performed in the Krick-Ensslin technique. As the fluoride assay result is based on the total neutron count rate, the degree of correction was small (<~10%). This result was produced for comparison with the results from the standard fluoride correction and the Krick-Ensslin correction techniques.

4.6. Offline Determination of the Uranium Mass

For the residue measurements there was a requirement to report the total uranium mass for accountancy purposes in addition to the ^{235}U mass content. The PPAM system has a simplified ability to report an indicative ^{235}U mass value if a significant 185.7 keV peak is measured. However, this technique takes no account of gamma ray attenuation and is therefore not considered to be accurate. As such a technique based on the PuF_4 correction method was developed.

This technique used the magnitude of the 1001 keV peak characteristic of ^{238}U decay and compared it to the 414 keV ^{239}Pu peak to determine the ^{238}U/^{239}Pu ratio. As in the fluoride correction techniques, correction was applied for the effect of attenuation in the residue material (using the 345 keV to 414 keV peak ratio). The ^{239}Pu mass of the sample was obtained from the calculated plutonium mass and the isotopic composition, which was then multiplied by the ratio of ^{238}U/^{239}Pu to determine the ^{238}U mass:

$$R_{U235} = \frac{186keVCountRate}{414keVCountRate} \cdot NuclearData \cdot DetectionEfficiencyRatios \quad \text{Eq. 4.6.1}$$

$$R_{U238} = \frac{1001keVCountRate}{414keVCountRate} \cdot NuclearData \cdot DetectionEfficiencyRatios \quad \text{Eq. 4.6.2}$$

If a 185.7 keV peak was measured, the ^{235}U mass was determined directly using the same methodology as for ^{238}U, again accounting for the effect of attenuation in the matrix. If no 185.7 keV peak was measured, natural uranium enrichment of 0.7% was assumed.

5. Results

5.1 Example Residue Container Measurement Result

For each container, the results from each measurement technique described above were compared. The example shown below in Table 1 was a high mass PuF_4 Residue container. In this example, the necessity of the application of the PuF_4 correction is evident as the results obtained using the PPAM (calculated offline) and the Revised Calibration are unphysically high.

In the case of high PuF_4 residues, the effect of the PuF_4 correction technique can be very significant. For example, in the case shown in Table 1, when using the α value of 63 calculated by the PuF_4 technique, the Krick-Ensslin technique calculates an M value of 1.036 and hence using the equations presented in section 4.4, calculates a Doubles rate correction factor (C_f) of approximately 0.15, indicating that 85% of the measured Doubles signal came from induced rather than spontaneous fission. This clearly highlights the fact that the standard PNCC technique used by the PPAM (and the Revised Calibration) which assumes negligible self-multiplication was not suitable for assay of these high PuF_4 containers.

For this particular container, the assay result from the PuF_4 technique with no correction for self-multiplication (i.e. making the assumption that M=1) was assigned as the Accountancy Pu mass of the item. This slightly more pessimistic result was chosen in this case because the total neutron count rate was on the limit of the tested range.

	Pu Accountancy Mass (g)	Overall Uncertainty (g) (1σ)	Nuclear Safety Mass (g)
PPAM System	Outside certified range[1]	Outside certified range	Outside certified range
Offline Recalculation	44,788.5	19,141.8	102,213.8
Revised Calibration	3,273.1	6,220.1	21,933.5
PuF_4 Technique with no correction for M	588.6	84.7	842.7
Krick-Ensslin with α from PuF_4	581.4	95.8	Method not used for Nuclear Safety Mass
PuF_4 correction with Krick-Ensslin derived M	568.4	81.8	Method not used for Nuclear Safety Mass

Table 1: Example Results Table Reported following Offline Analysis for a Residue Container.

[1] The PPAM system will not quote a measurement result over 999 g as this is outside the certified range and so instead reports a fault. The measurement data is saved and is analysed offline.

The selection of the attenuating matrix for the PuF_4 correction was determined by the comparison of the different PuF_4 calculation methods and by establishing an estimate of the thickness of attenuating material required to yield the observed peak intensity ratios. The relationship between the PuF_4 fraction reported for the different methods will vary with the selection of attenuating matrix material as they depend on different peak energies (Methods 1-3 use the 583 keV peak, whereas Method 4 uses the 891 keV peak and Method 6 uses 1274 keV peak). The effect of the selection of the different matrices is evident from Figure 5 where Fe has been used as the attenuating matrix and Figure 6, where PuO_2 was the matrix material. Figure 6 shows that the PuF_4 ratios vary widely and reports a PuF_4 fraction of 94.25 %, suggesting a poorly suited matrix. This is in contrast to Figure 5 where the ratios are more closely aligned and reports a PuF_4 fraction of 62.22%, demonstrating the importance of assigning an appropriate attenuating matrix material.

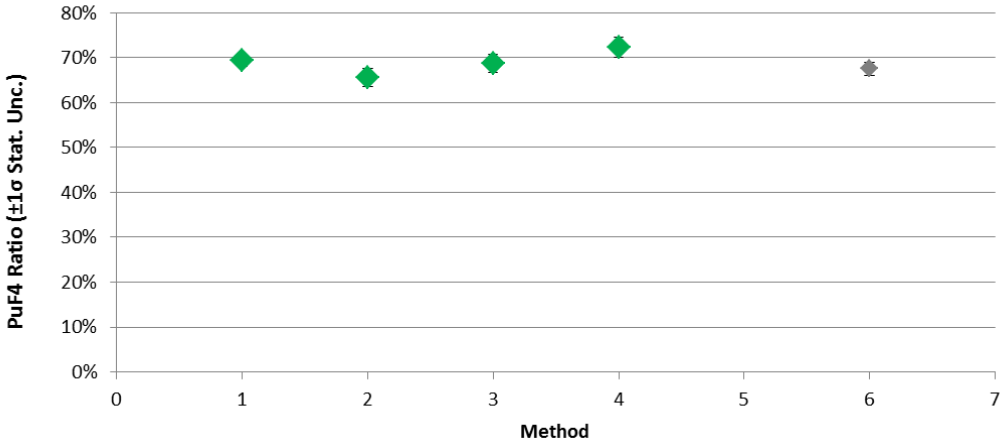

Figure 5: Comparison of PuF_4 Ratios for an Attenuating Matrix Material of Fe. PuF_4 fraction calculated as 67.6%.

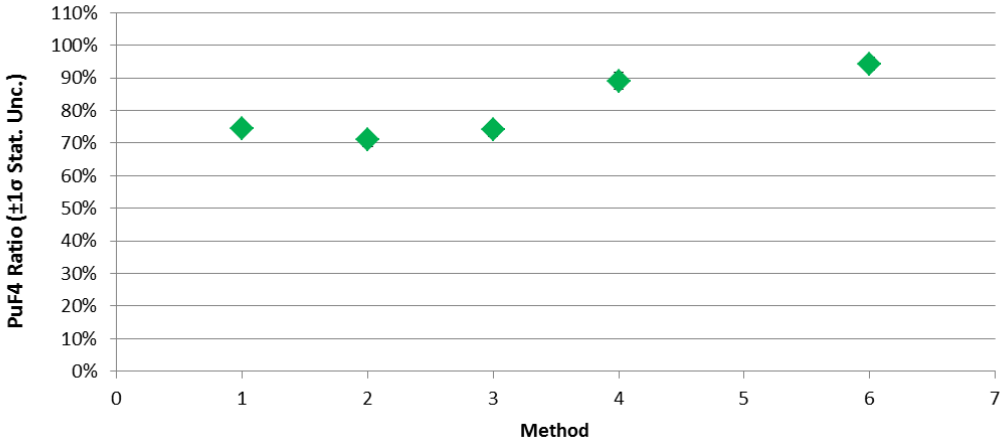

Figure 6: Comparison of PuF_4 Ratios for an Attenuating Matrix of PuO_2. PuF_4 fraction calculated as 94.25%.

5.2 Overall Summary of Results

The offline analysis was successfully applied to determine an Accountancy mass for each Residue container and both Nuclear Safety and Accountancy masses for each Dross bottle.

Four main techniques were found to be applicable for the containers (see Figure 7). The main method of analysis for the Dross bottles and the MOX Residue containers was the Revised Calibration, whilst for the Fluoride containing Residues, either the PuF_4 correction technique, or the PuF_4 correction technique with correction for M derived from the Krick-Ensslin method was applied.

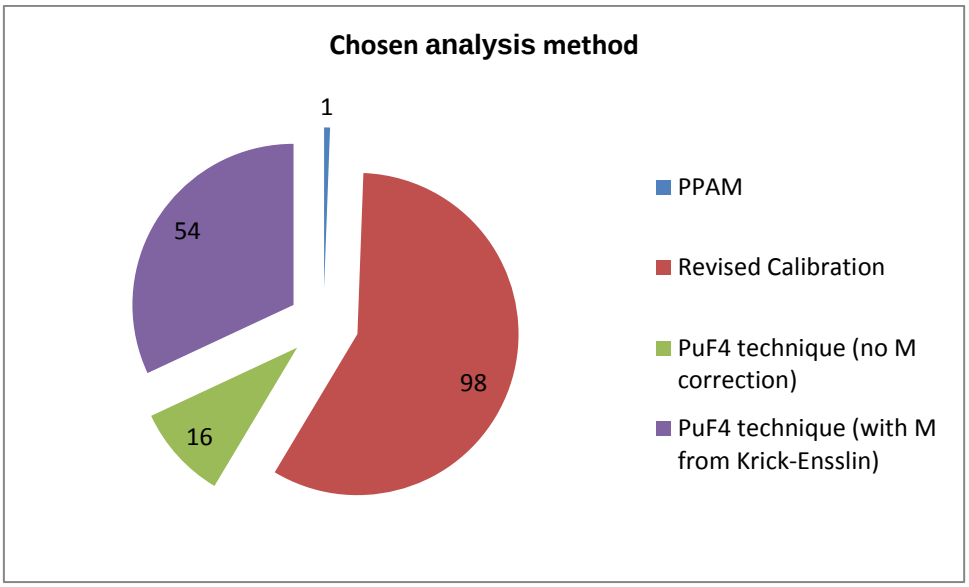

Figure 7: Chosen Analysis Method for the Dross and Residue Containers (Number of Containers or Bottles Measured Indicated).

The effectiveness of the measurement techniques is demonstrated in Figure 8 below. For the PuF_4 and MOX residues, it can be seen that the assay reported Accountancy Pu masses are significantly lower than both the net mass of the Residue and the expected Pu content of the Residues based on previous theoretical studies. For the PuF_4 Residues, the total Accountancy Pu mass from assay was only 58% of the expected value, and 77% for the MOX residues. Likewise for the Dross bottles, the Accountancy Pu mass is only a fraction of the net Residue mass.

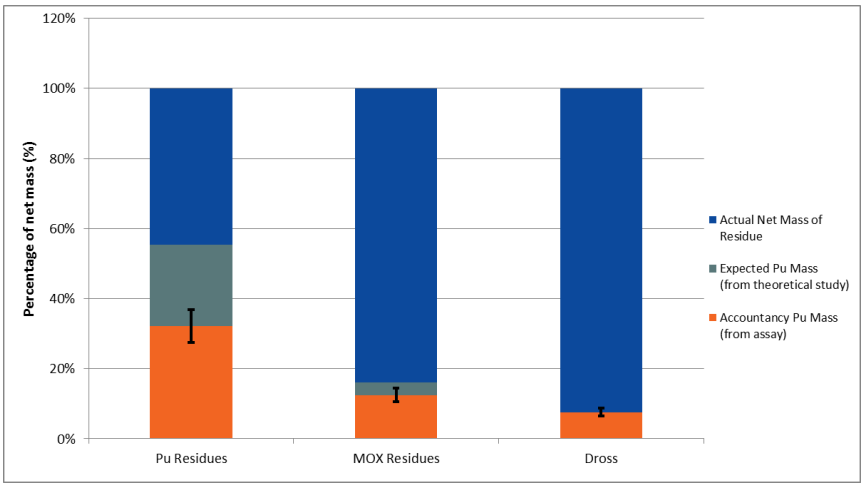

Figure 8: Showing Estimated and Measured Plutonium Mass as a Percentage of the Net Residue Mass.

6. Conclusions

The measurement of the Residue containers was technically challenging, requiring the development of multiple analysis techniques in order to account for high neutron emissions in challenging matrices. A toolbox of measurement techniques was developed such that the measurement of each container could be customised for its own properties, accounting for induced neutron emissions, or self-multiplication.

The PuF_4 technique facilitated measurement of containers with significant PuF_4 content. Had only the existing PPAM technique been applied, these would have resulted in unphysical results (i.e. the PuF_4

technique reported on average only 6% of the Pu Accountancy value determined using the PPAM technique). The same technique was also then extended to give accurate values for the ^{235}U and ^{238}U masses, which were required for Safeguards purposes.

The RRP saw each Residue container and Dross bottle successfully assigned an Accountancy mass and each Dross container assigned a Nuclear Safety mass. This enabled the export of the Residue containers to a long-term engineered store, reducing the radiological hazard. Furthermore, all Dross bottles measured were consigned as PCM waste, with a number of residue containers also identified as actually containing Dross material and consigned as PCM waste, which was a substantial cost-saving to Sellafield Ltd in terms of future waste processing cost. This project was achieved by modifying existing equipment in order to extend its calibrated measurement range and applying an innovative technique to allow accurate assay of large plutonium masses and high neutron emissions.

The benefits of providing accurate Accountancy masses are two-fold, both in terms of providing accurate data for Safeguards purposes and in enabling future decommissioning projects to make educated decisions on the basis of the true Pu masses present, rather than on the basis of Pu masses from conservative desktop technical studies.

8. References

1. *"Application Guide to Neutron Multiplicity Counting",* LA-13422-M, LANL, N Ensslin et al, November 1998.
2. *"The determination of the isotopic composition of plutonium by gamma-ray spectrometry",* Atomic Energy Estab. Report, AERE-R 8737, M Banham, 1977.
3. *"The application of offline analysis techniques to PCM monitor results to aid the efficient and cost effective repackaging of legacy PCM wastes containing calcium and potentially plutonium fluoride",* ICEM'09 -16034, D.J. Thornley et al., Oct 2009.
4. *"Passive Non-destructive Assay of Nuclear Materials",* LA-UR-90-732, LANL, D Reilly et al, March 1991.

Particle Swarm Imaging (PSIM) – A swarming algorithm for the reporting of robust, optimal measurement uncertainties

Dan Parvin, Sean Clarke

Cavendish Nuclear
Sellafield, Seascale, Cumbria, United Kingdom
E-mail: dan.parvin@cavendishnuclear.com, sean.clarke@cavendishnuclear.com

Abstract:

Particle Swarm Imaging (PSIM) is an innovative technique developed by Cavendish Nuclear used to enhance quantitative gamma-ray assay[1]. The innovation overcomes some of the challenges associated with the accurate declaration of measurement uncertainties of radionuclide inventories within waste items when the distribution of activity is unknown. Implementation requires minimal equipment, making use of gamma-ray measurements taken from different locations around the waste item, using only a single electrically cooled HRGS gamma-ray detector for objects up to a UK ISO freight container in size.

The PSIM technique iteratively 'homes-in' on the true location of activity concentrations in waste items. PSIM differs from conventional assay techniques by allowing only viable solutions - that is those that could actually give rise to the measured data - to be considered. Thus PSIM avoids the major drawback of conventional analyses, namely, the adoption of unrealistic assumptions about the activity distribution that inevitably leads to the declaration of pessimistic (and in some cases optimistic) activity estimates and uncertainties.

PSIM applies an optimisation technique based upon 'particle swarming' methods to determine a set of candidate solutions within a 'search space' defined by the interior volume of a waste item.

The positions and activities of the swarm are used in conjunction with a mathematical model to simulate the measurement response for the current swarm location. The swarm is iteratively updated (with modified positions and activities) until a match with sufficient quality is obtained between the simulated and actual measurement data. This process is repeated to build up a distribution of candidate solutions, which is subsequently analysed to calculate a measurement result and uncertainty along with a visual image of the activity distribution.

This paper provides examples of PSIM's ability to significantly reduce the levels of pessimism inherent in reported uncertainties.

Keywords: PSIM, Imaging, Non-destructive assay

1. Introduction

Cavendish Nuclear has over 50 years of experience in the development, delivery and operation of non-destructive assay systems both in the UK and internationally. As part of the on-going development and innovation strategy, a review of the existing technologies was performed with the aim of developing new and novel measurement techniques.

The concept of Particle Swarm Imaging (PSIM) was developed as part of this process, being driven by the increasing demand for novel techniques with improved levels of accuracy and performance whilst keeping the cost and complexity of measurement systems to a minimum.

[1] *In 2014 PSIM was the winner of the Sellafield Ltd. Supply Chain Awards for "Supply Chain Innovation – Large Supplier"*

2. Particle Swarm Imaging (PSIM)

To illustrate the concept of PSIM consider a measurement geometry comprising of an arbitrary volume (referred to as the 'search space') containing n point sources of activity, with each point source possessing an activity A_n. Consider the deployment of M detectors around the waste item (or alternatively M measurements using the same detector at M different positions) and let each individual point source have a detection efficiency with respect to each detector. The goal of the measurement is to determine the total activity within the search space. A schematic of the measurement arrangement is shown in Fig. 1.

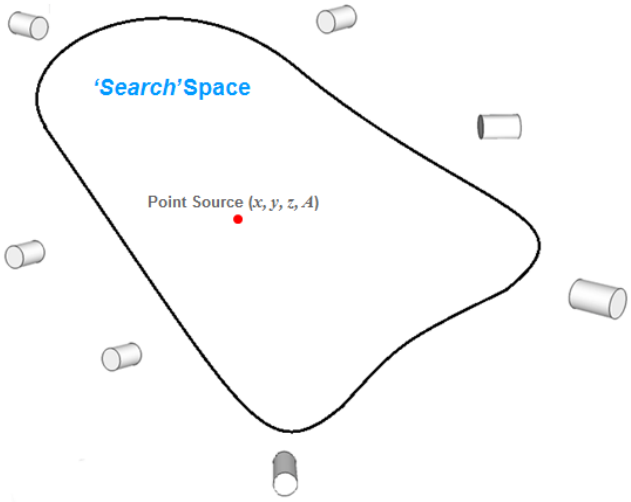

Figure 1: Measurement geometry containing point sources of activity which are constrained to lie within a 3-dimensional 'search space' such as the interior volume of a drum or box, the surfaces of a wall, interior of a glovebox etc.

Unlike many conventional assay techniques PSIM makes use of the information contained within each of the individual measurements taken around the search space shown in Fig. 1. The count rates measured at each of the M measurement positions must be dependent upon the position and activity of each source within the search space. Representing the source distribution as a sequence of source activities at discrete locations (x, y, z), the measured count rates may be written

$$\begin{aligned} C_1 &= A_1\varepsilon_{1,1} + A_2\varepsilon_{1,2} + \ldots A_n\varepsilon_{1,n} \\ &\vdots \\ C_M &= A_1\varepsilon_{M,1} + A_2\varepsilon_{M,2} + \ldots A_n\varepsilon_{M,n} \end{aligned} \qquad \text{Eq. (1)}$$

where:

C_i = count rate measured at position i = 1 to M

A_j = activity of source j

$\varepsilon_{i,j}(x, y, z)$ = detection efficiency of point source j at measurement position i

Although the number of point sources, activities and positions required to solve (Eq. 1) explicitly are not known, it is possible nevertheless to evaluate the 'quality' of the agreement between the count rates produced from any 'potential' distribution of activity within the search space and the actual count rates measured.

The PSIM approach initialises a 'swarm' of solutions within the search space. Representing the unknown point source activities and their positions as a vector $\mathbf{p}$ then the objective is to minimise

$$minimise: \sum_{i=1}^{M}\left[C_i - \hat{C}(\mathbf{p})_i\right]^2 \quad \text{Eq. (2)}$$

where:

$\hat{C}(\mathbf{p})_i$ = count rates due to the activity within the search space at measurement position i

The positions and activities of the swarm are used in conjunction with a mathematical model describing the measurement geometry to simulate the measurement response for the current swarm location. The swarm is iteratively updated (with modified positions and activities) until a match with sufficient quality is obtained between the simulated and actual measurement data i.e. until a solution to Eq. (2) is found. This process is repeated to build up a distribution of candidate solutions, which is subsequently analysed to calculate a measurement result and uncertainty along with a visual image of the activity distribution, a typical example of which is shown in Fig. 2.

The benefit of this approach is that only viable solutions - that is those that could actually give rise to the measured data - are considered. And this, in turn, facilitates accurate quantification of total activity and activity distribution.

PSIM avoids the major drawback of conventional analyses, namely, the adoption of unrealistic assumptions about the activity distribution that can lead to the declaration of pessimistic, or in many cases optimistic, activity estimates and uncertainties.

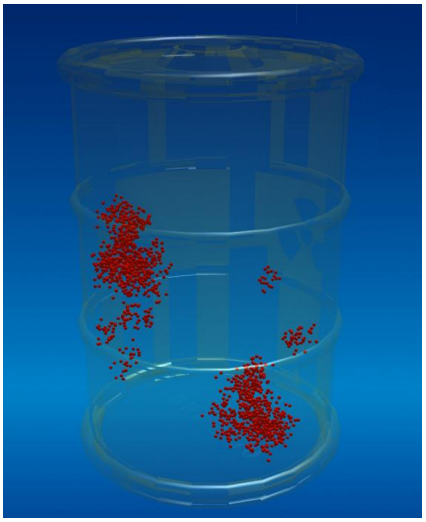

Figure 2: Example of PSIM image of the activity distribution within a 200 litre drum

2.1. Swarming Concept

Particle Swarming is a computational method that optimizes a problem by iteratively trying to improve a candidate solution with regard to a given measure of quality, see Eq. (2). The particle swarming approach used by PSIM is a hybrid of the 'Particle Swarm Optimisation' or PSO approach originally attributed to Kennedy, Eberhart, Ref. [1] and 'Artificial Bee Colony Optimisation' or ABC attributed to D. Karaboga, B. Basturk, Ref. [2].

The PSIM algorithm works by having a population (called a swarm) of candidate solutions (called particles). Each particle is assigned an activity value and position within the search space (for example the volume of a waste drum). The particles are moved around in the search space according to a few simple formulae. The movements of the particles are guided by their own best known position in the search space as well as the entire swarm's best known position. When improved positions are discovered these will then guide the movements of the swarm. The process is repeated until a match of sufficient quality is obtained with the measurement data.

Having established a good 'match' to the measurement data the swarm is allowed to evolve (either explore, expand or contract) seeking other candidate solutions that also produce a good 'match' to the measured data. Over time the swarm effectively searches the entire search space (exploration) producing a distribution of solutions from which the final activity result and associated uncertainties are derived.

The swarming pseudo - algorithm is shown in Fig. 3.

It is important to note that no assumption as to the physical size (number of particles) within the swarm is made as the swarm is able to adjust its size as necessary throughout its lifetime.

Furthermore the approach does not seek a 'global' minimum (i.e. a single 'best' solution) as it not possible to find a unique solution to most measurement scenarios. In reality there are many solutions that will match the measurement data, all of which will be equally valid.

However over the lifetime of the swarm, regions of 'preferred' space result, leading to regions where the solution density is higher. Regions of high solution density therefore correspond to the most likely position of the activity within the search space.

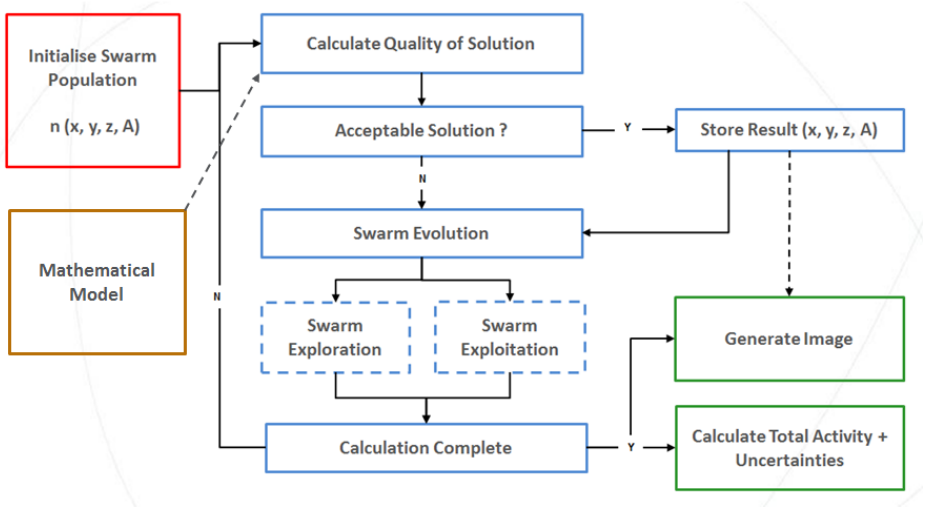

Figure 3: PSIM algorithm

2.2. Mathematical Model and Calibration

The distribution of activity within the search space can be represented as a sequence of point sources at discrete locations, producing count rates described by (Eq. 1). To calculate the count rates at the measurement positions we require a model that calculates the efficiencies for each point source of activity within the swarm. If the efficiencies are known then the count rates at the detector positions can be evaluated.

The PSIM model is defined firstly by a series of quadric surfaces which define the measurement geometry. A quadric surface is represented by the following expression:

$$Ax^2 + By^2 + Cz^2 + Dxy + Exz + Fyz + Gx + Hy + Iz + J = 0 \qquad \text{Eq. (3)}$$

where $A, \ldots, J$ are constants.

This notation allows the user to specify complex geometries including shapes that can be constructed from multiple planes, spheres, cylinders, cones etc. In addition to the surfaces that make up the measurement geometry it is necessary to define the cells within the geometry. Each cell is defined by a series of 'senses' with respect to each surface which uniquely defines the spatial extent of the cell volume within the measurement geometry. Each cell must be assigned a material density and mass attenuation coefficient appropriate to the gamma-ray of interest.

The PSIM model does not use pre-defined 'template' geometries instead specifying the geometry by a series of quadric surfaces providing the user with greater flexibility to specify more representative and complex geometries.

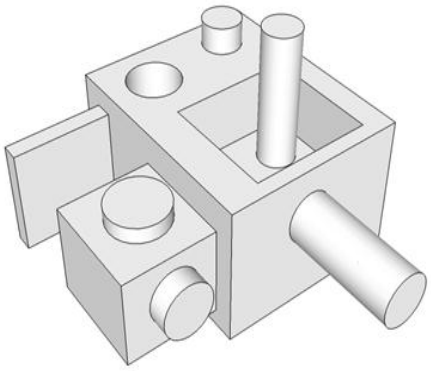

Figure 4: Complex geometries can be modelled by PSIM

'Source' cells are identified within the PSIM model. Only these cells are permitted to contain sources of activity (an example of a 'source' cell would be the matrix within a drum or a vessel within a glovebox). This definition ensures that the swarm does not explore regions of the geometry within which no activity can exist. There is no restriction on the number of source cells allowing complex geometries to be considered (an example may be the measurement of multiple waste items within a room, a scenario which may be difficult to interpret using only pre-defined geometries due to the measurement cross-talk between individual objects and the measurement positions).

The PSIM model is completed by defining the locations at which the measurements were performed as well as the detector response. The measurement positions are simply defined by the central co-ordinates of the front face of the detector within the measurement geometry. The orientation of the detector with respect to the search space is defined by the normal vector perpendicular to the front surface of the detector. The detector response is pre-calibrated as a function of the incident gamma-ray energy. This detector calibration is the only model parameter that requires any pre-calibration prior to performing a measurement.

2.3. Percentile Uncertainty Reporting

The PSIM model is used to calculate the count rates at each measurement position for the current swarm position, and the fit 'quality' of the count rates is compared to the measured data. If the quality of the solution is 'acceptable' then the solution is archived (this then becomes a 'candidate' solution).

Before continuing with the PSIM analysis, the model can be perturbed (i.e. the cell densities, material types, efficiency of the detector, detector positions and measured count rates are all sampled) before the analysis resumes. Thus PSIM is able to incorporate the effects of uncertainty components associated with the model and measurement data into the final result.

Having established a good 'match' to the measurement data the swarm is allowed to evolve (either by exploration or exploitation) seeking other candidate solutions that also produce a good 'match' to the measured data. Over time the swarm effectively searches the entire search space producing many candidate solutions. The PSIM analysis is terminated once the required number of candidate solutions has been exceeded (a typical PSIM analysis will be configured for a total of 2000 - 3000 candidate solutions before a result is generated).

On completion of the analysis a frequency histogram is produced showing the distribution of the total activity (i.e. the sum of the activities of each point source or particle) for each candidate solution. It is from this histogram that the final activity result and associated uncertainties are derived – see Fig. 5.

The activity results and uncertainties calculated by PSIM are based on a 'percentile' methodology. This method of confidence level reporting is ideally suited to PSIM because the set of activity solutions stored by PSIM are rarely normally distributed. In most cases the PSIM frequency histogram of solutions is skewed and contains important information that should be included when reporting robust measurement uncertainties.

To illustrate the percentile method employed by PSIM, consider Fig. 5, which shows a typical normalised frequency histogram constructed from a set of candidate solutions. A percentile is a measure used in statistics indicating the value below which a given percentage of observations in a group of observations (or PSIM solutions) fall. For example, the 20th percentile is the value below which 20% of the PSIM solutions may be found and the 90th percentile is the value above which 10% of the PSIM solutions would be found.

Suppose the histogram comprises 1000 different candidate solutions. After ranking the total activities from smallest to largest, let the values be denoted by $(A_1, A_2, \ldots, A_{1000})$. If we choose to report uncertainties at the 95% confidence interval, then the minimum and maximum activity values would therefore be $[A_{25}, A_{1975}]$ corresponding to the upper and lower 2.5% of solutions taken from each end of the distribution. Here A_{25} represents the lower activity value at 95% confidence and A_{1975} the upper activity value at 95% confidence (see both vertical lines shown in Fig. 5).

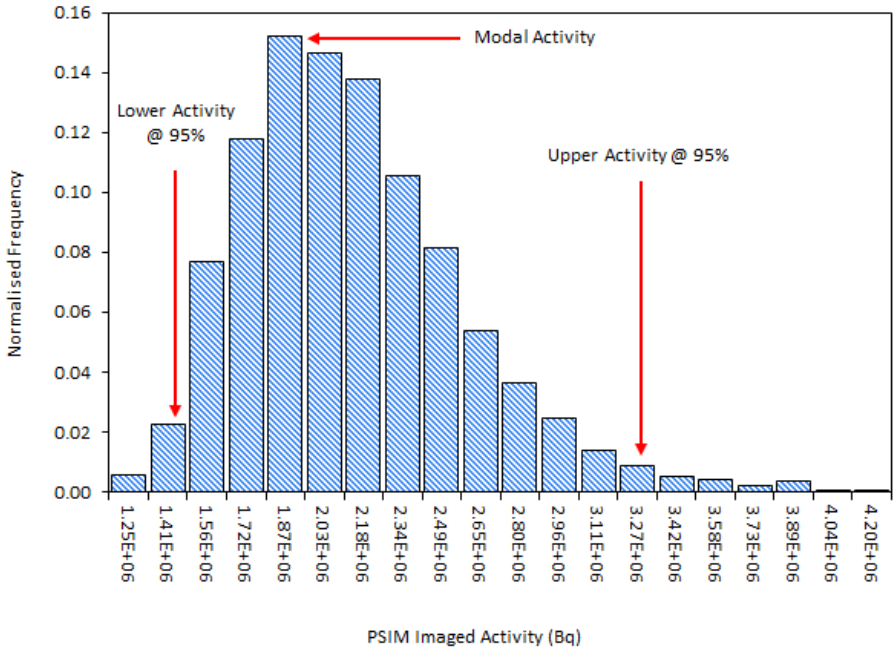

Figure 5: PSIM Imaged (total) activity frequency histogram

The PSIM 'best estimate' activity is usually reported as the modal value of the histogram, but other alternatives include the median or average value.

2.4. 'Hotspot' Imaging

This section presents examples of PSIM's ability to image the location of activity within a defined 3D search space; other examples are provided in Ref. [3]. This simulated example considers a 200 litre drum containing 2 x 1 MBq 'hotspots' of Cs-137 activity (the search space is defined as the interior volume of the drum consisting of concrete at a density of 1.2 g/cc). Two measurement scenarios are considered as shown in Fig. 6. The first considers 8 discrete measurements performed at the drum mid-height as shown in the left figure and the second a total of 8 discrete measurements taken at two different heights as shown in the right figure.

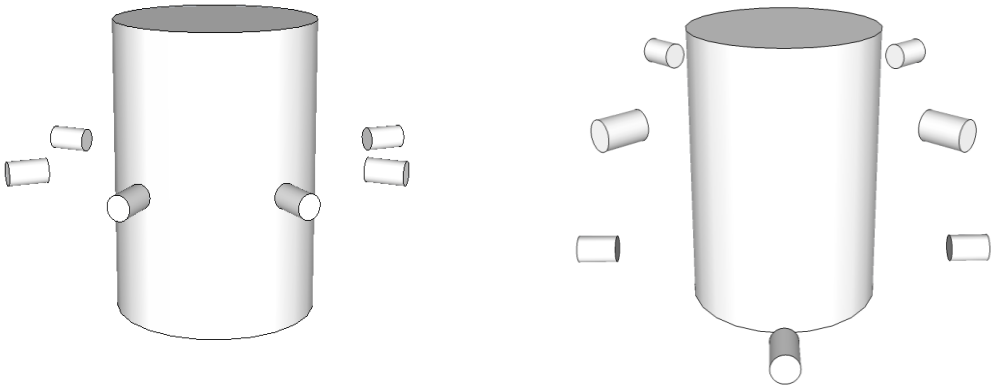

Figure 6: Detector deployments for PSIM imaging examples. Scenario #1 consists of 8 measurements at the drum mid-height (left) and Scenario #2 a total of 8 discrete measurements taken at two heights (right)

Fig. 7 shows a visual representation of the evolution of the swarm for Scenario #1. The bottom figure shows the final PSIM solution and the actual locations of the two hotspots of activity.

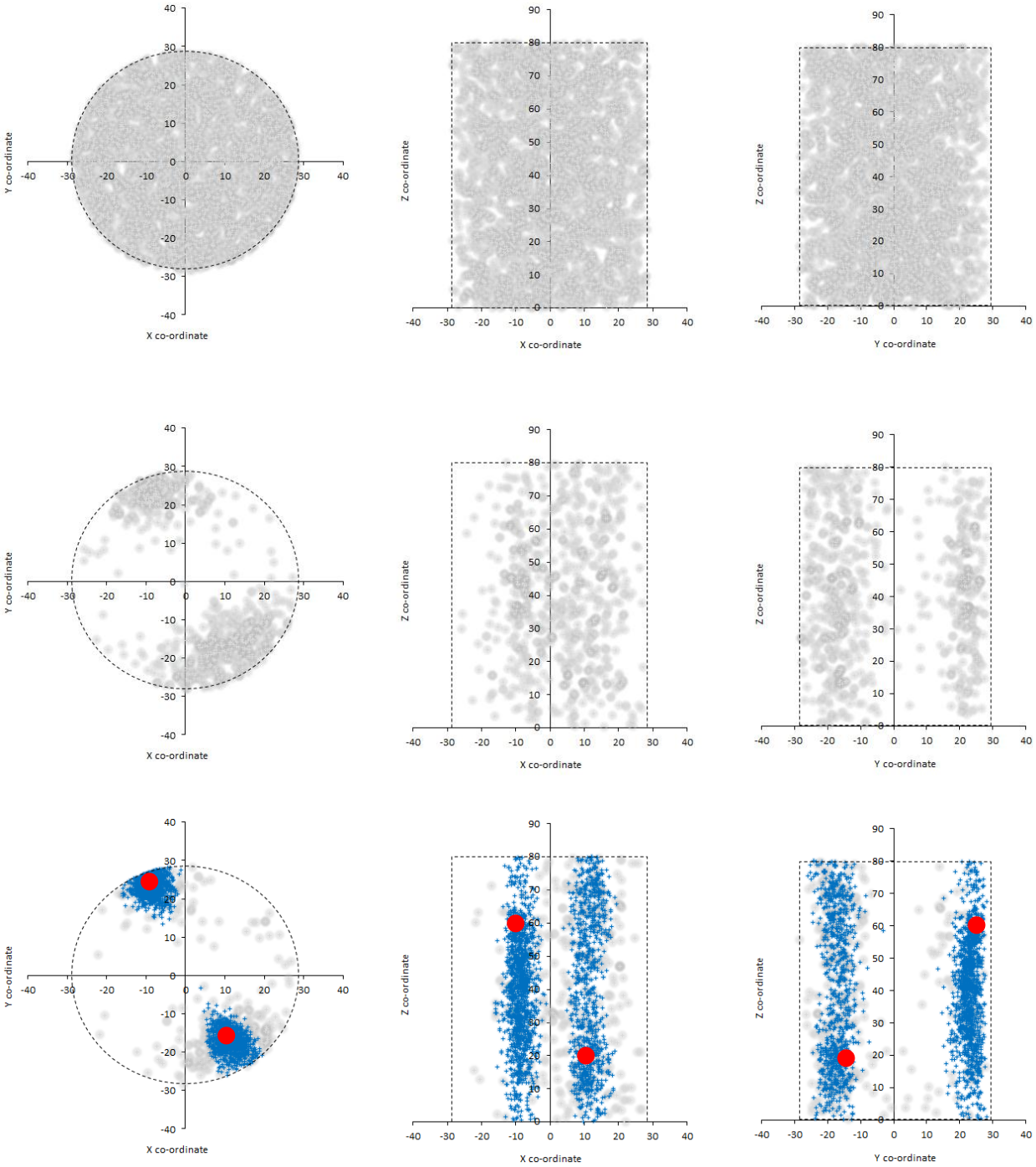

Figure 7: PSIM images for Scenario #1. The top figure shows the initial random swarm configuration. The middle figure shows the swarm after approximately 500 iterations. The bottom figure shows the final PSIM solution along with the actual location (red markers) of the two hotspots of activity within the drum. The data shown in blue represents locations within the drum contributing most to the overall 'quality' of the PSIM solution and represents therefore the most probable location of any activity within the drum.

The lack of height information associated with Scenario #1 (i.e. all the measurement positions are at the same height) is reflected in the image shown in Figure 7, showing solutions extending along the full height of the drum.

This should be compared to the PSIM image result for Scenario #2 shown in Fig. 8. The addition of height information into the PSIM solution allows the two hotspot positions to be correctly resolved into the top and bottom regions of the drum.

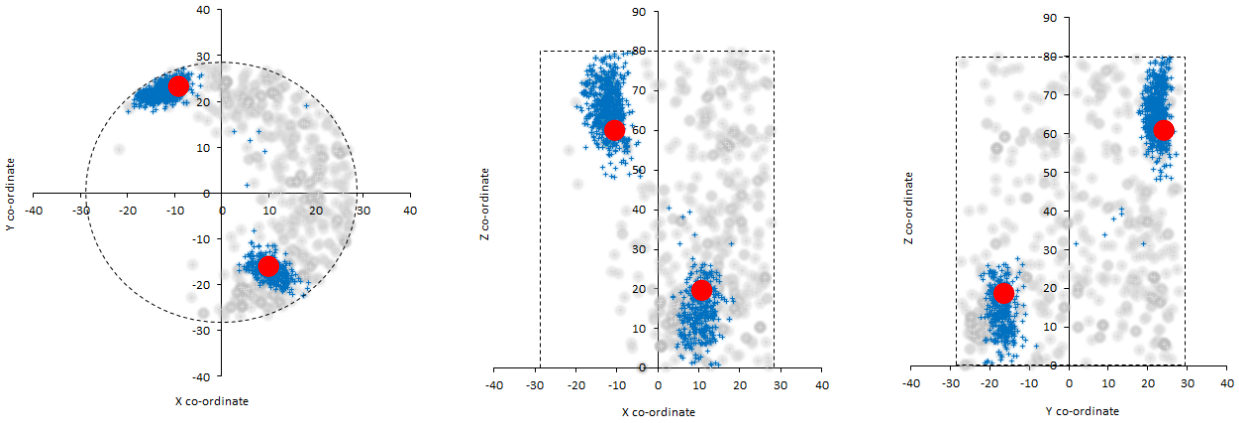

Figure 8: Final PSIM images for Scenario #2.

Fig. 9 shows the activity results returned by PSIM compared with those determined using more conventional analysis methods. In the conventional analysis method the calibration assumes the activity is 'uniformly' distributed throughout the drum volume, uses the sum of the count rates at each of the eight measurement positions, and the uncertainties are expressed at the 95% confidence intervals based on the assumption that any activity present has the potential to exist as a single point source located anywhere within the drum.

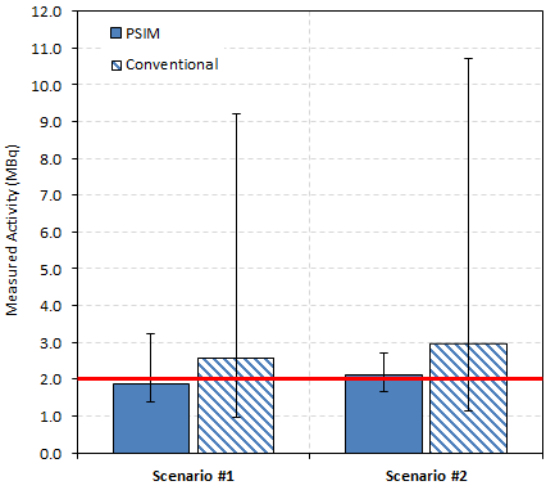

Figure 9: Comparison of PSIM and conventional analysis results for measurement Scenario #1 and Scenario #2 (note that the true activity within the drum is indicated by the solid red line and the uncertainties shown are at the 95% level of confidence generated using the percentile method described in Section 2.3)

In terms of accuracy, the best estimate PSIM value is closer to the true value because it has imaged the actual location of the activity. In terms of uncertainty, PSIM only considers those solutions that could have given rise to the count rates at the measurement positions and therefore avoids the major drawback of conventional analyses, namely, the adoption of unrealistic assumptions about the activity distribution that can lead to the declaration of pessimistic, or in some cases optimistic, uncertainty estimates. Both these facilitate accurate quantification of total activity and robust uncertainty declarations. The PSIM uncertainties are significantly smaller and the additional height information in Scenario #2 leads to a smaller uncertainty component than Scenario #1.

2.5. Dispersed Source Imaging

Waste items will not always contain discrete hotspots of activity, but rather multiple sources distributed in a random fashion throughout the waste volume. To compare the performance of PSIM in these circumstances against more conventional analysis methods a simulated trial was performed comparing the PSIM measurement uncertainties against those obtained using a conventional analysis approach.

The trial randomly located between 1 and 10 point sources within a 200 litre drum containing concrete having a bulk density of 1.2 g/cc. The measurement geometry used was that shown in Fig.6 (left). A total of 1,700 random trials were performed.

The conventional analysis is calibrated to assume the activity is 'uniformly' distributed throughout the drum volume, uses the sum of the count rates at each of the eight measurement positions, and the uncertainties are expressed at the 95% confidence intervals based on the assumption that any activity present has the potential to exist as a single point source located anywhere within the drum.

In contrast, the PSIM analysis makes no prior assumption as to the distribution of activity within the drum (i.e. no calibration is assumed prior to the measurement) and only required the generation of a model to reflect the measurement geometry.

Fig. 10 shows the results of the trial, comparing the uncertainties output by PSIM against those obtained from the conventional analysis approach described above. The uncertainty ratio shown equals the 95% upper uncertainty on the activity divided by the true activity within the drum. Thus ratio values greater than one would be expected in all cases. The PSIM uncertainty ratios have been sorted in order of increasing value and then plotted against the corresponding conventional value.

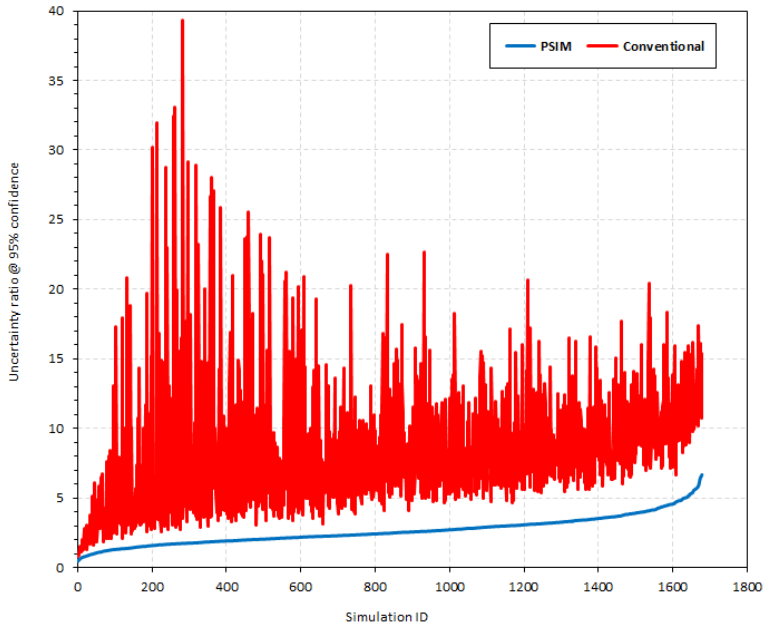

Figure 10: Comparison of PSIM and Conventional analysis methods. The uncertainty ratio shown equals the 95% upper uncertainty calculated using both analysis methods divided by the true activity within the drum.

The result of the trial clearly demonstrates that the uncertainty ratios generated by PSIM are in every case less than those generated using the conventional analysis. For only a few cases is the uncertainty ratio less than unity and these represent 2.5% of the total trials performed and therefore entirely consistent with the confidence level of 95% chosen.

The PSIM uncertainties are on average approximately three times smaller (the average uncertainty ratio for the PSIM data being 2.6 compared to a value of 8.2 for the conventional analysis results).

Because PSIM only considers those solutions that could have given rise to the count rates actually measured it avoids the overly pessimistic uncertainty estimates seen in the conventional results.

3. PSIM Projects (United Kingdom)

PSIM has been used by Cavendish Nuclear to perform measurements at nuclear facilities across the United Kingdom to confirm the suitability of waste to be consigned to LLWR and ILW and VLLW waste disposal and treatment facilities to support waste hierarchy re-categorisation. The PSIM technique has been used successfully for both characterisation and verification monitoring, including in-situ HRGS assay of a wide range of waste streams, waste item types and radionuclide species.

Recent projects include:

- VLLW bagged combustible wastes, for Sellafield / Environment Agency
- Legacy waste vault characterisation, for Sellafield
- Over 70 VLLW and LLW Isofreight containers, for LLWR / Sellafield / Environment Agency
- Drummed waste arising from low active drain operations, Sellafield
- Drummed wastes at other UK-wide nuclear sites such as Magnox Trawsfynydd, EDF Hunterston and EDF Heysham (ILW – containing concrete-shielding legacy wastes, VLLW and LA-LLW – containing asbestos and PPE, LLW – containing pond reactor and laundry waste, LLW – containing redundant plant and PPE)
- Multi-element bottles (MEBs) and other large metallic items prior to recycling at Studsvik.

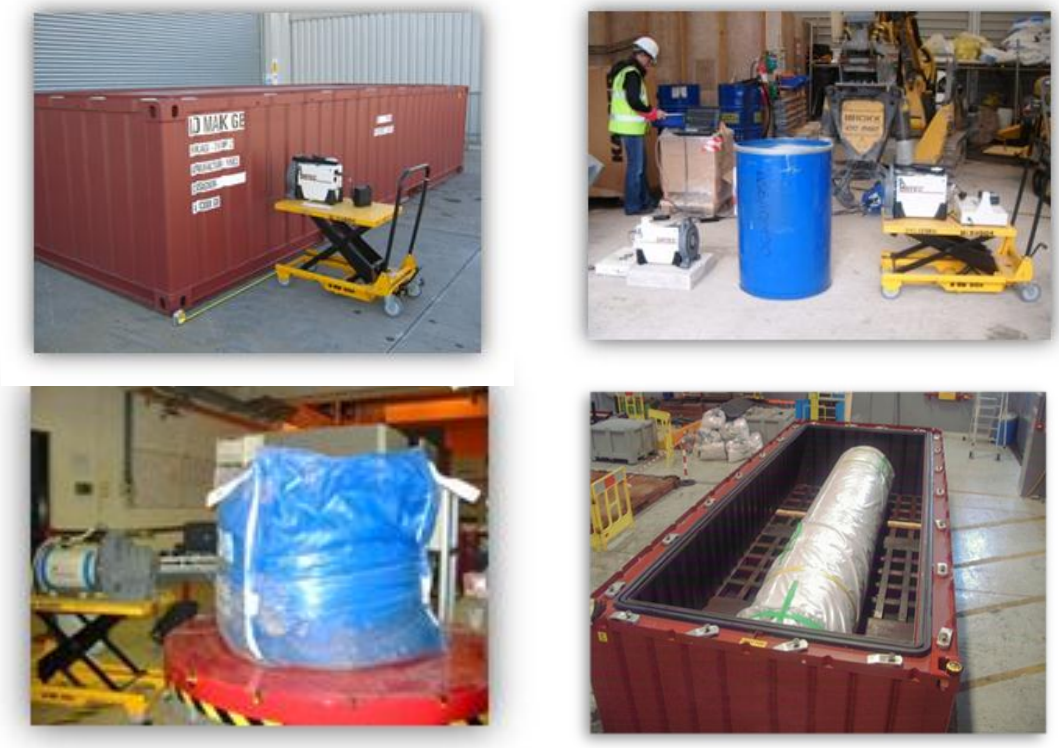

Figure 11: PSIM measurements performed at various sites in the UK

4. Future Developments – Neutron Swarm Imaging (NSIM)

PSIM is equally applicable to the assay of neutron emitting material such as plutonium (stored in waste drums, crates etc.) as well as monitoring and verification of material in process plant such as gloveboxes.

Whilst the modelling required to determine the response of the swarm is more complex, the algorithm shown in Fig. 3 is readily adapted to neutron based measurements. In fact neutron based measurements benefit from producing both totals and reals (coincidence) count rates, therefore providing the swarm with more information for use in the optimisation process.

Fig. 12 shows the module mapping between PSIM and NSIM.

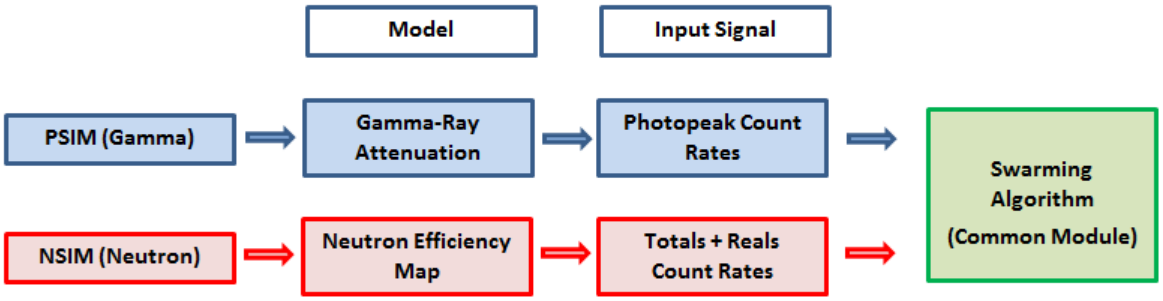

Figure 12: Module mapping between current PSIM algorithm and NSIM (Neutron Swarm Imaging)

As well as imaging the location of neutron emitting material, Cavendish Nuclear is currently developing methods for including both alpha (the ratio of (α, n) to spontaneous fission neutrons) and neutron multiplication as additional swarming variables in the solution eliminating the requirement to know or make assumptions for their values.

MCNP modelling is being used to test and validate the development of the NSIM algorithms. Fig. 13 (left) shows a 3D visual of a glovebox surrounded by 18 polythene moderated He-3 neutron detectors containing three process vessels as shown in the right hand figure.

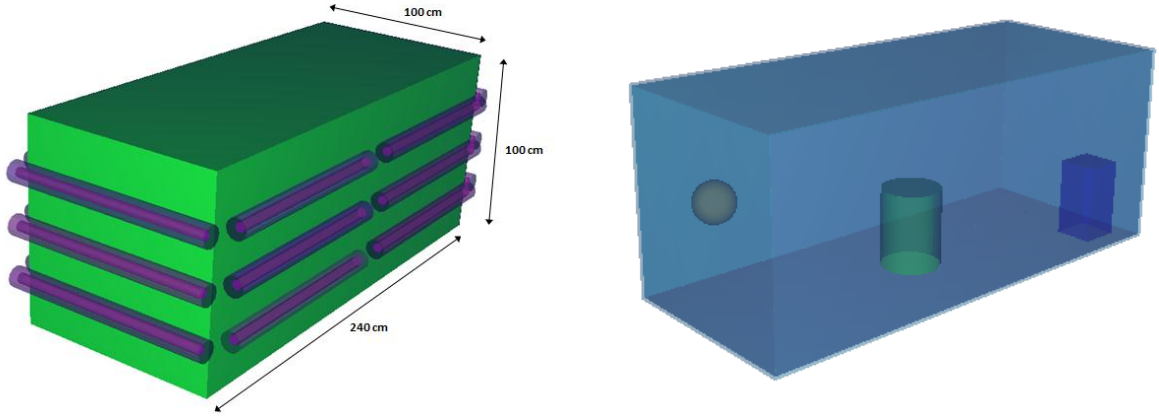

Figure 13: Example of an MCNP model used to validate the development of NSIM

The 3D schematic shown in Fig.14 is an example of NSIM imaging the neutron emitting material in the three process vessels as well as material located on the floor of the glovebox.

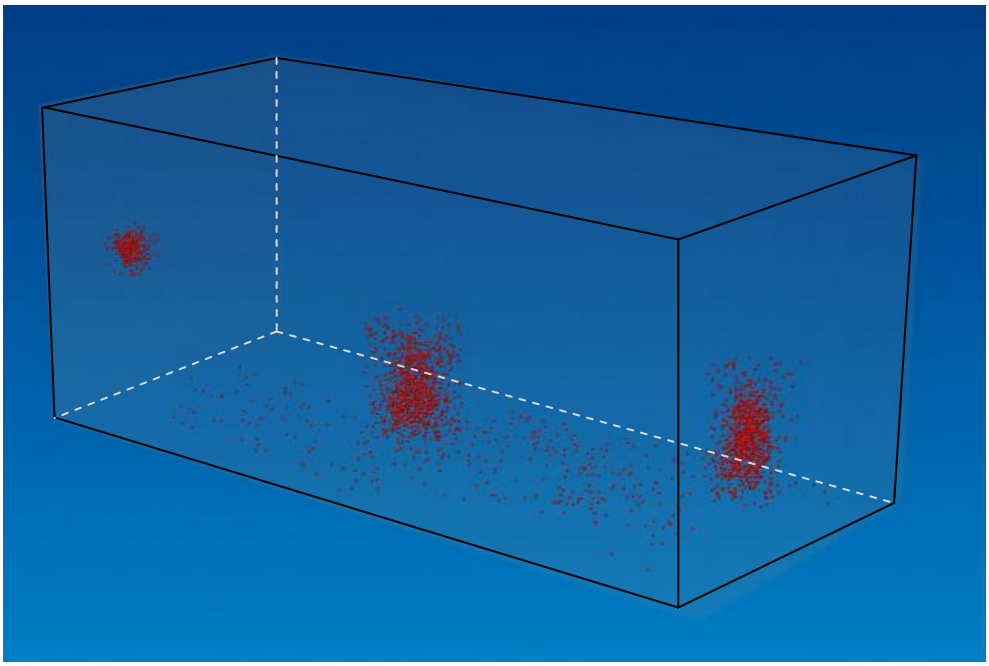

Figure 14: Example of NSIM imaging in process vessels and glovebox floor

5. Summary

Particle Swarm Imaging (PSIM) is an innovative approach developed by Cavendish Nuclear to perform gamma-ray assay.

PSIM has been successfully used to perform verification and characterisation measurements at nuclear facilities across the United Kingdom to confirm the suitability of waste to be consigned to LLWR and ILW and VLLW waste disposal and treatment facilities

The innovation overcomes some of the challenges associated with the accurate declaration of measurement uncertainties of radionuclide inventories within waste items when the distribution of activity is unknown. Implementation requires minimal equipment, making use of gamma-ray measurements taken from different locations around the waste item.

PSIM avoids the major drawback of conventional analyses, namely, the adoption of unrealistic assumptions about the activity distribution that inevitably lead to the declaration of pessimistic (and in some cases optimistic) activity estimates and uncertainties.

PSIM is being developed for the assay of neutron emitting material such as plutonium (stored in waste drums, crates etc.) as well as monitoring and verification of material in process plant such as gloveboxes.

6. References

[1] Kennedy, J.; Eberhart, R. (1995), "Particle Swarm Optimization", Proceedings of IEEE International Conference on Neural Networks. IV. pp. 1942–1948.

[2] D. Karaboga, B. Basturk, “A Powerful and Efficient Algorithm for Numerical Function Optimization: Artificial Bee Colony (ABC) Algorithm”, Journal of Global Optimization, Volume 39, Issue 3, pp: 459–471, Springer Netherlands, 2007.

[3] Parvin D, *Particle Swarm Imaging (PSIM) - Innovative Gamma-Ray Assay,* 132497, WM2013 Conference, February 24 – 28, 2013, Phoenix, Arizona USA.

Monte Carlo modelling of EURATOM neutron detectors for operational purposes

D. Ancius, P. De Baere, P. Schwalbach

Nuclear Safeguards Directorate, DG Energy, European Commission,
L-2920 Luxembourg, Luxembourg.
E-mail: darius.ancius@ec.europa.eu

Abstract:

EURATOM operates around 90 neutron coincidence and multiplicity detectors which are portable or permanently installed in nuclear installations across the EU. They are used to verify operators' declarations – to carry out quantitative evaluation of the amount of nuclear material in certain items. Installed equipment is often used to verify flow and contents of items moving to/from Material Balance Areas (MBA). To assure their sound performance the detectors are regularly maintained and tested. Monte Carlo techniques allow modelling of failure scenarios as well as simulation of variation of their parameters such as the efficiency, Rho-0, die-away time, and more.

This paper presents MCNP™ modelling of two EURATOM coincidence detectors permanently installed in two MOX fuel fabrication plants. It is demonstrated that changing the boundary conditions of a detector may significantly modify its performance and certain parameters, e.g. after its installation where the detector is surrounded by shielding such as concrete or JABROC. Such effects are also confirmed by tests performed with a ^{252}Cf source. The paper investigates how the Monte Carlo technique may be applied for numerical calibration of the neutron detectors in the cases where the measured items containing nuclear material change their shape or physical features such as the density, cans' void ratio, etc.

Uncertainties due to the model's geometry and material composition, as well as uncertainties due to the nuclear data are estimated. As a matter of validation of the MCNP™ model, the use of a well characterized spontaneous fission source is very important. For operational purposes this raises the demand for source longevity and for precision of its neutron yield estimation.

Keywords: Monte Carlo; MCNP; neutron detectors; measurement system; uncertainty estimation.

1. Introduction

Implementation of EURATOM Safeguards requires quantitative verification of operators' declarations of nuclear materials. Plutonium containing materials represent high strategic value and thus EURATOM inspectors are frequently present in MOX fuel fabrication and spent fuel reprocessing plants. Quantitative verification of materials involves the use of NDA tools such as mobile or permanently installed (unattended) gamma and passive neutron coincidence and multiplicity detectors. EURATOM owns and operates around 90 units (including active neutron coincidence detectors used for Uranium mass determination, mainly in LEU fuel assemblies). To assure reliability of the results, periodic preventive maintenance and calibration checks are executed. Repairs are carried out in case of malfunction or failure and extensive upgrades might be required after a couple of decades of continuous operation, an example was reported by Ancius [1]. Differently from mobile detectors the unattended detectors are frequently located in difficult-to-access locations - often in radiation controlled or high security zones. Data is acquired automatically and transmitted via the autonomous EURATOM data network to unattended data acquisition systems such as RADAR and operated in combination with the data evaluation programs CRISP or iRAP [2].

The remote location of EURATOM detectors in European nuclear installations and their limited accessibility during plant's active operation set some restrains on preventive maintenance and repairs in terms of the duration of intervention. This implies very rigorous planning, availability of proper tools as well as good knowledge of the detectors. In addition to the above given number of the neutron detectors it is important to highlight that their incorporation in plant's industrial line often requires custom-designed rather than the commercially available detectors [3, 4]. This is why their variety is very large. In some cases where the operator of the facility has its own installed NDA assay system, EURATOM Safeguards is based on branching of an authenticated detector's signal(s) [5, 6]. Operators' systems do not require EURATOM maintenance, but good knowledge of the system is necessary to assure an independence of the measurement analysis.

Use of numerical modelling methods for design of neutron counting systems is not new and witnesses a history of several decades. A good practice guide for numerical modelling in Safeguards was prepared by the ESARDA NDA Working Group [7]. With the increasing availability of powerful computational systems the use of Monte Carlo techniques became more and more popular.

This paper shows applications of the Monte Carlo computational code MCNP^{TM} (Briesmeister' [8]) for operational purposes such as maintenance, failure analysis or estimation of alteration of detector's calibration characteristics in various circumstances. An alternative way to calibrate detectors using Monte Carlo modelling is investigated. The modelling uncertainties are estimated and discussed.

2. Motivation for Monte Carlo modelling

What else may be expected from numerical modelling once neutron detector is designed, calibrated and tested? The answer to this question is closely related to specificities of operation of EURATOM detectors and some aspects unique to this matter that normally are not seen in scientific laboratories operating such detectors.

2.1. Alteration of detector's parameters

One of such specificities is that we are often limited in the possibility to collect enough knowledge about detector's operational characteristics after installation. In some cases, especially when the detector is installed in an already operational plant, the time to test and to perform maintenance may be very short as in case of the D0 detector in Melox [4]. The D0's operational parameters, such as the Rho-0, the die-away time, and the dead-time correction coefficients were obtained from the Factory Acceptance Tests (FAT). Then it was calibrated with reference sources. We discuss below how, after installation in the facility, some of the characteristics were influenced by surrounding materials like concrete and significantly altered. By performing normalization measurements with a certified source and finding such altered characteristics one may reach wrong conclusions about good performance of the detector. Monte Carlo based estimation of neutron albedo from surrounding construction materials is relatively simple and may substantiate or not such conclusions. Moreover, when supported by the tests with certified spontaneous fission source this modelling may re-establish the realistic detector's in-situ characteristics.

2.2. Failure scenarios

EURATOM Safeguards are based on multi-layer verifications from accountancy to physical quantitative and qualitative checks of items at different points of interest inside a facility. This is why the failure of an individual detector may not lead to a failure of overall material balance verification in the facility. Thus, in case of a "bad measurement" involving significant discrepancy between the mass of nuclear material declared by an operator and that measured by an inspector, questions may arise whether the declaration or the measurement itself is wrong. Detector's performance showing repeated "bad measurements" involving similar items may become seriously questionable. Usual procedure for this case is that the inspector would request the measurement of the reference item or ask the test source. However, a validated Monte Carlo model may support the estimation of the detector's response function for a given item and allow making the definite conclusions. In case of a failure an accurate Monte Carlo model in combination with the tests source may assist in the failure diagnostics and save intervention time and costs.

2.3. Calibration of the detectors

Calibration of detectors requires significant experimental effort and suitable reference standards. Monte Carlo technique allows modelling of a large variety of masses, obtaining of detectors response functions, as well as establishment of calibration curves. Furthermore, the Monte Carlo techniques allows for "real-time calibration" described by Peerani [9]. Last mentioned technique may be especially very useful in the cases of "non-standard" items for which the application of point model (used in an absolute majority of cases) has some particularities.

2. Modelling of two MOX fabrication plants' detectors

Two EURATOM neutron coincidence detectors installed in two MOX plants – SMP in U.K. and Melox in France – were modelled with MCNPX and MCNP6 codes (there are multiple versions of original MCNP^{TM}, the MCNP6 being the last version). The general computational scheme and validation of built Monte Carlo model is presented in **Fig. 1.**

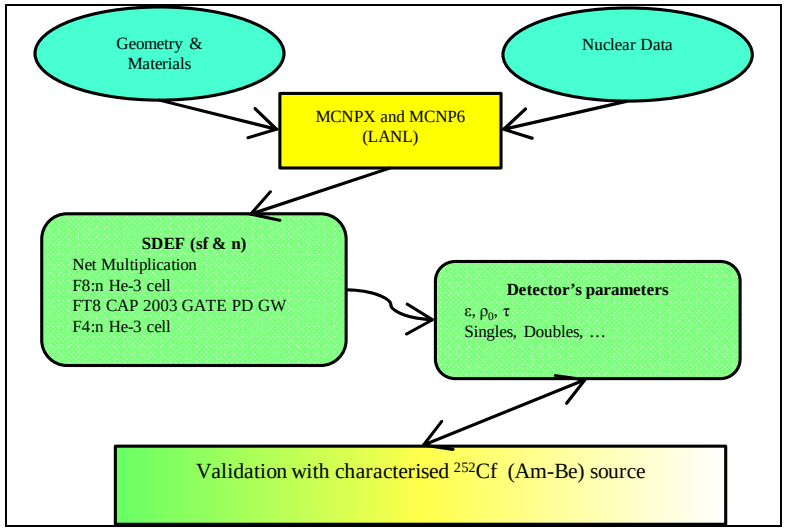

Fig. 1. Computational scheme and validation of the Monte Carlo model

All neutron detectors' components like ^{3}He tubes, polyethylene moderator, cadmium and stainless steel liners, as well as the constructions surrounding the detectors (concrete slabs, JABROC shielding and their material compositions etc.) were input and modelled to our best knowledge. The measured items, i.e. the cans and MOX assemblies were modelled accurately taking into account the real structure of the item, as for example the annular hole of the pellet and the cladding or the internal, intermediate and outer cans in case of PuO_2 items.

MCNP^{TM} uses the nuclear data like nuclear reactions cross-sections, multiplicity of spontaneous and induced fissions, etc. All that nuclear data is organized in nuclear data libraries and constitutes an integral part of the computational code. However, the users may select the version(s) of nuclear data libraries. In this case we have employed the ENDF/B-VII.0 [10] libraries for continuous neutron energy cross-sections: **ENDF70** with the identifiers ZAID.70c and its previous version **ENDF66** with the identifiers ZAID.66c. As concerns the fission multiplicity data, the default multiplicity data (available for 18 isotopes) were used at this stage of calculations.

For the source definition the **SDEF** card with the particle identifier **sf** – for spontaneous fission neutrons and **n** – for the neutrons from (α;n) reactions in PuO_2 or MOX was used. The Watt spectrum and its default values were fixed for spontaneous fission spectrum. To establish a realistic (α;n) neutron spectrum we have applied the probability distribution tables specified by Chard [7]. Thus, the

input file was run twice for a given problem: once to sample the tallies from the spontaneous fission and once more for the tallies from (α;n) reactions.

As a result of the Monte Carlo simulation and the neutron's track length (**F4:N** tally) estimation, the probabilities of the neutron's capture in a cell (cells) representing the ^{3}He tube may be calculated. For the detector's efficiency estimation the item's leakage multiplication has to be known as well. This is why the **net multiplication** calculated by MCNP^{TM} is very important (also for calibration purposes - to be explained later). The **net multiplication** well approximates the leakage multiplication (used in the plutonium mass calculation algorithms) if its numeric value is smaller than 1.5 [11].

MCNP^{TM} pulse-height tally **F8:N** in conjunction with the **CAP**, also known as the coincidence capture tally, and the **GATE** card permits simulation of the shift register's logics and evaluation of the factorial moments. Setting of different pre-delay and gate widths for processing of simulated pulse trains from the neutron captures in ^{3}He tubes allows estimation of detector's characteristics like the die-away time τ and the Rho-0.

For the evaluations of the Singles (Totals), the Doubles (Reals), the Triples and so on, the MCNP^{TM} results need to be normalized against the source strength. In this case the source strength of the particles **sf** (spontaneous neutrons) and **n** (neutrons from (α;n) reactions) may be calculated from the isotopic composition of Uranium, Plutonium and Americium in the simulated item. It is important to underline that the dead-time effects taking place in the real detectors are not simulated by MCNP^{TM}, except its specific versions like MCNP-PTA [12]. In this work the measured count rates of the Singles and the Doubles are corrected for dead-time effects using the reported dead-time correction coefficients of the detector. Then the dead-time corrected Singles and Doubles are compared with the values obtained from Monte Carlo modelling.

For the modelling of ^{252}Cf spontaneous fission source the small geometrical cell (equivalent to the point source comparing to detector's dimensions) containing the low density of the isotope (to exclude the self-multiplication effects) has been introduced. To model the Americium-Beryllium (Am-Be) non-coincidence neutron source the probability function corresponding to the neutron spectrum from (α;n) reaction in Am-Be source was used [13]. Obtained MCNP^{TM} results were normalized with the decay-corrected source's strength from its characterisation certificate.

The leakage multiplication mentioned earlier or its MCNP^{TM} approximation the **net multiplication** becomes very important at the stage of validation of Monte Carlo models built for calibration purposes. Contrary to the Rho-0 (the ratio of the Doubles to Singles for a non-multiplying sample of ^{240}Pu) whose incorrect value - technically speaking - may be compensated by the calibration parameters, the leakage multiplication shall not be lower than 1. However, an arbitrary or wrong Rho-0 value may lead to such situations (in some cases of the automated plutonium mass calculation algorithms the leakage multiplication may be forced to 1). This is exactly why in the detectors' modelling we want to achieve realistic values of the **net multiplication** and of the Rho-0.

2.1. Case of D5 SMP neutron coincidence detector

EURATOM's neutron coincidence detector D5 in the Sellafield MOX plant (SMP) was integrated into the Fuel Assembly Handler and used to measure the MOX fuel assemblies when placed into the fuel assembly store. The design is described in [14]. D5 has 24 ^{3}He tubes imbedded in the polyethylene moderator and surrounded by a thick layer of JABROC (material used in neutron radiation shielding). The detector has an internal and external 0.5 mm cadmium liner protected by a stainless steel sheet. D5 has not been in use for several years but will be re-activated as the SMP fuel store takes over a new function [15].

The MCNPX model of D5 detector is presented in **Fig. 2.** The JABROC (in grey) surrounds the polyethylene moderator (in blue) and the ^{3}He tubes (red). The MOX PWR fuel assembly (shown only partially – the model takes into account its total length) is positioned in the centre of D5 and is protected against accidental damage by the stainless steel sheath. The shown assembly's vertical position corresponds to the EURATOM verification measurement position. The lower part of the assembly remains in the concrete well. The stainless steel plate (in green) supports D5 from beneath.

For simulation of the detector's response to ^{252}Cf and Americium-Beryllium sources a small cylindrical source was modelled in the centre of D5's cavity.

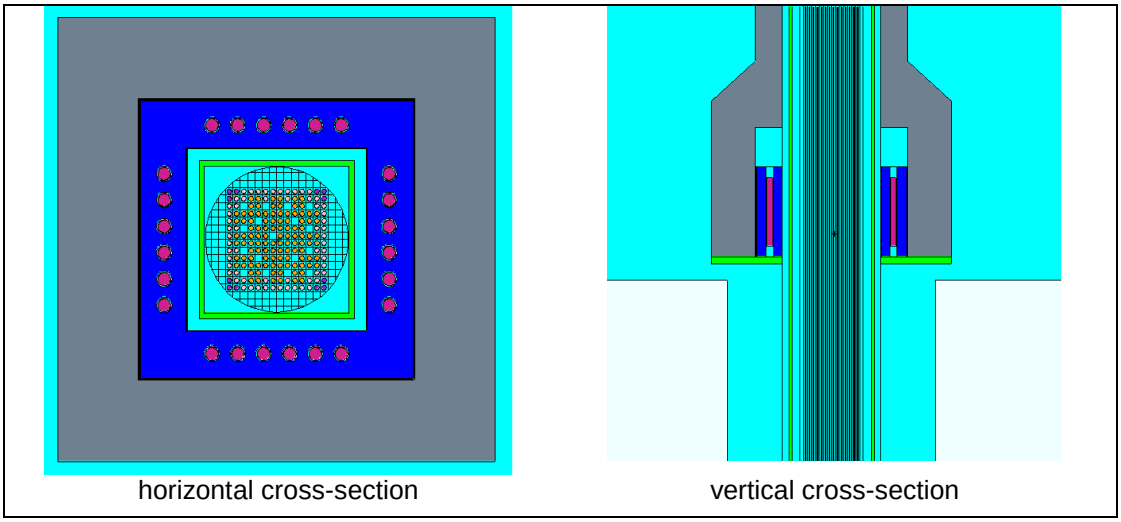

Fig. 2. MCNPX model of D5 MOX assembly coincidence detector

2.1. Case of D0 Melox neutron coincidence detector

EURATOM D0 neutron coincidence detector was custom–designed [4] for a specific location in Melox. It was installed into a concrete ceiling and is used to measure the PuO_2 cans moving to the store one level higher. The PuO_2 cans are packaged in a transport container which is lifted through D0 where actual measurements are done in 3 different vertical positions. D0 has 40 ^{3}He tubes imbedded in the polyethylene moderator and surrounded by the ceiling's concrete. The detector has an internal and external 0.5 mm cadmium liner protected by a stainless steel sheet. The MCNPX model of D0 detector is presented in **Fig. 3.**

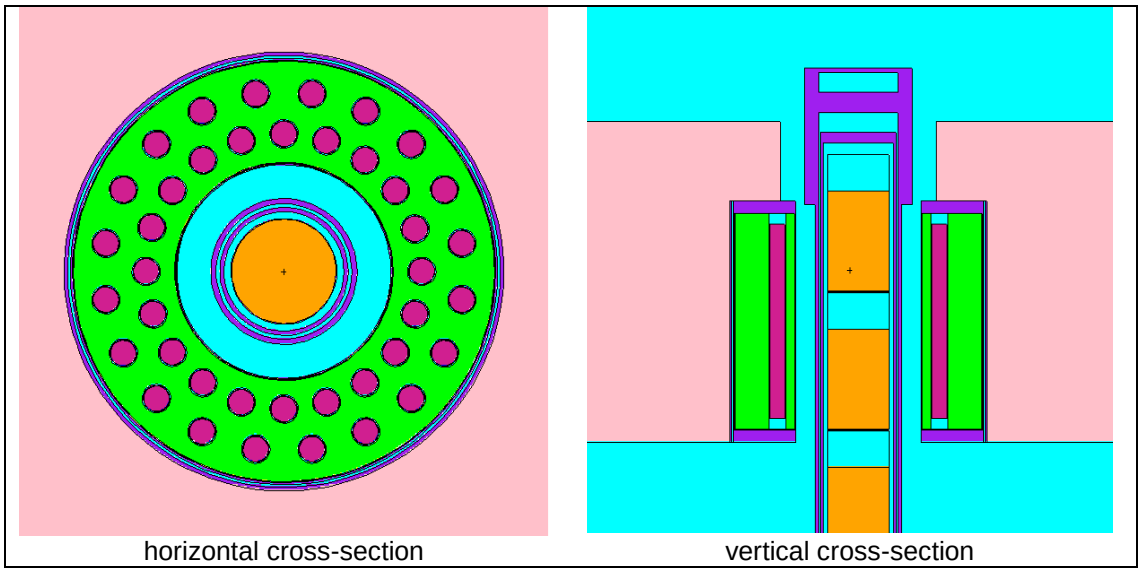

Fig. 3. MCNPX model of D0 PuO_2 coincidence detector

The concrete (in pink) surrounds the polyethylene moderator (in green) and the ^{3}He tubes (red). PuO_2 cans in their transport container (shown only partially – the model takes into account all length and all

cans) are inserted to the D0. The shown vertical cross-section corresponds to one of the three EURATOM verification measurement positions.

For simulation of the detector's response to ^{252}Cf source a small cylindrical source was modelled in the centre of D0's cavity.

3. Modelling results

3.1. Validation of Monte Carlo models

Both D0 and D5 models were built based on information about their construction materials and dimensions available in technical documents. Some information has been re-verified in place. In order to validate the models recent preventive maintenance measurements with ^{252}Cf and the Americium-Beryllium neutron sources were taken into account. **Table 1** presents a comparison of Monte Carlo and measurement results.

DETECTOR'S CHARACTERISTIC	Monte Carlo estimation	Measured with ^{252}Cf source*	$\frac{\text{Measured} - \text{Monte Carlo}}{\text{Measured}}$
D0 MELOX DETECTOR			
Singles, cps	6929.7 ± 1.4	7039 ± 145	+1.55%
Doubles, cps	1761.3 ± 1.1	1776 ± 60	+0.84%
Efficiency, %	25.27 ± 0.005	25.66 ± 0.53	+1.52%
Rho-0	0.1445 ± 0.0001	0.1434 ± 0.019	-0.77%
Die-away time, µS	40.52 ± 0.16	41.8	+3.06%
* ^{252}Cf source's neutron yield = 27427 ± 521 n/s (1.90%) for the measurement day of 6-March-2014			
D5 SMP DETECTOR			
Singles, cps	27438 ± 8	22846 ± 216	-20.09%
Doubles, cps	2203 ± 3	1551 ± 44	-42.04%
Efficiency, %	8.56 ± 0.00003	7.13 ± 0.07	-20.06%
Rho-0	0.046 ± 0.0001	0.039 ± 0.009	-16.92%
Die-away time, µS	61.48 ± 0.39	57.96 ± 9.39	-6.09%
* ^{252}Cf source's neutron yield = 320575 ± 2853 n/s (0.89%) for the measurement day of 12-November-2014			

Table 1. Comparison of MCNPX and measurement results for validation of the detectors' models

For D0 the modelled and measured discrepancies of Singles, Doubles, Rho-0, and Efficiency are small and within their statistical uncertainties. Whenever such discrepancies are within 10%, it is recommended to introduce the fixed correction factors [7]. However, in our case the main uncertainties stem from the test measurements (measurement statistics and the uncertainty of neutron yield of the test source). This is why at this stage we consider our model valid.

Test measurements on D5 showed larger discrepancies, not in line with the model. An effort to improve the D5 model did not give considerably better results. Additional test measurements with Americium-Beryllium neutron source (nominal yield 2.2E+5 n/s) have been made. The neutron energy spectrum of an Americium-Beryllium source, which differs significantly from that of Californium (fission), has been used for Monte Carlo modelling. Once more the measured and calculated efficiencies were significantly different: 5.56 ± 0.84% (measured) and 7.16 ± 0.002% (calculated). The discrepancy was -22.35%. This points towards a loss of efficiency during this long non-operation period. One of the possible verifications of this assumption is to validate the model using the pre-operational measurements, e.g. Factory Acceptance Tests (FAT). To test the FAT conditions the above model of D5 was modified by "removing" the JABROC, the stainless steel plate, and the concrete slab. The results of this altered model, compared with FAT measurements are presented in **Table 2**.

DETECTOR'S CHARACTERISTIC	Monte Carlo estimation	Measured during FAT with ^{252}Cf source*	$\frac{\text{Measured} - \text{Monte Carlo}}{\text{Measured}}$
D0 MELOX DETECTOR			
Singles, cps	926.8 ± 0.2	945	+1.89%
Doubles, cps	211.5 ± 0.2	-	-
Efficiency, %	22.66 ± 0.005	23.10	+1.89%
Rho-0	0.130 ± 0.0001	-	-
Die-away time, µS	40.30 ± 0.17	40.6	+0.74%
* ^{252}Cf source's neutron yield = 4090 ± (n.d.) n/s for the measurement day of 20-December-2007.			
D5 SMP DETECTOR			
Singles, cps	461.2 ± 0.18	463.1 ± 2.2	+0.40%
Doubles, cps	30.18 ± 0.05	30.80 ± 0.32	+2.01%
Efficiency, %	6.778 ± 0.0003	6.805 ± 0.033	+0.40%
Rho-0	0.0372 ± 0.00006	0.038 ± 0.005	+2.11%
Die-away time, µS	59.32 ± 0.46	57.18	-3.74%
* ^{252}Cf source's neutron yield = 6804 ± 31 n/s (0.46%) for the measurement day of 28-May-1997.			

Table 2. Comparison of MCNPX and Factory Acceptance Tests (FAT) results

Monte Carlo simulation of the FAT test shows good agreement of calculated and measured values and excludes significant modelling errors. During preventive maintenance test on D5 the instability of the count rates was observed. This, together with the results of Monte Carlo calculations led us to decide to dismantle the detector from the Fuel Handling Machine for in-depth maintenance. This operation is not easy and requires prior preparations and justifications convincing the operator of the facility about the need for such intervention. In the meantime, it has been done.

Our experience with D5 motivated us to make the same verification for D0. And this is why the identical approach of modelling of the FAT conditions has been used. The MCNPX results of the simplified model of D0 were compared with the FAT results. The comparison is presented in **Table 2**.

Existing FAT records do not contain uncertainty estimations and this is why the modelled and measured discrepancies could not be verified properly. Some other quantities like the Doubles or the Rho-0 were not measured and could not be compared. However, in general, the discrepancies are not large and this proves once more that our Monte Carlo model is trustworthy.

3.2. Estimation of alteration of detectors' characteristics after their installation

The validation of the Monte Carlo models for FAT of D0 and D5 has highlighted significant alterations of detectors' characteristics, such as the Efficiency, the Rho-0 and the Die-away time after the detectors' installation in the plant. The summary of such altered characteristics of D0 and D5 detectors is shown in the **Table 3**.

DETECTOR'S CHARACTERISTIC	Monte Carlo estimation	Measured with ^{252}Cf source in 2014
	D0 MELOX DETECTOR	
Efficiency	+11.52%	+11.08%
Rho-0	+11.15%	-
Die-away time	+0.55%	+2.96%
	D5 SMP DETECTOR	
Efficiency	+26.28%	+4.78%
Rho-0	+22.58%	+2.56%
Die-away time	+3.64%	+1.36%

Table 3. Alteration of FAT characteristics of D0 and D5 after their installation in the plant

Comparison of Monte Carlo calculated alteration of detector's characteristics to the measurements with a certified ^{252}Cf source is in good agreement for D0. As concerns the D5 there is no agreement, but we have to bear in our mind that the ^{252}Cf measurements were performed at the moment where the detector had probably already lost some efficiency.

This alteration of characteristics as calculated by MCNPX is very different for D0 and D5, but there is a principal difference which explains this: the concrete (D0 case) is a less good reflector of the neutrons leaving the detector than the JABROC (D5 case). In fact, the JABROC with its density of 1.3 g/cm^3 contains ~50% of carbon and even 6% of hydrogen (by mass), which makes it a very efficient neutron shielding material but also an excellent neutron reflecting medium [16]. In this specific case the neutron backscattering in D5 due to JABROC and the related increase of detector's efficiency (+26.28%) is even higher than it would have been if the detector was shielded with high density polyethylene (+23.47%) and is comparable to the graphite's case (+40.27%). In both cases these magnitudes were obtained by MCNPX modelling. Of course, this estimated change will be once again verified with the ^{252}Cf source as soon as the good functioning of D5 is confirmed after its maintenance. However, the alteration of D5 efficiency by JABROC as evaluated by MCNPX above is not lacking for explanations.

3.3. Investigation of possibility to use Monte Carlo for calibration of detectors

Detector's calibration using physical reference materials for the items such as measured by D0 and D5 is almost hypothetic. First of all, the items are of high complexity and contain significant plutonium masses: the canisters contain several cans with potentially different isotope composition (D0 case), the MOX assemblies may have different matrixes - 14x14, 16x16 grids and even more complex

hexagonal shape like fast breeder's sub-assemblies (D5 case). Secondly, the fact that the measured item is only partially inserted into the detector makes that both D0 and D5 operate beyond the point model's mode. Thus the assumptions like the constant neutron emission and invariable multiplication (as in case of a typical reference material) are not valid anymore. This is why the "physical calibration" procedure is based on the use of the "reference items" which known isotopic composition and the plutonium mass may be confirmed and verified by other safeguards means (as destructive analysis upstream in the process). On the other hand it is very convenient to have such reference item(s) for re-verification of the detector's response at any time. However this is not always possible because in the high throughput facilities they end up into the industrial process and are not available anymore. Another aspect which is also important to mention here is that any calibration process involves significant preparatory work, selection of representative items, verifications and sometimes repeated measurements which require additional operators' and inspectors' efforts.

At this point the use of Monte Carlo modelling may become very attractive because of its simplicity (providing that the model has been already validated), flexibility, and relatively low computational time resources. With the following example we want to demonstrate our attempts to model one item measurement in D0 detector and to discuss the uncertainties of such modelling.

The container has several PuO_2 cans and is measured in three different insertion positions. **Table 4** compares measured (dead-time corrected) and our calculated Singles and Doubles. Both MCNPX and MCNP6 calculation results are presented.

D0 DETECTOR (arbitrary density of PuO_2 is 2.5 g/cm^3)	**Measurement Position 1**	**Measurement Position 2**	**Measurement Position 3**	**Average**
		$\frac{\mathbf{MCNPX - Measured^{DT-CORR}}}{\mathbf{MCNPX}}$		
Singles	-7.6%	-5.5%	-2.5%	**-5.5%**
Doubles	+18.4%	+20.3%	+20.7%	**+19.7%**
		$\frac{\mathbf{MCNP6 - Measured^{DT-CORR}}}{\mathbf{MCNP6}}$		
Singles	-7.3%	-5.0%	-2.0%	**-5.0%**
Doubles	+16.9%	+18.5%	+19.7%	**+18.2%**

Table 4. Comparison of MCNPX and MCNP6 calculated and measured Singles and Doubles, D0

Following the good practice recommendations [7], the <20% difference can still be compensated by benchmarking of our model and then used for calibration of D0. However the achievement of the minimum differences is not in the objectives of this paper. We want to reveal the types of uncertainties one may encounter in Monte Carlo model built for calibration of detectors for complex items and to point out how better results may be achieved.

3.4. Uncertainties of Monte Carlo modelling of the D0 detector

3.4.1. Geometrical position and physical form of an item

The uncertainties of D0 calculation results due to geometrical inaccuracy of D0 components may be evaluated from model validation involving the ^{252}Cf source. The geometrical reality of the item (container with several cans, not always filled to the same degree) is more challenging to model with

high certainty, because the operator does not always declare all the details. The position of the cans inside the long container (in particularly the distance of the bottom can from container's foot – due to for example the use of a shock-absorber or any other material) is not well known. Fortuitously, it does not matter for the establishment of measurement based calibration curves unless these characteristics change from campaign to campaign. Three measurement positions are fixed by the step motor cams and this mechanism assures the invariance of conditions established during the calibration exercises. But for Monte Carlo simulation such uncertainty of the "active column" of cans may introduce noteworthy uncertainties, especially for top and bottom measurement positions, 1 and 2.

The void factor of the cans or the density of PuO_2 is another aspect which when unknown makes the Monte Carlo estimations indefinite due to neutron multiplication assessment. Accurate density of PuO_2 is not declared by the operator, but by taking its variation from 2.0 to 3.0 g/cm^3 we assume that the true density is situated in between. Therefore, we have chosen an arbitrary value of 2.5 g/cm^3 for our calculations. They show that the variation of the density of 20%, between 2.0 and 3.0 g/cm^3 changes the multiplication of the neutrons in the item correspondingly from 1.14 to 1.19 in the measurement position 2 and from 1.13 to 1.19 in the measurement positions 1 and 3. In the uncertainty terms of our measurables this would translate to ± 3% for the Singles and to +10 and -11% for the Doubles (from the arbitrary density of 2.5 g/cm^3).

3.4.2. Dead-time correction

The dead-time correction of D0 as recommended in the FAT report is based on a single dead-time constant ***a*** (0.312 µS) for the Doubles and it was determined by the method of one correlated and one non-correlated neutron source. The uncertainty ***Δa*** was not assessed during FAT, but using the reported FAT measurement raw data and through uncertainty estimations using partial derivatives we have established that its conservative value is 0.052 µS. This results to a relative uncertainty of 6.20% for the dead-time corrected Doubles and 1.55% for the dead-time corrected Singles (***a***/*4* was used for the correction of the Singles).

3.4.3. Nuclear data

The user of MCNP^{TM} may define himself the nuclear data he is going to apply. It starts with the definition of the cross-section libraries for the materials used in the problem. To evaluate the influence of different libraries to calculation results we have compared two sets of libraries represented as **ENDF66** (MCNPX) and **ENDF70** (MCNP6). The results of such comparison are given in **Table 5**.

D0 DETECTOR (arbitrary density of PuO_2 is 2.5 g/cm^3)	**Singles (not DT corrected)**	**Doubles (not DT corrected)**
$\frac{\mathbf{ENDF66 - ENDF70}}{\mathbf{ENDF66}}$	-0.43%	+1.84%
(ENDF66): $\frac{Watt-(\alpha;n)^*}{Watt}$	+2.0%	-1.0%
(ENDF70): $\frac{Watt-(\alpha;n)^*}{Watt}$	+2.0%	-0.7%
***** the probability distribution of (α;n) neutron spectrum is reproduced taking into account the neutron production probabilities in ref. [7] and the isotopic composition of Plutonium and Americium of the measured cans.		

Table 5. Uncertainties of D0 detector simulation due to nuclear data: selection of cross-section libraries and use of Watt vs. (α;n) neutron spectra for (α;n) neutrons simulation

The differences of the Singles and the Doubles derive from slightly different results of induced fission estimations in MCNPX (ENDF66) and in MCNP6 (ENDF70). Renewed cross-section library **ENDF70**

differs from previous **ENDF66** version by several new features, which permitted better treatment of unresolved resonances and processing of the delayed neutrons (not taken into account in **ENDF66**).

The definition of the source of fissionable material and the neutron spectrum in MCNP^{TM} especially for (α;n) reactions is complex. However, the average energy of spontaneous and (α;n) neutrons in oxides (in the point model there is only one value of efficiency for both) is close [17]. Thus, the source definition in modelling may be significantly simplified by using the Watt fission spectrum for both spontaneous fission and (α;n) neutrons. We have estimated what would be the uncertainties due to such choice. These estimations are also shown in the **Table 5**. In this case of the D0 detector the α=0.74 (the ratio of neutrons from (α;n) and spontaneous fission) and the contribution of spontaneous fission neutrons is more important. But for the items with higher α, e.g. the scrap material, the contribution from (α;n) becomes significant and thus the differences of the results due to the use of Watt and (α;n) neutron spectra for (α;n) neutrons simulation would increase.

4. Conclusions

Modelling of EURATOM neutron detectors with MCNP^{TM} permits verification of characteristics like the efficiency, the Rho-0, and the die-away time. These may change after the detector's installation in the plant due to changed boundary conditions and surrounding materials such as concrete or JABROC.

Validations of MCNPX models for D5 and D0 were performed on the basis of the records of the Factory Acceptance Tests (FAT) executed with the ^{252}Cf spontaneous fission neutron sources. Recent test measurements of D0 were in good agreement with Monte Carlo predicted values. Such prediction for D5 detector differed significantly and raised doubts about the good functioning of the detector after its long inactivity period. The detector is being prepared for an in-depth maintenance. In particularly the example of D5 shows how the Monte Carlo simulation may be efficiently used in the failure analysis of EURATOM detectors. Given the usual remote location of EURATOM detectors and complexity of the access to the detectors in an operating plant, the Monte Carlo modelling may significantly complement failure diagnostics and shorten repair-after-failure times.

Uncertainties of Monte Carlo simulation depend first of all on good knowledge of the detector's construction components and also on the knowledge of its surroundings, after installation. Test measurements involving ^{252}Cf source may reduce these uncertainties to 1-2% both for the Singles and the Doubles. As the analysis above shows, the magnitude of these uncertainties is largely caused by the uncertainties of the neutron yield from ^{252}Cf source. This raises the demand for the availability of well characterised spontaneous fission sources permitting to achieve lower measurement uncertainties. The short longevity of ^{252}Cf source is an essential motivation for investigations on spontaneous fission sources with longer half-lives.

As concerns the modelling of PuO_2 items, characteristics such as the density and the internal position of cans in the transport container may become the primary source of uncertainties. These may be ignored during the "physical calibration" exercises unless they change between different measurement campaigns. The dead time effects of the electronics of the detector may not be modelled with the classic version of MCNP^{TM}. This is why the good knowledge of the dead-time correction constants and their uncertainties (FAT or established during post-tests) is important for the reduction of Monte Carlo simulation uncertainties.

Selection of nuclear data libraries may slightly vary the Monte Carlo calculation results. In particularly for the prediction of the Doubles this difference is smaller than 2%. Monte Carlo calculation results depending on the way the neutron spectrum from (α;n) reactions is modelled (Watt vs. (α;n) reaction data [7]) differ by 1-2% for the Singles and the Doubles. For the items with an increased α (the ratio of neutrons from (α;n) and spontaneous fission) the selection of Watt or (α;n) spectra may further increase above estimated difference.

5. References

1. Ancius D., Berndt R., Mortreau P., Löschner J., De Baere P., Levert J.F., Eestermans W., Schwalbach P., *"Modernization of EURATOM's unattended measurement stations at Melox MOX Fuel Fabrication and La Hague Reprocessing Plants"* 35th ESARDA Annual Meeting p. 1 – 9. Bruges, Belgium, 2013.
2. Smejkal A,, Linnebach R,, Longo J,, Nordquist H,, Regula J., *"Joint Partnership – a New Software Development Paradigm", Proceedings of Symposium on International Safeguards: Linking Strategy, Implementation and People, IAEA CN-220"*, October 2014.
3. De Baere P., Chare P., Schwalbach P., Swinhoe M., *"A custom designed Pin Tray Detector for an Automatic MOX Plant"*, Proceedings 17th ESARDA Symposium, Aachen, 9-11 May, 1995, p. 605-607,
4. Tagziria H., Peerani P., Schwalbach P., *"Neutron coincidence detector for the verification of PuO2 cans"*, Nucl. Instrum. Methods Phys Res A 580, 2007, p. 377 - 379.
5. Bourva L., Caspall-Askew P., Ancius D., Smejkal A., Wilkins C., Lahogue Y., *"Continuous Can Content Monitoring for Special Nuclear Material Control and Accountancy at the Sellafield Product and Residue Store"* 35th ESARDA Annual Meeting p. 1 – 9. Bruges, Belgium, 2013.
6. Burke K.J., Ancius D., Chaudry A., Gunn R.D., Looman M.R., Maina D.J., Mason J.A., Paton D., Towner A.C.N., Wood G.H., *"Design Development and Testing of a Combined Neutron and Gamma ray Assay System for Measuring Fissile Material in Fuel and Waste Items -15340"*, WM2015 Conference, Phoenix, Arizona, USA March 15 – 19, 2015.
7. Chard P. (editor), *"A Good Practice Guide for the use of Modelling Codes in Non Destructive Assay of Nuclear Materials"*, ESARDA BULLETIN, No. 42, November 2009.
8. Briesmeister J.F., *"MCNP - A general Monte Carlo N-particle transport code"*, LA-13709-M, Los Alamos National Laboratory, March 2000.
9. Peerani P., Tagziria H., Looman M., *"Real-time simulation of neutron counters"*, Radiation Measurements 43, 1506–1510, 2008.
10. Chadwick M.B. et al, *"ENDF/B-VII.0: Next Generation Evaluated Nuclear Data Library for Nuclear Science and Technology"*, Nuclear data Sheets, vol. 107 pp. 2931 – 3060, 2006.
11. Swinhoe M. T. (LANL), *Private communication*, 2014.
12. Looman M. R., Marin Ferrer M., Peerani P., *"Simulations of neutron multiplicity counters with MCNP-PTA"*, Proceedings of the 29th Annual Symposium on Safeguards and Nuclear Material Management, Aix-en-Provence, France, 22–24 May 2007.
13. Reilly D., Ensslin N., Smith H Jr., Kreiner S., *"Passive Non-destructive Assay of Nuclear Materials"*, NUREG/CR-5550, LA-UR-90-732, (March 1991).
14. Croft S., Chard P.M.J., Hutchinson I. G., Price P. J., Schwalbach P., *"Design and Performance of Neutron Detector Assemblies for a MOX Fuel Fabrication Plant"*, Proceedings 19th Annual Symposium on Safeguards and Nuclear Material Management, Montpellier, France, 1997, p. 245-249.
15. Persson L., Synetos S., Ozols A., Ayranov M., Lahogue Y., Kiewiet A., Ancius A., Homer A., Wheeler I., Harrison R., Anderson A., Beaman M., "*Consolidation of NM in the UK: Optimising the EURATOM approach"*, Proceedings IAEA Safeguards Symposium 2014.
16. Permali Gloucester Ltd., *"Typical properties of JABROC N"*, Permali Gloucester Ltd. Publication 8.200/1.
17. Swinhoe M. T., Hendricks J. S., *"Calculation of the Performance of ^{3}He Alternative Detectors with MCNPX"*, LA-UR-11-03050, 2011.

6. Legal matters

"We agree that ESARDA may print our name/contact data/photograph/article in the ESARDA Bulletin/Symposium proceedings or any other ESARDA publications and when necessary for any other purposes connected with ESARDA activities."

Session 5

Spent Fuel Verification

Extension of the SCK•CEN spent fuel inventory library

A. Borella[1], M. Cometto[1,2], R.Remetti[2], R. Rossa[1,3], K. van der Meer[1]

1) SCK•CEN, Nuclear Science and Technology unit, Boeretang 200, B-2400 Mol, Belgium
2) Sapienza, Università di Roma, Via Antonio Scarpa 14, 00161 Roma, Italy
3) Université libre de Bruxelles, Ecole polytechnique de Bruxelles - Service de Métrologie Nucléaire (CP 165/84), Avenue F.D. Roosevelt, 50 - B1050 Brussels, Belgium

Email: aborella@sckcen.be

Abstract:

SCK•CEN is performing R&D work related to the development of Non Destructive Assay on spent fuel elements. Due to difficulty in accessing spent fuel, having an accurate and validated model of the measurement equipment and a characterization of the source term is important for this type of studies. To better understand and develop methods based on neutron counting and gamma spectroscopy, a significant effort was done to determine the source terms associated to spent fuel with depletion and evolution code calculations.

This paper reports about the extension of the SCK•CEN spent fuel inventory library with the ORIGEN-ARP code. The cases considered a Low Enriched Uranium 17×17 PWR fuel with an initial enrichment of 2.0, 2.5 and 3.0 %. This set of enrichments complements the data published previously for enrichments between 3.5 % and 5 %. In addition, results obtained with Mixed Oxide (MOX) fuel are presented and discussed. The impact of the initial enrichment, for LEU fuel, and the Pu mass, for MOX fuel, on the neutron emission and production of the main neutron emitters, are also studied.

Keywords: Evolution and depletion calculation; Spent Fuel Inventory; Neutron emission; Gamma emission; Spent Fuel; Non Destructive Assay;

1. Introduction

In the last decade, a significant research and development effort on Non-Destructive Assay (NDA) measurements methods used for spent fuel verification has received world-wide attention [1,2]. Several measurements technologies have been and are being investigated [3] with the aim of reducing the uncertainties associated with spent fuel verification. While some of the technologies rely on novel approaches [4], others rely on measurements concepts either already used in spent fuel verification [5] or more technologically mature [6].

Despite the large inventory of spent fuel, this material is often stored under water in difficult-to-access areas. Access to spent fuel is granted in agreement with the nuclear operators and authorities in charge of the spent fuel management, and stringent safety regulations must be respected when manipulating spent fuel and carrying out the measurements. These limitations and the non-existence of adequate reference material, result in a difficulty on the possibility to verify the performances of the measurement methods being developed or investigated. Therefore, studies of the considered techniques are carried out by means of numerical calculations, often based on Monte Carlo methods [7].

Studies with Monte Carlo methods are based on models of the measurement environment. Such model typically includes the geometry and composition of the measurements equipment, the measurement environment and the characteristics of the radiation source. Moreover, other modelling

and physics options can be adjusted or enabled in the model. In case of spent fuel modelling, its geometry and composition are specified. In addition, in order to estimate the absolute detector response, a description of the source term associated to the spent fuel is needed. For example, the source term can be the neutron or gamma energy differential distribution.

The determination of the spent fuel composition and the characteristics of the emitted radiation can be achieved by means of evolution and depletion codes such as Origen-ARP [8,9,10] and ALEPH2 [11]. These codes are validated against experimental data on the composition of spent nuclear fuel [12,13,14]. Previous work [15,16], indicated how the interpretation of Fork detector spent fuel measurement data benefits from the combined use of the detector responses, obtained with Monte Carlo simulations, and spent fuel composition and emitted radiation, obtained with evolution and depletion codes.

In this framework, SCK•CEN started to develop a spent fuel library and investigate the impact of different factors on spent fuel composition and emitted radiation. The characteristics of spent fuel depend on quantities such as fuel type, irradiation history and initial composition of the fuel. We focussed on 17x17 PWR fuel element and studied the change of the neutron emission by varying parameters such as initial uranium enrichment (IE), average power level (AP), duration of the irradiation cycle (DIC) and cooling time between two complete irradiation cycles (CTIC), burnup (BU and cooling time (CT) after discharge [17,18].

The spent fuel library consists of entries, each corresponding to a specific irradiation case. In one entry the total neutron emission, total gamma emission, and the corresponding energy spectra are given. In addition, the abundances of 50 selected nuclides are present. All the data are available in a format which is compatible with the one of an MCNP [19] input file. To process the large amount of data generated by the codes and extract only the indicated entry data an ad-hoc tool was developed. It is envisaged that the library content will be made available to the scientific community.

In this work, we first describe the current status of the library. We then describe how the results of the output of the used evolution and depletion codes are processed. In addition, we report about the results of calculations that were carried out for Low Enriched Uranium (LEU) fuel for with an initial enrichment of 2.0%, 2.5% and 3.0%. In addition results with Mixed Oxide (MOX) fuel are also presented.

Conclusions and outlook on future work are also presented.

2. Spent Fuel Library – current status

The SCK•CEN spent fuel library is based on the results obtained with Origen-ARP code. The cases refer to LEU 17×17 PWR fuel with an initial enrichment between 2.0% and 5.0%. All the quoted percentages are weight percent. The burnup ranged between 5 and 70 GWd/t_{HM} and 30 values of cooling time, from 0 up to 3 million years, were considered. An average power of 40 MW/t_{HM} was used; this value was obtained from the irradiation histories of the spent fuel data in [20].

In addition to LEU fuel also MOX fuel was considered. Four different percentages of plutonium on the total fuel mass (i.e. 4, 6, 8 and 10%) were studied. The range of burnup was limited to 60 GWd/t_{HM} due to limitations in the cross sections libraries of ORIGEN-ARP. The following Pu/U isotopic vector was taken from literature data [21] and was kept constant through the simulations:

Plutonium:		Uranium:	
^{238}Pu	2.5%	^{234}U	0.00119%
^{239}Pu	54.7%	^{235}U	0.25%
^{240}Pu	26.2%	^{238}U	99.7488%
^{241}Pu	9.5%		
^{242}Pu	7.2%		

With this choice of the isotopic vector, a MOX fuel with 6 % of Pu has approximately the same amount of fissile material as a LEU fuel with 4.0% initial enrichment.

In previous works [17,18], we reported on the results obtained with LEU 17x17 PWR with an initial enrichment between 3.5% and 5%. In addition, the impact of several parameters such as the Average Power, the Duration of the Irradiation Cycle and Cooling Time between two complete Irradiation Cycles, affecting the irradiation history, was also studied for a reference case with IE=4.5%.

The content of the library is given in Table 1. The new contributions to the spent fuel library are highlighted. For each group of entries, the quantities that are varied with respect to the reference case (IE=4.5%, AP=40 MW/t_{HM}, DIC=360 days, CTIC=30 days) are shown in bold.

IE / %	AP / MW/t_{HM}	DIC / days	CTIC / days
2.0	40	360	30
2.5	40	360	30
3.0	40	360	30
3.5	40	360	30
4.0	40	360	30
4.5	40	360	30
5.0	40	360	30

IE / %	AP / MW/t_{HM}	DIC / days	CTIC / days
4.5	**30**	360	30
4.5	**35**	360	30
4.5	**40**	360	30
4.5	**45**	360	30
4.5	**50**	360	30
4.5	40	**270**	30
4.5	40	**360**	30
4.5	40	**420**	30
4.5	40	360	**15**
4.5	40	360	**30**
4.5	40	360	**45**
4.5	40	360	**60**
4.5	40	360	**90**

Pu mass / %	AP / MW/t_{HM}	DIC / days	CTIC / days
4.0	40	360	30
6.0	40	360	30
8.0	40	360	30
10.0	40	360	30

Table 1: Overview of the SCK•CEN spent fuel library. The new additions are shown in yellow background.

3. Data processing

For each simulated case, the output file of Origen-ARP contains the composition of the fuel during the irradiation history. In addition, the characteristics of the neutron and gamma sources are given after each irradiation period. Since we have decided to track information on all the available nuclides throughout the irradiation, the corresponding output file size is several Mbytes. In order to handle efficiently the extraction of the relevant information, several scripts working under the *Cygwin bash shell* environment were developed. With these scripts, it is possible to extract the following information associated to a given entry of the spent fuel library:

- Total neutron emission
- Total neutron emission components (spontaneous fission, (n,α), delayed neutrons)
- Neutron emission due to a given nuclide and its components (spontaneous fission, (n,α), delayed neutrons)
- Abundance of a given nuclide or a set of nuclides

The user needs to specify the irradiation or decay case and cooling time(s) for which the information is requested and the scripts generate the requested information in text files.

In addition, a dedicated script was written to determine the 50 most important nuclides for the neutron transport and generate an MCNP input file for the composition of the spent fuel. This script determines this information based on the abundance of all nuclides at a given time and a weight factor associated to each nuclide. A ranking is then determined based on the product of the nuclide abundance and the weight factor; the first 50 nuclides of the ranking are selected and included, in addition to oxygen isotopes, in a material entry in MCNP format where their abundance is given in g/t_{HM}.

The weight factor was determined with ad-hoc MCNP calculations, from the nuclide neutron absorption cross section averaged on an isolethargic flux from 10^{-9} to 100 MeV. The average absorption cross section normalized to the maximum obtained value is shown in Fig. 1. An example of the material entry in MCNP format obtained with the processing scripts is given here:

```
008016 -1.341270E+05 &
008017 -5.426640E+01 &
008018 -3.085850E+02 &
092238 -9.353740E+05 &
092235 -1.851200E+04 &
094239 -5.859370E+03 &
094240 -1.753320E+03 &
095241 -6.989090E+02 &
094241 -4.187120E+02 &
092236 -4.930160E+03 &
060143 -8.552370E+02 &
062151 -1.540490E+01 &
064155 -3.731280E+00 &
062149 -4.620770E+00 &
054131 -4.159840E+02 &
062152 -1.154340E+02 &
093237 -4.190830E+02 &
045103 -4.449080E+02 &
055133 -1.084190E+03 &
060145 -6.561470E+02 &
060144 -1.153380E+03 &
092234 -2.842850E+02 &
062147 -2.689780E+02 &
058142 -1.048250E+03 &
062150 -2.675470E+02 &
094238 -8.899680E+01 &
043099 -7.469910E+02 &
063153 -9.141050E+01 &
094242 -2.629840E+02 &
059141 -1.047370E+03 &
042095 -7.329210E+02 &
054136 -2.039950E+03 &
057139 -1.137010E+03 &
063151 -2.594210E+00 &
060148 -3.358500E+02 &
044101 -7.127980E+02 &
060146 -6.245410E+02 &
064157 -1.037900E-01 &
054134 -1.401980E+03 &
042097 -7.529560E+02 &
040091 -5.904900E+02 &
040093 -6.864520E+02 &
040094 -7.329250E+02 &
042100 -8.551440E+02 &
054132 -9.467280E+02 &
044102 -6.874880E+02 &
046105 -2.988980E+02 &
047109 -5.272200E+01 &
095243 -4.368760E+01 &
056138 -1.204980E+03 &
042098 -7.525010E+02 &
055135 -3.762380E+02 &
058140 -1.174420E+03
```

For the future, the development of additional scripts allowing to generate the neutron and gamma energy spectra associated to entries of the spent fuel library, is foreseen.

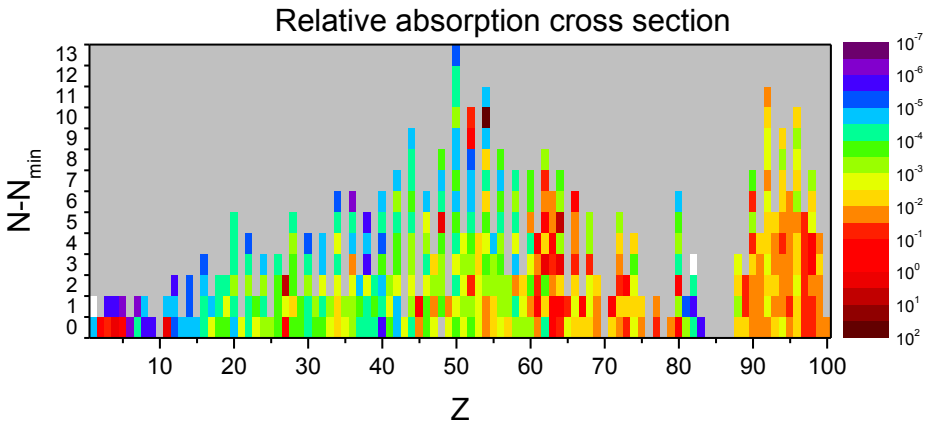

Figure 1: Relative average absorption cross section as a function of the atomic number (Z) and the neutron number N. The maximum value is set to 100. N_{min} is the minimum number of neutron for a given element for which nuclear data are available.

4. Neutron emission study for LEU and MOX 17x17 PWR fuel

4.1. LEU fuel

The total neutron emission and the nuclides contributions were determined as a function of BU and CT for LEU of different IE. The results for the total neutron emissions are compared with the one obtained for an IE=5.0%, which is taken as reference case in this work, in Fig. 2.

To correctly interpret the obtained results, we studied how the nuclide contribution to the total neutron emission varies with BU and CT. The nuclides contribution for the most important nuclides is given in Table 1 for a LEU with IE=2.5% and in Table 2 for a LEU with IE=4.0% for different BU and CT values. The data reveal that at low BU and CT less than 1 year, ^{242}Cm is the main neutron emitter. For intermediate and high burnup, ^{244}Cm contributes the most to the neutron emission until 10^2 y. Between 10^2 and 10^4 y, ^{240}Pu and ^{246}Cm are the main neutron emitters. Above 10^4 y, ^{242}Pu dominates, while the importance of ^{241}Am is limited to specific values of Bu and CT. By comparing the data in Table 1 and Table 2; one can conclude that the roles of the main neutron emitters do not vary strongly with IE.

The data in Table 1, allow an interpretation of the structures present in the data of Fig. 2, as a function of CT. The fact that different nuclides account for the neutron emission for different CT and BU values, explains why such structures can be present. By varying the IE, the production/depletion of the dominant nuclides is enhanced, compared to the reference case, due to the increased neutron flux. Therefore, different structures can be observed.

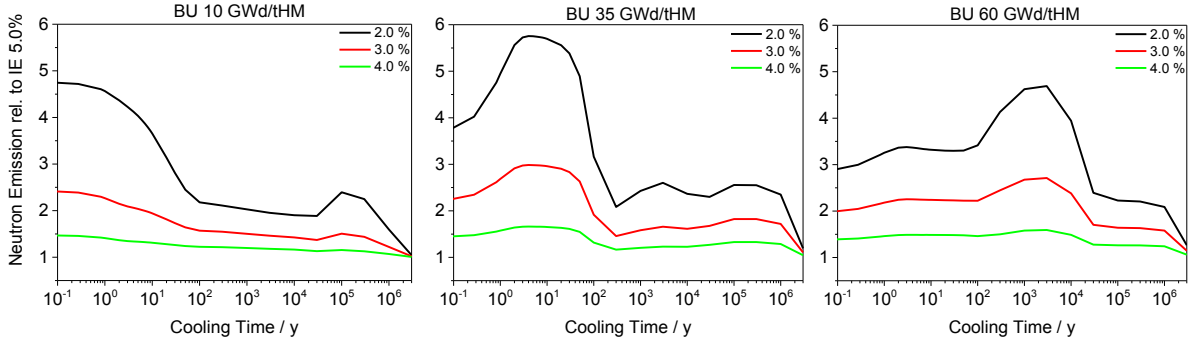

Figure 2: Total neutron emission for LEU fuel as a function of BU, CT and IE. The data are relative to the one for LEU with IE=5.0% at each BU value.

BU	10 GWd/t_{HM}						35 GWd/t_{HM}						60 GWd/t_{HM}					
CT	^{242}Cm	^{244}Cm	^{246}Cm	^{240}Pu	^{242}Pu	^{241}Am	^{242}Cm	^{244}Cm	^{246}Cm	^{240}Pu	^{242}Pu	^{241}Am	^{242}Cm	^{244}Cm	^{246}Cm	^{240}Pu	^{242}Pu	^{241}Am
1 d	73	15		8	1		35	64					12	82	1			
10 d	73	16		8	1		34	65					12	83	1			
100 d	65	20		10	1		26	73					9	86	1			
1 y	37	35		18	1	1	10	88					3	92	1			
3 y	3	51		29	2	4	1	98					0	96	1			
10 y		43		31	2	13		98	1	1				97	2			
30 y		23		36	3	28		94	1	1	1	1		95	4			
10^2 y		2		44	3	40		55	10	12	5	13		58	32	3	2	3
10^3 y				66	5	16			31	38	17	11			84	7	5	2
10^4 y				62	13				19	34	40				71	8	16	
10^5 y					66						96						81	
10^6 y					36						90						80	

Table 1: Percentage share of different nuclides to the total neutron emission as a function of CT and BU for LEU fuel of IE=2.5%.

BU	10 GWd/t_{HM}						35 GWd/t_{HM}						60 GWd/t_{HM}					
CT	^{242}Cm	^{244}Cm	^{246}Cm	^{240}Pu	^{242}Pu	^{241}Am	^{242}Cm	^{244}Cm	^{246}Cm	^{240}Pu	^{242}Pu	^{241}Am	^{242}Cm	^{244}Cm	^{246}Cm	^{240}Pu	^{242}Pu	^{241}Am
1 d	73	9		12			49	50					21	77				
10 d	72	10		12			48	51					20	78				
100 d	64	12		16			39	60					15	83				
1 y	36	21		28	1	1	17	80					5	92				
3 y	3	29		42	2	6	1	96		1				98				
10 y		23		42	2	15		96		1				98	1			
30 y		10		41	2	30		90		3		3		95	3			
10^2 y				44	2	37		40	4	18	5	22		60	23	4	3	5
10^3 y				64	3	14			12	50	17	16			71	14	9	4
10^4 y				59	7				7	45	38				55	16	25	
10^5 y					43						95						91	
10^6 y					18						84						88	

Table 2: Percentage share of different nuclides to the total neutron emission as a function of CT and BU for LEU fuel of IE=4.0%.

Burnup / GWd/t_{HM}	10			35			60		
IE / %	**2.0**	**3.0**	**4.0**	**2.0**	**3.0**	**4.0**	**2.0**	**3.0**	**4.0**
Nuclide	**Mass at discharge**								
^{240}Pu	2.12	1.56	1.22	1.38	1.25	1.11	1.08	1.07	1.04
^{242}Pu	5.79	2.82	1.60	2.66	1.89	1.36	1.76	1.49	1.23
^{242}Cm	4.87	2.54	1.52	1.91	1.56	1.25	1.10	1.10	1.07
^{244}Cm	12.62	4.34	1.92	5.94	3.06	1.69	3.27	2.23	1.49
^{246}Cm	41.24	8.61	2.60	16.28	5.79	2.27	6.89	3.70	1.92

Table 3: Nuclides abundances as a function of IE and burnup. The data of each nuclide are relative to the ones for an IE of 5% at the indicated burnup value.

The data in Fig. 2 reveal also that the neutron emission increases when decreasing the initial enrichment, given the BU and CT. To obtain the same BU levels in the same DIC, i.e. keeping the same AP, LEU fuels with lower IE are irradiated with a neutron flux that is higher compared to the one for LEU fuel with higher IE values. Under higher flux the production of transuranic, and the one of neutron emitters such as ^{242}Cm and ^{244}Cm, happens at a faster rate and this explains why a higher neutron emission is obtained for LEU fuel with lower enrichment.

This interpretation is confirmed by looking at the production of specific neutrons emitters during irradiation for different IE. The concentrations of the main neutron emitters, relative to the one for a 5.0% IE, are given in Table 3, for different values of IE and BU. At all BU values, the nuclides concentrations decrease with IE. The neutron emission, consequently, follows the same pattern. As shown in Fig. 2, at low BU, the fuel has been exposed to relatively low neutron fluence and the nuclides are mainly generated as a consequence of irradiation and their depletion is limited, especially for the Cm isotopes due to their higher mass number. At higher BU, the neutron fluence is higher and also the depletion of the nuclides plays a role in addition to their production. This explains the decreasing sensitivity to IE as BU increases.

4.2. MOX fuel

4.2.1. Comparison with LEU fuel

The total neutron emission and the nuclides contributions to the neutron emission were determined as a function of BU and CT for MOX with different amounts of Pu. The results for the total neutron emissions are compared with the ones obtained for a LEU IE=4.0%, which has approximately the same fissile content, in Fig. 3.

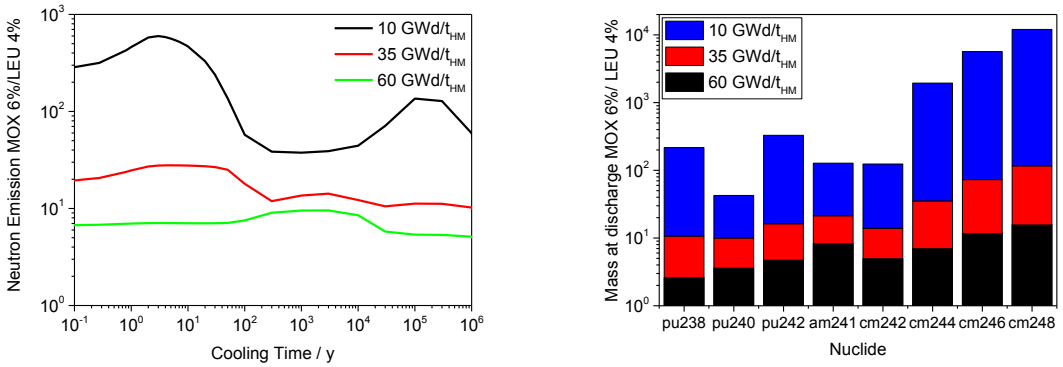

Figure 3: Total neutron emission as function of BU and CT (left) and mass at discharge (right) for the main neutron emitters for different BU values. All the data are for a 6% MOX fuel relative to a 4% LEU fuel.

Due to the presence of Pu isotopes already at the beginning of irradiation, and the consequent earlier production of Cm isotopes, the neutron emission is always higher for MOX fuel. The relative difference decreases as BU increases, as shown in Fig. 3.

Also the nuclides contribution to the total neutron emission strongly differs between LEU and MOX fuel, as indicated in Table 5 and Table 2, at low and intermediate BU values.

BU	**10 GWd/t_{HM}**						**35 GWd/t_{HM}**						**60 GWd/t_{HM}**					
CT	^{242}Cm	^{244}Cm	^{246}Cm	^{240}Pu	^{242}Pu	^{241}Am	^{242}Cm	^{244}Cm	^{246}Cm	^{240}Pu	^{242}Pu	^{241}Am	^{242}Cm	^{244}Cm	^{246}Cm	^{240}Pu	^{242}Pu	^{241}Am
1 d	30	66		1			23	76					15	81		1		
10 d	29	67		1			23	76					15	81		1		
100 d	22	74		2			17	82					11	85		1		
1 y	9	86		2			6	93					4	92		1		
3 y		93		2				98						96		2		
10 y		91		3	1	1		98						97		2		
30 y		82		6	2	4		96	2					94		4		
10^2 y		25		25	10	23		63	15	7	3	8		56	36	2	2	3
10^3 y				56	26	14			52	25	14	8			87	6	4	2
10^4 y				43	50				36	25	36				75	7	14	
10^5 y					98						97						80	
10^6 y					96						96						81	

Table 5: Percentage share of different nuclides to the total neutron emission as a function of CT and BU for MOX fuel with 6% of Pu.

4.2.2. Impact of Pu mass

Both the variation of total neutron emission and the nuclides contributions were studied for MOX fuel with different Pu mass, as function of BU and CT. We refer to the data of Table 5, for the nuclide contribution to the total neutron emission vs BU and CT for a MOX with 6% Pu mass. For all BU values, ^{244}Cm is the main neutron emitter until 10^2 y. Between 10^2 and 10^4 y, ^{240,242}Pu and ^{246}Cm are the main neutron emitters depending on the BU. Above 10^4 y, ^{242}Pu dominates, while the importance of ^{241}Am is limited to specific values of BU and CT. This pattern is present also at other values of Pu mass.

The results for the total neutron emissions are compared with the one obtained for a Pu mass of 10.0%, which is taken as reference case for MOX fuel, in Fig. 4.

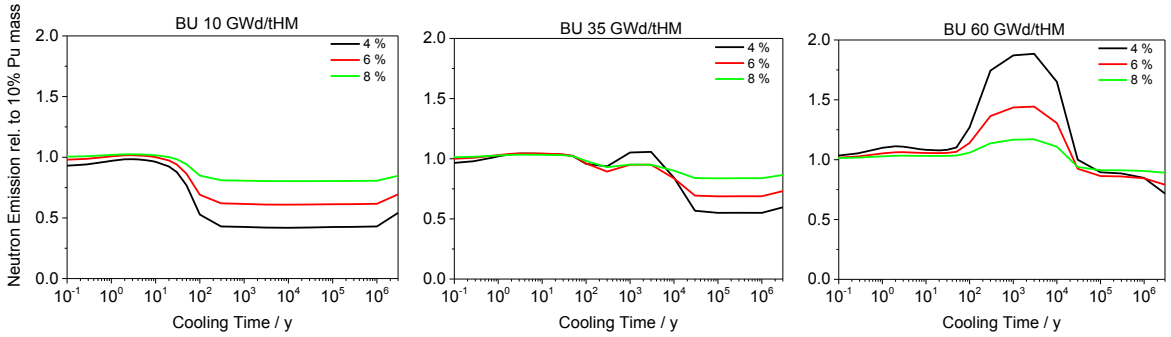

Figure 4: Total neutron emission for MOX fuel as a function of BU, CT and Pu mass. The data are relative to the one for MOX with 10.0% Pu mass at each BU value.

The interpretation of the data in Fig. 4 is not straightforward as for the corresponding data for LEU, given in Fig. 2. In the case of MOX fuel, by varying the Pu mass, we do not change only the amount of fissile material initially present in the fuel, but also overall the mass of Pu (fissile and not fissile isotopes). Therefore two competing phenomena, from the neutron emission point of view, take place during the irradiation: on one hand, at low Pu masses, to achieve the same BU levels in the same DIC, i.e. keeping the same AP, a higher flux is needed; therefore, a higher production of transuranic

and transplutonium nuclides take place; on the other hand, at higher Pu masses, a higher presence of transplutonium nuclides is due to the higher initial mass of Pu isotopes.

Burnup / GWd/t_{HM}	10			35			60		
Pu mass / %	4.0	6.0	8.0	4.0	6.0	8.0	4.0	6.0	8.0
Nuclide	Mass at discharge								
^{240}Pu	0.41	0.60	0.80	0.37	0.57	0.79	0.32	0.53	0.76
^{242}Pu	0.42	0.61	0.80	0.53	0.68	0.84	0.60	0.74	0.87
^{242}Cm	0.78	0.88	0.95	0.71	0.86	0.94	0.53	0.76	0.91
^{244}Cm	1.06	1.07	1.05	1.04	1.05	1.04	1.05	1.04	1.03
^{246}Cm	2.99	1.93	1.37	2.74	1.85	1.34	2.41	1.75	1.31
^{248}Cm	6.61	3.09	1.71	6.35	3.03	1.68	5.81	2.94	1.65

Table 2: Nuclides abundances as a function of Pu mass and burnup. The data of each nuclide are relative to the ones for a Pu mass of 10% at the indicated burnup value.

The interpretation of the data in Fig. 4 and the explanation given above, are supported by the data about the change in the production of specific neutrons emitters during irradiation as a function of Pu mass. The concentrations of several nuclides, relative to the one for a 10% Pu mass, are given in Table 2, for different values of CT, BU and Pu mass. The data reveal a different pattern compared with the data for LEU shown in Table 3. Only for the nuclides with the highest mass numbers (^{246}Cm and ^{248}Cm), the nuclides concentrations decrease with Pu mass at all BU values. For nuclides with lower mass number (^{240}Pu, ^{242}Pu and ^{242}Cm) the nuclides concentrations increase with the Pu mass, while ^{244}Cm shows little sensitivity with Pu mass and BU values.

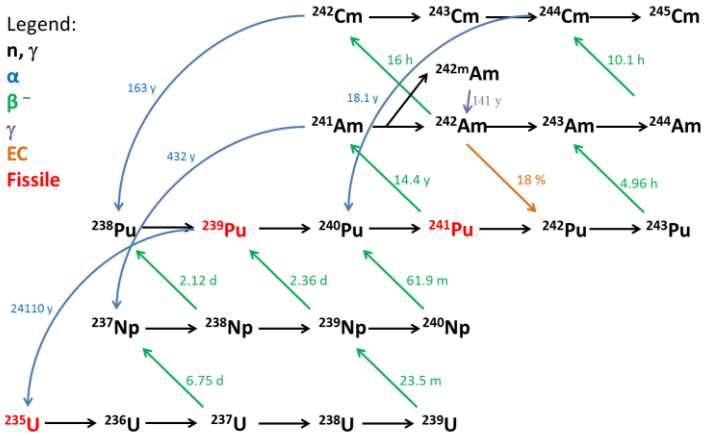

Figure 5: Production of transuranic nuclides during irradiation.

By changing the Pu mass, the initial amount of Pu isotopes changes. The amount of ^{240}Pu and ^{242}Pu, relative to the 10% Pu mass case, almost does not change with BU, indicating the production of nuclides is balanced by their depletion. A similar interpretation is valid for the ^{242}Cm and ^{244}Cm, which, however, are not present initially in the fuel. The ^{242}Cm is produced by beta decay of ^{242}Am and ^{242m}Am, following neutron capture on ^{241}Am, produced from decay of ^{241}Pu, as shown in Fig. 5. This explains why its abundance follows a similar trend as the one observed for Pu isotopes. The production of ^{244}Cm requires more neutron captures from ^{242}Pu, so the variation of its abundance with Pu mass is influenced both by the initial Pu amount and, in the opposite direction, by the higher neutron fluence associated with lower Pu masses. These phenomena explain the obtained data for ^{244}Cm in Table 4.

The neutron emission, consequently, follows a similar pattern. Up to 10^2 y, ^{244}Cm dominates the neutron emission and its production is almost insensitive to Pu mass. Above 10^2 y and at low burnup,

^{240}Pu and ^{242}Pu dominate the neutron emission and their impact scales with the Pu mass. For intermediate and high burnup, ^{246}Cm is the main neutron emitter and the trend of its production with Pu mass explains the structure in the data in Fig. 4, in a similar way to as already seen for LEU fuel.

5. Conclusions and outlook

To better understand and develop methods based on neutron counting and gamma spectroscopy, a significant effort was done at SCK•CEN to determine the source terms associated to spent fuel with depletion and evolution code calculations. The extension of the SCK•CEN spent fuel inventory library with the ORIGEN-ARP code was presented in this paper. The results obtained for a Low Enriched Uranium 17×17 PWR fuel with an initial enrichment of 2.0, 2.5 and 3.0 % were presented and compared with previous work. In addition, results obtained with Mixed Oxide (MOX) fuel with a reference isotopic vector were presented and discussed.

For LEU fuel the impact of the initial enrichment on the neutron emission and production of the main neutron emitters was discussed. To achieve the same burnup value, a higher neutron flux is needed at lower values of the initial enrichment. This has direct impact on the total neutron emission and the production of neutron emitters. In the case of MOX fuel, the impact of the Pu mass on the neutron emission and the production of neutron emitting nuclides was also studied. Both the initial mass of Pu and the neutron fluence required to obtain a given burnup value play an important role in the productions of different neutron emitters. Moreover, specific dynamics, depending on cooling time and burnup values, need to be accounted for to explain the obtained results.

Future work will focus on extending the LEU data up to an initial enrichment of 6.0%, investigate the impact of the isotopic vector on the neutron emission associated to MOX fuel, develop scripts to generate gamma ray and neutron spectra and make available the obtained results to the scientific community.

6. Legal matters

6.1. Privacy regulations and protection of personal data

"I agree that ESARDA may print my name/contact data/photograph/article in the ESARDA Bulletin/Symposium proceedings or any other ESARDA publications and when necessary for any other purposes connected with ESARDA activities."

6.2. Copyright

The authors agree that submission of an article automatically authorises ESARDA to publish the work/article in whole or in part in all ESARDA publications – the bulletin, meeting proceedings, and on the website.

The authors declare that their work/article is original and not a violation or infringement of any existing copyright.

7. References

[1] *Coordinated Technical Research Meeting on Spent Fuel Verification Methods*, IAEA March 3-6 2003

[2] M.T. Swinhoe, D. Beddingfield, and H.O. Menlove, *A Survey Of LWR Spent Fuel And Measurement Methods*, Los Alamos Report, 2002, LA-UR-02-6996

[3] S. Tobin, H. Menlove, M. Swinhoe, M. Schear, *Next Generation Safeguards Initiative research to determine the Pu mass in spent fuel assemblies: Purpose, approach, constraints, implementation, and*

calibration, Nuclear Instruments & Methods In Physics Research Section A, 2011, doi 10.1016/j.nima.2010.09.064

[4] V. Mozin, S. J. Tobin, A. Hunt, J. Vujic, *Delayed Gamma Assay for Spent Nuclear Fuel Safeguards*, LA-UR 11-00261, 2011

[5] P.M. Rinard and G.E. Bosler, *Safeguarding LWR Spent Fuel with the FORK Detector*, Los Alamos National Laboratory report LA-11096-MS (March 1988)

[6] S. Jacobsson, A. Bäcklin A. Håkansson, and P. Jansson, *A Tomographic Method for Experimental Verification of the Integrity of Spent Nuclear Fuel*, Applied Radiation and Isotopes 53 (2000) 681- 689

[7] R.Rossa, A.Borella, K. van der Meer, *Investigation of the Self-Interrogation Neutron Resonance Densitometry applied to spent fuel using Monte Carlo simulations*, Annals of Nuclear Energy 75 (2015) 176–183

[8] S.M. Bowman , O.W. Hermann, L.C. Leal, C.W. Parks, ORIGEN-ARP, A Fast and Easy-to-Use Source Term Generation Tool, ORNL/CP-104231, Oak Ridge 1999

[9] Germina I., et al. *Overview of ORIGEN-ARP and its Application to VVER and RBMK*. Oak Ridge National Laboratory, Oak Ridge, TN, 2007

[10] I. Gauld, S. Bowman, J. Horwedel, *Origen-ARP: automatic rapid processing for spent fuel depletion, decay, and source term analysis,* ORNL/TM-2005/39. January 2009

[11] A. Stankovskiy, G. van den Eynde *ALEPH 2.2 A Monte Carlo Burn-up Code,* SCK•CEN-R-5267, September 2012

[12] C. Gauld, G. Ilas, G. Radulescu, *Uncertainties in Predicted Isotopic Compositions for High Burnup PWR Spent Nuclear Fuel*, NUREG/CR-7012, ORNL/TM-2010/41, United States Nuclear Regulatory Commission (US-NRC). January 2011

[13] A. Stankovskiy, G. van den Eynde, T. Vidmar, *Development and Validation of ALEPH Monte Carlo burn-up code*, Nuclear Measurements, Evaluations and Applications – NEMEA-6. October 2010

[14] B. Lance, *REBUS International Programme, REBUS-PWR Final Report*, Ref. No. File 0501320/221-1 (RE2005/37), SCK•CEN, Belgium. 2006

[15] Borella A., *The Fork Detector for Spent Fuel Measurements: Measurements and Simulations*, In: Proceeding of the 53rd INMM Annual Meeting, Orlando, Florida, United States, 15-19 July 2012

[16] Vaccaro S. et. al., *A New Approach to Fork Measurements Data Analysis by RADAR-CRISP and ORIGEN Integration*, ANIMMA conference proceedings 2013

[17] Rossa R., et al., *Development of a reference spent fuel library of 17x17 PWR fuel assemblies*, ESARDA BULLETIN, No. 50, December 2013

[18] A. Borella, M. Gad, R. Rossa, K. van der Meer, *Sensitivity Studies on the Neutron Emission of Spent Nuclear Fuel by Means of the Origen-ARP Code*, In: Proceeding of the 55th INMM Annual Meeting, Atlanta, Georgia, United States, July 2014.

[19] D. B. Pelowitz (Ed.), MCNPX™ User's Manual Version 2.7.0, LA-CP-11-00438, Los Alamos, 2011

[20] Borella A., et al., *Spent Fuel Measurements with the Fork Detector at the Nuclear Power Plant of Doel*, 33rd ESARDA Annual Meeting, Budapest, Hungary, May 16-20 2011

[21] P.R. Thorne, G. J. O'Connor and R.L. Bowden, *Problem Specification for the OECD/NEANSC Burnup Credit Benchmark Phase IV-B: Mixed Oxide (MOX) Fuels*, BNFL, Risley, Warrington, Cheshire, U.K., Updated February 2002

Influence of fuel composition on the spent fuel verification by Self-Interrogation Neutron Resonance Densitometry

Riccardo Rossa[1,2], Alessandro Borella[1], Pierre-Etienne Labeau[2], Nicolas Pauly[2], Klaas van der Meer[1]

1) SCK•CEN, Belgian Nuclear Research Centre, Boeretang, 200 - B2400 Mol, Belgium

2) Université libre de Bruxelles, Ecole polytechnique de Bruxelles - Service de Métrologie Nucléaire (CP 165/84), Avenue F.D. Roosevelt, 50 - B1050 Brussels, Belgium

E-mail: rrossa@sckcen.be

Abstract:

The Self-Interrogation Neutron Resonance Densitometry (SINRD) is a passive Non-Destructive Assay (NDA) that is developed for the safeguards verification of spent nuclear fuel. The main goal of SINRD is the direct quantification of ^{239}Pu by estimating the SINRD signature, which is the ratio between the neutron flux in the fast energy region and in the region close to the 0.3 eV resonance of ^{239}Pu. The resonance region was chosen because the reduction of the neutron flux within 0.2-0.4 eV is due mainly to neutron absorption from ^{239}Pu, and therefore the SINRD signature can be correlated to the ^{239}Pu mass in the fuel assembly.

This work provides an estimate of the influence of ^{239}Pu and other nuclides on the SINRD signature. This assessment is performed by Monte Carlo simulations by introducing several nuclides in the fuel material composition and by calculating the SINRD signature for each case. The reference spent fuel library developed by SCK•CEN was used for the detailed fuel compositions of PWR 17x17 fuel assemblies with different initial enrichments, burnup, and cooling times.

The results from the simulations show that the SINRD signature is mainly correlated to the ^{239}Pu mass, with significant influence by ^{235}U. Moreover, the SINRD technique is largely insensitive to the cooling time of the assembly, while it is affected by the burnup and initial enrichment of the fuel. Apart from ^{239}Pu and ^{235}U, many other nuclides give minor contributions to the SINRD signature, especially at burnup higher than 20 GWd/t_{HM}.

Keywords: SINRD, neutron resonance densitometry, reference spent fuel library, Non-Destructive Assay, spent fuel verification

1. Introduction

The International Atomic Energy Agency (IAEA) has the task to ensure that all nuclear activities in the Member States are devoted exclusively to peaceful applications. In order to achieve this objective, the Nuclear Material Accountancy (NMA) is the primary verification tool, and it is supported by Containment and Surveillance (C/S) measures [1].

As part of the NMA for spent nuclear fuel, the non-destructive assays (NDA) are playing an important role for the verification of operator data. Moreover, they can be used for the characterization of spent fuel both for safeguards verification and for other applications such as the disposal of spent fuel in a geological repository [2]. Many NDA methods are currently under investigation to improve the capabilities of current NDA techniques [3], and the Self-Interrogation Neutron Resonance Densitometry (SINRD) is proposed to directly quantify the ^{239}Pu mass in a fuel assembly [4].

However, in addition to ^{239}Pu, spent fuel contains a wide variety of radioactive elements that are resulting from the irradiation in the reactor core. In order to evaluate the influence of several nuclides on the results of the SINRD technique, a set of simulations were carried out considering fuel with different fuel compositions. The impact of single nuclides included in the fuel composition was evaluated following a multi-step procedure. Starting from fuel containing only ^{238}U and ^{16}O other nuclides were added sequentially to estimate the effects of each isotope on the SINRD signature and on the neutron energy distribution. Moreover, the SINRD signature was calculated for fuel with different initial enrichment, burnup, and cooling time, to evaluate the sensitivity of SINRD to the fuel irradiation history.

This paper first describes the approach chosen to investigate the SINRD technique, together with a description of the Monte Carlo model developed for the simulations and the details of the fuel compositions used in the study. Then the influence of single nuclides on the SINRD signature is evaluated in Section 4, whereas the impact of the fuel irradiation history is analyzed in Section 5.

2. Background on the SINRD technique

The SINRD technique is a passive NDA method that has the unique feature to directly quantify the ^{239}Pu content in a spent fuel assembly, and this goal is achieved by measuring the attenuation of the neutron flux in the 0.2-0.4 eV energy region. This energy region is close to the significant resonance of ^{239}Pu, and therefore the reduction of the neutron flux is expected to be correlated to the ^{239}Pu concentration in the fuel [5], [6], [7], [8].

The ^{239}Pu content is estimated using the SINRD signature, which is defined in Formula (a) as the ratio between the neutron flux in the fast energy region (*FAST*) and in the region close to the resonance (*RES*).

$$SINRD = \frac{FAST}{RES} \qquad (a)$$

A ^{238}U fission chamber and a ^{239}Pu fission chamber are envisaged to measure the fast neutron flux and the flux around the 0.3 eV resonance region, respectively. The term "self-indication" can also be used in the acronym of SINRD instead of “self-interrogation” because the isotope quantified with the technique is also used as active material in the detector to increase the detection of neutrons in the resonance region. Apart from the SINRD technique, self-indication measurements are a well-established method for cross-section measurements [9], [10], [11]. In the approach proposed for SINRD the ^{239}Pu resonance region is selected by wrapping a foil of Gd or Cd around the ^{239}Pu fission chamber. These elements are also called filters because they exhibit a cut-off energy for neutron absorption slightly below and above 0.3 eV. Therefore by taking the difference between the neutron fluxes transmitted through each filter, the estimation of the neutron flux around 0.3 eV is possible.

3. Description of the model

3.1 Monte Carlo model of the fuel assembly and detector

The PWR 17x17 fuel assembly geometry was taken as reference for the development of the Monte Carlo model. The MCNPX code [12] was used to create the model of the fuel assembly and of the 12 cm thick layer of polyethylene surrounding it. By simulating this configuration the neutron moderation occurred mainly outside the fuel assembly and this leads to a clearer reduction of the neutron flux at 0.3 eV due to ^{239}Pu absorption. In fact, the neutron moderation within the fuel pins occurring when the fuel assembly is stored under water is detrimental for the SINRD technique, because it reduces the indication of the neutron absorption due to ^{239}Pu as mentioned in [13], [14].

The neutron flux was calculated in the central guide tube of the assembly in a void cavity that can host the neutron detector and filter. No model of detector or filter was placed at this stage in the simulation, and the flux transmitted through the filter (φ_{tr}) used for the calculation of *RES* was estimated as:

$$\varphi_{tr} = \varphi_{in} \cdot exp(-d \cdot l \cdot \sigma_{tot}^{D}) \qquad (b)$$

where *d* is the atom density, *l* is the thickness, and σ_{tot}^{D} is the Doppler broadened total cross-section of the filter. Therefore, the transmitted flux is directly related to the total cross section and the area density of the elements present in a sample [15]. Considering the results in [16], a 0.1 mm Gd filter and a 1.0 mm Cd filter were used in the calculations to achieve a good balance between significant sensitivity to ^{239}Pu and large total neutron counts.

For the estimation of *FAST*, Formula (b) was modified by neglecting the exponential term since a bare ^{238}U fission chamber is used for the measurement.

3.2 Characteristics of the spent fuel compositions

Fuel compositions containing the 50 main neutron absorbers were selected for this study in order to account for the influence of single nuclides on the SINRD signature. The reference spent fuel library was developed for more than 1600 case studies according to several variables such as initial enrichment, fuel burnup, and cooling time after discharge [17], [18].

In this paper the fuel compositions calculated for 4 values of initial enrichment (i.e. 3.5, 4.0, 4.5, 5.0%), 6 values of burnup (i.e. 5, 10, 15, 20, 40, 60 GWd/t_{HM}), and 5 values of cooling time (i.e. direct discharge, 30 days, 5, 10, 50 years) were included in the Monte Carlo simulations.

The simulations in Section 4 evaluated the influence of single nuclides on the SINRD signature, and the ^{239}Pu concentration was selected first as additional nuclide apart from ^{238}U and ^{16}O. Then several nuclides were added sequentially and the SINRD signature was calculated for each case. The concentration of each nuclide added in the fuel composition was taken from the reference fuel library, and the quantity of ^{238}U was adjusted to keep a constant total fuel mass. The study in Section 5 compared the SINRD signature calculated for fuel with different irradiation histories. The fuel composition for these simulations contained the 50 main neutron absorbers as calculated in the reference spent fuel library.

4. Influence of single nuclides on the SINRD technique

4.1 SINRD signature

One of the objectives of this paper is to investigate the influence that single nuclides have on the SINRD signature. To reach this goal, several simulations were performed starting from fuel containing only ^{238}U and ^{16}O, and then adding one nuclide sequentially as described in Section 3.2. The nuclides chosen in this section represent the nuclides that have the highest macroscopic cross-section in the energy region around 0.3 eV and therefore are expected to give the major contributions to the SINRD signature [14].

Figure 1 shows the normalized SINRD signature as a function of the ^{239}Pu content for the cases selected in this study. The simulations considered fuel with 3.5% initial enrichment, 10 years of cooling time, and burnup up to 60 GWd/t_{HM} as indicated in the plot. The values of the SINRD signature were normalized to the case obtained for fuel containing only ^{238}U and ^{16}O. Several groups of data points can be identified on the plot as a function of the ^{239}Pu content, and they reflect the different fuel burnup considered in this study.

At low burnup fuel the SINRD signature obtained with a detailed fuel composition is almost the same as the signature obtained with only ^{239}Pu and ^{235}U as additional nuclides. Moreover, the ^{235}U gives the major contribution up to 20 GWd/t_{HM}. By increasing the burnup the contribution from other nuclides becomes more relevant, and Table 1 shows the share of SINRD signature due to the single nuclides added in the fuel composition for fuel with 3.5% initial enrichment, 10 years cooling time, and 60 GWd/t_{HM} burnup. For the cases reported in Table 1 the two main fissile isotopes in spent fuel, namely ^{239}Pu and ^{235}U, account only for about 60% of the SINRD signature.

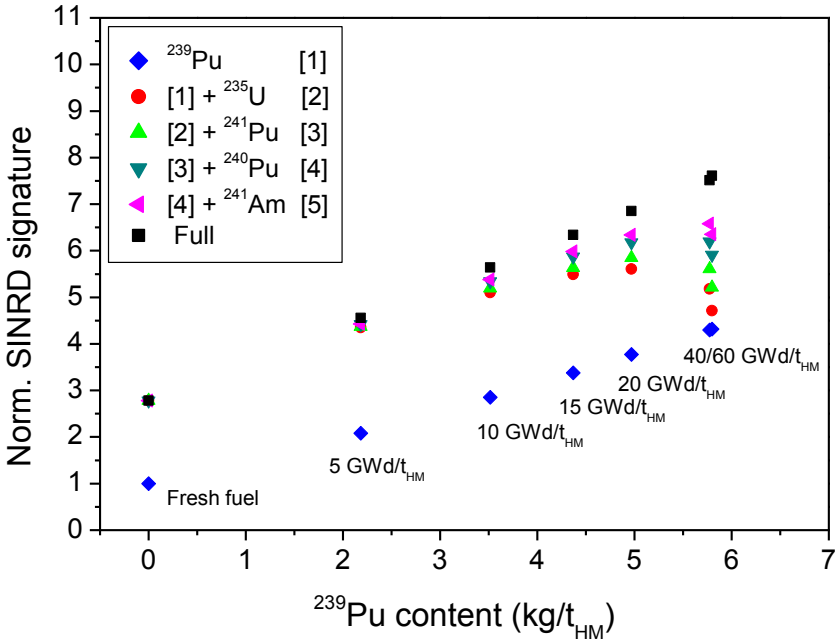

Figure 1: Normalized SINRD signature as a function of the ^{239}Pu content. The legend shows the additional nuclide added in the simulation starting from ^{238}U and ^{16}O. The values reported close to the data points refer to the fuel burnup.

Nuclide		SINRD signature	Share of full material card
^{239}Pu	[1]	4.3	57 %
[1] + ^{235}U	[2]	4.7	62 %
[2] + ^{241}Pu	[3]	5.2	68 %
[3] + ^{240}Pu	[4]	5.9	78 %
[4] + ^{241}Am	[5]	6.4	83 %
Full card		7.6	100 %

Table 1: Normalized SINRD signature and share compared to the full material card. The values refer to fuel with burnup of 60 GWd/t_{HM} and the uncertainty associated to the SINRD signature was always lower than 0.1%.

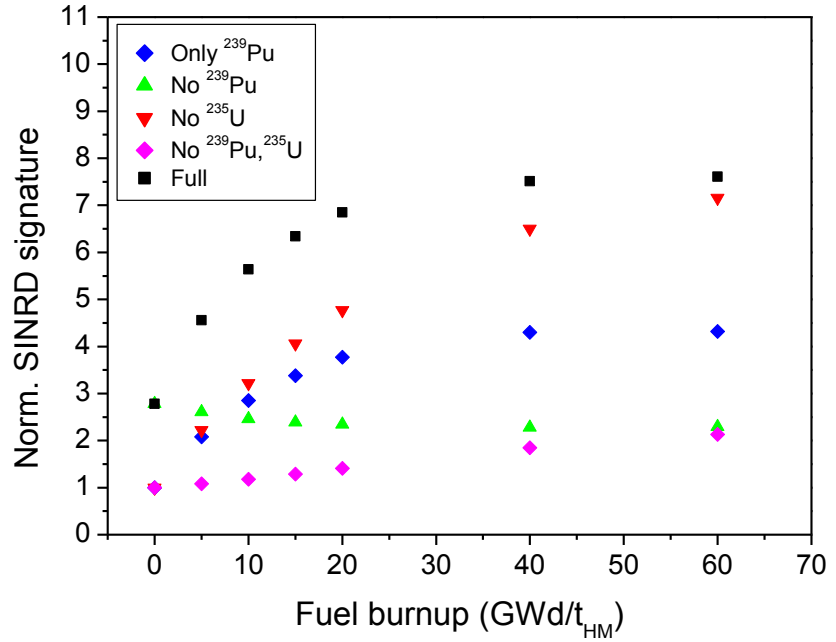

Figure 2: Normalized SINRD signature as a function of the fuel burnup for different fuel compositions.

Additional simulations were performed to evaluate the influence of both ^{239}Pu and ^{235}U on the SINRD signature. Figure 2 shows the normalized SINRD signature as a function of the fuel burnup for several fuel compositions. The plot contains the results obtained for full material cards and for fuel with only ^{239}Pu, ^{238}U, and ^{16}O. In addition, the SINRD signature was calculated for fuel where ^{239}Pu, ^{235}U, or both ^{239}Pu and ^{235}U were removed from the material composition. All cases reported in the figure show almost constant SINRD signatures for fuel with burnup higher than 40 GWd/t$_{HM}$, because the ^{239}Pu content in the fuel is not varying at high burnup. Moreover, the figure shows that by excluding the ^{239}Pu from the fuel composition the SINRD signature is almost independent from the fuel burnup, and this supports the concept that the SINRD signature is mainly affected by the ^{239}Pu fuel content.

4.2 Energy distributions of the neutron flux

As shown in Figure 1 the SINRD signature is influenced by several nuclides, and the mass of each nuclide in the fuel composition depends on the fuel burnup. To investigate the results included in the previous section, Figures 3 and 4 show the energy distributions of the neutron fluxes in the resonance and in the fast energy regions for fuel with burnup of 15 GWd/t$_{HM}$ and 60 GWd/t$_{HM}$ respectively. The color scheme used in the figures to indicate the fuel composition is the same of Figure 1.

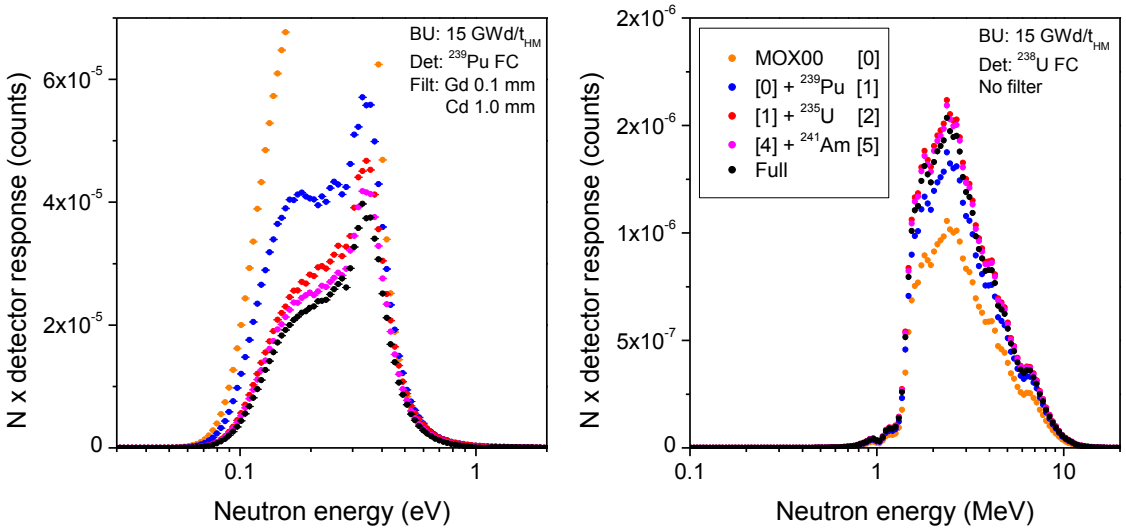

Figure 3: Energy distributions of the neutron fluxes in the resonance *(left)* and fast *(right)* energy regions. The color scheme used to indicate the fuel composition is the same as Figure 1 and the compositions refer to fuel with burnup of 15 GWd/t$_{HM}$.

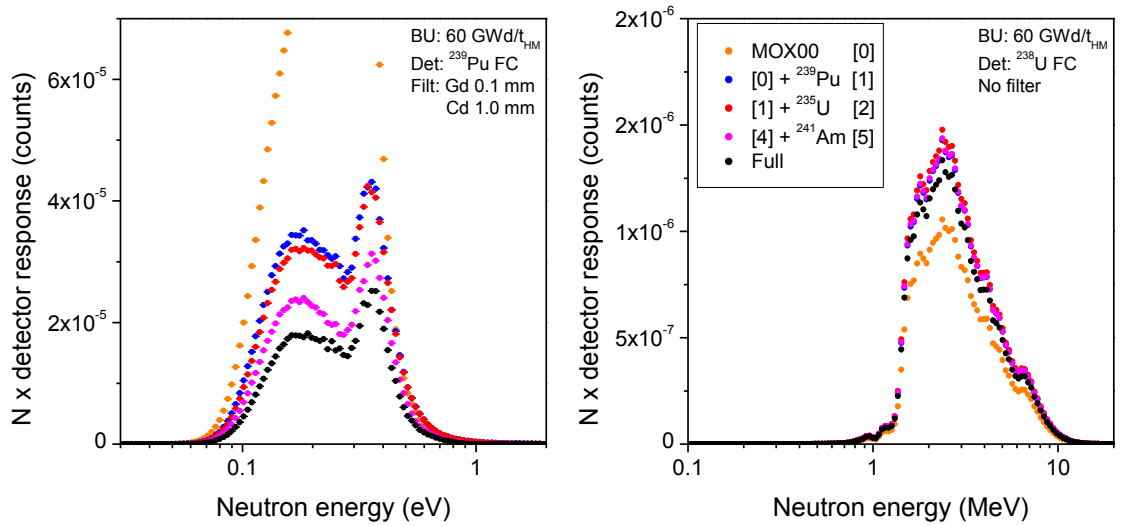

Figure 4: Energy distributions of the neutron fluxes in the resonance *(left)* and fast *(right)* energy regions. The color scheme used to indicate the fuel composition is the same as Figure 1 and the compositions refer to fuel with burnup of 60 GWd/t$_{HM}$.

The energy distribution in the resonance region was calculated as the difference between the transmitted fluxes through Gd and Cd filters, and by considering ^{239}Pu as active material in the detector, while for the fast energy region the response of a bare ^{238}U fission chamber was calculated.

The plots of the resonance region show a decrease when nuclides are added to fuel containing only ^{238}U and ^{16}O (MOX00), while an opposite trend is shown in the graphs of the fast energy region. The reduction of the neutron flux in the resonance region is due to the neutron absorptions from different nuclides, while the increase in the fast energy region is linked to the increase of the total fissile material in the fuel. For both burnup values there is a significant decrease of the neutron flux in the resonance region due to ^{239}Pu absorption, while significant effect is due to ^{235}U only for fuel with burnup of 15 GWd/t_{HM}. Moreover, for fuel with burnup of 60 GWd/t_{HM} several nuclides are responsible for the reduction of the neutron flux in the resonance region, while the curves for fuel with burnup of 15 GWd/t_{HM} and containing only ^{239}Pu and ^{235}U are rather similar to the results obtained with full material composition.

Focusing on the fast energy region, this region is less influenced by the fuel composition compared to the resonance region. However, still significant contributions can be seen from ^{239}Pu and ^{235}U for fuel with burnup of 15 GWd/t_{HM}, while ^{239}Pu alone gives the main influence for fuel with higher burnup.

5. Impact of the fuel composition on the SINRD signature

The nuclides included in the fuel composition have an influence on the energy distribution of the neutron flux and therefore result also in a variation of the SINRD signature.

Figure 5 shows the SINRD signature calculated for the fuel compositions mentioned in the previous section starting from data obtained in the reference spent fuel library. The values are normalized to the SINRD signature calculated for fuel containing only ^{238}U and ^{16}O.

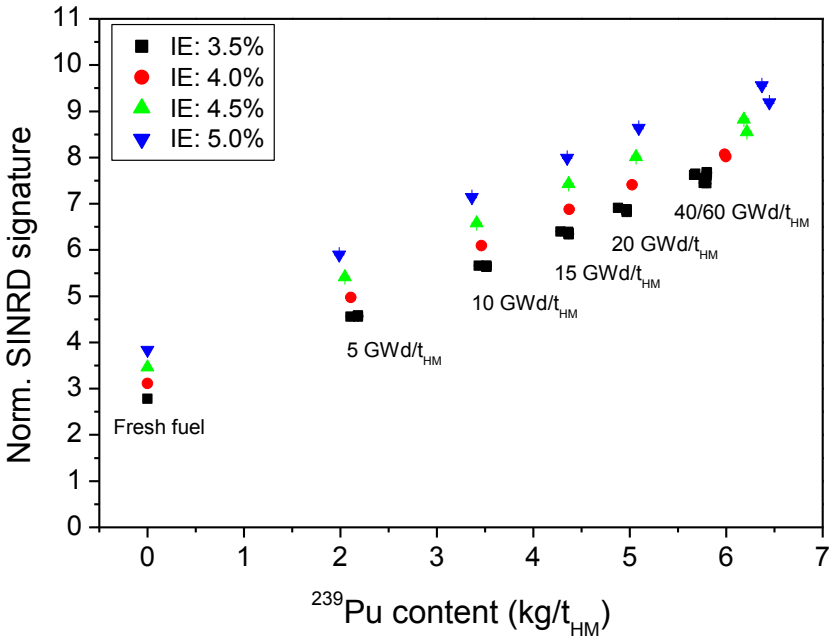

Figure 5: Normalized SINRD signature as a function of the ^{239}Pu content for several fuel compositions. The burnup values corresponding to different data groups are reported in the figure.

A significant trend can be observed with the initial enrichment and burnup of the fuel; the increase of the SINRD signature with the initial enrichment is due to the increasing ^{235}U content, while the increase with the fuel burnup is due to the increasing ^{239}Pu concentration. Only the results from simulations with burnup of 40 and 60 GWd/t_{HM} give similar SINRD signatures because the ^{239}Pu content in these cases is similar.

The SINRD signature is reported in Figure 5 for several cooling times only for the fuel with 3.5% initial enrichment. As shown in the figure, the cooling time of the fuel assembly does not influence significantly the SINRD signature, and this is because both ^{235}U and ^{239}Pu concentrations are not affected by this parameter. Therefore, the SINRD signature shown in Figure 5 for other initial enrichments refers only to the cooling time of 10 years.

The results from these simulations agree with previous results [14] that concluded that the SINRD signature was mainly influenced by the ^{239}Pu and ^{235}U concentrations and minor effects were due to other nuclides.

6. Conclusions

The SINRD technique aims at the direct quantification of ^{239}Pu in a fuel assembly by measuring the attenuation of the neutron flux close to 0.3 eV due to the neutron absorptions of this nuclide. However, since all isotopes present in the fuel assembly determine a variation in the energy distribution of the neutron flux, this paper estimated the influence that single nuclides have on the SINRD technique.

By using the results of the reference spent fuel library developed by SCK•CEN, ^{239}Pu and ^{235}U were the isotopes that influenced mostly this parameter, but for burnup higher than 20 GWd/t_{HM} significant contributions from other nuclides such as ^{240}Pu, ^{241}Pu, and ^{241}Am were observed. Finally, the correlation between the SINRD signature and the ^{239}Pu fuel content was confirmed because the simulations of fuel without ^{239}Pu did not show any significant trend for the SINRD signature.

The energy distribution of the neutron flux calculated with different fuel composition confirmed the major role of ^{239}Pu and ^{235}U on the SINRD signature, and highlighted the balance between the neutron absorptions in the resonance region due to multiple nuclides and the increase of the fast neutron flux due to the presence of fissile material.

Considering the 50 main neutron absorbers present in the spent fuel, the SIRND signature was calculated for fuel compositions reflecting several combinations of initial enrichment, burnup, and cooling time. It was found that the SINRD signature increases with initial enrichment and burnup because of the increase of the ^{235}U and ^{239}Pu concentrations respectively. On the other hand, the cooling time did not influence significantly the results because the ^{235}U and ^{239}Pu contents are not affected by this parameter.

7. Acknowledgment

This work is sponsored by GDF SUEZ in the framework of the cooperation agreement CO-90-07-2124 between SCK•CEN and GDF SUEZ.

8. Legal matters

8.1. Privacy regulations and protection of personal data

"I agree that ESARDA may print my name/contact data/photograph/article in the ESARDA Bulletin/Symposium proceedings or any other ESARDA publications and when necessary for any other purposes connected with ESARDA activities."

8.2. Copyright

9. References

[1] International Atomic Energy Agency (IAEA), 2011. *"Safeguards Techniques and Equipment: 2011 Edition"*, IAEA/NVS/1/2011 (Rev. 2). Vienna, IAEA.

[2] International Atomic Energy Agency (IAEA), 2008. *"Spent Fuel Reprocessing Options"*, IAEA-TECDOC-1587. Vienna, IAEA.

[3] Tobin S. J., et al., 2013. *"Prototype Development and Field Trials under the Next Generation Safeguards Initiative Spent Fuel Non-Destructive Assay Project"*, proceedings of the 35th ESARDA Symposium.

[4] Menlove H. O., et al., 1969. *"A Resonance Self-Indication Technique for Isotopic Assay of Fissile Materials"*. Nuclear Applications Vol. 6.

[5] LaFleur A. M., 2011. *"Development of Self-Interrogation Neutron Resonance Densitometry (SINRD) to Measure the Fissile Content in Nuclear Fuel"*. PhD dissertation at Texas A&M University.

[6] LaFleur A. M., et al., 2012. *"Comparison of Fresh Fuel Experimental Measurements to MCNPX Calculations Using Self-Interrogation Neutron Resonance Densitometry",* Nuclear Instruments and Methods Section A, 680 (2012) 168-178.

[7] LaFleur A. M., et al., 2013. *"Development of Self-Interrogation Neutron Resonance Densitometry to Improve Detection of Partial Defects in PWR Spent Fuel Assemblies",* Nuclear Technology, 181, (2013) 354 – 370.

[8] LaFleur A. M., et al., 2015. *"Analysis of experimental measurements of PWR fresh and spent fuel assemblies using Self-Interrogation Neutron Resonance Densitometry",* Nuclear Instruments and Methods Section A, DOI:10.1016/j.nima.2015.01.029.

[9] Fröhner F. H., et al., 1966. *"Accuracy of Neutron Resonance Parameters from Combined Area and Self-Indication Ratio Measurements".* Proceedings of the Conference on Neutron Cross Section Technology, P. Hemmig (ed.), CONF-660 303, Washington D.C. (1966) Book 1, pp. 55-66.

[10] Bakalov T., et al., 1980. *"Transmission and self-indication measurements with U-235 and Pu-239 in the 2 eV-20 keV energy region"*, NBS Special Publications, (594), 692-697.

[11] Massimi C., et al., 2011. *"Neutron resonance parameters of 197Au from transmission, capture and self-indication measurements"*, J. Korean Phys. Soc. 59, 1689 – 1692.

[12] Pelowitz D., 2011. *"MCNPX User's Manual Version 2.7.0"*. Los Alamos National Laboratory. LA-CP-11-00438.

[13] Hu J., et al., 2012. *"The performance of self-interrogation neutron resonance densitometry in measuring spent fuel"*. Journal of Nuclear Material Management, Volume XL, No.3.

[14] Rossa R., et al., 2015. *"Investigation of the Self-Interrogation Neutron Resonance Densitometry applied to spent fuel using Monte Carlo simulations"*, Annals of Nuclear Energy 75 (2015) 176-183.

[15] Schillebeeckx P., et al., 2011. *"Neutron resonance spectroscopy for the characterization of materials and objects"*. 2nd International Workshop on Fast Neutron Detectors and Applications.

[16] Rossa R., et al., 2015. *"Neutron absorbers and detector types for spent fuel verification using the Self-Interrogation Neutron Resonance Densitometry"*, submitted for publication in Nuclear Instruments and Methods Section A, forthcoming.

[17] Rossa R., et al., 2013. *"Development of a reference spent fuel library of 17x17 PWR fuel assemblies"*, ESARDA Bulletin Issue 49.

[18] Borella A., et al., 2014. *"Sensitivity Studies on the Neutron Emission of Spent Nuclear Fuel by Means of the Origen-ARP Code"*. Proceeding of the 55th INMM Annual Meeting, Atlanta, Georgia, United States.

Development of a Differential Die-Away Instrument for Characterization of Swedish Spent Nuclear Fuel

Tomas Martinik[1,2], Vladimir Henzl[2], Sophie Grape[1], Peter Jansson[1], Martyn T. Swinhoe[2], Alison V. Goodsell[2], Stephen J. Tobin[2]

[1]Department of Physics and Astronomy
Division of Applied Nuclear Physics
Box 516, Uppsala, Sweden
E-mail: tomas.martinik@physics.uu.se

[2]Los Alamos National Laboratory
P.O.Box 1663, Los Alamos
NM 87545, USA

Abstract:

An active non-destructive assay technique - differential die-away (DDA) - is being investigated within the Next Generation Safeguards Initiative Spent Fuel project as one of several promising alternatives to currently available instruments used for spent nuclear fuel assemblies (SFAs) characterization.

An external neutron generator produces interrogating neutrons which thermalize while penetrating the SFA to induce fission primarily on the fissile content, typically ^{235}U, ^{239}Pu and ^{241}Pu. The strength of the signal and the time distribution of detected neutrons depend on a balance between the amount of fissile isotopes and neutron absorbers, and reflect the overall SFA isotopic composition and irradiation history. Taking advantage of differences in dynamic evolution of the detected signal, the DDA instrument can determine various characteristics of SFAs, be it multiplication, total Pu content, fissile content, initial enrichment, burn-up and presence of certain types of partial defects.

Given the demand from the Swedish Nuclear Fuel and Waste Management Company for an instrument for spent fuel characterization, the DDA instrument is being developed to independently verify both boiling water and pressurized water reactor fuel assemblies. The first prototype of DDA instrument is customized for deployment in the central interim storage facility (Clab) in order to perform test measurements on 50 SFAs with different characteristic parameters. A future DDA instrument is considered to reliably characterize more than 40 000 SFAs at the encapsulation facility (Clink) before the fuel is deposited into the geological repository.

Within the scope of this paper, the selection and design of individual components as well as operational aspects of the DDA instrument developed for its specific use in Clab will be described. Additionally we provide justification for individual decisions made accompanied by a discussion of potential changes in the DDA instrument performance should the individual components be chosen differently.

Keywords: differential die-away, spent nuclear fuel, non-destructive assay, prompt fission neutron detection, Clab

1. Introduction

In 2009, The Next Generation Safeguards Initiative Spent Fuel project (NGSI-SF) of the United States Department of Energy [1] began the effort of researching new alternatives to existing non-destructive assay (NDA) techniques for nuclear safeguards with a particular emphasis on the capability of an integrated NDA system. The primary goals of the project are to (1) detect the diversion or replacement of pins, (2) determine Pu mass in spent fuel, (3) verify initial enrichment (IE), burn-up (BU) and cooling

time (CT) of the spent nuclear fuel (SNF) declared by the facility's operators, and (4) estimate the heat content.

The NGSI-SF project initially suggested the use of 14 different techniques, each of which was evaluated in terms of their possible application to SNF characterization. One of these techniques, differential die-away (DDA), has been chosen for further research because initial simulation results indicated the potential for independent verification of various fuel parameters. Following the simulation results from the earlier stage of this project, the DDA method revealed the potential for this technique to be comprehensive. The DDA based instrument is expected to be able to measure spent fuel assembly (SFA) multiplication [2] determine total Pu content [3], and measure total fissile content [4], IE, and BU [5].

An SFA, after being irradiated inside the reactor core during several operational cycles, contains a considerable amount of nuclear material, which can be used for illicit purposes. To prevent the illegal proliferation of nuclear material, SFAs are required to be characterized and verified in accordance with international safeguards agreements. After the irradiation, the SFAs are placed and kept inside a temporary storage facility, before a final decision is made on how to deal with the nuclear waste. In principle, the three main options are to (1) reprocess the SFA, (2) deposit the fuel in a repository, or (3) postpone the final decision. In Sweden, the current plan is to encapsulate the SFAs in dedicated copper containers, which are inserted in a long-term geological repository. The process of encapsulation is expected to start in 2023 in a newly built facility named Clink, which will be located in close proximity to the current interim storage facility Clab in Oskarshamn. The estimated operational time of Clink is until approximately 2070, when all the SFAs are expected to be encapsulated and transported by ship to the long-term geological repository in Forsmark. There the canisters will be placed 500 meters below the surface in the granite rock.

Given the objective to accurately characterize the SFAs before the final encapsulation, the Swedish Nuclear Fuel and Waste Management Company (SKB) has joined the NGSI-SF in a collaborative effort to develop instrument(s) for SFA characterization in a future Swedish encapsulation facility. The participation of Sweden in the collaboration has created an opportunity for the project to test the performance of instruments researched within the NGSI-SF on commercially used SFAs. The DDA instrument was designed to be deployed and tested in Clab. If the expected performance of the DDA instrument is successfully confirmed, the same or an improved version may be used at Clink. The DDA prototype, as described in more detail in [6], has been designed and will soon be under construction at Los Alamos National Laboratory (LANL). Following the completion of the prototype construction, the performance of the DDA instrument is planned to be first tested on fresh fuel assemblies (FFAs) at LANL, and then on a set of 25 pressurized water reactor (PWR) and 25 boiling water reactor (BWR) SFAs at Clab.

As the DDA instrument is expected to share certain structural components with other instruments designed for Clab, e.g. the differential die-away self-interrogation instrument (DDSI), some construction modifications have been made to the design proposed in [6]. Within the scope of this paper, we summarize the individual components of DDA design as described together with the simulation results in [6], and we list major modifications that are based on practical considerations of a real-life industrial type of deployment. In addition, the consequences of such changes on the DDA performance and operation are discussed.

2. The Differential Die-Away Technique

The DDA is an NDA technique based on the active interrogation of fissile isotopes of an item that contains nuclear material, e.g. SFAs, by neutrons from an external source. A neutron generator (NG), which is commonly used as a source of these neutrons, injects short and intense pulses of fast neutrons to the SFA. The highly energetic neutrons penetrate deep into the SFA, thermalize, and induce fission primarily in fissile isotopes (i.e., ^{239}Pu, ^{241}Pu, and ^{235}U). The induced fission leads to the emission of prompt fission neutrons, which are either detected by detectors surrounding the SFA, are absorbed in the material, or induce another fission reaction. While the NG neutrons that hit the detector directly without any previous fission reaction (so-called "burst neutrons") die away on the order of tens of μs, the induced fission neutrons remain inside the SFA for longer time, and are

absorbed with die-away time approximately in the range of 80 – 180 μs. The name of the DDA method is derived from the difference in die-away times of these two different groups of neutrons.

The DDA instrument provides the information primarily from two measurable quantities: (1) the integral sum of the DDA signal detected in a certain time domain following the end of the interrogation neutron pulse; and (2) the die-away time, which can be determined in various time domains by least square exponential fit of the DDA signal distribution. Both of these quantities are driven by SFA composition and are dependent on the balance between the amount of fissile material and the amount of neutron absorbers in the fuel. The DDA signal is typically stronger for FFAs that usually have higher fissile content than the irradiated fuel assemblies, which also contain a significant amount of neutron absorbers. The die-away time in the early time domain reflects the amount of present neutron absorbers but in the later time domain reflects the SFA multiplication. The die-away time tends to decrease with higher BU as the amount of neutron absorbers also increases. The DDA signal and die-away time may be used to characterize the SFAs (i.e., to determine the IE, BU, CT, and Pu mass and total fissile content) [3,4,5].

3. Differential Die-Away Instrument Proposed for Clab

The design of the first DDA deployment-ready prototype as introduced in [6] and illustrated in Fig. 1 has been developed with special consideration for deployment in Sweden. The DDA design initially introduced by [7] has been subject to extensive research and underwent significant evolution before the design of the first prototype was released [6]. The first modification of the DDA instrument with the objective of practical operation and deployment in Sweden was done by Lundkvist et al. [8], and was later further developed in [6]. The first DDA design simplifications were made in [8] investigating also a light weight version of the DDA instrument, which is designed to be more easily transportable. However, this concept was later abandoned as not perspective for the Swedish application given the operators requirement not to use fission chambers in the instrument design. As a result, the conceptual design by Blanc et al. [9] using ^{3}He detectors was taken to be a starting point for a new research path of the Clab design. The latest design proposed for use in Clab as described in [6] features many components similar to the Blanc conceptual design. A significant difference is the choice of commercial off-the-shelf components that, once combined together, provide a fully functioning instrument able to operate in the high radiation environment and handle the high neutron detection rates expected on individual ^{3}He detectors. Several of the components that are critical for the proper functionality and that essentially dictate the final layout [6] are summarized below:

- **Neutron generator** - The selected NG is a ThermoScientific™ model P 385 [10]. It provides a nominally highest achievable neutron yield of ~$3\cdot10^{8}$ n/s that should be sustainable over long (months to years) periods of operation. It is anticipated to be operated at a minimum yield of $1\cdot10^{8}$ n/s with a 5% duty cycle and 2500 Hz pulse frequency.
- **Detectors + polyethylene moderator** – In total, twelve ^{3}He detectors were placed around the SFA. The detectors are 5 cm in active length, have a 1.25 cm diameter, and have a gas pressure of 7.5 atm. Small detectors were chosen to limit the count rate and to assay only a limited region of the SFA in the vertical direction as the BU distribution of the SFAs can vary significantly along the vertical axis, i.e. edges of PWR SFAs and the entire length of BWR SFAs. The decreased efficiency due to limited length is compensated by an increased inner pressure which improves the detection efficiency. All detectors are enclosed in a 1.4 cm thick polyethylene sleeve which is covered by a 0.1 cm thick cadmium (Cd) liner to make the detector exclusively sensitive to the prompt fission neutrons.
- **Cd liner around SFA** – Previous research [8] suggests that a Cd liner around SFA should be used to prevent the return of thermalized neutrons from the water back to the SFA. This component is essential especially if the SFA is surrounded by a relatively thick (> 1 cm) layer of water.
- **Lead shielding of detectors** – The preamplifiers of ^{3}He detectors and detector themselves must be shielded from gamma rays emitted by SFA; therefore, a 5 cm thick and 50 cm high lead collar was placed between the SFA and detectors to minimize the exposure of ^{3}He detectors.
- **Tailoring material between the NG and SFA** – Based on the simulation study by Goodsell et al. [11], the tailoring material between SFA and NG, be it tungsten, lead, stainless steel, water, or even in an extreme case, ^{238}U, does not indicate a significantly improved or worsened

active signal on the detectors. Therefore, the function of the tailoring material, the primary purpose of which was to slow down the neutrons and produce additional neutrons by (n,2n) reaction, was omitted here in favour of placing the NG closer to the SFA which leads to additional improvement of the expected signal-to-background ratio (S/B).

- **Shielding of NG –** The inner components of the NG (e.g., the NG target, tube, and electronics) are also sensitive to gamma rays. Consequently, extreme gamma exposure of the NG may lead to the overall paralysis of the NG. In [6] the position of the NG was chosen as a compromise between keeping the NG close enough to have relatively high (S/B) ratio, and a sufficient distance that ensures a low gamma ray exposure from the SFA. As a result, it was suggested that a 3 cm thick, 50 cm high rectangular tungsten block be placed between the NG and SFA to minimize the gamma dose rate on the NG target while still keeping the satisfactory S/B ratio. This block may be alternatively replaced with a 5 cm thick lead block.
- **Neutron flux monitor** – In addition to the ^{3}He detectors, an independent flux monitor is required to monitor the neutron output from the NG during every single measurement campaign, as well as over the entire lifetime of the NG tube. In [6], several options (^{3}He, ^{4}He, and various types of fission chambers) were presented as potential candidates for this purpose.

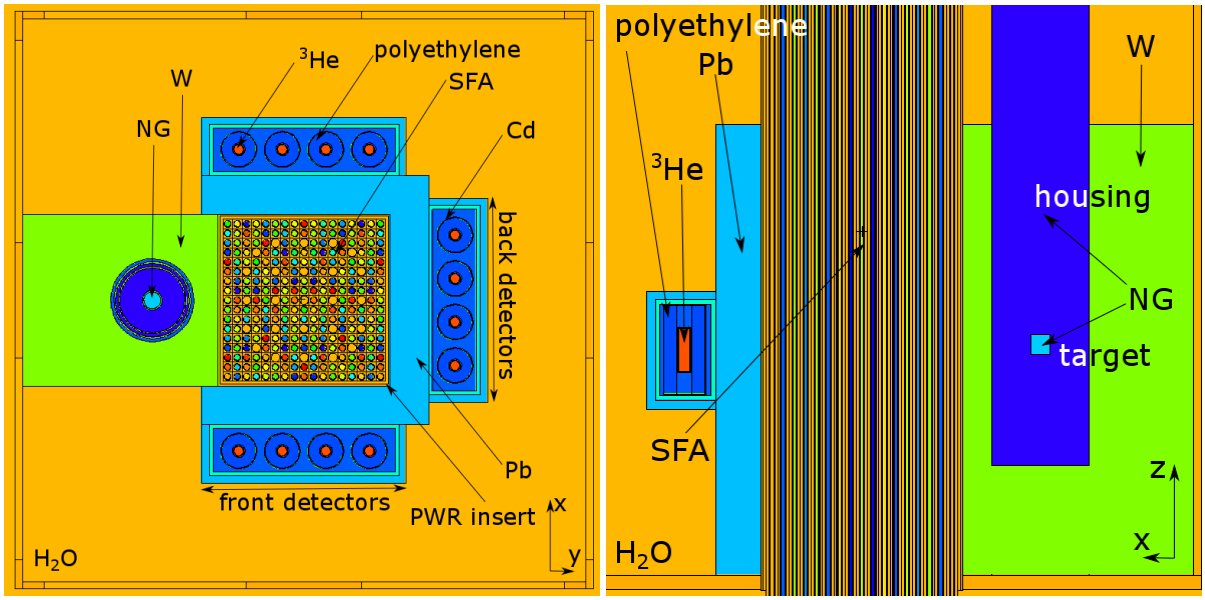

Figure 1: Horizontal (left panel) and vertical (right panel) cross-sectional view of the DDA design as simulated and proposed for the deployment in Clab [6].

4. Impact of various design modifications on the DDA instrument performance

The conceptual design of the DDA instrument for Clab, as summarized in Section 3 and thoroughly described in [6], is still expected to be modified due to various fabrications constraints and in order to benefit from mechanical design features of other instruments (e.g., DDSI). The initial idea of sharing the majority of the components and building one integrated instrument for DDA and DDSI has been abandoned because of too large number of compromises it entailed that were threatening the very performance of individual instruments. However, the external basket of DDSI [12], which accommodates the entire instrument, will be used to house DDA instrument as it is preferred by SKB and provides enough space to house all necessary instrument components. However, several components as suggested in Section 3 and depicted in Fig. 1 have been modified or replaced. This section of the paper describes the main alterations that have been implemented into the most recent design to be fabricated at LANL. Some of the modifications may have an impact on the performance of the DDA instrument, and within this paper we discuss the potential magnitude of such effects in terms of longer measurement times and different levels of accuracy from those described in [6].

4.1. Shielding of the NG

The NG, if operated in vicinity of another SFA, must be effectively protected to ensure optimum operation. The most sensitive part of the NG is the high voltage section, which accelerates the ions to the target. In [6], several different materials of various thicknesses were simulated using Monte Carlo Neutron Particle transport code (MCNP) [13]. Given the compromise between the position of the NG and the gamma dose rate on the NG's target, a 3 cm thick tungsten block was preferred over lead because given the same thickness the more dense tungsten blocks gamma rays more effectively than lead. However, the high cost of tungsten alloys made this option generally less desirable. Therefore, the decision was made to limit the use of tungsten to only the space between the NG and SFA. More recently, that decision was reversed and the originally suggested 3 cm of tungsten between the NG and SFA was replaced with 5 cm of lead shielding. Thorough MCNP simulations have shown that the 5 cm of lead is about as efficient in shielding gammas as 3 cm of tungsten. The consequences of shifting the NG 2 cm farther from the SFA on the active signal yield are discussed in Section 4.2.

In addition to the gamma-ray shielding between the NG and SFA, the NG has to be shielded from gamma rays originating from other external sources (e.g., the SFAs stored nearby). However, since the exact layout of the encapsulation facility and thus the measurement conditions has not yet been decided, it is difficult to predict the exact thickness of this additional shielding that needs to be placed around the NG. In anticipation of need to provide at least some additional shielding of the NG the initial idea was to use a simple 1 to 3 cm thick lead collar covering the external side of the NG as shown in the figures of [6], the final decision was made to house the entire NG into a compact 2.5 cm thick lead enclosure, which effectively protects the NG from exposure to external gamma sources.

4.2. Shift of the NG Position

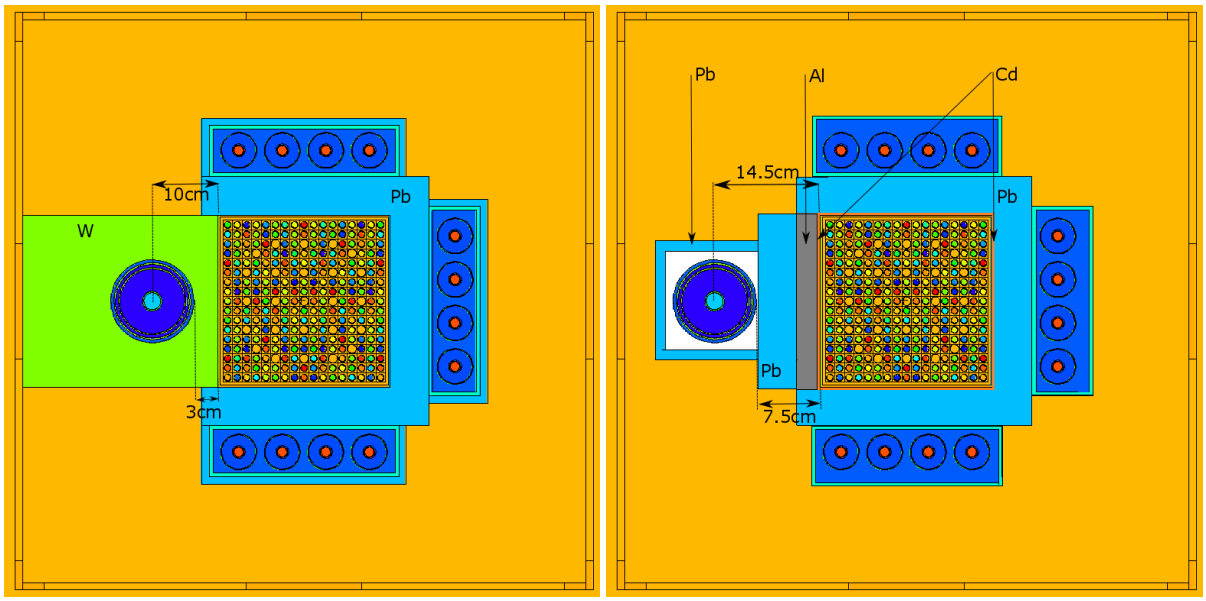

Figure 2: Schematic drawing of the DDA detector layout and position of NG dictated by the use of different shielding material and other design modifications. The left panel illustrates the situation for initially modelled position in [6], the right panel displays the current configuration.

The results in [6] suggest placing the NG as close as possible to the SFA without compromising the gamma shielding of the NG. But as described in Section 4.1, the 3 cm thick tungsten shield of NG [6] has been replaced by a 5 cm thick lead brick, which requires altering the position of the NG from that projected in [6]. In addition to this 2 cm shift, the NG will be also need to be shifted by another 2.5 cm to accommodate the insert and the upper funnel of the assembly. In total the NG will be shifted by 4.5 cm farther from the SFA (relative to the position suggested in Fig. 1). The effect of the gap necessary for the insertion of the funnel may significantly influence the performance of the instrument For example, if water is used to fill this gap, many fewer neutrons from the NG would actually reach the

SFA because many will thermalize and then will be captured by the Cd liner. Therefore, it has been suggested that this space should be filled with aluminum, which is expected to be nearly transparent to fast neutrons. The new layout (right panel) is compared to the original (left panel) in schematic drawing in Fig. 2. Reference [6] shows how shifting the NG by 3 cm impacts the active neutron count rates on detectors and consequently also the S/B ratio in comparison with the position without any shielding material between the NG and SFA. Following the same approach as that applied in [6] for the estimation of the change of the S/B ratio, the active signal is expected to decrease by a factor of approximately 0.7 ± 0.1 if the NG is shifted by the additional 4.5 cm discussed above. In total, the simulated S/B ratio for the summed signal from all detectors is expected to be approximately 1.5 ± 0.2 for the worst case SFA (i.e., 5% IE, 60 GWd/tU, 5y CT, and a 300 s measurement time). For the SFA with the highest active signal (i.e., 5% IE, 15 GWd/tU, 5y CT, and a 300 s measurement time), the resulting S/B ratio is approximately $6.0 \cdot 10^2 \pm 0.8 \cdot 10^2$. The S/B ratio for all other PWR SFAs is expected to stay within this range.

4.3. Use of Cd Liner around the SFA Insert

Lundkvist et al. [8] studied an important issue arising from neutron return to SFA after its thermalization in water. This neutron return impacted the distribution of the neutron population considerably if the SFA without a Cd liner was placed in water as it induces more fission in the front region of the SFA, resulting in an oversampling of this region relative to the rest of the assembly and eventually distorting the entire DDA signal. Thus, using a Cd liner was suggested to reduce such thermal neutron return. A similar use of the Cd liner was also studied in [6]. For the case of the “full scale” DDA instruments such as designed by Blanc and Menlove [9] or the proposed Clab design [6], the Cd liner was observed to be unnecessary if the water gap between the SFA and lead shielding remained below 1 cm. The primary reason for this conclusion is that the detectors and various shielding material surrounding the SFA provides enough neutron absorption that the effects of thermal neutron return are significantly suppressed and become negligible. As a result, the decision was made to use a 60 cm tall, removable Cd liner around the PWR SFA insert for situations where the water gap exceeds 1 cm. The Cd liner is vertically centered at the level of the target plane extending 30 cm up and down.

4.4. The Effect of Different Polyethylene Thickness around the Detector

The twelve ^{3}He detectors with a 1.4 cm thick polyethylene sleeve moderator, which were simulated in [6] and suggested for use in the Clab instrument, are expected to be slightly altered. Following the recent measurements of the fresh fuel with a laboratory DDA setup at LANL [14], the detectors located closest to the NG (also referred as front detectors) experienced difficulties in handling the high count rates which are also expected during real-life measurement at Clab. The fast neutron flux is the highest at the position of the front detectors because a significantly higher fraction of neutrons come directly from the NG. Despite the dedicated studies of front and back detector count rates in [6] which resulted in adjusting the ^{3}He tube and moderator dimensions, the preliminary experimental results from the LANL indicate potential issues with too high dead time. A conservative estimate to ensure the data from all detectors are valid and not compromised by high count rates, forces us to reduce the efficiency of the individual ^{3}He detectors. The most practical way to do that is reducing the polyethylene moderator thickness around the detectors preventing thus a more costly replacement of current detectors by smaller models. At this stage, the decision has not yet been made regarding how much to reduce the polyethylene thickness and whether to do it on all the detectors - a conservative response - or to only modify the front set of the detectors, since the back detectors experience approximately an order of magnitude lower peak detection rate.

The change of the polyethylene thickness would alter the absolute levels of both active, as well as passive signal count rates, as simulated in [6]. This in turn means the S/B would remain the same and therefore general performance of the instrument is also expected to remain unchanged. But as the active signal is overall decreased, the projected measurement times in the range of 5 to 10 minutes [6] may be prolonged in order to achieve same statistical accuracy.

4.5. Independent Monitoring of NG Output

One of the last few unresolved questions that need to be addressed is the selection and design of the independent neutron flux monitor. It is however expected to be decided based on the experience with

the fresh fuel measurement campaign that is currently ongoing at LANL. The independent flux monitor is expected to provide information proportional to the immediate neutron flux emitted from the NG over the span of the individual measurement and for the duration of the entire NG operation. The system of independent monitoring is required to verify the actual NG's output, which is known to be slowly decreasing during routine use that exceeds several hours as well as the gradual decrease of the maximum achievable intensity as the tritium inside the NG target is depleted. For this purpose, a dedicated cavity behind the NG has been suggested to accommodate the independent flux monitor. At the time of writing this paper, the approximately 18 cm, active length fission chamber with 2 grams of depleted uranium is suggested and considered to be adequate for this purpose.

4.6. BWR Insert and Position of SFA in the Instrument

The majority of the study dedicated to finalization of the Clab design was performed only with PWR SFAs. However, the majority of spent fuel in Sweden consists of BWR SFAs, which are dimensionally (but also by shape of the BU distribution) different from PWR SFAs. BWR SFAs have not been simulated with the Clab design primarily because of associated high computational demand compared with PWR SFAs. However, the DDA performance with BWR SFAs has been tested on the conceptual DDA design in [4], where the design by Blanc and Menlove [9] was modified to enclose the BWR SFA. In [4], the lead shielding dimensions and detector positions were changed to enclose the SFA similarly as for the PWR in [9]. The comprehensive set of 216 SFAs was simulated and analyzed. The results did not indicate a significant change in the DDA instrument performance when benchmarked with results obtained from PWR SFAs. Therefore, the Clab design, which is similar to the conceptual design by Blanc and Menlove is anticipated to work with BWR SFAs as well.

In case of the Clab design, the BWR assemblies are expected to be assayed by the same DDA instrument as the PWR SFAs which can be modified to accommodate both dimensionally different PWR (~ 21 x 21 cm) and BWR (~ 14 x 14 cm) SFAs. While the volume of BWR assemblies is significantly lower, the space between the SFA and the DDA instrument needs to be filled with material that does not significantly alter the neutron transport. If water is not prevented from occupying this place, the majority of fast fission neutrons from SFA would thermalize and get captured on Cd liner of the individual detectors. Thus, the DDA instrument performance could be significantly degraded.

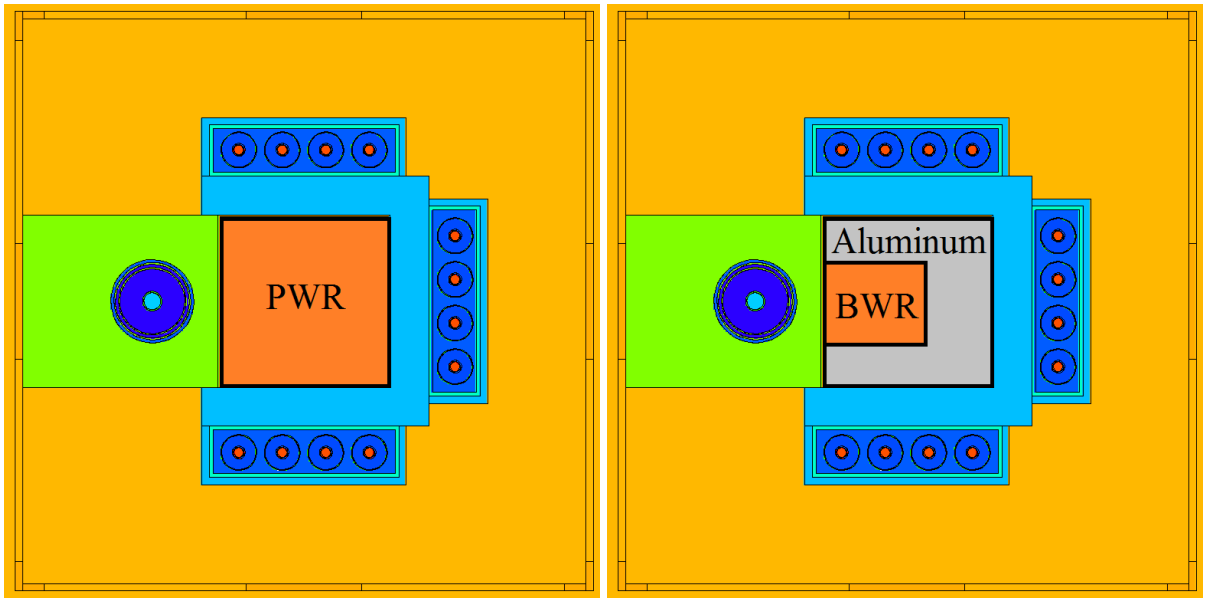

Figure 3: The comparison of the DDA instrument with the inserted PWR SFA (left) [6] and BWR SFA together with aluminum insert (right).

In general, the gap around the SFA when the BWR is assayed has been recommended in [6] to be filled by material such as air, aluminum, iron or stainless steel to minimize the neutron interactions with this material. The position of the BWR assembly during the assay is also suggested to be as close to

the NG as reasonably possible (right panel of Fig. 3) because the solid angle of the injected neutrons that target the SFA is larger improving thus the S/B ratio. However, at this point we are unsure about the details of operations with the BWR assemblies and whether off center position inside the DDA instrument can be permitted by the facility operator. The alternative is that the BWR is centered inside the DDA cavity resulting in a uniform gap of app. 3 cm around the SFA. Fig. 3 (right panel) schematically illustrates the preferred position of BWR SFAs and filling of the gap with aluminum, as proposed to the Swedish operators.

5. Planned Measurement and Operational Scenarios

The test measurements are planned to use the interrogation scenario with a 5% duty cycle and the interrogation pulse length of 50 μs resulting in the pulse frequency of 1000 Hz. This interrogation scenario was suggested in [6] as the best compromise to improve S/B ratio without compromising DDA signal quality by mixing neutrons from various time domains. In [6], the statistical uncertainties were investigated for measurement times of 5 and 10 minutes, which both indicated a satisfactory relative statistical uncertainty below 1%. This time is dedicated only to a measurement of a single SFA orientation, which in many cases is expected to be sufficient. However, some of the SFAs may require assay of all four SFA orientations [15]. In such case, the data acquisition time would be prolonged by factor of 4 to be approximately 20 to 40 minutes per SFA. But, that time does not account for additional time necessary to maneuver (i.e. to insert, to extract, and to rotate) the SFA. The time required for maneuvering the SFA is expected to be 5 to 10 minutes for single-sided assay, and 20 to 40 minutes for multi-sided assay, respectively. The estimated total handling time of SFA including both measurement and maneuvering is approximately 10 to 20 minutes for single-sided assay, and 40 to 80 minutes for a multi-sided assay, respectively. Whether this anticipated time is compatible with future Clink operation, which is anticipated to encapsulate one canister per 8 hour working day (i.e., 12 BWR or 4 PWR SFAs), is beyond the scope of this paper and will need to be evaluated in the future.

6. Summary and Conclusions

The DDA instrument that was designed and proposed for Clab deployment has undergone several modifications because of various limitations in construction, expected deployment conditions, and financial or other technical reasons. The most significant changes in the design that may impact the instrument performance are: (1) different shielding for the NG, (2) increased separation of the NG from the SFA, (3) use of a Cd liner around the SFA, (4) monitoring of the NG output, and (5) positioning of the BWR SFA in the instrument. The effect of these changes has been evaluated leading to a conclusion that despite remaining uncertainty in actual operational conditions the DDA instrument design proposed for Clab deployment is still expected to provide statistically significant results in practical measurement times.

7. Acknowledgments

The authors would like to acknowledge the support of the Next Generation Safeguards Initiative (NGSI), Office of Nonproliferation and Arms Control (NPAC), National Nuclear Security Administration (NNSA), and Uppsala University.

8. Legal matters

8.1. Privacy regulations and protection of personal data

"I agree that ESARDA may print my name/contact data/photograph/article in the ESARDA Bulletin/Symposium proceedings or any other ESARDA publications and when necessary for any other purposes connected with ESARDA activities."

8.2. Copyright

9. References

[1] Humphrey, M. A., Tobin, S. J., and Veal, K. D.; *"The Next Generation Safeguards Initiative's Spent Fuel Nondestructive Assay Project"*, Journal of Nuclear Materials Management Vol. 40, No. 3 (2012) pp 6.

[2] Henzl, V., Swinhoe, M. T., Tobin, S. J., and Menlove, H. O.; *"Measurement of the Multiplication of a Spent Fuel Assembly with the Differential Die-Away Method within the Scope of the Next Generation Safeguards Initiative Spent Fuel Project"*, Journal of Nuclear Materials Management Vol. 40, No. 3 (2012) pp 61.

[3] Henzl, V., Croft, J., Richard, J., Swinhoe, M. T., and Tobin, S. J.; *"Determination of the Plutonium Content in a Spent Fuel Assembly by Passive and Active Interrogation using a Differential Die-Away Instrument"*, Nuclear Instruments And Methods A 712, 83-92, 2013, doi:10.1016/j.nima.2013.02.006

[4] Henzl, V.; *"Evaluation of Differential Die-Away Technique Potential in Context of Non-Destructive Assay of Spent Nuclear Fuel",* Los Alamos National Laboratory report LA-UR-14-29224 (2014).

[5] Henzl, V., Swinhoe, M. T., and Tobin, S. J.; *"Direct Measurement of Initial Enrichment and Burn-up of Spent Fuel Assembly with a Differential Die-Away Technique Based Instrument"*, Proceedings of Institute of Nuclear Materials Management conference, Orlando, Florida, 2012.

[6] Martinik, T., Henzl, V., Grape, S., Jansson, P., Swinhoe, M. T., Goodsell, A. V., and Tobin, S. J.; *"Determination of the Plutonium Content in a Spent Fuel Assembly by Passive and Active Interrogation using a Differential Die-Away Instrument"*, Expected to be submitted for publication to NIM-A in 05/2015.

[7] Lee, Tae-Hoon, Menlove, H. O., Swinhoe, M. T., and Tobin, S. J.; *"Monte Carlo simulations of differential die-away instrument for determination of fissile content in spent fuel assemblies"*, Nuclear Instruments And Methods A 652, 103-107, 2011, doi:10.1016/j.nima.2010.08.094

[8] Blanc, P. C., Tobin, S. J., Croft, S., and Menlove, H. O.; *"Plutonium Mass Determination in Spent Fuel-Delayed Neutron Detection in an Integrated Delayed-Neutron and Differential Die-Away Instrument with ^{3}He Detectors and a DT Generator",* Los Alamos National Laboratory report LA-UR-11-01912 (2011).

[9] Lundkvist, N., Goodsell, A. V., Grape, S., Hendricks, J. S., Henzl, V., Swinhoe, M. T., and Tobin, S.J.; *"A Qualitative Analysis of the Neutron Population in Fresh and Spent Fuel Assemblies during Simulated Interrogation using the Differential Die-Away Technique", Submitted for publication to ESARDA bulletin.*

[10] *"Thermo Scientific webpage"*, available online at: "http://www.thermoscientific.com/en/product/p-385-neutron-generator.html", [2015-04-29]

[11] Goodsell, A. V., Henzl, V., and Swinhoe, M. T.; *"Notes on Differential Die-Away (DDA) instrument performance with Sodern G16 neutron generator",* Los Alamos National Laboratory report LA-UR-14-20016 (2014).

[12] Kaplan, A. C., Henzl, V., Menlove, H. O., Swinhoe, M. T., Belian, A. P., Flaska, M., and Pozzi, S. A.; *"Determination of spent nuclear fuel assembly multiplication with the differential die-away self-interrogation instrument"*, Nuclear Instruments and Methods A 757, 20-27, 2014, doi:10.1016/j.nima.2014.04.023

[13] Pelowitz, J. F. (Editor), MCNPX™ User's Manual Version 2.7.0, Los Alamos National Laboratory Report LA-CP-11-00438, April 2011

[14] Goodsell, A. V., Henzl, V., Swinhoe, M. T., Rael, C. D., Desimone, D. J., and Charlton, W.; *"Comparison of fresh fuel experimental measurements to MCNPX results using the differential die-away instrument for nuclear safeguards applications"*, Proceedings of 37th ESARDA Symposium, Manchester, United Kingdom, 2015.

[15] Martinik, T., Henzl, V., Grape, S., Jacobsson Svärd, S., Jansson, P., Swinhoe, M. T., and Tobin, S. J.; *"Simulation of differential die-away instrument's response to asymmetrically burned spent nuclear fuel"*, Nuclear Instruments and Methods A 788, 79-85, 2015, doi:10.1016/j.nima.2015.02.058

Improving the prediction model for Cherenkov light generation by irradiated nuclear fuel assemblies in wet storage for enhanced partial-defect verification capability

Erik Branger, Sophie Grape, Peter Jansson, Staffan Jacobsson Svärd

Uppsala University, Uppsala, Sweden
E-mail: erik.branger@physics.uu.se

***Abstract**:*

The Digital Cherenkov Viewing Device (DCVD) is one of the tools available to an inspector performing verification of the irradiated nuclear fuel inventory in wet storages at a nuclear facility. For gross defect verification, the presence of Cherenkov light and its qualitative properties are sufficient to verify the presence of an irradiated fuel assembly. For partial defect verification, the measured Cherenkov light intensity is quantitatively related to the intensity that is expected from the assembly under investigation, given the operator declarations for that assembly.

While the currently used method for predicting the Cherenkov light emission intensity has performed well, data have also shown that enhanced methods incorporating more details may improve the prediction capabilities even further, in particular for short-cooled fuel assemblies. Fuel parameters such as initial enrichment, burnup, cooling time, as well as the fuel irradiation history and fuel type affect the total emitted Cherenkov light intensity, and should be taken into account in the prediction process. Furthermore, a larger number of fuel types and geometries need to be incorporated into the methods to take geometric effects into account.

This paper describes a new and fast method to predict the Cherenkov light intensity of an irradiated fuel assembly, taking the fuel irradiation history and fuel geometry into account. The proposed method takes advantage of pre-computed Monte Carlo simulations of the Cherenkov light generated by a fuel, and is fast enough to be used in the field. The improved prediction method will also allow for more stringent detection limits, which may improve the partial defect detection capabilities of the DCVD.

Keywords: DCVD; partial defect verification; Cherenkov light

1. Introduction

One of many safeguards tasks undertaken by authority inspectors is the verification of irradiated nuclear fuel assemblies. The fuel assemblies are often stored in water for decay heat removal and for radiation protection. The electromagnetic radiation emitted from the fuel assemblies will interact with the water and gives rise to Cherenkov light in the water, which can be measured. A commonly used method for verifying irradiated nuclear fuel assemblies is to detect and quantify the Cherenkov light emission from spent fuel assemblies, and compare the quality and/or intensity of the detected light to what is expected from a fuel assembly.

To do quantitative measurements with the DCVD, the measured Cherenkov light intensity of a set of fuel assemblies are compared to predicted intensities. The currently used prediction method (referred to as CPM in this text) works by first simulating the Cherenkov light intensity in a fuel assembly for a range of burnups and cooling times of the fuel. Based on the operator declared values for burnup and cooling time, the relative intensity of a fuel assembly is then interpolated from the previously simulated data. This paper presents a next generation prediction method (referred to as NGM in this text) for the Cherenkov light intensity, which also takes fuel geometry and irradiation history into account when predicting the intensity.

1.1. Measurements with the DCVD

One of the instruments available to an inspector for measuring the Cherenkov light emitted from a fuel assembly is the Digital Cherenkov Viewing Device (DCVD) [1]. The DCVD has for a long time been used for gross defect verification, where the inspector verifies that an object is an irradiated fuel assembly as opposed to a non-fuel object. The DCVD can also be used to perform partial defect verification, with the purpose of detecting missing and/or substituted fuel rods according to the IAEA's definition of a partial defect, currently at a level of 50%.

In a measurement situation, the DCVD is mounted on the railing of a bridge above the fuel, looking down into the water, as shown in Figure 1. This allows for quick, non-destructive measurements of fuel inventories.

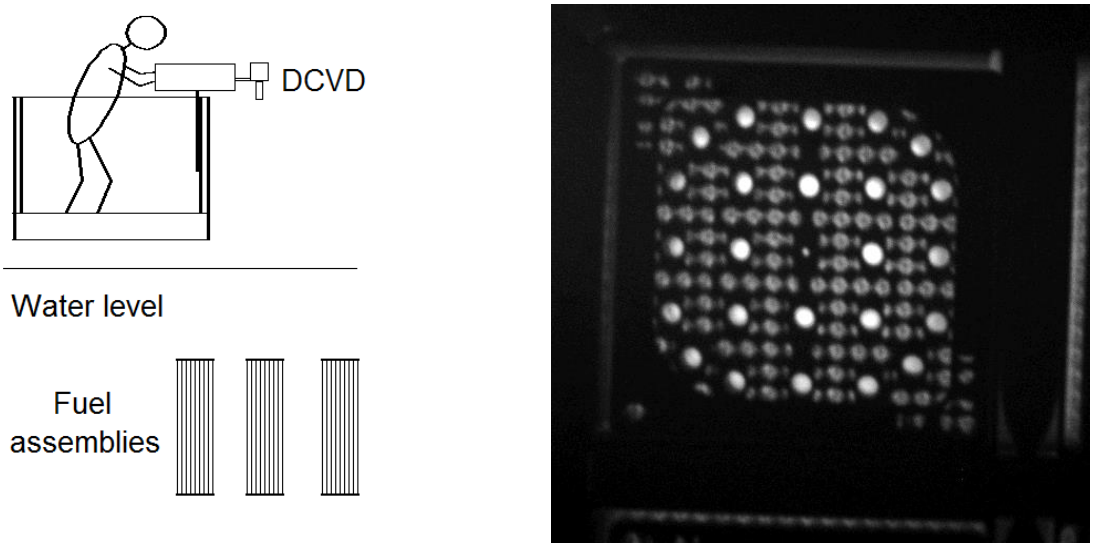

Figure 1 Left: the typical measurement situation when measuring irradiated nuclear fuel assemblies with a DCVD. Right: an example of a gray-scale DCVD image of a PWR fuel assembly.

Depending on whether an inspector wants to perform a gross or a partial defect verification campaign, the measurement scenario looks slightly different. For gross defect verification, the inspector studies the detected Cherenkov light intensity and light characteristics from each fuel item separately, in order to determine whether the object under study is a fuel item or a non-fuel item. For partial defect verification a collection of spent fuel assemblies of the same type is measured, and the measured (quantified) intensities are compared to expected intensities, which have been estimated from the fuel burnups and cooling times. Conclusions on whether the fuels are intact or suffer from partial defects are drawn after measurements have been performed. Currently, an inspector enters information about the fuels to be measured into a program that estimates the Cherenkov light intensity by interpolating pre-computed data for fuels with varying burnup and cooling time. Entering the fuel data into the program doing the interpolation is often done manually, but can be done automatically if there are scripts available to read the data in the format provided by the operator.

As can be understood, the prediction method for the Cherenkov light intensity needs to be both fast and accurate in order to be useable in the field. The CPM, which takes only the final burnup and the cooling time since end-of-irradiation into account, has performed well in most measurement campaigns. However, it has not been able to accurately predict the Cherenkov light intensity from short-cooled fuel, with a cooling time shorter than a few years. For such short-cooled fuels, the irradiation history influences the Cherenkov light intensity to a relatively large extent. Furthermore, implementing a more detailed method will improve the capability of the DCVD to detect partial defects, by putting more stringent limitations on both the expected intensity value and its uncertainties. For these reasons, the method presented here was developed.

1.2. Next-generation prediction tools

To model the Cherenkov light generation in a fuel assembly, a Geant4 [2] based simulation toolkit has previously been developed [3]. This toolkit has now been updated to work with the latest version of Geant4, and scripts have been developed to launch the simulations and collect the data with limited

efforts from the user of the toolkit. This work is a continuation of the work in [4], further developing the models and procedures used for the simulations of predicted Cherenkov-light intensities.

The updated toolkit uses a Geant4 standard physics list, with optical physics added separately. The gamma source in the simulations can be chosen to be one of the following: 1) a monoenergetic source, 2) an arbitrary spectrum provided in a format the program can read, or 3) an output file from the fuel depletion calculation program ORIGEN [5]. The geometry of the fuel assembly, including rods with cladding and a fuel box surrounding the fuel is specified in an input file. The standard simulation settings are applicable to most cases, but via input files the user may alter settings such as cut-off energies of gammas and electrons, and what data to save during a simulation run.

2. **Current prediction method (CPM) for predicting the Cherenkov light intensity**

The CPM used to predict the Cherenkov light intensity from an irradiated nuclear fuel assembly is based on a method developed by Rolandson [6]. In this method, the Cherenkov light intensities for a selection of boiling water reactor (BWR) fuels with varying burnups and cooling times were obtained through Geant3 simulations. In the analysis, these results are used to interpolate the expected Cherenkov light emission intensity for a fuel assembly, given its burnup and cooling time. The method was later extended by others to work for a larger range of burnups and cooling times, as well as to give predictions for short-cooled fuel, with cooling time shorter than one year.

2.1. Description of the CPM

The simulations of the data that form the basis of the CPM were performed in two steps. The first step was to calculate the concentration of fission product isotopes in a fuel assembly using a fuel burnup calculation program, and create a gamma spectrum as emitted by the fuel. The second step was to transport the gamma rays from their place of emission inside the irradiated nuclear fuel, which includes tracking them through their interaction with e.g. electrons in water and in the Cherenkov light generation process in the surrounding water. The last step also included the transport of the Cherenkov photons to the place of detection.

The first step was done using the ORIGEN fuel depletion code, and as a result the gamma spectra emitted from the selected BWR assemblies with different burnups were calculated. In the original studies the fuels were irradiated during four to six irradiation cycles, with each cycle having an irradiation period of 330 days followed by 35 days of cooling. The length of the final cycle was adjusted so that the fuels had the desired total burnup. The power level was chosen to be equal at all times of irradiation. However, for high-burnup fuels, more irradiation cycles were added, while for low-burnup fuels, four irradiations cycles were used with a lower power level. After irradiation, the gamma spectrum was saved for several cooling times in the range of 1 to 50 years. To simplify the calculations, the original investigations concerned only the contributions from the six isotopes Y-90, Rh-106, Cs-134, Cs-137, Pr-144 and Eu-154, which together contributed to more than 96% of the total gamma ray intensity at energies which may result in Cherenkov light being produced for the burnups under consideration. All these nuclides are gamma emitters, except for Y-90. This isotope emits high-energy electrons that cause Bremsstrahlung in the fuel, which contributes to the total gamma spectrum. All recent updates of these simulations, including results presented here, include not only these six isotopes, but the full inventory of gamma emitters. This is especially important when extending the simulations to more short-cooled fuel, where many short-lived isotopes are present and contribute to the total Cherenkov light intensity.

The second step was to simulate the transport and interaction of the gamma rays in the fuel geometry. This was done in the Monte Carlo code Geant3. The code simulated the gamma ray interactions with surrounding matter (fuel, cladding and the water), the creation of electrons and the generation of Cherenkov light. The propagation of the Cherenkov photons to a detector position 5 m above the fuel was also simulated. A “shadow factor” was also introduced, to take into account the effect of spacers and top structures in the fuel. This factor was multiplied with the simulated intensity to get an estimate of the measured intensity. Later simulations used a simplified geometry, and the total emitted Cherenkov light intensity was used as an estimate rather than a simulated intensity at a detector position.

2.2. Limitations of the CPM

The CPM has worked well so far. However, since it does not take into account the irradiation history, it has proven to be less accurate in predicting the Cherenkov light intensities from short-cooled fuel. Furthermore, a simplified geometry is used and the results from the simulations of a specific BWR fuel type are taken to approximately describe all types of fuels. The impact of these two factors is described in the following two sections.

2.2.1. Irradiation history

The CPM works very well when the decays of Cs-137 are the dominating contribution to the emitted Cherenkov light. Since Cs-137 is long-lived with a half-life of 30.2 years and since it is proportional to burnup, the knowledge of the burnup and cooling time of a set of fuel assemblies is sufficient to estimate their relative Cherenkov light intensities. However, for fuels with a cooling time on the order of or less than two years, the irradiation history of each fuel assembly and its location inside the reactor core becomes more important. A typical fuel in a power producing reactor is placed near the center of the reactor core for the first cycles, where it has a relatively high power level, and spends the last cycles near the edge of the core, with a lower power level. For short-cooled fuels, the short-lived gamma-emitting isotopes which were generated in the last irradiation cycle are still present. This means that the assumption of an equal power level in all irradiation cycles is not fully valid, especially if the burnup of the last cycle deviated significantly from the average of the previous ones.

While the “typical” fuel has a high burnup in the first cycles and low burnup in the last ones, it is also common that fuels may have an irradiation history which differs from this. If a fuel spends a cycle outside the reactor before being irradiated again, or if the final cycle is high-power, this can greatly affect the gamma spectrum of the fuel at discharge. Thus, for short-cooled fuel, the fuel irradiation history must be taken into account to accurately predict the Cherenkov light intensity.

2.2.2. Geometry

The foundation for the CPM is based on simulations of 8x8 BWR fuel. It is currently being investigated to what extent, and with which accuracy, the results can be applied to predict the Cherenkov light intensity from other types of spent nuclear fuels. In addition, it is being investigated whether the simulations can be simplified by simulating and extrapolating the Cherenkov light emitted by one single fuel rod, rather than a full assembly, in order to speed up the process. Work is ongoing in both areas, but it is worth mentioning that by using simplified geometries there is a risk of neglecting differences between different fuel types. This may e.g. impact the Cherenkov light generation process and the transport of the Cherenkov photons from their place of emission to the DCVD, and hence increase the errors in the predicted intensity for other fuel types. Thus, there is a need for a prediction method which also takes the fuel geometry into account.

3. Proposed next generation method (NGM) for predicting the Cherenkov light intensity

In this paper, it is argued that more accurate predictions of the Cherenkov light emission from a fuel assembly can be obtained through simulation of its actual fuel irradiation history and detailed Monte Carlo modelling of the Cherenkov light generation in the entire fuel assembly, and for this reason the NGM has been developed. As in the case of the CPM, the fuel depletion step is done in ORIGEN, and the particle transport is done in Geant4. The modelling of the particle transport takes into account the full fuel geometry including all rods, the cladding and the fuel box. The process of repeating the generation of the source term (i.e. the gamma spectrum) for different fuel geometries also allows for an investigation of possible differences between different fuel types. To speed up the prediction process, the Cherenkov light production due to gamma rays of a given energy in an assembly can be pre-computed, and given a gamma spectrum from e.g. ORIGEN, the Cherenkov light intensity can be estimated quickly based on the pre-computed values.

3.1. Simulating Cherenkov light from BWR and PWR fuel geometries

To investigate the difference between the CPM and the proposed NGM, and to study if the gamma spectrum and Cherenkov light production depends on fuel type, simulations have here been performed for an 8x8 BWR and a 17x17 PWR fuel design. The fuel history simulated in ORIGEN was chosen to be rather similar to the one used in [6] so that the results may be compared. However in this

work all the cycles were of equal length, while the previous work adapted the length of the final cycle in order to meet the desired total burnup.

For all simulations, an initial enrichment of 2% was assumed, to allow comparison with the earlier results. Fuels with 10, 20 and 30 MWd/kgU burnup were irradiated for four cycles, where each cycle had 312.5 days of irradiation and 46 days of cooling. The power levels for the three burnups were 8, 16 and 24 kW/kgU, respectively. For the 40 MWd/kgU case, the power level remained at 24 kW/kgU, and the fuel was irradiated for 5 cycles. For all burnup levels, separate gamma spectra were saved at 0.25, 0.5, 1, 2, 3, 5, 7, 10, 15, 20, 30, 40, 50 and 60 years of cooling time after discharge. The same irradiation histories, initial enrichment and power levels were used for both the BWR and the PWR studies.

The gammas rays from the fission products inside the fuel were generated in the vertical center of the full fuel rod length, and at randomly distributed positions in the horizontal fuel rod plane. The momentum directions of the gamma rays were isotropic. To save computer time, gamma rays with energy below 300 keV were not simulated, since simulations show that for gammas just below 300 keV only one or two Cherenkov photons are generated per 10 million gammas, which is negligible. Further, electrons with energy less than 257 keV were discarded in the simulations, since these have too low energy to produce Cherenkov light. Once a gamma ray had energy lower than 257 keV it was also discarded, since it cannot produce electrons with sufficient energy to produce Cherenkov light.

Geometrically, the 8x8 BWR fuel geometry was matched to the one used in [6], with the same fuel and cladding diameters and rod pitch (center distance between rods). The chosen PWR geometry was a 17x17 Westinghouse type with water filled guide tubes for control rods and a central instrumentation tube. The geometrical fuel information for the BWR and PWR fuels is given in Table 1. The inner radius of the cladding is chosen to be the same as the fuel pellet radius, corresponding to a closed gap in between the fuel and the cladding. Since the fuel types simulated are rotationally symmetric, it was sufficient to simulate one octant of the fuel, and the information could be used to predict the Cherenkov light contribution from the rods that were not simulated.

Property	**BWR 8x8**	**PWR 17x17**
Fuel size [mm]	130 * 130 * 3985	214*214*3852
Pellet radius [mm]	5.22	4.09
Cladding outer radius [mm]	6.13	4.75
Pitch [mm]	16.3	12.6

Table 1 Geometry details of the implemented BWR and PWR geometries.

The Monte Carlo simulations were run on the UPPMAX computer cluster at Uppsala University, with each fuel rod submitted as a separate job, enabling all rods to be simulated in parallel. For each rod, 10 million fission product gamma rays were simulated, with the energy distribution given by the gamma spectrum from ORIGEN. The results of all the separate jobs were merged, to give a total emitted Cherenkov light intensity for the given gamma spectrum of the fuel. The statistical uncertainty in the total emitted Cherenkov light intensity of an assembly with a given gamma spectrum, due to the Monte Carlo nature of the simulation, was estimated to be less than 0.4% for all BWR simulations, and less than 0.1% for all PWR simulations.

3.2. Pre-computing the Cherenkov light intensity of a fuel assembly

While a simulation of a complete assembly is expected to give accurate results, such simulations are too comprehensive to be executed during a measurement campaign. One way to speed up the process of predicting the light intensity is by pre-computing the Cherenkov light intensity for each rod at a number of different gamma energies. These pre-computed intensities can then be combined with the assembly gamma spectrum to quickly obtain an estimate of the Cherenkov light intensity in the fuel.

The first step in predicting the Cherenkov light intensity is to use a program such as ORIGEN to simulate the fuel irradiation history, to obtain a gamma spectrum of the assembly. The gamma ray spectrum is then combined with pre-computed values of how much Cherenkov light is generated in an assembly by gammas of various energies. Since the gamma spectrum is typically binned, the pre-computed values can be the number of Cherenkov photons generated in a fuel assembly per gamma quantum in each bin which occurs in the gamma ray spectrum. This makes it very easy to estimate the

Cherenkov light intensity from an assembly, since there is information about the gamma ray intensity per bin, as well as the Cherenkov light production per gamma for each energy bin.

To test this method and to compare it with the simulations done in section 3.1, simulations were run for both a BWR and for a PWR fuel assembly. The simulations were run for one octant of the fuel assembly, using the symmetry of the fuel to obtain the intensity values for the other rods. For each rod and for each gamma ray energy bin, a simulation of 10 million gamma rays was run. This corresponds to about 4000 CPU-hours to simulate both the BWR and the PWR fuels. This work is extensive, but only needs to be done once for every fuel geometry.

Due to the large amount of simulated particles, the statistical uncertainties in the resulting Cherenkov light emission are very low, typically around 0.03% per gamma ray energy bin. Although the statistic uncertainty in the gamma ray spectra from ORIGEN is low [7], larger systematic uncertainties arise due to not modelling e.g. the complete fuel history including every control rod movement during irradiation, and one may thus relax the statistical precision somewhat in the Cherenkov emission simulations without affecting the overall uncertainties significantly. Accordingly, simulating a complete assembly may be done in a few hundred CPU-hours while still having a statistical uncertainty much lower than the systematic uncertainty of the gamma ray spectrum.

4. **Results**

This section presents the results of the simulations. The first subsection compares the results of BWR simulations using the CPM in [6], with the complete assembly simulations done using the NGM here. In the next subsection, a comparison is made between the Cherenkov light intensity from BWR and PWR fuel assemblies with identical irradiation history.

4.1. Comparison of the current and next generation methods

The results of the CPM and the NGM are shown in Figure 2, where the results have been scaled to be equal at 10 years. As can be seen, the new simulations stretch into shorter cooling times than the results from the CPM.

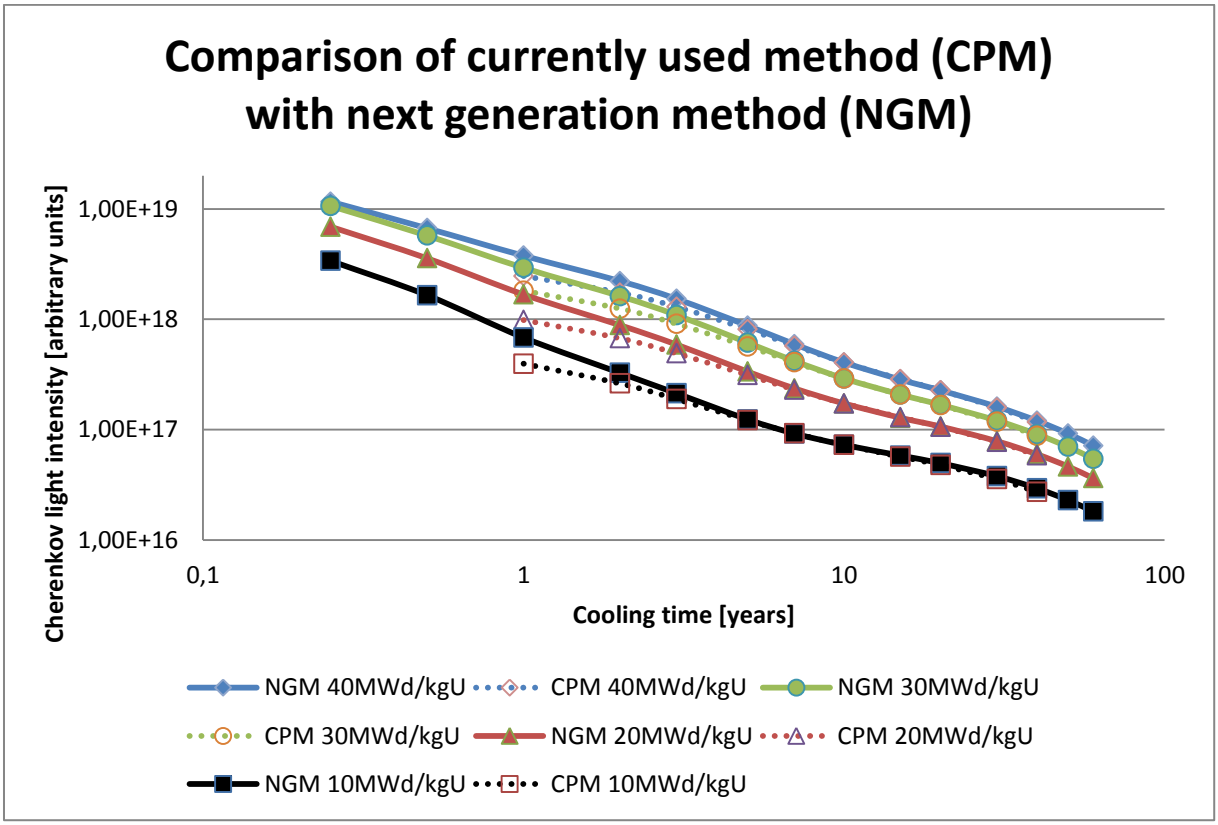

Figure 2 Comparison of a full BWR assembly simulation with the currently used method (CPM) **[6]** and the next generation method (NGM), normalized to 10 years cooling time. Statistical uncertainties of simulated values are smaller than 0.4% of the value.

The results from the CPM and the NGM are quite similar for fuel with a cooling time of more than 10 years, but for short-cooled fuels the results deviate. The simulations done here suggest a higher relative intensity compared to the CPM. This can be expected since the new simulations include the contribution of all isotopes in the fuel, while the older results only considered six long-lived isotopes. The difference may also depend on small differences in the fuel irradiation history used. Investigating how the irradiation history affects the Cherenkov light intensity is the subject of future work. Further, the differences may also be due to updates in nuclear cross sections in ORIGEN and updates in physics models used in Geant4 compared to the older versions of the code.

The results also differ from those found in [4], where a somewhat lower intensity was found. The cause of this is under investigation, but possible reasons are improved methods to introduce ORIGEN spectra into Geant4 and updates in the physics models used in Geant4.

Done in an automated way, the ORIGEN burnup calculations and the estimation of the Cherenkov light intensity using pre-computed simulations can be performed in a few seconds per fuel, which is fast enough to be practically useable during measurements.

4.2. Cherenkov light emission from different fuel types

The CPM is based on simulations of a BWR fuel respectively on simulations of a single rod. If the results of such simulations are applied to other types of fuels, the predictions become more uncertain since the effect of fuel geometry on Cherenkov light production is not taken into account. To investigate what effect the fuel geometry has on the Cherenkov light production, simulations were run for a BWR and a PWR fuel assembly with identical irradiation history.

Comparing the simulated emission of Cherenkov light from a PWR fuel to that of a BWR fuel reveals that the intensity profiles as a function of time differ, as shown in Figure 3. With a normalization of data to 10 years' cooling time and the same uranium mass, the Cherenkov light emission appears to be higher for PWR fuels as compared to BWR fuels for short cooling times. This is most noticeable for the simulated fuel assemblies with low burnup, where the difference is largest at 2-8 years, depending on the burnup. For very short cooling times of less than one year, the intensity is instead lower for PWR fuels, which may be explained by the difference in how short-lived isotopes are built up in BWR and PWR reactors. For a cooling time longer than 10 years, the Cherenkov light intensity for the PWR fuel appears to be lower compared to a BWR fuel.

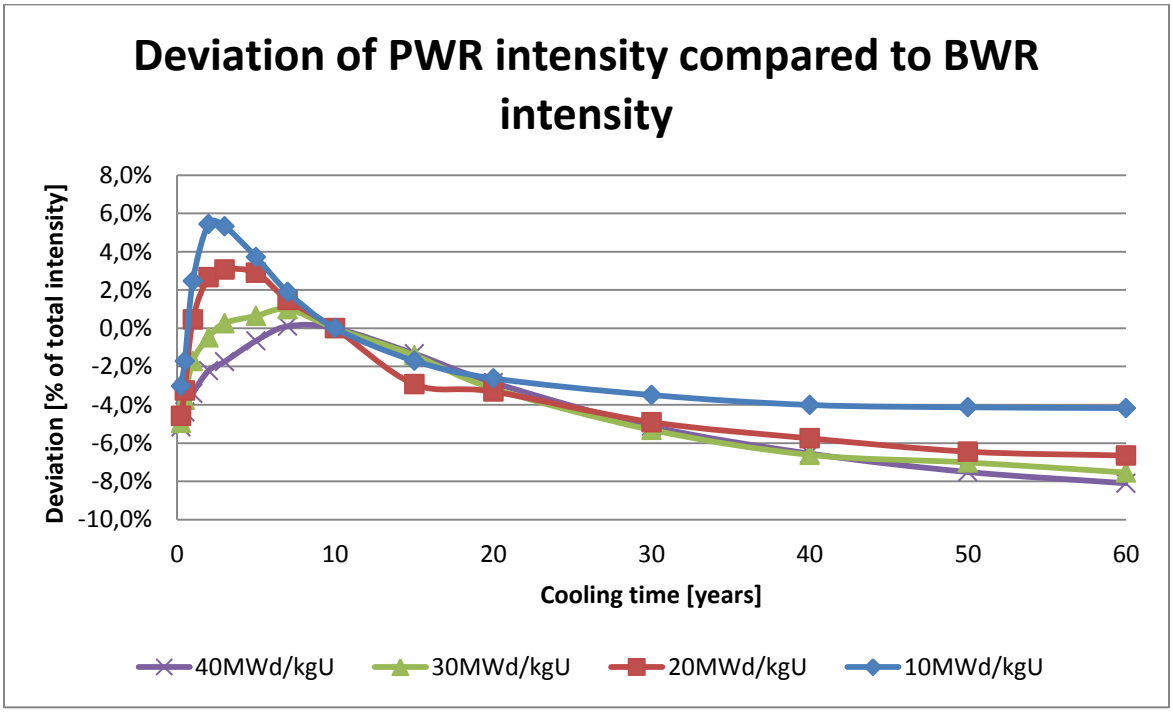

Figure 3 Deviation of the simulated emitted PWR Cherenkov light intensity compared to the BWR intensity, normalized to 10 years cooling time and the same uranium mass content. The uncertainties of the values are smaller than 0.5 percent units.

These effects are on one hand due to differences related to the reactor core design of BWR and PWR reactors, such as the presence of void in the BWR reactor and on the other hand due to differences in the fuel geometry such as fuel and cladding size, pitch, and guide tubes which affect the amount of water inside the fuel assembly. The statistical uncertainty of the total Cherenkov light intensity in the BWR simulations were typically between 0.2% and 0.4%, while for the PWR case it was smaller than 0.1%, which means that the difference between the two are significant.

As a consequence, if Cherenkov light emission intensities based on BWR simulations are used to predict corresponding intensities for PWR assemblies or vice versa, a noticeable error is introduced. For accurate estimations of the Cherenkov light intensity, one may conclude that each fuel type should have its own set of intensity estimates.

5. **Conclusions**

This paper describes the currently used method for predicting the Cherenkov light intensity emitted from irradiated nuclear fuel assemblies in wet storage. It also presents results from the new proposed method for predicting the Cherenkov light intensity generated in an assembly for both BWR and PWR fuels, and suggests a new, quick and accurate way to obtain the same information. The new method makes use of pre-calculations to estimate the contribution to the total Cherenkov light intensity in the assembly for gamma-rays of various energies from each rod. It takes into account both the fuel history and fuel geometry, while still being fast enough to allow for use during field measurements or when only limited computational resources or time is available. The increase in prediction accuracy can aid in setting more stringent limits on how much a measured intensity may deviate from a predicted value, which, in turn, may be used to improve the partial defect detection capability of the DCVD. The simulations performed also show that the new method gives very similar results to the currently used method for fuels with a cooling time longer than 10 years, but shows a different behavior for short-cooled fuel.

The new method requires computationally expensive pre-calculations, done separately once for each fuel type, preferably on a computer cluster. For long-cooled fuel, or for fuel where a detailed irradiation history is unavailable, a standard irradiation history may be applied. Using such a standard fuel history, the intensity estimates can be obtained with the same amount of work as the currently used prediction method. However, for short-cooled fuels, with a cooling time on the order of one or two years, the irradiation history must be taken into account, which is possible using the methodology suggested here. It is also possible to automate the input of the fuel history into ORIGEN, running it, and extracting the resulting gamma ray spectra. A modern laptop is capable of producing around 2000 such estimates per hour, which includes the ORIGEN simulations of the fuel history. This will allow for predictions taking into account the fuel history, while still not adding to the workload of converting the operator declaration to a Cherenkov light intensity estimate.

6. **Outlook**

One possible extension to the suggested method is to not only pre-calculate the total emitted Cherenkov light intensity, but to also handle the transport of the Cherenkov light to a detector position. This will further increase the accuracy of the method, since it predicts what the DCVD can actually detect. This will however require additional information on the geometrical details of the fuel assembly such as spacers and top structure to be taken into account, as well as the axial burnup distribution and the absorption of light in water. A related question is to what extent this information is available to an inspector on site. Furthermore, material deposits on fuel rod surfaces (CRUD) may alter the optical properties and thus change the absorption and reflectivity of UV light, which must also be taken into account. Also, if the prediction takes into account the light intensity which the DCVD can measure, it may also be possible to directly compare the Cherenkov light intensity of fuel assemblies of different types.

7. **Acknowledgements**

This work was supported by the Swedish Radiation Safety Authority (SSM), under contract SSM2012-2750. The computations were performed on resources provided by SNIC through Uppsala Multidisciplinary Center for Advanced Computational Science (UPPMAX) under project p2007011.

8. **References**

[1] International Atomic Energy Agency (IAEA), *"Safeguards Techniques and Equipment: 2011 Edition,"* IAEA/NVS/1/2011, 2011.

[2] Agnostelli, S, et al (the Geant4 collaboration), *"Geant4 - a simulation toolkit,"* Nuclear Inst. and Meth. in Physics Research Section A: Accelerators, Spectrometers, Detectors and Associated Equipment, Volume 506, Issue 3, 1 July 2003, Pages 250-303.

[3] S. Grape, S. Jacobsson Svärd, B. Lindberg, *"Verifying nuclear fuel assemblies in wet storage on a partial defect level: A software simulaiton tool for evaluating the capabilities of the Digital Cherenkov Viewing Device,"* Nuclear inst. and Meth. A, Volume 698, 11 January 2013, Pages 66-71, ISSN 0168-9002, 10.1016/j.nima.2012.09.048.

[4] S. Grape, S. Jacobsson Svärd, *"Recent modelling studies for analysing the partial-defect detection capability of the Digital Cherenkov Viewing Device,"* ESARDA bulletin no 51, December 2014.

[5] Bowman S. M et. al, *"ORIGEN-ARP, a fast and easy to use source term generation tool,"* Paper submitted to ICRS - 9, Ninth International Conference on Radiation Shielding, August 6, 1999.

[6] S. Rolandson, *"Determination of Cherenkov light intensities from irradiated BWR fuel,"* IAEA task ID JNTA0704, SKI Report #: SE 1-94, 1994.

[7] J.J. Klingensmith, I.C. Gauld, *"ORIGEN-S Gamma Decay Spectra Characterization and Benchmarking,"* Trans. Am. Nucl. soc. 94, 385-387, 2006.

Underwater Testing of Detectors and Electronics Hardware for Spent Fuel Measurements

K. D. Ianakiev, M. T. Swinhoe, M. L. Iliev, S. J. Tobin

Los Alamos National Laboratory, Los Alamos, NM 87545

Anders Sjöland[1], Henrik Liljenfeldt[1], Peter Jansson[2]

[1]Swedish Nuclear Fuel and Waste Management Company, [2]Uppsala University

Abstract

Underwater gamma and neutron spent fuel measurement techniques are being researched to meet the combined needs of the international safeguards community and the Swedish Nuclear Fuel and Waste Management Company (SKB), which is responsible for fuel encapsulation and repository operation in Sweden. Both SKB and the involved regulators anticipate measuring each spent fuel assembly individually before encapsulation; such a measurement plan presents a real challenge for the performance and long-term behavior of detectors and electronics hardware. The reliability and radiation hardness of the electronics and detectors are a big challenge for users of this technology. For instance, the gamma detectors and electronics may have to operate at count rates up to few million counts per second while maintaining good spectral resolution to detect lines from ^{137}Cs, ^{134}Cs, and ^{152}Eu. If the ^{10}B proportional counters are to replace the difficult-to-transport ^{235}U fission chambers, they must tolerate a gamma dose rate of many thousand R/h (many tens of Sv/h) without gain changes due to space charge effects or long-term degradation of the gas mixture. To address these challenges, a special underwater enclosure was developed for testing these detectors and electronics in parallel with the design and deployment of nondestructive assay options for characterization of the spent fuel. In this paper we describe the hardware and modeling components of the testing setup.

Keywords: spent fuel, underwater measurements, passive gamma spectroscopy, high counting rate, ^{235}U fission chambers, ^{10}B detectors, scintillation detectors, radiation resistance, front-end electronics, collimator modeling

1. Introduction

In-situ spent fuel measurements for safeguards are needed, which creates particular requirements for underwater radiation detection instrumentation. This paper will inform the safeguards community about (1) the challenges encountered by the current detector/electronic technologies for underwater gamma spectroscopy and total neutron flux measurements; (2) new detector electronics and modeming that have been developed to resolve these challenges.

Passive gamma emission from fission products in the spent fuel contains important information about a range of characteristics (e.g., the level of burnup, cooling time, initial enrichment, Pu mass, reactivity, and heat) of spent fuel assemblies [1]. Using high-purity germanium (HPGe) detectors and scintillation detectors outside of a spent fuel pool [2] is a mature measurement approach. Recent measurements substituting the HPGe detector with moderate-resolution, but much faster light response LaBr scintillation detectors demonstrate the promising potential of this technology to eliminate the need for long air collimators [3].

The deployment of scintillation detectors in-pool enables the acquisition of high-quality spectral information more readily, thus enabling practical safeguards deployment, as well as enabling the development of advanced techniques such as gamma tomography [4]. This technique requires a low dead time and very good pileup rejection to mitigate the interference between the 1274-keV line of ^{154}Eu and the 1324-keV sum peak created by the pileup of 662-keV lines of ^{137}Cs. The following limiting factors hinder the fulfillment of the above requirements:

1. A fundamental count rate limitation is caused by the duration of the scintillation process. The use of LaBr as a scintillator reduces this limitation because it has an exceptionally fast light response (95% of scintillator light is collected in the first 60 ns). This fast response does not present a practical count rate limitation for most envisioned deployments as much as the electronics does. In contrast, the widely used and much more inexpensive NaI(Tl) scintillator has a slower light response. In particular, the slow components of the scintillation are many times longer than the decay time of the Tl activation center [5], which is the main limiting factor for deterioration of the pulse height spectrum at high count rates.

2. The gain in a photomultiplier tube (PMT) is unstable at high count rates. It is well known that PMT operation at both a high gain and a high count rate causes fluctuation of the voltage on the dynodes (and thus fluctuation in the PMT gain), resulting in spectrum degradation. Typically, the light response of a LaBr detector with a Hamamatsu R6232 PMT to a 662-keV gamma would provide an anode current pulse with an ~20-mA amplitude and therefore about a 750-mV amplitude at the output of a 75-ohm terminated cable. Transporting small-amplitude, very short (tens of nanoseconds) pulses is not very practical; therefore, a preferred option is amplifying and transforming the detector's current pulses into voltage pulses with longer exponential decay in a charge-sensitive amplifier before transmitting through the cable.

3. All industry standard multichannel analyzers (MCAs) require a preamplifier signal with an exponential decay of a minimum 40 μs and maximum amplitude of a few volts. Because of the extensive pileup of preamplifier pulses, the amplitude of preamp pulses should be in the range of a few hundred mV; thus, there is a voltage mismatch. To preserve the highly desired resolution of a LaBr detector (about 3% FWHM for the 662-keV line), the contribution of high count rate and electromagnetic interference (EMI) noise in a long cable should be less than 1% or 10–20 mV. A classical charge-sensitive preamp cannot fulfill the conflicting requirements of (2) and (3).

Replacement of the ^{235}U fission chamber faces many challenges. The ^{235}U fission chamber has been the main choice for the fork detector measurements of spent fuel because of its exceptional tolerance to gamma doses. Special designs of ^{235}U fission chambers and fast electronics have been used for reactor

core measurements at gamma dose rates up to 10^6 R/h (10^4 Sv/h); however, that exceptional gamma resistance comes with heavy penalties:

- Increasing the scrutiny for shipping and handling detectors containing special nuclear material makes them very difficult to use in safeguards applications.
- Lower sensitivity (about 20–50 times lower that of a ^{10}B proportional counter with the same size) requires longer measurement times for assemblies with low activity;
- It is a few times more expensive than a ^{10}B proportional counter of the same size.
- Despite the higher energy of ^{235}U fission fragments, the signal is on the order of the lower range of the ^{3}He tube signal (a few fC at a 6-MeV threshold), which aggravates the problem of operating with long cables.

The ^{10}B proportional counters have gamma resistance and neutron detection efficiency somewhere between ^{235}U fission chambers and ^{3}He tubes [8] and therefore could be an attractive alternative for replacing the radioactive ^{235}U fission chamber in fork detector measurements [9]. However, the experimental results in both of these publications encountered severe space charge effects, leading to a change of tube gain, and thus of detection efficiency. In addition to that limitation, the organic gas admix used for the improvement of charge collection time and count rate capabilities, is known to cause long-term instability problems due to the decomposition of organic gas molecules and photo-polymerization of the gas on the anode wire.

2. Measurement Setup

This section describes the proposed setup testing the detectors at Clab. The underwater testing is planned to take place in the upper pool. The side and top views of the proposed measurement arrangement are shown in Fig. 1a and Fig. 1b.

The cylindrical underwater enclosure will be immersed in the pool at a fixed position along the concrete wall; a structural support extending down from the edge of the pool will hold the detector at a fixed location above the floor of the pool. The detector enclosure is built with 0.25-in.-thick aluminum tubing having a length of 24 in., and an internal diameter of 7.5 in. Two 12-in. square flanges are welded onto both sides. The enclosure is sealed via a third flange with an outlet for ¾-in.-thick flexible watertight electrical conduit. The LaBr gamma detector and front-end electronics are placed in a cylindrical hole behind the Pb shielding, whereas the ^{10}B detector and small ionization chamber are placed in front of the shielding. A diagonally placed, 2-mm-diameter cylindrical hole serves as a collimator for the LaBr. The diagonal arrangement of the collimator geometry was chosen to maximize the shielding effect for the fixed thickness of Pb. Since the Pb collimator is designed to be inserted into the enclosure, a separate coaxial shielding geometry with the front collimator is possible. The signal cables connecting the data acquisition electronics outside the pool with the front-end electronics inside the underwater enclosure are placed in a watertight electrical conduit.

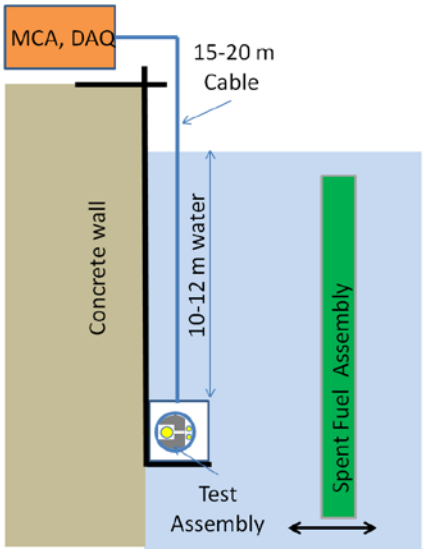

Fig. 1a. Side view of the measurement arrangement.

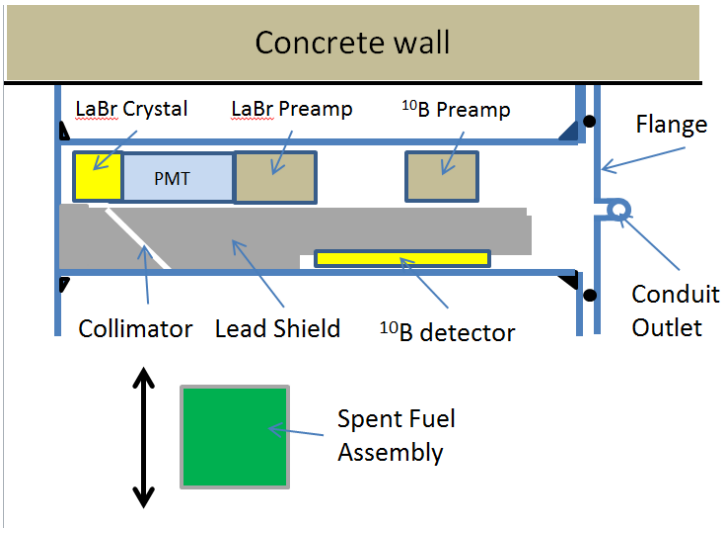

Fig. 1b. Top view of the measurement arrangement. A cross section of the testing enclosure shows the arrangement of its components.

3. New Detection Technology for Passive Gamma Measurements

3.1. Scintillation Detector

The need to improve the count rate capabilities of NaI detectors to be used for the Spent Fuel Attribute Test [7] led to the development of a novel electronics approach that overcomes the fundamental limitation of NaI detectors by cancelling the slow decay component in the preamplifier signal [8]. That approach was refined [9] and successfully implemented in the detectors used for transmission-based, online enrichment monitoring technology [10]. The off-the-shelf PMT dividers and decoupling circuitry are not optimized for high count rate applications. The problem is aggravated additionally for PMTs with positive high voltage (which most commercial PMTs for scintillation counting are), where all decoupling capacitors have values that are getting impractically high.

3.2. Electronics

Fulfilling the conflicting requirements for a high amplitude preamplifier signal needed for improved immunity from ground looping and EMI encountered during the previous measurements and, small (hundreds of mV) amplitude at the MCA input is not possible with the off-the-shelf instrumentation. Therefore, we propose a novel approach based on our prior experience with industrial noises encountered in UF_6 Blend Down Monitoring Systems [10] and our current United States Department of Energy, Next Generation Safeguards Initiative (NGSI) work for noise immunity of front-end electronics for unattended monitoring [11, 12]. A simplified block diagram explaining that approach is shown in Fig. 2. The +/-12-V power supply cables and interconnections, as well as the more complex-charge sensitive feedback described in [10], are omitted for simplicity.

The charge sensitive preamplifier (simple RC feedback configuration is shown) has a short-time constant, on the order of a few μs, thus enabling the generation of pulses with a few volts of amplitude without reaching the voltage rails of the preamplifier.

The Time Constant and Gain Conditioning Module (TCGCM) converts the high-amplitude, but short-time constant pulses into signals with lower amplitude but with the 50-μs long-time constant necessary for proper operation of the MCAs (just the opposite function of classical pole/zero cancellation).

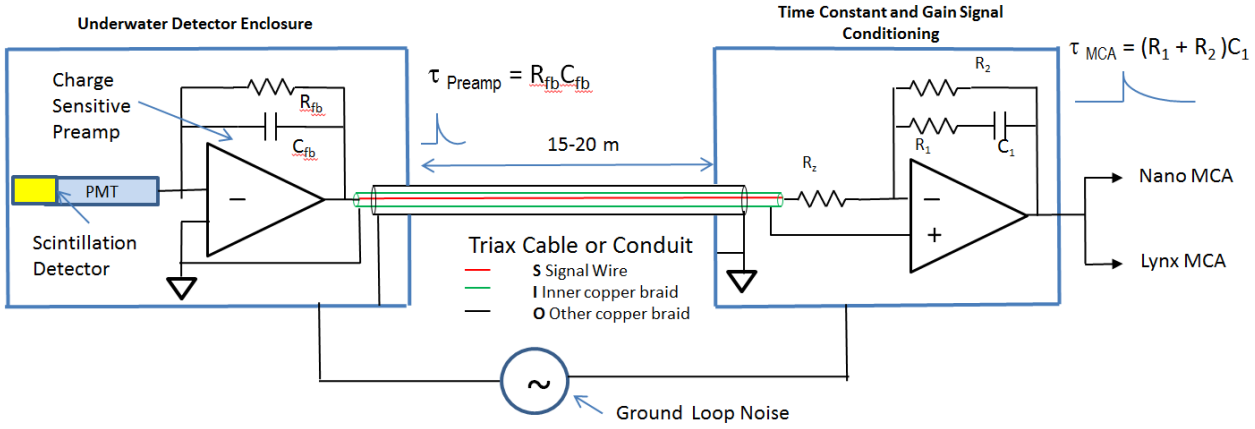

Fig. 2. A simplified block diagram of the scintillation detector and electronics for passive gamma measurements. The charge-sensitive amplifier and detector are installed in the underwater enclosure, whereas the TCGCM is installed outside the spent fuel pond next to the Data Acquisition (DAQ) electronics. The facility ground loop noise is presented as a voltage source connected between the enclosures.

3.3. Modeling

A set of Monte Carlo calculations has been performed using MCNP 5 [15] to estimate the effects of shielding against gamma radiation when measuring close to a used nuclear fuel assembly using a LaBr detector. A worst-case scenario with no shielding was simulated as a base case with which simulations incorporating various shielding thicknesses could then be compared. The geometry for the calculations was simplified, as compared with the geometry shown in Section 2 on the measurement setup, while still providing useful information regarding necessary shielding for future applications of the technologies presented in this work [e.g., as a spectral resolved gamma detector used in combination with a differential die-away (DDA) instrument]. The detector was placed just outside the corner of the fuel assembly, where it is planned to be used in the DDA instrument.

3.4.1 No shielding A calculation with the detector in its enclosure without any shielding was performed to get a base line with which to compare cases with added shielding. For this case, the average flux of gamma radiation in the detector was tallied for the following combinations of sources: (1) for each of the gamma energies 605, 662, 796 and 1274 keV, emitted homogenously and isotropically from each fuel rod; and (2) from each individual fuel rod in the 17-x-17 fuel assembly.

As can be seen in Fig. 3, the contribution to the average flux in the LaBr detector is dominated by the fuel rods closest to the detector. It is also evident that contributions from fuel rods in the upper right part of the

assembly that is further away from the detector are negligible. Fig. 3 shows that the flux contributions are symmetric around the (8,8)-(-8,-8) diagonal of the fuel assembly.

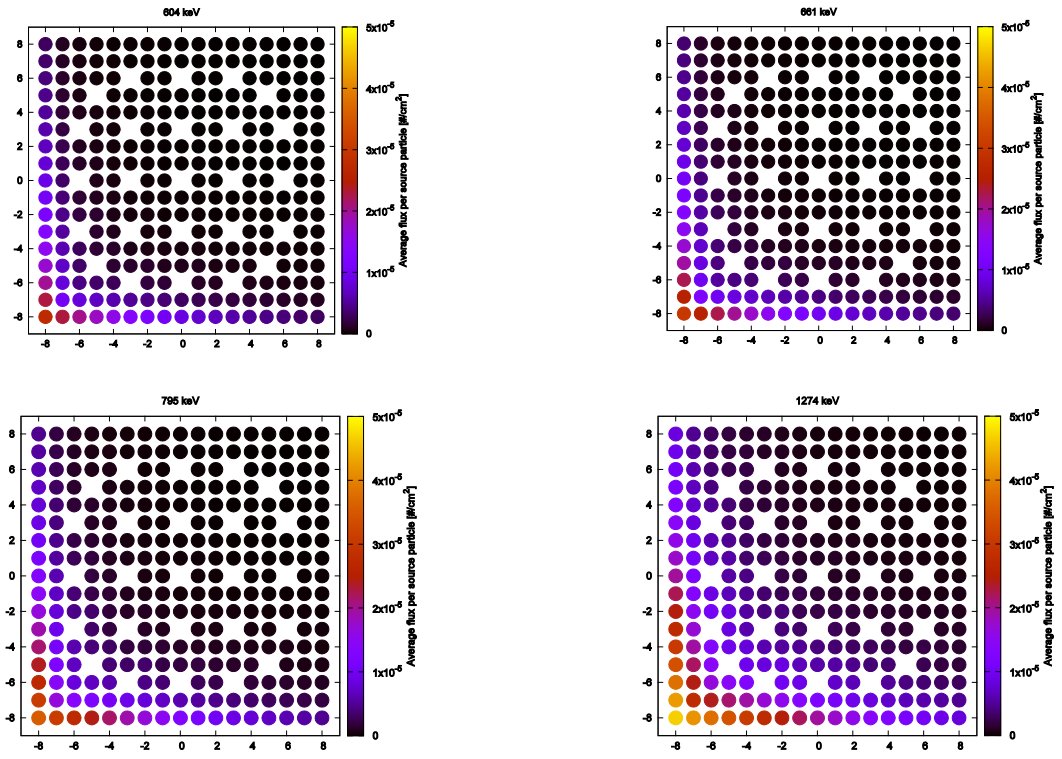

Fig. 3. Contribution to the average flux in the LaBr detector without shielding for different gamma-ray source energies.

3.4.2 With shielding As can be seen in Fig. 3, the calculations for the no-shielding case showed that the contribution to the flux from fuel rods in the upper right part of the assembly was negligible compared with the contribution from the bottom left part that is closer to the detector. Therefore, for calculations incorporating shielding, the source was considered to be originating only from the contributing part of the assembly (primarily towards the bottom left as shown in Fig. 3). Also, the calculations for the no-shielding case showed that the geometry has a large degree of symmetry. Therefore, when shielding was included in the geometry, we performed calculations only for a quarter of the fuel assembly that is closer to the detector, with the results corrected for the missing source.

We present results for calculations with shielding using a 1274-keV (Eu-154) gamma source in Fig. 4. Increasing the thickness of the Pb shielding from 1 to 4 cm will decrease the photon flux by a factor of about 6 for the 1274-keV gamma radiation.

Planned experiments at Clab will be informed by these calculations regarding how much shielding must be added to a LaBr detector when the DDA instrument is equipped with it.

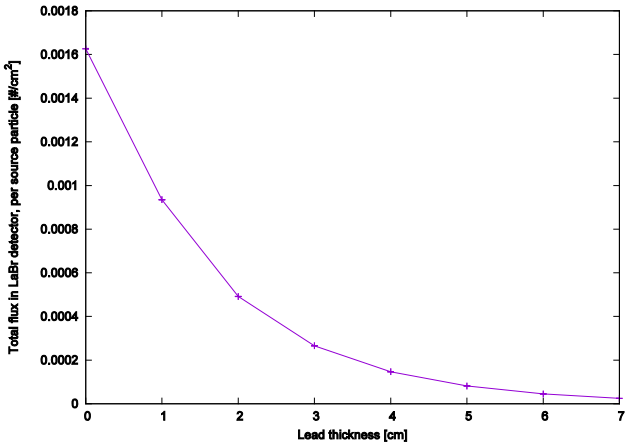

Fig. 4. Contribution to the average flux in the LaBr detector for different thicknesses of Pb shielding for a 1274-keV gamma source. The figure shows the total flux, per source particle, as a function of Pb thickness (where the statistical uncertainty in the calculated values is too small to be visible in the plot).

4. New ^{10}B Detector and Electronics for Total Neutron Flux Measurements

Despite encouraging results, current off-the-shelf ^{10}B proportional counters are not suitable for direct replacement of ^{235}U fission chambers for fork measurements because, as discussed in the introduction, problems exist with the short- and long-term degradation of detection sensitivity. Because the gamma signal in gaseous detectors originates from a pileup of Compton electrons generated in a tube wall, the gamma sensitivity depends in a very complex way on energy deposition in the gas, signal formation on anodes, and shaping time of the front-end electronics. These effects need to be taken into consideration in the system design.

4.1 Detector

To assess the status of current technology and address its limitations, we present the analysis of the available experimental results from [9] obtained with an RS-P7-0405-201 ^{10}B proportional counter (tube diameter of 0.5 in., anode wire diameter of 0.001 in., active length of 5 in., and sensitivity of 1.3 cps/nv) and a PDT-210 preamplifier based on an Amptek-A111 chip. The plots in Fig. 5a and Fig. 5b show the plateau of counting characteristics at different gamma dose rates taken with and without 2-cm-thick tungsten shielding (an attenuation factor of about 55 for the 662-keV line).

The currently used ^{10}B detector and PDT-210 electronics in a fork cannot accurately measure the entire range of spent fuel assemblies, and still requires two types of neutron detectors for assay. Using an organic gas admix will cause additional long-term degradation of gain stability and the requirement for tedious and labor-intensive periodic recalibration.

Based on our experience with high count rates in ^{3}He proportional counters developed under the NGSI program [15], we believe that the main reason for a space charge gain shift is the very high nonuniformity of the electrical field due to the use of a thin (0.001-in.-thick) anode wire.

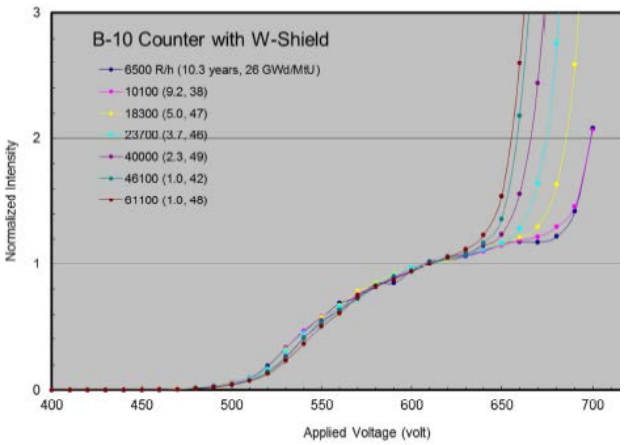

Fig. 5a. Shielded detector counting characteristics (detector dose rates 100 to 1000 R/h). The gain loss due to space charge effects is noticeable at 520 V, which is far below the 620-V normalization voltage.

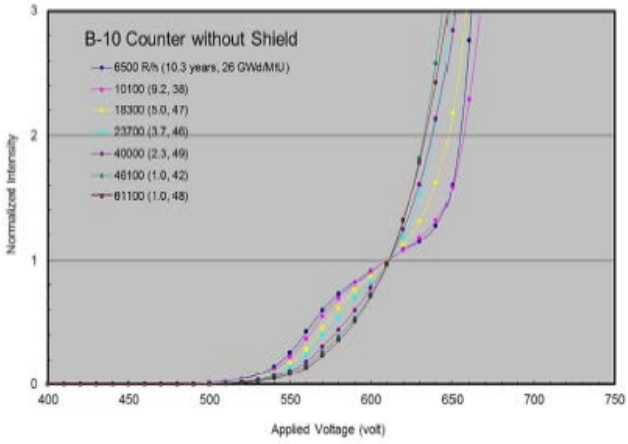

Fig. 5b. Unshielded detector counting characteristics (detector dose rates (6500 to 61,000 R/h). Severe gain loss can be seen across the entire range of the dose rate.

To address these two major limitations of ^{10}B detectors, a special radiation-hardened design of ^{10}B detectors has been specified and built by GE Reuter-Stokes (GE-RS). The detector has a 5-in. active length, a 3/4-in. tube diameter, and a 0.004-in.-thick anode wire that provides a space-charge-free geometry electrical field. Because of the larger tube diameter, this detector has about 60% higher sensitivity than the RS-P7-0405-201 used in the fork measurements. The GE-RS proprietary inorganic gas admix does not decompose by radiation effects, and thus, the detector does not require periodic recalibration. This gas admix has very low stopping power for Compton electrons generated in the wall, resulting in a lower amplitude of gamma pulses, but also will be prone to double pulsing due to a slower charge collection time. The front-end electronics needed to resolve that problem are described in the next section.

4.2 Electronics

The lack of a real plateau in the ^{10}B counting characteristic and the possibility for infiltration of gamma pulses above the detection threshold reduces the possible range of measured spent fuel. Based on the Los Alamos National Laboratory (LANL)-designed for Amptek A-111 replacement basic KM-200 electronics that may be commercialized by Ludlum Measurements, an experimental proof of principle dual-channel architecture prototype has been built to expand the measurement capabilities of ^{10}B detectors over the entire range of measured fuel. The prototype and the block diagram depicting the principles of operation are shown in Fig. 6a and Fig. 6b respectively.

The simultaneous measurement at two points (on the slope far below the gamma pileup and at the quasi plateau) will be used to expand the measured range of spent fuel assemblies with only one instrument. The ratio of the two count rates is very sensitive to gamma pileup but not to neutron flux and therefore will be

used as an indicator for excessive gamma pileup. If gamma pileup is detected, the count rate of the fast channel, corrected by the initially calibrated ratio in a pure neutron flux, can be used.

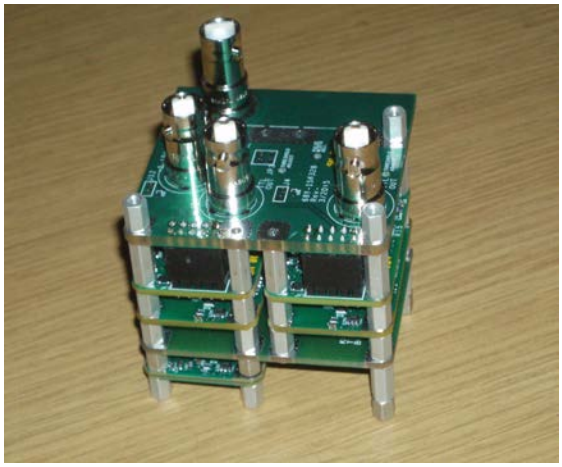

Fig. 6a. An assembled KM-200 dual-channel prototype: preamplifier, signal distribution, fast and slow shapers, fast and slow discriminators, power regulators, and connector boards.

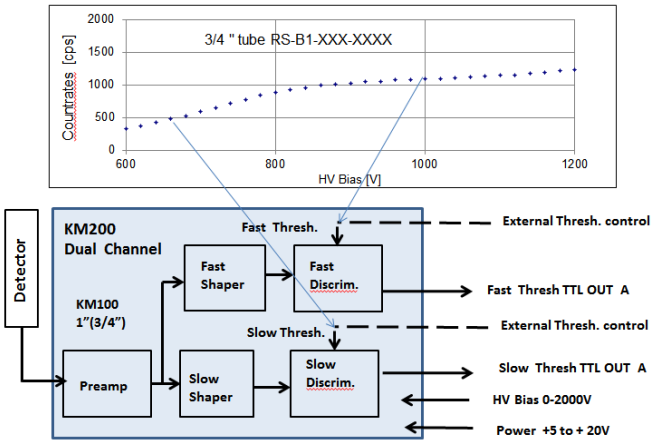

Fig. 6b. KM-200 dual-channel functional diagram and ^{10}B counter characteristics showing the position of fast and slow detection thresholds.

5. Future Work

Measurements in the spent fuel pool are expected to take place in August 2015 and during the next year.

6. Conclusions

In situ spent fuel measurements are needed, which creates particular requirements for underwater radiation detection instrumentation (neutron and gamma). It is hard to meet these requirements with current off-the-shelf technology. For neutrons, recent advances in detectors and electronics may help to address this problem. Electronics for spent fuel passive gamma measurements with scintillation detectors that may lead to significant improvements in performance have being developed. The research is guided by modeling at many different points in the development process. An important point is that we must consider the complete measurement system (detector, signal processing and data acquisition electronics as well as the data analysis software) to obtain optimum performance, rather than simply plugging together available components.

We are taking advantage of an excellent opportunity to benefit from real-world testing provided at the Clab facility, which will benefit many of the stakeholders in the spent fuel community. It should be noted that regardless of the results of these tests, long-term testing of the equipment will be needed.

Acknowledgments

The authors wish to thank the NGSI Program and the Swedish Nuclear Fuel and Waste Management Company (SKB) for their support of this work. We also wish to thank Nathan Jonson (GE-RS) for his fruitful discussions and help with the radiation-hard ^{10}B detector.

7. References

1. S.J. Tobin et al., "Experimental and Analytical Plans for the Non-Destructive Assay System of the Swedish Encapsulation and Repository Facilities," IAEA-CN-220/238, Proceedings of 2014 IAEA Symposium. Vienna, October 2014
2. P. Jansson, "Studies of Nuclear Fuel by Means of Nuclear Spectroscopic Methods," Uppsala: Comprehensive Summaries of Uppsala Dissertations from the Faculty of Science and Technology, 2002. ISSN 1104-232X, ISBN 91-554-5315-5. http://urn.kb.se/resolve?urn=urn:nbn:se:uu:diva-2057.
3. K. Ianakiev, A. Favalli, "Passive Gamma Measurements with LaBr Detector," Clab 2013 Personal communication
4. P. Janson et al., "Gamma Transport Calculations for Gamma Emission Tomography on Nuclear Fuel within the UGET Project", Vienna, October 2014.
5. K. Ianakiev and R. Arlt, "High Count Rate Preamplifier for Spent Fuel Attribute Test Measurements," 1992 personal communication
6. K. McKinny et al., "Neutron Detector Sensitivity Measurements and their Variations," N11-7, 2011, Nuclear Science Symposium, Conference record.
7. Young-Gil Lee et al., "Development of 'Fissioon Cahmner Free' Fork Detector (FDET) for Safeguards Measures on LWR Spent Fuel Assemblies," Proceedings of 2014 IAEA Safeguards Symposium Vienna.
8. K. Ianakiev et al., "Apparatus and Method for Temperature Correction and Expanded Count Rate of Inorganic Scintillation Detectors, USPTO#20050269513 A1,"
9. K. Ianakiev et al., "Improving the Accuracy of a Uranium Enrichment Monitor Based on a NaI(Tl) Spectrometer and Transmission Source," 2007 ESARDA Conference. Aix-en-Provence,
10. M. Iliev, Master of Science Thesis http://scholarworks.csun.edu/bitstream/handle/10211.2/3504/Iliev-Metodi-thesis-2013.pdf?sequence=1 , May 2013.
11. E. Smith et al., "Front-End Electronics for Verification Measurements: Performance Evaluation and Viability of Advanced Tamper Indicating Measures," Proceedings of 2014 IAEA Safeguards Symposium. Vienna.
12. K. Ianakiev et al., "LANL Advanced Tamper Indication Method Based on Time Domain Analysis and Correction of Signal Integrity,"
13. K. Ianakiev, M. Iliev, M. Swinhoe, and Nathan Johnson, "High Count Rate Thermal Neutron Detectors and Electronics," Proceedings of 2014 IEAE Safeguards Symposium, Vienna.

14. (MCNP5) X-5 Monte Carlo Team, “MCNP—A General Monte Carlo N-Particle Transport Code, Version 5, Volume 1: Overview and Theory,” Los Alamos National Laboratory report LA-UR-03-1987 (April 2003).

In-Field Performance Testing of the Fork Detector for Quantitative Spent Fuel Verification*

I. Gauld[1], J. Hu[1], P. DeBaere[2], S. Vaccaro[2], P. Schwalbach[2], H. Liljenfeldt[3], S. Tobin[4]

[1] Oak Ridge National Laboratory
P.O. Box 2008, Oak Ridge, TN 37831-6170 USA
E-mail: gauldi@ornl.gov
[2] European Commission, DG Energy, Directorate Nuclear Safeguards
[3] Swedish Nuclear Fuel and Waste Management Company
[4] Los Alamos National Laboratory

Abstract:

Expanding spent fuel dry storage activities worldwide are increasing demands on safeguards authorities that perform inspections. The European Atomic Energy Community (EURATOM) and the International Atomic Energy Agency (IAEA) require measurements to verify declarations when spent fuel is transferred to difficult-to-access locations, such as dry storage casks and the repositories planned in Finland and Sweden. EURATOM makes routine use of the Fork detector to obtain gross gamma and total neutron measurements during spent fuel inspections. Data analysis is performed by modules in the integrated Review and Analysis Program (iRAP) software, developed jointly by EURATOM and the IAEA. Under the framework of the US Department of Energy–EURATOM cooperation agreement, a module for automated Fork detector data analysis has been developed by Oak Ridge National Laboratory (ORNL) using the ORIGEN code from the SCALE code system and implemented in iRAP. EURATOM and ORNL recently performed measurements on 30 spent fuel assemblies at the Swedish Central Interim Storage Facility for Spent Nuclear Fuel (Clab), operated by the Swedish Nuclear Fuel and Waste Management Company (SKB). The measured assemblies represent a broad range of fuel characteristics. Neutron count rates for 15 measured pressurized water reactor assemblies are predicted with an average relative standard deviation of 4.6%, and gamma signals are predicted on average within 2.6% of the measurement. The 15 measured boiling water reactor assemblies exhibit slightly larger deviations of 5.2% for the gamma signals and 5.7% for the neutron count rates, compared to measurements. These findings suggest that with improved analysis of the measurement data, existing instruments can provide increased verification of operator declarations of the spent fuel and thereby also provide greater ability to confirm integrity of an assembly. These results support the application of the Fork detector as a fully quantitative spent fuel verification technique.

Keywords: Fork detector; iRAP; spent fuel verification; ORIGEN; spent fuel safeguards

1. Introduction

Spent fuel safeguards rely primarily on material containment and surveillance with item counting and non-destructive assay (NDA) verification measurements. Such measurements are required for spent fuel assemblies before they are transferred to long-term dry storage, final disposal at a repository or, in general, to other facilities where assemblies are not easily accessible. Verification measurements may also be required to re-establish continuity of knowledge. The instruments currently accepted by

the International Atomic Energy Agency (IAEA) for spent fuel measurements are the Fork detector and the Cerenkov Viewing Device (CVD) [1].

Activities related to spent fuel storage and disposal are increasing in Europe and worldwide as spent fuel pools reach their storage capacities and many countries are expanding dry storage operations and some are seeking extended interim storage options. In Europe, the increasing use of dry cask storage has increased the demands on safeguards authorities to perform inspections during cask loading. Measurements are routinely performed using the Fork detector during joint inspections by the IAEA and the European Atomic Energy Community (EURATOM). The Fork instrument relies on passive gross gamma-ray and total neutron counting as a means to indirectly verify the operator declarations of the fuel. The Fork detector has been used for safeguards since the 1980s; the underlying technology has remained largely unchanged over 30 years, owing to its simplicity, durability, transportability, and the fast and relatively low-intrusive nature of the measurements.

To address increasing demands on inspection resources and to improve the efficiency of data collection, EURATOM developed the Remote Acquisition of Data and Review (RADAR) unattended data acquisition software application, which can operate without the presence of an inspector [2]. Data analysis, review, and reporting are performed by the Integrated Review and Analysis Program (iRAP), developed jointly by EURATOM and the IAEA. To enable analysing the Fork measurement data quantitatively and identifying potential discrepancies between operator declarations and measurements, an automated spent fuel data analysis module has been implemented in iRAP. This module is based on the ORIGEN code [3], developed and maintained at the Oak Ridge National Laboratory. Software development, integration, and testing have been done under a collaboration agreement between the US Department of Energy (DOE) and EURATOM. Unlike some research initiatives focusing mainly on new and advanced detector technologies, the current research focuses rather on improving the accuracy and efficiency of the data analysis for a proven technology (the Fork detector), thereby minimizing the impact on existing inspector requirements or facility operations.

Benchmarking and validation of the spent fuel analysis module in iRAP have been performed using measurement data acquired through cask loading campaigns in Europe during joint inspections using both EURATOM and IAEA Fork instruments and electronics. In the past two years, data from more than 15 loading campaigns and more than 200 assemblies have been evaluated [4, 5]. However, cask loading data are inherently limited by low assembly diversity. Frequently, the assemblies have the same or similar enrichments, burnup, and cooling times. Consequently, the limited assembly properties do not provide sufficient challenges to test the analysis capabilities. Additionally, finding patterns or trends within such limited data set has proven to be difficult.

The research presented in this paper includes an analysis of recent Fork measurements performed on assemblies at the Swedish Central Interim Storage Facility for Spent Nuclear Fuel (Clab), in Oskarshamn, Sweden. These assemblies have been selected for measurements under the US DOE Office of Nuclear Nonproliferation and Arms Control's Next Generation Safeguards Initiative Spent Fuel (NGSI-SF) Project, in collaboration with the EURATOM Directorate for Nuclear Safeguards, and the Swedish Nuclear Waste Management Company, Svensk Kärnbränslehantering AB (SKB). The assemblies selected under this experimental program cover a very wide range of spent fuel characteristics that are representative of commercial fuels. Extensive fuel design and detailed operating history data are also available for all assemblies included under this program. Such a diverse data set provides a valuable opportunity to quantify the performance of the Fork detector and data analysis methods. Furthermore, the results discussed in this paper, which are representative of current technology capabilities, can be used to benchmark results obtained with the more advanced instruments and techniques.

2. Facility and experimental program

Under the DOE NGSI-SF project, several advanced NDA instruments have been developed for assembly measurements to advance the state-of-the-art in NDA techniques for spent fuel verification [6]. Under the US International Nuclear Safeguards Engagement Program (INSEP) and in the framework of the EURATOM-DOE Technical Cooperation Agreement on nuclear safeguards and security, an Action Sheet has been agreed between SKB, EURATOM, and DOE. Several instruments are being deployed for testing and performance evaluation at the Clab facility in Sweden. Operated by SKB, Clab is the central interim storage facility for all spent nuclear fuel from 12 commercial reactors

in Sweden. More than 30,000 spent fuel assemblies are currently stored in the pools at Clab, with plans for a final repository in Forsmark to become operational after 2030.

Within the experimental program, 50 spent fuel assemblies were selected for measurements that span the wide range and diversity of fuels that are intended to go in the Swedish repository. The fuel design and operating characteristics of 25 assemblies from pressurized water reactors (PWRs) and 25 from boiling water reactors (BWRs) are listed in Table 1. The PWR assembly designs include 15×15 and 17×17 lattice types, while the BWR assembly designs include 8×8 (with and without water rods), 10×10 SVEA and 10×10 ATRIUM lattice designs.

The 25 PWR assemblies have an enrichment range from 2.1% to 4.1% and a burnup range from 19.6 to 52.6 GWd/tU. The cooling times span from 4.2 to 29.2 years. The 25 BWR assemblies have enrichments from 1.3% to 4.0%, burnups from 9.1 to 46.4 GWd/tU, and cooling times between 7.2 and 29.2 years.

In addition, several assemblies had complex irradiation histories, where the assembly was unloaded from the reactor for several cycles between its initial loading and final discharge. The irradiation history is indicated approximately in Table 1 by the percent effective full-power days (%EFPD). This parameter represents the percentage of time that a particular assembly is irradiated at full power rate between its initial loading and final discharge. Assemblies with low %EFPD values generally experienced either significant outages (within cycle and/or between cycles) or long periods of low power operation while irradiated in the core. For example, assembly PWR24 was out of core for about 10 years before it was re-loaded in the core, resulting in a low %EFPD of 11%. BWR25 was loaded in the first cycle of the reactor and it experienced long periods of low power operation, resulting in a %EFPD of 31%.

Assembly Identifier	Assembly Design	Enrichment (^{235}U%)	Burnup (GWd/tU)	Cooling time (yr)	Loading date (month/day /year)	Discharge date (month/day /year)	%EFPD
Pressurized water reactor fuel assemblies							
PWR1	15x15 AFA3GAA	4.10	52.630	4.2	5/4/2005	5/28/2009	89
PWR2	15x15 AFA3GAA	3.93	49.555	4.2	5/4/2005	5/29/2009	83
PWR3	17x17 Fra	3.69	48.175	13.1	7/6/1996	6/21/2000	83
PWR4	17x17 HTP	3.93	46.873	5.2	9/26/2004	6/4/2008	87
PWR5	17x17 HTP	3.94	46.866	5.2	9/26/2004	6/2/2008	87
PWR6	17x17 AA	3.60	45.658	14.1	7/8/1993	6/23/1999	52
PWR7	17x17 Siemens	3.94	44.483	6.1	9/5/2003	6/27/2007	80
PWR8	17x17 W	3.30	44.375	24.9	8/20/1984	9/11/1988	75
PWR9	15x15 W	3.71	45.846	6.0	6/15/2003	8/1/2007	76
PWR10	17x17 Fra	3.70	43.474	15.1	7/1/1994	6/17/1998	75
PWR11	17x17 Fra	3.51	43.225	13.1	7/1/1994	6/21/2000	50
PWR12	17x17 W	3.30	42.969	24.9	8/20/1984	9/11/1988	72
PWR13	15x15 KWU	3.20	40.920	26.3	7/25/1982	4/25/1987	59
PWR14	17x17 Fra	3.51	40.745	16.1	7/8/1993	6/24/1997	70
PWR15	17x17 W	2.80	40.473	26.0	4/17/1982	8/27/1987	52
PWR16	17x17 Fra	3.60	40.410	17.1	6/23/1993	6/21/1996	92
PWR17	17x17 Fra	3.70	40.294	13.9	9/22/1994	9/1/1999	56
PWR18	17x17 Fra	3.52	39.756	18.2	7/9/1989	6/9/1995	46
PWR19	15x15 KWU	3.20	35.027	28.3	5/17/1980	5/1/1985	48
PWR20	17x17 W	3.10	34.032	27.1	7/4/1980	6/18/1986	39
PWR21	17x17 W	3.10	34.019	27.1	7/4/1980	6/18/1986	39
PWR22	17x17 W	2.80	31.165	27.0	4/18/1982	8/10/1986	50
PWR23	17x17 Fra	3.60	28.499	17.1	7/7/1993	6/21/1996	66
PWR24	17x17 W	2.10	23.151	18.2	7/2/1980	6/9/1995	11
PWR25	17x17 W	2.10	19.607	29.2	7/3/1980	5/24/1984	35
Boiling water reactor fuel assemblies							
BWR1	SVEA-96S	4.01	46.41	8.3	10/28/1999	8/29/2006	62
BWR2	SVEA-100	3.2	43.76	10.3	6/9/1999	8/17/2004	77
BWR3	SVEA-100	3.4	44.36	12.3	10/13/1993	8/3/2001	51
BWR4	SVEA-100	3.4	41.89	12.3	10/28/1999	8/29/2006	57
BWR5	SVEA-96S	3.14	42.02	8.3	10/28/1999	8/29/2006	56
BWR6	8x8	2.65	38.15	29.2	10/11/1993	8/3/2001	48
BWR7	SVEA-100	3.15	41.24	10.3	6/9/1999	8/17/2004	73
BWR8	ATRIUM 10B	3.15	39.75	9.5	8/29/2001	5/19/2005	97
BWR9	SVEA-96S	4.01	40.44	7.2	8/29/2001	9/7/2007	61
BWR10	SVEA-96S	3.14	39.50	8.3	8/29/2001	8/29/2006	72
BWR11	8X8-1	2.09	31.53	22.3	9/15/1995	7/25/2003	45
BWR12	SVEA-96	2.96	33.51	9.5	6/24/1997	6/10/2005	38
BWR13	SVEA-96	2.96	36.83	9.5	6/24/1997	6/10/2005	42
BWR14	8x8	2.65	30.49	29.2	9/3/1987	8/12/1992	67
BWR15	8x8-1	2.09	29.42	25.3	8/26/1988	5/21/1996	42
BWR16	8x8-1	2.09	26.82	27.5	8/29/1988	10/14/1993	64
BWR17	8x8	2.31	32.71	28.4	3/1/1975	7/15/1986	26
BWR18	8x8-1	2.09	21.52	22.3	7/23/1994	8/30/2000	48
BWR19	8x8	1.27	30.80	25.5	10/17/1984	6/10/1989	60
BWR20	SVEA-96	2.96	26.43	9.5	8/2/1998	6/10/2005	35
BWR21	8x8	2.31	27.67	27.4	3/1/1975	7/1/1987	20
BWR22	SVEA-96	2.96	20.41	9.5	7/14/2001	6/10/2005	48
BWR23	SVEA-96	2.96	15.99	9.5	5/24/1999	6/10/2005	24
BWR24	8x8	1.27	13.32	27.4	10/17/1984	7/10/1987	45
BWR25	8X8	1.27	9.13	27.4	10/17/1984	7/10/1987	31

Table 1: Fuel characteristics for the measured PWR and BWR assemblies

3. Fork detector design

Measurements were performed with PWR and BWR Fork detector instruments provided by EURATOM. Each arm of these instruments contains a gamma ionization chamber operated in current

mode and two neutron fission chambers. One fission chamber is bare to measure primarily thermal neutrons; the other is embedded in a polyethylene region covered by cadmium to measure epithermal and fast neutrons. The gamma detectors are LND model 52110, filled with Xe gas at 10 bars, with a 16 mm diameter and an active length of 86 mm. The neutron fission chambers, CENTRONIC model FC167, contain approximately 160 mg ^{235}U (93% enriched) and are filled with Ar and N at 4.5 bars; they have a diameter of 25.4 mm and an active length of 127 mm.

The PWR Fork detector assembly used in the measurement is shown in Fig. 1. A cross-sectional view of one detector arm containing the three chambers and their arrangement is shown in Fig. 2. The neutron signals from the two fission chambers of the same kind (bare or cadmium-covered) in each arm of the detector are integrated to compensate for potential radial burnup gradients in the fuel assembly. The signals from the bare fission chambers are registered in Channel A, and the signals from the cadmium-covered chambers are registered in Channel B.

Fig. 1 PWR Fork detector assembly.

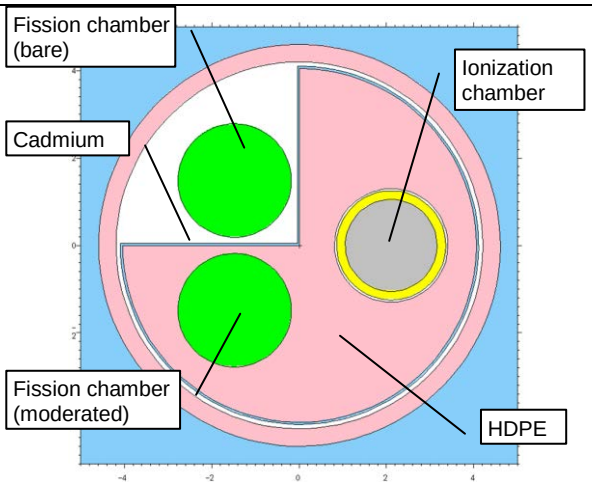

Fig. 2 Cross section of Fork detector arm showing configuration (MCNP detector model).

4. Spent fuel data analysis module

The iRAP review and analysis software includes a spent fuel analysis module that performs automated analysis of Fork detector measurements based on operator-declared information on each assembly. This verification approach does not try to estimate enrichment, burnup, or cooling time independently of the operator information; rather, it uses the declared data to predict the neutron and gamma signals, compares the predictions to the measurements and thus identifies potential discrepancies in operator declarations.

The spent fuel analysis module uses the ORIGEN code [7] to perform the burnup and decay calculations. This module can use all information available on the irradiation history of an assembly to calculate the neutron and gamma ray emission rates and energy distribution in the fuel. The ORIGEN calculations use cross-section libraries that have been developed for most classes of fuel assembly designs. For each assembly design, cross-section data are tabulated in libraries as a function of initial enrichment, burnup, and moderator density (for BWR designs). The Fork detector signal is determined by combining the emission rates in the fuel predicted by ORIGEN with energy-dependent detector response functions that have been pre-calculated for the fuel assembly–detector configurations using MCNP. This procedure allows neutron and gamma ray signals to be calculated from assembly declarations in typically less than 5 seconds. The information returned to iRAP by the calculation includes (1) irradiated uranium isotopic contents, (2) plutonium isotopic contents, (3) the gamma ion chamber response, and (4) the neutron fission chamber response for both the bare and cadmium-covered detectors. This system has been described previously [3-5].

A limitation of the spent fuel analysis software identified in previous research [5] is that subcritical neutron multiplication in an assembly was not considered. The methods described above for the neutron response include only the primary emission neutrons without neutron multiplication. The neutron source calculated by ORIGEN includes the delayed neutron emission from spontaneous fission (^{242}Cm and ^{244}Cm are usually dominant) and from (α, n) reactions from ^{17}O, ^{18}O, and any other light element in the fuel. Subcritical neutron multiplication in the assembly is dependent on the composition of the fuel (the amount of residual fissile material and neutron absorber nuclides); the geometry (leakage); and absorption in water, which may contain soluble boron. Most discharged fuel generally has a similar effective neutron multiplication factor (k_{eff}) and therefore similar induced neutron source multiplication. However, for the fuel assemblies measured at Clab with diverse characteristics, the neutron multiplication varies significantly from one assembly to another. For assemblies that were irradiated beyond typical burnup, neutron multiplication will be reduced, leading to lower neutron counts. For assemblies with low burnup, the higher residual fissile content will increase multiplication and will increase the Fork detector count rate.

A correction for neutron multiplication was added to the spent fuel module for the analysis of the Clab measurements in this work. Neutron multiplication is given approximately as $M = 1/(1 - k_{\text{eff}})$.To avoid time-consuming criticality calculations to determine k_{eff} for each assembly, neutron multiplication is approximated using the infinite neutron generation factor k_∞ calculated directly by ORIGEN as the neutron production rate divided by the neutron absorption rate in the fuel:

$$k_\infty = \frac{\sum_{i=1} n_i \sigma_{f,i} \bar{\nu}}{\sum_{i=1} n_i \sigma_{abs,i}},$$

where n is the number density of a given nuclide, σ_f is the fission cross-section, $\bar{\nu}$ is the average neutrons per fission, and σ_{abs} is the total absorption cross-section. The summation is carried over all nuclides in the system. This expression does not consider neutron absorption in assembly structures or water, or leakage. A non-leakage probability factor (P_{NL}) for a single assembly in water is applied, so that $k_{eff} = k_\infty P_{\text{NL}}$, where P_{NL} is determined for each assembly design class using a detailed neutron transport calculation. A value $P_{\text{NL}} = 0.7$ was applied for analysis of the Clab measurements. This value depends on the soluble boron level in the storage pool. The storage pool at the Clab facility does not contain boron. In pools that contain boron, provided the boron level remains constant at the facility, the effect of boron can be captured in the neutron calibration factor for the instrument.

5. Measurement campaigns

Fork detector measurements were performed by EURATOM in two campaigns at Clab. Fifteen of the 25 PWR assemblies (as shown in Table 1) were measured during October 14-15, 2014. The remaining assemblies are scheduled to be measured later in 2015. The 25 BWR assemblies (Table 1) were measured on March 22, 2015. Separate Fork detectors were used for the PWR and BWR measurements due to the different sizes of the assemblies. At the time of the present analysis, detailed operating history data were not available for 10 of the 25 BWR assemblies. Therefore, only results for the 15 BWR assemblies with detailed data are included in the present analysis.

The data acquisition time was approximately 3 minutes per assembly. The relative standard deviation of the measurements was approximately 1% to 3%. Channel A count rate exhibited some erratic behaviour during the BWR measurement campaign, as identified by anomalies in the ratio of the Channel A and B count rates. Consequently, only the results from channel B were used in the analysis presented here. The measurement results for the PWR and BWR assemblies are listed in Table 2. This table shows the calculated neutron and gamma ray signals, both uncorrected and corrected, based on detailed information of the fuel provided by SKB. This detailed information may not always be provided by a reactor operator. The comparisons between measurement (M) and calculation (C) are also included in the table. For the neutron count rates, the correction was made to account for the subcritical neutron multiplication as described in Section 4. For the gamma ray signals, the correction was made to account for the nonlinearity of the ion chamber response (more detailed explanations are included in the next section). Discussions about the comparisons are provided in the next section.

Assembly	Measured		Calculated				C/M-1(%)			
			Uncorrected		Corrected		Uncorrected		Corrected	
	Neutron (cps)	Gamma (units)	Neutron (cps)	Gamma (units)	Neutron (cps)	Gamma (units)	Neutron	Gamma	Neutron	Gamma
Pressurized water reactor fuel assemblies										
PWR1	2162.1	1223182	2321.1	1441610	2263.1	1253397	7.4	17.9	4.7	2.5
PWR2	1837.9	1126913	1795.3	1259584	1828.6	1125102	-2.3	11.8	-0.5	-0.2
PWR3	1246.4	612000	1312.1	588625	1216.1	612183	5.3	-3.8	-2.4	0.0
PWR4	1522.0	934477	1404.3	1020117	1468.0	950452	-7.7	9.2	-3.6	1.7
PWR6	1049.3	562908	1105.8	525230	1034.0	558843	5.4	-6.7	-1.5	-0.7
PWR7	1169.3	802432	1091.0	852702	1167.6	823471	-6.7	6.3	-0.1	2.6
PWR9	1395.5	859405	1408.2	890628	1432.4	852644	0.9	3.6	2.6	-0.8
PWR10	798.5	531171	798.2	488502	785.7	527356	0.0	-8.0	-1.6	-0.7
PWR11	817.4	517900	829.8	489221	818.8	527976	1.5	-5.5	0.2	1.9
PWR14	666.2	486164	622.0	439165	625.8	484298	-6.6	-9.7	-6.1	-0.4
PWR16	590.0	480941	570.5	420549	577.0	467804	-3.3	-12.6	-2.2	-2.7
PWR19	245.8	338518	258.2	257907	256.5	316360	5.0	-23.8	4.3	-6.5
PWR22	205.5	319391	209.9	243437	209.3	302078	2.1	-23.8	1.9	-5.4
PWR23	163.1	359146	130.3	298237	165.8	355353	-20.1	-17.0	1.7	-1.1
PWR24	149.9	263198	162.2	202231	170.0	260428	8.2	-23.2	13.4	-1.1
Boiling water reactor fuel assemblies										
BWR1	1034.7	501985	1140.3	567202	1050.4	531017	10.2	13.0	1.5	5.8
BWR2	843.2	477075	883.5	506707	839.4	485204	4.8	6.2	-0.4	1.7
BWR5	738.4	494300	768.2	518009	750.1	493842	4.0	4.8	1.6	-0.1
BWR7	756.7	451088	744.3	475366	731.9	461043	-1.6	5.4	-3.3	2.2
BWR8	679.0	463648	646.7	498980	658.4	479275	-4.8	7.6	-3.0	3.4
BWR9	641.0	520513	664.8	549400	675.2	517642	3.7	5.5	5.3	-0.6
BWR10	629.8	505537	617.8	519270	635.1	494804	-1.9	2.7	0.8	-2.1
BWR12	375.0	397132	343.4	377655	374.5	383526	-8.4	-4.9	-0.1	-3.4
BWR13	525.3	427656	490.5	415504	503.3	413979	-6.6	-2.8	-4.2	-3.2
BWR19	193.3	234132	182.5	215353	180.3	244702	-5.6	-8.0	-6.7	4.5
BWR20	164.8	341681	134.9	308797	175.3	326480	-18.1	-9.6	6.4	-4.4
BWR22	52.9	268423	32.6	223775	57.7	252329	-38.3	-16.6	9.0	-6.0
BWR23	23.6	220091	9.6	169824	22.7	202357	-59.5	-22.8	-3.9	-8.1
BWR24	21.4	109311	21.8	88574	24.6	120216	2.0	-19.0	14.9	10.0
BWR25	7.1	81625	5.1	59782	7.1	87776	-28.4	-26.8	0.7	7.5

Table 2: Comparison of measured neutron (channel B) and gamma detector signals with calculations. Neutron calculations are shown with and without correction for subcritical multiplication. Gamma calculations are shown with and without correction for nonlinearity of the ion chamber response

6. Analysis

6.1 Gamma signals

An initial review of the gamma data (uncorrected) in Table 2 showed significant deviations of up to +18% and -27% compared to measured signals. The discrepancies exhibit clear trends with the gamma signal intensity, indicating a nonlinear detector response. This behaviour does not exhibit saturation at high gamma ray intensities, but rather, exhibits a strong power relationship over the range of the predicted signals.

Detector response of the LND model 52110 gamma ion chambers used in the measurements has previously been measured using a calibrated Keithly ionization chamber and a ^{60}Co source in water. Nonlinear behaviour is also evident in the calibrated response data, yielding a well-defined power relationship of $y = x^p$, where $p = 0.575$ with an R^2 fit coefficient of 0.9995 over more than 5 orders of magnitude of gamma ray dose rate.

The gamma ion chamber response for both the PWR and BWR measurement campaigns at Clab also indicates a nonlinear power relationship, as was observed in the ^{60}Co calibration data. However, a power coefficient of $p = 0.8$ with an R^2 value of 0.996 was found over the range of the Clab data,

representing a factor of more than 30 in ion chamber response. The cause of the differences in ion chamber response may be due to the detectors, electronics, sources, or detector performance in a mixed neutron and gamma environment. Assuming a power relationship for the gamma detector response, the predicted gamma ray signals were corrected for the nonlinear behaviour. The results, shown in Table 2 as corrected gamma data, show that the discrepancies observed before correction are largely eliminated and that most results are within ± 5%. The gamma results, plotted in Fig. 3, show the predicted gamma signal as a function of the measured signal before and after correction. The BWR assemblies have lower signals, caused primarily by the smaller assembly size and lower quantities of actinides and fission products.

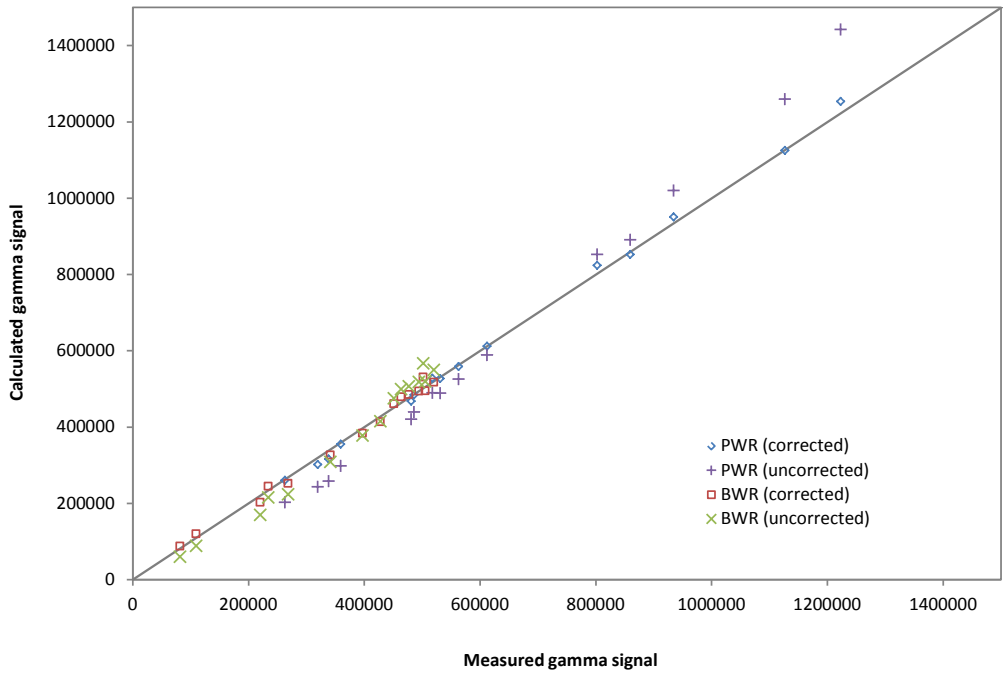

Fig. 3. Comparison of measured and calculated (uncorrected and corrected for ion chamber response) gamma ion chamber signals for PWR and BWR assemblies.

6.2 Neutron count rates

The measured and calculated neutron count rates in Table 2 are illustrated in Fig. 4. Results with and without the correction for subcritical neutron multiplication are given. Good agreement is generally observed between calculations (corrected) and measurements for most assemblies, with only one PWR and one BWR assembly exhibiting a difference greater than 10%. The range of neutron data spans more than a factor of 100 in fission chamber response. The largest deviations are observed for both the lowest burnup PWR and BWR assemblies. Assembly BWR #24 had a count rate of 21 cps compared to more than 1000 cps for BWR #1, and also had a very low burnup of 13 GWd/tU and an enrichment of only 1.27 wt% ^{235}U.

The impact of the neutron multiplication correction for the SKB assembly analysis is seen to be significant. Excluding the correction resulted in larger deviations for almost all assemblies. For example, assembly PWR #23 experienced a burnup that was less than most assemblies with similar enrichments, resulting in relatively more residual fissile material in the assembly that increases neutron multiplication. Including the neutron multiplication correction decreased the discrepancy with measurements from 20% to less than 2%. The effect of the multiplication correction was not as evident in previously evaluated loading campaign data due to the similarity of many of the assemblies.

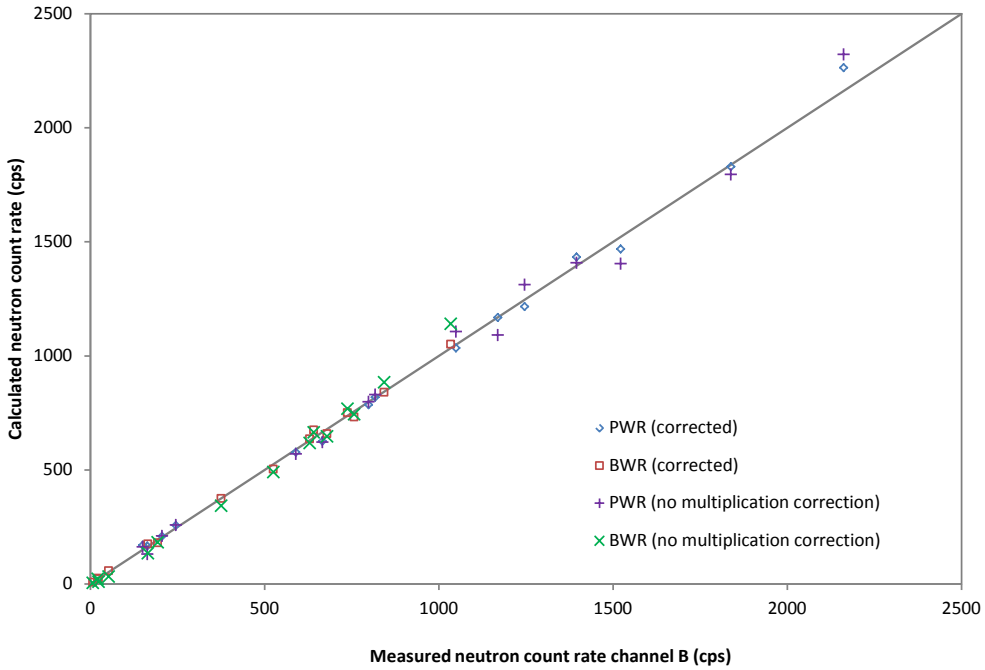

Fig. 4. Comparison of measured and calculated (uncorrected and corrected for subcritical neutron multiplication) neutron fission chamber count rates for PWR and BWR assemblies.

The relative standard deviation of the percent differences between calculated (after correction) and measured gamma signals, shown in Table 2 and plotted in Fig. 5, is 2.4% for the 15 PWR assemblies and 5.2% for the 15 BWR assemblies. The largest deviations occur for the BWR assemblies #23, #24, and #25. These assemblies experienced very low burnup and had the lowest gamma signals of all measured assemblies. Using a 95/95 two-sided tolerance interval and 15 measurements, and assuming a normal distribution, 95% of measured PWR assemblies are expected in an interval of ± 7% of the predicted values based on declarations with a 95% probability. For the BWR measurements, the 95% tolerance interval is ± 15%.

The relative standard deviation of the percent differences between calculated and measured neutron signals (Fig. 5) is 4.6% for the 15 PWR assemblies and 5.7% for the 15 BWR assemblies. Similar to the gamma results, the largest deviations occur for the low-burnup assemblies that had the smallest neutron signals. Using a 95/95 two-sided tolerance interval and 15 measurements, a 95% tolerance range of ± 14% is expected for the PWR measurements. For the BWR measurements, the 95% tolerance interval is ± 17%. All assemblies measured at SKB are within these tolerance ranges.

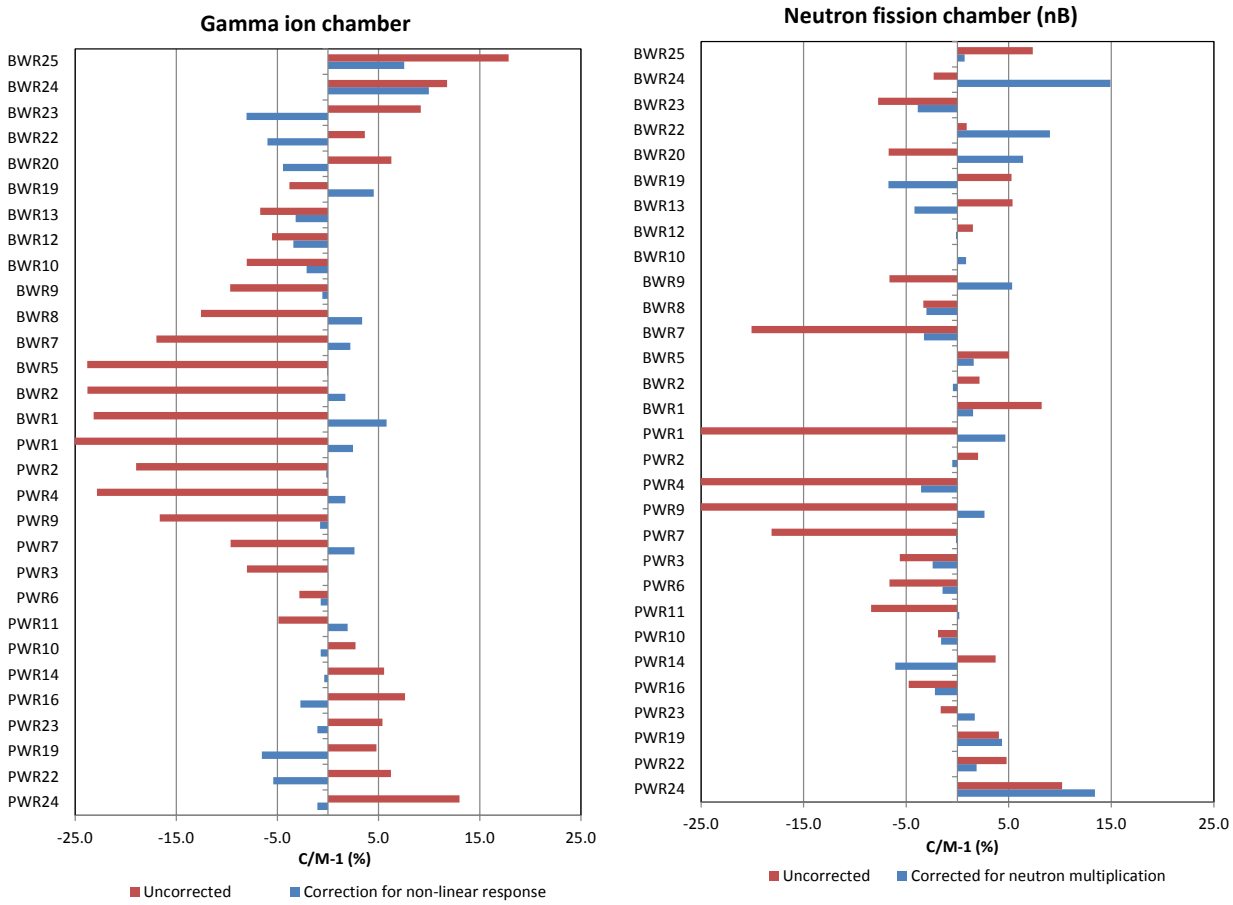

Fig. 5. Percent deviation between calculated and measured gamma ion chamber results (left) and neutron fission chamber (Channel B) results (right) for the SKB assemblies.

7. Uncertainties

Uncertainties are attributed to the measurements (counting and assembly positioning uncertainties), the declarations, and the analysis. These uncertainties define the ability to identify discrepancies in declarations and verify the integrity of the nuclear material. The main contributors to uncertainty in the spent fuel analysis method are described in this section.

7.1 Accuracy of the records

The assembly burnup declaration is obtained from reactor simulation codes and is generally accurate to 2% to 3% [8]. For typically discharged fuel, this burnup uncertainty results in an uncertainty in the gamma signal of similar magnitude (2% to 3%) and an uncertainty in the activity of the major neutron-emitting actinides of up to 6% for ^{242}Cm and 13% for ^{244}Cm. Therefore, achieving accuracy in the neutron count rate verification of less than ~10% will be limited by the uncertainty in the reactor records.

7.2 Operating history

Information on the operational details of an assembly may not be available to the inspector, including dates when the assembly resided in the reactor and the accumulated burnup by operating cycles that can be used (if available) to derive the specific power of the assembly during its irradiation history. Information on non-continuous assembly irradiation in the reactor (if removed for some cycles and then re-loaded in the core) can have a significant effect on both neutron and gamma signals due to the half-lives of the dominant nuclides: ^{154}Eu (8.6 yrs), ^{134}Cs (2.07 yrs), ^{137}Cs (30 yrs), ^{242}Cm (163 days), and ^{244}Cm (18.1 yrs). Other operational variables include the exposure to control absorbers, discrete burnable absorber rods, or control blades.

Detailed operating histories for the assemblies measured at Clab were provided by SKB and they were used in this analysis. To further quantify the uncertainties introduced by the lack of detailed data, additional analysis using only standard safeguards data (e.g., just fuel burnup without cycle history information) on these measurements are being performed and the results will be reported in the future.

7.3 Fuel and assembly design

Assembly designs are modelled using representative design information that approximates the range of design variations in use, and these approximations contribute to uncertainty. Although the class of assembly design(s) in a facility is usually known, other variables, such as presence of integral burnable absorber rods (e.g., gadolinium) and enrichment zoning (variation of rod enrichments in the assembly), are typically unknown to the inspector.

7.4 Axial burnup distribution

The assembly average burnup is reported by the operator; however, Fork detector measurements are typically performed at the mid-section of the assembly. The assembly burnup is adjusted in this analysis using a factor of 1.06 for PWR assemblies and 1.16 for BWR assemblies. This factor is estimated as the ratio of assembly centreline burnup to the assembly average burnup.. An analysis using the actual centreline burnup of each measured SKB assembly indicates that the variability in the axial burnup profile introduces an uncertainty of less than 1.5% in the centreline burnup, with variations of up to 5% observed for several low-burnup assemblies that have larger axial peaking factors.

7.5 Repeatability of the measurements

Uncertainty attributed to positioning of the assembly in the Fork detector was evaluated and the variability was found to be generally less than 1% in the gamma signal. The neutron channel B results showed differences of 1% to 2% and the neutron channel A showed differences of 3% to 5% when the same assembly was measured multiple times. The larger sensitivity observed in channel A may be due to the fact that the bare neutron fission chambers measure primarily thermal neutrons that are sensitive to any changes in moderation.

7.6 Assembly rotational uncertainty

The two Fork arms, each containing separate detectors, are designed to compensate for potential burnup gradients in the assembly that may lead to non-uniform neutron and gamma emission rates. The Fork measurements were repeated on three PWR assemblies with small and large radial burnup gradients after the assemblies were rotated in 90° steps. The gamma signal was found to have a small dependency on rotation (~1% variation). The neutron channel B also exhibited low dependence (about 1% to 2%); the neutron channel A had the largest dependence (about 2% to 4%).

7.7 Nonlinear gamma detector response

Corrections to the LND gamma ion chamber signals were required to compensate for apparent nonlinear response. The correction factor between the minimum and maximum gamma signal was larger than 40% over the range of the PWR assemblies. The gamma response was different from responses observed in earlier LND detector calibration measurements performed using a ^{60}Co source. It has not yet been determined whether the response is associated with the source energy spectrum, the ion chamber design, detector performance in mixed gamma and neutron fields, the detector operating regime, and/or the associated electronics. Linear response behaviour, or the ability to reliably correct for nonlinear response, will be a critical requirement to apply the Fork detector for quantitative spent fuel verification applications.

8. Conclusions

Safeguards agencies are facing increasing near-term spent fuel verification challenges from the expanding use of dry cask storage and with the planned repositories in Sweden and Finland.

EURATOM has identified data quality (better instruments and improved data evaluation to reduce false alarms) and resources (better efficiency and reduced costs) as key near-term support needs.

The research described in this paper addresses both improved data evaluation efficiency and improved accuracy by using rigorous modelling and simulation software and nuclear data. The analysis methods implemented in iRAP have been upgraded based on initial instrument testing and applied to measure a very diverse set of assemblies at the SKB Clab facility. These developments enable advancement of the Fork detector from a qualitative measurement instrument used frequently as an attribute test, or with limited semi-empirical analysis, to a fully quantitative instrument capable of verifying operator declarations with improved accuracy.

This research also points to a need for instrument improvements. The ion chamber response was found to be nonlinear with the gamma ray signal, which represents a potential roadblock for wider quantitative application of the Fork detector. Alternative gamma instruments, such as the Cadmium-Zinc-Telluride (CdZnTe) detector, that have been previously investigated for application to the Fork [9, 10] may provide a practical and cost-effective near-term solution.

Finally, while verification of operator declarations of spent fuel is one of the goals of the IAEA, safeguards inspections must also verify the integrity of a fuel assembly to determine that nuclear contents have not been diverted from intended use. Quantitative application of the Fork detector will enable improved partial defect detection by identifying statistically significant discrepancies between the predicted and measured signals. The level of partial defect detection (fraction of fuel being removed from the assembly) will be dependent on the detector performance, as is quantified in this paper. With improved quantitative analysis and review of the measurement data, the ability to detect partial defects is likely to be significantly better than the current 50% partial defect level, as is frequently cited for the Fork detector.

9. Acknowledgements

This work has been funded by the International Nuclear Safeguards Engagement Program (INSEP) under the Office of Nonproliferation and Arms Control of the National Nuclear Security Administration, U.S. Department of Energy, and by the European Commission. The Fork measurements performed at the Clab facility in Sweden were made possible with the support of the Swedish Nuclear Fuel and Waste Management Company, SKB.

10. References

1. A. Lebrun, S. Jung, S. Zykov, and A. Berlizov; *Status of NDA Techniques in Use for the IAEA Verification of Light Water Reactor Spent Fuel*; INMM (ISBN: 978-1-62993-580-5); 2013.
2. Schwalbach, P., et al.; *RADAR: EURATOM's Standard for Unattended Data Acquisition*; Proc. Int. Atomic Energy Agency Symposium Int. Safeguards, Wien, Austria; 2001.
3. Gauld, I. C., et al.; *Applications of ORIGEN to Spent Fuel Safeguards and Non-Proliferation*; Proc. of INMM 47th Annual Meeting, Nashville, Tennessee, 2006.
4. Vaccaro, S., et al.; *Enhanced Spent Fuel Verification by Analysis of Fork Measurements Data Based on Nuclear Modelling and Simulation*; INMM Information Analysis Technologies, Techniques and Methods for Safeguards, Nonproliferation and Arms Control Verification Conference, Portland; May 12–14, 2014.
5. Vaccaro, S., et al.; *A New Approach to Fork Measurements Data Analysis by RADAR-CRISP and ORIGEN Integration*; *Trans. Nucl. Sci*. **61**(4); 2014; p 2161.
6. Tobin, S. J., et al.; *Experimental and Analytical Plans for the Non-destructive Assay System of the Swedish Encapsulation and Repository Facilities*; IAEA Safeguards Symposium 2014, Vienna, Austria; 2014.
7. Gauld, I. C., et al.; *Isotopic Depletion and Decay Methods and Analysis Capabilities in SCALE*; *Nuclear Technology* **174**, 2; 2011; p 169.
8. Electric Power Research Institute; *Determination of the Accuracy of Utility Spent Fuel Burnup Records—Final Report*; EPRI TR-112054; July 1999.
9. Tiitta, A., et al.; *Investigation on the Possibility to Use Fork Detector for Partial Defect Verification of Spent LWR Fuel Assemblies*; STUK-YTO-TR 191; 2002.
10. Doering T. W., and Cordes, G.A.; *Status of the Multi-Detector Analysis System (MDAS) and the Fork Detector Research Programs*; IAEA-TECDOC-1241; 2000; p. 286.

Session 6

Integrated Measurement and Monitoring

Progress and Status of Remote Data Transmission in EURATOM Safeguards

Konrad Schoop, Johan Stronkhorst, Jean-Francois Levert, Carlo Demartini, Juha Pekkarinen, Marcel Garrisi, Sylvain Kurek, Kai Ruuska,

European Commission, DG Energy, Directorate Nuclear Safeguards, Unit E1,
L-2920 Luxembourg
E-mail: konrad.schoop@ec.europa.eu

Abstract:

Based on some successful achievements and several years of experience the authors want to compare the advantages of Remote Data Transmission (RDT) against the costs and effort for secure implementation. An overview of the current and planned RDT implementation in the EU will be given. Furthermore the generic 'Security Plan' describing the principles and details of data transfer, distribution and storage, the results of risk analyses of data transfer with and without RDT, the security aspects and approaches, as well as the Incident Handling Plan will be presented. Last but not least we will discuss how EURATOM safeguards are monitoring the continuous functioning of the remote installed equipment. Details of the practical cooperation with the IAEA, including handling of remote maintenance, will be described. In addition, we will present the different challenges for the acquisition, evaluation and transfer of safeguards data within large facilities, focussing on large reprocessing and fuel fabrication plants. Recently, a successful network, equipment and software upgrade in a French fuel fabrication plant gave us important feedbacks that have been applied to upgrade the networks in other reprocessing plants in the EU.

1. Introduction

The European Commission (EC) and the IAEA have installed optical surveillance systems, electronic sealing and data acquisition systems in most of the European nuclear facilities based on their obligations stipulated in international safeguards treaties and agreements. These systems operate completely isolated from all other systems in the nuclear facility. The data from these systems are stored on removable storage devices, and where no remote data transmission (RDT) is installed, they are transported by the inspectors to Luxembourg and Vienna headquarters for review. In case of installed RDT the data is transferred automatically to the EC Headquarters (HQ).

In order to separate data from different sources, three isolated systems are in operation in the HQ (details see chapter 4)
- the UK RDT system, operational between Sellafield site and EC HQ since 2007 [1], will soon be extended to also cover Dounreay and Sizewell sites,
- the France RDT system, currently under negotiation, preparation and construction and
- the EU Non-Nuclear Weapon States (NNWS) RDT system [2,3], operated jointly with the IAEA since 2009 and being extended step by step to connect nearly all nuclear sites in the EU.

After the introduction of IAEA Integrated Safeguards with Short Notice Random Inspections (SNRI) in the EU NNWS, the EC guarantees a permanent optical surveillance in the nuclear facilities in order to cover the time period following the SNRI announcement until presence of inspectors. To do this the EC is installing RDT in concerned facilities, while the systems on-site remain in principle unchanged. Only if necessary, few components in the existing housings are changed by EC technicians. If Member States or nuclear operators require specific individual measures for IT security reasons, they might be implemented. For example the British Office for Nuclear Regulation (ONR) and the German Bundesamt (BSI) have required the use of specific VPN devices approved by them and the German operators have required an additional time delay of 24 h.

2. Description of the RDT implementation

2.1. The basic principles

The basic principle of the RDT link is the creation of a Virtual Private Network (VPN) tunnel between the fully isolated data acquisition system (i.e. optical surveillance or sealing system) inside the nuclear plant and the isolated collecting server at EC HQ in Luxembourg over an internet broadband connection. The VPN is created often over a DSL line by Netscreen VPN routers with firewall and encryption/decryption functionalities. In most cases, the daily files of the previous day will be pulled once a day by the collect server in Luxembourg from the remote facilities and the data from the NNWS is simultaneously forwarded to IAEA HQ in Vienna using a second VPN tunnel (see Fig.1). In the secured review rooms at the Luxembourg EURATOM HQ dedicated systems are available to review the acquired inspection data on the Storage Server.

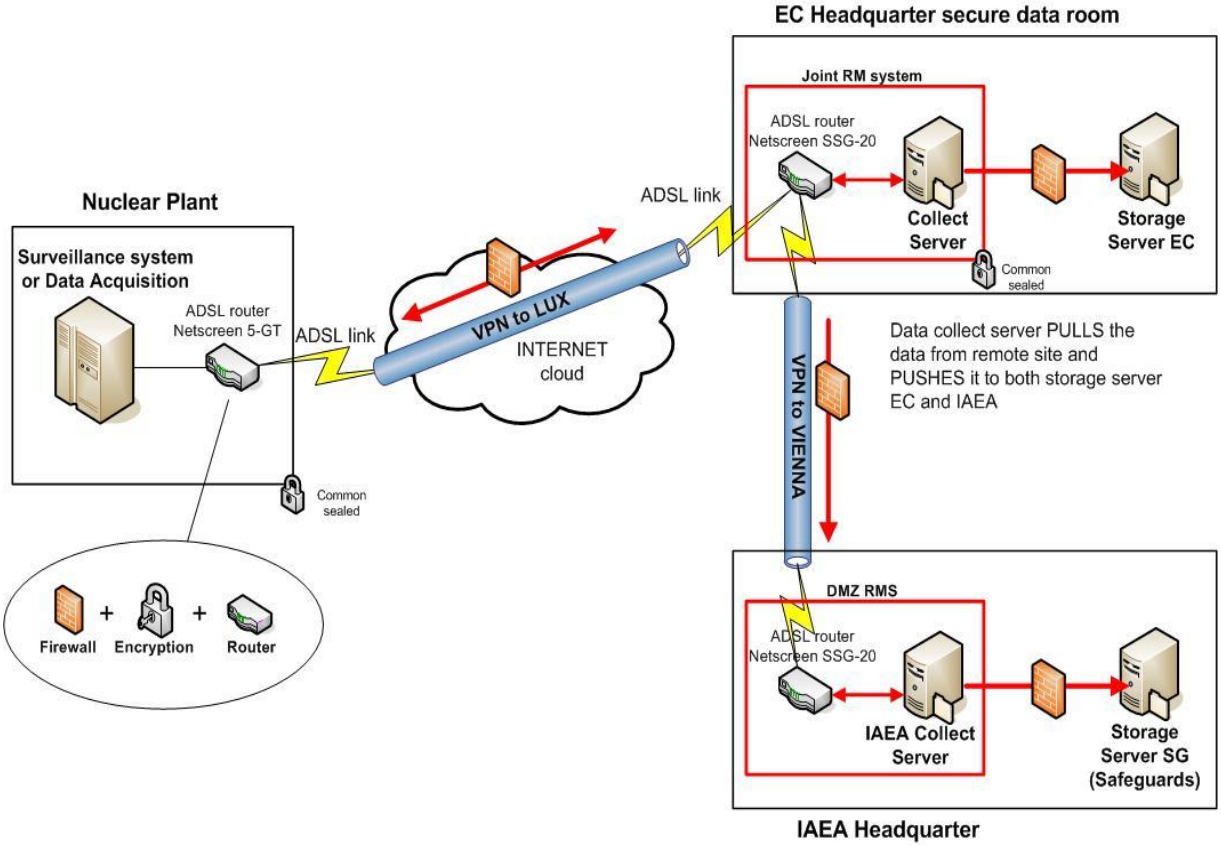

Fig. 1: Concept of Remote Data Transmission for EU NNWS

2.2. Routine data transmission

The implementation of RDT is based on a bidirectional VPN tunnel, but the data flow for routine transmission is unidirectional from the facility to the HQs and occurs often only once a day with data from the previous day. So the transferred images are typically between 2 and 30 hours old and there is no real time image transmission.

The collect server in the secured area in Luxembourg pulls routinely the data of the previous day from the remote site over the secured VPN tunnels at pre-defined times. This data set is a copy of the data stored on the removable storage media of the remote (surveillance) system. Then the data is copied simultaneously to isolated data servers in Luxembourg and Vienna (via an additional VPN) using a push routine. The pull routine by the collect server was chosen for security reasons because if the traffic is initiated from inner (trusted) side to the untrusted outside the firewall rules can be greatly simplified. All traffic request from outside will be blocked; only a creation of a VPN tunnel where certificates will be checked and ping requests are allowed to pass the firewall for testing the

connection from the remote site. All download jobs are automated and run unattended. The data flow for routine data transmission is shown in figure 2.

The hardware used for the VPN has several security certifications including FIPS 140-2 and NATO-Restricted. These devices are already being used by the EC and the IAEA at several nuclear sites. The integrated site-to-site IPsec and VPN features allow a secure link to be established between the plant and EC premises. The data packages are encrypted by a state of the art AES process while non-authorised requests or packages are blocked by the firewall. The hardware both in nuclear plants and at EC headquarters is placed in cabinets with common IAEA/Euratom seals. The access to the VPN device setup is password protected and the remote management function is only possible via the VPN tunnel. Thus the configuration changes are only possible by authorised personnel in the presence of both inspectorates.

2.3 The EC HQ Infrastructure

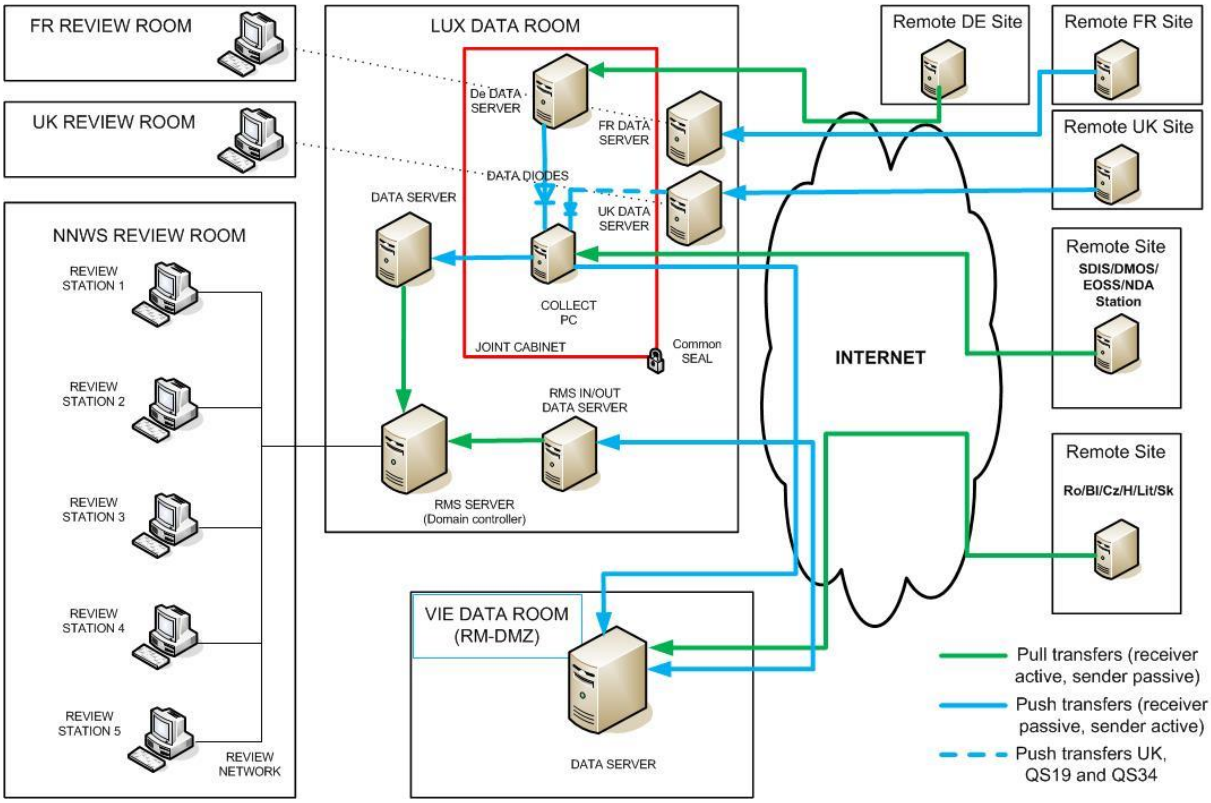

Fig. 2: The data flow in the RDT systems HQ infrastructure (incl. safeguards review and archive)

The data generated by remote safeguard systems are pulled from remote sites and copied in batches routinely on both Luxembourg and Vienna data servers. For most of the new EU member states installations the IAEA had already RDT installed before INFCIRC 193 came into force. For this historic reason data from these facilities are often still collected by the IAEA in Vienna and then automatically transferred to Luxemburg using the second VPN channel. For better upgrades of these old systems it was agreed with the IAEA in 2009 to transfer them step by step to the common system. For historical reasons the file naming and structure are different on both servers. To allow a single centralized repository in EC HQ with a common file structure, a centralized server named RMS-SERVER has been put in place.

The RMS server in Luxembourg receives and stores all safeguards data (including those manually transported by inspectors or received remotely from Vienna) and makes it available to the 5 NNWS review stations. This very small "review net" is fully isolated from any other networks. Intermediate servers, firewalls and data diodes are in place between external systems (remote sites and IAEA in Vienna) and the RMS-SERVER, so there is no direct contact from outside to the RMS-SERVER itself and therefore no possibility to enter RMS-SERVER from outside or to use it as a bridge between different external sites. This and the firewall rules on the VPN router ensure that the systems at the nuclear sites have no contact to any other systems.

The whole RDT system performance is evaluated daily by the Review Officer to check for missing files, anomalies and breakdowns. Automatic procedures (log file parser) have been put in place on RMS-SERVER to check all incoming daily files against their presence and appropriate length and some abnormal values in the log files (power, temperature, UPS battery status, etc.). If files are not present or abnormal conditions are detected, an alarm is raised and the Review Officer can verify the alarm condition and perform the necessary actions. Reviews will be performed usually in the review room using the five review stations directly connected to the RMS-SERVER on the dedicated review network.

If needed, data may be manually copied across an air-gap to the DG ENER secure network where it can be further evaluated by the inspectors. This secure network is fully separated from the normal Commission office network and is highly secured against access from outside. After evaluation the data are deleted from the secure network. The data on the RMS-SERVER are backed-up and archived for 5 years and deleted after that period.

In case of problems in the routine data transmission, the EC technical services will be active to solve the issue. If no problem is found on the data transmission equipment in Luxembourg, the operator of the nuclear facility might be asked for help to verify the presence of main power to the surveillance equipment and the functionality of the internet connection. If the remote connection cannot be restored then the EC will send a technician to repair the surveillance or transmission system. These activities are not time critical, because the on-site systems are storing the data for more than half a year.

2.4 Joint-Use Remote Maintenance System

Besides the automated routine data transmission it is intended to use the VPN connection also for remote administration of the installed data acquisition systems to further increase the efficiency. Examples of such interventions are remote diagnostics, rebooting of a system, control and change of camera settings without modification of the field of view on-site (because camera position and lenses are fixed) or adding new sites or remove certificates in the HQ configurations. In 2009 the EC and the IAEA agreed on the joint-use remote maintenance (JURM) system for NNWS. It has been installed in Luxembourg allowing a shared joint access to remote transmission systems and the corresponding data in nuclear facilities (see Fig.3).

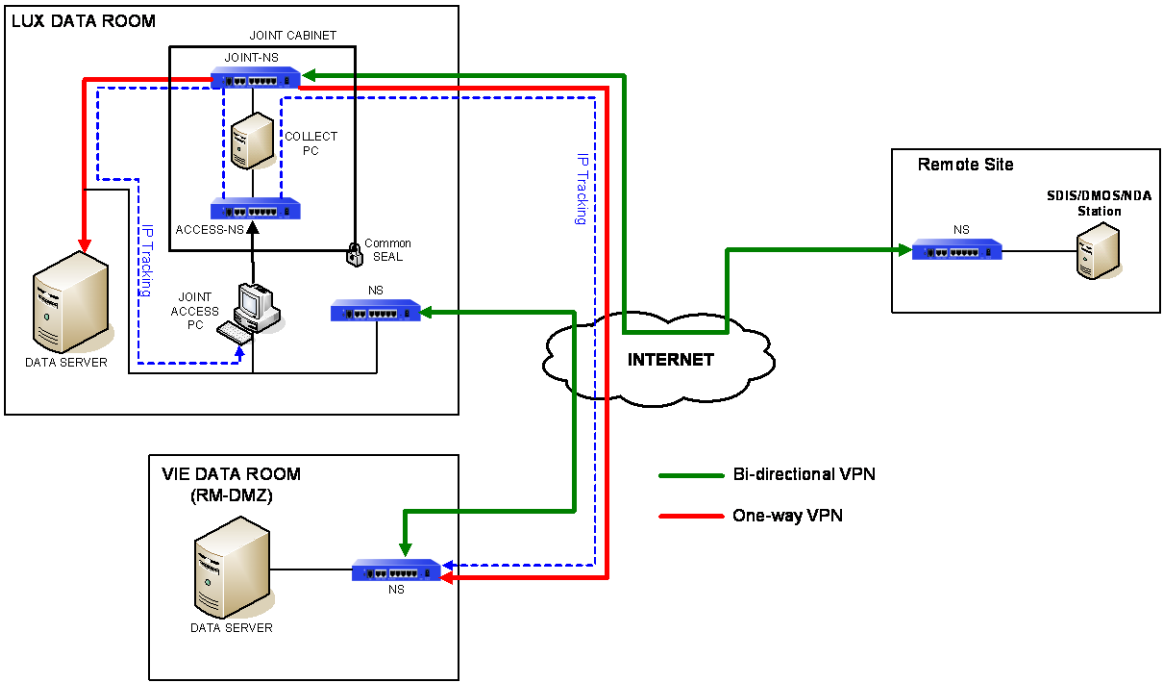

Fig. 3: The JURM system overview

The maintenance or check of a camera set-up requires the EC, the IAEA and, if necessary, the operator to agree upon a date for turning on the Joint-Access-PC in the EC premises. After synchronisation of the PC in Vienna with the Joint-Access-PC via a second VPN the IAEA can open the access to the Collect-Server using IP tracking. Then a bidirectional connection to the site can be established via the Collect-Server and the necessary maintenance or checks can be done. Each party

has the right to "pull the plug", meaning that there must always be a consensus for changes and near real time image transmissions.

3. Advantages of RDT vs. Effort

The RDT implementation is not available for zero effort. Therefore the advantages of RDT have to be compared with the effort for implementation – for the inspectorates as well as for the operators. Highest priorities are efficiency and effectiveness of inspections and very high IT security.

3.1. The Advantages of RDT implementation

RDT has obvious advantages if manpower can be saved, for the inspectors as well as for the operator. In installations where safeguards procedures require more than 1 to 2 inspections per year - the obligatory PIV (Physical Inventory Verification) and possibly their preparation - the RDT has the potential to be more effective, as verification and maintenance activities can be carried out in the HQ. That includes mostly installations with HEU and fresh PU, bulk handling facilities and stores with material difficult to access. Examples are special research and MOX power reactors, fuel fabrication, reprocessing and encapsulation plants. The inspectors are saving manpower and travelling costs and the operators save the administrative workload for preparing and accompanying inspections.

Since 2007 the EC is operating RDT from the EURATOM network in Sellafield (more details in 4.2.) [1]. The UK data server and review terminals are connected via a bidirectional VPN channel to the isolated EURATOM network in Sellafield allowing full access to all network connected EC systems on-site. The savings in manpower are considerable;

- for inspectors, having only to walk 100m to access all data from Sellafield at any time. Much of the safeguards data evaluation work can be carried out in HQ instead of the on-site office or on local machines,

- for the technicians, being able to daily check and intervene on the system performance. Many of the detected issues can be corrected by remote adjustments, reboots or software updates or with the help of inspectors present on site.

- for operators, because the request for inspectors document preparation and escorts are reduced and sensitive information will not be transported outside the secured environments.

Since the implementation of IAEA Integrated Safeguards it seems that RDT does not save effort in the LEU power reactors and spent fuel storages, but the RDT allows the EC to check daily the status of health of the systems and to react quickly in case of technical problems. This also serves the purpose to reduce consequences and effort for the operator in case of e.g. loss of continuity of knowledge.

For NNWS, a certain savings potential is expected for RDT linked to the spent fuel cask loading with Ion-fork measurements. Ideas already exist in EURATOM, but they have to be agreed with IAEA and operators first.

Another important advantage of RDT is the possibility to transport the image data in a more secure and timely manner compared to hand delivery made by the inspectors. This notably increases the data and IT security and allows safeguards inspectors to carry out certain inspection tasks even before their arrival at the nuclear facility. Therefore, this approach has advantages for both, the operators and the inspectors.

3.2. The effort for RDT implementation

The effort for implementation of RDT includes the administrative effort for agreements between stakeholders concerning IT security and modalities, the HQ infrastructure preparation, hard and software purchase and the remote site infrastructure preparation and hardware implementation as well as communication and maintenance expenses.

The time for administrative negotiations and agreements is very difficult to quantify. This is a process That may last over several years, especially for countries with a large nuclear infrastructure. For example, during the negotiation with France it was required to make a detailed risk analysis and

establish a security plan in line with the ISO 27000 series on IT Security and the related Commission regulations C(2006) 3602, 2015/443 and 2015/444. For this task the EC has hired an external IT security expert for several years who has not only performed the risk analyses but is also updating existing agreements with other stakeholders. Due to the existence of a Security Plan, agreements in principle could be achieved with Sweden and Spain in a very short period, shorter than 1 year.

However, the implementation of RDT depends also from specific installation in the country. Very often, the surveillance systems have to be upgraded before because the old single camera system is not 100% RDT compatible. The quickest installations have been done in Krsko and, thanks to the support from STUK and the operator FORTUM, in Loviisa

In the HQ the IT infrastructure for pulling, checking and pushing the data to other servers had to be prepared and maintained. The initial effort for the NNWS system can be roughly estimated to about 2 person-years and about 80 k€, of which about a half person-year was spent for the software development for the State of Health evaluation system and about 40 k€ was used to purchase the data diode from German collect PC to the (joint) Collect PC. The maintenance and follow up of the system requires about 80 persons-days per year, each adding of a new installation about 2 person-days (EC HQ effort only).

On the remote site usually installation costs occurs on cable placing from the safeguard system to the switchboard and for reimbursement of the DSL line costs. A good average is about 7000€ per MBA plus about four times 700 € for 4 year DSL line reimbursement. Several installations, mostly German and Eastern European, are charging much less because they only request reimbursement for external costs and don't take into account their internal cost.

The installation effort for a new site is much larger for the EC technical and financial service and can be estimated to 12 person-days per new site, where more than half of it is used for the administrative procedures in our HQ (writing of specifications, request for cost estimation, evaluating of cost and preparation of reimbursement agreement).

3.3. Comparison

Having in mind that the HQ infrastructure had to be built up only once and that an addition of a new installation is a reasonable effort, especially when combined with other activities onsite such as surveillance system upgrade etc. [6], it can be stated that RDT always makes sense in installation where more than 1 to 2 inspections per year are necessary. The costs and effort are still moderate but the savings can be enormous. Even for LEU reactor with cask loading and no static spent fuel storages it is useful to have RDT to transport the data in a secured and timely manner to prevent that data get lost or disclosed and to react quickly on malfunctions. In cases of shut down LEU reactors where the remaining fuel will be loaded into cask after the complete pond verification by DCVD it has to be decided if a redundancy of permanent surveillance is the best approach.

A real story of success is the RDT from Sellafield which allow the EC to have the same inspection performance with reduced staff available. We try to repeat this story also with the large reprocessing and fuel fabrication plants in France, but during the ongoing pilot phase in La Hague some restrictions have to be accepted and common trust has to be built first.

4. Progress in the last years and status of RDT

In the last few years [2, 3] a lot of effort has been spent mainly by the authors themselves to

- improve the EC HQ infrastructure and documentation set (risk analysis, security plan),
- develop and implement State of Health (SoH) data evaluation software,
- get principal agreements with all EU Member states having nuclear installation where RDT is useful and connect further installation to the NNWS RDT system,
- refurbish the onsite network systems to have reliable and secured connections to all data acquisition systems and
- upgrade the data acquisition and evaluation software and hardware [4] to newer operating systems like Win7 or higher. This action is not only important for higher IT security; it is a precondition for reliable unattended systems and for saving of human resources with RDT [5].

4.1 The RDT system with France

The RDT with France is still under development but the road map has been agreed and has to be implemented gradually. As a pilot project the data transfer from La Hague was chosen. The detailed risk analysis based on the EBIOS approach was agreed by the common working group of French authorities (CET, ANSI,…), operator (AREVA) and EC (ENER E2 and E1) and the security plan in line with ISO norms and EC regulations was established. The security plan describes the scope and principles of RDT, the hardware and software, the detailed risk analysis of the existing approach, the counter measurements and the remaining residual risk, the internal laws to be followed and the physical access, training and indoctrination of staff. The result of this very systematic work was also adapted to all other RDT applications so that today we have templates for all different RDT systems. The risk analysis has shown that the manual transport of data is the biggest risk concerning data disclosure and data loss. From the IT security point of view it is a necessity to implement state of art RDT as soon as possible.

The French authorities require for this pilot project a delay of 2 days for transmission of certain data. This delay is not an issue for the safeguards data evaluation, but has consequences for the structure of the network. The UP2 and UP3 network should be interconnected and only the near real-time network will be accessible from the inspector's offices on-site. The data will be mirrored with 2 days delay over a data diode to an additional server which is accessible from EC HQ. The use of a data diode guarantees that the data transfer can go only in one direction from real-time to the delayed network or server, but never back. The data on the delayed network are accessible via VPN from the EC HQ and can be remotely evaluated and maybe corrected. If these evaluated data have to be transferred back to the real-time network than it can be done only onsite with dedicated USB stick which should never leave the inspector offices there. The SoH data can be transferred immediately so that we have near real-time information about the functioning of our systems available in our HQ but the remote maintenance is very limited. Nevertheless, ideas and experience exist to solve this issue in the future.

Today the network refurbishment in La Hague is ongoing, aiming to be in line with the security plan. The network will be documented in detail (UP3 is already finished), the new switches and server hardware will be installed soon and the local SoH system will be fine-tuned to be use it immediately if RDT is in place. Furthermore, the hardware and software replacement and network restructuring in the inspector office is ongoing so that an audit of the system against the security plan can be performed in the second half of the year. We hope to have the RDT with La Hague in place around the end of this year already.

In the Melox plant we are at a final stage. In 2013 the network refurbishment was performed to have a network ring topology with modern routers which redirect the traffic over to the other side if one side is interrupted. Also most of the Data Acquisition (DA) cupboards with in total 60 sensors (gamma or neutron detectors with their dedicated electronic, door monitors, ID readers, balances …) connected to 16 DA-PCs were modernised. In 2014, after testing and qualifying our new release or data acquisition and evaluation software RADAR and iRAP [5] for Win7 operating systems we have first upgraded the historical databases to a newer Oracle version, then we migrated to the new RADAR and iRAP versions and finally we replaced the inspector office hardware by a complete virtual system comprising two hot redundant servers sharing a common NAS and hosting a part of the IT infrastructure. All these activities were done on running 24/7 systems without any data loss and very low interference with the inspection schedules.

4.2. The Sellafield RDT system

The Sellafield network has historically grown over the last 20 years [4] starting from small local surveillance, sealing and DA systems in Thorp, SMP, Magnox and SPRS. They have been gradually connected to each other by different technologies (Fibre optic, ATM, TCP/IP,…) and connected via VPN to a server located the EC HQ secured data room in 2007 so that a full access to the entire judge network in Sellafield is possible. A network and hardware refurbishment was really necessary [3] to achieve reliability and redundancy in future using state of art hardware and routers.

In 2013 the existing network status was well documented in detail and a plan for restructuring and additional lines was established. Fig. 4 gives an overview about the logical fibre optic network only. In

total 134 sensors are connected to 37 DA-PCs. In this figure the surveillance system PCs and the data evaluation PCs in the inspector office are not included. In 2014 gradually the network was upgraded during full operation of the entire systems without any data loss. Now the activities as in Melox above will be repeated, first the databases will be upgraded, then the RADAR/iRAP software and office hardware – this time under consideration to perform it together to save time and human resources.

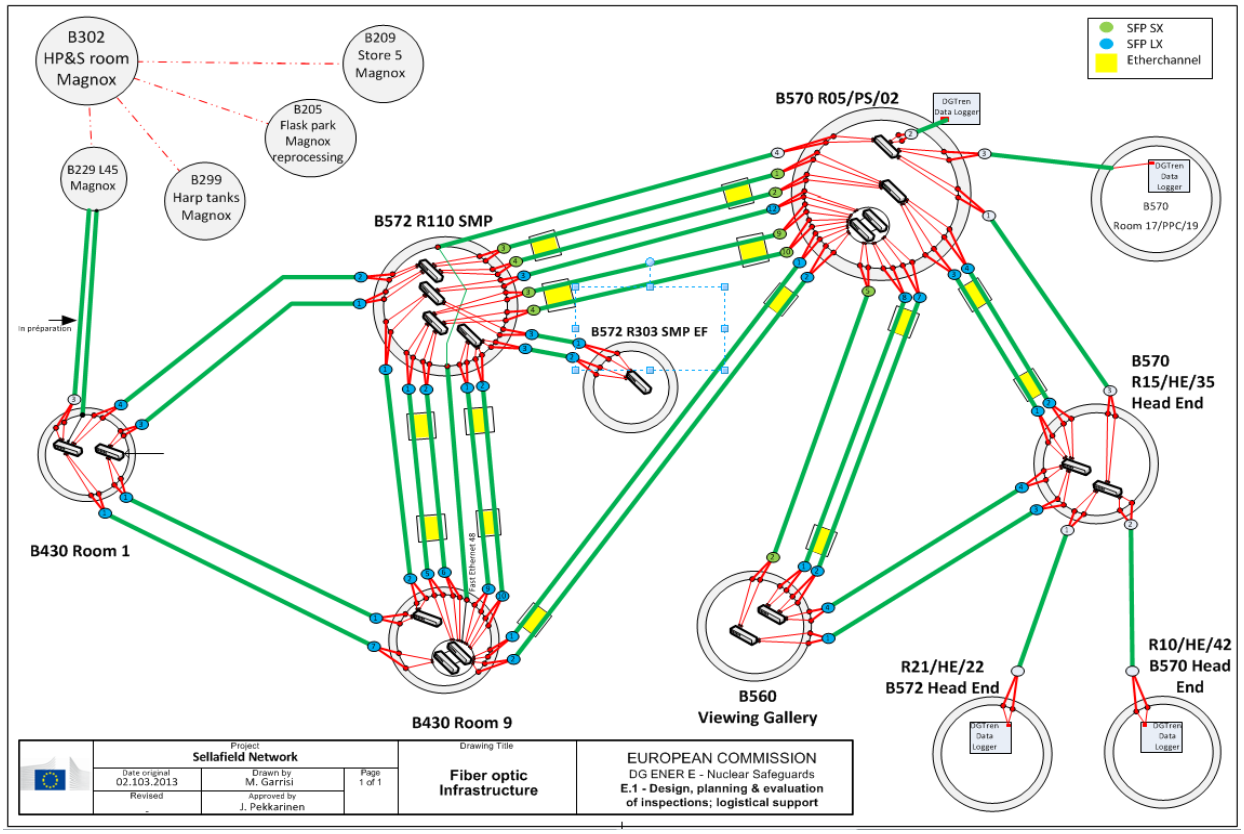

Fig.4: Sellafield Network Fibre Optic infrastructure

Concerning RDT documents the "Accreditation Document Set" [1] upgrade is ongoing to a "Code of Connection" which establishes together with the Sellafield Security Plan the legal framework for the data transmission between the Sellafield operator and EC. Until now an unsolved issue is the limited band width of DSL connection from Sellafield site to the next DSLAM but here the operator and EC are depending from the British Telecom. A better connection is envisaged for the next years, which will then allow us also to transmit several images regularly.

4.3 The NNWS RDT system

In the recent years, principle agreements for RDT could be achieved with Germany, Finland, Sweden and Spain. There is only one country in the EU still missing, mainly due to lack of sufficient human resource in the EC. One reason for the quick results in few countries is the existence of the security plan template. It gives the security experts of national authorities and installations an easy way to quickly find answers to their questions. The discussion with Finland was very helpful in this process because a chapter about protection of privacy was included in the security plan and a penetration test of the VPN connections was carried out on the initiative of FORTUM.

Gradually more and more installations will be connected to the system described in chapter 2. The connection to RDT, however, often requires an upgrade of the connected system, i.e. the single optical surveillance systems. The successor system NGSS is well tested and ready for deployment since October 2014 [6]. First installations were already done in Loviisa, Sellafield and Spain; Sweden, Italy, the Netherlands and Germany will follow soon.

The HQ infrastructure has been improved and restructured as mentioned in chapter 2.3. and a software for automated check of the system's performance was developed. The so-called log file

parser is running on the RMS server every day in the morning or on request and is checking if all expected files from previous day of all listed systems are available, if the file size is in the adjustable range (i.e. +/- 10 % of the average of the last 10 days) or if in the RADAR log file some parameters have strange values. Based on the checking result the errors will be shown on an alarm page where the review officer can flag them according to actions he has taken. The history page is showing the alarm history of the last 30 days over all listed systems with different colours. A wizard allows managing the different systems to be included in the parser. This parser can also been used in local systems in La Hague and Melox where historically the Nagios software was used to record the SNMP traps (predefined alarm messages from operating systems).

By upgrading the HQ data room internet connections we no longer have bandwidth issues with the downloads, but the limited upload speeds of asymmetric connections used to forward the data to the IAEA can still be a bottleneck at times. However, it seems that this issue can be solved later this year.

From the about 80 installations (with 143 MBAs) in the EU NNWS where we get regularly data, one third (27) is connected to the RDT system. That includes installations from Slovenia, Italy, Czech Republic, Slovakia, Hungary, Romania, Bulgaria, Poland, Lithuania, the Netherlands, Germany, Finland and soon Sweden and Spain. Additional 15 installations could be connected in the next months because all the administrative issues are solved, the reimbursement agreements are in progress and the necessary hardware and software is available on stock. The biggest issue is the limited human resources but by sharing installation work with the surveillance team and getting help from the IAEA SGTS and EC inspectors we hope to solve this issue too.

5. Summary

In the past few years a lot of effort has been spent to prepare the necessary network documentation, to adapt the HQ infrastructure, to automate the SoH checks and modernise and upgrade the infield infrastructure and networks for remote data transmission and maintenance. Milestones were the creation of the security plans, implementation of local and central automated SoH data evaluation, the review net installation (Fig. 2) as core part of HQ RDT infrastructure, and the successful complete upgrade of the Melox safeguards infrastructure.

We hope that by the end of this year certain other milestones can be achieved, like the first RDT from France, the nearly completed modernisation of the Sellafield data acquisition and evaluation infrastructure, and the connection of more than 50 % of installations to the NNWS RDT system. But there are also plenty of other tasks and projects on the horizon, so that the available human resources will play a deciding role.

6. References

1. M. Beaman, P. Chare, P. Schwalbach, W. Stanley, J. Vigo, Scope for Remote Monitoring in Large Scale Plutonium Facilities, Proceedings of 27th ESARDA Annual Meeting, London, 2005
2. K. Schoop et.al., Developments in Implementation of Remote Data Transmission, IAEA Symposium 2010 (CN-184/239)
3. K. Schoop, et.al., Reference Configuration for reliable and secured Data Acquisition and Remote Data Transfer, Proceedings of 33rd ESARDA Annual Meeting, Budapest 2011.
4. P. Schwalbach et.al., RADAR and CRISP – Standard Tools of the EC for remote and unattended data acquisition and analysis for nuclear safeguards, IAEA Symposium 2006 (CN-148/195)
5. A. Smejkal et.al., Automated Processing of safeguards data: Perspective on software requirements for a future "All in One Review Platform" based on iRAP, Proceedings of 37th ESARDA Annual Meeting, Manchester, 2015
6. J. Pekkarinen et al., EURATOM experiences on NGSS infield implementation preparation, Proceedings of 37th ESARDA Annual Meeting, Manchester, 2015

An update on the implementation of remote data transmission (RDT) in the dry interim storage facilities in Germany

A. Jussofie[1], W. Graf[1], K. van Bevern[2], W. Geißler[3] I. Niemeyer[4], A. Rezniczek[5], W. Trautwein[6], K. Schoop[7]

[1]Gesellschaft für Nuklear-Service mbH, Frohnhauser Str. 67, 45127 Essen, Germany
[2]VGB PowerTech e. V., Deilbachtal 173, 45257 Essen, Germany
[3]RWE Power AG, Kraftwerk Biblis, 68647 Biblis, Germany
[4]Forschungszentrum Jülich GmbH, IEK-6: Nuclear Waste Management and Reactor Safety, 52425 Jülich, Germany
[5]UBA Unternehmensberatung GmbH, An Gut Forensberg 40, 52134 Herzogenrath, Germany
[6]Bundesministerium für Wirtschaft und Energie, Villemombler Str. 76, 53107 Bonn, Germany
[7]European Commission, DG ENER E1, L-2920 Luxembourg

E-mail: astrid.jussofie@gns.de, katrin.vanbevern@vgb.org, Wolfram.Geissler@kkw.rwe.com, i.niemeyer@fz-juelich.de, Rezniczek@uba-gmbh.de, wolfgang.trautwein@bmwi.bund.de, Konrad.Schoop@ec.europa.eu

Abstract:

The importance of dry interim storage for SF management is emphasized by the enactment of the Law on Site Selection from 23rd July 2013 for a repository to store heat generating radioactive waste, which requires the definite repository site to be selected until 2031. As long as no operating repository is available, the intermediate storage of spent fuel and heat-generating waste, which storage licence is currently limited to 40 years, is the only legal possibility in Germany. The remote transmission of Safeguards data from the dry interim spent fuel storage facilities (SFSFs) to EURATOM and IAEA HQs is not only important in the light of maintaining the continuity of knowledge (CoK) during announcement of short notice random inspections, since it allows to detect a failure of the systems on a daily basis by monitoring the Safeguards equipment. Furthermore, RDT improves substantially the security of data transport.

Since in Germany the interim dry SFSFs underlie different license and supervising authorities, a fully functional RDT solution was developed by EURATOM and IAEA by implementing also the recommendations by the Federal Office for Information Security (BSI) and established by means of a field trial in the dry SFSF at Ahaus under the German Support Programme to the IAEA. The promising results of the field test from September 2012 to January 2013 needed to be confirmed by a longer follow up operation in order to demonstrate the long-term reliability of the unattended RDT system.

The paper will summarize the progress made over the last two years in achieving a RDT implementation approach top-down from the federal level to the individual operators of nuclear facilities. An update of the experiences gained and the current status of RDT implementation in the German interim dry SFSFs will be given.

Keywords: Remote data transmission, field trial, continuity of knowledge, interim dry storage facilities

1. Introduction

The political decision in 2011 to shut down immediately eight of a total of 17 German reactors that started in or before 1980 and the remaining nine reactors stepwise by 2022 [1, 2] as well as the enactment of the Law on Site Selection from 23rd July 2013 for a repository to store heat generating radioactive waste provide a unique situation in Germany regarding spent fuel management [3]. The new act determines no preference for a specific host rock type and foresees the restart of the search for high level radioactive heat generating waste with participation of the public in all process steps as a necessary precondition for a site selection supported by a

broad consensus; major decisions are finally made by law. Based on the three legally fixed temporal milestones of the current site selection act, operation of the repository is foreseen after completing the site selection process until 2031 as well as after completion the following licence and construction phases.

Germany's accelerated exit from nuclear energy that is associated with the need for defueling of nuclear power plants as soon as possible by temporarily increasing the loading of SF into casks on one hand, the timeline deriving from the current site selection act on the other hand – both emphasize the importance of dry interim storage for SF management and the need for long-term reliable unattended Safeguards (SG) measures in order to preserve the continuity of knowledge (CoK). With regard to a sustainable SG concept for long-term interim SF storages the importance of the failure-free operation of optical surveillance and, hence, the importance of remote image transmission will grow in consequence of a decreasing diversity of suitable seal types. It can be assumed that maintenance-free passive seal types will be preferred to battery containing electronic seals as EOSS. Through the increasing application of the passive Cobra seal, the optical surveillance in conjunction with RDT may contribute to the preservation of the "dual principle of Safeguards instrumentation" since the application of different technology types increases failure resistance.

The implementation of RDT in the German SFSF was mainly motivated by the concern that the failure-free operation of the unattended Safeguards instruments is to be ensured under the Integrated SG-regime, where the camera function has to be guaranteed within the short notice random inspection (SNRI) notification period of 48 h. Since without RDT, malfunctions or a functional loss of the SG cameras are not automatically returned to the inspectorates, EURATOM used to check the functional state of the camera / video system and to exchange the hard disk with the stored image files on-site once a year in the absence of IAEA in addition to the inspections performed by both inspectorates as a joint team.

Hence, the implementation of RDT in 15 dry SFSF in Germany (12 on-site dry SFSF, the two centralized SFSF at Ahaus and Gorleben and the SFSF at Lubmin) is for EURATOM also under the aspect of budgetary constraints of major interest, since RDT enables EURATOM to reduce their inspection efforts by increasing the efficiency of routine Safeguards. In Germany without a national Safeguards authority, EURATOM is in charge of establishing and maintaining the state's system of accounting for and control of nuclear material subject to Safeguards under the agreement INFCIR/193. In compliance with this obligation, EURATOM can only reduce their inspection frequency with the application of compensating measures in order to keep the quality of their control function.

A further reason for the implementation of RDT is the confidentiality of the collected images what the main concern is for the operators. The SG data have been stored compressed but unencrypted on removable hard disks so far so that the risk of an unauthorized data disclosure through a theft during their physical transport to Luxembourg and Vienna is higher than during their remote transmission.

2. Security arrangements for sensitive data

The protection against unauthorized data access through unauthorized users that could gain access to the RDT system to make unauthorized changes to the IT-system or to the transmitted and stored data is the major requirement of the operator. The particular situation in Germany is a result of the decades-long anti-nuclear movement that opposes the use of nuclear power. Images from a SFSF in publicity would demonstrate that the issue of information security has not been dealt properly with. This is just what nuclear opponents are waiting for in order to jeopardize the reputation of the whole nuclear industry.

Because of the fundamental importance of confidentiality of SG data for German operators the BSI, the ultimate Federal Office for IT-security in Germany, was involved to check the concept of RDT developed by EURATOM and IAEA with respect to the operators' main concern of a risk of an unauthorized access to Safeguards data. A technical solution approved by BSI is of additional advantage for the German operators, since thereby the suitability of the security level for RDT is agreed on a federal level. Hence, this approach ensures a pilot solution that is applicable in principle to all SFSF regardless of the different license and supervising authorities the operators underlie

in consequence of the federal structure of Germany.

Basically, the original RDT concept of EURATOM and IAEA differentiates between state of health (SoH)-data and sensitive Safeguards data, which deserve special protection. In compliance with the German security requirements for sensitive data, the BSI recommended a modification of the basic RDT system developed by EURATOM and IAEA by installing two German developed devices in the RDT-system:

I. The SINA Box LE from Fa. Secunet AG, which has been approved by BSI for use at the national level VS-nfD (Germany) as well as at the international level EU restricted and NATO restricted, ensured a secure handling of image data.

II. The Data diode (SINA OWG2 Gateway with input and output server) in order to ensure a unidirectional data transfer. It was installed between the PC that collects the Safeguards data from Germany and the PC that collects the data from other non-weapon states of the EU. The data diode decouples the German RDT-network from other RDT networks so that a potential access from installations outside Germany to EURATOM IT systems or installations in Germany could be excluded.

The increasing concern for security in data transmission over the networks has resulted in virtual private network (VPN) solutions being the most preferred technology for secure networking. Accordingly, the technical solution of EURATOM and IAEA for RDT is based on a virtual private network (VPN) tunnel between the data acquisition system in the respective dry SFSF and the data collecting server in the EURATOM headquarter at Luxembourg using a broadband internet connection which is separated from the operator’s IT network. Following the transfer of data to Luxembourg the data are immediately transmitted to Vienna via a further VPN tunnel. The SINA box at the respective SFSF encrypt the SG data to be transmitted and the SINA-box at EURATOM headquarter decrypt the encrypted data transmitted. The Safeguards data are encrypted according to the Advanced Encryption Standard (AES)-algorithm by a 256 bit key which is only known by the two SINA-boxes.

The Point-to-Point Protocol Over Ethernet (PPPoE)-protocol is ensuring that during the transmission over the internet all data packages from the sender will arrive at the receiver without loss. All images are signed with an authentication signature, calculated already during the image capturing process in the DCM14 camera module. This signature is automatically verified during the review in the inspector's headquarter to ensure the genuine of the image. Further details of the technical solution adapted to German security requirements are given in the security plan for RDT connections with Germany [4].

3. The field trial - An essential step in implementation of RDT

In the next step the practicability of the RDT-system, which had been modified according to the recommendations of the BSI / adapted to the German security requirements was demonstrated under daily use conditions during a field test as part of the German support programme for the IAEA. The field test had been carried out at the central dry SFSF at Ahaus between 6/9/2012 and 31/01/2013 in two test phases. The first test phase was limited to the transmission of SoH data, which consist of SDIS-log-files and data from an EOSS which had been opened and closed for test purposes outside the storage hall by the operator at Ahaus. The times of seal openings and closings were recorded for comparison with the signals received at Luxembourg. The second test phase was extended to the transmission of sensitive data in the form of original images from the four surveillance cameras installed in the dry SFSF at Ahaus. The image transmission with a delay of 24 h is a crucial precondition for the German operators who have thus the opportunity to be on the same level of information as EURATOM and IAEA. The data flow for routine transmission occurs once a day with the data from the previous day so that the time required by the collect server Germany to acquire the transmitted data varies between 3 and 30 hours. Since the timeliness goals of IAEA and EURATOM do not require an image transmission in real time, the image data were delayed by additional 24 hours.

In summary, the RDT field trial in the SFSF at Ahaus has been evaluated as successful by all parties involved BMWi (Federal Ministry of Economic Affairs and Energy), BSI (Federal Agency for Security in Information Technology), FZJ (Forschungszentrum Jülich),

WKK (Nuclear Fuel Cycle Association) and VGB (Association for Power and Heat Generators). The RDT system ensured a complete and reliable data transmission applicable under daily use conditions. It could be demonstrated that all the images were genuine, recorded and transmitted with the valid (authentic) signature and the correct recording interval. Interruptions of the RDT-operation for several days remained without consequences due to the local storage capacity of the RDT system and its subsequent automatic synchronization. The field trial proved that the RDT-system based on the concept of EURATOM and IAEA in consideration of the German security requirements offers a technically fully functional solution applicable as a prototype to implement RDT in all German interim dry SFSF [5].

4. Further basic arrangements for RDT implementation in German dry SFSF

Apart from the German security requirements to be considered for the remote transmission of images, further basic arrangements were agreed on for implementing RDT in German SFSF:

- No connection to the operator's own data network: RDT transmission occurs via a separate communication line, which is the easiest and most effective measure to protect the network on-site from the introduction of malicious software when implementing RDT. In addition, RDT via a separate communication line also excludes the transmission of operating data.
- No impact on the plant operation: It is a general concern across the whole nuclear industry that SG measures may not impede the operational processes.
- No increase of the operators' effort by RDT:

  The daily transmission of images may not lead to increased inquiries by EURATOM with the potential consequence of an increasing inspection frequency, a higher control density or other operators' efforts.

Specific considerations were made regarding the compliance of RDT with the operator's Privacy Policy. For this purpose the operator's data protection officer was consulted on the remote data transmission of images since it can not be excluded that the transmitted images, which are taken inside the dry storage facility in order to follow the path of SF - currently only into and within the material balance area (MBA)- coincidentally may also show facility staff. However, the view angle of the camera is chosen such that movements of the big-sized transport and storage casks can be monitored within a large area of the MBA. The review of the transmitted images by the inspectorates is limited to images that indicate movements of big objects such as casks. As long as no movement is registered by the review software program, the review of images is carried out automatically by comparing consecutive images and triggering a human review in case of differences between images. Since no personal data is collected, nor any records are kept that can be linked to an individual, the inspection data collection will not be in conflict with the operator's Privacy Policy

This applies equally to the physical protection of the dry SF storage facilities. In case of the SF storage facility at Ahaus print outs of images were handed over to the data protection officer on request in order to demonstrate the respect of privacy.

Under the aspect of data protection, it was necessary to assure that the recommendations of BSI have been implemented and that the storage of the transmitted data is only temporary. Accordingly, after the review, the images will be archived for 5 years, after that period the storage media (HDD and/ or DVDs) will be physically destroyed. It was concluded that from a data protection perspective, no objection against the remote transmission of SG-related images exists.

In addition, the works council was informed on the field trial of remote transmission of Safeguards data. It was emphasized that the operators are legally obliged to tolerate and support the control of nuclear material by the relevant supervising organizations EURATOM and IAEA. According to the body of Safeguards rules and Safeguards regulations, EURATOM and IAEA have the right to record images and to review them. It was pointed out that the information content of the transmitted images remains unchanged by RDT and only the path for transmitting SG data from the storage site to EURATOM's headquarter has changed. It was assured that EURATOM is the

owner of all collected data and that the operator has no access to the image data. Hence, a control of staff performance is a priori impossible.

5. Considerable progress in the administrative field

The legal situation in Germany concerning the RDT to EURATOM and IAEA is incomplete, since the Implementation Act that is mandatory for the operators, does not cover Article 14 of the Additional Protocol especially regarding RDT. Therefore an approach top-down from the federal level to the single operator was necessary in order to pave the way for an implementation of RDT in all German dry storage facilities, which underlie different competent Federal Land authorities. The approach includes the following steps:

- Consultation of the relevant Federal Agencies via the Federal Ministry of Economic Affairs and Energy (BMWi) to ensure an approval of RDT implementation on the federal level
- Instructing the German Federal Land authorities to support the implementation of RDT in German SFSF
- Official Informing of the operators of the German dry SFSF about Implementation of RDT by BMWi

In consideration of the extensive preparatory work, the adherence to the basic arrangements agreed on and the successful field trial, the BMWi endorsed the RDT implementation in German interim dry storage facilities. After the approval of RDT implementation by the Federal Ministry for the Environment, Nature Conservation, Building and Nuclear Safety and that of BSI in 2014, BMWi instructed the competent German Federal Land authorities by letter dated 28 May 2014 to support the implementation of RDT in the dry interim SF storage facilities. Finally, BMWi informed the operators of the German SF storage facilities by a letter dated 17 June 2014 on the intended RDT implementation.

6. Status quo of RDT implementation

The implementation of RDT has been completed in three dry interim SF storage facilities in Germany including the SFSF at Ahaus. The two are the “Zwischenlager Nord” (ZLN) close to Lubmin, which was connected in 10/2014, and the storage at Biblis as the first on-site dry SFSF, which was connected in 03/2015.

The connection of the SFSF Krümmel, Lingen and Gundremmingen is coming soon, since the contract has been concluded. Start of RDT operation is expected for 06/07 2015.

In the SFSF Brunsbüttel, Philippsburg, Neckarwestheim and Gorleben the preparatory works are ongoing; the necessary infrastructure adaptations have been identified and cost estimates are in preparation.

7. Experiences

7.1 Reliability

After completion of the field trial the period of observation was extended for reliability estimations. Since the start of operation on 06.09.2012 an interruption of RDT from SFSF Ahaus to the headquarter of EURATOM occurred three times, namely in 09/2012, 11/2014 and 03/2015. It can be stated that until today virtually no additional effort of the operator is required for routine RDT operation.

In the storage ZLN an initial faulty cable connector caused RDT interruptions, which had no effect due to automatic synchronisation and data transmission later on.

Overall, based on the current experience an effort reduction should be achieved on the part of the operators as well as on the part of EURATOM and IAEA by implementing RDT, since the RDT system works reliably under daily use conditions and the Safeguards data are transmitted completely.

7.2 RDT-setup

Due to the experience from the Ahaus field trial, no technical problems occurred in the other two SF storage facilities, neither during installation of the RDT components on-site nor

their start-up. A stable VPN tunnel was created at the first attempt.

7.3 Lessons learnt

It can be stated that technically no significant problems emerged during the installation of the RDT-systems. However there is a potential for improvements in the administrative area field. For instance the execution of the reimbursement agreement in English would be easier in the official language of RDT implementing MS. Likewise, the availability of EURATOM's IT security plan in the official languages of the EU would facilitate the preparatory works for RDT. One of the major issues is the responsibility that has to be clarified between operator and EURATOM in the legal sense.
The approach of performing a pilot project with the involvement of all parties concerned (EURATOM, BMWi, BSI, Federal Land authorities and operators) and administrative provisions for implementing RDT in in the dry interim SF storage facilities could be recognized as a best practice.

8. Outlook

Completion of RDT-implementation in all German dry SFSF is foreseen in 2015/2016. Meanwhile EURATOM already aims at performing a pilot field trial for RDT from a German reactor. The implementation of RDT in nuclear reactors is only worthwhile if their operation time still lasts at least for 5 years. From the operators' point of view, however, the experience gained with RDT from dry SFSF has to be evaluated in the first step before starting a field test in a reactor thereby enabling a final evaluation of the experience gained with RDT from SFSF. However, arrangements and the concept made for SFSF are not fully applicable to reactors, since not all reactors are equipped with a communication line that is separated from the operator's IT network. In addition, the higher protection requirements to data and IT-systems in nuclear power plants have to be complied with.

9. References

[1] *Gesetz zur geordneten Beendigung der Kernenergienutzung zur gewerblichen Erzeugung von Elektrizität vom 22. April 2002* (BGBl. I 2002, Nr. 26, S. 1351).

[2] *Dreizehntes Gesetz zur Änderung des Atomgesetzes vom 31. Juli 2011* (BGBl. I 2011, Nr. 43, S. 1704)

[3] *Gesetz zur Suche und Auswahl eines Standortes für ein Endlager für Wärme entwickelnde radioaktive Abfälle und zur Änderung anderer Gesetze (Standortauswahlgesetz – StandAG) vom 23. Juli 2013* (BGBl. I 2013, Nr. 41, S. 2553).

[4] Jussofie A, Graf W, K. van Bevern, Niemeyer I, Rezniczek A, Trautwein W, Schoop K; *Ahaus remote data transmission (RDT) field test – from the operators' point of view*; Proceedings of 35th SARDA annual meeting in Bruges, Belgium, 27-30 May 2013.

[5] Jussofie A, Schoop K (EURATOM); *Feldversuch im Transportbehälterlager-Ahaus - Pilotstudie zur Implementierung der Datenfernübertragung in den Standortlagern (Abschlussbericht*); German Support Programme Report, JOPAG D.37/E1859 2013.

Verification of Spent Fuel Transfers in Germany

I. Tsvetkov[a], J. Araujo[a], G. Morris[a], Z. Vukadin[a], B. Wishard[a], W. Kahnmeyer[b], L. Matloch[b], W. Trautwein[c]

[a] International Atomic Energy Agency, A-1400 Vienna;
[b] European Commission – Directorate-General for Energy
Directorate E – Nuclear Safeguards, L-2920 Luxembourg:
[c] Federal Ministry for Economic Affairs and Energy
D-53107 Bonn, Germany

Abstract:

Following the decision of the German Federal Government to completely phase out nuclear energy by 2022, safeguards inspectorates are facing an increasing number of spent fuel (SF) transfers from nuclear power plants (NPP) to dry SF storage facilities. Verification of these transfers in the period 2014-2017 using standard approaches would have required about 1500 additional calendar-days in the field by inspectors. To meet the verification requirements with the available resources, the Agency together with the European Commission (EC) designed an innovative approach. The approach is making full use of safeguards cooperation with the EC and Germany's NPP operators to reduce the inspector's efforts, while fully adhering to the Agency's safeguards policy and requirements.

The approach includes verification for partial defect test using digital Cerenkov viewing device (DCVD) of SF inventories in a reactor pond(s) before and after a SF loading campaign; during the SF loading campaign all SF in pond(s) is kept under continuous surveillance, while the containment measures on SF casks, i.e. fibre-optic and electronic seals, and corresponding fibre-optic cables, are applied by the NPP operator in accordance with the agreed procedure. While the above approach allows for a substantial reduction of the Agency inspector presence during the SF cask loading campaign, it can only be implemented when good cooperation exists between the Agency, the facility operator, and, as in the case of Germany, the regional safeguards authority.

Keywords: verification; spent fuel; partial defect; Germany; IAEA

1. Introduction

The German Government's decision to permanently shut down eight NPPs in 2011 and to completely phase out nuclear energy by the end of 2022 by gradually shutting down the remaining nine NPPs was taken in the wake of Fukushima nuclear accident on 11 March 2011. The decision became part of the German Atomic Law on 31 July 2011 and is continuing to be implemented. As a result, the number of SF transfers from reactors to SF dry storages in Germany has increased substantially. The IAEA and the EC are facing an increased workload related to verification of these transfers, which for the period 2014 -- 2017 would require about 1500 additional calendar days in the field (CDFs) of the inspector's efforts, if current practice for verification was to be continued.

2. Development of the Safeguards Approach and relevant State-specific Factors

To meet the verification requirements with the available resources, the IAEA together with the EC designed an innovative safeguards approach. The approach is making full use of safeguards cooperation with the EC and Germany's NPP operators to reduce the inspectors' efforts, while fully adhering to IAEA safeguards policy and requirements. The following State-specific factors are essential for full utilisation of this approach:

a) A Comprehensive Safeguards Agreement (CSA) with an Additional Protocol (AP) should be in force in the State, and broader safeguards conclusion on the absence of undeclared material and activities should be drawn for this State by the IAEA
b) Appropriate State-level Safeguards Approach, e.g. integrated safeguards approach, should be developed and implemented in the State
c) Permanent surveillance measures should be applied to the spent fuel pond areas at relevant NPPs in the State
d) Facility operator and the State/Regional authorities should agree to apply IAEA containment measures without presence of IAEA inspectors, in accordance with agreed procedure.

The factors a) and b) allow for application of optimized safeguards measures, while factors c) and d) provide for substantial increase in efficiency gain of the approach.

For Germany, the broader safeguards conclusion was drawn for the first time in 2008 and was reaffirmed every year since; integrated safeguards has been implemented since January 2010; permanent surveillance measures are applied to the spent fuel pond areas at all NPPs; and the facility operators of German NPPs and the EC are willing to support the IAEA by applying containment measures without presence of IAEA inspectors. Thus, in Germany, all relevant State-specific factors for implementation of safeguards measures outlined below are present, and the safeguards approach for verification of SF transfers is expected to meet the required verification activities without substantial increase in utilized resources.

3. Safeguards Measures applied to SF Cask Loading Campaigns at NPPs in Germany

After SF has been discharged from a reactor to a SF pond, it is jointly verified by IAEA and EC inspectors by item counting (100%) and for gross defect test with PIV[1]-level detection probability, normally by Cerenkov Viewing Device (ICVD). The SF is then cooled in the SF pond for at least 5 years prior to its transfer to the dry storage. As the fuel assemblies at German NPPs are of the types that can be easily dismantled, a partial defect test is required to verify SF loading to SF cask, using the best available method approved for inspection use with random high (RH) detection probability. Currently, Digital Cerenkov Viewing Device (DCVD) and, if DCVD is not available or feasible, Fork Detector Irradiated Fuel Measuring System (FDET) are the best available NDA methods.

Traditionally, verification of SF for partial defect is carried out for each SF cask separately. Between the time of SF verification and until placement of the SF cask in the dry storage, continuity of knowledge (CoK) is maintained on each SF cask by surveillance and later by containment measures, e.g. seals, applied by the inspectors after loading of every SF cask. This approach requires approximately 7 CDFs of IAEA inspectors' efforts for each SF cask loading; therefore, it is not very efficient.

For States with broader conclusion, where a State-level safeguards approach has been implemented, e.g. Germany, the IAEA policy is to allow for certain relaxation of timeliness requirements for verification of SF transfers, i.e. when SF has been previously verified to the required level and has remained under successful Containment/Surveillance (C/S) measures, verification of SF prior to its transfer to SF cask is not required.

Based on this policy, the Agency and the EC have considered various conditions in the facilities in question in Germany and determined the optimal verification strategy for verification of SF transfers. Particularly for the shut-down NPPs where no incoming flow of SF is expected, the safeguards approach for verification of SF transfers to dry storage has been worked out as follows:

a. **Before** the beginning of SF loading campaign the SF inventory in the reactor pond(s) is verified with the required detection probability for partial defect test by DCVD

[1] Physical Inventory Verification

b. **During** the SF loading campaign all SF in the reactor pond(s) is kept under continuous surveillance, while the containment measures on SF casks, i.e. fibre-optic and electronic seals, and corresponding fibre-optic cables, are applied by the NPP operator in accordance with the agreed procedure
c. **After** the SF loading campaign the SF left in the reactor pond(s) is again verified to the same requirements as before the campaign
d. The containment measures applied by the operator on SF casks will be finally verified by both the Agency and EC inspectorates upon SF casks arrival at the receiving interim dry storage facility (verification for a group of casks).

This approach allows for substantial efficiency gains during SF cask loading campaigns, as it requires only limited IAEA and EC inspector presence for verification of SF assemblies and sealing of casks; however, substantial efforts are expected for verification of SF pond(s) inventory by DCVD before and after the campaign. Training of the facility operator for application of containment measures should also be taken into account. Thus, application of the above safeguards measures during SF cask loading campaigns should be carried out on a case-by-case basis, considering the operational status of the reactor, number of SF casks involved in the campaigns, operator's readiness to provide required information and apply containment measures. It is a further advantage of this approach that verification using DCVD and cask loading are decoupled in time, i.e. there is a certain flexibility regarding the timing of verification by DCVD. Sealing by operators also considerably reduces the need for coordination between the operator activities and inspection needs if compared with sealing by the inspectors. The approach thus results in added benefits for both inspectorates and the operator.

4. Provision of Information by the NPP Operator

For proper evaluation of surveillance measures, the NPP operator should provide the IAEA and EC with detailed information on the schedule of the entire SF cask loading campaign in advance, normally as soon as it is available. The information will include, *inter alia*:

- the start and end date of the SF cask loading campaign(s)
- the number of SF casks planned to be loaded during each campaign
- the number of SF assemblies and pins to be loaded (total and cask by cask amounts)
- the schedule of the loading of individual SF cask
- cask/container ID and IDs of all SF assemblies to be loaded in the cask
- presence and planned movement during the campaign of any other casks suitable for storing or transporting SF assemblies and pins in the area covered by surveillance
- number of pins to be loaded in SF casks (this activity would take place after the loading of all fuel assemblies or when loading the last SF cask)
- planned pin removal activities before and during the campaign.

It is expected that the spent fuel assemblies will be loaded and shipped ahead of any fuel pins. Any change in the schedule should be communicated to the IAEA and EC as soon as information becomes known to the operator.

5. Verification of Spent Fuel for Partial Defect using DCVD

The DCVD is a tool for Cerenkov Light examination of spent nuclear fuel, with partial defect test capability, to the visual pin level. A quantitative measurement of the light emission by SF assembly is possible and can be linked to the operator declarations of initial enrichment, burnup, and cooling time [1]. This quantitative measurement is a relative measurement; the evaluating software performs a consistency check on the Cerenkov light emission computing a normalization factor. For this reason it is mandatory that items that are compared to one another must have the same emission profile. Hence, it is necessary to receive detailed information from the NPP operator on the irradiation history, removed pins, fuel inserts, etc. for the whole SF inventory of a pond prior to verification. The verification with DCVD has three components:

1. Qualitative verification for consistency with declaration on item type, fuel map position and for missing pins

2. Qualitative verification of Cerenkov light emission profile, to distinguish between irradiated fuel and non-irradiated items (dummies or fresh fuel)
3. Quantitative verification of total Cerenkov light emitted against predictions.

Two thresholds are applied for the quantitative verification for partial defect:

1. A threshold of 30% represents a low intensity warning level and a threshold of - 30% represents a high intensity warning level
2. A threshold of +/-50% represents a potential inconsistency with regards to the Partial Defect Test objective.

Fig.1 represents an evaluation diagram of SF verification for partial defect using DCVD.

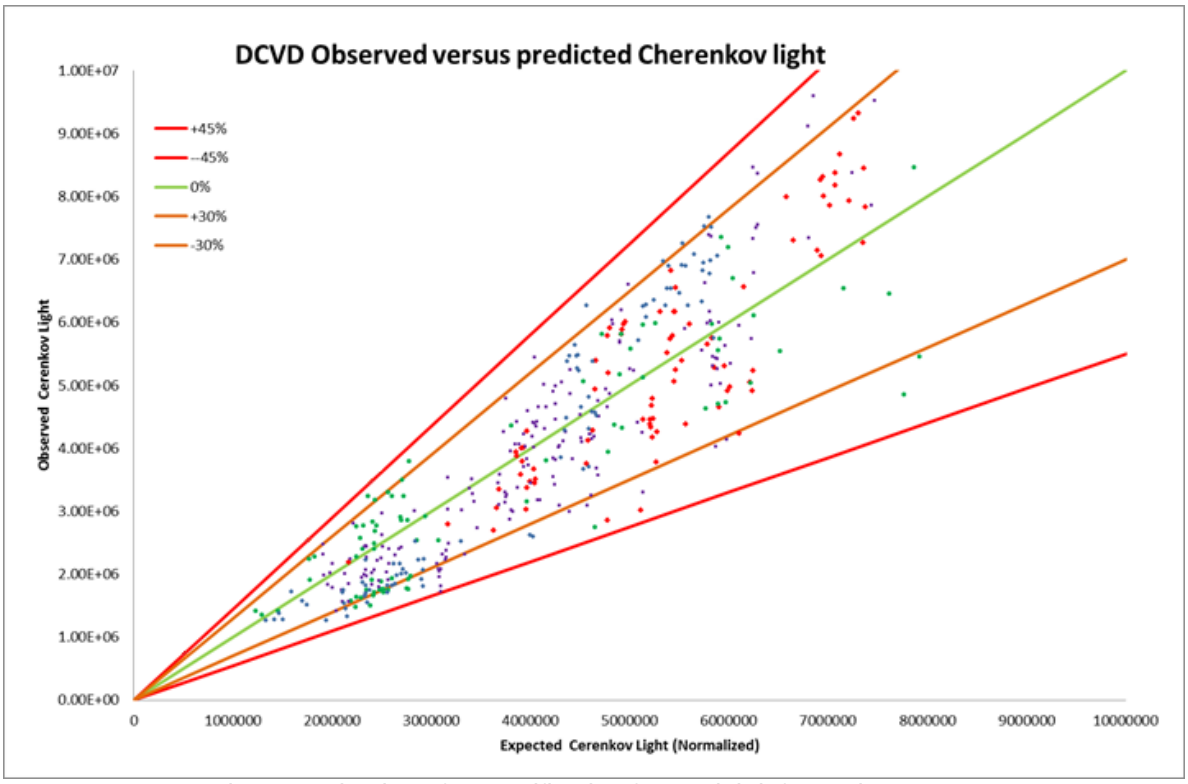

Fig. 1. Evaluation of SF verification for partial defect using DCVD

6. Application of Containment Measures by Facility Operator

Containment measures (optical COBRA and electronic EOSS seals) on SF casks are applied by the NPP operator when both the IAEA and EC inspectors are not present. The attachment (or detachment) of seals as well as the recording of the containment application activities will be carried out by the Operator, without the presence of inspectors, using specially adapted standard IAEA/EC equipment while the continuity of knowledge will be maintained on the seals and the sealed nuclear material.

Application of containment measures by operator requires special arrangements, equipment, and training for operator. In Germany, NPP operators require assurance on the correct application of COBRA and EOSS seals, for which purpose a special interface tool was developed by the EC for NPP operators to have assurance on successful EOSS attachment. The sealing reader system on Fig. 2 was developed by Dr. Neumann Elektronik GmbH under a contract with the EC to allow the NPP operators to read, save and generate a printout with the status of EOSS closure. This tool facilitates the sealing by the German NPP operators by providing documentary evidence of the successful handling of the sealing operation.

Fig. 2. Sealing Reader System.

7. Conclusion

The safeguards approach utilizing DCVD for verification of SF transfers and sealing by operators in Germany allows for substantial efficiency gains during SF cask loading campaigns, as it requires only limited IAEA and EC inspector presence for verification of SF assemblies and sealing of SF casks.

However, the approach should be implemented at each reactor on a case-by-case basis, after taking into due account the operational status of the reactor, number of SF casks involved, and the operator's readiness to provide required information and apply containment measures. Operators may also profit from this approach through a reduced number of inspections.

8. Acknowledgement

The authors wish to acknowledge great contribution to DCVD verification of SF for partial defect test done by IAEA technical experts, in particular Messrs D. Parise and S. Lackner.

9. References

[1] CSSP Report 123, SKI Report 02:25, *Development of a High Sensitivity Digital Cerenkov Viewing Device,* 15 May 2002.

Automated processing of safeguards data: Perspectives on software requirements for a future "All-in-one Review Platform" based on iRAP

Authors: Andreas Smejkal[a], Ralf Linnebach[a], Peter Schwalbach[a]

[a]European Commission
Directorate-General for Energy
Directorate E - Nuclear Safeguards
Luxembourg

***Abstract**:*

Acquiring, processing and analysing information to confirm and verify declarations on mass or flow of nuclear material is an essential part of EURATOM safeguards. Unattended measurement systems and automated review platforms are installed at all larger nuclear facilities in Europe and at the EURATOM headquarters in Luxemburg.

The information to be processed and analysed originates from a variety of sources and sensors acquiring data autonomously by EURATOM's standard data acquisition system RADAR (Remote Acquisition of Data and Review). Large amounts of data need to be analysed and compared with operator declarations by safeguards inspectors. To cope with this challenge, the use of adequate automated review tools is inevitable.

The integrated Review and Analysis Package iRAP, the successor of CRISP (Central RADAR Inspection Support Package), is a modular software package developed by EURATOM. It has been used for years successfully by EURATOM inspectors and has been recently adopted by the IAEA as a future review tool. Under a licence agreement with the IAEA, iRAP will be developed jointly towards an "All-in-one review platform".

Whilst the software package meets current requirements, it is essential to enhance the effectiveness of safeguards measures and the efficient use of existing resources. In addition, the construction of new facility types (geological repositories and encapsulation plants) in Sweden and Finland requires a careful adjustment of the existing solutions in order to prepare for future challenges and requirements.

This paper describes ongoing projects, like the integration of operators' branched and authenticated data into iRAP via EDAS, the Enhanced Data Authentication System developed by Sandia National Laboratory, and ongoing developments to automatize the verification of spent fuel measurements using a specifically packaged version of ORNLs ORIGEN code. A major challenge is the incorporation of video information into iRAP. A concurrent analysis of correlated video, seal and NDA data would be a significant improvement of the current review process.

All modifications and enhancements of this complex software system are managed under a legal agreement with the IAEA. A framework based on inter-institutional relationships between research centres and safeguards authorities has been established. It prioritizes and assesses software requirements coming from multiple stakeholders with various perspectives.

Keywords: unattended data acquisition; automated review; software development

1. Introduction

Unattended data acquisition and automated review have become an important part of modern nuclear safeguards. As a matter of fact, requirements on safeguards software have changed significantly in the last 10 years. Today nuclear material verifications at larger nuclear plants are highly dependent on automated measurements controlled and triggered by software modules without any human intervention.

Whilst unattended data acquisition systems as deployed by EURATOM are more or less invisible to inspectors, completely different requirements are applied to review and analysis tools.

The increasing number of unattended systems providing a great amount of information to inspectors and the need to optimize human resources in operational units have made it necessary to develop an automated data review platform which supports inspectors in their daily work.

Even if safeguards software is developed for a very small, but technically skilled, user group (EURATOM employs 163 nuclear inspectors [1]), non-functional requirements are getting more and more important. Standards and expectations on software have changed along the years. In order to get a software package accepted by the end user, it is very important not only to focus on what the software does, but as well on how the software will do it. Complex mathematical operations and nuclear analysis methods need to be provided to the inspectors by intuitive and easy to use user-interfaces.

Another major aspect when developing safeguards applications is data security. Data security does not only involve the confidentiality of data. It must also include data authentication. It has to be guaranteed that data has not been modified during transmission or storage, and it needs to be assured to the receiver that data come from a valid sender.

All new and ongoing developments need to take those additional specific requirements into account. Support in the field of new safeguards techniques and on the growing requirements on data security is provided by European and US research centres and consultants. Therefore, the number of contributing parties has increased significantly. This requires a careful project management in order to coordinate successfully contributions from various stakeholders.

2. RADAR and iRAP, two software platforms developed by EURATOM

2.1. Unattended Data Acquisition by RADAR

The software package RADAR (Remote Acquisition of Data and Review) is a modular and standardized software platform for data acquisition from different sensors. The development of RADAR started in 1997 and it has been financed by the European Commission (EC) [2], [3].

RADAR is EURATOM's standard software for unattended measurements and has been successfully deployed in all large facilities in Europe. RADAR has replaced all other acquisition tools, like NEGUS, BUD and NOVIS [4] which had been tailored for facility specific needs.

RADAR was originally developed as a resident system for large facilities [2]. In facilities like Sellafield RADAR operates more than 100 sensors. In total, RADAR controls several hundred sensors which continuously monitor nuclear operations in European facilities.

Furthermore, a portable system was developed which indicates visually state of health information of system components (Fig. 1). This system was designed to support spent fuel (Castor) loading campaigns. The data acquisition hardware (SMC2100 [5] and the PC are in a sealable, portable box with a transparent front panel. In order to visualize state of health information of certain system components, a special data acquisition module was developed and integrated into the RADAR

system, the so called Alarm-Agent. This module checks the system permanently and turns on red or green status lights indicating operability of all relevant system components. In combination with other sensors ensuring continuity of knowledge, the permanent presence of an inspector during a spent fuel loading campaign is no longer required.

Fig 1: A portable Fork measurement system indicating State of Health information: Two modules are active under RADAR. One module controls the Fork measurement electronics; the other indicates status of system components.

2.2. Data evaluation by iRAP

The development of iRAP, the successor of CRISP (Central RADAR Inspection Support Package), started in 2001 and was based on principles of modularity and standardization openness to 3rd party suppliers [3].

iRAP was designed to be a software package with several tools to configure or to access a database system for a full data analysis. The database contains all the necessary information to perform an automated data analysis. It accepts plant information and operator declarations on material moves and item contents including the timing. Furthermore, the database contains a number of algorithms to extract information (events) out of RADAR produced raw data files and process these events. A considerable number of evaluation algorithms are already integrated into the iRAP system. They are the core of iRAP and can be either in-house developed (e.g. Pu Mass Calculation, Flow verification [6]) or integrated as a third party development into the system (MGA [7], INCC [8], ORELLA/ORIGEN [9], [10]).

Once iRAP is configured it can perform an automated analysis for each selected system. This process can be described as a sequence of predefined tasks in separated evaluation layers (Fig. 2). Each layer uses special algorithms to perform the requested operation. In the first step iRAP reads data from a number of selected sensors; these sensors are combined to a measurement system. A typical system could be a combined measurement station for Gamma, Neutron and ID reading in order to perform an automated Pu mass calculation. Measured data originate from corresponding RADAR modules. These modules control all necessary electronics like multichannel analysers, shift registers and ID readers.

Subsequently corresponding events at a selected measurement system are correlated and evaluated by using preconfigured algorithms like MGA or PuCalc Mass to calculate the isotopic composition and the mass of Pu. In a final step the result is compared to the operator’s declaration.

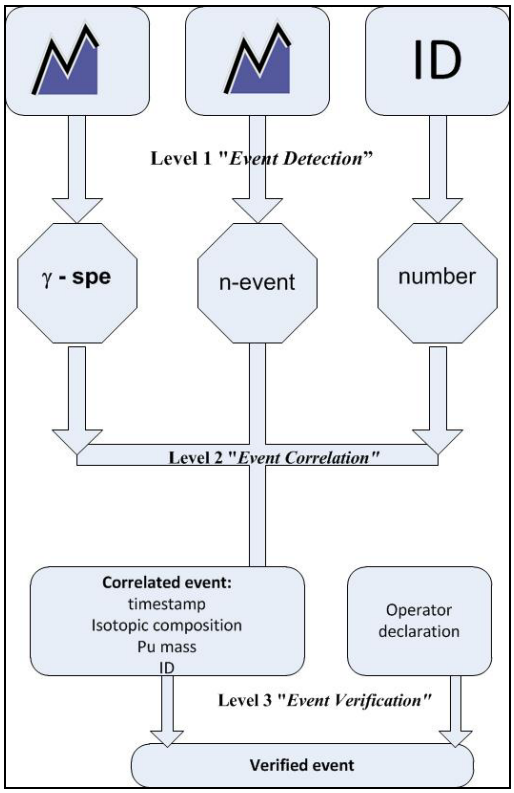

Fig. 2: The iRAP data flow outline for a Pu mass calculation

In Evaluation Level 1 "Event Detection" iRAP accesses the raw data. Adjustable event detection algorithms extract the relevant information out of the data. A typical event can be for instance the mean value of a neutron measurement plateau, an ID or balance reading.

Evaluation Level 2 "Event Correlation" will correlate corresponding events (e.g. neutron plateau, gamma spectrum and ID reading) to a single correlated event and will then evaluate this newly created event by using algorithms to calculate for instance mass and isotopic composition.

Verification of the results is done in Evaluation Level 3 "Event Verification" by comparing the result with imported operator‘s declarations

3. What are the requirements for future iRAP and RADAR developments?

Even if both software packages meet current requirements, it will be inevitable to consider major changes or a complete re-engineering of certain modules in the near future. The RADAR framework is based on principles defined in 1997. The development of CRISP, the predecessor of iRAP, started in 2001. A sustainable software management requires at a certain time a complete status review in order to identify potential deficits and to react in due time.

Safeguards software is used by a small number of users, nuclear inspectors and safeguards technicians working either in field or at the HQ. A nuclear measurement is a highly complex process. A measurement system contains many different components and needs to be installed, configured and maintained, often under harsh conditions and time constraints, in a nuclear facility.

The analysis of nuclear data acquired by those systems requires a broad understanding of safeguards principles and nuclear physics.

In order to use human resources efficiently, safeguards inspectors need to be trained quickly on tools and techniques provided to them; this includes of course training on software tools as well. For this reason new developments in the field of safeguards software need to focus much more on:

- Usability of software: For the time being RADAR controls about 20 different sensor types, all with characteristic configuration parameters. iRAP uses a number of sophisticated algorithms in order to detect and evaluate measurement events automatically. Even if configuration interfaces are standardized, look and feel principles are applied to the design, it requires a sound knowledge of measurement electronics, detectors and evaluation algorithms to configure a reliable and stable data acquisition system and a corresponding review platform. In order to enhance the usability of a system, simple dialogues are required. The majority of the users should be able to complete typical tasks without requiring assistance. The use of

installation and configuration wizards may support the user. Interactive user interfaces with precise and constructive on-screen help and documentation would help to achieve the aim.

- Maintainability of the software: As a matter of fact, data acquisition systems and review platforms are usually installed at nuclear facilities at remote places. In order to minimize travel of technical support teams and/or to optimize a planned technical intervention, a software system needs to be maintainable to a high degree via remote connections (if available). Back-up procedures after catastrophic failures need to be achievable remotely.

- Data protection is a major challenge for all stakeholders, i.e. the safeguards authorities, the nuclear operator and national authorities, especially when using remote data transmission. Data is provided either by independent safeguards measurement systems or by branched sensors provided by the facility operator. In both scenarios it needs to be assured that data is protected. Data encryption provides only authorized parties with the possibility to read, whilst data authentication reduces the risk that data has been tampered with during a transfer, and it also verifies that data comes from an expected sender.

In order to meet these requirements, EURATOM has started a number of initiatives to address upcoming needs.

4. Joint development of iRAP by the IAEA and EURATOM

The IAEA was seeking an IT tool for an automated analysis of safeguards inspection data. After closely evaluating the CRISP code, they concluded that CRISP provided a good basis and already had a good part of the features which the IAEA had identified as needs. Consequently, the IAEA offered EURATOM the possibility to jointly develop the software for common use by safeguards inspectors of both organisations. The joint development of the Central RADAR Inspection Support Package (CRISP), later re-named to iRAP, by EURATOM and the IAEA can be described as a typical model for sharing development effort, resources and the resulting source code. Nevertheless, two main questions had to be answered in advance: "Who owns what?" and "Who does what?"

The first question addresses the ownership of intellectual property (IP) rights. If this is not examined in advance, there may be a potential problem for an organisation not obtaining all necessary intellectual property rights for modifying or further developing a product. If a nuclear safeguards authority like IAEA or EURATOM does not obtain the necessary intellectual property rights to adapt a certain product to specific needs, the results can be disastrous and range from loss of certain functionalities to a complete uselessness of the product. This led to the conclusion that a licence agreement was needed to assess licensing issues.

CRISP/iRAP has been solely owned by the European Commission (EC). Therefore, it was possible to allocate development and IP rights to the IAEA. The IAEA, as a new end-user, is now an active participant in the software development process of iRAP and will share ownership of newly created intellectual property. IAEA specific tasks are carried out by contractors selected and financed by the IAEA.

Finally, a licence agreement, negotiated between the EC department for intellectual property and technology transfer and the IAEA office of legal affairs (OLA) was signed in October 2013 [11]. This legally binding agreement was necessary as all stakeholders needed to understand who owns the IP for a jointly developed safeguards software package and whether the packages can be shared with 3rd parties.

The second question ("Who does what") addresses the use of financial and human resources and was described in the "All-in-One Software Configuration Plan" agreed by both parties. It clearly defines the processes by which the software tool is modified, enhanced and maintained by the two organisations and any third-party developers and how a new product should be developed by one party or jointly by both parties. Nevertheless, this plan describes the general framework of the partnership. Specific projects, jointly or individually developed, need to be decided on a case by case basis.

For this reason the joint development of iRAP is coordinated and supervised by a Change Control Board (CCB) of IAEA and DG ENER experts. The CCB meets regularly in order to bring developers, users and technicians together in the very early phase of a development cycle, to define the scope and requirements of projects, to avoid potential conflicts among different user groups and to review new releases. This enhances communication and relations between inspectors and technical personnel of both organisations.

The modularity of the iRAP software package offered quickly and with minimal financial effort the possibility to easily modify and adapt the existing package to IAEA data formats. iRAP is now able to read and display all kind of data types from various IAEA specific data sources. In addition, a configuration wizard was developed which supports users in the set-up of simple analysis scenarios.

Further developments cover the integration of analysis algorithms for the VXI Integrated Fuel Monitor (VIFM) for Bundle Counters and Core Discharge Monitors (CDMs) [12]. Those systems are widely deployed by the IAEA and are used at CANDU reactor sites to detect and automate the accounting of spent fuel transfers. VIFM is jointly used by both organisations in Romania (NPPs at Cernavoda).

Projects of common interest have been identified and will be launched soon. First activities will cover enhancements of the iRAP core and the enhancements of the user interface, which needs to be adapted to current user expectations. A new user interface needs to be highly interactive; it should allow for manual marking of events and on-screen writing of notes and remarks.

The integration of the widely used INCC [8] software into iRAP as an external algorithm will allow users to apply all INCC core functionalities within the iRAP framework. For this reason the existing version of INCC needs to be upgraded in order to be compliant to iRAP requirements on external algorithms. Necessary changes will be done by LANL (Los Alamos National Laboratory) staff. This work is coordinated by the IAEA.

A milestone of upcoming joint developments will be the integration of video information into iRAP and correlation of images with NDA events. A careful preparation of this step towards an All-in-One Review Platform is inevitable as this will extend the range of functions significantly. A concurrent analysis of NDA, seal and image data is envisaged; correlation of events either coming from sensors or cameras should be possible. Both organisations are drafting their user requirements and development work is planned to start before the end of 2015.

5. US-DOE/EURATOM cooperation:

Under the US-DOE EURATOM Agreements on nuclear safeguards and security, first concluded in 1995 and revised 2010 [13], a number of Action Sheets have been launched which directly address certain needs, for instance in the field of usability improvements or data protection.

5.1. Automated burn-up calculation - iRAP meets SCALE

iRAP has been developed in a way that it is easily adaptable to facility specific needs without any major effort or development necessary. In a recent development, functionalities of the SCALE [9, 10] package can be called by iRAP using the newly-developed ORELLA module to allow automated evaluation of Fork measurement campaigns. ORELLA takes basic information on the assembly design and declared operating history from operator declarations imported into iRAP, creates input files for the ORIGEN code, executes that code, and returns the expected Fork detector signals.

This is a significant improvement of the usability of the ORIGEN code and the iRAP package, as inspectors are not required anymore to transfer measurement data into spreadsheets or perform consistency checks manually.

In the next development step it is planned to automate the complete evaluation process and transfer the result to the operator. This new method to be developed and integrated into iRAP would allow

performing loading campaigns in absence of safeguards inspectors but with the assurance that spent fuel is verified.

Final storage projects envisage conditioning of spent fuel in an encapsulation plant - the fuel will be encapsulated in copper canisters to be disposed in a final repository. Most advanced are Finland [14] and Sweden which target start of operations for the 2020s. In other EU countries packaging of spent fuel in casks for interim storage is continuing at growing rates. Both situations present a considerable challenge to the safeguards authorities.

Implementation of EURATOM and IAEA safeguards are expected to require all assemblies to be verified [15]. Inconsistencies will need to be communicated to the operator instantly to interrupt the loading process before a container is closed and moved to the repository. Consequently, the measurements and their evaluation need to be fully unattended and automated. This automation can now be implemented by a combination of ORNL's ORIGEN code (Oak Ridge Isotope GENeration) [9] and the IAEA/EURATOM package iRAP.

In combination with the EURATOM system for unattended Fork measurements, this approach will allow the design of a completely autonomous spent fuel verification station [16]. The system could be an integral part of a comprehensive IAEA/EURATOM safeguards verification scheme; it could be linked to the safeguards HQs and indicate any inconsistencies to the operator autonomously. Before the operation of the encapsulation facilities, important parts of the system can be applied immediately to current spent fuel cask loading operations for intermediate storages.

5.2. Data security - EURATOM coordinates field test for EDAS

The Enhanced Data Authentication System (EDAS) is a technical concept to securely “branch” measurement data from operator-owned equipment while assuring the integrity of the operator’s communication link. While safeguards normally depend on measurements that are completely independent from operator measurements, certain situations may call for the sharing of information from facility systems for both operations and verification purposes. Nevertheless, the inspector must be confident that this branched information is a secure, true and complete duplication of the operator’s device. At the same time, an operator must have the assurance that the branching does not modify or interrupt his measurements.

The EDAS project is a joint collaboration between the European Commission Directorate-General for Energy (EURATOM), the European Commission Joint Research Centre (JRC), the U.S. Department of Energy, and Sandia National Laboratories.

An EDAS field test was launched at the Westinghouse fuel-fabrication plant at Springfields in the United Kingdom early 2015 [17]. Two EDAS units were installed at the entry point of the Oxide Fuel Complex. Those units are connected to the operator’s weighing and identification system. Information on weight and ID of incoming and outgoing UF6 cylinders is branched, encrypted, signed and transferred to a data acquisition station either via USB or Ethernet.

Once connected, EDAS is capturing the complete data stream. All data packages, either sent to the device or transmitted from the device, are stored in a single file. Therefore, EURATOM developed a RADAR component based on existing modules to filter those data packages, write them to individual files compatible to iRAP and indicate their encryption and authentication status.

The result of the field test will prove if EDAS is able to meet inspector and operator requirements.

EDAS may also have additional valuable applications, not for branching but for inspector's equipment. Successful laboratory tests have already shown that the concept of encrypting and signing data in real time by attaching an EDAS system, as close as possible to the signal output of the measurement electronics, has a lot of potential for further use in the field of safeguards measurements and instrumentation. Fig.3 shows a system set-up as it could be used for spent fuel verification. The Fork electronics, a SMC 2100 [5] is directly connected to EDAS and provides by that way two separated outputs, an original data stream and a branched stream, encrypted and authenticated.

This set-up allows even remote configuration of the electronics as EDAS does not interrupt or modify the communication between control software and electronics.

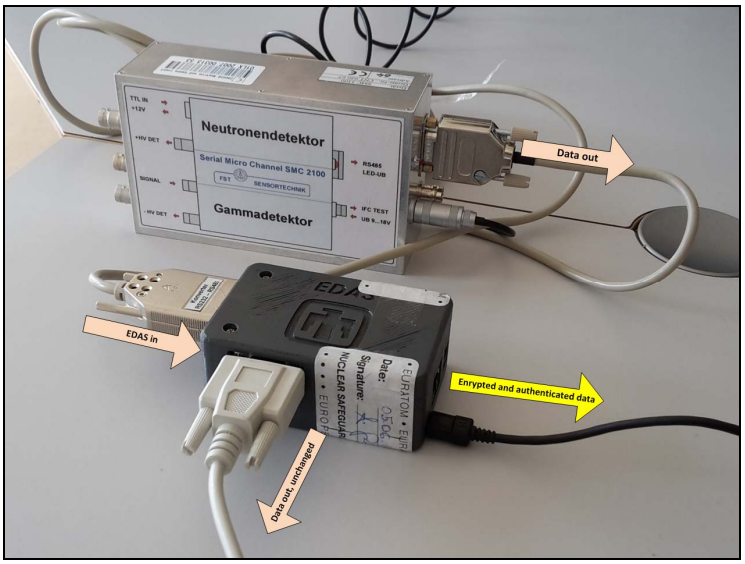

Fig. 3: EDAS connected to measurement electronics for spent fuel measurements.

6. Summary

Nuclear safeguards organisations, regardless if international or regional, depend on the provision of specific IT tools and software tailored to the needs of nuclear inspectors allowing them to analyse and review nuclear data in a reliable and efficient manner. As a matter of fact, commercial off-the-shelf software for nuclear safeguards purposes hardly exists. Analysis and evaluation tools are mostly provided by some manufacturers of measurement electronics or research centres. Most of these products are not developed for operating conditions in nuclear facilities. Furthermore, maintenance of such products is either problematic or time consuming due to missing IP rights.

EURATOM decided already in the late 1990's to avoid these problems by starting an in-house development for a data acquisition system (RADAR) and some years later a corresponding review platform (CRISP/iRAP). In recent years, EURATOM started a number of initiatives to improve cooperation between stakeholders. EURATOM shares all IP rights on iRAP with the IAEA. A joint licence agreement allows now both organisations to develop new features and tools with individual software developers according to each organisation's specific needs, but as well to share resources for common needs. The benefits for both organisations are obvious; as the IAEA now holds all necessary IP rights, they can start developments on the basis of an approved and recognised software package. In addition, EURATOM has gained a lot of experience in the use of iRAP in automated Pu handling facilities. The IAEA will boost the development with new ideas and approaches. Common needs like the integration of INCC or video review are expected to become less expensive as costs will be shared.

In addition, a number of Action Sheets with the US DOE have provided valuable scientific input to the software. A combined use of software packages iRAP and SCALE, provided by Oak Ridge National laboratory, allows user friendly automated consistency checks of declarations on spent fuel. A possible use at the future encapsulation plants in Sweden and Finland and CASTOR loading campaigns is envisaged.

The important aspect of data encryption and authentication as close as possible at the signal source is taken into account in the EDAS project of SANDIA National Laboratories.

7. REFERENCES

[1] Report on the Implementation of Euratom Safeguards in 2013, https://ec.europa.eu/energy/sites/ener/files/documents/201405_euratom_safeguards_2013_report.pdf

[2] P. Schwalbach, P. Chare, T. Girard, L. Holzleitner, S. Jung, W. Kloeckner, A. Smejkal, M. Swinhoe, RADAR: EURATOM's Standard for Unattended Data Acquisition;; Proceedings IAEA Symposium on International Safeguards, Wien 2001, Austria

[3] P. Schwalbach, A. Smejkal, E. Roesgen, T. Girard, RADAR and CRISP - Standard Tools of the European Commission for remote and unattended data acquisition and analysis for nuclear safeguards; Proceedings IAEA Symposium on International Safeguards, Wien 2006, Austria

[4] P. Chare, W. Kloeckner, P. Schwalbach, M. Swinhoe, Unattended Measurement Systems of Euratom; INMM 1999, Naples, USA.

[5] http://www.fst-sensortechnik.com/seiten/frms1.html

[6] A. Smejkal, P. Schwalbach, M. Boella, D. Ancius, E. Roesgen, "Automated Flow Verification of Nuclear Material with CRISP (Central RADAR Inspection Support Package)", INMM Annual Meeting 2010

[7] R. Gunnink, W.D. Ruhter, MGA: A Gamma-Ray Spectrum Analysis Code for Determining Plutonium Isotopic Abundances, Volume I and II, Lawrence Livermore National Laboratory, Livermore, CA., UCRL-LR-103220, 1990

[8] M.S. Krick; W.C. Harker, P.M. Rinard; T.R. Wenz, W. Lewis, P. Pham, P. de Ridder The IAEA neutron coincidence counting (INCC) and the DEMING least-squares fitting programs;; [IAEA]; Inst. of Nucl. Mater. Mgmt. XXVII (39th Proceedings, Naples, FL (United States), 26-30 Jul 1998

[9] I. C. Gauld; S.M. Bowman; B. D. Murphy; P. Schwalbach, Applications of ORIGEN to Spent Fuel Safeguards and Non-Proliferation, , Proc. of INMM 47th Annual Meeting, July 16–20, 2006, Nashville, Tennessee

[10] S. Vaccaro, J. Hu, J. Svedkauskaite, A. Smejkal, P. Schwalbach, P. De Baere, and I. C. Gauld, A New Approach to Fork Measurements Data Analysis by RADAR-CRISP and ORIGEN Integration, IEEE TRANSACTIONS ON NUCLEAR SCIENCE, Vol 61, 2014, p 2161 ff

[11] COMMISSION DECISION of 30.10.2013 on the granting of a licence for the development and use of the CRISP software, C(2013) 7421

[12] Bot, D., Keeffe, R., Messner, R., Autonomous Data Acquisition Module for Radiation Monitoring in Integrated Systems or Stand-Alone Modes, Canadian Nuclear Safety Commission. Paper presented at the 19th ESARDA Annual Symposium on Safeguards and Nuclear Material Management, Montpellier, France, 13-15 May 1997.

[13] AGREEMENT Between THE UNITED STATES DEPARTMENT OF ENERGY and THE EUROPEAN ATOMIC ENERGY COMMUNITY Represented by THE EUROPEAN COMMISSION in the field of NUCLEAR MATERIAL SAFEGUARDS AND SECURITY RESEARCH AND DEVELOPMENT, http://www.state.gov/documents/organization/154334.pdf

[14] Park W.S., J Coyne, M Ingegneri, L Enkhjin, L.S. Chew, R Plenteda, J Sprinkle, Y Yudin, C Ciuculescu, K Baird, C Koutsoyannopoulos, M Murtezi, P Schwalbach, S Vaccaro, J Pekkarinen, M Thomas, A Zein, T Honkamaa, M Hämäläinen, E Martikka, M Morink, O Okko, Safeguards by design at the encapsulation plant in Finland, Proceedings IAEA Symposium on International Safeguards, Wien 2014, Austria

[15] M. Murtezi, C. Koutsoyannopoulos, A. Zein, W.Kahnmeyer, P. Turzak, P. Schwalbach, A. Smejkal, V. Sequeira and E. Wolfart, Application of safeguards in the geological disposal of spent nuclear fuel: data requirements and arrangements for very long lasting records and knowledge retention (this conference)

[16] A. Smejkal, M. Boella, P. Schwalbach, K. Schoop, D. Ancius, S. Vaccaro, I. C. Gauld, D. Wiarda, Improvements for spent fuel verifications by safeguards inspectors , Proc. of INMM, Annual Meeting 2012, Orlando, Florida

[17] M. Thomas, G. Baldwin, R. Hymel, A. Smejkal, P. Schwalbach, M. Rue, L. Dechamp, J. Goncalves, Enhanced Data Authentication System: Converting Requirements to a Functional Prototype, 35th ESARDA Symposium proceedings p. 1 – 7, 2013

The role of the VARO inspection software for the implementation of an Integrated Management System (IMS) at the EURATOM Safeguards Office

P. Dossogne, W. Koehne, J. Lupo
P. Kaypaghian, M. Vlietinck, M. Vassart, F. Rowie
C. Cosmo, A. Terrasi, P. Schwalbach, O. Alique

European Commission, Directorate General for Energy,
Directorate E Nuclear Safeguards, Luxembourg

E-mail: wilhelm.koehne@ec.europa.eu

Abstract:

With the implementation of an Integrated Management System (IMS) within EURATOM issues like coherence of inspection approaches, data quality, traceability, and the evaluation of inspection data become more essential than ever. In combination with ever shrinking resources and the increased complexity of plants in the nuclear fuel cycle there is no other way than to rely on software to help inspectors carrying out their verifications in a comprehensive, harmonised and least time consuming but still fully documented way.
Some years ago EURATOM started to develop the VARO software package (Verification of Accountancy Records of Operators) to support their inspectors with the evaluation of accountancy declarations received from the nuclear operators at HQ against on-site accountancy records, operational data and verification results. The VARO application aims to make safeguards conformity assessment activities coherent without limiting inspectors in their inspection scope. A generic application, centrally managed at HQ, reduces the resources needed for development, maintenance and training, thus leading together with the central data storage to a more consistent evaluation of safeguards data.
The application is part of the standard inspection software package used by EURATOM inspectors, which is available in a so called Mobile Kit, thus allowing inspectors to work almost seamlessly while being on site and allowing them to synchronise their inspection results upon return to HQ. The centralisation of inspection data allows for a direct comparison of their performance regarding safeguards between installations and helps focussing inspection resources.
With the IMS aiming for an ISO 17020 compliant inspection management system based on inspection documentation, preparation, execution and recording, VARO is the choice that ensures EURATOM management and inspectors to have the necessary tools at hand for their inspection co-ordination and work, like central criteria setting, seamless workflow between HQ and installation. The central inspection data management and documentation at HQ allows for direct comparison of safeguards activities and detailed statistical evaluations of their results as required by the IMS.

Keywords: software; inspection; standardisation; management; quality

1. Introduction

The EURATOM Treaty is law in the European Union (EU) and implemented by the European Commission (EC). One of the major challenges for the EC over the next years will be to find the right balance between available resources, in particular personnel, on the one hand and credible safeguards verification schemes on the other. A number of industrial operations will generate extra workload, such as the defueling of nuclear power reactors because of the decision in some Member States (MS) to phase out nuclear power, the production and export of large numbers of nuclear fuel elements for overseas markets, the consolidation of strategic material in the UK, as well as the

construction of encapsulation plants and final repositories in Finland, Sweden, France, Spain and elsewhere.

Despite the increasing workload and the challenging staff reduction targets of the EC, EURATOM Safeguards is aiming to maintain and where possible increase its effectiveness. The introduction of an Integrated Management System (IMS) supplementing the procedures of the Directorate-General and the Internal Control Standards (ICS) of the European Commission is a way to cope with the additional challenges. The IMS is based on ISO standards for quality management and conformity assessment and compliance of the directorate's internal processes with the ICS of the European Commission.

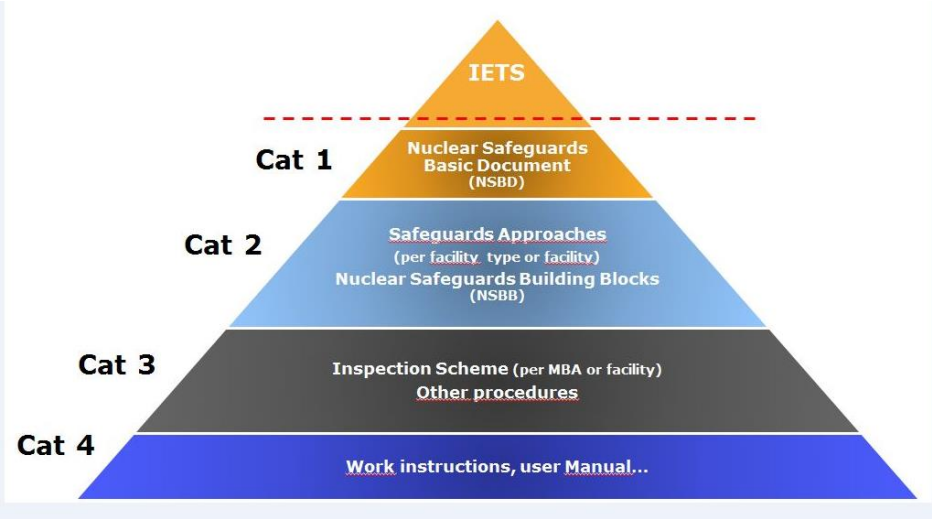

In this context it is essential to ensure that the right safeguards tools are available to support the IMS concept and to cope with reducing resources at a time when the complexity of the safeguarded facilities, the amount of nuclear material under control, and verification activities continue to grow steadily.

2. Development of standardised software tools

The use of standardised software tools is one way to save resources in several aspects, such as development, harmonisation, training, documentation, etc., to apply coherent verification standards at all installations under EURATOM Safeguards, to evaluate data provided by the operators in a consistent way, to have fully documented and recorded inspection results, and to support the EURATOM Safeguards Directorate in drawing its safeguards conclusions.

All nuclear operators in the European Union are required to maintain a system of accountancy and control for nuclear materials in their possession. According to EURATOM Regulation 302/2005, these systems shall include accounting and operating records with information on quantities, category, form, composition and location of these materials, together with information on recipients or shippers, when nuclear materials are transferred. Accounting and operating records shall be made available to the inspectors in electronic form if they are kept in this form by the installation. The amount of these data might be limited for small installations and by consequence the related safeguards verifications could be done manually. However, this has proven to be very resource demanding or even impossible in bigger or more complex installations. It is therefore essential to provide inspectors with efficient software tools to allow them to carry out their verifications in an efficient and coherent manner.

Almost immediately when computing power became more widely available, nuclear safeguards inspectors started to use it. The new technology was deployed to evaluate nuclear accountancy declarations and related operational records. From simple spreadsheet type evaluations these developments evolved in a number of cases into very specific and complex applications that became essential for the successful execution of inspections. However, the constant development of the hardware and software platforms, combined with staff mobility and the constant evolution of nuclear installations, have made it very difficult to maintain a large number of individual installation-specific applications, to keep them in working order and adapted to the inspection needs. Apart from the

difficult maintenance and long-term development, these different applications created a constant need for inspectors training. When being on inspection, inspectors are facing all sorts of different tasks and the use of different software applications at the installations for similar tasks is a further complicating factor that needs to be avoided whenever possible.

In addition to these issues, the statutory reporting format was changed from 80 character lines to XML records with EURATOM Regulation 302/2005 coming into force, thus making most of the existing installation specific applications obsolete due to the incompatibility of the input format of at least parts of the data.

The EURATOM VARO software project addresses these aspects. It provides a common verification tool for safeguards data that the inspectors can use at a broad range of installation types. During inspections as well as at headquarters it helps inspectors to verify that declarations and accountancy records correspond, and whether these are supported by operational records. The evaluation of conformity assessment activity results falls also under the scope of VARO.

3. EURATOM Safeguards IT concept for inspection data

EURATOM Safeguards uses database systems at their Luxembourg headquarters to process, store and evaluate the declarations that nuclear operators are required to send according to Regulation 302/2005 for most of the installations on a monthly basis. These declarations are first checked for compatibility with the required reporting format, checked for internal consistency, and then loaded into the accountancy database. The declarations are then checked against the reporting rules of the Regulation and facility specific criteria stored in a database called Rulebook. For installations under IAEA safeguards, these declarations are also translated into the IAEA format and subsequently forwarded to the IAEA.

Nuclear safeguards inspectors carry out onsite inspection activities to verify the completeness and correctness of these declarations by comparing them with the physical reality at the installations. Nuclear operators transmit on a monthly basis declarations about the flows of nuclear material in and out of Material Balance Areas (MBA). This declaration is called the Inventory Change Report (ICR). The deadline for the transmission of the ICR of a given month to EURATOM is the fifteenth of the following month, thus creating a gap of at least two weeks between the accountancy data available on site and the accountancy declaration available in the EURATOM HQ. This gap has to be updated by the inspectors onsite.

When preparing for their onsite inspection activities, the inspectors download the relevant declarations sent by the operators, from the HQ accountancy database system (CMF) for the relevant Material Balance Areas (MBA) together with other relevant data like the seals applied in the installation, installation related documentation, procedures etc. into a so called "Mobile Kit" for their onsite inspection activities.

On arrival at the installations the HQ data are complemented with accountancy records kept by the operator to update the declarations to the day before the start of the inspection. This accountancy update is straightforward if the operator is prepared to provide the required inventory change data in the XML format of the EURATOM Regulation 302/2005. In some installations the accountancy systems do not allow interim ICRs without creating the monthly file for EURATOM, thus creating a new report number. To avoid any issues with the report numbering all operators are asked to implement a functionality to produce an interim report without an increment of the report number. However, many operators at reactors and smaller facilities, who only declare a few lines per month, do not have their own accountancy system and use the ENMAS (EURATOM Nuclear Material Accountancy System) application to prepare their monthly declarations. Since the accountancy systems in these installations are often paper based or use incompatible data systems, there is no other way for the inspectors than to transcribe these data into the required XML format using the ENMAS application. During onsite inspection activities this can be relatively time-consuming and some inspectors prefer to do this upon return in HQ. When loaded, these local accountancy records are checked for consistency and compliance with the reporting requirements to allow the inspectors to establish an updated book stock. Then, they are compared with operating records for consistency.

Depending on the size and variation of the inventory, physical verifications are carried out based on stratification by splitting the inventory into the different material categories, e.g. Plutonium, high and low enriched, natural and depleted Uranium and further sub-strata depending on the verification methods used. Established sampling plans are used to calculate sample sizes and to select items out of the different strata to be chosen for physical verification activities.

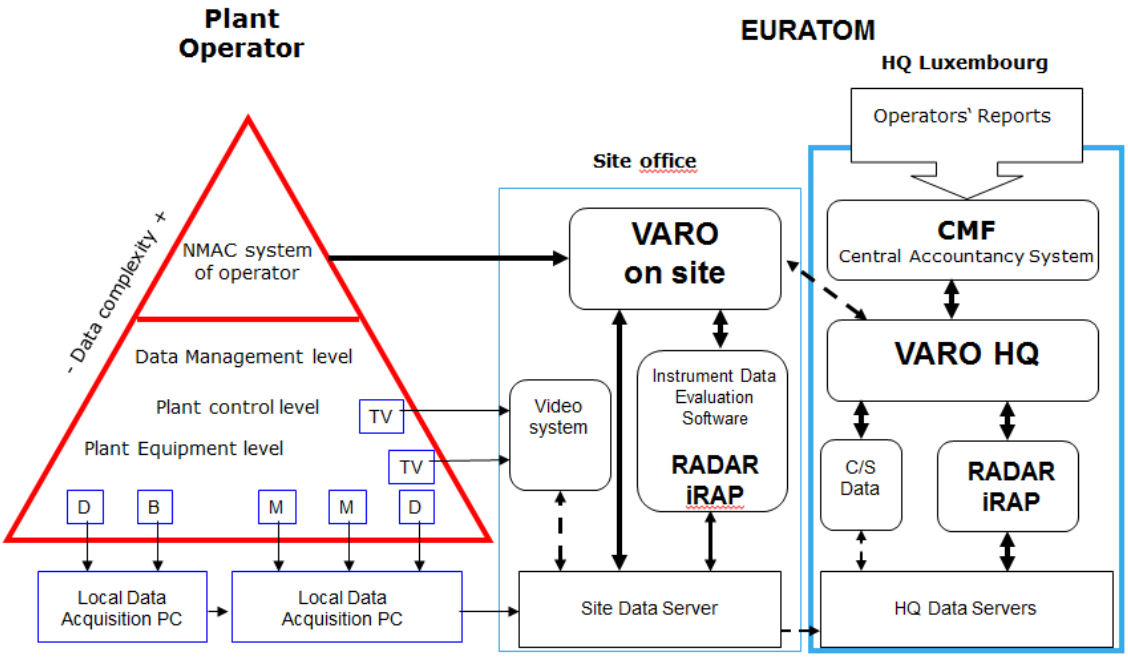

The data loading routines use mapping files to translate the operating records and verification data into the standardised internal database format. A powerful, easy to use, query engine has been developed to display and compare the different data sources in a coherent and common, but also user defined way. Several output functions allow the inspectors to view and export data in different formats for reporting and further evaluation.

The "Mobile Kit" concept enables the inspectors to work seamlessly while being on site. The uploading of data into the HQ database on their return allows for a full data trail from nuclear materials declarations through accountancy and operating records to verification measurement results.

These functionalities described above are an important step forward regarding the requirements of ISO 17020 for standardisation of sampling and inspection techniques, including the traceability and recording of inspection results, thus an important element of the IMS of EURATOM.

To be compatible with other EURATOM software projects, the VARO application is designed using web technology with an underlying Oracle database system, which is running either on a HQ server or as a mobile version using a so called Mobile Management System (MMS) on the inspector's PC. The MMS is used to create so called Mobile Kits containing the required safeguards applications and the relevant data for the specific on site activities. These "Mobile Kits" are either copied onto encrypted storage devices for transfer to and use on onsite PCs or directly deployed on the inspectors' notebooks with encrypted hard drives. Inspectors therefore always leave HQ with the latest software versions and data, which are synchronised with HQ, in a secured way as required for sensitive safeguards data.

The look and feel of the mobile version of VARO is exactly the same as with the HQ version. With the development of the MMS it is now possible to control the software development centrally, thus ensuring that the infield version is fully compatible with HQ, that there are no conflicts with software versions and that data are handled in a coherent way both in HQ and on inspections. This is resulting in a significant reduction of necessary, resource demanding software maintenance at the sites.

4. VARO Project Phases

Phase 1 of the project was focused on the accountancy declaration checks. This part of the application is needed at all installations and addresses the most urgent requirements of the inspectors. Phase 2 of the project is focused on the loading and evaluation of operating records and their comparison with the accountancy. Phase 3 addresses the stratification, sampling and comparison of verification activities with the operating records and is in development. Additional phases are foreseen for the material balance evaluation, batch operation of commands, automatic routines to interface with instruments, and the creation of a HQ data repository allowing data warehouse functionalities together with the other HQ applications.

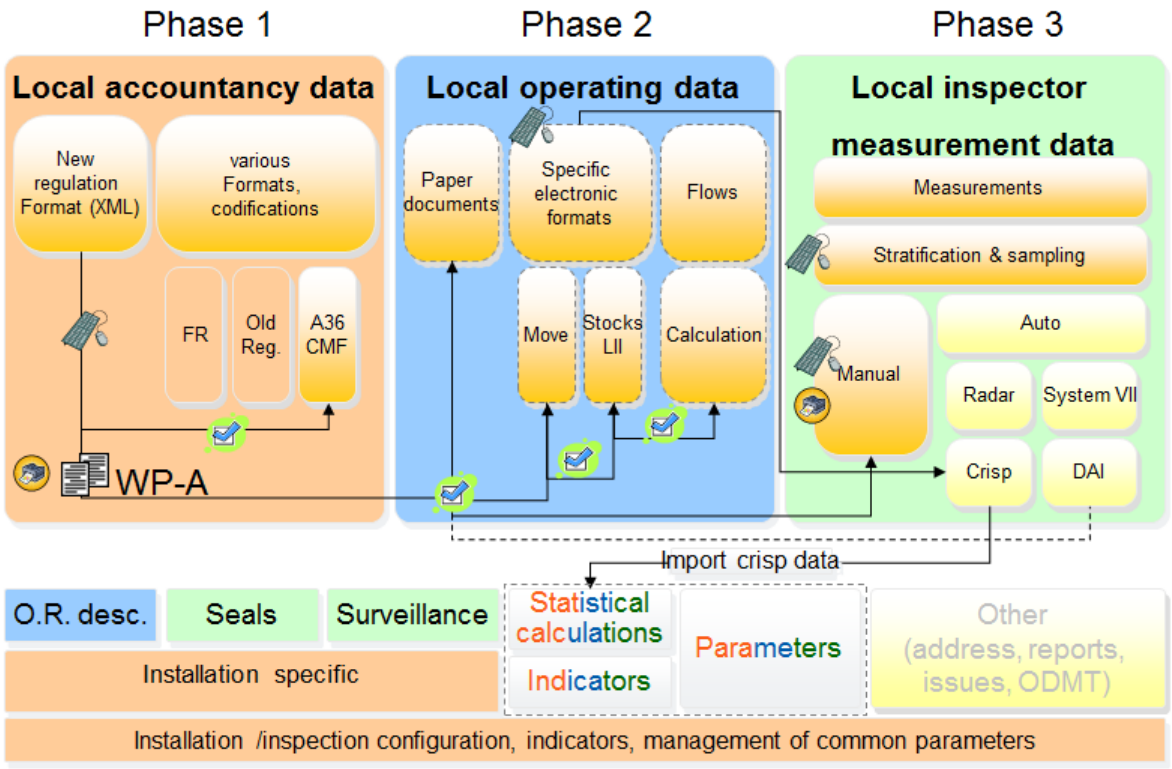

Similar to other large and complex software projects running over a longer period of time, it is difficult to define all functionalities in sufficient detail at the conception phase to allow for a writing of the full specification. Since the VARO development team is relatively small in relation to the size of the project, this stepwise approach was chosen, splitting the project in different phases. The definition of these phases was mainly based on the functionalities in question. Since the loading and verification of accountancy data is the most generic of the functions required, the project was started with a tool for the loading and checking of these data. This function is used in all facility types and was after the change of the reporting format the one in most urgent need. Subsequent project phases incorporate the treatment of operating and measurement data, statistical evaluations and the central storage of inspection related data for reference. However, since some of the functionalities needed in these phases are common, the start-up development effort was significant. The development of the Mobile Management System (MMS) was a significant step to allow the inspectors using safeguards applications while being away from HQ. This also required a relatively high upfront investment. Also the storage and sharing of user defined queries were brought forward to avoid a repeated loss of definition work done by the users, which could have caused an acceptance problem.

The development is done in iterations, with four versions managed in parallel. The developers are working on version N, while version N-1 is being tested by professional software engineers, while version N-2 is in user acceptance testing (UAT) and version N-3 is operational. At the moment iteration 33 is operational. This sequence is ensuring a close feedback cycle for the development team and allows the analyst to define the way forward in close cooperation with the project committee,

which consists of representatives of all units of the safeguards directorate. Whereas the project committee meets at different intervals to discuss strategic issues and to review functionalities, a smaller team meets at shorter intervals for status meetings to review user comments and more imminent development issues.

A user feedback function *"Problems? Questions? Remarks?"* at the bottom of the application interface allows users to send messages to the applications helpdesk at any time by e-mail. Attachments can be used to explain the issue using screenshots or other documents and with the e-mail a list of the last commands used is sent to allow the development team to establish the operational background for the comments. All user comments and bug reports are followed up in a database, thus allowing the project team to prioritise and monitor progress. This development environment is ensuring a short iteration cycle and clear guidance for the development team.

5. Mobile Kit

All new EURATOM safeguards applications are now based on web interfaces, using Oracle databases. With the start of the development of VARO it was decided to develop a mobile working environment for essential safeguards applications to run on, called "Mobile Kit". Besides VARO, applications for seal management (ESAM) and reporting (IMIS) have or will have mobile versions, thus allowing the inspectors to use their HQ tools when being out of the office. This system ensures that the actual software versions are only kept and maintained at HQ, thus reducing drastically the need for onsite software maintenance.

Since the sensitivity of safeguards data does not allow to use fully web based applications, these mobile versions work within an inspection context and are run either on the inspectors' notebooks, which have encrypted hard drives and are security cleared to be used for the storage, treatment and transfer of sensitive data or on local PCs in the on-site safeguards offices.

Before leaving HQ for an inspection the inspectors define the content of their specific Mobile Kits by selecting the required applications, the inspections to be covered, and the data to be copied from the HQ systems. Once the selections are made, the Mobile Kit is prepared as a self-extracting jar-file serving as a data container. These files are password protected and are either copied to the encrypted hard drives of the inspectors' notebooks or any other approved storage medium for sensitive safeguards data, like encrypted USB sticks with biometric (fingerprint) user identification. These jar-files can be deployed directly on the inspectors' notebooks or at big installations, with safeguards IT infrastructure, on a server, thus allowing multi user access. In this respect the web based applications are versatile as they are multi-user capable by design, thus allowing inspectors to work in teams with them in a networked environment.

At the end of the inspection activities the preparation of inspection outcome kits is necessary for the return of safeguards and verification data to HQ. The inspectors have the option to delete some of the data fields in the outcome kit, like the location in inventory listings, to address security concerns in some Member States. This outcome kit is used to upload the inspection data to the HQ database. It is to be noted that there is no backward synchronisation of accountancy data with HQ, but all data are stored in the inspection context of VARO for later reference.

6. Accountancy data

One of the first activities at the start of an inspection is to check whether inventory changes have happened since the last declaration was sent to HQ in order to establish the book inventory at the start of the onsite inspection activities. To do so, the operator is asked to provide an update of the inventory change reports (ICR) to the day before the inspection starts. These ICRs are loaded into VARO, checked for syntax, consistency and errors, and can be merged with the HQ data to establish the running totals of the declarations received.

It is essential that inspectors use coherent verification rules when loading accountancy data. VARO uses the same rules as the HQ application (CMF). So there is only one reference used for verifications and the inspectors are sure that they are using the correct, up to date syntax for these checks as used in HQ and by the accountancy unit in charge of the nuclear materials declaration checks at HQ.

After loading of the accountancy declarations, errors and warnings can be checked and the inspectors have the option to compare and combine HQ and onsite declarations. Different browse and filter options allow adapting the views on the data and help the inspectors with consistency and coherence checks. Since the application is based on a query editor, predefined queries can be created at HQ by experienced inspectors being in charge of the installation, thus sharing the knowledge and allowing for specific checks that are adapted to the plants. All queries can be saved and selected to be shared amongst the inspectors.

7. Operating records

The consistency of accountancy and operating records is one of the essential checks that inspectors carry out during the onsite inspection activities. Operating records are very plant specific and their detail and structure depends on the plant type, operational concept and size, but also on the inspection activities to be performed and reporting requirements for the operators as laid down for example in the Particular Safeguards Provisions (PSP) foreseen in the EURATOM Regulation and the Facility Attachments (FA) foreseen in the safeguards agreements, e.g. INFCIRC 193, for installations under IAEA safeguards.

Whereas in small installations the nuclear material tracking by the operator's is done mainly manually using paper documentation, more complex installations with higher throughputs use IT systems that allow for online tracking of material flows and quantities in the different areas. This serves many purposes, like process and criticality control, quality assurance, product documentation and is also important for nuclear material accountancy and control. Plants using fully integrated material tracking systems normally have a very good documentation of their operations and are able to provide this information in electronic format. However, also smaller installations use mostly electronic tools to keep their records up to date and these data are often in the form of spreadsheets or databases, which can relatively easily be converted into a format suitable for evaluation by software tools. Mapping files are used to relate the different formats of operating data to the internal data structure of VARO. This is another area where the use of common software tools is of help to get to more coherent data structures. New installations providing operational data in electronic formats can use already existing data formats for which mapping files already exist.

Operating records are needed for flow and inventory verifications. Depending on the inspection context the required data are different. For inventory verifications the operating records consist of inventory listings and related documentation. Flow verifications are normally based on documentation related to material movements, like shipments in automated plants, where containers or fuel assemblies pass through unattended measurement stations, solvent flows in reprocessing plants, weighing data in bulk handling facilities etc. and these results are compared with the flow information.

8. Measurement data

Physical verifications are the essential part of inspection activities. After the accountancy records have been verified against operating records, these are used to divide the nuclear material into different more homogeneous strata depending on the material type, category, quantity, location and available instrumentation for safeguards verifications. Depending on the inspection type, the List of Inventory Items (LII), store inventory listings or movements at strategic points of the plant are used to select items for measurements.

The number of items to be selected for verifications is calculated either by using the Jaech sampling algorithm, depending on the required detection probability, the number of items, the goal quantity and the average nuclear material quantity of the strata or using predefined percentages / fixed numbers, like 10% or 5 items out of a stratum. These requirements are part of a Material Balance Area (MBA) specific set up, which is pre-defined by the facility officer at HQ, thus ensuring that all inspectors use the same criteria when carrying out their physical verifications. These requirements are stored in installation specific operational setup data and queries, which are part of the mobile version of VARO that travels with the inspectors in the Mobile Kits.

In the stratum setup the facility officer also defines the verification methods, instruments to be used and the data to be recorded, if manual measurements are carried out by the inspectors.

Once the item selection is done, the inspectors prepare their paper print-outs of working papers for use in the plant. These working papers provide information specific to the verifications to be done, like area listings for tag checks sorted by location or measurement data sheets for specific instruments. There is also the option to use electronic spreadsheets as an output for the working papers that can be filled in by the different inspection teams whilst carrying out their verifications.

After having carried out the physical verifications the inspectors have to enter the measurement data into the application. This can be done either by manual transcription from the working papers, by re-importing the electronic spreadsheets, or by importing instrument specific data files. The measurement data are linked with the operating data using item IDs or time related information.

Some of the mobile instruments in use have an internal memory for measurement results that can be exported as instrument data files. Specific mapping files will be used to import these data and feed them into the VARO application for evaluation and comparison. The use of these routines is essential to avoid transcription errors, gain traceability, archiving of data and to save inspection resources.

For unattended measurement systems EURATOM uses its own Remote Acquisition of Data and Review (RADAR) software, which allows for remote control of and data gathering from unattended instruments. So called DAMs (Data Acquisition Modules) are used as interfaces for the different instruments, like ID readers, Neutron Coincident Counters (NCC), High Resolution Gamma Systems (HRGS), transducers etc. The recorded data of the DAMs are collected on local PCs and at bigger installations are automatically copied to central servers in the inspectors' offices. EURATOM's evaluation software CRISP is moving to its next generation under the name of integrated Review & Analysis Package (iRAP). iRAP is now a common software project with the IAEA, evaluates the recorded data and detects safeguards relevant events based on triggering devices like limit switches, ID readers or signal patterns, like weighing processes or level readings of vessels being filled or emptied. If more than one signal is used for the event definition, like neutron and gamma measurements with an ID reader or level and density measurements for tank transfers, these are combined to establish safeguards relevant information, like element or isotopic data or material quantities.

If operating data are needed to evaluate the measurement data, like isotopic data for a NCC without a HRGS, or tare weights of containers for weighing, VARO will provide these data to iRAP using inspector defined queries and iRAP specific protocols. After iRAP has evaluated the data and formed the measurement events, these are exported to VARO for comparison with the operating data.

The sequence above allows for a comparison of safeguards verifications with accountancy declarations through operating records and related statistical analysis. With related measurement uncertainties the inspectors get immediate feedback if and when measurement results are outside of predefined acceptance criteria. They can trigger follow-up actions, e.g. re-check or re-measure and/or seek for background information. This avoids late surprises and ensures that re-verifications are done as early as possible to avoid unnecessary interference with plant operations later. At the end of the physical verifications specific routines and listings will allow the inspectors to calculate overall statistics on measurement uncertainties related to their measurements. Related operator / inspector differences and their uncertainties will support the inspectors in their judgement on the acceptability of their verifications and related declarations of the operators.

9. Query engine

One of the main challenges of the project is to be generic enough to cover all installation types under EURATOM Safeguards and being at the same time specific enough to allow inspectors to carry out their verifications. In this respect one of the main features of the application is the query engine, allowing inspectors to filter, organise and display the available information in a very flexible, but specific way to support the detection of inconsistencies and errors. These queries are using a SQL type syntax, which is relatively easy to use with pull-down menus for the available commands and data fields. Since the queries are displayed in a window at the top of the result list, immediate feedback is given to the user when defining the criteria. Complemented by sorting and display options the user has the full flexibility to display and check the data available. This query engine is used for all data sets, accountancy, operating data (moves, inventory listings) and measurement data. The queries, sorting and display settings can be saved by each user under his/her preferences and can

also be made available to others by sharing them. This allows the management and facility officers to define standard verification routines without limiting the inspectors in any way to carry out the verifications under their responsibility.

10. Document checks and versioning

During the course of an inspection it is sometimes necessary for the operator to update the documentation provided. Since inspectors often immediately process information made available, each updated set of data causes a problem for the inspectors to know which data were changed and if these changes have an impact on the verifications already performed or the conclusions already drawn. A typical example is the List of Inventory Items (LII), which as an operational document is sometimes updated by the operator during a Physical Inventory Verification. It is therefore essential to have a routine to check updated data files against the original and to highlight changes found. This also allows for a statistical evaluation on the quality of original documents, e.g. how precise they were, the number of errors corrected etc. However, verifications already carried out and their established relation to operating records should not be compromised. Therefore, the application has to be able to detect changes in updated data sets, whilst at the same time maintaining record relations between operating and measurement data based on the item ID.

11. Legal restrictions on data transfers to HQ

Normally the inspectors enter all relevant data into the VARO application for data transfer to HQ to be able to continue working with them and for documentation and archiving. However, some Member States have very specific legal restrictions on the transfer of data related to nuclear material quantities and locations. To address these restrictions it is possible to limit the data travelling back with the inspectors to HQ by taking only pre-defined data back, i.e. without location information, in order to respect these local requirements.

12. Data storage

On return to HQ the inspectors are required to upload their inspection data by using a created outcome kit for uploading to the HQ database. After this upload, it is possible to continue working with the data and their evaluation seamlessly. The use of the mobile version allows for the inspectors' independence from on-site data and takes away from them the time pressure to finish evaluations on-site. Dedicated data output formats and print-outs allow the inspectors to record their inspection activities and verification results. These documents are used as annexes to the inspection reports, which are the overall record of the inspection activities.

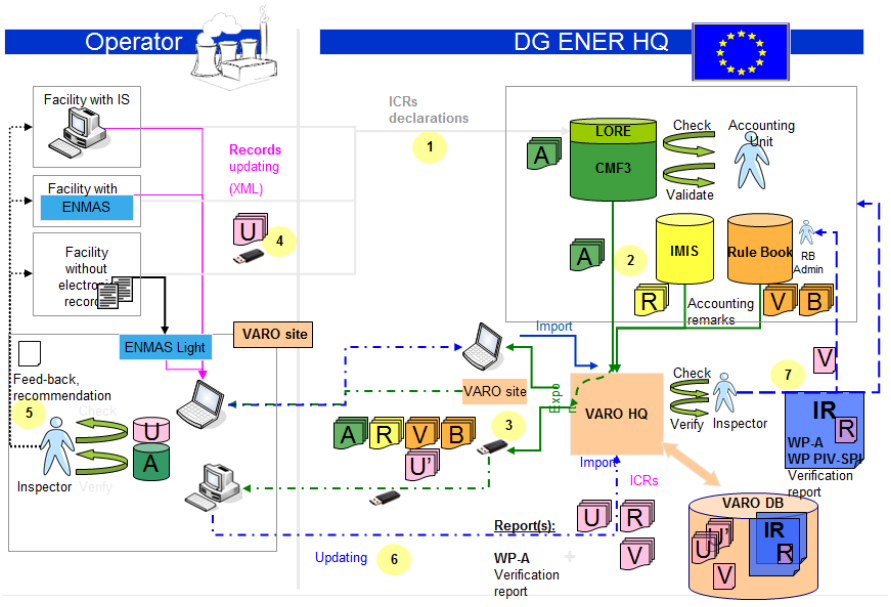

After the evaluations are finished it is the responsibility of the head of the inspection to close the inspection. This is the moment when the inspection data are fixed, cannot be modified anymore and

considered as reference. In the IMS context the increased traceability and seamless data transfer between HQ, site and vice versa is to be seen as an asset in striving for improved quality of inspection results.

Whereas the HQ database for accountancy data is to be seen as reference, similar central repositories for operational and measurement data do not exist yet. These data are normally stored at the installations and taken, if possible, back to HQ as separate files. These files have different structures, depending on their origin and are not stored in a single, compatible data format. With the start of the VARO project it was decided to normalise operating and measurement data using an internal data structure that allows for a central storage. So far all inspection related data are stored in the inspection context.

However, depending on the installation type, it might be necessary for the inspectors to reference back to data received at earlier inspections or to have older measurement data available for comparison and to complement data. This is for example necessary at storage locations used at fabrication and reprocessing facilities, where isotopic composition details are needed for later in-process measurements or re-verifications. Other aspects are that along the fuel cycle data from enrichment plants are used for input verifications at fuel fabrication plants or that nuclear data from fabrication plants are also useful for spent fuel verifications at reactors. Since the VARO concept is relying on HQ data as reference, it is essential that inspectors are able to take relevant operating and measurement data for predefined areas and periods with them when leaving for an inspection. Central data repositories are planned to allow for referencing and cross comparison outside the inspection context, across different installations and over time.

13. Material Balance Evaluation

The centralised HQ storage of relevant inspection data allows not only for evaluation in the inspection context, but also for data analysis over several inspections and years. It is foreseen to have routines allowing for periodical evaluations on MBA and installation level. This will help the inspectorate to better focus the inspection effort and to adapt it regularly to requirements.

At bulk handling facilities, the evaluation of the difference between the book stock and the physical inventory, called Material Unaccounted For (MUF), is an important indicator for the quality of the Nuclear Material Accountancy and Control (NMAC) system of the operator. MUF can be an essential indicator for a possible protracted diversion. Since all the data required for a MUF evaluation are available in VARO, MUF is calculated automatically by VARO. An essential element of the MUF evaluation is to know the related operator's measurement uncertainties, which are needed to establish acceptance limits for verifications and for the sigma MUF calculation.

The operators are required pursuant to EURATOM Regulation 302/2005 to describe in the Basic Technical Characteristics (BTC) of their installation the methods for measurements, sampling and analysis and are also required to provide derived estimates of random and systematic errors with the operating records. If these uncertainties are not available, the International Target Values for Measurement Uncertainties in Safeguarding Nuclear Materials are used in a top down approach as an estimate. It is foreseen to implement a MUF and sigma MUF calculation using these uncertainties to support the Material Balance Evaluation (MBE) at the end of the Material Balance Period (MBP) after the Physical Inventory Taking (PIT) of the operator and its verification at the Physical Inventory Verification (PIV) by the inspectorates. Long-term trending of the MUF and the Cumulative MUF (CUMUF) helps to detect possible bias effects, operational changes, measurement deficiencies, protracted diversion of nuclear material etc. With the storage and evaluation of related data it is foreseen to automate this process, as far as possible, allowing for a direct comparison of the different installations and a better focusing of inspection resources.

14. Co-operation with the IAEA

The functionalities of VARO are tailored to the needs of the EURATOM Safeguards Directorate. However, all of its functions are needed by IAEA inspectors as well. The IAEA is aware of the development and with the common development of the iRAP instrument interface software the use, exchange and comparison of operating data is an essential VARO feature to encompass the different operating data formats. The exchange of inspection data is an obligation stemming from the

safeguards agreements of EURATOM with the IAEA. The exchange of EURATOM's inspection results, as foreseen in the safeguards agreements, could be done in the future by making the relevant "Mobile Kit" for an inspection available through the existing VPN channel used for the transmission of surveillance data. This could significantly improve the exchange of data with and the use of them by the IAEA.

15. Difficulties encountered

Due to the complexity of the project and the required start-up time until the first version came into common use, it proved to be difficult to keep stability in the IT project team. Because of termed contracts and existing mobility of staff within the organisation, the project management changed several times. However, resilience on the user side has ensured that the project did not lose track. Due to the differences between the installations, ranging from small laboratories handling milligram quantities to complex reprocessing plants handling tons of sensitive nuclear material, the use of data tools varies strongly between the different inspection groups. The harmonisation and centralisation of inspection concepts and documentation is still a matter of continued discussion with all stakeholders.

16. Co-operation of all stakeholders required

The aim of the VARO application is, besides other elements, to increase the efficiency of the limited inspection resources available and to help with the implementation of IMS. It is in the interest of all stakeholders to carry out inspections as smooth, efficient and effective as possible, without any unnecessary delays. A fundamental requirement is a coherent and seamless data processing. Whereas in almost all installations the use of computerised material tracking systems is an established practice, the data exchange with the safeguards authorities is often done in a patchwork fashion. To avoid cumbersome and time consuming manual data treatment during on-site inspection activities, it is essential that inspectors receive predefined datasets, which can be loaded and evaluated automatically. To support the use of VARO, inspectors are required to agree common data interfaces with the operators. This will save time and effort at all sides, but requires an initial investment and co-operation to get these arrangements into routine operation. The operators of nuclear installations have a crucial role in this context and their co-operation is an essential element for the standardisation of operating data and the related implementation of VARO. On the other hand, VARO will be an essential building block for a coherent safeguards implementation in the different installation types and Member States of the European Union as foreseen in the IMS.

17. References

[1] P. Schwalbach et. al; Data acquisition systems in large nuclear facilities - challenges, experiences, solutions; IAEA Safeguards Symposium 2010, Vienna

[2] P Schwalbach et. al; RADAR and CRISP – Standard Tools of the European Commission for remote and unattended data acquisition and analysis for nuclear safeguards; Proceedings Symposium on International Safeguards, Vienna 2006, Austria

[3] A Smejkal et al; Automated processing of safeguards data: Perspectives on software requirements for a future "All in One Review Platform" based on iRAP; ESARDA Symposium 2015, Manchester, UK

[4] W Koehne et al; VARO - A Euratom software project for safeguards data evaluation; Proceedings of the ESARDA Symposium, Budapest, 2011

[5] IAEA-Tecdoc-261; IAEA Safeguards Technical Manual, Part F: Statistical Concepts and Techniques

[6] IAEA STR-368; International Target Values 2010 for Measurement Uncertainties in Safeguarding Nuclear Materials

Applying the Data Analysis and Interpretation Software to Analyze Feed and Withdrawal Operations

Jim Garner, Michael Whitaker

Oak Ridge National Laboratory, P. O. Box 2008, Oak Ridge, Tennessee 37831

Abstract:

The number of facilities and quantities of nuclear material and other items under International Atomic Energy Agency (IAEA) Safeguards are continuing to increase, but the Agency's financial resources have not risen commensurately. In recognition of this emerging challenge, the IAEA and its Member States are investigating new safeguards measures to enhance inspection efficiency without sacrificing effectiveness. One new concept being investigated for safeguards at gas centrifuge enrichment plants (GCEPs) – one of the more labor-intensive types of nuclear facilities to safeguard – is to leverage operators' load cells at feed and withdrawal (F/W) stations to monitor the flow of material transferred to or from the enrichment process. **This would help the IAEA achieve one of its primary safeguards objectives at declared GCEPs: the detection of undeclared feed which could lead to excess low enriched uranium (LEU) production.[*] The detection of excess undeclared LEU production at an existing enrichment facility is important because the excess material could be shipped to a small clandestine facility where it could be further enriched to a level suitable for nuclear weapons.**

Oak Ridge National Laboratory (ORNL) has assembled a small-scale F/W system [1,2] and platform-scale testing center [3] to generate load cell data representative of that produced during GCEP F/W operations. A major benefit of the simulated data produced by these systems is that the information is neither sensitive nor propriety and thus can be shared and discussed with all stakeholders. The ORNL F/W system has also been used to generate data that cannot be easily produced in operating facilities, namely, data resulting from a variety of facility misuse scenarios (e.g., diversion, undeclared feed, etc.). The authors installed the OSIsoft PI data historian to store F/W cycle data, which was then analyzed using the Data Analysis and Interpretation (DAI) software package developed by the European Commission – Joint Research Center – ITU Ispra. The DAI software has been used extensively at reprocessing plants like THORP and La Hague [4], and the IAEA has used a related software system called the Solution Monitoring Software at the Rokkasho reprocessing plant in Japan [5]. However, the IAEA has not yet approved this type of software for use at GCEPs. This paper explores how DAI might be used by the IAEA to strengthen the efficiency of safeguards at large-scale GCEPs and demonstrates a proof-of-concept application of this approach by analyzing data generated using ORNL's F/W system for both normal cycles and potential misuse scenarios.

Keywords: Gas centrifuge enrichment plant safeguards, load cell monitoring

Applicability for IAEA safeguards

The primary objectives for applying international safeguards at declared nuclear facilities are to verify that declared nuclear material is not being diverted and that the facilities are not being misused for undeclared production or processing of nuclear material. ORNL and other researchers have been evaluating the potential application of process monitoring techniques to strengthen the application of IAEA safeguards at GCEPs and other facilities that process Uranium Hexafluoride (UF_6) cylinders – UF_6 conversion and fuel fabrication plants.

[*] The primary safeguards objectives for GCEP are (1) the detection of diversion of declared material, (2) the detection of enrichment levels that exceed declared levels (especially highly enriched uranium (HEU)), and (3) the detection of excess LEU product using undeclared feed material.

Gas centrifuge enrichment plants are of particular nonproliferation concern because they can potentially be misused to directly produce highly enriched uranium (HEU) for a weapons program. Currently, the IAEA safeguards GCEPs in five non-nuclear weapons states (NNWS): Brazil, Germany, Iran, Japan, and the Netherlands.

The IAEA has three main safeguards objectives for declared GCEPs:

1) the timely detection of the diversion of declared nuclear material;
2) the timely detection of the enrichment of uranium above the declared level (particularly HEU); and
3) the timely detection of excess production of LEU via undeclared feed.

The IAEA uses nuclear material accountancy, containment and surveillance (C&S), and Design Information Verification (DIV) to detect diversion of declared nuclear material. The IAEA uses limited-frequency, unannounced access (LFUA) to the cascade area with nondestructive assay, material sampling, containment and surveillance, environmental sampling and DIV to detect enrichment of uranium above the declared level. The IAEA is currently exploring new process monitoring techniques to assist in achieving these safeguards objectives (i.e., on-line enrichment monitoring systems [6] and unattended cylinder verification stations [7]). Detecting excess production of LEU, however, continues to be a challenge because the IAEA has fewer proven “tools in its tool box” to achieve this safeguards objective. Previous IAEA publications have suggested that continuous unattended monitoring of load cell data may provide an option to address this challenge: “Load-cell monitoring supports the detection and deterrence of excess production scenarios in a way that other unattended instrumentation cannot” [8]. One promising tool to help inspectors harness the value of load cell data is automated analysis using software tools like the Data Analysis and Interpretation (DAI) software package.

Currently, there are limited safeguards measures for monitoring the transfer of UF_6 between the enrichment process and the cylinders. Typically, feed cylinders are not continuously monitored by the IAEA after they have been initially verified, so material could potentially be removed prior to feeding the cylinder contents to the process. Empty product and tails cylinders are not all verified by the IAEA prior to being filled, so the calculated net UF_6 content (gross weight – empty weight) is based on an unverified empty weight value (i.e., the cylinder tare weight). Finally, there is no continuous monitoring (or camera surveillance) of the F/W stations using current safeguards approaches, so possibilities exist to process undeclared cylinders in between inspections.

Monitoring cylinder weight data from load cells in F/W stations offers a capability that could significantly strengthen the IAEA’s ability to meet its safeguards objectives of detecting the diversion of declared materials and undeclared production scenarios within declared facilities by providing the following safeguards capabilities:

- confirmation that weights of declared cylinders (full and empty) do not change between the F/W stations and the accountability scales;
- a capability to confirm the number of cylinders processed (e.g., no undeclared feed, product, or tails cylinders were processed in the declared F/W stations);
- a capability to more quickly resolve discrepancies or anomalies that would normally have to wait until the annual Physical Inventory Verification (PIV); and
- the ability to calculate a more timely, approximated material balance (e.g., a rough snapshot in time).

Load cell data collection, analysis, and comparison

One of the IAEA’s current tools to detect excess production relies upon short-notice access to the F/W areas; this is referred to as Extended Limited Frequency Unannounced Access (ELFUA[*]). At facilities where ELFUAs are performed, the operator submits a feed occupancy list information daily to an in-

[*] An EFLUA provides for short notice access to the F/W area in addition to the cascade areas once an LFUA has been announced.

situ mailbox.* When the inspectors arrive for ELFUA inspections, they retrieve the feed occupancy list and verify that only the F/W stations declared to be in use are occupied.

New informal operator declarations to the in-situ mailbox would be used as the baseline for comparison against the process load cell data. Official declarations often take a longer path through the state system for accountancy and control and so may be given to the IAEA months after actual inventory changes occur. For timely detection and anomaly resolution, the operator will need to declare all cylinder movements into or out of feed or withdrawal stations to the in-situ mailbox.

Modern F/W stations typically have integrated weighing systems that operators use for process control. Monitoring the existing load cells in F/W stations is one of the most promising options to detect excess production [9]; however, there are serious challenges to its use as a safeguards measure. For example, the operators are required to protect proliferation-sensitive data, and the IAEA wishes to receive authentic data. ORNL researchers are testing a variety of systems for collecting and analyzing load cell data for safeguards purposes including methods to improve the IAEA's confidence in the authenticity of the shared weight data.

If data is collected very frequently (e.g., once a second), operators have expressed concerns that sensitive details about the centrifuges, cascade design, or efficient plant operations can be revealed. However, our investigations are showing that very frequent data collection is not needed for the IAEA to reach safeguards conclusions. Studies are under way to identify an optimal data frequency collection range that is both short enough to meet safeguards objectives and long enough to protect the operator's proprietary information [10, 11].

To meet the IAEA's objective for detecting excess production of LEU, load cell data would need to be collected to confirm that it is consistent with continuous feed operations by identifying key markers such as the date† and the gross weight of the full cylinder when it is first put into the station and the date and gross weight when the emptied cylinder (containing residual UF_6 after the UF_6 transfer process had been completed) is removed from the station. Only minimal periodic data is required between these points to support the conclusion that the station was continually occupied by a declared cylinder. Additionally, continual monitoring with only minimum data would be required to support the conclusion that undeclared cylinders were not processed in stations reported to be empty.

Algorithms can be written to identify the key cycle markers and time periods where manual evaluation is required to enable the inspectors to quickly verify the number of cylinders processed between inspections. Additionally, the cylinder weight data could be compared with the operator's cylinder change reports. Currently the IAEA inspectors verify a statistically significant subset of declared cylinder full and empty weights, but in the future, the process-scale full and empty weights from load cell data could be compared against the accountability values reported by the operator to provide greater confidence that declared material isn't diverted between the declared F/W stations and accountancy scale. The net amount of material transferred to and from the process through all the F/W stations can be calculated to provide an estimate of the process inventory changes to compare with operator declarations for a more timely, approximated material balance.

A number of options exist to identify these key markers to count cylinders or perform advanced analysis. A key consideration is whether the method is local to each feed or withdrawal station or if the method employs a centralized data collection and analysis architecture.

John Howell (formerly a Reader at the University of Glasgow) developed a concept and reference implementation for a basic cylinder counting algorithm on a data logger to log local load cell data and analyze it in real time. This technique leverages a simple programmable logic device to provide minimal output information to the inspector at each station. ORNL researchers assembled a system

* The IAEA has deployed in-situ mailboxes at several Gas Centrifuge Enrichment Plants. The IAEA defines mailbox declarations as "Declarations of operational activities at facilities that are submitted electronically, time-stamped and irretrievable, which can be randomly validated by the Agency [IAEA]." State Level Concept Supplementary Document (footnote 53).

† The precision required will depend on the feed/withdrawal cycle period. For example if a cylinder can be fed in less than a day then the software would need to identify these key markers with more than day precision (e.g. hour precision).

based on the reference implementation and tested it using data from the small-scale F/W system.* More details will be discussed in a forthcoming paper. A local logging and analysis technique may be appropriate at facilities with a limited number of stations; however, larger facilities would likely require a centralized logging and analysis technique because it requires less inspector time to review the data and reduces the maintenance burden on the inspectorate.

Application of DAI to ORNL cycle data

The DAI software was developed for process monitoring in reprocessing facilities [4]. Researchers at the Joint Research Centre (JRC) in Ispra, Italy, have managed the development of DAI and a closely related spin-off called the Solution Monitoring Software, which is used by the IAEA at the Rokkasho Reprocessing Plant [5]. Researchers at the JRC have also proposed using DAI for GCEPs [12].

DAI analyzes process data by evaluating time series data against rules. DAI organizes sets of rules as a "comportment" that relates to what is physically happening in the process that is being monitored. These comportments are strung together to form cycles, but DAI requires a starting or reset comportment be configured. The starting comportment for ORNL's feed cycles was configured to require the data match two rules—first, that the slope before the evaluation time was less than -0.2 and, second, that after the evaluation time the slope was between 0.05 and -0.05. This is displayed graphically in Figure 1.

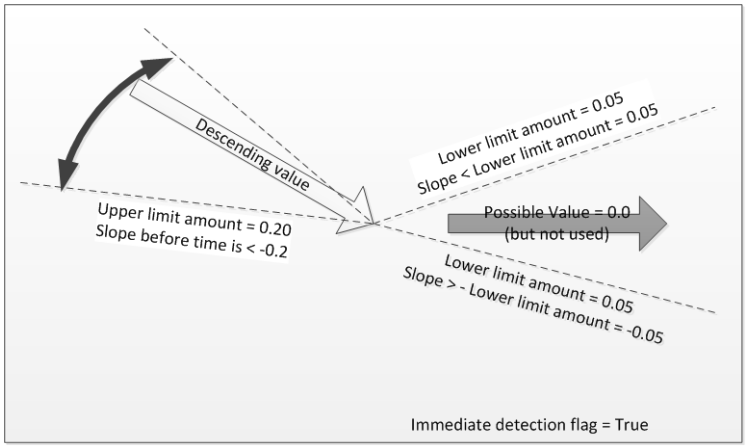

Figure 1: To find the starting point of the ORNL cycle, DAI is trying to find a time period where the slope of the load cell data is less than -0.2, followed by a time period where the slope of the load cell data is between 0.05 and -0.05.

DAI has a useful test feature that shows in real time how the algorithms are interpreting and matching the rules to the data. An example of the test feature is shown in Figure 2 with an arrow drawn to point out where the rule previously described first matched the data.

*In 2008, ORNL established a small-scale F/W system that uses water as a surrogate for UF_6. This system has been leveraged by several researchers to evaluate different load cell monitoring techniques including both local and central logging and analysis techniques. In 2010 and 2011, David Hooper and James Henkel, while working at ORNL under a contract with Oak Ridge Associated Universities (ORAU), used a central collection approach to obtain load cell data sets that simulated both normal F/W operations as well as abnormal operations that included several plausible diversion scenarios.

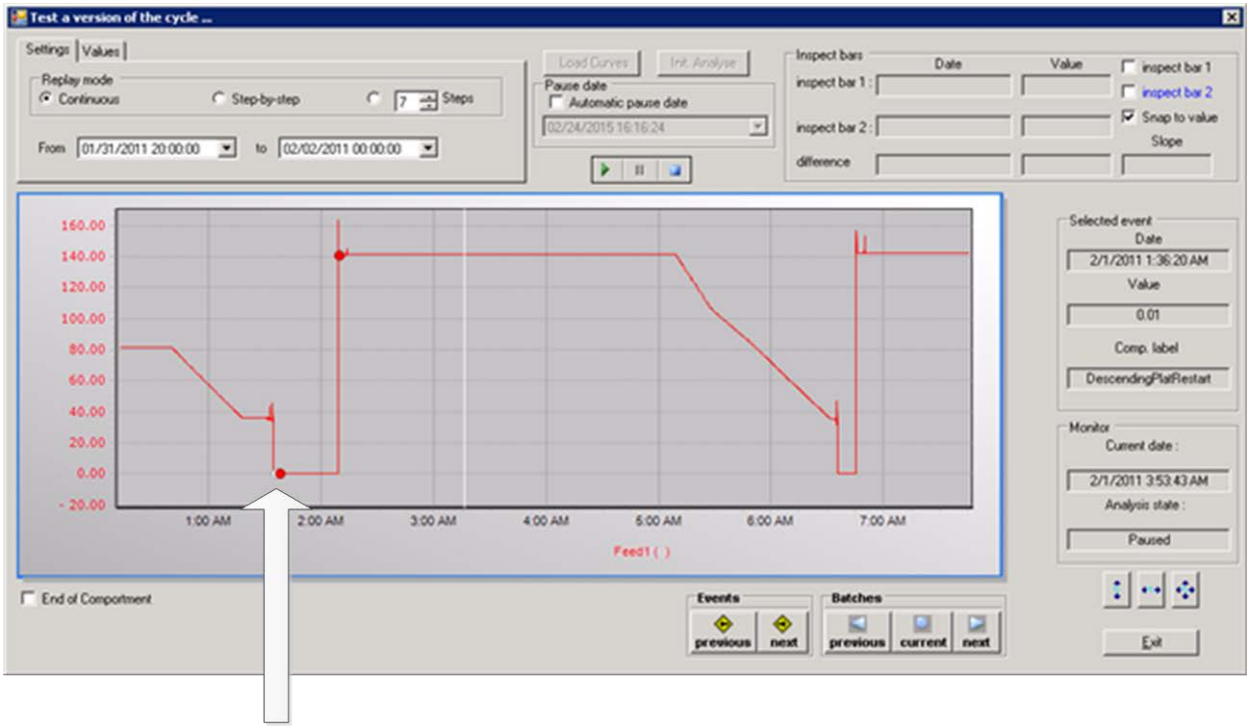

Figure 2: An example feed cycle with arrow showing where DAI found the starting point for the cycle.

DAI allows for comportments to be dragged onto the control surface and linked together, as shown in Figure 3. This set of comportments, each with its own set of rules, was used to analyze ORNL load cell data.

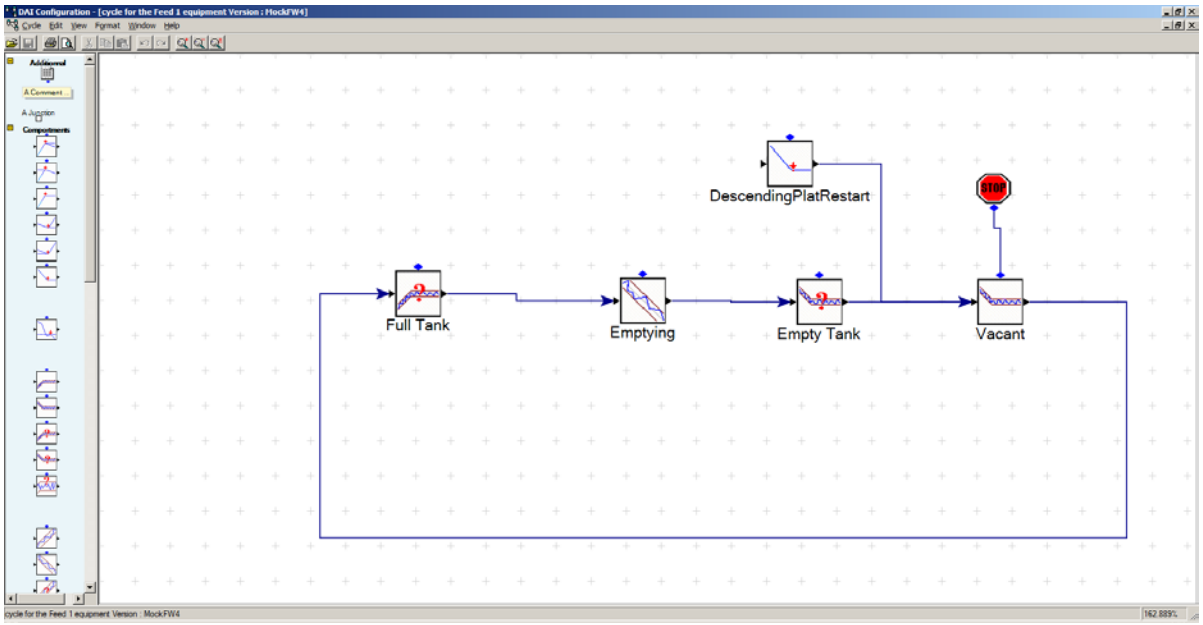

Figure 3: Comportments can be dragged from the left pane to the control surface and linked together.

Henkel and Hooper stored their data into a general-purpose relational database called PostgreSQL. However, DAI was built to use the OSIsoft PI data archive. OSIsoft's PI is purpose built for time series data. In order to get the Henkel and Hooper data into OSIsoftPI, the raw data was extracted from the PostreSQL database as comma separated values (CSV), manipulated in Excel to eliminate the time between independent runs, exported as a CSV file, and then imported into OSIsoft's PI data archive using OSIsoft's Universal File Loader. When data is imported into OSIsoft PI, exception and compression algorithms are typically run on the incoming data to minimize the data that is actually

stored. This feature maintains enough details from the time series data to fully describe trends or disturbances, while helping to reduce the storage required when a sensor reports the same value for consecutive periods and helping to expedite the retrieval and analysis of the data. If the operator and the IAEA could agree, the exception and compression settings built into OSIsoft PI may be a sufficient information filter to ensure that the IAEA has a safeguards significant set of data that satisfactorily limits the data frequency to protect the operator's sensitive or proprietary interests.

The configuration in Figure 3 was able to identify both expected transition events and abnormal weight profiles when it was used to analyze the ORNL small-scale F/W system load cell data. Figure 4 demonstrates the analysis on this load cell data. The round markers in this figure indicate normal transition events, while the red triangles indicate that DAI recognized an abnormal event.

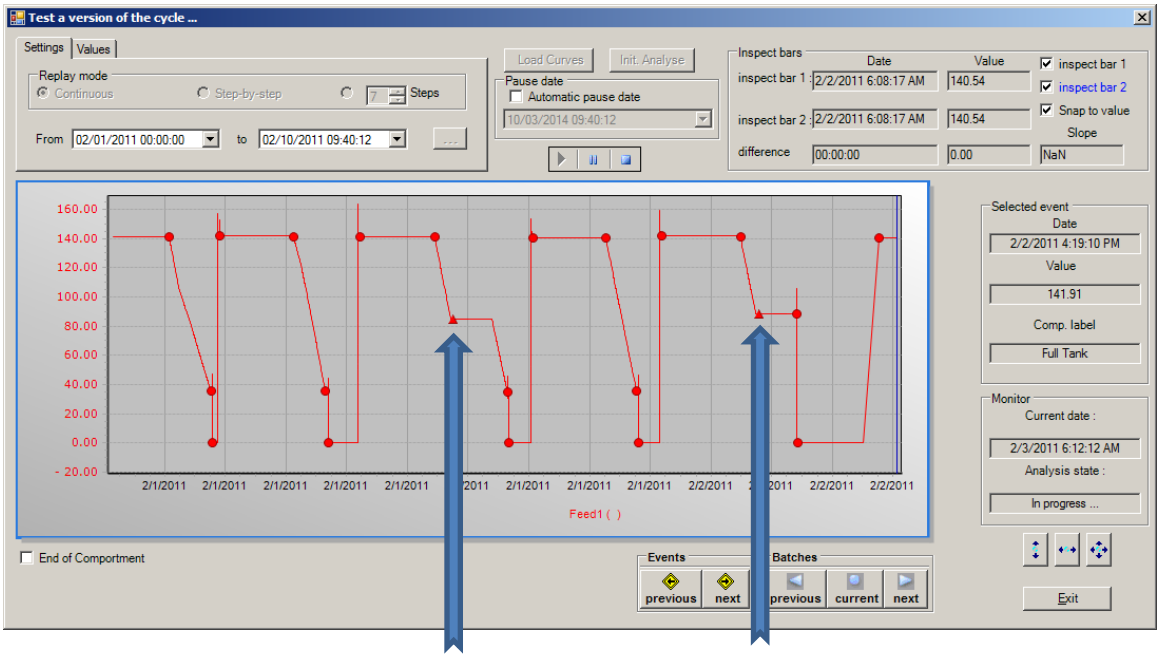

Figure 4: The configuration shown above correctly identified normal cycles and alerted when abnormal events were encountered.

Installation and use at a GCEP

OSIsoft PI offers flexible options to import data. Standard industrial protocols like ModbusTCP or OPC could be used to import data into the OSIsoft PI data archive. An installation could also leverage the IAEA's emerging data transmission standard (RAINSTORM*) to import data.

Figure 5 shows a hypothetical GCEP load cell data transmission architecture using RAINSTORM to transmit the load cell data. In this environment, weighing systems at each F/W station could collect raw data into simple text-based files. The IAEA's GetRainstorm† application could then be used to retrieve the most recent data and move it to the input folder for OSIsoft PI's Universal File Loader (UFL). The UFL is a configurable software application that can parse incoming file data into the OSIsoft PI data archive. Optionally, exception and compression algorithms could filter data and permanently store only time series significant events in the OSIsoftPI data archive. This would discard consecutive data points if they have the same value so that only data points that vary significantly from the norm would be stored.

*The IAEA is developing and adopting the RAINSTORM (Real-time And INtegrated STream-Oriented Remote Monitoring) protocol as a standard way to retrieve data from remotely monitored instruments. The RAINSTORM protocol leverages the same underlying communication protocol (HTTP) that delivers web pages to deliver data files from sensors to centralized collection computers or IAEA headquarters. The IAEA has developed some reference implementations of RAINSTORM for Windows and Linux computers.

†The IAEA has also developed the GetRainstorm application to retrieve files from IAEA instruments using the RAINSTORM protocol.

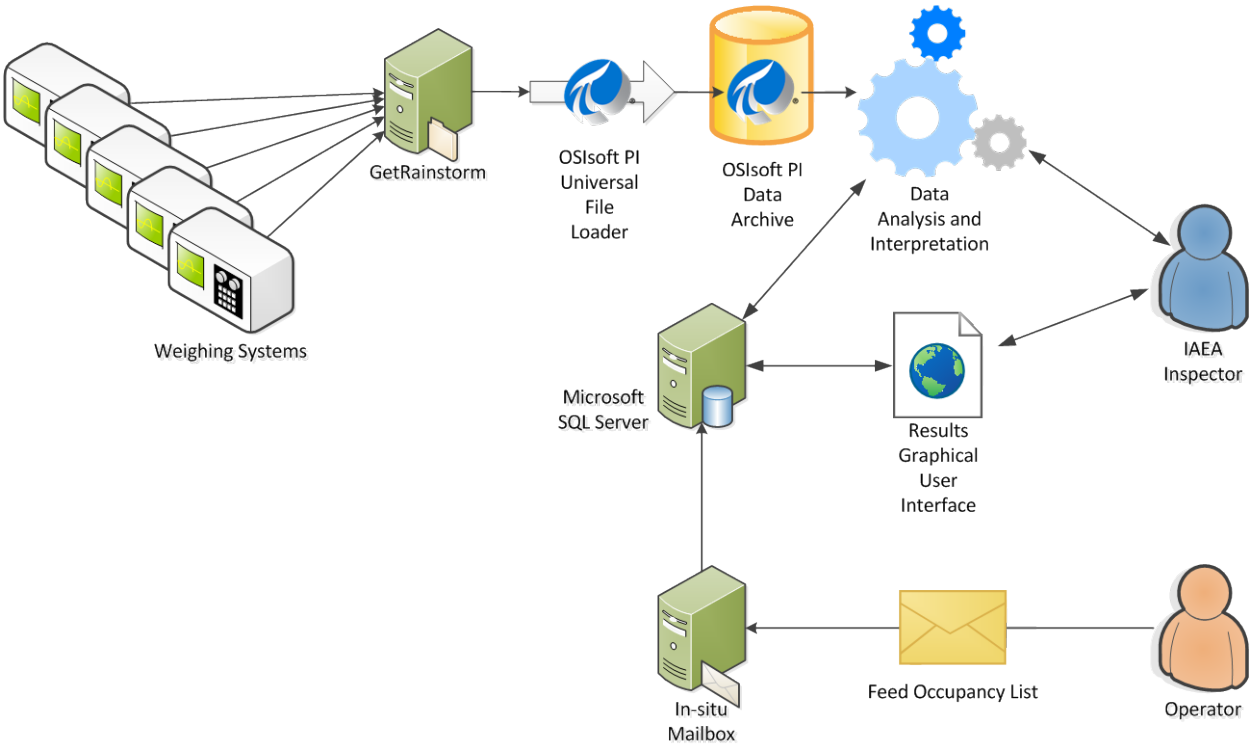

Figure 5: Weighing systems at each F/W station could provide a Rainstorm interface. A central system could use GetRainstorm to pull text files from each of the systems. The OSIsoft PI Universal File Loader can be easily configured to parse text files and import data into the OSIsoft PI data archive. DAI pulls raw data from the OSIsoft data archive, automatically analyzes the data, and can save the analysis results into Access or SQL server databases. Initially, IAEA inspectors would configure the analysis algorithms using the DAI software. IAEA inspectors would then routinely use an extension to the existing DAI software or a stand-alone graphical user interface to compare the analysis results with operator declarations.

Once the raw data is in the OSIsoft PI data archive, the DAI analysis algorithms can be run automatically to identify the significant F/W events and complete cycles. These results could then be saved into a SQL server or Access database. While the IAEA inspectors would need access to the load cell data to configure DAI, they may not need routine access to the raw periodic process load cell data.

If the algorithms correctly identified all key cycle markers and did not identify any time periods that needed additional review, the IAEA inspectors would only need to use an extension to DAI or a separate application to display the analysis results in order to compare them to the operator's declarations. A sample screenshot is provided in Figure 6 showing the comparison of mock operator declarations corresponding to the feed cycles in Figure 4 as an example of how an inspector might be able to view the data. If, on the other hand, DAI identified a weight difference that differs significantly from the declared mass transfer or a time period that was abnormal, then the corresponding cell or row would be highlighted to indicate this time period needs additional evaluation.

Drill down functionality to click the highlighted cell to display the raw periodic cycle data in DAI would likely be the most useful for inspectors if they were investigating analogous events. In order to protect this more sensitive data, access controls could be applied in order to limit access to the raw data to a subset of inspectors from approved states. Another way to control this sensitive information while allowing inspectors to investigate the region of interest would be to use a mutually agreed upon data release mechanism that requires operator involvement for a small subset of data near the time period of interest.

Operator Declaration	DAI			Operator Declaration
Cylinder ID	Start Date	End Date	Weight Difference	Mass Transferred
5980	2011-02-01 07:XX	2011-02-01 11:XX	106.21	106.10
61789	2011-02-01 12:XX	2011-02-01 15:XX	56.40	105.20
52338	2011-02-01 18:XX	2011-02-01 21:XX	104.79	104.90
37174	2011-02-01 22:XX	2011-02-02 01:XX	107.00	106.20

Figure 6: An extension to DAI or a stand-alone graphical user interface could display DAI analysis results and the operator declaration. A simple table could show the first level of detail and highlight cycles that require additional investigation.

Using OSIsoft PI and DAI with a graphical user interface to compare the key markers (full and empty weights with times) against declared values could greatly improve the IAEA's effectiveness to detect excess production; however, these gains do not come without costs. Localized data analysis solutions installed at each station may be appropriate at smaller facilities but will require more inspector time to use and will be more difficult to maintain (making configuration changes on one centralized system would be significantly easier than making changes at multiple stations all under seal). Larger facilities with more stations and higher cylinder throughput are probably better suited for centralized analysis solutions, but data sharing policies need to be negotiated between the operator and inspectorates.

Remaining questions

A key question that needs to be addressed for the IAEA to utilize DAI is how to perform the initial configuration of the software in a large-scale GCEP plant. Other topics that need further discussion and resolution include what data (and at what frequency) can be shared, how can sensitive data be adequately protected, how shared process data can be used to support IAEA safeguards conclusions, and what level of authentication is necessary for the data to be useful to the IAEA. The specific needs and requirements resulting from these discussions can then be tested and evaluated at mock F/W stations and then demonstrated in operating facilities.

Conclusions

Strengthening the application of IAEA safeguards at GCEPs is a priority for the United States and the IAEA. While the IAEA currently has relatively effective safeguards measures at GCEPs to detect (1) the diversion of declared material (e.g., nuclear material accountancy), and (2) the production of UF_6 with higher-than-declared enrichment (e.g., environmental sampling and NDA measurements during LFUA to cascade halls), it does not have many proven tools to detect excess production.

To improve the IAEA's ability to efficiently detect excess production, the IAEA needs to be able to continuously monitor the transfer of material between the cylinders and the process. A potential cost-effective solution would be to share data from the operator's already installed load cells; however, operators must protect proliferation-sensitive information and the IAEA needs to be confident about the authenticity of the data.

ORNL, sponsored by the Next Generation Safeguards Initiative (NGSI), has been investigating solutions. These projects include the development of a small-scale F/W system, in addition to the more recent development of a larger platform-scale testing center, to evaluate innovative ways to improve the IAEA's confidence in the authenticity of data. These systems provide ORNL researchers and our collaborators with representative data free from the sensitivities associated with data from a real facility. Another NGSI-funded project at ORNL involves using Monte Carlo analysis to identify a frequency of data transmissions which may protect the operator yet satisfy IAEA safeguards needs. ORNL is also evaluating how minor enhancements to how existing information that is already reported

to the in situ mailbox is used and how additional information could further strengthen the value of this tool.

This study furthers ORNL's work to strengthen the IAEA's tools by examining how the DAI software might be used in a large-scale GCEP plant to detect excess production. For this study, the authors installed the OSIsoft PI data archive and universal file loader to leverage data sets previously collected on the small-scale water-based F/W system. **Centralized analysis software, such as DAI, is the only cost-effective and efficiently maintainable choice for collecting and analyzing large data sets**. Currently, in cooperation with JRC, the DAI software is being used to analyze this data and to investigate how a similar architecture could be deployed for IAEA safeguards. DAI or other centralized analysis applications could be used to automatically analyze load cell data for better detection of excess feed at large GCEPs.

Preliminary feed, product, and withdrawal configurations were developed and tested for this study. During the configuration process, the authors had full access to the raw data from the small scale F/W system. During the configuration process at a GCEP, inspectors or technicians would likely need full access to the raw weight data. An automated tool, once properly configured with allowances for the IAEA to access the weight data upon request to resolve discrepancies, may provide an effective information filter to provide the IAEA with sufficient data to draw safeguards conclusions while also protecting the raw data in order to satisfy operators' concerns.

The findings from this study continue to emphasize the point that monitoring weight data from load cells in F/W stations could provide confirmation that weights of declared UF_6 cylinders (full and empty) do not change between the time they are weighed at F/W stations and the time they are weighed by accountability scales, which in turn could enhance existing methods to detect excess LEU production. This new capability could also confirm that the number of cylinders processed matches the number declared (e.g., no undeclared feed, product, or tails cylinders were processed in the F/W stations). In addition, monitoring load cell data could provide the IAEA with a capability to more quickly resolve discrepancies or anomalies that would normally have to wait until the annual PIV. Load cell monitoring could also provide the IAEA with ability to calculate a more timely, approximated material balance (e.g., a rough snapshot in time).

Further dialog is needed with stakeholders to address the remaining questions. Past consultancies among technology holders have been useful for promoting valuable dialogs between operators, inspectorates, and researchers, and a follow-up consultancy would help to clarify some of the remaining questions.

Acknowledgments

The authors would like to thank the European Commission for the use of the Data Analysis and Interpretation software and Pascal Dransart, Patrice Richir, and Luc Dechamp of the Institute for the Protection and the Security of the Citizen at the Joint Research Centre Ispra for hosting several visits to install and configure DAI.

References

1. Hopper, David A., Henkel, James J., Hines, J. Wesley , Krichinsky, Alan M.; "Improvements and Operation of the Oak Ridge Mock Feed And Withdrawal Facility," Institute of Nuclear Materials Management (INMM), 2011.

2. Krichinsky, A., Bates, B., Chesser, J., Koo, S., and Whitaker, J. M.; *A Mock UF_6 Feed and Withdrawal System for Testing Safeguards Monitoring Systems and Intended for Nuclear Fuel Enrichment and Processing Plants*; Oak Ridge: Oak Ridge National Laboratory, TM report, 2009.

3. Garner, J. R., Whitaker, J. M., Dabbs, B.T.; "Platform Scale Testing To Substantiate Load Cell Monitoring for Nuclear Safeguards," Institute of Nuclear Materials Management (INMM), 2014.

4. Richir, P., Dechamp, L., Janssens-Maehout, G. et al.; "Data Analysis and Interpretation Software from Solution Monitoring towards Near Real Time Accountancy," Institute of Nuclear Materials Management (INMM), 2007.

5. Van Handenhove, Carl, Breban, Domnica, Creusot, Christophe, Dransart, Pascal, Dechamp, Luc, Jardé, Eric; *Development of Solution Monitoring Software for Enhanced Safeguards at a Large Scale Reprocessing Facility*; ESARDA Bulletin, No. 46, December 2011.

6. Ely, J., Pochet, T., Younkin, J., Garner, J., March-Leuba, J., Smith, E., Lebrun, A.; "On-Line Enrichment Monitor (OLEM): Supporting Safeguards at Enrichment Facilities," IAEA Safeguards Symposium, 2014.

7. Smith, E., Miller, K., Garner, J., Poland, R., McDonald, B., March-Leuba, J.; "An Unattended Verification Station for UF_6 Cylinders: Development Status," IAEA Safeguards Symposium, 2014.

8. Smith, L. Eric, Lebrun, Alain R., Labella, Rocco; "Potential Roles for Unattended Safeguards Instrumentation at Centrifuge Enrichment Plants," *JNMM*, Fall 2013.

9. "Conceptual Approach for Applying Safeguards at a Large Gas Centrifuge Enrichment Plant, Neville Whiting 2nd Japan-IAEA Workshop on Advanced Safeguards Technology for the Future Nuclear Fuel Cycle 10–13 November 2009 Japan Atomic Energy Agency, Tokai-mura Ibaraki Japan.

10. Garner, J. R., Whitaker, J. M.; "A Monte Carlo Analysis of Gas Centrifuge Enrichment Plant Process Load Cell Data," ESARDA Annual Conference 2013.

11. Garner, J. R.; "A Monte Carlo Analysis of Gas Centrifuge Enrichment Plant Product and Tails Withdrawal Station Load Cell Data," Institute of Nuclear Materials Management (INMM) Annual Conference, 2014.

12. Carchon, Roland, Dechamp, Luc, Eklund, Lars Gustav, Janssens, Willem, Mercurio, Giovanni, Peerani, Paolo, Richir, Patrice; "Load Cell Monitoring in Gas Centrifuge enrichment Plants: Potentialities for Improved Safeguards Verifications," *Nuclear engineering and Design*, vol. 241 no. 1 pp. 349-356, 2011, jrc n°: jrc59958. issn: 0029-5493.

Session 7

Safeguards Concepts

Exploring Operational Safeguards, Safety, and Security by Design to Address Real Time Threats in Nuclear Facilities

M Schanfein
S Mladineo

Pacific Northwest National Laboratory
P.O. Box 999
Richland, Washington 99352

Corresponding Author:
Mark Schanfein (208) 569-6199 or mark.schanfein@pnnl.gov

Abstract

Over the last few years, significant attention has been paid to both encourage application and provide domestic and international guidance for designing in safeguards and security in new facilities.[1,2,3] However, once a facility is operational, safeguards, security, and safety often operate as separate entities that support facility operations. This separation is potentially a serious weakness should insider or outsider threats become a reality.

Situations may arise where safeguards detects a possible loss of material in a facility. Will they notify security so they can, for example, check perimeter doors for tampering? Not doing so might give the advantage to an insider who has already, or is about to, move nuclear material outside the facility building.

If outsiders break into a facility, the availability of any information to coordinate the facility's response through segregated alarm stations or a failure to include all available radiation sensors, such as safety's criticality monitors can give the advantage to the adversary who might know to disable camera systems, but would most likely be unaware of other highly relevant sensors in a nuclear facility.

This paper will briefly explore operational safeguards, safety, and security by design (3S) at a high level for domestic and State facilities, identify possible weaknesses, and propose future administrative and technical methods, to strengthen the facility system's response to threats.

Introduction

The impetus for safeguards by design started in 2010 with the recognition that, with few exceptions, International Atomic Energy Agency (IAEA) safeguards systems were installed in facilities after completion of construction.[4] This resulted in a safeguards system that was costly, less efficient, and less effective than if it had been incorporated during facility design. To mitigate this problem, guidance for all nuclear fuel cycle facility types, with the outreach focused on architect/engineers, vendors, builders, State Regulatory Authorities, and facility operators is now being issued by the IAEA.[3] The goal for this guidance is to raise awareness and effect a positive change to the project management process so that safeguards is considered during the earliest conceptual design phases. Ideally, safeguards would be accorded attention similar to safety, a discipline that went through an evolutionary process so that it is always included in designing a facility, and is considered as part of any initial concept for any type of nuclear facility.

Nuclear facility designers have long considered the importance of safety by design. More recently initiatives have focused on safeguards by design and security by design. With the incipient expansion of nuclear technology to newcomer countries, the IAEA has developed a milestone approach to building a nuclear infrastructure.[5] The process of building this infrastructure suggests consideration of the potential synergies from addressing all three disciplines of safety, safeguards, and security (3S) holistically.

Since its introduction by Japan in 2008, and acceptance as a concept by the Group of Eight (G8) at their Hokkaido summit, there have been a number of papers and presentations on the history and possible synergies of 3S, including some by one of the present authors.[6] For example, at the Hokkaido summit some of the shared principles include: [7]

> "…peaceful use of nuclear energy accompanied by commitments to implement 3S is a sound basis for international transparency and confidence in the sustainable development of nuclear energy."
>
> "Implementation of 3S constitutes an indispensable objective for the development of the infrastructure necessary for the introduction of nuclear power generation."
>
> "…international cooperation can greatly contribute to the development of such infrastructure."

At the Workshop on Effective Management of Safety, Security, and Nonproliferation Issues at Operating Nuclear Facilities held at Oak Ridge National Laboratory the Chairperson suggested that among the challenges for organizations and facilities:[8]

> "There is a general understanding of the potential benefits of the 3S concept. However, there is a lack of fundamental understanding of what are the interfaces and synergies between safety, security and safeguards and how they can be practically implemented."

Several papers by experts trying to address the challenge of applying the 3S concept can be found in archive proceedings of the Institute of Nuclear Materials Management and the European Safeguards Research and Development Association. In this paper, the authors seek to demonstrate the importance of close coordination among the three disciplines in emergency situations and propose a mechanism that would enhance nuclear security, while taking advantage of the capabilities of the other disciplines.

Discussion

The disciplines of safety,[9,10] safeguards,[11] and security[12] have been refined over many decades in nuclear fuel cycle facilities. A number of risk assessment approaches have been used for each one. The boundaries for each discipline with respect to each other have areas of complete independence as well as areas of overlap, and can be represented as in Figure 1. This paper will emphasize the common area among these three disciplines as indicated in the shaded region where all three intersect.

Figure 1

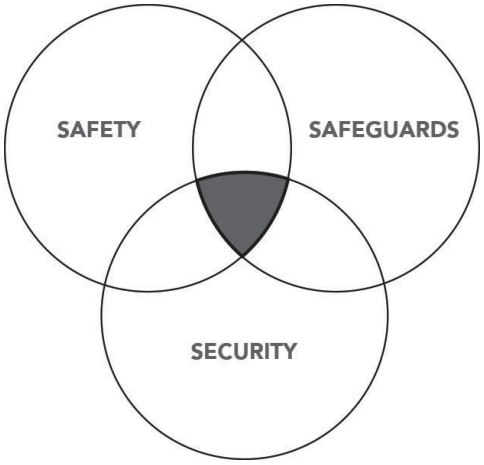

To illustrate an area in which these disciplines overlap, consider the following example: a requirement for a second door in a nuclear material vault. Safeguards and security would prefer that there not be a second door to reduce the risk of loss or theft of material by limiting egress points. Safety, on the other hand, requires the second exit to ensure personnel on staff have a second egress point should the primary door not be accessible in an emergency. One possible set of solutions to this dilemma is for safeguards to install a collimated radiation portal monitor to detect the removal of nuclear material through the door, and for security to install a balanced magnetic switch and alarm on the door to detect when it opens and to announce the opening to local staff members. In this way, solutions to the requirements and needs of all three disciplines can be optimized.

Focusing on the overlap of safeguards, security, and safety even further, we consider emergency response, including insider and outsider threats. This is where real-time cooperation has the potential for the greatest positive impact on a facility's response to threats. Planning, implementation, and training for a coordinated approach are critical to realize the most effective application of the limited resources available to counter various threats. Table 1 shows some example events to illustrate how a joint response operation could perform in a coordinated and supportive manner.

Safeguards by Design for Pyroprocessing Facilities in the ROK

Ho-Dong Kim, Eun-Ha Kwon and Se-Hwan Park

Korea Atomic Energy Research Institute, Daejeon
Nonproliferation System Research Division
Daedeok-daero 989-111, Yuseng-gu, Daejeon, 305-353 Republic of Korea
E-mail: khd@kaeri.re.kr, kwoneh@kaeri.re.kr, ex-spark@kaeri.re.kr

Abstract:

Safeguards by Design (SBD) is expected to improve the efficiency and effectiveness of safeguarding new nuclear facilities. Application of the SBD to the design of new nuclear facility will minimize the proliferation risks and facility retrofit for safeguards equipment. The KAERI has been developing pyroprocessing technology for the recycling of the useful resources from the spent fuel, and the SBD is incorporated into the conceptual design and system development phase of the pyroprocessing facilities. Safeguards approach of the Reference Engineering-scale Pyroprocessing Facility (REPF), which is an engineering-scale model facility, was developed through the IAEA Member State Support Program (MSSP) and its performance was evaluated by analysing the MUF uncertainty. As a result of the review by the safeguards experts for the REPF safeguards approach, it was recommended to the technology development in the field of input accountancy, viability of the Cm ratio method, NDA and DA measurements of U and U/TRU ingots, and process monitoring in argon hot cell. The close collaboration on the SBD of the pyroprocessing facilities is continued through the IAEA MSSP.

Keywords: SBD; Safeguards Approach; Safeguards Measures; Nuclear Fuel Cycle; Pyroprocessing

1. Introduction

KAERI has been developing pyroprocess since 1997 to resolve the issue of spent fuel accumulation and produce metal-based fuel for future fast reactors. Figure 1 shows a flow diagram of the process: (1) pretreatment (decladding, voloxidation, and sintering), (2) electroreduction, (3) electrorefining (including uranium recovery), (4) electrowinning, and (5) waste salt treatment [1]. The nuclear fuel cycle facilities related to the pyroprocess such as DFDF(DUPIC Fuel Development Facility), ACPF(Advanced spent fuel Conditioning Process Facility), and PRIDE(PyRoprocess Integrated inactive DEmonstration facility) have been constructed in ROK, and the safeguards system for each facility was designed from the beginning of the facility design [2].

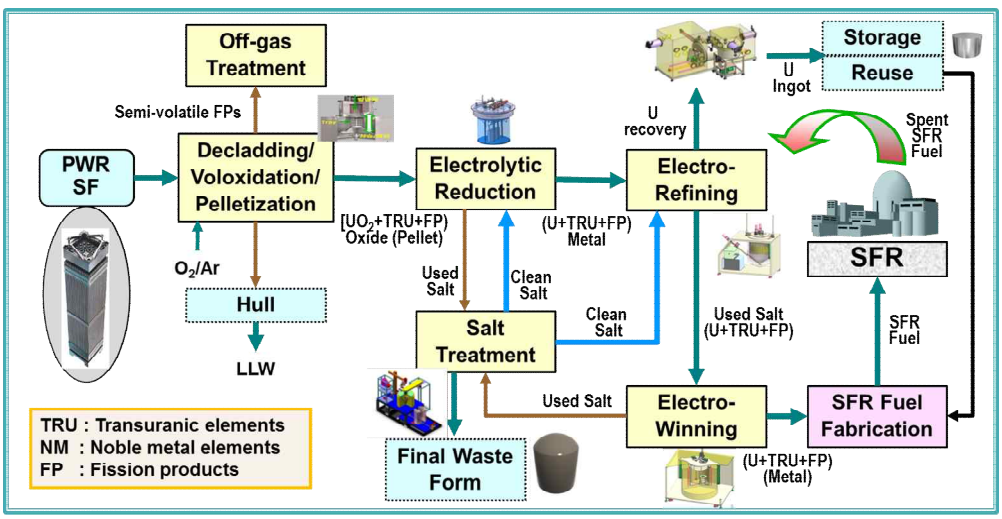

Figure 1. Flow Diagram of Pyroprocessing

Safeguards-By-Design (SBD) is an approach in which international safeguards requirements and objectives are fully integrated from the design stage of a nuclear facility. By integrating all regulatory issues, including safeguards requirements, the project risks can be minimized. The ROK has the experience of developing safeguards systems for nuclear fuel cycle facilities and is actively developing safeguards technologies for the pyroprocessing facility, using the SBD approach [3]. In this paper, the main features of SBD for pyroprocess by the KAERI, which include the nuclear fuel cycle facilities and its implemented safeguards system, the development of NDA instruments, and the study of reference pyroprocessing facility concept, are introduced and discussed.

2. Development of Safeguards System for Pyro-related Facilities

KAERI has been developing a head-end processing step for spent oxide fuel that applied to pyroprocessing technology. This processing step employs the feed material fabrication activity to produce granules and pellets from the voloxidized powder using spent PWR fuel at DFDF. The granules and pellets could be used for the hot test of electrolytic reduction process in pyroprocess. The main objectives of the feed material fabrication activity at DFDF are to demonstrate technology for developing optimal process conditions to produce granule and low density pellet from the spent PWR fuel by only utilizing the thermal and mechanical processes, and to supply the feed material to the electrolytic reduction process of ACPF.
DFDF consists of one concrete hot cell used for the technology development of the DUPIC (Direct Use of Pressurized Water Reactor Fuel in CANDU) fuel fabrication as well as for vol-oxidation of irradiated PWR fuel rod cuts. During the vol-oxidation process, volatile fission products are removed and trapped, e.g. Cs-137 is significantly reduced. The safeguards system development of the DUPIC fuel cycle has been considered from the beginning of the R&D process. Two aspects of its safeguards R&D technology have been developed and demonstrated. The first involves nuclear material accountancy in a hot-cell with the DUPIC Safeguards Neutron Counter (DSNC), and the second involves containment and surveillance with an unattended image and radiation monitoring system. Fugure 2 shows an overview of DFDF.

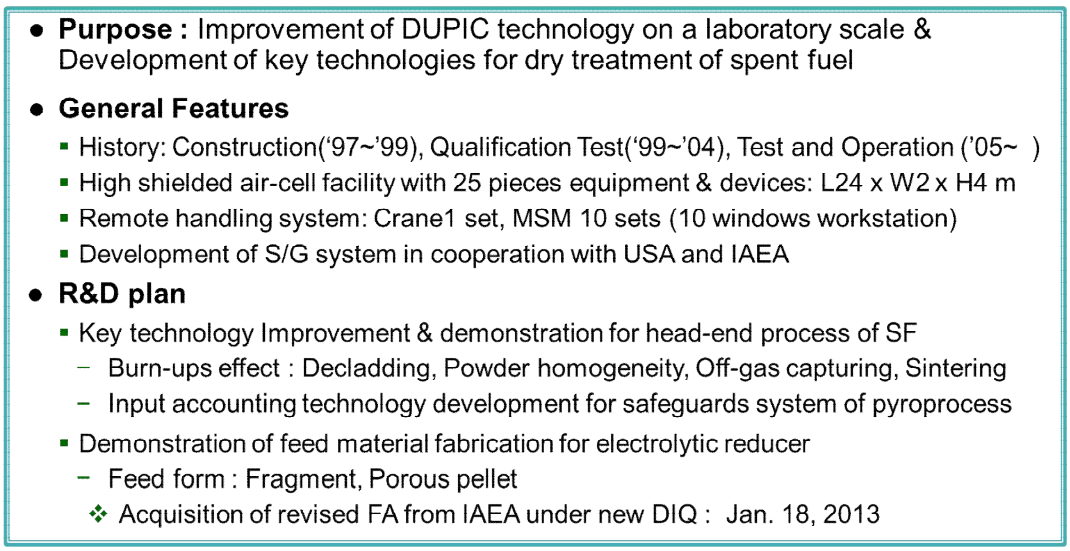

Figure 2. DFDF Overview

KAERI is currently developing an electrolytic reduction process to demonstrate the laboratory scale operation in ACPF, in which spent fuel materials will be used. ACPF is an R&D facility consisting of two concrete hot cells, one of which contains an argon compartment, for research into the electrolytic reduction process. The ACPF process involves only one step of the full pyroprocess for the electrolytic reduction of oxide into metal form in the argon compartment. The demonstration test is divided into two phases, in which the cold test with natural and depleted uranium and hot test with up to 10 kg-U of feed material from DFDF (PWR irradiated fuel rod cuts after vol-oxidation process in the form of low density pellets or granules) will be performed. Figure 3 shows an overview of ACPF.

- **Purpose** : To verify feasibility of an Electro-reduction process for PWR spent fuel in combination with DFDF
- **General features**
  - History: Const'n('03~'05), Inactive Test('06~), Refurbishment('13~'14), Op'n('15~)
  - High shielded hot cell(L11 x W2 x H4 m) with a modular type Ar compartment
  - Remote handling system: Crane1 set, MSM 5 sets (5 window workstations)
- **Future R&D plan**
  - Key technology development for electrolytic reduction process
    - Assessment of electrochemical reaction behaviors : Potential of electrodes, Reduction yields(U/TRU/NMs), and FPs behaviors (Ar cell: L1.8 x W1.8 x H2.4 m)
    - Assessment of ER system : Stability, remote operability and maintainability
  - R&D to enhance safeguardability for electrolytic reduction process
    - Demonstration of ASNC(ACP Safeguards Neutron Counter)
    - Study of LIBS(Laser-Induced Breakdown Spectroscopy Instrumentation)

Figure 3. ACPF Overview

KAERI has been developing a passive-mode neutron coincidence counter for material accounting of the ACP. This well-type neutron counter, so-called ACP Safeguards Neutron Counter (ASNC), is for conducting NDA of the materials that exist during the ACP process. The basic concept of the ASNC is the Pu to Cm ratio method which uses the Cm mass determined by measuring the coincidence neutrons from Cm-244 and the pre-determined Pu-to-Cm ratio to calculate the Pu mass. The ASNC contains 24 3He tubes, which are symmetrically located in high density polyethylene moderator. Each 3He tube is connected to an individual pre-amplifier. The 24 signals from the tubes are divided into 4 groups, and each group is combined into 1 signal. The signal cable was designed to be replaced by remote manipulators. There is lead shield inside the sample cavity to protect the 3He tubes and electronics from the intense gamma rays of the process materials. Lead and HDPE shields outside the ASNC reduce the background gamma rays and neutrons from the hot cell environment. The ASNC was installed inside the hot cell of the ACPF in 2005, and the performance tests were conducted with 252Cf sources. A verification test using spent fuel rod-cuts was performed with experts from the IAEA and LANL in 2007. The results were satisfactory, and the ASNC could measure spent fuels with Triplet counts [4]. The ASNC also has remote operation capabilities, and maintenance can be performed while the ASNC is in a hot cell. It is currently under the minor modification of modularization into several components to meet the load limit requirement of the in-cell crane.

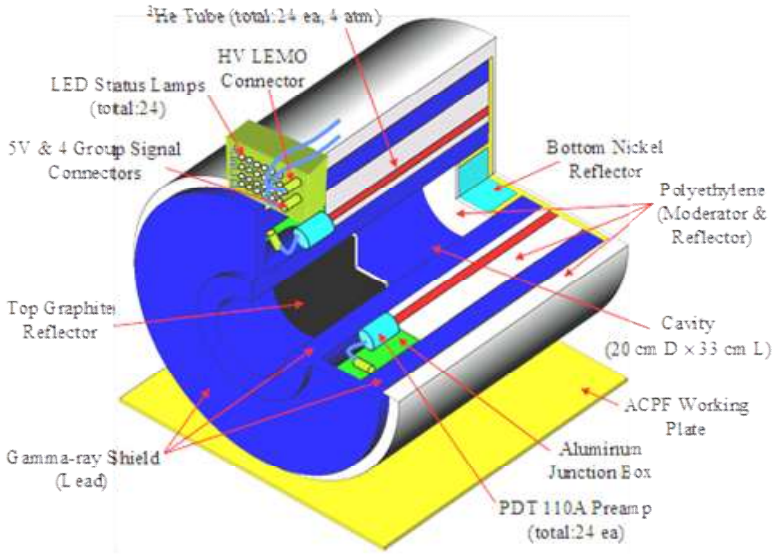

Figure 4. Structure of ASNC

The ASNC is a key NDA device for nuclear material accounting. The accounting data of the ASNC are provided to the IAEA periodically. The IAEA's slab detector is used for independent verification of the nuclear material accountancy for the ACPF. Three IAEA cameras and three IAEA neutron monitors were installed at the rear and side doors of the ACPF hot cells to monitor any activities related to the nuclear material movement through the doors. The cameras and neutron monitors are connected to the IAEA safeguards server located in the working area of the ACPF.

Since 1997, the laboratory-scale unit process of pyroprocessing has been carried out, and the design and construction of an engineering-scale integrated system was developed by KAERI. PRIDE is the integrated engineering-scale mock-up pyroprocessing facility, and it was constructed in 2013. The PRIDE consists of a large scale argon-atmospheric cell (40.3 m length, 4.8 m width and 6.4 m height), an argon system, in-cell equipment (transfer lock, in-cell crane, feed through, etc.) and remote operation devices. The purpose of the PRIDE is to test the unit process performance, the remote-equipment operability, the integrity of the unit process, the system operation under argon conditions and the safeguards technology. Only uranium and depleted uranium will be treated in the PRIDE. The processes in the PRIDE consist of a voloxidation, oxide reduction, electrorefining, electrowinning, and waste treatment processes. Air-atmosphere processes such as fabrication of UCl3, ingot production and voloxidation are carried out on the first floor and large argon cell is positioned on the second floor. The throughput of the facility is 10 tonU/yr.
The construction and installation works for the facility have been completed and the cold operations of unit process are now by using DU, while the integrated works of full spectrum will be started soon. The key pyroprocessing technology will be tested and demonstrated using natural and/or depleted uranium with surrogate materials, and the system engineering studies including the design study for facility and equipment, remote operation and maintenance, advanced safeguards and radioactive materials transportation etc. will be performed. The PRIDE will also support the near-term mission to evaluate and produce reliable data in order to resolve scale-up issues of full-spectrum pyroprocessing technology [5]. Figure 5 and 6 show the overview and equipment of PRIDE facility.

- **PRIDE :** *PyR*oprocessing *I*ntegrated inactive *DE*monstration facility *(10 ton-HM/yr)*
  - **Purpose**: Demonstration of full-spectrum pyroprocessing performance with depleted uranium and surrogate materials in an Ar-environment cell (L40 x W4.8 x H6.4 m)
  - **Milestones:** Design (‘07~’08), Installation (‘09~’12.6), Blank tests (‘12.7~)
  - **Operation:** Salt test (’13), DU test (’14), SimFuel(surrogate) test (‘15~‘16)
- **R&D plan**
  - Demonstration of Eng-scale integrated pyroprocessing facility with surrogates (DU and SimFuels)
  - Experiences in scale-up and in-cell remote handling systems and utilities
  - Securing commercialization technology in connection with JFCS results
  - Development of safeguard technology through cooperation with IAEA

Figure 5. Facility Overview of PRIDE

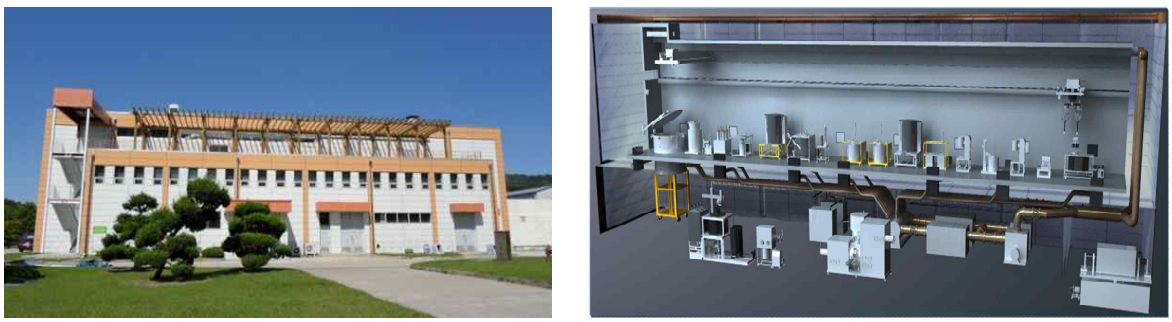

Figure 6. Exterior and Equipment of PRIDE Facility

A safeguards system of the PRIDE has been designed and is being developed. Because natural and depleted uranium are the process materials in the PRIDE, the mass measured at the Key Measurement Point (KMP) is the most important parameters in the accounting system. The 235U

amounts will also be accounted for with a unified NDA system. This instrument is an integrated device with three independent techniques of neutron counting, gamma-ray spectroscopy, and weighing and called the 'Unified NDA' of PRIDE facility. The figure 7 shows an MCNPX model of the Unified NDA instrument. The Unified NDA instrument was designed to be flexible for several containers, which are largely different in their size. Thus the inner cylindrical neutron counter can be removed for larger containers to be accommodated. The basic principles of each technique will remain intact but some improvement in measurement error is expected by the synergy of the combined techniques. Although there will be only natural or depleted uranium materials to be used in the PRIDE facility, the Unified NDA concept could be applied to the nuclear material measurement for future pyroprocessing facilities. Gamma detectors are installed inside the argon cell to evaluate the possibility of tracking the uranium process flow. Key measurement parameters such as current, voltage, temperature, and humidity will be monitored from process equipment. Cameras are installed to survey the movement of nuclear material. An integrated safeguards system, which combines the on-line NDA signals and process monitoring signals, is being developed to implement Near Real Time Accountancy (NRTA) at PRIDE.

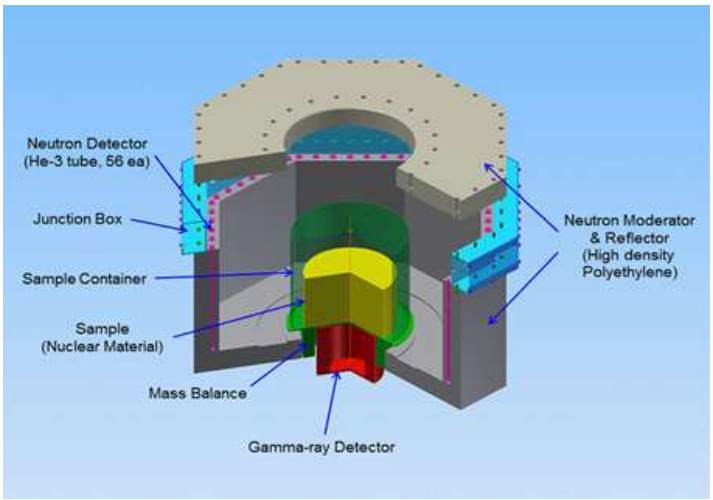

Figure 7. The Unified NDA Instrument

3. Safeguards by Design for REPF

A Member State Supporting Program for Agency Safeguards (MSSP) for the 'Support for Development of a Safeguards Approach for a Pyroprocessing Plant' was contracted between the IAEA and the ROK in 2008. Six pyroprocessing facility concepts suggested by the US, Japan, and the ROK were analyzed, and the Reference Engineering-scale Pyroprocessing Facility (REPF) concept was developed. The input material for the REPF is PWR spent fuel, and the output materials are U ingot and U/TRU ingot. The size of the process batch is 50 kgHM, the throughput per campaign is 500 kgHM, and the throughput per year is 10 MTHM.

The main processes performed in the REPF consist of receipt and storage of spent fuels, the head-end process, the electrolytic reduction process, the electro-refining process, the electro-winning process, and waste salt regeneration and solidification. The head-end process has five steps: disassembling and rod extraction, chopping, decladding, homogenization, and pretreatment of the oxide fuel. In the electrolytic reduction process, the oxide fuel is converted to a metallic form. The electro-refining system, which is composed of an electro-refiner, a salt distiller, and a melting furnace, recovers pure uranium from the electrolytically reduced fuel. The electro-winning system is able to recover actinides from salt after the electro-refining operation. The waste salts are fabricated into durable waste forms in the waste salt regeneration and solidification process.

Three Material Balance Area (MBA)s were identified for the REPF, which consists of the spent fuel receiving area, the storage and head-end process area (MBA-1), the main pyroprocessing area (MBA-2), and the product and waste storage area (MBA-3). Key Measurement Point (KMP)s should be identified in which the nuclear materials are present to make it possible to measure them and determine the material flow or inventory [6].

Since the main nuclear materials that should be accounted for are uranium and plutonium in the REPF, and the most important KMPs for accounting these materials are the point before the main pyroprocessing, and two points where the final U ingot and U/TRU ingot products of the pyroprocessing are placed. A unified NDA equipment, a PNAR detector and a fission chamber were suggested as material accounting instruments at three KMPs [7].

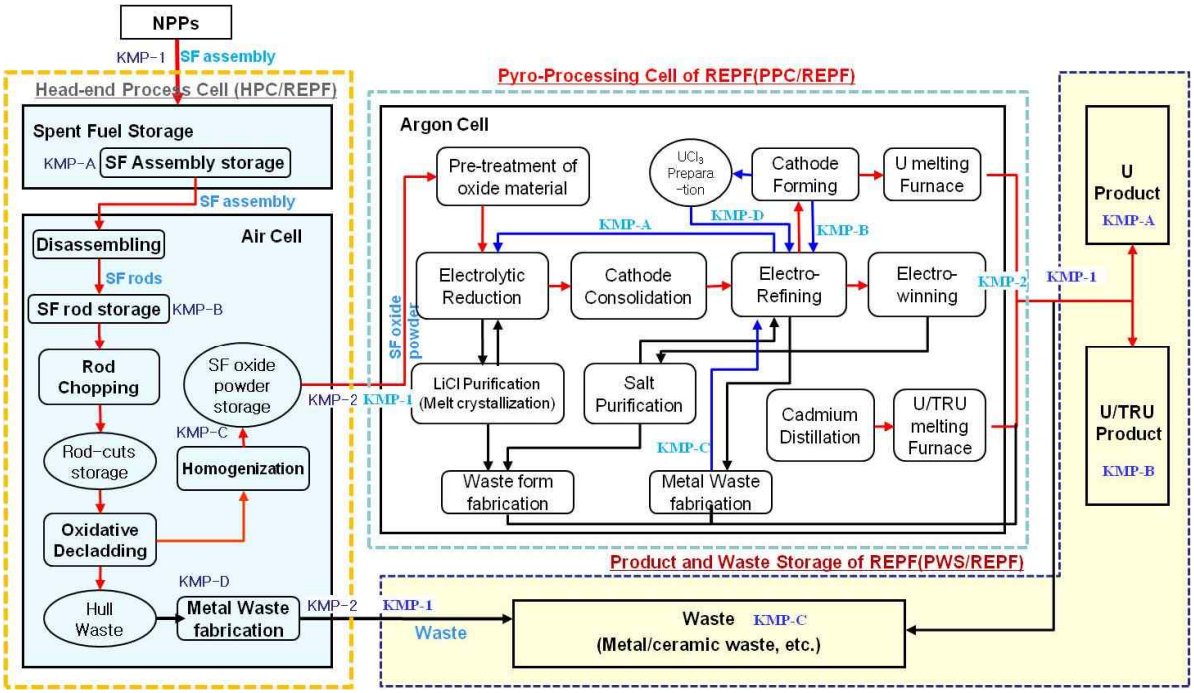

Figure 8. Key measurement points in MBAs of the REPF

Near-real time accountancy (NRTA) system will be established to timely detect a diversion during pyroprocessing. NRTA system could be based on NDA equipment and a Destructive Assay (DA) would also be applied to the three important KMPs to increase the accuracy of material accounting. Considering the time required for a DA, a three-level method was suggested. In the first level, the DA samples are obtained at the three important KMPs, and the samples are analyzed by the DA method. In the second level, the NRTA equipment in NRTA system are continuously performed at three important KMPs while the DA samples are analyzed. In the third level, the NRTA results from the NRTA system are updated and corrected by comparing with the DA results.

A simulation program called Pyroprocessing Material flow and Material unaccounted for Uncertainty Simulation (PYMUS), has been developed to analyze the nuclear material flow in the REPF and to calculate the MUF uncertainty. DA-based material accounting in the REPF can give accurate information for the necessary accountability, and the NDA-based accounting can also yield useful accounting information in a timely manner.

Although the REPF concept was mainly based on safeguards concerns and the analysis under these conditions may give limited results, the efforts to design a reference facility and to develop a safeguards approach for pyroprocessing will be helpful in implementing the safeguards-by-design concept [8].

4. Conclusions

Pyroprocessing is a new and advanced proliferation-resistant technology that could help reduce the volume and the radioactivity of spent fuels, and potentially allow the spent fuel to be recycled. The safeguards approach for pyroprocessing should be established to determine the Pu inventory accurately, track the nuclear material flow, and ensure that there is no diversion.

The ROK has successfully developed and implemented NDA instruments and safeguards systems for pyroprocess-related facilities. Currently, the R&D efforts to develop NDA measurement equipment, advanced C/S and process monitoring systems, and modeling and simulation for the safeguards of the

pyroprocessing facilities continue. The SBD approach is based on these efforts. From the beginning of the design phase, these projects have proceeded in cooperation with facility designer. The REPF concept was established to develop the safeguards approach, and to analyze the safeguardability.
While incorporating the SBD concept early in the design phase is being emphasized for commercialization of next-generation nuclear systems, KAERI has dedicated itself to developing technologies that are required to implement an international safeguards system for pyroprocess, which is a promising and/or advanced nuclear fuel cycle technology in Korea. KAERI is expanding its R&D scope to integrate safeguards with other safety and security objectives in the overall design process of pyroprocessing. The ultimate goal is to achieve an optimum design technology for pyroprocessing that incorporates the enhanced 3S features. By addressing the concepts of 3S at an initial stage of development, the credibility of the state will be enhanced, which will lead to a pyroprocessing-based fuel cycle being realized in Korea.
The application of SBD to these efforts will contribute to improving nuclear transparency and safeguards technology so that pyroprocessing technology can be realized in the future.

5. Acknowledgments

This work was supported by the National Research Foundation (NRF) grant funded by the Ministry of Science, ICT & Future Planning, Republic of Korea (No. 2012M2A8A502594).

6. References

[1] K. C. Song, H. Lee, J. M. Hur, J. G. Kim, D. H. Han, and Y. Z. Cho, “Status of pyroprocessing technology development in Korea”, Nuclear Engineering and Technology, Vol. 42(2), 131 (2010).

[2] W. Bekiert, M. Basturk-Tatlisu, F. Gao, M. Hori, M. Pellechi, L.A. Re Falo, D. Y. Song, S. H. Park, I. J. Cho, G. I. Park, H. D. Kim, S. W. Kim, L. J. Park and S. H. Ahn, “Safeguarding Pyroprocessing Related Facilities in the ROK’, Proceedings of IAEA Safeguards Symposium (2014).

[3] H. D. Kim, H. S. Lee, D. Y. Song, T. H. Lee, B. Y. Han, S. K. Ahn, and S. H. Park, “Application of safeguards-by-design for the pyroprocessing facilities in the ROK’, JNMM, Vol. XL(4), 24 (2012).

[4] T. H. Lee, H. O. Menlove, S. Y. Lee, and H. D. Kim, “Development of the ACP safeguards neutron counter for PWR spent fuel rods”, Nuclear Instruments and Methods in Physics Research A 589, 57 (2008).

[5] S. I. Moon, W. M. Chong, G. S. You, J. H. Ku, and H. D. Kim, “Preliminary conceptual study of engineering-scale pyroprocess demonstration facility”, Nuclear Engineering and Design, Vol. 259, 71 (2013).

[6] S. K. Ahn, H. S. Shin, and H. D. Kim, “Safeguardability analysis for an engineering scale pyroprocess facility”, Journal of Nuclear Science and Technology, Vol. 49(6), 632 (2012).

[7] B Y. Han, H. S. Shin, and H. D. Kim, “Analysis of measurement uncertainty of material unaccounted for in the reference pyroprocessing facility”, Nuclear Technology, Vol. 182, 369 (2013).

[8] S. K. Ahn, C. S. Seo, E. H. Kwon, and H. D. Kim, “Linkage option between unit process to enhance proliferation resistance of pyroprocessing”, Annals of Nuclear Energy, Vol. 75, 184 (2015)

An Operators' Experience of Applying Safeguards by Design

Alan Homer*, Virginia Ferguson, Cameron Frears

Nuclear Materials Accountancy & Safeguards Department
Sellafield Limited, Seascale, Cumbria, CA20 1PG, UK
*Corresponding Author: alan.homer@sellafieldsites.com

Abstract

Safeguards-by-design is defined as the consideration of safeguards throughout the lifecycle of a nuclear facility, from conceptual design to decommissioning. Sellafield Limited are currently designing, constructing and moving into operations with a number of new facilities, most notably a nuclear material storage facility as part of the UK strategy for consolidating nuclear material from other UK facilities to allow for their declassification. Although safeguards-by-design has not introduced any new safeguards requirements to the various projects, it has provided an opportunity for Sellafield Limited to engage voluntarily with DG ENER earlier than legally required in order to reduce project risk. It has been in the interests of both Sellafield Limited and DG ENER to collaborate in order to facilitate the effective implementation of safeguards. The Safeguards-by-design process has facilitated enhanced understanding of various facilities and their capabilities and the suitability for safeguards implementation, whilst driving value for money and ensuring safeguards related issues are addressed in line with the project schedule. This paper shares learning from the safeguards-by-design process at various lifecycle phases in a number of facilities. Typically, to meet the safeguards requirements, a close dialogue has been established between the interested parties on a consistent basis and early contact at the concept and design stages has provided the operator with high-level safeguards principles to work to and has facilitated the inclusion of safeguards instrumentation into the overall design and subsequent facility construction. Detailed discussion at the early design stages has raised the profile of nuclear material safeguards within the wider Sellafield community. While nuclear materials accountancy and safeguards generally has a small impact on project cost and overall schedule, lack of sufficiently detailed consideration early in the design process can result in a much larger impact. The task of avoiding such increases is assigned to the facility design and construction project management, with the support of safeguards specialists, who can better address issues when informed at an early stage.

Keywords: safeguards by design; project management; facility design

1. Introduction

The Energy Act (2004) [1] requires that the United Kingdom (UK) has a strategy [2] to safely and securely manage nuclear material in the most practical and cost effective way. This Act sets out the formation of the Nuclear Decommissioning Authority (NDA) which manages this strategy on behalf of the UK Government. The NDA mission is to deliver safe, sustainable and publicly accepted solutions to the challenge of nuclear clean-up and waste management. The NDA estate consists of 19 sites across the UK, including Sellafield.

Sellafield Limited are responsible for safely delivering decommissioning of the UK's nuclear legacy on the Sellafield site in West Cumbria, as well as fuel recycling and the management of low, intermediate and high level nuclear waste activities. As Sellafield Limited comes towards the end of this decade, reprocessing operations will cease and more emphasis will be placed on post-operational clean out (POCO), waste management and decommissioning. This in itself means the design, construction and commissioning of new facilities, enabling the site to transition towards new operations covering novel waste streams arising from the clean-up activities.

Another area for consideration is the UK strategy for plutonium and uranium disposition to ensure the safe management and ultimate disposition of UK-owned plutonium and uranium. Many plutonium-bearing materials are being consolidated at Sellafield for long-term storage. This approach retains future options for either re-use or direct disposal of the material and allows for consolidation of nuclear material and wastes to enhance security and reduce overall lifetime costs to the UK nuclear estate.

Nuclear safeguards are measures to verify that states comply with their international obligations not to use nuclear materials (plutonium, uranium and thorium) from their civil nuclear programmes to manufacture nuclear weapons. The application of safeguards measures in the UK derives from the Euratom Treaty [3] and the Treaty on the Non-Proliferation of Nuclear Weapons (NPT) [4]. The safeguards measures involved are implemented by the safeguards inspectorates of the European Commission (DG-ENER) and the International Atomic Energy Agency (IAEA). In the UK, the Office for Nuclear Regulation (ONR) acts as the national authority for safeguards [5].

Sellafield Limited has recognised the need and importance of embedding "safeguards by design" as a prerequisite into their guidance for project management. This approach allows for a more complete description of the nuclear materials accountancy, control and safeguards (NMAC&S) expectations early in the design process and the involvement of all relevant stakeholders at key decision making points. Some of the main drivers for this inclusion are:

- recognition from historical experience of the difficulties involved in retro-fitting NMAC&S requirements to facilities,
- the potential for project cost increases associated with late intervention from NMAC&S,
- the potential for schedule over-runs due to design change requirements, and
- the avoidance of NMAC&S requirements ending up on the project critical path.

This paper will briefly describe the process put into practice by Sellafield Limited to embed NMAC&S into its project management approach, consider whether or not it is ever too early to engage the safeguards authorities in the safeguards by design process and then discuss best practice and potential pitfalls observed by operators at Sellafield Limited involved in various safeguards by design activities.

2. Sellafield Gated Process

Any work performed on Sellafield site that is delivered as a project is developed and managed using the Sellafield Gated Process (SGP). Work activities towards the completion of a task are progressed through two phases, programmes and projects. Programmes confirm the

need for work to be carried out and coordinate any studies required to select a single viable option to meet the specifications of a new plant or process. Projects then take this single option through design, procurement, construction and commissioning. Once the project demonstrates that it meets the required specifications, operations can begin.

Major projects can be broken down into five key areas:

1. Project Concept
2. Preliminary Design
3. Detail Design
4. Construction
5. Active Commissioning

There are also a number of review points as part of the SGP, which together with the various stages involved in project delivery are illustrated in figure 1. These stages and associated review points will be discussed in the following sections, together with NMAC&S involvement and learning from various projects.

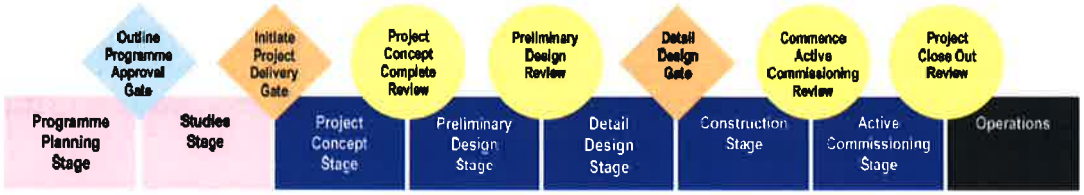

Figure 1: A diagram indicating the various stages of the Sellafield Gated Process and their associated review points.

2.1. Programme Planning Stage

The purpose of the Programme Planning Stage is to manage the performance gap between the current and required capabilities of the Sellafield site according to the site strategy. The programme plan must balance the identified performance gap with current site capability and existing study and project activities to develop one interdependent programme of work.

The Outline Programme Approval Gate verifies that an initial technology readiness assessment has been performed to understand any technology gaps and to identify any associated technology development requirements. The outline programme approval gate also ensures that synergies between existing programmes of work have been identified and reconciled and that key specialist resources required for the work have been identified (including any relevant subject matter experts (SMEs).

2.2. Studies Stage

The purpose of the Studies Stage is for the programme to select the best technologically viable option before the project is initiated. The selected solution must meet a customer developed functional specification and be sufficiently mature to provide confidence that it can be engineered. As many concurrent activities are managed throughout the Programme Planning and Studies stages, it should be noted that this early part of the SGP is highly iterative and every study does not result in initiation of a project.

The SGP requires the project team to establish an interdisciplinary team comprising of SMEs during the studies stage. This approach ensures early participation of NMAC&S SMEs, providing clear direction from NMAC&S from the project outset. Project risks associated with NMAC&S can be identified early and incorporated into the overall project risk management strategy. These risks are typically managed using a conservative approach towards the need for NMAC&S measures early in the design, and when the design and discussions evolve, this conservatism is relaxed.

The Initiate Project Delivery Gate marks the end of this stage and the official beginning of the project. Safeguards relevant information is gathered and incorporated into a Project Execution Plan, covering activities from the Initiate Project Delivery Gate through to the Detail Design Gate (see figure 1).

2.3. Project Concept Stage

The purpose of the Project Concept Stage is to confirm that there is a single fit-for-purpose, cost effective scheme that will deliver the required business benefits before commencing preliminary design. It is typically during this stage that initial engagement with DG ENER would commence to build on the high level NMAC&S advice provided by the Sellafield Limited safeguards SMEs in the studies stage. Formal notification of preliminary design information is provided to DG ENER via ONR in the format of a Basic Technical Characteristics (BTC) or Design Information Questionnaire (DIQ) document.

The Project Concept Complete Review validates that the project is ready to move into the Preliminary Design Stage. The early engagement of DG ENER is essential at this stage as it has been estimated that in the total lifetime costs of a project, conceptual design decisions can account for up to 80% of a projects cost [6].

2.4. Preliminary Design Stage

The purpose of the Preliminary Design Stage is to deliver an engineering solution that is sufficiently mature to deliver performance requirements and allows the project to move into detailed design. At this stage in the process a more detailed NMAC&S assessment of the project solution is completed and an initial safeguards approach formulated with DG ENER.

As preliminary design progresses, the basic technical characteristics (BTC) document is produced and initial design information verification (DIV) can be performed to ensure that DG ENER have the opportunity to verify the facility design, proposed flow and inventory locations and investigate any potential nuclear proliferation scenarios. The safeguards requirements outlined in the initial safeguards approach and the BTC allow a procurement strategy to be developed for safeguards-related equipment.

2.5. Detail Design Stage

The purpose of the Detail Design Stage is to confirm that the project definition has been developed to enable engineering procurement to be completed and that the project is ready to commence major procurement, manufacture and construction activities.

A BTC will be formally issued to DG ENER on completion of the preliminary design review in advance of the legally required 200 days notice prior to planned start of construction. A detailed safeguards assessment of the project solution is completed based on the BTC and the safeguards approach is finally agreed with DG ENER. A review of the project at this point validates that the project definition and maturity has been developed to the point where construction is possible.

2.6. Construction Stage

The purpose of the Construction Stage is to complete all procurement, manufacture, construction and inactive commissioning activities. It is during this stage that the operational safety and design performance will be achieved and a regulatory permission for operation granted.

Usually, for large projects, the definition of the BTC will be revised, completed and issued to DG ENER via ONR at this stage and an initial facility design information verification mission can be performed. Notification is required at least 200 days before the first consignment of SNM is due to be received by the facility and construction generally takes longer than this. Also, the nuclear materials accountancy systems to be used for the facility are demonstrated as far as is practicable without the introduction of active material.

2.7. Active Commissioning Stage into Routine Operations

The purpose of the Active Commissioning Stage is to confirm that all functional requirements have been met for the project. A post investment appraisal is completed to assess the realised business benefits and to validate that learning from the delivery performance has been captured to inform future delivery strategies. Before moving into routine operations all necessary regulatory interfaces must be satisfied.

3. Is it ever too early to inform the Safeguards Authorities of a New Project?

In recent times, Sellafield Limited, through the SGP, has communicated new projects and modifications to existing facilities to DG ENER as soon as a project has been formally sanctioned (towards the end of the project concept stage, section 2.3). Especially with more complex facilities, sharing of information with the safeguards inspectorates can result in a significant amount of effort in order for them to assess the information, provide feedback to the designer / operator and begin engagement in safeguards discussion.

There have been examples where site strategy has changed or there have been budgetary constraints that have led to a project being put on hold or even cancelled well into the preliminary design phase. Careful consideration must be given to the amount of design information provided, the urgency of the safeguards inspectorate response required and the confidence that a project will been seen through to completion. Whilst in a perfect world, all

projects will be completed, the dynamic environment of the nuclear industry can sometimes lead to disconnect between the strategists and the designers, and whilst the designers are continuing with their projects, they are unaware of a higher strategic view.

This can also have an impact on the relationship between the safeguards inspectorates and the operator. Where pressure is applied from the operator to the safeguards inspectorates to review design information, and to provide advice and guidance on safeguards approach so that the project can progress and then a project is then curtailed, then it can be frustrating that the resource and effort could have been better utilised in another area. In these times of increasing financial constraints and resource issues for both the operator and the safeguards inspectorates, all should be mindful of the consequences of their actions.

4. Best Practices

4.1. Project Dossier

The compilation of project dossiers has been essential in providing traceability for key NMAC&S decisions made in projects, the reasons for those decisions, and any formal / informal correspondence between Sellafield Limited and the safeguards authorities. Key information captured within the dossiers includes:

- Formal project information
- Minutes of meetings and plant visits (including any photographs taken and shared)
- Formal correspondence
- Any design information which has been shared with the safeguards inspectorates
- Iterations of the safeguards approach and BTC
- Cost estimates and the associated justification
- Any supporting nuclear materials accountancy information.

In the early stages of a project, there is often a lot of iteration in terms of design, technology concepts and personnel involved in decision making. The dossier is a tool which consolidates this information to provide traceability and transparency of the decision making processes.

4.2. Communications Strategy

The consistent use of a clear, structured approach to communicating with the safeguards authorities when dealing with projects has resulted in habitual information sharing and a common expectation of how a project will unfold. Initial high-level face to face discussions in the project conceptual design stage allows the safeguards authorities to identify their key personnel for a given project, an initial discussion surrounding high-level safeguards concepts to be considered by the project team and a frequency of information share to be established.

Regular communication early in the project lifecycle has facilitated positive, open engagement on often difficult safeguards challenges, involving various facilities and forms of nuclear material. A flexible, pragmatic approach from the key stakeholders, without the time pressure associated with late engagement and the subsequent short timeframes, allows development and agreement of more comprehensive and efficient safeguards arrangements.

Routine video conferencing has been found to be extremely effective in managing actions and for information sharing. It allows the safeguards authorities to attend in person if at Sellafield on mission and also allows technicians, inspectors, management and the project team to attend. This platform of regular communication has assisted in the timely turnaround of documents for review, updating of design information and the development of safeguards solutions.

4.3. Safeguards Requirements List

The development of a list of required safeguards-related equipment has facilitated efficient resource allocation throughout project lifecycles and allowed for early resolution of equipment delays / technology issues. The table specifies:

- What equipment is required and in what quantity
- The purpose of the equipment
- The responsibilities of both Sellafield Limited and the safeguards authorities for each piece of equipment
- Contact details for the responsible people for each piece of equipment
- Key dates required for provision of design information, when the equipment is required in location on site and when installation is required
- Current status of each piece of equipment work stream.

An example of a safeguards requirements list is simulated in table 1. This table was developed to address the various pitfalls discussed in section 5. It provides clarity of information for personnel introduced to and leaving the project and ensures a clear understanding of what must be delivered by all parties. Used in conjunction with a strong communications plan this table often acts as an agenda for discussion as a given project develops and helps to provide a focus for both the project team and safeguards authorities.

5. Pitfalls

5.1. Lack of NMAC&S Knowledge in the Project Team

Whilst the safeguards by design concept has been formally captured within the Sellafield Limited approach to project management through the SGP, the question still remains as to how an individual project identifies whether or not it is safeguards significant. Whilst safety and security are often obvious areas for consideration, the field of nuclear materials accountancy and safeguards is not as well known outside of its immediate practitioners.

If the design team are not aware of the safeguards implications of their project then the engagement with both NMAS SMEs and with the safeguards inspectorates doesn't happen. Subsequently, this can lead to late engagement of the relevant parties, potential re-design and retro-fitting of plant if the design and construction have progressed sufficiently through the SGP, short term notice of a cost and resource requirement and potential project schedule delays.

It is essential that the designers and project teams have enough NMAC&S knowledge in order to identify whether or not there are any safeguards implications for their projects.

Table 1: A table setting out requirements for NMAC&S equipment required for a given project. The data in this table is simulated and does not refer to a specific project.

Item	Video Surveillance Camera's (4)	Door Neutron Monitors (2)	Package Unloading Weigh Balance	Pen Detector for Endoscope
NMAC&S Function	Real-time video surveillance of storage area	Indication of passage of Pu bearing material	Provision of gross mass for each package	Gross measurement in-channel
DG-ENER Responsibility	Identify location, specify and procure cameras / cabling	Identify location, specify and procure monitors / cabling	N/A	Specify and procure equipment
DG-ENER Lead	Inspector A	Inspector B	Inspector C	Inspector D
Sellafield Responsibility	Install cabling / cameras in specified location	Install cabling / monitor in specified location	Specify, procure, install. Ensure independent output signal available, agree data protocol with DG-ENER	Provide mechanism for fixing to endoscope
Sellafield Lead	Operator A	Operator B	Operator C	Operator D
Date Design Information Required	08/2013	01/2014	01/2014	04/2014
Date Required on Site	02/2014	08/2014	03/3014	07/2014
Date Required in Service	03/2014	10/2014	04/2014	09/2014
Current Status	Available	Monitor location and set-up uncertain – discussions ongoing	Available	Mechanism to move detector along channel not agreed and fixing mechanism not designed

5.2. Projects Covering a Long Timeframe

When a project covers an extended period of time there are often changes in the personnel involved within both the project team and within the safeguards inspectorates. It is not uncommon for a new safeguards inspector to have different ideas on the required safeguards approach, or for a project team member to suggest an alternative method, process or design. This causes problems, especially the more advanced the project is as design changes or retro-fitting of equipment installation can cause project delays, increase the project cost and introduce a degree of frustration within both Sellafield Limited and the safeguards authorities.

Constant variability in the financial situation at both Sellafield Limited and within the safeguards inspectorates has resulted in increased pressure on cost savings, efficiencies and an adaptation to inspection approach. The power of a robust project dossier and safeguards requirements list can not be overstated at this point to provide traceability as to the decision making processes and confirm managerial buy-in to existing agreements. It is key at this point to reinforce that the safeguards approach adopted by the safeguards authorities should not negatively impact on or interfere with plant operations. Once arrangements have been agreed and a project progresses into late detailed design and the subsequent construction phase, any design changes or safeguards approach changes are likely to negatively impact on the project and future operations.

5.3. Developing Relationships

It is common in the initial stages of a project for all safeguards related queries to be directed through the NMAC&S SME who forms part of the project team. As a project develops and engagement begins with the safeguards inspectorates, this relationship typically holds to begin with. The project team will correspond with the safeguards inspectorates through the NMAC&S SME, and vice-versa. This allows a robust project dossier to be compiled and clear communication lines are established.

As the project progresses further, it is not uncommon for key links between the project team and the safeguards inspectorates to develop and direct communication between the parties occurs. Whilst this approach is more efficient for the individuals involved, without a robust reporting mechanism to capture all decisions made and the reasons for them, important project knowledge and traceability can be lost and decisions questioned later on in the project if new project team members or safeguards inspectors are involved. Decisions can also be made without all individuals being in possession of all of the facts.

6. Conclusions

The main conclusions of this paper are:

- The safeguards by design process is key in supporting project progression to ensure timely delivery and effective management of project costs.
- Clarity of the formal NMAC&S requirements to key stakeholders not directly working in the field of NMAC&S is essential. The increased NMAC&S awareness helps to avoid confusion with project deliverables and ensure the NMAS department and the safeguards inspectorates are engaged.
- Consideration must be given as to the correct time and the correct level of information with which to engage the safeguards inspectorates.
- Early stage engagement may aid the safeguards inspectorates in developing new safeguards approaches and new equipment/technologies.
- The integration of safeguards by design into a clear, phased project delivery structure ensures that NMAC&S requirements are identified, considered, discussed and implemented in a timely manner. Proactive engagement enables workable NMAC&S arrangements to be agreed to meet this challenge.
- Using an open, early engagement approach with the safeguards inspectorates, time, resource and as a result money can be saved. By focussing attention on proposals

that Sellafield Limited know have the broad support of the safeguards inspectorates, NMAC&S expectations are met.

- Scheduled, clear communication between relevant subject matter experts and the safeguards inspectorates ensures that regulatory expectations are met. This allows for all stakeholders to retain awareness of their requirements and the timescales involved.
- Nuclear materials accountancy and safeguards requirements should not affect the project critical path.

7. Privacy regulations and protection of personal data

The author agrees that submission of this work automatically authorises ESARDA to publish the work in whole or in part in all ESARDA publications – the bulletin, meeting proceedings, and on the website.

The author declares that this work is original and not a violation or infringement of any existing copyright.

8. References

[1] Great Britain, *Energy Act 2004*, Department of Energy and Climate Change, Chapter 20, 22/07/2004.

[2] Nuclear Decommissioning Authority, *Strategy*, 01/04/2012.

[3] European Commission, *Treaty Establishing the European Atomic Energy Community (EURATOM)*, 25/03/1957.

[4] United Nations, *Treaty on the Non-Proliferation of Nuclear Weapons, opened for signature 01/07/1968*, 21.U.S.T 483, 729 U.N.T.S 161.

[5] Office for Nuclear Regulation *http://www.onr.org.uk/safeguards* (10th April 2015)

[6] International Council on Systems Engineering, *Systems Engineering Handbook – A Guide for System Lifecycle Processes and Activities*, Version 3.1, ICOSE, Seattle, Washington, 08/2007.

Clandestine Proliferation: A Stochastic Process Model

Nicholas Kyriakopoulos, Xuan Zhou

Department of Electrical and Computer Engineering
The George Washington University
Washington, DC 20052 USA
E-mail: kyriak@gwu.edu; zhouxuan@gwmail.gwu.edu

Abstract:

Under the State-level concept for safeguards embodied the objective is to develop a safeguards protocol that covers activities, items and locations in the entire State. Although these additional elements have legitimate uses, they could contribute to or be part of a clandestine nuclear program. The challenge is how to develop and implement a safeguards approach that does not rely on detailed nuclear material accountancy, or a mechanistic verification, yet, it is objective transparent and non-discriminatory.

The decision of a State to develop a nuclear weapons program at any given time may depend on the existence of conditions that are conducive to proliferation. However, these conditions by themselves do not necessarily imply proliferation and may change over time. A*lthough there is a relationship between proliferation and certain conditions such as presence of conflicts, that relationship is neither deterministic nor causal. It is more appropriate to treat these conditions as random variables. Similarly, the data collected under the Additional Protocol do not have a specified direct causal relationship to proliferation, although they could be related to some yet to be determined degree. Thus, at best they can be characterized in terms of their statistical properties which can form the basis of calculating the probability of detecting deviations from legitimate activities.*

This paper addresses the problem of detecting the state of development of clandestine processes along diversion paths such as those enumerated in the Critical Path Analysis approach. The undeclared activities of a State are modeled as a stochastic system, because of the uncertainties inherent in the clandestine development of nuclear weapons. The state of the system is represented as a state vector. Similarly, the evaluation of the State as a whole, under the Additional Protocol is also stochastic, because of the uncertainty in the connection between the data collected by the IAEA and the existence of a clandestine process. A modified form of the Kalman filter equations has been developed that makes it possible to estimate the state of clandestine development as long as the clandestine process remains stable. Examples illustrating the uses of the approach are presented.

Keywords: clandestine proliferation; stochastic model; detection; safeguards concepts

1. Introduction

The integrated safeguards approach envisions the evaluation of a State as a whole to determine whether the State is engaging in any clandestine activities in violation of its obligations under the Nuclear Non-proliferation Treaty. The IAEA in its effort to strengthen the effectiveness and improve the efficiency of the safeguards through the application of the Additional Protocol is facing the challenge of developing an “objective” mechanism for verifying the declarations under this protocol without employing a “mechanistic” approach. While the safeguards applied to the declared nuclear facilities under INFCIRC/153 are based on the materials balance approach to detect diversion, the Additional Protocol explicitly excludes “detailed nuclear material accountancy”. In addition, the IAEA

may not “systematically seek to verify” the information collected under the Protocol [1]. At the same time, the evaluation of a State needs to be objective, transparent and non-discriminatory. An even bigger challenge is to develop a methodology for detecting undeclared activities in the absence of empirical data about the characteristics of clandestine nuclear development programs.

Acquisition path analysis is being investigated as a potential approach to State-level evaluation [2]. It provides an exhaustive list of possible paths to develop nuclear weapons. Each path consists of a sequence of steps that could eventually lead to a nuclear weapon. Each potential clandestine path originates at some declared activity. Thus, for States for multiple declared activities in the nuclear fuel cycle, there are multiple starting points for clandestine activities. For a given State, some of the paths might not be feasible or desirable, because one or more processes in the path do not exist in the State.

Using game theory, acquisition path analysis seeks to identify which path a State might choose to follow in order to develop a nuclear weapon on the basis of the least cost to the State. Estimation of the cost includes the cost associated with detection by the IAEA. In calculating optimal strategies, the model assumes that implementation of the Additional Protocol by the IAEA has a high probability of detecting clandestine activities, while the application of INRCIRC/153 safeguards provides a low probability of detection. These probabilities are assumed probabilities and, to our knowledge, are not based on any detailed analysis of processes taking place in clandestine development paths and the detection mechanisms for each of the possible paths.

In order to make the approach more robust, one needs to develop a methodology for evaluating probabilities of detection of clandestine activities under all possible acquisition paths. It is not an easy task. To assign realistic probabilities of detection one needs to needs to have a fairly good description of the activities involved in a clandestine path. Also, for each such set of activities a corresponding set of measurements are needed for detecting them. When a State initiates a clandestine program it is not clear whether it has a well-developed plan, it experiments with different approaches or both. As a starting point and in the absence of any specific information, it would be reasonable to treat the parameters of the clandestine process random variables. Similarly, the measurement system, i.e., the types of information collected by the IAEA under the Additional Protocol may also possess some degree of randomness, because it may not necessarily be associated with a particular stage of the clandestine process

In this paper we describe clandestine proliferation as a process with the variables being the state of development of a nuclear weapon and the parameters of the process being random variables. We also treat as random variables the measured parameters and the measurement data in order to denote the inherent uncertainties in both. In the first part of the paper we have a process model for a clandestine weapons program followed by the development of stochastic models for the clandestine process and the measurement system under the Additional Protocol. To estimate the state of the clandestine proliferation process, we have derived a modified form of the Kalman filter equations that takes into account the uncertainties in the state and measurement system matrices. In the third section of the paper, absent any empirical data, we have used two hypothetical scenarios to demonstrate the applicability of the model.

2. Clandestine proliferation as a process

As identified in the paper by Lister et al [2], there are multiple starting points for a clandestine nuclear weapons program depending on the state of the legitimate nuclear industry in a given State. Any given clandestine weapons development scenario, comprises more than one paths existing in parallel and secretly. For example, one path would lead to the acquisition of highly enriched uranium, another

to the acquisition of highly accurate timing circuitry, yet another to the acquisition of capabilities for precision tooling. In the present context, the term acquisition denotes capability either developed indigenously or imported. The starting points of a clandestine weapons program are unique to each State. For example, in a State with indigenous advanced electronics manufacturing, the capability to acquire the trigger mechanism would already be present in the form of advanced circuitry and engineering personnel. On the other hand, the same path for a State with non-existent or minimal electronics manufacturing capabilities would consist of many steps until the attainment of the capability to manufacture a working trigger mechanism. Similar reasoning applies to the paths for the clandestine acquisition of highly enriched uranium or plutonium. Thus, although the various acquisition paths have been well documented, their internal structure, namely, how many steps each of those paths contain, is not well-defined and it is correlated with the technological capabilities of each State.

As with any product development, each acquisition path is a multi-step process. One can classify the clandestine acquisition paths into two categories an *ab initio* clandestine and spin-off from existing processes. An example of the first category is the case of a State without legitimate and declared nuclear activities that starts the entire process of acquiring highly enriched uranium clandestinely. The second category may involve starting a clandestine enrichment process at some point of a declared nuclear fuel cycle, or the development of weapon-related technology as a spin-off from legitimate production processes. These two categories apply to all possible weapons development paths that lead and converge to a nuclear explosive device.

The starting point of a clandestine nuclear weapons program is the decision by a State to embark on one. In a previous paper [3] we have identified some conditions such as regional conflicts, militarization, etc., that could become the trigger mechanism for a State to embark on such a program. Once such a decision has been taken, the development process, typically, consists of multiple parallel paths for the complementary technologies that are essential for the assembly of the final device. Regardless how each of the paths starts, the development of the relevant technologies is a discrete step process. Each step involves, *inter alia*, planning, design, experimentation, testing, and verification of design prior to the next step of development. A first order approximation is that for the case of a spin-off path, the clandestine process once started remains completely separate from the legitimate one. Figure 1 illustrates these two categories; part (a) indicates an *ab initio* development path where $cp_i(k)$ is the k^{th} step of the i^{th} clandestine acquisition path with $cp_i(0)$ the initial step consisting of the decision to start the program; part (b) indicates an acquisition path as a spin-off of a legitimate path p_i where the decision to embark on a clandestine program is taken at some stage $p_i(n)$ of the legitimate path. For example, a State with a declared enrichment program at 5% makes a decision to start a clandestine program to obtain highly enriched uranium. In such a case the starting point of the clandestine path would be the expertise and technology associated with the enrichment level of 5%. Similar analogies apply to the complementary technologies needed to assemble a nuclear device.

The two types of clandestine paths are similar in form, but differ on the initial conditions and possibly on the transition parameters between successive steps. For example, initial conditions in terms of technology and expertise for a spin-off path can be assumed to be stronger than those of an *ab initio* one. For either path, the transition between sequential development steps can be expressed as

$$cp_i(k+1) = f_i(cp_i(k)) \qquad (1)$$

The function $f_i(cp_i(k))$ relates the $(k+1)^{th}$ stage of the development process to the preceding one. We will use the uranium enrichment process to illustrate this relationship. The process to obtain HEU from NU or LEU is sequential consisting of multiple steps. Each step involves varying degrees of effort measured in terms of kilogram Separative Work Unit commonly abbreviated as SWU. At each step, the effort is a function of the concentration of uranium in the feed material, the enriched output and

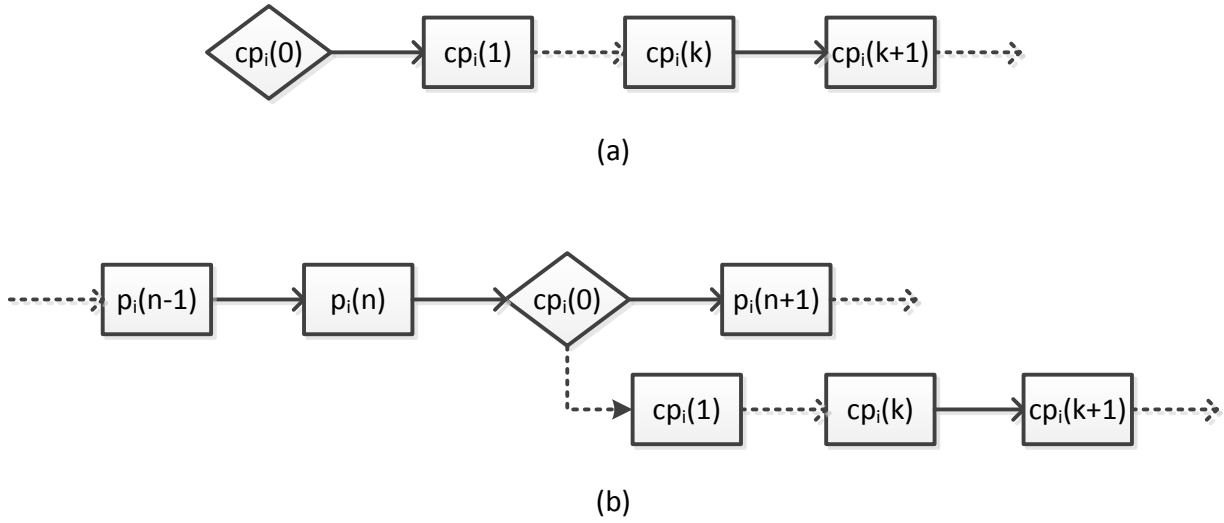

Figure 1. Two general categories of clandestine acquisition paths, *ab initio* (a) and spin-off (b).

the depleted stream. For example, the number of SWU required to attain a given level of enrichment varies inversely with the amount of uranium left in the depleted stream and vice versa. Similarly, for a given level of enrichment, the number of SWU decreases as the concentration of uranium in the feed material increases [4],[5].

A number of factors affect the transition from one level of enrichment to the next, such as the arrangement of centrifuges into cascades which consist of groups of centrifuges connected in parallel to form stages that are connected in series. There are different categories of cascades depending on the number of centrifuges per stage and the handling of the waste per stage. There are simple and recycle cascades, symmetric and asymmetric cascades, tapered and square cascades to name some of the most common configurations. Regardless of the configuration, factors affecting the efficient operation of the enrichment process include, in addition to the optimization of performance of each centrifuge, the flow rate and the material passes from one stage to the next. In addition to the complexity of the enrichment process, the centrifuges are constructed from special alloys of high quality steel and aluminum. Furthermore, although gas centrifuge is the most widely used method of enrichment, there are additional methods of enrichment, some less efficient such as the older gas diffusion method as well as experimental ones. They fall into the broad categories of laser separation, chemical and ion exchange, thermal diffusion aerodynamic separation and electromagnetic isotope separation [6], [7].

Another factor entering into the equation for the transition from one step of the process to the next may be the potential asymmetry of the effort involved in the transitions between steps. For example, one tonne of uranium feed requires approximately 800 SWU-900 SWU to achieve an enrichment level of 4% - 5% for power reactors, 1100 SWU for an enrichment level of 20% for research reactors power reactors and 1300 SWU for an enrichment level of 90% for nuclear weapons [8].

The foregoing example illustrates the complexity of the processes involved in the development of a nuclear weapons program. Similar examples of complex processes can be developed for the technologies required to transform an explosive nuclear device into a usable nuclear weapon. Thus, the function $f_i(\bullet)$ has obviously many parameters with unknown interrelations. However, if one bears in mind that technological improvements generally take place incrementally, one can refine the successive steps in a given product development line to consist of small increments. Under such assumption, within each development step, the transition function can be assumed to be linear and expressed as

$$\mathbf{x}(k) = \mathbf{P}(k)\mathbf{x}(k-1) \tag{2}$$

where $\mathbf{x}(k)$ is the state of development at the k^{th} stage of the i^{th} clandestine path and $\mathbf{P}(k)$ a matrix of the parameters that determine the transition from the $(k-1)^{st}$ to the k^{th} stage of development.

There is no known model in the open literature for the development of a clandestine product related to nuclear weapons. There is, however, a wealth of literature on product development and technological innovation [9], [10], [11], [12], [13], [14]. Some of those models describing the process of innovation are rather simplistic in that they describe a sequence of steps basic research, applied research, and development. Such a broad definition has come into existence primarily as a mechanism for achieving public policy objectives through the allocation of funding rather than as a tool for predicting innovation [15]. More substantive and promising work has been on processes for the development of commercial products. Models describing the development of products fall into four general categories. There are models that describe actual product development processes, theoretical models for ideal processes, didactic models that are used as tools to visualize and simplify actual development activities, and management tools used in specific companies to visualize and organize their internal development activities. Some of the theoretical models for product development are partitioned into new product development models and incremental development models, which refer to products that are based on but are substantially different from existing product lines. A substantial amount of research is devoted to the so called “fuzzy front end” in product development that comprises all activities before the formal product design stage. Fuzzy front end is the first stage in a new product development process. It is a set of activities that take place from the moment an idea is generated until it is either discarded or approved for the development of the product. The extensive research in the area of commercial new product development has not resulted in the development of predictive models for technological innovation, because the processes involved in technological progress are neither orderly nor understood. Some have described the process as chaotic with non-predictable steps involving learning through feedback [16].

3. A stochastic model

The foregoing cursory review of models of commercial product development illustrates the challenges inherent in the efforts to develop objective procedures for detecting clandestine nuclear programs when no predictive process models are available even for commercial products. For a given State there is uncertainty first on how the effort to develop a particular technology critical to the development of a clandestine weapon is organized and second whether or not the effort would be successful. In other words, for practical purposes there is total lack of measurable information concerning any clandestine activity.

3.1. A clandestine proliferation model

In the absence of a deterministic predictive model for the evolution of technology and the high degree of uncertainty surrounding the existence of a clandestine program or the lack there off, it would be reasonable to consider the parameters of the matrix $\mathbf{P}(k)$ to be random variables as a starting point for the development of a process model. As an example, if the process at each step consists of two variables, the transition between successive stages is given by equation (3).

$$\begin{pmatrix} x_1(k) \\ x_2(k) \end{pmatrix} = \begin{bmatrix} p_{11} & p_{12} \\ p_{21} & p_{22} \end{bmatrix} \begin{pmatrix} x_1(k-1) \\ x_2(k-1) \end{pmatrix} \tag{3}$$

Each of the elements of the matrix $\mathbf{P}$ denotes the strength of the transition of each process variable in the development path and has a range $[-1, 1]$. For example, $p_{12} = p_{21} = 0$ and $p_{11} = p_{22} = \pm 1$

indicate that process variable $x_1(k)$ depends only on process variable $x_1(k-1)$ and is not affected by process variable $x_2(k-1)$, in other words, the two variables are completely decoupled. On the other hand, if the two variables a fully coupled, $p_{11} = p_{12} = p_{21} = p_{22} = \pm 1$.

In general, a clandestine development process at the k^{th} state of development may be described by equation (4).

$$\mathbf{x}(k) = \mathbf{P}(k-1)\mathbf{x}(k-1) + \mathbf{G}\mathbf{w}(\mathrm{k}) \tag{4}$$

where $\mathbf{P}$ is an n x n matrix relating the transition of the n states within each development step and $\mathbf{w}(\mathrm{k})$ a vector denoting the process noise at each transition.

3.2. Measurements under the Additional Protocol

Although the Additional Protocol requires the collection of a broad range of data, it explicitly excludes material accountancy and a "mechanistic" approach as tools for verification. At the same time, the IAEA is charged with developing an "objective" approach for detecting clandestine activities. Under such constraints, the challenging task for the IAEA is to devise a measurement system that seeks to identify the unknown $\mathbf{x}(k)$ of development. Since the IAEA has no direct access to the clandestine development paths, if such paths exist, it cannot have in place a specified measurement system for an unknown clandestine development stage. Thus, the information obtained under the Additional Protocol, since it is provided by the State, may or may not have some relationship to the state of development of the clandestine stage that is not clearly specified. This relationship is given by equation (5).

$$\mathbf{y}(k) = \mathbf{C}(k)\mathbf{x}(k) + \mathbf{v}(k) \tag{5}$$

where $\mathbf{y}(k)$ denotes the measurements (data) obtained by the IAEA under the Additional Protocol, $\mathbf{C}(k)$ is a matrix relating the unknown states at the k^{th} measurement instant to the state of clandestine development and $\mathbf{v}(k)$ is the measurement noise. In the absence of an *a priori* known relationship between the data collected by the IAEA and the clandestine state of development, the elements of the matrix $\mathbf{C}(k)$ may also be characterized, at first, as random variables until more experience is gained in the collection of relevant data.

4. Estimating the state of clandestine development

The problem of estimating the state $\mathbf{x}(k)$ of a process corrupted by noise on the basis of periodic noisy measurements has been solved through the design of Kalman filters [17], [18], [19]. These are linear, recursive filters that minimize the variance of the error between the actual state $\mathbf{x}(k)$ and the estimate of the state $\hat{\mathbf{x}}(k)$. The basic operation involves two steps. First, the best estimate at the measurement instant $(k-1)$, $\hat{\mathbf{x}}(k-1|k-1)$, is projected to next measurement instant (k), i.e., $\hat{\mathbf{x}}(k|k-1)$. The projected estimate is given by equation (6), where $\mathbf{P}(k-1)$ is the process at $(k-1)$.

$$\hat{\mathbf{x}}(k \mid k-1) = \mathbf{P}(k-1)\hat{\mathbf{x}}(k-1 \mid k-1) \tag{6}$$

Also, projected from $(k-1)$ to (k) is the error covariance matrix given by equation (7), where

$$\mathbf{Q}(k \mid k-1) = \mathbf{P}(k-1)\mathbf{Q}(k-1 \mid k-1)\mathbf{P}^T(k-1) + \mathbf{G}(k-1)\mathbf{W}(k-1 \mid k-1)\mathbf{G}^T(k-1) \tag{7}$$

Subsequently, the projected estimate is corrected on the basis of the new information obtained from the measurements $\mathbf{y}(k)$ to yield the updated best estimate $\hat{\mathbf{x}}(k|k)$ given by equation (8).

$$\hat{\mathbf{x}}(k|k) = \mathbf{P}(k-1)\hat{\mathbf{x}}(k-1|k-1) + \mathbf{\Gamma}(k)\left[\mathbf{y}(k) - \mathbf{C}(k)\mathbf{P}(k-1)\hat{\mathbf{x}}(k-1|k-1)\right] \quad (8)$$

The filter gain $\mathbf{\Gamma}(k)$ is calculated from the projected error covariance $\mathbf{Q}(k \mid k-1)$, and the measurements $\mathbf{y}(k)$ and is given by equation (9) where $\mathbf{R}(k)$ is the covariance matrix of the measurement noise.

$$\mathbf{\Gamma}(k) = \mathbf{Q}(k|k-1)\mathbf{C}^T(k)\left[\mathbf{C}(k)\mathbf{Q}(k|k-1)\mathbf{C}^T(k) + \mathbf{R}(k)\right]^{-1} \quad (9)$$

Using the filter gain $\mathbf{\Gamma}(k)$ the updated error covariance becomes (eq.10)

$$\mathbf{Q}(k|k) = \left[\mathbf{I} - \mathbf{\Gamma}(k)\mathbf{C}(k)\right]\mathbf{Q}(k|k-1)\left[\mathbf{I} - \mathbf{\Gamma}(k)\mathbf{C}(k)\right]^T + \mathbf{\Gamma}(k)\mathbf{R}(k)\mathbf{\Gamma}^T(k) \quad (10)$$

In contrast to conventional state estimation problems where the processes and the measurement systems are known and deterministic, the clandestine processes being unknown by their nature, can be viewed as stochastic and the elements of the state transition matrix $\mathbf{P}(k)$ be independent random variables. The measurement system $\mathbf{C}(k)$ can either be described either as deterministic or stochastic. In the case of the safeguards under INFCIRC 153, where the relationship between the nuclear fuel cycle and the measurements is well defined, the elements of $\mathbf{C}(k)$ are deterministic. This is not the case where a clandestine process is not well defined. Under these conditions, the closest one can come to describing the elements of the measurement system is to consider them as independent random variables.

In this paper we have developed a modified set of Kalman filter equations by taking into account the stochastic nature of both the state transition matrix $\mathbf{P}(k)$ and the measurement matrix $\mathbf{C}(k)$, in other words, the state transition matrix is given by $E\{\mathbf{P}(k)\} = \left[E\{p_{ij}\}\right]$ where p_{ij} are independent random variables, and the measurement matrix $E\{\mathbf{C}(k)\} = \left[E\{c_{ij}\}\right]$. The projected state estimate is given by equation (6a) where $E\{\mathbf{P}(k-1)\}$ denotes the expected value of the state transition matrix.

$$\hat{\mathbf{x}}(k \mid k-1) = E\{\mathbf{P}(k-1)\}\hat{\mathbf{x}}(k-1 \mid k-1) \quad (6a)$$

The projected error covariance given by equation (6a) takes into account the statistical properties of the state transition matrix where q_{ii} is the i^{th} diagonal element of the error covariance matrix, $\sigma^2_{p_{ji}}$ is the variance of the $(ji)^{th}$ parameter of the state transition matrix, w_{ii} is the i^{th} diagonal element of the system noise covariance matrix and $\sigma^2_{g_{ji}}$ is the variance of the $(ji)^{th}$ element of the measurement noise matrix.

$$\begin{aligned}\mathbf{Q}(k \mid k-1) = {} & E\left\{\mathbf{P}(k-1)\right\}\mathbf{Q}(k-1 \mid k-1)E\left\{\mathbf{P}^T(k-1)\right\} \\ & + \left[\operatorname{diag}\left\{\sum_{i=1}^{n} q_{ii}(k-1 \mid k-1)\sigma^2_{p_{ji}}(k-1),\ j = 1,\cdots,n\right\}\right] \\ & + E\left\{\mathbf{G}(k-1)\right\}\mathbf{W}(k-1 \mid k-1)E\left\{\mathbf{G}^T(k-1)\right\} \\ & + \left[\operatorname{diag}\left\{\sum_{i=1}^{n} w_{ii}(k-1 \mid k-1)\sigma^2_{g_{ji}}(k-1),\ j = 1,\cdots,n\right\}\right]\end{aligned} \quad (7a)$$

The updated state estimate is given by equation (8a) where the state transition matrix and the measurement matrix are expressed in terms of their statistical properties.

$$\hat{\mathbf{x}}(k|k) = E\{\mathbf{P}(k-1)\}\hat{\mathbf{x}}(k-1|k-1) + \mathbf{\Gamma}(k)\left[\mathbf{y}(k) - E\left\{\mathbf{C}(k)\right\}E\{\mathbf{P}(k-1)\}\hat{\mathbf{x}}(k-1|k-1)\right] \quad (8a)$$

The Kalman filter gain is given by equation (9a), where q_{ii} is the $(ii)^{th}$ element of the error covariance matrix and $\sigma^2_{c_{ji}}$ is the variance of the $(ji)^{th}$ element of the measurement matrix.

$$\mathbf{\Gamma}(k) = \mathbf{Q}(k|k-1)E\left\{\mathbf{C}^T(k)\right\} \bullet \left[\left[E\left\{\mathbf{C}(k)\right\}\mathbf{Q}(k|k-1)E\left\{\mathbf{C}^T(k)\right\} + \mathbf{R}(k)\right] + \left[\operatorname{diag}\sum_{i=1}^{n} q_{ii}(k \mid k-1)\sigma^2_{c_{ji}}(k)\right],\ j = 1, m\right]^{-1} \quad (9a)$$

Finally, the updated error covariance is given by equation (10a) where γ_{ji} is the $(ji)^{th}$ element of the filter gain $\mathbf{\Gamma}(k)$.

$$\mathbf{Q}(k|k) = \left[\mathbf{I} - \mathbf{\Gamma}(k)E\{\mathbf{C}(k)\}\right]\mathbf{Q}(k|k-1)\left[\mathbf{I} - \mathbf{\Gamma}(k)E\{\mathbf{C}(k)\}\right]^T + \mathbf{\Gamma}(k)\mathbf{R}(k)\mathbf{\Gamma}^T(k) - \left[\operatorname{diag}\left\{\sum_{i=1}^{n}\gamma_{ji}(k)q_{ii}(k \mid k-1)\sigma^2_{c_{ji}},\ j = 1,\cdots,n\right\}\right] \quad (10a)$$

5. Some illustrative examples

Let $\mathbf{x}(0)$ denote the starting point of the diversion process that can be considered as the state of development at the breakout instant. Successful achievement of a desirable objective for the particular development path is indicated by the equilibrium state $\mathbf{x}_e = \mathbf{0}$. On the other hand, if the clandestine process is not successful in achieving the desirable goal, the equilibrium state will not be reached and the norm of the state vector will be greater than the norm of $\mathbf{x}(0)$, i.e. $\|\mathbf{x}(k)\| > \|\mathbf{x}(0)\|$. The information collected by the IAEA from the State is indicated by $\mathbf{y}(k)$ and is updated annually. Thus, the interval between successive measurements is one year. During any such interval, the clandestine process transition matrix $\mathbf{P}(k)$ remains constant, but it may change between successive measurement instances, i.e. $\cdots\mathbf{P}(k-1) \neq \mathbf{P}(k) \neq \mathbf{P}(k+1)\cdots$. In evaluating the State as a whole, the objective of the IAEA would be to estimate the state of development of the particular clandestine process on the basis of the information obtained from the annual measurements regardless whether the process has been successful and reached equilibrium or unsuccessful. The noises corrupting the process and the measurement system are considered Gaussian with zero mean and specified variances, i.e., $E\{\mathbf{w}(k)\}=E\{\mathbf{w}(k-1)\}=0$, $\mathrm{E}\{\mathbf{w}(k)\mathbf{w}^T(j)\}=\mathbf{W}(k)$, for $j = k$ and $E\left\{\mathbf{v}(k)\right\} = E\left\{\mathbf{v}(k-1)\right\} = 0$, $E\left\{\mathbf{v}(k)\mathbf{v}^T(j)\right\} = \mathbf{R}(k)$ for $j = k$. For the purposes of this analysis we limit the number of state variables for the particular process to five, i.e., $\mathbf{x}^T(k) = [x_1(k)\ x_2(k)\ x_3(k)\ x_4(k)\ x_5(k)]$. If the particular effort is based on trial and error, it might or might not be successful. In such a case, the elements of the state transition matrix can be considered random with values $p_{ij}(k) \in [-1,1]$ with +1 and -1 indicating strong positive and negative feedback, respectively, for a particular state. In assigning values to the elements of the measurement matrix $\mathbf{C}(k)$ we have considered the combination of the total lack of information available to the IAEA about the particular clandestine process and the accumulated experience by the IAEA in safeguards implementation. The accumulated experience can be represented as positive elements in the measurement matrix modified by the uncertainties concerning the connection between the actual state of the clandestine process and the information given to the IAEA by the State. For the purpose of these illustrative examples we have used the following values:

$$\mathbf{W}(k)=\begin{bmatrix}0.1 & 0 & 0 & 0 & 0\\ 0 & 0.3 & 0 & 0 & 0\\ 0 & 0 & 0.3 & 0 & 0\\ 0 & 0 & 0 & 0.2 & 0\\ 0 & 0 & 0 & 0 & 0.4\end{bmatrix};\quad \mathbf{G}(k)=\begin{bmatrix}1 & 0 & 0 & 0 & 0\\ 0 & 1 & 0 & 0 & 0\\ 0 & 0 & 1 & 0 & 0\\ 0 & 0 & 0 & 1 & 0\\ 0 & 0 & 0 & 0 & 1\end{bmatrix}$$

$$\mathbf{C}(\mathrm{k})=\begin{bmatrix}1 & 1 & 0 & 0 & 0\\ 0 & 0 & 1 & 1 & 0\\ 0 & 0 & 0 & 0 & 1\end{bmatrix};\quad \mathbf{R}(k)=\begin{bmatrix}0.4 & 0 & 0\\ 0 & 0.5 & 0\\ 0 & 0 & 0.4\end{bmatrix}$$

5.1. Case I – Clandestine process completely chaotic

In an extreme case, consider a State without any substantive experience with technological development that initiates a clandestine process. In this case, the elements $\left[p_{ij}(k)\right]$ are uniformly distributed in the range $[-1,1]$ with $E\{p_{ij}(k)\}=0$. Normally, one would perform a Monte Carlo simulation. For this paper, we use only some sample calculations to illustrate the applicability of the proposed approach. To illustrate a completely chaotic development process, we used a (5 x 5) state transition matrix with each of the elements generated randomly with uniform distribution in the range [-1,1].

$$\mathbf{P}(k)=\begin{bmatrix}0.6276 & -0.2131 & -0.8928 & -0.2499 & 0.5500\\ -0.6694 & 0.8244 & -0.3616 & -0.3404 & -0.5915\\ 0.5344 & -0.8601 & 0.9001 & -0.6836 & -0.4271\\ 0.3743 & -0.7177 & 0.0242 & 0.4427 & 0.8577\\ 0.4642 & 0.4996 & -0.1854 & -0.5210 & 0.0417\end{bmatrix}$$

The following cases were investigated. In Case Ia, the elements of the state transition matrix remained constant for every iteration, i.e., $\mathbf{P}(0)=\mathbf{P}(1)=\mathbf{P}(2)=\cdots=\mathbf{P}(k)\cdots$ denoting the same level of chaos at each stage of the process. In Case Ib, the elements of the state matrix were modified randomly in the range $[0.9,1.1]p_{ij}$, and the elements of the measurement matrix were modified randomly in the range $[0.75,1.25]c_{ij}$ where p_{ij} and c_{ij} are the values of the initial matrices. In Case Ic, the elements of the state and measurement matrices were assigned values at random in the ranges $[0.5,1.5]p_{ij}$ and $[0.75,1.25]c_{ij}$, respectively.

For each of the three cases, the initial state $\mathbf{x}(0)$ of the diversion path is assumed to be known, because it the state of the declared process from which the particular clandestine path diverged. As expected, the clandestine process did not converge to an equilibrium state, because the eigenvalues of the state matrix were outside the region of stability of the process, which is the interior of the unit circle. Figure 2 shows the norm of the state vector as a function of the iterations. As the uncertainty about the value of each parameter of the state transition matrix increased, the divergence became more rapid, which of course, was not unexpected. In other words, a completely chaotic development process would be unlikely to converge.

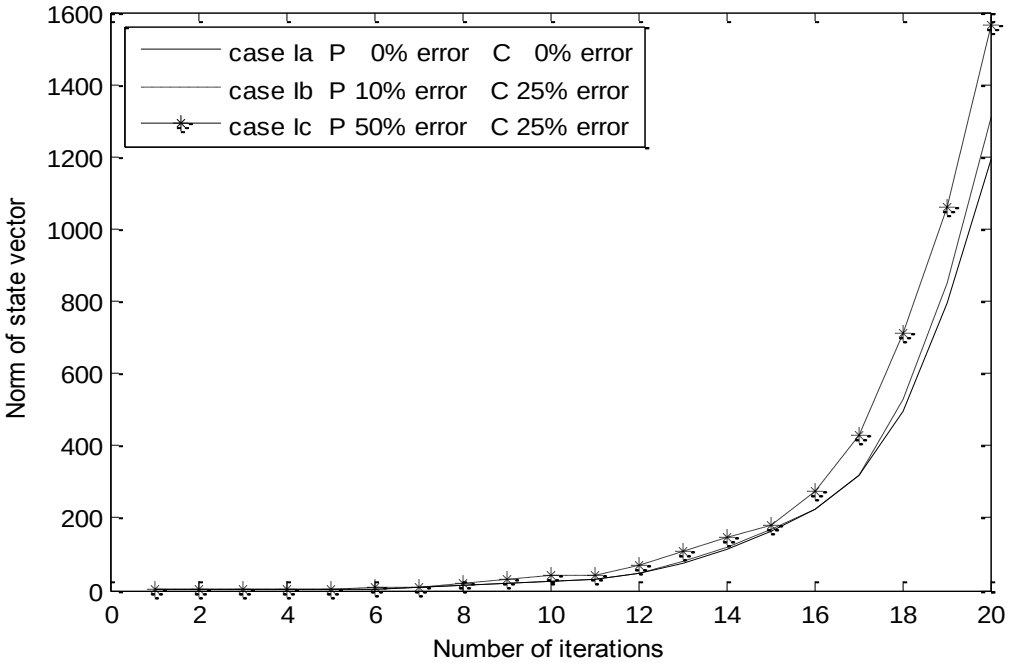

Figure 2. State trajectories for Case I; the elements of the state transition and measurement matrices are random variables.

The interest, however, was to determine whether the estimator would be able to track the state vector. As shown in Figure 3, that plots the norm of the error vector $\left\|\mathbf{x}(k)-\hat{\mathbf{x}}(k)\right\|$, the estimator was able to track the state trajectory only in the case where the values of the elements of the state transition matrix and the measurement matrix remained constant for each iteration. In other words, although the parameters of both matrices were selected arbitrarily, and the process diverged, the estimator was able to follow the state trajectory and converge to a steady state estimation error within a few iterations.

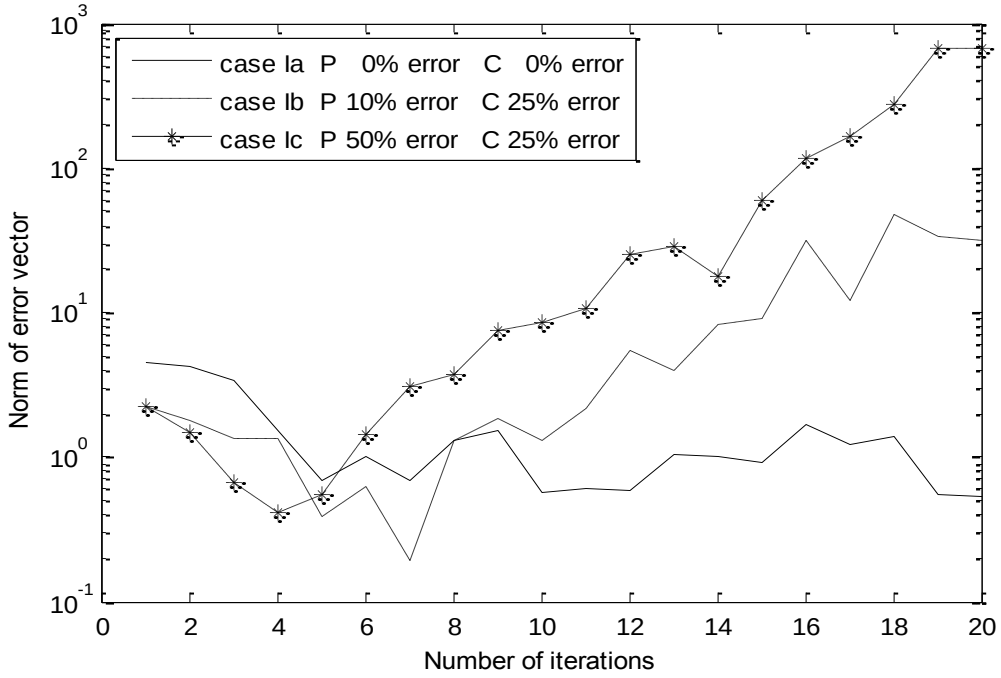

Figure 3. Trajectories of the norm of the estimation error vector for Case I.

5.2. Case II – Clandestine process achieves desirable objective.

At the other extreme, a State with substantial technological expertise could organize a clandestine process with high level of confidence that the process will result in the desirable outcome, i.e., the equilibrium state will be reached starting from some initial state. For this case, the elements of the state transition matrix are not completely random, because they represent parameters of a well-organized process. In such cases, for the system to converge to an equilibrium state, the eigenvalues of the state transition matrix must be located inside the unit circle. The stochastic nature of the process is reflected in randomness of the elements of the state transition matrix subject to the constraint that the eigenvalues remain in the interior of the unit circle. For this case, the elements of $\mathbf{P}(k)$ were arbitrarily selected such that $p_{ij}(k) \in [-1,1]$ subject to the preceding constraint and are given by

$$\mathbf{P}(k) = \begin{bmatrix} 0.7 & 0.2 & 0.1 & 0 & -0.1 \\ 0.2 & 0.2 & -0.1 & 0.3 & 0.2 \\ 0.1 & -0.1 & 0.3 & 0.3 & 0.2 \\ 0 & 0.3 & 0.2 & 0.2 & -0.1 \\ -0.1 & 0.2 & 0.3 & -0.1 & 0.5 \end{bmatrix}$$

The eigenvalues of $\mathbf{P}(k)$ are $\{-0.3641,\ 0.8149,\ 0.7060,\ 0.3716 \pm j0.0252\}$

As in the preceding case, three cases were examined. For case IIa, the elements of the state matrix remain constant for every iteration, i.e., $\mathbf{P}(0) = \mathbf{P}(1) = \mathbf{P}(2) = \cdots = \mathbf{P}(k) \cdots$ indicating the clandestine process is equally well coordinated at every step of the given diversion path. For case IIb, the elements of the state matrix were modified randomly in the range $[0.9, 1.1]p_{ij}$, and the elements of the measurement matrix were modified randomly in the range $[0.75, 1.25]c_{ij}$ where p_{ij} and c_{ij} are the values of the initial matrices. In Case IIc, the elements of the state and measurement matrices were assigned values at random in the ranges $[0.5, 1.5]p_{ij}$ and $[0.75, 1.25]c_{ij}$, respectively. For the last two cases, the random variations in the parameters of the state transition matrix and the measurement matrix have been introduced to indicate the uncertainties in both the process and the measurements inherent at each stage of the clandestine path.

For each of these cases, the state converges to an equilibrium state, i.e., the objective of the clandestine operation is achieved as shown in Figure 4 even with uncertainties as large as 50% in the values of the elements of the state transition matrix. Thus, the estimator would be able to track the state trajectory as shown in Figure 5. In other words, a clandestine diversion path would ultimately lead to a successful outcome under a reasonably planned effort. Similarly, the application of the safeguards under the Additional Protocol should be able to detect such a diversion path after a number of iterations. It should be noted, however, that, for the present measurement schedule at one-year intervals, it would take a number of years for the estimator to converge to some equilibrium value where the estimation error reaches a steady state. Furthermore, the estimation error will never converge to zero, due to the uncertainties in the values of the process and measurement parameters. In other words, no definitive conclusion can be reached about the existence of a clandestine diversion path.

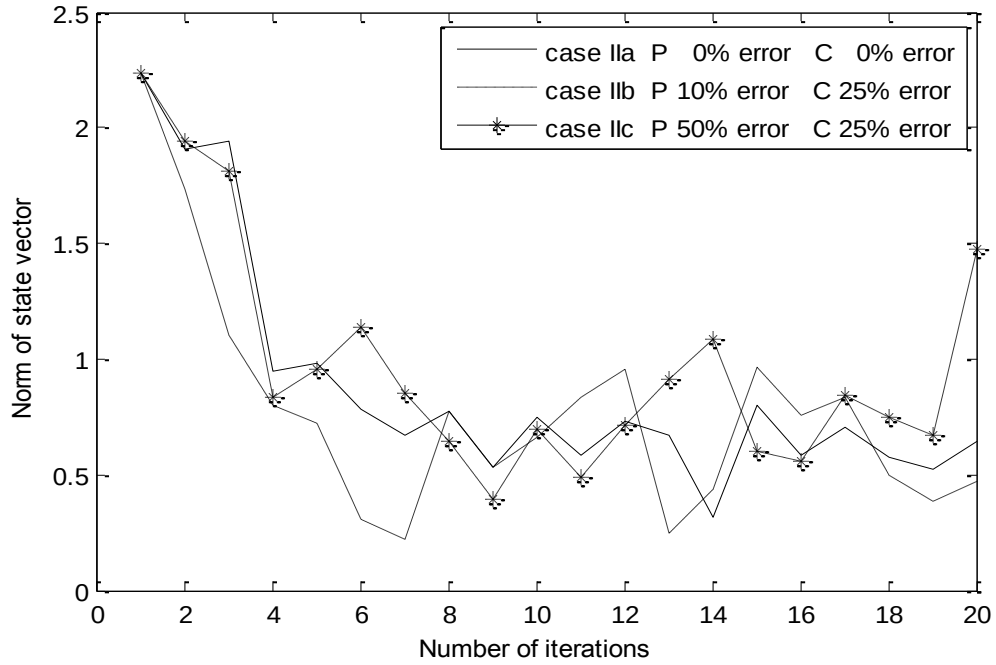

Figure 4. State trajectories for Case II; the elements of the state transition matrix and the measurement matrix are random variables subject to the constraint that the process is stable.

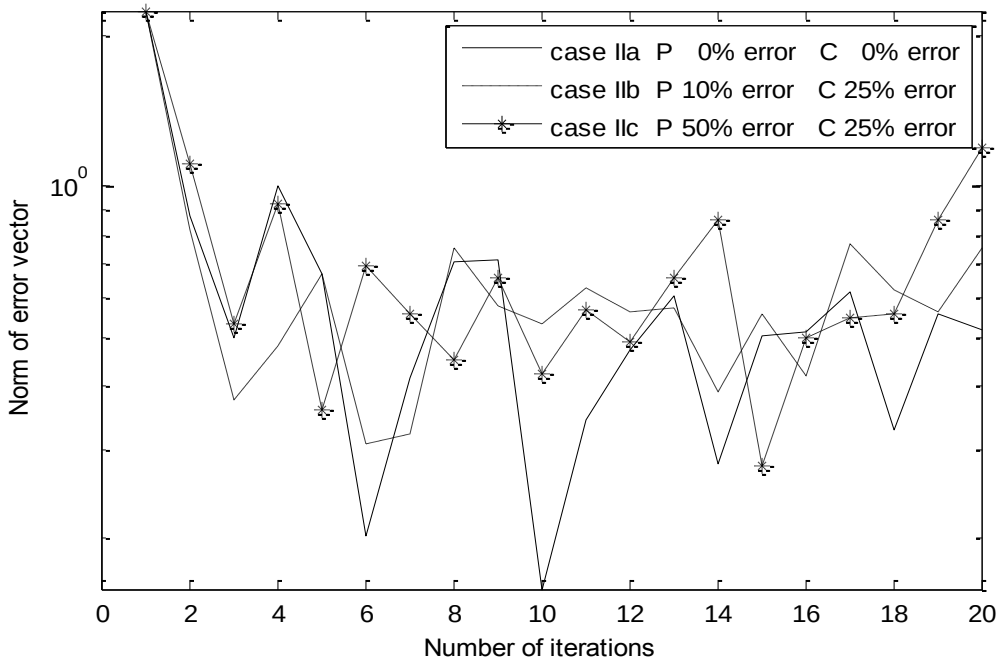

Figure 5. Trajectories of the norm of the estimation error vectors for Case II indicating that the estimation error has reached a non-zero equilibrium.

6. Conclusions

In this paper we have addressed the problem of applying an objective criterion to the evaluation of a State as a whole in the absence of a monitoring system designed to detect clandestine operations using some optimality criterion. In typical state estimation problems, the processes are generally

known both in terms of their variables and their structure. For such problems recursive estimation of the values of the internal variables is a well-developed field even for processes that are characterized by some variability in their parameters. However, the problem of detecting clandestine nuclear weapons development programs presents unique challenges for two main reasons. There is no reliable model for a typical clandestine development process. Also, the Additional Protocol restricts the ability of the IAEA to verify all information supplied by the State and collect any other data that might be needed for detection. Under those constraints, the development of techniques for evaluating sparse information to characterize an unspecified process is a very difficult task. In such cases one option available is to use statistical techniques that rely on incomplete specification of a clandestine process and uncertainties about the values of the available information. In this paper we have shown that, even under great uncertainty, it is possible to converge to a solution in cases where a clandestine process achieves its objective. However, to achieve detection, multiple measurement steps are needed. This process can be improved, by pursuing two parallel paths. One avenue of research would be to build upon the foundation of Critical Path Analysis. For each of the possible critical paths, one could develop one or more corresponding process models that a clandestine development program could follow. The data collected under the Additional Protocol would be used to evaluate the performance of such process models and, also, to determine the sufficiency of the information for detecting the state of a given clandestine process. Such an iterative process would be used as a learning mechanism for improving the measurement system. In other words, the type of information collected by the IAEA on an annual basis would be modified and augmented on the basis of the results of the evaluation of the preceding year.

References

[1] International Atomic Energy Agency; Model Protocol Additional to the Agreements(s) Between the State(s)and the International Atomic Energy Agency for the Application of Safeguards; INFCIRC/540 (Corrected); September 1977

[2] Listner, C., Canty, M. J., Rezniczek, A., Stein, G., Niemeyer, I; “Approaching acquisition path analysis formally - a comparison between AP and non-AP States”; *Proceedings of the 35rd ESARDA Annual Meeting*, Bruges, Belgium; 27-30 May 2013.

[3] Kyriakopoulos, N; “The Impact of Interdependencies on the Effectiveness and Efficiency of Safeguards”, *ESARDA Bulletin No*. 37; June 2012; pp.56-64.

[4] Arjun Makhijani, A., Chalmers, L., Smith, B; *Uranium Enrichment*; Report, Institute for Energy and Environmental Research; 15 October 2004; http://ieer.org/resource/reports/uranium-enrichment/

[5] Barzashka, I., Oerlich, I; Separation Theory;
http://www.fas.org/programs/ssp/nukes/fuelcycle/centrifuges/separation_theory.html

[6] Barzashka, I., Oerlich, I; Enrichment Cascades;
http://www.fas.org/programs/ssp/nukes/fuelcycle/centrifuges/cascades.html

[7] Wood, H; “Uranium Enrichment: Guns or Butter?”; i*n Assessing the Threat of Weapons of Mass Destruction*, J.L. Finney and I. Šlaus, (Eds); IOS Press; 2010; pp.191-198.

[8] World Nuclear Association; *Uranium Enrichment*; January 2015;
http://www.world-nuclear.org/info/Nuclear-Fuel-Cycle/Conversion-Enrichment-and-Fabrication/Uranium-Enrichment/#.UWrver-IRAs

[9] Verworn, B. and Herstatt, C; “The innovation process: an introduction to process models”; Department for Technology and Innovation Management, Technical University of Hamburg; Working Paper No. 12; January 2002;
http://www.tuhh.de/tim/downloads/arbeitspapiere/Working_Paper_12.pdf

[10] Song, X. M., Montoya-Weiss, M. M; “Critical Development Activities for Really New versus Incremental Products”; *Journal of Product Innovation Management*; 1998:15; pp.124-135.

[11] Verworn, B., Herstatt, C. and Nagahira, A; “The fuzzy front end of Japanese new product development projects: impact on success and differences between incremental and radical projects”; *R&D Management*; Vol. 38, Issue 1; January 2008; pp.1–19.

[12] Verworn, B; “A structural equation model of the impact of the “fuzzy front end” on the success of new product development”; *Research Policy*; Vol. 38, Issue 10; December 2009; pp.1571–1581.

[13] Lynn, G. S., Akgun, A. E; “Innovation Strategies Under Uncertainty: A Contingency Approach for New Product Development”; *Engineering Management Journal*; Vol. 10, Issue 3; 1998; pp. 11-17.

[14] Sperry, R., Jetter, A; “Theoretical Framework for Managing the Front End of Innovation Under Uncertainty”; *PICMET 2009 Proceedings*; Portland, Oregon USA; August 2-6 2009; pp. 2021-2028.

[15] Godin, B; “The Linear Model of Innovation: The Historical Construction of an Analytical Framework”; Project on the History and Sociology of S&T Statistics, Working Paper No. 30; Institut national de la recherche scientifique (INRS); 2005; http://www.csiic.ca/PDF/Godin_30.pdf

[16] Cheng, Y. T. and van de Ven, A. H., "Learning the Innovation Journey: Order out of Chaos?", *Organization Science,* vol. 7, 1996, pp. 593-614.

[17] Gelb, A; *Applied Optimal Estimation*; MIT Press, Cambridge, Mass; 1974

[18] Grewal, M.S., Andrews, A.P; *Kalman Filtering: Theory and Practice with MATLAB, 4th Edition*; Wiley-IEEE Press; 2014.

[19] Calafiore, G., Dabbene, F. and Tempo, R; “Research on probabilistic methods for control system design”; *Automatica*; vol. 47; 2011; pp. 1279–1293.

Formalizing Acquisition Path Analysis for the IAEA's State-Level Concept

Clemens Listner[1], Irmgard Niemeyer[1], Morton J. Canty[1], Gotthard Stein[2] and Arnold Rezniczek[3]

[1]Forschungszentrum Jülich, Germany
[2]Consultant, Bonn, Germany
[3]UBA GmbH, Herzogenrath, Germany

Abstract

The IAEA's Department of Safeguards has embarked on an evolutionary process to more fully develop and apply the State-level concept for safeguards implementation. In an attempt to direct safeguards to areas of greatest proliferation risk, this concept makes use of all safeguards-relevant information available in order to focus and prioritize its safeguards activities for a State.

A key component is the development of a State-level Approach which consists of analyzing acquisition paths, establishing and prioritizing technical objectives, and identifying applicable safeguards measures. The methodology to accomplish this is based on a three-step-approach: network modeling, network analysis, and strategic assessment. The network modeling step assesses and formalizes the State's nuclear capabilities as well as other state-specific factors concerning relevant proliferation scenarios. The network analysis step gives a ranking of all plausible acquisition paths including a visualization of the paths. Finally, the strategic assessment evaluates the State's proliferation and compliance options as well as the IAEA's set of technical objectives and subsequent safeguards measures.

In this paper, a hypothetical State model was developed in order to test the methodology's performance. Therefore, an Excel spreadsheet with all necessary state-level factors has been created. Afterwards, a Python software module based on graph theoretical algorithms was applied to produce a comprehensive list of ranked acquisition paths including their visualization. The following step of the strategic evaluation is mainly based on the concept of the Nash equilibrium resulting in a stable combination of the State's and the IAEA's strategies. This formal and automatic procedure offers the advantage of gaining results in a comprehensive and non-discriminative manner.

1 Introduction

Since the first ideas for supervising nuclear material, the verification system has evolved constantly. After gaining first experiences with item-specific safeguards according to the commitments in INFCIRC/66, the system of international safeguards was established by the signature and ratification of the Non-proliferation Treaty (NPT) in 1970. The treaty

implementation has mainly been governed by comprehensive safeguards agreements (CSA) and later the additional protocol (AP) with Integrated Safeguards.
In order to verify the State's compliance to these provisions, the IAEA has been carrying out a mechanistic, check-list approach to safeguards with limited success. This method has been superseded over the past years by a holistic approach called the State-level concept (SLC). The SLC's main idea is to move away from material centric approaches to a system analysis view of nuclear proliferation which clearly identifies the actors, their possibilities and their risks. Due to its general and comprehensive nature, the SLC has great potential to replace voluntary offer agreements (VOA) in nuclear weapon States (NWS) and to be used in other fields of treaty verification.
Underneath the new paradigmatic view to nuclear verification, the State-level concept essentially consists of three processes which help to develop State-level safeguards approaches (SLA) [1]:

1. Identification of plausible acquisition paths.
2. Specification and prioritization of State-specific technical objectives (TO).
3. Identification of safeguards measures to address the technical objectives.

This paper concentrates on the first step of this process which is also known as acquisition path analysis (APA). APA is defined as the analysis of all plausible sequences of activities which a State could consider to acquire weapons usable material [2]. The purpose of the APA is to determine whether a proposed set of safeguards measures is sufficient. Therefore, some overlap to the second step, the definition of technical objectives, is obvious.
The approach to acquisition path analysis used in this paper has advanced over the past years [3, 4, 5, 6, 7]. Motivated from the fact that the SLC tries to come up with adaptive safeguards approaches, the main idea of this approach to APA is to account for differentiation without discrimination. In order to accomplish this, the available safeguards-relevant information is processed in an objective, transparent, reproducible, standardized and well-documented way in contrast to classical reasoning-with-words or black-box-approaches.
Besides the methodology and its progress, the new verification paradigm has to be compatible with the existing approach to nuclear material accounting, a major element of traditional safeguards. Therefore, it will be shown how performance targets can be derived from a risk assessment of the State's as well as the inspectorate's strategic options.
In the following, the methodology and its recent enhancements will be presented. Then, a discussion on the relationship between game theory and performance targets will be carried out. Afterwards, a case study focusing on the strategic assessment part of the method will be shown. Finally, conclusions of the paper and an outlook on future work will be presented.

2 Materials and Methods

The given approach to acquisition path analysis consists of three general steps: First, the potential acquisition network is modeled based on the IAEA's physical model and experts' evaluations. Second, using this model all plausible acquisition paths are extracted automatically. Third, the State's and the inspectorate's options are assessed strategically. The workflow is depicted in Figure 1. In the following, a description of the three stages will be given. A more in depth discussion can be found in Listner et al. [8].

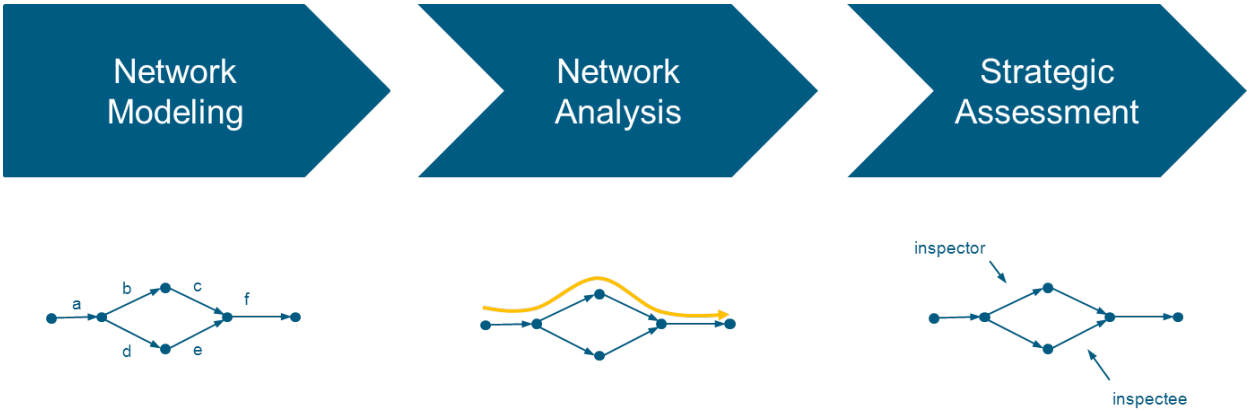

Figure 1. Three step approach to acuisition path analysis.

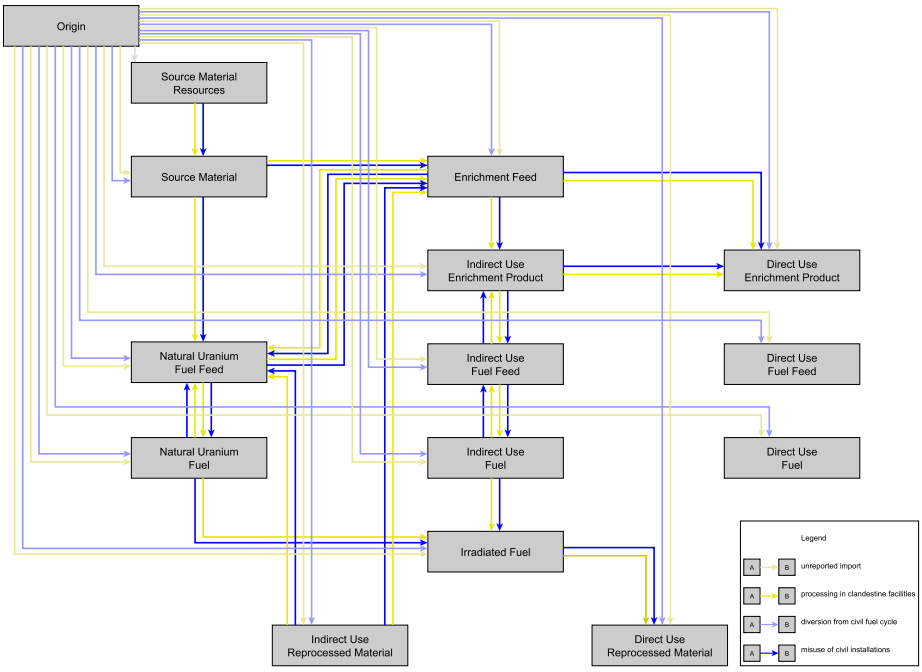

Figure 2. Generic Phyiscal Model.

During the first step of the process, also known as network modeling, a State-specific acquisition model is set up. Mathematically, such a network can be seen as a directed graph with material forms represented by nodes and processes represented by edges. The IAEA's physical model [9] serves as a starting point, where all proliferation relevant materials and processes are formally described in a general acquisition model for nuclear weapons usable material.[1] Based on the IAEA's physical model, a mathematical model has been derived that encodes all the potential materials and activities in a single directed graph (see Figure 2).

There are four categories of processes in this model: diversion from existing facilities (div), undeclared import (imp), misuse of existing facilities (mis), processing in clandestine facilities (cland). When assessing a State's options for acquiring nuclear weapons usable material,

[1]In principle, also the weaponization step itself could be modeled using a graph theoretic approach. However, due to the definition of acquisition path analysis given in International Atomic Energy Agency (IAEA) [2], this paper's approach ends at weapons usable material.

specific processes of these four types are included in or excluded from the model. E.g. if a State does not have an enrichment facility on its ground, all edges of type misuse in connection with enrichment will be removed from the model. On the other hand, there will be always the option for enriching in clandestine facilities and hence these processes will remain in every State's case.

Besides the mere presence of edges in the model, these edges will be assessed in terms of attractiveness for the particular State. Three dimensions of attractiveness are used which originate in the GIF methodology [10]: Technical Difficulty (TD), Proliferation Time (PT) and Proliferation Cost (PC).[2] For each process, the three dimensions are graded based on expert judgment. The grades range from 0 meaning a very attractive option to 3 being very unattractive. Using the arithmetic mean for each edge e, a single edge weight w_e is calculated from these figures.

After having specified the edge weights, it is necessary to model the inspectorate's side i.e. the possible technical objectives t with their respective non-detection probability $\beta_e^{(t)}$ on a specific edge e. Also the inspectorate costs c_t generated by technical objective t have to be quantified. Although no specific safeguards measures have been determined at this point, an expert can estimate the costs for attaining a given detection probability based on experience and knowledge about the State's capabilities, fuel cycle as well as existing safeguards approaches. While these figures can be specified for the edges related to the declared fuel cycle, i.e. misuse and diversion, deriving this information for the undeclared processes, i.e. undeclared import and clandestine processing, is yet an unsolved task. However, the given approach assumes that such a quantification can in principle be done for all types of processes, no matter whether they take place in declared facilities or elsewhere in the State.

As a result of the first step, a directed multi-graph is produced that represents the State's options for acquiring weapons usable material including their attractiveness in terms of time, cost and technical difficulty. Furthermore, also the inspectorate's options to control the activities are given, including the costs and non-detection probabilities in specific areas of the State's acquisition network.

This directed multi-graph is now analyzed in terms of all technically plausible acquisition paths. In order to accomplish this, a fully automated software extracts all paths from node 'Origin' to any node representing weapons usable material by applying the Depth-First Search (DFS) algorithm [11, pp. 540-549]. For each path p_i, the overall attractiveness is calculated by the sum of the weights of the constituting edges $E(p_i)$, i.e.

$$l_i = \sum_{e \in E(p_i)} w_e. \tag{1}$$

The list of paths is then reordered by attractiveness and all paths are visualized. It has to be emphasized that not only the shortest path but all technically plausible paths are considered. Therefore, this approach is comprehensive and avoids to ignore technically less attractive paths which could be strategically interesting.

Using the results of the first and second step, especially the list of paths with their respective attractiveness as well as the non-detection probabilities of technical objectives, the third step assesses the strategies of both parties, i.e. the State and the inspectorate. On the one hand, all acquisition paths and the option of compliant behavior are considered to be the State's strategy set. On the other hand, the strategies of the IAEA are all combinations of technical

[2]These dimensions only represent technical aspects of proliferation as if no inspectorate was present. The interplay of State and inspectorate will be considered separately in the third stage of the process.

	No Alarm	**Alarm**
Compliant Behavior	$(0, 0)$	$(-f, -e)$
Non-compliant Behavior along path i	$(d_i, -c)$	$(-b, -a)$

Table 1. Game Theoretic Payoffs.

objectives (TOC) that have been defined in the first part of the process. The overall non-detection probability of TOC_j for a given path p_i can be calculated using the product rule for probabilities by

$$\beta_{ij} = \prod_{e \in E(p_i), t \in TOC_j} \beta_e^{(t)}. \tag{2}$$

For each strategy combination a pair of payoff values for State and Inspectorate (H_1, H_2) can be defined (see Table 1). For the IAEA, the strategic outcomes in increasing order of preference are undetected non-compliance $(-c)$, detected non-compliance $(-a)$, false alarm $(-e)$ and compliance without alarm (0). These parameters can be selected freely as long as the ordering is kept.
Regarding the State, the strategic outcomes ordered increasingly by preference are detected non-compliance $(-b)$, false alarm $(-f)$, compliance without alarm (0) and successful acquisition along path i (d_i). The path length l_i calculated in step two is used to obtain the payoff values for successful acquisition by

$$d_i = \frac{l_1}{l_i}. \tag{3}$$

The decision whether an alarm is raised by the inspectorate depends on the non-detection probabilities. Hence, for each strategy combination an expected outcome for both players can be calculated. In case the State decides to follow an acquisition path i and the IAEA has TOC j in place, this payoff for the State is given by the expected benefit from a successful acquisition plus the risk of getting caught red-handed, i.e.

$$H_1^{(i)} = d_i \beta_{ij} - b(1 - \beta_{ij}). \tag{4}$$

For the IAEA, the expected payoff can be derived from the sum of the risks of detected and undetected non-compliance , i.e.

$$H_2^{(i)} = -c\beta_{ij} - a(1 - \beta_{ij}). \tag{5}$$

In case the State behaves in compliance with its given commitments, the outcome for both sides is only determined by the false alarm risk with false alarm probability α, i.e.

$$H_1^{(compliant)} = -f\alpha \tag{6}$$

for the State and

$$H_2^{(compliant)} = -e\alpha \tag{7}$$

for the IAEA.
Based on these considerations, a stable strategy combination (H_1^*, H_2^*) known as the Nash equilibrium can be calculated using the Lemke-Howson-algorithm [12]. The Nash equilibrium is characterized by the fact that its impossible for either of the two actors to deviate unilaterally from the equilibrium strategy and increase its expected payoff. Hence, it seems

rational for both players not to deviate and pursue the equilibrium strategy. This very limited definition of rationality only means that the actors care for the risks and benefits they are facing.
Using the equilibrium payoff value for the IAEA and scaling the IAEA's payoff parameters to $c = 1$, it is possible to define effectiveness as

$$E = 100\% + H_2^*. \tag{8}$$

In case of 0% effectiveness, the equilibrium ends in non-compliance with no possibility of detection. For 100% effectiveness, compliance with no false alarm is achieved almost surely. As the ultimate goal of acquisition path analysis is the selection of a TOC inducing compliant behavior (expressed by the term sufficient in the APA definition), this paper proposes to use a TOC leading to a high effectiveness value in the Nash equilibrium.
Moreover, in cases where compliant behavior can be induced in the Nash equilibrium, it is also possible and reasonable to gain an increase in efficiency. By iterating over a cost threshold W and calculating the Nash equilibrium for this range of values, a strategy with a given level of effectiveness at minimum costs can be selected.

3 Strategic Assessment using Performance Targets and Game Theory

In the previous section, it has been shown how a game theoretic, highly quantitative approach to technical objectives determination could look like. Alternatively, a more qualitative approach based on the idea of performance targets [13] can be used, which gives more flexibility to the analyst. This section will show that the philosophy behind these two different approaches to APA can be considered to be equivalent.
A performance target on the path level can be defined as the minimum detection probability that is needed in order to deter a State from pursuing this path. This means that if performance targets are properly defined for a given set of acquisition paths, these paths can be considered to be adequately covered by safeguards measures. Hence, the State is likely to act in compliance with its given commitments.
More formally, one can say that for given acquisition path i and technical objectives combination j, path coverage is achieved if the risk for the State to get caught along the path is higher than the benefit of a successful acquisition[3], i.e.

$$d_i\beta_{ij} - b(1 - \beta_{ij}) \leq 0. \tag{9}$$

In the past, the IAEA has considered it to be sufficient to obtain a detection probability of 90% in nuclear facilities with high potential to be used in nuclear weapons programmes. Transferring this to the idea of acquisition path analysis, for the most attractive path a performance target of 90% should be reached. As it has been shown in Avenhaus and Canty [14], this directly influences the choice of the payoff values in Equation 9, i.e.

$$\begin{aligned} 0 \geq \quad & d_1 \cdot 0.1 - b \cdot 0.9, \\ 9 \geq \quad & {}^{d_1}\!/_{b}. \end{aligned}$$

[3]For reasons of simplicity, false alarm risks are ignored in this paper. A similar argument can be made, if false alarm risks are included in the model.

Because the payoff values are ranging from 0 to 1 (see Equation 3) with $d_1 = 1$, dethe State's payoff for a successful acquisition is $b = 1/9$.
Using these parameter values derived for the most attractive path, one can reinsert them into Equation 9 which leads to

$$\beta_{ij} \leq \frac{b}{d_i + b} = \frac{1}{9\frac{l_1}{l_i} + 1}. \tag{10}$$

This gives a rationale to define the path performance targets for the detection probability based on its attractiveness as

$$PT_i = DP_i^{(min)} = 1 - \beta_{ij}^{(max)} = \frac{l_1}{l_1 + l_i b}. \tag{11}$$

This calculation of performance targets can be used within the methodology of Budlong Sylvester et al. [15] in order to specify the appropriate technical objectives. If all performance targets are fulfilled, it is guaranteed under the assumptions of the model that the State will chose to behave in compliance with its commitments.
While the methodology in Budlong Sylvester et al. [15] leaves the decision up to the analyst which technical objectives to choose, the methodology in Section 2 uses an optimization technique to determine them. From the standpoint of the underlying philosophy however, both methods are equivalent.

4 Example Case Study

In order to prove the feasibility of the concept described in the previous sections, a case study was carried out. Therefore, a hypothetical State with a complex civil nuclear fuel cycle and comprehensive capabilities was modeled. Attractiveness values as well as costs and detection probabilities for technical objectives were determined using expert judgement. Following that, a set of 2060 plausible acquisition paths was calculated and sorted according to their attractiveness. Furthermore, a visualization was generated (see Figure 3).
In order to allow for a manual determination of technical objectives according to Section 3, 21 paths out of the 2060 paths were selected for further analysis. At this stage of the process, performance targets were calculated for the selected paths using Equation 11. The selected paths with their associated attractiveness, payoff values and performance targets are displayed in Table 2.
Finally, the strategic assessment, restricted on the 21 paths, was carried out using an approach which iterated over the cost limit W as it was described in Section 2. As previous studies have shown, the results are highly dependent on the detection probability for clandestine activities, DP_{cland}, the algorithm ran for different values of this parameter. The results are displayed in Figure 4. The alternative approach to technical objectives selection as described in Budlong Sylvester et al. [15] was beyond the scope of this paper.

5 Conclusions and Outlook

This paper shows how acquisition path analysis can be carried out using a comprehensive methodology which is yet compatible with the principles defined in Cooley [1]. Furthermore, two possibilities for determining technical objectives were proposed and evaluated. The first

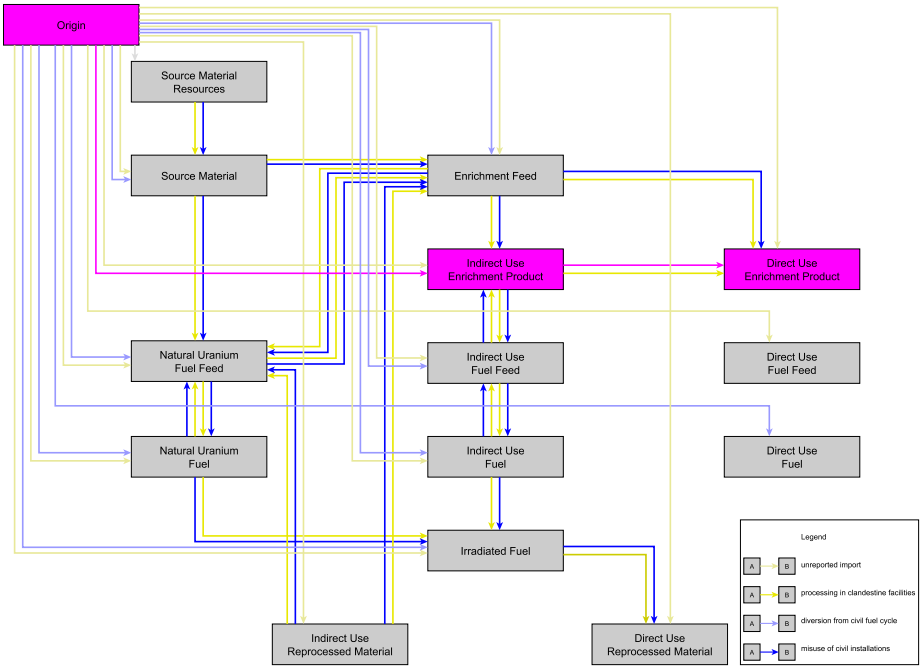

Figure 3. Visualization of the 5th most attractive path. The path highlighted in magenta represents the diversion of low enriched UF6 from the declared enrichment facility and misusing the enrichment facility in order to produce direct use material.

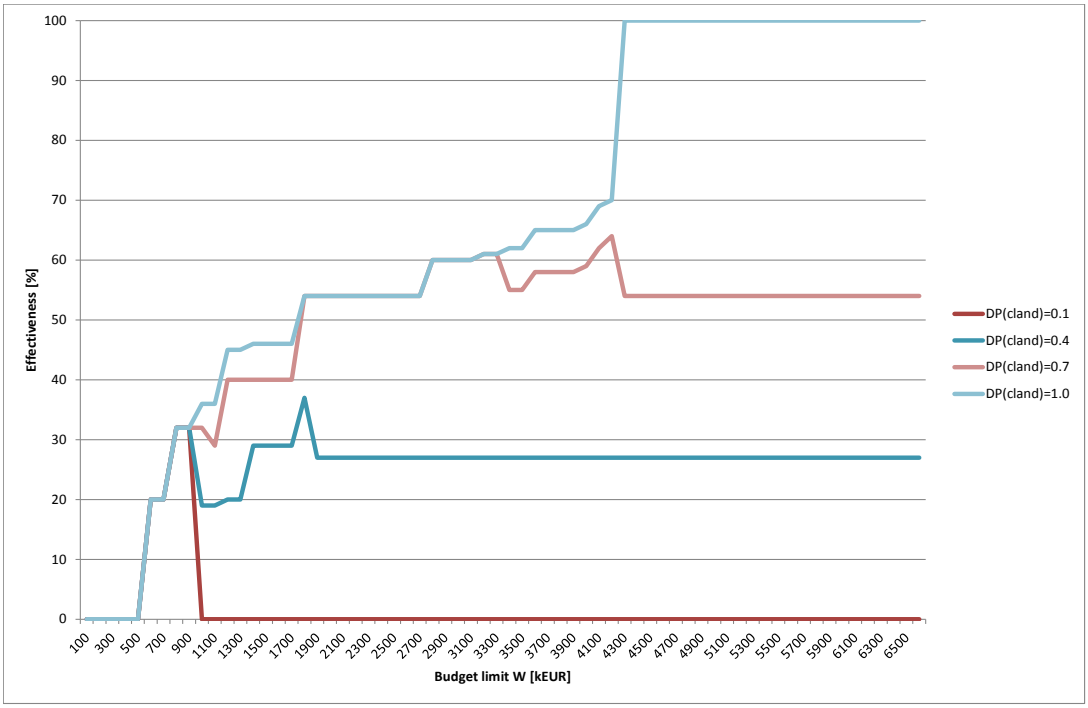

Figure 4. Effectiveness chart retrieved from game theoretic analysis.

i	Description	l_i	PT_i	d_i
1	Origin -imp- Direct Use Enrichment Product	2.33	90%	1.0
5	Origin -div- Indirect Use Enrichment Product -mis- Direct Use Enrichment Product	3.0	88%	0.78
8	Origin -div- Irradiated Fuel -mis- Direct Use Reprocessed Material	3.67	85%	0.64
14	Origin -div- Enrichment Feed -cla- Direct Use Enrichment Product	4.33	83%	0.54
22	Origin -div- Indirect Use Fuel -mis- Irradiated Fuel -mis- Direct Use Reprocessed Material	4.33	83%	0.54
27	Origin -imp- Indirect Use Reprocessed Material -mis- Enrichment Feed -mis- Direct Use Enrichment Product	4.67	82%	0.5
39	Origin -div- Source Material -mis- Enrichment Feed -cla- Direct Use Enrichment Product	5.0	81%	0.47
40	Origin -imp- Source Material -cla- Enrichment Feed -mis- Direct Use Enrichment Product	5.0	81%	0.47
44	Origin -imp- Natural Uranium Fuel -mis- Irradiated Fuel -cla- Direct Use Reprocessed Material	5.0	81%	0.47
58	Origin -div- Indirect Use Fuel -cla- Irradiated Fuel -cla- Direct Use Reprocessed Material	5.33	80%	0.44
65	Origin -imp- Natural Uranium Fuel -mis- Natural Uranium Fuel Feed -mis- Enrichment Feed -mis- Direct Use Enrichment Product	5.33	80%	0.44
67	Origin -imp- Indirect Use Fuel -mis- Indirect Use Fuel Feed -mis- Indirect Use Enrichment Product -mis- Direct Use Enrichment Product	5.33	80%	0.44
68	Origin -div- Source Material Resources -cla- Source Material -cla- Enrichment Feed -mis- Direct Use Enrichment Product	5.33	80%	0.44
73	Origin -div- Enrichment Feed -mis- Indirect Use Enrichment Product -cla- Direct Use Enrichment Product	5.67	79%	0.41
88	Origin -imp- Source Material -mis- Enrichment Feed -mis- Indirect Use Enrichment Product -mis- Direct Use Enrichment Product	5.67	79%	0.41
95	Origin -imp- Natural Uranium Fuel -mis- Natural Uranium Fuel Feed -cla- Enrichment Feed -mis- Direct Use Enrichment Product	5.67	79%	0.41
125	Origin -div- Source Material Resources -cla- Source Material -cla- Enrichment Feed -cla- Direct Use Enrichment Product	6.0	78%	0.39
164	Origin -div- Source Material Resources -mis- Source Material -mis- Natural Uranium Fuel Feed -mis- Natural Uranium Fuel -mis- Irradiated Fuel -mis- Direct Use Reprocessed Material	6.33	77%	0.37
262	Origin -imp- Indirect Use Reprocessed Material -mis- Natural Uranium Fuel Feed -mis- Natural Uranium Fuel -mis- Irradiated Fuel -cla- Direct Use Reprocessed Material	7.33	74%	0.32
538	Origin -div- Source Material Resources -mis- Source Material -mis- Enrichment Feed -mis- Indirect Use Enrichment Product -mis- Indirect Use Fuel Feed -mis- Indirect Use Fuel -mis- Irradiated Fuel -mis- Direct Use Reprocessed Material	9.0	70%	0.26
1509	Origin -div- Source Material Resources -cla- Source Material -cla- Enrichment Feed -cla- Indirect Use Enrichment Product -mis- Indirect Use Fuel Feed -cla- Indirect Use Fuel -mis- Irradiated Fuel -mis- Direct Use Reprocessed Material	12.0	64%	0.19

Table 2. List of paths selected for strategic assessment along with path index i, description of the path, overall path attractiveness l_i, performance target PT_i and payoff value d_i.

more quantitative approach delivers a set of technical objectives with optimal effectiveness under the assumptions of a game theoretic model. Besides the high degree of automation, this approach also allows for an inherent randomization of technical objectives. However, the analyst has to specify a set of parameters in this approach. Therefore a good understanding of the model is necessary, as the influence of the parameters on the model's outcome is very complex.
The alternative approach overcomes these drawbacks by a higher degree of interaction with the analyst. Moreover, it allows for re-prioritization of paths based on possible indications. On the other hand, this flexibility leads to less reproducibility of the results when transferring the task to a different analyst.
In summary, while the underlying philosophy is the same, both methodologies have their advantages and disadvantages. However, it also has been shown that the underlying philosophy is the same.
In the future, further case studies need to be carried out. Also, the outcomes sensitivity on the selected parameters in both approaches will be investigated. Furthermore, the applicability of the presented ideas to other applications in the area arms control and disarmament will be investigated. Finally, the methodology will be iteratively improved with the help of experts at the IAEA.

6 Acknowledgments

This paper was prepared as an account of work sponsored by the Government of the Federal Republic of Germany within the Joint Programme on the Technical Development and Further Improvement of IAEA Safeguards between the Federal Republic of Germany and the IAEA.

References

[1] J. N. Cooley. "Progress in Evolving the State-level Concept". In: *Seventh INMM/ESARDA Joint Workshop Future Directions for Nuclear Safeguards and Verification*. 2011.

[2] International Atomic Energy Agency (IAEA). "IAEA Safeguards Glossary". In: *International Nuclear Verification Series No. 3* (2001).

[3] C. Listner et al. "A Concept for Handling Acquisition Path Analysis in the Framework of IAEA's State-level Approach". In: *Proceedings of the 53rd INMM Annual Meeting*. INMM. 2012.

[4] C. Listner et al. "Approaching acquisition path analysis formally - experiences so far". In: *Proceedings of the 54th INMM Annual Meeting*. INMM. 2013.

[5] C. Listner et al. "Approaching acquisition path analysis formally - a comparison between AP and non-AP States". In: *Proceedings of the 35rd ESARDA Annual Meeting*. 2013.

[6] C. Listner et al. "Evolution of Safeguards - What Can Formal Acquisition Path Analysis Contribute?" In: Institute of Nuclear Materials Management 55th Annual Meeting, Atlanta(USA), 07/20/2014 - 07/24/2014. 2014.

[7] C. Listner et al. "Quantifying Detection Probabilities for Proliferation Activities in Undeclared Facilities". In: Symposium on International Safeguards: Linking Strategy, Implementation and People, Vienna(Austria), 10/20/2014 - 10/24/2014. 2014, p. 28.

[8] C. Listner et al. *A Concept for Handling Acquisition Path Analysis in the Framework of IAEA's State-level Approach*. Tech. rep. JOPAG/04.13-PRG-400. 2013.

[9] International Atomic Energy Agency (IAEA). "The Physical Model". STR-314. 1999.

[10] GEN IV International Forum. *Evaluation Methodology for Proliferation Resistance and Physical Protection of Generation IV Nuclear Energy Systems*. 2006.

[11] T.H. Cormen et al. *Introduction to Algorithms*. 2nd. Cambridge, MA, USA: MIT Press, 2001.

[12] M. J. Canty. *Resolving conflicts with Mathematica: algorithms for two-person games*. AP, 2003.

[13] C.L. Murphy et al. "Evolution of Safeguards - An Information-driven Approach to Acquisition Path Analysis". In: *Proceedings of the 55th INMM Annual Meeting*. INMM. 2014.

[14] R. Avenhaus and M.J. Canty. "Formal Models of Verification". In: *Verifying Treaty Compliance*. Ed. by R. Avenhaus et al. Springer, 2006, pp. 295–319.

[15] K. W. Budlong Sylvester et al. "The Use of Performance Targets in the State-Level Concept". In: *Proceedings of the 55th INMM Annual Meeting*. INMM. 2014.

Methodological Aspects on the IAEA State Level Concept and Related Acquisition Path Analysis

Lance K. Kim, Guido Renda, Giacomo G. M. Cojazzi

Institute for Transuranium Elements
Joint Research Centre, European Commission
Via Fermi, Ispra 21020 (VA) Italy
E-mail: giacomo.cojazzi@jrc.ec.europa.eu

Abstract:

International Atomic Energy Agency (IAEA) safeguards designed to deter nuclear proliferation continue to evolve to respond to new challenges. Within its State Level Concept, the IAEA envisions a State Level Approach for safeguards implementation that considers a State's nuclear and nuclear-related activities and capabilities as a whole within the scope of the State's safeguards agreement to meet generic safeguards objectives. For a State with a Comprehensive Safeguards Agreement, these generic safeguards objectives are to detect diversion of declared nuclear material in declared facilities or LOFs, to detect undeclared production or processing of nuclear materials in declared facilities or locations outside facilities (LOFs), and to detect undeclared nuclear material or activities in the State. Under the SLA, States will be differentiated based upon State-Specific Factors (SSF) that influence the design, planning, conduct and evaluation of safeguards activities. Proposed categories of factors include both technical and legal aspects, spanning from the deployed fuel cycle and the related state's technical capability to the type of safeguards agreements in force and the IAEA experience in implementing safeguards in that State. SSFs related to a State's technical capabilities are captured through an Acquisition Path Analysis (APA) that identifies plausible routes for acquiring weapons-usable material. In order to achieve this goal, the APA will have to identify possible acquisition paths, characterize them and eventually prioritise them. A key issue affecting the SLC's ability to satisfy effectiveness, efficiency, and nondiscrimination principles is the objectivity of technical SSFs captured through the APA. A review of proposed APA methods and historical evidence indicates that assessments of a State's technical capabilities and pathway completion times may not be as objective as has been suggested. Process modifications are proposed to improve pathways characterization supporting the SLC, such as developing a sounder basis for technical plausibility, formalizing considerations of intrinsic technical difficulty, assessing uncertainties in collected information and issuing guidance on omitted SSFs that may influence pathway completion times.

Keywords: Safeguards, State Level Concept, Acquisition Pathways Analysis

1. Introduction: The IAEA State-Level Concept for Improving the Effectiveness and Efficiency of International Safeguards Implementation

International Atomic Energy Agency (IAEA) safeguards designed to deter nuclear proliferation continue to evolve to respond to new challenges. With the introduction of the Additional Protocol (AP), approaches for detecting the diversion of material and the misuse of declared facilities have been complemented by additional measures to strengthen the detection of possible undeclared activities within the State. The IAEA's State-Level Concept (SLC) envisions a holistic approach to nuclear safeguards considering the State as a whole with safeguards implementation tailored to the State. Within the SLC, the IAEA envisions a State Level Approach (SLA) for safeguards implementation that considers a State's nuclear and nuclear-related activities and capabilities as a whole within the scope of the State's safeguards agreement to meet generic safeguards objectives – the detection of diversion, misuse, and undeclared material or activities.[1]–[3]

Improving the effectiveness and efficiency of safeguards implementation are among the key goals of the SLC.[3] While these aspirations are uncontroversial, demonstrably achieving them are empirical questions. While the IAEA envisions reductions of safeguards intensity informed by the Broader Conclusion (BC) [3], assuring the absence of undeclared activities may be costly to achieve.[4] Perceived over-spending in States with substantial nuclear infrastructure thought to present low proliferation risk [5] may reflect non-technical factors (e.g. security environment, form of government, etc.) rather than technical State Specific Factors (SSF) – potentially engendering accusations of discrimination and requiring a level of transparency that some consider generally lacking.[6] While these scenarios are deliberately provocative, they underscore the importance of an evidence-based approach to safeguards effectiveness and efficiency.

1.1. Program Theory

Towards an evidence-based approach, a program theory or logic model [7] assesses the mechanisms by which the SLC might achieve effectiveness and efficiency goals. Figure 1 outlines the processes supporting the implementation of safeguards at the State-level as envisioned by the IAEA.[3] The SLC program theory in Figure 2 developed from the IAEA's diagram (excluding feedbacks), reflects the premise that differentiating States on the basis of SSFs will lead to improvements in safeguards effectiveness and efficiency.

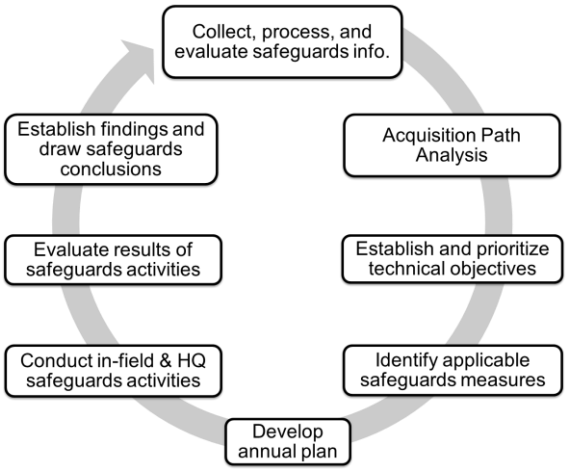

Figure 1: Flow chart of processes supporting State-level safeguards implementation, adapted from [3]

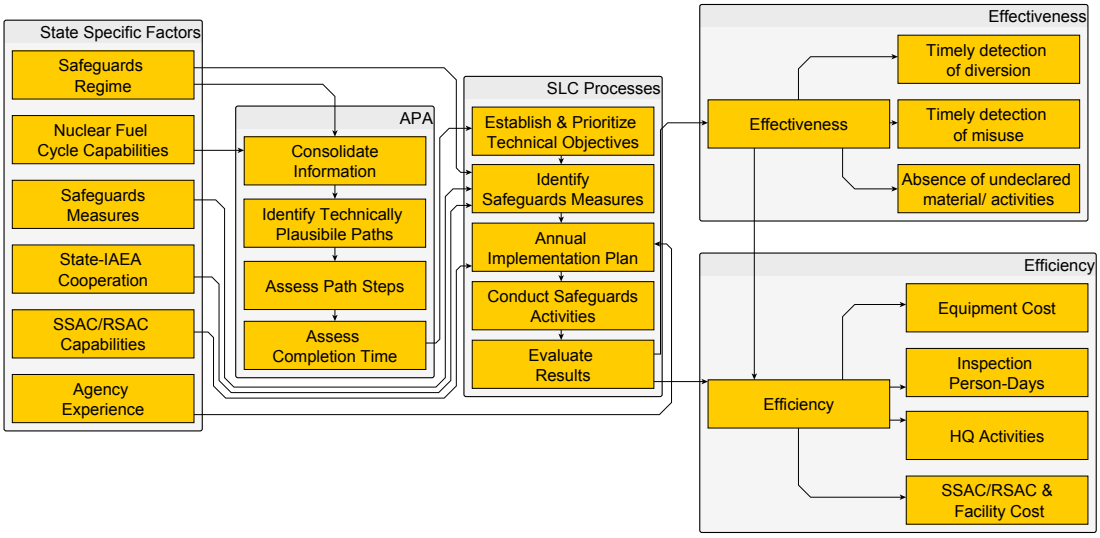

Figure 2: Notional sketch of SLC program theory linking State Specific Factors to Acquisition Pathways Analysis and effectiveness and efficiency measures

A key issue affecting the ability to improve effectiveness and efficiency in a non-discriminatory manner is the extent to which information on the SSF related to "the nuclear fuel cycle and related capabilities of the State" can be utilized objectively within Acquisition Pathways Analysis (APA). Though an exposition of the program theory diagram is beyond the scope of this paper, the "tail" of the program theory diagram is discussed first to identify measures of safeguards effectiveness and efficiency (Section 2). The "head" is then discussed (Section 3), summarizing the impact of SSFs upon effectiveness and efficiency. The focus then turns to features of a State's nuclear fuel cycle captured by the APA to identify methodological improvements that enhance analytical rigor and address uncertainties (Section 4). Processes supporting the SLA closely linked to the APA, including the prioritization of technical objectives and developing an annual implementation plan, are also discussed (Section 5).

This paper is a snapshot of on-going APA development in support of the State Level Concept for safeguards implementation. This paper captures concepts derived primarily from open sources of information, including publications, presentations, and workshops on the APA by the IAEA, various Member States Support Programs (MSSPs), and relevant work found in the open literature. It also builds upon previous JRC contributions in the area of methodological considerations for the APA process and the potential of open sources of information for supporting the APA.[8], [9] As the APA and the SLC are continuing to evolve, the topics covered here should be considered a snapshot in time, does not reflect finished products, and does not necessarily reflect official views.

2. The Tail: Evaluating Effectiveness and Efficiency

Defining goals is an important step to the design of any system. When evaluating whether or not a program has had the desired outcomes, evaluations of effectiveness and efficiency generally focus on improving processes or proving causal relationships.[7] Towards the latter, the impact of the nonproliferation regime on the behavior of States has been studied extensively. Some have suggested anecdotally that the nonproliferation regime is an overwhelming success as early fears of the number of nuclear-armed States have not yet materialized.[10],[11] But proving causality is more elusive as "States might simply join the NPT because they do not plan to acquire nuclear weapons".[12] Quantitative analysis suggests that the "presence of traditional IAEA safeguards" was not among "proliferation inhibitors" but was a "proliferation promoter", finding statistically significant correlations between safeguards and decisions to "explore" and "pursue" (but not to "acquire") nuclear weapons.[13],[14] Others have suggested that the safeguards system is, paradoxically, a victim of its own success as the rarity of safeguards events hampers assessment.[15] Looking forward, while widespread adoption of the AP is expected to inhibit proliferation, data is not yet available to assess its impact.[14]

Lacking the "gold standard" of a program evaluation – a randomized controlled study [7] – evaluations of safeguards effectiveness are inherently subjective. A report written in 1995 by the U.S. Office of Technology Assessment notes that, "Despite the objective, systematic way in which the IAEA nuclear safeguards system has been codified and implemented…the underlying judgment as to what the safeguards system needs to be able to do and how well it needs to do it is inherently a subjective one."[16] The IAEA's effectiveness measures reflect this reality. Effectiveness indicators essentially come in two categories: "the scope of achievement resulting from safeguards implementation" and "the level of assurance attained".[15] Whereas the former is quantifiable (e.g. the percentage of nuclear material/facilities under safeguards for which inspection goals have been fully attained), the level of assurance is more difficult to ascertain.[1], [15], [17]

The generic State-level safeguards objectives proposed by the IAEA [18] and other proposals for performance-based measures [19], [20] contribute to the scope of achievement and level of assurance. For example, the three State-level objectives are:

- "to detect any diversion of declared nuclear material at declared facilities or LOFs
- to detect any undeclared production or processing of nuclear material at declared facilities or LOFs; and
- to detect any undeclared nuclear material or activities in the State as a whole."[3], [18]

Though efficiency is not formally defined in the IAEA safeguards glossary, [1] it is commonly understood as the ratio of effectiveness and cost - presenting obvious difficulties when assessing levels of assurance. *Ceteris paribus*, alternative safeguards measures could be evaluated based on the effort, cost, and impact to the Agency and State.[21]

3. The Head: Differentiating States with State-Specific Factors

Turning to the head of the program theory diagram, the IAEA has stated that States are to be differentiated based upon objective State-Specific Factors (SSFs) that influence the design, planning, conduct, and evaluation of safeguards activities and has identified six categories of SSFs as listed in Table 1.[3] Though the IAEA has stated that no other factors would be considered, [18] others have suggested that these SSFs may be incomplete (e.g. democratic government, multinational nuclear companies, etc.) – potentially missing effectiveness and efficiency gains.[22], [23] Some have characterized these SSFs as being based on "indisputable facts" or "more open to disagreement", but still based on shared implementation experience, and without "inherently subjective" factors such as the State's political situation, intentions, etc.[24] Others appear more skeptical, with one commenter characterizing four of the six SSFs as "hardly quantifiable" or "discretionary".[23] In contrast, the SSF related to "the nuclear fuel cycle and related capabilities" is considered to be "well quantifiable" [23] and based on "…indisputable facts and thus not open to misinterpretation or ambiguity."[24] (Table 1)

State Specific Factors [3]	**Medici, 2014** [23]	**Burton, 2014** [24]
The type of safeguards agreement in force for the State and the nature of the safeguards conclusion drawn by the Agency	"well quantifiable"	"…indisputable facts and thus not open to misinterpretation or ambiguity."
The nuclear fuel cycle and related capabilities of the State	"well quantifiable"	"…indisputable facts and thus not open to misinterpretation or ambiguity."
The technical capabilities of the State or regional system of accounting for and control of nuclear material (SSAC/RSAC)	"hardly quantifiable"	"…more open to disagreement between the IAEA and the State, but are still based on the shared experience in implementing safeguards in the State."
The ability of the Agency to implement certain safeguards measures in the State (e.g. remote monitoring, unannounced/short notice inspections)	"discretionary"	"…indisputable facts and thus not open to misinterpretation or ambiguity."
The nature and scope of the cooperation between the State and the Agency in the implementation of safeguards	"discretionary"	"…more open to disagreement between the IAEA and the State, but are still based on the shared experience in implementing safeguards in the State."
The Agency's experience in implementing safeguards in the State	"discretionary"	"…more open to disagreement between the IAEA and the State, but are still based on the shared experience in implementing safeguards in the State."

Table 1: Summary of the quantifiability and objectivity of State-Specific Factors, examples, and impacts on safeguards implementation, derived from [3], [23], [24]

4. Nuclear Fuel Cycle Capabilities and the APA

To begin to address how quantifiable is "well quantifiable", this section explores how information about a State's nuclear fuel cycle capabilities is used by Acquisition Pathways Analysis (APA). As the technical backbone of the SLA process, APA is utilized to estimate the speed by which a State might acquire weapons-usable material and used to allocate limited safeguards resources. The APA consists of a four stage process:

- Information Collection: "Consolidating information about the State's past, present, and planned nuclear fuel cycle-related capabilities and infrastructure"
- Path Identification: "Identifying and visually presenting technically plausible acquisition paths for the State"

- Path Characterization: “Assessing acquisition path steps (State's technical capabilities and possible actions) along the identified acquisition paths”
- Path Prioritization: “Assessing the time needed to complete a technically plausible acquisition path” [25]

4.1. Information Collection

As depicted in the program theory diagram, what can be known about a State’s nuclear fuel cycle capabilities is influenced by the safeguards regime in place. Considerably more information is available about a State with an Additional Protocol (CSA+AP) than one with only a Comprehensive Safeguards Agreement (CSA-only). Much as verification of a State’s declarations has been the basis of safeguards conclusions for decades, analysts must confront the possibility that the evidence in hand may be incomplete, unreliable, ambiguous, and even deceptive.[9] As the pendulum of relative advantage swings from competition between hiders and seekers, the probability of detection may be difficult to characterize at any particular moment. As will be discussed further below, these information asymmetries between the State and the IAEA contribute to misestimates of a State’s capabilities and to the potential for unpleasant surprises.

4.2. Path Identification

Overall, the process of path identification appears to be based on solid foundations, leveraging the IAEA’s Physical Model [26] to identify safeguards-relevant flows of materials. Two features are notable about the IAEA’s process: the process of addition (vs. subtraction) and the definition of technically plausible paths.

4.2.1. Path Identification: Additive vs. Subtractive Processes

Enhancing the robustness of pathway identification will be important to avoid inadvertently excluding plausible paths. The process of addition defined by the IAEA adds technically plausible path segments to declared facilities, excluding pathways deemed to be technically implausible.[27] A suggestion engine augmenting an analyst-driven process promotes completeness by suggesting potentially overlooked pathways and warning of inconsistencies. The engine might also consider other factors, such as reducing reliance upon importation with increasing economic development.[28] Alternatively, a process of elimination that systematically “prunes” implausible pathways may also promote completeness. Computational tools may accelerate this process as well, identifying implausible pathways based on logical (e.g. utilizing “if-then” relationships [29]) or physical relationships (e.g. the IAEA physical model [26]). Differences in workload between a process of addition and elimination may depend upon the complexity of a State’s infrastructure and capabilities, but may not be substantial if all path segments are assessed for plausibility.

4.2.2. Technical Plausibility as a Screening Criterion

The IAEA employs technical plausibility essentially as a screening criterion to “prune” technically implausible pathways. A pathway is considered technically plausible if “…a State could, from a technical point of view, acquire at least one significant quantity of weapons-usable nuclear material within five years…”.[25] Presumably, implausible pathways that are deemed too far off into the future to warrant further consideration are pruned to reduce analytical burdens. However, as currently defined, this concept has procedural, definitional, and conceptual issues. As technical plausibility is essentially a preliminary estimate of completion time, the associated definitional and conceptual issues associated with estimating completion time are addressed later in this paper.

On procedural grounds, a determination of technical plausibility appears premature at this stage of process. As the technical capability of a State is assessed later in the process, analysts will depend upon previous assessments, theoretically leading to a vicious cycle of declining safeguards attention. For this reason, analysts should err on the side of caution by excluding only the most implausible path segments and implausible pathways should be reassessed periodically so that all pathways face the possibility of detection. The IAEA has recognized this possibility, noting that the “… State evaluation process will continue to look for indications that a State may be developing related capabilities and their technical plausibility will be reassessed periodically.”[25]

Despite this precaution, a sounder criterion for technical plausibility is desirable as the five year criterion appears arbitrary. A plausibility threshold based on detection by *semper vigilans* safeguards measures (such as those associated with the State evaluation processes including the monitoring of open source information, third-party sources of information, etc.) may be a more defensible basis for pruning pathways while maintaining complete coverage. For a given measure with an annual detection probability, P_{annual}, the probability of detection after t years is, assuming independence of events, $P(t) = 1-(1-P_{annual})^t$. A safeguards measure assessed to have a 37% annual probability of detection results in a 90% probability of detection within five years. By doing so, the threshold for plausibility establishes detection goals for implausible pathways without sacrificing full coverage. These goals, however, may be largely aspirational as they may elude quantification.

4.3 Path Characterization

Drawing upon the consolidated information about a State, characterizing paths is largely descriptive in nature – a structured collection of facts about a State's technical capabilities – and appears to be well developed. Relevant details of a State's capabilities depend on the type of acquisition path step e.g. indigenous production, diversion, misuse, clandestine, import. In the case of a path step involving e.g. the diversion of spent fuel from a declared Light Water Reactor (LWR), relevant technical details include inventories of material and their characteristics. In the case of potential undeclared activities, factual information include assessments of the State's knowledge, R&D, current capabilities to manufacture or purchase equipment, and experience with operating related processes. State actions (i.e. proliferation scenarios) are then identified and assessed for each plausible acquisition path step. In the case of diversion, State actions include the diversion of spent fuel assemblies with replacement by dummies and the diversion of spent fuel rods through the disassembly of fuel assemblies. Misuse includes such actions as using excess capacity and concealed modifications or upgrades. Clandestine paths are assessed with respect to the actions necessary to acquire the missing capability through indigenous development and/or importation.[25]

4.4. Path Prioritization by Estimating Completion Time

Following the identification and characterization of paths, the "…ease (technical capabilities) and speed by which a State could acquire one significant quantity of nuclear material using that path" are then estimated.[25] Path completion time is a concept useful for establishing timeliness goals for safeguards planning and should not be mistaken for path likelihood as "…the most likely path is not necessarily the quickest path".[30] That being said, estimating ease and speed are perhaps the most analytically challenging element of the APA process. As noted by the developers of the Program Evaluation Research Task (PERT) process, analysts must consider several factors including, "…resources, in the form of dollars, or what 'dollars' represent – manpower, materials, and methods of production, technical performance of systems, subsystems, and components, and time."[31] As discussed below, estimating how fast or how slow must also contend with sources of informational and analytical uncertainties.

4.4.1. Assessing Ease: Intrinsic Technical Difficulty and State Capabilities

The IAEA appears to emphasize the technical capabilities of the State when assessing the "ease" of a path. The ease of the task itself is also important, without which, completion time cannot be estimated. Analytical models demonstrate that path priorities are sensitive to the ratio between the intrinsic technical difficulty and a State's capabilities.[32] As defined in the Generation IV International Forum's Proliferation Resistance and Physical Protection (PR&PP) evaluation methodology, the intrinsic technical difficulty of a path step (defined as "technical difficulty" by PR&PP) is, "The inherent difficulty arising from the need for technical sophistication, including material-handling capabilities, required to overcome the multiple barriers to proliferation."[33]

Caution is necessary when evaluating intrinsic technical difficulty as qualitative statements can be misleading. For example, as reported in a recent review study, some analysts have claimed that "…all enrichment techniques demand sophisticated technology in large and expensive facilities", suggesting that enrichment is out of reach of all but the most capable States. In contrast, others suggest that a small centrifuge plant is "…feasible for countries with no prior experience, 'that possess relatively little technical skills and which have relatively little industrial activity'".[34] Quantitative descriptions may

help narrow these discrepancies by specifying costs and labor requirements in addition to necessary materials and physical processes.[30], [35]–[39]

Provided that a path is well-specified in terms of its intrinsic technical difficulty, the IAEA's process appears well-suited for collecting information about a State's nuclear-specific and related capabilities.[25] Broader consideration of a State's economic status may also be necessary to reflect generalizable capabilities that can be redeployed to nuclear programs. These linkages are evidenced by the correlation between proliferation decisions and, *inter alia*, general economic development in addition to nuclear specific capabilities.[14], [40] General capabilities also impact technology choices and reliance on imports – more sophisticated States may choose to be less reliant upon importation to maintain secrecy.[28] Furthermore, even non-nuclear industrialized States may have plausible pathways. After all, over half a century ago, only seven years elapsed between the discovery of fission and the first use of a nuclear weapon. States that exploded or deployed nuclear weapons had an average GDP per capita of $8000 (in 2015 U.S. dollars) and many States were below that average.[40] Though the use of economic status may be contrary to IAEA guidance against the use of SSFs to "rate or grade States",[3] the rationale for this prohibition is unclear as SSFs could also be misused to rank States and economic status may be rationally related to assessing a State's technical capabilities.

4.4.2. Assessing Speed: Sources of Informational and Analytical Uncertainty

Once a task has been defined in sufficient detail, engineering management methods can estimate completion times in light of a State's capabilities and resources. Approaches such as the Program Evaluation and Review Technique (PERT) that capture "The effects of resources and technical performance changes" on time, [31] have been used to plan complex projects, including the Hanford Engineer Works during the Manhattan Project.[41] The importance of uncertainties, particularly for research and development activities, was recognized early on. The PERT method itself quantifies uncertainties with a combination of optimistic, likely, and pessimistic task times.[31]

Evidence suggests that these uncertainties might be sufficiently large to warrant consideration. A retrospective study of U.S. intelligence estimates concluded a State's nuclear capabilities have tended to be overestimated i.e. States have tended to acquire capabilities later than expected.[42] However, our review of the cited cases indicates that foreign nuclear fuel cycle capabilities (excluding estimates involving weapons development and testing) tend to be underestimated i.e. States have acquired capabilities sooner than expected. Of these 35 cases, 13 were underestimated, 13 were correct, and nine were overestimated. Quantitative time estimates were available for nine of these 35 cases with an average underestimate of approximately five years along with a number of unexpected surprises (Table 2).[42] While it is difficult to know if these cases are a representative sample, this evidence suggests that the potential for underestimation may be large enough such that capabilities judged to be implausible within five years may already exist within a State.

Direction	Cases	Quantified Cases	Average Error (Years)
Underestimated	13	5	4.8
Correct	13	1	-
Overestimated	9	3	1.8

Table 2: Estimates of foreign nuclear fuel cycle capabilities from a recent study of US intelligence estimates, derived from [42]

This history of misestimation suggests that even a well-structured collaborative process emphasizing early warning may lead to significant underestimates of a State's capabilities. Political, cultural, bureaucratic, and organizational distortions contributed to these misestimates (Table 3). Cultural biases may be particularly concerning (Table 4). Not only might these "…cultural or racial biases…" engender accusations of discrimination, these biases also include "…failure[s] to understand an economic system" that can distort assessments.[42]

Type	Distortion Hypothesis
Political	• The ideology of the executive may encourage or promote those estimates that conform to the desired view • Policy initiatives, past, present, and future, can affect estimates (e.g. existing policy makes difficult or precludes objective analysis, whether logistically or psychologically, not enough importance attached to an area of geography or analysis, likelihood of major action resulting from estimate) • Likelihood of disclosure / politicization of estimate
Cultural	• Cultural biases create mistaken assumptions of capabilities • Misestimating intent / motives / resolve of subject State • Analysts misinterpret the involvement of outside sources
Bureaucratic	• Multiple advocacy among agencies causes compromise and/or domination • A fragmented bureaucracy stalls the dissemination and aggregation of useful data
Organizational	• Data overwhelms the analytic system, signals not separated from noise • Preference for secret over open sources [and vice versa?] • Recent experience with intelligence failures • Mistaken induction / conceptual rigidity: assumptions derived from historical experiences may not apply

Table 3: Categories of intelligence distortion hypotheses, summarized from [42]

State	Program Period	Direction of Cultural Bias	Description
Germany	1941-1945	Overestimation	"Culturally, beliefs about the abilities of the German scientists and a motivated misinterpretation of the slightly delayed publications where absence of evidence was considered evidence also contributed to distortion."
France	1954-	Overestimated	"… it is likely that cultural biases were positive in the French case, causing analysts to downplay the probability of inevitable problems and pushing estimates forward."
Israel	1955-	Underestimated	"… underestimated Israeli technical capabilities, as it was believed that Dimona could not be completed without US or French assistance"
China	1956-	Underestimated	"… underestimation of native Chinese production capabilities was a major factor in skewing earlier estimates, which expected reliance on Soviet assistance."
Iraq	1973-1991	Underestimated	"The program's underestimation was driven by a prior underestimation of Iraqi manufacturing capabilities, as evidenced by the expected reliance on foreign sources."
Libya	1970-2003	Underestimated	"Prior views of Libya's incompetence (although justified) may have contributed to the six-year gap between Libya's decision to seek a nuclear program through assistance from the A.Q. Khan network and the CIA reports of Libyan attempts to acquire materials from abroad."

Table 4: Examples of cultural biases impacting assessments of a State's technological capability, table based on text extracted from [42]

Technical process issues may also contribute to misestimation. In the context of the APA, two principal sources of uncertainty are important to recognize: informational and analytical.[9] Analytically, even assuming certain input data, the certainty of path completion times estimates will likely vary by the type of pathway under consideration and depend upon the degree to which factors of production are fixed or variable. In the parlance of production economics, factors of production (e.g. land, labor, capital equipment) are fixed if they are not readily altered over the short-run. In the long-run, all factors of production are variable.[43] Along this continuum, diversion scenarios can assume largely fixed

factors of production and well understood means of moving nuclear material. Misuse paths are more complicated as production factors are more variable and a State's capabilities are more salient, leading to greater analytical uncertainties. Clandestine paths have considerably more degrees of freedom that include the possibility of indigenously produced material, imported material, and equipment, with the potential to produce widely divergent estimates.

Some of this divergence is addressable through guidance on the degree of conservatism to be exercised when specifying end states and path step scheduling. Similar to considerations of intrinsic technical difficulty, estimates of time depend upon the end state of a path. Evaluating a range of technological options of varying intrinsic technical difficulty challenges analysts to consider scenarios that might otherwise go unnoticed or downplayed. For example, for a State known to have conducted basic radiochemistry experiments, a large production reprocessing facility that takes a decade to complete may be implausible, but a small pilot reprocessing facility completed is nearly plausible, and a "quick and dirty" reprocessing system may be faster yet. (Table 5).[38], [39], [44] Path step scheduling can also have dramatic impacts on time estimates. As evidenced by a Gannt chart timeline of the Hanford facility form the Manhattan project, a path step that could have taken nearly two decades in peacetime was claimed to have been substantially accelerated to about a third of that time during wartime by performing steps more quickly and in parallel.[41]

Technology	Estimated Time to "Quick and Dirty" Facility	Average Time to Pilot Plant (years)	Average Time to Production (years)
Enrichment (diffusion)		-	6
Enrichment (centrifuge)		8	14
Enrichment (EMIS)		2	3
Enrichment (chemical)		6	11
Enrichment (aerodynamic)		7	18
Enrichment (laser)		-	-
Graphite-moderated production reactors		1	2-11
Heavy-water-moderated production reactors		1	2-6
Research reactors			4-5
Reprocessing	4-6 months	6	10

Table 5: Estimated and historical timelines for various fuel cycle technologies, derived from [38], [39], [44]

Though engineering management methods have been used to estimate pathway time, some have claimed that such estimates are often wrong without accounting for motivational factors and institutional barriers that may hasten or slow progress. A review of related literature on estimating proliferation time and latency suggests that the proposed APA process may omit factors that impact time, including the influence of budgets, proliferator goals, and organizational issues.[37], [45] As noted by a study on latency, "…if one uses [an engineering management] approach for specific known cases, the time predicted for a State to develop its first nuclear device tends to be incorrect" as "…pathway decisions are determined by various motivations and institutional impediments that often outweigh the pure engineering resource management decisions."[35]

Difficulties in quantifying these omitted factors (e.g. information related to the demand for nuclear weapons, institutional issues, and budgetary resources) limits their practicality and their use may be perceived as subjective and discriminatory. Nonetheless, guidance on these omitted State level factors that influence pathway times may be necessary to limit analyst discretion and assure uniform implementation across States. For example, analysts may be instructed to assess multiple challenging scenarios and make assumptions that minimize path time e.g. assuming a motivated state with large budgetary resources and competent management pursuing technologies that are easier than commonly perceived.

5. Beyond the APA: Technical Objectives, Safeguards Measures, and Implementation Planning

The APA directly impacts processes of the SLA that establish the frequency and intensity of safeguards measures.[25] As APA development requires an understanding of the SLC as a whole, this section turns its attention to the processes following the APA that support the SLA, namely the:

- Establishment & prioritization of technical objectives
- Identification of safeguards measures
- Development of an annual plan[3]

As described by the IAEA, safeguards technical objectives and safeguards measures are established on the basis of the results of the APA as diagrammed in Figure 3. Technical objectives are identified for each path segment and safeguards measures are selected to satisfy the technical objective with a frequency and intensity dependent upon path completion times and the effectiveness of safeguards measures.[25] A SLA for safeguards implementation is then developed and executed through an annual implementation plan.

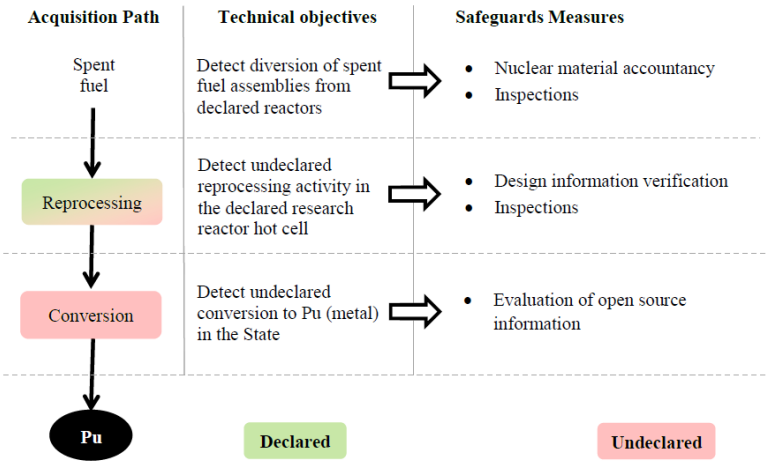

Figure 3: Identification of technical objectives and safeguards measures from an acquisition path analysis, reprinted from [18]

5.1. Technical Objectives

Informed by APA results, State-specific technical objectives are formulated and prioritized to achieve the three generic safeguards State-level objectives as illustrated in Figure 3. The process of establishing technical objectives translates path step information into safeguards-relevant terminology by identifying what needs to be safeguarded and where. For example, a high priority pathway might involve the clandestine reprocessing and conversion of diverted spent fuel from a declared reactor to produce metallic plutonium. For this pathway, one of several technical objectives is the detection of undeclared reprocessing activities in the State.

While the establishment of technical objectives appears relatively straightforward, the extent to which their prioritization should reflect additional factors beyond those considered in the APA is unclear. In the previous example, technical objectives can include the detection of diversion of spent fuel, detection of undeclared reprocessing activities, detection of undeclared conversion, detection of undeclared reprocessing R&D activities, etc. Whether all technical objectives should assume the same or different priorities as the pathway is unspecified. For example, strong indicators of the pathway that can be obtained at lower cost may be of greater interest than higher cost weaker indicators.

5.2. Safeguards Measures

Presumably, safeguards measures and associated sampling/inspection plans are selected from a set of technologies developed for a particular technical objective with defined performance characteristics (e.g. measurement uncertainties, desired probability of detection and false alarm rate, cost, etc.). For example, safeguards techniques and equipment used for material accountancy, containment and surveillance, environmental sampling, and data security are described by the IAEA as are target measurement uncertainties.[46], [47] Performance characteristics of safeguards measures to detect undeclared activities may be less certain.[17], [48]

5.2.1. Model Facility and Pathway Approaches

Given possible variations in the application of safeguards measures, model pathway safeguards approaches extending the model facility concept may support more consistent implementation of the SLC. Under classical safeguards, model facility safeguards approaches developed for a postulated reference facility serve as a starting point for the identification of applicable safeguards measures. Similarly, modifications to model pathway approach would arise from the APA through the channels of quantity and timeliness goals, facility-specific design and operational features, and other SSFs associated with the capabilities of the SSAC and safeguards implementation issues. Much as model facility approaches are modified on the basis of State-specific information, model pathway safeguards approaches clarify the impact of SSFs on safeguards implementation, for instance, by defining modifications to path priorities in response to previous instances of noncompliance.[49]

5.3. Annual Implementation Planning

While many details relevant to implementation planning are lacking, the IAEA appears to have adopted a collaborative expert judgment approach.[18] Whether these collaborative State Evaluation Groups (SEGs) will operate with the aid of formal expert elicitation techniques, with decision support tools, or in a more ad-hoc manner remains to be seen. Moreover, to assure equal treatment and dispelling potential accusations of discrimination, States may request extraordinary access to internal deliberations and safeguards implementation data.

5.3.1. Algorithms vs. Human Judgment

Algorithmic approaches to safeguards implementation planning are an alternative to expert judgement – the latter of which, as mentioned previously, can be subject to various biases. While any analytical result, particularly those reliant upon models of the strategic interaction between the State and inspectorate (e.g. game theoretic approaches [50]), should be treated with caution, algorithms may nonetheless achieve more consistent results and outperform expert judgment on average. This may be particularly true in “low validity” and “high validity” environments. In “low validity” environments, humans have difficulties detecting weak causal linkages, make inconsistent decisions, and yet may develop an illusion of skill. Predicting the future value of stocks and long-term political prognostications are examples. In “high-validity” environments with frequent objective feedback, humans can develop true skill, but algorithms might still outperform humans who are subject to lapses in attention. Medicine and firefighting are examples where true skill can develop.[51]

Where safeguards analysis lies on this spectrum of validity is debateable. Some safeguards activities, such as spent fuel counting, may be “high-validity” activities – though tedium is also a source of error.[51] Though analysts can learn “best practices” for designing an annual safeguards implementation plan, the relationship between cause and effect may be vague as the effectiveness of a safeguards implementation plan is difficult to evaluate objectively. Coupled to the rarity of proliferation events, the short tenure of safeguards analysts, and the limitations of institutional memory, safeguards implementation planning may have aspects resembling a “low validity” type of activity. Algorithms will face similar issues without adequate data for verification and validation, but they may nonetheless outperform human analysts on average and contribute to non-discrimination goals through sheer consistency.

6. Summary

Based upon a comprehensive study of methods proposed by the IAEA and member states and drawing upon evidence available in the literature, this paper evaluates the technical basis of Acquisition Pathways Analysis (APA) by assessing the influence of technical State Specific Factors related to "the nuclear fuel cycle and related capabilities of the State" [3] upon safeguards implementation. In addition to theoretical considerations, evidence was sought to derive process insights. While the APA process appears conceptually sound at a high level, considerations of theory and evidence suggests that there may be considerable uncertainties when assessing a State's nuclear fuel cycle and related capabilities.

Methodological insights are identified to support continued development. These insights reflect the fact that estimating completion time is a complex task that not only may lead to inconsistent assessments between individual analysts, but may leave safeguards implementation open to unpleasant surprises should States acquire capabilities sooner than estimated. Process improvements essentially boil down to the need for a "surprise-sensitive" [42] and strategic safeguards planning approach, including an APA process that explicitly postulates a highly motivated, resourceful State that rapidly pursues pathways that are easier than might be implicitly assumed and where information asymmetries favor the "hider". These types of analytical assumptions might be incorporated into model pathway approaches to promote consistent implementation, constrain analyst discretion to limit the potential for discriminatory biases, and clarify how safeguards implementation might change under the SLC.

The use of algorithmic approaches supporting the implementation of safeguards will continue to be an area of debate. While algorithmic consistency contributes to nondiscrimination, decision models are an imperfect science. Decision support tools can support expert judgment, but processes may be time consuming and subject to cognitive biases leading to subjective and inconsistent outcomes that may be construed as discriminatory. A resolution to the debate ultimately requires an evidence-based, not faith-based, approach evaluating the impacts of safeguards on a State's behaviour. Such evidence is likely not forthcoming as a randomized controlled study of safeguards effectiveness is impractical. Nevertheless, some insights may be derived by considering the validity (e.g. low vs. high) of the safeguards environment. Such thinking, as noted in early work on collaborative human-machine approaches for safeguards, [52] may better harness the consistency of algorithms while bringing human reasoning to bear where it is needed most.

7. Acknowledgements and Disclaimer

The work here presented is being carried out within the project "Innovative Concepts and Methodologies for Nuclear Safeguards" funded within the European Commission (EC) Euratom Horizon 2020 Research and Training Programme, also as a contribution to the EC Support to the IAEA task JNT C 1871: "Acquisition Path Analysis Methodology and Software Package". The views expressed in this document are those of the authors and do not necessarily represent the official views of the European Commission.

8. References

[1] International Atomic Energy Agency, "IAEA Safeguards Glossary," Austria, IAEA/NVS/3, 2002.
[2] "Guidance for States Implementing Comprehensive Safeguards Agreements and Additional Protocols," International Atomic Energy Agency, Vienna, Austria, 21, Mar. 2012.
[3] "The Conceptualization and Development of Safeguards Implementation at the State Level," International Atomic Energy Agency, GOV/2013/38, Aug. 2013.
[4] V. Bragin, J. Carlson, and R. Leslie, "Integrated Safeguards: Status and Trends," *Nonproliferation Rev.*, vol. 8, no. 2, pp. 102–110, 2001.
[5] J. Carlson, R. Leslie, P. Riggs, and A. Berriman, "Back to Basics - Re-Thinking Safeguards Principles," presented at the Annual Meeting of the Institute of Nuclear Materials Management, Phoenix, Arizona, 2003.

[6] T. McIntosh and W. Burr, “International Atomic Energy Agency Lacks Transparency, Observers and Researchers Say,” *The National Security Archive*. [Online]. Available: http://nsarchive.gwu.edu/nukevault/ebb512/. [Accessed: 28-Apr-2015].
[7] P. H. Rossi, M. W. Lipsey, and H. E. Freeman, *Evaluation: A Systematic Approach*, 7th ed. Sage Publications, Inc., 2004.
[8] G. G. M. Cojazzi, G. Renda, L. K. Kim, C. Versino, and E. Wolfart, “Acquisition Paths Analysis: Some Methodological Considerations,” presented at the Acquisition Path Analysis Workshop, Vienna, Austria, 24-Feb-2014.
[9] G. Renda, L. K. Kim, R. Jungwirth, F. Pabian, E. Wolfart, and G. G. M. Cojazzi, “The Potential of Open Source Information in Supporting Acquisition Pathway Analysis to Design IAEA State Level Approaches,” presented at the Symposium on International Safeguards: Linking Strategy, Implementation and People, Vienna, Austria, 2014.
[10] “Nuclear Proliferation Safeguards,” *World Nuclear Association*, Sep-2014. [Online]. Available: http://www.world-nuclear.org/info/Safety-and-Security/Non-Proliferation/Safeguards-to-Prevent-Nuclear-Proliferation/. [Accessed: 07-Jul-2014].
[11] P. Lavoy, “The Enduring Effects of Atoms for Peace,” *Arms Control Today*, Dec. 2003.
[12] D.-J. Jo and E. Gartzke, “Determinants of Nuclear Weapons Proliferation,” *J. Confl. Resolut.*, vol. 51, no. 1, pp. 167–194, Feb. 2007.
[13] J. Li, M.-S. Yim, and D. N. McNelis, “An Open Source Based Approach to Predict Nuclear Proliferation Decisions,” presented at the INMM, 2009.
[14] J. Li, M.-S. Yim, and D. N. McNelis, “Model-Based Calculations of the Probability of a Country’s Nuclear Proliferation Decisions,” *Prog. Nucl. Energy*, vol. 52, no. 8, pp. 789–808, Nov. 2010.
[15] H. Gruemm, “Safeguards Verification - Its Credibility and the Diversion Hypothesis,” *IAEA Bull.*, vol. 25, no. 4, 1983.
[16] “Nuclear Safeguards and the International Atomic Energy Agency,” U.S. Congress, Office of Technology Assessment, Washington, DC, OTA-ISS-615, Jun. 1995.
[17] J. A. Larrimore, “Timely Detection Under the State-level Concept,” presented at the INMM Annual Meeting, 2012.
[18] “Supplementary Document to the Report on the Conceptualization and Development of Safeguards Implementation at the State Level (GOV/2013/38),” International Atomic Energy Agency, Vienna, Austria, GOV/2014/41, Aug. 2014.
[19] K. Budlong Sylvester, J. Pilat, and T. Burr, “Evaluating International Safeguards Systems,” in *Nuclear Safeguards, Security, and Nonproliferation: Achieving Security with Technology and Policy*, 2008.
[20] K. Budlong-Sylvester and J. Pilat, “Performance-Based International Safeguards System,” presented at the 27th ESARDA Annual Meeting, Symposium on Safeguards and Nuclear Material Management, London, 2005.
[21] A. Vincze, “Experiences with the Development and Implementation of Integrated Safeguards (IS) in Some European States,” presented at the ESARDA, 2013.
[22] M. Hibbs, “The Plan for IAEA Safeguards,” *Carnegie Endowment for International Peace*, 20-Nov-2012. [Online]. Available: http://m.ceip.org/publications/?fa=50075. [Accessed: 06-Mar-2014].
[23] F. Medici, “Traditional/Integrated Safeguards vs. State Level Concept: Where is the IAEA heading to?,” presented at the ESARDA Joint Meeting on IAEA State Level Concept, Ispra, Italy, 12-Nov-2013.
[24] P. Burton, “A Canadian Perspective on the IAEA’s State-level Concept,” presented at the Symposium on International Safeguards, Vienna, Austria, 2014.
[25] T. Renis, Y. Yudin, and M. Hori, “Conducting Acquisition Path Analysis for Developing a State-Level Safeguards Approach,” presented at the INMM, 2014.
[26] Z. Liu and S. Morsy, “Development of the Physical Model,” in *Proceedings of the IAEA Safeguards Symposium*, 2007.
[27] A. El Gebaly, R. Grundule, K. Gushchyn, R. Higgy, W. Mandl, A. Nakao, and I. Tsvetkov, “Acquisition Path Analysis as a Collaborative Activity,” presented at the Symposium on International Safeguards, Vienna, Austria, 2014.
[28] J. Ullom, “Enriched Uranium Versus Plutonium: Proliferant Preferences in the Choice of Fissile Material,” *Nonproliferation Rev.*, 1994.
[29] J. King, “Improved Analysis of Information of States’ Nuclear Activities,” presented at the INMM, 1994.
[30] D. J. Sweeney and W. S. Charlton, “Proliferation Pathway Decision Analysis for Nuclear Weapons Latency,” in *Proceedings of the INMM 52nd Annual Meeting*, Palm Desert, CA, 2011.

[31] D. G. Malcolm, J. H. Roseboom, C. E. Clark, and W. Fazar, “Application of a Technique for Research and Development Program Evaluation,” *Oper. Res.*, vol. 7, no. 5, pp. 646–669, 1959.
[32] A. Vincze and A. Nemeth, “Effect of State-specific Factors on Acquisition Path Ranking,” presented at the IAEA Safeguards Symposium, 2014.
[33] “Evaluation Methodology for Proliferation Resistance and Physical Protection of Generation IV Nuclear Energy Systems,” Generation IV International Forum, GIF/PRPPWG/2011/003, Sep. 2011.
[34] R. S. Kemp, “The Nonproliferation Emperor Has No Clothes,” *Int. Secur.*, vol. 38, no. 4, pp. 39–78, Apr. 2014.
[35] D. J. Sweeney, J. M. Slanker, W. S. Charlton, and R. Juzaitis, “Quantifying Nuclear Weapons Latency,” in *Proceedings of the 2009 Annual Meeting of the Institute of Nuclear Materials Management*, Tucson, AZ, 2009.
[36] D. J. Sweeney and W. S. Charlton, “Simulating State Proliferation for Nuclear Weapons Latency,” presented at the INMM 54th Annual Meeting, Palm Desert, California, 2013.
[37] R. Harney, G. Brown, M. Carlyle, E. Skroch, and K. Wood, “Anatomy of a Project to Produce a First Nuclear Weapon,” *Sci. Glob. Secur.*, vol. 14, no. 2–3, pp. 163–182, 2006.
[38] E. B. Staats, “Quick and Secret Construction of Plutonium Reprocessing Plants: A Way to Nuclear Weapons Proliferation?,” U.S. General Accounting Office, Washington, DC, Oct. 1978.
[39] V. Gilinsky, M. Miller, and H. Hubbard, “A Fresh Examination of the Proliferation Dangers of Light Water Reactors,” Nonproliferation Policy Education Center, Washington, DC, Oct. 2004.
[40] S. Singh and C. R. Way, “The Correlates of Nuclear Proliferation: A Quantitative Test,” *J. Confl. Resolut.*, pp. 859–885, 2004.
[41] H. Thayer, *Management of the Hanford Engineer Works in World War II: How the Corps, DuPont, and the Metallurgical Laboratory Fast Tracked the Original Plutonium Works*. New York, NY, USA: ASCE Publications, 1996.
[42] A. H. Montgomery and A. Mount, “Misestimation: Explaining US Failures to Predict Nuclear Weapons Programs,” *Intell. Natl. Secur.*, 2014.
[43] S. Rasmussen, *Production Economics: The Basic Theory of Production Optimisation*, 2nd ed. Springer, 2013.
[44] M. D. Zentner, G. L. Coles, and R. J. Talbert, “Nuclear Proliferation Technology Trends Analysis,” Pacific Northwest National Laboratory, PNNL-14480, Sep. 2005.
[45] J. E. C. Hymans, “Botching the Bomb,” *Foreign Affairs*, Jun-2012.
[46] “Safeguards Techniques and Equipment: 2011 Edition,” International Atomic Energy Agency, Vienna, No. 1 (Rev. 2), 2011.
[47] “International Target Values 2010 for Measurement Uncertainties in Safeguarding Nuclear Materials,” International Atomic Energy Agency, STR-368, Nov. 2010.
[48] J. Pilat, K. Budlong Sylvester, and W. Stanbro, “Expert Elicitation and the Problem of Detecting Undeclared Activities,” presented at the INMM, 2002.
[49] B. Boyer, K. Budlong Sylvester, C. L. Murphy, and J. Pilat, “Prioritizing Paths and the Use of Performance Targets,” presented at the Acquisition Path Analysis Workshop, Vienna, Austria, 24-Feb-2014.
[50] C. Listner, M. J. Canty, A. Rezniczek, and G. Stein, “Approaching Acquisition Path Analysis Formally - A Comparison Between AP and Non-AP States,” presented at the ESARDA, 2013.
[51] D. Kahneman and G. Klein, “Conditions for Intuitive Expertise: A Failure to Disagree.,” *Am. Psychol.*, vol. 64, no. 6, pp. 515–26, Sep. 2009.
[52] F. L. Greitzer, R. V. Badalamente, and T. S. Stewart, “Collaborative Human-Machine Nuclear Non-Proliferation Analysis,” Pacific Northwest Laboratory, PNL-8922, Oct. 1993.

Session 8

Neutron Measurements

LA-UR-15-23252

Comparison of fresh fuel experimental measurements to MCNPX results using the differential die-away instrument for nuclear safeguards applications

Alison V. Goodsell[1,2], Vladimir Henzl[1], Martyn T. Swinhoe[1], Carlos Rael[1], David Desimone[1], William S. Charlton[2]

[1] Los Alamos National Laboratory
P.O. Box 1663, Los Alamos, NM 87545, USA
[2] Nuclear Security Science & Policy Institute
Texas A&M University, College Station, TX 77840, USA
E-mail: alisong@lanl.gov

Abstract:

A non-destructive assay technique, the Differential Die-Away (DDA) Instrument, is currently being investigated at Los Alamos National Laboratory (LANL) to better understand the development and deployment challenges. The DDA instrument is based on an active neutron interrogation technique which uses an external deuterium-tritium (DT) neutron generator to induce fission in a fuel assembly. The time of arrival (list-mode data) of the prompt fission neutrons are detected by nine ^{3}He detectors positioned around the fuel assembly. The characteristics of an assayed fuel assembly, such as the enrichment and presence of neutron absorbers, change the time required for the DDA signal to die away. Previously performed spent fuel Monte Carlo N-Particle eXtended transport code (MCNPX) simulations have shown that the dynamic evolution of the DDA signal can reveal various characteristics of a spent fuel assembly. The principal DDA instrument capabilities include measurement of multiplication, total effective fissile mass, total plutonium content, estimation of basic fuel assembly parameters such as initial enrichment and burnup, and identification of certain partial defects. In this work, results of experimental measurements using fresh pressurized water reactor (PWR) nuclear fuel in a water tank are compared with MCNPX simulations. The primary observables used in the comparison are the die-away times in several time domains. The ability to reliably reproduce the experimental measurement results using MCNPX is critical in the development and eventual deployment of the DDA instrument. We present results of our efforts to identify possible discrepancies and to quantify sources of uncertainty in the experiment and the simulation.

Keywords: differential die-away, nuclear fuel, non-destructive assay, safeguards, active interrogation

1. Introduction

The differential die-away (DDA) instrument is an active, non-destructive assay neutron interrogation technique for nuclear safeguard applications currently being investigated at Los Alamos National Laboratory (LANL). The instrument uses short pulses from an external deuterium-tritium (DT) neutron generator to induce fission in the fissile material of a fuel assembly. The DDA signal depends on the amount of fissile material in the fuel and the neutron absorber content. The time-dependent signal is recorded using multiple helium-3 (^{3}He) detectors positioned around the fuel assembly on a list-mode data acquisition system.

Spent fuel simulations using Monte Carlo N-Particle eXtended (MCNPX) [1] performed under the US National Nuclear Security Administration's Defense Nuclear Nonproliferation Next Generation Safeguards

Initiative Spent Fuel project (NGSI-SF) [2] showed the capability of the DDA instrument to characterize properties of a wide range of spent fuel assemblies (SFAs) [3]. Based on results of MCNPX simulations, the predicted DDA instrument capabilities include determination of SFAs multiplication, burnup and initial enrichment, as well as the total fissile content, effective fissile mass, and identification of certain types of partial defects. [4]

Previously, the DDA technique has been used to assay drums of nuclear waste for storage. [5] Compared to the traditional use, we are investigating a new application for the DDA technique in the time domain nearly directly after the short (~20 μs) neutron generator pulse. These short time scales require data acquisition system to reliably operate in a very high counting rate environment.

2. Fresh Fuel Experimental Setup

2.1. DDA Components

The DDA instrument consists of nine ^{3}He detectors inside three stainless steel detector pods, and an external DT neutron generator inside of a waterproof cylinder (Fig. 1). These components are all submerged in a water tank. A template made of high-density polyethylene (HDPE) is positioned on the bottom of the water tank to align the experimental components. A second HDPE template is used to position the detectors, which are inserted into HDPE cylinders wrapped with cadmium (Cd), inside the stainless steel pods. Neutron detection data from individual detectors are recorded using a list-mode data acquisition system such that the time of arrival of each pulse is recorded.

Figure 1. The DDA instrument setup with the experimental components slotted into the base template (left) and the setup submerged in the water tank (right).

2.2. Fresh Fuel and Assembly Specifications

Fresh fuel rods containing uranium dioxide (UO_2) were used for the active assay with the DDA instrument. A 15x15 PWR-like fuel lattice with 204 fuel pin positions and 21 guide tubes was used. The fresh fuel at LANL consists of low-enriched uranium (LEU) and depleted uranium (DU) fuel pins with an average enrichment of 3.19% and 0.22% ^{235}U, respectively. The fuel assembly and fuel pin specifications are provided in Table I.

PWR Assembly			
Lattice geometry	15 x 15		
Assembly width	21.5 cm		
Fuel pin pitch	1.4 cm		
Number of fuel pin slots	204		
Number of guide tube slots	21		
Fuel Pin Information			
Fuel type	UO_2		
Cladding type	Zircaloy-2		
Average LEU rod enrichment	3.19% ^{235}U		
Average DU rod enrichment	0.22% ^{235}U		
Fuel pellet density	10.48 g/cm^3		
Fuel pellet radius	0.4525 cm		
Cladding thickness	0.0875 cm		
Outer pin radius	0.54 cm		
Total fuel rod length	130 cm		
Active fuel length			
LEU rod	102 cm		
DU rod	120 cm		
Inert fuel regions	LEU	DU	
Top	17 cm	6 cm	
Bottom	12 cm	5 cm	

Table I: LANL PWR 15x15 fresh fuel and assembly specifications.

2.3. DT Neutron Generator

The Thermo Scientific P 385 DT neutron generator produces an approximate maximum yield of $5 \cdot 10^8$ n/s of 14.1 MeV neutrons from fusion. During experiments, the neutron generator is operated within standard manufacturer recommended parameters of 125 kV or 90 kV high voltage, 70 μA beam current, 5% or 10% duty cycle, and 2500 Hz pulse frequency. The neutron generator output is monitored using a ^{3}He flux monitor positioned outside of the water tank. The flux monitor data are compared between experimental runs to verify the consistency of the neutron generator output over time.

2.4. Detectors and Electronics

During the course of the experimental campaign, we have tested a variety of detector models and associated electronic components. In particular, we have performed a range of experiments using the PDT-10A pre-amplifiers with an AMPTEK A-111 chip for fast pulse processing [6]. These pre-amplifiers are specifically designed to operate in high count rate environments.

2.5. List-Mode Data Acquisition System and Analysis

List-mode data are acquired using a data acquisition system assembled at LANL from all commercially available parts. The DAQ system, nicknamed ARIEL, can record 32 individual data channels at up to 2MHz each and is rugged and portable with 6 TB data storage. List-mode data acquisition and analysis software was also designed at LANL for the fresh fuel DDA project.

3. Experimental Data

3.1. Deadtime Correction

The data was corrected for the deadtime of the electronics using the infinite exponential method [7]. The coefficients were determined by comparing the shape of the counting rate distributions at low and high neutron generator intensities. The deadtime correction coefficient was slightly varied to determine the impact on the die-away time magnitude in two time domains, 60-100 μs and 100-150 μs. The deadtime correction coefficient was set to 800 ns, 850 ns, and 900 ns. The die-away time of the DDA signal was determined using these three values for several fresh fuel enrichments.

As expected, we found that in the early time domain (60-100 μs), the die-away times of detectors closest to the DT neutron generator (detectors 1 and 2) were most sensitive to changes (up to 12%) in the correction coefficient. Also, cases with more fissile material (higher enrichment), were affected more than lower enriched cases. Detectors positioned further from the neutron generator (and therefore experiencing lower count rates) were considerably less affected by changes to the deadtime correction coefficient (Fig. 2A).

For the later time domain (100-150 μs), we found the detectors were not as sensitive to the deadtime correction coefficient (Fig. 2B). However, there was still a small change (0%-3%) in the determined die-away time magnitudes which should be considered when comparing experimental data to simulation results.

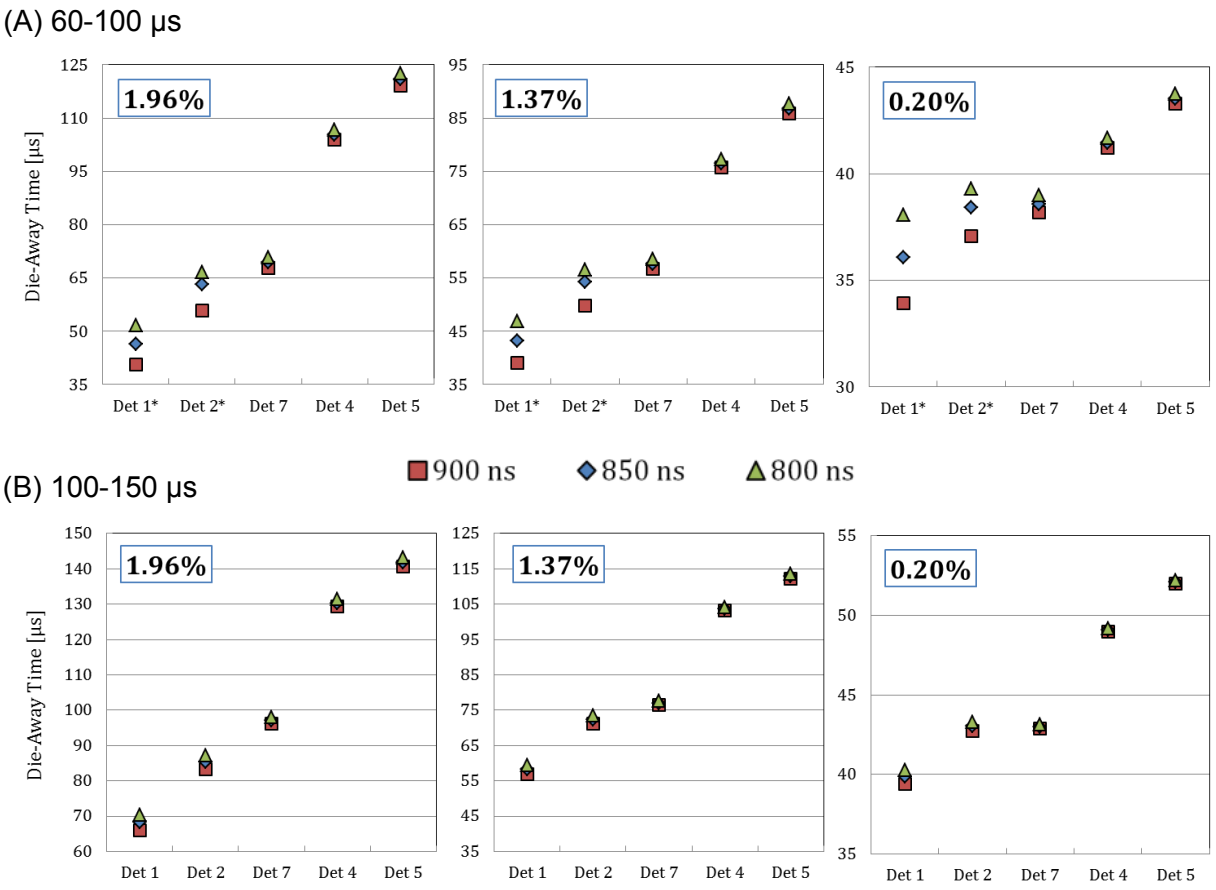

Figure 2. The experimentally measured die-away times in two time domains (A) 60-100 μs and (B) 100-150 μs for three different FFA enrichments (1.96%, 1.37%, and 0.20% ^{235}U) were calculated using different deadtime correction coefficients: 800, 850, and 900 ns. The die-away times measured by detectors 1 and 2 exhibited significant sensitivity to changes in the deadtime correction coefficient in the early time domain with die-away time values ranging ±5 μs. In the later time domain, the sensitivity of the measured die-away times on the deadtime correction coefficient nearly vanishes.

3.2. Estimation of Die-Away Time Uncertainty

The uncertainty in the experimentally determined die-away times was estimated by recording a series of 10 measurements each 30 s for three fresh fuel assembly configurations with different average enrichments (1.67%, 1.08%, and 0.49% ^{235}U) and the empty assembly without any fuel pins. For the empty fuel assembly, the DDA signal die-away time magnitude depends on the detector system properties, such as the amount of moderating material around the detectors. For each measurement, we determined the die-away time value in the 100-200 μs time interval. The mean die-away time, standard deviation of the mean, and relative uncertainty were determined for the four cases (Table II). Overall, within each set of measurements, the experimental die-away times generally differed by less than 0.5 μs, or less than 0.5%, from the mean. The relative uncertainty in the die-away time increased marginally as the amount of fissile mass in the fuel assembly decreased. Based on these results, we concluded that a measurement time of 30 s was sufficient for an accurate die-away time determination of fresh fuel. Typical uncertainties for the measured die-away times are less than 1% per detector.

	Die-Away Time [μs]			
	Average Enrichment (% ^{235}U)			
Run	1.67%	1.08%	0.49%	Empty
1	102.03	81.75	61.13	32.24
2	102.50	82.13	61.29	32.79
3	101.38	81.34	60.44	32.74
4	101.84	82.30	61.25	32.63
5	101.92	82.17	61.35	32.40
6	102.17	82.00	61.18	32.22
7	101.85	81.85	61.05	32.55
8	101.85	81.63	61.26	32.41
9	102.05	81.42	61.21	32.45
10	101.43	82.33	61.27	32.24
Mean [μs]	101.90	81.89	61.14	32.47
SDOM [μs]	0.1	0.1	0.1	0.1
SDOM [%]	0.1%	0.1%	0.1%	0.2%

Table II: The results of ten 30 s measurements: the die-away time in the 100-200 μs time interval, the mean value, standard deviation, and relative uncertainties were determined for three fresh fuel cases (1.67%, 1.08%, and 0.49% ^{235}U) and the empty setup. The relative error gradually increased as the amount of fissile mass decreased.

4. MCNPX Fresh Fuel Simulations

4.1. Simulation Setup

The DDA instrument in the MCNPX simulations was designed to reproduce the experimental setup as accurately as reasonably achievable. All of the main experimental components, including the fresh fuel assembly, water tank, three stainless steel detector pods containing a total of nine ^{3}He detectors, and the DT neutron generator in a waterproof stainless steel cylinder were modeled (Fig. 3). Material definitions from a Pacific Northwest National Laboratory report [8] were used to standardize the materials in the simulations.

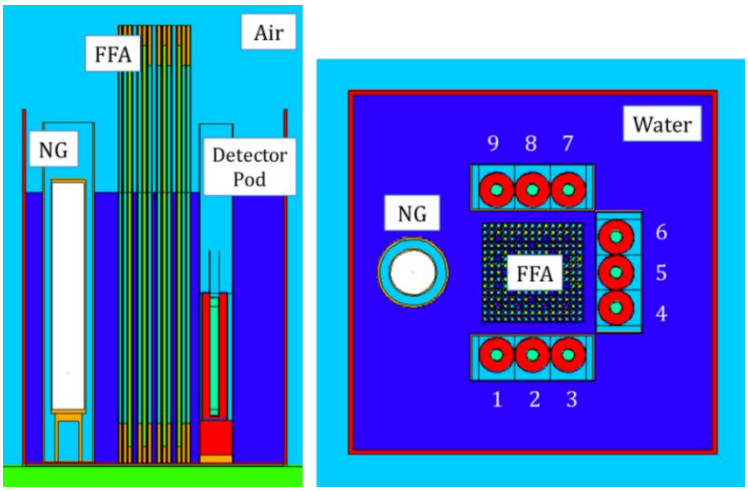

Figure 3. Schematic drawing of the DDA instrument setup as modeled in the MCNPX simulations.

4.2. Sensitivity Studies

Small variations of several parameters of the MCNPX simulations were investigated to determine the effect on the overall results. The sensitivity studies included study of the statistical variation in MCNPX results, neutron generator pulse wrap-around effects, and small changes to the detector positions.

4.2.1. Statistical Variation in MCNPX

The uncertainty of MCNPX tally results is calculated by the code based on analysis of sub-sections of the simulation. In order to estimate the uncertainty on values obtained when the MCNPX results are processed further, such as calculating the die-away time, we performed multiple MCNPX simulations with different starting random numbers and evaluated the variance of the final results.

Five nearly identical simulations, differing only by the random number, were run for two different cases, a 1.96% ^{235}U fresh fuel enrichment and an empty assembly (no fissile material). The die-away times for the nine detectors positioned around the fuel assembly were determined from the DDA signal. The mean value and the standard deviation of the die-away times were found for three different time domains: 0-50 μs, 100-150 μs, and 150-200 μs (Table III).

The variance of die-away times has been found to be relatively small when different random numbers were used, indicating that the statistical quality of each simulation was satisfactory. The 1.96% ^{235}U case seems more affected by the different random number than the empty fuel assembly case. The back detectors, primarily detector 5, experienced the largest variance. The relative error for all detector positions for both fuel assembly configurations increased with time after the neutron pulse. Typical uncertainties for the simulated die-away time values ranged from less than 1% to approximately 3.5% per detector position for the two fuel configurations.

	1.96% ^{235}U: DDA Signal Die-Away Time [μs]					
Time domain:	**50-100 μs**		**100-150 μs**		**150-200 μs**	
	Mean	SDOM	Mean	SDOM	Mean	SDOM
Detector 1	46.6	0.1	60.2	0.2	90.6	0.6
Detector 3	59.2	0.2	85.6	0.6	125.4	1.8
Detector 5	88.5	1.0	138.6	1.5	165.9	3.2
Detector 7	59.3	0.1	85.7	0.9	124.8	2.2
Detector 9	46.7	0.1	60.3	0.2	90.7	0.3

	Empty: DDA Signal Die-Away Time [μs]					
Time domain:	**50-100 μs**		**100-150 μs**		**150-200 μs**	
	Mean	SDOM	Mean	SDOM	Mean	SDOM
Detector 1	35.2	0.1	33.1	0.1	32.6	0.1
Detector 3	35.2	0.1	33.4	0.2	32.6	0.3
Detector 5	35.3	0.2	33.2	0.4	33.2	0.4
Detector 7	35.4	0.1	33.2	0.1	33.9	0.3
Detector 9	35.2	0.1	33.1	0.1	33.0	0.2

Table III: The standard deviation of the mean simulated die-away time in three time domains was calculated from five MCNPX simulations starting with different random numbers to determine the statistical variation of the results. The relative error increased in the later time domains. The back detector (detector 5) was most affected by statistical variation in the transport code. The average and standard deviation values are in units of microseconds.

4.2.2. Neutron Generator Pulse Wrap-Around Effects

In each MCNPX simulation, essentially only one neutron generator pulse is simulated. However, during an experiment, the neutron generator pulses tens of thousands of times as the DDA signal is typically acquired over several minutes. We investigated how neutrons from the previous pulse which may still be lingering in the vicinity of the fuel assembly and detectors could change the die-away time magnitude in simulations.

For experiments, the DT neutron generator is typically operated at 2500 Hz with a 20 μs long pulse. Therefore, every 400 μs a new pulse from the generator arrives to interrogate the fuel assembly. To reproduce the wrap-around effects, the tally signal from the 400-800 μs time domain respective time bins were summed with the signal from the 0-400 μs time domain. Simulated data not including the wrap-around neutrons (Fig. 4, “Original”) and including the residual neutrons (Fig. 4, “Wrap Around”) were plotted. Including the residual neutron population slightly increased the overall number of neutrons detected in the 0-400 μs time domain and slightly increased the DDA signal and die-away time magnitudes. The residual neutron (Fig. 4, “Residual Neutrons”) population is approximately two orders of magnitude less than the DDA signal from the subsequent pulse but still influences the recorded signal. On average, the pulse-wrap around effect increased the DDA die-away time magnitude by approximately 2% for all detector positions and fuel configurations (Fig. 5). The empty FFA case was not affected because our detectors are not sensitive to thermal neutrons and therefore some fission is required to create detectable signal. The results in this study have been corrected for the wrap-around effect, which

is however not expected to significantly change the uncertainty estimate discussed in the previous sections.

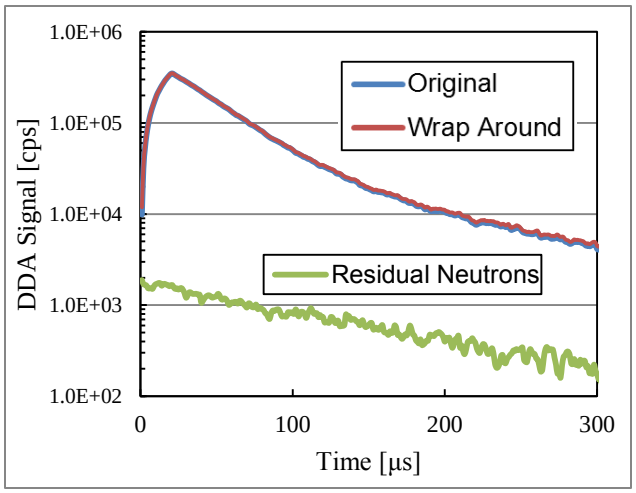

Figure 4. (Left) The simulated DDA signal from a single MCNPX simulation ("Original") was compared to the previous pulse wrap around effects included signal ("Wrap Around") from Detector 5. (Right) The magnitude of the residual neutron population from the previous pulse ("Residual Neutrons") was compared to the DDA signal magnitudes.

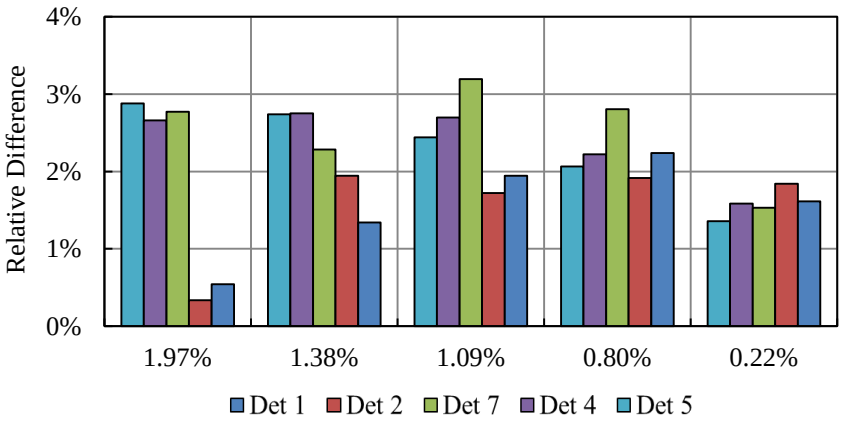

Figure 5. The relative differences between the simulated die-away times in the 100-200 μs time domain of the original and the wrap-around corrected DDA signal. The wrap around corrected die-away time magnitude was consistently larger than the original, due to neutrons still present in the vicinity of the fuel. The empty FFA die-away time was not affected by pulse wrap-around effects.

Another potential effect is the influence of delayed neutrons on the DDA signal. Technically, delayed neutrons are included in the MCNPX simulations; however, the time cutoff of the tally for a single neutron history (1 ms) effectively excludes delayed neutrons from contributing to the tally. We expect delayed neutrons to contribute a constant background to the DDA signal. We intend to investigate the influence of delayed neutrons on the DDA signal in a future study.

4.2.3. Detector Position

The effect on the DDA signal magnitude by changing the detector positions with respect to the FFA and the effect on the DDA signal die-away time when moving the detectors horizontally along the side of the FFA were investigated through MCNPX simulations.

Moving the detectors 4 mm away (relative to the best known position) from the fuel assembly resulted in a 1-2% decrease of the DDA signal magnitude recorded from most detectors. Shifting the detectors 4 mm closer to the FFA resulted in a 1-4% increase of the DDA signal recorder by most detectors. Horizontal shifts of the detectors also caused changes to the DDA signal die-away times; however, the magnitude of the effect of the shift was partially dependent on the detector position and time domain over which the die-away time was determined. Moving the detectors ±2 mm from the best known position resulted in the largest changes to the back detector (detectors 4-6) die-away times in the 70-100 μs and 100-130 μs time domains. The back detector die-away times changed approximately 1-5% with the horizontal detector shifts. The die-away times in the front detectors were more affected in the 100-130 μs time interval (1-4% change) than directly after the neutron generator pulse.

In future experiments, we will use additional components to strictly fix the positions of the detectors relative to the FFA as small changes to the DDA instrument geometry results in measurable changes to the DDA signal magnitude and die-away time.

5. Comparison of Experiment and Simulation

The experimental and simulated results were compared to determine how accurately we are able to model the complex DDA signal using MCNPX. We evaluated two observables from both the experimental data and the simulation results: the time-dependent behavior of the DDA signal and the DDA signal die-away time magnitude in two time domains.

From previously performed niobium foil irradiations, the DT neutron generator yield at the operating high voltage of 90 kV was estimated to be $1.8 \cdot 10^8$ n/s ± 5%. A deadtime correction coefficient of 875 ns was used to correct the experimental data. Both the experimental and simulated data were acquired in 5 μs bins; the DDA signals were then converted to counts per second.

5.1. The Dynamic Evolution of the DDA Signal

The experimental (red) time-dependent DDA signal is plotted with the MCNPX simulation results (blue) in Figure 6. Overall, we found the experimental and simulated DDA signal distributions compared well within experimental and simulation uncertainties. The DDA signals trend well for multiple enrichments and detector positions. (Note: Detectors 3 and 7 are positioned symmetrically around the FFA such that we expect statistically identical results for uniform assembly configurations.)

Detector 1 was heavily impacted by deadtime directly after the neutron generator pulse. The deadtime effects are due to the very high count rate experienced by the detector and electronics due to its position close to the DT neutron generator. The count rates in the front detectors (detectors 1 and 2) were so high that the deadtime correction model failed at the earliest times (<70 μs) times, giving rise to signal excursions (seen above the pulse peak in red). In the future, we intend to upgrade our experimental detector/electronics packages by using LANL-made faster post-burst recovery electronics [9] to improve the data quality in the early time domains. We will also consider reducing the efficiency of the front detectors by decreasing the radial thickness of the HDPE sleeves.

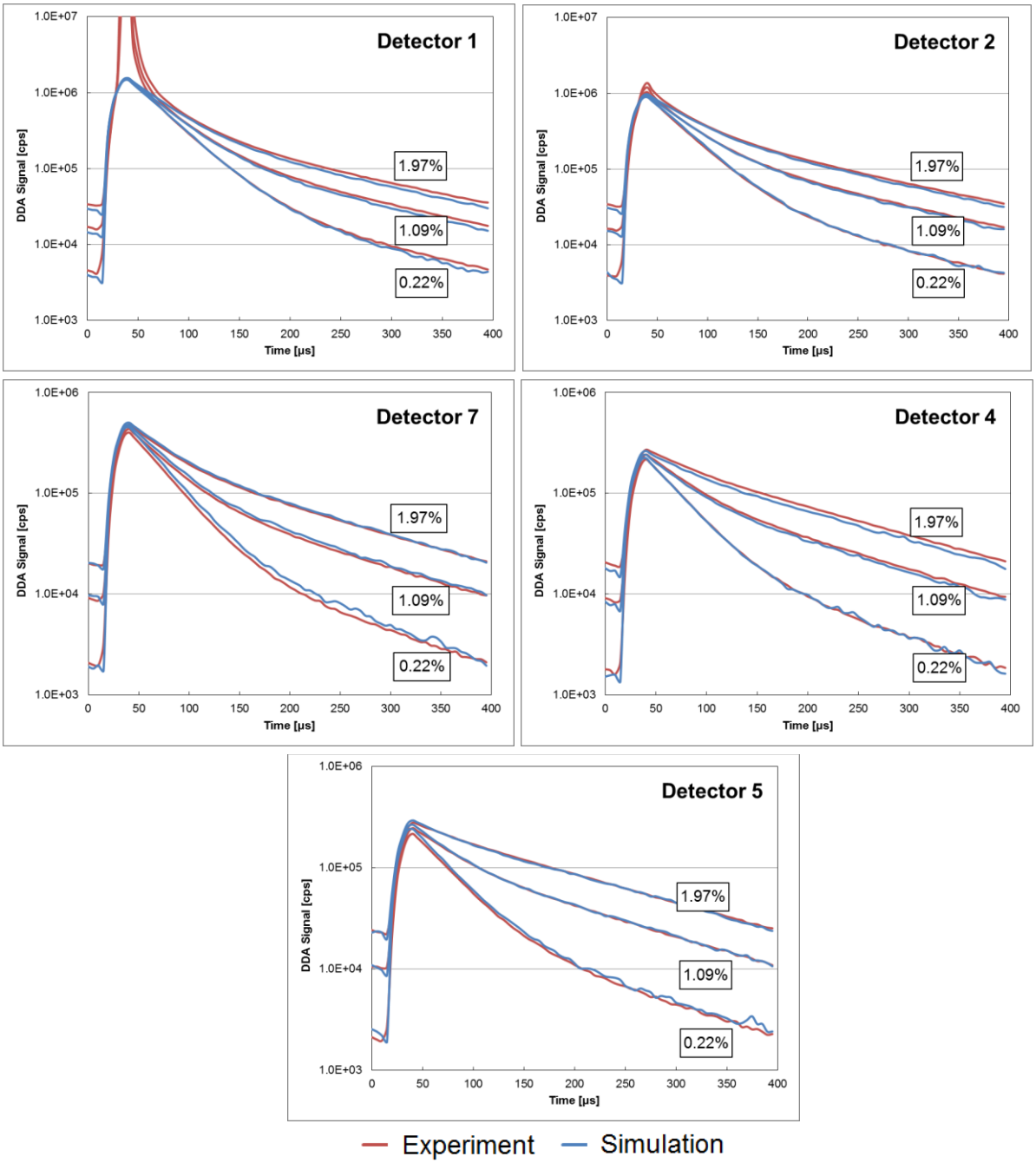

Figure 6. The dynamic evolution of the DDA signal is plotted for three fresh fuel enrichments for five detectors positioned around the FFA.

5.2. Die-Away Time as a Function of Enrichment

The DDA signal die-away time values for the 70-100 μs and 100-150 μs time periods were determined from the experimental and simulated results and compared. In the early time domain (70-100 μs), the MCNPX simulated die-away times trended well with the experimental die-away times (Fig. 7). Detectors 1 and 2 were particularly sensitive to deadtime correction in the early time domain due to the very high count rates recorded by the front positions (close to the DT neutron generator). The die-away times for

detectors 7, 4, and 5 compared well for all fresh fuel enrichments and the empty case. We also found good agreement between the experimental and simulated die-away times in the later time domain (100-150 µs) when deadtime was no longer significantly affecting the DDA signal.

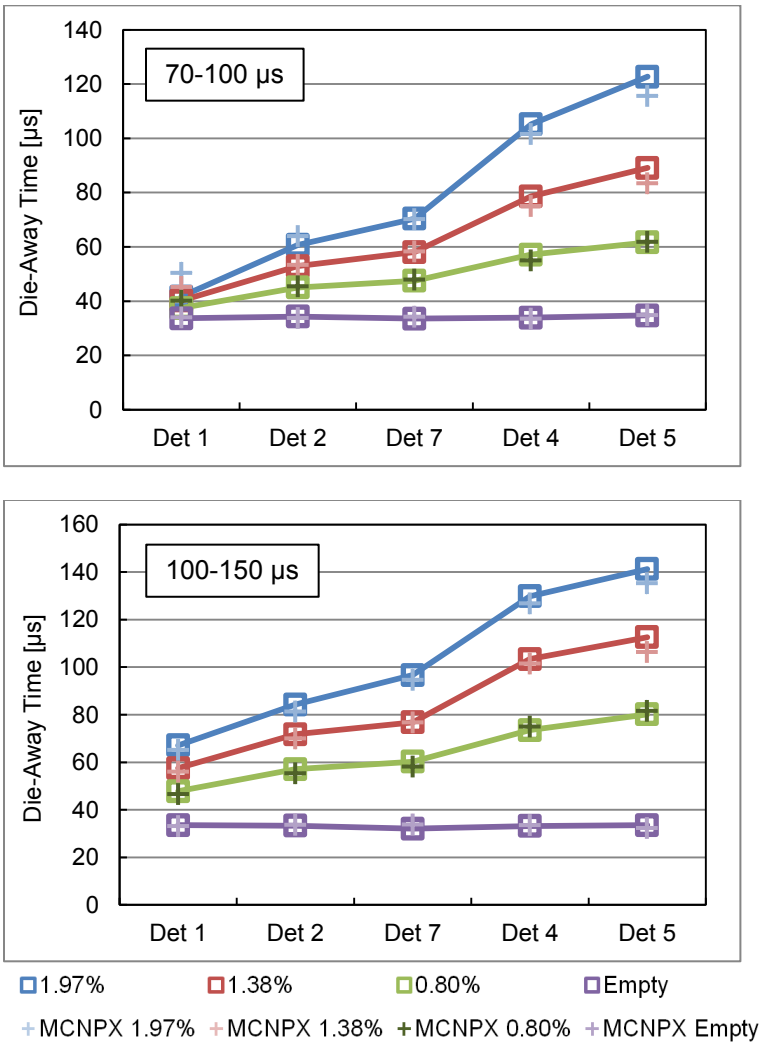

Figure 7. Comparison of the experimental (square) and simulated (cross) die-away times of the DDA signal in the 70-100 µs and 100-150 µs time domain for four FFA enrichments.

We determined the relative differences between the experimental and simulated DDA signal die-away times for the 70-100 µs and 100-150 µs time domains (Fig. 8). We found good agreement between the experimental and simulated die-away times both in terms of trending with the average enrichment of the fresh fuel assembly and the magnitude. In the early time domain (70-100 µs), the experimental DDA signals from detector 1 was recovering from the DT neutron generator burst which affected the die-away time magnitude. However, the die-away time values from detectors 2, 7, 4, and 5 compared well with the simulated results, with an average relative difference of approximately ±2.3%. In the later time domain (100-150 µs), the die-away time values compared well for all detectors for all fresh fuel arrangements, with an average relative difference of approximately ±2.6%.

From the mainly positive relative difference values for both time domains, the simulation generally underestimated the DDA signal die-away time. The minor discrepancies between simulation and

experiment die-away time magnitudes may have been caused by small geometry errors or the lack of delayed neutrons contributing to the DDA signal in simulation.

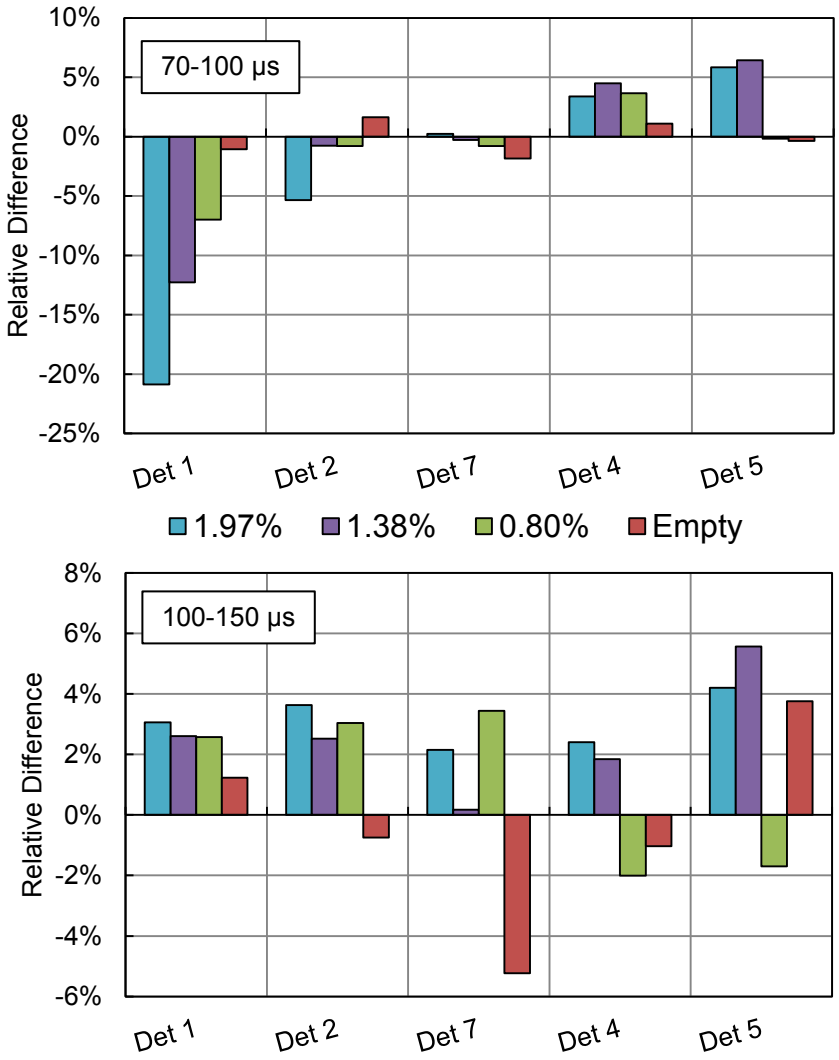

Figure 8. In the early time domain (70-100 µs), the die-away times as a function of average FFA enrichment from Detectors 2, 7, 4, and 5 compares fairly well with the simulated results, with an average relative difference of approximately ±2.3%. Detector 1 was overwhelmed by deadtime which affected the die-away time determination. In the later time domain (100-150 µs), the die-away times as a function of average FFA enrichment from all detectors compared well with the experimental results, with an average relative difference of ±2.6%.

6. Discussion and Conclusions

Overall, we found good agreement between the experiment and simulation, with the relative difference (approximately 3%) between the die-away time results within uncertainty (approximately 5%). The uncertainty on the die-away time is dependent on statistical variation in the exponential fit (<1%) and small discrepancies between the experimental setup and simulation geometry (up to 5%). Other uncertainties affecting the DDA signal magnitude include the DT neutron generator yield and the absence of delayed neutrons in the simulations. The die-away time comparison has less uncertainty because it is

independent of the absolute neutron generator strength but is still affected by the uncertainty in the deadtime correction coefficient, particularly for the front detectors in the early time period.

We plan to continue to perform experiments and simulations of the fresh fuel assay by the DDA instrument. We are planning to upgrade our detector and electronics packages by using faster post-burst recovery systems. Improved electronics will decrease deadtime effects and allow for more accurate analysis of the DDA signal closer to the DT neutron generator peak. We also intend to investigate the effect of delayed neutrons on the DDA signal through the experiment.

We have shown that the DDA instrument is capable of practically measuring the complex time-dependent signal from a fuel assembly that is interrogated by pulsed external neutron source. Through the experiments and simulations described in this paper, we demonstrate that MCNPX produces a reliable and accurate DDA model. These results lend credibility to the previously performed spent fuel simulations which showed the capabilities of the DDA instrument to characterize spent fuel for nuclear safeguards applications.

8. Acknowledgements

The authors would like to acknowledge the support of the US National Nuclear Security Administration's Office of Defense Nuclear Nonproliferation Research and Development.

9. Legal Matters

We agree that ESARDA may print our names/contacts data/photograph/article in the ESARDA Bulletin/Symposium proceedings or any other ESARDA publications and when necessary for any other purposes connected with ESARDA activities.

10. References

[1] D. Pelowitz and et al., "MCNPX User's Manual, Version 2.7.0," Los Alamos National Laboratory, LA-UR-11-00438, 2011.

[2] M. Humphrey, S. Tobin and K. Veal, "The Next Generation Safeguards Initiative's Spent Fuel Nondestructive Assay Project," *Journal of Nuclear Materials Management,* vol. 40, no. 3, 2012.

[3] V. Henzl, M. Swinhoe, S. Tobin, H. Menlove, J. Galloway and D. Won Lee, "Direct Measurement of Initial Enrichment, Burn-up and Cooling Time of Spent Fuel Assembly with a Differential Die-Away Technique Based Instrument," in *Institute of Nuclear Materials Management*, Orlando, 2012.

[4] V. Henzl, "Evaluation of Differential Die-Away Technique Potential in Context of Non-Destructive Assay of Spent Nuclear Fuel," Los Alamos National Laboratory, LA-UR-14-29224, 2014.

[5] K. Coop, "Neutron dieaway methods for criticality safety measurements of fissile waste," in *Winter meeting of the American Nuclear Society*, San Francisco, 1989.

[6] AMPTEK, "A111 Charge Sensitive Preamplifier & Discriminator," AMPTEK, [Online]. Available: http://www.amptek.com/products/a111-charge-sensitive-preamplifier/. [Accessed September 2014].

[7] A. Goodsell, M. Swinhoe, V. Henzl, K. Ianakiev, M. Iliev, C. Rael and D. Desimone, "Differential Die-Away Instrument: Report on Neutron Detector Recovery Performance and Proposed Improvements," Los Alamos National Laboratory; LA-UR-14-27369, 2014.

[8] R. McConn, C. Gesh, R. Pagh, R. Rucker and R. Williams III, "Compendium of Material Composition Data for Radiation Transport Modeling," PNNL-15870 Rev. 1, Richland, 2011.

[9] K. Ianakiev, M. Iliev and M. Swinhoe, "High Count Rate Thermal Neutron Detectors and Electronics," IAEA-CN-220, 2014.

Detection of fission signatures induced by a low-energy neutron source

A. Ocherashvili[a], V. Mayorov[b], A. Beck[a], G. Heger[c], E. Roesgen[b], J.-M. Crochemore[b], M. Mosconi[b], B. Pedersen[b]

[a] Physics Department
Nuclear Research Center Negev
P.O. Box 9001, 84190 Beer-Sheva, Israel

[b] Nuclear Security Unit
Institute for Transuranium Elements (ITU)
Joint Research Centre, European Commission
Via E. Fermi 2749, Ispra 21027 (VA), Italy
bent.pedersen@jrc.ec.europa.eu

[c] Israel Atomic Energy Comission
P.O. Box 7061, 61070 Tel Aviv, Israel

Abstract:
We present a method for the detection of special nuclear materials (SNM) in shielded containers which is both sensitive and applicable under field conditions. The method uses an external pulsed neutron source to induce fission in SNM and subsequent detection of the fast prompt fission neutrons. The detectors surrounding the container under investigation are liquid scintillation detectors able to distinguish gamma rays from fast neutrons by means of the pulse shape discrimination method (PSD). One advantage of these detectors, besides the ability for PSD analysis, is that the analogue signal from a detection event is of very short duration (typically few tens of nanoseconds). This allows the use of very short coincidence gates for the detection of the prompt fission neutrons in multiple detectors while benefiting from a low accidental (background) coincidence rate yielding a low detection limit. Another principle advantage of this method derives from the fact that the external neutron source is pulsed. By proper time gating the interrogation can be conducted by epithermal and thermal source neutrons only. These source neutrons do not appear in the fast neutron signal following the PSD analysis thus providing a fundamental method for separating the interrogating source neutrons from the sample response in form of fast fission neutrons. The paper describes laboratory tests with a configuration of eight detectors in the Pulsed Neutron Interrogation Test Assembly (PUNITA). The sensitivity of the coincidence signal to fissile mass is investigated for different sample and configurations and interrogation regimes.

Keywords: Nuclear security, SNM detection, PSD, neutron generator

1. Introduction

Passive and active non-destructive assay (NDA) methods have potential in practical applications as a means to detect special nuclear materials (SNM). The prompt emission from fission of neutrons and γ-rays appear to be useful signatures for the detection of SNM in shielded containers. One reason for this is that a component of the prompt γ-rays from fission are of high energy and thus very penetrating and difficult to deliberately shield from detection. Furthermore identifying the detected radiation to be originating from fission events is evidence of the presence of SNM in the object under investigation. To this end it is useful to arrange the detection system to take advantage of the fact that during the fission event multiple prompt γ-rays and neutrons are emitted simultaneously [1-3].
Using an external neutron source to induce fission extends the usefulness of this detection method to apply not only to spontaneous fissile elements but also to elements with a cross-section for neutron induced fission. Pulsing of the external neutron source can provide further advantages to be exploited in the detection method. This includes the fact that by proper timing (gating) of the detection period

with respect to the neutron emission from the external source, the object can be interrogated by a low energy neutron flux (epi-thermal or thermal neutron flux) only, providing the possibility to distinguish the fast fission neutrons from the low energy source neutrons in the neutron detection system [4].
In the present work we study epi-thermal neutron interrogation only. The thermal interrogation has been demonstrated to yield a response proportionally to the fissile mass. In the epi-thermal interrogation, which is desirable for nuclear security purposes, the response is harder to interpret due to the large proportion of gamma detection events in the detector during slowing-down of the source neutrons.

2. Experimental setup

The Pulsed Neutron Interrogation Test Assembly (PUNITA) of the Joint Research Centre is designed for experimental studies in non-destructive analysis (NDA) methods for nuclear safeguards and security. Figure 1 shows a cross section of PUNITA and the positioning of the detectors used in this work. The facility is composed of a large graphite liner surrounding a central cavity of volume 50x50x80 cm^3. The (D-T) pulsed neutron generator, the sample under investigation and the scintillation detectors used for coincident detection are located inside the cavity. In total 96 one metre long ^{3}He neutron detectors are embedded in polyethylene modules and shielded by cadmium (fission neutron counters in Figure 1). In the present experiments these detectors are used as reference detectors of the prompt fission neutrons.

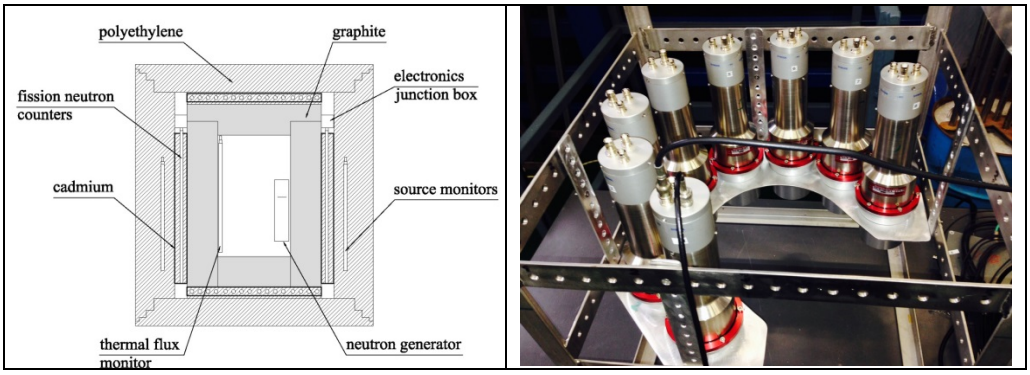

Figure 1: Sketch of PUNITA showing the permanently mounted neutron detectors and the neutron generator mounted inside the sample cavity (left picture). The right hand picture shows the positioning of the eight liquid scintillation detectors within the sample cavity of PUNITA.

In Figure 1 is also indicated, as source monitors, bare ^{3}He neutron detectors which are used to normalize detector readings in all experiments to the same total neutron emission from the generator target. The neutron generator (Model A-211 from Thermo Fisher Scientific Inc.) is pulsed at 100 Hz which is chosen based on the average thermal neutron lifetime in the graphite/cavity configuration. The thermal flux generated by source neutrons being thermalized in the graphite peaks at about 250 μs after the 14-MeV neutron burst [6]. The generator is able to produce short and intense bursts of neutrons with no neutron emission between bursts. This fact, together with the very short duty-cycle of one per mille, allow separation of the neutron interrogation into a fast/epi-thermal period from zero to 120μs, and a thermal period from 250 μsec to 9 msec, respectively [4].

We use of an array of eight 3”x3” liquid scintillation detectors EJ-309 from Eljen Technology [5] for the detection of the prompt radiation from fission events (Figure 1). These detectors can distinguish fast neutron interactions from other interactions by means of pulse shape discrimination (PSD). The detection principle is based on the simple fact that detection of fast (fission) neutrons is evidence for the presence of fissile material. The performance of scintillation detectors with respect to γ/n discrimination in the PUNITA facility is described in [4]. Due to the very fast response of the scintillation detectors the effect of the neutron generator burst can be followed in detail [7].

The anode output of the photomultiplier is connected directly to a signal digitizer. Each detector was supplied with individual high voltage (NDT1740) [8] to allow having same response in all detectors to a given photon source. The detectors were calibrated using the following photon sources: ^{133}Ba (Eγ=356 keV), ^{137}Cs (Eγ=662 keV), ^{54}Mn (Eγ=835 keV), and ^{22}Na (Eγ=511,1274 keV). The upper end of the dynamic range is set to eliminate the 2.223 MeV photons produced by thermal neutron capture in

hydrogen, and the lower end of the dynamic range is set to the PSD resolution value at 120.6 keVee as achieved with a ^{252}Cf source.

The signal digitizers used in this work are from Signal Processing Devices Sweden AB (http://spdevices.com/). Figure 2 shows the triggering and data processing scheme used in these experiments.

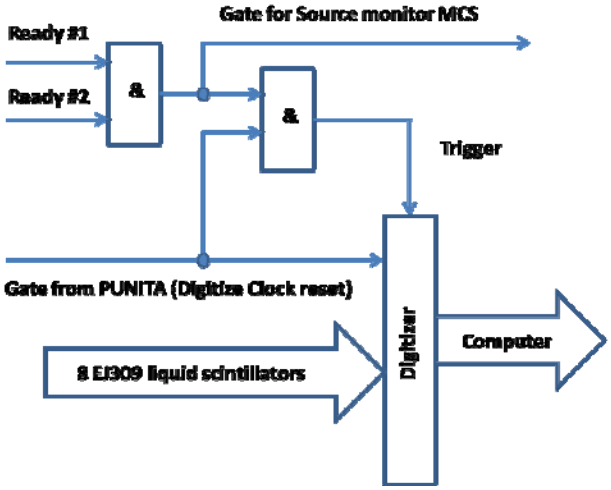

Figure 2: Data triggering scheme.

By delaying the data recording period from the neutron generator burst (Figure 2, "Gate from PUNITA") the data acquisition can be tailored to a certain neutron energy range. In an earlier work interrogation was done by thermal neutrons only using a triggering scheme based on detection of multiple signals [7]. In the present work concerned with epi-thermal neutron interrogation this triggering scheme is not efficient due to the very high rate of photon detections during the slowing down of the generator neutrons. In contrast the present triggering scheme (Figure 2) is very simple. A data stream from the eight scintillation detectors is recorded following a "ready" signal from the digitizers and for the duration of the PUNITA Gate. The recorded waveforms are 95 μs long, digitized at 1 GS/s and 12-bit resolution and constitute a single data cycle. Such data streams are recorded at 100 Hz.

All recorded waveforms are analyzed offline in MATLAB [9]. A signal is defined as having an amplitude larger than 3σ of the baseline variation. Examples are shown in Figure 3. All signals are extracted by such criteria.

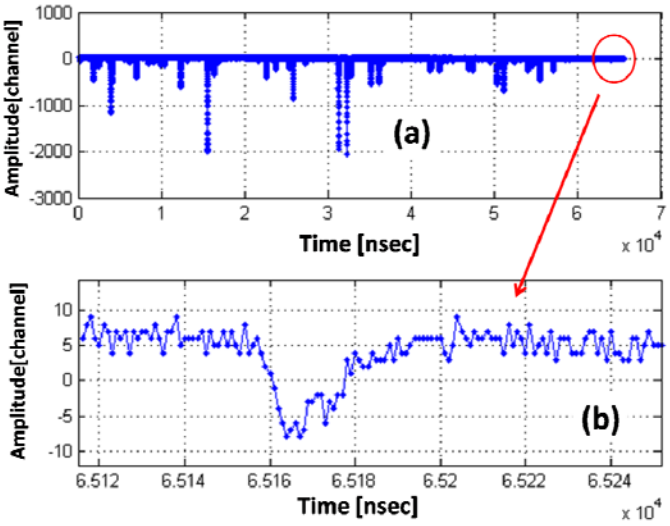

Figure 3: Typical waveform of epithermal data (a), in picture (b) is shown analyzes of the last signal.

The initial data analysis produces a list of all signals. The signals are described in terms of: signal amplitude, time stamp (t_0), detector number and PSD value. From this list the neutron signals can be selected as in standard list-mode operation of neutron multiplicity analyzers. This allows us the possibility of using standardized principles from passive neutron multiplicity analyses. In addition we can analyze mixed photon/neutron streams.

3. Measurements of uranium samples in PUNITA

A series of standard CNNM U_3O_8 sources [10] are used in conjunction with the pulsed neutron interrogation and eight EJ-309 scintillation detectors. The five CBNM standards are identical in all aspects (total U mass of about 169 grams, density, geometry, container type) except for the ^{235}U enrichment. The mass of the fissile ^{235}U component is 0.52 g (0.31%), 1.12 g (0.71%), 3.28 g (1.94%), 4.99 g (2.96%) and 7.54g (4.46%), respectively. Also measurements of an empty CBNM container are included for the purpose of comparison. The sample is placed centered among the eight detectors at a distance of 150 mm.

Figure 4 shows the MCNP simulated source neutron spectrum in discrete periods of the range 27 μs to 135 μs after the 14-MeV burst. In the present analysis we use the period 28 μs to 123 μs i.e. 95 μs. Also shown in Figure 4 are the capture and fission cross-sections of some isotopes. Clearly in the selected time period fission is only induced in the ^{235}U isotope. One can also estimate that for CBNM samples of small ^{235}U content, the capture reaction in ^{238}U becomes relatively important compared to fission in ^{235}U.

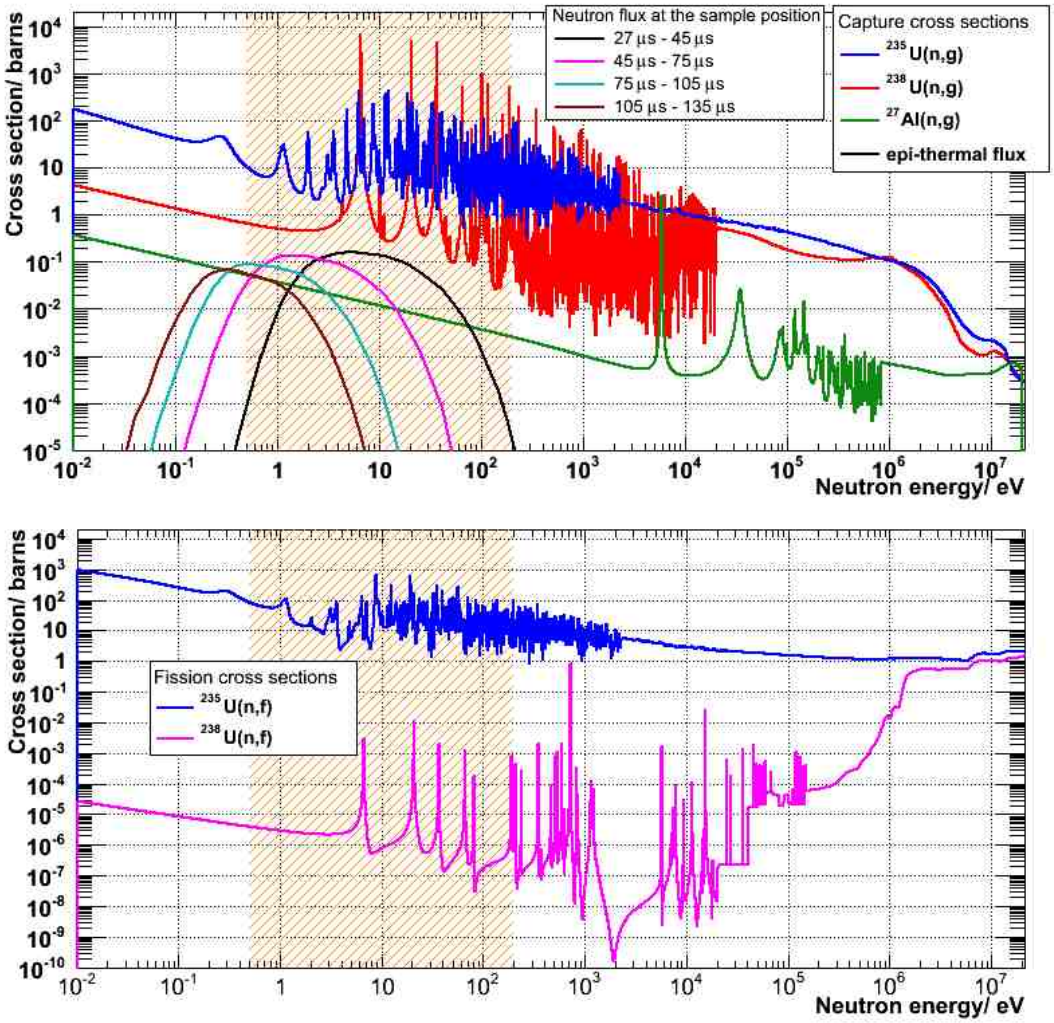

Figure 4: Epi-thermal neutron cross section for ^{235}U(n,γ), ^{238}U(n,γ), and Al((n,γ), (top picture) and ^{235}U(n,f), ^{238}U(n,f) (bottom picture).

3.1 Neutron multiplicity counting

As mentioned above continuous waveforms of 95 μs length were recorded, starting at 28 μs delay after the 14-MeV neutron burst. Figure 5 shows a distribution of the pulse time stamp (t_0) for neutrons only.

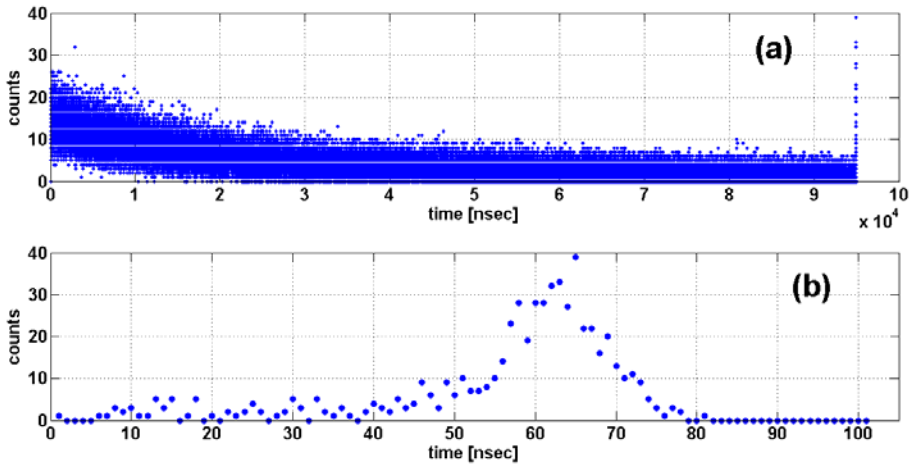

Figure 5: Distribution of time stamps (t_0) for neutron associated pulses (a), picture (b) shows zoom of last 100 ns of the waveform for the CBNM446 sample (4.46% ^{235}U).

In Figure 5(a) the detected neutron counts decreases until about 30 μs. The neutron detections in this range are mostly fast neutrons from the generator. Neutrons of energy below about 700 keV do no longer produce a signal (PSD) in the detectors associated with neutron detection. After 30 μs most detected neutrons are fast fission neutrons. The slowly falling rate of neutron detections is due to the decaying neutron flux (in spite of the increasing fission cross section for lower energies). We divide our data analyses into three parts: 28-59 μs, 59-81 μs and 81-123 μs. For this data we use a kind of Shift Register analysis on the neutron associated "Rossi-alpha" kind of distributions.

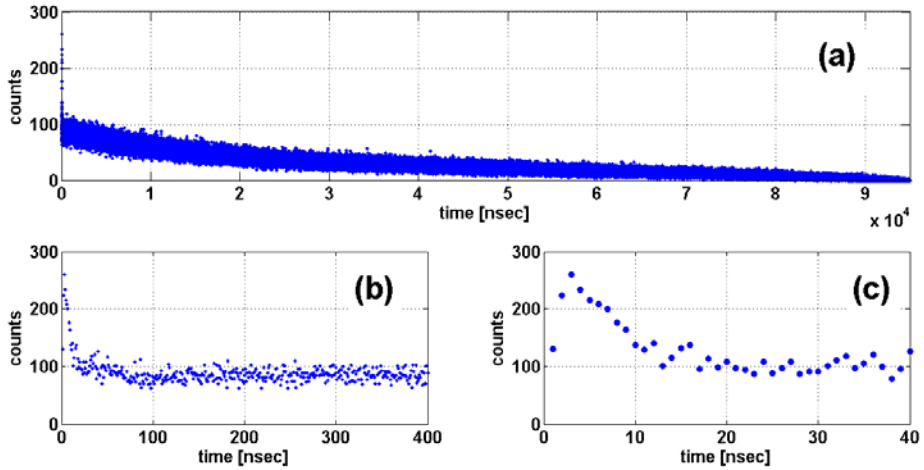

Figure 6: Neutron asosiated "Rossi-alpha" kind of distribution for CBNM446 sample: (a) entire picture, (b) zooming of first 400 ns and (c) zooming of first 40 ns.

As can be seen in Figure 6(b) a "Rossi-alpha" distribution of detected neutrons quite similar to what is observed in standard passive neutron counting of spontaneous fission events although the time scale is quite different. We consider two time gates: one immediately following a neutron signal of length 20 ns (called the prompt gate (PG)), and another in the period 250÷270 ns after the first (called the delayed gate (DG)). We form frequency distributions of number of neutron detections in the gates, calculate the 1st factorial moment from the distribution, and make the subtraction PG – DG. For different samples measurements this result is normalized to the Source Monitor (SM) counts

(proportional to the neutron emission from the generator). Figure 7 shows the results of the CBNM uranium samples.

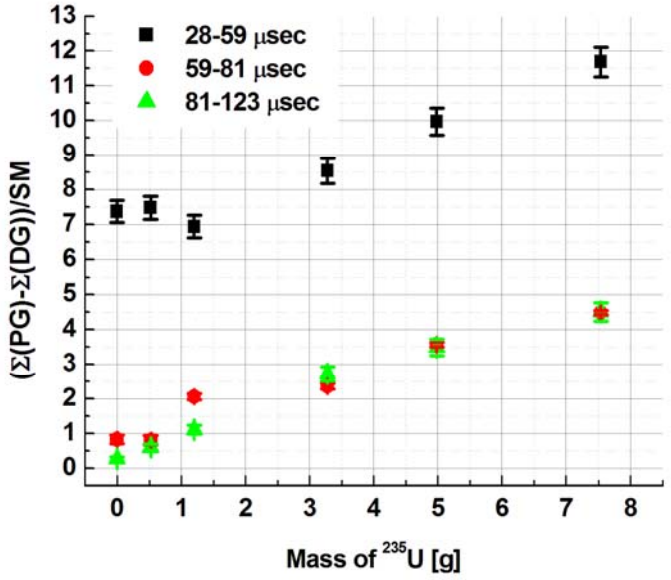

Figure 7: Difference between PG and DG gates of neutron pair events normalised to the neutron emission of the neutron generator.

For the time period of 28-59 µs the linearity is not good for the smallest sample and the empty container. The reason might be that fast source neutrons still persist in this range.

The result for counting the total number of neutron detection events (single neutrons) is presented in Figure 8. In this case the earlier period (28-59 µs) does not show linearity with fissile mass. The reason is likely due to source neutrons still being observed as fast neutrons in the detectors.

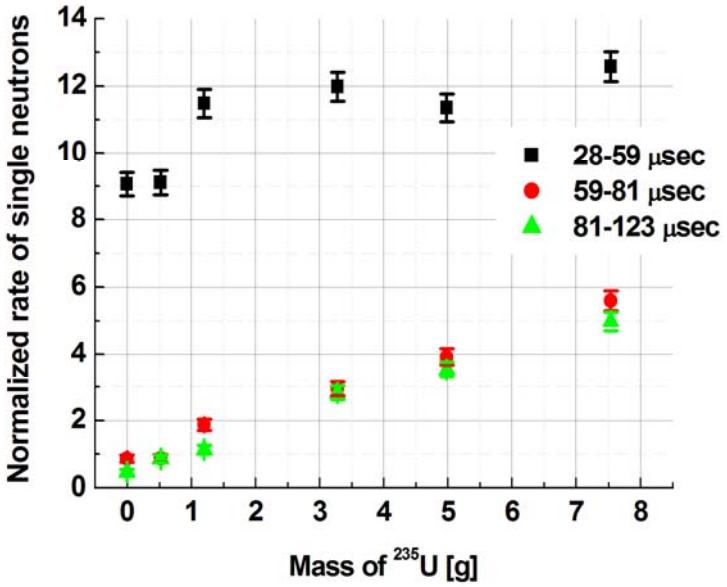

Figure 8: Detected normalized rate of single neutrons.

4. Conclusions

In the present work we have investigated a detection method for special nuclear material based on an epi-thermal source of neutrons inducing fission is fissile isotopes, and the detection of fast prompt fission neutrons as a signature of the presence of fissile material. The advantage of this method is that epi-thermal neutrons have sufficiently low energy not to leave a neutron signature in the liquid scintillation detectors, while the neutron energy is sufficiently high for the neutrons to pass through thermal neutron shielding, and induce fission in fissile isotopes. The suitable source neutron energy range is selected by varying the delay of interrogation following a burst of 14-MeV neutron from a pulsed neutron generator placed in a strongly moderating detection assembly. The difficulty in epi-thermal interrogation is the overwhelming photon response in the detectors during the slowing-down of the source neutrons. By recording all detection events in eight scintillation detectors in a selected period of about 30 μs during slowing-down of the source neutrons, a clear signature, proportional to the fissile mass, of prompt neutrons from induced fission by epi-thermal neutrons was observed.

The purpose of this work is to investigate the feasibility of a device for the detection of SNM that would combine epi-thermal and thermal neutron interrogation, and would be both sensitive to the presence of fissile materials and be able to overcome potential thermal neutron absorbers placed around the fissile material.

5. References

[1] Enqvist A, Flaska M, Dolan J L, Chichester D L, Pozzi S A; *A combined neutron and gamma-ray multiplicity counter based on liquid scintillation detectors;* Nucl. Instr. Meth. A; 652; 2011; p. 48-51.

[2] Pozzi S A, Clarke S D, Flaska M, Peerani P; *Pulse-height distributions of neutron and gamma rays from plutonium-oxide samples*; Nucl. Instr. Meth. A; 608(2); 2009; p. 310-315.

[3] Clarke S D, Flaska M, Pozzi S A, Peerani P; *Neutron and gamma-ray cross-correlation measurements of plutonium oxide powder*; Nucl. Instr. Meth. A; 604(3) 2009; p. 618-623.

[4] Ocherashvili A, Roesgen E, Beck A, Caspi E N, Mosconi M, Crochemore J M, Pedersen B; *SNM detection by means of thermal neutron interrogation and a liquid scintillation detector*; JINST, 7 CO3037, 2012

[5] www.eljentechnology.com

[6] Favalli A, Mehner H-C, Crochemore J-M, Pedersen B; *Pulsed Neutron Facility for Research in Illicit Trafficking and Nuclear Safeguards*; IEEE Transactions on Nuclear Science; 56(3); 2009; p. 1292-1296.

[7] A. Ocherashvili, M. Mosconi, J-M. Crochemore, A. Beck, E. Roesgen, V. Mayorov, B. Pedersen, Fast neutron coincidences from induced fission as a method for detection of SNM, ESARDA Bulletin, Issue No 49, p42-51, July 2013.

[8] CAEN High Voltage unit NDT1740, http://www.caen.it/

[9] MATLAB 7.0 and Statistics Toolbox 7.1, The MathWorks, Inc., Natick, Massachusetts, United States.

[10] Carpenter B S, Gramlich J W, Greenberg R R, Machlan L A, DeBievre P, Eschbach H L, Meyer H, Van Andenhove J, Connelly V E, Trahey N M, and Zook A; Standard Reference Materials: Uranium 235 Isotopic Abundance Standard Reference Materials for Gamma Spectrometry Measurements; National Bureau of Standards Special Publication 260-96; U.S. Government Printing office Washington; 1986.

[11] X-5 Monte Carlo Team Diagnostics Applications Group Los Alamos National Laboratory; MCNP – A general Monte Carlo N-Particle Transport Code, Version 5, Volume I: Overview and Theory; LA-UR-03-1987; 2003; Los Alamos National Laboratory

Preliminary Results of the 2014 Field Trial of the Advanced Experimental Fuel Counter (AEFC) for Verification of Research Reactor Spent Fuel at the Institute of Nuclear Physics (INP)

K. Miller[1], H. Menlove[1], C. Rael[1], S. Baytelesov[2], F. Kungurov[2], J. Yusupov[2], U. Salikhbaev[2], M. Mayorov[3], U. Yavuz[3], B. Reid[4], C. Gesh[4], J. Marlow[1], L. Szytel[5]

[1] Los Alamos National Laboratory, Los Alamos, New Mexico, USA
[2] Institute of Nuclear Physics, Tashkent, Uzbekistan
[3] International Atomic Energy Agency, Vienna, Austria
[4] Pacific Northwest National Laboratory, Richland, Washington, USA
[5] U.S. Department of Energy, Washington, D.C., USA

E-mail: kamiller@lanl.gov, hmenlove@lanl.gov, cdr@lanl.gov, baytel@inp.uz, fkungurov@inp.uz, yusupovdjalil@inp.uz, salikhbaev@inp.uz, m.mayorov@iaea.org, u.yavuz@iaea.org, bruce.reid@pnnl.gov, gesh@pnnl.gov, jmarlow@lanl.gov, lisa.szytel@nnsa.doe.gov

Abstract:

The Advanced Experimental Fuel Counter (AEFC) is a nondestructive assay (NDA) system developed at Los Alamos National Laboratory (LANL) and designed for underwater measurement of research reactor spent fuel assemblies. The system has components for active and passive neutron coincidence counting and an ion chamber for gross gamma-ray counting. The basic measurement objective of the AEFC is to verify the residual fissile mass (i.e., $^{235}U + ^{239}Pu$) in spent fuel assemblies using active neutron interrogation. Extended analysis of the passive neutron and gamma-ray signatures provides a consistency check on the operator declaration of parameters such as burnup, cooling time, and initial enrichment. The passive signatures can provide quantitative assessments of these parameters if combined with burnup and detector modelling codes. In 2014, the Institute of Nuclear Physics (INP) in Tashkent, Uzbekistan hosted an AEFC field trial. This paper summarizes the preliminary results of the measurements at the INP WWR-SM research reactor.

Keywords: NDA; neutron; gamma; spent; fuel

1. Introduction

The Advanced Experimental Fuel Counter (AEFC) is a nondestructive assay (NDA) system developed at Los Alamos National Laboratory (LANL) and designed for underwater measurement of research reactor spent fuel assemblies. The system uses active and passive neutron coincidence counting and an ion chamber for gross gamma-ray counting. The basic measurement objective of the AEFC is to verify the residual fissile mass (i.e., $^{235}U + ^{239}Pu$) in spent fuel assemblies using active neutron interrogation. Extended analysis of the passive neutron and gamma-ray signatures provides a consistency check on the operator declaration of parameters such as burnup, cooling time, and initial enrichment. The passive signatures can provide quantitative assessments of these parameters if combined with burnup and detector modelling codes. This paper summarizes the preliminary measurement results of the 2014 AEFC field trial at the Institute of Nuclear Physics (INP) in Tashkent, Uzbekistan.

There have been two previous field tests of the AEFC. The first occurred in 2006 in Australia,[1] and the second occurred in 2011 at the INP WWR-SM reactor in Uzbekistan.[2] The field trial that is the subject of this paper was also performed at the INP WWR-SM reactor. Participants measured a total of

twenty-one spent fuel assemblies, which included twelve IRT-4M and nine EK-10 assemblies. The field trial introduced a new three-point fuel scanning procedure and successfully demonstrated that ^{252}Cf can be used as the active neutron interrogation source for the AEFC in lieu of AmLi. Interrogation with ^{252}Cf is based on the Time-Correlated Induced Fission (TCIF) concept.[3] This paper describes the AEFC design, operating parameters, measurement procedure, and preliminary results of the IRT-4M measurements.

2. AEFC Design

2.1. Signatures & Observables

Verification of spent fuel assemblies is complicated by the fact that there are multiple fuel parameters folded into the radiation signatures. Where active neutron measurements can provide an unambiguous measure of the residual fissile mass in spent fuel for a given fuel type, the passive neutron and gamma-ray signatures are generally a function of burnup, cooling time, and initial enrichment. Furthermore, the fuel parameters often affect the passive signatures in competing ways (e.g., increased burnup increases passive neutron and gamma-ray signals, while increased cooling time decreases them). Analysis of AEFC data can be extended beyond the basic functionality of the active neutron signal to include the passive neutron and gamma-ray signatures.

Figure 1 shows a diagram that maps relationships between the fuel parameters to the radiation signatures they affect. The arrows marked with a plus sign (+) indicate positively-correlated relationships, those marked with a minus sign (-) indicate negatively-correlated relationships, and those with no marking have more complex relationships. For example, an increase in burnup is positively correlated with the passive neutron count rates, but the burnup affects the shape of the passive neutron profile with plutonium, and possibly curium, growing in more quickly in the middle of the fuel assembly compared to the top or bottom of the assembly.

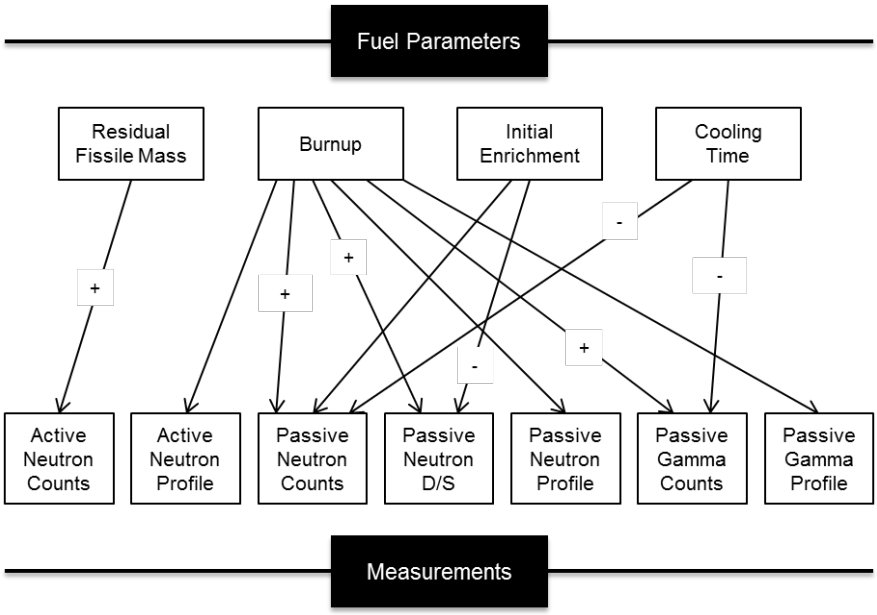

Figure 1: Diagram mapping spent fuel parameters to AEFC measurements.

2.2. Mechanical Design

The AEFC is comprised of neutron and gamma-ray counters, high-density polyethylene (HDPE) moderating material, and lead shielding inside a watertight stainless steel shell as shown in Figure 2. The main detector body is cylindrical in shape with a 117-mm through-hole for fuel assemblies. There is a funnel on top of the through-hole that helps guide assemblies into the measurement position. The neutron and gamma-ray counters are positioned on the opposite side of the through-hole from a slot

for the active neutron interrogation source, and there is a crescent-shaped piece of lead shielding on the detector side of the through-hole.

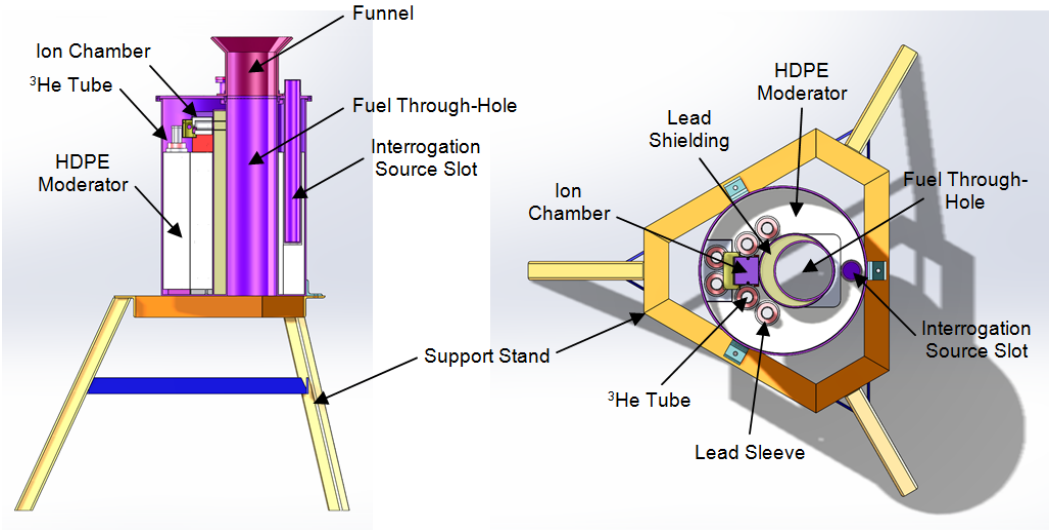

Figure 2: Mechanical design of the AEFC.

For neutron detection, the AEFC has six boron-lined ^{3}He tubes with 4 atm of gas pressure, each surrounded by a 10-mm-thick lead sleeve and embedded in the HDPE moderator. The ion chamber used for gross gamma-ray counting is located on top of the HDPE, next to a collimator hole that creates a window to the fuel assembly through the crescent-shaped lead pillar. When the system is underwater, detector signal and voltage cables run to the top of the spent fuel pool inside waterproof Tygon tubing. The interrogation source is contained inside a HDPE holder and connected to a Teleflex cable. It is moved into and out of the AEFC through a PVC guide tube that runs from the AEFC to the top of the spent fuel pool.

2.3. Data Acquisition

For the 2014 measurements, neutron data was collected in parallel with both a JSR-15 shift register and a PTR-32 list mode module being tested by the International Atomic Energy Agency (IAEA). The shift register data was collected on a laptop and analysed in “Rates Only” mode using IAEA Neutron Coincidence Counting (INCC) software version 5.1.2 to obtain the singles and doubles count rates. INCC 6, which is currently under development, will include list mode data analysis capability that supports the PTR-32.[4] The gamma-ray signal cable was connected to a current-to-pulse converter (CPC) that detects input current from the ion chamber and produces transistor-transistor logic (TTL) pulses at a rate proportional to the input current. The resulting TTL pulses were counted with the JSR-15. This allowed the INCC software to record the gamma rate, time synchronized with the neutron count rates, without the need for an additional software package to collect and analyse the gamma data. INCC outputs the neutron and gamma count rates for each assembly to a single file.

3. Operating Parameters & Measurement Procedure

In this field trial, the AEFC operated with a predelay of 4.5 µs and gate length of 128 µs. The ^{252}Cf interrogation source was supplied by INP and had a strength of 7.4×10^5 n/s. Before the AEFC was lowered into the spent fuel pool, we measured a high voltage plateau for the neutron detectors with the ^{252}Cf source. Once the system was in the pool, we measured a high voltage plateau with the spent fuel assembly expected to have the highest gamma-emission rate (i.e., highest burnup level, shortest cooling time). This allowed us to choose an operating voltage below the point of gamma interference. Figure 3 shows a plot of both high voltage plateaus for comparison. The ^{252}Cf curve shows the count rate level off at the plateau; whereas, there is a sharp increase in counts after ~1640 V for the IRT-4M curve due to gamma interference. For this field trial, the AEFC operating voltage was set at 1620 V to be below the point of gamma interference, which resulted in a 5% loss in efficiency.

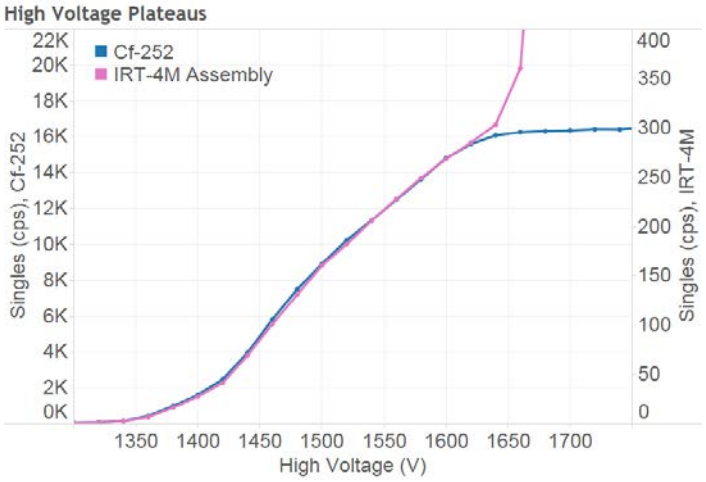

Figure 3: High voltage plateaus for the neutron detectors showing the point of gamma interference.

The AEFC measurement procedure was refined for the 2014 field trial. The development team tested a new three-point fuel scanning technique motivated by the fact that most of the residual ^{235}U is located at the ends of the fuel. Figure 4 shows a photograph of the AEFC being lowered into the spent fuel pool at INP with an overhead crane (top left) and at the measurement location on top of the fuel storage grid (bottom left). Previous field trials of the AEFC included only one measurement position near the middle of the fuel assembly. In order to provide a full-length scan, we measured the top, middle, and bottom of each assembly using a positioning jig attached to the fuel handling pole, shown in Figure 4 (right). The jig was set on a platform that spanned the width of the pool during the measurements to hold the fuel assembly in place. For each position, we took a 5-min. passive and 5-min. active measurement for a total of 30 min. of count time per assembly.

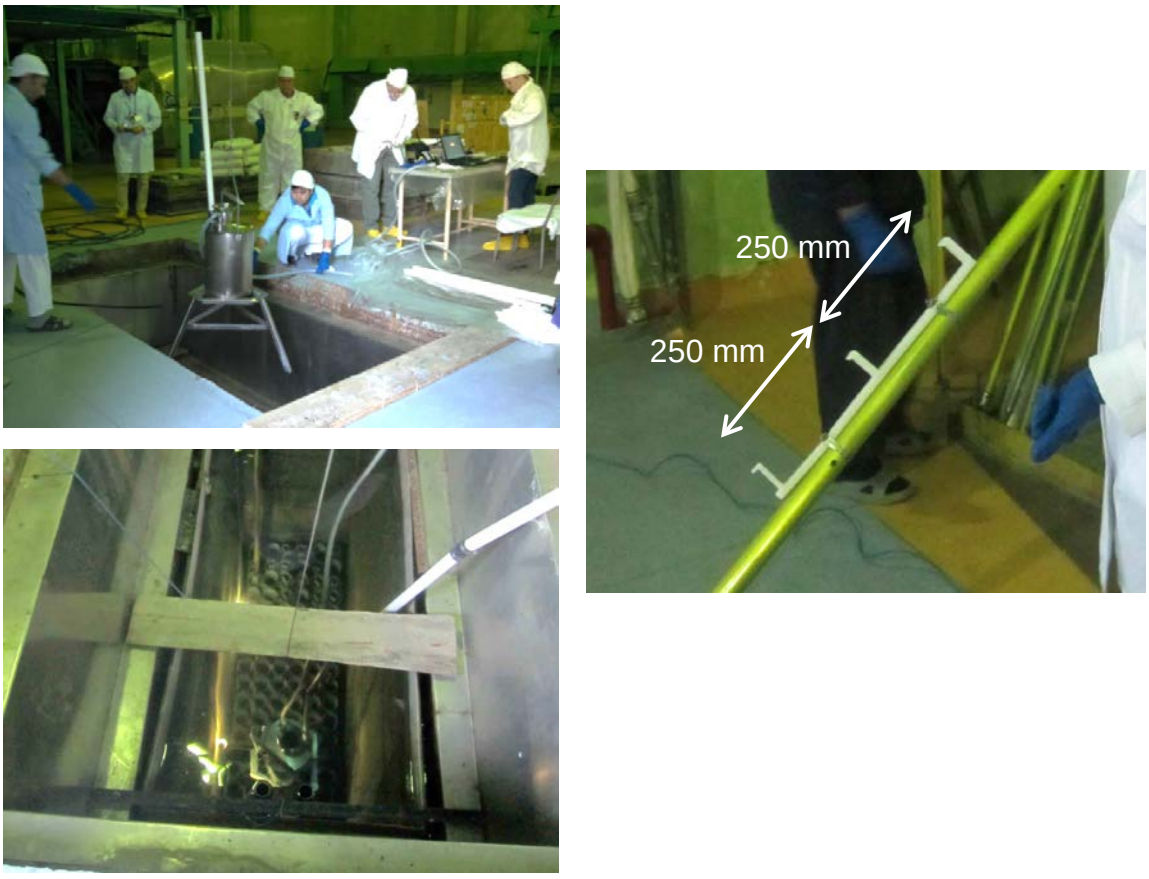

Figure 4: Photographs of the AEFC being lowered into the spent fuel pool at INP (top left), at the measurement location on top of the fuel storage grid (bottom left), and the positioning jig attached the fuel handling pole (right).

4. Measurement Results

The field trial included measurement of twelve IRT-4M and nine EK-10 assemblies. Here, we summarize the preliminary results of the IRT-4M measurements. The IRT-4M fuel assemblies have 19.75%-enriched UO_2-Al fuel with a total length of 882 mm and an active length of 600 mm. The plate fuel elements are oriented as concentric squares. The IRT-4M fuel assemblies measured have two configurations: the six-plate model with ~266 g ^{235}U when fresh and the eight-plate model with ~300 g ^{235}U when fresh. Eleven of the IRT-4M assemblies measured at INP are the six-plate type and one is an eight-plate type (assembly 04M). All of the IRT-4M assemblies measured have a declared burnup level near 60%. Two were discharged in 2002 and nine were discharged in 2011-12.

4.1. AEFC Basic Analysis

The basic measurement objective of the AEFC is to verify the residual fissile mass (i.e., ^{235}U + ^{239}Pu) in spent fuel assemblies using active neutron interrogation. In this section, we refer to this value as residual ^{235}U mass because the analysis is based on the operator declaration of ^{235}U mass. Figure 5 shows a comparison of the active count rates as a function of the residual ^{235}U mass for the middle position only versus the average of the top, middle, and bottom positions (the active singles and active doubles provide a redundant signature in the AEFC).

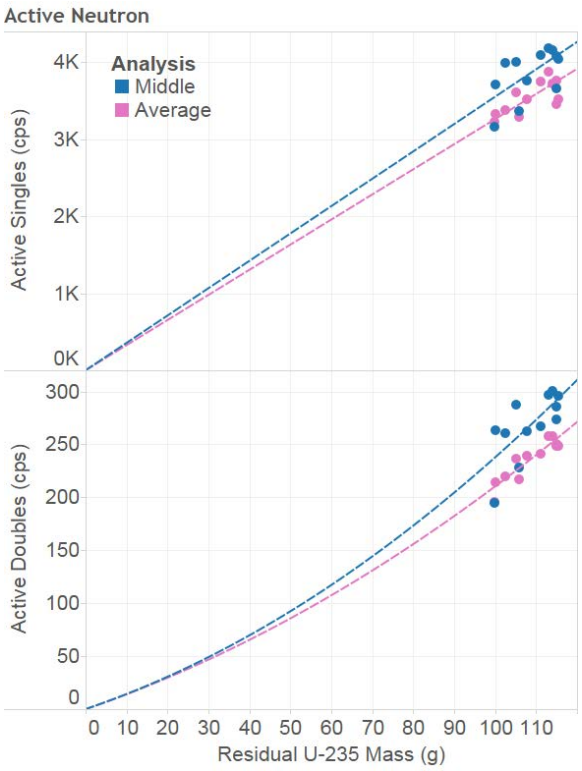

Figure 5: Comparison of the middle and three-point average active neutron count rates as a function of the operator-declared residual ^{235}U mass.

The active singles are fit with a linear calibration curve forced through the origin, and the active doubles are fit with a second-order polynomial forced through the origin. The functional forms of these curves should be verified with Monte Carlo simulations that cover a wider range of residual mass values than measured in this field trial. We calculated residual ^{235}U mass based on the measured count rate and the calibration curve for each assembly along with the relative difference between the declared and calculated value. Table 1 provides the relative standard deviation (RSD) from the operator-declared residual ^{235}U mass with the three-point average analysis compared to analysis of the middle position only for both the active singles and doubles signatures. The large improvement in the doubles assay for the three-point average is partially due to improved counting statistics (i.e., three-times longer measurement time), but counting statistics do not play a significant role in the improvement of the singles assay.

Table 1: Comparison of Middle versus Three-Point Average Relative Standard Deviation (RSD) from the Operator-Declared Residual ^{235}U Mass for the Active Neutron Measurements

Singles	Middle	Average
%RSD	7.0%	4.2%
Doubles	**Middle**	**Average**
%RSD	6.2%	2.2%

2.2. AEFC Extended Analysis

In addition to the basic analysis of the active neutron measurements for verifying residual fissile mass, extended analysis of the AEFC signatures provides a consistency check on the operator declaration of parameters such as burnup, cooling time, and initial enrichment. The extended analysis can provide quantitative assessments of these parameters if combined with burnup and detector modelling codes. For example, Figure 6 (left) shows a plot of the passive doubles count rate as a function of the operator-declared burnup. In low-burnup fuels, the passive doubles come primarily from plutonium; however, ^{242}Cm and ^{244}Cm become the dominant sources of passive doubles in high-burnup fuels, with neutron emission rates four orders of magnitude larger than that of ^{240}Pu. Here, the dramatic increase in passive doubles as a function of burnup suggests that curium is present in the IRT-4M fuel assemblies. Furthermore, the passive singles are proportional to ^{239}Pu (α,n) neutrons in low-burnup fuels. The dual-axis plot in Figure 6 (right) shows an overlay of the passive singles and doubles count rates. This plot shows that the singles are dominated by spontaneous fission neutrons in this case.

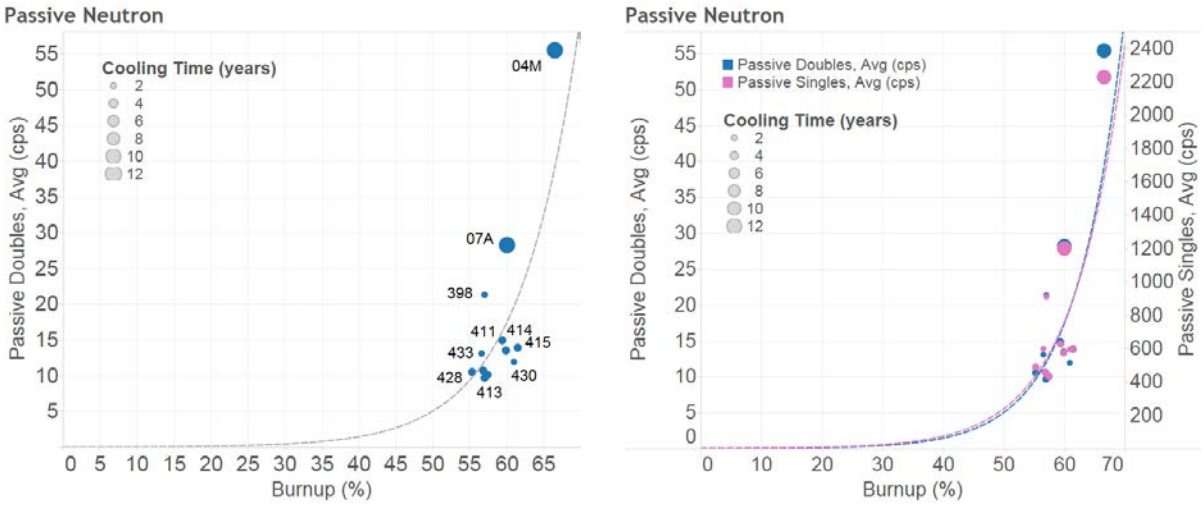

Figure 6: Passive neutron signatures as a function of operator-declared burnup level.

Figure 7 shows a plot of the passive doubles versus gamma count rates where the operator-declared burnup is indicated by the color gradient of the data point and cooling time is indicated by the size of the data point. This type of plot allows the analyst to examine multivariate relationships between the passive signals, burnup, and cooling time and can be used to identify structure within the data. As expected, we see a positive correlation between the passive neutron and gamma count rates. We also see the dependence of these signatures on both burnup and cooling time. The passive neutron and gamma signatures increase with burnup level but have a reduced gamma contribution for longer cooling times. There is a clear distinction between the assemblies discharged within the past three years compared to those discharged twelve years ago, where the short-lived gamma emitters have decayed away. The assemblies with similar cooling times are clustered together on the plot.

Finally, Figure 8 shows the active and passive neutron profiles and position ratios for all of the neutron and gamma-ray measurements (the gamma data only includes measurements for the top half of the fuel). As with the data in Figures 6 and 7, the profiles facilitate consistency checks with the declared burnup and cooling times based on the relative magnitude of the signatures. The top-to-middle and bottom-to-middle position ratios facilitate analysis of the shape of the burnup profile to check for anomalies. The position ratios for the IRT-4M assemblies show a high degree of uniformity, which is consistent with the operator declaration that all of the assemblies have a similar burnup level.

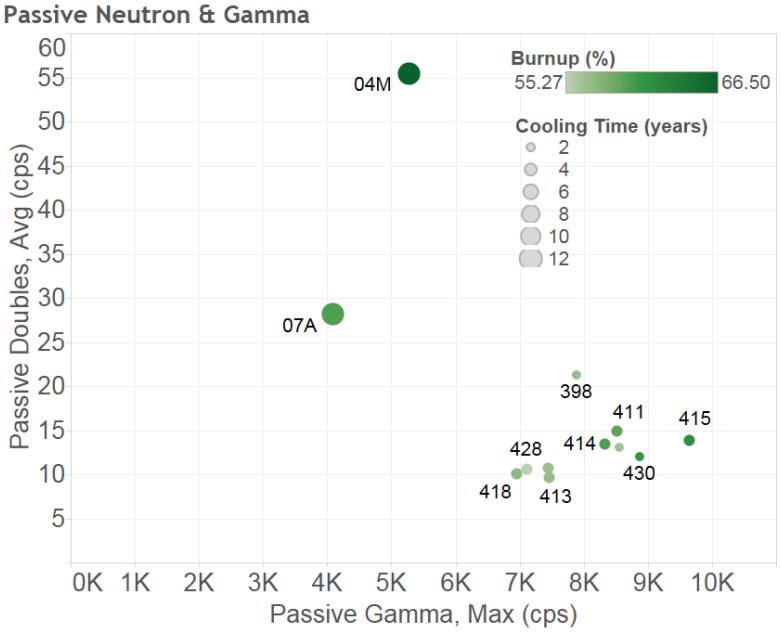

Figure 7: Passive neutron versus gamma count rates showing operator-declared burnup and cooling time.

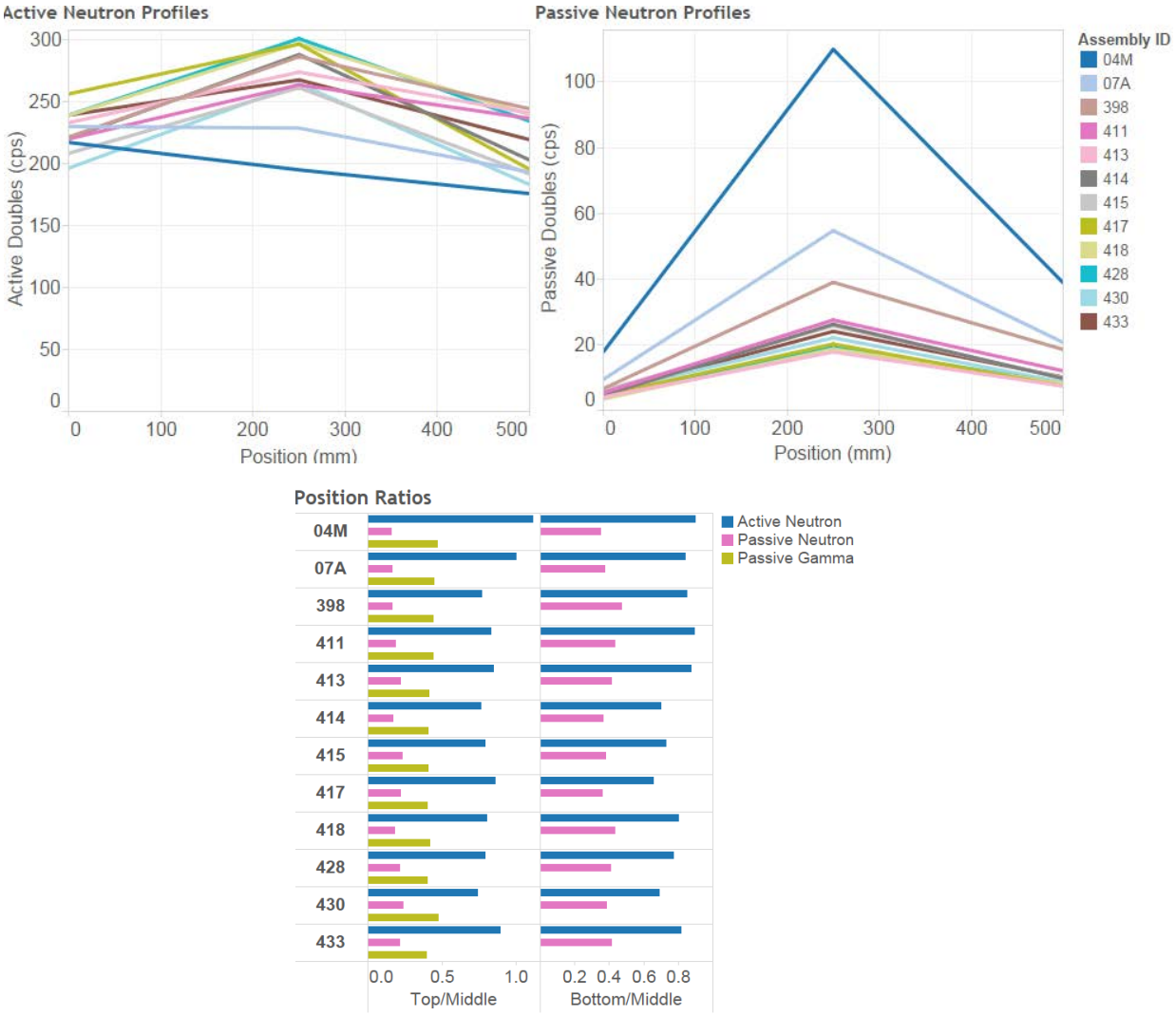

Figure 8: Active and passive neutron profiles (top) and position ratios for neutron and gamma measurements.

5. Conclusions

The 2014 field trial of the AEFC at the INP WWR-SM reactor was a successful demonstration of the measurement system, helped the development team refine and simplify the implementation procedures, and significantly enhanced our understanding of the AEFC signatures. The new three-point fuel scanning technique was motivated by the fact that most of the residual ^{235}U is located at the ends of the fuel and shows promise to improve the accuracy of the residual fissile mass estimate. We recommend continued use of this technique in subsequent AEFC measurements. The field trial also demonstrated the viability of the ^{252}Cf TCIF concept in lieu of AmLi as the active interrogation source. The current-to-pulse converter was a key enabling technology new to the AEFC kit in 2014. It provides a simple solution for the collection of time-synchronized neutron and gamma signals, which are both collected using INCC and output to a single file.

Follow-on work from the field trial includes a focused study to generate an active calibration curve for the AEFC based on ^{252}Cf interrogation. We also plan to use a combination of burnup and detector modelling codes to study the evolution the passive signatures as a function of burnup, cooling time, and initial enrichment. By isolating the effects of these fuel parameters on the AEFC signatures, we hope to strengthen the technical basis for the extended analysis capability.

6. Acknowledgements

Funding for this work was provided by the Nuclear Noncompliance Verification (NNV) program of the U.S. National Nuclear Security Administration (NNSA) Office of Nonproliferation and International Security (NIS).

The AEFC development team would like to thank the staff at the INP in Uzbekistan for their hospitality in accommodating these measurements and providing us the unique opportunity test the AEFC at their reactor. We would also like to thank Lisa Szytel, Bruce Reid, and Chris Gesh for their extensive support during the measurement campaign and contributions to this paper; Mikhail Mayorov and Ufuk Yavuz for their technical insights; and Roy Boyd for his health physics support.

7. References

[1] Menlove HO, et al.; *Field Application of a Portable Detector for the Verification of Research Reactor Spent Fuel*; proc. ESARDA Symposium; Aix-en-Provence, France; 2007.

[2] Menlove HO, et al.; *Field Tests of the AEFC for Verification of Research Reactor Spent Fuel at the WWR-SM Reactor at the Institute of Nuclear Physics Uzbekistan*; proc. INMM Annual Meeting; Orlando, Florida USA; 2012.

[3] Menlove HO, et al.; *The development of a new, neutron, time correlated, interrogation method for measurement of ^{235}U content in LWR fuel assemblies*; *NIM-A*; 701; p. 72-79; 2013.

[4] Longo J, et al.; *Sustaining IAEA Neutron Coincidence Counting (INCC), Past, Present and Future*; proc. IAEA Safeguards Symposium; Vienna, Austria; 2014.

A theoretical and experimental investigation of using Feynman-Y functions for the total and gamma detections in a nuclear and radioactive material assay

Dina Chernikova[a,*], **Kåre Axell**[a,b], **Anders Nordlund**[a]

[a]Chalmers University of Technology, Department of Applied Physics, Nuclear Engineering, Fysikgården 4, SE-412 96 Göteborg, Sweden
[b]Swedish Radiation Safety Authority, SE-171 16 Stockholm, Sweden

Abstract:

Recently a new one-group Feynman-alpha theory was derived and experimentally (as well as numerically) evaluated for total (neutron and gamma without pulse shape discrimination) as well as gamma detection [1]. Extension of this theory to detection of gamma and total neutron and gamma opened a possibility to use separately gamma and total variance-to-mean ratios for the evaluation of nuclear and radioactive material mass without need for applying neutron-gamma discrimination techniques. However, the preliminary evaluation showed differences between theoretical predictions and experimental (and numerical) results. Analysis of the root for these discrepancies indicated that a possible reason might be hidden in the one-group theoretical approximation used, which does not include removal of particles from the fast particle group available for detection to the thermal particle group. Therefore, the subject of this paper is related to theoretical derivations and analysis of a new theoretical model for two-group Feynman-alpha theory for total and gamma detections. The new theory is tested against the previous one [1] experimentally and numerically in a realistic setup. Results of these tests and conclusions drawn are presented in this work.

Keywords: variance to mean, Feynman-alpha, Feynman-Y, gamma Feynman-Y, total Feynman-Y, fast detection

1. Introduction

An ability to use gamma-based time stamping measurement methods, such as Rossi-α or Feynman-α methods, in evaluating nuclear material characteristics or detection of nuclear material attracts a lot of attention in the Safeguards community. Despite the fact that this type of analysis represents a rather complex problem due to the number of the processes which gamma particles can undergo, it is worth doing. Therefore, recently a few attempts were done to approach this task [1, 2], in particularly, a new one-group Feynman-alpha theory was derived, numerically and experimentally evaluated for gamma detections. To our disappointment, experimental results were shown to be deviating from theoretical predictions for only gamma detections [1]. A few hypotheses have been suggested to explain this disagreement. One of them was related to the importance and influence of cascade gammas, or in other words importance of careful analysis of energy information for gamma detections. This paper reports on preliminary tests of this hypothesis and present a new theoretical model for two-energy groups for gamma particles.

2. Theoretical model

2.1. The main concept and assumptions

The neutron-gamma variance to mean (Feynman-alpha) formulas for separate gamma detection in two-energy intervals and total gamma detection will be derived by using the Kolmogorov forward approach the same way as described in [3, 4]. In the model that will be used for the derivations we assume that there are one neutron and two gamma populations: neutrons (denoted as particles of type 1) and gammas (denoted as type 2 and 3). Neutrons can undergo the reactions (i) listed below:

- absorption ($i = a$) with no gammas emitted,

*Corresponding author, email: dina@nephy.chalmers.se

- absorption ($i = 2g$) with one gamma emitted in the energy group 2,
- absorption ($i = 3g$) with one gamma emitted in the energy group 3,
- absorption ($i = cg$) with s gammas emitted in the energy group 2 and d gammas emitted in the energy group 3,
- fission ($i = f$) with corresponding gamma emission.

Gamma particles can be absorbed ($i = a$), detected ($i = d$) or removed ($i = 2r$) from energy group 2 to energy group 3. As mentioned, the assumption behind the model is the same as with the traditional Feynman-alpha theory, i.e. that the medium is infinite and homogeneous with space-independent reaction intensities.The total transition intensities for neutrons and gammas are denoted as λ_1, λ_2 and λ_3. In the model we include a compound Poisson source of neutrons and gammas with emission intensity S. The source is assumed to release m neutrons, n gammas in the energy group 2 and j gammas in the energy group 3 in one emission event with the probability distribution $p(m,n,j)$.

2.2. Separate and total detection of gamma particles in two energy groups: derivation

In order to derive the two-group (for gammas) one-point Feynman-alpha theory for separate detection of gammas in two energy intervals, let us assume that the source S is switched on at the time $t_0 \leq t$, whereas the separate detection processes are started at the same fixed time instant t_d, where $t_0 \leq t_d \leq t$. Let the random process $N_1(t)$ represents the number of neutrons at the time $t \geq 0$, the random processes $N_2(t)$ and $N_3(t)$ represent the number of gammas in two energy groups at the time $t \geq 0$, and $Z_2(t,t_d)$ and $Z_3(t,t_d)$ - the number of gamma detections in two energy groups in the time interval $[t_d,t]$, respectively. Thus, the joint probability of having N_1 neutrons, $N_2(t)$ and $N_3(t)$ gammas (in two energy groups) at time t in the system, and having detected Z_2 gammas in energy group 2 and Z_2 gammas in energy group 3 during the period of time $t - t_d \geq 0$ can be defined as $P(N_1,N_2,N_3,Z_2,Z_3,t|t_0)$. By summing up the probabilities of all mutually exclusive events of the particle not having or having a specific reaction within the infinitesimally small time interval dt, one obtains the forward Kolmogorov or forward master equation

$$
\begin{aligned}
&\frac{dP(N_1,N_2,N_3,Z_2,Z_3,t)}{dt} \\
&\qquad = -(\lambda_1 N_1 + \lambda_2 N_2 + \lambda_3 N_3 + S)P(N_1,N_2,N_3,Z_2,Z_3,t) \\
&\qquad + \lambda_{1a}(N_1+1)P(N_1+1,N_2,N_3,Z_2,Z_3,t) \\
&\qquad + \lambda_{2a}(N_2+1)P(N_1,N_2+1,N_3,Z_2,Z_3,t) \\
&\qquad + \lambda_{3a}(N_3+1)P(N_1,N_2,N_3+1,Z_2,Z_3,t) \\
&\qquad + \lambda_{2g}(N_1+1)P(N_1+1,N_2-1,N_3,Z_2,Z_3,t) \\
&\qquad + \lambda_{3g}(N_1+1)P(N_1+1,N_2,N_3-1,Z_2,Z_3,t) \\
&\qquad + \lambda_{cg}\sum_{s}^{N_2}\sum_{d}^{N_3} v(s,d)(N_1+1)P(N_1+1,N_2-s,N_3-d,Z_2,Z_3,t) \\
&\qquad + \lambda_{1f}\sum_{k}^{N_1+1}\sum_{l}^{N_2}(N_1+1-k)f(k,l)P(N_1+1-k,N_2-l,N_3,Z_2,Z_3,t) \\
&\qquad + \lambda_{2d}(N_2+1)P(N_1,N_2+1,N_3,Z_2-1,Z_3,t) \\
&\qquad + \lambda_{2r}(N_2+1)P(N_1,N_2+1,N_3-1,Z_2,Z_3,t) \\
&\qquad + \lambda_{3d}(N_3+1)P(N_1,N_2,N_3+1,Z_2,Z_3-1,t) \\
&\qquad + S\sum_{m}^{N_1}\sum_{n}^{N_2}\sum_{j}^{N_3} p(m,n,j)P(N_1-m,N_2-n,N_3-j,Z_2,Z_3,t)
\end{aligned}
\tag{1}
$$

where, the initial condition reads as

$$
P(N_1,N_2,N_3,Z_2,Z_3,t = t_0 \mid t_0) = \delta_{N_1,0}\delta_{N_2,0}\delta_{N_3,0}\delta_{Z_2,0}\delta_{Z_3,0} \tag{2}
$$

The various moments of the particle numbers and detection numbers can be obtained from this equation by using the generating function technique in a way similar to as described in [3]. By defining the following generating function for the probability distribution $P(N_1,N_2,N_3,Z_2,Z_3,t)$:

$$G(X,Y,L,W,V,t) = \sum_{N_1}\sum_{N_2}\sum_{N_3}\sum_{Z_2}\sum_{Z_3} X^{N_1}Y^{N_2}L^{N_3}W^{Z_2}V^{Z_3}P(N_1,N_2,N_3,Z_2,Z_3,t) \tag{3}$$

with the initial condition for $t_0 \leq t$

$$G(X,Y,L,W,V,t = t_0 \mid t_0) = 1, \tag{4}$$

the following partial differential equation is obtained:

$$\begin{aligned}
&\frac{\partial G}{\partial t} \\
&\quad = [\lambda_{1a} + \lambda_{2g}Y + \lambda_{cg}V(Y,L) + \lambda_{3g}L - \lambda_1 X + F(X,Y)\lambda_{1f}]\frac{\partial G}{\partial X} + [\lambda_{2a} + \lambda_{2d}W + \lambda_{2r}L - \lambda_2 Y]\frac{\partial G}{\partial Y} \\
&\quad + [\lambda_{3a} + \lambda_{3d}V - \lambda_3 L]\frac{\partial G}{\partial L} + S[P(X,Y,L) - 1]G.
\end{aligned} \tag{5}$$

Here the generating functions of the number distributions of neutrons and gamma photons in a source event (spontaneous fission) and an induced fission event were introduced in a way similar to [1, 2].

Thus, a steady subcritical medium with a steady source, a stationary state of the system exists when $t_0 \to -\infty$. For that case the following solutions are obtained for the constant neutron and gamma populations $\bar{N}_1$, $\bar{N}_2$, $\bar{N}_3$ and the time-varying detection counts $\bar{Z}_2(t)$, $\bar{Z}_3(t)$:

$$\begin{aligned}
\bar{N}_1 &= \frac{SP^{(1,0,0)}}{\lambda_1 - \lambda_f F^{(1,0)}} \\
\bar{N}_2 &= \frac{SP^{(1,0,0)}\left(\lambda_{cg}V^{(1,0)} + \lambda_f F^{(0,1)} + \lambda_{2g}\right)}{\lambda_2\left(\lambda_1 - \lambda_f F^{(1,0)}\right)} + \frac{SP^{(0,1,0)}}{\lambda_2} \\
\bar{N}_3 &= \frac{S\left(\lambda_{2r}P^{(0,1,0)} + \lambda_2 P^{(0,0,1)}\right)}{\lambda_2\lambda_3} - \frac{SP^{(1,0,0)}\left(-\frac{\lambda_{2r}\left(\lambda_{cg}V^{(1,0)} + \lambda_f F^{(0,1)} + \lambda_{2g}\right)}{\lambda_2\lambda_3} - \frac{\lambda_{cg}V^{(0,1)} + \lambda_{3g}}{\lambda_3}\right)}{\lambda_1 - \lambda_f F^{(1,0)}} \\
\bar{Z}_2(t) &= \lambda_{2d}\bar{N}_2 t \\
\bar{Z}_3(t) &= \lambda_{3d}\bar{N}_3 t
\end{aligned} \tag{6}$$

By introducing the modified second factorial moment of the random variables a and b as follows

$$\begin{aligned}
\mu_{aa} &\equiv \langle a(a-1)\rangle - \langle a\rangle^2 = \sigma_a^2 - \langle a\rangle \\
\mu_{ab} &\equiv \langle ab\rangle - \langle a\rangle\langle b\rangle
\end{aligned} \tag{7}$$

and then taking cross- and auto-derivatives, the following system of differential equations is obtained for the modified second factorial moments $\mu_{N_1N_1}$, $\mu_{N_1N_2}$, $\mu_{N_2N_2}$, $\mu_{N_1N_3}$, $\mu_{N_2N_3}$, $\mu_{N_3N_3}$ of the neutron and gamma

populations:

$$\begin{aligned}
\frac{\partial}{\partial t}\mu_{N_1N_1} &= \lambda_f F^{(2,0)}\bar{N}_1 + 2\mu_{N_1N_1}\left(\lambda_f F^{(1,0)} - \lambda_1\right) + SP^{(2,0,0)} \\
\frac{\partial}{\partial t}\mu_{N_1N_2} &= \mu_{N_1N_1}\left(\lambda_{\mathrm{cg}} V^{(1,0)} + \lambda_f F^{(0,1)} + \lambda_{2g}\right) + \lambda_f F^{(1,1)}\bar{N}_1 + \mu_{N_1N_2}\left(\lambda_f F^{(1,0)} - \lambda_1\right) + SP^{(1,1,0)} - \lambda_2\mu_{N_1N_2} \\
\frac{\partial}{\partial t}\mu_{N_2N_2} &= \bar{N}_1\left(\lambda_{\mathrm{cg}} V^{(2,0)} + \lambda_f F^{(0,2)}\right) + 2\mu_{N_1N_2}\left(\lambda_{\mathrm{cg}} V^{(1,0)} + \lambda_f F^{(0,1)} + \lambda_{2g}\right) + SP^{(0,2,0)} - 2\lambda_2\mu_{N_2N_2} \\
\frac{\partial}{\partial t}\mu_{N_1N_3} &= \mu_{N_1N_1}\left(\lambda_{\mathrm{cg}} V^{(0,1)} + \lambda_{3g}\right) + \mu_{N_1N_3}\left(\lambda_f F^{(1,0)} - \lambda_1\right) + SP^{(1,0,1)} + \lambda_{2r}\mu_{N_1N_2} - \lambda_3\mu_{N_1N_3} \\
\frac{\partial}{\partial t}\mu_{N_2N_3} &= \lambda_{\mathrm{cg}} V^{(1,1)}\bar{N}_1 + \mu_{N_1N_3}\left(\lambda_{\mathrm{cg}} V^{(1,0)} + \lambda_f F^{(0,1)} + \lambda_{2g}\right) + \mu_{N_1N_2}\left(\lambda_{\mathrm{cg}} V^{(0,1)} + \lambda_{3g}\right) + SP^{(0,1,1)} + \lambda_{2r}\mu_{N_2N_2} - \lambda_2\mu_{N_2N_3} - \lambda_3\mu_{N_2N_3} \\
\frac{\partial}{\partial t}\mu_{N_3N_3} &= \lambda_{\mathrm{cg}} V^{(0,2)}\bar{N}_1 + 2\mu_{N_1N_3}\left(\lambda_{\mathrm{cg}} V^{(0,1)} + \lambda_{3g}\right) + SP^{(0,0,2)} - 2\lambda_3\mu_{\mathrm{LL}} + 2\lambda_{2r}\mu_{N_2N_3}
\end{aligned} \tag{8}$$

In a stationary system, these modified moments are constant, and can be easily obtained by solving the algebraic equation resulting from setting the l.h.s. of (8) equal to zero.

After a lengthy algebra the well-known Feynman-alpha expression is obtained for the gammas in the energy group 2.

$$\frac{\sigma^2_{Z_2Z_2}(t)}{\bar{Z}_2} = 1 + Y_{g1}\left(1 - \frac{1-e^{-\omega_{g1}t}}{\omega_{g1}t}\right) + Y_{g2}\left(1 - \frac{1-e^{-\omega_{g2}t}}{\omega_{g2}t}\right) \tag{9}$$

where the two roots ω_{g1} and ω_{g2} are obtained as

$$\begin{aligned}
\omega_{g1} &= -\lambda_{1f}F^{(1,0)} + \lambda_1 \\
\omega_{g2} &= \lambda_2
\end{aligned} \tag{10}$$

The functions Y_{g1}, Y_{g2} in the gamma Feynman-alpha formula (13) are given in the form:

$$\begin{aligned}
-Y_{g1} &= \frac{2\lambda_{2d}\left(\lambda_{\mathrm{cg}}\mu_{N_1N_2}V^{(1,0)} + \lambda_f\mu_{N_1N_2}F^{(0,1)} - \lambda_f\mu_{N_2N_2}F^{(1,0)} + \lambda_{2g}\mu_{N_1N_2} + \lambda_1\mu_{N_2N_2} - \omega_1\mu_{N_2N_2}\right)}{\omega_1\left(\omega_1 - \omega_2\right)\bar{N}_2} \\
-Y_{g2} &= \frac{2\lambda_{2d}\left(\lambda_{\mathrm{cg}}\mu_{N_1N_2}V^{(1,0)} + \lambda_f\mu_{N_1N_2}F^{(0,1)} - \lambda_f\mu_{N_2N_2}F^{(1,0)} + \lambda_{2g}\mu_{N_1N_2} + \lambda_1\mu_{N_2N_2} - \omega_2\mu_{N_2N_2}\right)}{\omega_2\left(\omega_2 - \omega_1\right)\bar{N}_2}
\end{aligned} \tag{11}$$

It can be shown that:

$$Y_{g0} = \frac{2\lambda_{2d}\left(\lambda_{\mathrm{cg}}\mu_{N_1N_2}V^{(1,0)} + \lambda_f\mu_{N_1N_2}F^{(0,1)} - \lambda_f\mu_{N_2N_2}F^{(1,0)} + \lambda_{2g}\mu_{N_1N_2} + \lambda_1\mu_{N_2N_2}\right)}{\omega_1\omega_2\bar{N}_2} \tag{12}$$

In the case when detection of gamma particles in the energy group 3 is considered the final expression for the Feynman-alpha formula will have a three exponential form as below:

$$\frac{\sigma^2_{Z_3Z_3}(t)}{\bar{Z}_3} = 1 + Y_{g13}\left(1 - \frac{1-e^{-\omega_{g13}t}}{\omega_{g13}t}\right) + Y_{g23}\left(1 - \frac{1-e^{-\omega_{g23}t}}{\omega_{g23}t}\right) + Y_{g33}\left(1 - \frac{1-e^{-\omega_{g33}t}}{\omega_{g33}t}\right) \tag{13}$$

The three roots ω_{g13}, ω_{g23} and ω_{g33} are obtained as

$$\begin{aligned}
\omega_{g13} &= -\lambda_{1f}F^{(1,0)} + \lambda_1 \\
\omega_{g23} &= \lambda_2 \\
\omega_{g33} &= \lambda_3
\end{aligned} \tag{14}$$

The functions Y_{g1}, Y_{g2} in the gamma Feynman-alpha formula (13) are given in the form:

$$\begin{aligned}
&-Y_{g1} \\
&= -\frac{1}{\bar{N}_3\omega_1(\omega_1-\omega_2)(\omega_1-\omega_3)}(2\lambda_{3d}(\omega_1(-\lambda_{cg}\mu_{N_1N_3}V^{(0,1)}+\lambda_f\mu_{N_3N_3}F^{(1,0)}-\lambda_{3g}\mu_{N_1N_3}-\lambda_1\mu_{N_3N_3}-\lambda_2\mu_{N_3N_3} \\
&+\omega_1\mu_{N_3N_3}-\lambda_{2r}\mu_{N_2N_3})+\lambda_{cg}\lambda_{2r}\mu_{N_1N_3}V^{(1,0)}+\lambda_2\lambda_{cg}\mu_{N_1N_3}V^{(0,1)}-\lambda_2\lambda_f\mu_{N_3N_3}F^{(1,0)}+\lambda_f\lambda_{2r}\mu_{N_1N_3}F^{(0,1)} \\
&-\lambda_f\lambda_{2r}\mu_{N_2N_3}F^{(1,0)}+\lambda_{2g}\lambda_{2r}\mu_{N_1N_3}+\lambda_2\lambda_{3g}\mu_{N_1N_3}+\lambda_1\lambda_2\mu_{N_3N_3}+\lambda_1\lambda_{2r}\mu_{N_2N_3}))
\end{aligned} \tag{15}$$

$$\begin{aligned}
&-Y_{g2} \\
&= \frac{1}{\bar{N}_3(\omega_1-\omega_2)\omega_2(\omega_2-\omega_3)}(2\lambda_{3d}(\omega_2(-\lambda_{cg}\mu_{N_1N_3}V^{(0,1)}+\lambda_f\mu_{N_3N_3}F^{(1,0)}-\lambda_{3g}\mu_{N_1N_3}-\lambda_1\mu_{N_3N_3}-\lambda_2\mu_{N_3N_3} \\
&+\omega_2\mu_{N_3N_3}-\lambda_{2r}\mu_{N_2N_3})+\lambda_{cg}\lambda_{2r}\mu_{N_1N_3}V^{(1,0)}+\lambda_2\lambda_{cg}\mu_{N_1N_3}V^{(0,1)}-\lambda_2\lambda_f\mu_{N_3N_3}F^{(1,0)}+\lambda_f\lambda_{2r}\mu_{N_1N_3}F^{(0,1)} \\
&-\lambda_f\lambda_{2r}\mu_{N_2N_3}F^{(1,0)}+\lambda_{2g}\lambda_{2r}\mu_{N_1N_3}+\lambda_2\lambda_{3g}\mu_{N_1N_3}+\lambda_1\lambda_2\mu_{N_3N_3}+\lambda_1\lambda_{2r}\mu_{N_2N_3}))
\end{aligned} \tag{16}$$

$$\begin{aligned}
&-Y_{g3} \\
&= \frac{1}{\bar{N}_3(\omega_1-\omega_3)\omega_3(\omega_3-\omega_2)}(2\lambda_{3d}(\omega_3(-\lambda_{cg}\mu_{N_1N_3}V^{(0,1)}+\lambda_f\mu_{N_3N_3}F^{(1,0)}-\lambda_{3g}\mu_{N_1N_3}-\lambda_1\mu_{N_3N_3} \\
&-\lambda_2\mu_{N_3N_3}+\omega_3\mu_{N_3N_3}-\lambda_{2r}\mu_{N_2N_3})+\lambda_{cg}\lambda_{2r}\mu_{N_1N_3}V^{(1,0)}+\lambda_2\lambda_{cg}\mu_{N_1N_3}V^{(0,1)}-\lambda_2\lambda_f\mu_{N_3N_3}F^{(1,0)}+\lambda_f\lambda_{2r}\mu_{N_1N_3}F^{(0,1)} \\
&-\lambda_f\lambda_{2r}\mu_{N_2N_3}F^{(1,0)}+\lambda_{2g}\lambda_{2r}\mu_{N_1N_3}+\lambda_2\lambda_{3g}\mu_{N_1N_3}+\lambda_1\lambda_2\mu_{N_3N_3}+\lambda_1\lambda_{2r}\mu_{N_2N_3}))
\end{aligned} \tag{17}$$

It can be shown that:

$$\begin{aligned}
&Y_{g0} \\
&= Y_{g1}+Y_{g2}+Y_{g3} = \frac{1}{\bar{N}_3\omega_1\omega_2\omega_3}(2\lambda_{3d}(\lambda_{cg}\lambda_{2r}\mu_{N_1N_3}V^{(1,0)}+\lambda_2\lambda_{cg}\mu_{N_1N_3}V^{(0,1)}-\lambda_2\lambda_f\mu_{N_3N_3}F^{(1,0)} \\
&+\lambda_f\lambda_{2r}\mu_{N_1N_3}F^{(0,1)}-\lambda_f\lambda_{2r}\mu_{N_2N_3}F^{(1,0)}+\lambda_{2g}\lambda_{2r}\mu_{N_1N_3}+\lambda_2\lambda_{3g}\mu_{N_1N_3}+\lambda_1\lambda_2\mu_{N_3N_3}+\lambda_1\lambda_{2r}\mu_{N_2N_3}))
\end{aligned} \tag{18}$$

In the case of total detection of gammas in two groups the assumptions below theory are similar to the ones used above for the separate detection with the only difference that now $Z(t,t_d)$ represents the number of total gamma detections in two groups in the time interval $[t_d,t]$. Thus, the joint probability of having N_1 neutrons and N_2, N_3 gammas at time t, and Z gammas in two energy groups together having been detected during the period of time $t-t_d \geq 0$ can be defined as $P(N_1,N_2,N_3,Z,t|t_0)$. Repeating the same procedure as before, one obtains the following generating function equation:

$$\begin{aligned}
&\frac{\partial G}{\partial t} \\
&= [\lambda_{1a}+\lambda_{2g}Y+\lambda_{cg}V(Y,L)+\lambda_{3g}L-\lambda_1X+F(X,Y)\lambda_{1f}]\frac{\partial G}{\partial X}+[\lambda_{2a}+\lambda_{2d}W+\lambda_{2r}L-\lambda_2Y]\frac{\partial G}{\partial Y} \\
&+[\lambda_{3a}+\lambda_{3d}W-\lambda_3L]\frac{\partial G}{\partial L}+S[P(X,Y,L)-1]G.
\end{aligned} \tag{19}$$

In a steady subcritical medium with a steady source the solutions for neutron and gamma populations $\bar{N}_1$, $\bar{N}_2$, $\bar{N}_3$ are the same as in the case of separate detection of neutrons and gammas, though, the time-varying detection counts $\bar{Z}(t)$ represents the sum of $\bar{Z}_1(t)$ and $\bar{Z}_2(t)$ (taken from the case of separate detection of neutrons and gammas):

$$\bar{Z}(t) = \lambda_{2d}\bar{N}_2t+\lambda_{3d}\bar{N}_3t \tag{20}$$

The final expression for the Feynman-alpha formulas for total counts is given as below:

$$\frac{\sigma^2_{ZZ}(t)}{\bar{Z}} = 1+Y_{g1}(1-\frac{1-e^{-\omega_{g1}t}}{\omega_{g1}t})+Y_{g2}(1-\frac{1-e^{-\omega_{g2}t}}{\omega_{g2}t})+Y_{g3}(1-\frac{1-e^{-\omega_{g3}t}}{\omega_{g3}t}) \tag{21}$$

The three roots ω_{g1}, ω_{g2}, ω_{g3} are obtained as

$$\begin{aligned} \omega_{g1} &= \lambda_2 \\ \omega_{g2} &= -\lambda_{1f} F^{(1,0)} + \lambda_1 \\ \omega_{g3} &= \lambda_3 \end{aligned} \tag{22}$$

The functions Y_{g1}, Y_{g2} and Y_{g3} in the gamma Feynman-alpha formula (21) are given in the form:

$$\begin{aligned} -Y_{g1} &= \frac{\omega_1 \left(-\frac{2K_1\lambda_{2d}}{\omega_1(\omega_1-\omega_2)} + \frac{2K_0\lambda_{2d}}{\omega_1^2(\omega_1-\omega_2)} - \frac{2L_2\lambda_{3d}}{(\omega_1-\omega_2)(\omega_1-\omega_3)} + \frac{2L_1\lambda_{3d}}{\omega_1(\omega_1-\omega_2)(\omega_1-\omega_3)} - \frac{2L_0\lambda_{3d}}{\omega_1^2(\omega_1-\omega_2)(\omega_1-\omega_3)} \right)}{\bar{N}_3\lambda_{3d} + \bar{N}_2\lambda_{2d}} \\ -Y_{g2} &= \frac{\omega_2 \left(\frac{2K_1\lambda_{2d}}{(\omega_1-\omega_2)\omega_2} - \frac{2K_0\lambda_{2d}}{(\omega_1-\omega_2)\omega_2^2} + \frac{2L_2\lambda_{3d}}{(\omega_1-\omega_2)(\omega_2-\omega_3)} - \frac{2L_1\lambda_{3d}}{(\omega_1-\omega_2)\omega_2(\omega_2-\omega_3)} + \frac{2L_0\lambda_{3d}}{(\omega_1-\omega_2)\omega_2^2(\omega_2-\omega_3)} \right)}{\bar{N}_3\lambda_{3d} + \bar{N}_2\lambda_{2d}} \\ -Y_{g2} &= \frac{\omega_3 \left(\frac{2L_2\lambda_{3d}}{(\omega_1-\omega_3)(\omega_3-\omega_2)} - \frac{2L_1\lambda_{3d}}{(\omega_1-\omega_3)\omega_3(\omega_3-\omega_2)} + \frac{2L_0\lambda_{3d}}{(\omega_1-\omega_3)\omega_3^2(\omega_3-\omega_2)} \right)}{\bar{N}_3\lambda_{3d} + \bar{N}_2\lambda_{2d}} \end{aligned} \tag{23}$$

It can be shown that:

$$Y_{g0} = \frac{2\left(K_0\omega_3\lambda_{2d} + L_0\lambda_{3d}\right)}{\omega_1\omega_2\omega_3\left(\bar{N}_3\lambda_{3d} + \bar{N}_2\lambda_{2d}\right)} \tag{24}$$

where

$$\begin{aligned} K_0 &= \lambda_{cg}\lambda_{3d}\mu_{N_1N_3}V^{(1,0)} + \lambda_{cg}\lambda_{2d}\mu_{N_1N_2}V^{(1,0)} + \lambda_{3d}\lambda_f\mu_{N_1N_3}F^{(0,1)} + \lambda_{2d}\lambda_f\mu_{N_1N_2}F^{(0,1)} - \lambda_{3d}\lambda_f\mu_{N_2N_3}F^{(1,0)} \\ &- \lambda_{2d}\lambda_f\mu_{N_2N_2}F^{(1,0)} + \lambda_{3d}\lambda_{2g}\mu_{N_1N_3} + \lambda_{2d}\lambda_{2g}\mu_{N_1N_2} + \lambda_1\lambda_{3d}\mu_{N_2N_3} + \lambda_1\lambda_{2d}\mu_{N_2N_2} \end{aligned} \tag{25}$$

$$K_1 = \lambda_{3d}\mu_{N_2N_3} + \lambda_{2d}\mu_{N_2N_2} \tag{26}$$

$$\begin{aligned} L_0 &= \lambda_{cg}\lambda_{3d}\lambda_{2r}\mu_{N_1N_3}V^{(1,0)} + \lambda_{cg}\lambda_{2d}\lambda_{2r}\mu_{N_1N_2}V^{(1,0)} + \lambda_2\lambda_{cg}\lambda_{3d}\mu_{N_1N_3}V^{(0,1)} + \lambda_2\lambda_{cg}\lambda_{2d}\mu_{N_1N_2}V^{(0,1)} \\ &- \lambda_2\lambda_{3d}\lambda_f\mu_{N_3N_3}F^{(1,0)} + \lambda_{3d}\lambda_f\lambda_{2r}\mu_{N_1N_3}F^{(0,1)} + \lambda_{2d}\lambda_f\lambda_{2r}\mu_{N_1N_2}F^{(0,1)} - \lambda_{3d}\lambda_f\lambda_{2r}\mu_{N_2N_3}F^{(1,0)} - \lambda_{2d}\lambda_f\lambda_{2r}\mu_{N_2N_2}F^{(1,0)} \\ &- \lambda_2\lambda_{2d}\lambda_f\mu_{N_2N_3}F^{(1,0)} + \lambda_{3d}\lambda_{2g}\lambda_{2r}\mu_{N_1N_3} + \lambda_{2d}\lambda_{2g}\lambda_{2r}\mu_{N_1N_2} + \lambda_2\lambda_{3d}\lambda_{3g}\mu_{N_1N_3} + \lambda_2\lambda_{2d}\lambda_{3g}\mu_{N_1N_2} \\ &+ \lambda_1\lambda_2\lambda_{3d}\mu_{N_3N_3} + \lambda_1\lambda_{3d}\lambda_{2r}\mu_{N_2N_3} + \lambda_1\lambda_{2d}\lambda_{2r}\mu_{N_2N_2} + \lambda_1\lambda_2\lambda_{2d}\mu_{N_2N_3} \end{aligned} \tag{27}$$

$$\begin{aligned} L_1 &= \lambda_{cg}\lambda_{3d}\mu_{N_1N_3}V^{(0,1)} + \lambda_{cg}\lambda_{2d}\mu_{N_1N_2}V^{(0,1)} - \lambda_{3d}\lambda_f\mu_{N_3N_3}F^{(1,0)} - \lambda_{2d}\lambda_f\mu_{N_2N_3}F^{(1,0)} + \lambda_{3d}\lambda_{3g}\mu_{N_1N_3} + \lambda_{2d}\lambda_{3g}\mu_{N_1N_2} \\ &+ \lambda_1\lambda_{3d}\mu_{N_3N_3} + \lambda_2\lambda_{3d}\mu_{N_3N_3} + \lambda_{3d}\lambda_{2r}\mu_{N_2N_3} + \lambda_{2d}\lambda_{2r}\mu_{N_2N_2} + \lambda_1\lambda_{2d}\mu_{N_2N_3} + \lambda_2\lambda_{2d}\mu_{N_2N_3} \end{aligned} \tag{28}$$

$$L_2 = \lambda_{3d}\mu_{N_3N_3} + \lambda_{2d}\mu_{N_2N_3} \tag{29}$$

2.3. Theoretical prediction for evaluation of variance-to-mean ratios for detection of gamma emitted from ^{22}Na

This case was chosen because of its similarity to the measurement setup. The comparison of the variance to mean ratios for gammas in two energy groups and total gamma (two energy groups are combined) is made by using quantitative values of the transition probabilities and reaction intensities obtained in a way similar to that described in [4–9]. A detection efficiency (ε) for gammas is assumed to be equal to 9%, $\lambda_d = \varepsilon \cdot \lambda_a$ in which the geometric efficiency is intended to be included.

As shown in Figure 1, the behavior of the dependence of the variance-to-mean ratio for the number of gammas in two energy groups and total gammas (two energy groups are combined) shows that for a Group

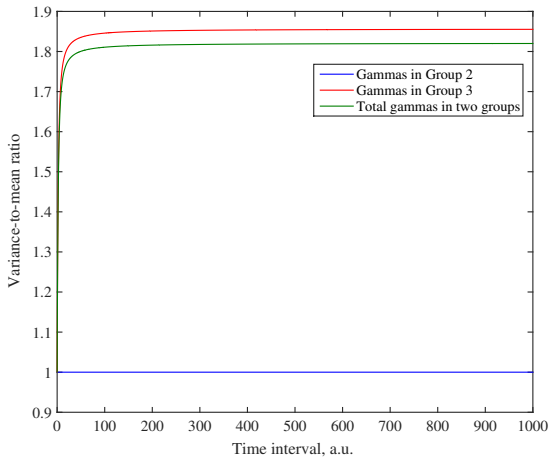

Figure 1: Theoretical prediction for evaluation of variance-to-mean ratios for detection of gamma emitted from ^{22}Na.

2 variance-to-mean ratio is unity, which means that gamma particle in this energy range are not correlated. At the same time, gamma particles in Group 3 appear to be correlated.

The alarming sign is that an asymptotic value of the Feynman-Y functions is higher for correlated gamma detections in Group 3 in comparison with the total gamma detections. This means that most probably the variance-to-mean ratio of the total gamma detections do not represent a reliable indicator in a situation when cascade gammas are present.

3. Experimental evaluation

In the experimental evaluation we used the same setup and procedure, as described in [1] for ^{22}Na correlated gamma source ($\sim$ 2125 kBq) with the only difference that the detection threshold was set to 0.06 V as compared to 0.2 V in [1]. Measurement time was chosen to 100 seconds sharp. As shown in Figure 2

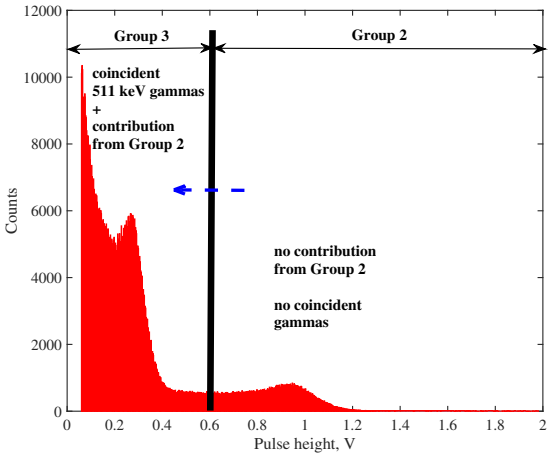

Figure 2: Pulse height spectra obtained for two detectors/channels with a ^{22}Na source.

in order to perform the variance-to-mean ratio analysis we sorted data (time stamps) for two energy groups (Group 2 and Group 3) with a threshold 0.6 V.

Finally, as it is shown in Figure 3 the behavior of variance-to-mean ratio for the number of gammas in two energy groups and total gammas (two energy groups are combined) are in a good agreement with

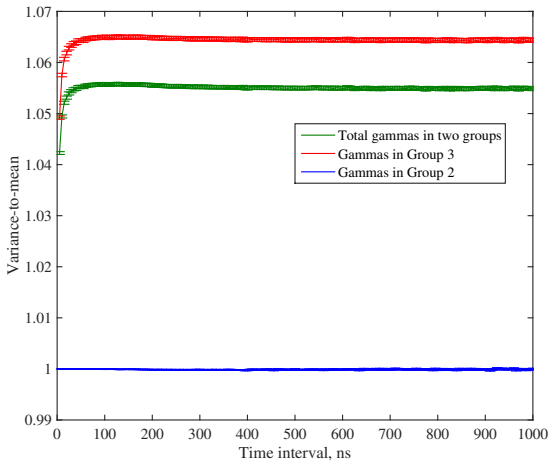

Figure 3: Experimental evaluation of variance-to-mean ratios for detection of gamma emitted from ^{22}Na.

a theoretical prediction. Again the asymptotic value of the Feynman-Y functions is higher for correlated gamma detections in Group 3 in comparison with the total gamma detections.

Thus, we shall conclude that in the case when cascade gammas are present it is very important to perform time-analysis of energy-dependent data. The reasons, effects and the way to account for differences caused by energy-related effects are to be investigated in future work.

4. Conclusion

In this paper a new theoretical formalism was created in order to account for energy-related information of gamma particles when they are analyzed by using a Feynman-alpha approach. Theoretical formulas are tested against experimental results obtained for a ^{22}Na correlated gamma source ($\sim$ 2125 kBq). Results show a good agreement between theoretical and experimental behavior of the variance-to-mean ratio. This indicates the importance of performing a time-analysis of energy-dependent data if gamma particles is to be considered. At the same time the difference between asymptotic values of the Feynman-Y functions for correlated gamma detection in Group 3 and the total gamma detection raises new questions to be answered in a future work.

5. Acknowledgement

This work was supported by the Swedish Radiation Safety Authority, SSM.

References

[1] Dina Chernikova, Kåre Axell, Senada Avdic, Imre Pázsit, Anders Nordlund: The neutron-gamma Feynman variance to mean approach: gamma detection and total neutron-gamma detection (theory and practice) Nuclear Instruments and Methods in Physics Research A 782 (2015), 4755.

[2] Dina Chernikova, Imre Pázsit, Stephen Croft, Andrea Favalli, The effect of capture gammas, photofission and photonuclear neutrons to the neutron-gamma Feynman variance-to-mean ratios (neutron, gamma and total), submitted to ANS MC2015, Nashville, Tennessee, April 19, 2015.

[3] I. Pázsit, L. Pál, Neutron Fluctuations: A Treatise on the Physics of Branching Processes, Elsevier Science Ltd., London, New York, Tokyo, 2008.

[4] D. Chernikova, W. Ziguan, I. Pázsit, L. Pál, A general analytical solution for the variance-to-mean Feynman-alpha formulas for a two-group two-point, a two-group one-point and a one-group two-point cases, The European Physical Journal Plus, 129 (2014) 259.

[5] P. Cartemo, A. Nordlund, D. Chernikova, Sensitivity of the neutronic design of an Accelerator-Driven System (ADS) to the anisotropy of yield of the neutron generator and variation of nuclear data libraries, ESARDA meeting, Brugge, 2013.

[6] D. Chernikova, I. Pázsit, W. Ziguan, Application of the two-group - one-region and two-region one-group Feynman-alpha formulas in safeguards and accelerator-driven system (ADS). ESARDA meeting, Brugge, 05/2013.

[7] J. Anderson, D. Chernikova, I. Pázsit, L. Pál, S.A. Pozzi, Two-point theory for the differential self-interrogation Feynman-alpha method, The European Physical Journal Plus, 127 (2012) 90.

[8] J. Anderson, L. Pál, I. Pázsit, D. Chernikova, S. Pozzi, Derivation and quantitative analysis of the differential self-interrogation Feynman-alpha method, The European Physical Journal Plus, 127 (2012) 21.

[9] D. Chernikova, I. Pázsit, L. Pál, Z. Wang, Derivation of two-group two-region Feynman-alpha formulas and their application to Safeguards and accelerator-driven system (ADS). INMM 54th Annual Meeting, JW Marriott Desert Springs, Palm Desert, California USA, 07/2013.

Improved Holdup Blender Assay System (IBAS) Slope Validation Measurements to Improve Nuclear Material Accountancy of High Alpha Holdup

Adrienne M. LaFleur[1], Hironobu Nakamura[2], Howard O. Menlove[1], Yasunobu Mukai[2], Martyn T. Swinhoe[1], Johnna B. Marlow[1], Tsutomu Kurita[2]

[1]Los Alamos National Laboratory, Los Alamos, NM 87545 USA
[2]Tokai Reprocessing Development Center, Japan Atomic Energy Agency, Tokai-mura, Ibaraki-ken, Japan

Email: alafleur@lanl.gov; nakamura.hironobu@jaea.go.jp; hmenlove@lanl.gov; mukai.yasunobu@jaea.go.jp; swinhoe@lanl.gov; jmarlow@lanl.gov; kurita.tsutomu@jaea.go.jp;

Abstract:

The IBAS (Improved Holdup Blender Assay System) ^{3}He slab detector system was developed at LANL in collaboration with JAEA to improve the existing HBAS detector system for safeguards and nuclear material accountancy (NMA) of holdup measurements at the Plutonium Conversion Development Facility (PCDF). The IBAS consists of two slabs (one on each side the glovebox) where each slab consists of 20 ^{3}He tubes embedded in high-density polyethylene. The purpose of this detector is to measure the doubles rate from each glovebox in order to determine the mass of Pu holdup. In order to establish calibration curves for the IBAS detector and improve the holdup measurement methodology, JAEA conducted the IBAS calibration exercise with LANL support using MOX standards in 2010. In 2011, a cleanout exercise was performed and the results showed that the holdup removed from the glovebox had a significantly higher alpha term (α=15.8~31.5) than the MOX standards (α=0.67) used to establish the 2010 calibration curves. To further investigate these findings, JAEA conducted slope validation measurements in 2013 to confirm the validity of IBAS calibration slopes for the case of high alpha holdup. This paper describes the IBAS slope validation tests, analysis of the experimental results, and the evaluation of the need for a correction factor for the high alpha holdup. Quantifying the alpha term of the holdup in each glove box and understanding how this value changes over time is important to improving the overall NMA at PCDF. The results from this work will provide invaluable experimental data that directly supports safeguards and NMA measurements of plutonium holdup in gloveboxes.

Keywords: holdup, nuclear safeguards, non-destructive assay, plutonium

1. Introduction

The IBAS (Improved Holdup Blender Assay System) ^{3}He slab detector system was developed at LANL in collaboration with JAEA to improve the existing HBAS detector system for holdup measurements at PCDF. The purpose of this detector is to measure the doubles rate from each glovebox (GB) in order to determine the mass of Pu holdup. In order to establish calibration curves for the IBAS detector and improve the holdup measurement methodology, JAEA conducted the IBAS calibration exercise with LANL support using MOX standards in 2010. From May to June 2011, JAEA conducted the IBAS validation test at PCDF. This test consisted of measuring GB P14B01 with IBAS before and after MOX holdup was removed. The holdup removed from the glove box was measured using the non-destructive assay (NDA) equipment available at PCDF, which included the Plutonium Scrap Multiplicity Counter (PSMC) and Waste Drum Assay System (WDAS). The results from the 2011 cleanout showed that the holdup removed from the glovebox had a significantly higher alpha term (α = 15.8~31.5) than that of the MOX standards (α = 0.67) used to establish the 2010 calibration curves where alpha (α) is defined as the ratio of the (α,n) neutron yield to the spontaneous fission (SF) neutron yield. We believe that the change in the doubles rate being measured by IBAS may be driven by the high alpha of the holdup. The

high alpha values of the holdup samples create a situation where the sample itself acts as a neutron random driver such as the AmLi source used in the Active Well Coincidence Counter (AWCC) [1] and induces fissions in the sample. In this case, the doubles rate in the holdup from induced fission reactions increases even when the multiplication (M) is nearly 1.0. Thus, the induced fission rate is a function of alpha (the driver term), the Pu fissile mass (induced fission target), and the geometric distribution of the MOX holdup powder. To further investigate these findings, a new methodology for validating the IBAS calibration slopes was proposed.

This report describes the IBAS slope validation tests, analysis of the results, and the evaluation of the need for a correction factor for converting ^{240}Pu effective mass to Pu mass to account for high alpha holdup. Quantifying the high alpha term of the holdup in each glove box is important to improving the overall nuclear material accountancy (NMA) at PCDF. Furthermore, understanding what the alpha term of the existing holdup is and how it changes with time is essential to establishing a baseline calibration for distinguishing the different fuel types. The results from this work will provide invaluable experimental data that directly supports safeguards and NMA measurements of plutonium holdup in gloveboxes.

2. NDA Equipment

2.1. IBAS (Improved Holdup Blender Assay System)

The IBAS system was developed and calibrated in 2010 to improve the existing HBAS detector system for holdup measurements at PCDF. Figure 1 shows (a) side view of the measurement positions for a glovebox and (b) top-down schematic of the IBAS detector slabs in position A2/B2. Each slab consists of 20 ^{3}He tubes embedded in high-density polyethylene. The ^{3}He tubes are 2.54-cm in diameter with a 152-cm active length. Four AMPTEK preamplifiers are used in each IBAS slab and are located in the junction box housing on top of the slabs. The AMSR-150 multiplicity shift register with fast accidentals was used to count and record the total number of pulses and the time correlation of coincidence pulses in the IBAS slabs. IAEA Neutron Coincidence Counting (INCC) software [2] version 5.04 was used to set the operating parameters for IBAS, as well as collect and archive all of the measurement data.

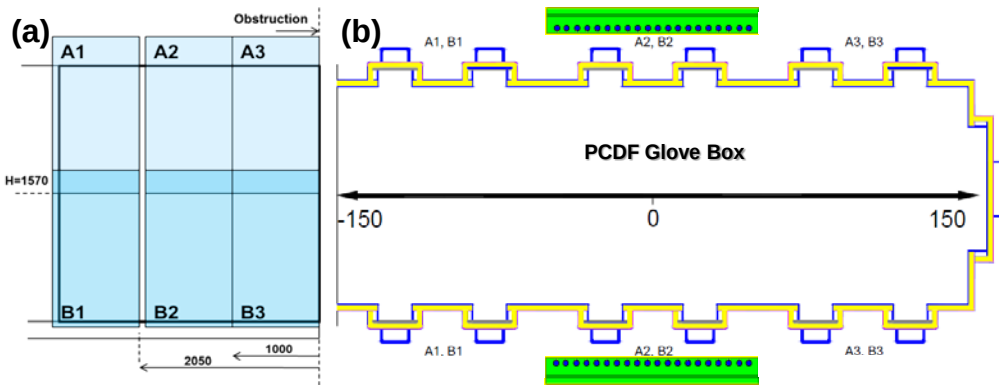

Figure 1. (a) side view of GB measurement positions and (b) top-down view of IBAS slabs in position A2/B2.

Figure 2 shows a picture of IBAS measuring a glove box and the detector operating parameters used in INCC. As illustrated in Figure 1, the IBAS detector needs to measure 6 positions, A1 to B3 (depending on the size of the GB), in order to obtain a representative doubles count rate for the GB. The doubles rates collected from each position are then averaged to get the representative doubles count rate for the GB.

IBAS Detector Parameters	
Detector Efficiency	5.0%
High Voltage	1680 V
Pre-Delay	2.0 μs
Gate Width	90 μs
Die-Away Time (τ)	61 μs
Deadtime Coefficient A	0.680
Deadtime Coefficient B	0.220

Figure 2. Picture of IBAS measuring a glove box and the detector operating parameters used in INCC.

2.2. PSMC (Plutonium Scrap Multiplicity Counter)

The PSMC is a high efficiency well counter that is used to measure impure plutonium and MOX samples with masses ranging from grams to several kilograms. Figure 3 shows a diagram of the PSMC modeled in MCNPX. This detector consists of 80 ^{3}He tubes at 4-atm pressure embedded in high-density polyethylene. The outer dimensions of the PSMC are 66-cm x 66-cm x 80-cm [3].

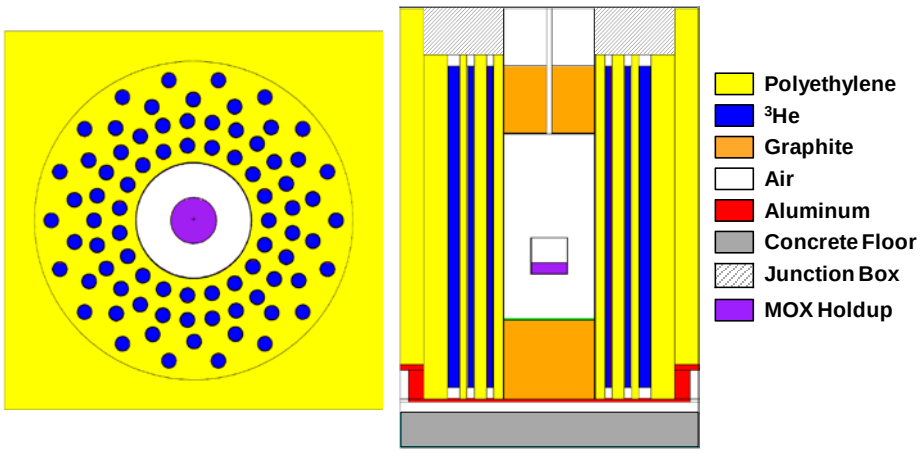

Figure 3. Diagram of the PSMC modeled in MCNPX.

At PCDF, the PSMC is jointly used by both operator and inspectorate. The operator uses the PSMC for MOX powder standards (α = 0.67), sludge (PuO_2-$Na_2U_2O_7$; α = ~25) and scrap holdup powder removed from the glove boxes. The inspectorate uses the PSMC for inventory verification of the MOX powder standards, sludge and the scrap holdup powder. Figure 4 shows the detector parameters currently used for the PSMC at PCDF [4] and pictures of the PSMC and scrap container used for MOX holdup samples. The scrap container is made out of polyethylene and has an inner diameter of 8.0-cm.

For the holdup measurements, the purpose of the PSMC was to measure the MOX cleanout scrap from the glove boxes at PCDF. The scrap was bagged out of the glove box and placed into small containers that fit inside the PSMC. The singles (*S*), doubles (*D*), and triples (*T*) were measured in the PSMC using long measurement times (15 to 23-hours) to obtain reasonably small statistical errors. The INCC software uses the measured rates to solve for the $^{240}Pu_{eff}$ mass, the multiplication (M) and the alpha value (α). The $^{240}Pu_{eff}$ mass [Eq. (1)] is defined as the mass of ^{240}Pu that would give the same doubles coincidence response as that obtained from all the even Pu isotopes in the sample:

$$^{240}Pu_{eff} = Pu_{Total}\left(2.52\,^{238}Pu + {}^{240}Pu + 1.68\,^{242}Pu\right) \quad (1)$$

where $^{240}Pu_{eff}$ and Pu_{Total} are masses (grams) and ^{238}Pu, ^{240}Pu, and ^{242}Pu are isotopic fractions (wt%).

Scrap Container for PSMC Measurements

PSMC Detector Parameters	
Detector Efficiency	54.3%
High Voltage	1700 V
Pre-Delay	4.5 μs
Gate Width	64 μs
Die-Away Time (τ)	49 μs
Doubles Gate Fraction	0.615
Triples Gate Fraction	0.400
Multiplicity Deadtime	112 ns
Deadtime Coefficient A	0.379
Deadtime Coefficient B	0.123

Figure 4. Detector parameters used for the PSMC at PCDF and pictures of the PSMC and scrap container used for MOX holdup samples.

3. IBAS Slope Validation Procedure

For the IBAS slope validation test, holdup samples from two gloveboxes, P13B04 and P15B01, were cleaned out into scrap containers (see Figure 4) and measured with the PSMC. The location of these gloveboxes in room A126 at PCDF is shown in Figure 5.

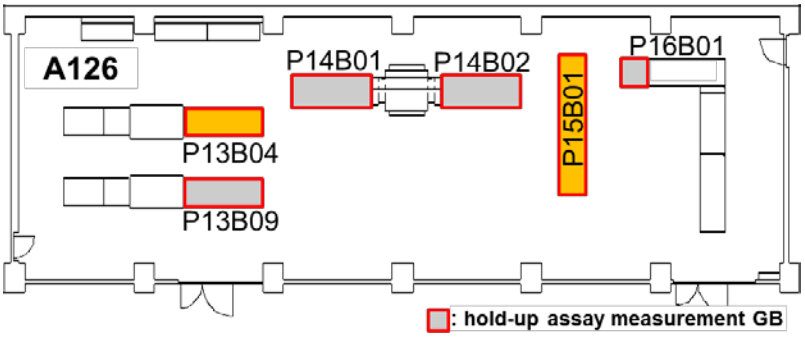

Figure 5. Location of gloveboxes used for holdup assay measurements in room A126.

The IBAS slope validation test was conducted by JAEA using the following procedure:

1) IBAS health check, background, and normalization measurements were performed.
2) The condition of the gloveboxes (port cover and location of the boats) was checked prior to beginning IBAS measurements **before** cleanout.
3) IBAS measurements were performed for every GB in room A126 **before** cleanout using a count time of 45min/face except for P13B04 and P15B01 which were measured for 60min/face to reduce the counting statistical error.
4) Holdup from P13B04 and P15B01 was collected, put into plastic bottles and then bagged out of the gloveboxes.
5) PSMC measurements of the recovered MOX powder were performed to determine alpha (α), multiplication (M), $^{240}Pu_{eff}$ mass, and total Pu mass.
6) After the PSMC measurements were completed, the net weight of the MOX scrap powder was measured and DA samples were taken to determine the Pu and impurity content in the recovered scrap powder.
7) The condition of the gloveboxes (port cover and location of the boats) was checked prior to beginning IBAS measurements **after** cleanout.

8) IBAS measurements were performed for every GB in room A126 **after** cleanout using a count time of 45min/face except for P13B04 and P15B01 which were measured for 60min/face to reduce the counting statistical error.

9) The recovered Pu mass and 1σ standard deviation determined by the PSMC and weight/DA measurements was compared to the recovered Pu mass determined by the IBAS measurements (difference before and after cleanout) and the difference was calculated.

10) The results from step 9) were evaluated to determine the significance to the 2010 IBAS calibration slopes and if a correction factor might be needed.

4. Analysis of Measurement Results

4.1. Validation of 2010 Calibration Slopes

Prior to performing the IBAS slope validation tests, several samples of MOX holdup were taken from different locations in each GB and each sample was measured using the PSMC to determine the alpha value of the holdup. The purpose of these measurements was to assess the alpha distribution of holdup in each GB. These results were then used to calculate the weighted average alpha for each GB at PCDF. The IBAS slope validation tests were performed after these alpha map measurements so that the measured average alpha values for each GB could be used to help evaluate the need for a correction factor to the 2010 IBAS calibration slopes. It is important to note that the results from the alpha map measurements confirmed that the alpha values of the actual holdup (α = 0.9~41) were much higher than the alpha values of the MOX standards (α = 0.7) used during the 2010 calibration exercise.

The measured IBAS doubles rates before and after cleanout at each position for gloveboxes P13B04 and P15B01 are given in Table 2. A count time of 60 minutes was used for each measurement position. This enabled the relative 1σ uncertainty in the measured doubles rates to be reduced to approximately 4-5%. It should also be noted that for both gloveboxes we see a measureable decrease in the average doubles rates after cleanout indicating that a sufficient mass of MOX holdup was removed from each GB which is necessary for validation of the 2010 calibration slopes.

Position	P13B04 Doubles ± 1σ [cps]	
	Before Cleanout	After Cleanout
A1	42.22 ± 11.10	36.36 ± 9.55
A2	87.06 ± 14.18	90.48 ± 8.97
A3	96.42 ± 14.54	87.10 ± 10.35
B1	139.6 ± 14.55	154.4 ± 13.91
B2	272.1 ± 15.87	216.6 ± 16.55
B3	247.2 ± 19.32	145.3 ± 12.19
Average	**147.4 ± 15.1 (10%)**	**121.7 ± 12.2 (10%)**

Position	P15B01 Doubles ± 1σ [cps]	
	Before Cleanout	After Cleanout
A1	40.58 ± 7.95	42.03 ± 6.69
A2	38.55 ± 6.18	38.33 ± 7.55
A3	17.12 ± 3.73	9.707 ± 3.35
A4	9.699 ± 2.24	7.541 ± 1.99
A5	5.254 ± 1.22	1.806 ± 1.61
B1	127.6 ± 12.7	128.7 ± 13.1
B2	116.6 ± 11.1	103.4 ± 10.6
B3	42.39 ± 4.89	36.55 ± 4.67
B4	20.15 ± 3.16	14.54 ± 2.81
B5	10.95 ± 2.25	9.46 ± 2.06
Average	**42.9 ± 6.7 (16%)**	**39.2 ± 6.6 (17%)**

Table 1. Measured IBAS doubles rates before and after cleanout for gloveboxes P13B04 and P15B01.

Table 3 shows the comparison of the results for the $^{240}Pu_{eff}$ mass measured by IBAS and the PSMC. For IBAS, the $^{240}Pu_{eff}$ mass was calculated by dividing the difference in the doubles rate before and after cleanout by the 2010 calibration slope measured for each GB. For the PSMC, the $^{240}Pu_{eff}$ mass was calculated using the passive multiplicity analysis method in INCC. Based on these results, we see that for both gloveboxes (P13B04 and P15B01) there is **not** a significant difference (>3σ) between the $^{240}Pu_{eff}$ mass measured by IBAS and the PSMC. Thus, this confirms that the 2010 calibration slopes are still valid.

Glovebox	Alpha	$^{240}Pu_{eff}$ Mass ± 1σ		Significant Difference (>3σ)
		PSMC	IBAS	
P13B04	37.5	35 ± 10	99 ± 31	**No**
P15B01	3.10	50 ± 3	45 ± 37	**No**

Table 2. Comparison of results for recovered $^{240}Pu_{eff}$ mass measured by IBAS and the PSMC.

In order to obtain a better understanding of how alpha (α) and multiplication (M) can impact the calibration slopes, the point model equations [5] were used to calculate the doubles rate as a function of $^{240}Pu_{eff}$ mass using for two different values of α (0.7 and 34) and M (1.001 and 1.010). The results are shown in Figure 6. It should also be noted that the alpha and multiplication values given in the table next to the plot were determined from the alpha map measurements and represent the average for each glovebox. Based on these results, we see that the high alpha value only has a significant effect on the doubles rate when the multiplication is significantly greater than 1.00. This is an important result because we expect that the multiplication values of the holdup in the gloveboxes in PCDF to be approximately equal to 1.00. Furthermore, this also reiterates the conclusion above that the 2010 calibration slopes are still valid.

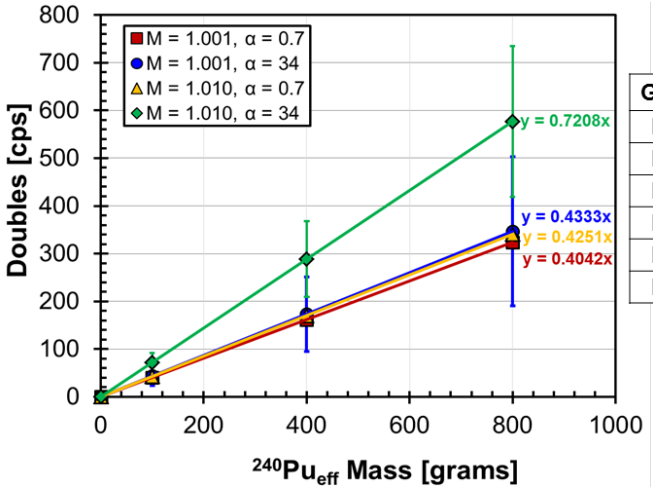

Glovebox	Alpha	Multiplication
P13B04	37.46	1.001
P13B09	18.10	1.002
P14B01	2.522	1.002
P14B02	7.263	1.001
P15B01	3.095	1.000
P16B01	3.111	1.001

Figure 6. Point model calculations for Doubles rate versus $^{240}Pu_{eff}$ mass for different values of alpha and M.

Another important factor that should be considered is that the PSMC measured alpha values may be higher than the actual alpha values inside the GB prior to clean-out, especially for higher mass samples. This may be attributed to the fact that the holdup is dispersed in the GB and then lumped together in a container when measured in the PSMC which increases the multiplication and alpha. The doubles to singles ratio can be used as an additional check for alpha since we expect changes in alpha to primarily affect the singles rate. Figure 7 shows the (a) average doubles rate and (b) average doubles / singles (D/S) ratio from each glovebox from 2010 through 2013. Based on the results, we see that the average doubles rates and D/S ratios are relatively constant for all gloveboxes except P13B04 which may be attributed to the removal of holdup.

Since the increase in the multiplication of holdup with high alpha values affects the integrity of current calibration slopes, it is necessary for operator to determine the holdup location and recover the holdup as a cleanout activity prior to PIT (Physical Inventory Taking) in order to maintain the appropriate measurement conditions for nuclear material accountancy and inspection. Therefore, JAEA has reflected this knowledge into an operational procedure at PCDF.

Figure 7. (a) average doubles rate and (b) average D/S ratio from each GB from 2010 through 2013.

5. Summary and Conclusions

We have conducted the IBAS slope validation test and analysis in order to confirm the validity of 2010 IBAS calibration slopes for the condition of high alpha holdup. The slope validation tests were performed after the alpha map measurements so that the measured average alpha values for each GB could be used to determine if any corrections were needed for the 2010 calibration curves. The results from the alpha map exercise confirmed that the alpha values of the actual holdup (α = 0.9~41) were much higher than the alpha values of the MOX standards (α = 0.7) used during the 2010 calibration exercise.

It is important to note however that the results from IBAS slope validation test confirmed that the 2010 calibration slopes are valid even for high alpha holdup. Quantifying the alpha term of the holdup in each glovebox and understanding how it changes over time is important to improving the overall nuclear material accountancy at PCDF. The doubles to singles ratio can be used as an additional check for alpha since we expect changes in alpha to primarily affect the singles rate. The results from this work have provided invaluable experimental data that directly supports safeguards and NMA measurements of plutonium holdup in gloveboxes.

6. Acknowledgements

We would like to acknowledge the Department of Energy National Nuclear Security Administration's Next Generation Safeguards Initiative (NGSI) / International Nuclear Safeguards Engagement Program (INSEP) in the Office of Nonproliferation and International Security for supporting this work.

7. References

[1] H.O. Menlove, J.E. Pieper, "Description and Operation Manual for the Active Well Coincidence Counter," *Los Alamos National Laboratory Report*, LA-7823-M (1979).

[2] B. Harker, M. Kirk, "INCC Software User's Manual," *Los Alamos National Laboratory Report*, LA-UR-01-6761, March 2009.

[3] H.O. Menlove, J. Baca, M.S. Krick, K.E. Kroncke, D.G. Langner, "Plutonium Scrap Multiplicity Counter Operation Manual," *Los Alamos National Laboratory Report*, LA-12479-M.

[4] H. Nakamura, Y. Mukai, T. Kurita, "Information on Current NDA Systems (PSMC, WDAS, M-SBAS)," *PAS-14 JAEA Communication Report*, July 2011.

[5] N. Ensslin, M.S. Krick, D.G. Langner, et al., Chapter 6 Passive Neutron Multiplicity Counting, *Passive Nondestructive Assay Manual Addendum*, LA-UR-07-1403 (2007).

Session 9

Training and Knowledge Management

Canada's Standardized Program for Training Safeguards Inspection Staff

Paula Creary, Karen Owen-Whitred, Robert Chamberlain

Canadian Nuclear Safety Commission
Ottawa, ON K1P 5S9 Canada
Paula.Creary@cnsc-ccsn.gc.ca, Karen.Owen-Whitred@cnsc-ccsn.gc.ca, Robert.Chamberlain@cnsc-ccsn.gc.ca

Abstract

Training is fundamental to success in a new position at the Canadian Nuclear Safety Commission (CNSC) or any organization. Training is particularly important to the area of safeguards as it is a specialized field in which a unique set of skills is required, including communication, mediation and diplomacy. The safeguards staff of the CNSC remained static for many years, but an increase in turnover is expected due to an increasing retirement rate as well as the reality of increased staff mobility. Historically, there has been a lack of documentation with regards to training, but due to the factors mentioned above it has become evident that a documented and standardized program for training was necessary. The CNSC's safeguards training program exists within the larger CNSC Inspector Training and Qualification Program (ITQP), a standardized process launched by the CNSC in 2009 with the goal of improving consistency and efficiency amongst all its inspectors. All employees in a designated inspector position at the CNSC must enroll in this program. The ITQP requires that new inspection staff complete a variety of knowledge-based activities and on-the-job training (OJT) activities – some of these are generic or core activities common to all CNSC inspectors and some are tailored to the specific field in which the inspector is working. The OJT is of particular importance in the area of safeguards as some of the unique skills required in this position can only be learned by observing experienced staff in the field as opposed to self-study. This paper will provide a brief description of the CNSC's ITQP, and of training for safeguards staff in particular, including on the job training, with the focus ultimately shifting to what has worked well and what could potentially be improved upon.

Keywords: training, on- the- job, inspectors, ITQP

1. Introduction

The Canadian Nuclear Safety Commission (CNSC) regulates the use of nuclear energy and materials to protect health, safety, security and the environment and to implement Canada's international commitments on the peaceful use of nuclear energy; and to disseminate objective scientific, technical and regulatory information to the public. The Commission is an independent administrative tribunal set up at arm's length from government, with no ties to the nuclear industry. The role of State System of Accounting for Control of Nuclear Material (SSAC) is fulfilled by the CNSC, specifically the International Safeguards Division (ISD). Figure 1 depicts the placement of Canada's SSAC within the CNSC.

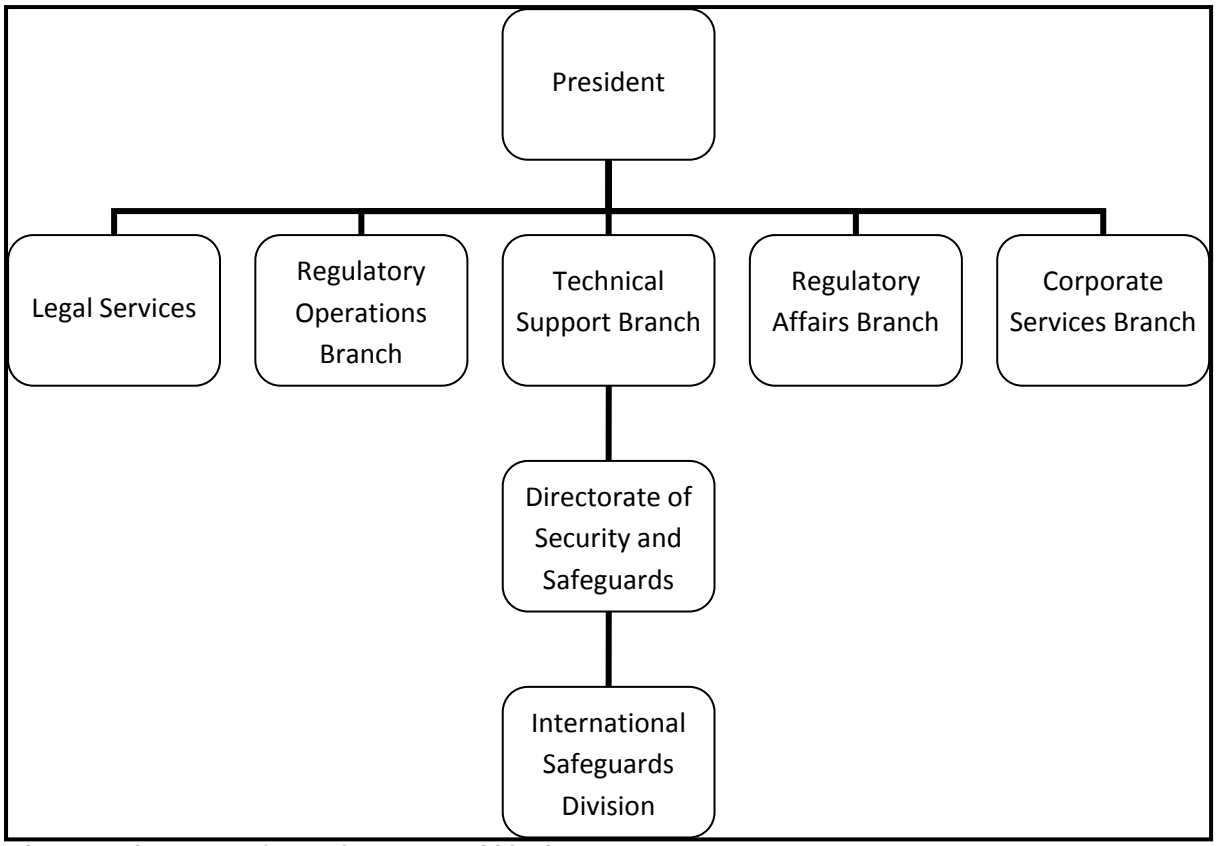

Figure 1: Placement of Canada's SSAC within the CNSC

Historically, Canada did not have a domestic safeguards inspectorate. The role of an ISD inspector during International Atomic Energy Agency (IAEA) inspections is to ensure that the licensee complies with all of their safeguards obligations, thereby enabling the IAEA to carry out its inspection and to ensure that the IAEA limits its inspection activities to those permitted under the Integrated Safeguards procedure and/or the Safeguards Agreements for the facility. The largest role for the CNSC during an inspection is to facilitate communication between the licensee and the IAEA, for instance, translating CNSC regulatory requirements into IAEA requirements (and vice versa). In all cases, it is paramount to ensure that the inspections are performed safely and in compliance with the CNSC's and the licensee's health and safety regulations. The Canadian domestic safeguards program differs from some other safeguards programs in that the IAEA does not necessarily have to be accompanied by the State, although the CNSC makes every effort to be present for all inspections.

The advent of the State-Level Integrated Safeguards Approach (SLA) in 2005 has shifted that slightly, introducing the concept of Physical Inventory Taking Evaluations (PIT-E). Under the SLA, a selection probability was introduced in which not all facilities in Canada were selected in a given year for a Physical Inventory Verification (PIV). With the CNSC's domestic safeguards program, those facilities not selected by the IAEA for a PIV will be subject to a PIT-E in order to be able to give assurances to the IAEA that those facilities were adequately prepared had they been chosen for a PIV.

2. Safeguards at the CNSC

The field of safeguards is a specialized field with a unique set of challenges. Safeguards staff at the CNSC remained static for several years, however, with the increasing retirement rate as well as the CNSC's initiative promoting staff mobility within the organization, the CNSC has seen an influx of new safeguards staff in the last few years. New staff typically has limited knowledge of safeguards and without the benefit of knowledge transfer from seasoned staff members, it became evident that a documented and standardized program was necessary. The development of this standardized program is also part of a broader corporate initiative. The CNSC launched its Inspector Training and Qualification Program (ITQP) in 2009 with the goal of introducing a consistent set of training and

qualification requirements for all inspectors across the organization. This program was also developed to continue to ensure the highest calibre of professional knowledge and experience among CNSC inspectors, give inspectors full confidence in their skills and abilities, and better support the authority of the CNSC.

Another unique challenge associated with safeguards is the set of skills required to participate in IAEA led inspections. As the CNSC must act as a point of contact between the facility and IAEA, communication, diplomacy and mediation are key. These skills cannot be taught by self- study and are best learned by observing seasoned staff in the field.

3. Overview of CNSC Inspector Training

Canada's Nuclear Safety and Control Act gives authority to the CNSC to designate as an inspector, for the purposes of the Act, any person whom the CNSC considers qualified. The inspector's authority and powers are also described in the Act. Given the extensive authority and powers of a CNSC inspector, only those who are qualified and whose duties and responsibilities require them to be an inspector will be issued a certificate. Trained and qualified inspectors are issued certificates in accordance with the Act and the CNSC General Nuclear Safety and Control Regulations. Under the Act, any person designated as an inspector shall be provided with a certificate in the prescribed form certifying the person's designation. The Regulations prescribe the form of the inspector's certificate and the information, in addition to that required by the Act, which must be included on it.

The CNSC has approximately 800 employees, with an inspector population of approximately 160 staff comprised of inspectors and inspectors- in-training. ISD currently has six active inspectors and five inspectors- in- training for a total of eleven inspectors.

The CNSC has dedicated significant effort to formalize its training program for domestic inspectors across all CNSC directorates and divisions responsible for conducting inspections. The purpose of this centralized CNSC-wide program, termed the Inspector Training Qualification Program (ITQP) is to:

- establish a consistent approach to train, qualify and assess CNSC inspectors-in-training across all service lines;
- empower inspectors-in-training with the skills and knowledge required to perform their duties;
- ensure inspectors-in-training possess the necessary qualifications and can demonstrate a high level of competencies required to conduct inspections;
- support the mandate of the CNSC.

The ITQP is comprised of three components: core training, service line-specific training and on-the-job (OJT) training. These three components will be discussed in greater detail below. The program also includes initiation training and an assessment of the employees' understanding of the CNSC Regulations. Inspectors-in-training and their director are responsible for ensuring that the inspector-in-training has met all the requirements of the ITQP. A standardized template is used by all inspectors-in-training to record his or her progress.

Typically, completion of all the training components of the program takes between 12 and 24 months. Completion of the program is dependent on many factors such as previous experience, operational requirements, timelines, and schedules.

Once all the training is acquired, an overall evaluation is completed by a coach, whom is a senior employee, and by the director. A successful evaluation is followed by a recommendation for certification from the director to a CNSC Designated Officer. A Designated Officer is an individual from CNSC's upper management authorized by the CNSC to make decisions on specific licensing actions and activities, such as designating inspectors.

3.1. Core Training

All inspectors-in-training must complete the core training which consists of basic and transferable knowledge and skills required by all CNSC inspectors. This training is based on the fundamentals of conducting a CNSC inspection, which are derived from international standards and good practice, including the IAEA Safety Standard Series titled Governmental, Legal and Regulatory Framework for Safety. All core training is offered through in-house classroom sessions or online modules and is followed by an exam.

3.2. Service-Line Specific Training

Service-line specific training is specific to the licensed activities and facilities that are inspected by each division. Each division must identify the service-line specific training required for their inspectors. For example, inspectors working within the power reactor licensing divisions are required to take a course on the fundamentals of the CANDU nuclear reactors. There is no service-line specific training that is required to be completed for safeguards staff to obtain an inspector's certificate. However, all safeguards inspectors are expected to take the IAEA's International Training Course on Implementation of State System of Accounting for and Control of Nuclear Material (SSAC course) at some point in their careers. The CNSC attempts to get safeguards inspectors-in-training and inspectors on this course at the first available opportunity.

3.3. *On-the-job Training (OJT)*

OJT teaches the skills, knowledge and competencies that are required to perform a specific job. It occurs within the normal working environment an employee will experience on the job. OJT uses workplace resources (personnel, equipment, documents) which allow an inspector-in-training to effectively learn how to perform his or her job. The OJT process relies on and uses the experience of senior employees as coaches.

In addition to the completion of the ITQP, inspectors-in-training must also complete training specific to their division. The additional training required for safeguards inspection staff is detailed in the next section.

4. International Safeguards Division (ISD) Specific Training

New ISD inspectors that facilitate IAEA inspections and conduct CNSC inspections are required to complete a variety of knowledge based activities and OJT under the guidance of a qualified ISD inspector. The training program specific to safeguards includes a Safeguards Orientation Plan and On-the-Job Training (OJT) Guide for International Safeguards Inspection Staff (hereafter, the Guide)

4.1. Safeguards Orientation Plan

The Safeguards Orientation Plan consists of six modules intended to introduce the subject of international safeguards on both a generic level and also with respect to implementation at specific facility types and locations in Canada. The staff presenting each module will discuss the subject area and make reference to their experiences, past presentations and relevant reference documents.

Module 1 starts with an overview of safeguards in Canada including the Non-Proliferation Treaty, the IAEA Statute and Canada's safeguards agreements and arrangements with the Agency; safeguards procedures for Canadian facilities; CNSC regulatory requirements and documentation; the CNSC's safeguards mandate; and future direction of safeguards in Canada.

Module 2 provides a high level familiarity with nuclear material accountancy in Canada, including an overview and introduction to nuclear materials accounting (NMA) in Canada, reporting requirements of licensees and the Nuclear Materials Accounting System (NMAS) used by ISD staff.

Modules 3 to 6 cover safeguards at Canadian facilities in more detail. Module 3 covers uranium processing and fuel fabrication facilities as well as Locations Outside Facilities (LOFs), Module 4 covers CANDU reactors, Module 5 covers research reactors and Module 6 covers Chalk River Laboratories and static spent fuel dry storage facilities. Each of these modules includes:

- an overview of a facility or site;
- terminology
- an overview of safeguards implementation at the facility/site and how it relates to the State-level approach;
- a detailed review of the current IAEA safeguards procedures and how they are applied at the facility/site; and
- a review of the applicable CNSC regulatory requirements and the CNSC internal safeguards procedures related to the different types of IAEA activities.

Other topics relevant to safeguards in Canada are also covered in these modules, such as the annual Additional Protocol update, and future direction of safeguards at the facility/site under the State-level concept.

4.2. On-the-Job Training Guide (OJT) for International Safeguards Division Inspectors

The purpose of this manual is to provide ISD with a standardized approach for training new inspectors who will participate in ISD inspections. Such an approach supports the CNSC's objective of having safe and effective inspections.

The Guide contains the learning tasks for successfully participating in inspections and consists of four sections:

- Role of an inspector
- Prepare for an Inspection
- Conduct an Inspection
- Document the Inspection and Follow-Up

Each section contains learning tasks, the role of the coach, the role of the inspector- in- training and any relevant references.

5. On-the-Job Training (OJT)

All components of the training program are important, but as OJT is of particular importance, this section will be devoted to OJT. Safeguards inspections differ from other types of inspections performed by the CNSC in that the IAEA is present. This uniqueness requires safeguards staff to have not only technical knowledge, but effective communication and mediation skills. As mentioned previously, these skills cannot be taught and are best learned by observing seasoned staff in the field. The importance of OJT in the field of safeguards has resulted in a training manual specifically for OJT, referred to as the Guide in this paper.

The suggested OJT training process, as outlined in the Guide, is divided into three sections: prior to the inspection, during the inspection and immediately following the inspection. Each section details recommendations for both the coach and the inspector-in-training such as focus of the training, review of tasks and relevant documentation, expectations and feedback.

ISD strives to follow a three phase approach with respect to OJT. During the initial phase of OJT, the coach demonstrates each inspection task and explains why it is important, while encouraging questions from the inspector-in-training. The inspector-in-training is an observer, rather than an active participant, during the initial phase. The second phase involves the coach and the inspector-in-training completing the inspection together. This phase allows the coach to guide and monitor the inspector-in-training during the inspection. The third and final phase allows the inspector-in-training to

complete the inspection with minimal guidance from the coach. The final phase can be performed as many times as required until the coach is satisfied that all inspections are being effectively completed.

When the coach and inspector-in-training mutually agree that the inspection learning tasks are performed to an acceptable level, the coach recommends to the Director of ISD that the inspector-in-training can be evaluated for that particular inspection process. A senior inspector accompanies the inspector-in-training into the field and evaluates the inspection process for completeness. As each evaluation is completed, the evaluator signs off on the OJT Evaluation Record.

Under the ITQP, all inspectors in training must document their OJT training in the training log provided by the CNSC. A new inspector will continue to participate in inspections until such time that the evaluation criteria is met to the satisfaction of the director.

6. Lessons Learned

As for all CNSC employees, the inspector's learning needs continue to be assessed on an ongoing basis using a performance based approach. Effective April 2016, an inspector's qualifications will be assessed against the existing ITQP qualifications prior to the expiry of the inspector's certificate. As a result, in addition to mandatory retraining in radiation protection and occupational health and safety, the inspector will have to retrain in areas determined to be required to confirm the qualifications have been maintained. The inspector will also have to demonstrate commitment to continuous learning, by having attended five days of relevant learning activities - such as workshops, conferences and self-directed learning - throughout the period he or she held an inspector certificate.

The Guide for ISD staff was implemented in 2014 and like any new implementation, this program is subject to continuous improvement. New safeguards staff are fortunate in that they are afforded several opportunities to observe and participate in field inspections with qualified safeguards inspectors. This experience is invaluable to not only the inspector- in- training, but also to the division. Often times, ISD is participating in two or three inspection activities simultaneously, with limited resources, so it is important for ISD to have a full complement of trained inspectors. Throughout this paper, the importance of OJT has been stressed and the greater the OJT opportunities, the sooner inspectors-in-training gain the confidence and competence to become qualified inspectors.

7. Conclusion

The President of the CNSC is responsible for ensuring that the CNSC meets its obligations to Canadians and abides by all Government of Canada laws and policies, which includes implementing measures on the non-proliferation of nuclear weapons and nuclear explosive devices. It is the vision of the President and the CNSC to be the best nuclear regulator in the world. The fundamental principle of transparency plays an important role in achieving this goal. The CNSC achieves transparency by being open and evident. This involves ensuring that all regulatory requirements and expectations are available to stakeholders and that the CNSC's inspection activities are open to formal scrutiny by the Government of Canada, stakeholders and the public, via reports and information requests. The concept of transparency can be applied across the organization. Informed decisions are documented within regulatory programs, processes, procedures and work instructions. By documenting our inspection training process, we demonstrate transparency and help to ensure a quality, consistent and effective regulatory program.

The Belgian approach in education and training in nuclear safeguards

Klaas van der Meer[1], Alessandro Borella[1], Riccardo Rossa[1,2], Michèle Coeck[1], Rozle Jakopic[3], Yetunde Aregbe[3], Peter Schillebeeckx[3], Bent Pedersen[4], Klaus Mayer[5]

[1] Studiecentrum voor Kernenergie•Centre d'Etude de l'Energie Nucléaire SCK•CEN, Boeretang 200, Mol, Belgium
[2] Université libre de Bruxelles, Ecole polytechnique de Bruxelles - Service de Métrologie Nucléaire (CP 165/84), Avenue F.D. Roosevelt, 50 - B1050 Brussels, Belgium
[3] Institute for Reference Materials and Measurements, JRC Geel, Belgium
[4] Institute for TransUranium Elements ITU, JRC Ispra, Italy
[5] Institute for TransUranium Elements ITU, JRC Karlsruhe, Germany

Abstract:

Since 2008 SCK•CEN provides a short safeguards course for mainly students in nuclear engineering. This is done in collaboration with the Institute for Reference Materials and Measurements (IRMM) of the Joint Research Centre in Geel, Belgium. This course is part of the BNEN (Belgian Nuclear higher Education Network) programme, a master-after-master specialization course in nuclear engineering. An adapted version has been provided to members and collaborators of the Flemish Parliament.
Based on these first initiatives, SCK•CEN and IRMM participate in the FP7 GENTLE project and have provided an updated course in 2014 to a group of international students. Next to theoretical classes, the course was extended with practical exercises in gamma and neutron NDA measurements and a workshop on safeguarding a country with a specific nuclear fuel cycle. These additional practical parts enabled trainees to enrich and illustrate their acquired knowledge with the practice of real-life situations.
In line with the European EQF and ECVET principles, learning outcomes for this course were defined in terms of knowledge, skills and attitudes.

In this paper we will describe the development of the Belgian safeguards course from an almost purely lecture-based course into an interactive course with hands-on practices. The integration into several national and international course programmes is described. Lessons learned from the pilot sessions and the planned implementation of additional elements to optimise the effectiveness of the Belgian safeguards courses are discussed.

***Key words**: safeguards course, nuclear engineering*

Introduction

The present ESARDA Working Group on Training & Knowledge Management (TKM WG) was established in the beginning of 2004 as the ad hoc Working Group on Modules of Courses by the ESARDA Steering Committee. Whereas the traditional focus of academic nuclear engineering programmes is the front-end of the nuclear fuel cycle and reactor safety, the ad hoc Working Group on Modules of Courses wanted to broaden that focus by introducing non-proliferation aspects to nuclear engineering students. At the end of their study nuclear engineers may well not have heard at all of non-proliferation aspects of nuclear energy. In addition to this, a significant loss of safeguards experience was expected for the next years due to the retirement of many experienced safeguards experts. Without the instream of new, young professionals this would pose serious problems for the safeguards community.

In 2005 a first ESARDA safeguards course was given on the premises of the Joint Research Centre of Ispra, Italy, under the auspices of the ESARDA TKM WG. It was attended by 20 participants from various backgrounds and institutes. Students of the Belgian Nuclear Higher Education Network BNEN could acquire 2 ECTS (European Credit Transfer System) points for attending the course and writing a small essay.

With the financial support of JRC Ispra the course is continued annually with growing success. In 2007 the TKM WG published a syllabus for the standard part of the course. This was required by the European Nuclear Education Network (ENEN) to allocate 3 ECTS points to the course.

From 2008 the course attracts so many students that a numerus clausus of 60 students per year had to be established. At the same time it was decided to start a limited version of the ESARDA course with the safeguards essentials at the Belgian Nuclear Research Centre SCK•CEN in Mol, Belgium. This course was a topical course in the curriculum of BNEN and 2 ECTS points were allocated to students that successfully wrote an essay. Similar initiative has been taken by Sweden, where a safeguards course was given at the University of Uppsala.

Development of the Belgian safeguards course

Since 2008 SCK•CEN provides a short safeguards course for mainly students in nuclear engineering. This is done in collaboration with the Institute for Reference Materials and Measurements (IRMM) of the Joint Research Centre in Geel, Belgium. This course is part of the BNEN (Belgian Nuclear higher Education Network) programme, a master-after-master specialization course in nuclear engineering. An adapted version has been provided to members and collaborators of the Flemish Parliament. This version contained a simple introduction to nuclear physics.

The BNEN safeguards course is not part of the obligatory programme of the nuclear engineering master-after-master, but is optional. This means that not all BNEN students will follow the safeguards course. However, the BNEN safeguards course has been given almost every year since 2008 and attracted each time 15-20 participants. The participants were mostly BNEN students, but also young professionals from JRC Geel and SCK•CEN that were interested in safeguards.

The content of this BNEN safeguards course is given in the Appendix A [1]. The course was based on vocational training only and lasted for two days. It discussed the legal basis of safeguards in the form of the various treaties and the safeguards systems (INFCIRC/66, /153, /540), safeguards concepts and the specific techniques used in safeguards (NDA, DA, C/S, …). Some country cases were discussed, like e.g. DPRK, Iran, Iraq.

Whereas the first editions discussed at length basics of nuclear physics and the nuclear fuel cycle, it was decided to eliminate the basics of nuclear physics since nuclear engineers encounter this already in other parts of the BNEN curriculum, while the nuclear fuel cycle part was transformed to a lecture in which for each nuclear fuel cycle installation the safeguards approach was discussed, rather than the technical details of the installation itself.

Based on these first initiatives, SCK•CEN and IRMM participate in the FP7 GENTLE project with the purpose to develop a safeguards course that makes an integral part of a nuclear engineering academic course. The pilot GENTLE safeguards course was provided in 2014 to a group of international students.

We took the occasion to rethink the whole concept of the safeguards course in order to make it more attractive for the students and to provide them with much more hands-on practice in safeguards. To this end, we wanted to provide more practical training in both the more conceptual part of safeguards, i.e. how to inspect a state and the development of safeguards approaches for nuclear fuel cycle installations, and the practical aspects of measuring the quantity and quality of nuclear material by NDA methods. These are discussed in the next section.

The pilot course will be adapted on basis of the feedback that was received by the students. The developed course with extended hands-on training will also be integrated in the BNEN training curriculum.

The new aspects in the GENTLE safeguards course

As mentioned in the previous section, the GENTLE safeguards course aimed at providing more hands-on training in safeguards than its predecessor the BNEN safeguards course.
To this end, new modules were developed to perform practical NDA measurements on nuclear material and to develop a safeguards approach for a state with a well-developed nuclear fuel cycle.

Practical NDA measurements

The students were divided into small groups of 6-7 persons and could perform gamma measurements and neutron measurements on nuclear material with the help of NDA experts from JRC-Geel, JRC-Ispra and SCK•CEN.

Gamma measurements were performed on uranium samples in order to assess the enrichment of the uranium. The measurements were carried out with the so-called CBNM standards by applying the infinite thickness method. For four samples the enrichment was known to the participants, who had then to determine the enrichment for a sample whose enirichment was unknown to them.

Neutron measurements were performed on plutonium samples in order to quantify the plutonium mass. Aspects like necessary knowledge of the isotopic composition and related uncertainties, single, double and triple neutron measurements were discussed during this session.

The focus of this practical session was more on the analysis of the measured data than on the measurements itself, given the limited time available.
For this practical measurement workshop one day was allocated.

Workshop on safeguards approach of a nuclear fuel cycle

In the workshop on safeguards approach a fictitious country with a well-developed nuclear fuel cycle was presented. Students were divided in several groups and each group discussed separately following aspects. First a general discussion was held on the proliferation concerns of the presented fuel cycle. Based on the results of this discussion and further input on the history of the nuclear fuel cycle research in the country, the groups were asked to make an acquisition path analysis of the country's nuclear fuel cycle.

The groups were allocated different roles (inspector, proliferator) and each group had to develop specific inspection strategies/acquisition paths with the purpose to defeat the adversary group.
Finally, a discussion was held dealing with Additional Protocol aspects of inspections and how this would change the possibility to divert nuclear material.

Feedback

The participants of the pilot safeguards course were asked to provide feedback about the course. Some requested less theory and even more practical sessions, and overall the practical workshops were very well appreciated. Remarks were received about too much content in the presentations, while other remarks mentioned that the lectures were given sometimes too slow. In general more practical examples were asked for.

Some remarks were received about the practical organisation of the practical and vocational sessions. Due to limited availability of lecturers and support for the practical sessions it will not always be possible to take these remarks completely into account.
One specific problem for the group of students that attended the pilot GENTLE session was that their knowledge of the nuclear fuel cycle was more limited than that of nuclear engineering students. Therefore there was a need to explain the nuclear fuel cycle in more detail, while it had been decided to skip this based on the assumption that the students would have this knowledge.
In general the course was appreciated between good and excellent and so were the course lecturers.

Learning outcomes

In line with the European EQF and ECVET principles, learning outcomes for this course were defined in terms of knowledge, skills and attitudes. Given the relative short duration of the course (3 days), the learning objectives for the vocational training sessions were often limited to the aspects of comprehension and description of the subjects treated. However, with help of the practical training sessions and workshop we succeeded in establishing a higher level of use of knowledge, i.e. the ability to apply the acquired knowledge to actually design a safeguards approach for a well-developed nuclear fuel cycle and discuss the advantages and disadvantages of the designed safeguards

approach. Likewise, the students were able to make an analysis of gamma and neutron measurement results and discuss the influence of uncertainties on the conclusions that can be drawn regarding isotopic composition and quantity of nuclear material present.

Summary and conclusions

Thanks to the GENTLE FP7 project, the BNEN safeguards course has developed from a set of purely vocational lectures to a combination of vocational lectures and practical training and workshops.
The use of practical sessions makes it possible to lift the students' acquired knowledge to a higher level, i.e. that they are not only able to repeat the treated knowledge but are also able to actually use the knowledge in a more independent way.

From the feedback received from the students the practical sessions and workshop were highly appreciated, showing that this development should be maintained in the future and possibly more developed.

Although the students indicated they wanted even more practical sessions, there should remain a balance between more theoretical (vocational) training and practical sessions. Without any background in safeguards principles it will not be possible to have a workshop on safeguarding a nuclear fuel cycle.

Next sessions will be aimed to provide a better balance between vocational and practical training on each individual day.

Acknowledgements

We would like to express our thanks to the technical staff of IRMM, JRC Geel, who supported the NDA measurement sessions.

References

[1] R. Carchon, K. van der Meer, "*Safeguards course in the framework of BNEN (Belgian Nuclear higher Education Network)*", 4th International Conference on Education and Training in Radiological Protection ETRAP 2009, 8-12 November 2009, Lisbon, Portugal

Appendix A: Content of the first editions of the Belgian safeguards course [1]

2.1. Introduction

The course provides a specialised overview of all the elements needed to understand the basic principles of Safeguards, the verifications that take place within the framework of the Treaty on the Non-proliferation of Nuclear Weapons.

2.2. Basics of Nuclear Physics

A repetition of basic concepts of nuclear physics was considered mandatory, because part of the students had a background in sociology. Concepts of atomic and nuclear structure, nuclear stability and the nuclide chart, radioactivity, natural radioactivity and fission, the chain reaction were discussed.

2.3. Nuclear Fuel Cycle

An overview was given of the nuclear fuel cycle: mining, milling, conversion, enrichment, fuel fabrication (uranium and mixed-oxides), reactor operation, reprocessing, waste, final disposal.

2.4. International Treaties

Safeguards originates from the Treaty on the Non-proliferation of Nuclear Weapons (the Non-proliferation Treaty – NPT) and some prior bilateral agreements. To better position the NPT, a comprehensive overview of international treaties was given, including those that are related to disarmament.

2.5. The general safeguards picture

In the sub-part on Safeguards principles, the objective (political and technical) and limitations of safeguards are explored. Safeguards principles for declared material were clarified, such as starting point of safeguards, Safeguards measurement techniques (in general), some definitions (material categories, significant quantity, timeliness goal, detection probabilities), diversion strategies, types of inspection. Safeguards principles for undeclared activities are also discussed.

The sub-part on Safeguards approaches contains a historical overview of the different approaches existing, evolving from bilateral agreements on specific installations, towards full scope safeguards in the States that signed the NPT (since 1970). The Additional Protocol (INFCIRC/540) was developed after the discovery of an undeclared weapon programme in Iraq, and was explained in detail.

In the sub-part on Case studies in (non-)proliferation, specific attention was given to historical and actual problematic cases: North Korea, Iran, South Africa, Libya, Pakistan, India, Israel, Iraq.

2.6. Techniques

There were various sub-sections:
Nuclear Material Accountancy
The sub-section on Nuclear Material Accountancy explained Nuclear Material Accountancy as the basis of safeguards.

C/S
The sub-section on C/S contained the legal basis of C/S, some Application Examples, the underlying safeguards requirements, Digital Systems, current C/S equipment, C/S in the context of integrated safeguards, and current R & D projects and needs.

NDA
The sub-section on Non Destructive Analysis NDA dealt with nuclear techniques and other physical properties instruments. The aim of the topic was to give a flavour on how a single measurement, or a combination of, can contribute for the inspector to make independent conclusions in his verification activities. The recommended NDA methods are also part of the IAEA safeguards criteria, discussed in 2.7.

The nuclear related NDA deals with Gamma-Ray Instruments and Neutron Instruments, with details on the detectors and associated electronics, and methodology.
The non-nuclear related NDA deals with weighing and load-cells, ultrasonic thickness gauge, Cerenkov glow measurement devices, with details on the physical principles and methodology.
Performance was considered in detail, as well as the different types of NDA Instruments, Equipment authorization for inspection use in the IAEA, and Equipment information.

DA
The sub-section on DA dealt with the currently applied techniques, such as Thermal Ionization Mass Spectrometry (TIMS), Isotope Dilution Mass Spectrometry, Inductively Coupled Plasma Mass Spectrometry (ICP-MS), alpha Spectrometry, Hybrid K-Edge, Compucea, which were described in detail.
Particle analysis proved to be very powerful tool for detection of undeclared activities, considering that the highest sensitivity, accuracy and precision are required for answering specific questions.

AP methods
The sub-section on AP methods showed briefly the particular inspection techniques inflicted by the Additional Protocol: Open source information, Satellite monitoring, Environmental sampling (Swipes, Wide-area sampling).
The link was made to safeguards inspection techniques in general, with DA methods in particular, and the complementarities highlighted.

2.7. Verification measurement tables

The structure of the IAEA Safeguards Criteria was explained following the structure of the 12 chapters corresponding to the different fuel cycle installations.
The verification measurement tables were explained for the LWR and the RRCA.

2.8. Import/export control

Export controls on nuclear materials exist since the entering into force of the Treaty on the Non-proliferation of Nuclear Weapons (NPT). An extension to dual-use items was activated after the first Gulf war, and the detection of an undeclared weapons oriented programme in Iraq. This module explains in a historic context the various treaties related to export control.

2.9. Physical protection

Physical protection was explained as complementary to safeguards verification activities, in the sense that it is a first step in protecting sensitive goods from diversion or theft.
The Convention on Physical protection of Nuclear Materials (INFCIRC/274 Rev 1) was explained.

2.10. Design Information

A special chapter was devoted to Design information, regarded as “information concerning nuclear material subject to safeguards under the agreement and the features of facilities relevant to safeguarding such material”, as it is considered vital for effective Safeguards.

2.11. IAEA Member State Support Programmes

A short overview was given of the IAEA Member State Support Programmes, their way of working, the projects involved, and some details about the Belgian Support Programme, as an example.

The UK's Long Term Commitment to Training and Development in the International Safeguards Community

Stephen Francis

National Nuclear Laboratory, B709, Springfields Salwick Lancashire, United Kingdom
stephen.m.francis@nnl.co.uk

Abstract

The UK has maintained a long term commitment to provide support to the International Safeguards community in the form of training and development activities for safeguards inspectors and analysts. The majority of this support has been provided and funded through the UK's Safeguards Support Programme to the IAEA. The assistance offered centres around offering access to its nuclear facilities for the conducting of a specific safeguards training courses and activities in the UK. More theoretically based training events are also provided directly to IAEA in Vienna. This involves the utilisation of various leading UK technical experts in various fields across the breadth of the nuclear fuel, as well as in more specific safeguards related fields. Some of the longer standing training events have histories dating back over 25 years and these form the baseline for UK support. However, with the current evolutionary nature of IAEA safeguards, new events are developed and existing courses are constantly adapted to meet the changing needs of IAEA

1. Introduction

The UK Safeguards Support Programme (UKSSP) is currently funded through the Department of Energy and Climate Change (DECC), with programme management being sub-contracted to the UK's National Nuclear Laboratory. The majority of the budget is dedicated to offering technical support to the IAEA's Department of Safeguards, with a large proportion of this spending being dedicated to the provision of training courses and exercises.

There are established procedures for IAEA requests of support from Member State Support Programmes (MSSPs). On receipt of such requests, UK then has to decide whether it is technically able to offer such support and whether it has the budgetary means to do so. With only a finite budget available in any given financial year, not all requests for support can be accepted. UK strategy in this regard is generally to offer support in areas where the UK is able to offer technical resources which are either unique to the UK or not readily available to the IAEA elsewhere. The provision of specialist training support related to UK nuclear facilties and technology experts fits very well this criterion.

The UK has always operated a variety of nuclear facilities in all areas of the nuclear fuel cycle, with a particularly varied and high density of facilities being located in the north-west of England. Importantly, UK facility operators have always been extremely receptive to requests for access to their facilities, and for the involvement of their personnel for the purpose of providing training opportunities for safeguards inspectors from IAEA. This coupled to relatively short travel times from Vienna and easy transport links within the UK, has led to the steady development of an on-going portfolio of training support provided to IAEA.

2. Long Term Evolution of UK Training Portfolio

The origins of UK training support to the IAEA go back over 25 years. Initial support was in the form of facility based training exercises for IAEA Inspectors, primarily at fuel fabrication and reprocessing facilities. It was events following the discovery of the Iraqi clandestine nuclear weapons programme and the subsequent initiative to improve and strengthen IAEA safeguards that began a steady process of increased training provision by the UK

Safeguards Support Programme over the past 20 years.

The main basis for this increased involvement of UK in IAEA training provisions was the initial development of training in the area of proliferation pathways and proliferation indicators. The training was aimed directly at providing the IAEA with assistance in building a capability for the identification of clandestine activities. Indeed it was stated during the introduction to the early training events that discussion and questions relating to traditional safeguards inspections would not be allowed.

The Proliferation Pathways Course proved extremely successful and received universally excellent feedback. This started a process of the UK being asked to provide follow-up training for individual groups such as the Iraq Action Team and subsequently to develop more and advanced in-field training.

At the same time, the IAEA was in the process of expanding the number and variety of training courses on offer to both its inspectors and staff in other Division. With an already increased profile, and good feedback from existing courses, the UK was suddenly being asked to assist with training in a number of new areas. This process has continued to the present time and the provision of training services now makes up a large proportion of the support offered by the UK Safeguards Support Programme to the IAEA.

3. Recent UK Training Support to IAEA

3.1 Proliferation Pathways and Indicators

This was the first UK training course developed specifically as a consequence of the IAEA 93+2 Programme to introduce new and strengthened safeguards measures following the discovery of the Iraqi clandestine nuclear programme. The course was developed in the mid to late 1990's and still continues to the present day with 2 events held most years, with over 30 events to date.

IAEA requested a technology based training course based around all the major elements of the nuclear fuel from a technical rather than safeguards perspective. So rather than being a conventional nuclear fuel cycle technology course focused on safeguarding processes and nuclear materials, the course was designed to cover all supporting processes, equipment, materials and technical expertise required. As such, the course lecturers selected were technical experts in their respective fields and not safegaurds experts.

Due to the intensive nature of the course and the volume of technical material presented, the event is always held away from IAEA HQ in Vienna at a remote venue. From a pure training angle, this allows for the course participants to be able to concentrate fully on the training event, without any of the day to day work distractions that can be evident when training is conducted in the Vienna International Centre.

In addition to the base presentational material and associated technical exercises, the course documentation produced includes detailed technical narratives on the Conversion, Enrichment, Reactor and Reprocessing modules. As well as describing all the major processes, there is an emphasis on the description of the main proliferation indicators, which are also assigned relative strengths.

In many ways one of the initial aims of the training was to change the mindset of the IAEA inspectors. The term "inquisitive inspector" was used frequently; this was an attempt to remind the inspectors that the new and developing safeguards regime would not be solely aimed solely at meeting prescriptive safeguards criteria and inspection goals.

Although initially aimed at more senior IAEA inspectors, the course was soon opened up to all inspectors. In more later years, with the rapid development of Integrated Safeguards and the State Level Approach, the course is now offered to safeguards staff across all Divisions of the Department of Safegaurds.

3.2 Advanced Nuclear Fuel Cycle (ANFC) Course

This course was designed as a follow on to the lecture based Proliferation Pathways Course. The aim was to take the IAEA participants into the field and let them see and "experience" the processes and indicators described. The initial

week-long course itinerary included 2 days at the Sellafield reprocessing facility, 2 days at the Springfields fuel fabrication and conversion facility and a single day the Capenhurst enrichment facility. At present, 2 events are held each year in the UK and the course has now been running for over 10 years.

Access to UK nuclear fuel cycle facilties for the carrying out of training events remains key to being able to offer this type of training to the IAEA. Fortunately, UK facilities have always been extremely co-operative in allowing access to their sites and where necessary will make local staff available to provide expert technical assistance. However, access should never be taken for granted and it is vital to maintain a strong relationship with all the facility operators - a task not helped by the splitting up of the UK nuclear industry following the break up British Nuclear Fuels.

The ANFC course has continued to evolve over the years, mainly to reflect changes in the way IAEA safeguards has developed in recent times. As the IAEA moves to safeguards based on a State Level Concept, the use and involvement of safeguards analysts in the IAEA has increased. Originally this course was designed just for IAEA inspectors, however it has now been modified to accommodate the participation of safeguards analysts too. As such, the course now considers and includes the use of satellite imagery and open source information analysis into its programme.

3.3 Design Information Verification (DIV) Training at Bulk Handling Facilities

Originally called the Bulk Handling Course, this is the oldest UK training course that is still offered to IAEA. Current records for this course go back in to the 1980s, when the course was a mixture of plant tours, technical lectures, accountancy exercises and some on-plant measurement exercises. The course has always included weeks at both the Sellafield and Springfields facilities in the UK. Over the years the course has undergone various iterations to meet the changing needs of the IAEA and has finally evolved in to a Design Information Verification course, but still based around fuel fabrication, conversion and reprocessing facilities.

This course requires very close support from the facilties involved. As well as the provision of technical guides to support on-plant inspection exercises, the facilties are also extremely co-operative in the provision of technical plant details along with detailed process and plant drawings for the course participants to work with. There is a strong emphasis in training the course participants in the use and understanding of technical engineering drawings.

The overall 2 week course itinerary includes almost equal time in the classroom and on-facility. Extensive time is spent prior to the on-plant exercises in the examination of Design Information Questionnaires (DIQs) and a multitude of supporting documents such as building floor plans and elevations along with engineering and process flow diagrams

3.4 Comprehensive Inspection Exercise at Bulk Handling Facilities

This course more than any other required the greatest degree of support from a facility operator. Hosted by the Springfields fuel fabrication and conversion facility, the course encompassed exercises in the measurement of a number of different types of material using a range of measurement techniques. The course was aimed solely at IAEA inspectors is one of the basic technical training courses required by inspectors visiting LEU conversion and fuel fabrication facilities. IAEA also provided 4 technical experts, to cover the different measurement exercises.

The main requirement of the course was to provide the opportunity for participants to carry out measurements on low enriched UF6, UO2 powder, UO2 pellets, PWR fuel rods and PWR fuel assemblies. A demonstration of UF6 sampling was also provided and the participants were also provided with a detailed uranium accountancy exercise to undertake.

The courses were held over a period of 2 weeks. The first 3 days were reserved for the set up of equipment by the IAEA instructors who arrived in advance of the course participants. Some 400kg of equipment was sent in advance from

Vienna to Springfields. Amongst other things, this comprised, sodium iodide and germanium detectors, hand held detectors and a neutron collar. Measurements were carried out in 4 separate plant locations, requiring extensive effort in preparation of the training environments. The remaining 2 days of the first week were given over to technical lectures on measurement techniques, a description of the measuremnet exercises and the group based nuclear materials accountancy exercise. The second week involved rotation of the 4 groups of 3 participants around the different measurement exercises; with one day being spent in each area. The final day was reserved for the write up and presentation of the findings of the exercises.

As can be seen from the course description, the course essentially involved 4 distinctly separate exercises, each in a different plant area controlled by a different plant management team. It was this aspect that made the course particularly difficult to plan, organise and administer. Extra complications were created by other aspects, such as the need to keep the germanium detectors constantly re-filled with liquid nitrogen for the duration of the course.

3.5 Ad Hoc Support

Further training support is offered by UK to IAEA on an ad hoc basis - usually related to one off requests for training needs that arise from time to time in niche technical areas, or for groups of staff from specific Departments or Divisions.

In recent years technical visits have been made by a number of groups to many different facilties in the UK. These sometimes involve requests for more in-depth access to facilities already covered by existing training, but also involve facilities not routinely offered for training purposes.

4. Concluding Remarks

The UK continues to offer wide ranging support to the IAEA through its Safegaurds Support Programme. Traditionally this support was always facility based, making use of the wide ranging nuclear facilties operated within the UK's nuclear fuel cycle. The extent of this support has developed rapidly, particularly in the last 15 years.

The main challenge facing the UK at present is to be able to maintain this level of support in the light of the changes that are currently occurring within the UK fuel cycle. As some facilities enter a period of planned shutdown and eventual decommissioning, the facility based training provided will need to be adapted to meet these changes. In some ways the process of closing a facility can also provide new opportunities, as often this enables a better opportunity to inspect equipment that would otherwise be difficult to see close up whilst it was operating. However, this period of opportunity is obviously limited.

Challenges are also imposed by the ever increasing levels of security and security procedures surrounding nuclear facilities. This trend makes the process of obtaining clearance for IAEA staff to visit UK nuclear facilities increasingly painstaking and time consuming.

Increasingly the UK is being asked to provide training in many different areas, some even non-technical. The UK remains committed to its continued support to IAEA through its Safeguards Support Programme and will continue to respond positively to these requests as far as it is able to do so in terms of technical and budgetary constraints.

Nuclear knowledge management in higher education. Case of Tomsk Polytechnic University.

Demjanjuk D.G., Perminova M.V.

National Research Tomsk Polytechnic University.
Lenin Avenue, 30, Tomsk, 634050, Russia
E-mail: masha199303@gmail.com

Abstract:

*Leave three line spaces after the authors' addresses. Use the title '**Abstract**' as shown. The abstract should be about 300 words in length, describing only the main themes/ideas presented in the article.*

*Leave two line spaces after the abstract and write the title '**Keywords**:' as shown below. List not more than five keywords on the same line separated with semicolons. The objective of listing keywords is to facilitate the selection/classification of articles, to facilitate the establishment of the sessions in the conferences, and to allow for an easy retrieval by keywords. Please stick to words and not phrases.*

Keywords: publication; guidance; editing; standardisation

1. Introduction

The problem of knowledge loss is the issue of the present day in all types of industry. Special attention should be paid to nuclear industry. Nuclear energy technologies have a long life cycle, an obvious example is a nuclear power plant. Designing of a nuclear power plant takes at least ten years; its construction is also a long-term process, which needs the required knowledge and past experience. The next step is operation of nuclear power plant and the last one is shutdown. The whole process requires fixing of stored knowledge in the process of operation and in addition, it requires build-up and improvement of knowledge. For example, Fermi identified the concept of fast reactors development in 1944. In 1946, an experimental plutonium-fuelled reactor was created (Climentina, USA). To date, over twenty experimental and development fast breeder reactors have been created, the first industrial prototypes of fast power reactors, cooled by liquid metal (sodium), are in operation: in Russia (BN-600), France (PHENIX). These facts required knowledge transfer to the next three generations of researchers. Countries, which had no knowledge transfer of fast neutrons reactors technologies and closed nuclear fuel cycle, lost this knowledge considerably. The losses of experience and knowledge are not just economic losses. It is full-on scientific and technology disaster, which consists of losses of skilled workers, strong system of higher education, research and trial facilities, generation of young researchers. It may take decades for the government to recoup the losses.
Often, the knowledge and experience of past years have not been documented. The reason for the loss of nuclear knowledge, can serve a variety of factors such as aging of employees, decline of technological skills and loss of know-how, potential reduction in the safety and feasibility of innovation potential disappearance. In reference with the above nuclear knowledge stakeholders such as governments, international organizations, and industry have a vigorous activity in development of knowledge management. It includes strategies and programs to collect, exchange, store and transfer information to new generation.

Incidentally, knowledge management is needed to be applied to academic institutions too. Knowledge management formation in National Research Tomsk Polytechnic lets us provide an access to legacy of the past, present and future of nuclear industry.

2. IAEA and nuclear knowledge management

The IAEA nuclear knowledge management activities assist in transferring and preserving knowledge, exchanging information, establishing and supporting cooperative networks, and training next generation of nuclear experts. These activities in assisting Member States in the preservation and enhancement of nuclear knowledge and in facilitating international collaboration have been recognized by the General Conference of the International Atomic Energy Agency. Much work has been done by the IAEA in addressing the knowledge management needs of different nuclear organizations [1].

3. International experience

Experience of other international organizations, not just in nuclear industry, shows there are no universal systems of knowledge management for any kind of organisation. Each system has unique elements, tools and technologies. All knowledge systems is developed according to the purposes of a company, kind of activity and specificity of company`s knowledge. For the moment, the concept of knowledge management is integrated in developed global scale companies. This can be exemplified by Siemens AG, where in 1999 an information exchange system ShareNet29 started operating in Siemens Information and Communication network (ICN) [2]. The next example is Skanska Group, which has IT-platform called Skanska Knowledge Network [3]. Skanska Knowledge Network helps corporate employee to find necessary information in inhouse database. The example of application of nuclear knowledge management system is Canadian project CANTEACH [4]. This knowledge repository provides high quality technical documentation relating to the CANDU nuclear energy system. The CANTEACH Project aims to provide an information exchange network for people interested in the CANDU energy system. Contributors are industry experts who hold valuable knowledge and experience in diverse aspects of CANDU technology and its applications, and unique expertise in the areas of science and technology, nuclear power design and construction, project management and development of engineering tools [4].
Consequently, one of the main points of successful usage of stored knowledge is systematization and management. Nuclear industry needs individual approach for integration of knowledge management system.

4. Nuclear knowledge management system in National Research Tomsk Polytechnic University

National Research Tomsk Polytechnic University (TPU) is one of the leading nuclear universities of Russia. Today TPU consists of twelve institutes, thirteen management units and has its own nuclear reactor. Also, the university is included in association of consortium of main academic institutions of Rosatom State Atomic Energy Corporation (Rosatom). Rosatom is integrating nuclear knowledge management system in all branches of company.TPU with such complex organizational structure has a significant knowledge and information flow. This flow needs to be managed. The goal of the present work is to investigate the Rosatom`s experience in creating of nuclear knowledge management system and, as a result, integrate this system in the Institute of Physics and Technology (IPT). The introduction of the concept into the structure of the Institute will provide access to the existing legacy of nuclear expertise, ensure the transfer of knowledge to a new generation, and will fill the gaps emerged in connection with the loss of nuclear knowledge.
Organizational structure of IPT is detailed in figure 1. The structure includes Academic office, Science office, Material Properties Measurements Centre (MPMC), Engineering support office, Nuclear research rector, Information office. In addition, the institute consists of eleven departments and seventeen laboratories. Authority of IPT is headed by the Director, Deputy Director for Academic Affairs and Deputy Director for Research.

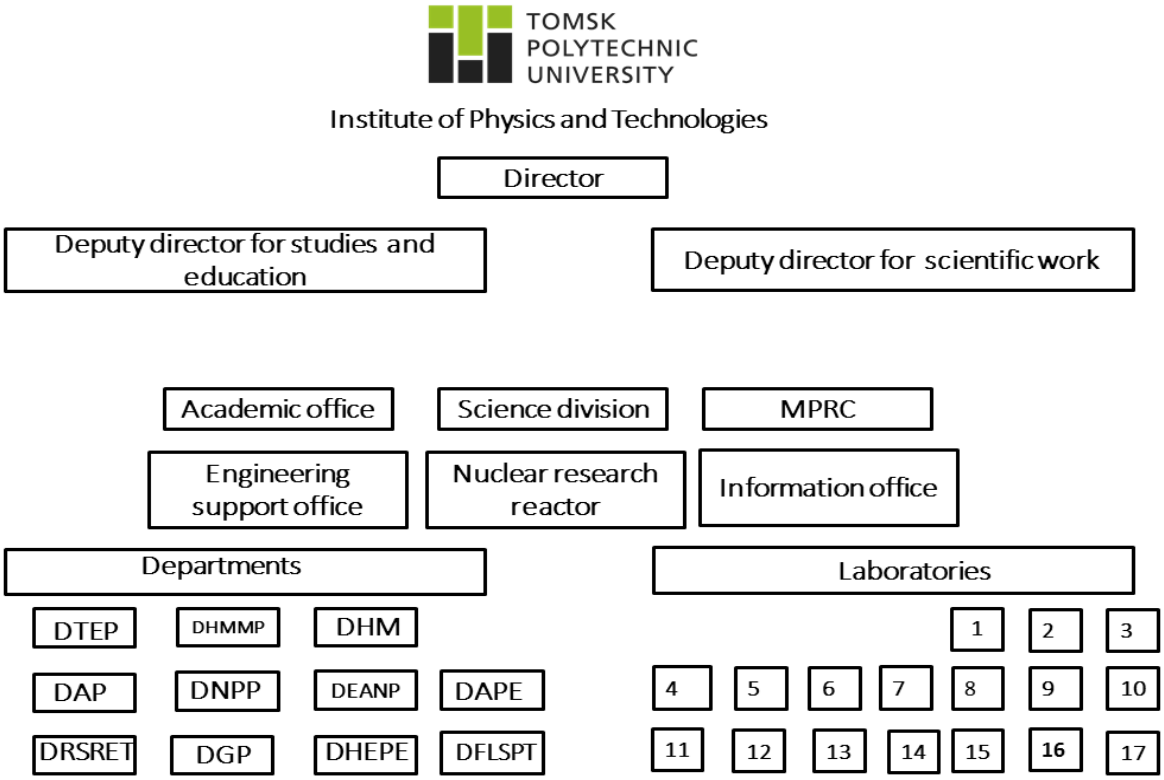

Figure 1 Organizational structure of Institute of Physics and technologies

R&D results obtained by IPT staff and students need to be structured and preserved. The diagram of knowledge generation processes is shown on figure 2.

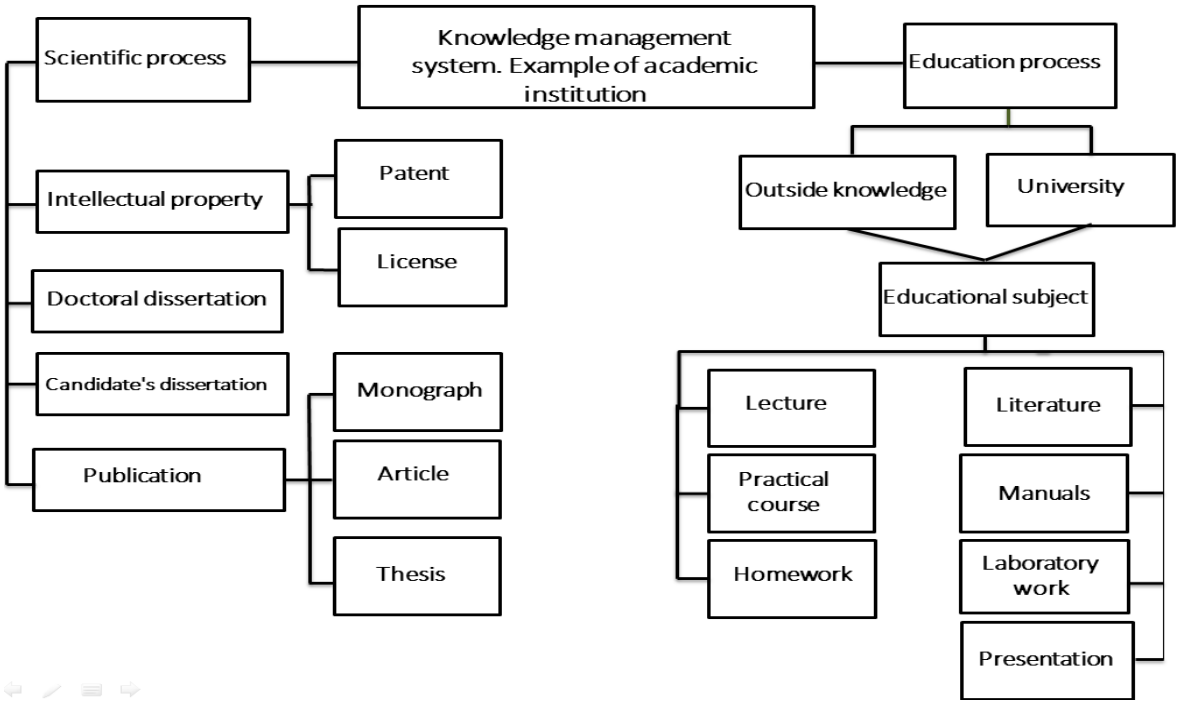

Figure 1 Information processes

Scientific and technical information portal of IPT has the form of library, which collects all scientific research, projects, IPT employees and students' publications; in addition, it consists of work experience of last generations. All this information is available for both employees and students, thereby reducing the time for information search.
Using a web-browser users connect to the portal and can perform the following actions:
• view information collections;
• add, edit and delete the items in information collections;
• perform a full-text, attributive search, and a search using the industry classifier or the thesaurus;
• create permanent thematic queries;
• use the "Calendar of scientific and technical activities".
Home page includes general information about this project, a newsportal, and materials of knowledge management system with operating manual and history of the project. One can also find contact information, and technical support line, where users can seek the advice of the portal content administrators and technical experts on issues related to the preparation of documents and their posting on the Scientific and Technical Information portal.
Portal includes nine information sections (figure 3).
1. Publication. This section includes articles, reports, presentations of employees and students that were publish in national and foreign journals.
2. Repository of scientific and technical documentation. Catalogue of digitized scientific and technical documentation of the Institute (research paper, developmental work. Inoperative patents, etc.).
3. R & D works ready for commercialization.
4. Intellectual property. This section consists of IPT employees' intellectual property.
5. Content of scientific events. This section consists of conference, seminar, and symposium information.
6. Specialists. The details about specialists of IPT in different scientific fields.
7. Scientific online resource. Hyperlink for informative sources.
8. Trade journals.

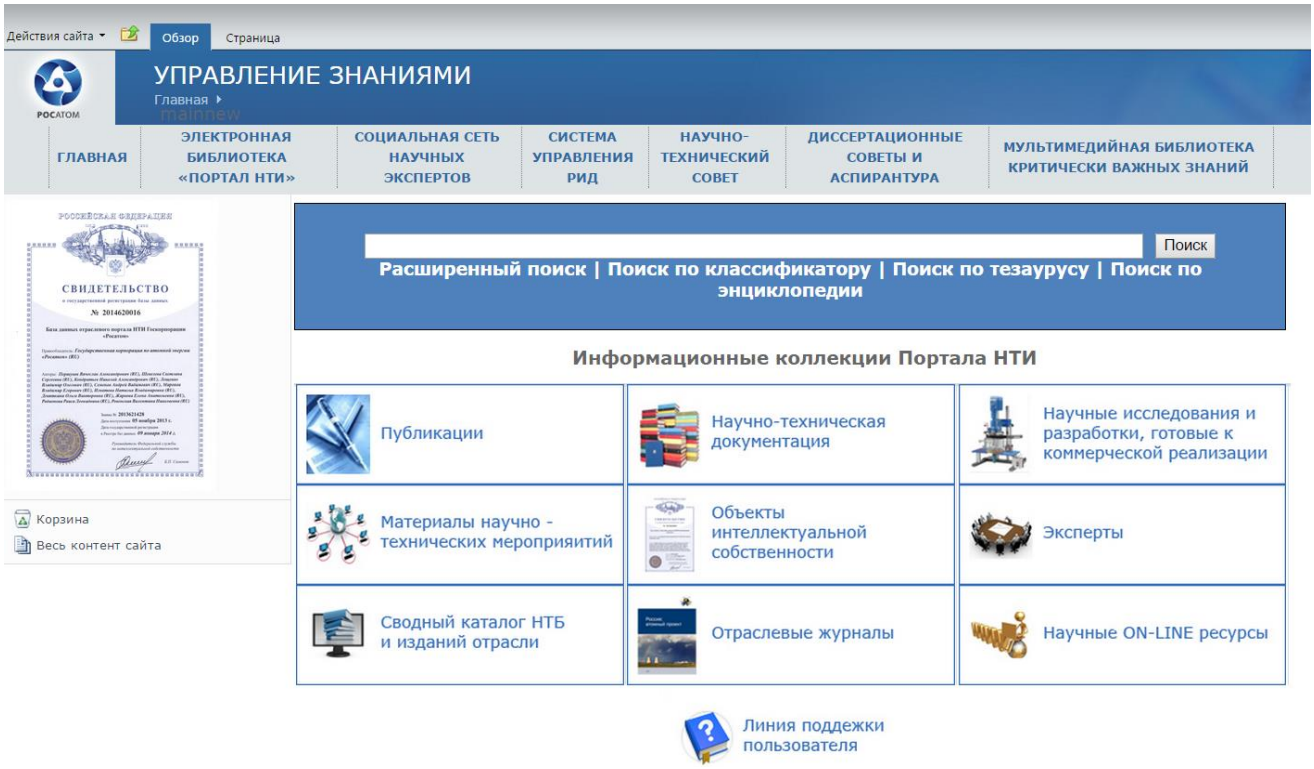

Figure 3 Scientific and Technical Information portal of IPT

5. Conclusion

At the beginning of scientific work, a researcher spends eighty percent of time for solving old tasks and just twenty percent for searching innovation solutions. Thanks to the Scientific and Technical Information portal of IPT this proportion can be changed exactly the opposite. Currently, TPU is integrating into knowledge management system of Rosatom. The process of developing IPT system is on the early stage. Digitisation of IPT stored knowledge and filling-in of the library have already started. After successful application in IPT, it is planned to expand and integrate the system into all institutes of TPU.

8. References

[1] International Atomic Energy Agency; Knowledge Management for Nuclear Research and Development Organizations; 2012.

[2] Hauke Heier, Hans P. Borgman, Andreas Manuth; Siemens: Expanding the Knowledge Management System ShareNet to Research & Development; Idea group Publishing, USA, 2005.

[3] Mikael Ericsson, Sebastian Reismer; Knowledge Management in Construction: an approach for best practice diffusion in Skanska Sweden AB; Chalmers reproservice, Göteborg, Sweden 2011.

[4] Bill Garland, Yulia Kosarenko, Dan Meneley; .Preserving CANDU Technical Knowledge. The CANTEACH Project; Bulletin Can. Nuc. Soc., 2003.

Building a Strategy for ESARDA - Education, Training and Knowledge Management

Sophie Grape, Karin Persson, Erik Andersson Sundén

Department of Physics and Astronomy
Division of Applied Nuclear Physics
Box 516, Uppsala, Sweden
Uppsala University
E-mail: sophie.grape@physics.uu.se

Abstract:

This document proposes a new strategy for how the ESARDA organization could work with education, training and knowledge management in nuclear safeguards. With this document we want to anchor these ideas within the organization and its management, in order to have a broad support for this initiative. We propose to activate all ESARDA working groups in the process of identifying, selecting and preparing material for module based education and training. ESARDA could then more effectively broaden its education and training activities and strengthen the connections with academia. In this way, we would also create a way to export knowledge on nuclear safeguards to nuclear education programs on the European level.

We propose to create a task force that addresses a set of identified questions; examples are how to implement the new strategy, how to interact with academia and young professionals and how to develop, maintain, and structure the educational modules. By the end of 2015, the findings of the task force should be presented to the ESARDA management in order to be able to make a more informed decision on how to proceed with the new strategy.

Keywords: strategy, education, training, knowledge management, module

1. Introduction

ESARDA is an association of European organisations formed to advance and harmonise research and development in the area of safeguards. It provides a forum for the exchange of information and ideas between nuclear facility operators, safeguards authorities and persons engaged in research and development. ESARDA was formed in 1969 with the purpose of facilitating collaboration in R&D in the field of safeguards and in the application of such R&D to the safeguarding of source and special fissile materials. Activities take place via

- annual meetings and symposia,
- working groups (WGs),
- education,
- the ESARDA Bulletin and website

The ESARDA Training and Knowledge Management Working Group (ESARDA TKM WG) is one of several working groups in the ESARDA organization. The primary objective of this group has been to offer the ESARDA nuclear safeguards and non-proliferation course to students and young professionals at least once per year. However, there has been a wish from ESARDA to spread the knowledge about nuclear safeguards to more students than those of the ESARDA course, e.g. students taking courses in nuclear technology. Furthermore the wish had been also to encourage these individuals as well as young professionals to join and remain in the safeguards field.

1.1. Vision: Building a strategy for ESARDA education, training and knowledge management

This document describes a vision of how the ESARDA organisation could implement knowledge management in a practical way. In addition, we believe that the ESARDA organisation should work actively to increase awareness of nuclear safeguards by making educational and research material available, thereby promoting education and training in nuclear safeguards to a broad audience.

In the consideration of broadening the education and training activities of the ESARDA organization, we propose to map such activities performed by other networks, institutions and organizations to – if possible – benefit from collaborations and coordination of work.

Preliminary ideas how to develop a strategy for ESARDA and ESARDA TKM were published in the ESARDA Bulletin No. 51 [1]. This document deviates from those ideas to some degree, mainly because we now consider to a larger extent what is realistically doable. One of the differences concerns the degree of control that ESARDA has on the education offered by other institutions e.g. via train-the-trainer courses.

1.2. Objective of this report

The objective of this document is to anchor the proposed vision in the ESARDA organization in order to have this initiative approved for further investigations. Specifically, we need a broad support from the ESARDA management to create a task force comprising individuals representing the ESARDA management (Executive Board and Steering Committee) as well as the different WGs. We also believe that the entire WG TKM should be involved in the process. Of course, other alternatives to the creation of this task force could be discussed, such as including one or two members from the Executive Board and/or Steering Committee as well as members of the Editorial Committee and the other working groups into WG TKM. In both cases, a dedicated group of people working with this issue is required.

1.2.1. Task force

The purpose of the task force should be to investigate a number of questions. Some of them have already been identified, while others will most likely be revealed later on in the process.

Already identified tasks which the task force will need to address and answer are:

- Map external educational and training networks for possible future collaboration
- Identify possible ways of implementing the suggested vision, taking available resources into account
- Identify ways to develop, maintain and structure the educational modules and the content of a train-the-trainer course
- List what material that may already be available for inclusion in the modules
- Consider to what extent the available material should be open-source and to what degree, and using what resources, it should be quality controlled.
- Identify ways to interact with universities, university teachers, students and young professionals
- Engage the different WGs in the process
- Identify possible sources for funding for the proposed work
- To develop a time-plan and suggest responsible actors (persons or organizations) for the implementation

Ideally, the task force would work with these issues and come up with a realistic way to move forward with this initiative during 2015. After presenting the results of this work, it would be up to the ESARDA management to make a decision on what parts to implement and how.

We are aware of that ESARDA as an organization has no available funding and that ESARDA members are involved at their own expense. We also know that any suggestions that require the involvement of people are associated with a cost in terms of time and money. A question whether

universities have funding for this has come up, but we cannot see that it is possible. Another option is to ask if and to what extent different ESARDA member organizations may contribute. In conclusion, it is crucial for the task force to investigate what sources of funding that may be available to finance the implementation of the proposed changes which are associated with the new strategy.

1.3. Knowledge management

Considering the comprehensive knowledge of ESARDA, we believe that there is plenty of room for improvement on how to benefit from, and make use of, this knowledge. We need to raise awareness of knowledge management (KM) itself, and at the same time discuss how we best deal with it internally, as it constitutes a new challenge for the organization.

KM is a way to handle and align the knowledge inventory of an organization. By doing this, people, work processes and technology interact constructively and the work as well as the decision making is made effectively and in line with the organization's goals. The knowledge itself can be abstract or know-how, stored on a media or applied in practise. The knowledge is associated to the people in the organization, to the programmes or tools that are used by the people and to the organizational culture and the practises within it. Unless the knowledge within the organization is transferred, shared, transformed, adapted, updated and applied it becomes useless, making the organization more vulnerable to external factors.

KM is since long time an important issue in fields of business administration, management and information sciences, but it is becoming more important as part of the business strategy also in several other fields. Within the IAEA, a special subprogram on nuclear knowledge management is in place [1]. It is aimed at helping governments and nuclear organizations to clearly recognize and meet their responsibilities for managing nuclear knowledge, having a focus on developing and implementing methodologies for KM, facilitating information exchange and providing services related to nuclear KM.

We believe that ESARDA has much to learn about KM and that we may benefit from implementing it. We also acknowledge that we do not need to reinvent the wheel, and that there are several actors that may be very useful to us in this process. In the long run, we believe that ESARDA may be able to become one of those who are able to educate others on how to implement KM in practise.

1.3.1. NuSaSET

ESARDA currently has a portal for advertising activities of nuclear safeguards relevance. We would like to broaden its use because it constitutes an excellent platform for interaction. We envisage that NuSaSET could be the place for interaction between ESARDA WGs, safeguards lecturers, students at universities, professionals as well as researchers in the fields and the new initiative ESARDA Young Generation. We will elaborate further on the possible expansion of NuSaSET in section 4 of this document.

2. Education and training in nuclear safeguards

The education and training activities of ESARDA are currently restricted to organizing and giving the ESARDA course, arranged by JRC Ispra. It is a very popular course, attended by participants with various academic background and experience, and we think that there is both room and interest for an expansion of education and training activities beyond this course. The new education and training activities could be fitted to different target groups and it is not necessarily ESARDA members or JRC Ispra who are expected to do the actual teaching.

2.1. Module based education and training

When the TKM WG was discussed and established in 2003-2004, the purpose of the WG was to develop several safeguards modules that could be made available to and used by universities in a broader context of education of technical and non-technical students. We revisit these ideas and suggest to develop module-based knowledge repositories for research and educational material. The modules should be made available by ESARDA. This strategy serves several purposes:

- To give researchers and individuals involved in education and training in nuclear safeguards an overview of the current state of knowledge.
- To structure the work performed within ESARDA by clarifying what research that is ongoing and by whom. This would in turn improve the possibilities of internal collaboration by stating what the area of expertise is within each WG.
- To categorize and tag (associate with material with descriptive keywords such as e.g. “Non-Destructive Analysis”) research and educational material
- To make nuclear safeguard material available (e.g. slides together with explaining text in order to minimize the risk for misinterpretation of information) for internal as well as for external use. The idea is that anyone may choose material from different modules to create his or her own safeguard course (see Figure 2).

The actual content of each module could be e.g. one or several texts, e-books, case studies, published research papers, further references, video material etc. Seeing that ESARDA would not perform the teaching but only provide material, we have chosen not to include material for e.g. calculating and laboratory exercises. Instead we suggest to let the user of the material determine how it should be used. In a module based training package, a number of modules can be combined to suit different audiences with different needs. The module material should be kept in an electronic format which is easy to update, edit and “keep alive” and the course participants should be given easy access to download the selected modules. We foresee two levels of difficulty: an overview level, and an in-depth level. Furthermore, we suggest a digital tagging system for each piece of material in order to make it easy to search and access. The material should preferably represent the full competence of the WGs, and the material of each module should be available in the NuSaSET portal. A graphical representation of a module can be found in Figure 1.

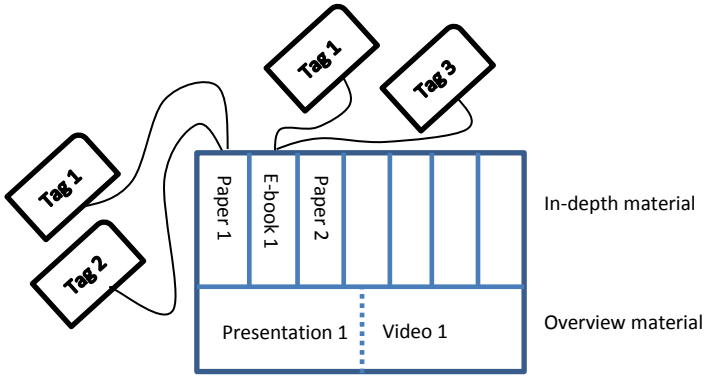

Figure 1. A module is a collection of material on a specific topic. The material is categorized as overview material or in-depth material (represented by the horizontal level in the figure). Each module could contain different material such as videos, books, scientific papers etc. The material is tagged to provide an easy navigation through the material.

Each module is meant to comprise material sufficient to educate participants on a particular subject. The subject matter could be technical or non-technical in its nature, but should be of relevance to nuclear safeguards or a specific ESARDA WG. Modules could for example exist for the following topics: non-destructive assay (NDA), KM in practice, safeguards for geological repositories, the legal framework of nuclear safeguards etc. Modules which are not explicitly part of research on nuclear safeguards and non-proliferation such as nuclear security could be encouraged by the ESARDA management via the Revision Board (see section 2.3). In that case, the topic could become part of an existing WG or constitute a new WG, and the development of the module then becomes the responsibility of that particular WG. It could also be possible to develop modules together with ESARDA partners such as research institutes, universities, educational networks etc. In the more distant future, this could lead to an exchange of modules between several partners.

In the creation of a specific course, e.g. *Non-proliferation and nuclear safeguards for non-technicians*, material could be selected from a number of different modules. Which modules and what level of

difficulty depends on the target group for that specific course and it is the person responsible for giving the course who makes the selection.

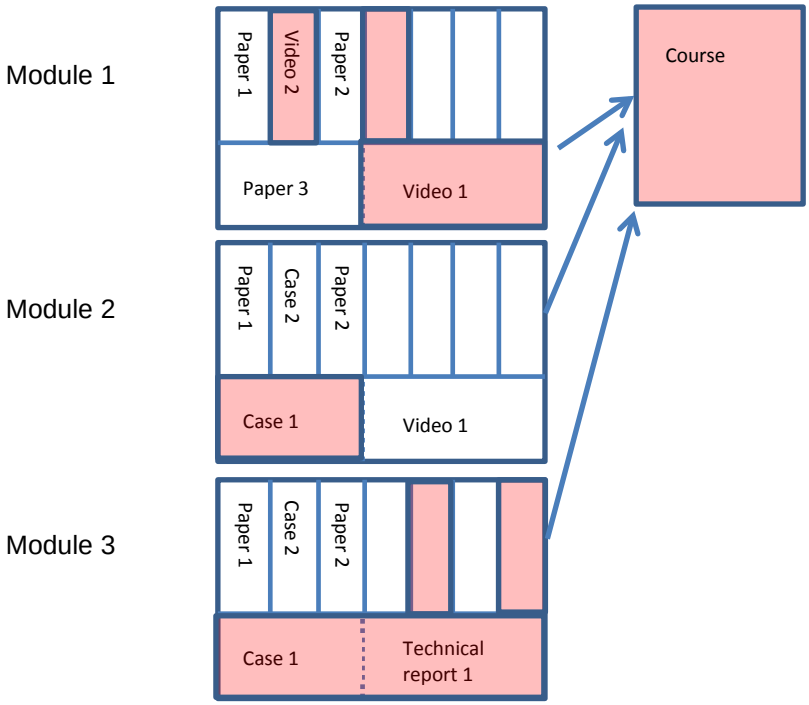

Figure 2. An illustration of how material from different modules is selected to for a specific course.

2.2. The role of the WGs

ESARDA is currently divided into several WGs (discipline oriented, facility oriented, ad-hoc, Training and Knowledge Management –TKM, and Editorial Committee). Each WG consists of experts in that particular field, and each WG is in principle independent of other WGs and consequently the communication between the WGs is sparse. The development of the module-based knowledge repository for research and educational material would allow for a larger overlap of activities, since all WGs would need to make their material and expertise available to a broader audience and hence be part of promoting education, training and knowledge management. More specifically, the WGs should, beside their current activities, engage in the following specific tasks:

1) ***Identify and update module material*** that is suitable for education and training. The material is created by members or fractions of the WG and can be research papers, reports, videos etc.Each WG shall identify material which they judge is suitable teaching material. The WG categorizes this material into one or several modules and suggests an appropriate tagging for each material. This material should be (continuously) revised by the WG so that it contains also recent research results. We suggest that each WG selects one member who is responsible for the material identified and collected by the WG. This person should in addition participate in the Revision Board for the module-based knowledge repository for research and educational material. In this way, the work of the WGs becomes formalised and become part of the annual assessments of the Executive Board of the WG activities.
2) ***Scrutinize the material*** provided by the WGs in order to ensure that it is comprehensive and on the right level. In some cases, WG needs to identify complementing background material, references etc. For each module, a video and/or documentation could be made available, explaining the scope and content of that specific module.
3) Actively work to ***attract and keep the involvement of students and (young) professionals*** in ESARDA. In order to be attractive to this target group, the WGs must be able to offer something. We have identified a number of things which the WGs could offer this target group:

a. Bachelor and Master thesis projects
b. Scientific scrutinizers for projects
c. Research material and specialist competence
d. Mentors
e. Internships
f. Job opportunities

The list can be made longer, but what is important is to prioritize this wish-list for students and young professionals and then to identify how we best contribute to that.

2.2.1. WG TKM

Knowledge management within ESARDA is currently done via the annual meetings and symposia, as well as the publishing of the ESARDA Bulletin. We believe that WG TKM, together with the aid from other WGs, also should deal with knowledge management by:

1) ***Managing the module material*** that is suitable for education and training as follows:
    a. Select the format(s) in which the available material should be made available.
    b. Regularly invite the module responsible persons to a Revision Board meeting. In this forum each module content is presented to
        i. spread the current status of the research field within the consortium
        ii. inspire other module responsible persons how to organise their modules
2) ***Offer the ESARDA course*** at Ispra and/or other places
3) ***Identify new research fields*** that should be included in the ESARDA network.

Note that we need to ensure that the knowledge management activities by different actors become constructive and not competitive. We invite representatives of the Editorial Committee to specifically take part in discussions on knowledge management within ESARDA.

2.3. Revision Board

In our current version of this strategy, we propose to create a Revision Board that should make sure that the module material is up to date. However, we are open for other options, proposed by the task force or other actors.

The purpose of the Revision Board is to update the module material that is suitable for education and training during regular meetings. The Revision Board should comprise members of the ESARDA management and each WG. In case there is module material which is not tied to any particular WG, the person responsible for that module should also be in the board.

The Revision Board should meet in connection to the annual meeting and review the material of each module. Depending on the scope and tags of that material, the Revision Board may become aware of material which is beyond the scope of existing WGs. It should then be up for discussion how this knowledge is best managed and if it is motivated to create a new WG.

3. Networks

3.1. Young Generation

The establishment of an ESARDA Young Generation (ESARDA-YG) is an initiative that may tie well into this strategy of promoting education, teaching and knowledge management. It is meant to support and work within ESARDA, and at the same time pay special attentions to its young members. YG will provide a meeting point for students and young professionals involved in different aspects of nuclear safeguards, and the aim is to contribute in the promotion and increase awareness of nuclear safeguards. Via ESARDA-YG, the ESARDA organization will be given access to students and young professionals who are interested in this field. This will hopefully lead to a larger fraction of people who will continue their careers this specific field.

The main objectives of the ESARDA-YG are to:

- Facilitate the attendance to the ***ESARDA Symposium***
- Encourage the participation to the ***ESARDA Working Groups***
- Plan ***technical visits*** to nuclear facilities and research centers
- Organize ***lectures and workshops*** related to nuclear safeguards
- Provide opportunities for ***interactions and networking***
- Create an ***informal forum*** for students and young professionals interested in nuclear safeguards

Like many organizations dealing with nuclear topics, the ESARDA-YG is limited by the low number of young people working with this subject. Therefore, by grouping students and young professionals at European level it is possible to find sufficiently many people to create an active organization.

The ESARDA-YG could offer its members an introduction to the safeguards community. The ESARDA association will benefit from the interactions with motivated students and professionals that bring innovative approaches to tackle current R&D. ESARDA-YG consequently benefits both safeguards newcomers and field experts.

3.2. Partners and partner organizations

There are a number of other organizations which engage in education and training activities related to nuclear power and nuclear education (such as e.g. INSEN, ENEN). The scope of activities within these organizations is not known to the authors at this moment, but we have identified a need to map them in order not to duplicate work and to possibly initiate collaboration.

In addition, we have also identified a need to map initiatives and organizations that more generally deal with nuclear safeguards. Such organizations are e.g. be the IAEA and Institute for Nuclear Material's Management (INMM), with which ESARDA already now has collaborations, but also possible new partners should be included.

4. The connecting hub – the NuSaSET portal

The **Nu**clear **Sa**feguards & **S**ecurity **E**ducation and **T**raining portal (www.nusaset.org) is an international initiative of the INMM, ESARDA and the IAEA. The portal provides support to professionals in the field of Nuclear Safeguards and Security, specifically to promote the provision of training and education of students. We would like to expand the use of NuSaSET in several ways since we see it as the natural platform for internal as well as external collaboration.

1) Each WG should make their module material that is suitable for education and training available for lecturers and students here.
2) It could constitute a forum for discussions and the sharing of experience on how to educate and train people on specific modules. It could also be the place where teachers could upload their own material (e.g. slides and exercises) and keep in touch with other professionals etc.
3) University students taking nuclear safeguards courses could sign in on NuSaSET in order to download the course material as well as getting information on thesis subjects and PhD positions among the ESARDA community.
4) YG members could interact with each other and with professionals and students.
5) By activating both students and young professionals on NuSaSET , we allow for
    - cross-European collaborations among students, and
    - a (further expanded) platform for advertisement of thesis subjects, nuclear safeguards courses, future PhD positions as well as positions in companies all over Europe.
6) The "train-the-trainer" course could be made available through NuSaSET.

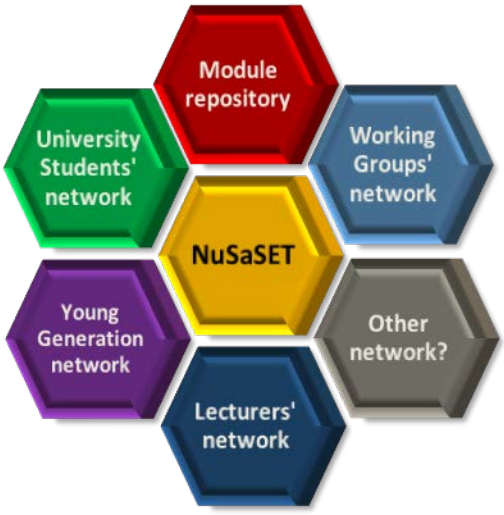

Figure 3. Different actors on NuSaSET.

5. Summary

In this document, we have described a vision of how ESARDA could deal with education as well as training and knowledge management in a more effective way. We have described a development towards a module-based knowledge repository for research and educational material, aimed to facilitate awareness of nuclear safeguards and non-proliferation to both students and young professionals. In the process of developing and maintaining the material, we foresee a larger overlap between the ESARDA WGs and a way to implement knowledge management in practice into the organization.

We believe that the proposed strategy will greatly expand the extent to which ESARDA engages in education and training. It will make education and training more flexible and provides the possibility to offer different nuclear safeguards courses depending on different needs and target groups.

We also suggest that the TKM WG should take steps to develop a train-the-trainer course in order to stimulate further interest in academia for teaching in the safeguards and nuclear non-proliferation field.

6. Outlook

In the nearest future we suggest to form a Task Force that will develop the thoughts in this document as well as implementing them. Ideally the task force consists of members from all WGs (including steering committee). Therefore we urge the steering committee to rally a Task Force from the members of the WGs.

During 2015 this Task Force develops and deepens the thoughts presented in this document and pays special attention to the funding of further development. By the end of 2015 the Task Force presents a more detailed plan for 2016. This plan should consist of an action plan for how and who to implement the changes.

7. Acknowledgement

This report has been supported by the Swedish Radiation Safety Authority (SSM).

8. References

[1] S. Grape, K. Persson and T. Jonter, *Visions for the development of ESARDA and ESARDA TKM WG*, ESARDA Bulletin No 51, December 2014

[2] IAEA program on knowledge management - Nuclear Knowledge Management (NKM), www.iaea.org/nuclearknowledge

Session 10

Quality Control in Destructive Analysis

Quality control tools for age dating in nuclear safeguards and forensics

Célia Venchiarutti[1], Adelheid Fankhauser[1], Zsolt Varga[2], Rožle Jakopič[1], Stephan Richter[1], Yetunde Aregbe[1], Klaus Mayer[2], Christophe Maillard[3], Cédric Rivier[3] and Danièle Roudil[3]

[1]European Commission, Joint Research Centre (JRC),
Institute for Reference Materials and Measurements (IRMM)
Retieseweg 111, B-2440 Geel
[2]European Commission, Joint Research Centre (JRC),
Institute for Transuranium Elements (ITU)
Postfach 2340, 76125 Karlsruhe, Germany
[3]Commissariat à l'énergie atomique et aux énergies alternatives (CEA/DEN)
Centre de Marcoule BP 17171 l 30207 Bagnols-sur-Cèze cedex

E-mail: rozle.jakopic@ec.europa.eu

Abstract:

Nuclear safeguards conclusions are based to a large extent on comparison of measurement results between operator and safeguards laboratories. Nuclear forensics deals with consistency of information, coherence between materials or samples, conformity of findings with declared processes and comparison of external and internal data. Representative samples are measured by respective networks of laboratories. For nuclear safeguards these are the Euratom safeguards and the IAEA Network of Analytical laboratories (IAEA-NWAL). For nuclear forensics, the laboratories are mainly members of the Nuclear Forensics International Technical Working Group (ITWG). Metrological quality control tools are a means to establish accurate, traceable and comparable measurement results. The European Commission-Joint Research Centre (EC-JRC) has therefore put effort into the development of certified reference materials and the provision of conformity assessment tools, particularly for "age-dating" of uranium and plutonium samples, which is of importance to both communities. In this context the new IRMM-1000a and IRMM-1000b, certified for the production date based on the $^{230}Th/^{234}U$ radiochronometer, will be presented, and the results from the Regular European Inter-laboratory Measurement Evaluation Programme (REIMEP-22) on 'U Age Dating' will be discussed. Furthermore the status of the on-going development of a ^{243}Am spike reference material in the frame of the recently signed collaboration agreement between the EC-JRC and the CEA/DEN will be presented. This spike is intended for use in the determination of the last separation date of plutonium samples by Isotope Dilution Mass Spectrometry (IDMS) using the $^{241}Pu/^{241}Am$ radiochronometer.

Keywords: nuclear forensic; nuclear safeguards, quality control tools; age dating; IDMS

1. Introduction

Nuclear forensics is a key element of nuclear security aiming at the identification and characterisation of illicit nuclear material, such as uranium or plutonium, to re-establish the history of nuclear material of unknown origin. By applying advanced analytical techniques to determine the isotopic compositions, elemental concentrations, chemical impurities and physical dimensions or microstructure of the nuclear material in question, the origin of an unknown material can be determined. More recently, the determination of the "age" of the material has drawn increased interest, not only in nuclear security but also in nuclear safeguards. The "age" of a nuclear material refers to its production date, *i.e*. the time elapsed since the last chemical separation of the daughter nuclides from the mother radionuclide. This

specific signature allows a narrowing of the possible origins of the material in question and provides valuable information on its history [1-4]. In order to address the emerging need of the nuclear forensic and safeguards communities for suitable reference materials, the European Commission - Joint Research Centre (EC-JRC) is joining efforts within JRC institutes and with other national organisations.

The JRC - IRMM (Institute for Reference Materials and Measurements) and the JRC - ITU (Institute for Transuranium Elements) jointly produced the first uranium reference material certified for the production date based on the $n(^{230}Th)/n(^{234}U)$ radiochronometer. This certified reference material was produced in compliance with ISO Guide 34 and ISO 17025 [5,6] in two sizes, 20 mg (IRMM-1000a) and 50 mg uranium (IRMM-1000b) as dried uranyl nitrate to be applied for mass spectrometric and radiometric analytical techniques. Such reference materials are a prerequisite for validation of measurement procedures and establish traceability of the measurement results to the SI.

Prior to the release of IRMM-1000a and IRMM-1000b, the REIMEP-22 inter-laboratory comparison (ILC) entitled "U Age Dating- Determination of the production date of a uranium certified test sample" was organised in support to the Nuclear Forensics International Technical Working Group (ITWG). This ILC aimed particularly at the ITWG members, as well as the Network of Analytical laboratories of the International Atomic Energy Agency (IAEA-NWAL), laboratories from industry and experts in the fields of nuclear and environmental (geological) sciences. Inter-laboratory comparisons, such as REIMEP-22, allow participants to benchmark their results against independent and traceable reference values, to identify possible problems, and to improve their measurement procedures, if necessary. Participants in REIMEP-22 received either a 20 mg and/or 50 mg certified test sample with an undisclosed value for the production date and were asked to apply their routine measurement procedure and to report the calculated production date with associated measurement uncertainty.

As a follow-up to a recommendation from the IAEA Technical Meetings on Reference Materials for Destructive Analysis in the Nuclear Fuel Cycle, CEA/DEN and JRC-IRMM joined efforts and engaged in the future production of a ^{243}Am spike reference material certified for the amount content and isotope amount ratios, using an americium base material available at CEA/DEN/Marcoule. Currently there is no ^{243}Am spike commercially available, although a certified reference material is needed for method validation in nuclear forensics, nuclear security and nuclear safeguards for the accurate measurements of ^{241}Am content in nuclear materials. A particular application of this spike material would be in the "age dating" of Pu samples using the $^{241}Pu/^{241}Am$ radiochronometer.

2. IRMM-1000a and IRMM-1000b

IRMM-1000a and IRMM-1000b were prepared at the JRC-ITU from a mixture of low enriched uranium dioxide pellets resulting in a relative mass fraction $m(^{235}U)/m(U)$ of 3.6% in the final material. From the dissolved uranium dioxide, a mother solution containing about 20 g of uranium in nitric acid (c = 3 $mol \cdot L^{-1}$) was prepared. An aliquot of this mother solution (about 6 g) was used to produce the reference materials. Four chemical separation steps by extraction chromatography (TEVA® Resin, Triskem International, Bruz, France) were performed in order to completely remove ^{230}Th from its parent ^{234}U uranium to the maximum extent achievable. The completeness of the separation and the recovery were monitored by γ-ray spectrometric measurements and by Inductively Coupled Plasma-Mass Spectrometry (ICP-MS) using a ^{232}Th tracer [7-9]. The individual units were prepared by dispensing the purified solution into PFA vials with a subsequent evaporation to dryness. This reference material is available in two different unit sizes of 20 mg uranium for mass spectrometric methods and 50 mg uranium for radiometric methods, corresponding to IRMM-1000a and IRMM-1000b respectively. The production date of IRMM-1000a and IRMM-1000b corresponds to the date and the carefully recorded time of the last (fourth) chemical separation [10].

The characterisation, homogeneity and stability assessments of the material were carried out in accordance with the ISO Guide 34:2009 [5] and the associated uncertainties by the Guide to the Expression of Uncertainty in Measurement [11]. Details on establishing the certified value and its final uncertainty can be found in the certification report [10]. The following value was assigned to IRMM-1000a and IRMM-1000b:

IRMM-1000a/IRMM-1000b	Certified value dd/mm/yyyy	Uncertainty(k = 2) [day]
Production date based on $n(^{230}\text{Th})/n(^{234}\text{U})$ radiochronometer	09/07/2012	13

Table 1: IRMM-1000a/IRMM-1000b certified value and its uncertainty.

3. REIMEP-22

REIMEP-22 on "U Age Dating–Determination of the production date of a uranium certified test sample" was organised in parallel to the production of the IRMM-1000a and IRMM-1000b in support to the ITWG and the IAEA-NWAL and in compliance with ISO/IEC 17043:2010 [12]. Besides experts in nuclear forensics, other laboratories that are at the stage of acquiring capabilities in this field were particularly encouraged to participate in REIMEP-22. The measurand of interest was the production date of the certified test samples. However, the participants were asked to report in addition either the $n(^{230}\text{Th})/n(^{234}\text{U})$ amount ratio or the activity $A(^{230}\text{Th})/A(^{234}\text{U})$ ratio for the two uranium certified test samples, respectively. This made it possible to distinguish whether a deviation from the reference value was due to mistakes in the measurements or in the calculations. Moreover, the participants had the possibility to report the production date based on the $n(^{231}\text{Pa})/n(^{235}\text{U})$ amount ratio or the $A(^{231}\text{Pa})/A(^{235}\text{U})$ activity ratio although the material was not certified based on the $^{241}\text{Pa}/^{235}\text{U}$ radiochronometer. The production date had to be reported as dd/mm/yyyy with the associated expanded uncertainty in days. The participant results were evaluated against the reference value by means of zeta-scores in compliance with ISO 13528:2005 [13].

3.1. Participant results

Fourteen laboratories registered for REIMEP-22; however three laboratories could not report their results due to technical problems. Finally, eleven different laboratories reported results; among these, two laboratories submitted results both for the 20 mg and 50 mg uranium certified test samples, making thirteen participant results in total. Nine participants reported results for the 20 mg sample and four participants reported results for the 50 mg sample. Additionally, two laboratories reported the production dates based on the $n(^{231}\text{Pa})/n(^{235}\text{U})$ amount ratios. The results for the 20 mg uranium certified sample based on $n(^{230}\text{Th})/n(^{234}\text{U})$ amount ratio and 50 mg uranium certified sample based on $A(^{230}\text{Th})/A(^{234}\text{U})$ activity ratio are presented in Figure 1 and in Figure 2. Details about the participant results and REIMEP-22 can be found in the report [14].

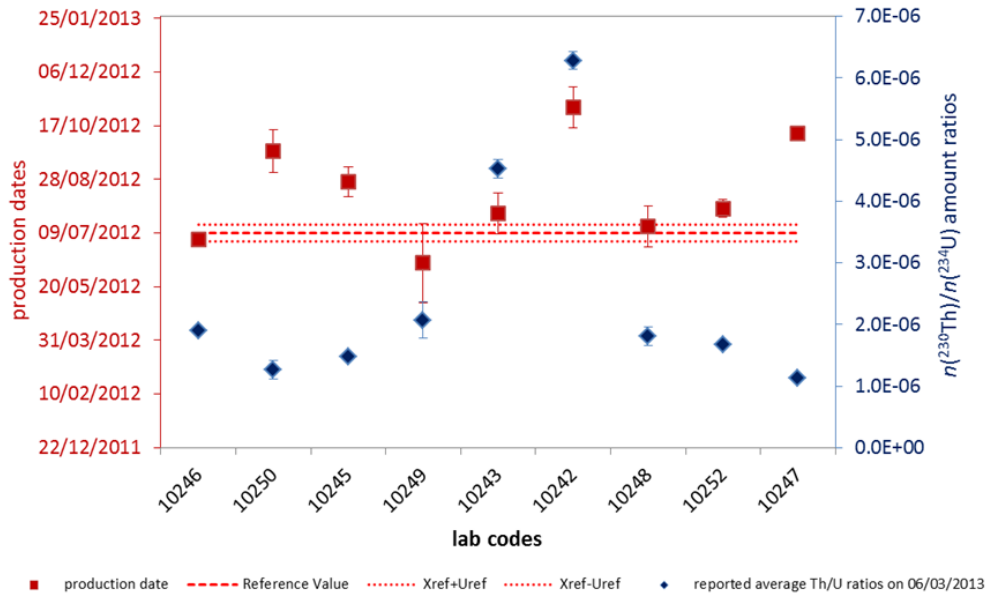

Figure 1: Reported results for the 20 mg uranium certified sample with uncertainties for production date (red squares) and $n(^{230}Th)/n(^{234}U)$ amount ratios (blue diamonds) normalized to March 6, 2013 (reference date). The reference value and its uncertainty are shown by the dashed red lines.

The challenge in REIMEP-22 was to determine the date of the last separation of ^{230}Th from ^{234}U in a young sample, *i.e.* with a very low amount of ^{230}Th. Based on the calculated production dates and ratios reported by the participants, it can be concluded that the participants in REIMEP-22 performed well for both mass spectrometric and alpha-spectrometric measurements; however, the spread of results was larger for the activity ratio results measured by alpha spectrometry.

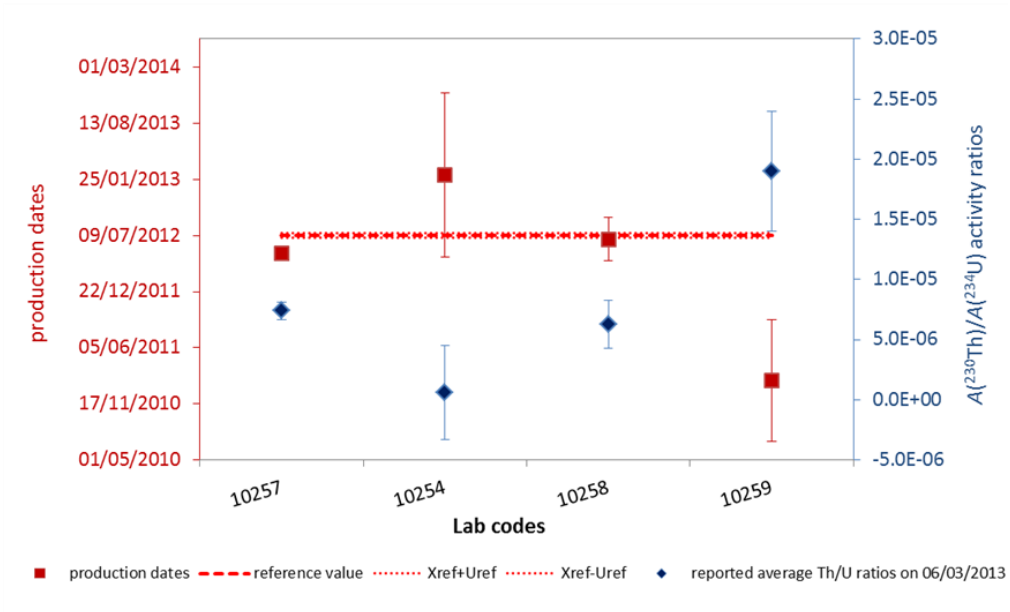

Figure 2: Reported results for the 50 mg uranium certified sample with uncertainties for production date (red squares) and $A(^{230}Th)/A(^{234}U)$ activity ratios (blue diamonds) normalized to March 6, 2013 (reference date). The reference value and its uncertainty are shown by the dashed red lines.

The evaluation of the laboratory performance was done by means of zeta-scores in accordance with ISO 13528 [13].

$$zeta = \frac{x_{lab} - X_{ref}}{\sqrt{u_{ref}^2 + u_{lab}^2}}$$

Where

x_{lab} is the measurement result reported by a participant,

X_{ref} is the reference value (assigned value),

u_{ref} is the standard uncertainty of the reference value,

u_{lab} is the standard uncertainty reported by a participant

The laboratory performance expressed as zeta-scores can be interpreted as satisfactory for zeta score ≤ 2 (green), questionable for 2 < zeta score ≤ 3 (yellow) and unsatisfactory for zeta score > 3 (red). This score provides an indication whether the estimate of the uncertainty is consistent with the laboratory's deviation from the REIMEP-22 reference value, X_{ref} = 09/07/2012 ± 7.8 days (k = 2). An unsatisfactory laboratory performance may be caused by an underestimated uncertainty or by a large

deviation from the reference value. The zeta-scores per participating laboratory for the 20 mg and 50 mg REIMEP-22 samples are presented in Table 2 [14].

Lab codes	Zeta-scores		
	20 mg sample $n(^{230}Th)/n(^{234}U)$	20 mg sample $n(^{231}Pa)/n(^{235}U)$	50 mg sample $A(^{230}Th)/A(^{234}U)$
10246	1.3	7.6	/
10250	-7.1	/	/
10245	-6.0	/	/
10249	1.5	/	/
10243	-1.8	/	/
10242	-6.0	/	/
10248	-0.6	/	/
10252	-2.6	-0.5	/
10247	-20.4	/	/
10257	/	/	2.5
10254	/	/	-1.5
10258	/	/	0.3
10259	/	/	4.8

Table 2: Overview of the zeta-scores for the 20 mg and 50 mg uranium certified test sample.

Six participants out of thirteen reported results obtained satisfactory performance and two participants achieved questionable performance based on the zeta scores evaluation. The results confirmed the analytical capabilities of laboratories for this type of measurements. The results also showed that more care still needs to be brought to the estimation of measurement uncertainties, which were generally underestimated. Two participants also reported $n(^{231}Pa)/n(^{235}U)$ amount ratios and the associated production dates (Table 2). Nevertheless, this is already a good indication that the certified production date of IRMM-1000a and IRMM-1000b may also be applicable for the $^{231}Pa/^{235}U$ radiochronometer, although these CRMs are not certified for this specific radiochronometer and further work is needed to verify that.

4. ^{243}Am spike CRM (IRMM-0243)

JRC-IRMM and CEA/CETAMA (CEA/DEN Marcoule, France) will jointly produce and certify a ^{243}Am spike reference material. Currently there is no ^{243}Am certified spike reference material commercially available to measure the ^{241}Am content in a sample by IDMS. 3 mg of Am base material (88% ^{243}Am and 12% ^{241}Am) made available by CEA/CETAMA was purified by extraction chromatography and impurity analyses was performed by ICP-AES. Subsequently the Am material was shipped to JRC-IRMM and further processing and certification in accordance with ISO Guide 34 is currently on-going [5]. The Am solution will be diluted with nitric acid (c = 2 mol·L^{-1}) to achieve a mass fraction of 1.5 µg·g^{-1} and will be dispensed into screw-cap glass ampoules. About 600 units will be prepared; each unit will contain about 3.5 mL of a solution. The reference material will be certified for the ^{243}Am and ^{241}Am amount contents and Am isotope amount ratios by ID-TIMS and TIMS, respectively. A flow-chart of the various steps of this joint project is presented in Figure 3.

To certify the ^{243}Am, in principle, a ^{241}Am spike reference material would be required. In the absence of any certified ^{241}Am, a rather unorthodox approach for certification had to be chosen. For certification purpose, a ^{241}Am in-house spike will be prepared from a high enriched ^{241}Pu (99.3%) material available at JRC-IRMM. The ingrown ^{241}Am, produced by beta decay of ^{241}Pu (14.325 ± 0.024 y, [15]), will be used as the spike reference material for IDMS. The initial ^{241}Pu material was purified by anion exchange (Bio-Rad, AG-1X4). The completeness of the separation (the absence of ^{241}Am in the purified ^{241}Pu) was confirmed by γ-ray spectrometry. The purified spike solution (kept under weight control) was characterised by TIMS to determine the isotopic composition and by IDMS using a ^{242}Pu spike CRM (IRMM-049d) to determine the ^{241}Pu amount content. Before the release of the new ^{243}Am

CRM CEA/CETAMA will organise an interlaboratory comparison exercise for this candidate reference material, similar to what was done in REIMEP-22 before the release of IRMM-1000a and IRMM-1000b. This ILC will be open to all (expert) laboratories in the field but also to laboratories that would like to gain experience in the field of americium measurements.

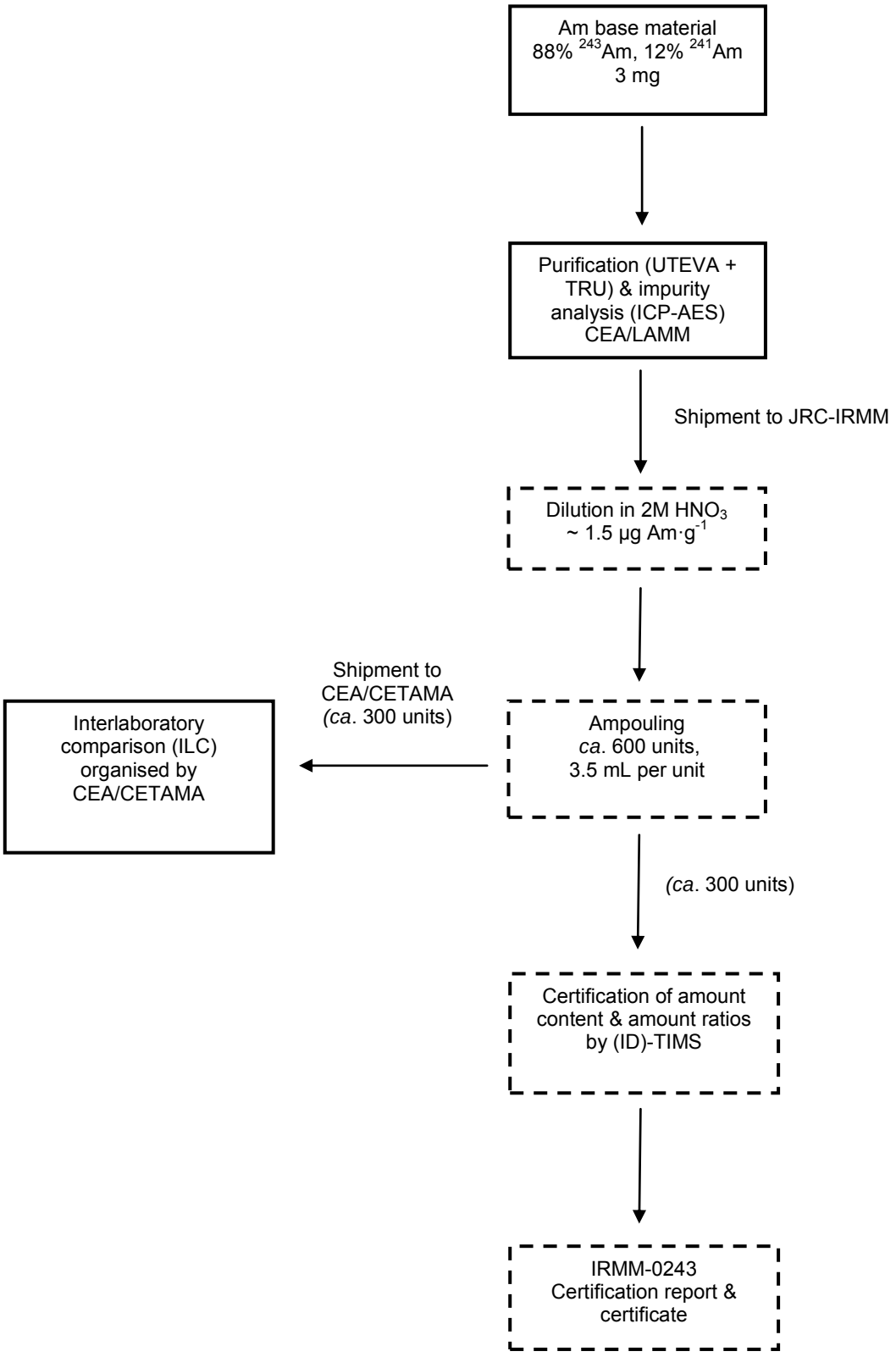

Figure 3: Various steps for the preparation and certification of ^{243}Am spike CRM (IRMM-0243). In full line squares are the steps carried out by CEA/CETAMA, in dashed line squares the steps carried out by JRC-IRMM

5. Conclusions

The IRMM-1000a and IRMM-1000b uranium reference materials were jointly produced and certified by the JRC - IRMM and JRC - ITU according to international guidelines for the production date based on the $^{230}Th/^{234}U$ radiochronometer. The certified reference value of the IRMM-1000a and IRMM-1000b and its expanded uncertainty was determined as: 09/07/2012 ± 13 day (k = 2). These novel CRMs will contribute to more reliable measurements of the "age" and characterisation of intercepted uranium materials in nuclear forensic and will improve method validation in nuclear safeguards. In parallel, the REIMEP-22 interlaboratory comparison was organised on the certified uranium test samples. This ILC gave the participating laboratories the opportunity to demonstrate that their measurement results for the determination of the age of uranium nuclear or radioactive materials are fit for the intended purpose and within the required measurement uncertainties of the current best practice in Nuclear Forensics. Furthermore laboratories still acquiring capabilities in nuclear forensics could benchmark their state-of-practice via participation in REIMEP-22. The evaluation of the laboratories' performances showed that the participants performed well for this kind of measurements using either mass spectrometry or alpha-spectrometry, although the spread of the results was larger for the measurements performed by alpha-spectrometry. It also showed that there is still room for improvement in the estimation and reporting of measurement uncertainties. The ongoing preparation of a ^{243}Am certified spike reference material required for the measurement of the last chemical separation of plutonium samples by IDMS is one more example that cooperation within and between institutes with expertise in the field of nuclear material analysis and quality control is an asset for the nuclear safeguards and nuclear security communities.

6. References

[1] Mayer, K., Wallenius, M., Ray, I; *Nuclear forensics - a methodology providing clues on the origin of illicitly trafficked nuclear materials*; Analyst; 130; 2005; 433-441.
[2] Mayer, K., Wallenius, M., Fanghaenel, T.; *Nuclear forensic science - from cradle to maturity;* Journal of Alloys and Compounds*;* 444-445; 2007; 50-56.
[3] Morgenstern, A., Apostolidis, C., Mayer, K.; *Age Determination of Highly Enriched Uranium: Separation and Analysis of 231Pa;* Analytical Chemistry*;* 74; 2002; 5513-5516.
[4] Wallenius, M., Mayer, K.; *Age determination of plutonium material in nuclear forensics by thermal ionisation mass spectrometry*; Fresenius J Anal Chem; 366; 2000; 234-238.
[5] ISO Guide 34; *General requirements for the competence of reference materials producers,* International Organization for Standardization; Geneva; Switzerland; 2009.
[6] ISO/IEC 17025:2005; *General requirements for the competence of testing and calibration laboratories,* International Organization for Standardization; Geneva; Switzerland; 2005.
[7] Varga, Z., Suranyi, G.; *Production date determination of uranium-oxide materials by inductively coupled plasma mass spectrometry*; Analytica Chimica Acta; 599; 2007; 16-23.
[8] Varga, Z., Nicholl, A., Wallenius, M., Mayer, K.; *Development and validation of a methodology for uranium radiochronometry reference material preparation;* Analytica Chimica Acta; 718; 2012; 25-31.
[9] Wallenius, M., Morgenstern, A., Apostolidis, C., Mayer, K.; *Determination of the age of highly enriched uranium*; Anal Bioanal Chem; 374; 2002; 379–384.
[10] Venchiarutti C., Varga Z., Richter S., Nicholl A., Krajko J., Jakopic R., Mayer K., Y. Aregbe; *Preparation and certification of IRMM-1000a (20 mg) and IRMM-1000b (50 mg);* Report EUR 27146; 2015.
[11] ISO/IEC Guide 98-3; *Guide to the Expression of Uncertainty in Measurement; (GUM 1995);* International Organization for Standardization; Geneva; Switzerland; 2008.
[12] ISO/IEC 17043:2010; *Conformity assessment - General requirements for proficiency testing; 2010.*
[13] ISO 13528:2005; *Statistical methods for use in proficiency testing by inter-laboratory comparisons;* 2005.
[14] Venchiarutti C., Varga Z., Richter S., Nicholl A., Krajko J., Jakopic R., Mayer K., Y. Aregbe; *REIMEP-22 U Age Dating - Determination of the production date of a uranium certified test sample;* Report EUR 27124; 2015.
[15] Wellum R.; Verbruggen A.; Kessel R.; *A new evaluation of the half-life of ^{241}Pu*; J. Anal. At. Spectrom.; 24; 2009; 801-807.

Experimental estimation of the uncertainties associated to low-background alpha-spectrometry measurements

Nadia Cherubini [(1)], Alessandro Dodaro [(1)], Roberto Iacovacci [(2)], Giuseppe Augusto Marzo [(1)], Giorgio Giorgiantoni [(1)], Massimo Sepielli [(1)],

[(1)] ENEA, C.R. Casaccia
Via Anguillarese 301, 00123 S.Maria di Galeria, Rome – Italy
E-mail: nadia.cherubini@enea.it, alessandro.dodaro@enea.it, giuseppe.marzo@enea.it, giorgio.giorgiantoni@enea.it, massimo.sepielli@enea.it

[(2)] SCK-CEN, C.R. Mol
Boeretang 200, 2400 Mol, Belgium
E-mail: Robertolako@libero.it

Abstract

The alpha spectrometry techniques aim to determine the activity of alpha-emitting radioisotopes contained in soil samples, various materials (cement, iron), or liquid samples.
The identification and quantification of alpha-emitting radionuclides have a key role in the field of radiation protection and the characterisation of nuclear materials. They have a fundamental role in safeguards and security in general, since the relevant samples are often alpha-contaminated.
The experimental activities are carried out using certified alpha sources at the ENEA Casaccia Nuclear Materials Characterisation Laboratory with an integrated alpha spectrometer for measuring low-activity samples. The quantitative analysis of alpha-particle spectra is aimed to the determination of the positions of bands in units of channel numbers and of the areas of bands in units of counts. Both quantities must be determined together with their associated uncertainties. Using the energy - and efficiency - calibration data, along with an appropriate nuclides library, these positions and areas are then converted into absolute activities of the nuclides contained in the source.
A measurement repeated in identical conditions does not necessarily coincide with the previous one because the emission mechanisms and detection of alpha particles are stochastic. The variability of the measurements is characteristic of the physical phenomenon but is also a function of parameters associated to the measurement system, such as the geometry of the detector, the properties of the sample to be measured, and the electronics of the instrument. Therefore it is necessary to quantify the extent of the variability of the measurements in order to estimate the associated uncertainty.
The present paper describes the methodologies for the alpha spectrometer characterisation to quantify the inherent variability of the measured values both in terms of energy of the particles revealed (position of the spectral bands) and in number (intensity of spectral bands).

Keywords: alpha spectrometry; uncertainties; nuclides; safeguards.

1. Introduction

The alpha spectrometry [1] is employed to measure natural radionuclides (polonium, uranium, thorium) and anthropogenic (plutonium, americium, neptunium) alpha emitters in samples deriving from different kind of matrices (water, sediments, dry atmospheric aerosols).
Alpha spectrometry is the process of measuring the energy and the number of alpha particles emitted from a sample containing radioactive elements alpha-emitters. The alpha spectrometry techniques aim to determine the activity per unit mass of radioisotopes alpha-emitters present in soil samples, various materials (cement, iron), or liquid samples.
The identification and quantification of alpha-emitting radionuclides has a key role in the characterization of nuclear materials and radiation protection in general and is an essential part of safeguards and security.

The alpha-emitting radioisotopes spontaneously produce alpha particles to energies characteristics included between 4 and 6 MeV.
A typical energy spectrum of alpha particles emitted from a radioactive source is therefore constituted by one or more lines, corresponding to the various possible transitions for that particular isotope.
The energy spectrum of the alpha particles can be detected by a silicon detector, placed in a vacuum environment, since the alpha can be stopped even by small thicknesses of air.
The silicon detectors used for measurement of the energy of the alpha particles generally have a good resolution in terms of energy, which may allow in many cases to distinguish the peaks corresponding to different isotopes or different transitions of the same isotype.
The detector efficiency for these particles is virtually 100% and the linearity of the response with the energy is very good over a wide range.
From an operational point of view, the sample should be as thin as possible and the path of the alpha particles between the sample and the detector must be done in a chamber in which have been made vacuum conditions. The reduced range value that characterizes the interaction of the alpha particles with matter involves, in fact, a significant attenuation within the sample and within each material interposed between the sample and the detector. From the spectrometer point of view it results in an asymmetrical deformation of the spectral bands characterized by a low energy tail, which limits the instrumental performances.
In both cases, the sample must be prepared to be measured and the sample pre-treatment depends on the type of measurement of choice.
The experimental activities are carried out using certified alpha sources at the ENEA Casaccia Nuclear Materials Characterisation Laboratory with an integrated alpha spectrometer for measuring low-activity samples.
In this work our goal is to provide an initial estimate of the performances and limitations of the ENEA alpha spectrometry system in terms of the uncertainties associated with the energy and efficiency calibrations obtained by means of specific certified radioactive sources.

2. Experimental set-up

2.1. Sample preparation

The material undergoing the measurement has to be deposited on a substrate to obtain a thin layer, in a form chemically isolated that can be placed in a spectrometer and analysed with minimum interferences and self-absorption.
Generally, the main steps for such a pre-treatment of the sample for alpha spectroscopy are the following:

- homogenization and preparation of the sample for subsequent chemical processes;
- chemical separation: used to isolate elements of interest;
- production of thin source.

The sample preparation consists therefore in:

- extraction of the analyte from the matrix (co-precipitation, liquid-liquid extraction, ion-exchange chromatography);
- separation of the analyte from potentially interfering nuclides;
- production of thin source by electrodeposition.

The source of the radioactive material must be very thin and homogeneous (ideally the substrate should be coated with a single layer of radioactive atoms, without other impurities), and then the raw material has to undergo various changes before be able to perform the measurement.
The initial matrix material is treated with suitable methods to obtain a solution containing the radionuclides of interest; the final sample, ready for to be measured, is obtained by electrodeposition solution containing the radioisotopes on a metal disk, the latter being the substrate of choice. This procedure allows to obtain, in contrast to other methods, very thin and uniform sources in which the layer of radioactive material on the surface of the substrate approaches very well the ideal case of a monoatomic layer.
Various methods of electrodeposition have been studied to obtain the maximum yield and efficiency of the process. The methodology used in this case was developed by N.A. Talvitie [2] and is the most suitable for the electrodeposition of Pu, Th, U, Np, Cm and Am as hydrous oxides.

2.2. Energy and efficiency calibration.

The instrumentation used to perform the measurements is composed by:

1) a Passivated Implanted Planar Silicon (PIPS) A-600-23AM, 600 mm^2 surface, 140 μm thickness, 23 keV resolution;
2) a vacuum chamber and electronic equipment (power supply voltage, preamplifier, amplifier, analog-to-digital, multi-channel analyser);
3) a vacuum pump and connecting pipe.

In Figure 1 the ENEA spectrometry alpha system is illustrated.

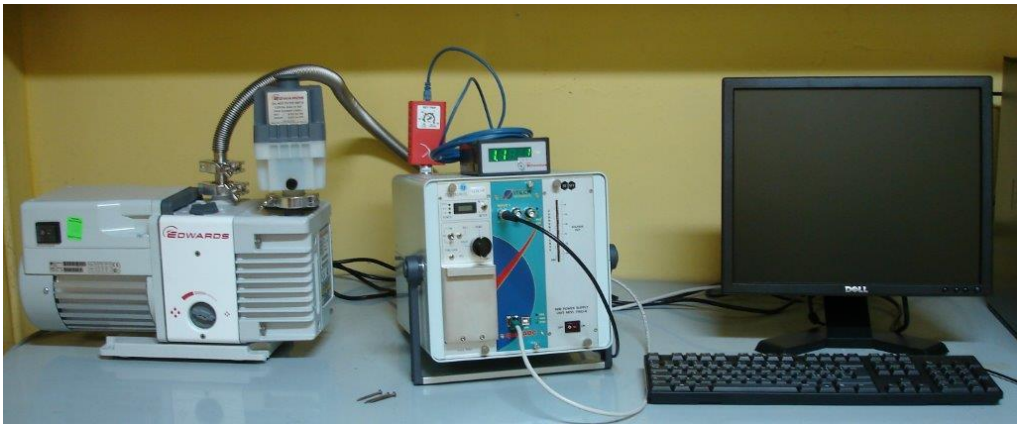

Figure 1: Experimental setup for the alpha spectrometry.

The PIPS semiconductor detectors combine the techniques of ion implantation and photolithography to produce detectors with very low leakage currents, input windows very thin, and excellent operational characteristics.
The thin entrance window of the PIPS detectors provides increased resolution and the reduction of the distance detector-source is required to have high efficiencies. The low leakage current helps to minimize the drift of the peak with the temperature change. The ratio of the background count is typically less than 0.05 counts/cm^2 hr in the energy range from 3 to 8 MeV.
In order to determine the capabilities of alpha spectrometry system [3], different measurement were executed to determine the correct value of efficiency and to execute a correct efficiency calibration. To pursue such a goal, certified alpha sources, with activity going from 10 kBq to 55 kBq, were placed with different geometries (i.e., distances with respect to the PIPS detector; Fig. 2):

- mixed source ^{239}Pu ^{241}Am ^{244}Cm with total activity of 5550 Bq;
- alpha source of ^{239}Pu with activity of 2630 Bq;
- mixed source ^{239}Pu ^{241}Am ^{244}Cm with total activity of 1018 Bq.

Table 1 shows energies and the corresponding branching ratio of the radionuclides in the certified alpha sources.

Nuclide	Energy (MeV)	Branching ratio (%)
^{239}Pu	5105.5	11.9
	5144.3	17.1
	5156.6	70.8
^{241}Am	5442.8	13.1
	5485.6	84.8
^{244}Cm	5762.6	23.1
	5804.8	76.9

Table 1: Characteristics of the certified alpha sources

The detection efficiencies for the nine different distances of the source from the detector, for each alpha certified sources, are shown in the Figure 2.

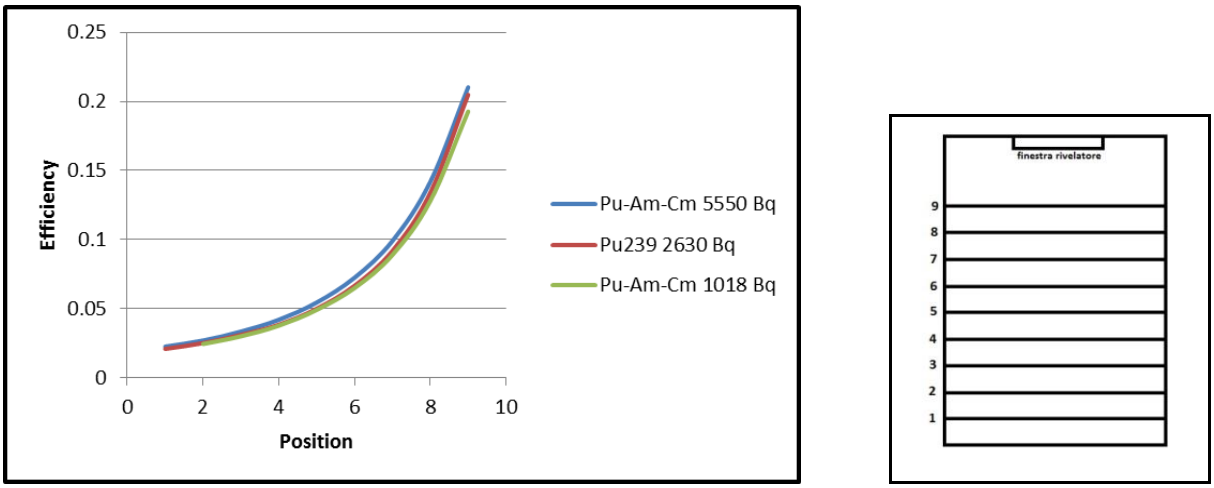

Figure 2: Detection efficiencies as a function of the position of the sample in the vacuum chamber, with all calibration sources.

Below, the uncertainties associated with the calibration potentially obtained using these described sources are evaluated.

3. Uncertainties associated with the measurements

A measure repeated in identical conditions does not necessarily coincide with the previous because the mechanisms of emission and detection of alpha particles are stochastic. The variability of the measurements is characteristic of the physical phenomenon under examination (i.e. alpha decay) but is also a function of the characteristics of the measuring system such as the geometry of the detector, the properties of the sample to be measured, the electronics of the instrument. It follows that it is necessary to quantify the extent of the variability of the measures in order to estimate the uncertainty associated.
At this stage, the instrument has been characterized by the inherent variability of the measured values both in terms of energy of the particles revealed (i.e., position of the spectral bands) and in number (i.e. intensity of spectral bands).

3.1. Position of the spectral bands at different measurement geometry

The association between spectral bands with a source, that decays by emitting alpha particles of known energy, and acquisition channels of the instrument determines the energy calibration of the instrument. A spectrometer calibrated in terms of energy identifies the alpha particles energy of unknown samples and then it allows to identify which alpha-emitters radioactive elements are present in the sample.
The variability of the position of the spectral band at 5.157 MeV of the certified ^{239}Pu source has been studied by varying the position of the sample with respect to the detector.
Ten different measurements have been performed for each position from number 9 (position closest to the detector) to number 6 (Figure 2), with an acquisition time of 100 seconds each. Then, the mean acquisition channel corresponding to the band peak, for each position, has been evaluated assuming, in first approximation, a Gaussian profile of the spectral band (in this work we omit the complete description of the asymmetries affecting the spectral bands), fitted by a Marquardt-Levenberg non-linear minimization algorithm [5] (Figure 3).
The mean value of the peak position in the four positions falls on the channel 1796 with a maximum uncertainty of 1.2 acquisition channels (relative uncertainty of 0.06%) corresponding to about 28 keV (= 1.2 x 23 keV).

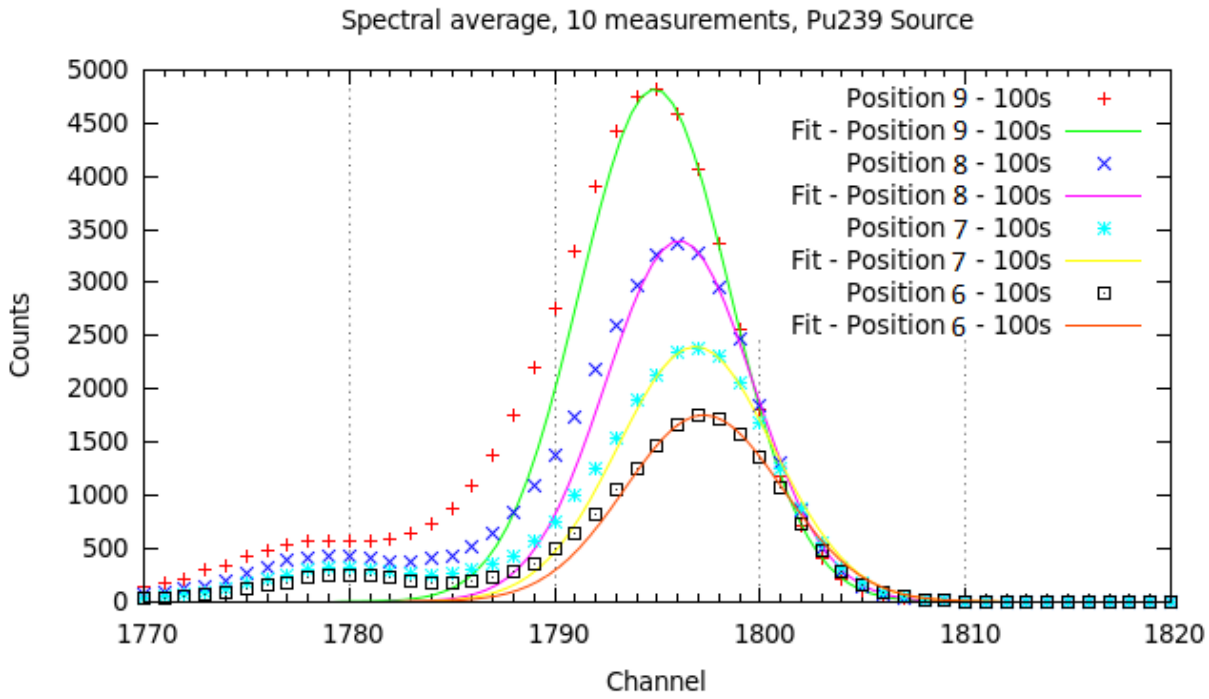

Figure 3: Average size (symbols) and their functions interpolate (solid lines) at different geometry measurement

3.2 Intensity of the spectral bands

The intensity of the spectral bands is proportional to the number of alpha particles detected by the instrument and therefore provides information on the amount of alpha-emitting material contained in the unknown sample. The association between intensity of the bands and quantity of the alpha-emitter of a known source determines the efficiency calibration of the instrument.
A preliminary study of the variability of the intensity of the spectral bands was carried out using a certified ^{239}Pu ^{241}Am ^{244}Cm mixed source characterized by an activity of 5550 Bq. Ten measurements were made for each of the following three cases:
position 9: 100 seconds of acquisition,
position 8: 100 seconds of acquisition and
position 8: 200 seconds of acquisition (Figure 4).
It has been observed that the relative uncertainty of the peaks of the spectrum (Figure 4, bottom panel) is substantially constant for both the different energies of the alpha particles revealed that for different geometries and acquisition times.
Quantitatively this uncertainty is very low and roughly of the order of 0.2 %.

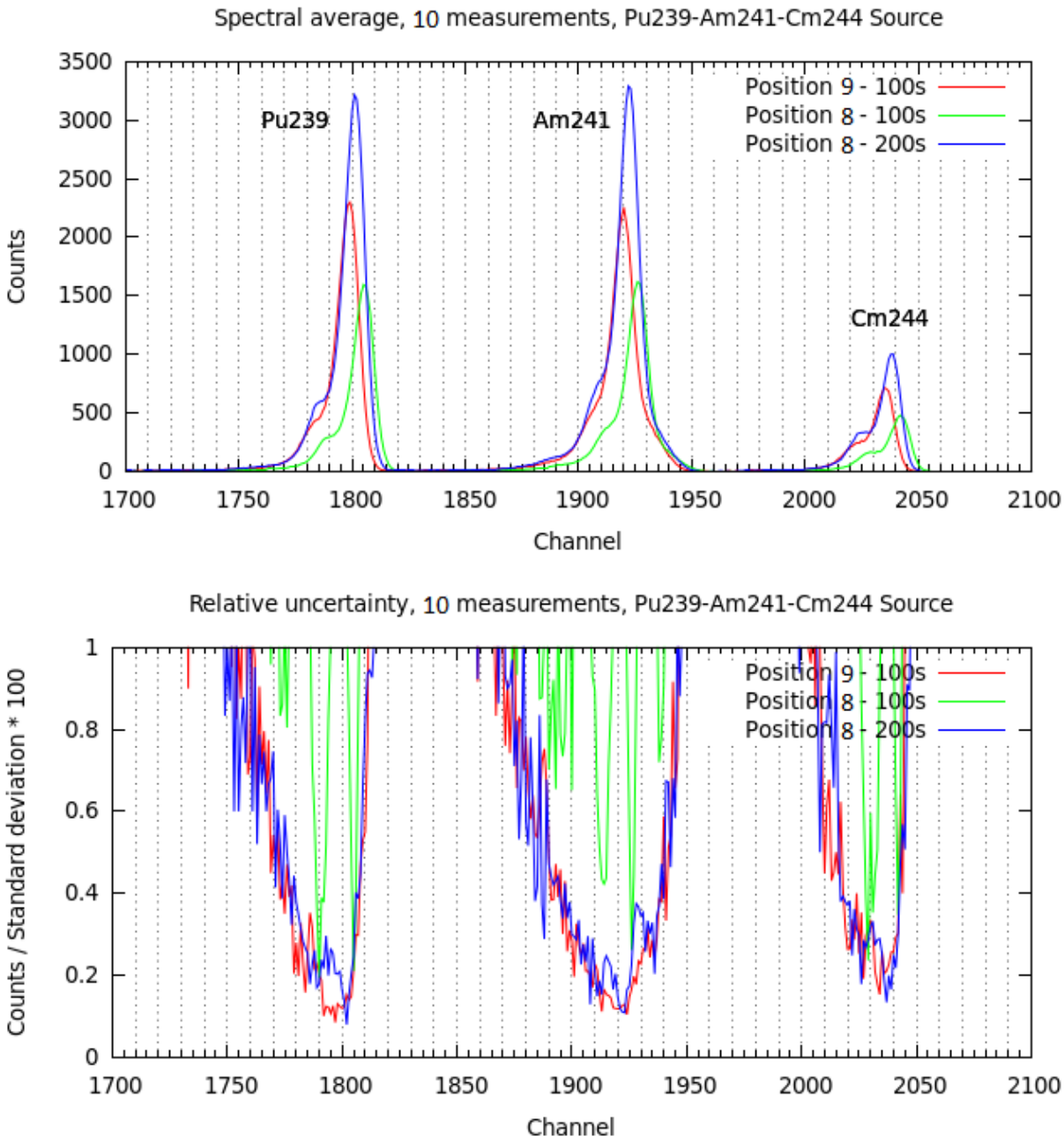

Figure 4: Measurements medium (top panel) and uncertainties relating percentages (lower panel) to vary the geometry of the measurement and the time of acquisition of the same.

The results presented show that the uncertainty associated with the efficiency calibration is greater than that associated with the energy calibration even if an uncertainty of 28 keV on the average value of the peak does not always allow to uniquely identify the isotope alpha-emitter eventually present in an unknown sample. This disadvantage can be partially solved by performing the calibration in specific energy for each different measurement geometry.

4. Conclusions

Due to the stochastic processes involved in the alpha decay and its detection, a measurement repeated in identical conditions does not coincide with the previous one. For such a reason here we quantify, in first approximation and with an empirical approach, the extent of the variability of the measurements in order to estimate the associated uncertainty. This allows us to know the limitations

of the energy and efficiency calibration obtained by means of certified alpha sources and, in turn, of our alpha spectrometer.
Our results show that the energy calibration is accurate within 0.06% and the efficiency calibration accuracy is roughly of the order of 0.2%.
Future work will include to consider an appropriate line shape (i.e., considering the asymmetries of the spectral bands) in our fitting procedure and extend such evaluations to other parameters characterizing the measurements (i.e., sample thickness).

5. References

[1] Helmbold, M.; *Alpha particle spectroscopy,* Nuclear Instruments and Methods in Physics Research; v. 223(2/3) p. 386-391.

[2] N.A. Talvitie: *Electrodeposition of actinides for alpha spectrometric determination*, Analytical Chemistry, vol 44, No. 2, February 1972.

[3] C. R. Hill; *A method of alpha particle spectroscopy for materials of very low specific activity*; Nuclear instruments and methods 12 (1961) 299--306.

[4] Eduardo Garcıa Torano; *Current status of alpha-particle spectrometry,* Applied Radiation and Isotopes 64 (2006) 1273–1280.

[5] K. Levenberg; *A Method for the Solution of Certain Non-Linear Problems in Least Squares*. The Quarterly of Applied Mathematics, 2: 164-168 (1944).

Preparation of Uranium Micro-Particles as Reference Material for Nuclear Safeguards

R. Middendorp, A. Knott, M. Dürr

Forschungszentrum Jülich GmbH
IEK-6: Nuclear Waste Management and Reactor Safety
52428 Jülich, Germany
E-mail: ma.duerr@fz-juelich.de

Abstract:

Over the past few years, particle analysis of environmental swipe sampling has progressed significantly. For example, the minor isotope fractions of analysed uranium particles are routinely determined, requiring accurate and precise mass spectrometric measurements. Quality control measures play a major role in obtaining reliable analysis data. To this end, reference material in form of micro-particles with characterized or even certified properties may be used for quality control purposes of particle analysis methods.

During the last years Forschungszentrum Jülich has developed a system for the production of mono-disperse uranium micro-particles. The system is based on the production of an aerosol where droplets containing uranyl nitrate solution are dried and sintered to form solid uranium oxide particles with a diameter of approximately 1 µm. Such a system allows the production of particles with uniform properties which may serve as a reference material for particle analysis methods. Some results from the characterization of produced particles will be presented and some follow-up procedures will be discussed. This includes the further treatment of particles in order to get stable samples for handling, storage and transport, which is required when particles are to be certified with respect to isotopic composition and the elemental content.

Keywords: Environmental Sample Analyses**;** Particle Analysis; NWAL; Reference Material

1 Introduction

The destructive analysis of safeguards samples forms part of the various verification measures applied by the International Atomic Energy Agency (IAEA) to derive safeguards conclusions. Stringent requirements are applied to analytical measurements in which performance targets need to be reached, in order to ensure that the IAEA draws information from sound measurement data. Therefore analytical laboratories rely on the use of validated techniques and methods, where (certified) reference materials play an important role. Performance assessment of techniques and laboratories is undertaken by organizing interlaboratory comparisons or by blind QC sample analysis. In the area of destructive analysis used for verification of nuclear material accountancy certified reference materials are commercially available and performance targets have been established [1], the area of reference standards for particle analysis performed on environmental swipe samples is far less matured.

The IAEA undertakes sample analysis relying on in-house analytical services (SGAS – Safeguards Analytical Services) as well as on a worldwide network of certified analytical laboratories within the member states (NWAL- Network of Analytical Laboratories). According to the 2013 IAEA Annual Report [2], 371 swipe samples were taken by the IAEA for analysis in the laboratories during that year, which justifies development and production of dedicated material for quality control and/or reference material. Various approaches on particle reference material have been reported (see [3] and references therein). Currently, particle analysis is routinely performed using (Large-Geometry) Secondary Ion Mass Spectrometry and the Thermal Ionization Mass Spectrometry. However, as procedures and techniques are developed and refined, the requirements on the reference material evolve. At Forschungszentrum Jülich, a setup for the synthesis of particles with certain properties was

established. Such material may be used for different purposes in particle analysis used in safeguards applications:

(1) Validation
(2) Calibration
(3) Quality Control
(4) Proficiency Testing

This paper presents the setup for production of particles, operating parameters and some characteristics of synthesized particles. The particle properties are bound to the production process, which therefore imposes certain boundary conditions for quality management related applications in particle analysis. These constraints will have to be considered for their use as reference material or as standard for quality control. On the basis of the current operational particle production setup some considerations on further preparation will be presented.

2 Particle Production at Forschungszentrum Jülich

2.1 The particle production setup

The particle production setup was designed with the aim to prepare mono-disperse uranium oxide microspheres with a nominal diameter of about 1 µm. The particles should have a well-defined isotopic composition and the determination of the elemental content of individual particles may be of interest. In order to prepare the micrometer-sized particles, a system similar as described by Erdmann et al. [4] has been constructed at Forschungszentrum Jülich [3]. In short, the production process involves the generation of droplets out of a prepared feed solution using a commercial aerosol generator. The droplets are transported within a gas stream (e.g. Air) through the so-called drying column, in which the volatile component of the droplets evaporates. The particle within the air-stream passes a heat treatment (realized through one or several ovens), in which the particle is chemically transformed in order to bring it into a chemically and physically stable form (see Figure 1). The essential feature is that the particles are produced from mono-disperse aerosol implying that the resulting particles are homogeneous in size, elemental content and their physical and chemical form. The degree of homogeneity among the produced particle population makes such particles an interesting candidate for quality control purposes or as material for the purposes (1) - (4) described above. The production process allows for adjustment of specific characteristics of produced particles, which can be kept under control during the process. Most importantly for their application in analytical measurements, the isotopic composition of particles and elemental content is determined by the isotopic composition and the concentration of non-volatile part of the feed solution used for aerosol generation, respectively. This concentration also determines the final size of the particle. Each vibration of the orifice creates a droplet, as it virtually ‘chops’ a stream of liquid into individual droplets constituting the precursor of the actual final particle. The volume of the droplet V_d is simply the liquid volume flow-rate Q divided by the chopping Frequency f. The mass of the particle m_P is equal to the amount of non-volatile material in the individual droplet which is determined through the concentration c of the non-volatile component in the feed solution. The operation principle expresses itself in few simple relations:

$$V_d = Q/f \qquad (1)$$

$$m_P = V_d * c \qquad (2)$$

When it is desired to obtain a uniform particle distribution in terms of elemental content and size (i.e. identical particles), the droplets should be as mono-disperse as possible. The production process yields particle of a certain physical and chemical composition, which so far has not yet been fully determined.

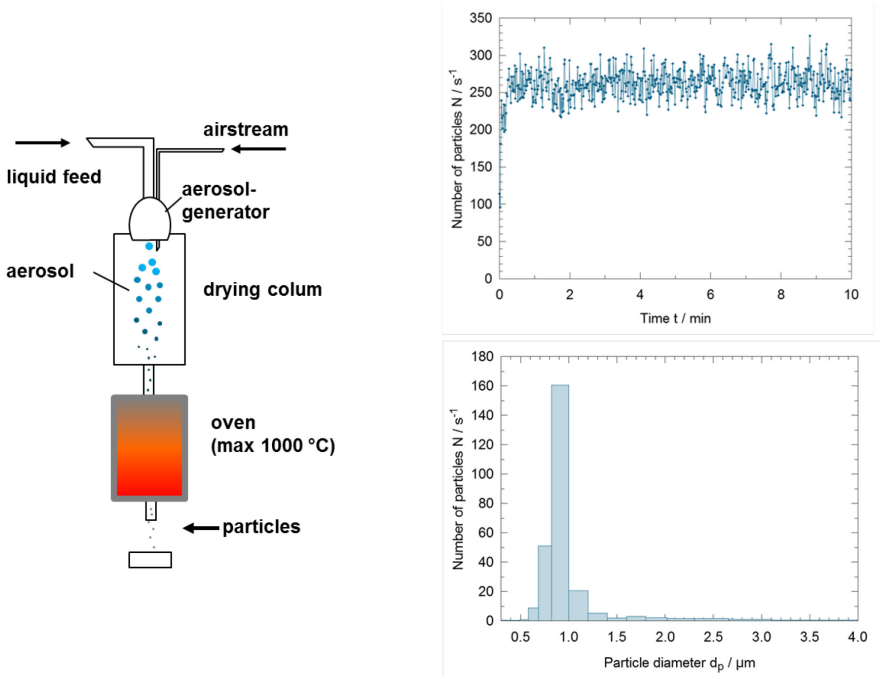

Figure 1: Schematic overview of microparticle production system (left) and online measurements of particle concentration (right-top) and particle size distribution (right-bottom). Online measurements performed using an optical particle sizer.

There are multiple parameters determining the process, such as the non-volatile fraction of the feed solution, the heat treatment temperature and the heating time. Significant effort was spent to evaluate the different setting parameters of the production setup. With the setup outlined in the scheme of Figure 1 (left), routine production of uranium particles is possible. The typical operation mode for particle production will be reported in the following paragraphs. It needs to be mentioned, that the system provides some flexibility in terms of production output, where the entire parameter space has not yet been fully evaluated.

2.2 Particle Production Tests

In usual operation, uranyl nitrate aerosol is prepared using a vibrating orifice aerosol generator (VOAG) (TSI Inc. VOAG Model 3450). In order to produce micro-particles with a diameter of about 1 µm an orifice with 20 µm diameter is used. A liquid feed rate Q = 2.32 10^{-9} m^3 s^{-1} has been applied with a frequency f = 69 kHz. According to equation (1), aerosol droplets with a total volume V_d = 3:36 10^{-14} m^{-3} are produced. As liquid feed a 1:1 mixture of a uranyl nitrate solution and ethanol has been used. The uranyl nitrate solution is obtained by dilution of certified reference material IRMM-183, a depleted, reprocessed uranyl nitrate solution with a precisely characterized isotopic composition. Beside the isotopic composition, the uranium concentration and HNO_3 content are given as informative values as $w(U) \approx 0.2$ g g^{-1} and $m(HNO_3) \approx 6$ mol kg^{-1}, respectively. For the preparation of the liquid feed solution, the CRM is diluted gravimetrically (Mettler-Toledo XP205 DeltaRange) with ultra-pure water to an uranium content of about 250 µg g^{-1}. In order to allow faster evaporation, the diluted sample is further diluted with ethanol to obtain a solution with a uranium content of approximately 125 g g^{-1}. All solutions used have been analyzed by ICP-MS (PerkinElmer/SCIEX Elan 6100 DRC) to determine the uranium content. Based on the droplet volume and uranium content, particles with a uranium content m(U) ≈ 3.76 pg are expected to be produced, calculated using equation (2). In order to minimize the impurities of the produced particles, all dilutions have been performed using ultra-pure water obtained using a Elga PURELAB Ultra installation which produced water with a resistance of 18.2 MΩ cm and Merck Millipore absolute ethanol. The prepared aerosol solution is dispersed with an air dispersion stream to prevent coagulation of aerosol droplets and for further transport.

Some issues with the corrosion of the orifice were encountered, where the orifice plate made of a thin stainless steel diaphragm suffered from perforation induced by corrosion caused by the uranyl nitrate

solution. Using in-house available electroplating, a protective gold coating was applied in order to increase the durability of the orifice plate. Comparative corrosion tests have shown the increased stability of the gold-coated orifice as compared to the unmodified orifice. So far the production system shows promising performance using the modified orifice plate. Typical operation consists of a production cycle of ca. 1 h operation, in which ca. 10 ml of a prepared feed solution consisting of uranyl nitrate diluted in a 1:1 water-ethanol solution with an uranium concentration adjusted such to reach the desired final particle diameter is used. An optical particle counter (OPS) (TSI inc. Model 3330) is connected in parallel to the main particle air stream allowing for on-line monitoring of particle number and particle size distribution. It should be noted, that the OPS provides an indicative value, as optical and geometric diameter may differ on the micrometre length scale. An example of typical operation is displayed in Figure 1 (right) over a period of 10 min clearly showing that stable output of mono-disperse particles can be maintained. After switching off the aerosol generator the particle count of the particle counter drops to nearly zero and far below the particle count level in the ambient air of the laboratory. This implies that the air stream within the closed system is clean and that remnant particles within the tubing of the system are not a source of possible contamination from previous particle production runs. It therefore seems feasible of performing production runs of various particle species without need for replacement of parts used for transport and treatment of the aerosol. To avoid any contamination of the liquid feed from prior usage it is necessary to thoroughly flush the liquid feed system.

2.3 Uranium chemistry of particle formation

The heat treatment leads to chemical transformation of the intermediate product consisting of the particle that resulted from the drying droplet. We assume that the intermediate particles (or precursor) is chemically composed of uranyl nitrate hexahydrate, $UO_2(NO_3)_2 \cdot 6H_2O$, which is one of the most common hexavalant uranium compounds. Uranyl nitrate hexahydrate is commonly used in the uranium industry as intermediate product and has been studied intensively in the past (e.g. [5]). One of the main areas of interest is the thermal decomposition of uranyl nitrate hexahydrate to uranium trioxide, UO_3. The thermal decomposition has been described in two main phases; first the thermal dehydration followed by the thermal denitration. The influence of the temperature with which particles are treated during the production becomes evident from literature data on thermal dehydration and denitration of uranyl nitrate. The dehydration process is complete at temperatures above 300 °C (Figure 2 – left). UO_3 is the first oxide formed when uranyl compounds are heated in air or oxygen and is stable up to temperatures around 550 °C (Figure 2 – right). The difference in temperatures at which transformation is observed in the experiments reported in the literature stems from the different experimental conditions. Currently, the production setup is operated with a compact air heater at a final air temperature set to 500 °C. It must be noted, that the actual temperature of the particle within the air stream is unknown and that the heating component provide merely an indicative temperature value. Therefore, systematic analysis of the production output is necessary. So far systematic tests of the influence of heating temperature on produced particles can be interpreted according to the transformation of uranyl nitrate hydrate as reported in literature [5-10] by analysing the size and morphology with SEM accompanied with elemental analysis using EDX. The actual final particle diameter can be reproduced quite well, as has been confirmed by analysing a series of batches over time (October 2014 - May 2015) using different feed solutions with varying uranyl concentration.

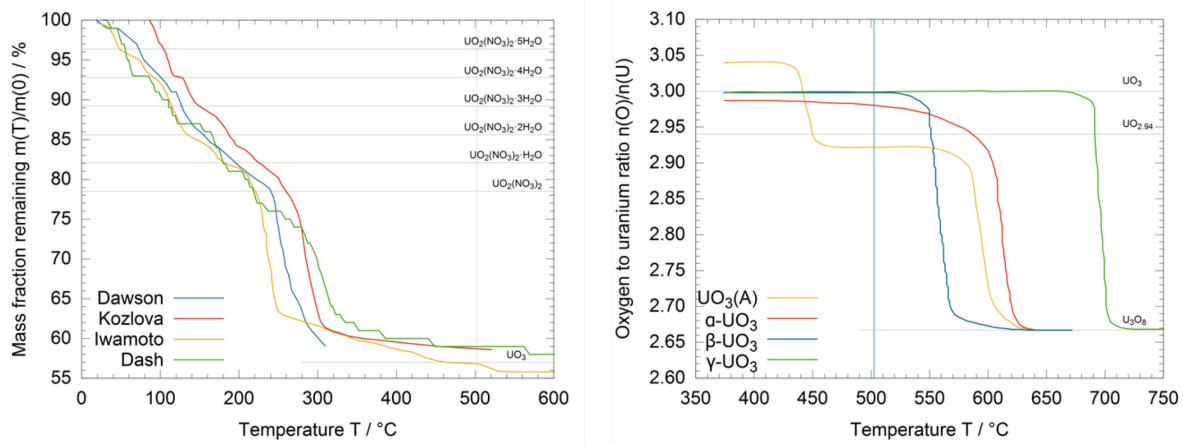

Figure 2 The graphs represent data of the thermal decomposition of uranyl nitrate hexahydrate in an air atmosphere (left), measured by thermal gravimetrical analysis [5-8] and the reduction of various modification of UO_3 to U_3O_8 (right) [9,10].

2.4 Particle sampling and characterization

The particles in the air stream are sampled using impaction on a substrate, as similarly practiced in particle collection from swipe samples. This way, ca. 10,000 particles can be collected on an uncoated substrate (e.g. 1" diameter glassy carbon planchet) within 5 min deposition time. It has been reported in literature, that the IAEA impaction technique suffers from poor collection efficiency, which, however, can be increased by application of an adhesive coating. Such coating would have interfered in particle handling and characterization and in the currently evaluation phase the particle collection is not optimized for collection efficiency.

For SEM characterization uranium particles are readily identified in the backscatter-electron imaging mode. A particle search was conducted and EDX elemental analysis has confirmed that the particles consist of uranium. Under optimal conditions the particles are spherical and mono-disperse. In previous work undertaken to characterize particles produced using the VOAG, it was reported that some voids may be present [11]. Under the currently optimized production parameters (500°C heating temperature), produced particles had been selected for preparation using a Focused Ion Beam (FIB) apparatus (Zeiss Nvision 40 Cross Beam Workstation). The FIB apparatus features high-resolution SEM such that the shape and surface of particles can be studied with high detail (Figure 3 – bottom left). The FIB technique allows for surface modification with an ion-beam thus serving as a 'milling machine' on the nano- and micro- scale and is ideally suited to study the internal morphology of particles (Figure 3 – right-bottom). A random selection of six uranium particles from a production run (heat treatment temperature 500 °C) was sliced to study the internal of produced particles. All particles on the sample were spherical and free of voids. Some porosity is observed in the centre of the particles, with higher density at the perimeter (see Figure 3 - right-bottom). The particle being formed from an evaporating droplet that is subsequently treated in an oven for a relatively short time, the presence of a certain degree of porosity is to be expected. Using the prior knowledge of the expected amount of uranium per particle allows an estimation of particle density assuming the particle consists of UO_3, has a spherical shape and by determining the diameter of the particle population from the SEM analysis. With the production settings from above the estimated density amounts ca. 4.3 g cm^{-3}, close to the value observed in quantitative analysis performed on uranium oxide particles [11]. The production of a range of particle sizes was undertaken, yielding spherical particles in the range of 0.8 to 1.5 micrometers. At the smaller diameters the particle collection on uncoated substrates becomes increasingly inefficient. The density of the particles was consistent at the same value for the entire range of produced particle sizes and we conclude that the density within that range is determined by the heat treatment on not by the droplet evaporation dynamics.

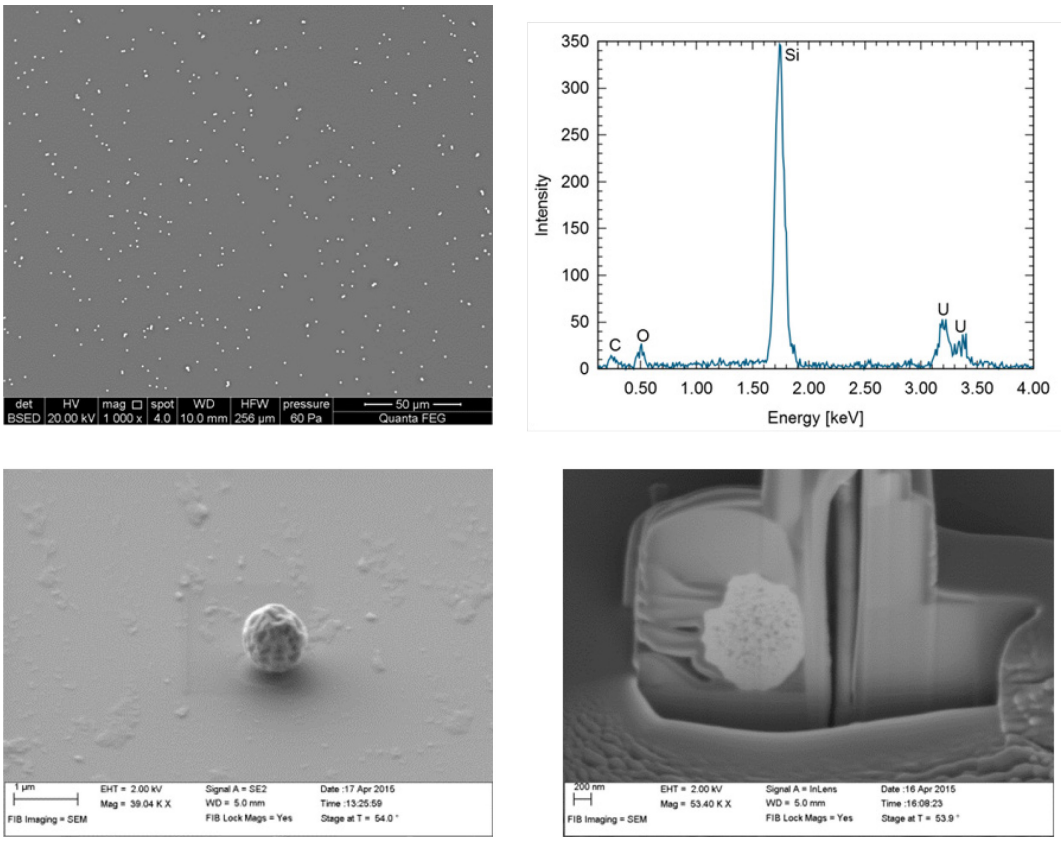

Figure 3: SEM (left) and EDX (right-top) of produced microparticles deposited on a Si wafer and a cross-section prepared by FIB milling (right-bottom).

3 Considerations for Particles as Reference Material

As most results of analytical methods, such as mass spectrometry, are used for further decisions, meeting certain quality goals like measurement accuracy and precision, or interfering background contributions is of high importance. A number of documents of the International organisation for standardization (ISO) describe quality control (QC) processes to assure that measurements are performed under proper conditions and the risk of obtaining incorrect results is minimized. One of the most important standards for analytical laboratories is EN ISO/IEC-17025:2005 [12]. With the current set of production parameters particles can be produced under certain boundary conditions. At this stage the suitability as material for quality control processes depends on the target application.

3.1 (Certified) Reference Material

In most cases, a certified reference material (CRM) is used as sample with a precisely known true value. A CRM is a type of reference material (RM). In the international vocabulary of metrology (VIM) [13] a reference material is defined as

"material, sufficiently homogeneous and stable with reference to specified properties, which has been established to be fit for its intended use in measurement or in examination of nominal properties".

A certified reference material is a reference material, but instead of fit for purpose, the properties are well characterized. The VIM has defined a certified reference material as

"reference material, accompanied by documentation issued by an authoritative body and providing one or more specified property values with associated uncertainties and traceability, using valid procedures".

As not only the property value is of importance, but also the associated uncertainty, the characterization of these certified reference materials is rather complicated and has been covered by

the international organization for standardization in a series of guides, where the production and characterization of (certified) reference materials is mainly covered in ISO guide 34:2009 [14] and ISO guide 35:2006 [15].

3.2 Particles as Reference Material

For particles this means, that at least a homogeneity and stability assessment is required. With the stipulated quality goals in particle analysis where the isotopic ratios are determined, at minimum the isotopic ratios of uranium isotopes U-234/U-238, U-235/U-238, U-236/U238 property values of particles would have to be assessed with respect to the homogeneity and stability criterion. Further property values of particles like size and shape, elemental composition, uranium content and chemical form may be also relevant or can be provided as information values.

For certification of particle properties significant additional effort would be required due to the stringent requirement, e.g. determination of uncertainties of the property value including uncertainties stemming from in-homogeneity and instability.

Unlike (certified) reference materials that is usually available in solutions or powder form, it so far has remained undetermined, in which configuration particles will be prepared as material for the intended purpose (Validation, Calibration, Quality Control or Proficiency Testing).

4 Particle Preparation Options

With the production process delivering mono-disperse particles described in the previous section of this paper, the present chapter will discuss several options on how particles are packaged and implications on homogeneity and stability of the property value(s). In these considerations we will limit ourselves to the isotopic composition of the particles as the relevant property in safeguards analysis. Once the packaging of particles 'fit for purpose' is accomplished or property values have been certified, it constitutes a product that fulfils certain requirements as stipulated by the application in analytical measurements. Each option brings certain advantages and disadvantages in consideration of their use as material or use in quality control or reference material. Following options are currently being considered (see also Figure 4):

(A) Impaction on substrate: The simplest strategy would be directly depositing particles onto a solid substrate (e.g. Si-wafer or glassy carbon planchet). Such deposition leads to a batch production of particle-loaded substrates. In terms of homogeneity and stability, a sampling scheme for statistical sampling of particles on selected planchets could be applied, along the lines followed by the NUSIMEP-6 and NUSIMEP-7 particle analysis interlaboratory comparison [16].

(B) Transfer into suspension: Another option is to directly collect a large number of particles in a suspension or the transfer of particles collected on the substrate(s) into a suspension. Liquid suspensions have a great advantage for subdivision and as they allow users to use any substrate material of their preference, e.g. from a single certified batch of micro-particle suspensions. Another interesting feature is offered by creating mixtures of different particle species (e.g. NU and LEU particle mixtures) by mixing several single species particle suspensions.

However, the stability of particles in a suspension could prove difficult, as a number of processes could take place. Problems may arise for the stability of particles within the solution and possible isotopic exchange between the remaining uranium background in the solution and the uranium of the micro-particles.

(C) Transfer on substrate: As a third option, the suspension is processed further to transfer onto a substrate of choice. This would mitigate the stability issues that may be present in option (B). Compared to option (A) mixtures of suspensions of varying particle species could be mixed prior to transfer thus facilitating creation of substrates with certified particle mixtures.

(D) Transfer in matrix: A possibility for the stabilization of the micro-particles is by embedment into a solid matrix. An advantage is that the particle stability might be increased and that it might be more convenient for production. Fixation of embedded particles may also be of interest for certain analytical procedures for which the particles would have to fulfil the purpose as a reference material.

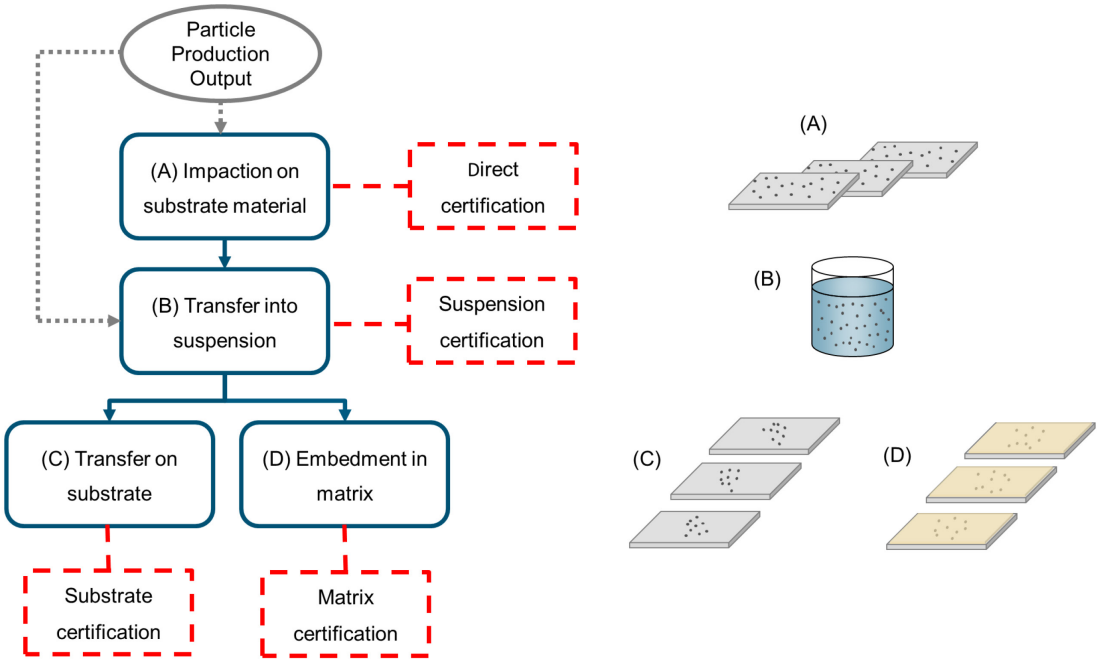

Figure 4 : Possible procedures for further processing of produced micro-particles before certification.

In the current stage, option (A) seems realizable without little development effort. In the current setup, the particle collection would have to be modified to enable batch production of substrates. The preparation of particle suspensions has some challenges, like creation of clusters and the stability of particles within the solution.

It is noteworthy to mention, that processing of particles can also include arrangement of particles in a regular pattern which offers better controlled measurement conditions in the analytical application of interest (e.g. LG-SIMS or LA-ICP-MS). Here, technologies using patterned masks and substrates may be of interest where larger numbers of particles from a solution (i.e. option (C) and (D)) can be arranged in regular patterns which is rather resource intensive when applying single particle deposition using micro-manipulation.

5 Summary and Outlook

A production process for uranium-oxide micro-particles of spherical shape and with diameter of ca. 1 µm based on mono-disperse aerosol generator provides promising candidate material for use in quality control or as (certified) reference material. A number of particle properties have been characterized, such as size, shape, elemental composition and internal morphology have been characterized using SEM/EDX and FIB. Further particle properties like chemical composition may be of importance in terms of the stability over extended storage period and therefore characterization of particles using appropriate techniques (micro-raman, transmission electron microscopy, X-ray diffraction) will be of great interest.

The production process, including the implemented particle collection and further processing to package particles into a suitable form that meets the analytical needs, needs to be considered. In particular certification of particle properties requires extensive analytical effort and therefore careful attention is required to properly determine the suitable form. Currently, the preparation of uranium particles in a suspension seems to provide attractive features in terms of handling by the end-user. However, open questions remain concerning stability of particles within the suspension which are currently being addressed by systematically studying processes like dissolution and isotope exchange on particles produced with the setup presented in this paper.

6 Acknowledgements

We thank M. Klinkenberg and M. Güngör from Forschungszentrum Jülich for SEM and FIB analysis of particles.

This work was supported under task C.45 / A1961 by the German Support Programme and by Bundesministerium für Wirtschaft und Energie "Neu- und Weiterentwicklung von Safeguardstechniken und -methoden" (FKZ 02W6263).

7 References

[1] IAEA, *International Target Values 2010 for Measurement Uncertainties in Safeguarding Nuclear Materials*, IAEA-STR-368, Vienna, November 2010

[2] IAEA*, Strengthening the Effectiveness and Improving the Efficiency of Agency Safeguards*, Report by the Director General 58th General Conference of the IAEA, August 2014

[3] Knott, A. and Duerr, M.*, Production of monodisperse uranium particles for nuclear safeguards applications*. ESARDA Bulletin, **49,** 40, 2013

[4] Erdmann, N., Betti, M., Stetzer, O., Tamborini, G., Kratz, J., Trautmann, N. & van Geel, J.*, Production of monodisperse uranium oxide particles and their characterization by scanning electron microscopy and secondary ion mass spectrometry*, Spectrochimica Acta Part B: Atomic Spectroscopy, **55**, 565, 2000.

[5] Dawson, J. K., Wait E., Alcock, K. and Chilton, D. R.*, Some aspects of the system uranium trioxide-water*. J. Chem. Soc., **353**, 1956.

[6] Kozlova, R., Matyukha, V. and Dedov, V., *Mechanism and kinetics of thermal decomposition of uranyl nitrate hexahydrate under the nonisothermal conditions,* Radiochemistry, **49(2)**, 130, 2007.

[7] Iwamoto, K.*, Thermal decomposition of uranyl nitrate hexahydrate in the presence of graphite,* Journal of Nuclear Science and Technology, **1(4)**,113, 1964.

[8] Dash, S., Kamruddin, M., Bera, S., Ajikumar, P., Tyagi, A., Narasimhan, S. and Raj, B., *Temperature programmed decomposition of uranyl nitrate hexahydrate,* Journal of Nuclear Materials, **264(3)**, 271, 1999

[9] Hoekstra, H. R., Siegel S., *The uranium-oxygen system: U_3O_8-UO_3,* J. Inorg. Nucl. Chem., **18**,154-165, 1961

[10] Wheeler, V. J., Dell, R. M., Wait, E., *Uranium trioxide and the UO_3 hydrates*, J. Inorg. Nucl. Chem., **26**,1829-1845, 1964

[11] Kraiem, M., Richter, S., Erdmann, N., Kühn, H., Hedberg, M., Aregbe, Y., *Characterizing uranium oxide reference particles for isotopic abundances and uranium mass by single particle isotope dilution mass spectrometry, Anal. Chim. Acta, **748**, 37, 2012*

[12] ISO 17025:2005 *General requirements for the competence of testing and calibration laboratories*, 2005.

[13] BIPM, IEC, IFCC, ILAC, ISO, IUPAC, IUPAP, and OIML. *International vocabulary of metrology - Basic and general concepts and associated terms*, volume 3. 2012

[14] ISO Guide 34:2009 *General requirements for the competence of reference material producers*, 2009.

[15] ISO Guide 35:2006 *Reference materials - General and statistical principles for certification*, 2006

[16] Truyens, J, Stefaniak, E.A., Aregbe, Y, *NUSIMEP-7: uranium isotope amount ratios in uranium particles, J*ournal of Environmental Radioactivity, 125, 50, 2013

Stabilisation of Uranium/Plutonium dried spikes with a cellulose matrix

R. Carlos-Marquez, R. Buda, K. Lützenkirchen,
A. Sánchez Hernández, P. van Belle

Institute for Transuranium Elements (JRC-ITU)
Joint Research Centre, European Commission
Hermann-von-Helmholtz-Platz 1, 76344 Eggenstein-Leopoldshafen, Germany
E-mail: Ramon.CARLOS-MARQUEZ@ec.europa.eu

Abstract:

Large Scale Dried (LSD) spikes are used in nuclear safeguards laboratories world-wide for an accurate Isotope Dilution Mass Spectrometric (IDMS) determination of physical nuclear material inventories, with relative uncertainties for U and Pu of better than 0.28 % (k=1). IDMS fully relies on the mechanical integrity of the spikes. The spikes need to be robust during transport and storage for their guaranteed life-time of 3 years. Mechanically damaged spikes are no longer fit for purpose (ISO-guide 34 on "General requirements for the competence of reference material producers").

LSD spikes are produced by dispensing accurately-weighed quantities of a nuclear material reference solution into penicillin vials, after which the solution is evaporated to dryness. Some commercially available spikes are additionally covered with an organic coating to prevent unintented losses of nuclear material when the spike vials are opened for use. The main requirements for such coatings are good adherence to glass, mechanical stability, resistance to radiation and long term stability. Furthermore, the coating should readily dissolve in nitric acid and should not interfere with chromatographic chemical separation and subsequent mass spectrometric measurements.

JRC-ITU carried out research and development to improve on traditional coatings based on Cellulose Acetate Butyrate (CAB) that is used in spikes such as JRC-IRMM 1027. CarboxyMethyl Cellulose Sodium Salt (CMC) is proposed as an alternative to current CAB coatings that fail to offer the desired shelf-life. In the JRC-ITU procedure, CMC is dissolved in water, changed to a nitrate form with a high viscosity and added to spike vials containing the dried deposits of nuclear reference material. After warming, the CMC forms foam that is extremely robust to mechanical impact and appears to have a long shelf-life. The CMC foam coatings were scrutinized by Scanning Electron Microscopy and Energy Dispersive X-ray Spectroscopy (SEM/EDX) and preliminary IDMS studies indicate that CMC does not interfere with IDMS assays. CMC appears to be a promising coating material for LSD spikes.

Keywords: spike; safeguards; Carboxymethyl Cellulose;

1. Introduction

To be relevant, Nuclear Material Safeguards measurements need to be carried out to high accuracy. Isotope Dilution Mass Spectrometry (IDMS) using high quality spikes is one of the primary measurement techniques that offer the highest possible measurement accuracy (IAEA/ESARDA International Target Values (ITV) [1]. The spikes used in IDMS are produced starting from ultra-pure plutonium and uranium reference metals. Accurate masses of these metals are gravimetrically dissolved to obtain a spike mother solution with known element mass fractions. Accurately weighed portions of the mother solution are subsequently dispensed into vials and then dried. Each spike produced in this manner will therefore, contain known amounts of Pu and U. Successful and accurate IDMS analyses require the nuclear material isotopic composition in the spike mother solution to be deliberately different from the corresponding isotopic composition for the Safeguards samples. The dried deposits of the spike reference material are prone to damage by alpha-radiation, which readily

converts the deposits to powder / dust. It is therefore desirable that the deposits are covered by an organic coating to prevent unintended escape of nuclear material when the spike vials are opened for use because unknown losses of nuclear material will render the IDMS results valueless. An ideal coating needs to be mechanically robust, be resistant to radiation damage, needs to have good adherence to glass, be long-term stable, be readily dissolved and destroyed by acid whenever the spikes are used for nuclear material assay and the material used for coating should not interfere with essential IDMS steps such as chromatographic chemical separation and mass spectrometry.

From the perspective of the spikes themselves, the accuracy of the results obtained through IDMS assay depends, amongst others, on the accurate characterisation of the material used for spike production both in terms of quantity and in terms of isotopic composition, the integrity of the spikes and the ability to homogenise spike and sample material. One problem with the current CAB coatings used on U/Pu spikes is that they have a rather short shelf-life and after this period they become brittle and start to flaking soon after.

2. Chemistry and properties of the CMC

Carboxymethyl cellulose (CMC) sodium salt is a cellulose fiber with sodium hydroxide and chloroacetic acid (see Figure 1). This anionic polysaccharide is a commercial product that finds uses in an increasing number of applications (for instance as suspending agent, in adhesives, as a stabilizer, etc.). Hercules Inc. [2] describes most of the physical and chemical properties of CMC, but here we highlight only the most pertinent properties.

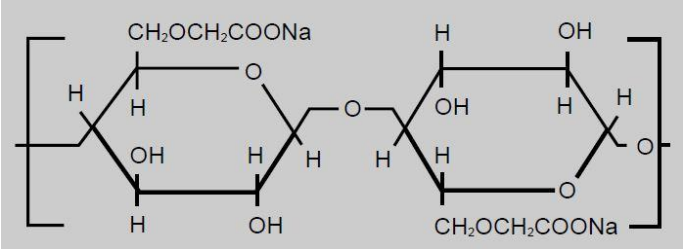

Figure 1: Structure of Carboxymethycellulose.

Cellulose ethers, such as CMC, are long-chain polymers. Their solution characteristics depend on the average chain length or degree of polymerization as well as the degree of substitution, both of which determine the molecular weight of the polymer. The viscosity of CMC solutions increases markedly with increased molecular weight. Approximate values (weight averages) for the degree of polymerization and molecular weight of several viscosity types of CMC are given in Table 1 (Hercules Inc. [2]).

Viscosity Type	Degree of Polymerization	Molecular Weight
High	3,200	700,000
Medium	1,100	250,000
Low	400	90,000

Table 1: Typical Molecular Weights and Viscosity.

2.1. Dispersion and dissolution of CMC

CMC is soluble in aqueous solutions (hot or cold), is insoluble in pure organic solvents, but can be dissolved in certain mixtures of water and water–miscible solvents, such as ethanol or acetone.

CMC particles have a tendency to agglomerate or lump, when first added to water. Adding water to the dry solid produces clumps of solid CMC that are very difficult to dissolve. To obtain good solutions, the dissolving process should be carried out in a two-steps operation:

1. Dispersing the dry powder in water. Individual particles should be wet and the dispersion should not contain lumps.
2. Dissolving the wetted particles

Hercules Inc. [2] proposes several dissolution methods, and when the proper technique is used, good dispersion is obtained and the CMC will go into solution rapidly.

2.2. CMC Stability and Chemical Degradation

CMC is subject to microbiological attack and chemical degradation, but in the JRC-ITU procedure, the CMC used for the preparation of spike coatings is combined with concentrated nitric acid, which makes the solution more resistant to the microbiological attack.

Under certain conditions, solutions of CMC are susceptible to chemical degradation. CMC with high viscosity offers better resistance to viscosity degradation and precipitation. Sunlight, exposure to oxygen and prolonged exposure to high temperatures are known to adversely affect the stability of CMC solutions (Hercules Inc. [2])

2.3. CMC interaction with nuclear material

Although the applications of CMC in the food industry are well-researched, there are not many studies on the interaction of CMC with nuclear materials. Popescu et al. [3] have proposed a structure for a uranium-CMC polymer, which is shown in Figure 2 (red for O atoms, cyan for C atoms, white for H atoms and purple for U atoms) and Figure 3:

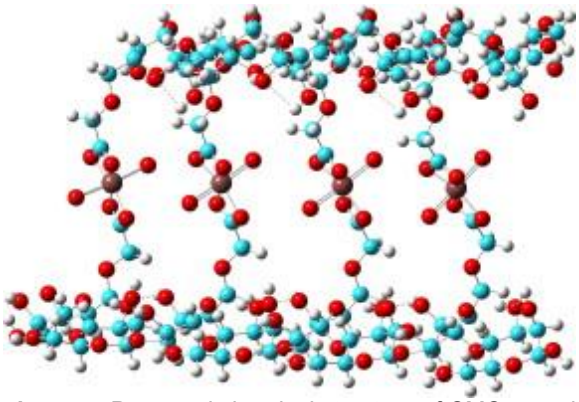

Figure 2: Proposed chemical structure of CMC-uranyl complex

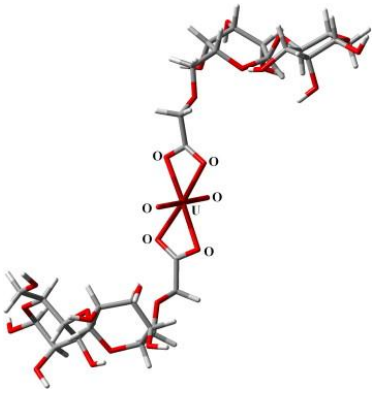

Figure 3: Spatial structure of $UO_2(CMC)_2$ molecular system

We have not been able to find similar studies on the interaction of CMC with plutonium. Nevertheless, the known chemistry of plutonium needs to be taken into account when applying CMC to materials containing plutonium-nitrate. As described by Neck et al. [4] and Walther et al. [5] plutonium forms readily and partly irreversibly PuOx colloids at pH values exceeding 1.5. IDMS requires the plutonium from both spike and sample to be available in the form of mobile ions and the formation of colloids needs to be avoided at all cost. It is therefore, essential that CMC solutions are prepared at pH values below 1, e.g. using nitric acid. Our studies have shown that, under acidic conditions, CMC mixes very well with both plutonium- and uranyl-nitrates. The presence of the nitric acid is believed to generate modest amounts of CO_2 which would explain the formation of a CMC foam, as opposed to a solid CMC coating, when the CMC solution is gently warmed to dryness. The foam, so produced, creates a spike coating with highly desirable properties.

3. Materials and equipment

The materials and equipment needed for the preparation are listed below:

- Milli-Q purified water.
- CMC HV: Carboxymethyl cellulose sodium salt, High Viscosity; cat: 217274, CAS: 9004-32-4; pH: 7.3; Viscosity: 2550.0 mPa.s, Loss on drying: 4.5%, Company: CALBIOCHEM
- CMC LV: Carboxymethyl cellulose sodium salt, Low Viscosity; cat: 217277; CAS: 9004-32-4; pH:6.8 Viscosity: 42.0 mPa.s Assay: 99.61% Company: CALBIOCHEM
- Nitric Acid (HNO_3): SUPRAPUR 65%; Cat: 1.00441.1000; Company: MERCK,
- Glass Vials: vo. 10 mL; 20.5 x 54.5 mm, flat-clear-Crip neck N20; Company: Macherey-Nagel
- Heater: VLM BIO1 GmbH, Type: V.668.061.624, supply: 230V, 50-60Hz; Power: 300W
- Erlenmeyer: 100mL-glass; Company: Schott&Gen;
- Syringe: OMNIFIX 20mL; Ref: 4616200V, sterile/nonpirogenic

4. Experimental CMC solutions

Several parametric variations with regards to CMC concentration, nitric acid molarity, and drying temperature were carried out before good CMC-gels and desirable CMC-foam structures were obtained. In these tests we controlled three main variables:

- Concentration of CMC in HNO_3
- Viscosity of the CMC
- Molarity of the HNO_3

The first attempts were done using low viscosity CMC in different concentrations and with different molarities of the HNO_3. The best foam structures were obtained using a CMC concentration of 70 mg/mL and a nitric acid molarity of 4 M. However, the gel itself is not perfectly stable due to the low viscosity of the CMC (low molecular weight of the polymer chains).

Thereafter experiments were carried out using high viscosity CMC. However, in this case the nominal CMC concentration of 70 mg/mL combined with a nitric acid molarity of 4 M produces a very dense and viscous gel that is not easily dispensed into the spike vials. The concentration of CMC was therefore, reduced to 50 mg/mL while keeping the HNO_3 molarity at 4 M. The resulting gel is less viscous and can be dispensed with ease. In addition, the CMC gel is stable over time. Subsequent evaporation of the latter gel produces a stable white to beige foam that is remarkably resistant to strong mechanical impact. Spike vials are typically charged with approximately 2.5 mL of the gel and will therefore have a CMC inventory of approximately 125 mg of CMC. After gently heating most of the water and acid will evaporate and will leave approximately 3-5 mL of CMC-foam behind.

When coated spikes are used in IDMS assays, it is essential that the coating dissolves easily to allow intimate homogenization between the nuclear material of the spike and that of the sample. Less than perfect homogenization falsifies the basic assumptions that underpin Isotope Dilution Mass Spectrometry and will lead to biased results. Tests on the foam show that more than 95% of the foam dissolves instantly on contact with 4 mL of 8-Molar nitric acid. Some 5% of the foam appears to resist instant dissolution, but can be totally dissolved / destroyed after 2 hours of heating at 60 °C.

5. Stability test: degradation by heat, shocks and radiation

Many stability studies have been carried out and reported in the literature on CMC in gel form, but not many studies report on CMC foam. In JRC-ITU, CMC in gel form is only used as an intermediary in the production of a stable, impact-resistant foam. As it is this foam that protects and binds the nuclear material present in the spike, the stability tests in JRC-ITU have focussed on the foam itself.

Temperature tests: the CMC foam produced has been exposed for three months to an elevated temperature of 40°C. After this test, no flakes were detected inside the glass vials and the foam remained resistant to mechanical shocks. Prolonged exposure to elevated temperatures does

however, changes the consistency and colour of the foam, which changes from white to beige to a darker brown (see Figure 4). Nevertheless, the valuable features of the coating material are preserved as no lose particles were noticed.

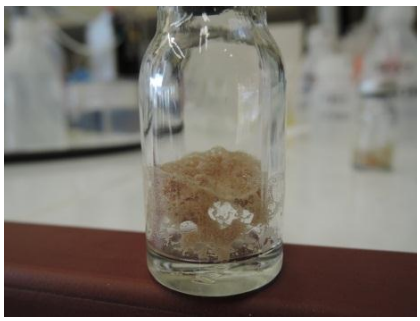

Figure 4: CMC Foam exposed to temperature.

Shock tests: In order to check the resilience of the material, the vials containing the foam were hammered hard against a solid surface without any damage to the foam. In addition, the vials were subjected for 2 minutes in an ultrasonic bath. The ultrasonic treatment has been applied to a freshly produced foam as well as to a foam that has been warmed for three months at 40°C. In either case, no evidence of damage or flaking was seen.

Irradiation tests: 5 vials with CMC foam were exposed inside Hot Cells to a dose rate of 1Sv/h for one month (a total aggregated dose of 730 Sv). After visual and microscope inspection no damage or flaking has been detected. The only visible change was in the colour of the foam, which had changed from white to beige. At this moment, more irradiation tests at the same high dose rate are running for longer periods, 3 and 6 months. Choi et al. [6],[7],[9] and Lee et al. [8] have tested the degradation under irradiation of CMC hydrogel and report a loss in viscosity.

6. Final process for the preparation of the CMC

6.1. Preparation of CMC in aqueous solution

The first step entails the dissolution of CMC in water as this produces a final product with a higher viscosity as when CMC is dissolved directly in nitric acid. In this step High Viscosity CMC sodium salt powder is used and 3 g of CMC is dissolved in 50 mL of distilled H_2O while heating at 60 °C. To prevent the formation of carboxymethylcellulose lumps, the mixture is stirred for two hours until total dissolution of the CMC is achieved and a transparent solution is obtained. After this step the solution is cooled down to room temperature, resulting in a transparent high viscosity gel.

6.2. Preparation of CMC in nitric acid solution

Once the CMC in aqueous solution has cooled down and while stirring at room temperature, concentrated HNO_3 is added until a HNO_3 4 M solution is obtained with a CMC concentration of approximately 50 mg/mL The CMC nitric solution is then ready to be dispensed into glass spike vials using a 20 mL syringe, (see Figure 5)

6.3. Evaporation and foam production

The CMC nitric solution present in the vials is then heated at 40°C for three days. During this process more water is lost from the gel with a corresponding rise in nitric acid molarity. When the gel has almost dried, the interaction between the nitric acid and the CMC causes a gentle production of CO_2 gas, which causes the remainder of the gel to turn into foam (Figure 6).

Figure 5: CMC nitric solution.

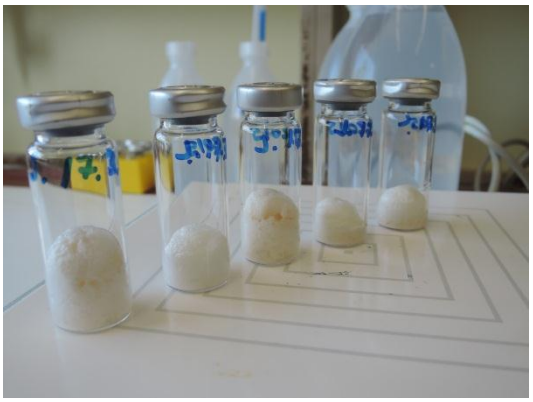

Figure 6: CMC foam state.

7. Test with foam-coated spikes

To prove that the CMC coating does not interfere with Isotope Dilution Mass Spectrometry, a test has been carried out in which an accurately known quantity of approximately 3 mg of plutonium originating from a high burn-up plutonium nitrate solution (known as SM4) was dried, coated with CMC gel and finally heat-treated to produce foam. In parallel, another known quantity of approximately 3 mg of SM4 plutonium was deposited in a spike vial and received an identical treatment, but without the addition of CMC gel (see Figure 8). After some weeks, the plutonium present in either vial was assayed using a plutonium reference solution produced by gravimetric dissolution of a known quantity of CETAMA MP2 weapon grade plutonium metal (97.76 % ^{239}Pu). The assay largely follows the procedure routinely used in JRC-ITU for the verification of spikes produced by external customers (van Belle and Zuleger [10]). The test showed that the presence of CMC does not affect the outcome of an IDMS assay at the level of 0.035% (k=1). More such tests will be carried out in future to improve that level of uncertainty.

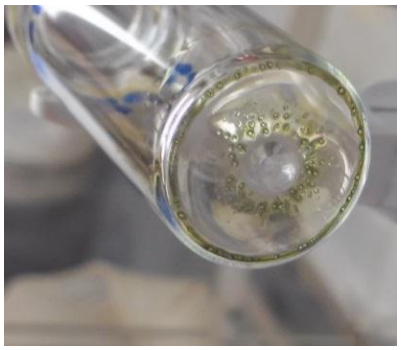

Figure 7: Pu metal dried

Figure 8: Pu in foam

Foam-coated U/Pu spikes have been also made using the (U/Pu) REIMEP17A solution Jakopič et al. [11]. Foams charged with the REIMEP material were subsequently subjected to Scanning Electron Microscopy and Energy Dispersive X-ray Spectroscopy (SEM/EDX) to obtain a detailed view of the mechanical structure of the foam and to verify homogeneity in the distribution of both U and Pu (see Figures 9, 10 and 11).

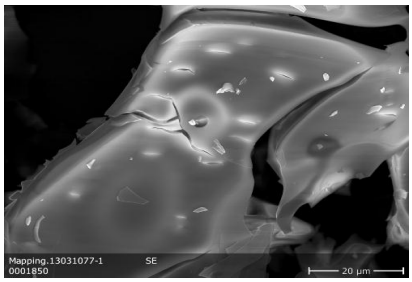

Figure 9: SEM image

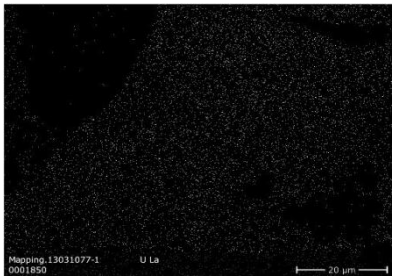

Figure 10: Distribution of U in SEM image

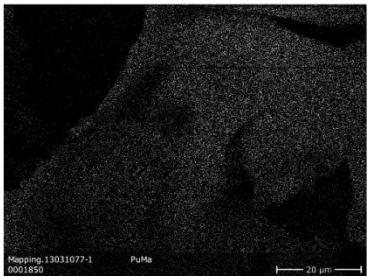

Figure 11: Distribution of Pu in SEM image

8. Conclusions

The preliminary tests carried out in JRC-ITU show that CMC foam is a promising coating material for LSD spikes. The first part of the research has been dedicated to the development of the CMC solution with a good consistency for ease of application to spike vials and one that produces a robust, impact-resistant foam coating. Chemical, mechanical and irradiation tests have been performed on some samples to establish the properties and stability of the CMC foam.

The foam appears to offer a good adsorption capability for the dried U and Pu nitrates and the U and Pu element distribution within the foam appears homogenous. The CMC foam is easily dissolved and destroyed in nitric acid when heating at 60°C for about 2 hours.

These preliminary investigations suggest CMC foam to be a suitable candidate to stabilize Large Scale Dried U/PU Spikes for use in Nuclear Safeguards Inventory Verification Measurements.

More research is needed to obtain better information on ageing effects with the aim of providing a better estimate of the shelf-life of foam-coated spikes. Absolute proof that CMC does not affect the outcome of IDMS assays will require a larger number of comparisons between coated and non-coated spikes and a collaboration between JRC-ITU and JRC-IRMM has been set up to carry out a large-scale study using 24 U/Pu Large Sized Safeguards spikes from JRC-IRMM batch 1027Q.

9. Acknowledgements

This research was supported by the Analytical Service of the JRC-ITU. The microscopy studies were also performed at the laboratories of JRC-ITU. The authors are grateful to our colleagues Karin Casteleyn, Lily Duinslaeger and Evelyn Zuleger, who provided much of the insight and expertise that assisted the research.

10. References

[1] IAEA; *International Target Values 2010 for Measurement Uncertainties in Safeguarding Nuclear Materials*, IAEA-STR-368, 2010.

[2] HERCULES Incorporated; *AQUALON® Sodium Carboxymethylcellulose: Physical and Chemical Properties;* Technical report, 1999.

[3] Popescu IC, Filip P, Humelnicu D, Bligh Scott T, Crane R; *Removal of Uranium (VI) from aqueous systems by nanoscale zero-valent iron particles suspended in carboxy-methyl-cellulose*. *Journal of Nuclear Materials;* Volume 443; 2013; p 250-255.

[4] Neck V, Altmaier, Seibert A, Yun JI, Marquardt CM, Fanghänel Th; *Solubility and redox reactions of Pu(IV) hydrous oxide: Evidence for the formation of* PuO_{2+x}*(s, hyd)*; *Radiochimica Acta*; Volume 95; 2006; p 193-207.

[5] Walther C, Rothe J, Brendebach B, Fuss M, Altmaier M, Marquardt CM, Buechner S, Cho H-R, Yun J-I, Seibert A; *New insights in the formation processes of Pu(IV) colloids*; *Radiochimica Acta*; Volume 97; 2009; p 199-207.

[6] Choi JI, Kim JH, Lee KW, Song BS, Yoon Y, Byun MW, Lee JW; *Comparison of gamma ray and electron beam irradiations on the degradation of carboxymethylcellulose*; *Korean Journal of Chemical Engineering;* Volume 26; 2009; p 1825-1828.

[7] Choi JI, Lee HS, KimJH, Lee KW, Chung YJ, Byun MW, Lee JW; *Effect of electron beam irradiation on the viscosity of carboxymethylcellulose solution*; *Nuclear Instruments and Methods in Physics Research Section B*; Volume 266; 2008; p 5068-5071.

[8] Lee HS, Choi JI, Kim JH, Lee KW, Chung YJ, Shin MH, Byun MW, Shin MG, Lee JW. 2009. *Investigation on radiation degradation of carboxymethylcellulose by ionizing irradiation*; *Applied Radiation and Isotopes;* Volume 67; 2009, p 1513–1515.

[9] Choi JI, Lee HS, Kim JH, Lee KW, Lee JW, Seo SJ, Kang KW, Byun MW; *Controlling the radiation degradation of carboxymethylcellulose solution*; *Journal: Polymer Degradation and Stability;* Volume 93; 2008; p 310-315.

[10] Van Belle P, Zuleger E; *Procedure for the verification of large scale U/Pu dried spikes*, Technical Note JRC-ITU-TPW-2009/22; 2009.

[11] Jakopič R, Aregbe Y, Buják R, Richter S, Buda R, Zuleger E; *Results of the REIMEP-17 interlaboratory comparison for the measurement of the U and Pu amount content and isotope amount ratios in the synthetic input solution*; *European Commission Report EUR 26667 EN;* 2014.

Poster Session

Chromatographic separation and on-line detection of long life alkali, alkaline earth and transition metal radionuclides by ICP-MS

Andrius Budreika [1], Deivis Plausinaitis [1,2], Evaldas Naujalis [3], Birutė Knasiene [3] Aleksandr Prokopchik [4].

[1] Company LOKMIS, Visoriu str. 2, LT-08300, Vilnius, Lithuania
[2] Department of Physical Chemistry, Vilnius University, Naugarduko str. 24, LT-03225, Lithuania
[3] Laboratory for Metrology in Chemistry, State Research Institute Center for Physical Sciences and Technology, A. Gostauto str. 11, LT-01108, Vilnius, Lithuania
[4] Chemical technology department, Ignalina Nuclear Power Plant, Druksiniu km., Visagino sav. LT-31500, Lithuania
E-mail: andriusb@lokmis.lt, deivis@lokmis.lt

Abstract:

A flow injection analysis system was developed for simultaneous detection and activity determination of long life alkali, alkaline earth and transition metal radionuclides, such as ^{90}Sr, ^{135}Cs, ^{59}Ni and ^{63}Ni. Highly active gamma emitters such as ^{134}Cs, ^{137}Cs, and ^{60}Co which were detected at the same time, were used as references for measurements. The measurement system was composed of two coupled devices: interchangeable ion and liquid chromatograph (IC and HPLC), and a mass-spectrometer with inductively coupled plasma (ICP-MS). The method was based on the use of cation exchange chromatographic column. The proposed procedure was compared with two chromatographic columns: a strong cation exchange Zorbax SCX300 and an anionic/cationic mixed bed IonPac CS5A. Oxalic acid neutralized with ammonia was used as the main component of the mobile phase for the separation of ^{90}Sr and ^{135}Cs from isobaric mass (^{90}Zr and ^{135}Ba). Separation of ^{59}Ni and ^{63}Ni was achieved with a mobile phase containing tartaric acid neutralized with ammonia. Application of the method for determination of ^{134}Cs, ^{135}Cs, ^{137}Cs, and ^{90}Sr in samples from spent nuclear fuel storage has been demonstrated.

Keywords: long-life radionuclide; ICP-MS; ion chromatography; radioactive waste

1. Introduction

The detection of radionuclides of alkali, alkaline earth and transition metal in various samples is one of the most important fields of research related to nuclear energy [1]. The nature of these radionuclides is twofold. The alkali and alkaline earth radioisotopes such as ^{134}Cs, ^{135}Cs, ^{137}Cs, and ^{90}Sr are usually nuclear fission products. Therefore, these pollutants can accumulate in the spent fuel storage. Meanwhile, the transition metal or specifically radionuclides of 3d elements are products of neutron activation. When these metals are in a nuclear reactor core, neutron activation generates a whole range of radioactive isotopes of Fe, Ni, Mn and Co. During the corrosion process these radioactive contaminants are easily transported through pipelines and other constructional elements from a nuclear reactor core. Additionally, the concentrations of 3d radionuclides in the radioactive waste can be sufficiently high [2]. Therefore later they must be collected and properly insulated.

Short-lived isotopes such as ^{134}Cs, ^{137}Cs, and ^{60}Co are easily identified using gamma-spectrometry. However, ^{90}Sr, ^{135}Cs, and ^{63}Ni are only β-emitter, so it could be determined by other radiometric methods such as β-spectrometry [3,4]. ^{59}Ni emits low energy X-ray by electron capture, thus it can be determined by X-ray spectrometry [5]. The methodology of β-spectrometry is relatively complex, because the target radionuclide must be precisely separated from the sample matrix. This fact complicates application of β-spectrometry for routine analysis.

Currently, the most progressive method for the analysis of element isotopes is a mass spectroscopy (ICP-MS). Both the stable (natural) and the radioactive (technogenic) isotopes can be detected using ICP-MS, and their detection limits are often are as low as ppt levels. The main problem in the ICP-MS is the interference of masses. In order to determine a concentrations of radioactive ^{90}Sr , ^{135}Cs, ^{59}Ni, and ^{63}Ni in a sample, one needs to know the concentrations of stable ^{90}Zr , ^{135}Ba, ^{59}Co, and ^{63}Cu [6,7]. For the aforementioned reason, direct application of ICP-MS method can not be done to determine the exact concentrations of ^{90}Sr, ^{135}Cs, ^{59}Ni, and ^{63}Ni. High-resolution mass spectrometers, such as SF-ICP-MS, can not be applied for this purpose alone. One of the most suitable solutions of this problem is using ion chromatography (IC) high performance liquid chromatography (HPLC) when detection is performed with ICP-MS.

2. Materials and methods

2.1 Instrumentation

For developing methods of detection, we used two measurement systems. One was a metal-free Dionex ICS-3000 ion chromatograph (IC, Dionex, Sunnyvale, CA, USA) connected to the inductively coupled plasma quadrupole-type mass spectrometer Agilent 7500 (ICP-QMS, Agilent Technologies, Japan). The ion chromatography system consisted of the following modules: gradient elution was carried out using a dual pump (DP) to control the eluent percentage and flow rate as a function of time; for the direct injection procedure a 6-port two-positions sampling valve (in conductivity detector module DC) with 100, 300 or 1000 μL volumes of sample loops was used. Test solution loop was filled using a manual syringe. Ion chromatographic system was controlled by Chromeleon (v6.8, 2006, Dionex) chromatographic software. ICP-QMS quartz Scott-type spray chamber with MicroMist glass concentric nebulizer was connected to the column effluent through a PTF and 0.25 mm I.D. polyetheretherketone (PEEK) tubing. The ICP-QMS system was controlled and data were processed, by a means of Agilent ICP-MS Chemstation (B.03.02, 2004) software.

The second measurement system consisted of Agilent 1100 series modular high performance liquid chromatograph (HPLC, Agilent Technologies, Waldbronn, Germany) connected to the inductively coupled plasma high resolution (sector field) mass spectrometer Element2 (ICP-HRMS, Thermo Finnigan GmbH, Bremen, Germany). HPLC was composed of a four-channel gradient pump G1311, a vacuum degasser G1322 and a 6-port two-positions valve G1158 for injections with sample loops. The same volumes of sample loops as in HPLC-ICP-HRMS system were used there as well. All HPLC couplings were made through a 0.25 mm I.D. polyetheretherketone (PEEK) tubing. The column effluent was connected directly to the nebulizer with a Scott double-pass quartz spray chamber. The operating conditions for the both ICP-MS are summarized in the Table 1.

	Agilent 7500 ICP-QMS	Element2 ICP-HRMS
Rf power	1500 W	1200 W
Rf frequency	-	27.12 MHz
Sampling depth	7.00 mm	-
Reflected power	-	<5 W
Gas flow rates:		
Cooling gas	15 L/min	14 L/min
Carrier gas	0.8 L/min	1-1.3 L/min
Makeup gas	0.3 L/min	0.75 L/min
Masses monitored for ^{90}Sr and ^{135}Cs detection	85, 87, 88, 90, 133, 134, 135, 136, 137,138	85, 87, 88, 133, 134, 135, 137
Masses monitored for ^{59}Ni and ^{63}Ni detection	52, 54, 55, 57, 59, 60, 63, 64	52, 54, 55, 56, 59, 60, 63, 64
Number of acquisition points per mass	3	-
Scan type	-	E scan over small range
Integration time per acquisition point	0.1 s	-
Sampling time	2.42 s	-
Mass window	-	150%

Table 1: Operation conditions of the ICP-MS's

Two different columns were used in our measurements. The Dionex IonPac CS5A 4 mm ID and 250 mm length analytical column with IonPac CG5A 4 mm ID guard column was used in the IC-ICP-QMS system. The CS5A can be operated at flow rates up to 2.0 mL/min, but in all our experiments the recommended flow rate 1.2 mL/min was used. Zorbax 300SCX (Agilent Technologies) 4.6 mm ID and 150 mm length cation exchange column with 4.6 mm ID and 12.5 length guard column were used in the HPLC-ICP-HRMS system. 1.0 mL/min eluent flow was used in this system.

A high purity germanium detector (HPGe) GC1020 (relative efficiency of 30%) with Genie2000 (v3.0, 2004, Canberra Industries) gamma spectroscopy analysis software was used to acquire and analyze gamma spectra.

2.2 Reagents and Solutions

Ultrapure water for rinsing and dilutions was produced by reverse osmosis of distilled water followed by deionization NanoPure (Barnstead, USA) to yield 17.8 MΩ cm resistivity reagent. All plastic labware were cleaned by immersion in 10% (v/v) HNO_3 (Suprapur, Merck) for at least 24 h and thoroughly rinsed with deionized water afterwards.

Eluent was prepared by dissolution of the oxalic acid dihydrate (Suprapur®, Merck) in freshly deionized water and adjusted to the desired pH with 25% ammonia (Suprapur®, Merck). The same procedure was followed in preparation of L(+)-tartaric acid (analytical grade, Merck) as well as citric acid (analytical grade, Merck) eluents.

Working standard solutions of Cs, Sr, and Ba were prepared just before use by mixing and after stepwise dilution of a 1000 mg L^{-1} stock standard solutions (ICP Standard Certipur®, Merck, respectively $RbNO_3$, $CsNO_3$, $Sr(NO_3)_2$ and $Ba(NO_3)_2$ in Suprapur® HNO_3 2-3% Merck). The Agilent Multi-element calibration standard (10 mg/L element concentration in 5% high purity grade HNO_3 solution) was used for detection of retention time of Ni, Co, Mn, and Cu.

3. Results and discussion

Before the measurements both columns were preconditioned with the appropriate solutions. Dionex IonPac CS5A column was washed with 200 mL of 0.5 mol/L (~3%) HNO_3 solution and with a small volume of deionized water. To clean strongly retained materials from the Zorbax 300SCX, the column was flushed with 100 mL of 1 mol/L $NaClO_4$ (flow rate 1.0 mL/min) and then with 20 mL of water. After that both columns equilibrated with eluent before resuming normal operation. After each sample measurement the columns were washed with the eluent ensuring removal of the interfered elements such as barium, cobalt, and copper. Before the chromatographic measurements both ICP-MS were tested directly with prepared standards solutions.

The main aim of our study was to create a chromatographic method for detection of long life alkali, alkaline earth and 3d transition metal radionuclides by IC-ICP-MS system. We have begun determination of the chromatographic conditions from selection of the proper eluent. Three eluents were prepared using citric, tartaric and oxalic acids. pH of all eluents was standardized by adding NH_4OH. The chromatograms of 10 μL injection of 100 ppb standard of Cs, Sr, and Ba using IonPac CS5A column when the mobile phases were: (a) - oxalic acid, (b) - citric acid, and (c) - tartaric acid, are presented in Figure 1. As it can be seen, the retention times of Cs are practically independent of the nature of acid. Meanwhile, the eluent composition has a significant influence for Sr and Ba retention times (Ba ion retention time in oxalic and tartaric acids eluents was over 15 minutes). This effect can be explained by the fact that alkali metals and carboxylic acids do not form stable complexes, therefore Cs retention times are independent of the nature of acid. The data show that the shortest retention times of Sr and Ba are when the mobile phase consists of citric acid. It is related to the formation of citrate complexes of strontium and barium in the mobile phase. Retention time observed in oxalic eluent is comparable with that of Sr and Ba in tartaric acid eluent. A small difference is likely due to the slightly different stability of oxalate and tartarate complexes and different acidity constants of these acids. As the IonPac CS5A column manufacturer recommends the oxalic acid solution as the main eluent, the further research was carried out with oxalate mobile phase.

A similar experiment was performed with 3d metal ions. In figure 2 there are presented the chromatograms of 30 μL injection of 10 ppb standard of Mn, Co, Ni, and Cu using Zorbax 300SCX column when the mobile phases were: (a) - oxalic acid, (b) - citric acid, and (c) - tartaric acid. In this case, one can observe that the best separation of elements took place in tartaric acid solution. This result can most probably be explained by the specific complexing ability of tartaric ions. As the tartrate is a weakly complexing anion, therefore, only part of a metal ion are converted to a complexed form, which has a lower positive charge than the free metal ion. Meanwhile oxalate and citrate has a slightly stronger complexing property therefore, is difficult to separated different metal ions from each other. For these reasons in the further research we have used eluent of tartaric acid.

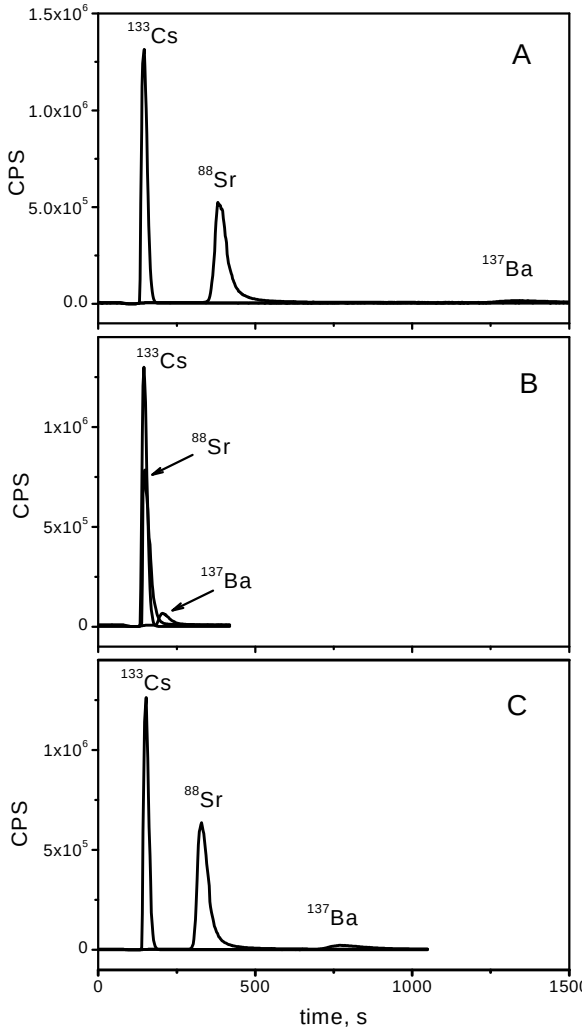

Figure 1: Chromatograms of ^{88}Sr, ^{133}Cs, and ^{137}Ba recorded using 0.1 mol/L concentrations of 3 eluents (pH=6.8): (a) oxalic acid, (b) citric acid, and (c) tartaric acid. 10 μL injection of 100 ppb standard Sr, Cs, and Ba solution.

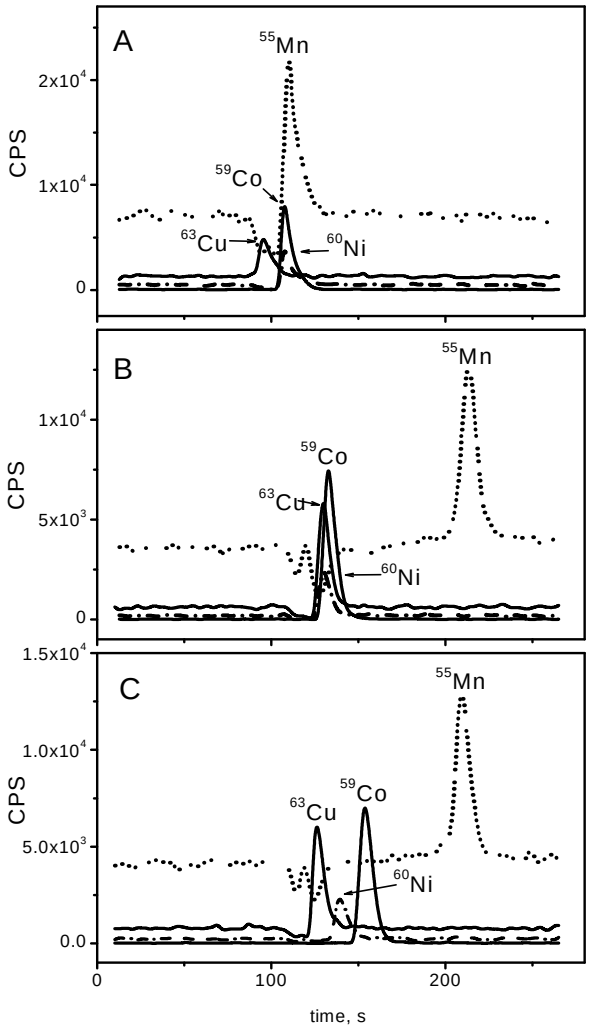

Figure 2: Chromatograms of ^{55}Mn, ^{59}Co, ^{60}Ni, and ^{63}Cu recorded using 0.1 mol/L concentrations of 3 eluents (pH=4.0): (a) oxalic acid, (b) citric acid, and (c) tartaric acid. 30 μL injection of 10 ppb standard Mn, Co, Ni, and Cu solution.

While optimizing the chromatographic conditions it was noticed that retention times of ions were dependent on concentration and pH of the mobile phase. To verify influence of mobile phase concentration on the retention times of Cs, Sr, and Ba using column Zorbax SCX300 three oxalic acid eluents with concentration of 0.05, 0.1 and 0.2 mol/L were made. pH of these eluents was standardized to 5.0. As expected, the retention times decreases with increase of eluents concentration. The slopes of linear tendencies for Cs, Sr, and Ba are respectively 468, 1816 and 3731

$s \cdot L \cdot mol^{-1}$. Similar experiments were conducted with the aim of evaluating the effect of pH. Retention times were determined using 0.1 mol/L oxalic acid solutions with pH 2.0, 4.0, and 5.5. It has been observed that with increase of pH of the mobile phase, retention times of all ions become shorter. The slopes of these tendencies for Cs, Sr, and Ba are respectively 18, 206, and 568 $s \cdot pH^{-1}$.

Based on the results of these experiments it was decided that the optimal eluent for detection of Cs and Sr isotopes by using IC-ICP-MS system are 0.1 mol/L oxalic acid at pH 4.5 – 5.0. As it can be seen in figure 3, the total time of chromatographic measurement can reach ~30 minutes, i.e. until Ba ions elute from the column. When required, the total time of analysis can be reduced by significantly increasing the pH of eluent.

With the aim of optimizing the chromatographic condition for detection of 3d metals, six eluents of tartaric acid were made: 1) three solutions of different concentration, but with the same pH, i.e. 0.025, 0.05, 0.1 mol/L and pH 4.5; 2) three solutions of different pH, but equal concentration, i.e. pH 4.0, 4.5, 5.0 and 0.05 mol/L. Based on the obtained data, it was observed that retention times of Mn, Co, Ni, and Cu increase along with decreasing of either concentration and/or pH of an eluent. This result can be explained as a weaker metals' complexation in a solution with low concentration of tartarate ions and low pH. The slopes of function of the retention times from concentration for Mn, Co, Ni, and Cu are respectively 3660, 5294, 3288, and 505 $s \cdot L \cdot mol^{-1}$. In case of pH changes, the slopes are 235, 110, 68, and 16 s per one pH unit respectively. As it can be seen, the tendencies of retention times' changes are stronger with concentration variation rather than with the variation of pH. The best separation of Ni from Co and Cu is typically obtained when mobile phase is 0.05 mol/L and pH 4.5 solution of tartaric acid neutralized with NH_4OH. Figure 4 shows the chromatograms of ^{55}Mn, ^{59}Co, ^{60}Ni, and ^{63}Cu. It can be seen that the total time of analysis when using of Zorbax SCX300 is approximately 10 min. and its limited by the retention time of manganese.

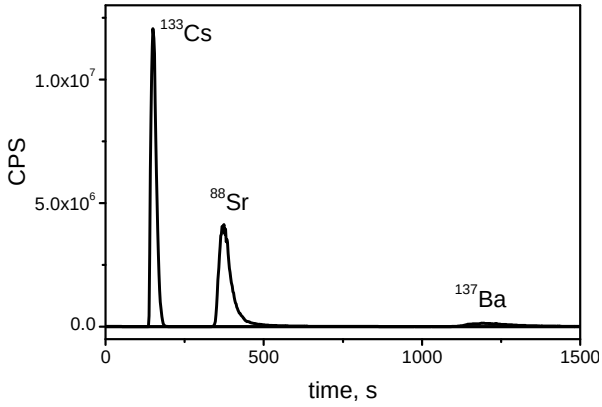

Figure 3: Chromatograms of ^{88}Sr, ^{133}Cs, and ^{137}Ba in a mobile phase containing 0.1 mol/L oxalic acid at pH 4.5 and isocratic flow rate of 1 mL/min; 1 mL injection of 10 ppb standard solutions.

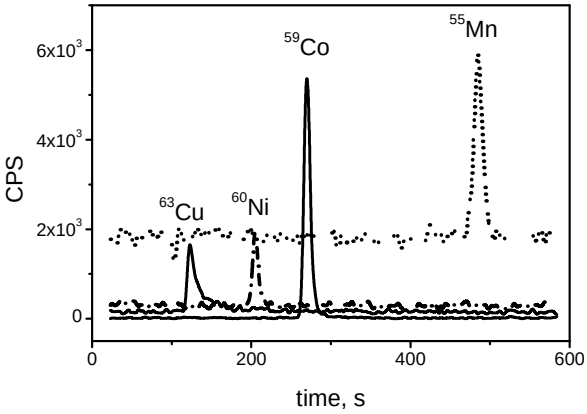

Figure 4: Chromatograms of ^{55}Mn, ^{59}Co, ^{60}Ni, and ^{63}Cu in a mobile phase containing 0.05 mol/L tartaric acid at pH 4.07 and isocratic flow rate of 1 mL/min; 30 μL injection of 100 ppb standard solutions.

Using these optimized conditions the main analytical characteristics, such as linear range of the calibration curve, slope (sensitivity of measurement system), relative standard deviation (RSD) of the mean value under the repeatability conditions, the limit of detection (LOD) and the limit of quantification (LOQ) were determined [8]. The slopes of the calibration curves of ^{88}Sr and ^{133}Cs were $2.25 \cdot 10^7$ cps/ppb $\pm$ 6.7 % and $2.60 \cdot 10^7$ cps/ppb $\pm$ 8.0% respectively. To verify the developed method, measurement of real sample was carried out. The sample was taken from the spent nuclear fuel storage. Since the sample matrix was deionized water, it was not necessary to treat it additionally. The chromatograms of Cs, Sr, and Ba isotopes were recorded using the IonPac CS5A column. The measurement was carried out in isocratic conditions using 0.1 mol/L oxalic acid eluent neutralized to pH 4.8 (NH_4OH). In Figure 5, it can be noticed that ^{134}Cs, ^{135}Cs, and ^{137}Cs radionuclides are separated from the isobaric masses, i.e. from ^{134}Ba, ^{135}Ba, and ^{137}Ba. Referring to the previously described calibration, the concentrations of ^{134}Cs, ^{135}Cs, and ^{137}Cs have been determined. Also traces of ^{90}Sr

can be qualitatively observed in the sample. However, quantity of ^{90}Sr is smaller than its LOQ (0.047 ppb). The calculated activities of ^{134}Cs, ^{135}Cs, and ^{137}Cs are given in the Table 2. A very slight difference was seen between the experimental results obtained from ICP-MS compared with the γ-spectroscopy measurements. The authors of the source [9] also provide the data that ratio ^{134}Cs /^{137}Cs from γ-spectroscopy is a little bit higher than when measured by HPLC-ICP-MS.

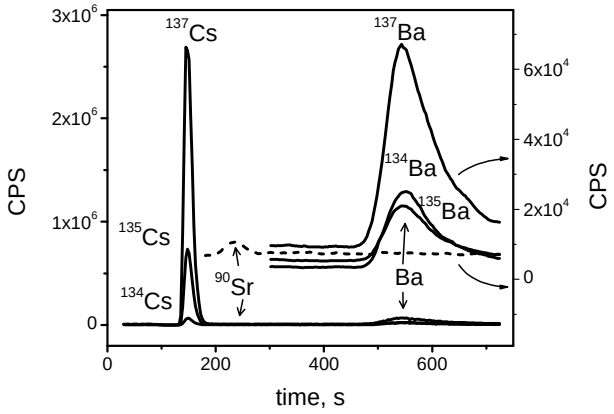

Figure 5: Chromatograms of Sr, Cs, and Ba isotopes in the sample from the spent nuclear fuel storage; eluent 0.1 mol/L oxalic acid pH 4.8, 1 mL injection.

	Activity ± SD, MBq/kg	
	IC-ICP-QMS measurements	γ-spectroscopy measurements
^{134}Cs	5.33 ± 0.11	7.25 ± 0.27
^{135}Cs	(5.69 ± 0.12) × 10^{-5}	n.a.
^{137}Cs	16.4 ± 0.35	20.0 ± 0.70

Table 2: Activity of cesium radionuclides in the sample from the spent nuclear fuel storage.

4. Conclusion

It has been demonstrated that IC-ICP-MS system can be exploited for simultaneous determination of alkali and alkaline earth radioactive nuclides. The chromatographic method developed was able to separate ^{134}Cs, ^{135}Cs, ^{137}Cs from all interfering barium isotopes. In one run ^{90}Sr also can be detected. It has been found that the most suitable eluent is oxalic acid solution neutralized by adding NH_4OH. The optimum concentration of oxalic acid is 0.1 mol/L, when the eluent pH is 4.5-5.5.

In the second part of this research, it has been shown there is a possibility to adapt the same chromatographic columns for separation of 3d metals. It was found that the best eluent to achieve this aim is the 0.05 mol/L solution of tartaric acid neutralized by adding NH_4OH to pH 4 – 4.5. In such case separation of ^{59}Ni and ^{63}Ni from interfering isotopes of cobalt and copper can be executed.

5. Acknowledgements

The authors would like to acknowledge the company LOKMIS, which partially supported the study under its own project *Nuclear Waste Characterization Research*. Furthermore, the authors would like to acknowledge Ignalina NPP for the opportunity to measure actual samples in general and, personally, Aleksandr Oryshaka, head of Radioactive Waste Management Department for his help and support.

6. References

[1] International Atomic Energy Agency. *Determination and use of scaling factors for waste characterization in nuclear power plants*. Vienna, 2009

[2] United States Nuclear Regulatory Commission. *Radionuclide Characterization of Reactor Decommissioning Waste and Neutron-Activated Metals*. Rep. NUREG/CR-5894, NRC, Washington DC 1993

[3] Hou, Xiaolin; Frøsig Østergaard, L.; Nielsen, S.P. *Determination of ^{63}Ni and ^{55}Fe in nuclear waste samples using radiochemical separation and liquid scintillation counting*. Analytica Chimica Acta, 2005**,** 535, 297-307

[4] Chang Heon Lee, Myung Ho Lee, Sun Ho Han, Yeoung-Keong Ha, Kyuseok-Song. *Systematic radiochemical separation for the determination of ^{99}Tc, ^{90}Sr, ^{94}Nb, ^{55}Fe and ^{59,63}Ni in low and intermediate radioactive waste samples*. J.Radioanal.Nucl.Chem., 2011, 288, 319-325.

[5] Taddei, M. H. T.; Macacini, J. F.; Vicente, R.; Marumo, J. T.; Sakata, S. K.; Terremoto, L. A. A.. *Determination of Ni-63 and Ni-59 in spent ion-exchange resin and activated charcoal from the IEA-R1 nuclear research reactor.* App. Rad. and Iso., 2013, 77, 50-55

[6] Barrero Moreno, J.M.; Betti, M.; Nicolaou, G. Determination of caesium and its isotopic composition in nuclear samples using isotope dilution-ion chromatography-inductively coupled plasma mass spectrometry. *J. Anal. At .Spectrom.,* 1999*, 14,* 875-879

[7] H.Geckeis, D.Hentschel, D.Jensen, A.Gortzen, N.Kerner. *Determination of Fe-55 and Ni-63 using semi-preparative ion chromatography a feasibility study*. Fresenius.J.Anal.Chem., 1997, 357,864-869

[8] D. Plausinaitis, E. Naujalis, A. Prokopchik, A. Budreika. *Method for Detection of Cs and Sr Isotopes Avoiding Interferences of Ba and Rb in Radioactive Samples using Ion Chromatography Coupled with ICP-MS*. Current Analytical Chemistry, 2014, 10, 140-148

[9] Caruso, S.; Guenther-Leopold, I.; Murphy, M. F.; Jatuff, F.; Chawla, R. *Comparison of optimized germanium gamma spectrometry and multicollector inductively coupled plasma mass spectrometry for the determination of ^{134}Cs, ^{137}Cs and ^{154}Eu single ratios in highly burnt UO_2*. Nucl. Instr. Meth. Phys. Res. A, 2008, 589, 425-435

An Efficient and Sensitive Optical Sensor based on Furosemide as a New Fluoroionophore for Determination of Uranyl ion

O. A. Elhefnawy, A. A. Elabd

Nuclear Safeguards and Physical protection Department,

Nuclear and Radiological Regulatory Authority, Cairo, Egypt

E-mail: oliveaeaea@yahoo.com, a.a.elabd@gmail.com

Abstract

A new, simple and sensitive optical sensor for determination of uranyl ion (UO_2^{2+}) in aqueous solutions by spectrofluorimetric technique was introduced. The fluorescence spectra and response characteristics of 4-chloro-2 (furan-2-ylmethylamino) - 5-sulfamoylbenzoic acid (Furosemide) to UO_2^{2+} was investigated. It showed preferable fluorescence response to UO_2^{2+}. Thereby, an efficient and sensitive optical sensor based on the fluorescence enhancement of Furosemide as a new fluoroionophore for UO_2^{2+} determination at low concentration levels has been developed. The reaction was extremely rapid at room temperature, and the fluorescence intensity remains unchanged for at least 24 h. Also, the response mechanism of the present sensor is discussed. This optical sensor is useful owing to the sufficient capability for determination of UO_2^{2+} in various real samples. Apart from the high sensitivity, the procedure is very simple, fast, wider linear range and gains a low detection limit without any complicated equipment. The present sensor has been successfully tested for determination of UO_2^{2+} in real samples and the results obtained are comparable to inductively coupled plasma optical emission spectrometry measured which could be used as a promising tool in nuclear safeguards material accountability measurements.

Keywords: Furosemide; Optical sensor; UO_2^{2+}; Fluorescence; enhancement.

1. Introduction

Uranium is an important element in a view of nuclear safeguards due to its wide applications in many nuclear industries such as mining, nuclear fuel preparation and waste management. Uranium found in nature in the earth crust as a uranium ore [1]. The most interesting species of uranium is uranyl ions (UO_2^{2+}) because it is the most widespread in nature. It can be found in low-pH water runoff, soil, around nuclear waste sites and processing facilities [2]. There are many different methods used for UO_2^{2+} determination in all stages of nuclear industry such as spectrophotometry, inductively coupled plasma-mass spectrometry, inductively coupled plasma optical emission spectrometry, atomic fluorescence spectrometry, gamma spectrometry, fluorimetry, potentiometry, colorimetric, voltammetric, x-ray fluorescence, ion chromatography, neutron activation analysis and alpha spectrometry have been used [3-15]. Although, these methods have a high sensitivity and favorable detection limits, but some of them require expensive equipment. Moreover, utilizing from some methods needs preliminary separation steps, such as solid phase extraction and ion-exchange procedures for sample preparation. Also, some of these procedures include using of large volumes of organic solvents and acids resulting of large volumes of waste [16-18].

Optical sensors have been used for UO_2^{2+} determination, because of their advantages such as high sensitivity, good selectivity and low cost.

Depending on simple instrumentation, they are simpler and lower cost to be used than any other analytical method available, also enabling final products with high homogeneity and purity [19]. Development of optical sensor has been mostly based on the immobilization of a reagent in/on the membranes by either physical method such as adsorption, encapsulation, sol–gel, etc. or chemical covalent bond methods like formation of stable complexes. Optical sensors are used based on different analytical techniques such as absorbance, fluorescence, or reflectance measurements [20, 21]. Up to date the studies on the using of fluorescence optical sensors for UO_2^{2+} determinations in aqueous solution remain rare [22]. Therefore, we insist to pay more attention to a new, simple, stable and sensitive fluorescence optical sensor for UO_2^{2+} determination in aqueous solutions. Due to the radius of actinide ions (from Ac^{3+} to Cf^{4+} with the range of 1.12 – 0.82 Á, respectively), these elements have different properties such as charge densities, size and hydration energy. Thus, by using 4-chloro-2 (furan-2-ylmethylamino) - 5-sulfamoylbenzoic acid (Furosemide) as a new fluoroionophore for determination of UO_2^{2+} which have an intermolecular cavity and relatively high flexibility, it is possible to construct a sensitive actinide ion sensor. The existence of donating nitrogen and oxygen atoms in Furosemide structure which causes a semi or intermolecular cavity and forms a template complex with UO_2^{2+} and considering the charge density and the size of UO_2^{2+}, expect that Furosemide can form sensitive complex with UO_2^{2+}. Thus, fluorescence study of the complexation in aqueous solution was carried out as a primary test. In the present work, a new, stable and sensitive optical sensor by fluorescence technique for determination of UO_2^{2+} in aqueous solutions was introduced.

2. Experimental

2.1. Materials and reagents

All chemicals were of analytical grade was used without further purification throughout the experiments. Uranyl nitrate hexahydrate, $UO_2(NO_3)_2{\cdot}6H_2O$ was manufactured by Mallinckrodt Company. 4-chloro-2 (furan-2-ylmethylamino) - 5-sulfamoylbenzoic acid (Furosemide) from National Authority for Control and Pharmaceutical Research, High molecular weight poly (vinyl chloride) (PVC), dioctyl adipate (DOA), dioctyl sebacate (DOS), tributylphosphate (TBP), dibutylphthalate (DBP), ortho-nitrophenyl octyl ether (o-NPOE), sodium tetraphenylborate (NaTPB), tetrahydrofurane (THF), 1,2-cyclohexylene dinitrilotetraacetic acid (CyDTA), all from Sigma–Aldrich (Saint Louis, USA) or Fluka (Buchs, Switzerland) chemical companies.. All other solvents and salts used in this work were purchased from Alpha Company. Standard stock solutions (1.0×10^{-3} mol L^{-1}) of UO_2^{2+} and Furosemide were prepared by dissolving appropriate amounts of $UO_2(NO_3)_2{\cdot}6H_2O$ and Furosemide in deionized water, respectively.

2.2. Instruments

All fluorescence measurements were recorded with a Meslo- PN (222-263000) Thermo Scientific Lumina fluorescence Spectrometer in the range (190 – 900 nm), USA. Inductively Coupled Plasma Optical Emission Spectrometry (ICP-OES), an iCAP 6500 ICP-OES from Thermo Fisher Scientific, UK, with ITEVA operating software for full control of all instrument functions and data handling, was used for determination of UO_2^{2+} and interfering ions concentration as a reference measured. The experimental work was carried out at safeguards analytical laboratory (ETZ-, KMP-I), Egyptian Nuclear and Radiological Regulatory Authority (ENRRA).

2.3. Membrane preparation

The membrane was prepared by dissolving 32.0 mg of PVC, 58.0 mg of o-NPOE, 8.0 mg of Furosemide and 2.0 mg NaTPB in 1.0 mL THF. The solution was immediately shaken vigorously to achieve complete homogeneity. A quartz plate was cleaned with pure THF to remove any organic impurities and then placed in the spin-on device. Ninety microliter of the above solution was injected to the quartz plate. After 30 s spinning, at rotation frequency of 600 rpm, the membrane was located in ambient air and allowed to dry in air.

2.4. The fluorescence measurement of UO_2^{2+}

To determine the concentration of UO_2^{2+}, the sensing membrane was placed in a 1.0 cm quartz cell filled with 3 mL of the test solution containing CyDTA (as masking agent) [23] and different concentration of UO_2^{2+} at pH 5.5. After 5 min the fluorescence emission intensity was measured at λ_{ex} / λ_{em} = 320 / 522 (nm). The fluorescence emission intensity linear range of the optical sensor is detected between $7.0x10^{-7}$ - $4.0x10^{-6}$ mol $L^{-1}$of UO_2^{2+} concentrations. By plotting the calibration curve of the fluorescence

emission intensity on the y axis versus the UO_2^{2+} concentration on the x axis, the unknown UO_2^{2+} concentration can be read from the calibration curve.

2.5. ICP-OES measurement

An aliquot of an ICP standard solution of uranium (1000 mg L^{-1}) containing is used in the preparation of calibration solutions. Working standard solutions are prepared by dilution of the stock standard solutions to desired concentration. The ranges of the calibration curves (5 points) were selected to match the expected concentrations (0 – 1 mg L^{-1}) for samples measured by ICP-OES. The correlation coefficient R^2 obtained for all cases was 0.999. In addition, U concentrations calculated from emission intensities measured at two wavelengths as follows: U(385.958{87}) and U(409.014{82}) confirmed that each dataset is consistent in itself. To ensure the accuracy of U concentration, certified reference material was analyzed in regular intervals during the measurement sequence. While no perfectly matrix-matched reference materials are available.

3. Results and discussion

3.1. Preliminary investigations

Furosemide can exhibit fluorescence emission band owing to the conjugated double bond system and the mobility of its π - electrons. It was observed that by optimized fabricating a sensor from immobilization of Furosemide and NaTPB in a plasticized PVC membrane containing o-NPOE, the determination of UO_2^{2+} could be practicable spectrofluoreometric technique. When UO_2^{2+} diffused into the membrane, it formed a complex with Furosemide. Fig. 1 shows the fluorescence emission spectra of Furosemide membrane and in different concentrations of UO_2^{2+}. As seen, the membrane spectrum without UO_2^{2+} has no fluorescence emission band at λ_{ex} / λ_{em} = 320 / 522 (nm). Upon addition of increasing amount of UO_2^{2+} to membrane, it subsequently reacts with excited state of UO_2^{2+} to generate a fluorescent product. Furthermore, with the proper selection of excitation wavelength at 320 nm, this reaction is selective for UO_2^{2+} over other common interferences. The fluorescence emission intensity of Furosemide membrane is linearity enhanced with the increase amount of UO_2^{2+}, which demonstrates that the chelating reaction of Furosemide membrane with UO_2^{2+} can be used to establish a fluorescent optical sensor for determination of UO_2^{2+}.

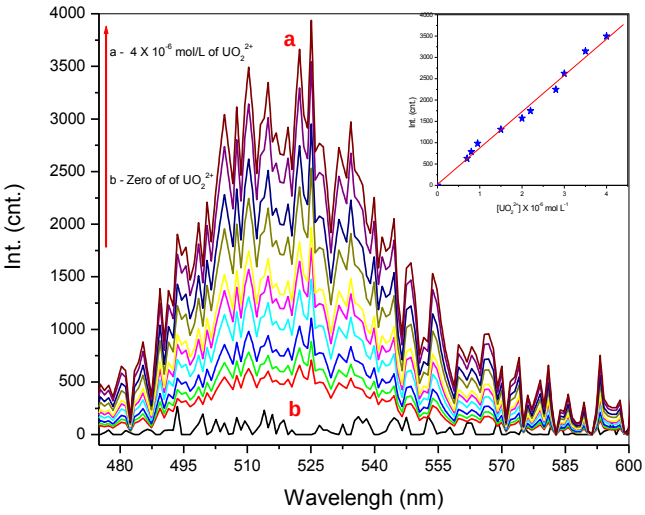

Figure 1. Fluorescence spectra of the present sensor upon increasing amount of UO_2^{2+} concentrations: (a) 4.0X10^{-6} mol L^{-1} of UO_2^{2+} ions, (b) Zero of UO_2^{2+}; conditions: pH 5.5; T=25 ◦C; response time= 5 min; membrane layer contained 32.0 mg of PVC, 58.0mg o-NPOE, 2.0mg NaTPB and 8.0 mg Furosemide (inset (the fluorescence emission intensity of UO_2^{2+} at λ_{ex} / λ_{em} = 320 / 522 (nm) by the present sensor versus the concentration of UO_2^{2+})).

3.2. Mechanism

The enhancement of the fluorescence emission intensity was occurred upon addition of the UO_2^{2+} to the optical sensor. The optimized experimental conditions revealed that the formation of the complex between UO_2^{2+} and Furosemide is 1:1 molar ratios. The mechanism of the binding of the present sensor to the UO_2^{2+} can be explained by a diffusion of UO_2^{2+} through the sensor layer. Once the UO_2^{2+} existed on the surface of the sensor, it reacts with one molecule of Furosemide through a highly electronegativity site (hydroxyl group, -0.22) and (amine group, -0.12) releasing protons and forming complex. By addition of 0.01M HCl, this increasing the concentration of protons in the sensor, reprotonates the sensor and releasing the UO_2^{2+} into the medium, as shown in Fig. 2.

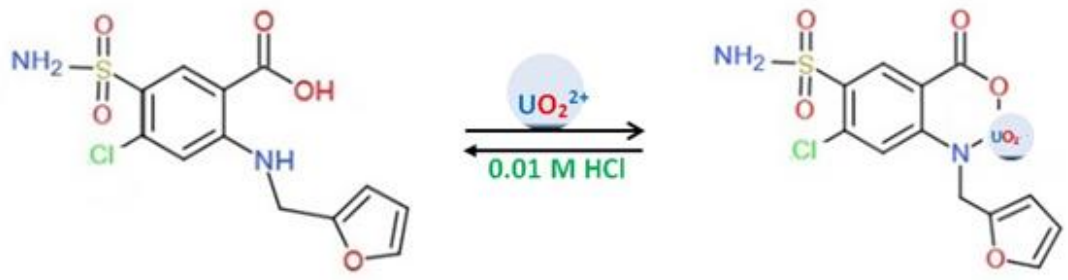

Figure 2. The proposed mechanism of the reaction between Furosemide and UO_2^{2+}

3.3. Optimization of the method

To take full advantages of the sensor, amounts of the sensor ingredients and reaction conditions should be optimized.

3.3.1. Effect of membrane composition

The response characteristics and working concentration range of each optical sensor depends significantly on the different ingredients such as base matrix, solvent mediator, fluoroionophore and the necessary additive used in the membrane structure. Therefore the sensor matrix should be selected. It was observed that high molecular weight PVC could be used as the membrane base. This selection was due to several parameters such as appropriate transmittance, suitable immobilization of Furosemide as a fluoroionophore without any leakage, good mechanical stability and reliable permeability to UO_2^{2+}.

In order to have a homogenous organic phase, solvent mediators (plasticizer) must be physically compatible with the polymer used in membrane preparation. In this work, several solvents such as DOA, DOS, TBP, DBP and o-NPOE were tested as potential plasticizers. As shown in Fig. 2 plasticizers of DOS and DOA showed good sensitivity but membranes containing these plasticizers showed leakage of the reagent. The membranes containing TBP and DBP were showed low sensitivity. The membrane containing o-NPOE was the appropriate selection with respect to high sensitivity and minimum leakage of Furosemide from the membrane

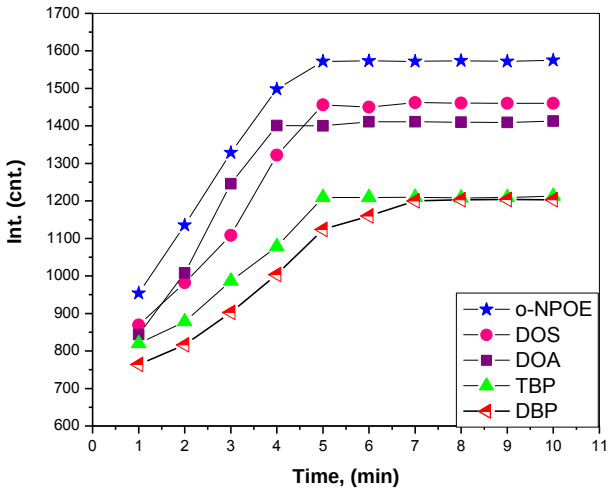

Figure 3. Effect of plasticizer nature on the response of the membrane, conditions: pH 5.5; T=25◦ C; response time= 5 min; membrane layer contained 32.0 mg of PVC, 58.0 mg o-NPOE, 2.0 mg NaTPB and 8.0 mg Furosemide.

As listed in Table 1, the membrane sensors with 32.0 mg of PVC and 58.0 mg of o-NPOE were provided better fluorescence emission intensity. Thus, it was selected as optimal amount in the membrane composition. In the present sensor, Furosemide acts as a fluoroionophore. Therefore, it is necessary to optimize its amount in the membrane composition. Due to the complete mass transfer of UO_2^{2+} into the membrane and also decreasing of the response time, the presence of an anionic additive such as NaTPB facilitates the ion-exchange equilibrium. As listed in Table 1, the presence of NaTPB caused to increasing of the sensor responses and reagent leakages from the all membranes. It is obvious that the membrane containing o-NPOE was the suitable selection in order to the maximum response and also minimum leakage of

Furosemide from the membrane. The amount of NaTPB was investigated in the range of 1.0–4.0 mg as listed in Table 1. It is obvious that the highest fluorescence emission intensity is recorded by using 2.0 mg of NaTPB. But at lower amounts of NaTPB the fluorescence emission intensity decrease, this is due to the less of UO_2^{2+} mass transfer, also at higher quantities of NaTPB the leakage of Furosemide caused a decreasing in fluorescence emission intensity. Therefore, 2.0 mg NaTPB was selected as an optimal amount in the membrane composition. Effect of different amounts of Furosemide on the membrane response is listed in Table 1. As resulted, the fluorescence emission intensity increased by increasing the amounts of Furosemide up to 8.0 mg and decreased at higher amounts that were resulted from membrane leakages. Therefore, 8.0 mg Furosemide was selected as an optimum value.

NO.	PVC (mg)	o-NPOE (mg)	NaTPB (mg)	Furosemide (mg)	Fluorescence at λ_{ex} / λ_{em} = 320 / 522 (nm)
1	28	62	2	6	1487
2	30	60	2	6	1510
3	32	58	2	6	1546
4	32	58	1	6	1501
5	32	58	3	6	1538
6	32	58	4	6	1533
7	32	58	2	4	1497
8	32	58	2	8	1572
9	32	58	2	10	1554

Table 1: Effect of membrane composition on the fluorescence emission intensity of the present sensor for the determination of (2.0×10^{-6} mol L^{-1}) UO_2^{2+}

3.3.2. Effect of pH

The complex formation between heavy metal ions and most of ligands is depending on the pH of the solution because of the protonation (or deprotonation) of ligand at various pH. The fluorescence emission intensity was measured at λ_{ex} / λ_{em} = 320 / 522 (nm) for 2.0×10^{-6} mol L^{-1} UO_2^{2+} at various pH values. The pH values were adjusted by the addition of dilute NaOH or HCl solution. The best response was obtained at about pH 5.5. At pH values more than 5.5, the response decreases. This could be due to the hydrolysis of the UO_2^{2+} in aqueous solutions, which results in the formation of different insoluble hydroxide forms of UO_2^{2+} [24]. Thus, it was not possible to examine pH effects in alkaline solutions, as UO_2^{2+} precipitated in these media. The decrease in the response of the present sensor at low pH must be due to the competition of hydrogen ions and UO_2^{2+} for Furosemide.

3.3.3. Effect of time

The response time of the sensor is defined as the diffusion time of the metal ions from solution into the membrane (the slowest step in complexation process). The effect of this parameter on the present sensor response was investigated in the range of 1–10 min. The response time of the present sensor was of the order of 5 min for 98 % attainment of the final value for 2.0×10^{-6} mol L^{-1} UO_2^{2+} concentration. It was observed that the fluorescence emission intensity of the membrane remained constant for more than 24 h. which implies that the fluoroionophore is quite stable in a membrane contacting with water.

3.4. Method validation

3.4.1. Analytical characteristics

A linear correlation was found between fluorescence emission intensity of the present sensor at λ_{ex} / λ_{em} = 320 / 522 (nm) and concentration of UO_2^{2+} in the range of $7.0x10^{-7}$ - $4.0x10^{-6}$ mol L^{-1}. The calibration curve was obtained by plotting the peak intensity of ions at λ_{ex} / λ_{em} = 320 / 522 (nm) versus the concentration of UO_2^{2+} and the graph (Fig. 1 (inset)) was described by the regression equation:

$$Y = a + bX$$

where Y = fluorescence emission intensity of the present sensor at λ_{ex} / λ_{em} = 320 / 522 (nm); a = intercept; b = slope and X = concentration in mol mL^{-1}. The limit of detection (LOD) and quantification (LOQ) calculated according to ICH guidelines [25] using the formulae: LOD= 3.3 s/b and LOQ= 10 s/b (where s is the standard deviation of blank luminescence intensity values, and b is the slope of the calibration plot) are listed in Table 2.

Parameter	Values
λ_{ex}, nm	320
λ_{em}, nm	522
Linear range, mol L^{-1}	$7.0x10^{-7}$ - $4.0x10^{-6}$
Limit of detection (LOD), mol L^{-1}	$4.6x10^{-7}$
Limit of quantification (LOQ), mol L^{-1}	$1.4x10^{-6}$
Regression coefficient (R^2)	0.994

Table 2: Analytical characteristics of the present sensor with UO_2^{2+}

3.4.2. Regeneration of the sensor

The fluorescence emission intensity of the present sensor was not recovered completely when the solution was switched from high to low concentrations of UO_2^{2+}. To regenerate the present sensor already immersed in UO_2^{2+} solution, several reagents including HCl, HNO_3, H_2SO_4 and NaOH were tested. Among all of them, HCl (0.01 M) fully regenerated the present sensor after 10 min. It should be mentioned that after regeneration step, and for the next analysis, the present sensor must be placed in buffer (pH 5.5) for at least 5 min.

3.4.3. Selectivity

For the selectivity investigation, the interference of different inorganic cations on the response of the present sensor was examined using a 2.0×10^{-6} mol L^{-1} of UO_2^{2+} and variable concentrations of the interfering cations in pH 5.5 The tolerance limit was fixed as the maximum amount of an ion causing an error not greater than 5% in fluorescence emission intensity of the consequent solutions. The resulting tolerance limits are listed in Table 3. It should be noted that some observed interfering effects of Th^{4+}, Al^{3+}, Fe^{3+} and La^{3+} were considerably diminished in the presence of CyDTA as a proper masking agent [23]. As it is clear from Table 3, the UO_2^{2+} content of solutions can be selectively determined using the present sensor in the presence of excess amounts of the potential interferences examined. These results indicate that the present UO_2^{2+} optical sensor can be applied for determination of UO_2^{2+} in real samples and in the presence of excess of several other coexisting cations.

Foreign ions	Tolerance limit (mg L^{-1})	Foreign ions	Tolerance limit (mg L^{-1})
Ba^{2+}	50	Ni^{2+}	35
Ca^{2+}	45	Zn^{2+}	30
Cd^{2+}	35	Al^{3+}	10 [a]
Co^{2+}	25	Cr^{3}	35
Cu^{2+}	30	Fe^{3+}	5 [a]
Mg^{2+}	40	La^{3+}	5 [a]
Mn^{2+}	40	Th^{4+}	5 [a]

[a] After addition of CyDTA.

Table 3: Effect of foreign ions on the determination of 2.0×10^{-6} mol L^{-1} UO_2^{2+}

3.4.4. Application

To test the practical application of the present sensor, various real samples spiked with different amounts of UO_2^{2+} were analyzed and the concentration of UO_2^{2+} were measured by using the present sensor and RSD % are calculated and listed in Table 4. To further investigate the performance of the present sensor, we compared the results obtained above with ICP-OES technique as a reference measured. As listed in Table 4, mean values are obtained with Student's t- and F-tests at 95% confidence limits. The results showed comparable accuracy (t-test) and precision (F-value), since the calculated values are less than the theoretical values, which confirmed that there is no significant difference between the performance of the present sensor and a reference measured. The results obtained are denoted on applicability of the present sensor

for the determination of UO_2^{2+} in various real samples.

Sample	UO_2^{2+} Spiked [a]	Proposed measured (n = 3)				Reference measured (n = 3)	
		UO_2^{2+} Average measured [a] ± CL [b]	%RSD [c]	t-test [d]	f-test [d]	UO_2^{2+} Average measured [a] ± CL [b]	% RSD [c]
Tap water	10	10.4 ± 0.94	3.63	0.50	2.05	10.3 ± 0.65	2.57
	20	20.3 ± 0.62	1.24	0.36	1.58	20.2 ± 0.49	0.99
	40	40.5 ± 1.08	1.08	0.20	1.33	40.4 ± 0.94	0.94
Well water	10	10.5 ± 1.08	4.15	0.43	1.84	10.4 ± 0.79	3.10
	20	20.3 ± 0.76	1.50	0.29	1.47	20.3 ± 0.62	1.24
	40	40.6 ± 1.22	1.22	0.27	1.49	40.5 ± 1.00	1.00
Synthetic wastewater	10	10.6 ± 1.23	4.67	0.37	1.70	10.4 ± 0.94	3.63
	20	20.4 ± 0.89	1.77	0.24	1.39	20.3 ± 0.76	1.50
	40	40.6 ± 1.29	1.28	0.17	1.27	40.5 ± 1.15	1.14

[a] The values are multiplied by 10^{-7} mol L^{-1} for measured.
[b] CL, confidence limits were calculated from: CL =±tS/(n)½. The tabulated value of t is 4.303, at the 95% confidence level; S = standard deviation and n = number of measurements, the values are multiplied by 10^{-7}.
[c] % RSD, relative standard deviation.
[d] Theoretical values of t- and f-tests at 95% confidence level are 4.303 and 19.0, respectively.

Table 4: The practical application of the present sensor for determination of UO_2^{2+} in various real samples

4. Conclusion

An efficient and sensitive optical sensor has been developed for the determination of UO_2^{2+} ions based on the fluorescence enhancement of Furosemide immobilized in a PVC based membrane. UO_2^{2+} can be determined by applying the optimum conditions which described in this study into the range of $7.0x10^{-7}$ to $4.0x10^{-6}$ mol L^{-1}. Also, the sensor showed short response time and higher selectivity to UO_2^{2+}. By the means of an easy and low-cost methodology, satisfactory experimental results were obtained for the determination of UO_2^{2+} by the present sensor.

References

[1] Biswasa S, Pathakb P, Roy S; *Development of an extractive spectrophotometric method for estimation of uranium in ore leach solutions using 2-ethylhexyl phosphonic acid-mono-2-ethylhexyl ester (PC88A) and tri-n-octyl phosphine oxide (TOPO) mixture as extractant and 2-(5-bromo-2-pyridylozo)-5-diethyl aminophenol (Br-PADAP) as chromophore*; Spectrochimica Acta Part A 91; 2012. 222– 227

[2] Nivens D, Zhang Y, Angel S; *Detection of uranyl ion via fluorescence quenching and photochemical oxidation of calcein*; Journal of Photochemistry and Photobiology A: Chemistry 152; 2002. 167–173

[3] Lutfullah A, Mohd N, Rahman N, Azmi S; *Optimized and validated spectrophotometric method for the determination of uranium(VI) via complexation with meloxicam*; Journal of Hazardous Materials; 155; 2008. 261–268

[4] Shariati S, Yamini Y, Zanjanim M; *Simultaneous preconcentration and determination of U(VI), Th(IV), Zr(IV) and Hf(IV) ions in aqueous samples using micelle-mediated extraction coupled to inductively coupled plasma-optical emission spectrometry;* Journal of Hazardous Materials 156; 2008. 583–590

[5] Tagami K, Uchida S; *Rapid uranium preconcentration and separation method from fresh water samples for total U and $^{235}U/^{238}U$ isotope ratio measurements by ICP-MS*; Analytica Chimica Acta 592; 2007. 101–105

[6] Rao T, Metilda P, Gladis J; *Preconcentration techniques for uranium(VI) and thorium(IV) prior to analytical determination—an overview;* Talanta 68; 2006. 1047–1064

[7] Nivens D, Zhang Y, Angel S; *Detection of uranyl ion via fluorescence quenching and photochemical oxidation of calcein;* J. Photochem. Photobiol. A: Chem. 152; 2002. 167–173

[8] Zheng Z, Kang M, Wang C, Liu C, Grambow B, Duro L, Suzuki-Muresan T; *Influence of gamma irradiation on uranium determination by Arsenazo III in the presence of Fe(II)/Fe(III);* Chemosphere 107; 2014. 373–378

[9] Anwar M, Mohammad D; *Potentiometric determination of free acidity and uranium in uranyl nitrate solutions;* J. Radioanal. Nucl. Chem. 134; 1989. 45–51

[10] Currah J, Beamish F; *Colorimetric determination of uranium with thiocyanate*; Anal. Chem. 19; 1947. 609–612

[11] McMahon A; *Application of analytical methods based on X-ray spectroscopy to the determination of radionuclides*; Sci. Total Environ. 130; 1993. 285–295

[12] Mlakar M, Branica M; *Stripping voltammetric determination of trace levels of uranium by synergic adsorption;* Anal. Chim. Acta 221; 1989. 279–287

[13] Haskins S, Kelly D, Weir R; *Comparison of neutron activation analysis with conventional detection techniques for the evaluation of trace elemental contamination in Mallard (Anas platyrhynchos) feathers;* Journal of Radioanalytical and Nuclear Chemistry 287; 2011. 471–478

[14] Wu M, Liao L, Zhao M, Lin M, Xiao X, Nie C; *Separation and determination of trace uranium using a double-receptor sandwich supramolecule method based on immobilized salophen and fluorescence labeled oligonucleotide;* Analytica Chimica Acta 729; 2012. 80– 84

[15] Dietz M, Horwitz P, Sajdak L, Chiarizia R; *An improved extraction chromatographic resin for the separation of uranium from acidic nitrate media;* Talanta 54; 2001. 1173–1184

[16] Moghimi A; *Solid phase extraction of thallium (III) on microcrystalline naphthalene modified with N,N-bis(3-methylsalicylidene)-orthophenylenediamine and determination by spectrophotometry*; Chin. J. Chem. 26; 2008. 1831–1836

[17] Elhefnawy O, Zidan W, Abo-Aly M, Bakier E, Elsayed G, *Synthesis and characterization of a new surface modified Amberlite-7HP resin by nano-iron oxide (Fe_3O_4) and its application for uranyl ions separation;* Journal of Radioanalytical and Nuclear Chemistry 299; 2014. 1821-1833

[18] Elabd A, Zidan W, Abo-aly M, Bakier E, Attia M; *Uranyl ions adsorption by novel metal hydroxides loaded Amberlite IR120*; Journal of Environmental Radioactivity 134; 2014. 99-108

[19] Ensafi A, Far A, Meghdadi S; *Highly selective optical-sensing film for lead(II) determination in water samples;* Journal of Hazardous Materials 172; 2009. 1069–1075

[20] Firooza A, Ensafib A, Hajyani Z; *A highly sensitive and selective bulk optode based on dithiacyclooctadecane derivative incorporating chromoionophore V for determination of ultra trace amount of Hg(II);* Sensors and Actuators B 177; 2013. 710– 716

[21] Maji S, Viswanathan K; *Sensitization of uranium fluorescence using 2,6-pyridinedicarboxylic acid: Application for the determination of uranium in the presence of lanthanides;* Journal of Luminescence 129; 2009. 1242–1248

[22] Vaughan A, Narayanaswamy R; *Optical fiber reflectance sensors for the detection of heavy metal ions based on immobilized Br-PADAP*; Sens. Actuators B 51; 1998. 368–376

[23]Cheng K; *Determination of traces of uranium with 1-(2-pyridylazo)-2- naphtol;* Anal. Chem. 30; 1958. 1027–1030

[24] Niboua D, Khemaissiab S, Amokranea S, Barkatb M, Chegroucheb S, Mellah, A; *Removal of UO_2^{2+} onto synthetic NaA zeolite. Characterization, equilibrium and kinetic studies;* J. Chem. Eng. 172; 2011. 296– 305

[25] *International Conference on Hormonisation of Technical Requirements for Registration of Pharmaceuticals for Human Use*; ICH Harmonised Tripartite Guideline; Validation of Analytical Procedures: Text and Methodology Q2(R1); incorporated in November 2005.

Image analysis methods for partial defect detection using tomographic images on nuclear fuel assemblies

Anna Davour, Staffan Jacobsson Svärd, Sophie Grape

Division of Applied Nuclear Physics
Department of Physics and astronomy, Uppsala University
Box 516, SE-75120 Uppsala, Sweden
E-mail: anna.davour@physics.uu.se

Abstract:

A promising non-destructive assay method for verification of irradiated nuclear fuel is gamma tomography, i.e. the use of measurements of the gamma radiation field around a nuclear fuel assembly to reconstruct detailed information about the internal source distribution.

Typically, tomographic reconstructions result in two-dimensional images of cross sections of the fuel. We demonstrate how such images can be searched for fuel rods using a template matching technique, which is a method commonly used in the field of image analysis. In this case, a template or mask corresponding to the size and shape of a fuel rod is translated across the image in order to find the region with the highest reconstructed activity, which is assumed to correspond to the location of a fuel rod in the image. This is done iteratively, allowing no overlap of the rods. By defining the threshold between background and fuel rod objects in the image, we can identify and count the fuel rods using no other assumptions than the rod radius.

Thus the rod identification procedure provides a possible means to verify whether all fuel rods are present, and it may also be implemented to identify the fuel type of the measured assembly. The procedure is robust in cases of irregularities, such as assembly bow or torsion, or the dislocation of individual fuel rods in the measured cross section.

Here we demonstrate fuel rod identification procedure, using authentic images collected with a tomographic measurement device on commercial fuel assemblies. The results show that image analysis can support tomographic partial defect verification of irradiated nuclear fuel assemblies, even on the single fuel rod level.

Keywords: image analysis; nuclear fuel; partial defect verification; nuclear safeguards; gamma emission tomography

1. Introduction

Digital image processing is an important technology with a wide variety of applications. A digital image is fundamentally a matrix of numbers – values that can be represented as colour. The image may be analysed with the help of computer algorithms. The human brain is exceptionally good at recognising certain types of pattern in images, but for many applications it is efficient to make use of automated pattern identification. We see this for example in the ubiquitous bar code scanners.

Here we will describe the use of image analysis for applications in nuclear safeguards, with special focus on non-destructive partial defect verification of used nuclear fuel assemblies using gamma emission tomography.

1.1. Image analysis for safeguards applications

Digital image processing has been used in various ways for nuclear safeguards applications. One example is the use for camera surveillance at nuclear facilities [1], another is the analysis of satellite images as a supporting technique for international treaty monitoring [2].

In our case the main focus is on verification of used nuclear fuel, in particular before deposition in underground storage which is difficult to access. A related application is the DCVD (Digital Cherenkov Viewing Device) [3][4], making use of the Cherenkov radiation emanating from used nuclear fuel in a storage pool. Image analysis techniques are implemented to reduce noise, and to improve measurement quality by centring the fuel within the image. The DCVD is approved by IAEA for gross defect verification as well as partial defect verification.

1.2. Tomography and image analysis in the UGET project

As part of the efforts to provide reliable tools for partial defect verification of used nuclear fuel, the IAEA has initiated the JNT 1955 project on Unattended Gamma-ray Emission Tomography, UGET.

Using the gamma radiation emanating from irradiated fuel, it is possible to reconstruct tomographic images of the source distribution within a nuclear fuel assembly. This is a powerful technique for non-destructive analysis of fuel, which can be enhanced by the use of digital image processing to extract quantitative information. The ongoing first phase of the UGET project is evaluating the feasibility of gamma emission tomography for attended and unattended partial defect testing, with the goal of presenting a design that could be constructed and tested if the project is continued in a phase 2.

Much of this work relies on experience from two previously operated gamma detection devices. Tomographic measurements on nuclear fuel were performed at the Forsmark NPP in 2002, using a test platform called PLUTO, which was constructed at Uppsala University [5]. Another device has been developed within the IAEA JNT 1510 project [6], and measurements using this device were performed at Olkiluoto in 2013 and Loviisa in 2014.

Both of these devices use detectors mounted in collimator packages which can be moved around the fuel assembly to perform measurements from different angles. In the JNT 1510 device, 208 semiconductor detectors are mounted in two opposite packages which are rotated around the fuel. In the case of PLUTO four scintillation detectors were used, within a collimator block that could be moved to different lateral as well as angular positions.

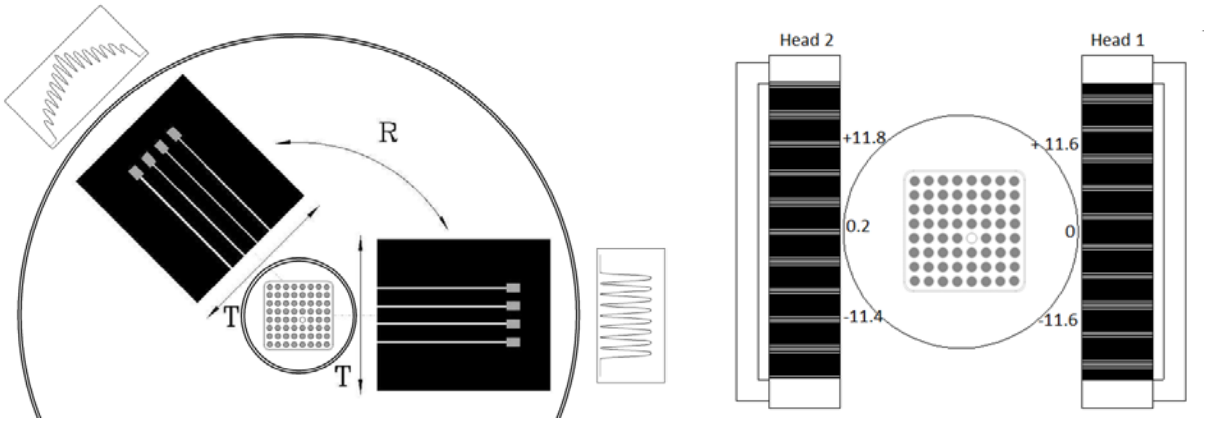

Figure 1: Schematic sketch of the PLUTO (left) and the more compact JNT 1510 devices (right), used for measurements of the gamma radiation field around used fuel assemblies. The images are not to scale (the relative size is indicated by the fuel at the centre). In PLUTO four BGO detectors are placed within one collimator package with 300 mm deep collimator slits, while the JNT 1510 makes use of 208 semiconductor detectors (CdZnTe) in two packages with a collimator slit depth of 100 mm..

2. Image analysis on SPECT images of nuclear fuel

The gamma emission measurements are taken as input to tomographic reconstructions, creating images of a two-dimensional cross section of the fuel. There are a variety of different tomographic algorithms, each with different strengths. Two types of reconstructions are the basis for the current work. One of them is a fast analytical method requiring minimal assumptions about geometry and the gamma attenuation within the fuel area [7], which is used to create the images used for image analysis. Another type of tomographic reconstruction method is based on an algebraic algorithm includes detailed modelling of the gamma attenuation within the fuel, returning the activity of each fuel rod. This method has previously been applied on measurements on irradiation commercial fuel assemblies, demonstrating that detailed information about the activity for each individual fuel rod can indeed be extracted from the measurements [8][9].

This second type of reconstruction requires taking into account accurate knowledge of the position of the fuel rods within the imaged area, and here image analysis can be used as a supporting technique. Image analysis can be used to very precisely find the position of the fuel bundle within the measuring device [10]. First, an analytic reconstruction is performed, calculating the source distribution from the measured gamma intensities. A template matching technique is applied to the resulting image in order to determine the precise location of the fuel bundle within the imaged area, which can then be used as input for the algebraic algorithm in order to quantitatively determine the activity of the individual fuel rods.

Template matching can also be used to individually identify and count the fuel rods within an image, and here lies the potential for automatic detection of missing rods also in cases when no operator declared information is available.

In the following sections, the template matching capabilities for position determination and for fuel rod counting are demonstrated.

3. Demonstration of positioning procedures on experimental images

3.1. Image analysis procedures used for assembly positioning

The resolution of the tomographic image is limited by the number of measurements and the reconstruction method. The images presented in this work have been reconstructed with 55x55 pixels, from a measurement set of about 10000 data points [7]. For example, the images of SVEA-96 fuel reconstructed from PLUTO data have sides corresponding to 138.6 mm with a pixel size of 2.52 mm. In order to be able to find the location of the fuel with the desired precision of 0.1 mm and 0.1° an interpolation technique has been applied, increasing the number of pixels to 1024x1024.

To find the position of the fuel assembly, a template corresponding to the known geometry of the fuel was compared with the image. This template is essentially an image with the value 1 where the fuel rods are located, and the value 0 where there is no fuel material. The template is translated and rotated across the tomographic image and multiplied with the fuel data, in search of the position with the highest intensity in the pixels covered by the template rods. In order to reduce the sensitivity to noise in the image and avoid finding a point in the coordinate space with randomly higher intensity, a function of the coordinates x, y and angle can be fitted to the intensities found for all tested template coordinates. This function constitutes a hyperplane which is then searched for the global maximum, taken as the position of the fuel.

3.2. Positioning of BWR fuel in the PLUTO device

The method described above was applied to PLUTO measurements on irradiated BWR fuel [10].

The results obtained in this way were cross checked with the independent measurements of the position of the fuel in the device, which were performed in connection with the tomographic

measurements. In this way it could be confirmed that a precision of 0.1 mm and 0.1° is indeed achievable using this method.

3.3. Positioning of VVER-440 fuel in the JNT 1510 device

When the reconstruction is not centred on the fuel, boundary effects can reduce the quality of the resulting image. In some of the measurements taken with the JNT 1510 device, the fuel was placed off-centre in the device. In such cases the positioning algorithm can be used to find the fuel position in the image, and a new image can be reconstructed with the centre of the image moved to correspond to the centre of the fuel. In figure 2 the reconstruction of a particularly misaligned VVER-440 fuel assembly is shown, together with a fuel mask (in red) showing where the fuel would be located if it had been perfectly centred in the device. The side of this image corresponds to 165 mm. Making use of the positioning algorithm, the actual position of this fuel was found to be +29.9 mm in the x direction and +10.2 mm in y, compared to centre of the measuring apparatus.

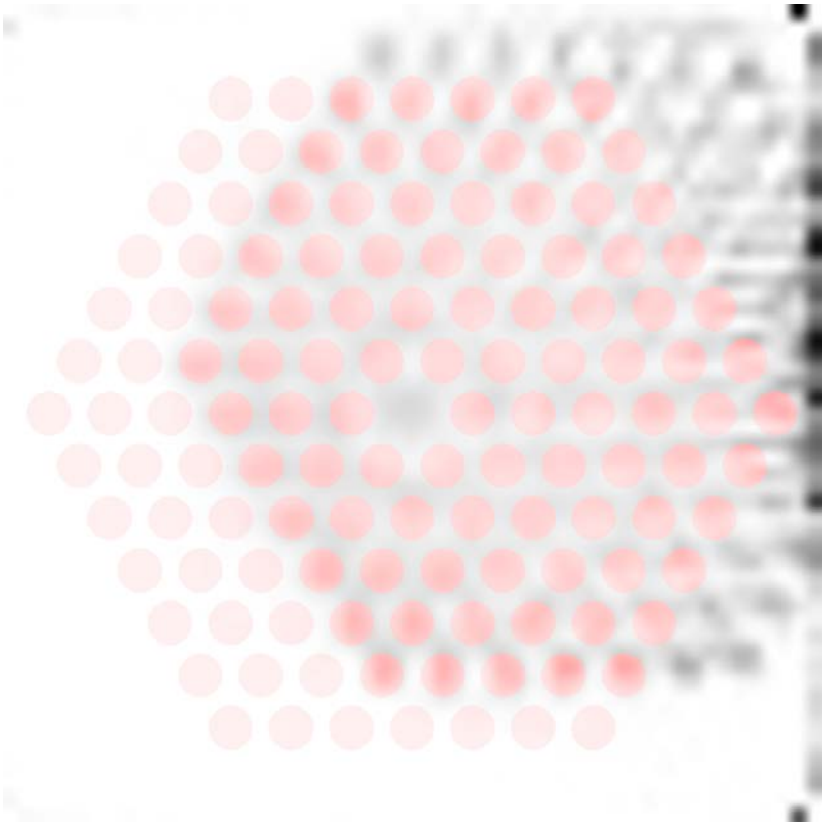

Figure 2: A reconstructed image of a VVER-440 fuel which was located off-centre in the measurement. A perfectly centred fuel mask is shown in red, demonstrating the misalignment. With the help of image analysis the misalignment was determined to be +29.9 mm in x and +10.2 mm in y.

4. Demonstration of rod counting on simulated and experimental images

Template matching can be used not only to find the location of a complete fuel bundle, but can also be applied to locate individual fuel rods in an image.

4.1. Image analysis procedures for fuel rod counting

We search an image for fuel rods without making any assumptions about the number and the location of these rods. The algorithm needs as input only a reasonable fuel rod radius. This radius is used to form a single rod template, rather than the complete fuel template discussed in section 3. The rod template is moved around the image, searching for the position giving the maximum intensity, i.e. the position corresponding to the maximum reconstructed activity in a rod-sized area. When this is found, the information is stored and the search is performed again, allowing no overlap with the result of the

first search. The search is iterated a pre-defined number of times, or until the whole image is covered. Earlier studies [10] have shown that the precision in the rod-positioning results is sensitive to the used radius of the rod template, and also indicated that assuming a rod radius slightly smaller than the actual imaged rods is better than using a radius that is too large.

4.2. Rod counting in images from simulated measurements of BWR fuel

In order to test and verify the reconstruction and the image analysis techniques, we used a simulation of the PLUTO device, modelling the 662 keV gamma emission from ^{137}Cs in a BWR fuel assembly of the SVEA-96 type. In this simulation all of the rods were identical, i.e. with equal activity.

The reconstructed image was searched for maximum activity positions corresponding to the size of a fuel rod. When 124 positions were found, there was no more room in the image to add any more rod candidates, as can be seen in the image in figure 3.

The intensities in the resulting positions were plotted in a histogram, in blue for the positions corresponding to actual fuel rods, and in red for the non-fuel image positions. There is a clear separation between the two groups, even with the spread in the distribution of rod intensities (the standard deviation is 17%) that is caused by the processes involved in the propagation and detection of the gamma radiation, and the subsequent image reconstruction.

It should be noted that this is the type of reconstruction including no a priori assumptions about the internal assembly geometry. Compare to a detailed modelling of the assembly geometry in a dedicated algebraic reconstruction, which results in an agreement with the simulation of 0.87% (1σ) [9].

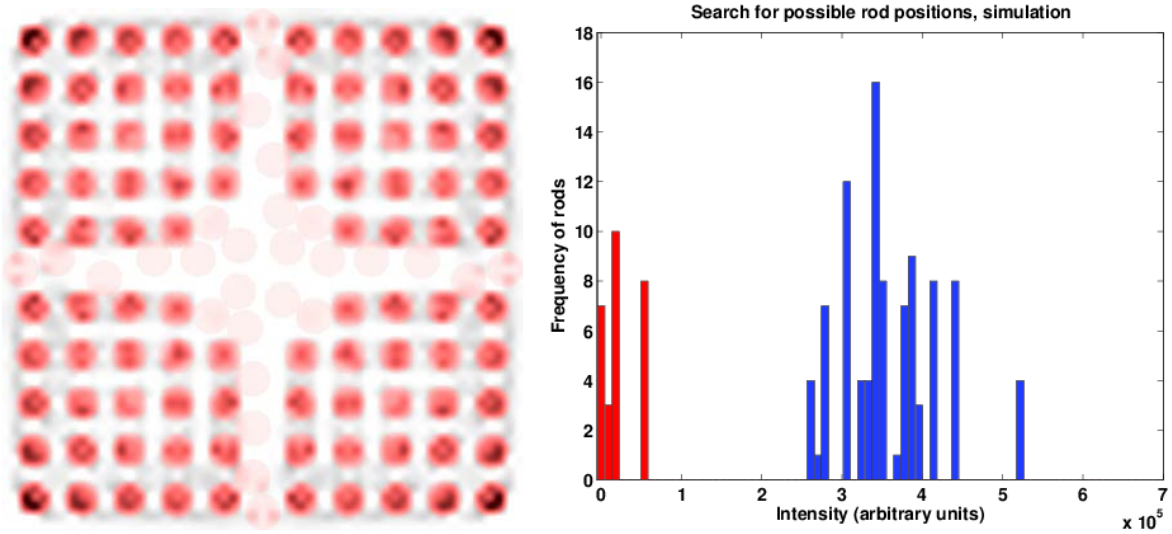

Figure 3: To the left is the result of the search for rod-sized parts of the image in decreasing order of intensity. The histogram shows the intensities corresponding to actual fuel rods in blue, and the other positions in red.

4.3. Rod counting in images from experimental measurements on irradiated BWR fuel

In an experimental campaign in 2002 the PLUTO equipment was used to measure the gamma radiation around a SVEA-96 fuel assembly. The 1596 keV peak from the ^{140}Ba/La decay chain was selected, and the data used in tomographic reconstructions. We apply the rod search method to this image and find 124 possible rod positions before the image is full, as shown in figure 4.

The standard deviation of the distribution is now larger, 33%, which reflects the variation in the actual activities of the rods (known to be 14% [8]), as well as the uncertainties from reconstruction and the stochastic processes involved in gamma transport and detection. There is still a clear separation between the activities of rods and non-rods, indicating that it would be possible to automatically discriminate between them. Again, note that this image is created using the type of reconstruction which includes no assumptions about the internal geometry, in contrast to the type of detailed

modelling in an algebraic reconstruction where the uncertainties are much smaller and we can get quantitative measures of the rod activities, as discussed in the references [8] and [9].

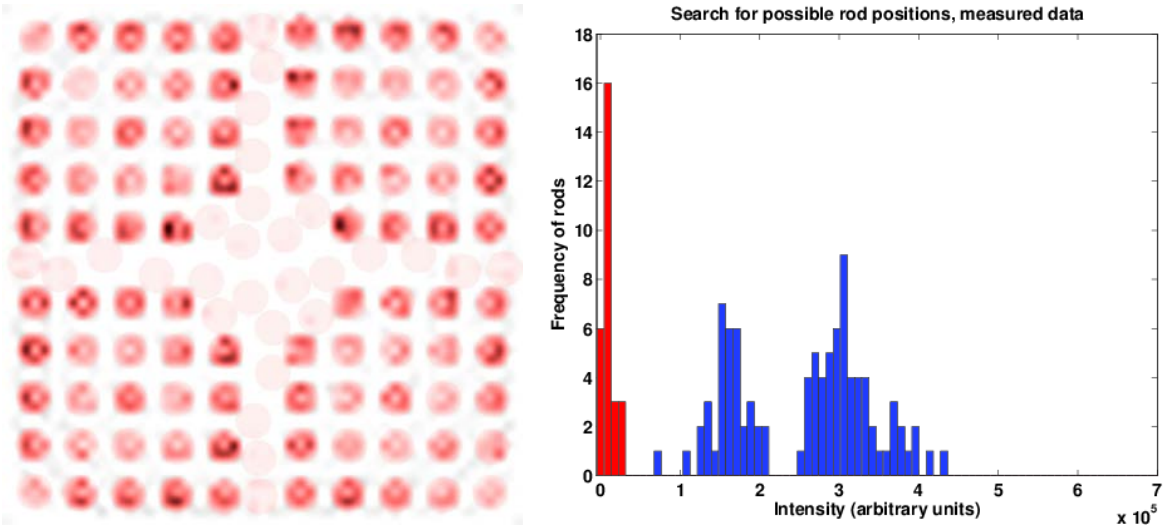

Figure 4: To the left is the result of the search for rod-sized parts of the image in decreasing order of intensity. The histogram shows the intensities corresponding to actual fuel rods in blue, and the other positions in red.

5. Conclusions and outlook

It has been demonstrated that image analysis of tomographic images of irradiated fuel assemblies can provide useful information for verification purposes.

The positioning method discussed in section 3 provides accurate information about the position of the fuel bundle, which is a prerequisite for the detailed quantitative rod-by-rod activity reconstruction discussed for example in [9]. This type of reconstruction algorithm is a powerful tool that can give an independent assessment of burn-up and cooling time of each fuel rod. This in turn can be used for verifying operator declared information and detecting anomalies.

Another useful procedure demonstrated in this work is individual fuel rod identification can be performed with an automatic algorithm in tomographic reconstructions of nuclear fuel assemblies. In the tested cases, including experimental as well as simulated data of various nuclear fuel types, all rods have been correctly identified. In all images the non-fuel parts had lower intensity, which indicates that a threshold level can be introduced to achieve full separation between true rods and false image artefacts arising from measurement noise and reconstruction errors. We conclude that this type of image analysis can support tomographic partial defect verification by providing a tool for counting of the fuel rods.

We can think of several additional ways these techniques can be put to use. For example, the output of the rod search algorithm described in section 4 could be used as the input to a pattern matching algorithm identifying the fuel assembly among a set of known fuel types. When gamma emission tomography is implemented for inspection use, verification of operator declared fuel information can be done with only minimal assumptions. In cases where operator information is missing, this type of test would compare the image to standard fuel types. An algorithm for rod and fuel type identification could be implemented to automatically flag images where the fuel geometry has some anomalies, making the method convenient to use on a large scale.

References

[1] Howell J A, Menlove H O, Rodriguez C A, Beddingfield D, Vasil A; *Analysis of integrated video and radiation data*; Institute of Nuclear Materials Management 36:th Annual Meeting, 1995

[2] Jasani B, Niemeyer I, Nussbaum S, Richter B, Stein G (ed); *International Safeguards and Satellite Imagery: Key Features of the Nuclear Fuel Cycle and Computer-Based Analysis*. Springer; Berlin Heidelberg; 2009.

[3] Grape S, Jacobsson Svärd S, Lindberg B; *Partial Defect Evaluation Methodology for Nuclear Safeguards Inspections of Used Nuclear Fuel Using the Digital Cherenkov Viewing Device; Nuclear Tecnology.* American Nuclear Society; vol 186; 2014. Pages 90-98.

[4] Branger E, Grape S, Jansson P, Jacobsson Svärd S; *Improving the prediction model for Cherenkov light generation by irradiated nuclear fuel assemblies in wet storage for enhanced partial-defect verification capability*; ESARDA 37th annual meeting, Manchester 2015.

[5] Jansson P, Jacobsson Svärd S, Håkansson A, Bäcklin A; *A Device for Nondestructive Experimental Determination of the Power Distribution in a Nuclear Fuel Assembly; Nuclear Science and Engineering*; vol 152; 2006. Pages 76-86.

[6] Sokolov A, Kontratjev V, Levai F, Honkamaa T; *CdTe linear arrays with integrated electronics for passive gamma emission tomography system*; Nuclear Science Symposium Conference Record; 2008. Pages 999-1002.

[7] Jacobsson Svärd S, Holcombe S, Grape S; *Applicability of a set of tomographic reconstruction algorithms for quantitative SPECT on irradiated nuclear fuel assemblies*. Nuclear Instruments and Methods in Physics Research A, vol 783, 2015. Pages 128-141.

[8] Jacobsson Svärd S, Håkansson A, Bäcklin A, Osifo O, Willman C, Jansson P; *Nondestructive experimental determination of the pin-power distribution in nuclear fuel assemblies*. Nuclear Technology, vol 151, 2005. Pages 70-76.

[9] Jacobsson Svärd S, Andersson P, Davour A, Grape S, Holcombe S, Jansson P; *Tomographic determination of spent fuel assembly pin-wise burnup and cooling time for detection of anomalies*; ESARDA 37th annual meeting, Manchester 2015.

[10] Troeng M; *Positioning of Nuclear Fuel Assemblies by Means of Image Analysis on Tomographic Data*; M Sc Thesis, Uppsala University; 2004.

Shielded Neutron Source Detection Option

Arturs Rozite

European Commission, Joint Research Centre
Institute for Transuranium Elements,
Nuclear Security Unit
Via Fermi, Ispra 21020 (VA) Italy
E-mail: arturs.rozite@jrc.ec.europa.eu

Abstract:

Possibility of detection of prompt gamma-rays emitted by shielded neutron source by means of high-purity germanium (HPGe) detectors is investigated. Properties of hydrogen, boron, cadmium and gadolinium based neutron-to-photon converters are studied. Special focus is made on the usage of HPGe spectrometers as neutron detection tool in different neutron shielding scenarios.

Keywords: Radiation Portal Monitor, HPGe detector, thermal neutrons, PGAA, nuclear security

1. Introduction

Research and development on detection of Special Nuclear Materials (SNM) by means of Radiation Portal Monitors (RPM) have been pioneered in Los Alamos in 1980th [1-4].
Basic efforts of scientists were focused on the development of passive automated system which could detect presence of gamma and neutron radiation emitted by SNM at distance of several meters and within couple of seconds.
Large volume plastic scintillation detectors have been chosen for detection of gamma radiation and later ^{3}He counters have been introduced for detection of neutrons [2].
NaI and HPGe photon detectors have been considered too, however higher manufacturing costs and technological constrains precluded their usage for a long time [1-4].
Initially RPMs have been installed to control exits from the objects dealing with storage and processing of nuclear materials and have been considered as a measuring tool used with complementary metal detectors and x-ray scanners and later they have found their place at the border crossing points [5] and thousands of systems have been deployed all over the world.
Properties of such passive systems have been well documented [7] and their advantages and limitations clearly defined [8].
Conventional RPMs installed at the border crossing points detect significant quantities [9] of SNM; however detection capabilities of conventional RPMs become questionable in case if SNM is shielded.
In this article prompt gamma-ray neutron activation analysis (PGAA) detection option for shielded neutron source is considered on the example of hand-held instruments. Considerations could be extended to RPM increasing sensitive volume of HPGe detectors to the level of sensitive volume of thermal neutron detectors such as ^{3}He used in conventional RPMs.

2. Materials and method

Radiation Portal Monitors are equipped with two types of radiation detectors. One type of detectors is used for detection of photons and second type of detectors is used for detection of neutrons. Basic purpose of RPM is in detection of Special Nuclear Materials, i.e. weapons-grade uranium (WGU) and weapons-grade plutonium (WGPu).

WGU consists mostly from ^{235}U (>90%) and ^{238}U (<10%). WGPu consists mostly from ^{239}Pu (<93%) and ^{240}Pu (>6%). Photons emitted by ^{235}U, ^{239}Pu and ^{240}Pu are characterized by relatively low energies

and therefore could be easily shielded using thin layer of material with high atomic number and high density. Photon detectors, particularly plastic scintillators are effective measurement tool only for detection of unshielded Special Nuclear Materials.

In terms of detection of high-Z shielded WGPu neutron detectors are used. Neutrons are emitted by ^{240}Pu at rate of about 1000 s^{-1} per gram [8]. Neutrons in general are more difficult to shield compared to photons due to the facts that photons interact with electrons of atom but neutrons interact with nucleus of atom and dimension of nucleus is thousands times less then dimension of atom.
For shielding against fission neutrons low-Z materials and material having high-cross section for absorption of thermal neutrons are used first to slow down neutrons and then to capture them. In the result of neutron capture in most cases characteristic photon is emitted.
Method used for analysis of material composition by irradiating material with neutrons and detecting photons emitted by material in the result of irradiation is called prompt gamma-ray neutron activation analysis (PGAA) [10, 11].

Neutrons emitted for example by shielded WGPu are captured by materials of shield and in the result prompt photons could be detected. Detected signal provides information about type of shielding material in case if specific full-energy absorption peaks are detected and about presence of source of artificial nature in case if photons with energies above 2614 keV are detected. This information is a useful signal which makes possible detection of shielded WGPu.

In the Table 1 characteristics of several effective neutron shielding materials are listed.

Table 1.

Converter	*Target nuclei*	*Natural abundance, %*	*Thermal neutron capture cross-section, barns**	*Nuclear reaction*	*Photon energies, keV*	*Emission probability for converter having natural isotopic composition***
HDPE	^{1}H	99.9885	0.332	$^{1}H + n \rightarrow {}^{2}H + \gamma$	2223	1
Boron	^{10}B	19.9	3846	$^{10}B + n \rightarrow \alpha + {}^{7}Li^{*}$ $^{7}Li^{*} \rightarrow {}^{7}Li + \gamma$	478	0.94
Cadmium	^{113}Cd	12.22	20770	$^{113}Cd + n \rightarrow {}^{114}Cd + \gamma$	558 651 above 2614	0.42 0.08 0.11
Gadolinium	^{155}Gd	14.8	60850	$^{155}Gd + n \rightarrow {}^{156}Gd + \gamma$	89 199	0.02 0.03
	^{157}Gd	15.65	255100	$^{157}Gd + n \rightarrow {}^{158}Gd + \gamma$	80 182 above 2614	0.04 0.07 0.09

** JEF-2.2 evaluated data library*
*** Data derived from Database for Prompt Gamma-ray Neutron Activation Analysis, IAEA*

High-density polyethylene could be considered both as a neutron moderator and as an absorber. In absolute case if HDPE is purely used as a neutron shield and thickness of HDPE allows absorb all neutrons emitted by source all of them will be converted into photons with energies 2223 keV.
This specific spectral line according to IAEA minimal technical requirements [7] for Radionuclide Identification Devices (RIDs) shall be included in library of RID.

Other materials such as Boron, Cadmium and Gadolinium having high thermal neutron capture cross-sections called neutron converters in combination with moderator such as HDPE could be used to suppress neutron signal from source. In this case specific prompt gamma-rays will be emitted at a lower than 100% rate. These specific spectral lines according to IAEA minimal technical requirements [7] for Radionuclide Identification Devices (RIDs) are not included in library of RID. Emission probabilities of prompt photons for specific converter materials are listed in last column of Table 1.

In this article on the example of ^{252}Cf source and HPGe detector properties of typical neutron shield materials are studied.

3. Experimental results for HPGe detector #1

3.1. Detection efficiency of HPGe detector depending on composition of neutron shield

In order to compare HPGe detector response to different neutron-to-photon converters number of measurements have been performed with HPGe detector #1 [12] using ^{252}Cf source and neutron shields of different compositions. Depending on neutron-to-photon converter material HPGe detector response in energy range from 50 to 3000 keV has been studied. Detection efficiency of prompt gamma-rays in under moderated and over moderated shielding scenarios has been measured. Results have been compared with reference ^{3}He detector. Parameters of detectors and intensity of ^{252}Cf source are listed in Tables 2 and 3.

Table 2.

Detector	***Diameter, cm***	***Length, cm***	***Sensitive volume, cc***
^{3}He counter	1.9	12.7	28
HPGe detector #1	50	30	53

Table 3.

Source	***Neutron flux into 4π steradian, s^{-1}***
^{252}Cf	160 000

^{252}Cf source was placed at 115 mm distance to HPGe detector endcap. Neutron moderator with dimensions 65x200x200mm (DxWxH) made from two HDPE bricks was placed between source and HPGe detector. Boron carbide powder, cadmium plate and gadolinium foil have been placed sequentially between moderator and HPGe detector. In Figure 1 experimental setup for HPGe detector is illustrated.

Figure 1. Example of experimental setup (source - moderator - converter - detector)

600 seconds live time spectra have been recorded by HPGe spectrometer, results of spectral measurements have been analysed and compared. Parameters and results of measurements are summarized in Table 4 and Figures 2 - 5 below.

Table 4.

Distance to endcap, mm	*Thickness of HDPE, mm*	*Thickness of Cd layer, mm*	*Thickness of Gd layer, mm*	*Thickness of Boron carbide powder, mm*	*Integral count rate in energy range from 2650 to 3000 keV, s^{-1}*	*Net count rate in prompt gamma-ray energy peak, s^{-1}*			
						^{1}H, 2223 keV	*^{157}Gd, 182 keV*	*^{113}Cd, 558 keV*	*^{10}B, 478 keV*
115	0	-	-	-	9	-	-	-	-
115	65	-	-	-	9.1	2.9	-	-	-
115	65	-	-	5	7	2.6	-	-	19.4
115	65	1	-	-	13.5	2.6	-	7.5	-
115	65	-	0.12	-	11.3	2.8	5.0	-	-

According to the analysis of measurement results the following conclusions could be made:

a) Intensity of 2223 keV spectral line is approximately the same for HDPE, HDPE/Boron, HDPE/Cadmium and HDPE/Gadolinium converters. This line could be used as a useful signal indicating presence of neutron source.

b) The highest count rate in characteristic full-energy absorption peak is obtained for 478 keV peak with HDPE/Boron converter. This is in good agreement with data of emission probabilities listed in Table 1.

c) The highest integral count rate in energy range from 2650 to 3000 keV is obtained for HDPE/Cadmium converter. This is also in good agreement with data of emission probabilities listed in Table 1.

d) The lowest integral count rate in energy range from 2650 to 3000 keV is obtained for HDPE/Boron converter. Count rate is less then count rate obtained with pure HDPE moderator. This could be related to presence of thermal neutrons on the output from pure HDPE moderator and to the absence of thermal neutrons on the output from HDPE moderator with Boron converter. Thermal neutrons are captured by Germanium isotopes of HPGe detector, prompt gamma-rays are emitted and in the result count rate above 2650 keV for pure HDPE moderator is higher than count rate above 2650 keV for HDPE moderator with Boron converter.

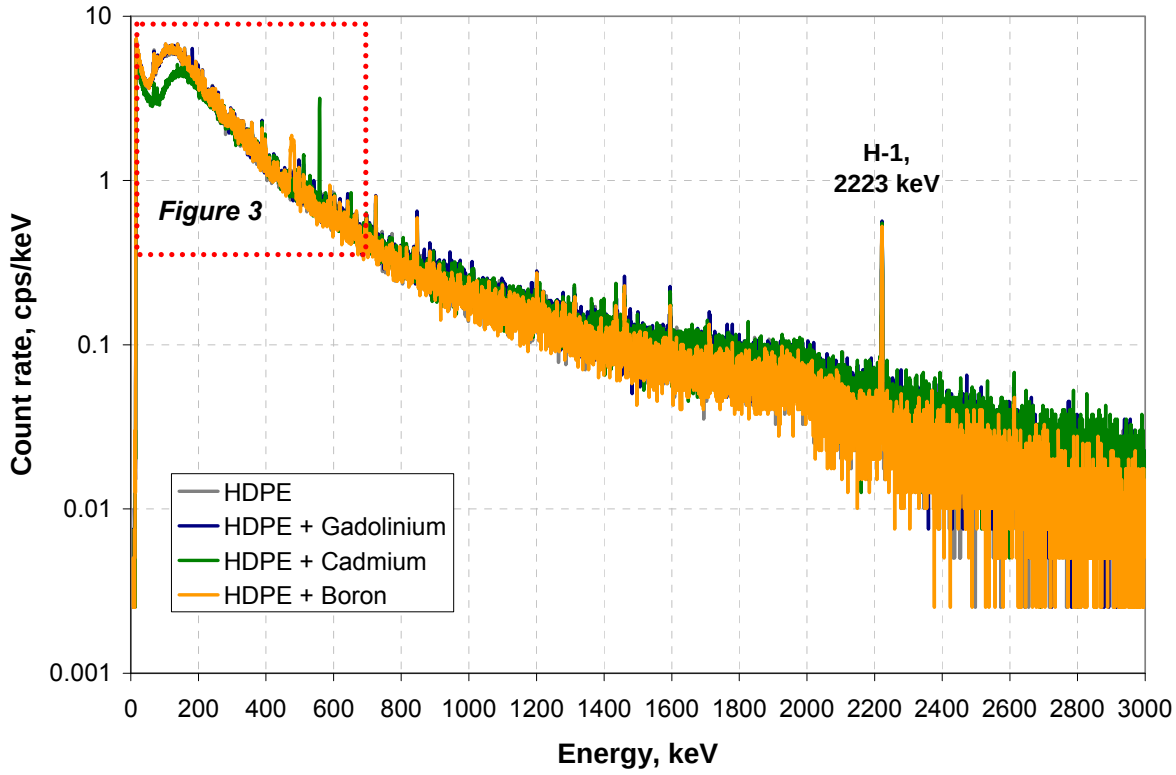

Figure 2. Comparison of HPGe detector response to different neutron-to-photon converters in energy range from 50 to 3000 keV

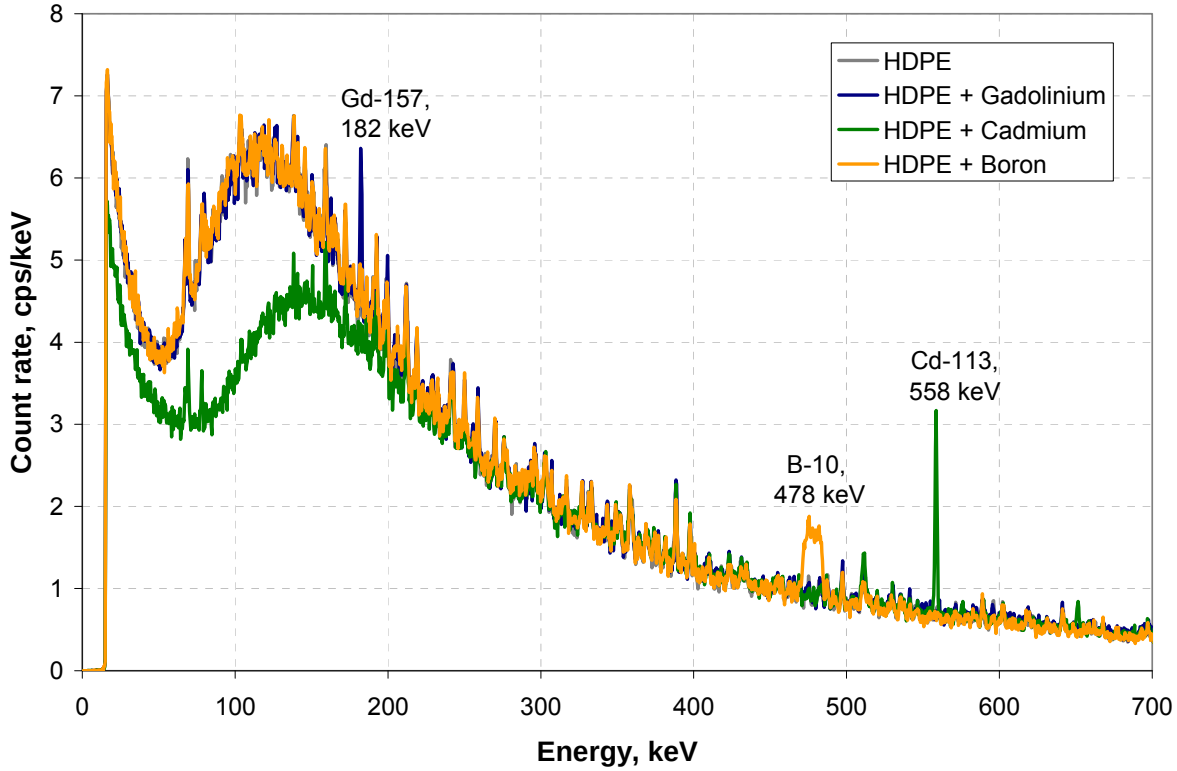

Figure 3. Comparison of HPGe detector response to different neutron-to-photon converters (full-energy absorption peaks)

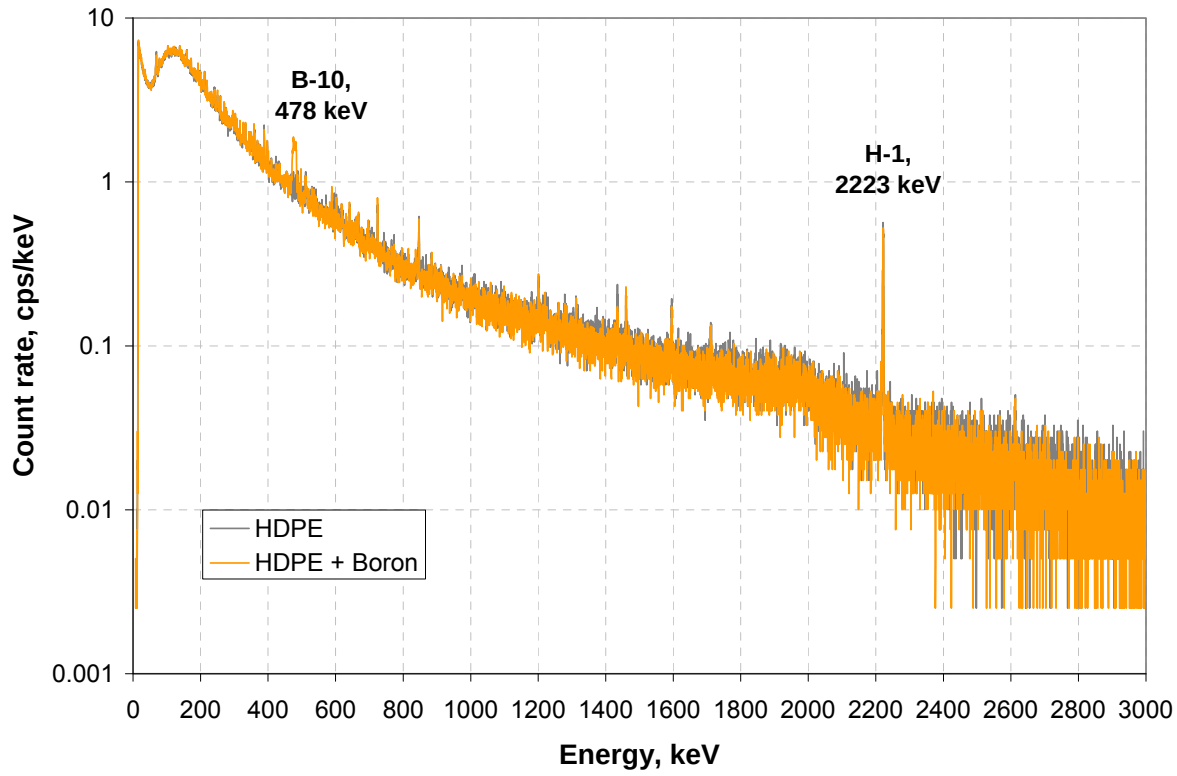

Figure 4. Comparison of HPGe detector response to HDPE and HDPE/Boron converters

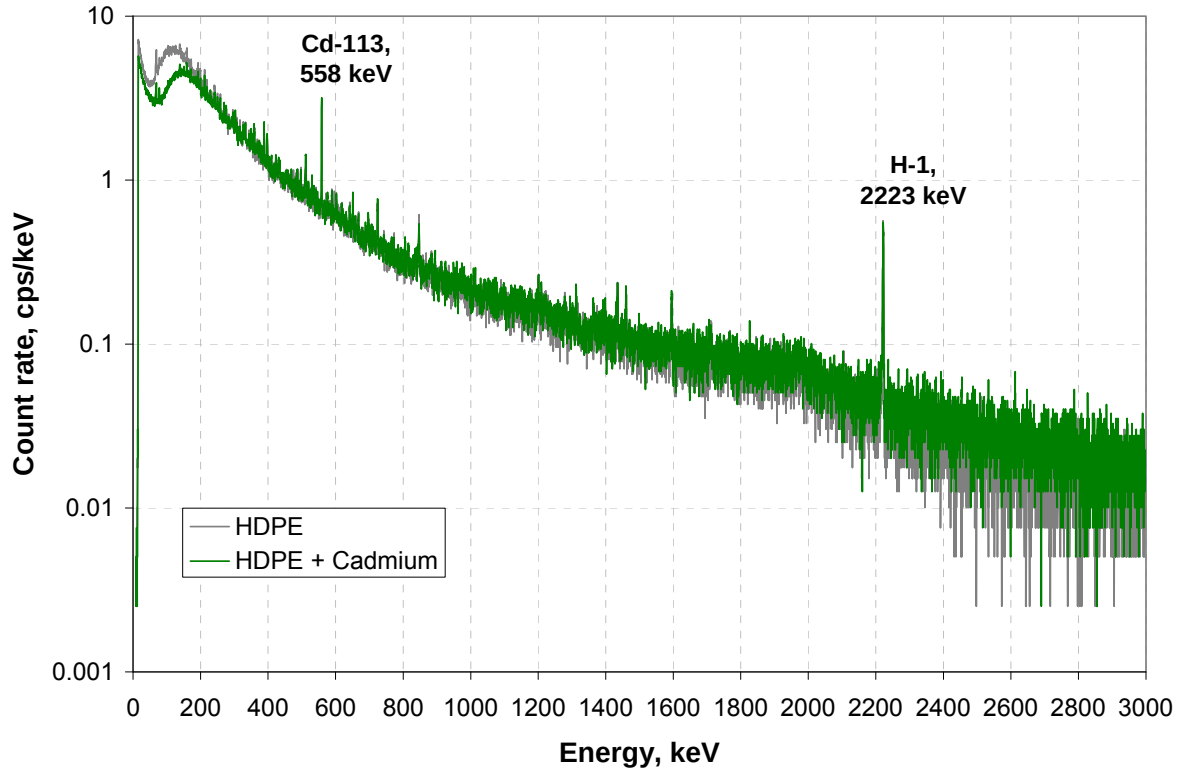

Figure 5. Comparison of HPGe detector response to HDPE and HDPE/Cadmium converters

3.2. Comparison of detection efficiency of HPGe detector with detection efficiency of ^{3}He proportional counter depending on composition of neutron shield

For the evaluation of detection efficiency of HPGe detector under different neutron shielding scenarios reference ^{3}He proportional counter embedded into TSA PRM-470CGN radiation monitor [13] was used. In order to improve its sensitivity to shielded neutron sources ^{3}He counter is under moderated i.e. surrounded just by about 1 cm thick HDPE.
In Table 5 measurement results of neutrons detection efficiency of TSA PRM depending on the thickness of additional HDPE moderator are shown.

Table 5.

Distance between source and detector, mm	*Thickness of additional HDPE moderator, mm*	*TSA PRM, neutron count rate, cps*
250	0	7.6
250	10	11.4
250	20	14.2
250	30	18.8
250	40	20.6
250	50	20
250	60	18.4

3.2.1. HDPE/Cadmium shield

For comparison of detection efficiency of HPGe detector and ^{3}He counter under HDPE/Cd shielding scenarios several measurements have been performed.
Cf-252 source was placed at 250 mm distance to HPGe detector endcap. Blocks of HDPE moderator with dimensions 195x200x200mm have been used. Thickness of HDPE moderator was increased from 0 to 195 mm with a step of 65 mm. Then measurement with HDPE moderator and single 0.15 mm thick plate of Cd placed between moderator and detector was performed.
Last measurement was performed using sandwich type arrangement of HDPE moderator and Cadmium converter i.e.:

1. Source
2. 65x200x200 mm HDPE
3. 0.15 mm Cd
4. 65x200x200 mm HDPE
5. 0.15 mm Cd
6. 65x200x200 mm HDPE
7. 0.15 mm Cd
8. Detector

10 sequential 20 seconds measurements were made using TSA PRM for each experimental setup and average values of signals were obtained.
600 seconds live time spectra have been recorded by HPGe spectrometer for each experimental setup.

Measurement results are summarized in Table 6.

Table 6.

Distance to endcap, mm	*Thickness of HDPE, mm*	*Thickness of Cd layer, mm*	*TSA PRM, neutron count rate, cps*	*Integral count rate in energy range from 2650 to 3000 keV*	*Net count rate in prompt gamma-ray energy peak, cps*	
					^{1}H, 2223 keV	*^{113}Cd, 558 keV*
250	0	-	7.6	2.3	-	-
250	65*	-	30	2.3	0.7	-
250	130	-	15.9	1.8	1.2	-
250	195	-	6.1	1.3	1.1	-
250	195	0.15	1.9	1.6	1.1	0.5
250	65+65+65	0.15+0.15+0.15	1.9	2.3	0.7	0.9

**Dimensions 65x200x200mm (DxWxH)*

According to the analysis of measurement results the following conclusions could be made:

a) Sensitivity of TSA PRM to unshielded neutron source is about 4 times less then to the neutron source shielded by 65 mm of HDPE.
b) Sensitivity of TSA PRM to unshielded neutron source is about the same as to the neutron source shielded by 195 mm of HDPE.
c) Sensitivity of TSA PRM to neutron source shielded by 195 mm of HDPE is about 6 times higher than sensitivity of HPGe detector
d) Sensitivity of TSA PRM to neutron source shielded by 195 mm of HDPE and single Cd layer is about the same compared to sensitivity of HPGe detector
e) Sensitivity of TSA PRM to neutron source shielded by sandwich type HDPE/Cadmium shield is about 1.4 times less then sensitivity of HPGe detector (but is about 1.4 times higher per unit of sensitive volume)

3.2.1. Borated HDPE shield

Neutron shield was made using borated HDPE bricks (5% Boron content by mass).
Cf-252 source was placed at 250 mm distance to HPGe detector endcap. Thickness of borated HDPE was increased from 0 to 200 mm with a step of 50 mm. 10 sequential 20 seconds measurements have been performed with TSA PRM for each experimental setup and average values of signals were obtained. 600 seconds live time spectra have been recorded by HPGe spectrometer for each experimental setup. Measurement results are summarized in Table 7.

Table 7.

Distance to endcap, mm	*Thickness of Borated HDPE, mm*	*TSA PRM, neutron count rate, cps*	*Net count rate in prompt gamma-ray energy peak, cps*
			^{10}B, 478 keV
250	0	7.6	-
250	50*	19.2	3.9
250	100	10	5.7
250	150	2.5	4.3
250	200	2.0	3.0

**Dimensions 50x200x200mm (DxWxH)*

According to the analysis of measurement results the following conclusions could be made:

a) 2223 keV full-energy absorption peaks are not registered in spectra due to uniform distribution of ^{10}B across volume of HDPE
b) Sensitivity of TSA PRM to neutron source shielded by 150 and 200 mm of borated HDPE is less then sensitivity of HPGe detector
c) Sensitivity of HPGe detector to neutron source first increases but then drops with increase of shield thickness due to increase of absorption of characteristic photons with energies 478 keV in the shield

4. Container for shipment of neutron sources

Container for shipment of neutron sources has been developed in Nuclear Security Unit of the European Commission, Joint Research Centre, Institute for Transuranium Elements. Container is made from borated HDPE and was fabricated by commercial vendor in 2014 in accordance with our design and specification. Container was made for TaskMED Project in the framework of Instrument Contributing to Stability and Peace.
Radiological characterisation of container was performed and comparison of the ^{3}He and HPGe detectors ability to detect presence of neutron source in this container was made.

4.1. Characterisation of container

Radiological characterisation of container was made using ^{252}Cf source with intensity 60000 s^{-1} and neutron and Gamma/X-ray dose rate measurement instruments. Results of neutron dose-rate measurements are listed in Table 8.

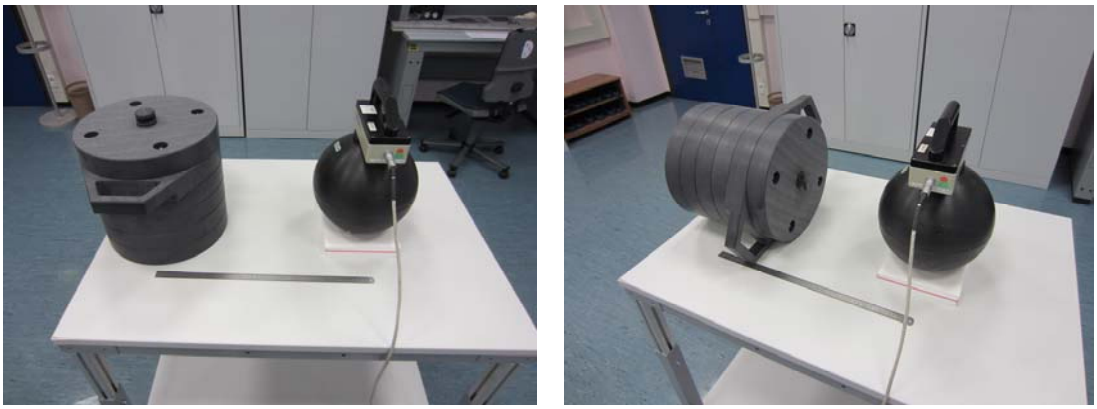

Figure 6. Radiological characterisation of container, neutron dose-rate measurements

Table 8. Shielding container from borated HDPE for shipment and storage of neutron sources

Parameter	***Value***	***Notes***
Diameter of container, mm	320	
Height of container, mm	300	
Source	^{252}Cf	
Activity, kBq (intensity, s^{-1})	518 (60000)	
Neutron background dose rate, μSv/h*	0.05	
Neutron dose rate at 50 cm distance to the unshielded source, μSv/h	3.1	from the geometrical centre of detector
Neutron dose rate at 50 cm distance to the source in container, μSv/h	0.32	from the side of container
Neutron dose rate at 50 cm distance to the source in container, μSv/h	0.43	from the top of container
**Neutron dose rate measurement instrument*	*Berthold LB6411*	

4.2. Comparison of detection efficiency of HPGe detector with detection efficiency of ^{3}He proportional counter for container made from borated HDPE

Measurements have been performed on the surface of container loaded with ^{252}Cf source using HPGe and ^{3}He detectors and at 160 mm distance to the open source.
10 sequential 20 seconds measurements have been performed with TSA PRM for each experimental setup and average values of signals were obtained. 600 seconds live time spectra have been recorded by HPGe spectrometer for each experimental setup.
Measurement results are summarized in Table 9.

Figure 7. Measurements of HPGe and ^{3}He detectors response on the surface of container

Table 9.

Distance to endcap, mm	*Thickness of Borated HDPE, mm*	*TSA PRM, neutron count rate, cps*	*TSA PRM + 3cm of HDPE, neutron count rate, cps*	*Net count rate in prompt gamma-ray energy peak, cps*
				^{10}B, 478 keV
160	0	13.4	45.4	0
160	160	9.3	10.5	23.6

According to the analysis of measurement results the following conclusions could be made:

a) Well moderated ^{3}He counter has more then 3 times better detection efficiency over under moderated ^{3}He counter for unshielded source
b) Under moderated ^{3}He counter has practically no advantage in terms of efficiency of neutrons detection over well moderated ^{3}He counter for this particular configuration of neutron shield
c) HPGe detector has approximately the same detection efficiency per unit of detector sensitive volume as reference ^{3}He counter in under moderated or well moderated configuration for this particular configuration of neutron shield

4.3. Evaluation of HPGe spectrometer as a neutron search device

In order to evaluate ability of HPGe spectrometer to detect presence of neutron source in container in search mode, series of 10, 5 and 2 seconds independent measurements have been performed measuring detector response at the surface of container (Figure 7). Results of measurements are summarized in Table 10 and Figure 8.

Table 10.

Number of measurement	*Net count rate in prompt gamma-ray energy peak, cps ^{10}B, 478 keV*			*TSA PRM, neutron count rate, cps*
	10 seconds measurement	*5 seconds measurement*	*2 seconds measurement*	*20 seconds measurement*
1	23.2	35.2	30.5	8
2	22.2	22.4	25.0	9
3	20.2	25.0	20.5	8
4	23.0	20.8	26.5	10
5	25.4	24.0	22.5	9
6	21.7	16.2	16.0	11
7	20.3	22.0	23.5	10
8	28.4	25.4	25.0	7
9	26.1	23.2	21.0	10
10	25.3	30.4	18.0	11
Average, counts	**23.6**	**24.5**	**22.9**	**9.3**
Standard deviation, counts	**2.7**	**5.2**	**4.2**	**1.3**

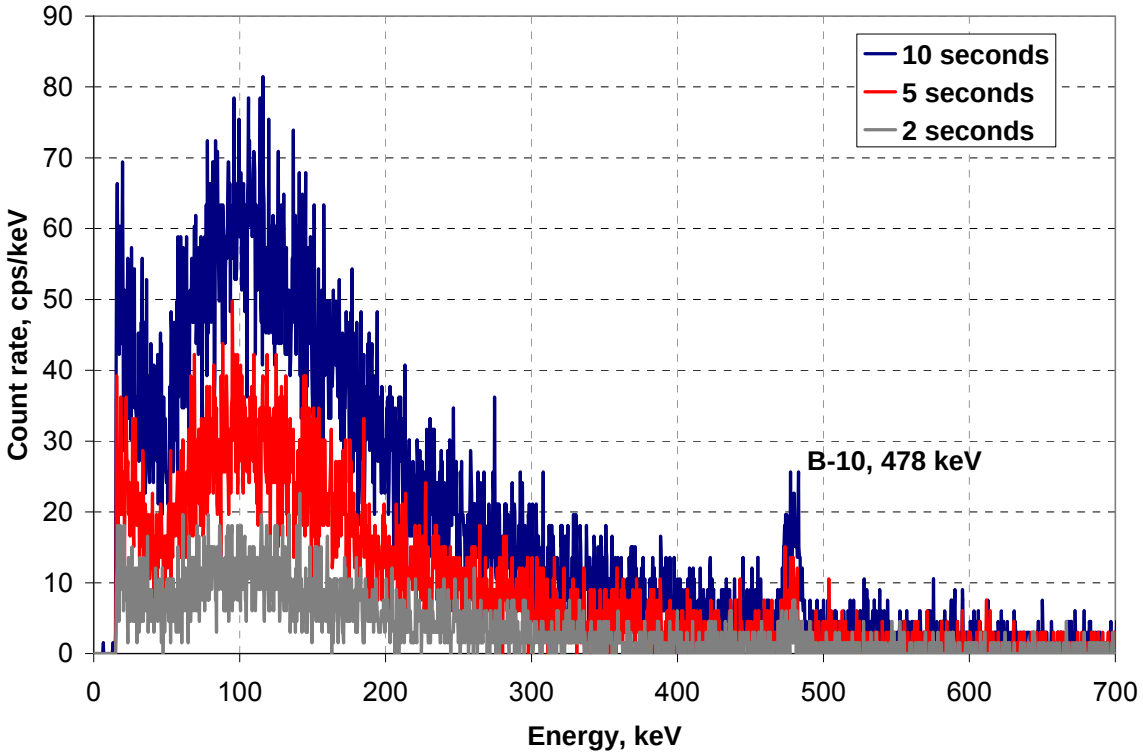

Figure 8. Measurements of HPGe and ^{3}He detectors response on the surface of container

5. Experimental results for HPGe detector #2

In order to evaluate HPGe detector response at energies above 2614 keV and up to 8500 keV, HPGe detector #2 [14] with higher sensitive volume compared to HPGe detector #1 was used and quite similar measurements to measurements described in Paragraph 3.1 have been performed. Basic parameters of detector, source and geometry of measurements are shown in Table 11 and Figure 9. Results of measurements are summarized in Table 12 and Figure 10.

Table 11.

Parameter	**Value**
HPGe detector #2	N-type coaxial
Diameter, mm	52
Length, mm	54
Sensitive volume, cc	111
Source	^{252}Cf
Neutron flux into 4π steradian, s^{-1}	160 000
Distance between source and HPGe detector endcap, mm	115

Table 12.

Thickness of HDPE, mm	***Thickness of Cd layer, mm***	***Thickness of Gd layer, mm***	***Thickness of Boron carbide powder, mm***	***Integral count rate in energy range from 2800 to 8500 keV, cps***	***Net count rate, cps***			
					^{1}H, 2223 keV	***^{157}Gd, 182 keV***	***^{113}Cd, 558 keV***	***^{10}B, 478 keV***
65			5	34.9	7.2			40.6
65	1			86.2	7.3		16.8	
65		0.12		68.4	7.5	-		

From the analysis of measurement results listed in Table 12 and Figure 10 it could be noted that HPGe detector #2 in contrast with HPGe detector #1 has better detection efficiency to HDPE/Cadmium converter then to HDPE/Boron converter due to higher sensitive volume compared to HPGe detector #1 and due to operation in extended up to 8500 keV energy range.

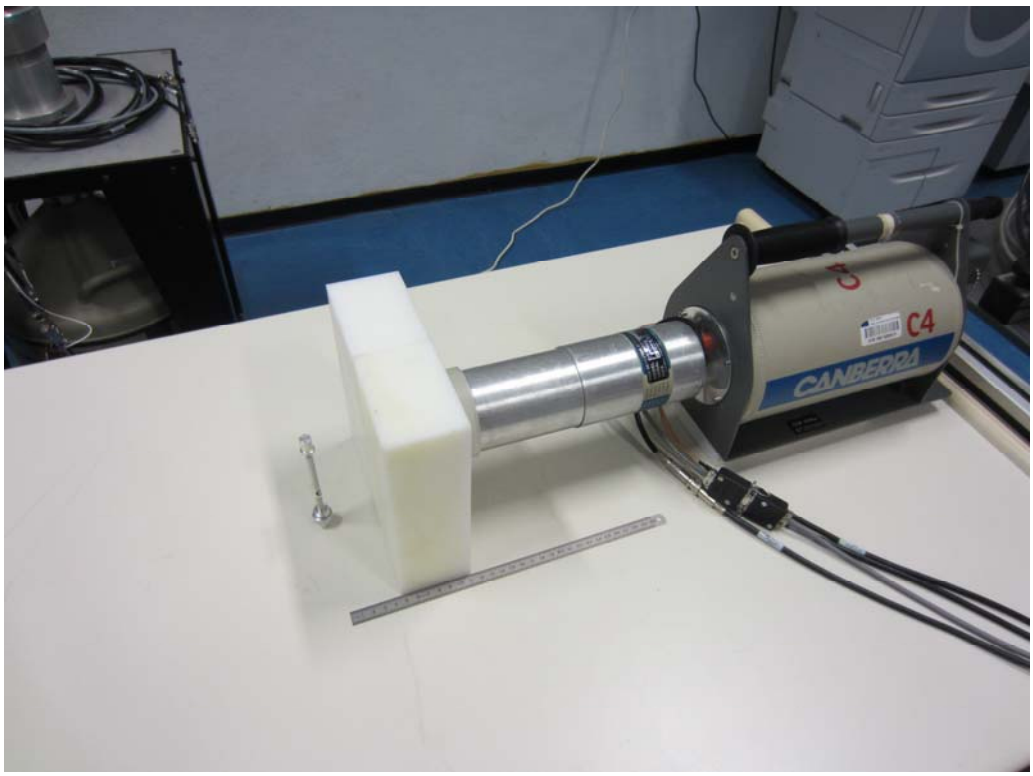

Figure 8. Experimental setup (source - moderator - converter - detector)

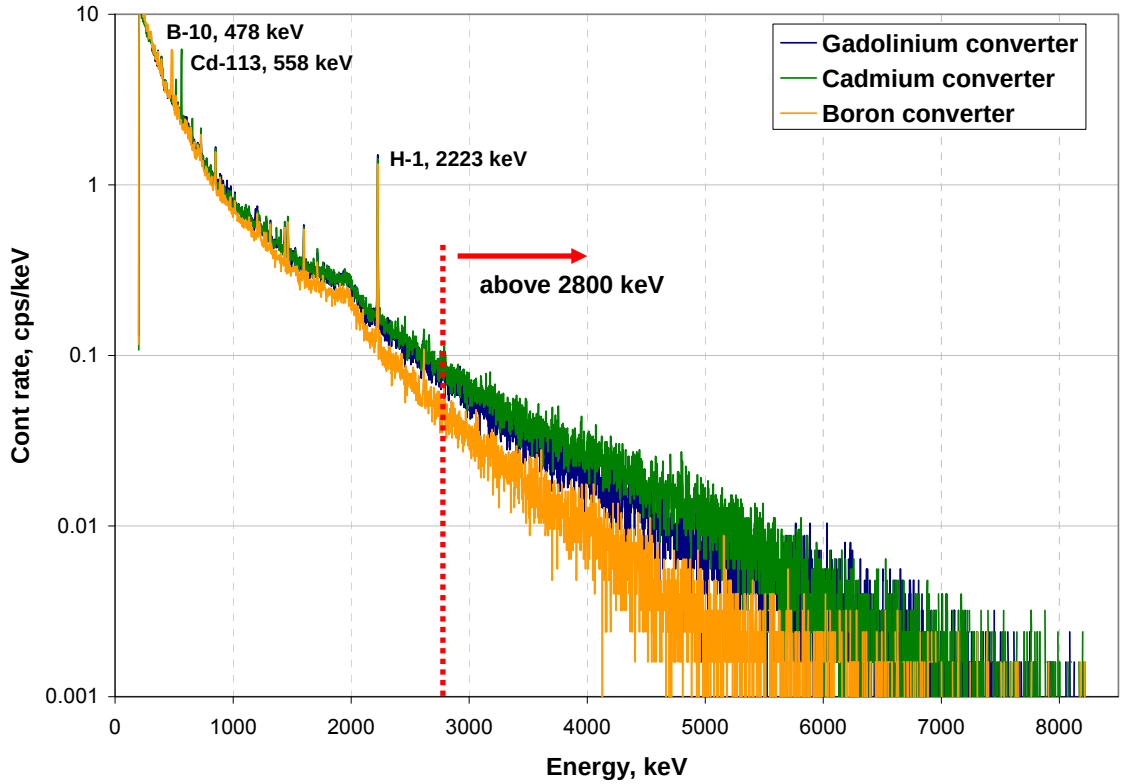

Figure 9. Comparison of HPGe detector response to HDPE/Gadolinium, HDPE/Cadmium and HDPE/Boron converters in energy range from 200 to 8500 keV.

6. Conclusions

In the results of competitive analysis of HPGe and ^{3}He detectors response in different neutron shielding scenarios feasibility study on possibility of PGAA detection option for shielded neutron source was performed and the following conclusion could be made:

a) It could be useful to include information about energy of most prominent prompt gamma-rays produced in the result of neutron capture on ^{10}B and ^{113}Cd into libraries of HPGe-based RIDs, for more exotic converter materials such as Gd this option could be considered.
b) Operational energy range of RIDs based on HPGe detectors could be extended from 3 MeV to 8 MeV, what could be useful for detection of sources of artificial nature or for detection of shielded WGPu when for example HDPE/Cadmium or HDPE/Gadolinium neutron shield is used.
c) Usage of HPGe detectors in RPM potentially allows detection of shielded WGPu with same or better detection efficiency compared to detection efficiency obtained with conventional thermal neutron detectors in case if comparable to conventional ^{3}He detectors sensitive volume is achieved.
d) Simultaneous usage of HPGe and thermal neutron detectors such as ^{3}He of comparable sensitive volume in RPM shortens requirement for thermal neutron detectors to be under moderated, so thermal neutron detectors used in conventional RPMs could be well-moderated and their detection efficiency to unshielded neutron source will be therefore improved.

7. Acknowledgements

Author would like to tell thank you to colleagues from Nuclear Security Unit for their support at different stages of this feasibility study.

Special thanks to Dr. Erica Fanchini from INFN (Italy).

8. References

[1] Chambers, W.H.; Atwater, H.F.; Fehlau, P.E.; Hastings, R.D.; Henry, C.N.; Kunz, W.E.; Sampson, T.E.; Whittlesey, T.H.; Worth, G.M. *Portal Monitor for Diversion Safeguards*. Los Alamos National Laboratory, LA-5681, 1974.

[2] P. E. Fehlau and G. S. Brunson. *COPING WITH PLASTIC SCINTILLATORS IN NUCLEAR SAFEGUARDS*. IEEE Transactions on Nuclear Science, Vol. NS-30, No. 1, February 1983.

[3] Paul E. Fehlau. *An Application Guide to Pedestrian SNM Monitors.* Los Alamos National Laboratory, LA-10633-MS, 1986.

[4] P. E. Fehlau. *An Application Guide to Vehicle SNM Monitors*. Los Alamos National Laboratory, LA-10912-MS, 1987.

[5] Rob L. York and Paul E. Fehlau. 1997 *Update for the Application Guide to Vehicle SNM Monitors*. . Los Alamos National Laboratory, LA-12347-MS, 1997.

[6] TSA Systems, Ltd. Vehicle *and Pedestrian Monitor VM-250AGN / PM-700AGN, Operations & Service Manual.* Doc: # 5000 Rev. A, January 30, 2006.

[7] IAEA. *Technical and Functional Specifications for Border Monitoring Equipment.* Nuclear Security Series No. 1. 2006.

[8] Steve Fetter, Valery A. Frolov, Marvin Miller, Robert Mozley, Oleg F. Prilutsky, Stanislav N. Rodionov and Roald Z. Sagdeev. *Detecting Nuclear Warheads.* Science & Global Security, 1990, Volume 1, pp. 225-302.

[9] Thomas B. Cohran and Christopher E. Pain. *The Amount of Plutonium and Highly-Enriched Uranium Needed for Pure Fission Nuclear Weapons.* NRDC, 1995.

[10] IAEA. Database for *Prompt Gamma-ray Neutron Activation Analysis.*
Available online: https://www-nds.iaea.org/pgaa/pgaa7/index2.htm

[11] IAEA, *Database of Prompt Gamma Rays from Slow Neutron Capture for Elemental Analysis*, 2007. ISBN: 92-0-101306-X.
Available online: http://www-pub.iaea.org/books/IAEABooks/7030/Database-of-Prompt-Gamma-Rays-from-Slow-Neutron-Capture-for-Elemental-Analysis

[12] R. Keyser, T. Twomey, D. Upp. *Performance of Light-Weight, Battery-Operated, High Purity Germanium Detectors for Field Use.* INMM, July 2003.

[13] TSA Systems, Ltd. *PRM-470CGN OPERATIONS MANUAL*. December 7, 2005.

[14] R. Berndt, P. Mortreau. *Monte Carlo modelling of a N-type coaxial high purity germanium detector.* Nuclear Instruments and Methods in Physics Research Section A: Accelerators, Spectrometers, Detectors and Associated Equipment. Volume 694, 1 December 2012, pp. 341–347.

Software Development for Radionuclide Analysis Applications

Kaiser, Matthias M.Sc.
Kim, Sergey M.Eng.
Baltic Scientific Instruments, Ltd.Ganibu dambis 26, LV-1005 Riga, Latvia
E-mail: m.kaiser@bsi.lv, s.kim@bsi.lv

Danilenko, Vladimir Ph.D.
Kovalsky, Eugene
LSRM, Ltd., General Alekseev avenue 15, Zelenograd, 124460 Moscow, Russia
E-mail: danilenko@lsrm.ru, kovalsky@lsrm.ru

Berlizov, Andrey Ph.D.
Division of Technical and Scientific Services, Department of Safeguards, IAEA, Vienna, Austria,
E-mail: a.berlizov@iaea.org

Abstract:

In the field of gamma-ray spectroscopy, high purity germanium (HPGe) detectors are widely known for their excellent energy resolution, which can't be reached by any other detector type. However, to be able to use this high energy resolution to the full extend, the spectrum has to be processed and analysed by highly sophisticated software applications. To offer the best possible solutions for our customers, we constantly improve our software and develop new software applications.

Software applications in gamma-ray spectroscopy have to fulfil a wide range of tasks. In laboratory applications, extremely precise measurements have to be obtained, analysed and later presented in a report. The analyzation process as well as the report have to fulfil national and international standards like ISO 11929. The user-friendly integration of these standards into the SpectraLine software was crucial to assure precise results and verifiability in the every-day laboratory routine.

In-situ measurements are, due to their diverse applications, a complicated field for the software development. To assure precise measurements of radioactive waste, nuclear or scientific facilities and other structures it is necessary to calibrate the detectors for a large variety of sample geometries. To avoid time consuming physical calibration processes, mathematical Monte-Carlo simulations, as implemented in the EffMaker software, are used. In the case of border controls, first-response or defence applications the software has to include next to the expert mode of operation, also an easy mode. These two user levels are implemented in the basic spectrometric software for handheld devices such as NitroSPEC or HandSPEC in such a way, that both user types can operate the device easily and get the best possible results.

Additional, the SpectraLine software allows to monitor the health of the detector closely to assure the quality of each measurement and to avoid the undetected deterioration of the detector specifications. This Quality Assurance (QA) system is user-friendly, to enable all users to monitor the detector health.

Keywords: spectroscopy; HPGe; software; analysis

1. Introduction

To offer our customers together with our spectrometers a high quality software solution, we constantly develop new software and improve the already existing solutions. These new developments and improvements are conducted in strong cooperation with our partner LSRM.

As the field of gamma spectroscopy is very broad, we offer different software packages for different applications. Additionally, we often develop and produce highly customized solutions, to address the specific needs of our costumer. In these cases, often also special software applications or add-ons have to be developed.

In section 2 we will give you a short introduction to the different software solutions Baltic Scientific Instruments offers.

To show you our solution, to avoid time consuming physical calibration in cases like in-situ measurements, body-scanners, and waste assay monitoring, applications, etc, we will introduce our **EffMaker** software in section 3.

Further, we will introduce our newest efforts to provide full, high quality solutions for the end-user in section 4 and 5, where we will talk about the implementation of the ISO 11929 and a QA system into our software.

Finally, we will give a short introduction into our new software language packages, which will enable more users to use our software without any language barrier in section 6.

2. Software Applications

The basic software module for all our devices is the **SpectraLine** software family. Depending on the application, we offer several specialized versions. For the most cases **SpectraLineGP** (Gamma Precision) is the software package of choice. It comes with an automatic calibration tool, nuclide library, activity calculation function, QA module (more in section 5), a report editor and an editor for reference materials (Etalon editor).

Other software applications of the **SpectraLine** software family, are **SpectraLineADA** (Alpha Decay Analysis) for our alpha spectrometers, **SpectraLineBG** (Beta Gamma) for beta-gamma spectrometers, **SpectraLineNM** (Nuclear materials) that is used for the measurement of the enrichment level of Pu or U in nuclear materials, **SpectraLineHandy** which includes attenuation corrections and an estimation tool for the activity calculation for hand held applications and the **SpectraLineDefender** that was specially designed for border controls, safe guard applications and other operations to detect illicit trafficking of radioactive materials.

All our hand held devices include a basic software application based on **SpectraLineGP.** This basic software allows the calibration of the device, the acquisition of spectra and includes basic analytical tools for radionuclide detection and the calculation of the activity. Additionally, it includes a gamma dosimeter and the possibility to connect wireless to the device.

We are often involved in R&D projects and new developments for costumers with special applications. A good example for that are automated systems like our **Automated Spectrometer** or the **FlowSPEC**. These highly automated spectrometers require a high level of software automation. The **SpectraLine** software family is flexible enough, to provide these automation possibilities with small modifications and add-ons. Other modifications are possible.

Additionally to the **SpectraLine** software family we offer the **NuclideMasterPlus** software that includes an extended nuclide library with the possibility to create customized nuclide libraries for the **SpectraLine** software, detailed decay chains, true-coincidence-summing corrections [1] and a basic module for the mathematical efficiency curve calculation using Monte-Carlo Methods for rotation symmetrical samples (for more information see section 3).

In case more advanced sample geometries have to be modelled, we offer the **EffMaker** software with a full Monte-Carlo simulation for the efficiency curve of the detector and any sample geometry (more in section 3).

3. Monte-Carlo Efficiency Simulations

We offer, as mentioned in section 2, two levels of efficiency curve simulations. Both options use Monte-Carlo simulation techniques to create an efficiency curve from the detector and sample geometry. The basic difference of the EffCalcModule as implemented in the **NuclideMasterPlus** software and the **EffMaker** software, is the level of complexity for the sample geometry.

The EffCalcMC module allows the efficiency simulation of semiconductor and scintillation detectors of arbitrary sizes and for basic laboratory sample geometries like Marinelli beakers, cylindrical objects and point sources of arbitrary size and composition.

Besides the efficiency calculation the option of calculation of true coincidence correction factors is supported in EffCalcMC module [1] [2]. These factors have a significant impact for geometries with great registration efficiency. The true coincidence modelling is performed using the decay schemes of radionuclides in ENSDF-file [3].

EffMaker has been developed for in-situ registration efficiency calibration of spectrometers. Since the package has been intended firstly for the modelling of objects with high attenuation of gamma-radiation, like the containers with radioactive wastes, transport containers for radioactive and nuclear materials, the importance sampling is used in the modelling process. Moreover the modelling process is broken down into 2 steps: 1) modelling of the function of the detector response to the monochromatic photon emission; 2) getting the sample radiation spectrum outside the detector.

The operation of convolution of the sample radiation spectrum and the detector response function is resulted in both the spectrometer efficiency in the geometry of the measured sample and the spectrum of the sample of the certain radionuclides composition.

The **EffMaker** software provides the possibility to model any detector or sample geometry. **EffMaker** uses for this purpose an in-built 3D GUI (see Figure 1) with preprogramed 3D patterns to simplify the modelling process. The software not just simulates the detector, but the whole spectrometer, which gives the possibility to calculate shielding effects of different components of the set up. The in-built 3D GUI enables the user to model even very complicated objects, like loaded trucks, human or animal bodies, complicated waste structures, etc. in a reasonable amount of time.

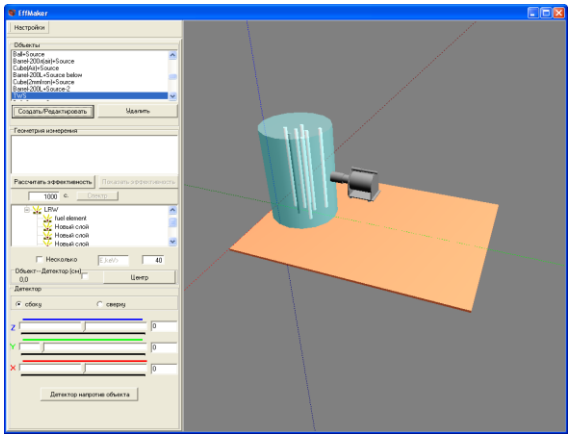

Figure 1: Example picture of the 3D GUI of EffMaker.

EffMaker has passed the metrological certification in one of the key metrological institutes in Russia as a part of the method of measurement detailed in the document «The method of measurement of activity of gamma- emitting radionuclides in the containers with radioactive wastes using the gamma-spectrometric system and SpectraLine-EffMaker software of LSRM Ltd».

4. Implementation of ISO 11929

Metrological Institutes and many research facilities have to apply national and international standards to their work routines. In the field of ionizing radiation measurement the ISO 11929 is one of the most important standards and defines the characteristic limits, their calculation and the presentation of the measurement results in a report. Laboratories have to prepare their measurement results often in accordance to this standard with additional requirements for their national standards.

The current version of the ISO 11929 is the ISO 11929:2011-01 [4], which was implemented into our **SpectraLine** software family. The main point of this standard is the calculation of the so called characteristic limits. The characteristic limits are an indicator of the reliability of the measurement results and consist of the decision threshold, detection limits and the limits of the confidence interval (for more information and the definition of these terms, please check [4]).

Classical software packages follow the formalism of Curie [5]. The ISO 11929, however, is breaking with this tradition and is using Bayes statistics instead of frequentist statistics as used by Curie. This allows to include uncertainties due to sample preparation, geometrical uncertainties and other effects that can influence the overall measurement uncertainty of a value.

In a mathematical sense that means, that any measurement value y is equal to a measurement specific model function G, which is a function of a set of estimated input values x_i :

$$y = G(x_1, \dots, x_m)$$

In which the x_i are the estimated values gathered from prior knowledge and the current measurement results. This leads to the formula for the standard uncertainty in Bayes statistics that is given by:

$$u^2(y) = \sum_{i=1}^{m} \left(\frac{\partial G}{\partial X_i}\right)^2 u^2(x_i)$$

In which the X_i are exact values that correspond to the estimated values x_i. The exact mathematical expression for G depends on the model that is used to describe the measurement process. I will not go further into the choice of the function G and the explicit calculation of the standard uncertainty, for more information, please check [4].

For our software package the usage of Bayes statistics for the calculations has two major impacts. The first difference is, that the software has to have the possibility for the user to input the information about the uncertainty he gathered prior to the measurement. For this purpose, an easy to understand user interface was created to enable the user to insert the pre-calculated uncertainties. The second major difference is the calculation of the resulting standard uncertainties and most important of the characteristic limits, which are used as an indicator for the reliability of the statistical calculations.

All results of the measurement, together with the characteristic limits and all information that characterize the circumstances of the measurement and analyzation are then presented in form of a report file, that is created in accordance with ISO 11929.

5. Implementation of Quality Assurance System

Quality Assurance Systems are a very important part of a modern Spectra analyzation software. These systems monitor the detector health in user defined intervals, to detect deterioration of the detector specifications at an early stage. This allows the user to proof the quality of his measurements and the service company to detect detector problems faster and to react before a fatal error occurs.

The QA system as integrated into the **SpectraLineGP** software will allow the user to monitor the temporal change of the FWHM values, peak position and efficiency for user selected energy peaks and the background level of the whole system. This data is acquired in user defined intervals and visualized in a graph (see Figure 2). The results can be printed in a user defined Report.

The resulting graph consist of three different coloured lines (user defined colouring) and the data points. The middle line is the average of the value, which is calculating at the installation of device with three separate measurements. The second pair of lines mark the borders of the warning level, which depends on the user defined confidence interval. If a value is outside the warning level, the measurement is marked. In case of warning, the system should be monitored strictly and the checking intervals should be minimized. In case the detector specifications deteriorate further, the producer or service company should be informed. The third pair of the lines are the lines that indicate the borders

of the alarm level. Is a value outside this alarm level it is marked red and is a strong indicator for a detector failure. In this case the producer or service company should be informed immediately.

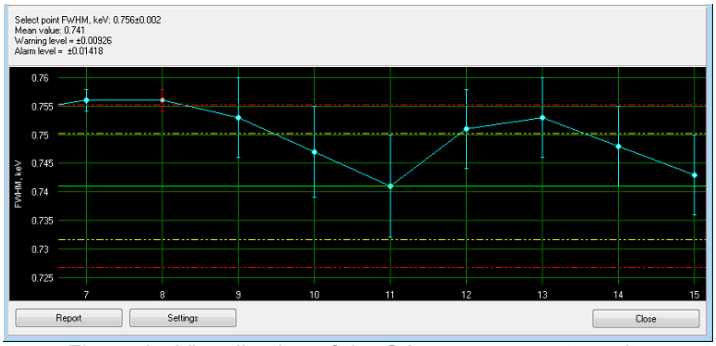

Figure 2 : Visualization of the QA measurement results.

6. Language Packages

To enable our international user community to use our software without barriers, we are constantly increasing the amount of languages our software is available in. Currently the software supports English, German, Russian and Chinese language visualization. In the near future we will add Spanish and French. Please contact our Team in case you need additional language packs, we are happy to help.

References

[1] Berlizov A.N., Danilenko V.N., Kazimirov A.S., Solovyeva S.L.,, "True coincidence correction factor calculation for cascade gamma — radiation based on statistical modeling with the use of evaluated nuclear data.," *Atomic Energu (RU),* vol. 100, no. 5, pp. 382-388, 2006.

[2] Berlizov A. N., Solovyeva S. L., A, "A Dynamic Link Library for calculating true-coincidence summing correction factors," vol. 276, no. 3, pp. 663-668, 2008.

[3] Tuli J. K., "Evaluated Nuclear Structure Data File. A Manual for Preparation of Data Sets," 2001.

[4] *ISO 11929:2011-01,* International Organization for Standardization (ISO), 2011.

[5] Curie L. A., "Limits for Qualitative Detection and Quantitative Determination," *Anal. Chem,* vol. 40, pp. 586-593, 1968.

Method and validation for the preparation of a plutonium age dating reference material

Zsolt Varga, Jozsef Zsigrai, Adrian Nicholl, Maria Wallenius, Klaus Mayer

European Commission, Joint Research Centre (JRC), Institute for Transuranium Elements (ITU)
Postfach 2340, 76125 Karlsruhe, Germany
E-mail: zsolt.varga@ec.europa.eu, jozsef.zsigrai@ec.europa.eu

Abstract:

The aim of the present work is the method development and validation of a plutonium age dating reference material. The principle is based on the complete separation of decay products at a well-known time and with a verified separation efficiency. The completeness of separation was verified by the addition of ^{233}U and ^{243}Am spikes to the starting material and their re-measurement from the final product. The final chemical purification of the material took place on 23 July, 2014. Altogether about 1.2 mg Pu age dating reference material was purified to produce 10 items, each containing ~120 μg Pu in solid form. The prepared material can be used for method validation and development in nuclear safeguards and forensics.

Keywords: plutonium; age dating; radiochronometry; reference material

1. Introduction

Several characteristics (so-called *signatures*) of the material can be used to verify the declaration of an unknown or questioned material, such as isotopic composition of Pu, U, Pb or Sr, elemental impurities, trace-level radionuclide content, crystal structure or anionic residues [1, 2]. Besides these parameters, the elapsed time since the last chemical purification of the material (commonly referred to as the *age* of the material) can also be measured for radioactive and nuclear materials. This unique possibility is based on the presence of radionuclides and their radioactive decay: during its production, the radioactive material is chemically purified from the impurities, including also its radioactive decay products. After the chemical separation of a radionuclide, its radioactive progenies start to grow-in into the material. The theoretical amount of daughter nuclide formed by the decay can be calculated by the use of the equations of the radioactive decays (Bateman equations) [3]. The ratio of the daughter nuclide amount relative to the amount of its parent nuclide can be calculated as follows:

$$\frac{N_{daughter}}{N_{parent}} = \frac{\lambda_{parent}}{\lambda_{daughter} - \lambda_{parent}} \left(e^{-\lambda_{parent} t} - e^{-\lambda_{daughter} t} \right) + \frac{N^0_{daughter}}{N_{parent}} e^{-\lambda_{daughter} t} \qquad (1)$$

where $N_{daughter}/N_{parent}$ is the amount (atom) ratio of the daughter and parent nuclides in the sample, $\lambda_{daughter}$ and λ_{parent} are the decay constants of daughter and parent nuclides, respectively, $N_{daughter}^0$ is the residual daughter nuclide after the chemical separation, and t is the elapsed time since the separation of the radionuclides. The daughter-to-parent ratio ($N_{daughter}/N_{parent}$) is often referred to as chronometer, while the elapsed time (t) is called the age of the material. If the residual daughter nuclide is completely separated ($N_{daughter}^0$ is equal to 0), the age of the material (t) can be determined after the measurement of the $N_{daughter}/N_{parent}$ ratio in the sample.

The obtained material age is a self-explaining parameter, and does not require any comparison sample or database for its interpretation. Therefore, it is highly useful to verify the declared origin in nuclear safeguards, or to identify the origin of an unknown illicit material in nuclear forensics [4-6].

This work describes a novel procedure for the preparation of a plutonium age dating reference material and the validation of the method. No such material is currently available to validate plutonium age dating. Our approach is based on the complete chemical separation of plutonium from its U and Am decay products at a well-known time. The completeness of U and Am separation was verified by the addition and re-measurement of ^{233}U and ^{243}Am at the beginning and after the chemical separation. Therefore, the Pu decay products present in the material shall derive solely from the decay of the Pu isotopes present in the material after the chemical separation and their ratio relative to the parent nuclide is governed by the radioactive decay laws. This method has already been proven for the production of U age dating certified reference material (IRMM-1000) [7]. Using this approach, a reference material with an accurately known production date can be prepared, together with a very low uncertainty down to a few hours. To validate the applied method the production date was measured by ICP-MS and gamma spectrometry following a known period of time after the preparation of the material and by comparing the measured ages with the known production date.

2. Experimental

2.1. Reagents and materials

All labware was thoroughly cleaned before use. Nitric acid was Suprapur grade (Merck, Darmstadt, Germany), which was further purified by subboiled distillation (AHF analysentechnik AG, Germany). For dilutions ultrapure water was used (Elga LabWater, Celle, Germany). Purum grade hydroxylamine nitrate solution (18% $NH_2OH{\cdot}HNO_3$ in H_2O) and analytical grade $NaNO_2$ were purchased from Sigma-Aldrich (Steinheim, Germany). ^{233}U and ^{242}Pu isotopic standards were used to spike the samples for the uranium concentration measurements. The ^{233}U concentration in the spike was calibrated against EC NRM 101 uranium metal by thermal ionization mass spectrometry (TIMS), while the ^{242}Pu spike was a IRMM-085 standard from the Institute for Reference Materials and Measurements (Geel, Belgium). Nominally 1% enriched uranium U-010 standard reference material from National Bureau of Standards (NBS, USA) was used to correct for instrumental mass discrimination. IRMM-185 (certified $n(^{235}U)/n(^{238}U)$ is $(2.00552 \pm 0.00060) \times 10^{-2}$) isotopic reference material was used to check the accuracy of the uranium isotope ratio measurements. TEVA extraction chromatographic resin (50-100 μm particle size, active component: aliphatic quaternary amine) supplied by Triskem International (Bruz, France) was used for the chemical separation. 0.4 mL of the TEVA resin was placed in plastic Bio-Rad holders (diameter: 6 mm, length: 14 mm) and was covered with a porous Teflon frit (Reichelt Chemietechnik Heidelberg, Germany) to avoid mixing. Before use, the column was cleaned with 1 mL of 0.02 M HF/0.02 M HNO_3 followed by conditioning with 4 mL 3 M HNO_3.

2.2. Preparation of the Pu age dating reference material

The Pu material was separated from U and Am progenies using extraction chromatography (TEVA resin). For the preparation approximately 2 mg Pu standard was dissolved with 5 mL 3 M HNO_3 solution in a perflouroalkoxy alkane (PFA) screw cap vial. The sample was mixed with a weighed aliquot of ^{233}U and ^{243}Am spikes, each containing of about 50 ng of the spike. The sample was thoroughly homogenized. The solution was mixed with 0.1 mL 1 M $NH_2OH{\cdot}HNO_3$. The $NH_2OH{\cdot}HNO_3$ serves to adjust the oxidation state of Pu to Pu(III). After a few minutes' waiting (the sample colour changes from dark green to pink), 0.3 mL 3 M $NaNO_2$ was added to the sample, which oxidizes the Pu to Pu(IV) oxidation state. Under such conditions Pu(IV) and Th(IV) retains strongly on the TEVA resin, while U and Am have little affinity to the resin. After loading the solution on the TEVA resin, the vial and the column were washed with 5 mL 3 M HNO_3, followed by the stripping of Pu as Pu(III) with 1 mL 3 M HNO_3/0.02 M $NH_2OH{\cdot}HNO_3$.After evaporation the TEVA separation was repeated twice. The time of the last chemical separation was registered (23 July, 2014, 11:00-11:40 a.m.), which serves as the production date of the material.

The separation was followed by ICP-MS and alpha spectrometry by taking samples from each step of the chemical separation (load, wash and Pu elution). The Pu chemical recovery was about 85%, however, relatively large portion of the Pu sample was taken and lost due to the fact that a sample aliquot was taken from each step of the procedure. The Am and U separation factors were calculated based on the ratio of the known ^{233}U and ^{243}Am amount added to the material before the separation (50 ng each) and their amount in the final, purified solution. The ^{233}U and ^{243}Am amount in the final solution was below detection limit, corresponding to minimum U and Am separation factors of 2.0 ×

10^4. This value results in that the residual U and Am amount correspond to less than 1 day if converted to age by Eq. 1.

2.3. Measurement of age by ICP-MS and gamma spectrometry

The sample preparation and Pu age measurement are described in details elsewhere [8]. The Pu and U isotopic measurements were carried out using a double-focusing magnetic sector inductively coupled plasma mass spectrometer (ICP-MS) equipped with a single electron multiplier (Element2, Thermo Electron Corp., Bremen, Germany). The ICP-MS instrument is attached to a nuclearized glove box in order to handle plutonium. All measurements were carried out in low resolution mode (R = 300) using a low-flow micro-concentric nebulizer operated in a self-aspirating mode (flow rate was approximately 50 μL min^{-1}) in combination with a stable introduction system (SIS) quartz glass spray chamber. The measured isotope ratios obtained by ICP-MS were corrected for instrumental mass bias using linear correction. All dilutions and spike additions for the isotope dilution analysis were done gravimetrically.

The gamma spectrometry measurements were carried out to measure the age based on the $^{241}Am/^{241}Pu$ chronometer. Spectra were taken by a planar high-purity Germanium detector (ORTEC SGD-36550), set to record spectra in the energy range 0-300 keV Total spectrum acquisition time was 60 hours. The $^{241}Am/^{241}Pu$ activity ratio and the corresponding age were calculated from the spectra by the software MGA v10 [9-11].

3. Results and discussion

The measured age results of the Pu certified reference materials are summarized in Table 1. The $^{241}Am/^{241}Pu$ chronometer was measured by gamma spectrometry, while the $^{234}U/^{238}Pu$, $^{235}U/^{239}Pu$ and $^{236}U/^{240}Pu$ chronometers were measured by ICP-MS. The measured ages are given relative to the measurement date for the gamma spectrometry or to the time of the sample preparation in case of ICP-MS, i.e. the calculated elapsed time (t) was subtracted from these specified reference dates. The obtained results agree well with the know production date of the material (23 July, 2014). Furthermore, the ages obtained by the different chronometers give identical results (concordant ages) proving that the both Am and U separations were complete.

	Chronometer			
	$^{241}Am/^{241}Pu$	$^{234}U/^{238}Pu$	$^{235}U/^{239}Pu$	$^{236}U/^{240}Pu$
Production date	19 July 2014 ± 10 days	23 July 2014 ± 3.1 days	21 July 2014 ± 4.1 days	23 July 2014 ± 1.5 days
Measured age in days (reference date)	189 ± 10 (24 January 2015)	222.3 ± 3.1 (3 March 2015)	224.1 ± 4.1 (3 March 2015)	222.1 ± 1.5 (3 March 2015)

Table 1: Measured ages and production dates of the Pu age dating reference material. Known production date of the sample is 23 July 2014. Uncertainties are expressed as expanded uncertainties (k = 2).

4. Conclusions

A novel method has been developed for the preparation of a Pu age dating reference material. It is based on the proven concept developed for the production of the IRMM-1000 uranium age dating material. Using these finding we have a possibility to produce Pu age dating reference material at larger scale, and also to tailor the reference material target characteristics to the needs of the safeguards and forensic laboratories (e.g. concentration, amount or Pu isotopic composition). Although the current work focuses on the bulk Pu age dating methodology, it can be extended in the future to produce Pu particles with known production date.

5. Acknowledgements

The EC-JRC-ITU Analytical Service is kindly acknowledged for their valuable assistance.

6. References

[1] Donohue DL; *Strengthened nuclear safeguards; Analytical Chemistry;* 2002; 74; p 28A-35A.

[2] Mayer K, Wallenius M, Varga Z; *Nuclear forensic science: Correlating measurable material parameters to the history of nuclear material; Chemical Reviews*; 2013; p 113:884-900.

[3] Bateman H; *Solution of a System of Differential Equations Occurring in the Theory of Radio-active Transformations; Proceedings of the Cambridge Philosophical Society, Mathematical and physical sciences*; 1910; p 423.

[4] Shinonaga T, Donohue D, Ciurapinski A, Klose D; *Age determination of single plutonium particles after chemical separation; Spectrochimica Acta - Part B Atomic Spectroscopy*; 2009; 64; p 95-8.

[5] Nygren U, Ramebäck H, Nilsson C; *Age determination of plutonium using inductively coupled plasma mass spectrometry; Journal of Radioanalytical and Nuclear Chemistry*; 2007; 272; p 45-51.

[6] Wallenius M, Mayer K; *Age determination of plutonium material in nuclear forensics by thermal ionisation mass spectrometry; Fresenius Journal of Analytical Chemistry*; 2000; 366; p 234-238.

[7] Venchiarutti C, Varga Z, Richter S, Nicholl A, Krajko J, Jakopic R, Mayer K, Aregbe Y; *Preparation and certification of IRMM-1000a (20 mg) and IRMM-1000b (50 mg) - Certified uranium reference material for the production date; EUR - Scientific and Technical Research Reports*; 2015.

[8] Varga Z, Nicholl A, Wallenius M, Mayer K; *Plutonium age dating (production date measurement) by inductively coupled plasma mass spectrometry; submitted to Journal of Radioanalytical and Nuclear Chemistry*; 2015.

[9] Gunnink R, *"MGA": A Gamma-Ray Spectrum Analysis Code for Determining Isotopic Abundances, Volume 1, Methods and Algorithms*, *Lawrence Livermore National Laboratory Report UCRL_LR-103220, Vol. 1*; 1990.

[10] Gunnink R, Ruhter WD; "*MGA": A Gamma-Ray Spectrum Analysis Code for Determining Isotopic Abundances, Volume 2, A Guide to Using MGA, Lawrence Livermore National Laboratory Report UCRL-LR-103220, Vol. 2*; 1990.

[11] Croft S, Bosko A, Gunnink R, Philips S, Lamontagne J, Koskelo M, McElroy R, *MGAv10: The Latest Evolution in the Multi-Group Analysis Code, Proceedings of the 12th International Conference on Environmental Remediation and Radioactive Waste Management, Liverpool, UK*; 2009.

Potential Causes of Inventory Differences at Bulk Handling Facilities and the Importance of Inventory Difference Action Levels

Alan Homer, Brendan O'Hagan

Nuclear Materials Accountancy & Safeguards Department
Sellafield Limited, Seascale
Cumbria, CA20 1PG, United Kingdom
E-mail: alan.homer@sellafieldsites.com

Abstract:

Accountancy for nuclear material can be split into two fundamental categories. Firstly, where possible, accountancy should be in terms of items which are objects that can be transferred as discrete packages and their contents are fixed at the time of their creation. All items must remain accounted for at all times and a single missing item is considered significant. Secondly, where nuclear material is unconstrained, for example in a reprocessing plant where it can change form, there is an uncertainty that relates to the amount of material present in any location. Cumulatively, these uncertainties can be summed and provide a context for any estimate of material in a process. Any apparent loss or gain between what has been physically measured within a facility during its physical inventory take and what is reported within its nuclear material accounts is known as an inventory difference. The cumulative measurement uncertainties can be used to set an action level for the inventory difference so that if an inventory difference is observed outside of such action levels, the difference is classified as significant and an investigation to find the root cause(s) is required. The purpose of this paper is to explore the potential causes of inventory difference and to provide a framework within which an inventory difference investigation can be carried out.

Keywords: inventory difference; action levels; uncertainty; measurement; investigation

1. Introduction

Accountancy for nuclear material falls into two fundamental categories. Firstly, where possible, accountancy is in terms of 'items'. Items are objects that can be transferred as discrete packages. Their contents are fixed at the time the discrete package or item is created. Generally, items are recognised in terms of being containers that can be counted, for example a uranium drum, a plutonium can or a transport flask. The safeguards criteria for areas where the nuclear material contents are only in the form of items is uncomplicated. Items are counted into and out of the area and all items must be accounted for. A single missing item is considered significant.

Where nuclear material is unconstrained, for example as part of a process within a reprocessing facility, then there is an uncertainty in any measure that relates to the amount of nuclear material present. Cumulatively these uncertainties can be summed and can provide a context for any estimate of material in the process. In summary, the aim is to know how much nuclear material is present by measurement and the level of confidence in that measurement by analysis of the uncertainty so as to demonstrate that the area is in control and to detect losses or diversion of nuclear material.

The difference between what is physically measured within a facility at a physical inventory take (PIT) and the amount of nuclear material declared within its nuclear material

accountancy system is known as the inventory difference (ID). The uncertainty of measurement defines what is known as the inventory difference action level (IDAL).

2. The Basic Units

For the remainder of this discussion, everything will be viewed in terms of quantity and proportion:

- Quantity is usually either volume or mass, however it can be the result of a more complicated indirect measurement system e.g. mass is equal to volume multiplied by density in plutonium nitrate (PuN) liquor transfers.
- Proportion is the concentration of a particular accountable nuclear material contained within an amount of some other substance e.g. the amount of plutonium in plutonium dioxide (PuO_2) powder.

Whether the nuclear material in question is an inventory item or the amount of nuclear material being transferred into or out of an area (a transaction), the nuclear material quantity is calculated in the same way, nuclear material is equal to quantity multiplied by proportion. For example, if a uranium trioxide (UO_3) drum contains 800 kg of UO_3, and its uranium assay is 88% (a proportion of 0.88), then 88% of the material in the drum is uranium, 704 kg.

3. What is Inventory Difference?

A minimum of once per calendar year (and at intervals of not greater than 14 months), each material balance area (MBA) will shutdown normal operations, move their nuclear material into an area where it can be measured and verified, and perform a PIT. During the period since the previous PIT, the nuclear material accountants will have maintained a book account (BA) where

Book **A**ccount = **O**pening Physical **I**nventory + **R**eceipts – **S**hipments (Eq. 1)

where the opening physical inventory (OI) is the amount of nuclear material in the MBA at the time of the previous PIT, and receipts (R) and shipments (S) are the amounts of nuclear material moved into and out of the MBA since the previous PIT. The results of the PIT are then compared with the book account. Theoretically these values should be identical, however in practice they usually differ producing an ID where:

$$\begin{aligned} ID &= PIT_{now} - BA \\ &= PIT_{now} - (OI + R - S) \end{aligned} \quad \text{(Eq. 2)}$$

and PIT_{now} is the amount of nuclear material measured at the current PIT. If there was no uncertainty involved with this process i.e. all measurements were exact, then the ID should be zero because everything would add up as expected. Although an observed ID will commonly occur due to the fact that it is not possible to measure all material exactly, the root cause of an ID can be due to many factors, some of which are examined later in this paper.

4. What is an Inventory Difference Action Level and why do we need it?

As nothing can be measured exactly, there are uncertainties associated with each measurement of inventory, receipts and shipments. These uncertainties can then be combined to calculate the total uncertainty on the ID (using Eq. 2). If the measured ID falls within the bounds given by the overall measurement uncertainty, then the statistical data supports a theory that the apparent difference is due to measurement uncertainty rather than a true difference. The IDAL is the maximum acceptable ID based on measurement uncertainty. If the ID is outside of these bounds then the difference must be investigated.

It is important that all measurement uncertainties for inventory, receipts and shipments are technically justified. This means that the uncertainties are underpinned with calibration data or reviewed technical papers justifying the parameters used. International Target Values (ITVs) [1] are primarily used as targets but can be used as a starting point for estimating uncertainties. The IDAL is required to ensure the plant is in control and, in the event of loss of control, to initiate the start of an investigation to determine the cause.

5. Who Needs an Inventory Difference Action Level?

Process facilities have nuclear material that is unconstrained (i.e. not confined to discrete containers) as the material is in a constant state of flux between holding vessels, with the material often undergoing a change in form. The measurement uncertainty then accumulates with each measurement which makes up the receipts, shipments and inventories. This can lead to an ID and hence an IDAL is required in these facilities.

Storage facilities do not need an IDAL since the material is constrained in containers such as drums and cans. There is however a need to count the containers to ensure none are missing. Exact knowledge of the number of containers does not imply exact knowledge of their contents. When the containers are put into the storage facility, the amount of material in each container is recorded in the inventory. Each container will have its own uncertainty which leads to a global uncertainty for the store. Take for example a PuO_2 storage can which consists of an inner can, a polyethylene bag and an outer can. The amount of nuclear material in the can is the gross mass minus the tare masses of the two cans and the bag making up the overall package. If the polyethylene bag mass was systematically being reported incorrectly, then the amount of nuclear material claimed to be in the store would be incorrect even though it can be confirmed that what went into the store is still in the store.

The storage area would not register an ID because the item count and the product can gross masses would be correct, but the supplying MBA would show a consistent ID as the shipments would be systematically biased. This type of problem is difficult to identify and the exact nature of the problem may only become truly apparent if the store and its contents are re-measured.

6. Causes of Inventory Difference

This work categorizes the main reasons why an ID may occur into six areas, shown diagrammatically in figure 1. It is not sufficient to identify a single cause without considering all contributory factors. Figure 2 shows that there are significant links that should be considered and it is worth noting that many of them lead back to the "personnel" category. These interconnections and the finer detail are discussed throughout the remainder of this paper. If learning from experience (LFE) is to have any meaning then it is important that all linking parts are examined.

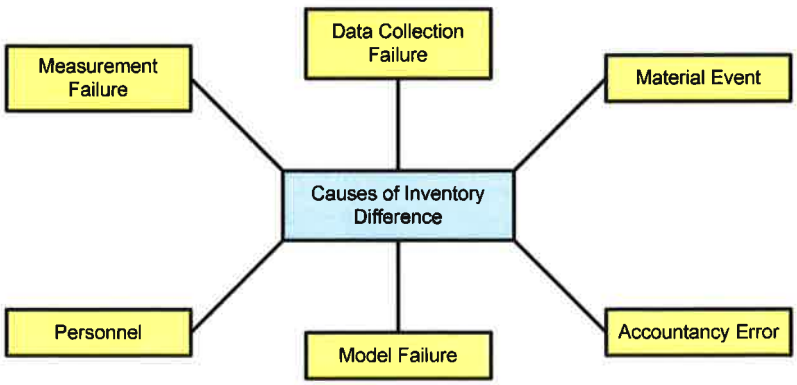

Figure 1: A diagram illustrating the main reasons why an inventory difference may arise.

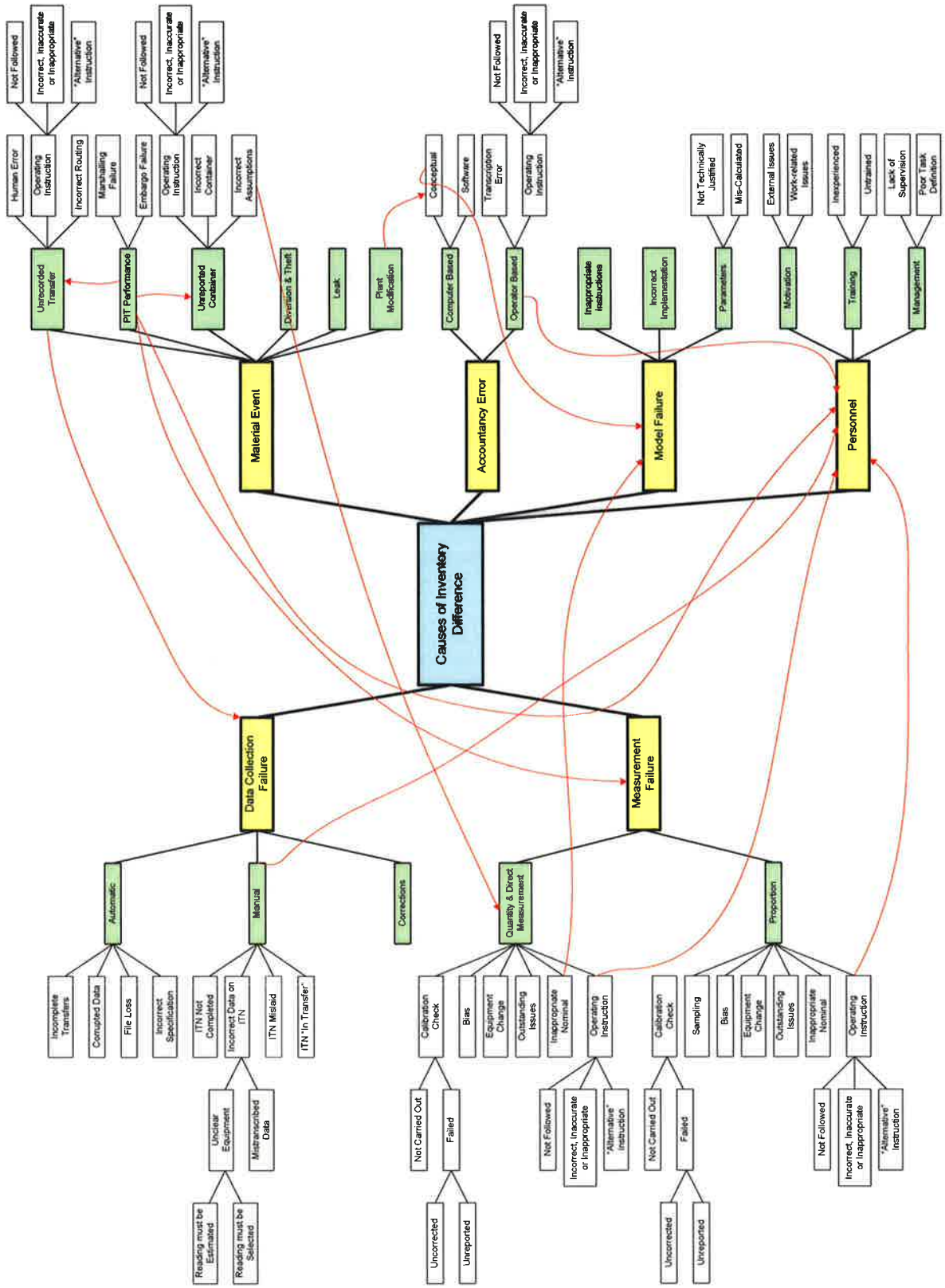

Figure 2: A diagram to illustrate potential causes of inventory difference and some of their various inter-dependencies.

When a potentially true ID is identified (i.e. an ID outside of the bounds of a calculated IDAL) an investigation must take place to explain what has happened within the associated material balance period (the period between two consecutive PITs). At Sellafield, the following framework for an investigation has been developed. The first phase of any ID investigation focuses on three main areas:

- Has there been a nuclear material event?
- Has there been a data collection failure?
- Has there been a failure of the nuclear materials accountancy model.

These questions will be considered in more detail in sections 6.1 – 6.3. If any of the questions are answered in the affirmative then they should be addressed immediately, the ID recalculated and if the issue is not resolved, the investigation should move into a second phase which is discussed in more detail in sections 6.4 – 6.6.

The second phase of the investigation focuses on whether or not there been a measurement failure, an accountancy error or if there are any personnel issues with people involved. Generally, the most common cause of an ID is measurement failure as particularly for flows, small errors can accumulate over a long campaign into very substantial amounts. It should also be remembered that, although measurement failures can also be associated with inventory measurements, these would apply to both opening and closing inventories and therefore the error would be associated with the difference between opening and closing values. Given that, under most circumstances, the facility should be minimising its inventory, the status of a facility at PIT is usually fairly constant and this difference is not usually that large.

6.1. Nuclear Material Event

Of all of the potential causes of ID, a nuclear material event is the most crucial. The underlying premise of a nuclear material event is that nuclear material is not where it is expected to be.

6.1.1. Diversion and Theft

From a safeguards perspective the worst scenario is that nuclear material has been diverted or stolen. Good practice therefore informs that any investigation should start from a position of no diversion or theft has occurred. It is essential to inform the Security Department as soon as there is thought to be an apparent breach of IDAL. This approach allows the Security Department to perform any preliminary investigations they see necessary, feedback their findings to provide assurance to the Nuclear Material Custodian / Controller and through them to other stakeholders.

6.1.2. Nuclear Material Leak

The Nuclear Material Custodian / Controller should arrange for those with direct oversight of the various areas within an MBA to perform a visual check of plant areas. Where a direct visual check is not possible, assurance should be sought through indirect measures such as sump checks, neutron monitor alarms etc. looking for any unusual readings or behaviours.

6.1.3. PIT Performance

When a PIT is performed, best practice informs that all movements should be embargoed in an area. In practice however, movements are often still required between a PIT and physical inventory verification (PIV). All such moves should be recorded and provided to the safeguards inspectorates. Failure to correctly record moves or lack of communication between the facility, the Nuclear Material Custodian / Controller and the Nuclear Materials Accountancy and Safeguards (NMAS) department can easily lead to nuclear material being

mislaid or double counted, its location being recorded incorrectly and general confusion surrounding nuclear material control.

6.1.4. Unrecorded Transfer and/or Unreported Container

An unrecorded transfer would tend to be caused by a procedural breakdown when a nuclear material move takes place with no paperwork generated, paperwork going astray, or a failure in an automated transfer system. An unreported container could be described similarly but in actuality would include finds[1] of nuclear material. The nuclear material status of a facility is recorded on a list of inventory items (LII) and the Nuclear Material Custodian / Controller must ensure that there is a direct correlation between the LII and the facilities physical layout. For example, it can be easy to overlook a sweepings container in a glovebox if it is normally present and empty. Similarly, the assumption that a hopper is empty is open to challenge if no physical assessment has been made and / or the location is unverifiable.

6.1.5. Facility Modification

Nuclear materials accountancy is based on a shared model with the actual facility. The Nuclear Material Custodian / Controller is responsible for the control of nuclear material in their area and therefore must inform the NMAS department of any modifications to the facility. There is also a regulatory obligation to inform the safeguards inspectorates in a timely manner to ensure they can verify such modifications. If there is disconnect between the facility model and the nuclear materials accountancy system then transfers could be lost and storage locations missed.

6.2. Data Collection Failure

The premise of data collection failure is that the nuclear material is where it should be but there has been a process failure in collecting the data.

6.2.1. Manual Failure

Data is often recorded on some type of form and failure to complete an appropriate form is not necessarily easy to detect. Such failures may only be identified through a check within the facility for missing or extra inventory items against the LII. Mislaid or in-transfer forms are easier to identify as most forms for nuclear materials accountancy purposes have a sequence number which can be checked. The latter should become clear to the NMAS department when performing a check of paperwork received. At this time the NMAS department should also perform a quality check of the data received to identify transcription errors e.g. wrong decimal places recorded or figures incorrectly transposed.

6.2.2. Automatic Failure

The initial testing and commissioning of automatic data transfer should be sufficient to give confidence in a systems performance, however, if a facility suffers an unexpected outage it is possible for errors to occur. Data may be lost or incorrect shutdown and restart procedures can give rise to file corruption or loss. Care must always be taken in the event of a power failure or unplanned shutdown to ensure that there is no effect on data transfer.

[1] A "find" is unforeseen nuclear material which is found in a material balance area.

6.2.3. Corrections

All corrections made to nuclear materials accountancy paperwork should be countersigned and be fully traceable. Similarly, where changes are made in the nuclear materials accountancy system, they should be logged, with an explanation to allow traceability in the event of an investigation.

6.3. Model Failure

The premise of a model failure is that measurements have been made correctly and the nuclear material is correctly located, but the interpretation of that data is inappropriate in some way. The Nuclear Material Custodian / Controller should commence an investigation utilizing both facility technical support and NMAS department as early as possible within the investigation. Such an investigation will effectively undertake a qualitative check on the nuclear materials accountancy model.

6.3.1. Inappropriate Assumptions

When a measurement is made there are usually some associated assumptions. For example, it is a reasonable assumption that the surface of a liquid is flat in a large vessel though not when estimating a level of a receptacle with a narrow diameter. Similarly, a container holding powders is unlikely to have a level surface where material has recently been dispensed. Also, powders in a vessel typically compact when left to settle, therefore the density will be different at the top and bottom causing sampling issues. The nuclear materials accountancy model must reflect physical reality as accurately as possible.

6.3.2. Incorrect Implementation

Generally, testing of software or spreadsheets which manipulate data should have been sufficiently detailed to ensure that the process exactly replicates manual calculation. It is possible, nonetheless, to generate incorrect data, especially if the implementer of the system and the user do not share a common set of assumptions. Equally important here is a review of the IDAL calculation itself because failure to capture all relevant details or incorrect estimations of associated uncertainties (both random and systematic) can lead to an ID uncertainty that is artificially small or large and consequently an IDAL that is simply unattainable or unrealistic.

6.3.3. Model Parameters

Where data manipulation takes place that involves the use of parameters then these parameters should be supported by a technical justification. Any that do not have an associated technical justification should be flagged for consideration.

6.4. Measurement Failure

The premise of measurement failure is that the nuclear material is where it should be but there has been an error in measuring the quantity or proportion of the material. Before investigating each and every measurement it is worthwhile assessing the probability of contribution to an ID that can be assigned to any particular flow or inventory location. By producing a list of all flows and inventory locations, a simple rule to prioritise areas of interest could be to assign the observed ID to each flow and inventory location and ask the question, what would it take to generate an ID of that magnitude from that specific flow or inventory point and what are the implications?

Such analysis should identify the most probable areas where measurement failure could produce or impact on ID and therefore provide some focus for the investigation. This does not

mean that smaller effects should be ignored – where identified they should still be corrected, but the most appropriate areas of concern should be targeted first.

6.4.1. Quantity and Direct Measurement

In general the first thought with quantity measures should be to analyse the routine verification activities of the measurement system. With weighing systems this should be relatively straightforward, with traceable evidence that the system has been recently calibrated and routine checks between calibrations have been performed to ensure the system is working as expected. With large vessels, and in general volumetric calibration, it may be extremely difficult to recalibrate after initial commissioning. The best option may be an inter-tank transfer comparison with other tanks in the processing stream.

Additional issues may occur where non-destructive analysis (NDA) equipment shares a joint function with safety and nuclear materials accountancy. Measurements generated for safety reasons can be deliberately biased to incorporate a 'worst-case' scenario for criticality purposes. Where such readings are used for nuclear materials accountancy without reference to a 'best estimate', these biases can accumulate. For example, PCM packets with an absolute plutonium content of less than half a gram should generate a zero accountancy value but the measurement system may typically record accountable quantities for safety purposes. It does not take many packets over a material balance campaign to generate a 1 kg ID.

6.4.2. Proportion

Where analysis for assay, concentration, or density takes place then it is important to confirm that no changes in the measurement process or equipment have occurred as these can affect both ID and IDAL. Where possible some repeat analysis for large bulk samples is useful confirmation as is the use of alternative procedures to ensure consistency and lack of bias.

6.5. Accountancy Errors

6.5.1. Computer-Based Errors

Computer based errors fall broadly into two areas, the first being conceptual issues. If there has been a plant modification, or change to a measurement process, does the accountancy system reflect physical reality? If not, there is a fundamental failure of the accountancy model and these changes can propagate errors throughout the accountancy system which could potentially result in material being unaccounted for, double counted or in the case where incorrect parameters are set in the underlying nuclear materials accountancy system code, incorrect data.

The second issue relates to the actual software itself which computes the nuclear material accountancy records. Where software is upgraded or operating systems are changed, robust testing of the accountancy system is required to ensure there are no bugs in the system. This is especially important when dealing with legacy accountancy systems which may have limited technical support and the expertise is not available to support transfer of the systems.

6.5.2. Operator-Based Errors

Ideally all nuclear materials accountancy systems would utilize automatic data capture and an operator or nuclear materials accountant would be responsible for peer-review and data verification. In many cases, especially with older plants, manual data entry by both plant operators and nuclear materials accountants is still required. An obvious error trap with manual data entry is transcription errors which can be difficult to recognise and correct. Therefore, a robust peer-checking process is essential.

The importance of clear, robust operating instructions must also be considered. Where operating instructions are not followed, are incomplete, inaccurate, inappropriate or there are multiple instructions for the same task, mistakes are likely to occur. Such issues also result in a lack of transparency, consistency and accuracy which is necessary for good nuclear materials accountancy.

6.6. Personnel

People work within systems and if those systems are properly constructed, supervised and appropriate training and understanding are given, then mistakes are less likely to happen. However, there always remains the 'human factor' meaning errors cannot be totally eliminated. To mitigate the propagation of repeatable errors it is good practice to undertake regular debriefs and post job reviews to ensure any LFE is captured.

A key personnel issue worth considering in an investigation is motivational issues. Are the individuals involved focussed on the task at hand? Has enough time been allocated to the operators for completing the PIT and the nuclear materials accountants for producing the relevant reports to the required quality? Secondly, are the individuals involved with the PIT, suitably qualified and experienced (SQEP'd). Mistakes can happen with both inexperienced and experienced personnel and it is key that all people involved with nuclear materials accountancy are aware of and maintain an awareness of their responsibilities and the impact that their actions may have. Finally, from a management perspective adequate supervision must be ensured to drive a high standard of plant condition at the time of the PIT, accountancy data is kept up to date and people involved have clear task definition.

7. Conclusions

The conclusions of this paper are as follows:

- In item accountancy areas of a facility, an IDAL is not required. A single missing item is considered significant, and an investigation required.
- In process areas of a facility, where material is changing form and measurements are being made, an IDAL is required. All measurements have an uncertainty and it is the cumulative sum of these uncertainties for all receipts into an area, shipments out of an area and for inventory measurements at a physical inventory take which determine the IDAL.
- An IDAL will change from one material balance period to the next as it depends on plant throughput and the amount of inventory change between successive physical inventory takes.
- If an ID falls outside of the bounds of a technically justified IDAL then an investigation should be performed.
- There are many potential causes of ID and this paper categorizes them into six key areas:

    1. Material Event
    2. Data Collection Failure
    3. Accountancy Error
    4. Measurement Failure
    5. Model Failure
    6. Personnel Issues

- Many causes of ID are interlinked and identifying the root causes of an ID is a complex task which must be fully examined. If a potential contributing cause to an ID

is identified early in an investigation, it should still be completed in its entirety to ensure all contributing factors are captured.

8. Privacy regulations and protection of personal data

The author agrees that submission of this work automatically authorises ESARDA to publish the work in whole or in part in all ESARDA publications – the bulletin, meeting proceedings, and on the website.

The author declares that this work is original and not a violation or infringement of any existing copyright.

9. References

[1] International Atomic Energy Agency, *International Target Values 2010 for Measurement Uncertainties in Safeguarding Nuclear Materials*, STR-368, Vienna, November 2010.

Session 11

Gamma Measurements

Best practices for determining uranium isotopic composition by MGAU and FRAM

T.Rüther[a,b], J.Zsigrai[a]

[a]European Commission,
Joint Research Centre (JRC),
Institute for Transuranium Elements (ITU),
Karlsruhe, Germany

[b]University of West Bohemia,
Faculty of Electrical Engineering,
Pilsen, Czech Republic

Abstract:

MGAU and FRAM are software codes which can be used for determining uranium isotopic composition by gamma spectrometry. The aim of this study is to establish best practices for using these codes to obtain the results as accurate as possible under given constraints. Uranium measurements can take place either in a laboratory (under optimal conditions) or in field (under non-optimal conditions). Both scenarios were investigated in this work. There are several factors affecting accuracy of analysis results. Some of the factors cannot be controlled. However, there are crucial factors that can be controlled such as the sample-to-detector distance and acquisition time. These two particular factors were studied. The study was based on using gamma-ray uranium spectra generated from real spectra of various certified materials and well characterized fuel pellets. The spectra were generated by Cambio software. This software randomly samples data from a real spectrum and allows generating "daughter spectra" having different number of total counts. This way enough statistically relevant data can be obtained. More than 10 000 spectra have been used in this study. This study also discusses influence of bismuth on the accuracy of MGAU and FRAM. The results of this work can help inspectors and analysts to appropriately set up gamma-spectrometric measurements of the uranium isotopic composition.

Key words: Gamma spectrometry, uranium isotopic composition, MGAU, FRAM

1 Introduction

MGAU and FRAM are software codes which can be used to determine uranium isotopic composition by analysing gamma ray spectra [1] [2]. Both codes are used by nuclear inspectors and analysts in many NDA applications. This study targets on establishing best practices for recording gamma spectra to by analysed MGAU and FRAM.

MGAU can report abundances of ^{235}U, ^{238}U and ^{234}U using gamma spectra in the energy range 0-300 keV. For certain samples MGAU is able to estimate $^{236}U/U$ ratio and detect the presence of ^{232}U. The code is capable of analysing uranium ranging from 0.3% to 93% ^{235}U enrichment [3]. FRAM possesses similar features to those of MGAU, however, gives advanced users more freedom to make their own customizations in the analysis procedure. Moreover, FRAM can also analyse plutonium and can utilize different energy ranges. However, this study deals solely with uranium and planar HPGe detectors to be used in the 0-300 keV energy range.

There are certain basic requirements that have to satisfy for using MGAU and FRAM and can be found in [4] [5]. The precision and accuracy of the MGAU and FRAM results is also influenced by other conditions and parameters. In this study, the particular interest is given to finding an optimal number of total counts and an optimal count rate. Results of this work may serve as guidelines for analysts and

inspectors to optimize their measurements and therefore determine the uranium isotopic composition by MGAU and FRAM more accurately.

2 Materials and equipment

The gamma spectrometers and software used in the study are listed in Table I and Table II, respectively.

Table I *Spectrometers used in the study*

Manufacturer	Internal Name	Detector	Type	Preamp	Cryostat	Rise time	Flat top
Canberra	AMM	GL0210R	LEGe Plnr.	2002CPSL	7600SL	5.6 µs	1.2 µs
Canberra	CP5	GL0210R	LEGe Plnr.	2002CPSL	CP5SL-Plus	5.6 µs	0.8 µs
Ortec	SGD	SGD-36550	LEGe Plnr.	-	Nitrogen Dewar	6 µs	0.8 µs

Table II *Software used in the study*

Software	Version	Year	Licence	Parameters
MGAU	4.2	2010	Canberra	-
FRAM	5.1	2011	Ortec	LEU_Plnr_060-250, HEU_Plnr_060-250
Cambio	120822	-	Freeware (U.S. DOE)	-

Following uranium samples have been used in the study:

- EC Certified Nuclear Reference Material 171 with various enrichments (0.7% - 4.5%) [6]
- 6 NBS standards (U_3O_8 powders) having various enrichments (from 3% up to 90%) [7]
- CRM 125A certified LEU fuel pellet [8]
- Two in-house characterized LEU fuel pellets[1] [9]

3 Optimal number of counts

Longer acquisitions lead to better counting statistics of gamma spectra. However, recording a spectrum beyond a certain acquisition time does not generate significantly better results. In other words, there is no sense to record a spectrum indefinitely, as the results of the analysis do not change after a certain time. The goal is to find the acquisition time after which the MGAU and FRAM results do not change anymore (or do not change significantly). Therefore this part of the study aims at finding the optimal acquisition time for MGAU and FRAM analysis with planar HPGe detectors

The optimal acquisition time depends on the count rate, which, in turn depends on many factors such as the sample activity, shielding, geometry, detector efficiency etc. Therefore, to be able to give general recommendations, the influence of the total number of counts in the spectrum on the accuracy of the results was studied. This resulted in finding an optimal number of total counts, above which the MGAU and FRAM results do not change anymore. Knowing the count rate, this can be easily converted to an optimal acquisition time, for any given sample and measurement setup.

3.1 Procedure for determining the optimal number of total counts

For carrying out a representative study, it is necessary to have a large amount of gamma spectra covering wide range of ^{235}U enrichments. Covering not only different kinds of samples (from depleted to high enriched uranium) but also different numbers of total counts for each of the samples would be almost impossible with real measurements. Therefore, so called "daughter spectra" were used in the study. They were generated by randomly sampling data from real high quality spectra recorded in our laboratories.

Spectra of the certified reference materials and well characterized fuel pellets were recorded. These so called "mother spectra" then served for generating sets of "daughter spectra" having different number of total counts (less than their mother spectra). This was done by using Cambio software [10]

[1] Detailed information on the isotopic composition and ratios can be found in [11].

which allows generating simulated spectra by randomly sampling data from real spectra. For each sample, 12 sets of 50 spectra were generated, each set having different number of total counts. More than 10 000 simulated spectra were used in this study. The results of the MGAU and FRAM analysis were then compared with certified isotopic ratios. Figure 1 illustrates the procedure of determining the optimal number of counts.

For comparing the MGAU and FRAM results with certified ratios, the so called MARD (Mean Average Relative Difference) was used. The MARD is described by Equation 1. To calculate the MARD, first the relative difference between measured and declared abundance of ^{235}U is determined. Then, the absolute value of this difference is taken and finally a mean for N spectra is calculated. In this particular case N is equal to 50 spectra that were generated for each of the sets of total counts.

Equation 1 *Mean Absolute Relative Difference (MARD). An indicator which has been used for comparing the MGAU and FRAM results with certified data of uranium abundances.*

$$MARD = \frac{\sum_{i=0}^{i=N} \left| \frac{M_i - D}{D} \right|}{N}$$

Where: Mi – Measured value
D – Declared value
N – Number of spectra

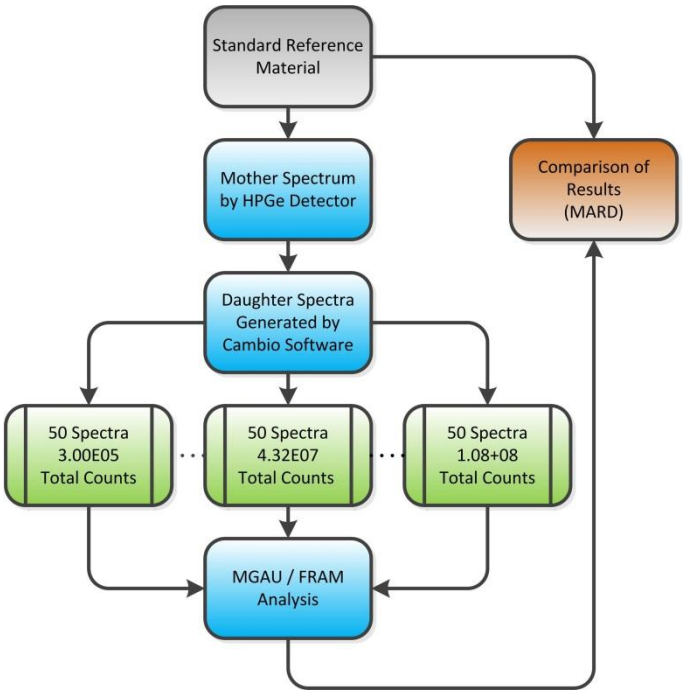

Figure 1 General procedure of determining the optimal number of total counts

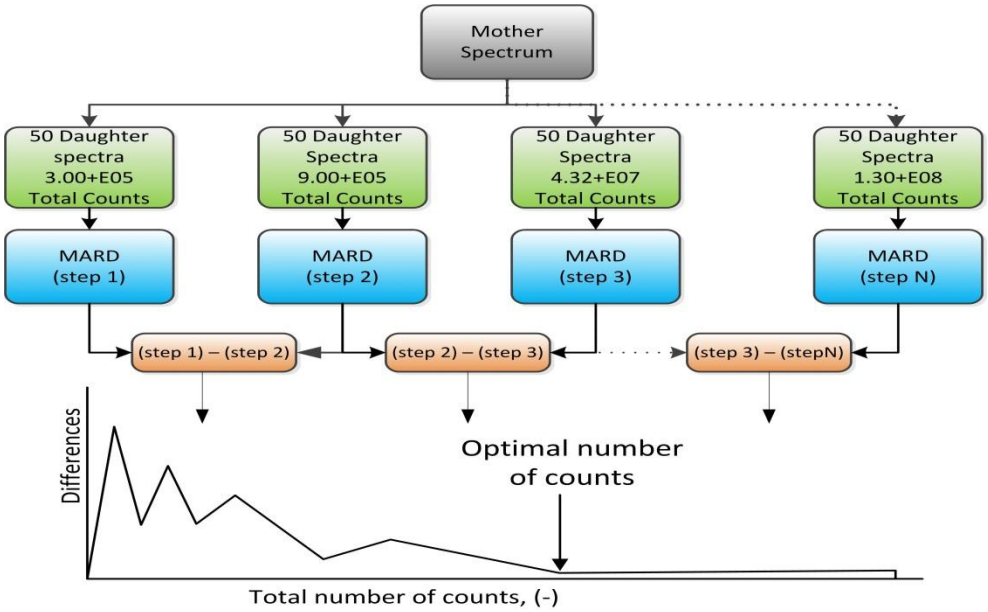

Figure 2 Detailed look at the procedure of determining the optimal number of counts, particularly at the process of getting the differences between the consecutive steps. The mother spectrum at the top serves for generating sets of daughter spectra having different numbers of total counts. For each individual set of 50 spectra the MARD value is calculated. In order to see how the MGAU and FRAM results change over the increasing number of total counts, the differences between every single step are calculated. The differences between consecutive steps are then plotted.

In order to determine the optimal number of counts, it was necessary to take a look at the development of the MARD values over the whole range of total counts. Differences between the consecutive steps (sets of 50 spectra) were calculated and plotted as it is illustrated in Figure 2. When the differences between consecutive steps become very low, it indicates that the results (expressed by MARD) do not change anymore or considerably. From this point onward, there is no sense to carry on recording gamma spectra because MGAU and FRAM results do not improve further or do not improve reasonably.

3.2 Results: optimal number of total counts for MGAU and FRAM

Figure 3 shows that above 4.32E+07 total number of counts in the spectra recorded by the AMM detector (see Table I) the MGAU results do not change considerably. Before this point, the values are spread over mainly due to poorer counting statistics. From this point onward the differences between the consecutive steps are negligible. In addition, most of the biases (expressed by the MARD) lie below 1%. One cannot reach significantly better results by performing longer acquisitions. Therefore it is recommended to acquire a gamma spectrum until reaching roughly **4.32E+07 total counts**[2]. This value is estimated to be the optimal number of total counts.

Analogous graphs were constructed for FRAM as well. For both investigated FRAM parameter sets, the graphs show that the results do not change after the 4.32E+07 total counts are reached. It was found that for all the detectors listed in Table I the optimal number of counts is close to 4.32E+07, both for FRAM and MGAU. Therefore, changing the detector does not affect the conclusion regarding the optimal number of counts as long as the detector satisfies the basic requirements for the applicability of MGAU and of the specified FRAM parameter sets.

[2] The stated optimal number of counts has its own statistical uncertainty, which is determined by the size of the steps between the numbers of total counts used in this work. By taking smaller steps, in principle, the value for the optimal number of total counts could be refined

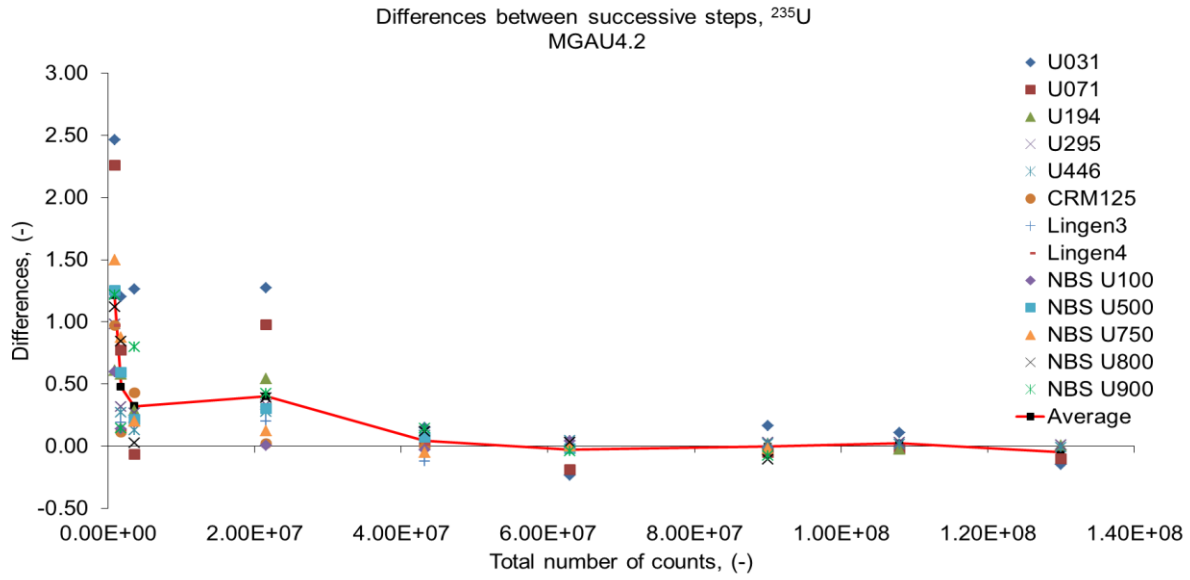

Figure 3 The graph shows differences between consecutive steps in MARD for MGAU4.2. The solid line represents average differences calculated for each of the steps. The average line converges to 4.32E+07 total counts. After this point the differences between consecutive steps are negligible and oscillate around zero, which means that the MGAU results (expressed by MARD) become nearly invariant. Therefore this number of total counts is estimated to be the optimal number of counts. For FRAM the corresponding graph looks alike

4 Optimal count rate (optimal sample-to-detector distance)

The purpose of studying the optimal count rate arose from unsureness about how to position samples to be measured by gamma detectors and analyzed by MGAU and FRAM. The sample-to-detector distance affects the final appearance of the sample's spectrum. Placing a sample too close to the detector may lead to coincidence summing, higher dead time and eventually result in distorted peak shapes. On contrary, positioning a sample too far from a detector makes it difficult to reach better counting statistics. The sample-to-detector distance and the respective count rate clearly affect accuracy of MGAU and FRAM results. The purpose of this part of the study was to determine the optimal count rate and corresponding optimal sample-to-detector distance giving best MGAU and FRAM results.

4.1 Procedure of determining the optimal count rate

In order to test the influence of different count rates on MGAU and FRAM results, an approach similar to the one in the previous chapter was employed. The certified materials CBNM 071, 194, 295, 446 and some of the NBS standards were measured for very long time (until reaching 2E+08 total counts) at various count rates. The count rates were set by adjusting sample-to-detector distances. Corresponding simulated spectra were then generated and subsequently analysed by MGAU and FRAM. The results of the analysis were compared with the certified data. Instead of using the MARD, the relative bias from declared values was calculated in order to find the optimal count rate. Since a bias is either positive of negative, it provides useful information whether the software overestimate or underestimate the abundance of ^{235}U.

4.2 Results: optimal count rate

The three detectors listed in Table I were used in this part of the study. The relative biases were plotted as a function of count rate for each of the detectors. Each point in the graph represents the average relative bias of a set of 50 spectra. Each set of the spectra has a certain number of total counts listed in the graph's legend. The points in the graph were fitted with a linear function and the intersections with zero were calculated for each of the trend lines. The intersections with zero represent the desired optimal count rate. As the count rate increases the bias lines go lower down from positive to the negative values. This declining trend is common for all of the CBNM samples and

detectors with some exceptions. As an illustration, the results for the SDG detector and CBNM 446 sample are shown in Figure 4.

As we have already published in [11], there is a dependence of the optimal count rate on the enrichment of ^{235}U. Furthermore, the study shows that the optimal number of counts depends also on the detector. Figure 4 clearly illustrates that the optimal count rate also differs for both MGAU and FRAM. There are a lot of factors affecting a detector's count rate such as the size of detector crystal, type of preamplifier, filter settings and many more. Therefore, it is not feasible to give a general recommendation on optimal count rates for all detectors available on the market. However, it is achievable for users to carry out this experiment in order for them to determine the optimal count rate for their detectors.

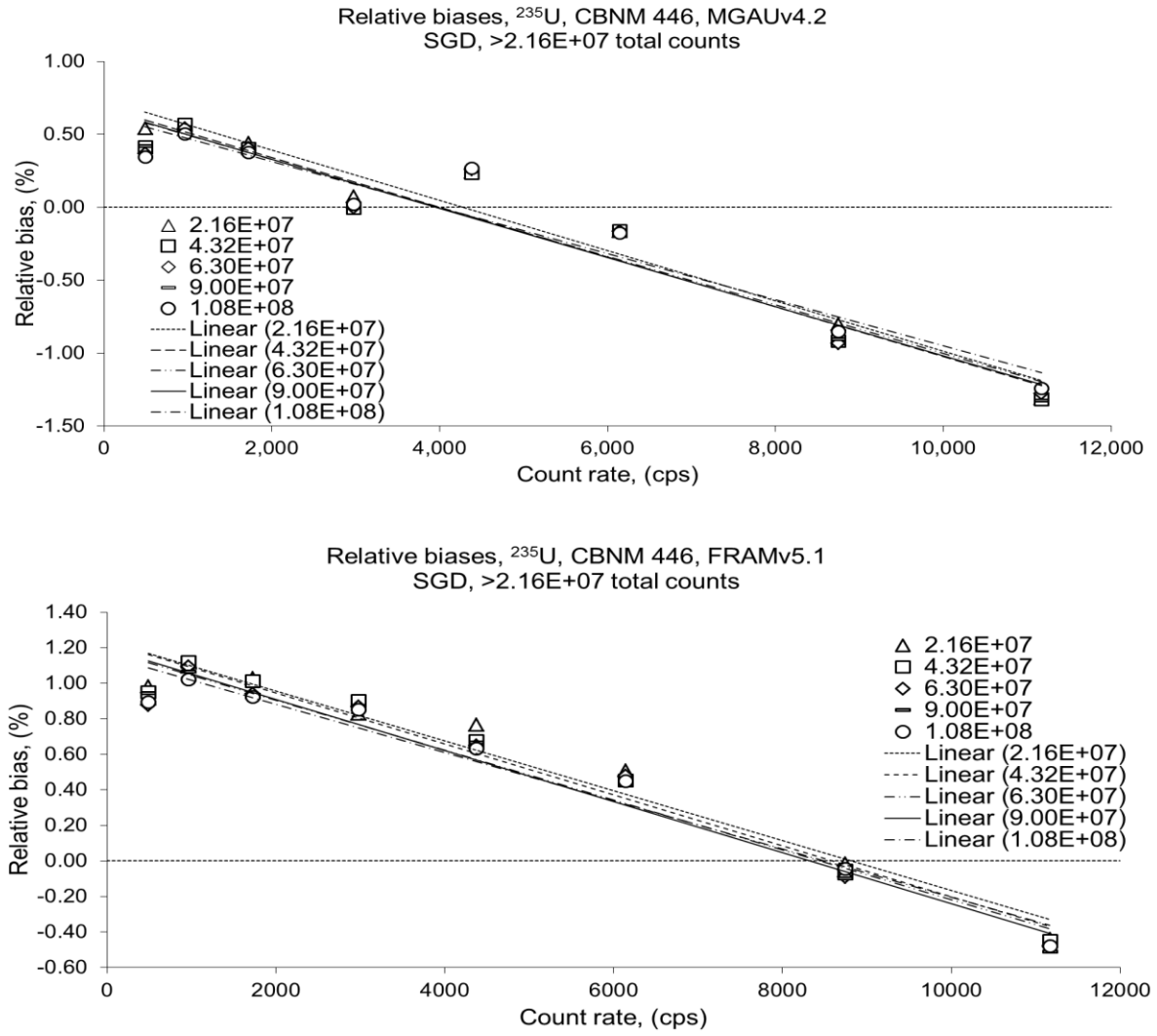

Figure 4 The graph displays relative biases of MGAU and FRAM results as a function of count rate for CBNM 446 when the number of total counts in the spectrum is more than 2.16E+07. Each point represents the average bias of 50 spectra having a certain number of total counts. The higher the count rate, the lines drop down to negative values. While for MGAU the optimal number of counts is close to 4000 cps, for FRAM the optimal number of counts is close to 9000 cps.

5 Validation of the approach

The spectra generated by Cambio are similar to their corresponding mother spectra but they have less total counts. They are created by randomly sampling data from their mother spectra. All the daughter spectra take after their parent the same information on background conditions, disturbances, interference etc. In reality, background and interference conditions vary over the time. Hence, the real spectra of the same sample measured in the same laboratory can differ from each other. Therefore the results of analysis could be also different. Since all the measurements have been done in a laboratory under controlled conditions, the real spectra should not be significantly different from one another. This approach of testing the software's performance had to be validated with real spectra. The simulated spectra were tested whether they correspond to real ones.

5.1 Procedure of validation

Two of the certified materials were chosen for the validation test. One sample from the enrichment range where the codes perform the best (CBNM U446) and another one from the high enrichment range where their performance is weaker (NBS U900). The samples were measured for certain periods of time listed in the Table II. In order to have enough spectra and to be able to calculate an average and standard deviation, each measurement was repeated ten times. After the acquisitions of real spectra were done, corresponding simulated spectra (having the same number of total counts) were generated. At the end, the MGAU and FRAM results for simulated spectra were compared with the results for real spectra.

5.2 Results of validation

Figure 5 depicts results of the validation test for one of the samples used in this study. Towards the greater number of total counts, as the statistics improves, the two points in the Figure 5 (triangle and rectangle) lie closer to each other and also their respective error bars are getting overlapped. The error bars represent the standard deviation of the MARD. There is also an apparent decreasing trend of the values along the x-axis. Having a similar decreasing trend line and having a similar standard deviation together with being in the same range, the simulated spectra correspond to the real ones in all aspects.

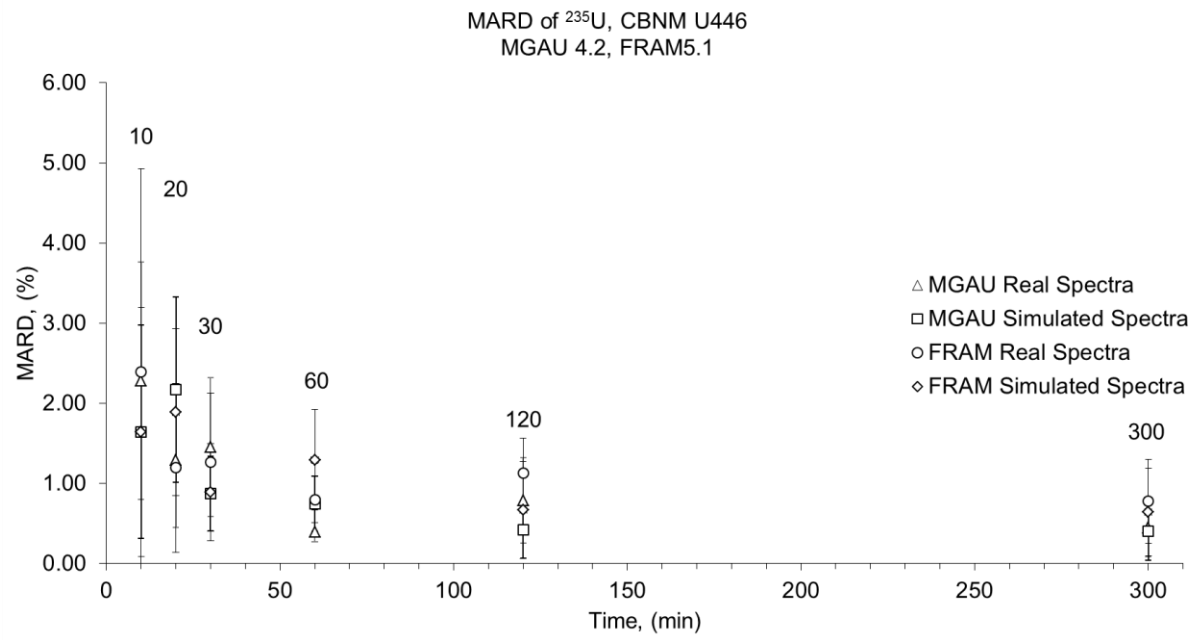

Figure 5 Comparison of the MARD values of real spectra versus simulated spectra. The sample comes from the enrichment range (4.46 %) where the code performs the best. For the other sample which was used in validation test the corresponding graph looks similar.

6 Ratio of counts in 0-300 keV and in 100 keV region

Uranium spectra are generally not as complex as plutonium spectra. Therefore, it was chosen to use the total number of counts as a parameter for deriving the optimal acquisition time - above referred to as the optimal number of counts. FRAM and MGAU use mainly the 100 keV region[3] for determining the isotopic ratios. Since samples from LEU to HEU were used in this study it was necessary to check if the ratio of the counts in the 0-300 keV and 100 keV region is similar for all of the samples. The study shows that the 300/100 keV region count ratio stays nearly constant over the whole range of ^{235}U enrichments for uranium oxides.

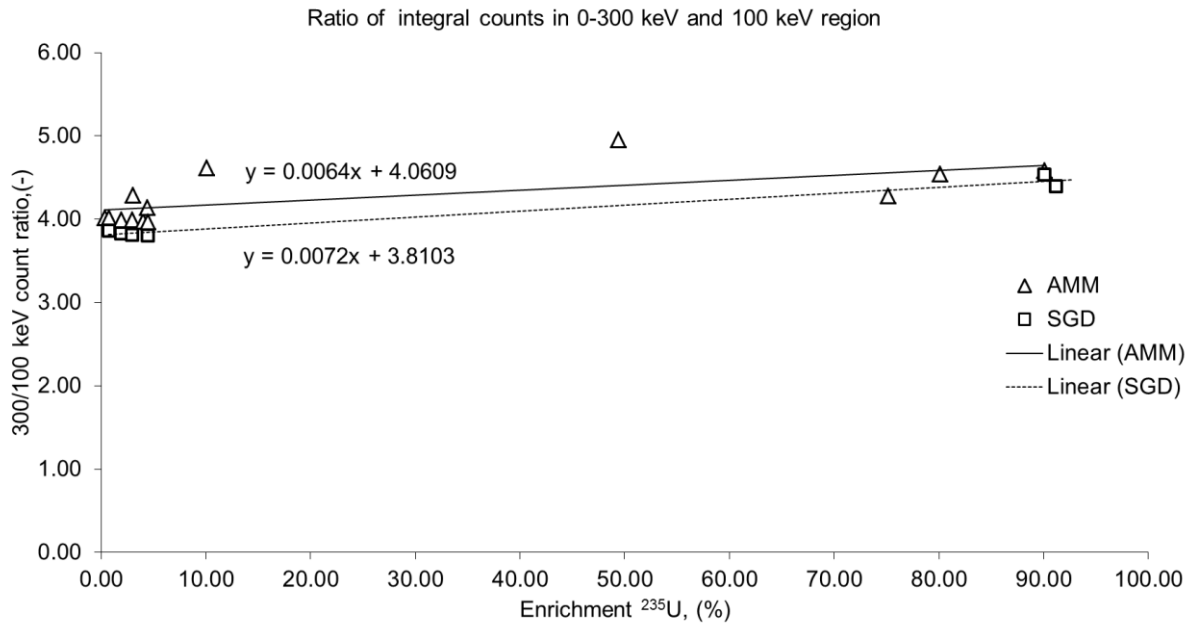

Figure 6 Ratio of the counts in the 300 keV region and in the complex 100 keV region. The 100 keV region is used by MGAU and FRAM for determining the uranium isotopic abundances. The linear trend-lines have very low slopes indicating that the 300/100 keV region count ratio is nearly constant for uranium oxides regardless of the enrichment.

7 In-field measurements

All the information above covers measurements in laboratories under controlled and nearly optimal conditions. In-field measurements usually have to be carried out under uncontrolled conditions within the shortest possible time. There is not that high demand on precision and accuracy as for laboratory measurements. MGAU and FRAM are also used for in-field measurement analysis. Therefore, it is of interest to establish best practices for measurements that are carried out on site.

Acquisitions of 5 min, 10 min, 20 min and 30 min in-field measurements were simulated using Cambio software. All the high quality mother spectra recorded for the optimal count rate test were reused for this purpose. Results of the evaluation should provide a clearer view on how to position a sample and how long to acquire a spectrum when it comes to in-field measurements.

Preliminary results indicate that the optimal count rates for in field measurements are slightly higher than those for laboratory measurements. Table III shows that for this particular sample and detector, the accuracy of the 5 min spectra stays roughly within ± 1%. The precision improves with the increasing time of acquisition (the standard deviation gets lower). Best practices for in field measurements are a subject of our ongoing research.

[3] 100 keV region refers to a complex area ranging from 89 keV to 101 keV. This region is mainly, but not solely, used for determining uranium isotopic ratios by MGAU and FRAM.

Table III *MARD and optimal count rate for in-field measurements*

CBNM 295, MGAU4.2, SGD detector	5 min	10 min	20 min	30 min
Optimal count rate [cps]	5377	5433	5088	4677
MARD [%]	0.754	0.685	0.479	0.542
Standard deviation of MARD	0.637	0.523	0.407	0.384

8 Bismuth as a source of bias

We observed systematic biases of ^{235}U/U from certified values for certain detectors and first could not find their origin. After careful examination of the detectors' spectra, we found bismuth x-rays which were not present in the background. Bismuth when struck by gamma rays emits fluorescence x-rays at similar energies to those of ^{235}U. MGAU and FRAM, in their default mode, are unable to unfold bismuth x-rays from the peaks originating from ^{235}U. Therefore, bismuth can be a source of bias when present in spectrometric measurements of uranium isotopic composition. Bismuth has been used for soldering as a substitute for toxic lead since a new European directive took effect in 2006 [12].

The 89.830 keV bismuth XRF peak falls into the area of two ^{235}U peaks and causes overestimation of the ^{235}U/U ratio reported by MGAU and FRAM. The overestimation ranges from 2% up to 7%. FRAM is customizable and bismuth peaks can be added into FRAM's algorithm. By doing so, the bismuth induced bias can be minimized. Figure 7 shows results of MGAU and FRAM with their default settings in comparison with customized FRAM's parameters. Adding bismuth peaks or removal of the ^{235}U peaks at 89 keV reduces the bias of ^{235}U/U ratio.

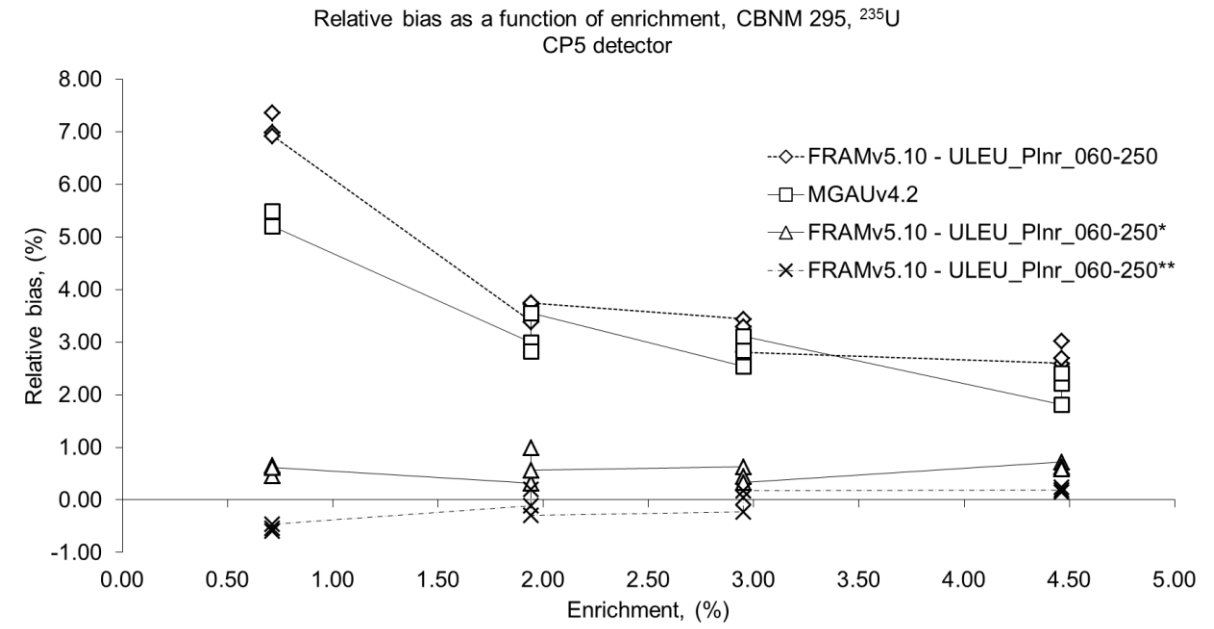

Figure 7 The figure shows how bismuth affects precision of MGAU and FRAM. The comparison between MGAU and three FRAM parameter sets is provided. FRAMv5.10-ULEU_Plnr_060-250* is similar to the default parameter set, but without the 89.957 keV peak of ^{235}U used for efficiency and activity calculations. FRAMv5.10-ULEU_Plnr_060-250** is also similar to the default parameter set, but with the 89.830 keV bismuth peak added. There is an apparent improvement in the accuracy of FRAM results for the modified parameters.

9 Conclusions

The optimal number of counts in the gamma spectrum for determining uranium isotopic composition by MGAU and FRAM was estimated to be 4.32E+07 counts. The study has shown that recording gamma spectra with more counts does not generate better results.

The optimal count rate differs for MGAU and FRAM. The optimal count rate was also found to be dependent on the ^{235}U enrichment and detector type. We were not able to give general recommendations for the optimal count rate. However users can carry out similar optimal count rate test for their detectors. The present work may serve as an example for doing so.

Simulated spectra were used for determining the optimal number of counts and optimal count rate. These spectra were generated by Cambio software. This software allows simulating acquisitions by generating daughter spectra from real mother spectra. It has been validated that these simulated spectra correspond to real ones in all aspects relevant for this work.

The ratio of the counts in the 0-300 keV region and in the 100 keV region was confirmed to be nearly constant over the whole range of ^{235}U enrichments for uranium oxide samples. Therefore, the optimal number of total counts in a spectrum is justified to be used as a parameter for classifying the statistical quality of uranium spectra.

The presence of bismuth can be an important source of bias in the measurement of U isotopic composition by MGAU and FRAM. Bismuth, when hit by gamma rays, emits fluorescence x-rays at energies similar to gamma and x-rays of ^{235}U. MGAU and FRAM attribute the counts from bismuth to ^{235}U and report results with biases ranging from 2% to 7%. The bismuth induced bias can be minimized by appropriately customizing parameters of the software.

The users of MGAU and FRAM can use the findings in this work to establish best practices for their spectrometric apparatus.

10 Acknowledgments

This work has been carried out with financial support by Graduate and Executive Nuclear Training and Lifelong Education Project, in short GENTLE Project: EU FP7 GENTLE. (http://www.gentleproject.eu/)

Special thanks go to Andrey Bosko who provided us with an extremely useful spreadsheet and helped us save a lot of time and efforts.

11 Works Cited

[1] R.Gunnink, W. Ruhter, P. Miller, J. Goerten, H. Wagner, M. Swinhoe, J. Verplancke, M. Bickel and S. Abousahl, "MGAU: A New Analysis Code for Measuring U-235 Enrichments in Arbitrary Samples," Lawrence Livermore National Laboratory, 1994.

[2] D. T. Vo and Los Alamos National Laboratory, “FRAM v.5: Simple Is Good,” in *Proceeding of the 51st Annual Meeting of The Institute of Nuclear Materials Management*, Baltimore, 2010.

[3] W.D.Ruhter, R.Gunnink, “Measurement of Plutonium and Uranium Isotopic Abundances by Gamma-Ray Spectrometry,” in *11th International Workshop on Accurate Measurements in Nuclear Spectroscopy*, Sarov, Nizhni Novgorod Region, Russia, 1996.

[4] T. E. Sampson, T. A. Kelley and D. T. Vo, “Application Guide to Gamma-Ray Isotopic Analysis Using the FRAM software,” Los Alamos National Laboratory, 2003.

[5] Canberra Industries, Inc, "Multi-Group Analysis for Uranium. Waste and Safeguards Measurement Systems and Software," [Online]. Available: http://canberra.com/products/waste_safeguard_systems/pdf/MGAU-SS-C39051.pdf. [Accessed 15 May 2014].

[6] Central Bureau for Nuclear Measurements, “Certificate of analysis: EC Certified Nucelar

Reference Material 171," Geel, Belgium, 1985.

[7] National Bureau of Standards, "Certificate of Analysis, Standard Reference Materia:l U-030, U-100, U-500, U-750, U-800, U-900," National Bureau of Standards, Washington D.C., USA, 1981.

[8] New Brunswick Laboratory, U.S. Department of Energy, "Certificate of Analysis, CRM 125-A, Uranium Oxide (UO2) Pellet Assay and Isotopic Standard," Argonne, Illinois, USA, 2008.

[9] Joint Research Centre - Institute for Transuranium Elements, "Analysis results SG1016," Karlsruhe, Germany, 2008.

[10] P. George P. Lasche, *Cambio Version 120822,* U.S. Department of Energy, Sandia National Laboratories.

[11] T. Rüther and J. Zsigrai, "Recommendations for Determining Uranium Isotopic Composition by MGAU," in *Symposium on International Safeguards: Linking Strategy, Implementation and People - IAEA CN-220*, Vienna, 2014.

[12] European Parliament and European Council, "Directive 2002/95/EC of the European Parliament and of the Council of 27 January 2003 on the restriction of the use of certain hazardous substances in electrical and electronic equipment," *Official Journal ,* vol. L, no. 037, pp. 0019 - 0023, 2003.

[13] Indium Corporation, "Product Data Sheets," 02 March 2015. [Online]. Available: http://www.indium.com/technical-documents/product-data-sheets/. [Accessed 02 March 2015].

[14] ORTEC, *FRAM 5.10 Ortec,* Safeguards Science and Technology Group, Los Alamos National Laboratory, 2011.

[15] H. Xiaolong and W. Baosong, "Evaluation of 235U decay data," *Applied Radiation and Isotopes,* vol. 67, no. 9, p. 1541–1549, 2009.

[16] A. Berlizov, R. Gunnink, J. Zsigrai, C. Gruyen and V. Tryshyn, "Performance testing of the upgraded uranium isotopics multi-group analysis code MGAU," *Elsevier,* vol. 575, no. 3, p. 10, 2007.

[17] N. GmbH, "Nucleonica - Nuclide Datasheets++," [Online]. Available: www.nucleonica.net. [Accessed 03 March 2015].

[18] A. A. Plionis, S. R. Garcia, E. R. Gonzales, D. R. Porterfield and D. S. Peterson, "Replacement of lead bricks with non-hazardous polymer-bismuth," *Journal of Radioanalytical and Nuclear Chemistry,* vol. 282, no. 1, pp. 239-242, October 2009.

Determination of Uranium enrichment with FRAM – comparison of electrically cooled Germanium detector Detective200 and U-Pu detector

T. Köble, W. Berky, H. Friedrich, M. Risse, W. Rosenstock, O. Schumann, E. Lieder, J. Glabian

Fraunhofer Institut Naturwissenschaftlich-Technische Trendanalysen (INT)
Appelsgarten 2, D-53864 Euskirchen, Germany
E-mail: theo.koeble@int.fraunhofer.de

Abstract: In the context of fissile material detection, the determination of Uranium enrichment and of the Plutonium isotopic vector is tremendously important. The negligence of such information may lead to drastic if not fatal consequences to the general public in case the material in question is used in explosive devices such as an Improvised Nuclear Devices (IND). The implemented automatic analysis routine of the electrically cooled Detective 200 detector has been investigated in earlier measurements measuring Uranium and plutonium sources of different enrichment respectively isotopic composition. The results have been partly disappointing. The object of the present work was to investigate the general ability and the quality of the spectra obtained with the Detective200 in comparison to the commonly used U-Pu detectors cooled with liquid nitrogen. To determine the uranium enrichment measurements were carried out with a source of depleted Uranium and different shielding materials. The evaluation of the spectra was performed with the isotopic analysis code FRAM. The results for the Uranium enrichment for the Detective200 system were compared to the enrichment result of the commonly used U-Pu detectors. The results of these measurements and an assessment of the ability of the FRAM software combined with the Detective200 system in determining the Uranium enrichment will be presented.

Keywords: gamma measurement, Uranium enrichment, U-Pu, FRAM

1 Introduction

The detection and identification of radioactive and especially nuclear material are crucial with respect to countermeasures against nuclear terrorism. Uranium and Plutonium play an especially important role in this context as these materials are the core substance of explosive devices such as an Improvised Nuclear Device (IND) which may be used to cause severe or even fatal injuries to the public in comparatively large areas, rendering them uninhabitable as a consequence. To prevent such acts from happening, this material must be tracked either before such devices are assembled of at least before they are ignited.

In order to achieve an identification of said material, highly sensitive gamma detectors with electrically cooled germanium semiconductors are a reasonable choice, primarily because of their excellent gamma energy resolution. U-Pu detectors cooled with liquid nitrogen (LN) are also a good option, although these devices have limitations with regard to on-site measurements due to the size and weight of their cooler and the availability of LN in the field.

The electrically cooled detectors are commonly equipped with an implemented identification routine. The ability of such analysis routines to reliably determine the isotopic composition of Pu or the degree of enrichment of U has been the subject of previous measurements [1, 2]. The results were, at least in part, quite disappointing although the quality of the gamma spectrum would have enabled an

appropriate identification. Therefore the special code called FRAM by Ametek/ORTEC was used for subsequent analysis of the measured spectra regarding uranium enrichment for a comparison of several electrically cooled germanium detectors with another germanium detector cooled with LN.

2 Measurement set-up

A series of measurements with low and high enriched as well as natural and depleted uranium was performed at the Institute for Transuranium Elements (ITU) in Karlsruhe, Germany, as low or high enriched uranium is not available at our institute. Additional measurements were performed with depleted uranium and a sample of mineral containing natural uranium at Fraunhofer INT.

2.1 Measurements at ITU

At ITU, four different uranium samples with different degrees of enrichment were available: 0.3% (depleted), 0.71 % (natural), 4.5 % (low enriched), and 91.4 % (high enriched). As shielding material 2 mm of lead and a combination of 1.5 cm of steel and 5 cm of an explosive simulate were used. The latter contained the same chemical components as explosive without actually being an explosive. This combination of steel and explosive simulate represented the configuration of an IND.

Four different measurement systems with electrically cooled germanium crystals were tested during this series: the Detective EX, the Micro Detective, the Detective 200 (all designed by Ametek/ORTEC), and the FALCON 5000 by Canberra. Figure 1 shows these detectors in a typical setup positioned around a source.

Figure 1: Measurement array with four detectors positioned around an unshielded source; the detectors are (clockwise starting on the bottom left): Detective EX, Micro-Detective, Detective 200 and Falcon 5000.

The main characteristic values of the detectors are given in table 1 as well as the outer dimensions of the systems. The three Detectives (Detective EX, Micro-Detective and Detective 200) differ from each other in respect of the Germanium crystal and the firmware. Detective EX and Micro-Detective are comparable concerning the crystal (see table 1) but differ in the firmware. Detective 200 and Micro-Detective both have the newer firmware V3, but the Detective 200 has a larger crystal.

Detector, Manufacturer	Weight of device [kg]	Size of Device [cm^3]	Crystal Size [cm] ø/Length	Energy Resolution [keV]		Relative Efficiency [%] for ^{60}Co	Battery Life [h]
				at 186 keV	at 662 keV		
Detective EX, ORTEC	12	37 x 18 x 34	5 / 3	1.3	1.7	16	> 3
Micro-Detective ORTEC	7	37 x 15 x 28	5 / 4	1.3	1.7	11	5
Detective 200, ORTEC	21	43 x 24 x 39	8.5 / 3	1.1	1.5	52	3
Falcon 5000, Canberra	15	40 x 35 x 16	6 / 3	1.1	1.4	18.5	6 - 8

Table 1: Overview of the detection systems and their specifications; the weight and the size of the Falcon 5000 do not include a necessary PC; weight and size figures for all systems include batteries; the relative efficiencies are obtained using the standard measurement procedure in which a ^{60}Co source is placed 25 cm away from the end-cap of the detector.

In all cases the spectra can be stored and the spectrum files can be exported and transferred to a specialist. The systems feature automatic identification and in particular special SNM (Special Nuclear Material) modes. The latter have been specially considered for these uranium measurements. In order to gain additional information concerning uranium enrichment and the isotopic composition of plutonium, the data were analyzed with the isotopic analysis software PC/FRAM 5.1 (ORTEC version) [3]. Thereby we used the existing parameter files u_cx_120-1010 for the Detectives and uleu_plnr_060-250 for the U-Pu detector after adapting the energy calibration but without any further optimization.

Compared to the firmware used by the Detective EX, the firmware of the Detective 200 and Micro-Detective has limited information output especially in the standard non-expert mode. To have a better comparability we therefore did not strictly use the recommended settings for the subsequent measurements although we wanted to evaluate the results which non-expert users would gain.

The identification mode displays of the Detective devices continuously update the results and run until they are manually stopped by the user. The Falcon 5000 can be operated with a preselected time or without a preset. However the result of the SNM Mode will be only displayed after the end of the measurement. The chronological development of the measurement results were specially observed for all detectors. Whenever possible, spectra with longer measurement times were obtained for example during midday or night.

2.2 Measurements at INT

These measurements were done to compare the performance of electrically cooled germanium detectors mentioned above to the quality of a U-Pu detector cooled with LN. The U-Pu detector yields gamma spectra in the lower energy region up to 300 keV which is a relevant region for measurements with nuclear material. Such type of detector is part of a wide-range collection of measurement systems at INT for detecting radioactive or nuclear material [4].

Measurements were performed with several detectors: the Detective 200, the Micro Detective, and a U-Pu detector cooled with LN. A 1.8 kg block of depleted uranium and a sample of mineral containing natural uranium were measured, both unshielded and shielded with 5 mm of Fe. Figure 2 shows a typical measurement layout with the depleted uranium shielded by Fe and the Micro Detective.

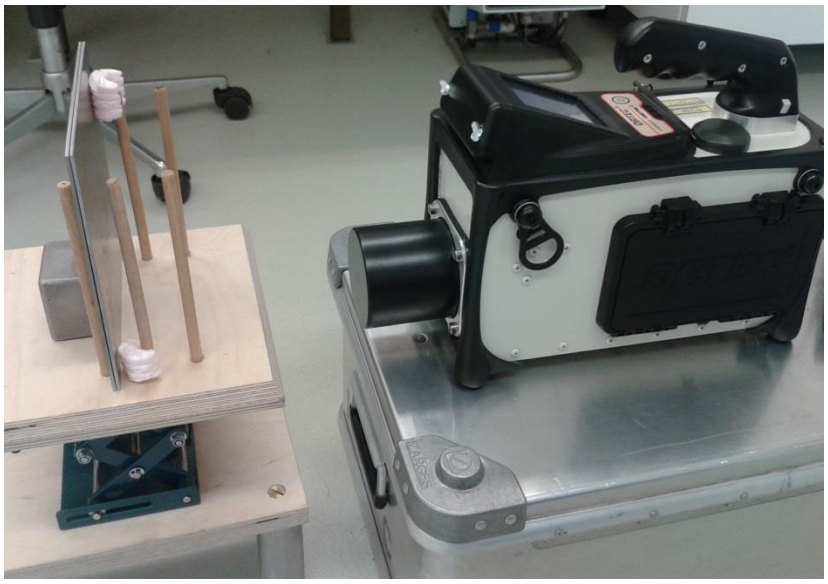

Figure 2: Measurement array with Micro Detective (on the right) and 1.8 kg block of depleted uranium (on the left) shielded by 5 mm of Fe.

3 Measurement Results

3.1 ITU Measurements

With each of the four uranium (depleted: DU, natural: nat. U, low enriched: LEU, and high enriched: HEU) at least one measurement was performed without shielding material and with the combination of steel and explosive simulate. LEU and HEU were additionally examined with lead shielding. Time permitting; multiple measurements were done with the same setup.

Tables 3 to 5 show comparisons of the identification results yielded by the implemented analysis routines of the devices and the results subsequently gained by the analysis with FRAM for the Detective 200, the Detective EX, and the FALCON 5000 for the uranium measurements. The derived results base on the categorization limits in table 2:

Material	Characterization limits
DU	$^{235}U < 0.64$ %
Nat. U	0.64 % < $^{235}U < 0.78$ %
LEU	0.78 % < $^{235}U <$ 20 %
HEU	$^{235}U > 20$ %
RGPu	$^{239}Pu < 90$ %
WGPu	$^{239}Pu > 90$ %

Table 2: Limits for the characterization of uranium and plutonium material

Sample	Shielding	Life Time (s)	Implemented Analysis	Result Derived From FRAM
DU	Unshielded	956	*Nucl. U*	DU
DU	Steel + Simulate	1458	*Nucl. U*	DU
Nat. U	Unshielded	874	*Nucl. U*	*LEU*
Nat. U	Steel + Simulate	1079	*Nucl. U*	*DU*
LEU	Unshielded	1189	*Nucl. U*	LEU
LEU	Steel + Simulate	7765	*Nucl. U*	LEU
LEU	Lead	255	*Nucl. U*	LEU
HEU	Unshielded	1575	*Nucl. U*, HEU	HEU
HEU	Steel + Simulate	691	*Nucl. U*, HEU	HEU
HEU	Lead	57613	*Nucl. U*, HEU	HEU

Table 3: Comparison of Detective 200 analysis results for the uranium measurements yielded by the implemented analysis routine and calculated with FRAM; color code: blue color refers to a correctly identified isotope or material, but the degree of enrichment or categorization is wrong, green color means both the identification and categorization are correct.

Sample	Shielding	Life Time (s)	Implemented Analysis	Result Derived From FRAM
DU	Unshielded	225	DU, elev. U concentration	DU
DU	Steel + Simulate	207	*elev. U conc.*	DU
Nat. U	Unshielded	890	–	nat. U
Nat. U	Steel + Simulate	596	*DU, elev. U conc*	*DU*
Nat. U	Steel + Simulate	712	*DU, elev. U conc.*	*DU*
LEU	Unshielded	1732	LEU, elev. U concentration	LEU
LEU	Steel + Simulate	302	*elev. U conc.*	*DU*
LEU	Steel + Simulate	6425	*nat. U, elev. U conc.*	LEU
LEU	Lead	352	*DU, elev. U conc.*	*DU*
LEU	Lead	152	*DU, elev. U conc*	*DU*
HEU	Unshielded	1004	*LEU*	HEU
HEU	Unshielded	212	*LEU*	*LEU*
HEU	Unshielded	137	*LEU*	*LEU*
HEU	Steel + Simulate	419	–	*DU*
HEU	Steel + Simulate	392	–	*LEU*
HEU	Steel + Simulate	157	–	HEU
HEU	Steel + Simulate	899	–	*LEU*
HEU	Lead	322	–	*LEU*
HEU	Lead	59771	*nat.U, elev. U conc.*	*LEU*

Table 4: Comparison of Detective EX analysis results for the uranium measurements yielded by the implemented analysis routine and calculated with FRAM; color code: red color refers to a completely incorrect identification result or no result at all, blue color refers to a correctly identified isotope or material, but the degree of enrichment or categorization is wrong, green color means both the identification and categorization are correct.

Sample	Shielding	Life Time (s)	Implemented Analysis	Result Derived From FRAM
DU	Unshielded	299	DU	DU
DU	Steel + Simulate	599	-	DU
DU	Steel + Simulate	937	DU	DU
Nat. U	Unshielded	201	*DU*	*DU*
Nat. U	Unshielded	89	*DU*	*DU*
Nat. U	Unshielded	103	*DU*	*LEU*

Sample	Shielding	Life Time (s)	Implemented Analysis	Result Derived From FRAM
Nat. U	Steel + Simulate	482	*DU*	*DU*
LEU	Unshielded	797	LEU, *WGPu*	LEU
LEU	Steel + Simulate	300	*DU*	*DU*
LEU	Steel + Simulate	221	*Nat. U*	LEU
LEU	Steel + Simulate	6199	*Nat. U*	LEU
LEU	Steel + Simulate	600	*Nat. U*	LEU
LEU	Lead	180	*DU*	*DU*
LEU	Lead	446	*DU*	LEU
HEU	Unshielded	264	*LEU*, WGPu	-
HEU	Unshielded	902	*LEU*, WGPu	HEU
HEU	Steel + Simulate	303	*LEU*	HEU
HEU	Steel + Simulate	617	*LEU*	*LEU*
HEU	Steel + Simulate	901	*LEU*	HEU
HEU	Steel + Simulate	22	*LEU*	*LEU*
HEU	Lead	179	*LEU*	-
HEU	Lead	58302	HEU, WGPu	HEU

Table 5: Comparison of FALCON 5000 analysis results for the uranium measurements yielded by the implemented analysis routine and calculated with FRAM; color code: red color refers to a completely incorrect identification result or no result at all, blue color refers to a correctly identified isotope or material, but the degree of enrichment or categorization is wrong, green color means both the identification and categorization are correct.

The Detective 200's implemented analysis routine does not include discrimination between LEU and HEU (merely "nuclear uranium" and HEU are defined) or between RGPu and WGPu (only "nuclear plutonium" is defined), respectively. Since the Micro Detective's routine is of the same type, no analysis results of this device are presented here as they were equally limited and therefore less interesting than the results by the Detective EX and the FALCON 5000, at least regarding the implemented routines.

In general, an obvious enhancement of the initial analysis results provided by the implemented routines was achieved with the FRAM analysis. The Detective 200 results benefitted most from the FRAM analysis as the latter produced the correct categorization in almost all cases. As for the other detectors, the FRAM analysis managed to enhance the previous identification result in some cases and failed to achieve this in others.

The use of FRAM appears to be most reasonable for the detector with the highest efficiency. The detectors mentioned above all cover a large range of gamma energy in order to analyse all types of radioactive and nuclear material. For cases when the focus of detection and identification is laid on nuclear material which emits photons in the lower energy region, specific U-Pu detectors are suitable. To evaluate if the FRAM analysis could be even more useful for a U-Pu germanium detector, a new series of measurements was done at INT with such a detector. Moreover, if the flaws of the detectors' implemented analysis routines were due to the large range of their gamma energy spectra and therefore due to limits of the energy resolution, these routines should be able to yield better results with spectra focussing on the lower energy region.

3.2 INT Measurements

The gamma energy spectra were collected by the detectors with the samples mentioned above. Tables 6 and 7 show, as examples, the comparison of the calculated mass percentages of ^{235}U in the sample of depleted uranium and the mineral sample, respectively, measured with the Detective 200, the Micro Detective, and the U-Pu detector, with 5 mm Fe shielding and without shielding.

Detector	No Shielding		5 mm Fe Shielding	
	Life Time (s)	^{235}U Content (%)	Life Time (s)	^{235}U Content (%)
Detective 200	26751	0.49 ± 0.01	6752	0.40 ± 0.03
Micro Detective	7005	0.16 ± 0.02	7030	0.17 ± 0.03
U-Pu Detector	7200	0.45 ± 0.06	7200	0.3 ± 0.1

Table 6: Mass percentages of ^{235}U in the sample of depleted uranium for three detectors as calculated by FRAM.

Detector	No Shielding		5 mm Fe Shielding	
	Life Time (s)	^{235}U Content (%)	Life Time (s)	^{235}U Content (%)
Detective 200	6752	1.0 ± 0.2	7200	0.0001 ± 0.0003
	28800	1.5 ± 0.1		
Micro Detective	3600	0.6 ± 0.3	28800	0.30 ± 0.06
	28800	0.6 ± 0.1		
U-Pu Detector	7200	3.2 ± 0.4	28800	2.4 ± 0.4

Table 7: Mass percentages of ^{235}U in the mineral sample for three detectors as calculated by FRAM.

The correct result of the ^{235}U mass percentage of the used depleted uranium would be approximately 0.25 % to 0.3 %. The Detective 200 and Micro Detective results were out of this range, even when taking the error figures into account. The results of the measurements with shielding, though, were closer to the expected value. The results for the U-Pu detector in general were higher than 0.3 %. The lower limit for the characterization as depleted uranium in general is ^{235}U < 0.64 %. This is fulfilled for all results, so an analysis would lead to the correct categorization.

For natural uranium the results were not in the correct range (0.64 % < ^{235}U < 0.78 %). In the shielded case the analysis was even more complicate. While the results for natural uranium are not correct this may not be of high concern for the decision makers. They are interested in correct results in terms of HEU/LEU in the case of uranium and of WGPu in the case of plutonium.

The fact that the FRAM analysis yielded not completely satisfactory results was primarily because of poor statistics leading to small numbers of counts in the relevant photo peaks. The samples used here emitted too weak a gamma radiation for an appropriate analysis. The FRAM analysis software was mainly designed for calculating enrichment of LEU or HEU samples and not for samples with such a low content of ^{235}U. In order to gain insight regarding the reasons for the flaws of the implemented analysis routines mentioned above by measurements with U-Pu detectors, other samples of nuclear material will be necessary. Therefore further measurements at institutions such as ITU must be taken into account.

4 Conclusions

Comparing the identification and categorization results of the detectors' implemented analysis routines to those achieved by means of the FRAM analysis with respect to measurements on uranium at ITU, a significant enhancement can be stated when using FRAM. In most cases, the implemented routines managed to identify the correct material, but the categorization was often false. Here the FRAM results were considerably superior, especially in the case of the Detective 200.

The measurements at ITU raised the question whether the flawed results obtained by the detectors' implemented analysis routines were due to limits of the measured spectra's energy resolution or because of weaknesses of the analysis routines themselves. To gain insight here, the additional measurements at INT with a U-Pu detector were performed. Unfortunately, the spectra measured with depleted uranium suffered from poor statistics due to the small amount of ^{235}U in the samples. Hence, other measurements with a U-Pu detector with low and high enriched uranium would be necessary to clarify this matter.

In general the quality of the spectra with electrically cooled germanium detectors was comparable to LN cooled germanium detectors. Therefore there is also a potential to enhance automatic analysis routines. Currently, the use of automatic analysis routines could be recommended only for unshielded or weekly shielded samples of SNM combined with a cautious review of the results.

5 References

[1] Risse, M.; Berky, W.; Friedrich, H.; Köble, T.; Rosenstock, W.; Rennhofer, H.; Pedersen, B.: *Identification of Nuclear Material with Hand-Held Gamma and Neutron Measuring Devices, INMM 51st Annual Meeting, Madison, Wisconsin: Omnipress, 2010, 10 S.*

[2] Risse, M.; Berky, W.; Friedrich, H.; Köble, T.; Rosenstock, W.; Schumann; O. Berndt, R.: *Identification Measurements of nuclear material – Detective EX versus Falcon 5000, INMM 53rd Annual Meeting, Orlando, 2012*

[3] Advanced Measurement Technology, http://www.ortec-online.com/download/PC-FRAM.pdf, downloaded on the 6th of July 2013

[4] Rosenstock, W.; Köble, T.; Risse, M.; *Measurement techniques to combat nuclear terrorism*; *Proceedings of the 25st annual meeting symposium on safeguards and nuclear material management*; Stockholm; 2003; 465

Analytical estimate of high energy gamma-ray emissions from neutron induced reactions in U-235, U-238, Pu-239 and Pu-240

Frederik Postelt, Fabio Zeiser, Gerald Kirchner

University of Hamburg
Carl Friedrich von Weizsäcker-Centre for Science and Peace Research
Beim Schlump 83, 20144 Hamburg, Germany
E-Mail: Frederik.Postelt@physik.uni-hamburg.de

Abstract:

Measurements of neutron induced gammas allow the characterisation of fissile materials. Most prompt gamma-rays from radiative neutron capture reactions in plutonium and uranium have energies between 3 and 6.5 MeV. High energy photons have a high penetrability and therefore minimise self-absorption and shielding effects. They are isotope specific and therefore may be well suited to determine the isotopic composition of fissile material. Since this measurement technique is non-destructive, its application in dismantlement verification is potentially attractive. Challenges are low transition probabilities, low detector efficiencies at high gamma energies, a high background of gammas from induced fission in the fissile material and delayed fission gammas from both radiative capture and induced fission. In addition, only few radiative neutron capture lines can be resolved, while most form a quasi-continuum.

The gamma emission rates of neutron interrogated fissile material are analytically estimated. From the variety of possible neutron sources, a DD-generator and a research reactor are selected. Additionally, the application of a chopper, neutron-gamma anti-coincidence counters, moderation of the neutrons and attenuation of the gammas by additional shielding have been investigated. The analytical estimates are compared to the few published measured spectra.

The results for plutonium with thermal neutrons from either a research reactor or a moderated DD-source are promising. Additional shielding to protect the gamma detector is indispensable. Highly enriched uranium has much lower transition probabilities and it is not very attractive to measure the enrichment with prompt gamma-rays from neutron capture. Potentials and limits of radiative neutron capture measurements are summarised and an outlook is given.

Keywords: dismantlement; verification; PGAA; plutonium; uranium

1. Introduction

It is possible to determine the isotopic vector of special nuclear material (SNM) with passive gamma-ray spectroscopy. However, the emitted photons are subject to strong self-attenuation and absorption. Active measurements present a promising alternative, especially if Information Barriers (IB) are required and a black box is measured [1, 2, 3]. Radiative neutron capture reactions in SNM isotopes lead to a gamma spectrum up to energies of 6.5 MeV. Such high energy photons have a much higher penetrability and therefore minimise shielding and self-absorption effects.

In this paper, the potential of (n,γ)-measurements for characterising fissile material is assessed and open questions are addressed.

2. State of research

Radiative neutron capture reactions were most researched in the 1990s and focused on low-Z materials, e.g. to identify explosives[1]. In the last decade research in the US has shifted to SNM, too, but only little information has been published. Examples of such research are the

[1] personal communication with Volker Dangendorf, PTB, in November 2011

"Nuclear Materials Identification System" (NMIS, which uses (n,γ) to identify explosives [4]), the "Nuclear Car Wash" (NCW, which uses (n,f) [5, 6]), Chemical Warfare Agents and Explosives PGAA (which focuses on (n,γ) to identify explosives [7, 8, 9, 10]) and the Nuclear Resonance Fluorescence (NRF, which uses gammas to activate the SNM [11]). Runkle *et al.* give an overview on active interrogation of SNM [12].

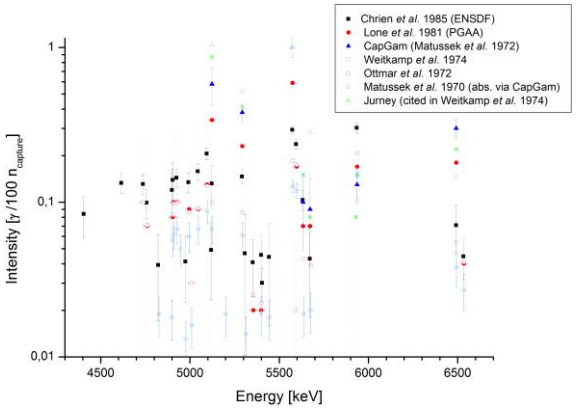

Figure 1: Measured plutonium-239 (n,γ)-intensities. The references are specified in the plot legend.

Most papers on (n,γ) in plutonium date in the 1970s and 1980s and do not discuss isotopic vectors [13, 14, 15, 16, 17, 18, 19, 20]. The measured intensities vary between one and two orders of magnitude between the different publications and databases, see Figure 1. Uranium has also been researched in the 2010s: Molnár *et al.* were able to assess the enrichment up to 36% U-235 [21] and Chichester *et al.* showed that a simple DD-generator set-up is not fit to identify highly enriched uranium [22].

There are two databases, which summarise (n,γ)-intensities and specific cross sections, respectively. The Prompt Gamma-ray neutron Activation Analysis database (PGAA [23]) was created from 1999 to 2003 by the International Atomic Energy Agency Nuclear Data Service (IAEA NDS) and contains the natural elements (up to uranium with Z=92). Plutonium is not included, but the PGAA database refers to Lone *et al.* [15]. The Thermal Neutron Capture gamma's database (CapGam [24]) by the Brookhaven National Laboratory National Nuclear Data Center (BNL NNDC) was last updated in 2013 and goes up to berkelium. Most publications and both databases refer to thermal neutron capture.

3. Assumptions

A Mathematica code has been written to analytically anticipate the neutron induced gamma spectra of fissile material above 3 MeV. Two different neutron sources and three different targets will be compared.

3.1. Neutron source

Two neutron sources are considered, a nuclear research reactor and a Deuterium-Deuterium Electronic Neutron Generator (DD-ENG). The research reactor estimates are oriented towards the existing PGAA set-ups in Garching and Budapest [25, 26, 27, 28, 29, 30, 31]. The assumed FRM-II reactor has a thermal equivalent neutron flux of $2.7 \cdot 10^{10}\ \mathrm{s}^{-1}\ \mathrm{cm}^{-2}$ at the target position and a cold source made of 25 K liquid D_2 [25]. In the following, we use the thermal equivalent flux because no comprehensive neutron flux spectrum is available. It is derived with the thin sample approximation [32]:

$$\int_0^\infty \sigma_\gamma(E_n)\,\Phi(E_n)dE_n = \sigma_{\gamma,0}\Phi_0$$

Deviations from the 1/v dependence are accounted for with the according Westcott *g* factors [33]. Their high neutron fluxes and low neutron energies are major advantages of research reactors, especially of the FRM-II.

For the DD-generator the continuous neutron energy distribution given by Fantidis *et al.* [34] is used. The total neutron flux is $10^5\ \mathrm{s}^{-1}\ \mathrm{cm}^{-2}$ at the target position and the peak energy $2.5\ MeV$ [35, 36]. The DD-source generates fast neutrons and a lower flux, but has the decisive asset to be portable.

3.2. Fissile material target

Target	Mass	ΔMass	Isotope	wt.%	Δwt.%
HEU [22]	610 g	1 g	U-235	90	1
			U-238	10	1
HEU	100 g	1 g	U-235	90	0.01
			U-238	10	0.01
WGPu	100 g	0.01 g	Pu-239	95	0.01
			Pu-240	5	0.01

Table 1: Characteristics of the simulated fissile material samples.

The assumed fissile material samples are summarised in Table 1. The first target is identical to a measured Highly Enriched Uranium (HEU) sample to allow comparison [22]. The masses of the other two samples are generic to facilitate extrapolation. All targets are assumed to have a cross section of $1\ cm^2$ perpendicular to the neutron beam and to

approximate a point source in respect to the HPGe detector.

3.3. Gamma detector efficiency

A point source in 10 cm distance of a HPGe detector (50% NaI) is assumed. The following efficiency calibration curve has been provided by Helmut Fischer, University of Bremen[2]:

$$\ln(\varepsilon) = \begin{cases} -294.7+273.70\ ln(E)-96.6700\ ln^2(E) \\ \quad +15.18\ ln^3(E)-0.89420\ ln^4(E) \end{cases}, \quad E \leq 100\ keV$$

$$\ln(\varepsilon) = \begin{cases} -28.50+16.260\ ln(E)-3.83000\ ln^2(E) \\ \quad +0.382\ ln^3(E)-0.01423\ ln^4(E) \end{cases}, \quad E \geq 100\ keV$$

Its uncertainty (including geometrical uncertainties) is set to 10%.

3.4. Nuclear reactions

The reaction of most interest here is the radiative neutron capture. In addition, the background from neutron capture, prompt fission gamma-rays and delayed fission gammas are considered and added to the signal. All other nuclear reactions, e.g. spontaneous fission and neutron scattering are neglected. The latter assumption is more justifiable for slow, than for fast neutrons, as non-elastic scattering with uranium and plutonium occurs only at high neutron energies.

3.4.1. Radiative neutron capture

Most gamma-rays from radiative neutron capture in fissile material form a quasi-continuum and only few gamma-rays, mainly at the extremes of the spectrum are distinct [32].

The radiative neutron capture signal is assessed by the (n,γ)-reaction rate. Their cross sections are taken from ENDF/B-VII.1 (duplicates were manually deleted[3]). As discussed in Section 2, the published intensities vary significantly. The gamma-ray intensities used here are from Chrien *et al.* [13] for Pu-239 and from the CapGam database [24] for U-235, U-238[4] and Pu-240[5]. These are the most reliable data sets in the view of the authors.

Only gamma-rays with energies $\geq 3MeV$ are considered here. The highest gamma energy is at $6.5\ MeV$ emitted by Pu-239, the lowest at $3.0\ MeV$, emitted by U-238. The gamma-ray energies for plutonium can be seen in Figure 4. All these energies are valid for thermal neutron capture; with moderately higher neutron energies, the capture gamma energies are shifted, too [19] and more and more transitions are possible. These effects are neglected here and the results for the DD source therefore preliminary.

The gamma-ray intensities per neutron capture range from $3.79 \cdot 10^{-6}$ (U-238) to $1.3 \cdot 10^{-1}$ (Pu-240). The sums of all regarded discrete (n,γ)-intensities for the four isotopes U-235, U-238, Pu-239 and Pu-240 are $8.49 \cdot 10^{-3}$, $4.09 \cdot 10^{-2}$, $3.06 \cdot 10^{-2}$ and $9.37 \cdot 10^{-1}$, respectively. On average, 3.78 gammas are emitted per radiative neutron capture [37] (for $E_n < 1.09\ MeV$), but most of these form a quasi-continuum and only very few gamma-rays at both ends of the (n,γ)-spectrum can be observed [32].

To consider the most important physical effect in the HPGe detector, each gamma-ray is broadened to a Gaussian distribution with a constant Full Width at Half Maximum (FWHM) of $4\ keV$.

The count-rate is estimated as

$$R_{n,\gamma}(E_\gamma) = N_{AX} I_\gamma(E_\gamma)\ \varepsilon(E_\gamma) \int_0^\infty \Phi(E_n)\ \sigma_{n,\gamma}(E_n)\ dE_n\ ,$$

where N_{AX} is the number of target atoms, $I_\gamma(E_\gamma)$ the intensity, $\varepsilon(E_\gamma)$ the detector efficiency, $\Phi(E_n)$ the neutron flux and $\sigma_{n,\gamma}(E_n)$ the (n,γ)-cross section.

3.4.2. Prompt fission gammas

The prompt fission background is assessed by the (n,f)-rate. Their cross sections are taken from ENDF/B-VII.1 [38][6]. On average, each neutron induced fission leads to the emission of 8.095 photons [37] (for $E_n < 1.09\ MeV$). Most fission gammas have energies smaller than 1 MeV. The gamma energy distributions used in the following have been measured by [37, 39, 40]. Spontaneous fission and induced fission by secondary neutrons are neglected. The prompt fission gamma background count-rate is calculated analogous to the (n,γ)-count-rate:

$$R_{n,f}(E_\gamma) = 8.095\ N_{AX} I_f(E_\gamma) \varepsilon(E_\gamma) \int_0^\infty \Phi(E_n) \sigma_{n,f}(E_n) dE_n$$

[2] personal communication, June 2013
[3] There exist more than one cross section for some energies
[4] The gamma-rays at 3913.1 keV and at 3406.9 keV are adapted from the according PGAA-database intensities by the authors.
[5] might be originally from White *et al.* [43], then arbitrary intensities
[6] Again after deleting duplicate entries

3.4.3. Delayed fission gammas and continuous capture gammas

An additional background is caused by delayed gammas from fission. To our knowledge no such data is recorded in ENDF. Thus, an estimate for the delayed fission gamma spectrum was obtained by calculating the ratio of delayed fission to prompt gammas for the spectra given in Matussek *et al.* [16]. This energy dependent ratio is then multiplied by the intensities estimated for prompt gammas.

Most gamma-rays from radiative neutron capture form a continuum. This additional background is estimated analogously to the delayed fission gammas.

A limitation of our approach is the incomplete data base of measured spectra. First of all, only Weapons-Grade Plutonium (WGPu) and HEU were measured by Matussek *et al.*, but not Pu-240 and U-238. Hence, here the WGPu data had to be used for Pu-239 and Pu-240 and the HEU data for U-235 and U-238. Secondly, the energy ranges covered only $4\,MeV$ to $6\,MeV$ and $4.2\,MeV$ to $6.5\,MeV$, respectively. Therefore the ratio had to be extrapolated to include all gamma lines (from $3.0\,MeV$ to $6.5\,MeV$). The uncertainties are accordingly high.

4. Results

This section is divided in three subsections. First, the application of a chopper and n-γ-anti-coincidence set-up is discussed; second, the estimate with a DD-generator; third, the estimate with a thermal reactor neutron spectrum.

4.1. Chopper and n-γ-anti-coincidence

It is possible to separate the (n,γ)-signal from part of the background by the use of a chopper and n-γ-anti-coincidence measurements as successfully applied by Matussek *et al.* [16]. A chopper or pulsed neutron beam allows a differentiation between prompt and delayed fission gammas, the n-γ-coincidence/-anti-coincidence method between fission and (n,γ)-reactions.

Figure 2 shows the simulated spectrum of the HEU target with 90% enrichment and a DD-source without delayed fission and prompt fission gammas. This corresponds to the application of a chopper and anti-coincidence set-up as used by Matussek *et al.* As a result, the (n,γ)-peaks become significantly more visible. This effect is more intense for lower energies, i.e. it favours the nuclei with an even number of neutrons, Pu-240 and U-238. Therefore, the U-238 peak at $4.060\,MeV$ is visible. Unfortunately, the fission product Rb-90 has a decay line at $4.062\,MeV$ [41], which gives additional background. The U-235 peak at $6.4\,MeV$ is also significantly more distinct, but still weak. This is due to the continuous (n,γ)-background. In addition the overall count-rate is very low. All (n,γ)-peaks above $4.81\,MeV$ are from U-235 and all below $4.64\,MeV$ from U-238.

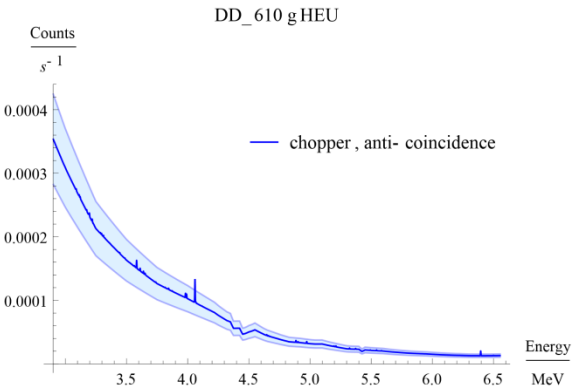

Figure 2: Theoretical (n,γ)-spectrum of a $610\,g$ 90% enriched HEU sample and a DD-generator with chopper and n-γ-anti-coincidence differentiation. Shaded areas represent uncertainties.

For all four simulated set-ups (HEU/WGPu with DD-ENG/FRM-II) the application of a chopper and the anti-coincidence method increases the signal to background ratio significantly, but does not change the general picture.

4.2. DD-generator

4.2.1. Comparison with measurement of uranium

For a $610\,g$ 90% enriched HEU sample our estimated (n,γ)-spectrum does not show any significant peak. Our estimations are in agreement with the finding of Chichester *et al.*, who used a similar set-up [22]. The background is mostly due to the delayed fission background and to a lesser degree due to prompt gammas from induced fission in uranium-235 and to the capture background.

4.2.2. Plutonium

The following results are produced with generic targets to allow easy extrapolation. However, due to self-absorption, a simple multiplication does not suffice.

The identical set-up with the same DD-generator, but a $1\,g$ WGPu target shows an lower count-rate, even if the mass difference is

accounted for. No single Pu-239 (n,γ)-line can be identified, at most some Pu-240 lines. For plutonium, the three different background contributors (Pu-239 fission, delayed fission and neutron capture gammas) are in the same order of magnitude up to $4\ MeV$. Thereafter, the delayed fission gammas become dominant.

4.2.3. Moderated DD-generator

The previous results indicate that an unmoderated DD neutron source does not allow the determination of the isotopic vector of neither SNM.

Moderation of the fast neutrons shifts the ratio between prompt fission (and following delayed fission) and neutron capture gammas to more desirable values. If one assumes a perfect moderator, all neutrons will be slowed down to the thermal state. Due to scattering, even with such a perfect moderator, a loss of neutrons still reaching the target will occur.

The used loss factor is established by MCNP (Monte Carlo N-Particle code [42]) simulations. An isotropic, mono-energetic 2.5 MeV neutron point source is assumed. The neutrons are moderated by $5\ cm$ thick and $10\ cm$ by $10\ cm$ wide polyethylene (PE) in $28\ cm$ distance of the sample. This distance is derived from the known total flux of the DD-ENG and that at the target position [34, 35, 36]. The sample is a sphere with $1.3\ cm$ radius, centred $6.3\ cm$ behind the PE. All neutrons entering the sample sphere are detected. The neutron energy distribution simulated by MCNP confirms the assumption that many neutrons are thermalised. Their number results in n_{mod}, whereas n_{com} is the number of neutrons that would enter the sample if it was located at the PE position (in $28\ cm$ distance of the source). The loss factor results in $L = \frac{n_{mod}}{n_{com}} = 0.28$.

A perfectly moderated neutron spectrum corresponds to the reactor spectra, which use a thermal equivalent neutron flux. The difference between the simulations of the moderated DD-source and the reactor spectra lies in the original relative neutron flux ratio times the loss factor L. Only the count-rates and uncertainties vary, while the shape of the gamma spectra can be expected to be almost identical. The potential of a maximally moderated DD-ENG can therefore be estimated with the reactor spectra, e.g. Figure 4. With the assumed loss factor of $L = 0.28$ and the relative flux difference between the FRM-II and the supposed DD-ENG, an overall factor of $F = 4.8 \cdot 10^4$ results.

4.3. Reactor spectra

This subsection is again divided in two parts. First, uranium is discussed, second, plutonium.

4.3.1. Uranium

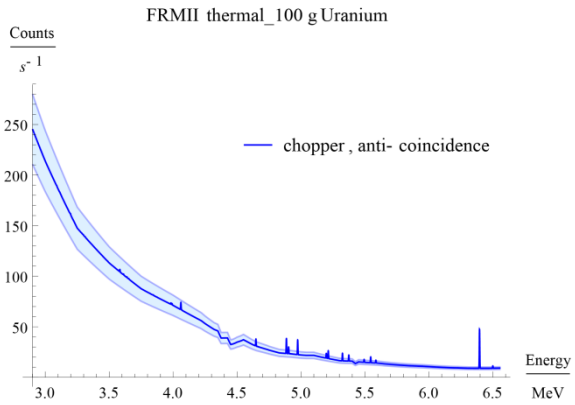

Figure 3: Theoretical (n,γ)-spectrum of a $100\ g$ 90% enriched HEU sample and neutrons from the FRM-II research reactor with "chopper" and n-γ-anti-coincidence differentiation. Shaded areas represent uncertainties.

As expected from the much higher neutron flux of the neutron source, the overall count-rate is much higher than with the DD-generator. It is so high that dead time effects will dominate and the detector might even be damaged. Therefore, additional shielding will be necessary, see Subsection 4.3.3.. However, the fission background is still suppressing most (n,γ)-peaks. The U-235 peak at $6.4\ MeV$ is by far the strongest peak. The U-238 $4.06\ MeV$ peak visible in the DD-spectrum (Figure 2) is not visible here, due to a shift in the cross section ratio $\sigma_{U-235}/\sigma_{U-238}$ and a high background from neutron capture and fission in U-235.

By the application of a chopper and an anti-coincidence set-up the (n,γ)-peaks become more distinct, see Figure 3. However, the general picture does not change. The U-238 peaks are still suppressed and the U-235 peak at $6.4\ MeV$ clearly dominates. This is consistent with Matussek *et al.* [16], who could identify this peak only. All (n,γ)-peaks above $4.81\ MeV$ are from U-235 and all below $4.64\ MeV$ from U-238.

As discussed, these results are transferable to an ideal moderated DD neutron source.

4.3.2. Plutonium

Figure 4 shows the simulated (n,γ)-spectrum of a 1 g WGPu target with 95% Pu-239 and 5% Pu-240 and the FRM-II research reactor as

neutron source. All (n,γ)-peaks above $5.08\ MeV$ are from Pu-239, all below $4.40\ MeV$ from Pu-240. The background is due to induced fission gammas in Pu-239, subsequent delayed fission gammas and continuous neutron capture gammas.

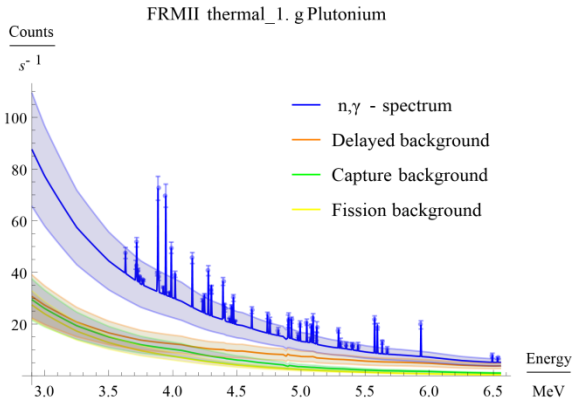

Figure 4: Theoretical (n,γ)-spectrum of a $1\ g$ WGPu sample with 95% Pu-239 and 5% Pu-240 and the FRM-II research reactor as neutron source (upper-most curve). Shaded areas represent uncertainties.

Again, the overall count-rate is much higher than with the DD-generator. Therefore, additional shielding will be required. For plutonium, most (n,γ)-lines are visible for both isotopes, Pu-239 and Pu-240.

4.3.3. Attenuation of prompt and delayed fission gammas

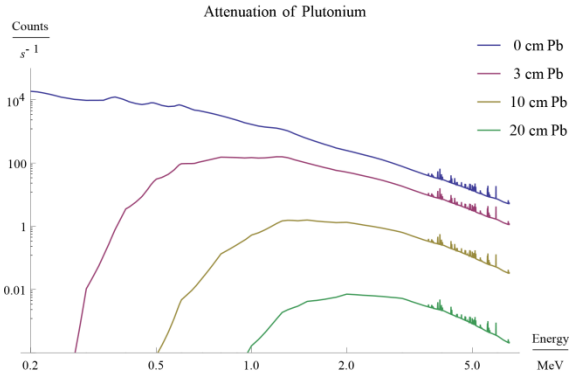

Figure 5: Pu spectrum (Figure 4, 95% Pu-235, 5% Pu-240, FRM-II), attenuated by 0-$20\ cm$ Pb.

The application of a chopper and anti-coincidence set-up does not sufficiently reduce the high gamma count-rates for the research reactor spectra. Therefore, the gamma-rays should be attenuated by additional shielding. Figure 5 compares the FRM-II plutonium spectrum in Figure 4 with the same spectrum attenuated by $3\ cm$, $10\ cm$ and $20\ cm$ of Pb[7].

[7] Mass attenuation coefficient data from Hubbel and Seltzer [44]

The spectrum is extrapolated below $4\ MeV$, see Subsection 3.4.3., resulting in high uncertainties. The peak/background ratio between 3 and $6.5\ MeV$ does hardly change. This also applies to the simulations with uranium as target and/or the DD-generator as neutron source.

5. Conclusion

The estimates presented here indicate that (n,γ)-spectroscopy with a simple DD-generator set-up is not possible, neither for uranium as already reported by Chichester *et al.* [22], nor for plutonium. Even suppression of the major external background effects (fission and delayed fission gammas) would not allow the determination of the isotopic compositions.

It is shown that the identification of Pu-239 and Pu-240 is possible with reactor neutrons. It also looks promising to measure the isotopic vector of plutonium with thermalised neutrons from a DD-generator.

This does not apply to uranium. A solution could be to use thermal neutrons to measure U-235, fast neutrons for U-238 and then combine both results to determine the enrichment.

Lead shielding poses an effective instrument in attenuating undesirable gamma-ray background without significant adverse mitigation of the (n,γ)-peaks between 3 and $6.5\ MeV$.

6. Outlook

The (n,γ)-measurement technique could expand current dismantlement verification techniques. It could solve the issue of an unknown shielding of the nuclear warhead or weapon pit in the container. Uncertainties could be reduced and therefore trust in the measurements and information barriers strengthened.

This measurement technique might also be useful in IAEA Safeguard applications and CBRN (Chemical, Biological, Radiological and Nuclear) defence. While active interrogation and the measurement of induced fission gammas might suffice to find hidden fissile material, it does not give information on the isotopic vector, although it may be crucial.

In order to show the feasibility of the (n,γ)-technique, we are going to perform measurements with research reactor and

moderated DD-ENG neutrons. For CBRN defense additional estimates with radioactive neutron sources such as americium-beryllium and californium-252 are carried out.

7. Acknowledgements

The authors thank Martin B. Kalinowski for the initial idea for this project. It would not have been possible without him, Reinhard Lieberei, Götz Neuneck, Caren Hagner and Malte Göttsche. Further thanks go to Erik Buhmann for proof-reading.

This research is funded by the German foundation for peace research (DSF).

8. References

[1] Committee on International Security and Arms Control, National Research Council, *Monitoring Nuclear Weapons and Nuclear-Explosive Materials: An Assessment of Methods and Capabilities*, J. P. Holdren and S. Fetter, Eds. National Academy of Sciences, 2005. http://www.nap.edu/-catalog.php?record_id=11265

[2] J. Carlson, J. Fuller, K. Hartigan, M. Dreicer, L. Duckworth, M. Göttsche, C. Hinderstein, S. Høibråten, D. Keir, D. B. Laird, M. Williamson, M. Bunn, A. Diakov, C. Hinderstein, R. Rajaraman, T. Renis, E. Rowan, J. Siegel, M. Smith, L. van Dassen, and T. Wood, *Innovating Verification: Verifying Baseline Declarations of Nuclear Warheads and Materials*, ser. Innovating Verification reports series. Nuclear Threat Initiative, July 2014. http://www.nti.org/analysis/reports/-innovating-verification-verifying-baseline-declarations-nuclear-warheads-and-materials/

[3] M. Göttsche and G. Kirchner, "Measurement techniques for warhead authentication with attributes advantages and limitations," *Science & Global Security*, vol. 22, pp. 83–110, 2014. http://-scienceandglobalsecurity.org/archive/2014/05/-measurement_techniques_for_war.html

[4] J. T. Mihalczo, J. K. Mattingly, J. A. Mullens, and J. S. Neal, *NMIS With Gamma Spectrometry for Attributes of Pu and HEU, Explosives and Chemical Agents*, May 2002. http://www.osti.gov/scitech/servlets/purl/799512

[5] J. Church, D. Slaughter, S. Asztalos, P. Biltoft, M.-A. Descalle, J. Hall, T. Luu, D. Manatt, J. Mauger, E. Norman, D. Petersen, and S. Prussin, "Signals and interferences in the nuclear car wash," *Nuclear Instruments and Methods in Physics Research*, vol. B 261, pp. 351–355, 2007.

[6] J. Hall, S. Asztalos, P. Biltoft, J. Church, M.-A. Descalle, T. Luu, D. Manatt, G. Mauger, E. Norman, D. Petersen, P. J., S. Prussin, and D. Slaughter, "The nuclear car wash: Neutron interrogation of cargo containers to detect hidden SNM," *Nuclear Instruments and Methods in Physics Research Section B: Beam Interactions with Materials and Atoms*, vol. 261, no. 1-2, pp. 337–340, August 2007. http://dx.doi.org/10.1016/j.nimb.2007.04.263

[7] A. Caffrey, J. Cole, R. Gehrke, and R. Greenwood, "Chemical warfare agent high explosive identification spectroscopy neutron induced gamma-rays," *IEEE Transactions on Nuclear Science*, vol. 39, no. 5, pp. 1422–1426, October 1992.

[8] E. H. Seabury and A. J. Caffrey, "Explosive detection and identification by PGNAA," Idaho National Engineering and Environmental Laboratory, Bechtel BWXT Idaho, LLC, Tech. Rep., November 2004.

[9] E. H. Seabury and A. J. Caffreys, "Explosives detection and identification by PGNAA," Idaho International Laboratory, Tech. Rep., April 2006. http://dx.doi.org/10.2172/-911698

[10] T. R. Twomey, A. J. Caffrey, and D. L. Chichester, "Nondestructive identification of chemical warfare agents and explosives by neutron generator-driven PGNAA," Idaho National Laboratory, Idaho Falls, Idaho 83415 USA, Tech. Rep., 2007.

[11] G. A. Warren and R. S. Detwiler, "Nuclear resonance fluorescence for material verification in dismantlement," Pacific Northwest National Laboratory, 902 Battelle Blvd, MSIN J4-65, Richland, WA, 99352 USA, Tech. Rep., 2011.

[12] R. C. Runkle, D. L. Chichester, and S. J. Thompson, "Rattling nucleons: New developments in active interrogation of special nuclear material," *Nuclear Instruments and Methods in Physics Research Section A: Accelerators, Spectrometers, Detectors and Associated Equipment*, vol. 663, no. 1, pp. 75–95, January 2012. http://dx.doi.org/10.1016/-j.nima.2011.09.052

[13] R. Chrien, J. Kopecky, H. Liou, O. Wasson, J. Garg, and M. Dritsa, "Distribution of radiative strength from neutron capture by Pu-239," *Nuclear Physics A*, vol. 436, no. 2, pp. 205 – 220, 1985. http://-www.sciencedirect.com/science/article/pii/-0375947485901964

[14] D. M. Drake, J. C. Hopkins, C. S. Young, and H. Condé, "Gamma-ray-production cross sections for fast neutron interactions with

several elements," *Nuclear Science and Engineering*, vol. 40, no. 2, p. 294, 1970.
[15] M. A. Lone, R. A. Leavitt, and D. A. Harrison, "Prompt gamma rays from thermal-neutron capture," Atomic Energy of Canadas Limited Chalk River Nuclear Laboratories, Ontario, Canada, Tech. Rep., 1981.
[16] P. Matussek, W. Michaelis, C. Weitkamp, and H. Woda, "Studies of radiative neutron capture and delayed fission gamma-ray spectra from uranium and plutonium as a basis for new non-destructive safeguards techniques," in *Safeguards techniques: proceedings of a Symposium on progress in safeguards techniques / organized by the International Atomic Energy Agency and held in Karlsruhe, 6-10 July 1970*, vol. 2, no. IAEA-SM133/33, 1970, p. 113.
[17] P. Matussek, H. Ottmar, I. Piper, C. Weitkamp, and H. Woda, "Measurement of gamma-ray spectra from thermal neutron interaction with U235," in *Conference on Nuclear Structure Study with Neutrons*, 1972, pp. A42, 84.
[18] P. Matussek, H. Ottmar, C. Weitkamp, and H. Woda, "Study of Pu240 by thermal neutron capture," in *Conference on Nuclear Structure Study with Neutrons*, 1972, pp. A43, 86.
[19] H. Ottmar, P. Matussek, C. Weitkamp, and H. Woda, "Average width of E1 and M1 radiative transitions from neutron capture states in Pu-240," in *Conference on Nuclear Structure Study with Neutrons*, 1972, pp. A44, 88.
[20] C. Weitkamp, P. Matussek, and H. Ottmar, "Nondestructive nuclear fuel assay by neutron capture gamma-ray spectrometry," in *Neutron capture gamma-ray spectroscopy: proceedings of the Second International Symposium on Neutron Capture Gamma-Ray Spectroscopy and Related Topics*, Petten, The Netherlands, September 2-6 1974.
[21] G. Molnár, Z. Révay, and T. Belgya, "Non-destructive interrogation of uranium using PGAA," *Nuclear Instruments and Methods in Physics Research*, vol. 213, pp. 389–393, 2004.
[22] D. L. Chichester, E. H. Seabury, J. Wharton, and S. M. Watson, "INL neutron interrogation R&D: FY2010 MPACT end of year report," Office of Scientific and Technical Information, Tech. Rep., August 2010. http://-www5vip.inl.gov/technicalpublications/-documents/4680348.pdf
[23] Prompt Gamma-ray neutron Activation Analysis database (PGAA). (1999-2003) International Atomic Energy Agency (IAEA) Nuclear Data Service (NDS). https://www-nds.iaea.org/pgaa/
[24] Thermal Neutron Capture Gamma's database (CapGam). (2013, September) Brookhaven National Laboratory (BNL) National Nuclear Data Center (NNDC). http://-www.nndc.bnl.gov/capgam/
[25] P. Kudejova, L. Canella, R. Schulze, N. Warr, A. Türler, and J. Jolie, "Characterization of the new PGAA and PGAI facility at the research reactor FRM II," in *NRC7 - Seventh International Conference On Nuclear And Radiochemistry*, 2008.
[26] W. Petry, "Advanced neutron instrumentation at FRM-II," in *IGORR 9: Proceedings of the 9. meeting of the International Group On Research Reactors*, vol. IAEA Ref. Number 36019445, 2003, p. 346.
[27] *Advanced Lab Course in Physics at FRMII*, TU München, 2010.
[28] W. Petry. (2014) Advanced neutron instrumentation at FRM-II. Forschungs-Neutronenquelle Heinz Maier-Leibnitz (FRM II). http://www.frm2.tum.de/aktuelles/infos-und-downloads/misc0/advanced-neutron-instrumentation/
[29] Z. Révay, T. Belgya, Z. Kasztovszky, J. Weil, and G. Molnár, "Cold neutron PGAA facility at Budapest," *Nuclear Instruments and Methods in Physics Research*, vol. 213, pp. 385–388, 2004.
[30] Neutron-Induced Prompt gamma-ray Spectroscopy (NIPS) and Neutron Optics and Radiography for Material Analysis (NORMA). (2014) Budapest Neutron Centre. http://-www.bnc.hu/?q=node/15
[31] Prompt Gamma Activation Analysis (PGAA). (2014) Budapest Neutron Centre. http://www.bnc.hu/?q=node/14
[32] G. L. Molnár, *Handbook of Prompt Gamma Activation Analysis with Neutron Beams*, G. L. Molnár, Ed., 2004.
[33] A. L. Nichols, D. L. Aldama, and M. Verpelli, "Handbook of nuclear data for safeguards: database extensions," International Atomic Energy Agency - Nuclear Data Section, Tech. Rep. IAEA INDC (NDS)-0534, August 2008.
[34] J. G. Fantidis, B. V. Dimitrios, P. Constantinos, and V. Nick, "Fast and thermal neutron radiographies based on a compact neutron generator," *Journal of Theoretical and Applied Physics*, vol. 6, no. 1, p. 20, 2012. http://dx.doi.org/10.1186/2251-7235-6-20
[35] J. Reijonen, K.-N. Leung, R. Firestone, J. English, D. Perry, A. Smith, F. Gicquel, M. Sun, H. Koivunoro, T.-P. Lou, B. Bandong, G. Garabedian, Z. Révay, L. Szentmiklosi, and G. Molnár, "First PGAA and NAA experimental results from a compact high intensity D-D neutron generator," *Nuclear Instruments and Methods in Physics Research*, vol. 522, pp. 598–602, 2004.

[36] J. Reijonen, "Compact neutron generators for medical, home land security, and planetary exploration," in *Proceedings of 2005 Particle Accelerator Conference, Knoxville, Tennessee*, 2005.

[37] R. E. Hunter and L. Stewart, "Evaluated neutron-induced gamma-ray production cross sections for 239Pu and 240Pu," Los Alamos Scientific Laboratory, Tech. Rep. LA-4901, 1972.

[38] M. Chadwick, M. Herman, P. Obložinský, M. Dunn, Y. Danon, A. Kahler, D. Smith, B. Pritychenko, G. Arbanas, R. Arcilla, R. Brewer, D. Brown, R. Capote, A. Carlson, Y. Cho, H. Derrien, K. Guber, G. Hale, S. Hoblit, S. Holloway, T. Johnson, T. Kawano, B. Kiedrowski, H. Kim, S. Kunieda, N. Larson, L. Leal, J. Lestone, R. Little, E. McCutchan, R. MacFarlane, M. MacInnes, C. Mattoon, R. McKnight, S. Mughabghab, G. Nobre, G. Palmiotti, A. Palumbo, M. Pigni, V. Pronyaev, R. Sayer, A. Sonzogni, N. Summers, P. Talou, I. Thompson, A. Trkov, R. Vogt, S. van der Marck, A. Wallner, M. White, D. Wiarda, and P. Young, "ENDF/B-VII.1: Nuclear data for science and technology: Cross sections, covariances, fission product yields and decay data," *Nuclear Data Sheets*, vol. 112, no. 12, pp. 2887–2996, December 2011.

[39] V. V. Verbinski, H. Weber, and R. E. Sund, "Prompt gamma rays from 235U(n,f), 239Pu(n,f), and spontaneous fission of 252Cf," *Physical Review C*, vol. 7, no. 3, pp. 1173–1185, March 1973.

[40] A. Oberstedt, T. Belgya, R. Billnert, F.-J. Hambsch, Z. Kis, T. M. Perez, S. Oberstedt, L. Szentmiklosi, K. Takács, and M. Vidalid, "New prompt fission gamma-ray spectral data and its implication on present evaluated nuclear data files," in *Physics Procedia: Scientific Workshop on Nuclear Fission Dynamics and the Emission of Prompt Neutrons and Gamma Rays, Biarritz, France, 28-30 November 2012*, 2012.

[41] R. Firestone. Table of radioactive isotopes. Lawrence Berkely National Laboratory. http://ie.lbl.gov/toi/radSearch.asp

[42] X.-. M. C. Team. (2003) MCNP - a general monte carlo n-particle transport code. Los Alamos National Laboratory. https://-mcnp.lanl.gov/

[43] D. H. White, R. W. Hoff, H. G. Börner, K. Schreckenbach, F. Hoyler, G. Colvin, I. Ahmad, A. M. Friedman, and J. R. Erskine, "Nuclear structure of 241Pu from neutron-capture, (d,p)-, and (d,t)-reaction measurements," *PHYSICAL REVIEW C*, vol. 57, no. 3, p. 1112, 1998.

[44] J. H. Hubbell and S. M. Seltzer. (1990) Tables of x-ray mass attenuation coefficients and mass energy-absorption coefficients from 1 kev to 20 mev for elements z = 1 to 92 and 48 additional substances of dosimetric interest. Radiation Physics Division, PML, NIST. http://www.nist.gov/pml/data/xraycoef/index.cfm

An investigation of impurities and associated neutron signatures of strong orphan source of alpha (α) particles

Dina Chernikova[a,*], **Kåre Axell**[a,b], **Anna Vesterlund**[c,d], **Henrik Ramebäck**[c,d], **Senada Avdic**[e]

[a]Chalmers University of Technology, Department of Applied Physics, Nuclear Engineering, Fysikgården 4, SE-412 96 Göteborg, Sweden
[b]Swedish Radiation Safety Authority, SE-171 16 Stockholm, Sweden
[c]Swedish Defence Research Agency, FOI, CBRN Defence and Security, SE-901 82 Umeå, Sweden
[d]Chalmers University of Technology, Department of Chemistry and Chemical Engineering, Nuclear Chemistry, Fysikgården 4, SE-412 96 Göteborg, Sweden
[e]University of Tuzla, Department of Physics, 75000 Tuzla, Bosnia and Herzegovina

Abstract:

The present paper reports on an investigation of the presence and nature of impurities in a 185 GBq ^{241}Am α-source and their influence on the associated neutron signatures. Originally this work was initiated by the appearance of a few highly energetic Doppler broadened gamma-ray peaks in the gamma spectrum measured with a Detective-EX HPGe detector. In order to explain the nature of these gamma-lines several hypothesis have been checked. As a part of this procedure, the source was measured for signs of neutron radiation. The results of a test using a neutron monitor detector indicated a presence of neutron emission in the source. Following investigations of the source using EJ-309 fast liquid scintillators, which enable a separation between neutron and gamma, confirmed the presence of neutrons. This allowed obtaining a neutron spectrum and a quantification of the neutron source. Together, the experimental results and the results of Monte-Carlo modeling of underlying processes which causes specific neutron and gamma emissions allowed to uncover the possible type and nature of impurities in the ^{241}Am alpha-source.

Keywords: impurities, alpha source, neutrons

1. Introduction

The presence of neutrons in the emission spectra of strong alpha-sources can obscure the correct identification of the material being investigated, leading, therefore, to confusing conclusions. For example, a 185 GBq ^{241}Am α-source discussed in this paper originally was automatically identified as a plutonium sample[1]. This was a result of measuring a specific combination of gamma and neutron signatures of the source.

In most of the cases, appearance of neutrons is quite easily explained by the (α,n)-reactions on the adjoint materials of the source, such as Be, Li or Al. However, it is not as simple to explain and trace neutrons originated from impurities-base reactions. Often impurities itself first become a subject for a separate investigation and only afterwards an origin of neutron emission is uncovered. The case which is considered in this piece of the research falls under the latter category. Thus, the complete investigation of age and impurities in the source is reported in [1]. The present paper is meant to be focused mostly on the investigation of associated neutron signatures and provide additional details in the study of impurities.

2. Description of an experimental set-up and procedure

In order to investigate the presence of neutron emission in a 185 GBq ^{241}Am sealed α-source and suggest hypothesis on possible origin of the neutron emission experimental studies were performed in two different setups. First experimental setup consisted of one EJ-309 (D76 x 76 mm) liquid scintillation detector placed at the distance of 19 cm from the source as shown in Figure 1. The source was enclosed into the lead container to decrease a contribution of low energetic gammas to the measurement data. Second experimental setup consisted of two EJ-309 (D76 x 76 mm) liquid scintillation detectors placed each at the distance of 23 cm from the source (at the 180°). This setup was used in order to evaluate a count distribution

*Corresponding author, email: dina@nephy.chalmers.se

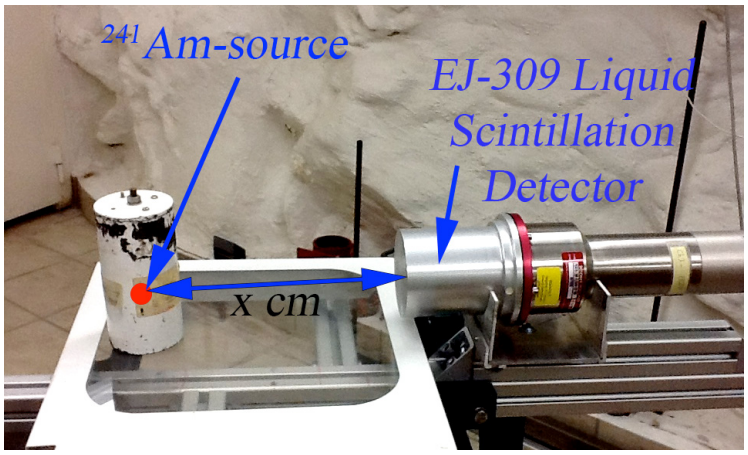

Figure 1: Photo of the configuration of the experimental setup (for one detector case).

for emitted neutrons. In all cases detectors were connected to the 8 channel, 12 bit 250 MS/s, VX1720E CAEN digitizer. A calibration procedure was performed with ^{137}Cs and ^{22}Na sources in the same way as described in [2]. As a result of this procedure, the high voltage bias and the DC offset were adjusted for each detector/channel individually as follows: Channel 0 (Ch 0, Voltage: 1915 V, DC offcet: -38.4) and Channel 3 (Ch 3, Voltage: 1750 V, DC offcet: -39.9). In the first experimental setup data were collected during 610 seconds and afterwards post-processed offline (pulse height threshold was equal to 0.06 MeVee). Time of data collection in the second setup was 877 seconds. Background was also measured and substructed when needed, as a routine part of the procedure.

3. Indicators of neutron presence

Originally, a presence of neutron emission in the ^{241}Am sealed α-source was discovered by using a Neutron Monitor 2222A He-3, Pig detector. Results obtained in that measurements indicated the need of careful separation between gamma and neutron particles which in the present study were approached by using liquid scintillation detectors to obtain signals and pulse shape discrimination signal processing procedure in a way similar to [3]. Pulse shape discrimination was performed by using a robust charge comparison method [4]. It should be noticed that better discrimination quality may be obtained with other methods, e.g. correlation-based techniques [5] or artificial neural networks [6, 7]. Although, as shown in Figure 2, the charge comparison method shows good performance in the present case, the neutrons and gammas are well separated. As it is shown, there is a clear presence of significant amount of neutrons in

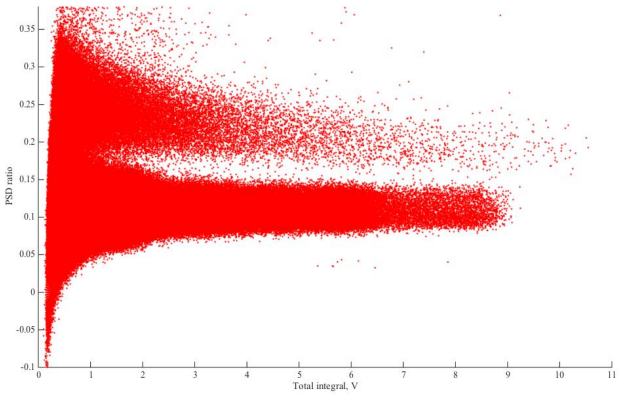

Figure 2: 2D plot of the counts as a function of the pulse energy and the PSD parameter[3].

the emission spectra of strong α-source. To achieve a sufficiently good separation between neutrons and gammas, the PSD parameter threshold was set to a value of 0.175.

Thus, by taking into account the solid angle and point source model, the first approximation of the neutron (with energy higher than $\sim$600 keV) emission intensity provides a value of $(1.9 \pm 0.1) \cdot 10^4$ neutrons per second. The corresponding value for gammas (with energy higher than $\sim$60 keV) is $(6.19 \pm 0.08) \cdot 10^5$ gammas per second. However, it should be mentioned that these values are still underestimated and are planned to be further investigated with a joint use of MCNPX modeling and experimental tests.

In order to investigate a neutron pulse height spectra measured by liquid scintillation detectors, measured light output in the units of MeVee was converted to the transferred neutron energy in the units of MeV by using following expression:

$$E(MeV) = 3.2169 + 1.223 * L(MeVee) + 3.368591 * LambertW(-0.367 * e^{-0.3632 * L(MeVee)}), \quad (1)$$

where LambertW is the Lambert W function (the omega function), L(MeVee) is the measured light output in the units of MeVee. Quantitative values of the expression implicitly corresponds to the experimental values of the exponential light curve 3-inch EJ-309 liquid scintillation detector measured in [8].

In Figure 3 one could see measured neutron pulse height spectra. In order to get any correspondence

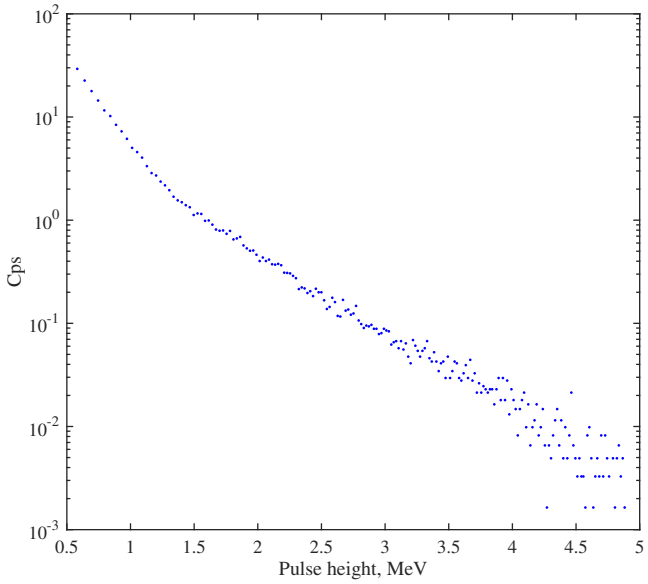

Figure 3: The neutron pulse height spectra measured by liquid scintillation detectors.

between the measured and source-related neutron spectrum an unfolding procedure shall be performed. This is, however, a subject for future work.

4. An investigation of impurities

4.1. Identified gamma lines and corresponding impurities

The analysis of impurities and their sources is well described in our paper [1]. However, it is important to recall some results. As a first step of impurities evaluation, the strong α-source was measured using a high purity germanium (HPGe) detector of coaxial type with high voltage bias set to -3000 V. The data was collected during 26100 seconds with a dead time of 13.66 %. The normalized results of these measurements are shown in Figure 4 together with a pulse height gamma spectrum obtained by EJ-309 liquid scintillation detector. The analysis of energies of gamma lines in the spectrum together with analysis of the slowing-

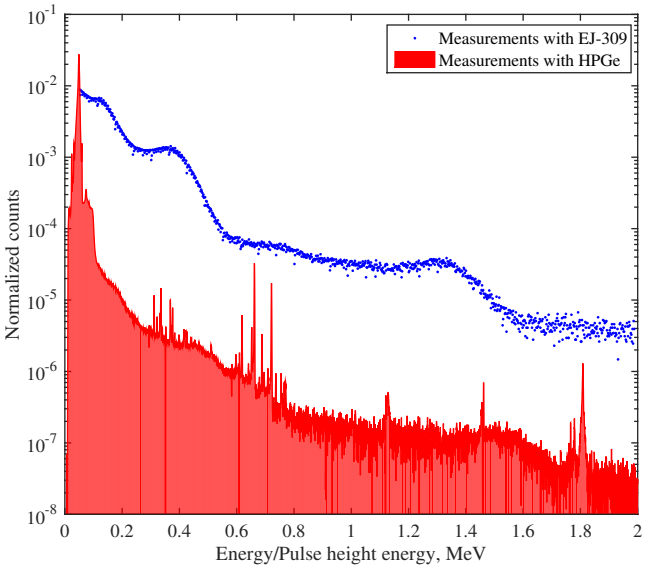

Figure 4: The gamma pulse height/energy spectra measured by liquid scintillation detector and HPGe detector (normalized).

down time of ions (^{23}Na, ^{26}Mg, ^{29}Si etc.) in a ^{241}Am source[1][1] and half-lives of the excited states of ^{23}Na, ^{26}Mg, ^{29}Si etc., in particular, analysis of Doppler shift in the gamma peaks, allowed us manually draw the conclusions on the presence of specific impurities in the source and on the possible scheme of their evolution within the source, as shown in Figure 5.

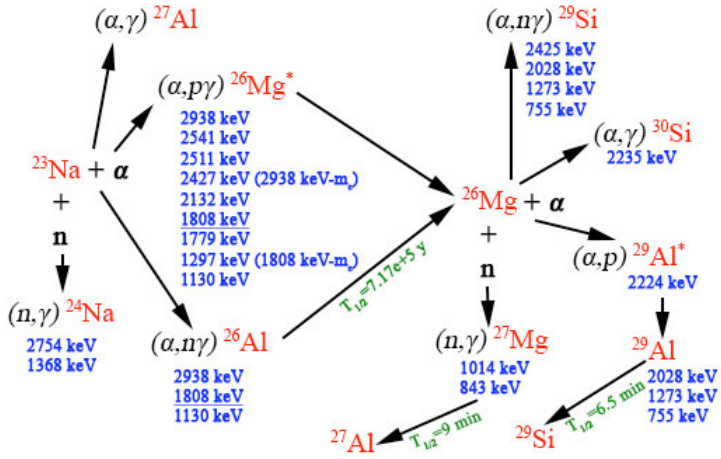

Figure 5: Identified gamma lines from nuclides other than ^{241}Am and its progeny, and suggested scheme of reactions.

One should mention that there are a number of programs which are normally used to evaluate origin of gamma-rays in the sources; most of them cover a wide range of energies and reaction types. However, as far as we are aware, none of them is polished enough to evaluate impurity types using specifically α particle induced gamma-rays. For example, even if ^{23}Na impurity can be identified by some of the programs, identification of the ^{26}Mg, ^{29}Si and ^{26,27,29}Al impurities (present at the same time) can lead to a confusion.

Therefore, in order to verify our ”half-manual” identification of impurities the artificial neural networks

[1]MCNPX simulations

were applied together with experimental data as a result of measurements of prompt gamma-rays induced by 5 MeV alpha-particles on 56 elements of periodic Mendeleev table[9].

4.2. Application of artificial neural networks

Artificial neural networks (ANNs) can be applied to many data processing applications, among them rapid pattern recognition. In order to identify impurities in the ^{241}Am source by using the ANN, we have created a library of 56 elements with gamma peak energy data obtained by bombarding the elements with 5 MeV alpha particles[9]. The first tests were performed for nine single elements and five combinations of two elements. It is planned in further work to include all 56 elements and their combinations.

The ANN used in this work is constructed from the Neural Network Toolbox in MatLab[10]. Different structures of networks and training algorithms were investigated and the best combination was selected by method of trials and errors. The ANN training procedure includes gamma-ray energies from individual elements as input data with a back-propagation (BP) algorithm.

The Levenberg-Marquardt (LM) back-propagation training algorithm was found to be the most effective one for the given task. The ANN is composed of an input layer with energy gamma peaks provided to each neuron of the input layer, two hidden layers with 35 and 15 neurons, respectively determined through trials and errors to be optimal and an output layer for 9 elements and 5 combinations of two elements. Each output neuron corresponds to one element or combination of elements and the output value corresponds to a probability of existence of the elements or their combinations. The log-sigmoid transfer function was used for the hidden and output layers, giving values between 0 and 1. The training target values were set to 1 for the correct element and 0 for the other elements or their combinations. The input data were pre-processed with histogram with energy step of 10 keV in the energy range between 700 and 3854 keV.

After the time-consuming training process, the identification procedure with the ANN is fast. The network was tested with the gamma spectrum of the source of ^{241}Am measured by a high purity germanium (HPGe) detector of coaxial type [1]. After subtraction of background gamma peaks and gamma peaks from the pure ^{241}Am, the rest of gamma peaks in the measured spectrum of ^{241}Am source is presented to the trained network in order to identify impurities.

Table 1 shows the list of elements and their combinations which were used in the training procedure, as well as probabilities of their recognition by the ANN for the measured spectrum of ^{241}Am (spectrum in question).

Table 1: Recognition of impurities by the ANN.

Element	Na	Mg	Cu	Al	Si	B	O_2	Fe	Zn	Na+Mg	Al+Si	Na+Cu	Mg+Cu	Cu+Si
Recognition	0	0	0	0	0	0	0	0	0	1	0	0	0	0

Results shown in the Table 1 indicate that the trained network with a high probability recognizes the presence of the combination of Na and Mg impurities in the strong ^{241}Am source.

Thus, ANN algorithm which was tested in the present work shows a potential to be used for high accuracy identification of combination of impurities present in a strong ^{241}Am α-sources. It may possibly be used for other types of α-sources but it is not adapted for this yet. This type of ANN approach is considered to be useful in situations that require rapid response without accurate quantification.

5. Possible sources of neutrons

Both manual and ANN-based analysis of impurities partially confirms the presence of ^{23}Na and ^{26}Mg impurities in the ^{241}Am source. Therefore, as shown in Figure 5 for the ^{241}Am source there are three main reactions which can lead to the production of neutrons in the strong α-source containing impurities:

$$\begin{aligned} {}^{23}Na + \alpha &\rightarrow (\alpha, n\gamma)^{26}Al \\ {}^{26}Mg + \alpha &\rightarrow (\alpha, n\gamma)^{29}Si \\ {}^{241}Am - spontaneous fission &\rightarrow p(n, \gamma) \end{aligned} \tag{2}$$

Regarding the last item in the list, i.e. a production of the neutrons in spontaneous fission of ^{241}Am itself, it should be mentioned that branching of ^{241}Am decay by spontaneous fission is very rare, i.e. the probability is 3.6(9)E-10 %. However, ^{241}Am has a high cross-section for induced neutron fission (both low energy and high energy neutrons), which may play a significant role in estimation of neutron emission intensity of the ^{241}Am source with impurities. Therefore, this effect was investigated additionally in the second experimental setup with two liquid scintillation detectors. The same data processing procedure was followed with the only difference that a time stamping information was retrieved and used to build a neutron count distribution in the time gate, as shown in Figure 6.

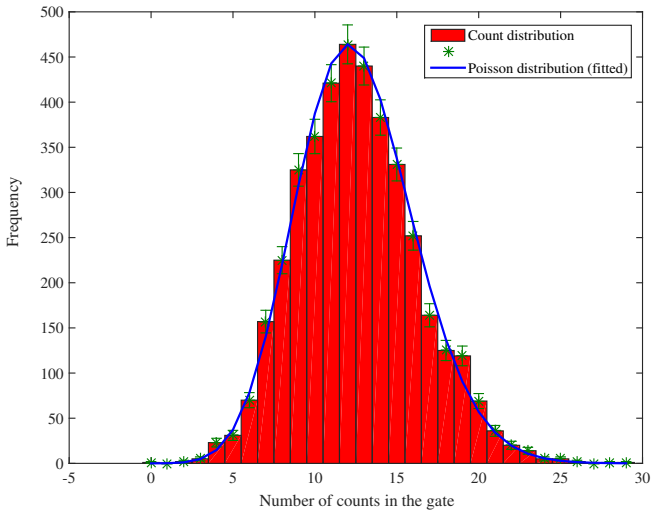

Figure 6: The neutron count distribution in the time gate.

In a case of induced fission neutrons present, the individual detections of neutrons should not be independent, instead rather positive correlations should exist between them due to the branching character of the fission process. At the same time, in the case of neutrons emitted from a source that follows simple Poisson statistics, the individual detections of neutrons are independent. Figure 6 indicates that with a high degree

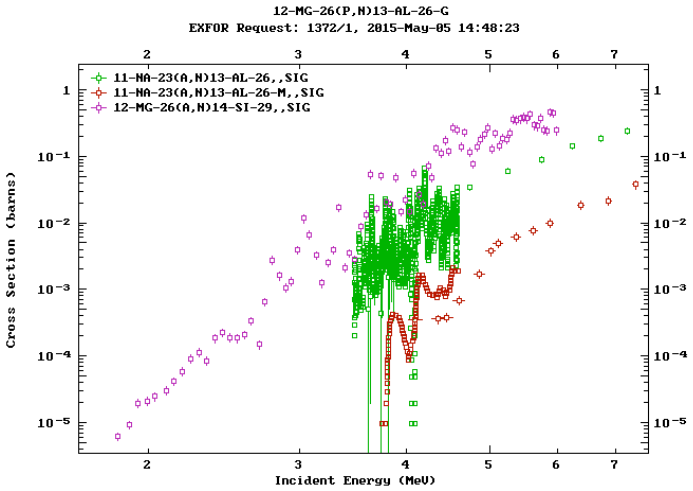

Figure 7: Cross-section data from Experimental Nuclear Reaction Data (EXFOR)[11].

of confidence it is possible to conclude that most of the neutrons emitted from the strong ^{241}Am α-source obey Poisson statistics. It means that certainly these are not fission neutrons, and therefore, most probably

these neutrons are emitted in $(\alpha, n\gamma)$ reactions (see discussion above). According to [12], in sodium a yield of neutrons per 10^6 alpha particles with average energy of 5.3 MeV is $\sim$ 1.5, which is $5.55 \cdot 10^6$ neutrons per second per Ci, or $2.49 \cdot 10^8$ neutrons per second per gram. At the same time in magnesium a yield of neutrons per 10^6 alpha particles with average energy of 5.3 MeV is $\sim$ 1.4, which is $5.18 \cdot 10^6$ neutrons per second per Ci, or $2.33 \cdot 10^8$ neutrons per second per gram.

However, as one can see in Figure 7 it is not clear which element, ^{23}Na or ^{26}Mg, contributes the most to the neutron emission. This therefore, is to be investigated further.

6. Conclusions

As a result of present study, the intensity of emission of neutrons with energy higher than $\sim$600 keV was evaluated as $(1.9 \pm 0.1) \cdot 10^4$ neutrons per second in a first approximation. Since most of the neutrons emitted from the strong ^{241}Am α-source are obeying Poisson statistics they are certainly not born in a fission process. Therefore, most of these neutrons are suspected to be emitted in two $(\alpha, n\gamma)$ reactions on ^{23}Na and ^{26}Mg. As shown by manual and ANN investigations, these are the main impurities in the strong ^{241}Am α-source. However, at the present state it is not possible to draw any conclusion on the individual contribution of each element ^{23}Na or ^{26}Mg to the neutron emission. This therefore, is to be investigated further.

Acknowledgement

This work was supported by the Swedish Radiation Safety Authority, SSM.

References

[1] Anna Vesterlund, Dina Chernikova, Petty Cartemo, Kåre Axell, Anders Nordlund, Gunnar Skarnemark, Christian Ekberg, Henrik Ramebäck, Characterization of strong ^{241}Am sources, Applied Radiation and Isotopes 99 (2015), 162-167

[2] Dina Chernikova, Kåre Axell, Senada Avdic, Imre Pázsit, Anders Nordlund: The neutron-gamma Feynman variance to mean approach: gamma detection and total neutron-gamma detection (theory and practice) Nuclear Instruments and Methods in Physics Research A 782 (2015), 47-55.

[3] D. Chernikova, K. Axell, I. Pázsit, A. Nordlund, R. Sarwar, A direct method for evaluating the concentration of boric acid in a fuel pool using scintillation detectors for joint-multiplicity measurements, Nuclear Instruments and Methods in Physics Research Section A: Accelerators, Spectrometers, Detectors and Associated Equipment, (11/2013) 90-97.

[4] F.D. Brooks, A scintillation counter with neutron and gamma-ray discriminators, Nuclear Instruments and Methods, 4 (1959) 151-163.

[5] D. Chernikova, Z. Elter, K. Axell, A. Nordlund, A method for discrimination of neutron and gamma pile-up events in scintillation detectors with a simultaneous identification of malfunctioning ones, INMM 55th Annual Meeting, Atlanta, Georgia, USA, 2014.

[6] T. Tambouratzis, D. Chernikova, I. Pázsit, Pulse shape discrimination of neutrons and gamma rays using Kohonen artificial neural networks, Journal of Artificial Intelligence and Soft Computing Research, Vol.3, No.1,pp.77-88, 2013.

[7] T. Tambouratzis, D. Chernikova, I. Pázsit, A Comparison of Artificial Neural Network Performance: the Case of Neutron Gamma Pulse Shape Discrimination, IEEE Symposium on Computational Intelligence for Security and Defense Applications (CISDA), Singapore, 2013.

[8] A. Enqvist, C. C. Lawrence, T. N. Massey, S. A. Pozzi, Neutron light output functions measured for EJ-309 liquid scintillation detectors, Proceedings of INMM Annual meeting, Orlando, FL July 15-19, 2012.

[9] Giles,I.S., Peisach,M.,A survey of the analytical significance of prompt gamma-rays induced by 5 MeV alpha-particles. J. Radioanalytical Chemistry 50, 307-360, 1979.

[10] Neural networks toolbox, Users guide, The Math Works Inc.

[11] https://www-nds.iaea.org/exfor/exfor.htm.

[12] ORAU Team Dose Reconstruction Project for NIOSH,ORAUT-OTIB-0024, 2005

A rapid sample digestion procedure to aid initial nuclear forensics investigations for uranium-bearing ores and concentrates prior to gamma spectrometry

David G. Reading, Ian W. Croudace, Phillip E Warwick

GAU-Radioanalytical Laboratories, Ocean & Earth Science, University of Southampton, National Oceanography Centre, European Way, Southampton, SO14 3ZH, UK.
E-mail: d.reading@noc.soton.ac.uk

Abstract:

A rapid and effective preparative procedure has been evaluated for the accurate determination of low-energy (40-200 keV) gamma-emitting radionuclides (^{210}Pb, ^{234}Th, ^{226}Ra, ^{235}U) in uranium ores and uranium ore concentrates (UOCs) using high-resolution gamma ray spectrometry. The measurement of low-energy gamma photons is complicated in heterogeneous samples containing dense, mineral phases. Attenuation corrections using mean density estimates result in an underestimation of the activity concentration where dense grains are dispersed within a less dense matrix (analogous to a nugget effect). The current method overcomes these problems using a lithium tetraborate fusion that readily dissolves all components including high-density, self-attenuating minerals/compounds in a matter of minutes. This is the ideal method for dissolving complex, non-volatile components in soils, rocks, mineral concentrates, and other materials where density reduction is required. This approach avoids the need for theoretical corrections or sample-specific matrix matching. The resulting homogeneous quenched glass produced can be quickly dissolved in nitric acid. The technique has been tested on uranium-bearing Certified Reference Materials and provides accurate activity concentrates compared to the underestimated activity concentration estimates derived from direct measurements of a bulk sample. The procedure offers an attractive solution for initial nuclear forensic studies where complex refractory minerals or matrices exist and is significantly faster, safer and simpler than alternative approaches and produces low-density solutions that can be counted by gamma spectrometry.

Keywords: *Borate fusion; photon self-attenuation; heterogeneous matrix.*

1. Introduction

The Nuclear Forensics International Technical Working Group recommend high-resolution gamma spectrometry (HRGS) on receipt of unknown, illicitly recovered materials such as uranium ore and uranium ore concentrate (UOC) [1–4]. In addition, the development of a database of gamma nuclide signatures for U-ores and UOCs of known provenance, combined with Principal Components Analysis (PCA) could aid in identifying the origin and history of recovered uranium ores and their concentrates.

The variance in sample matrices from HRGS calibration standards can cause an under or overestimation in photopeak efficiency for the detector due to the self-attenuation of low energy gamma photons within the matrix. Several radionuclides from the uranium and thorium series have low energy gamma emissions, which could be attenuated (table 1). Previous studies to overcome photon attenuation typically require direct transmission observations with a highly active source [5]; proxy measurements of higher energy gamma photons [6]; or theoretical density corrections derived from modelling photon interactions with the sample matrix [7]. This is not practical for rapid characterisation of recovered illicit materials. Additionally, adjusting the HRGS calibrations based on the relationship between photon efficiency and sample bulk density results in lower than expected activity concentrations. This problem is caused by dense U particles (uraninite = 8.5 g cm^{-3}) of varying size and concentration supported in less dense bulk matrices (typically < 2.0 g cm^{-3}).

Radionuclide	Energy (keV)	Gamma Yield (%)
^{210}Pb	46.5	4.3
^{241}Am	59.9	35.9
^{234}Th (^{238}U)	63.3	5.3
	92.4	13.7
	92.8	2.5
^{231}Th	84.2	6.7
	90.0	1.0
^{228}Th	84.4	1.2
	109.2	1.7
^{235}U	143.8	10.9
	163.4	5.1
	185.8	57.0
	202.1	1.1
	205.3	5.0
^{226}Ra	186.2	3.6

Table 1: Selected gamma emitting radionuclides where energy = < 200 keV and yield = > 1%.

A sample dissolution method using di-lithium tetraborate borate fusion was developed to reduce self-attenuation effects observed in U-bearing compounds to yield accurate activity concentrations from gamma-emitting radionuclides. This method does not require accurate characterisation of the sample prior to measurement, nor does it require any assumptions to be made about the samples composition or history.

2. Instrumentation

Radionuclide activity concentrations were determined with Canberra 50% N-type High Purity Germanium (HPGe) well-type detectors. Gamma spectra were acquired using Genie 2000 acquisition software (Canberra Industries, Harwell, UK) and analysed using Fitzpeaks spectral deconvolving software (JF-Computing, Stanford in the Vale, UK). The spectrometers were previously calibrated using a traceable, mixed nuclide source (NPL, Teddington, UK) with the addition of a ^{210}Pb solution standard (PTB, Braunschweig, Germany) mixed into a range of difference density matrices (cellulose, water, sand, steel and boron and a tin-tungsten ore) to produce a set of efficiency calibrations.

All samples were counted for one hour, as this was found suitable to obtain adequate counting statistics. The limit of detection values presented are based on the decision limit (or critical level) as defined by Currie [8].

3. Methodology

Three certified reference materials for uranium (CUP-1, BL-5 and CUP-2, Canadian Certified Reference Materials Project, Ottawa, Canada; table 2) were selected for this study.

	CUP-1 [9]	**BL-5** [10–12]	**CUP-2** [13]
Uranium (Wt%)	0.128 ± 0.002	7.09 ± 0.03	75.42 ± 0.17
^{238}U (Bq g^{-1})[a]	15.8 ± 0.3	876 ± 3.7	9313 ± 21
^{235}U (Bq g^{-1})[a]	0.70 ± 0.01	41.0 ± 0.2	434 ± 1
^{226}Ra (Bq g^{-1})	As ^{238}U	866 ± 21	< LOD
^{210}Pb (Bq g^{-1})	As ^{238}U	857 ± 38	< LOD

Table 2: Certified Reference Materials Data. [a]Activity concentration calculated from certified U wt% assuming natural ^{238}U/^{235}U abundances (99.275% and 0.72% respectively).

3.1 Initial characterisation of certified reference materials

All three certified reference materials were weighted into 20 mL polythene vials (CUP-1 = 28.1 g, BL-5 = 31.6 g, CUP-2 = 34.8 g) and the bulk densities were determined (1.36, 1.53 and 1.68 g cm^{-3} respectively). Apparent photon efficiencies of each measured radionuclide were calculated based on the bulk density of each reference material from the known relationship between photon detection efficiency and calibration standard density. The samples were characterised for ^{210}Pb, ^{234}Th, ^{226}Ra, ^{235}U and ^{234m}Pa activity concentrations. Protactinium-234m was measured as its high-energy gamma emissions (1001 keV) should not undergo sufficient photon attenuation in comparison to the lower energy radionuclides. Lead-214 and ^{214}Bi were not assessed for their extent of attenuation due to the possible disequilibria caused during sample preparation and radon de-gassing.

3.2 Lithium borate fusion

Borate fusion is well established as a sample digestion or dissolution method in geochemistry and is known to be effective in dissolving minerals and rocks comprising oxides, carbonates, chlorides, sulphates, sulphides, phosphates and metallic materials. Given the beneficial characteristics of borate fusions as a sample dissolution technique, it is surprising that there were no reported applications in the field or radioanalytical chemistry until the radiometric work of Croudace et al 1998 [14]. Prior to that study all reported radioanalytical preparations used a range of less effective and hazardous acid digestions or laborious alkali fusions.

The three certified reference materials were ignited at 600 °C for 3 hours to oxidise the sample and to inhibit volatilisation of elements such as Pb. An aliquot of 0.5 g of ignited reference material was weighed in to a platinum crucible at a 1:1 ratio with di-lithium tetraborate flux (Fluxana, Germany). The crucible is agitated to mix the two components and fused on a Vulcan Fusion Machine (Fluxana, Germany) where the sample is heated to 1200 °C and periodically agitated for approximately 10 minutes. The resulting melt is quenched in 50 mL of Milli-Q water and acidified with 50 mL concentrated nitric acid. Any residual material in the platinum crucible is collected and transferred to the digest. The sample is then heated at 80 °C to reduce the sample volume. Boric acid and silica may precipitate which requires filtering. The digest and precipitate is separated with a Whatman GF-C filter paper supported on a Whatman No 540 filter paper using vacuum filtration. The filters papers are then rinsed with 8M HNO_3 and effectively retained the precipitate resulting in a clear solution being collected. The precipitate contained no detectable radioactivity. The filtered solutions are reduced in volume to < 20 mL on a hot plate at 80 °C and then transferred to a 20 mL polythene vial with washing and made up to 20 mL. The samples were counted immediately for the same radionuclides identified above.

4. Results

The direct measurements for all three of the certified reference materials yielded low than expected activity concentrations for measured radionuclides (figure 1). The extent of the bias between the measured and certified activity concentrations is proportional to the increasing uranium content in the reference material. This can be observed with ^{234}Th where the activity concentration is 94%, 65% and 7% of the certified value for CUP-1, BL-5 and CUP-2 respectively. Where a certified activity concentration is not available for one of the measured radionuclides, the closest parent isotope value has been used. Reference material CUP-1 had no measurable ^{234m}Pa as it was not likely resolvable from the Compton background as the emission yield is very low (0.847%) in a low uranium concentration material (0.128%). Reference material CUP-2 had no measurable ^{226}Ra or ^{210}Pb due to the material being a uranium ore concentrate and insufficient time for ingrowth following the ore processing.

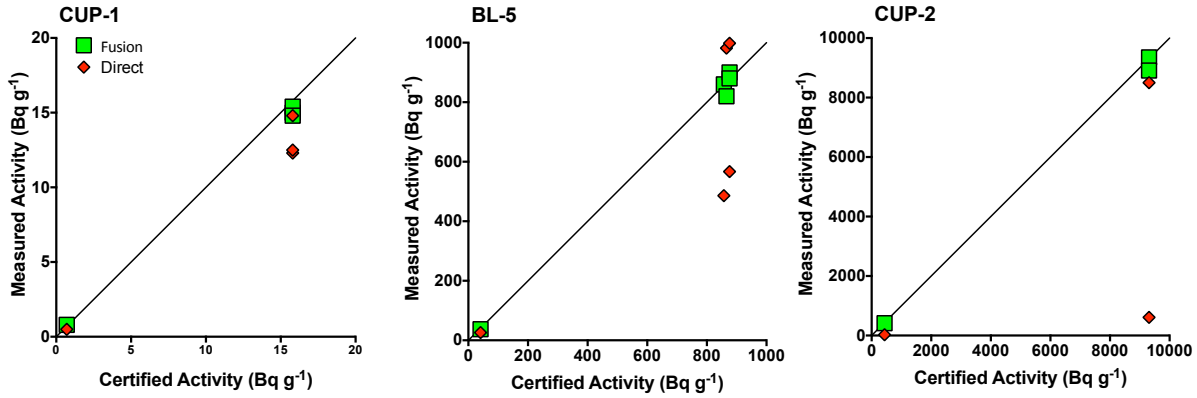

Figure 1: Activity concentrations for selected radionuclides of both solid and fused certified reference materials against the expected activity concentrations based on certified values.

The discrepancy with the direct measurements was identified as being proportional to the uranium concentration and the uranium particle size causing a "hot-particle effect" where the uranium is supported within a less dense bulk matrix. This characteristic would be difficult to matrix-match without significant sample characterisation and is the cause of the self-attenuation observed when directly measuring the certified reference materials.

The measured activities of the reference materials via the lithium borate fusion technique are all within uncertainty of the certified values. The fusion technique significantly reduces any matrix effects present in heterogeneously distributed uranium-bearing samples where grain size, density and concentration can vary. The average uranium weight percentage obtained from the fused materials yields 0.12 ± 0.02, 7.24 ± 0.33 and 75.2 ± 1.8 for CUP-1, BL-5 and CUP-2 respectively and are in agreement with certified values (table 2).

Both ^{235}U and ^{226}Ra emit ~186 keV gamma photons with a yield of 57.0% and 3.6% respectively. The deconvolving software uses lower energy ^{235}U gamma photons to determine how much of the 186 keV photopeak to assign to each radionuclide as ^{226}Ra only has one major emission energy. However, if the lower energy gamma photons of ^{235}U (143.8 keV with 11% yield) are being attenuated then this correction will be inaccurate resulting in lower ^{235}U and higher ^{226}Ra activity concentrations. This is observed in certified material BL-5 where ^{235}U and ^{226}Ra measured activity concentrations are 64 ± 12% and 113 ± 17% respectively and are not within uncertainty of one another. Once the reference material was fused, the activities were measured as 96 ± 7% and 95 ± 7% ^{235}U and ^{226}Ra respectively. This is important as a qualitative correction could produce an inaccurate ^{235}U activity concentration if the sample has been enriched in ^{235}U, does not contain the natural ^{238}U/^{235}U ratio, or has been processed whereby ^{226}Ra would not be expected to be present.

5. Conclusion

The lithium borate fusion technique achieves a highly effective and rapid dissolution of virtually any difficult to dissolve material (silicates, oxides, sulphates) as well as dissolving carbonates and halides. This ability makes it an attractive approach for rapid sample dissolution. The fusion process solubilises mineral particles removing the "hot-particle effects" and increases the detection efficiency of low-energy gamma-emitting nuclides such as ^{210}Pb and ^{234}Th in heterogeneous U-bearing samples. The high uranium content of CRM CUP-2 (75 Wt% U) had a ^{234}Th activity concentration of 7 ± 1% of the certified value when measured in its solid form using an efficiency correction based on its bulk density. After the borate fusion and digestion technique, the ^{234}Th concentration was 100 ± 2% of the certified value. The dense uranium-bearing grains are present within a lower bulk density matrix with variable grains sizes causing self-attenuation of low-energy gamma photons. The fusion technique avoids the need for sample-specific matrix matching or correcting and, combined with rapid sample preparation, offers an attractive, efficient alternative for accurate radiometric characterisation.

The procedure developed could be used to develop a database containing radionuclide activities, U-concentrations, ^{238}U:^{235}U / ^{238}U:^{232}Th ratios, and extent of secular

equilibrium for U-ores and uranium ore concentrates of known provenance so that recovered, illicit nuclear materials can be rapidly analysed and compared as part of a nuclear forensic characterisation.

The borate fusion technique can be used in other applications where accurate and rapid characterisation of low-energy gamma photons is required, such as accurately measuring ^{241}Am, ^{239}Pu or ^{241}Pu as part of a nuclear forensic effort or environmental monitoring. The technique was used to process and analyse >700 soil samples in only 12 weeks from the Greenham Common Airbase where an alleged nuclear incident took place in 1958. The fused samples underwent extraction chromatography of U and Pu in preparation for high precision radiometric and TIMS measurements [14,15].

Any material that may be affected by a "hot-particle effect" that requires accurate radiometric characterisation would benefit from the borate fusion technique, e.g. the accurate characterisation of hot-particles near nuclear sites such as Dounreay, UK [16] or Chernobyl, Ukraine [17,18] .The petroleum and mineral processing industries also regularly encounter NORM scales and deposits having high densities that contain Ba, Ra, U and Th and thorium. The accurate determination of the associated low-energy gamma radionuclides is critical for radiological assessment and for appropriately handling and disposing of waste and tailings. Such characterisations could also be facilitated using the lithium borate fusion-based technique.

6. Acknowledgements

The authors thank Giles Graham, Claire Watt, Nick Bright and AWE Plc. for their support and for funding this PhD project via the AWE Outreach Programme (AWE 30200056).

7. References

[1] I.D. Hutcheon, M.J. Kristo, K.B. Knight, N*onproliferation Nuclear Forensics, in: Uranium - Cradle to Grave*, Winnipeg, 2013: pp. 377–394.

[2] M.J. Kristo, *Handbook of Radioactivity Analysis,* Third edit, Elsevier, San Diego, 2012.

[3] R. Hanlen, *Round Robin 3 Exercise After Action and Lessons Learned Report. PNNL-20079,* Pacific Northwest Natl. Lab. U.S. Dep. Energy, Richland, WA. (2011).

[4] M. Wallenius, K. Mayer, I. Ray, *Nuclear forensic investigations: two case studies.*, Forensic Sci. Int. 156 (2006) 55–62.

[5] N.H. Cutshall, I.L. Larsen, C.R. Olsen, *Direct Analysis of 210Pb in Sediment Samples: Self-Absorption Corrections, Nucl.* Instruments Methods. (1983) 309–312.

[6] M. Długosz-Lisiecka, H. Bem, *Fast procedure for self-absorption correction for low γ energy radionuclide 210Pb determination in solid environmental samples*, J. Radioanal. Nucl. Chem. 298 (2013) 495–499.

[7] T. Pilleyre, S. Sanzelle, D. Miallier, J. Faïn, F. Courtine, *Theoretical and experimental estimation of self-attenuation corrections in determination of 210Pb by gamma-spectrometry with well Ge detector*, Radiat. Meas. 41 (2006) 323–329.

[8] L.A. Currie, *Limits for Qualitative Detection and Quantitative Determination. Application to Radiochemistry*, Anal. Chem. 40 (1968) 586–593.

[9] J.L. Dalton, W.S. Bowman, *Report CCRMP 86-2E - CUP-1: A Certified Uranium Reference Ore,* 1986.

[10] G.H. Faye, W.S. Bowman, W.S. Sutarno, R*eport 79-4 Uranium Ore BL-5 - A Certified Reference Material*, 1979.

[11] C.W. Smith, H.F. Steger, *Report 84-11e - Lead-210 in Certified Uranium Reference Ores DL-1a, BL-4a, DH-1a and BL-5*, 1984.

[12] C.W. Smith, H.F. Steger, *Radium-226 in Certified Uranium Reference Ores DL-1a, BL-4a, DH-1a and BL-5*, 1983.

[13] J.L. Dalton, W.S. Bowman, *Report 88-3E CUP-2 : A Certified Uranium Ore Concentrate*, 1988.

[14] I. Croudace, P. Warwick, R. Taylor, S. Dee, *Rapid procedure for plutonium and uranium determination in soils using a borate fusion followed by ion-exchange and extraction chromatography*, Anal. Chim. Acta. 371 (1998) 217–225.

[15] R.N. Taylor, I.W. Croudace, P.E. Warwick, S.J. Dee, *Precise and rapid determination of 238 Ur 235 U and uranium concentration in soil samples using thermal ionisation mass spectrometry*, Chem. Geol. (1998).

[16] F. Dennis, G. Morgan, F. Henderson, *Dounreay hot particles: the story so far*, J. Radiol. Prot. 27 (2007) A3–11.

[17] F.J. Sandalls, M.G. Segal, N. Victorova, *Hot Particles from Chernobyl : A Review*, J. Environ. Radioact. 18 (1993) 5–22.

[18] B. Salbu, T. Krekling, D.H. Oughton, V.A. Kashparov, T.L. Brand, J.P. Day, *Hot Particles in Accidental Releases From Chernobyl and Windscale Nuclear Installations*, Analyst. 119 (1994) 125–130.

Privacy regulations and protection of personal data

I agree that ESARDA may print my name, contact details, photograph, and the above article in the ESARDA 2015 Symposium Conference Proceedings and related ESARDA publications and activities.

David Reading.

Session 12

Export Control

Nuclear suppliers' enhanced export control compliance and communication with authorities

F. Sevini[1], A. Viski[1], R. Chatelus[1], C. Charatsis[1], Q. Michel[1,3], S. Zero[2]

[1]European Commission - Joint Research Centre
Institute for Transuranium Elements
Nuclear Security Unit
Via Fermi 2749, Ispra 21027, Italy
E-mail: filippo.sevini@jrc.ec.europa.eu

[2]AREVA, Paris, France
[3]Liege University, Belgium

Abstract

The relationship between industry and authorities represents one of the most pressing export control issues in Europe and worldwide.

The strategic export control legal framework in its regional or national formulations normally puts responsibility on exporters, whose awareness and compliance are key in making export controls an important non-proliferation tool. Without due collaboration with and contact to authorities, the licensing process would be less effective and illicit procurement could occur more easily, with enforcement measures the only possibly remaining effective barriers to an illegal shipment.

However, compliance could be seen by exporters as a burden slowing down trade, or even excessively controlling it, with unavoidable costs that not all exporters can afford, for example SMEs. At the same time, not all goods and destinations are equally sensitive. An adequate risk analysis, cost/benefit , discussion and consideration of incentives as well as enhanced collaboration could bring such an approach even further, providing useful information to the authorities and simplified procedures for exporters.

While the topic has been discussed repeatedly over the years, concrete and significant changes to the relationship have yet to be conceptualized or implemented.
The ESARDA export control working group recently held a meeting to identify concrete ways in which industry and authorities can communicate and cooperate more effectively in order to achieve common non-proliferation goals and aim towards a risk-based export control approach. The conclusions of the meeting and further reflections are presented in the paper.

1. Introduction

Strategic export control is one of the pillars of nuclear non-proliferation, complemented by the international safeguards and physical protection requirements.
Nuclear energy and nuclear proliferation programs are always potentially inter-twinned, which is a point to be taken into account when analysing the development of civil nuclear energy.

Since the end of WWII, the State-level proliferation in the 60's and 70's and the advent of transnational illicit procurement networks in the 90's and early 2000s, the awareness of WMD proliferation risks has grown, together with the risks for exporters. In this long period of time the control was extended to non-nuclear "dual-use" materials, technology and equipment.

UNSCR 1540 [1] "*Decides also* that all States shall take and enforce effective measures to establish domestic controls to prevent the proliferation of nuclear, chemical, or biological weapons and their

means of delivery, including by establishing appropriate controls over related materials..” and hence calls States to implement an efficient export control systems to prevent illicit trafficking.

In this respect it is clear that only States whose exporters comply with the DU export control regulatory framework can contribute to such a challenging effort.

In the EU, the legal framework is set by EC Regulation 428/2009 [2] and subsequent amendments, the latest of which brought the dual-use control list (Annex I) up to date with the changes decided by the international export control regimes [3,4,7,8] until 2013 (a new revision is already in progress).

The dual-use Regulation places an increased emphasis on the responsibility of the exporter. For instance, the catch-all provision in article 4 of the DU Regulation not only require a licence for non-listed items if the exporter has been informed by his national authority, but also if the exporter is aware or has grounds for suspecting that the items will be used for WMD proliferation purposes. The same applies in other legal frameworks, like the US one.

2. A system with many stake-holders

The scope and the efficacy of export control systems depend on the political will of governments, their legal systems and procedures, the awareness and training of their services, the international coordination of their efforts, their interaction with the industry and many more aspects of the complex machinery to put in place in order to mitigate the risk that legitimate trade is abused for illegitimate purposes.

Unlike other domains such as the regulation of nuclear energy or chemical agents, no law-based institution exists that oversees and sets international standards for strategic trade control. The so-called International export control regimes like the Nuclear Suppliers Group [3] are only politically binding for a, which have anyway a crucial importance because they define the control lists incorporated by national laws or regional regulations [4,5].

The implementation is responsibility of national authorities and therefore of all the other stake-holders involved, starting from the exporters. Indeed little would be effectively possible without informed, aware, collaborative and complaint suppliers and exporters. They are the primary actors to comply with requirements, starting from turning down unclear requests of export, to seeking the advice and authorisation of licensing authorities, and making correct declarations enabling enforcement of controls by customs.

The IAEA does not implement export controls, but benefits from their existence in terms of barrier to the uncontrolled diffusion of goods and technologies, and from the reporting duties foreseen under the Additional Protocol, although limited to the 1992 version of the Trigger List [9] meanwhile amended several times [10]. IAEA reporting requirements do not cover supply of Trigger List technology, although States may report such transfers, where they are known, on a voluntary basis.

Amongst the international organisations, the World Customs Organisation has made a significant step by launching its program on Strategic Trade Control Enforcement, which is geared to customs authorities but also has significant links to the other stake-holders. Just to mention one aspect, customs universally rely on the Harmonised System to identify goods, just as well as exporters have to use it in order to rate their goods first of all in order to calculate VAT and duties. Licensing authorities start from the different angle of the Dual Use coding system in 10 categories, which is not at all aligned with the HS. Correlation tables exist which trigger warnings on certain HS/CN codes as they may refer to dual-use items, but probably more efforts should be done to bring first of all the dual-use codes in line with the customs/exporters jargon.

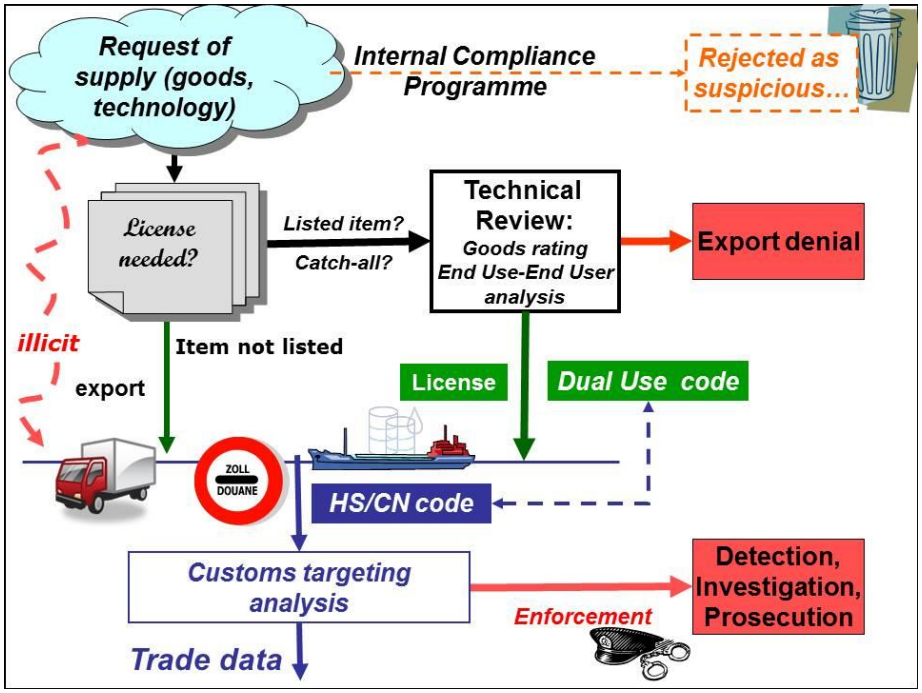

Figure 1 – Strategic export control scheme

3. Challenges

Strategic trade control's challenges apply to all stake-holders, from the private sector to governmental services. As recalled in [11], there are challenges intrinsic to export control regulations and systems and others deriving from continuous and sometimes spectacular evolutions of technology, communication and trade in an increasingly globalized environment.

They can summarised as:

- Interpretation of technical control text
- Intangible Technology Transfers
- Implementation and enforcement
- Catch-all clause
- Dual Use technology evolution
- Foreign availability of goods
- Technical capabilities of authorities
- Information exchanges among authorities
- Transit / Transhipment interpretation
- Brokering controls
- Sanctions
- Military control lists
- Extra-territorial controls, typically required by the US administration, as the control on re-exports and even deemed re-exports [JRC NNSA ESARDA seminar]

3.1 Technical challenges

The dual-use control list derives from the international export control regimes [3,4,7,8] and the Chemical Weapons Convention [13]. The EU list is contained in Annex I to EC Regulation 428/2009, lately amended as Regulation 1382/2014. Some EU national versions of the list may contain additions. The US Commodity Control List uses the same structure and adds about 25% more goods.

The interpretation of the very technical nature of controls on dual use items presents challenges to exporters and authorities. The controlled items are defined in advanced technical terms, difficult to understand by nonspecialists, as well as to relate to commercial products.

Sometimes, only manufacturers and users (sensitive or not) can easily assess whether their products meet specifications of control lists. Interaction and exchange with the authorities can help mutual understanding, also when deciding how to choose the relevant dual-use code and Harmonised System code, which is needed for both checking the possible duties in export countries, as well as a tool for customs enforcement at borders which may be triggered by warnings raised by possible correlation between DU and HS/CN. This is a complicated exercise supported by e.g. the TARIC correlation table.

Figure 2 – EU dual-use control list

Other technical lists are included in measures targeting certain countries, like Iran [14 and amendments] and DPRK [15].

3.2 Transparency and catch-all

As introduced by some regimes, the EU regulation and other national legal instruments allow the authorities to impose catch-all requirements on non-listed items that may contribute to proliferation programmes. It enables governments to request licenses for any transaction on the basis of the assessed risk of contribution to a WMD program, even if the item is not on a control list.

This is a complicated matter, as it creates a grey area around the official control list (which already has its degree of interpretation). The increased use of catch all clauses creates new uncertainties for the trade and manufacturing industry.

Sensitivity and security consideration may impose serious limits to the transparency of licensing decisions and to coordination between governments. In certain countries a catch-all requirement may lead to a no-license required, or automatically to a denial. The result is a certain level of uncertainty, unpredictability and inconsistency of licensing decisions which is uncomfortable for the private sector as much as for governmental implementers. It is prone to creating a uneven playing field among countries and hence the so-called “license shopping”.

As Figure 3 pictorially shows, also no concern states might be the target of a catch-all denial, because of fear for diversion and re-export to sensitive destinations, e.g. because the declared consignee/end user and/or the country’s legal and enforcement framework do not offer sufficient guarantees.

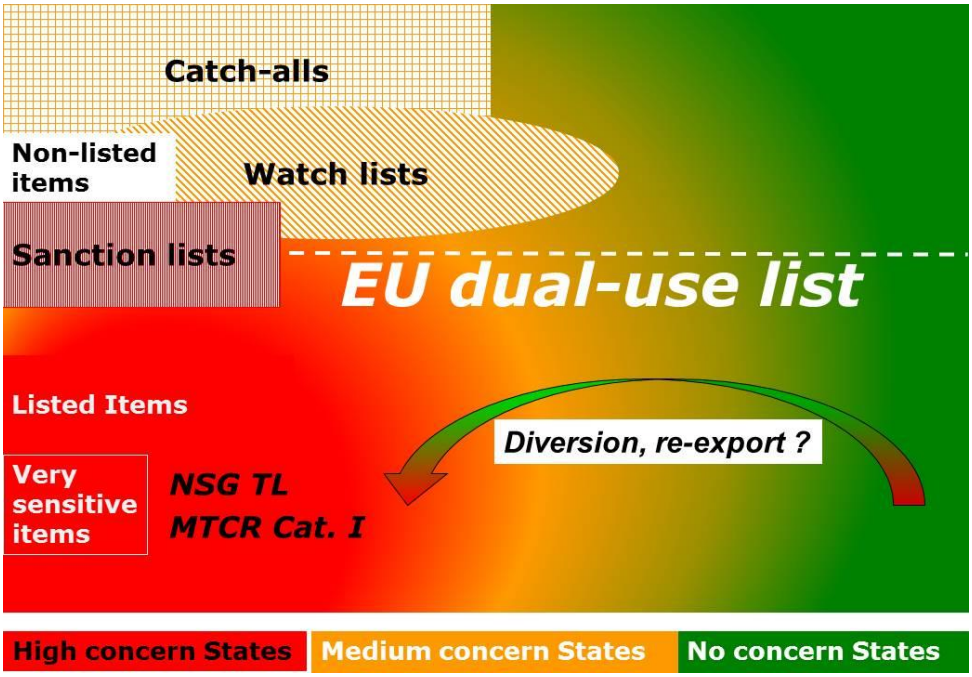

Figure 3 – Mapping of the various types of dual-use related controls versus countries of destinations.

3.3 Globalisation and foreign availability of goods

The globalisation of strategic trade was caused by a general increase in the flow of nuclear materials and equipment and technology in the past decade.

New countries engaging in nuclear trade are becoming able to supply nuclear dual-use goods and technology

Various important transit and trans-shipment points along supply routes.

It is hence increasingly important to have effective and efficient export control systems in partner countries along the supply chain route.

Industrial production apparatus have evolved to become worldwide integrated productions systems. Even without externalization, the functioning of large industrial groups involves many intra-company movements of commodities cross borders.

Production processes have been fragmented between multiple production sites and legal entities worldwide, in countries having its own export control regulation and practice.

Traditional technology holding countries delocalised their production only in countries where sufficient trade controls are in place. In this respect it can be said that having an export control system allowed these countries getting advanced technology and jobs. Some “trusted” countries even appear in the list of destinations for which General Export Authorisations or license exemptions apply.

A side aspects of globalised production is also that companies located in the EU or countries were controls are stringent may fear unfair competition by competitors based in countries with a lower level of controls. Exchange of information with authorities is hence key to provide evidence which can be used to try and establish a communication among governments to address the issue.

3.4 Intangible technology

New challenges are posed by intangible technology transfers (ITT) and the increasing importance of dual use research across national borders, which can also be exploited by front institutions in countries of concern. Awareness of dual-use controls in the research and academic community present particular challenges for regulators.

Monitoring technology transfers by intangible means poses its own set of problems. Cloud computing is a typical case. Centralised data storage and access are widely used and can pose export control issues even within large companies located in various countries. In this respect, the link to cyber-threats and data integrity is very close.

Export control systems are still best suited to control finished products physically crossing borders; when the production process and corporate organization fit within political boundaries. There may be opportunities associated. Modern technology provides new tools for detection, data processing and information analysis to enforcement services, licensing officers and compliance departments of companies.

Enhanced communication among stake-holders remains the only effective way of raising awarenss and duly implementing controls without suffocating business and research activities.

4. The role of exporters

4.1 Awareness

Awareness and compliance, triggering the export authorisation process in circumstances where this is required, are the primary elements of an effective export control system. The system cannot be effective if it relies solely on enforcement action, fines and imprisonment. It must be embedded in the company's policy and procedural arrangements.

Many small and medium size enterprises, the transportation industries or trade agents, may have difficulties staying up to date with their export control obligations and finding the means to be compliant.

More in general, if we take into consideration a sensitive, potentially WMD-related process and all the "actors" involved, we can reasonably say that all the suppliers directly dealing with controlled items are aware of sensitivities and, ideally, act consequently following all the necessary procedures. But the further we go from the central process, e.g. relying on sub-contractors, consultants and other professional (or research bodies) involved, the level of awareness, information and hence compliance may differ greatly.

Awareness is also perceived differently, depending on the "distance" from the core-controlled process and the type of business.

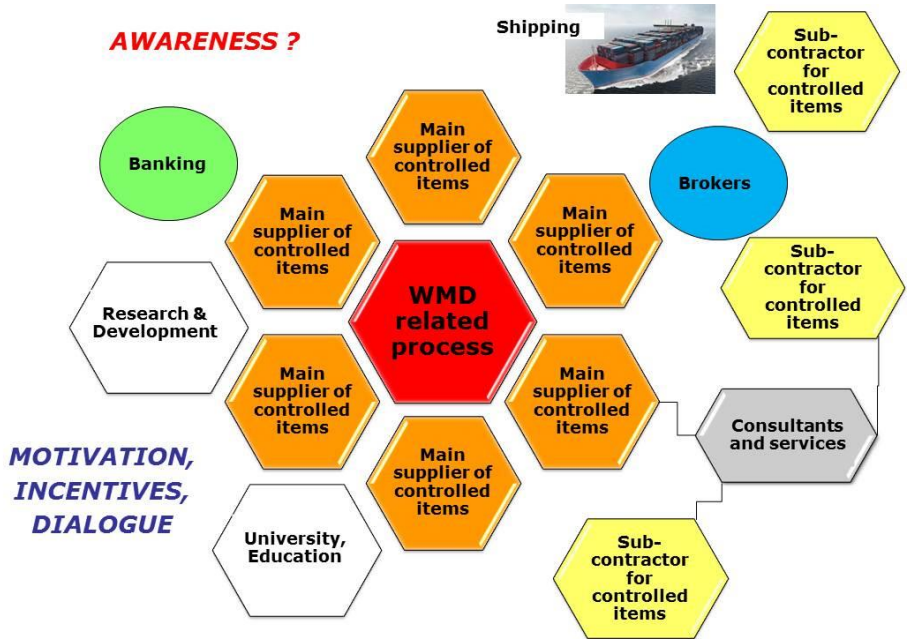

Figure 4 – The "awareness ring"

4.2 Internal Compliance

Internal Compliance Programs (ICPs) are a key instrument to promote suppliers' awareness raising and the fulfilment of export control requirements (e.g. the supply chain, systems integrators, distributors and others such as research centres).

A properly implemented ICP provides an organisation exporting sensitive items and technologies with a structured approach, and supports a culture of doing business in ways that ensure delivery of items to legitimate end-users thus minimizing the risk of diversion.

Compliance should be ensured all along the supply chain, by adequate information and training provided by the main contractor and of course the authorities, as long as they are correctly mapping the suppliers, or are informed by other sources.

Information exchange is hence the crucial point, of course on a cautious need to know basis.
In this respect, ICPs can also be a model enhancing communication and cooperation between the State and the exporter.

While the implementation of an ICP is the responsibility of the exporter, the State may also consider measures and stimuli in domestic laws and regulations encouraging to introduce an ICP, as well as foreseeing incentives following its adoption (e.g. global licenses). Having widespread ICPs favours export controls and creates an environment supportive of non-proliferation efforts.

However, no certified ICP models exist, although general guidelines are available, for example defined by the Wassenaar Arrangement or as reported in [11]. Certain national administrations attribute high value to company's ICP during audits, or even require it by law (e.g. Hungary). There is a tendency however to remove the legal obligation and maintain the requirement of an ICP for exporters seeking a global license.

4.3 Risks and incentives

Risks are perceived differently by exporters (sanctions, reputational loss) and authorities (violation of non-proliferation commitments)

Apart from the legal consequences of non-compliance, exporters also face risks in terms of reputation, with direct economic consequences for penal and financial sanctions.

Loosing good reputation is not just a matter of ethics and self-perception, it is also about losing the benefits of certifications, possibly appearing on US black-lists and being associated with risks that other players don't want to take by dealing with your supply chain.

5. Enhanced dialogue

Exchanges and communication among stake-holders, starting from exporters and authorities, have come up all along the previous paragraphs, for example related to detecting illicit requests or providing ground for catch-all controls.

Also the IAEA encourages suppliers to provide information on procurement attempts for nuclear-related (dual and single use) goods. This is a valuable source of information to enable the early detection of potential undeclared nuclear activities and help States identify covert procurement networks worldwide.

The ESARDA Export control WG debated the topic of enhanced dialogue in various meetings guided by a Concept paper which formulated key questions that the discussion should address.

Communication among trusted partners can be the cornerstone of a possible evolutionary export monitoring framework, proposed by AREVA.

Not all destinations are equally sensitive, and hence an evolutionary export control system might put more emphasis and resources where needed. Besides EU General Export Authorisations (corresponding to license exceptions in the US), also a different approach based on risk could be envisaged.

Proposals for a graded country-based approach were sent by AREVA [16] to the French national authority and the European Commission. These include e.g. reactor export free on licensing in the EU; EU General authorisations for exports to NSG-members; individual license for non-NSG trusted countries; prohibition to banned countries; training to raise exporter and authority awareness.

The concept is summarised in Figure 5, which actually reverses inside-out the scheme of Figure 3, by putting the emphasis on "automatically" agreeable exports to trusted partners, e.g. NSG members, leaving the requirement for an authorisation to other destinations. The "free" export would need to be notified instead of seeking individual authorisation.

This may be correctly seen as an extreme scenario, which anyway brings in the position and view of large exporters dealing with thousands of licenses. A possible alternative could be the definition of a EU General Export Authorisation for large projects, as well as a strong improvement in the procedures requested for Intra-EU transfers, also under discussion.

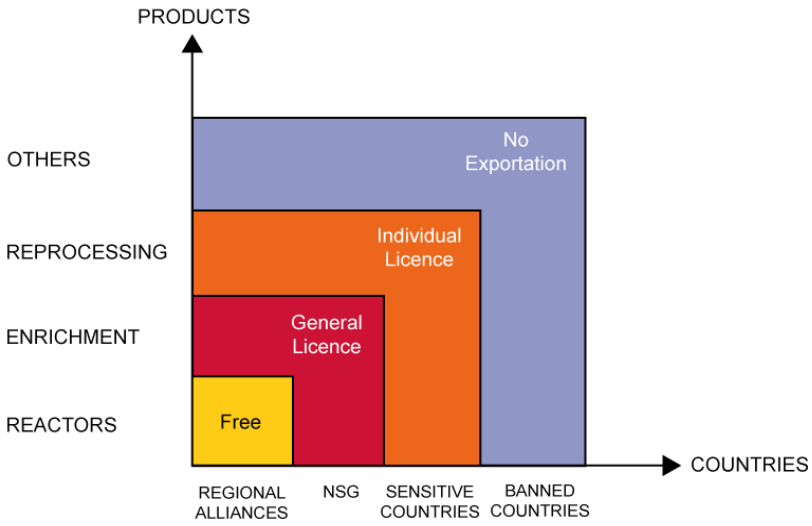

Figure 5 – Evolutionary export control model [16]

6. Way forward

6.1 EU revision of the export control framework

In October 2014 the EU held its annual open consultation EU industry forum, where exporters were invited to provide their views on the European Commission's Communication on the proposed improvements to the export control framework [18].

The discussions focused on the set of priorities and possible measures contained in the Communication. These include i.a. ITT, emerging threats, common criteria for catch-all, a risk-based approach, involvement of industry, more EUGEAs, capacity building initiatives and , Cooperative implementation of controls with partners. New EUGEA related to some category 0 items; removing Annex IV, or reducing its scope.

Procedural improvements are needed but must be legally justified and reasonably achievable

Unique export control guidelines are missing. In the EU, the control of intra-EU transfers is an historical burden probably used only for getting licensing data to be sent to IAEA for the AP declarations. That need could have other solutions (e.g. notifications).

The US has a general license for nuclear reactors, but no EU country has one (e.g. limit case of exports from France to Finland requiring 400 individual licenses)

Time is hence ripe to try and include new provisions safeguarding non-proliferation, but also meeting the needs outlined by exporters.

6.2 Doing the right thing: towards a strategic trade control culture

An interesting concept is expressed in [19]. Compliance and commitments to duly control trade should be fostered by the spreading of a Strategic Trade Control Culture, taking the inspiration for the nuclear security one.

International community, States, exporters, including of course research and academia, should all be encouraged to embed the concept of compliance not just in their procedural arrangements but also in their own mind sets. Non-proliferation would hence be reinforced by the necessity to do the right

thing, not just what it required. This would develop a *culture of compliance that* would see exporters understand, support, and adhere to official requirements— the most important being nonproliferation.

*Moreover, n*ow that strategic trade control is becoming not just the purview of a few officials in a few countries, but expanding as a legal obligation for all states and for many actors within states, the public also has a role to play in developing a basic level of awareness.

7. Conclusions

Many challenges apply to strategic trade controls.

Exchange of information is crucial to facilitate on the one hand the access to faster and more efficient instruments and procedures, on the other to improve the efficiency of the system and allowing to put more resources where the risk is higher.

Enhanced dialogue is hence key to establish a system of trusted partners, notwithstanding the necessary respect of each other's roles.

As anticipated in the Commission's Communication, a possible evolution in implementing export control encompasses introducing a risk-based framework. This may be part of a broader approach followed also by other like-minded partners.

Apart from legal obligations and requirements, success is also linked to the achievement of strategic trade culture fostering compliance as part of an overall striving for nonproliferaion goals.

8. References

1. United Nations Security Council. Resolution 1540 Adopted by the Security Council at its 4956th Meeting, on 28 April 2004, S/RES/1540, 2004
2. Council Regulation No 428/2009 of 5 May 2009 setting up a Community regime for the control of exports, transfer, brokering and transit of dual-use items (Recast), (2009).
3. Nuclear Suppliers Group, NSG, www.nuclearsuppliersgroup.org
4. IAEA INFCIRC/254/Rev.12/Part 1, GUIDELINES FOR NUCLEAR material, equipment and technology, available at www.nuclearsuppliersgroup.org
5. IAEA INFCIRC/254/Rev.9/Part 2 GUIDELINES FOR TRANSFERS OF NUCLEAR-RELATED DUAL-USE EQUIPMENT, MATERIALS, SOFTWARE, AND RELATED TECHNOLOGY, available at www.nuclearsuppliersgroup.org
6. Missile Technology Control Regime, www.mtcr.info
7. Australia Group, www.australiagroup.net
8. Wassenaar Arrangement www.wassenaar.org
9. Filippo Sevini, Renaud Chatelus, Malin Ardhammar, Jacqueline Idinger, Peter Heine, States' reporting of Annex II exports (AP) and the significance for safeguards evaluation, IAEA SG2014
10. F. Sevini, "Nuclear export controls update", 55th INMM, 2014, Atlanta, USA
11. R. Chatelus, F. Sevini, W. Janssens, Q. Michel, "Challenges to nuclear export controls today", Proceedings of ENS, Marseille 2014
12. Discussions at JRC-NNSA & ESARDA seminar, April 22-23, 2015, JRC Ispra, Italy
13. Organisation for the Prohibition of Chemical Weapons, OPCW, http://www.opcw.org/
14. Council Regulation (EU) No 267/2012 of 25 March 2012 on restrictive measures against Iran, later amended as 1263/2012
15. Council Regulation (EU) No 1283/2009 of 22 December 2009 amending Council Regulation (EC) No 329/2007 concerning restrictive measures against the Democratic People's Republic of Korea, later amended as 296/2013

16. F. Sevini et al. “Strengthening Strategic Export Controls by Internal Compliance Programmes’ Revision 2, JRC technical note, EUR 27059, ISBN 978-92-79-45042-6 (PDF), ISSN 1831-9424 (online)
17. Presentation by Sandro Zero at ESARDA Export control Working Group’s 5th meeting, Rome, November 4-5, 2014
18. COMUNICATION FROM THE COMMISSION TO THE COUNCIL AND THE EUROPEAN PARLIAMENT The Review of export control policy: ensuring security and competitiveness in a changing world COM(2014) 244 final
19. A. Viski, Building Strategic Trade Control Culture: Toward a New Phase in Nonproliferation, 1540 Compass, Issue n. 8, March 2015

SSM Research in Export Control

Jenny Peterson, Henrik Moberg, Elisabeth Koblet, Lars Hildingsson
Swedish Radiation Safety Authority (SSM)
Nuclear Non-proliferation and Transport unit
Solna Strandväg 96, SE-171 16 Stockholm, Sweden
E-mail: jenny.peterson@ssm.se

Abstract:

Nuclear export control is in part an assessment on goods potential use in a nuclear weapons program and assessment of the end-user. A credible export control must keep abreast of both technical developments to judge the potential use of the goods and of political developments in the recipient country. Technology development, in for example laser enrichment technologies and new reactor concepts, will have an impact on the type of goods that has to be controlled. Non-proliferation commitments and how it is manifested in internal control of the recipient country are also factors to take into account.

To ascertain that SSM has access to up-to-date information we have funded research covering both technical and political aspects of export control. This work is done in research institutes outside SSM. The technical research has been done by the Swedish Defense Research Agency, FOI, and covers areas as for example laser enrichment and accelerator driven reactors. The aim of the research is to have knowledge about new technologies but also other sensitive parts of the nuclear fuel cycle. A project on non-proliferation commitments examined the relationship between the NPT and various non-proliferation initiatives and institutions, such as NSG. An important aim of the research is to have access to groups outside SSM to judge export applications.

The paper will present more in detail how SSM work with research groups and how we use the results in our work with export applications and in our international engagement, such as ESARDA working group on export control. Some results of the research will briefly be presented as well as future challenges such as intangible technology transfers (ITT).

Keywords: export control; nuclear non-proliferation; research

1. Introduction

The Swedish Radiation Safety Authority (SSM) has a mandate within nuclear safety, radiation protection and nuclear non-proliferation, and may act as a regulatory authority as well as a supervising and a licensing authority. The Authority reports to the department of Environment and Energy and has around 300 employees with an office at Solna, north of Stockholm. With the vision of “a society safe from harmful effects of radiation” the Swedish Radiation Safety Authority strives at working proactively and preventively within the mandated areas. To meet the challenges of today and in the future the Swedish Radiation Safety Authority needs to keep abreast of developments within these areas, where technical issues represent a large part, but also for example safety culture and behavior science, as well as policy issues are of importance. Looking at the nuclear non-proliferation tasks of the Authority and especially the area of export control, the main challenges of today is linked to the ongoing technology advancements of material and equipment within the nuclear fuel cycle, together with an increasingly globalised world of cooperation, trade and technical solutions for communication. This paper gives an overview of the philosophy behind the research activities at the Swedish Radiation Safety Authority, with a focus on export control, and presents examples of financed research projects and other studies.

2. Export control and the role of the Swedish Radiation Safety Authority (SSM)

2.1. The export control framework

The Treaty on the Non-Proliferation of Nuclear Weapons, NPT, ratified in 1970, constitutes inarguably the foundation of the global non-proliferation community, export control included. The NPT is often interpreted as a three-pillar system:

- non-proliferation of nuclear weapons
- disarmament of nuclear weapons and
- the right to peaceful use of nuclear technology

One may view export control as a balance between the first and the third pillar, with the object to prevent the spread of nuclear weapons without hampering the legitimate civil nuclear trade, however, the main goal is off course to hinder proliferation, expressed in Article III.2 of the NPT:

"Each State Party to the Treaty undertakes not to provide:
(a) source or special fissionable material, or
(b) equipment or material especially designed or prepared for the processing, use or production of special fissionable material, to any non-nuclear-weapon State for peaceful purposes, unless the source or special fissionable material shall be subject to the safeguards required by this Article."

Each non-nuclear weapons state has, according to the NPT, to accept safeguards by the International Atomic Energy Agency (IAEA) to control that all nuclear material declared by the state is not misused, including that a shipment from one facility arrives at the designated recipient. The control is based on a safeguards agreement concluded with the state. The IAEA also keeps track of exports of nuclear related goods through an additional protocol to the safeguards agreement, where the state agrees to report all exports of goods listed in an annex to the protocol. The additional protocol is optional but is by many states seen as a fundamental part of safeguards.

Out of an export control perspective, the Article III.2 of the NPT was interpreted in the 1970's by a group of states later called the Zangger Committee. The Committee agreed on principles on conditions of supply of nuclear goods that fall under Article III.2 of the NPT, and the principles was published as IAEA Information Circular number 209, commonly referred to as the Trigger List. Today, however, the most potent export control association is rather the Nuclear Suppliers Group (NSG), consisting of 48 states with common principles on how to ensure that supplied goods are used solely for non-nuclear weapons purposes. The principles, together with annexes describing the type of goods that are considered to fall under export control, are published as the Guidelines of the Nuclear Suppliers Group (as IAEA Information Circular number 254). The Guidelines of the NSG go further than the Zangger Committee and have extended the scope of to control to include many products which do not fall under Article III.2 of the NPT but which clearly have a potential and crucial use in a nuclear weapons programme.

The Guidelines of the NSG, as well as of other export control regimes, are incorporated into the legislation of the European Union through Council Regulation (EC) No. 428/2009 on export control [1]. This regulation provides for common EU control rules and describes the scope of control including a list of all controlled goods with a dual use, i.e. with civilian applications but also useful in a military programme or weapons of mass destruction programmes. The regulation covers not only exports out of the EU but also intra-EU transfers, transit and brokering.

2.2. The role of the Swedish Radiation Safety Authority

As part of the national export control system (legislation, licensing, enforcement and sanctions) SSM's main role lies within the licensing and enforcement area.

The Swedish Radiation Safety Authority is the licensing office for exports out of the EU and intra-EU transfers of nuclear related goods, as well as brokering and transit. These goods include nuclear and other materials, complete nuclear plants and systems as well as individual equipment and components, plus related software and technology.

Before permitting a supply of nuclear goods, the following assessments need to be performed:

- Evaluate if the goods fall under the export control legislation.
- Evaluate the conformity between the exported goods and the stated addressee or end-user, the stated end-use as well as the risk of diversion
- Assess the non-proliferation commitment of the recipient state
- Assess if the intended export is in conformity with the non-proliferation commitments of Sweden and does not violate any international sanctions

To make solid decisions on export licensing and other forms of export control, in view of the above, the Swedish Radiation Safety Authority must ensure that there is adequate knowledge available. For some areas, the SSM has the competence in house, for other areas the Authority can rely on the expertise of other national authorities. In some cases other, external parties are preferred. The research strategy is formed around all these needs.

3. The SSM research strategy

The research funded by SSM provides valuable knowledge which can be used directly in its decision-making. SSM´s funding of research has also a purpose to develop and sustain an adequate competence in the relevant fields, both at SSM and nationally. The research should also support Sweden's international engagement and co-operation in areas relevant for SSM.

The SSM has an annual research budget totalling approximately 80 million Swedish kronor (approximately 8.5 million euros). The research covers mainly nuclear safety and radiation protection but also other areas, such as nuclear non-proliferation are included. The SSM has adopted a policy for more frequently use of advertising research projects broadly with the aim of having a transparent process and fostering competition to find the most competent researchers in the respective fields. The decision to qualify a research project for funding is based on requirements on relevance and scientific quality of course, but also a long-term plan is considered to ensure a sustainable research competence in the future within the fields of interest for the Authority. To ensure the appropriate use of the research budget an analysis of events and trends in the world which affect the Authority is performed regularly.

The research activities financed by the Swedish Radiation Safety Authority are in general mainly conducted by institutions of higher education and consulting firms in Sweden, since SSM does not have access to a dedicated Technical Support Organisation, TSO. However the export control has a little bit different approach as is described below.

3.1. Research strategy applied on export control

To sustain a credible export control, and perform the assessments listed in chapter 2, several areas of knowledge need to be attended, such as:

- The purpose of equipment and components in a facility and their technical requirements
- Technical developments of nuclear products
- Trade patterns and technical solutions to support trade
- Technical, political and social developments in the world
- International non-proliferation framework

The purpose of equipment and components in a facility and their technical requirements
Of the listed areas above, the first one is perhaps the most obvious; it is of course crucial to maintain a competence regarding the use and the technical requirements of material, equipment and components used in nuclear facilities. This includes both the technical and economical demands of the civilian nuclear power industry on these products as well as the usability of the products in a nuclear weapons program.

Technical developments of nuclear products
Knowledge of the technical progress of both materials and equipment is important to judge the potential use of the goods as well as to anticipate future needs to extend the export control regulations

to include new products. An example of this is new reactor concepts, both those belonging to the so-called Generation IV and those described as accelerator driven subcritical systems (both are described in section 4).

Trade patterns and technical solutions to support trade
To keep an effective export control, without hindering the legal trade, it is also important to follow the trends of company structures, which seem to get more and more globally integrated with each other, and to know how the trade of nuclear fuel and other materials and equipment works. One other element to keep track on is the development of technical solutions to support the trade, such as the use of the internet and servers which are physically placed in foreign countries.

Technical, political and social developments in the world
As the export control system also has to account to international relations, security policy and other policy studies are also relevant. Before exporting products related to the nuclear fuel cycle an analysis of the prerequisites of the recipient state, to handle and use the exported products as anticipated, is performed. It is therefore of significance to be informed on both political and social developments in the recipient state as well as other changes in the state which may affect the non-proliferation efforts. The technical developments in the nuclear industry are evaluated as well.

International non-proliferation framework
There is also a need to keep an eye on the work and the shifts within the international non-proliferation framework, both the NPT and the established export control regimes such as the NSG, but also all non-proliferation initiatives and institutions founded over the years. Furthermore, the IAEA and the development of both its activities and its role are of importance. All these developments affect the judgments on how to perform export control and how to use these groups and organisations in the most efficient and effective way for the benefit of non-proliferation. Understanding the non-proliferation framework and its history are also essential as guidelines when, as a licensing authority, SSM implements international commitments as well as EU legislation and national legislation. Policy studies and legal studies could support this.

3.2. Where the is knowledge found

The SSM has an in-depth knowledge of the use, function and technical developments of nuclear facilities corresponding mainly to the Swedish national nuclear plants, i.e. basically light water reactors, uranium conversion and fuel fabrication. The main part of the research funds is dedicated to nuclear safety and radiation protection and concentrates naturally on these types of facilities. This research does not focus on export control but it serves nevertheless as a valuable source of information for the technical evaluation of products within export control. The research on technical subjects related to export control includes these areas as well to bring a non-proliferation perspective, but the aim is to cover technical developments in all parts of the nuclear fuel cycle.

For the military dimension and the usability of a product in a nuclear weapons program, SSM has to turn to another source of information. Thus, since many years, SSM has a well-developed cooperation with the Swedish Defence Research Agency, FOI, being main governmental heir to the legacy of the Swedish nuclear research programs, the civilian but also the military program (in an era where many states explored both options, long time abandoned now for the sake of non-proliferation and disarmament) and with a commitment within the Swedish non-proliferation community as a support in technical and policy issues. FOI has the possibility to link the civilian and the military dimensions of the nuclear fuel cycle out of a proliferation point of view and make a judgement on the possible risk of misuse of materials, equipment and technology which may be supplied by Sweden. SSM therefore financially contributes to research projects and literature studies at the FOI with the aim at sustaining and developing this national competence. The choice of FOI is therefore reasonable even though it is a deviation from the general research approach of SSM aiming at competition and a transparent process. These research projects and other studies focus on technical issues, such as the technical ability of materials and equipment as well as the technical performance requirements depending on the purpose of the operation. A handful of these projects are described in section 4.

To find entities for conducting non-technical research projects and studies the SSM has in one case used the approach of advertising more broadly within the non-proliferation area. No specific research project was proposed, but it was left to the applicant to narrow down and interpret and fashion after its

own competence. Several interesting research projects of value were submitted and a proposal by the Peace Research Institute in Frankfurt was selected (see section 4.5). An advantage of advertising broadly is that SSM gets in contact with research groups that have not been familiar to the Authority before.

Further, SSM has initiated a study to map relevant research groups active within the non-proliferation field. The aim is to find and learn of entities, both in Sweden and abroad, with a potential to support the nuclear non-proliferation activities at SSM and to be funded by SSM.

4. A selection of research projects and studies through the years

The export control research budget is between 400 and 800 thousand Swedish kronor (approximately 42-85 thousand euros). Unfortunately these financial means do not allow all areas of concern to be covered and a priority has to be made based on considerations such as the following:

- What does the Swedish nuclear industry looks like? The answer gives us an idea of possible and plausible trade and transfers of nuclear related goods from Sweden.
- Which are the Swedish knowledge centres? This gives us an idea of possible transfers of technical know-how from Sweden.
- What exports are performed today? This gives us extra information on unmapped actors to be the objects for non-proliferation outreach.

The answers to these kinds of questions give a decision basis to focus the means on the areas where we can achieve the maximum effect on compliance to the export control legislation as well as minimisation of the proliferation risk. Some examples of financed research projects and other studies are presented below, and how the results are used in the export control activities of the Swedish Radiation Safety Authority.

4.1. Analysis of export data

This study was issued to partly answer the question regarding Swedish exports raised above. The project was conducted in 2013 by the Swedish Defence Research Agency (FOI) and consisted of screening and analysis of data of performed and declared exports out of Sweden. The screening was made through translating Customs commodity codes, stated in the export declarations, to product category numbers of the export control legislation, followed by a scan of the product portfolios of the exporters. Thereafter, exports and exporters were categorised using a three-step triage; “controlled goods”, “possibility of controlled goods”, “low probability of controlled goods”. The resulting list of ranked exports and exporters will serve as a basis for audits to companies and other entities in Sweden, to improve the level of compliance if needed, and for outreach programmes to raise awareness of the export control legislation and of proliferation.

4.2. New reactor concepts – a study on Generation IV reactor models

Any deployment of the so-called Generation IV reactors is still in the future, but advanced plans and studies already exist. There are major technical differences between the various proposals, but all are intended to be safer, cheaper and more efficient than the current generation of reactors. The study was initiated to explore potential risks that Generation IV could imply regarding the issue of nuclear proliferation and exports.

The study [2] showed that some of the proposed reactor types in Generation IV could pose a proliferation risk in the future. The current subsystems and components are similar only in part to those found in contemporary reactors, and the reactor core conditions require other materials than those used today. Because of this, the non-proliferation and export control community, both nationally and internationally, should monitor the development in this area closely, so that it can respond and act at an early stage to any deployment of reactors belonging to Generation IV.

4.3. Accelerator Driven Subcritical systems for use as a “nuclear reactor”

New, emerging technologies have to be evaluated from its potential use in a nuclear weapons program. Accelerator Driven Subcritical systems (ADS) have been drawing attention the last years because of the possibility to use such a system for the production of special fissionable material. A study on the issue was conducted by the Swedish Defence Research Agency (FOI) in 2013. An ADS consists of a subcritical core of fissionable material, very much like a conventional core in a contemporary nuclear reactor. A proton accelerator and a target are then used to create neutrons for sustaining a fission process in the core making it not only look like but also behave as a “nuclear reactor”, however with the difference that the neutron feed could be turned off at any time. This can be exploited for energy production, but also for the production of special fissionable material and therefore usable in a nuclear weapons programme.

The report [3] from the study presents an immature technology, still on the research stage. However the study also showed the clear potential of ADS to produce weapons-grade nuclear material. A conclusion was that even though exports of this kind of technology are not controlled today one should exercise some vigilance.

4.4. Technologies for separation of isotopes other than uranium and plutonium

This research project evaluated the differences and similarities between uranium enrichment and the separation of other elements. Although uranium enrichment is not strictly necessary to produce nuclear weapons, all known nuclear weapons programs have contained enrichment in some form. The export of equipment needed for uranium enrichment is strictly controlled. At the same time, a market for other more or less enriched elements has emerged, such as for use in the electronics industry or for medical applications. These substances can be enriched with equipment which, completely or partially, coincides with that used for uranium enrichment. As export control in its strictest interpretation applies only to equipment and technology exclusively for enrichment of uranium, this situation creates a potential gap that could be exploited for proliferation.

The resulting report, published in 2015 [4], compares different separation methods and their usability in a proliferation sense and draws conclusions valid for non-proliferation and export control. The results show that uranium enrichment and the separation of other elements are closely related, however generic rules on the usability of equipment for different elements are not self-evident, such conclusions require examinations of materials and specific technical solutions.

4.5. Relationship between the NPT and various initiatives and institutions

The study, conducted by the Peace Research Institute in Frankfurt (PRIF/HSFK), analysed the relationship between the Treaty on the Non-Proliferation of Nuclear Weapons, NPT and various initiatives and institutions (‘clubs’) based outside the NPT framework, which aims to improve and strengthen the Treaty. The study identified conflicts and possible synergies and proposed options for developing and improving the interaction between the NPT and ‘clubs’ in order to increase the overall efficiency.

The final report [5] describes facts about the various non-proliferation ‘clubs’, and also analyses and formulates conclusions about the various international initiatives in non-proliferation. The report contains several ideas that can be studied further.

4.6. The use of low enriched and high enriched uranium

The efforts to replace highly enriched uranium (HEU) with low enriched uranium (LEU) in research reactors and reactors for the production of medical isotopes have been going on for several decades. Still, HEU is in use in several countries, and there is an international discussion on how the amount can be reduced further in order to minimize the risk of diversion to military uses. If research reactors and radiation targets could be converted to use LEU, the amount HEU in circulation could be reduced, while also reducing the motives for further production of HEU.

The report [6] was commissioned to increase knowledge about how strong the arguments are to retain HEU in research reactors and other civilian use. The study provides an overview of the use of HEU in the world outside the military programs, and describes and analyzes the technical difficulties that a conversion to LEU may result in.

5. Export control challenges of today

Some of the challenges that the export control authorities are facing concern the globally integrated world of today and technical solutions which support communication. The progresses within information technology have brought an easy access to information across the globe, such as e-mail and remote access servers, and new solutions to store information, such as cloud storage, which bring an ambiguity regarding the physical location of information, and the national boundaries become less clear. The modern IT world therefore generates questions on how to practice an effective export control today. The practice of export control affects off course the way companies and other entities conduct their business. A glance at the company structures of the nuclear industry today, both regarding ownership and operation, show large multinational corporations with shared ownerships and local branches in many different states. The legitimate trade should off course not be hindered and a company needs to be able to communicate with its branches wherever based physically, at the same time there is a need to track all transfers out of a proliferation concern.

Related to the globally integrated world is the trend of migration of competence for manufacturing and supplying high-quality material and equipment to states outside the export control regimes, due to for example lower labour costs or better strategic locations for trade and shipments. In addition, within the nuclear area an increasing number of nuclear power nations can be seen, ranging from states in a start-up phase of a nuclear power programme to states reinitiating or reinforcing its existing nuclear fleet. There is no doubt that economic and educational developments are very positive things to be supported. However, the events create a much larger number of actors and potential recipients of nuclear related goods, and thereby an increased nuclear industry sector to follow. One challenge is to raise awareness in new and emerging nuclear countries. Another challenge is how the export control regimes, the NSG in particular, shall adapt to the growing number of nuclear supplier states that need to be involved in the non-proliferation community and be engaged to embrace the concepts of export control.

Another area of concern is new emerging technology concepts which have to be monitored. In addition there is a continuing technical development of equipment and materials, where the line between products specially designed or prepared for nuclear use and those products used in other industry becomes thinner, and for some products the line is nearly erased. Graphite is one of those materials where the industry use of very pure graphite is widely spread and the distinction between this graphite and the graphite for use as moderator in a nuclear reactor is not so much a matter of technical properties anymore. How to keep an effective export control without hampering the legitimate trade is therefore a challenge.

Harmonisation of the interpretation and implementation of the legislative text of the EU regulation is a challenge that also deserves mentioning. 28 sovereign member states of the EU share a common European market but have also national security, safety, foreign policy other concerns to consider as well. The level of export control beyond the minimum level stated in the Council (EC) regulation No. 428/2009 is therefore a summary of all these and the result may differ quite a bit between the states. We should nevertheless continue to strive towards a higher level of harmonisation within the EU for fair competitiveness within the EU.

6. Acknowledgements

The authors would like to acknowledge all those who have reviewed this article and contributed to its completion.

7. Legal matters

7.1. Privacy regulations and protection of personal data

We agree that ESARDA may print my name/contact data/photograph/article in the ESARDA Bulletin/Symposium proceedings or any other ESARDA publications and when necessary for any other purposes connected with ESARDA activities.

7.2. Copyright

The authors agree that submission of an article automatically authorises ESARDA to publish the work/article in whole or in part in all ESARDA publications – the bulletin, meeting proceedings, and on the website.

The author declares that their work/article is original and not a violation or infringement of any existing copyright.

8. References

[1] COUNCIL REGULATION (EC) No 428/2009 of 5 May 2009 setting up a Community regime for the control of exports, transfer, brokering and transit of dual-use items (as amended)

[2] Fjärde generationens reaktorer – en analys med fokus på icke-spridning och exportkontroll; SSM Reasearch 2013:18; Per Andersson, Mikael Meister, Fredrik Nielsen, Daniel Sunhede; Totalförsvarets forskningsinstitut, Stockholm; April 2013

[3] Acceleratordrivna subkritiska system - en analys med fokus på icke-spridning och exportkontroll; SSM Research 2013:05; Per Andersson, Fredrik Nielsen, Daniel Sunhede; Totalförsvarets forskningsinstitut, Stockholm; November 2012

[4] Samband mellan anrikning av uran och andra ämnen – en studie från ett icke-spridningsperspektiv; SSM Research 2015:13; Per Andersson, Fredrik Nielsen, Daniel Sunhede; Totalförsvarets forskningsinstitut, Stockholm; December 2014

[5] Global Non-proliferation ‘Clubs’ vs. the NPT; SSM Research 2014:04; Harald Müller, Carmen Wunderlich, Marco Fey, Klaus-Peter Ricke and Annette Schaper; PRIF/HSFK, Frankfurt; February 2014

[6] Användning av låg- och höganrikat uran – en studie från ett icke-spridningsperspektiv; SSM Research 2015:15; Per Andersson, Fredrik Nielsen, Daniel Sunhede; Totalförsvarets forsknings-institut, Stockholm; December 2014

Comparison between Additional Protocol Annex II and current NSG trigger list through semantic representation

**Luca Falconi, Giuseppe Augusto Marzo,
Giorgio Giorgiantoni, Massimo Sepielli**

ENEA, C.R. Casaccia
Via Anguillarese 301, 00123 S. Maria di Galeria, Rome – Italy
E-mail: luca.falconi.1@enea.it, giuseppe.marzo@enea.it,
giorgio.giorgiantoni@enea.it, massimo.sepielli@enea.it

Abstract:

The present paper describes some applicative examples of the comparison, by means of relational database techniques including a detailed content's analysis, of the Annex II of Additional Protocol (AP) to the Nuclear Non Proliferation Treaty, with reference to IAEA INFCIRC/193/Add.8, to the analogue trigger list from the Nuclear Suppliers Group (NSG), in particular Annex A of NSG Guidelines - Part 1 (2013).Such a comparison produces a potentially useful tool to every final user in different Institutions involved in activities related to the AP and Non Proliferation of Nuclear Weapons principles.
This work originated from the need of tracking technological upgrades occurred since the compiling of the AP Annex II (1998). This need inspired such an activity carried out by the ENEA AP Working Group. It can be divided into two parts: in the first we describe a methodology to define a common semantic, coherently with document's contents and structure. A XML file or equivalent database representation of documents is fully described in the paper and represents the first goal of the work. Having obtained a common semantic structure, the data collected from the two documents can be compared by an algorithm as a query, in some query language and tools. In the second part of the paper we provide possible applications and developments for the presentation, comparison, and integration, with technologies such as web semantic, of the data contained in the Annex II and the NSG Guidelines in order to make possible a higher fruition and comprehension of data.

Keywords: Additional Protocol; NSG Group; Database; Semantic

1. Introduction

This work originates from the need of tracking the technological upgrades occurred since the compiling of the Annex II of the Additional Protocol (Annex II hereafter) of the Treaty on the Non-Proliferation of Nuclear Weapons [1]. To address this challenging task, the Annex II is compared to the Trigger List [2] provided by the Nuclear Suppliers Group (NSG) and updated on a regular basis.

The Nuclear Suppliers Group is an organization which includes member States that are suppliers of nuclear components and technology to the industry. It operates in the context of the Treaty on the Non-Proliferation of Nuclear Weapons. It fosters exchanges between Countries for a peaceful development of nuclear technology. Documentation, in the form of Guide Lines, are produced by the NSG to consider changes due to scientific and technologic progresses of important items for the nuclear and non-nuclear industry.

Here we consider the June 2013 edition of NSG Guide Lines which, as usual, is labeled ‘Trigger List’. The goal of this work is to compare the Annex II the Trigger List by defining the appropriate criterions

and methods. The result is a list of differences between the information conveyed by such documents and, therefore, potentially, a list of implementations to be done in the Annex II to take into account the changes due to scientific and technologic progresses.

This complex goal translates in the definition of an appropriate database able to represent the structure and contents of the two documents.

2. Methodology for the database definition

The first step of the comparison process is to identify the appropriate documents to analyze and compare. Annex II is equivalent to the IAEA document INFCIRC/193/Add.8 [3]. The Trigger List [2] is provided directly from the NSG..

The second step is to identify the information contained in the two documents in terms of systems and components and their corresponding quantitative definitions. The latter are the variables used for their full description.

Then the data have to be described using a suitable architecture and format. In this work we use a relational database and a representation based on the Extensible Markup Language (XML) [4]. In such a way it's possible to define a semantic from our data and use query languages for retrieving back the information from it. Tables of the database and the corresponding relationships strongly depend on the structure adopted for the data architecture. This depends on the semantic structure defined for the documents.

3. Database layout

The documents [1], or rather [3], and [2] share the same layout. They are divided into chapters, sections, and subsections in the same order. In our view, the information is organized in the following categories: 'Structures', 'Components', 'Subcomponents', 'Variables', 'Materials', 'Constraints', and 'Function'. This choice is suggested by the original document layout allowing to sort out all the information easily. It looks a natural choice for defining the database tables (Figure 1).

Given this choice for the database tables, 'Structures', 'Components' and 'Subcomponents' are easily identified. The following is a simple example of table compiling. Chapters such as 'Nuclear reactor components' clearly represent the macro-containers of information, broken down in 'Components' and, where necessary, in 'Subcomponents'. 'Complete Nuclear Reactors' is the first occurrence and 'Complete Rotor Assemblies' is the second. 'Function' contains the information regarding the use of the component or subcomponent within the 'Structure', while 'Materials' indicates, of course, the type of material that it is made of. 'Variables' is a table populated with all the parameters characterizing the item. For example it may be a length, a mass, or the electric conductivity. In general it can be any physical quantity that characterizes the item. The value that each variable can take, that is a range of all the possible values, are contained in the table 'Constraints'.

All information is retrieved from the text of the two documents and populates the database. The result are two XML-type documents equivalent to the original documents which represent a relational database where the complete information of each original document is contained and is ready to be easily manipulated and interpreted by an algorithm. In Figure 2 a portion of the information coded into XML is provided.

The XML-type document is accessible by any software. For the purpose of the present work we used the Access format for representing the two original documents. They are named after the original names, specifically INFCIRC_193 and NSG_2013, respectively. The structure of the two databases, as discussed previously, is the very same and the information contained in each of them is splitted by adopting the same layout. Sharing the same layout makes the information immediately comparable, if the appropriate criteria are defined.

In general, such a layout choice makes a simple database query sufficient to highlight a particular relationship between items in terms of the value of a variable associated with it. The relationships between the tables are the key part of the comparison and the core of the search logic.

The process described so far is therefore proposed to define a semantic associated with the original documents. The XML representation is then used for building assertions like the following: X structure is divided into components Y1,...,Yn, each characterized by variables V_{11}, V_{12},...,V_{1n},...,V_{nn}, with data values C_{11},...,C_{nn}, made by materials M_1,...,M_n, and operating functions F_1,...,F_n.

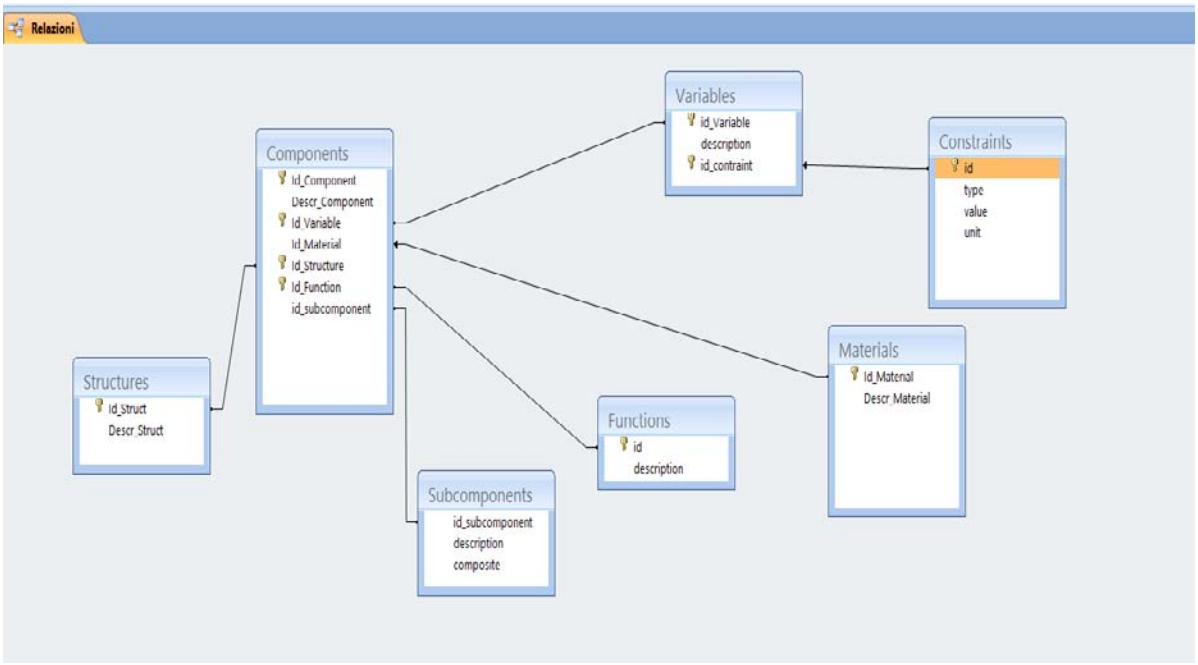

Figure 1 Relationships between tables.

```
- <Nsg2013>
    <Descr_Component>Gas centrifuges and assemblies and components for use in
      centrifuges</Descr_Component>
    <Descr_Material>Aluminium alloys</Descr_Material>
    <Subcomponents.description>Complete Rotor Assemblies</Subcomponents.description>
    <Variables.description>Specific modulus</Variables.description>
    <type>Minimum</type>
    <value>3.18*106</value>
    <unit>m</unit>
  </Nsg2013>
- <Nsg2013>
    <Descr_Component>Gas centrifuges and assemblies and components for use in
      centrifuges</Descr_Component>
    <Descr_Material>Filamentary materials</Descr_Material>
    <Subcomponents.description>Complete Rotor Assemblies</Subcomponents.description>
    <Variables.description>Specific tensile strength</Variables.description>
    <type>Minimum</type>
    <value>7.62*104</value>
    <unit>N/m2</unit>
  </Nsg2013>
- <Nsg2013>
    <Descr_Component>Gas Centrifuges and assemblies and components for use in
      centrifuges</Descr_Component>
    <Descr_Material>Aluminium alloys</Descr_Material>
    <Subcomponents.description>Complete Rotor Assemblies</Subcomponents.description>
    <Variables.description>Tensile strength</Variables.description>
    <type>Minimum</type>
    <value>0.46</value>
```

Figure 2 XML representation of the information

4. Potential applications

Here our main purpose is to show how to use the potential of the semantic layout definition to locate in a fast, simple way the unique differences between the documents examined.

Let's consider the Access implementation of the XML-type documents. In such a case the information retrieval can be made through the execution of SQL queries. The result is again in form of a table. Performing the same queries on the two databases it is possible to check(through a software application or even manually) for differences in the values of the table 'Constraints' in connection with 'Variables'. The comparison provides whether a given component has been modified in the documents prepared by the NSG, our reference and has then been subject to a relevant technological upgrade with respect to the Annex II.

The following is a brief description of a practical example for using our the semantic database. We are interested in determining the characteristics of a rotor tube ('rotor tubes' in our information system). The result of a simple query applied to both databases will provide the desired results. Figure 3 and Figure 4 show in tabular form the results of the appropriate queries.

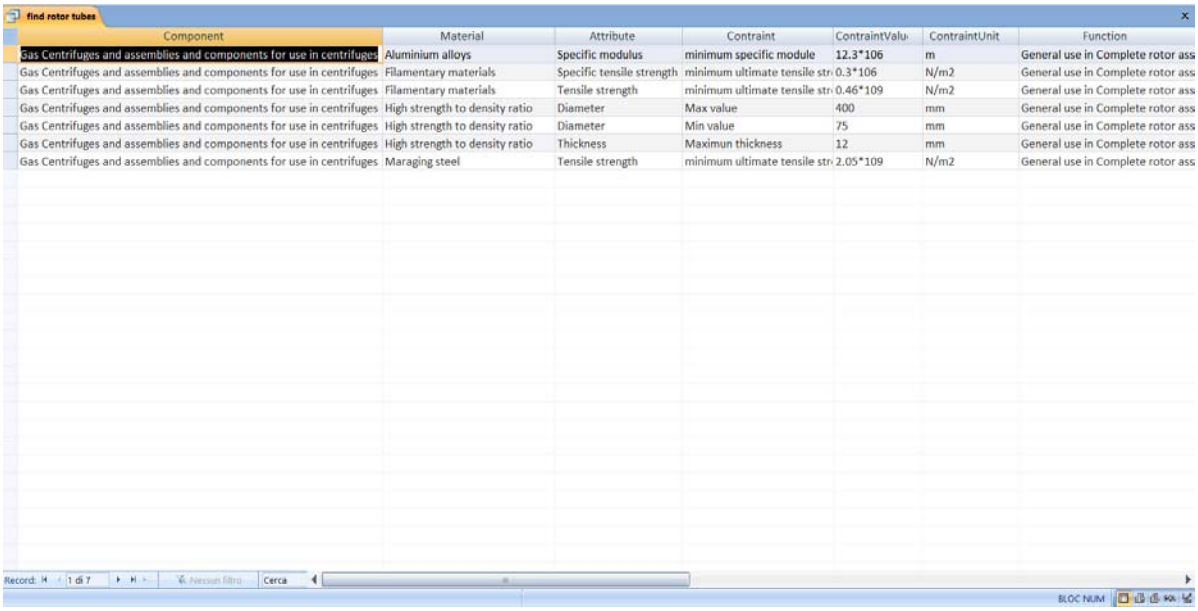
find rotor tubes

Component	Material	Attribute	Contraint	ContraintValu	ContraintUnit	Function
Gas Centrifuges and assemblies and components for use in centrifuges	Aluminium alloys	Specific modulus	minimum specific module	12.3*106	m	General use in Complete rotor ass
Gas Centrifuges and assemblies and components for use in centrifuges	Filamentary materials	Specific tensile strength	minimum ultimate tensile str	0.3*106	N/m2	General use in Complete rotor ass
Gas Centrifuges and assemblies and components for use in centrifuges	Filamentary materials	Tensile strength	minimum ultimate tensile str	0.46*109	N/m2	General use in Complete rotor ass
Gas Centrifuges and assemblies and components for use in centrifuges	High strength to density ratio	Diameter	Max value	400	mm	General use in Complete rotor ass
Gas Centrifuges and assemblies and components for use in centrifuges	High strength to density ratio	Diameter	Min value	75	mm	General use in Complete rotor ass
Gas Centrifuges and assemblies and components for use in centrifuges	High strength to density ratio	Thickness	Maximun thickness	12	mm	General use in Complete rotor ass
Gas Centrifuges and assemblies and components for use in centrifuges	Maraging steel	Tensile strength	minimum ultimate tensile str	2.05*109	N/m2	General use in Complete rotor ass

Record: 1 di 7 | Nessun filtro | Cerca | BLOC NUM

Figure 3 Rotor tubes information from the Annex II.

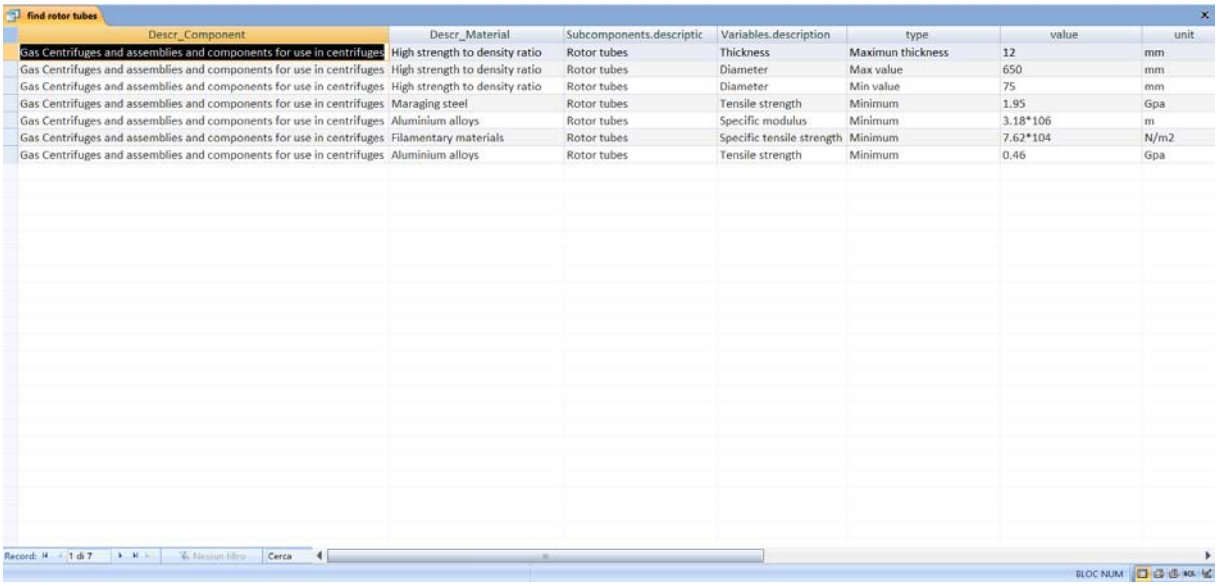

find rotor tubes

Descr_Component	Descr_Material	Subcomponents.descriptic	Variables.description	type	value	unit
Gas Centrifuges and assemblies and components for use in centrifuges	High strength to density ratio	Rotor tubes	Thickness	Maximun thickness	12	mm
Gas Centrifuges and assemblies and components for use in centrifuges	High strength to density ratio	Rotor tubes	Diameter	Max value	650	mm
Gas Centrifuges and assemblies and components for use in centrifuges	High strength to density ratio	Rotor tubes	Diameter	Min value	75	mm
Gas Centrifuges and assemblies and components for use in centrifuges	Maraging steel	Rotor tubes	Tensile strength	Minimum	1.95	Gpa
Gas Centrifuges and assemblies and components for use in centrifuges	Aluminium alloys	Rotor tubes	Specific modulus	Minimum	3.18*106	m
Gas Centrifuges and assemblies and components for use in centrifuges	Filamentary materials	Rotor tubes	Specific tensile strength	Minimum	7.62*104	N/m2
Gas Centrifuges and assemblies and components for use in centrifuges	Aluminium alloys	Rotor tubes	Tensile strength	Minimum	0.46	Gpa

Record: 1 di 7 | Nessun filtro | Cerca | BLOC NUM

Figure 4 Rotor tubes information from the NSG Trigger List.

The retrieved tables contain all the information which is conveyed by the Annex II and the Trigger List translated in a for which is easily interpretable by an algorithm or a human user.

From such a result, it is immediately clear that they are subcomponents used in the component 'Gas centrifuges and assemblies' and are characterized by properties such as the thickness which must not exceed the maximum value of 12 mm. They consist of materials that have, among other features, also a high strength to density ratio.

The next step is to identify the differences between the two tables. It is very easy to see that the value of the maximum diameter of this subcomponent went from 400 mm as reported in the Annex II to 650 mm as specified in the last Trigger List revision by the NSG.

5. Conclusions

Common textual documents can be represented by a XML database by defining table fields and an appropriate layout. This can be done with great precision by defining a semantic associated with the information conveyed by a document. the definition of such semantic is critical to make the document fully represented and its content available to users who do not share the same basic understanding of the technologies described. As an example, the XML tag that describes the 'Rotor tubes' may be associated with a URL containing information about the material 'Maraging Steel'.

The perspectives are definitely aimed to greater usability for allowing the dissemination of such information to a wider community potentially involved in these Safeguard regimes.

6. References

[1] https://www.iaea.org/publications/documents/infcircs/text-agreement-between-belgium-denmark-federal-republic-germany /

[2] http://www.nuclearsuppliersgroup.org/images/Files/Updated_control_lists/Prague_2013/NSG_Part_1_Rev.12_clean.pdf

[3] https://www.iaea.org/publications/documents/infcircs/text-agreement-between-belgium-denmark-federal-republic-germany /

[4] XML http://www.w3.org/XML/

International Secure Platform for Export-controlled Computing Tools

Timothy E. Valentine

Radiation Safety Information Computational Center (RSICC)
Oak Ridge National Laboratory
One Bethel Valley Road, Oak Ridge, Tennessee, USA 37831
E-mail: valentinete@ornl.gov

Abstract:

The Radiation Safety Information Computational Center (RSICC) at Oak Ridge National Laboratory is an information analysis center that collects, archives, evaluates, synthesizes and distributes information, data, and codes used in various nuclear technology applications. RSICC retains more than 2,000 software packages provided by code developers from various federal and international agencies. RSICC's customers (scientists, engineers, and students from around the world) obtain access to such computing codes (source and/or executable versions) and data to promote ongoing research, to help ensure nuclear and radiological safety, and to advance nuclear technology. However, in light of nonproliferation and national security concerns, it is prudent to explore alternatives to distribution of certain codes and data that pose a greater risk of diversion from their intended purposes or that could be utilized for nefarious activities. The international secure platform for export-controlled computing tools addresses the concern of providing access to export-controlled modeling and simulation (M&S) tools while also providing an avenue to foster cooperation among existing and new-entrant nuclear countries. This presentation provides a general overview of the secure cloud computing system, along with the access requirements and protocols established to permit use of certain export-controlled M&S tools and data.

Keywords: modeling, simulation, export, control, cloud, computing

1. Introduction

For the past five decades, the Radiation Safety Information Computational Center (RSICC) has served as the official repository for nuclear modeling and simulation (M&S) and data for the Department of Energy (DOE) and its predecessors and has collected and disseminated related information worldwide under specific distribution restrictions and guidelines set forth by the US government. RSICC maintains collaborations with other similar international organizations to foster cooperation and exchange of M&S tools and data to benefit to our customers. RSICC houses nearly 2,000 software packages provided by code developers supported from various research institutes and universities in the US, as well as international agencies and research centers. Many of these codes have a broad range of applications and uses.

One revolutionary challenge that RSICC has faced is the ever-expanding capability of computing technology accompanied by growing reliance on the need for M&S tools. In some part, the demand and reliance on M&S tools is a consequence of the increasing cost associated with operation of experimental nuclear facilities and the reduced availability of such facilities. Therefore, being able to provide quality-controlled software and data that can be utilized across a diverse set of computing

technologies is of growing importance, yet it is no easy task. Fortunately, RSICC has had the support of sponsors and code and data developers, along with access to a variety of computing resources to ensure that the packages that we supply to the user community span the breadth of resources for our users and address the range of the applications for which such software is needed.

RSICC's distribution of M&S tools and data helps to promote international cooperation in nuclear safety, ensures the safe development and deployment of nuclear technology, and provides those countries possessing or pursuing nuclear technology access to state-of-the-art software. However, in the light of nonproliferation and national security concerns, alternatives to distribution of certain codes and data that pose a greater risk of diversion from the intended purposes or that could be utilized for nefarious activities have been explored. Some of the most modern and versatile codes pose the greatest risk of diversion and/or theft. To help to resolve the dilemma between the open sharing of nuclear technology and the need to minimize the potential use of nuclear technology for nefarious purposes, RSICC developed, deployed, and implemented a system to provide access to modern software and data for which access would otherwise be limited or restricted. The deployment of this system also has additional benefit because some new entrant countries may lack access to sufficient computing infrastructure to effectively utilize modern M&S tools. In addition, the development and deployment of a secure computing architecture allows the user to access M&S tools installed under a controlled quality assurance process, thereby ensuring that the M&S tools function as designed. This paper describes the growing demand for M&S tools, along with a general description of the secure cloud system, as well as the protocols for accessing the system. Through its implementation, the system will help foster international cooperation in the peaceful uses of nuclear technology while minimizing the diversion of M&S software for other purposes.

2. Software Demand

The demand for state-of-the-art M&S tools has nearly doubled over the past 5 years, as shown in Figure 1. Over the past 4 years, RSICC has distributed over 4,000 software and data packages annually to customers and has seen a substantial growth in the number of packages delivered to customers who are not US citizens (shown in the figure as "foreign"). At the same time, RSICC has seen substantial growth in the number of requests from US universities at which a growing number of students are not US citizens.

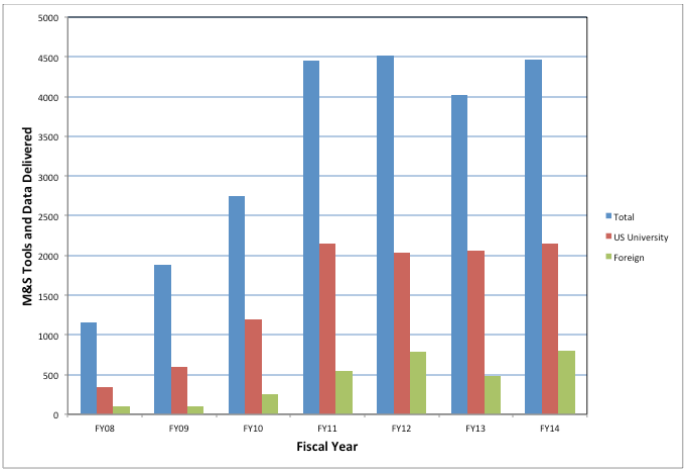

Figure 1. RSICC's annual software package distribution

Along with the growth in the demand for M&S tools and data, RSICC's customer base has expanded to include over 100 countries (Figure 2) and over 20,000 registered individuals. The greatest number of our customers is in the US, but RSICC has seen additional growth over the past 5 years in countries pursuing development and deployment of nuclear technology. Over 16,000 active customers from the US have requested or received software from RSICC since 2005. Outside the US, most of RSICC's clients reside in Canada, France, the United Kingdom, China, South Korea, and Germany.

As reliance on advanced M&S tools and data grows, RSICC anticipates further growth in the demand for its services.

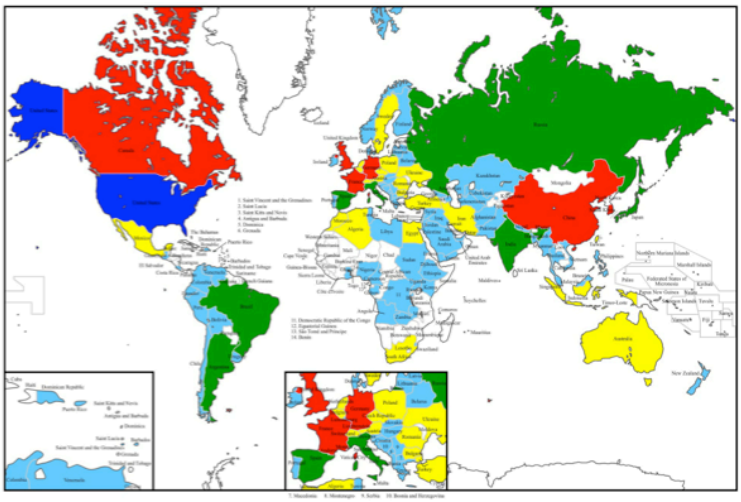

Blue >750; Red 350-749; Green 150-349; Yellow 50-149; Light Blue <50

Figure 2. RSICC's customer demographics.

The use of M&S tools spans a range of applications. The M&S software and data distributed by RSICC are being used for designing advanced reactor concepts, computing radiation source terms, designing and developing fusion devices, ensuring nuclear criticality safety, designing accelerators, implementing nuclear medicine applications, and implementing nuclear security applications. The Los Alamos Monte Carlo code MCNP [1] and the Oak Ridge National Laboratory SCALE system [2] can be applied across all of these areas and are in the most demand by our customers. These codes can also be used for other purposes when there are concerns regarding diversion, theft, or proliferation of the codes. Given these concerns, a balance between open sharing of advanced M&S tools and mitigation of improper code was sought through development and deployment of a secure cloud computing system. As previously stated, the primary purpose of this system would be to minimize national security concerns while allowing access to state-of-the-art M&S software and data for peaceful purposes.

3. System Description and Access Protocols

3.1. System Description

The general specifications of RSICC's secure cloud computing system are provided in Table 1. This is a capacity system capable of supporting 50 to 100 intermittent users. The system is comprised of 10 compute servers with 4 compute nodes per server and 2 processors per node. The system is built on "Abu Dhabi" Opteron eight core servers. The theoretical peak performance of the cluster is approximately 12 teraflops (TFlops). The system has 5,120 gigabytes (GB) of total memory, with more than 12 terabytes (TB) of disc space. The system is accessed through a log-in node using an RSA SecurID service for two-factor authentication as shown in Figure 3. The system is also segregated from other computing systems at Oak Ridge National Laboratory (ORNL) for network security purposes.

Secure cluster	Each node	Each server	Total cluster
10 compute servers/cluster		1	10
4 compute nodes/server	1	4	40
2 processors/node	2	8	80
16 cores/processor	32	128	1280
Memory	128 GB	512 GB	5,120 GB
Peak theoretical performance	0.307 TFlops	1.23 TFlops	12.3 TFlops

Table 1. RSICC's secure cloud computing system description.

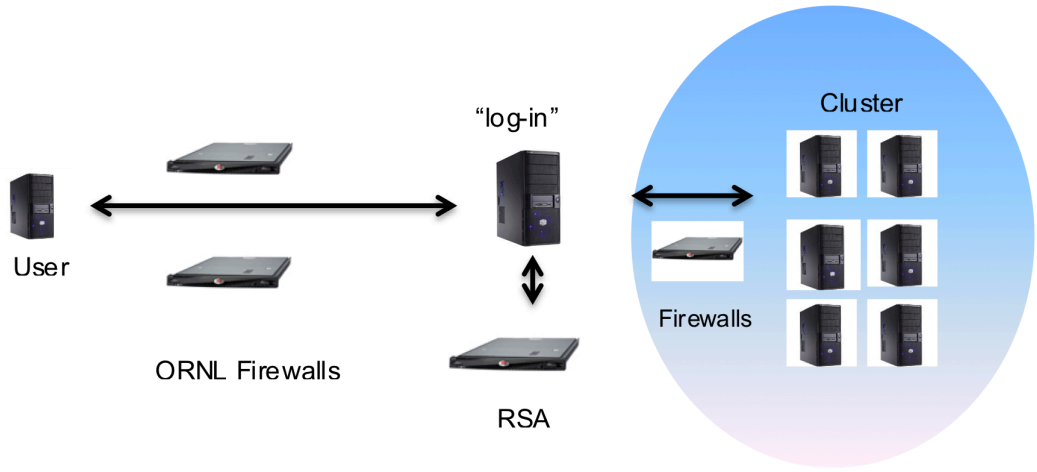

Figure 3. Graphical representation of RSICC's secure cloud computing system.

3.2. Access Protocols

As previously stated, individuals who otherwise cannot be provided access to certain M&S software will now be able to use state-of-the art M&S software on the secure cloud system. Currently, targeted users include foreign nationals collaborating or working at US national laboratories and universities. Additional users are likely to include individuals identified by the US Department of Energy for whom the use of the system is deemed to be in the interest of the US government.

The access process requires that the user register with RSICC by providing their contact information, including their physical address and their email address. After registering with RSICC, individuals can request software from our extensive collection. When foreign nationals who meet the selection criteria request MCNP, SCALE, and RELAP from RSICC, [3] they will be evaluated for access to the secure server, and instructions for access will be provided on approval. Approved users with access to the secure cloud system will be provided with instructions for using the system and will be provided with RSA SecurID tokens that are usable for a 5-year period. The RSA SecurID token will be mailed to the address the user provided during registration.

Each user will have a unique identifier and password associated with his or her account. The user will only be able to access the system remotely through a secure shell (ssh) using both the password and RSA SecurID token. The user will be permitted to upload and download ASCII text files and to send and/or retrieve input and output files. Each uploaded file will be scanned for viruses, and uploading of non-ASCII files will not be permitted. A users attempting to upload non-ASCII files will have his or her account suspended. Furthermore, a user will only have access to his or her personal area on the hard drive, and any attempt to access other areas of the system will result in the suspension of the user's account. Scripts have been written to execute MCNP, SCALE, and/or RELAP. The installed versions of these codes will be the production versions and will be updated as warranted. Beta versions of the codes will not be available on the secure cloud computing system.

4. Summary

Development and deployment of a secure cloud computing system at RSICC allows for controlled access to state-of-the-art M&S tools and data with extensive applications while simultaneously addressing concerns with diversion, theft, or nefarious uses of the codes. System deployment will also provide some users with computing infrastructure that may not be easily accessible in their own organizations. In addition, the system has been built to support 50 to 100 intermittent users at one time and can be accessed remotely using a unique customer identifier along with a secure token. Approved users will be able to use the production releases of MCNP, SCALE, and RELAP that currently reside at RSICC. Additional codes may be added to the secure cloud system as warranted.

The benefits of this system are notable. Individuals who otherwise would not be allowed access to these modern programs will now be able to use them on a rigorously tested and verified computing platform. System users will be able to focus on addressing scientific problems without being concerned with software installation or quality control. Individuals from some participant countries lacking modern computing infrastructure will now have access to a high-capacity computing system. Successful deployment of this system will permit sharing of state-of-the-art M&S tools and data to facilitate the safe application of nuclear technology while also fully addressing and mitigating proliferation concerns.

5. Acknowledgements

The author would like to acknowledge the support of the US Department of Energy Office of Nuclear Energy, the National Nuclear Security Administration, and the Office of Nonproliferation and Arms Control for development and deployment of the secure cloud computing system. The author would like to thank Mark Baird, Matt Disney, Ken Barker, and Brian Zachary of ORNL for their efforts to install, test, and validate the system's operation, as well as for their development of the network security protocols that enabled the system to be deployed.

6. References

[1] J.T. Goorley, et. al., "Initial MCNP6 Release Overview," *Nucl. Tech.,* **180**, 298-315 (2012).

[2] *SCALE: A Comprehensive Modeling and Simulation Suite for Nuclear Safety Analysis and Design*, ORNL/TM-2005/39, Version 6.1, Oak Ridge National Laboratory, Oak Ridge, Tennessee (June 2011).

[3] L. J. Siefken, et. al., "REPLAP5/MOD3.3 Code Manual Volumes 1-5," NUREG-6150 (September 2000).

3D Printing: Implications for Non-Proliferation

Grant Christopher

International Centre for Security Analysis
The Policy Institute, King's College London
22 Kingsway, London, WC2B 6LE, UK
E-mail: grant.christopher@kcl.ac.uk

Abstract:

Additive manufacturing—a technology that encompasses 3D printing—is a rapidly developing field. Use of this technology is now an industry standard for aiding production of high-strength components in the aerospace and automotive industries. Nor is 3D printing used only for rapid prototyping; it is now increasingly being used to produce final components. There have been significant recent advances in the strength and quality of printed components as well as the use of high strength metals. This paper will examine the implications of this technology on current issues in non-proliferation based on open source information.

Keywords: 3D printing, additive manufacturing, non-proliferation

1. Introduction

A day does not seem to pass without a groundbreaking application of 3D printing in such diverse areas as law enforcement [1], space [2], and medicine [3]. Advances appear to be so rapid any attempt to provide a comprehensive review of this field would be quickly outdated. Nevertheless, the technology referred to more broadly as digital manufacturing has been described by many societal commentators as a revolutionary technology [4] [5].

Discussions of 3D printing are typically centred around the ability to customise parts ("complexity is free"), the transformative effect on supply chains and uniform cost per unit changing economies of scale. However, the principal concern when looking through the lens of non-proliferation is the ability to print high strength or chemically resistant materials and the corresponding possibility of circumventing export and intellectual property controls.

There exists only a small body of previous work on 3D printing and non-proliferation [7], addressing export controls [8], perceptions and risks of 3D printing [9] and a general report on WMD and 3D printing [10].

Most recent advances in 3D printing have no direct relevance to non-proliferation; but of particular interest are advances in the aerospace industry which has in the last few years moved from a prototype R&D model to direct parts production [6]. Manufacture of high strength material, as is required in aerospace, is of special interest due to its applications in centrifuge production, one of the most sensitive technologies the nuclear fuel cycle. Overall, advances are being made in accuracy, detail, strength, time, cost, and materials used. However, significant challenges remain for 3D printing in increasing the ability to print multiple materials as well as warping effects when printing large items.

3D printing is the manufacturing step in the larger process known as additive manufacturing. Additive manufacturing (AM) includes the digital design of objects and the 3D scanning of existing objects. This, in practice, could create an enormous challenge for proliferation if sensitive objects are converted into a digital format useable in a 3D printer. Designs then could change hands through a targeted cyber attack, illicit digital exchange (for instance through email) or legal exchange through online marketplaces, where plans are available to download like any other digital good. Once a 3D

plan is available it has proven very difficult to control—the challenge of US law enforcement removing plans for the 3-D printed gun is a good example [11] [12].

The term “3D printing” actually encompasses multiple technologies that often bear little relation. Food and biomaterials printing are very different technologies to printing high-strength metals and plastics. The materials that can be printed depend on the method: metals can only be printed using lasers and the technologies that use molten plastics are not suitable for metals.

2. Overview of the Additive Manufacturing Process

Additive manufacturing is the full process from producing digital files by computer design or 3D scanning to production using a 3D printer. The moniker additive manufacturing is in contrast to traditional manufacturing that can be considered to be subtractive; the fundamental process being to take a piece of material and remove parts of it and then possibly stretch and manipulate it into the required final form.

Blurring the distinction between traditional, subtractive, manufacturing and additive manufacturing is the class of Computer Numerically Controlled (CNC) machine tools, or Computer Aided Manufacturing (CAM) tools. These machine tools are already in wide use. Indeed, whilst it is often said that 3D printing is ideal for rapid prototyping, subtractive manufacturing using CNC may be able to perform such activities faster.

CAM files are a shared property of AM and modern advanced manufacturing using CNC machine tools. A single file can be sent to any machine in the world and the item can be manufactured. The industrial process can therefore be split into two parts: the digital file design and the manufacturing process.

From a proliferation standpoint attribution is also a big question in this new supply chain. For most traditional goods the manufacturer is printed on the product. This is not the case for locally printed 3D items, especially those originating from consumer to consumer design exchange. Solutions to this problem that have been discussed include using chemical signatures and including particular nanoparticles in the final object that can be identified.

2.1. Additive Manufacturing Design Preparation

Files can be prepared for 3D printing by scanning a real object and using software to convert this information into a useable file format. Alternatively, software can be used directly to design an object.

2.1.1. 3-D Scanning

3D scanning technology can be used to produce a digital file from an object placed in a 3D scanning machine. The resulting file can be used in a 3D printer or digitally altered using an appropriate editing software application.

The technology used to scan is broadly split into two areas: contact scans and remote scans. Contact machines may damage sensitive delicate objects and are slower than remote methods.

Remote scanning techniques all exploit light in various methods such as Time of Flight (ToF) or structured light scanning. Methods that rely on a single beam are relatively slow and can suffer from inaccuracies. The structured-light technique, an especially active subject for current R&D is far more promising, allowing rapid scanning of an entire field of view simultaneously.

2.1.2. 3-D Printing Digital Files

Files for use in 3D printers use a number of different file formats. The STL is the industry standard format for printing and stores the object by storing the object surface as a series of triangles. Complex and curved geometries can be represented with a fine triangulation. Other file types are in use such as OBJ files but the vast majority of the industry uses STL.

2.1.3. 3D Printing Software

A large number of different software package are available for use in AM. Some are used in file conversion and producing the correct file type from information from 3D scanners or conversion from some CAD file to STL type. The key software for this technology is taking a 3D model and converting it into 2D layers suitable for printing, into slices on a scale of 40 μm. Other software can be used to manipulate existing digital design files to modify the produced product and often high-end 3D printers are accompanied by their own software package used for operation.

3D printing allows infinite customisation for the same price as an 'off the shelf' design and software is the ideal vessel for this creativity. For non-proliferation purposes these software manipulation packages are not especially relevant: only design files of certain objects are sensitive.

2.2. Additive Manufacturing: 3-D Printing

Once a file exists in the correct format the object can be printed using variety of different technologies available that are all considered to be 3D printing. The technology dictates the material available. The fundamental method for all these technologies is the same: to 2D print layer by layer in succession to build a 3D structure. The process is time-intensive for all technologies, requiring many hours to print anything but small items.

Once printed, 3D printed items require extensive quality control, which can include interior scanning for defects. Other post-production steps are necessary to polish and remove granularity. Many 3D printing techniques leave the object freestanding, so the supports that are in place will need to be removed.

A large number of different technologies are available. A non-exhaustive description of the most relevant technologies is provided below and for an in-depth review see [13].

2.2.1. Direct Metal Laser Sintering

Direct metal laser sintering (DMLS) uses a laser to sinter metal powder. The process is very similar to selective laser sintering. The powder is printed in layers and is sintered by a laser, whereby the boundary is heated between the materials to bind the structure in an adaptation of this common industrial process. The powder is pushed in layers to a bed of powder which is lowered as each layer is completed.

This technique was used to print the first 3D printed gun [11]. This is the most important process for non-proliferation concerns and can be used to print high-strength metals. The accuracy of this process is published to be +/- 0.05 mm but in practise accuracy is closer to +/-0.1mm per 100mm.

The process will leave residual material with a surface size of typically around 30 μm. Post-build finishing is also very important for this process. The object will be printed such that a small metal frame will hold in place for objects without a flat surface. Objects will also require surface smoothing and a heat treatment to relieve internal stresses applied. The process is also lengthy and may take several days for large components.

2.2.2. Selective Laser Melting

In Selective Laser Melting (SLM) a laser melts metal power into a solid homogenous mass. This is in contrast to laser sintering, which fuses homogenous small particles together at the boundary. Typically, lasers are used for this process, but electron beams can also be used. A sea of powder is also used in this technique in a similar manner to selective laser sintering. This technology is also important for high-strength metals.

2.2.3. Direct Metal Deposition

In this process the powder is injected via a nozzle onto a surface exposed surface, but in other respects is similar to DMLS.

2.2.4. Fused Deposition Modelling

In fused deposition modelling (FDM), also known as Fused Filament Fabrication (FFF), thermoplastic material is used. Plastic filament is melted and the molten plastic is injected with a nozzle. The plastic then hardens immediately. The technology is of interest due to the possibility to print fully fluorinated plastics. Stratasys is the leader in this technology (FDM their patent name of the technology) and it is used for prototyping in defence, aerospace, automotive and other technologies.

2.2.5. Stereolithography

In stereolithography, a photoactive resin is cured with a UV laser. A liquid resin is exposed to the laser in order to build up the layers of material from a pool to which successively more material is added in a technique similar to selective laser sintering and SLM. Beyond prototyping, there is little application of this technology to non-proliferation.

2.2.6. Other 3D Printing Technologies

Other 3D printing technologies, such as food, biotech and nanomaterials are available but not relevant to non-proliferation.

3. Available Hardware and Services

The marketplace for 3D printer production is increasingly global. However, the most technologically advanced printers that can be used to print high strength materials are restricted to states with advanced industrial bases. This is especially the case for metals production.

3.1. Available 3-D Printers

The number of suppliers of 3D printers is increasing and expanding globally. Stratasys, a US leader in 3D printer manufacture offers its cheapest printer from USD 3000 to USD 750,000 for its most advanced models and specializes in FDM [14]. XYZ Printing is another major manufacturer for household FDM printers which are available for USD 500 [15].

For printing metals there are fewer manufacturers and the printers are more expensive typically in the six-figure range (USD). Companies such as 3D Systems offer Direct Metal Printing machines (as well as stereolithography and SLS machines for plastic) [16]. Renishaw offers the AM250, a laser melting machine, which prints in a high-purity argon gas atmosphere for building reactive metals for around USD 500,000 [17]. The materials available include Stainless Steel, aluminium, titanium, cobalt chrome and inconel. Arcam, a Swedish 3D printing manufacturer have developed a series of printers for use in Aerospace and industry priced around USD 1m and able to print Titanium and cobalt-chrome [18]. Realizer, a German company offers SLM machines [19]. BeAM, a French company, offers a range of metal printers and is actively working towards developing new industrial applications for “aeronautics, aerospace defence and nuclear industries” with “multi-material capabilities” [20].

Independent developers are also developing 3D printers, in efforts to provide desktop printers in the thousands of dollars price range, rather than a six-figure industrial metal printer. A Kickstarter campaign to provide a low-cost printer was cancelled [21] but such low cost printers are already available, albeit with limited functionality [22].

A more comprehensive list of available printers is found at Aniwaa.com, a 3D printer comparison site which lists 37 printers capable of metal printing [23]. The ability to print high-strength metals is still restricted to a very small number of printers and is covered in more detail in section 4.

3.2. 3D Scanners

Commercially available 3D scanners are split into ‘hand-held’ battery operated and immobile systems. High-quality scanners are far cheaper than metal printers at around USD 40,000. At the high end of the range the GFMesstechnik TopoCAM uses structured light technology to a 2.5 µm resolution and is

priced at USD 100,000, although the scan volume is limited [24]. At a far lower price of under USD 50,000, the portable 3D Digital Corp Optix 500M has 50 μm resolution [25].

Academic literature is available on quality: various scanners have been assessed by biomedical academics to access their suitability for research [26].

3.3. Online Marketplaces

There are a wide variety of online marketplaces for exchanging 3D printing designs, typically in the form of STL files. They typically take the form of consumer-to-consumer sites, such as Thingiverse which varies from toys and jewellery to tool parts and household items. Most online marketplaces are variations on this theme, with some such as Cubify allowing software customisation. Defense Distributed, the company behind the first 3D printed weapon, has a site defcad.com, but this has been down since February, and the weapon design was removed by order of the US government [11]. Many sites are specifically catered to professionals and developers, such as Cubehero and 3DVIA. A non-exhaustive list of marketplaces is available from an aggregated list [27].

3.4. Exporting Hardware

There are no current export controls for 3D printers. The Nuclear Suppliers Group (NSG) dual use items list contains export controls for precision Computer Numerically Controlled manufacturing, such as spin-forming and flow-forming machines that are capable of manufacturing various materials associated with the nuclear fuel cycle [28]. The Wassenaar Arrangement manages export controls for conventional arms, and this control list also does not account for 3D printing [29]. Additive manufacturing equipment is controlled for the specific purpose of manufacturing of gas turbine engine blades, vanes or “tip shrouds” using single-crystal additive manufacturing equipment.

Some classes of 3D scanners could potentially be controlled under NSG item 1.B.3 from the dual use items list [28] and Wassenaar Arrangement item 2.B.6 [29] which control coordinate measuring machines operating on 2 or more axes operating with sufficient accuracy. It is not clear if this would control non-contact machines, particularly those using the structured light technology.

Materials used for printing themselves are not controlled unless manufactured in specific geometries [28].

4. Case Study: Can You Print a Rotor Suitable for Use in a Centrifuge?

Centrifuges used for enriching uranium rotate at such a rapid rate to require high-precision, high-strength material. Until very recently, these materials—carbon fibre, maraging steel and high strength aluminium—have only been available in a small number of countries with advanced manufacturing bases. If it were possible to 3D print high strength material for use in a centrifuge this would present a serious challenge to current export control regimes.

Is 3D printing a centrifuge possible? In comments to the American Association for the Advancement of Science, Michael Hopmeier from Unconventional Concept Inc., a Virginia-based defence consultancy company, stated that the technology already exists for 3D printing an entire centrifuge for uranium enrichment, without substantiating the comment [30]. There is not much literature available on this subject and we here attempt to examine this claim.

3D printers that can print maraging steel are already commercially available [31]. The mechanical properties “as built” are too weak for centrifuge use, according to NSG requirements [28] with an ultimate tensile strength (UTS) of around 1110 MPa. However, after age hardening the UTS exactly meets the NSG requirement of 1950 MPa. This clearly points to the technology being on the threshold—if not beyond—the capability to 3D print parts suitable for a centrifuge. In fact, a 2012 paper claims that mechanical properties comparable to conventionally produced maraging steel can be produced by SLM [32]. However, there are a number of important factors to consider.

The critical industrial process for maraging steel, though, is the age hardening, meaning a potential proliferator would require the infrastructure to perform this part of the manufacturing process for

maraging steel. Beyond obtaining the steel with the correct chemical composition martensic aging to alter the microscopic composition of the steel, commonly referred to as maraging, is the most difficult part of the industrial process. A 2014 paper leaves questions over the microscopic properties of maraging steel produced by SLM [33] but progress is consistently being made in this area. It should be pointed out that under current export controls only complete maraging steels that meet the required dimensions in addition to the UTS requirements are export controlled. The maraging steel powder that would be used in this process is not. Again we state that the printers themselves are also not currently export controlled.

The size of 3D printed objects is also an issue. Centrifuge rotors are longer than the current generation of commercial 3D printers allows: for instance the aluminium rotors of the Iranian IR-1 are about 1m in length and the carbon fibre IR-2m about 50 cm. A commercial system such as the EOS M 280 has a building volume of 25 x 25 x 32.5 cm^3 [34]; which is far too small.

4.1. Maraging Steel 3D Printers

The primary company that makes maraging steel capable 3D printers is Electronic Optical Systems (EOS). Others include the Matsuura, located in Japan [35]. The list of maraging steel capable 3D printers is provided in Table 1.

Maraging Steel Printers	Building Volume	Material
EOS M 270	25 x 25 x 21.5 cm^3	MS1
EOS M 280	25 x 25 x 32.5 cm^3	MS1
EOS M 290	25 x 25 x 32.5 cm^3	MS1
EOS M 400	40 x 40 x 40 cm^3	MS1
LUMEX Avance-25	25 x 25 cm^3	Matsuura Maraging II

Table 1: 3D printers of maraging steel.

Maraging steel capable 3D printers are not yet cheap, costing between USD 400k-750k. 3D Systems' Pro X range are also potentially maraging steel capable [16]. The Renishaw AM250, as discussed in section 3.1 may also be capable of printing maraging steel; a list of materials in development is was not available at the time of writing.

4.2. Maraging Steel Powder

The powder used for printing is EOS maraging Steel MS1 [31], a fine alloyed steel powder, which is designed to be used in the EOS M systems. The powder is US classification 18% Ni maraging 300, European 1.2709 and German X3NiCoMoTi 18-9-5. It is designed to be age hardened after printing at 490 Celsius. Other powders such as the Matsuura Maraging II are available [35].

4.3. Other High Strength Materials

High-strength aluminium is also suitable for centrifuges, although is far less desirable than maraging steel or carbon fibre. The EOS M systems can also print aluminium; however they are far below the strength needed for centrifuges [36].

4.4. Maraging Steel 3D Printing Services

Many Companies offer 3D printing services with 1.2709 Maraging Steel using EOS printers. These companies typically require CAD files, usually in the form of STL files and will use a professional 3D printer to print an item and then ship it to the customer. A selection of these service providers are listed in Table 2.

Company	Model	Location
3d-alchemy.co.uk	unknown	Shropshire, UK
axis proto	EOS M 270	Quebec, Canada
CDRM (3D systems)	unknown	Buckinghamshire, UK
GPI prototype & manufacturing	EOS M 270, 280	Illinois, USA
3D Material Technologies	EOS M 280	Colorado, USA
3trpd	EOS M 270, 280	Berkshire, UK

Table 2: 3D printing service providers offering maraging steel printing.

Not all information was available for all companies, but no printers were confirmed to be capable of printing maraging steel other than the machines previously identified. The list is certainly non-exhaustive, and the search methodology would likely miss non-English language companies.

5. Case Study: Printing UF6 Resistant Components

Uranium Hexafluoride (UF6) is a highly corrosive substance. Typically, Fully Fluorinated Materials (FFM)—that are resistant to UF6—are the only materials in contact with the gas during an industrial process. Other materials can be used such as aluminium, aluminium oxide, stainless steel nickel alloys such as inconel and phosphor bronze may also be used [28]. The piping between centrifuges is a typical component, as well as the contact point for pressure transducers and other applications in reprocessing. A complex object with moving parts such as a pressure transducer is not yet a realistic possibility. However, piping and other components required in a UF6 enrichment plant is a realistic object for a 3D printer.

5.1. Fully Fluorinated Materials

Fluoropolymers, the most common type of FFM, are a suitable material for chemical resistance of UF6. PTFE or Polytetrafluorethylene is polythene with a carbon chain and the hydrogen replaced with fluorine. However, this material does not melt when heated so would not be suitable for FDM 3D printing. Other materials include: FEP, PFA, PCTFE and Vinyidene fluoridehexafluoropropylene [26].

Currently, it does not seem that any FFM are being 3D printed. Current materials may not be suitable, due to melting requirements and would have to be developed.

5.2. Other Materials

Printing with metals such as stainless steel [37] and Inconel [38] is also possible. As these materials are in such common use they are only export controlled for very specific components [28].

6. Conclusions

Printing high strength components or corrosion resistant components for use in the nuclear fuel cycle is already possible with today's commercial 3D printers. However, due to the time it takes to print, as well as questions over cost, size and quality issues, it is highly unlikely that an actor pursuing a nuclear program would choose to 3D print unless it was not possible to obtain parts through traditional manufacturing supply chains. Complex multi-component parts are still beyond the current (and the next) generation of 3D printers as are parts with internal electronics.

3D printers and the high-strength materials used in them are not yet under export controls. Due to the digital nature of the files used in 3D printing, proliferation of sensitive designs could become a future issue in the current cyber security environment. The precedent for export controls for these items already exists with CNC machinery, which are controlled by the Wassenaar Arrangement and the Nuclear Suppliers Group.

7. Acknowledgements

Thank you to Paul Hooper and Mark Wenman for helpful conversations on post 3D printing treatment for maraging steel and Ian Stewart for a discussion on export controls.

8. References

[1] Eve C; *How Plymouth academics used state-of-the-art 3D printing to secure a murder conviction;* Plymouth Herald; 20 April 2015; http://www.plymouthherald.co.uk/Plymouth-academics-used-state-art-3D-printing/story-26359439-detail/story.html; accessed 20 April 2015

[2] NASA Press Release; *NASA Test Limits of 3D Printing with Powerful Rocket Engine Check;* 27 August 2013; http://www.nasa.gov/press/2013/august/nasa-tests-limits-of-3-d-printing-with-powerful-rocket-engine-check/#.VTdxdiFVhBd; accessed 22 April 2015

[3] Murphy S V, Atala A; *3D printing of tissues and organs;* Nature Biotechnology; 32; p773-785; 2014

[4] The Economist; *The Third Industrial Revolution;* 21 April 2012

[5] Berman B; *3-D Printing: The new industrial revolution;* Business Horizons; Vol. 55; I 2; March-April 2012; p155-162.

[6] Koreis; Rocke Robert; *Three Dimensional Printing of Parts;* US Patent & Trademark Office; Appl. No. 14/019129; 5 September 2013

[7] Richards A; *How The Evolution Of 3-D Printing Presents The Newest Challenge To Nonproliferation Norms And Global Export Controls,* PONI Fall Conf.; August 27-28, 2014

[8] Stewart I; *Export Controls and 3d printing;* Project Alpha; https://www.acsss.info/news/item/236-export-controls-and-3d-printing; 7 June 2013; accessed 4 February 2015

[9] Schneider T et al.; *3D Printing: Perceptions Risks and Opportunities;* Social Science Research Network; 4 November 2014; http://papers.ssrn.com/sol3/papers.cfm?abstract_id=2533681; accessed 22 April 2015

[10] Galamas F; *3D Printing WMD Proliferation and Terrorism Risks;* Fundacja im. Kazimierza Pulaskiego; March 2015; http://pulaski.pl/images/publikacje/raport/Raport_3DPrinting.pdf; accessed 20 April 2015

[11] Solid concepts Inc.; *Worlds First Printed Metal Gun;* YouTube; 6 Novermber 2013; https://www.youtube.com/watch?v=u7ZYKMBDm4M; accessed 22 April 2015

[12] Preston J; *Printable-Gun Instructions Spread Online After State Dept. Orders their Removal;* NY Times; 10 May 2013

[13] Zhai, Y; Lados, DA; Lagoy JL; *Additive Manufacturing: Making Imagination the Major Limitation;* JOM, Vol. 66, No. 5 2014

[14] Stratasys; www.stratasys.com ; accessed 3 February 2015

[15] XYZ Printing; www.xyzprinting.com ; accessed 10 March 2015

[16] 3D Systems; www.3dsystems.com ; accessed 10 March 2015

[17] Renishaw; *AM250 laser melting (metal 3D printing) machine;* http://www.renishaw.com/en/am250-laser-melting-metal-3d-printing-machine--15253; accessed 29 April 2015.

[18] Arcam; www.arcam.com; accessed 20 April 2015

[19] Realizer; http://www.realizer.com; accessed 20 April 2015

[20] BeAM, http://beam-machines.fr; accessed 20 April 2015

[21] Aurora Labs; *Affordable 3D Metal Printer – Aurora Labs;* Kickstarter; https://www.kickstarter.com/projects/460400892/affordable-3d-metal-printer-aurora-labs; accessed April 2015

[22] Pensa Labs; http://www.pensalabs.com; accessed 18 April 2015

[23] Aniwaa; www.aniwaa.com ; accessed 18 April 2015

[24] GF Messtechnik; http://www.gfmesstechnik.de; accessed 18 April 2015

[25] Optix; *Optix 500M 3D Scanner;* http://www.3ddigitalcorp.com/optix-500m-3d-scanner; accessed 28 April 2015

[26] Eder, M et al.; *Evaluation of Precision and Accuracy Assessment of Different 3-D Surface Imaging Systems for Biomedical Purposes;* Journal of Digital Imaging, April 2013, Vol. 26, Is. 2, p163-172; 15 May 2012

[27] 3D printing repositories; http://3dprintingforbeginners.com/3d-model-repositories/; accessed 21 April 2015

[28] Nuclear Suppliers Group; *NSG Guidelines Part 2 - June 2013;* 2013

[29] Wassenaar Arrangement; *Export Controls for Conventional Arms and Duel-Use Goods and Technologies;* Updated 23 March 2015

[30] NDIA; *Proliferation of Cheap 3-D Printers Raises Security Concerns;* November 2013; http://www.nationaldefensemagazine.org/archive/2013/November/pages/ProliferationofCheap3-DPrintersRaisesSecurityConcerns.aspx; accessed 20 April 2015

[31] *Maraging Steel MS1 Data Sheet*, http://proto3000.com/assets/uploads/Materials-Brochures/DMLS-MaragingSteel.pdf; accessed 5 February 2015

[32] Kempen K; Yasa, E; Thijs, L; Kruth, JP; Van Humbeeck, J; *Microstructure and mechanical properties of Selective Laser Melted 18Ni-300 steel,* Physics Procedia, Vol 12 Part A, 2011, p 255-263; 16 April 2011

[33] Jägle, EA; Choi, P-P; Van Humbeeck, J; Raabe, D; *Precipitation and austenite reversion behavior of a maraging steel produced by selective laser melting;* J. Mater Res., Vol. 29, No. 17, 14 September 2014;

[34] EOS M 280; http://www.eos.info/systems_solutions/metal/systems_equipment/eosint_m280; accessed 24 April 2015

[35] Matsuura LUMEX Avance-25; http://www.lumex-matsuura.com/contents/lumex04.html; accessed 28 April 2015

[36] *Aluminium AlSi10Mg Data Sheet*; http://proto3000.com/assets/uploads/Materials-Brochures/DMLS-Aluminum.pdf; accessed 27 April 2015

[37] *Stainless Steel PH1*; http://proto3000.com/assets/uploads/Materials-Brochures/DMLS-StainlessSteel.pdf; accessed 27 April 2015

[38] *Direct Metal Laser Sintering Inconel 718*; http://www.protolabs.co.uk/documents/united-states/inconel.pdf; accessed 27 April 2015

Session 13

Geospatial Information

Nuclear Verification from Space – Satellite Imagery within Nuclear Non-proliferation and Arms Control Verification Regimes

Irmgard Niemeyer

Forschungszentrum Jülich GmbH, IEK-6, 52425 Jülich, Germany

Abstract:

In the last decades, the international community has negotiated a number of multi or bilateral agreements on nuclear non-proliferation and arms control, partly including also provisions for the verification of compliance. Among the different verification measures, earth observation (EO) by scientific or commercial satellite imaging sensors has been considered as an important source of information. If the area of interest is not accessible, remote sensing sensors offer one of the few opportunities to gather almost real-time data over the area. The study reviews the technical progress in the field of satellite imaging sensors and explores the recent advances in satellite imagery processing as to the extraction of significant observables and signatures of possible non-compliance to non-proliferation and arms control. Some examples for potential applications of SI for nuclear verification in the context of the Non-proliferation treaty (NPT), the Comprehensive Nuclear Test Ban Treaty (CTBT) and a potential future Fissile Materials Cut-off Treaty (FMCT) will be given..

Keywords: satellite imagery, satellite sensors, image processing, verification regimes, arms control

1. Introduction

In the past years, research and development (R&D) activities related to the use of satellite imagery for non-proliferation and safeguards purposes have become less visible than in the 2000er years. One indication, among others, is the decreasing number of related topical papers at safeguards conferences. While earlier INMM or ESARDA conferences featured at least one technical session on satellite imagery, since some years it is increasingly difficult to fill a related topical session at all.

This is in some contrast to the actual technological developments in this area. 15 years ago, with the launch of the first very high resolution imaging sensor IKONOS, the space-based imaging technologies changed dramatically, in particular with regard to spatial resolution of optical data to 1 m and better. , and a more significant change is imminent. Video data from space is increasingly available, the spatial resolution of optical data has further enhanced up to 31cm, two of the most recent sensors also provide data from the shortwave infrared region of the electromagnetic spectrum at spatial resolution below 6m, and with the evolution of the so-called SmallSats, the temporal resolution has increased significantly. Besides the emerging space-based imaging technologies, also the image processing technologies are advancing, in line with the increasing computer performance improvements.

On the other hand, R&D on satellite imagery has been less considered by the safeguards-related Member State Support Programmes (MSSPs) in the past years. The European Framework Programme, which represented a source for funding in the past, e.g. through the Copernicus initiative [1-3] offers only very limited opportunities today. The Horizon 2020 calls issued so far, showed only limited links to advancing the application of satellite imagery for non-proliferation and safeguards purposes.

The contradiction between the technological advancements on the one hand, and the less funding contributions or options on the other hand could be due to the fact, that science and technology have solved

all relevant issues. And indeed, the potential of available satellite imagery (SI) for safeguards verification has been widely investigated and understood, and the IAEA is using SI on a routine basis. However, also the IAEA needs to keep pace with the technologic developments and therefore, feasibilities studies of the future SI are necessary. The IAEA may need to enhance the efficiency of using satellite imagery, e.g. by semi-automation of processes, and also the effectiveness by extracting more safeguards-relevant information from satellite imagery.

As far as other non-proliferation, arms control and disarmament agreements are concerned, satellite imagery has been considered as verification measure, in some case long time ago when the technical parameters of open source satellites were not as promising as they are today. Accordingly, these feasibility studies need to be updated or extended, taking the current and future technologies into account.

Against this background, the given paper will review the emerging satellite imagery technologies, both the imaging sensors and the image processing and give some examples for potential applications of SI for nuclear verification in the context of the Non-proliferation treaty (NPT), the Comprehensive Nuclear Test Ban Treaty (CTBT) and a potential future Fissile Materials Cut-off Treaty (FMCT).

2. Emerging Satellite Imagery Technologies

The era of civil Earth observation (EO) started 1972 with the launch of the first civil satellite by the US National Aeronautics and Space Administration (NASA). Earth Resources Technology Satellite (ERTS), later renamed as Landsat-1, provided image data in three spectral bands (green, red, near infrared) with a spatial resolution of 80 m. A number of papers demonstrated the application of Landsat, ASTER and SPOT imagery for nuclear safeguards applications (see e.g. [4,5]), however, the medium resolution of this imagery up to 15m does not allow for detailed analysis of nuclear facilities.

The first paradigm shift in the satellite industry and civil EO occurred in 1999, when the first very high-resolution satellite sensor IKONOS-2 was launched. Following the availability of this data, the use of satellite imagery in the nuclear safeguards system has tremendously gained in importance [6]. Today, commercial satellite imagery has become one of the most important information sources the IAEA's Department of Safeguards uses for monitoring nuclear sites and activities. The Department has implemented a customized geoinformation system (GIS) called the Geospatial Exploitation System (GES) based on industry-standard GIS server technologies, enterprise geodatabase and commercial relational database management system (RDBMS), which is deployed to process, analyse, visualize, and disseminate geospatial information at the IAEA [7].

Table 1 gives an overview on current and future very high-resolution optical imaging sensors providing a spatial resolution of 1.0 m or better. The sensors are ordered by their best spatial resolution and launch date. Following the merger of the former U.S. competitors GeoEye and DigitalGlobe in January 2013, DigitalGlobe has become the leading global provider of commercial satellite imagery, now operating six very high resolution sensors. In June 2014, the U.S. Department of Commerce lifted the restrictions to sell imagery at resolutions sharper than 0.50 m only to U.S. government authorities and not to any other customers in or outside the US and allowed DigitalGlobe to collect and sell imagery at the best available resolutions at that time. Beginning six months after the launch of WorldView-3, DigitalGlobe has been permitted to sell imagery at up to 0.25 m panchromatic and 1.0 m multispectral. The latest imaging satellite development by GeoEye dubbed GeoEye-2 was postponed in the course of the merger of the two companies in order to give launch space to WorldView-3; however, DigitalGlobe has now accelerated the completion of the satellite and plans to launch it as fourth-generation satellite in the WorldView series in mid-2016 providing customers with 0.30 m resolution imagery.

Besides the technical and economic supremacy of DigitalGlobe, another 11 satellites are under operation by the national space agencies or commercial companies of the Republic of Korea, France, Israel, Spain, India, and Dubai. Most of the sensors listed in Table 1 include multispectral bands from the visible and near infrared spectrum; the two most recent ones, Kompsat-3A (Korea) and WorldView-3 also provide image data

from the shortwave infrared spectrum of the electromagnetic spectrum at 5.5 m and 3.7 m resolution. All listed systems offer along- and cross-track stereo capabilities, and the scene size varies between 10 by 10 km² and 20 by 20 km².

Sensor	Company (Country)	Launch date	Spat. Resolution [m]	Swadth [km]
WorldView-3	DigitalGlobe (USA)	08/2014	0.31 (PAN), 1.24 (VNIR), **3.7 (SWIR)**	13.1
GeoEye-1	GeoEye/DigitalGlobe (USA)	10/2008	0.41 (PAN), 1.64 (VNIR)	15.2
WorldView-1	DigitalGlobe (USA)	09/2007	0.45 (PAN)	16
WorldView-2	DigitalGlobe (USA)	10/2009	0.45 (PAN), 1.84 (VNIR),	16.4
Kompsat-3A	Kari/EADS (Korea)	03/2015	0.5 (PAN), 2 (VNIR), **5.5 (SWIR)**	12
Pleiades-1A Pleiades-1B	Astrium (France)	12/2011 12/2012	0.5 (PAN), 2 (VNIR)	20
QuickBird-2	DigitalGlobe (USA)	10/2001	0.62 (PAN), 2.44 (VNIR)	16.5
Kompsat-3	Kari/EADS (Korea)	07/2006	0,7 (PAN), 2.8 (VNIR)	16
EROS B	ImageSat Int. (Israel)	04/2006	0.7 (PAN)	7
Deimos-2	Elecnor (Spain)	06/2014	0,75 (PAN), 3 (VNIR)	12
SkySat-1 SkySat-2	Skybox Imaging (USA)	11/2013 08/2014	0.85 (PAN), 2.0 (VNIR)	8
Cartosat-2 Cartosat-2A Cartosat-2B	ISRO (India)	01/2007 04/2008 07/2010	<1 (PAN)	10
DubaiSat-2	EIAST (Dubai)	11/2013	1 (PAN), 4 (VNIR)	?
Kompsat-2	Kari/EADS (Korea)	07/2006	1 (PAN), 4 (VNIR)	15
IKONOS-2	GeoEye/DigitalGlobe (USA)	09/1999	1 (PAN), 4 (VNIR)	11.3

Table 1: Very high spatial resolution optical imaging sensors (<=1m), ordered by spatial resolution. PAN: panchromatic; VNIR: visible and near infrared spectrum; SWIR: shortwave infrared spectrum. (Sources: Operators' websites, Earth Observation Portal at http://directory.eoportal.org/)

As a general trend, EO solutions continue to expand and diversify, in terms of spatial, spectral and temporal resolution, and in national ownership. More and more newcomer States plan to launch an EO satellite in order to respond to national policy or security interests, to assist in developing a national space infrastructure and to expand current commercial data offerings. From 2004–2013, 133 satellites for civil Earth observation (EO) were launched by civil governments and commercial entities from 33 countries. This number is expected to grow to 283 satellites for civil EO over 2014-2023 as further governments and commercial enterprises develop EO programs [8]. By 2016, more than 50 satellites are expected to offer commercial solutions [9]. Whether the increasing number of satellite will cause lower prices for satellite data or not, remains to be seen. While some developing EO programs use off-the-shelf solutions for their satellites, missions with a highly specialized sensor design providing for high ground resolution and geolocation accuracy, such as the WorldView series from DigitalGlobe, are expected to remain at the current price levels.

The second paradigm shift is just around the corner. After the first shift mainly addressed the spatial resolution of satellite imagery, the second shift will target its temporal resolution. Following the launch of SkySat-1 in November 2013, the U.S. company SkyBox Imaging has successfully demonstrated that also small satellites are capable to produce sub-meter imagery and high-definition videos. While small satellites or "SmallSats" are usually considered as satellites below 500 kg mass and smaller than a kitchen oven-size, must most of the EO SmallSats under development are far below these limit; in comparison: the WorldView series satellites get to 2.8 t. Due to much lower costs associated to development and launches, constellations of numerous SmallSats have become possible, allowing for more frequent revisits of areas of interest. SkyBox Imaging, acquired by Google in 2014, plans a total constellation of 24 satellites and there are other start-ups such as Planet Labs that has launched already 132 of its Dove satellites (a 3U CubeSat)

from the International Space Station (ISS) in 2014 [10], see Table 2 for other missions. For the sake of completeness, though not a satellite on its own, also the UrtheCast's developed world's first Ultra HD video camera Iris mounted on the ISS should be mentioned here, providing of true colour videos with 1 m spatial resolution and duration of up to 60-seconds.

Company (Country)	Launch date	Spat. Resolution [m]	Target number
Planet Labs (USA)	100/yr	3–5 (MS)	100 at any time
Skybox Imaging (USA)	15 by 2017	0.85 (PAN), 2.0 (VNIR)	24
Satellogic (USA)	16 in 2015	1 (PAN)	100+
OmniEarth (USA)	18 by 2017	2 (PAN), 5 (MS)	18
NorStar Space (CAN)	?	**hyperspectral, infrared**	40

Table 2: SmallSats. PAN: panchromatic; VNIR: visible and near infrared spectrum; MS: multispectral, band specification unknown. (Sources: Operators' websites, Earth Observation Portal at http://directory.eoportal.org/)

Although SmallSats do not offer the same very high spatial resolution as the mostly car- or truck-sized satellites listed in Table 1, its higher temporal resolution allows for other applications also for nuclear verification, such as more continuous change detection once their constellations are fully deployed. Once fully deployed, the SmallSats will be able to take a daily snapshot of the entire planet.

The last entry in Table 2, the development of SmallSats capable to acquire hyperspectral data by the Canadian company NorStar Space Data [12], points to another field of sensor advancements. While the multispectral sensors acquire data in a number of bands covering only parts of the electromagnetic spectrum, hyperspectral sensors record the reflected radiation in several hundreds of very narrow contiguous or overlapping wavelength bands and therefore provide a continuous spectrum from the visible to shortwave infrared. While the future and the technical details of the project is yet uncertain, it could mark the start of the third paradigm shift, now in terms of spectral resolution.

At the time being, there are just two satellite-based hyperspectral instruments in orbit, Hyperion, flying onboard the Earth Orbiter-1 (EO-1) spacecraft, launched by NASA in 2000 and CHRIS, flying on the Proba-1 spacecraft, launched by the European Space Agency (ESA) in 2001. Hyperion provides 220 spectral bands from 0.4 to 2.5 µm, CHRIS 62 bands from 0.4 to 1.05 µm. Besides the low temporal resolution (revisit), also the medium spatial resolution of 30 m and 20 m is a limiting factor for the application of hyperspectral data in a number of nuclear monitoring applications. This will also apply to other future missions, such as the German EnMAP (Environmental Monitoring and Analysis Program) or the Italian PRISMA (PRecursore IperSpettrale della Missione Applicativa).

Besides the optical sensors, State-of-the-art SAR (Synthetic Aperture Radar) sensors provide not only an all-weather, day and night monitoring capability, but also different information with regard to man-made structures and surface deformations (see Figure 1). For SAR data, the paradigm shift happened in 2007, when the first sensors providing 1m resolution were launched (see Table 3). Processing SAR data, however, needs some expert knowledge and often also optical imagery for interpretation. Though application of satellite data is usually restricted to very high-resolution optical data, SAR data have a lot of potential in order to assess movements and deformations due to drilling, mining or camouflage.

3. Potential Applications of Satellite Imagery for Nuclear Verification

Commercial high resolution imagery is routinely used within the IAEA's safeguards system as a reference source to aid in in-field and inspection planning, to verify the accuracy and completeness of information supplied by Member State, to detect changes and monitor activities at nuclear sites, to investigate undeclared activities, and to provide analytical input to the State Evaluation process. Geoinformation technologies further advance the use of satellite imagery to generate site plans and store and manage critical information related to sites and facilities.

Figure 1: Different information given by optical & radar sensors. Left: Optical image GeoEye-1 (Credit: GeoEye); Right: TerraSAR-X (Credit:Astrium)

Sensor	Company (Country)	Launch date	Frequency [GHz] (Band)	Spatial res. [m]	Swath [km] across/along	Temporal res. [days]
KOMPSAT-5	Kari/EADS (Korea)	2019 ??	(X)	< 1	?	?
PAZ	Hisdesat (Spain)	2015	9.65 (X)	1	10 / 5	11
KOMPSAT-5	Kari/EADS (Korea)	08/2013	9.66 (X)	1	5	?
Tandem-X	DLR/Astrium (Germany)	06/2010	9.65 (X)	1	10 / 5	11
TerraSAR-X	DLR/Astrium (Germany)	06/2007	9.65 (X)	1	10 / 5	11
COSMO-Skymed 1-4	ASI (Italy)	1: 06/2007 - 4: 11/2010	9.6 (X)	1	10 / 10	< 1 (4 Sat)
RADARSAT-2	CSA (Canada)	12/2007	5.405 (C)	3	10 / 10	24
SENTINEL-1A *SENTINEL-1B*	ESA (EU)	04/2014 *2016 ?*	5.405 (C)	5	20 / 20	6 (2 Sat)

Table 3: SAR sensors with spatial resolution <= 5m. (Sources: Operators' websites, Earth Observation Portal at http://directory.eoportal.org/)

In some contrast to the use of SI for verifying NPT compliance, the CTBT verification regime does not include SI as verification measure yet. However, the treaty text considers satellite monitoring as an additional technology whose verification potential should be examined (Article IV, paragraph 11). The CTBTO has investigated the application of airborne and space-borne imagery in the preparation of on-site inspections with regard to the specification of inspection area and point of entry, and for focusing activities during inspections [13]. The recent CTBT Integrated Field Exercise, which was held in Jordan end of 2014 (IFE14), included the use of multi-spectral imagery including infrared (MSIR) during on-site inspections for the first time. In addition, SI may also be used complementary for confirming information gathered from the International Monitoring System (IMS), including seismic, hydroacoustic, infrasound and radionuclide monitoring.

For verifying compliance with a potential future FMCT, SI should be considered as one tool among other verification measures in order to monitor declared shut-down facilities or undeclared facilities, and to prepare or initiate on-site inspections.

Due to the quality of today's satellite imagery, a variety of information can be extracted from this space-based data, such as spatial, spectral (reflective, emissive), polarization, temporal and/or semantic properties of image pixels or image objects by visual and/or computer-based analysis. For monitoring declared nuclear facilities or detecting clandestine activities using satellite imagery, specific object features related to the nuclear fuel cycle and its processes as well as geographical and cultural characteristics need to be surveyed. An imagery analyst has to identify objects regarding size, shape, height, color, surroundings, functionalities and temporal changes, and determine their significance [14].

Very high resolution optical satellite imagery provides a good basis for analyzing the facilities' installations and verifying design information and Additional Protocol declarations. Furthermore, the stereo capabilities of the sensors allow the extraction of high-resolution Digital Surface Models (DSMs) for 3D visualization of the sites and the surroundings [15].

DSMs can also be derived from high-resolution SAR imagery by applying either radargrammetric or interferometric techniques. Some current research studies have investigated whether SAR image analysis can meet the expectations with regard to safeguards applications [3,15,16].

Image acquired over the same area of interest at different acquisition times can be compared visually or by computer-driven processing techniques in order to assess the safeguards relevant changes, such as construction of buildings or streets, surface movements due to underground activities and others [3]. While a number of sophisticated image processing algorithms exist, the degree of robustness, automation and user-friendliness need to be improved. In particular (semi-)automated change detection techniques still suffer from too many false and negative false alarms that require extensive user interaction.

Thermal infrared data can be used to evaluate the operational status of facilities. After converting the thermal infrared data to emissivity and temperatures, image fusion with bands of higher spatial resolution facilitates the interpretation of the temperatures. Anomaly detection tools are useful for extracting "hot spots" in a specific region or the whole scene. Here, algorithms for temperature estimation and anomaly detection are well established for other applications [17]. However, as nuclear verification is generally restricted to space-borne remote sensing today, even the current sensors with their moderate spatial resolution of 60 to 100 m per pixel can provide relevant information.

Using well-calibrated hyperspectral imagery, surface materials can be characterised, identified and potentially tracked from source to destination [18]. By fusing the results of lower resolution hyperspectral analysis results with high-spatial resolution imagery, objects and information on materials can be identified simultaneously.

Besides information extraction from satellite imagery, information management, including the huge range of open source information and open source geospatial tools, manifold the application of geoinformation for non-proliferation and arms control. [19]

4. Summary & Conclusion

Satellite imagery (SI) generally represents a key source of information for the different national and international bodies involved in the implementation of (nuclear non-proliferation, arms control and disarmament) Treaties. SI has a lot of potential in verifying Treaties compliance by supporting the efficient management of arms control and non-proliferation issues, and by contributing to improve the performance of the Treaty.

As a general trend, the supply of EO solutions continues to expand and diversify, with newcomer States to launch an EO satellite in order to respond to national government policy interests, assist in developing a national space infrastructure and expand current commercial data offerings.

In order to keep track of these developments, more feasibility studies on the application and benefits of new and future SI for nuclear verification are required. Feasibility studies should focus on the use of SmallSats imagery (high temporal resolution, videos), KOMPSAT-3A (night imaging, hotspot detection, …), and hyperspectral & TIR imagery (high spectral resolution); for the latter, a case study based on airborne data could be useful. Moreover, studies investigating the identification of SI signatures of (preparations of) nuclear tests, operational status of nuclear facilities, and others need to be continued.

The role of SI within nuclear non- proliferation and arms control verification regimes should also be enhanced by improving SI processing tools as to increasing robustness and degree of automation. Besides, synergy effects when combining analysis of multisensor satellite imagery need to be strengthened.

In order to promote SI as effective, efficient and politically accepted verification measure also within the CTBT and potential FMCT verification regimes, more in-depth case studies and the development of sound image processing techniques for extracting relevant information are required. Research and development in the context of the CTBT should focus on off-site identifying relevant signatures of preparations and realisations of nuclear tests, providing information with regard to the specification of inspection area and point of entry, for focusing activities during inspections, and on complementing the information gathered from the International Monitoring System (IMS). Research and development in the context of a potential FMCT should look into procedures to monitor declared shut-down facilities or undeclared facilities, and to prepare or initiate on-site inspections.

References

[1] Canty, M., Jasani, B., Lingenfelder, I., Nielsen, A.A., Niemeyer, I., Nussbaum, S., Schlittenhardt, J., Shamoni, M. & H. Skriver (2009): Treaty Monitoring. In: Jasani, B., Pesaresi, M., Schneiderbauer, S. & G. Zeug (Eds.) (2009): *Remote Sensing from Space. Supporting International Peace and Security.* Springer, Berlin: 167-188

[2] Gonçalves J.G.M., Gutjahr, K.H., Listner, C., Loreaux, P., Marpu, P.R., Niemeyer, I., Patrono, A., Ussorio, A. & E. Wolfart (2010): Integrated Analysis of Satellite Imagery for Treaty Monitoring - The LIMES Experience. In: *ESARDA Bulletin* 43: 40-56

[3] Niemeyer, I., Canty, M.J., Lagrange, J-M., Listner, C., Schwartz, D., Uruñuela Hernández, S. & E. Wolfart: Integrated Analysis of Satellite Imagery for Nuclear Monitoring - G-SEXTANT Findings. In: Proc. 37th ESARDA Annual Meeting, Manchester, 18-21 May 2015

[4] Truong, Q.S., Keeffe, R., Baines, P. & J.P. Paquette (1999): Potential Applications of Commercial Imagery in International Safeguards. In: *Journal of Nuclear Materials Management (JNMM)*, Volume XXVII, Number 2, Winter 1999: 13-18

[5] Canty, M.J., Niemeyer, I., Richter, B. & G. Stein (1999): Wide-area Change Detection: The Use of Multitemporal Landsat Images for Nuclear Safeguards. In: *Journal of Nuclear Materials Management (JNMM)*, Vol. XXVII, No. 2, 1999, 19-24

[6] Niemeyer, I. (2009): Safeguards Information from Satellite Imagery. In: *Journal of Nuclear Management (JNMM), Vol. XXXVII*, No. 4, 2009, Special Issue: The Next Steps in International Safeguards: 41-48

[7] Steinmaus, K., Norman, C., Ferguson, M., Rialhe, A. & J. Baute (2013): The Role of the Geospatial Exploitation System in Integrating All-Source Analysis. In: Proc. INMM 54th Annual Meeting, Palm Desert, 14-18 July 2013

[8] Keith, A. (2015): Earth Observation, State of Play and Future Prospects. Presentation at ISPRS International Policy Advisory Committee (IPAC) Meeting, Berlin, May 12, 2015

[9] Keith, A. (2015): Emerging Programs, Markets Drive Earth Observation Growth. In: *Earth Imaging Journal* 12 (1), January/February 2015: 24-26

[10] Quinn, K. (2014): Great things from small packages. In: *Trajectory Magazine* 1, 2014: 28-34

[11] Hand, E. (2015): Startup Liftoff. How flocks of small, cheap satellites, hatched in Silicon Valley, will constantly monitor a changing Earth. In: *Science* 348 (6231): 172-177

[12] Ferster, W. (2015): Planned 40-satellite Constellation Would Monitor Earth and Space. In: *Space News*, May 4, 2015 (http://spacenews.com/planned-40-satellite-constellation-would-monitor-earth-and-space/ #sthash.qibDHh5e.dpuf)

[13] Rowlands, A. (2013): The Application of Airborne Remote Sensing for OSI. In: Proc. Science and Techology Conference 2013, Vienna, 17-21 June 2013

[14] Pabian, F. (2008): Commercial Satellite Imagery: Another Tool in the Nonproliferation Verification and Monitoring Toolkit. In: Doyle, J.E. (ed): Nuclear Safeguards, Security, and Nonproliferation. Elsevier, Burlington Oxford: 221–249

[15] d'Angelo, P., Rossi, C., Minet, C., Eineder, M., Flory, M. & I. Niemeyer (2014): High Resolution 3D Earth Observation Data Analysis for Safeguards Activities. In: Proc. IAEA Symposium on International Safeguards: Linking Strategy, Implementation and People, Vienna, 20-24 Oct. 2014

[16] Minet, C., Eineder, M., Rezniczek, A. & I. Niemeyer (2011): High Resolution Radar Satellite Imagery Analysis for Safeguards Applications. In: ESARDA Bulletin 46: 57-64

[17] Künzer, C.; Dech, S. (Eds.) (2013): Thermal Infrared Remote Sensing. Sensors, Methods, Applications. Springer, Netherlands

[18] Niemeyer, I., Listner, C. & S. Martens (2013): Monitoring Uranium Mining and Processing Sites Under Decommissioning Using Hyperspectral Imagery. In: Proc. 35rd ESARDA Annual Meeting, Brügge, 27-30 May 2013

[19] Pabian, F., Renda, G., Jungwirth, R., Kim, L.K., Wolfart, E. & G.G.M. Cojazzi (2014): Open Source Analysis in Support to Nonproliferation Monitoring and Verification Activities: Using the New Media to Derive Unknown New Information. In: Proc. IAEA Symposium on International Safeguards: Linking Strategy, Implementation and People, Vienna, 20-24 Oct. 2014

Remote Sensing Technique in Support to Nuclear Non-Proliferation Monitoring

Marc Lafitte (marc.lafitte@satcen.europa.eu), Jean-Philippe Robin (jean-philippe.robin@satcen.europa.eu), European Union Satellite Centre, Apdo de Correos 511, E-28850 Torrejon de Ardoz, Madrid, SPAIN

ABSTRACT

The mission of the European Union Satellite Centre (SatCen) is "to support the decision making and actions of the European Union in the field of the CFSP and in particular the CSDP, including European Union crisis management missions and operations, by providing, at the request of the Council or the HR, products and services resulting from the exploitation of relevant space assets and collateral data, including satellite and aerial imagery, and related services" [1].

The SatCen Non-Proliferation Team, part of the SatCen Operations Division, is responsible for the analysis of installations that are involved, or could be involved, in the preparation or acquisition of capabilities intended to divert the production of nuclear material for military purposes and, in particular, regarding the spread of Weapons of Mass destruction and their means of delivery [2].

For the last four decades, satellite imagery and associated remote sensing and geospatial techniques have increasingly expanded their capabilities. The unprecedented Very High Resolution (VHR) data currently available, the improved spectral capabilities, the increasing number of sensors and ever increasing computing capacity, has opened up a wide range of new perspectives for remote sensing applications. Concurrently, the availability of open source information (OSINF), has increased exponentially through the medium of the internet.

This range of new capabilities for sensors and associated remote sensing techniques have strengthened the SatCen analysis capabilities for the monitoring of suspected proliferation installations for the detection of undeclared nuclear facilities, processes and activities. The combination of these remote sensing techniques, imagery analysis, open source investigation and their integration into Geographic Information Systems (GIS), undoubtedly improve the efficiency and comprehensive analysis capability provided by the SatCen to the EU stake-holders.

The following document aims at reviewing the benefits of the suite of sensors and associated remote sensing capabilities afforded with regards to the monitoring of nuclear facilities.

1 INTRODUCTION

The number and capabilities of space-based electromagnetic sensors has increased dramatically over the last four decades. Meanwhile, the huge leaps in computing power, associated technology and communications has strongly supported the development of a wide range of applications utilising satellite imagery. Currently, almost any part of the earth can easily be imaged in High (HR) or even Very High Resolution (VHR) through web applications. However, remote sensing techniques based mainly on the three pillars commonly called spatial, spectral and temporal resolution remains a specialist domain.

This paper aims to review the potential techniques based on electromagnetic measurements acquired from space-borne platforms to support EU decision makers regarding Non-Proliferation of weapons of mass destruction issues dealing mainly with material diverted from the nuclear fuel cycle.

The nuclear fuel cycle is the set of industrial processes which make use of nuclear materials in the production of electricity. Most of these processes can be scrutinised and assessed using remote sensing techniques based on the analysis of satellite imagery [3].

Remote sensing is the art and science of obtaining useful information about an object or area acquired by a device that is not in contact with the object, area or phenomenon under investigation [4].

The first civilian remote-sensing sensor based on a space-borne platform launched on 23 Jul 1972, known as Landsat-1 (originally named ERTS-A - Earth Resources Technology Satellite) supplied satellite imagery with a ground sample distance (GSD) of 80 metres. [5].
However, military programs such as CORONA, the first US military satellite-based reconnaissance program, were already operating from August 1960 until May 1972.

Over the last decade, Hollywood movies have highlighted, and most of the time overstated, the abilities of satellite imagery.

Satellite imagery and associated remote sensing techniques are applied and analysed by humans. By nature this analysis is driven by a range of motivational and emotional factors which undoubtedly influence the processing of visual stimuli.

Our eyes do not send images to our brains. The images are constructed in our brain based on the very simple signals sent from our eyes. We only "see" after the brain has interpreted what was sent by the eyes. The human brain forms images based on pattern recognition learned from an early age.

2 THE SENSORS

Nowadays, more than 160 earth-observation satellites are commercially available worldwide [6].
Of the wide range of sensors available, the selection of the most suitable and efficient sensor is the key issue in order to broaden remote sensing techniques and to strengthen the analysis.

2.1 Space-based EO Sensors

Space-based sensors and in particular Electro-Optical (EO) sensors may be categorised by GSD capacity (Spatial resolution), electromagnetic capabilities (Spectral resolution) or revisit frequency abilities (Temporal resolution).

• Spatial Resolution is "a measure of the finest detail distinguishable in an image". The most commonly used descriptive terms for spatial resolution is the ground sample distance (GSD). It is commonly agreed on the following scale of spatial resolution

- Low Resolution: larger than 30 m
- Medium Resolution: 2 - 30 m
- High Resolution: under 2 m
- Very High Resolution: sub-metre

• The Spectral Resolution of the sensor is based on the number of bands, their location on the electromagnetic spectrum and how narrow the bands are. Spectral resolution is commonly applied to EO sensors, optical and infrared, which measure reflected or radiated energy. Panchromatic sensors acquire data from a single broad region of visible light, and sometimes also from the adjacent near-infrared of the electromagnetic spectrum. Multispectral sensors are capable of acquiring simultaneously from 3 to 10 wider bands while hyperspectral instruments can capture hundreds of narrow bands.

• The Temporal Resolution specifies the revisit frequency of a satellite sensor for a given location. It is commonly agreed on the following scale:

- High temporal resolution: < 24 hours - 3 days
- Medium temporal resolution: 4 - 16 days
- Low temporal resolution: > 16 days

High temporal resolution is significantly enhanced by the capability of on-board sensors to point both along and across the satellite track, providing a revisit capability of 1 to 3.5 days, depending on latitude. A constellation of satellites can also considerably shorten the revisit period.

2.1 SPACE-BASED SAR SYSTEMS

The Synthetic Aperture Radar (SAR) is an active and coherent sensor working in the microwave domain of the electromagnetic (EM) spectrum. It collects the backscatter signal of an electromagnetic wave. This electromagnetic wave is characterized by two fundamental properties: amplitude and phase.

• The amplitude is a function of backscattered energy displayed as intensity ($I = A^2$) and can be considered as the “visual” part of the information. The behaviour of the backscattered electromagnetic energy depends on the interaction between the electromagnetic wave and the physical and dielectric properties of the target; the roughness and the moisture. Some materials such as metal have a high reflective quality while other such as grass have a poor capacity to reflect incidental energy.

• The phase is a property of a periodic phenomenon which is the fraction of one complete sine wave cycle (from $-\pi$ to $+\pi$) corresponding to

the wavelength. It is a key element for the estimation of displacement (sensor-to-target distance) and thus used for interferometric measurement. The analysis of differences between phases of reflected radiation is called interferometry. There are two main possible sources of phase shift: vertical (terrain altitude) and horizontal (terrain motion).

The processing of the backscatter signal collected by the multiple antenna locations which form the synthetic antenna aperture allows the formation of a matrix of pixels in two dimensions: range and azimuth (cross range).
Space-borne SAR sensors use L, C or X-band and most of them are able to emit and receive with various polarizations (multi-polarization). These bands provide different spatial resolution and moreover a range of capabilities regarding ground and foliage penetration.

On 17 July 1991, the first Earth-observing SAR platform, the European Remote Sensing satellite (ERS) was placed into orbit. Since 03 April 2014, Sentinel-1A operates in the C-band and provides Copernicus, the European Programme for the establishment of a European capacity for Earth Observation, with SAR imagery/data at medium resolution [7].

3 REMOTE SENSING & IMAGE ANALYSIS

3.1 ANALYSIS OF MULTI-SPECTRAL IMAGERY

Despite a poor spatial resolution, the Terra (Aster) and Landsat series are the most useful space-borne sensors for multi-spectral analysis. The capability to simultaneously collect radiation from multiple narrow wavelength bands, in particular the reflected infrared (including near infrared "NIR" and shortwave infrared "SWIR") of the electromagnetic spectrum, enhances the ability to discriminate and characterise a wide range of natural elements which, by nature, have different spectral reflectance signatures.

This technique is particularly useful for the characterisation of soils by the discrimination of various minerals (eg. Uranium mines) or the classification of a range of vegetation/crops.

Amongst other wavelength bands, all high-resolution multi-spectral sensors provide at least one spectral band in the NIR, relevant for the analysis of vegetation stress or diseases by using NDVI techniques.

To a further extent, NIR bands are also frequently used to highlight moisture or vegetation growing on the roof of workshops, a main indicator for a derelict status.

WorldView-2 provides high-resolution 8-band multispectral imagery of which [8]:

- Red-Edge spectral band (705-745 nm) improves the accuracy and sensitivity of NDVI and plant studies. It can also enhance the discrimination between healthy vegetation, and those impacted by disease.
- Coastal Blue band (400-450 nm) strengthens the capabilities for "bathymetric" measurements. In addition, the absorption of this wavelength by chlorophyll in healthy plants may improve vegetation analysis.
- Yellow (585-625 nm) band enhances vegetation classification capabilities.

These spectral bands can also be very useful in determining the density and/or turbidity analysis of liquid ponds as well as demonstrating vegetation stress caused by toxic gas release or fire.

3.2 USE OF THERMAL DATA

The infrared (IR) wavelengths of the spectrum, lie between 1µm and 14µm and can be further broken down into two sub-domains respectively: the reflected infrared (1µm to 2.5µm) and the thermal infrared, also called TIR (3µm and 14µm). Due to atmospheric absorption windows, TIR is generally measured over two wavelength extents: 3µm - 5µm and 8 µm to 12 µm.

Terra (Aster) and Landsat series (Landsat 7 and 8) space-borne sensors acquire low spatial resolution (respectively 100 m, 60 m and 120 m GSD) temperature data between 8 µm and 12 µm.

In remote sensing, the radiance measured (radiant temperature) by thermal radiometers in the TIR are firstly converted into Digital Numbers (DNs) and subsequently to degrees Kelvin (Kinetic heat). The derived estimated surface temperature map is a significant asset for the analysis and assessment of various processes within the nuclear fuel cycle.

KOMPSAT-3A (Arirang 3A), successfully launched on 26 Mar 2015, hosting among other sensors an Infrared Imaging System (IIS) operating over the 3 µm - 5 µm wavelength region at high spatial (5m GSD) and thermal resolution [9]. Until now this type of imagery has not been commercially available. It will provide the community with a tremendous improvement in capability, in partic-

ular for the detection and monitoring of local processes where, for example, heat/steam is generated/inducted.

The use of the longer wavelengths of the infrared domain avoids anomalies from solar reflection and also therefore allows for the use of imagery collected by night.

3.3 Processing and Analysis of SAR Data

Synthetic Aperture Radar (SAR) is a coherent system. SAR images comprises of complex data which contains both amplitude and phase information.

A series of specific techniques are commonly used by SatCen image analysts to extract information from SAR data.

The analysis of single SAR data requires a lot of experience and a good understanding of SAR geometry regarding phenomenon such as layover, foreshortening, shadowing and texture. The visualisation (display) of the full range of SAR dynamic data is one of the main challenges. The SatCen routinely uses coloured dynamic look-up tables (LUT) and in particular the rainbow colour display. This coloured image enhances the analysis of high reflected radiation as well as features which do not reflect any, or very poor, radiation.

The Amplitude Change Detection (ACD) technique consists of comparing at least two examples of SAR data acquired using similar orbit and frequency parameters on different dates. The amplitude data is co-registered before being respectively assigned to the corresponding colour channel (Red, Green and Blue). Thus, changes appear according to the colour synthesis model defined. The monitoring of nuclear-related nocturnal activity is one of the main application of amplitude SAR data at the SatCen. However, the analysis derived solely from SAR amplitude imagery can only provide assumptions and therefore requires confirmation by electro-optical analysis.

One of the benefits of SAR systems is coherence. When two or more examples of SAR data have been collected along identical orbits with similar acquisition parameters, commonly known as interferometric acquisition conditions, a coherence map derived from the processing of a SAR interferometric pair can be generated. The Coherence Change Detection (CCD) techniques highlight coherence losses mainly due to structural changes between the two acquisition dates. It is particularly relevant for the monitoring and the activity assessment of large uranium mines.

The Multi-Temporal Coherence product combines the two previous techniques. It consists of the combination of two multi-temporal amplitude images and the corresponding computed coherence image. Each image is assigned to one of the colour channels (Red, Green and Blue). The MTC image highlights changes between two states of a target which appeared unchanged by ACD analysis. This technique is particularly relevant when surveying large storage areas (UO2 or UF6 casks) and often use to complement the CCD technique.

Ground-surface deformation phenomena induced by underground development may be detected using a Synthetic Aperture Radar differential interferometry subsidence map. Subsequent interferograms, formed by patterns of interference between the phase components of two SAR data acquired from the same orbit with slightly different incidence angle and at different times, provides high-density spatial mapping of ground-surface displacements. Under ideal conditions, it is possible to resolve changes in elevation in the order of a few millimetres.

Amongst the differential interferometric techniques, the permanent or persistent scatterer interferometry (PSI) [10] may provide evidence of tunnelling or ongoing underground activity. However, the amount of SAR data required for input to process and produce an accurate and reliable subsidence map, as well as the timeline for the acquisition of the required dataset, means that this technique is not very well suited for time sensitive operational usage. In addition, natural changes due to vegetation or seasonal variation will denigrate the relevant results. Thus, differential multipass Synthetic Aperture Radar Interferometry (DInSAR) is a technique useful for accurately detecting and estimating the ground displacement or land deformation. In this case, the phases of less SAR data (3 to 5), acquired from slightly different orbit configurations at different times, are combined in order to exploit the phase shift of the signals and compute a surface displacement map.

From the range of space borne SAR platforms available, the Italian COSMO-SkyMed constellation provides the SatCen with the most relevant advanced SAR capabilities, particularly regarding the high revisit frequency which allows relevant interferometry products [11].

3.4 Analysis of Multi-Temporal data (Monitoring/survey)

The accuracy of the assessment of a nuclear facility using remote sensing is based mainly on the capability to detect nuclear facilities at the earliest stage of construction. The foundations of the various constructions, the network of underground utility ducts, the internal layout and structure of the main buildings are crucial for the analysis of the facility.

Subsequently, the monitoring of a nuclear facility is driven mainly by the revisit capability commonly referred to as temporal resolution and the availability of the sensor.

Once the facility is operating, the analysis of the status of the facility from satellite imagery relies on indirect indicators of activity such as vapour plumes, efflux, liquid output, cooling fan rotation, vehicle activity, maintenance activity, damage, etc.

As an example, the analysis of snow covered imagery may reveal human activity, vehicle tracks, heat, etc. The low solar incidence during the winter period provides extended shadows which can significantly enhance the analysis of vertical features.

The monitoring of infrastructure and the analysis of changes can be visually strengthened by the processing of anaglyph views formed from two satellite images taken with slightly different angles. The image acquired with the larger incidence is assigned to the red-colour channel while the other imagery is allocated to the two remaining colour channels. This combination will create the illusion of relief and can be seen using bi-coloured lens glasses commonly RED/GREEN or RED/BLUE.

Monitoring data sets including heterogeneous sensor, viewing angle and season, can also be used to create 3D modelling [12]. The 3D models derived from satellite imagery provide the analyst with a more realistic contextual view of specific features.

3.5 Use of Digital Elevation Model (DEM)

An accurate Digital Elevation Model (DEM) can be obtained from the processing of an interferometric data pair as well as from an optical stereo-pair and can be used for the 3D rendering of an optical satellite imagery. This product provides the image analyst with an enriched contextual insight and a more realistic and natural perspective of the area of interest (AOI).

Furthermore, the difference between two DEMs may also be used to estimate volume variation, in particular in assessing spoil from underground extraction over a specific time period.

3.6 Open Source

Open Source Information (OSINF) includes any piece of information which can be obtained legally and ethically from public sources.

The amount of information or data available has grown exponentially over the last decade and new techniques are required nowadays in order to investigate the tremendous volume of data and be able to extract only the useful and relevant pieces of information.

Data Mining is a process which consists of analytical tools capable of exploring and analysing data from varying perspectives by investigating correlations or patterns amongst predefined key values.

As an example, the report which followed the visit to the Yongbyon Nuclear Complex on 12 Nov 2010 by Standford University experts provided, amongst other pieces of information, a detailed description of the “Uranium Enrichment Workshop” layout. The “transcription” of this textual depiction into a 3D model, based on satellite imagery along with knowledge of the current techniques for enrichment has provided the SatCen with a far greater understanding of the facility [13].

However, the reliability of open source information is an issue and all sources must be cross-checked and/or verified to become effective. Open source information which is knowingly biased, falsified or perverted is called deception. Over the recent years, the spread of false, edited or mocked-up pictures and imagery has become commonplace. Something as simple as the manipulation of the acquisition date (or time) of one satellite image may cause an entirely inaccurate assessment. In addition, the falsification of imagery is also widely used to serve propaganda or doctrine dissemination purposes.

The SatCen dedicates significant effort when using satellite imagery and open source information, in order to corroborate and verify reliability and accuracy across the whole range of data used.

4 CONCLUSION AND WAY AHEAD

The significant number of earth observation satellites placed into orbit for the last two decades, and the ensuing deterrence of steady overhead surveying, has not refrained the ambition of some states to develop or pursue undeclared or illicit nuclear programmes.

Although satellite imagery and subsequent remote sensing techniques will never supply all the relevant information required for the assessment of nuclear facilities, and moreover of undeclared facilities, the number of space-borne platforms, the progress in sensor techniques and the development of a range of applications described in this paper should contribute profoundly to a more comprehensive analysis.

The synthesis of the range of information acquired over various part of the electromagnetic spectrum, as well as the synergy of the remote sensing proficient techniques strengthen the SatCen's capabilities while assessing potential proliferation facilities. Subsequently this is of benefit to the EU stakeholders by providing reliable arguments and evidence.

The development of remote sensing techniques and in particular emerging novel space-borne sensors will most likely offer new favourable perspectives.

The High-Definition video sequences (Up to 90 seconds) already commercially available, will very soon provide multiple intra-daily acquisitions capabilities (eg. SkyBox constellation) while High Resolution imagery from Geostationary platform would improve (ESA study - 2025) scrutinize potential. In addition, medium-resolution (MR) hyperspectral sensors such as EnMAP (Environmental Mapping and Analysis Program), planned for 2018 and capable of collecting hundreds of narrow bands from 420 nm to 2450 nm with a spatial resolution of 30 m, will provide the community with an unprecedented capability to detect specific gases released during the different steps of the nuclear fuel cycle and also to distinguish a large collection of materials.

Finally, innovative technology such as Big Data will be needed to investigate the huge amounts of data for the extraction of valuable and relevant information (http://big-project.eu).

References

[1] Council Decision 2014/401/CFSP of 26 June 2014 on the European Union Satellite Centre and repealing Joint Action 2001/555/CFSP on the establishment of a European Union Satellite Centre
[2] European Council strategy against proliferation of Weapons of Mass Destruction - 15708/03 EU -10 December 2013
[3] Getting to the Core of the Nuclear Fuel Cycle "From the mining of uranium to the disposal of nuclear waste" - IAEA
[4] Remote Sensing and Image Interpretation - Lillesand and kiefer, 1979)
[5] http://landsat.usgs.gov
[6] Union of Concerned Scientists (UCS) database - http://www.ucsusa.org/
[7] SENTINEL-1 ESA's Radar Observatory Mission for GMES Operational Services - SP-1322/1 - March 2012
[8] WorldView-2 data sheet, Sep 2014- www.digitalglobe.com
[9] AIM-Space Cryocooler Programs M. Mai, I. Rühlich, A. Schreiter, S. Zehner
[10] Permanent scatterers in SAR interferometry. IEEE Transactions on Geoscience and Remote Sensing - Ferretti A, Prati C, Rocca F (2001)
[11] The COSMO-skymed very high resolution SAR satellites constellation for Earth observation and its applications in support of monitoring activities - L. Pietranera , F. Britti - e-GEOS, Rome, Italy
[12] www.sketchup.com
[13] A Return Trip to North Korea's Yongbyon Nuclear Complex - Siegfried S. Hecker - Center for International Security and Cooperation, Stanford University, November 20, 2010

Monitoring Uranium Mining and Milling using Commercial Observation Satellites

Lalitha Sundaresan[1], Chandrashekar Srinivasan[1] and Bhupendra Jasani[2]

1. Visiting Professors, International Strategic and Security Studies Programme, National Institute for Advanced Studies (NIAS), Bangalore, India

2. Department of War Studies, King's College London, London, UK

E-mail: sundaresan.lalitha@gmail.com, chandrashekar.schandra@gmail.com,

bhupendra.jasani@kcl.ac.uk

Abstract:

As several states have signed the Additional Protocol to their Safeguards Agreements with the International Atomic Energy Agency (IAEA), they will need to declare their nuclear activities in considerable detail, including their operational and shut down uranium mines. This could significantly increase the burden on the resources of the IAEA in carrying out its safeguards procedures. The IAEA could use space-based high-resolution panchromatic, multi-spectral and, to some extent hyper-spectral sensors to verify some aspects of uranium mining and milling. Such techniques could reduce the overall costs. The availability of such data cost free on the Google Earth web site and commercially from various imagery providers makes it possible for analysts to make assessments concerning the nuclear fuel cycle activities of various countries of interest. The mining of uranium and its conversion through a milling process into U_3O_8 (yellowcake) is the first step of a complex conversion cycle that determines how the mined material will be used.

Our study discusses the possible use of satellite imagery as well as open source information that includes ground and aerial photographs of facilities, for identifying and monitoring uranium mining and milling activities. In the study an attempt is made to answer the following questions:

1. Can we identify uranium mines using openly available satellite imagery?

2. Can we use various steps in uranium milling operations to identify such mills across the world?

3. Are there other extraction processes that share similar features with those for uranium? If so, then are there any special features present or absent in the sequence of operations for their extraction that helps an analyst separate a uranium operation from other operations that share some or all of the features present in the extraction of uranium?

4. Can satellite-based imagery be used to estimate the production capacity of a mill?

Based on empirically derived observables and signatures from satellite imagery for typical uranium extraction operations we have derived a decision making algorithm for determining whether a particular facility can be categorized as a uranium mill or whether it should be categorized as some other facility.

The method has been used to look at some copper mills across several locations and has shown that the decision making algorithm does help us to separate a uranium mill from a copper mill.

Keywords: Fuel cycle, Spatial features, Uranium mills, Uranium mines, International Safeguards, Satellite Images.

1. Introduction

The need to prevent nuclear material proliferation has been of serious concern for the last several decades. In fact the setting up of the International Atomic Energy agency (IAEA) was primarily to deter nation states from pursuing nuclear weapon programs. The States periodically declare all their activities according to the protocol agreed with the IAEA, specifically on nuclear material inventory control, containment and surveillance at facilities. Verification of these declared activities is a major task and with the Additional Protocol the verification has become more difficult; newer methods and technologies are always useful to strengthen the verification methods.

Verification measures include on-site inspections, visits, and ongoing monitoring and evaluation. Under the Additional protocols agreement, the signatory states are required to provide IAEA inspectors access to all parts of the nuclear fuel cycle – uranium mines, processing facilities, fuel fabrication, and enrichment plants, nuclear reactors potentially capable of producing weapons grade plutonium, nuclear waste sites as well as any other location where nuclear materials may be present.

This has vastly increased the amount and type of information that states will have to provide to the IAEA. At the same time, the burden of verification has also vastly multiplied as far as the IAEA inspectors are concerned. Given the security or the lack of it in the world in recent years, the IAEA is bound to find itself in a situation where physical verification of the declared nuclear facilities will become difficult. Undeclared facilities particularly in the early part of the nuclear fuel cycle such as uranium mining and milling could pose special problems. It is in this context that the role of satellite imagery in identifying nuclear fuel facilities becomes significant.

There have been several studies carried out to assess the usefulness of high resolution satellite images for verification of safeguard treaties between the IAEA Member States and the IAEA. [1] These efforts try to identify key features of a nuclear facility and seek to uniquely identify them from a satellite image.

It is well known that together with open sources of information including ground and aerial photographs, satellite images are useful for identifying and monitoring some nuclear facilities [2]. The IAEA has been using satellite images as a part of a routine toolset for safeguard purposes [3]. With the entry into force of the Additional Protocol, IAEA inspection involves more extensive monitoring the early part of the nuclear fuel cycle which includes uranium mining and milling. However, satellite images have not been used in a major way for looking at existing or newly created mining or milling operations for assessing whether they are used for the production of Uranium.

The present paper is an effort to demonstrate the possible use of openly available satellite imagery along with ground and aerial photographs for identifying and monitoring uranium mining and milling activities. Towards this end it seeks to answer the following questions:

- Can we use the various steps in uranium milling operations to identify such mills across the world using satellite imagery available in public domain particularly Google Earth images and other open sources of information?
- Are there other extraction processes that share similar features with uranium extraction processes? If so, how do we distinguish uranium mills from these mills in a satellite image?
- How can we make an assessment of the uranium production capacity of a mill identified in a satellite image?

2. Past Work

One of the earliest studies that attempted to demonstrate the use of satellite images for identifying uranium mines and mills was by Jasani et al. [4] The steps involved in the conversion of uranium ore to yellow cake were used to develop a set of keys to identify a uranium mill in a high resolution hyper-spectral satellite image. Taking the Ranger mine and mill as an example the study demonstrated that the potential observables which are present in the uranium mining and milling operation, but not in copper mining and milling, include the discriminator station, pyrolusite (manganese dioxide) which is used as an oxidant in leaching, the pregnant uranium leach liquor produced in the sulfuric acid leaching process, the concentrated uranium strip solution generated from solvent extraction, and

finally the yellowcake produced from the precipitation and drying steps. The study also pointed out that most of these features do not have unique spectral signatures and their identification is further complicated by their small spatial extents.

Using the Ranger mine and mill again as an example, researchers at the Sandia National Laboratory analysed the potential use of multi-spectral as well as hyper-spectral data from a number of remote sensing satellites to separate out any unique features of a typical uranium mining and milling operation [5]. Apart from magnesium chlorite the only other identifiable signature came from the Sulphur heaps at the Ranger site which is used to manufacture Sulphuric acid for the acid leaching process at the site. The study concluded that hyper-spectral data could not distinguish between uranium processes from other milling processes such as that of copper, zinc, vanadium, phosphorous and Rare Earths. Further the study pointed out that while high spatial resolution satellite systems such as Quickbird lack sufficient spectral resolution to uniquely identify many materials, spatial information provided by these systems could complement information obtained from high spectral resolution systems such as Hyperion. A unique aspect of this study however, was the creation of a decision tree that linked each step in the milling operation at Ranger to similar processes used in the extraction of other materials of commercial and strategic importance.

Another notable study demonstrated the use of satellite images for the IAEA to verify the reports submitted by the concerned country on the operational schedules of a uranium mine and mill [6].

An important conclusion that emerges from these studies is that it is difficult to identify a uranium mill using only spectral signatures be it multi spectral or hyper-spectral satellite images.

3. Our Approach

We identify a uranium mill using a novel approach which contrasts with the earlier studies. A set of keys for identification of a uranium mill is developed based on the spatial features of the equipment used in the milling operations. This is achieved by interpreting the Google Earth (GE) images of a large number of commercial uranium mills across the world.

A comprehensive understanding of the uranium operations at each site is built up using the process flow sheets of the mill along with publicly available information about the mill including ground and aerial photographs of the mill. Together with the GE image of the mill, the keys for identification are developed and these keys are then linked to the process taking place. Through such an approach we establish a pattern of connected signatures that are linked to specific process steps. The most commonly occurring features in the sample sets along with their signatures are then used to decide whether a mill seen on a satellite image is a uranium mill or not.

4. Uranium Milling Process

The process of uranium extraction is very well known [7]. However, to integrate it with our study, a schematic of a typical process for the extraction of uranium from its ore is shown in Figure 1. The associated equipment / reagents with each of these steps are also shown in the figure. Our objective is to determine which of these are unique to a uranium milling operation and are visible and identifiable in a satellite image. For the purpose of this study we have not considered those mills that use heap leaching as the only method for leaching. The reason for this omission is that the process steps involved in this case will differ slightly and it may not be possible to uniquely identify such mills in a satellite image.

We selected 11 uranium milling operations and our sample set is shown in Table 1.

The imagery available on GE for each of these mills and when possible ground and aerial photographs were studied in detail along with other publicly available information. For example, an aerial view of the Key Lake mill is used along with a Quickbird satellite image, to identify specific features (Figure 2). The flow sheet of the mill along with the site description of the mill provided by CAMECO further helps to identify some of the features. For instance, the solvent extraction building is

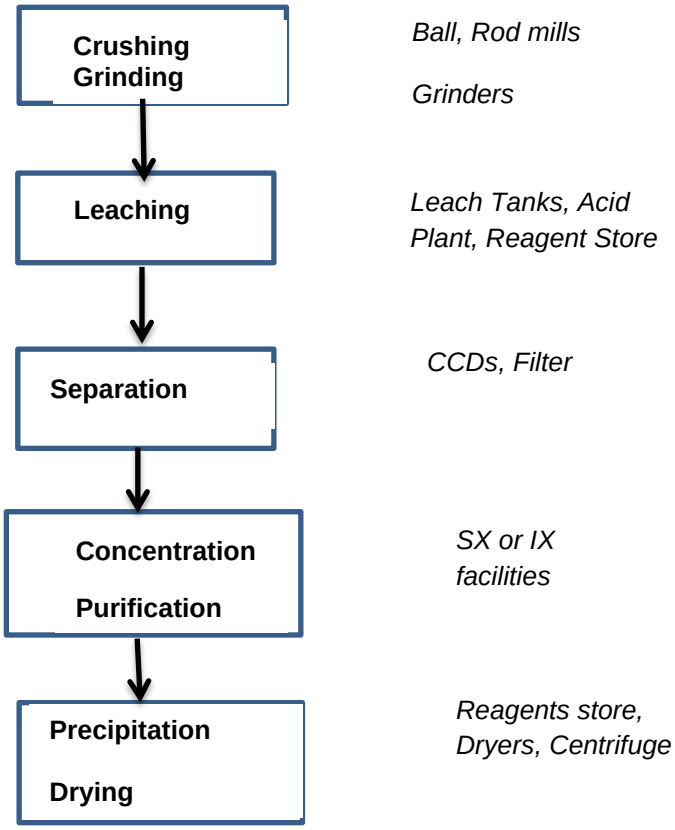

Figure 1 A Simplified Overview of the Steps involved in Uranium Milling Process

Country	Mill Name	Location (Lat / Long)	Owner	Start Year
USA	Sweet Water	42 03 N 107 54 W	Shut Down	1981
Canada	Rabbit Lake	58 15 N 103 40 W	CAMECO	1975
Australia	Ranger	12 41 S 132 55 E	ERA	1981
Canada	Mclean Lake	58 21 N 103 50 W	Areva	1999
Canada	Key Lake	57 13 N 105 40 W	CAMECO	1983
Niger	Arlit	18 47 N 7 21 E	Areva	1970
Namibia	Rossing	22 28 S 15 03 E	Rio Tinto	1976
Namibia	Langer	22 49 S 15 20 E	Paladin	2006
Russia	Krasnokamensk	50 06 N 118 11 E	Argun	1968
Czech Republic	Rozna	49 30 N 16 14 E	DIAMO	1958
Romania	Feldiora	45 50 N 25 30E	State Owned	1978

Table 1 Sample set of Uranium Mills

identified by the presence of the solvents stored alongside the building and by the connecting pipe that goes from the CCD to the building.

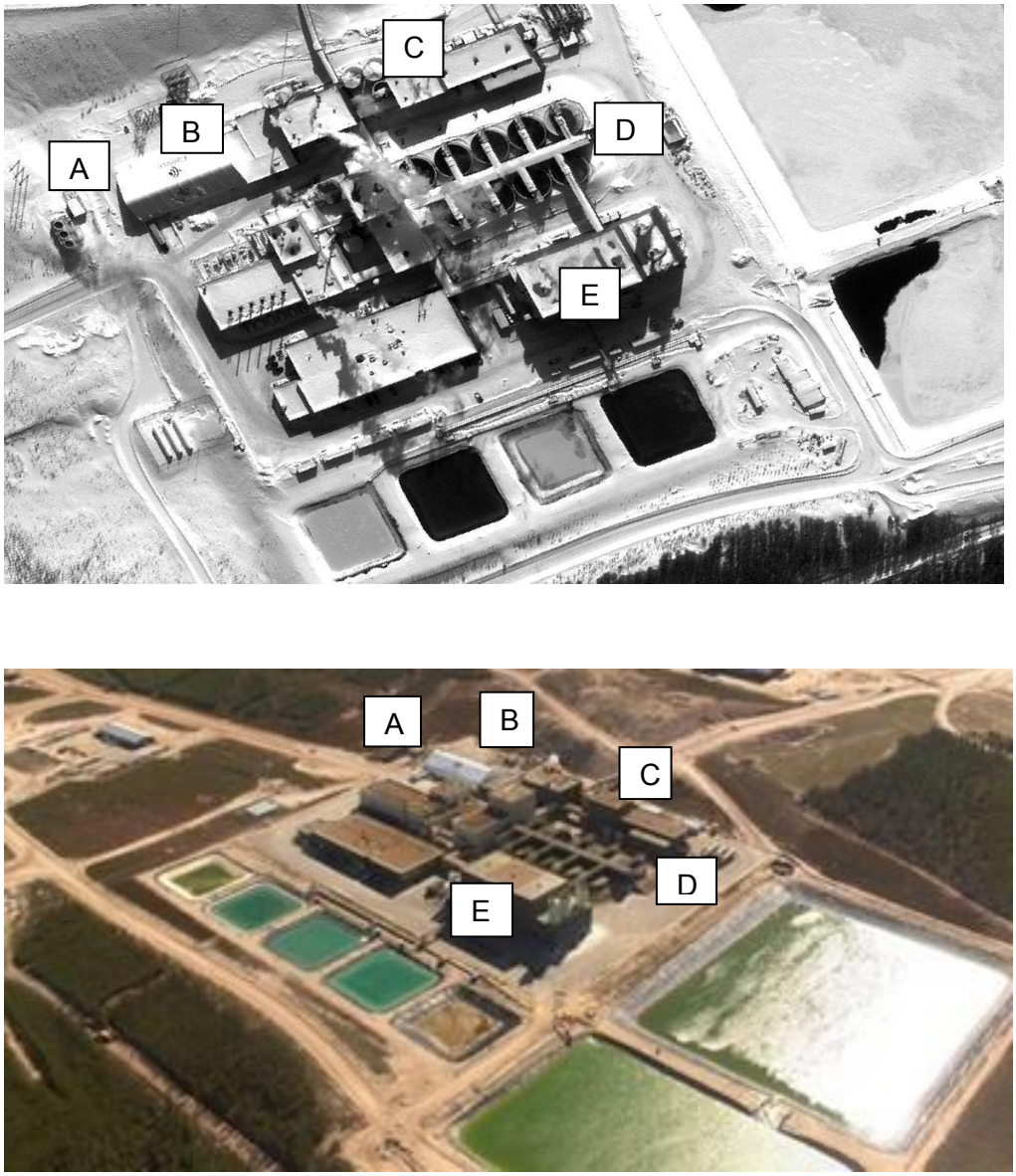

Figure 2 An Aerial Image (Bottom) and a QuickBird Image (top) of Key Lake Mill

(A – Heat Exchangers, B – Acid Plant, C – Leaching Section,

D – CCD, E – Solvent Extraction – precipitation)

5. What can be observed in a Satellite Image of a uranium mill?

The uranium mill features observable in a satellite image for the sample sites is summarised in Table 2. Though crushing, grinding and slurry preparation facilities are identifiable in most of the imageries they do not offer any special features associated with only a Uranium Milling operation.

Radiometric sorters are used in many Uranium mills to improve the ore quality. However they cannot be uniquely identified in a satellite image.

The most commonly visible feature in the satellite image is the Counter Current Decantation (CCD) unit, used in the solid / liquid separation process. Figure 3 shows some typical CCDs of some of the

Mill	Acid Plant	Sulphur store	Acid/ Alkali store	Hot Leach	Leach tanks	CCD	SX	IX Column	NH_3 tanks
Sweet Water	NA	NA	S	NS	NS	NS	Building?	NA	S
Rabbit Lake	S	S	S	NS	S?	S	Building?	NA	S
Ranger	S	S	S	NS	S	S	Pattern seen	NA	S
Mclean Lake	S	S	NS	NS	NS	S	Building?	NA	S
Key Lake	S	S	S	Smoke	NS	S	Building?	NA	S
Arlit	S	S	S	NS	S	S	Pattern Seen	NA	S
Rossing	S	S	S	NS	S	S	Pattern Seen	S	NS
Langer Heinrich	NA	NA	S	Heat Exch.	S	S	NA	S	NA
Krasno-kamensk	S	NS	S	Chimney Seen	Auto-clave	S	NA	S	NS
Rozna	NA	NA	S	Smoke	NS	S	NA	NS	NS
Feldiora	NA	NA	S	Chimney seen	Autocl ave	S	NA	S	NS

Table 2 Uranium Mill Features Observable in a Satellite Image (S - Seen, NS - Not Seen, NA – Not Applicable)

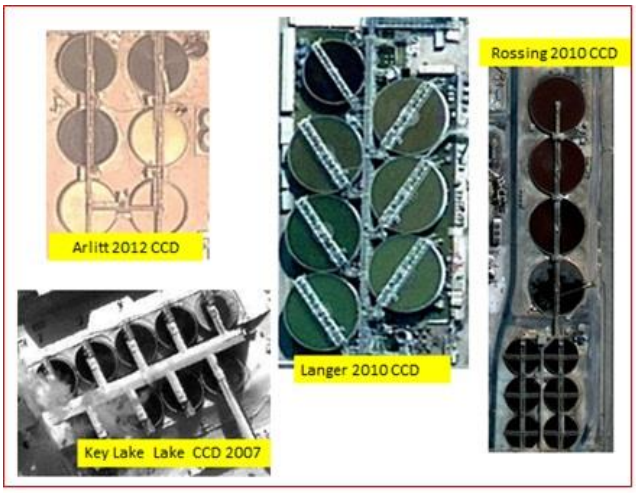

Figure 3 CCDs units as seen in a GE satellite image

mills. In all the cases except the Sweet Water mill, this feature is easily identifiable. The Sweet Water mill was closed down in 1984 and according to reports available the CCD is housed inside a

building.There are several features associated with the leaching process many of which can be seen in a satellite image. Some feature or the other that can be linked to a leaching step is seen in all the mills. Of the 11 mills Langer Heinrich, Rozna and Feldiora use alkaline leaching, while the other mills use acid leaching. Since alkaline leaching involves higher temperatures; one can look for evidence of chimney, heat exchangers or even smoke. Additionally in the case of acid leaching one can see either the acid plants or the leach tanks and in certain cases the acid storage tanks close to the leaching facility. Sulphur heaps or Sulphur storage can also be seen in some of the plants. Figure 4 shows typical leach tanks and leaching sections of some of the mills in our sample.

Unlike the CCDs, the leaching facility may need one or more features to be identified uniquely. However we do know that the leaching operation follows the ore preparation step and precedes the CCD step. This sequence of operation helps in the easy identification of the various features that can be linked to a leaching operation.

The next feature of interest is the equipment associated with the process of concentration and purification. In most mills this is done using either the Solvent Extraction (SX) or the Ion Exchange (IX) process. Occasionally a combination of both may be used. In our sample mill sites we noted that in many mills the Solvent extraction units are housed inside a sequence of identical buildings and linked to these are the storage tanks containing the solvents used in the process (Figure 5). In some cases such a sequence is however not seen though the presence of solvent storage tanks could provide an indirect indicator. The IX columns are usually left in the open and are visible in the satellite image (Figure 6).

The features associated with precipitation, drying and calcining are not uniquely identifiable in a satellite image. In most cases they have to be identified indirectly by the presence of containers holding solvents and reagents used for this purpose. Proximity to the SX or IX facilities of such features is another aspect that we can use to identify this facility. In some of the mills where ammonia is used, the ammonia cylinders are seen clearly in the satellite image.

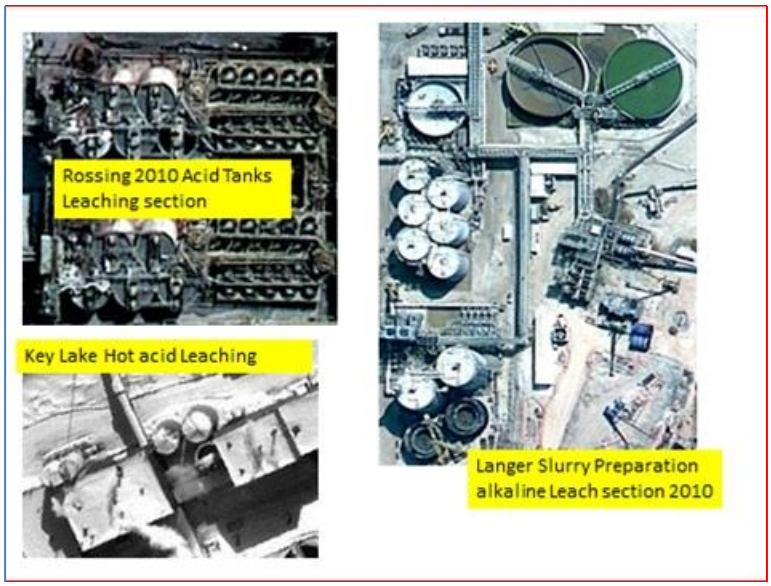

Figure 4 Leaching equipment as seen in a GE satellite imagery

To summarise the procedure for identifying a uranium mill from a GE image, we first identify the CCD circuit; then try to locate the leaching facility upstream. If the CCD process is followed by a SX or IX facility and some ammonia tanks are also seen we could conclude with high level of confidence that the facility is a uranium mill.

Figure 7 summarizes the likelihood of unique identification of a Uranium Mill from our sample set. The leaching as well as the solid-liquid separation process (CCD) provides robust signatures in a satellite image. The concentration step (Solvent Extraction or Ion Exchange) though easily identified in many

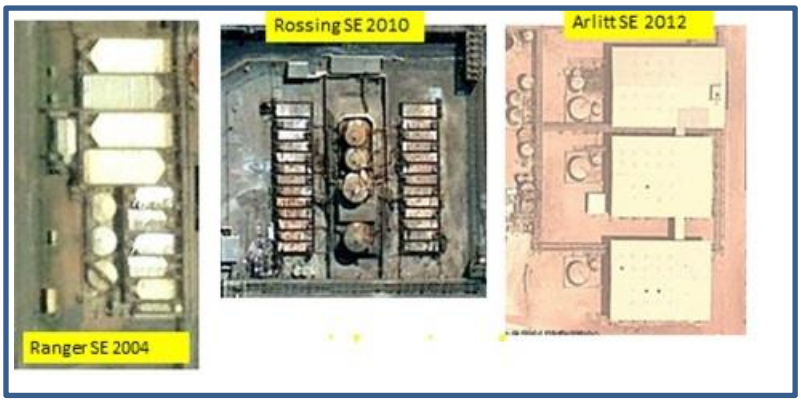

Figure 5 Solvent Extraction Buildings as seen in a GE satellite image

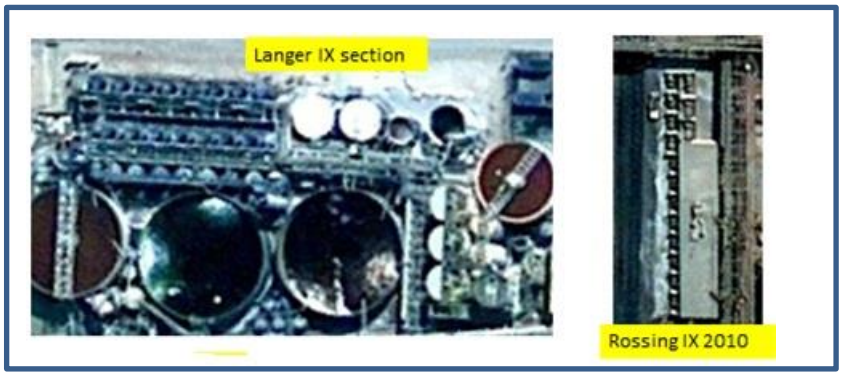

Figure 6 Ion Exchange columns as seen in a GE satellite image

mills does not always provide as robust a signature as the other two steps. The precipitation step also does not provide very reliable signatures that can be used under all circumstances. This therefore creates certain limitations because many other mineral extraction processes could share the leaching, CCD and solvent extraction steps as well. For instance the process steps of some copper, zinc and vanadium operations could be very similar to those of Uranium. If, however we are able to identify additional features which are unique to these mills, we will be able to improve upon our classification process.

Of all the commercially important elements the one whose signatures are most likely to be confused with a Uranium Mill is that of a Copper Mill. If we are therefore able to identify some feature in a copper mill that is not present in a Uranium Mill we can enhance the reliability of our Uranium mill classification.

In order to do this we need to examine the various operations associated with the extraction of copper and see whether copper mills offer satellite signatures that help separate a Uranium mill from a Copper mill.

6. Copper Extraction Process and Observables in a satellite image

The major steps involved in a copper extraction process are shown schematically in Figure 8.

A major difference between copper and uranium is the scale of operation. Invariably due to economic considerations, the copper processing facility will be several times larger than the uranium operation.

Copper occurs mostly in the Sulphide or Oxide forms. While the crushing and grinding steps are common to all extraction processes, the process steps in the case of a sulphide ore are different from those of the oxide ore. This is shown in the Figure 8.

Process	Image	Likelihood of seeing
Leaching		Signatures in all the mills
Separation		Seen in all mills except one
Concentration		Not always identifiable
Precipitation/drying		One of the features identifiable Not always present, however.

Figure 7 Likelihood of the features identifiable in a satellite image of a uranium mill

The sulphide ore goes through a froth flotation process after the initial crushing and grinding which concentrates the copper part. The froth from the flotation process contains the bulk of the copper. The froth is dried and then sent directly to a smelter. The smelter may be located at the mill site or may be located elsewhere. The smelter converts the copper concentrate into blister copper which is further refined to produce anodic copper and finally goes through an electro winning step to produce high purity copper.

The tailings from the froth flotation may also contain copper which could be recovered. These tailings are leached with sulphuric acid, passed through a series of CCDs followed by a solvent extraction step. The copper solution that comes out of the solvent extraction step is then sent to an Electro winning Facility for the extraction of copper.

Thus, a mill which processes low grade copper ore or a part of a copper mill which processes the tailings from a froth flotation process will look similar to a uranium mill. It will have the features such as CCD circuits, SX units in addition to the acid leach facilities that we have seen in a uranium mill.

However, the differentiating factor for the extraction of copper from flotation tailings is that after solvent extraction it goes to an electro winning facility instead of a precipitation facility. Since such an electro winning facility has a typical signature evidence of this step in a satellite image can be used to separate out a Uranium mill from a copper mill.

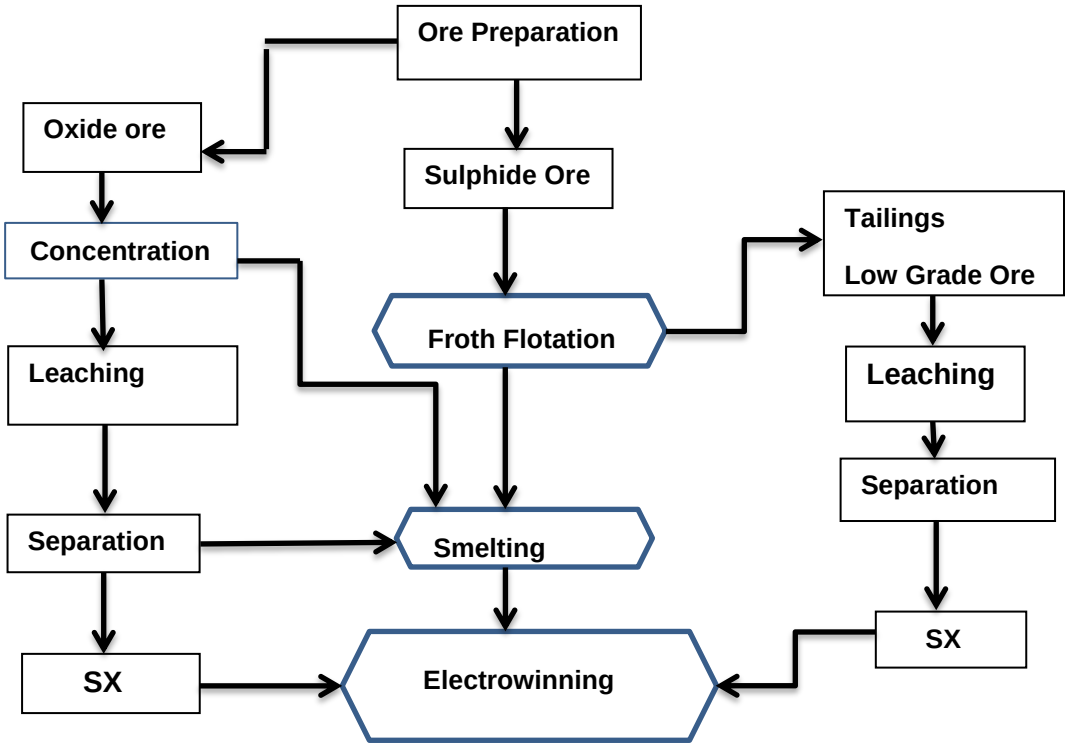

Figure 8 A Simplified Diagram showing the Copper Extraction Process Steps

In Figure 9 a typical electro winning facility as seen in a satellite image is shown. This is a GE image of the Nchanga copper tailings extraction plant in Zambia. In the figure the long building (D) is an electro winning facility which can be easily identified and this is co-located with the solvent extraction facility in the foreground (C). The CCD circuits and the acid leach facilities are also seen in the image

Copper occurring in the oxide form is leached using sulphuric acid after suitable crushing and grinding. Following concentration through a solvent extraction process the solution containing copper is sent to an electro-winning facility. Depending on the concentration of the ore the leaching step may also be followed by a CCD sequence prior to solvent extraction and electro-winning. Again the differentiating step between copper and uranium is the electro winning facility.

7. Key Differentiators for a Uranium Mill

The sequence of Acid or Alkaline leaching – CCD – solvent extraction – precipitation is typical of all Uranium mills.

The CCD unit of these mills is the most amenable to observation from satellite. Though its absence does not completely rule out Uranium, its presence is a robust indicator of a potential Uranium milling operation.

The leaching step is the next most visible feature in a satellite image. Both direct and indirect signatures are available to make inferences about this step. The absence of a leaching process rules out a Uranium mill.

Thus the sequence of CCD preceded by a leaching step provides a baseline signature for a possible Uranium Mill.

In many cases solvent extraction facilities have features such as repetitive identical buildings close to the CCDs that can be identified through satellite imagery.

Figure 9 GE image of Nchanga Copper mill (D – Electro winning, C – SX)

Ion exchange facilities can be seen in a satellite image unless in rare cases they are housed inside buildings.

In the case of precipitation, storage tanks for the various chemicals and their location in the flow of material provide some indications. Ammonia tanks used in many cases for the precipitation of Uranium are often identifiable in a satellite image. Along with a CCD and a leaching step Ammonia tanks provide a firm indication of a Uranium extraction operation.

Since the solvent extraction or ion exchange or even the precipitation steps in a Uranium mill do not always provide very robust signatures one way to enhance the reliability of our classification is to eliminate other materials that share the Leaching - CCD - Solvent Extraction sequence.

The presence of an electro-winning, smelting or froth flotation facilities along with the Leaching – CCD – Solvent extraction sequence is a clear indicator that the mill is not a uranium mill. The electro-winning, smelting and froth flotation equipment have clear spatial signatures and can be identified easily in a satellite image. Through such elimination of various alternatives that share the leaching step and in some cases the CCDs as well as solvent extraction steps, we can increase the probability that the mill we are seeing is indeed a Uranium Mill.

8. Assessment of the Production Capacity of a Uranium mill from a satellite image

Using the observables from the satellite image such as the number of CCD circuits, the diameter of the CCD in a mill along with the average ore grade, we have been able to arrive at an empirical equation to estimate the production capacity of the mill. The equation was derived linking the nominal production capacity data of the sample mills in our study with the measurements made on the satellite images of these mills.

The equation is in exponential form:

$$P = k * a^{G} * b^{N} * c^{A}$$

Where,

k = Constant

G = Ore grade in percentage

N = Number of CCDs

A = Area of the CCD in meter square

Expressed in log form and estimating the coefficients k, a, b and c using the sample data gives,

Ln P = 3.112976 + 0.457613*LnG + 0.956309*Ln N + 0.561587*Ln A

Country	Mill Name	Ore Grade (% U3O8) G	CCD Nos. N	CCD Diameter (meters) D	Nominal Capacity (Tonnes) P	Predicted Capacity (Tonnes)
USA	Sweet Water	0.048	6	9.75	350	401.41
Canada	Rabbit Lake	0.790	4	30.00	4615	3467.43
Australia	Ranger	0.130	8	34.65	4660	3463.12
Canada	Mclean Lake	1.220	8	12.85	3077	3166.65
Canada	Key Lake	3.400	8	20.00	7200	8320.77
Niger	Arlit	0.300	6	23.00	2330	2434.56
Namibia	Rossing	0.030	10	56.32	4000	3781.54
Namibia	Langer	0.050	7	23.15	1425	1251.39
Russia	Krasnokamensk	0.180	6	52.01	3000	4817.18
Czech Republic	Rozna	0.378	5	24.98	3200	2493.75
Romania	Feldiora	0.120	4	28.01	1120	1354.75

Table 3 Data from the Sampled Mills
(All data taken from Uranium 2009: Resources, Production and Demand, A joint Report by OECD NE Agency and IAEA, 2010, Also called the Red Book**)**

The data used for this purpose is shown in Table 3. The nominal capacity for the mills is taken from the Red Book. The estimated capacity values for the mills from the empirical equation are also shown in the table for comparison. The results are reasonably good except for the Russian Mill. Agencies such as IAEA having access to more accurate data will be able to improve upon these estimates.

This estimation process is applied to an Indian mill at Turamdih, Jharkhand. This mill uses acid leaching and ion exchange (Figure 8). The mill processes uranium ore of grade 0.034%. In the satellite image we can identify 3 CCDs of diameter 13m.

Using the empirical equation, we estimate the production capacity of the mill to be 244 tonnes which compares well with the nominal capacity of 190 tonnes.

9. Conclusion

This paper demonstrates how publicly available images from Google Earth and other open sources of information can be used for the purpose identifying a uranium mill.

It is possible to identify a uranium mill in a satellite image using the spatial features of the equipment used in the extraction process.

Figure 8 GE Image of Turamdih Mill, India (A –Sulphur heap, B – Ore Preparation, C – Leaching area, D – CCD, E – Ion Exchange, F – Leach tanks, G – Precipitation & Drying, H – Packing)

It is also possible to distinguish a uranium mill from a copper mill since the spatial features associated with the copper mill are different from those of the uranium mill. In particular, the presence of an electro-winning facility in a copper mill enables us to differentiate it from a uranium mill. By eliminating copper we can enhance the confidence that a particular sequence of operations associated with a Uranium mill is indeed only a Uranium Mill.

An empirical equation is provided to estimate the production capacity of a uranium mill identified on a satellite image. The number of CCDs, the diameter of the CCD and the ore grade are used to make this estimate.

10. Acknowledgement

We would like to acknowledge Digital Globe Inc. for providing us Quickbird satellite image of Key Lake mill. The authors would like to thank their colleagues Prof. R.Nagappa and Prof. N.Ramani for many useful suggestions while doing this study. We thank Ms.G.Vijayalakshmi for her assistance in data collection.

11. References

1. B Jasani, I Niemayer, S Nusbaum, B Richter and G Stein, *International Safeguards and Satellite Imagery*, Springer Verlag, 2009

2. Jasani, B., “Identification of Key Features of Nuclear Reactors for Interpretation of Images from Remote Sensing satellites”, *Journal of Nuclear Materials Management***,** Vol. XXXII, No. 3, Spring 2004; pp.28-36.

3. IAEA Information Series, *Tools for Inspection*, Division of Public Information, 04-46161/F S Series 3/03/E.

4. Jasani, B., Smart, H. A., Blair, D., Stork, C. T., Snoth, J and Canty, M , "Evaluation of remote sensor systems for monitoring uranium mines*", Proceedings of the 27th Annual Meeting, Symposium on safeguards and nuclear materials management*, ESARDA, 10-12 May 2005; London.

5. Christopher L. Stork, Heidi A. Smart, Dianna S. Blair, and Jody L. Smith, "Systematic Evaluation of Satellite Remote Sensing for Identifying Uranium Mines and Mills", *Sandia Report SAND2005-7791,* January 2006.

6. R. Leslie, P. Riggs and V. Bragin, Satellite Imagery for Safeguards Purposes: Utility of Panchromatic and Multispectral Imagery for Verification of Remote Uranium Mines, *Paper presented to Annual Meeting of the Institute of Nuclear Materials Management,* Orlando, Florida, 23-27, June 2002.

7. International Atomic Energy Agency, "*Uranium Extraction Technology*", Technical Report Series No. 359*,* International Atomic Energy Agency, Vienna 1993.

Integrated Analysis of Satellite Imagery for Nuclear Monitoring – G-SEXTANT Findings

Irmgard Niemeyer[1*], Clemens Listner[1], Mort Canty[1], Erik Wolfart[2], Jean-Michel Lagrange[3], David Schwartz[3], Susana Uruñuela Hernández[4]

[1] Forschungszentrum Jülich, Institute of Energy and Climate Research, IEK-6: Nuclear Waste Management and Nuclear Safety, 52425 Jülich, Germany
[2] European Commission - Joint Research Centre,, Institute for Transuranium Elements, Nuclear Security Unit, TP 421, 21020 Ispra (VA), Italy
[3] Commissariat à l'Energie Atomique et aux Energies Alternatives, Centre DAM / Ile-de-France / DASE / SLDG, Bruyères le Châtel 91297 Arpajon Cedex, France
[4] INDRA, Earth Observation Unit, 28830 San Fernando de Henares, Madrid, Spain

Abstract:

The FP7 project G-SEXTANT (Geospatial Intelligence Services in Support of EU External Action, 01/2013-03/2015) was intended to develop a portfolio of earth observation products and services to support the geo-spatial information needs of EU External Action users and stakeholders. G-SEXTANT was part of Copernicus, a European earth observation programme which combines the use of satellite imagery and other data with local, in situ, data sources to deliver geo-spatial information services and products to a wide range of end-users. Copernicus is expected to create an autonomous and operational European capability in environmental and security information services.
G-SEXTANT contained a work package entitled "Nuclear activities scenario", which provided tools in support of monitoring nuclear-related sites and activities using satellite imagery. The activities of the work package were grouped into two sub-scenarios, namely "Monitoring of nuclear decommissioning activities" and "Monitoring of nuclear activities in the context of the Nuclear Non-Proliferation Treaty (NPT)". The paper presents the developments of two sub-scenarios, in detail: i) SAR (Synthetic Aperture Radar) visualization tools, aimed at visualizing the changes maps over a SAR time series (e.g. multi-temporal coherence maps), and the automatic geometric correspondence between SAR/SAR and SAR/optical georeferenced data; ii) SAR time series analysis using the Method for generalized Means Ordered Series Analysis (MIMOSA), including the steps estimation of the amplitude distribution, computation of the probability density, and automatic thresholding. iii) SAR change detection using a complex Wishart algorithm for dual and quad polarimetric imagery in look-averaged covariance matrix format in order to define a per-pixel change/no-change hypothesis test. iv) Optical change detection using object-based techniques. v) GIS-based integration of the products in a system which provides access to all available products and information via standard web interfaces. The system is able to integrate and manage multi-temporal and multi-type information (satellite imagery, Open-Source documents, 3D-data information, GIS data).

Keywords: satellite imagery; Copernicus; G-SEXTANT; integrated analysis; SAR visualization; SAR change detection; optical change detection

1. Introduction

The goal of G-SEXTANT is to consolidate a portfolio of earth observation products and services that respond to geospatial information needs in support to EU External Action. The main objectives of G-SEXTANT are:

- Development and delivery of products within user-defined scenarios;
- Further enhancement of already mature products and mature products and users; and

* Corresponding author: i.niemeyer@fz-juelich.de

- Elaboration and definition of standardised portfolio.

G-SEXTANT is based on user defined scenarios covering potential application areas of interest identified by the previous working group “GMES-Security Support to External Action” (2010-2012) and mentioned in the Call SPA.201.1.1-03, e.g. humanitarian-aid-operations, border monitoring outside Europe, treaty monitoring and nuclear non-proliferation, illegal exploration of natural resources or monitoring of illicit crops and land use planning.

The objective of the scenario “Monitoring of nuclear sites and activities” is to monitor nuclear facilities and nuclear decommissioning areas. From the lessons learned (mainly from the users’ feedback on the previous Copernicus project GMOSS [1-3], LIMES [4] and G-MOSAIC), tools dedicated to the monitoring of nuclear facilities and decommissioning sites should provide additional information to complement the daily tasks carried out by satellite imagery analysts. Thus, this scenario aims at generating relevant tools in support of User’s activities related to monitor nuclear-related sites.

The activities covered in this scenario are organised in two sub-scenarios designed to meet the users’ requirements: (1) Monitoring of nuclear decommissioning and (2) Monitoring of nuclear activities in the context of the Nuclear Non-Proliferation Treaty (NPT).

The paper presents the tools developments in the context of both sub-scenarios, in detail:

i) SAR (Synthetic Aperture Radar) visualization plugin for the ERDAS IMAGINE processing software. Based on automatic geometric correspondence between slant range SAR images and optical images, the satellite model of each loaded image (SAR and optical) is used to automatically obtain the true ground coordinates of each pixel, thus allowing to link the views in ERDAS IMAGINE.
ii) SAR time series analysis plugin for the ENVI image processing software. The Method for generalized Means Ordered Series Analysis (MIMOSA) includes the following steps: estimation of the amplitude distribution, computation of the probability density, and automatic thresholding. The procedure is computationally efficient without need for spatial speckle filtering.
iii) SAR change detection plugin for ENVI and as (Python) stand-alone tool. The procedure uses the complex Wishart algorithm with dual and quad polarimetric imagery in look-averaged covariance matrix format in order to define a per-pixel change/no-change hypothesis test. The method includes approximations for the probability distribution of the test statistics, and so permits quantitative significance levels to be quoted for change pixels. The processing chain generates geo-coded change maps at the desired statistical significance level.
iv) Optical change detection plugin for the eCognition Developer image analysis software. Using object-based techniques, the procedure starts with the segmentation of the images of both acquisition times, and continues with the transformation of the feature space using multivariate statistical methods in order to emphasize and classify relevant changes.
v) GIS-based integration of the products in a geodatabase system which provides access to all available products and information via standard web interfaces. Using Google Earth and a HTML browser as graphical user interfaces, the system is able to integrate and manage multi-temporal and multi-type information (satellite imagery, Open-Source documents, 3D-data information, GIS data).

2. Developments

2.1. SAR Visualization Tool

The SAR visualization tool is composed by a set of modules aimed at achieving two main objectives:

- Visualization of the changes maps over a SAR time series (multi-temporal non-coherent, multi-temporal coherent);
- Automatic geometric correspondence between SAR/SAR and SAR/optical georeferenced data

For achieving the first objective, a set of modules were used to exploit the Multi-Temporal (MT) analysis and the Multi-Temporal Coherent change detection (MTC). The MT analysis is a simple change detection technique in which the different SAR complex images acquired over the same area of interest are co-registered, and their amplitudes are combined in a multi-band colour image. The

colour resulting from the combinations show the different changes occurred in the area of interest in the considered time interval.

This analysis allows working with temporal series of SAR images and shows the evolution of changes during long periods of time. Up to three SAR images obtained at different acquisition times can be combined in a Red-Green-Blue (RGB) image but commonly two SAR images are combined to form a MT RGB image

The interpretation of these changes depends on the terrain characteristics, as SAR images allow mainly to distinguish the terrain surfaces by roughness. The areas with changes can be interpreted as:

- Negative changes: The decrease of the radar backscatter signal in the second image may be caused by removed objects (e.g. vehicles, constructions), harvesting in cultivated zones, thus eliminating the elements that can cause backscatter, making the texture in the image darker and more fine and homogeneous. Flooded areas may appear darker because of the reflection of the radar signal on the water surface.
- Positive changes: The increase of the radar signal backscatter in the second image may be caused by new constructions, vehicle movements, vegetation growth in cultivated areas, drying of previously flooded areas.

The technique of MTC change detection starts with two co-registered Single Look Complex (SLC) SAR images (S1 and S2) captured with the same acquisition geometry. The interferometric complex coherence, which is a measure of phase correlation between them, is defined as the correlation coefficient calculated as ratio between coherent and incoherent summations:

$$\gamma = \frac{\left|\sum s_1(x) \cdot s_2(x)^*\right|}{\sqrt{\sum \left|s_1(x)\right|^2 \cdot \sum \left|s_2(x)\right|^2}}$$

The phase of the coherence is proportional to spatial elevation differences. The magnitude of the coherence is proportional to backscatter randomness and/or change in placement.

Coherence magnitude is 1 if backscattering phase and amplitude are the same on both images and it is equal to 0 when the backscattering has completely changed. The coherence value is influenced by the following factors:

- Systemic spatial decorrelation (orthogonal baseline between sensor positions at each acquisition times);
- Additive noise inherent to the sensor;
- Temporal decorrelation between the two scenes (typical of forested areas, water bodies);
- Atmospheric effects;
- Human activity.

For interferometric applications, such as the generation of digital surface and terrain models and 3D change detection, the coherence value is related to the phase noise in the interferogram, i.e. high coherence values represent good signal to noise ratios; therefore, height estimation is not possible in areas where the interferogram shows low coherence values. For the extraction of surface and terrain models, the SAR images should be acquired almost simultaneously in order to maintain a sufficient coherence degree and to reduce the temporal decorrelation. 2D change detection applications, however, exploit the temporal decorrelation of the coherence to find the changes in the area of interest.

The coherent change detection technique uses the so-called Multi-Temporal Coherence colour composite (MTC) RGB image for visualising the changes. The convention used is to compose the RGB image with the SAR image from the first acquisition time called master image in the red channel, the SAR image from the second acquisition time called slave image in the green channel, and the coherence map in the blue channel. The visualization of the composite image allows the interpreter to have a better representation and interpretation of change. The change map in Figure 1 can be interpreted as follows: Red and green indicate changes (negative and positive), yellow indicates low coherences zones (natural vegetation) with no changes, white indicates man-made objects with no

changes, light blue indicates flat/bare soil surfaces with no changes, and dark indicates water bodies or very flat areas with no changes.

Figure 1: Extract of a MTC product (produced from two different TerraSAR-X VHR images and the coherence image) showing the changes: red/green = changes (negative and positive); yellow = low coherences zones (natural vegetation) with no changes; white = man-made objects with no changes; light blue = flat/bare soil surfaces with no changes; dark colours = water bodies or very flat areas with no changes.

The second objective was to develop a customized tool for assisting the image interpretation process in the frame of nuclear decommissioning activities. For enabling the joint analysis of several SAR/optical images in their native geometry without any resampling process, geometric correspondence between SAR/SAR and SAR/optical georeferenced data is automatically established. The development focused on TerraSAR-X products and sensor model. The functionalities of the developed tool include:

- Ingestion of TerraSAR-X data and their metadata;
- Integration of TerraSAR-X sensor model using a preconfigured DEM of the area of interest;
- Refinement of geometric model for taking into account systematic errors

The tool, in addition, enables to dynamically navigate through one of the SAR images and to compute ground coordinates on the fly. It also allows the comparison of heterogeneous images (SAR/SAR and SAR/optical) and removes restrictions to the SAR acquisition geometry for time series analysis (see Figure 2).

The achieved accuracy in the sensor model application algorithm, using a precise DEM of the area, reaches sub-pixel level, when obtaining the row and column (pixel) in the SLC image from a geographic coordinate.

However, several problems were encountered during the development process when integrating the rigorous TerraSAR-X sensor model into the selected software framework. Therefore, the tool has some limitations by the time being, that are still under analysis with the objective of overcoming them:

- Due to the complexity of the applied model, the processing time slows down when moving from an area in the image to a far off area or the zoom level is changed not smoothly.
- The internal mechanism of the selected software framework for the implementation of the sensor model module and its behaviour implies the application of the sensor model in both directions: from ground coordinates to pixel, and from pixel to ground coordinates. The application of the sensor model in the latter direction is an iterative process that has been proven to be too complex and slow for its integration into the sensor model module. An alternative approach, which uses an approximation of the ground coordinates by interpolating them over a georeferenced grid, makes the sensor model module work but not as accurately

as expected: The coordinates shown for a given cursor position have a precision proportional to the density of the georeferenced grid, but as the results of the application of the sensor model in both directions is not coincident, the geographic link between the different images loaded is still imprecise.

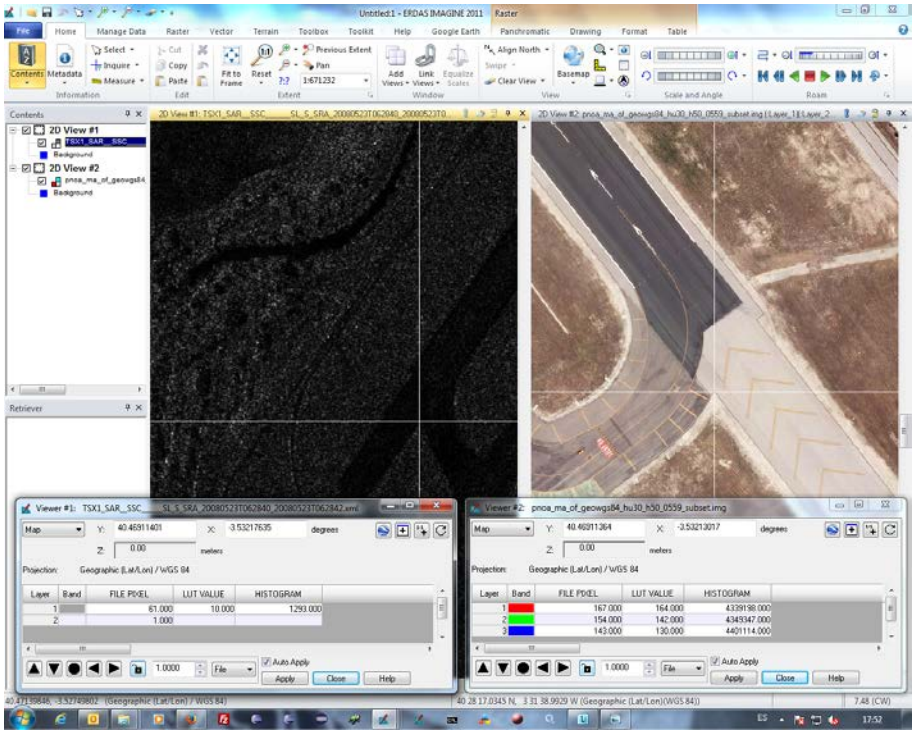

Figure 2: Screenshot showing the obtained on-the-fly coordinates of a TerraSAR-X (left) image in slant range geometry and the corresponding coordinates of an optical orthorectified image (right). NOTE: Due to the sensitivity of the selected area of interest for the sub-scenario, the screenshot has been taken with images from another area (Madrid Barajas Airport, Spain).

2.2. SAR Time Series Analysis using MIMOSA

The Method for generalIzed Means Ordered Series Analysis (MIMOSA) is a new technique that can detect changes between SAR image pairs or within time series [5]. Unlike many numerous existing techniques, this approach does not require any spatial filtering, uses the full resolution, is fully automatic and requires a single parameter. The only strong constraint is the acquisition mode as interferometric conditions are required.

The MIMOSA tool provides a complete chain for change detection using SAR imagery from pre-processing to post-processing. The MIMOSA tool is a set of three toolboxes presented as an ENVI menu (Figure 3).

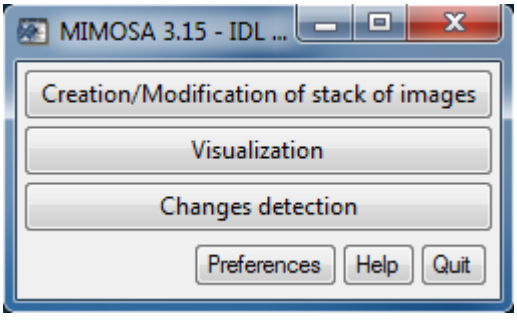

Figure 3: MIMOSA toolboxes implemented in the ENVI software.

After pre-processing of the SAR images, consisting of image co-registration and radiometric calibration, the algorithm requires tree steps. The aim of the first step is to estimate the three statistical parameters (i.e. μ, M and L) of the Fisher distribution in the amplitude images. The second step is, under previous assumption, the estimation of the joint probability density function $p_{m_0,m_k}(m_0,m_k)$ and of the conditional distribution of m_k under the knowledge of m_0, $p_{m_k|m_0}(m_k|m_0)$ between the pair of images, where m_0 (the geometric mean) and m_k (with $k > 0$) are two different Hölder means. Finally, the global change detection procedure consists in a double thresholding of $p_{m_0,m_k}(m_0,m_k)$ and $p_{m_k|m_0}(m_{k,A}|m_{0,A})$ according to the definition of a single parameter based on the false alarm rate, separating the changed from the unchanged pixels.

The MIMOSA interface allows then to superimpose the change detection results on images, showing appearance or disappearance over time. Isolated detections can also be eliminated through morphological filtering.

The MIMOSA tool has been deployed at CEA and tested in various situations and with different sensors, such as TerraSAR-X and COSMO-SkyMed X-Band. The false alarm rate in MIMOSA is taken as a constant value (equal to 1%) for general use and set between one and five percent for particular analyses.

Figure 4 shows the change detection results calculated based on a set of 24 images acquired during a campaign in which also ground information was provided. The detected changes, represented in green, confirm the good performance of the algorithm.

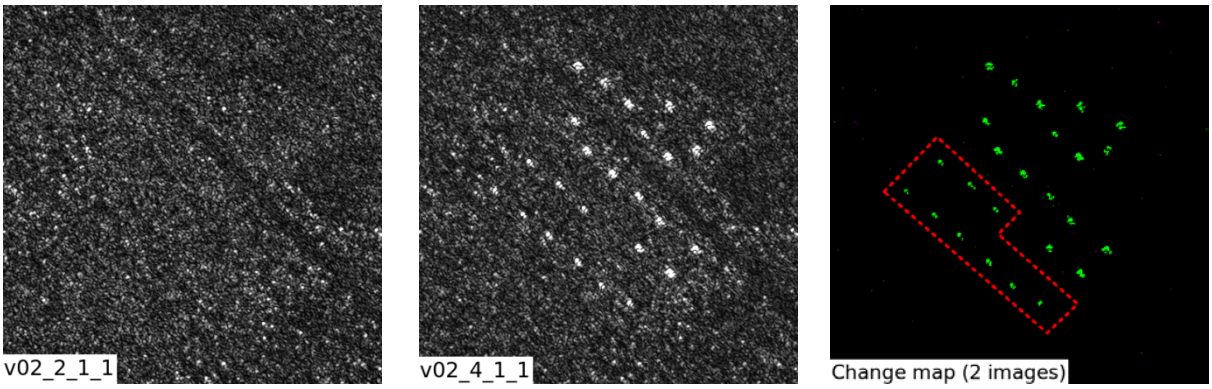

Figure 4: Left/middle: Amplitude images of the test site, where vehicle deployment is visible in the centre image and can be compared with the ground truth. Right: Automatic change detection; results obtained with MIMOSA are represented in green and represent appearance of vehicles between the two acquisition times.

2.3. Polarimetric SAR Change Detection

We investigated the application of multivariate statistical change detection with high-resolution polarimetric SAR imagery acquired from commercial satellite platforms for observation and verification of nuclear activities. A prototype software tool comprising a processing chain starting from single look complex (SLC) multitemporal data through to change detection maps has been developed.

Multivariate change detection algorithms applied to polarimetric SAR data are not common. This is because, up until recently, not many researchers or practitioners have had access to polarimetric data. However with the advent of several spaceborne polarimetric SAR instruments such as the Japanese ALOS, the Canadian Radarsat-2, the German TerraSAR-X, the Italian COSMO-SkyMed missions and the European Sentinal SAR platform, the situation has greatly improved. There is now a rich source of weather-independent satellite radar data, which can be exploited for nuclear safeguards purposes. The method will also work for univariate data, i.e. is also applicable to scalar or single polarimetric SAR data.

The change detection procedure investigated here exploits the complex Wishart distribution [6] of dual and quad polarimetric imagery in look-averaged covariance matrix format in order to define a per-pixel

change/no-change hypothesis test. It includes approximations for the probability distribution of the test statistics, and so permits quantitative significance levels to be quoted for change pixels. The method has been demonstrated previously with polarimetric images from the airborne EMISAR sensor, but is applied here for the first time to satellite platforms. In addition, an improved multivariate method is used to estimate the so-called equivalent number of looks (ENL), which is a critical parameter of the hypothesis test.

Figure 5 shows a processing sequence for generating a change map from two polarimetric SAR images available at the single look complex (SLC) processing level, in this case using open source software only. First of all, two geocoded multi-look polarimetric SAR images suitable for further processing with the change detection algorithm are generated from the SLC data with the open source software packages PolSARpro (European Space agency), together with MapReady (Alaska Satellite Facility). PolSARpro is first used to create multi-look images in covariance matrix format, which are then exported to MapReady for georeferencing with or without a DEM. MapReady will generate the covariance matrix images in the form of co-registered GeoTIFF files, one for each diagonal matrix element and two (real and imaginary parts) for each off-diagonal component. The python script `geo2polsar.py` is then used to combine these files to a single multi-band image in floating point format. The equivalent number of looks is a critical parameter for the statistical distribution of the image pixels and hence for a valid hypothesis test [7]. The Python script `enlml.py` implements a multivariate estimation procedure for the ENL, which is superior to univariate methods, especially in the presence of background clutter [8]. Finally, the Python script `wishart_change.py` calculates the per-pixel decision statistic $-2 \log Q$ and the probability of observing that value or smaller. A significance threshold may be set to generate a change map, that is, a classification image for change/no change. Single, dual, quad and diagonal polarimetric covariance matrix images can be processed with the script. In the context of G-SEXTANT the same processing chain has been implemented with the commercial software system ENVI/IDL/SARscape.

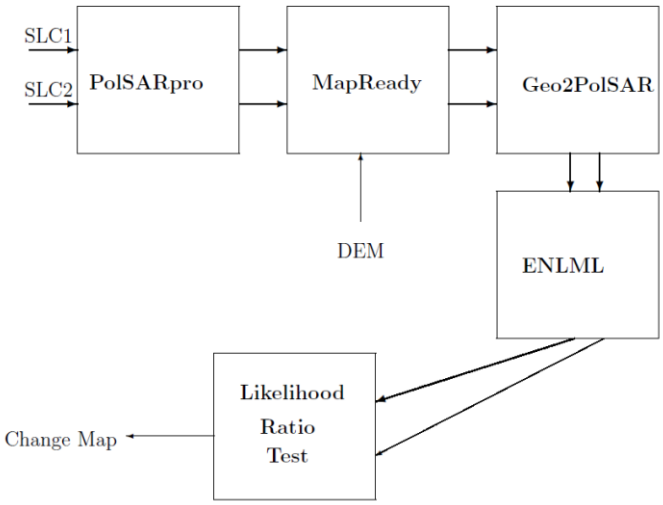

Figure 5: Processing Chain.

The method has been verified with quad polarimetric data, however, results are not shown here due to lack of space and we restrict discussion to two TerraSAR-X dual polarimetric images, which have been provided by the G-SEXTANT project. They were acquired on March 12 and September 26, 2013. The transmitted and received polarizations were HH and VV. Because of the hilly terrain, a DEM was used for geo-referencing in MapReady. It was downloaded from the freely available ASTER Global DEM V2 database. Ground resolution of the processed covariance images was 12.5m and the nominal number of looks was 6. The ENL estimates were 3.7 and 4.7 for the March and September data, respectively. Figure 6 (left) shows the HH intensity band of the March 12 image overlayed onto the DEM together with the one percent significant changes. Figure 6 (right) shows an enlarged projection of the changes around the fuel fabrication complex onto Google Earth. Lack of ground truth makes it difficult to interpret the changes seen, but there are no apparent changes to the on-site buildings.

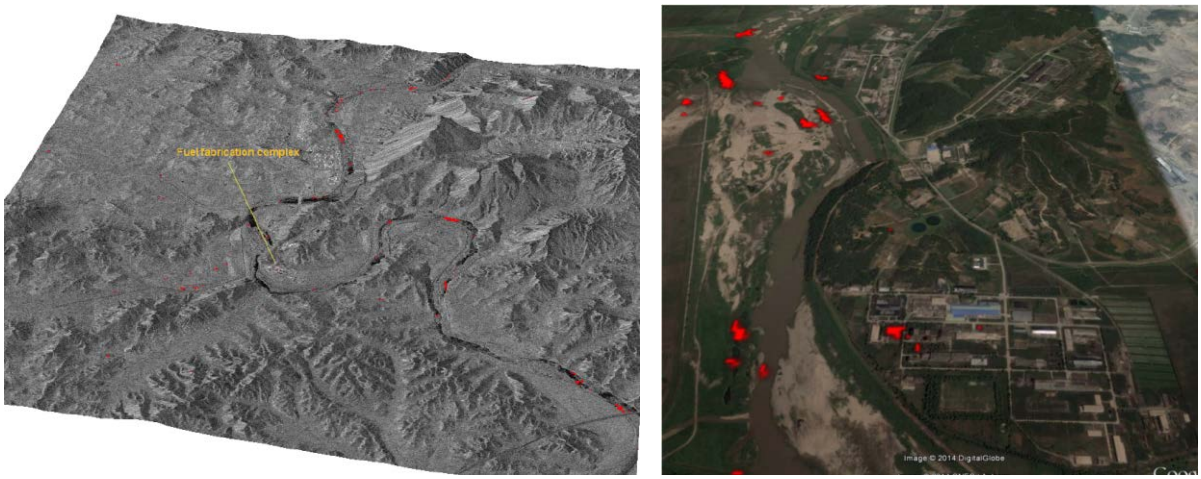

Figure 6: Left: Surface view of the March 12 TerraSAR-X dual polarimetric image over the Yongbyon nuclear facility in North Korea including 1% significance changes. Right: Google Earth projection of the March 12 TerraSAR-X dual polarimetric image over the Yongbyon nuclear facility in North Korea including 1% significance changes.

2.4. Object-based Optical Change Detection

Aiming at providing a robust approach to optical change detection, the procedure for object-based change detection described in [9] was adopted and extended to the needs of the sub-scenario. The method supports the analyst in monitoring relevant changes at nuclear facilities. The procedure includes six steps which will be explained in the following. Improvements achieved within G-SEXTANT compared to [9] will be highlighted.

a) Preprocessing: In order to accurately compare the remotely sensed data acquired at two different times, the method requires geometrically corrected input imagery. Therefore the input data is expected to be orthorectified and co-registered. Besides geometric correction, the image data is normalized spectrally using the relative correction method IR-MAD, which is described in [10].

b) Object extraction: The basis of each object-based image analysis method is the object extraction step also known as segmentation. Here, a bitemporal segmentation algorithm called Multiresolution Segmentation for Change Detection (MRS4CD) is applied. This algorithm produces stable results for different acquisition dates in areas where no changes in the objects' shape occurred, and adapted segmentation in areas where the objects' outlines did change. The result of this step is a segmentation for each of the two input images. For details on the method see [9].

c) Object correspondence: In order to allow an object-to-object comparison of the data, the two segmentations obtained in the previous step are linked using the method of Change Detection using Intersecting Objects (CDIO). This approach creates a third segmentation consisting of a spatial intersection of all object pairs from the two original segmentations (for details see [9]). Moreover, the object features used for change detection are selected in the third step. As possible correlations between the features are automatically removed in the next process step, the user can freely select the object features. The resulting pairs of feature vectors for each segment in the spatial intersection segmentation will serve as input to the next processing step.

d) Change detection: The objects' feature vectors are transformed using a combination of two multivariate statistical methods in order to emphasize changes between the two images. Firstly, the principal component analysis (PCA) is applied to the data in order to maximize the variance of each vector component. The resulting object vectors are then transformed using the canonical correlation analysis (CCA) which maximizes the variance of the difference in each vector component. The step results in uncorrelated difference images, the MAD variates, as well as a change intensity image, the so-called Z-value.

e) Change classification: Using the change intensity image obtained in the previous step, an extended version of the supervised classification method SEATH (see [11]) is used. The extended SEATH estimates the distribution of the change intensity for both classes, i.e. changed and unchanged objects, based on the samples given by the user. Then, an optimal threshold separating the two classes is calculated. Compared to [11], the methodology is now capable of applying also non-Gaussian distributions. The tool is implemented using the open source software GNU R.
Alternatively, also an iterative unsupervised classification scheme was developed within G-SEXTANT WP450 which takes advantage of a clustering algorithm called Fuzzy Maximum Likelihood Estimation (FMLE) (see [12]). At the beginning of each iteration, this method assigns a cluster to each of the objects using the MAD variates as input. Then, the cluster with the lowest average Z-value is removed from further analysis and the algorithm continues with the next iteration. In the current version, the user terminates the process based on visual inspection of the result.

f) Post-processing: In the last processing step, very small changes that are considered to be results of co-registration errors are removed. Also, the change objects' outlines are smoothed using the Douglas-Peucker algorithm (see [13]) in order to produce well legible maps.

The whole procedure was implemented in Trimble's eCognition software in combination with the GNU R statistical software package. Figure 7 shows input and products from optical change detection procedure.

Future developments of the methodology will comprise the implementation of the semi-automated change classification routine as an extension to the image processing software ENVI, going from scientific tools to software in an operative environment as well as training of the image analysts.

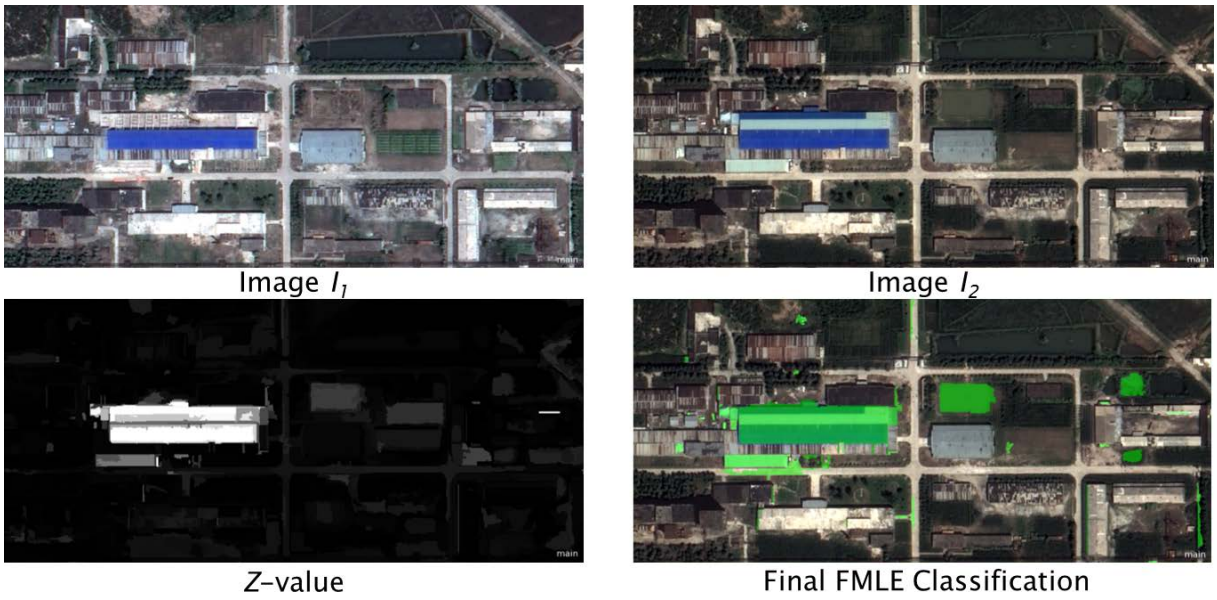

Figure 7: Input and products from optical change detection procedure.

2.5. Information Management and Integration

The work package provides an integrated platform to the non-proliferation image analyst which allows to retrieve, view and analyse all available (spatial and non-spatial) information for a given site, including satellite imagery, GIS information, external databases and open source information. It is based on a standard three-tier architecture - database (DB), application server (AS) and web client - as illustrated in Figure 8.

In order to support information of different types (both spatial and non-spatial), the platform incorporates three independent pillars each serving a particular purpose: a geographic information system, a Wiki system and a document repository:

- Geographic information system (GIS): The GIS provides an intuitive map-based interface to the user. It allows storing, retrieving and visualising spatial information. Each feature in the geo-database is context-sensitive, i.e. it can be selected from the user interface and cross-linked with other information, such as meta-information, collateral data and analysis results.
- Wiki system: The objective of the Wiki system is to capture unstructured, tacit information available in an organisation. For example, each feature in the geodatabase (e.g. a particular facility) can have a corresponding Wiki page containing relevant information or previous analysis.
- Document repository: The document repository is designed as a central archive for all relevant documents collected from various sources. In particular, open source information is becoming increasingly important to trigger, guide and support imagery-based analysis.

In order to facilitate information integration, the meta-data used to describe the information in all sub-systems is based on the same geographic and thematic taxonomy. This allows for example to automatically generate ‘country’ or ‘site’ pages, which provide direct access to all available information for the country or site of interest.

Figure 9 illustrates the concept with example snapshots of the Geo-Browser and HTML browser which show spatial and textual information related to the same nuclear site. The user interface provides links to easily navigate between the two environments.

The developments under G-SEXTANT focused on interfacing the GIS platform with the Nuclear Security Media Monitor (NSMM), which is used to monitor and review Open Source information related to Nuclear Security and non-proliferation [14].

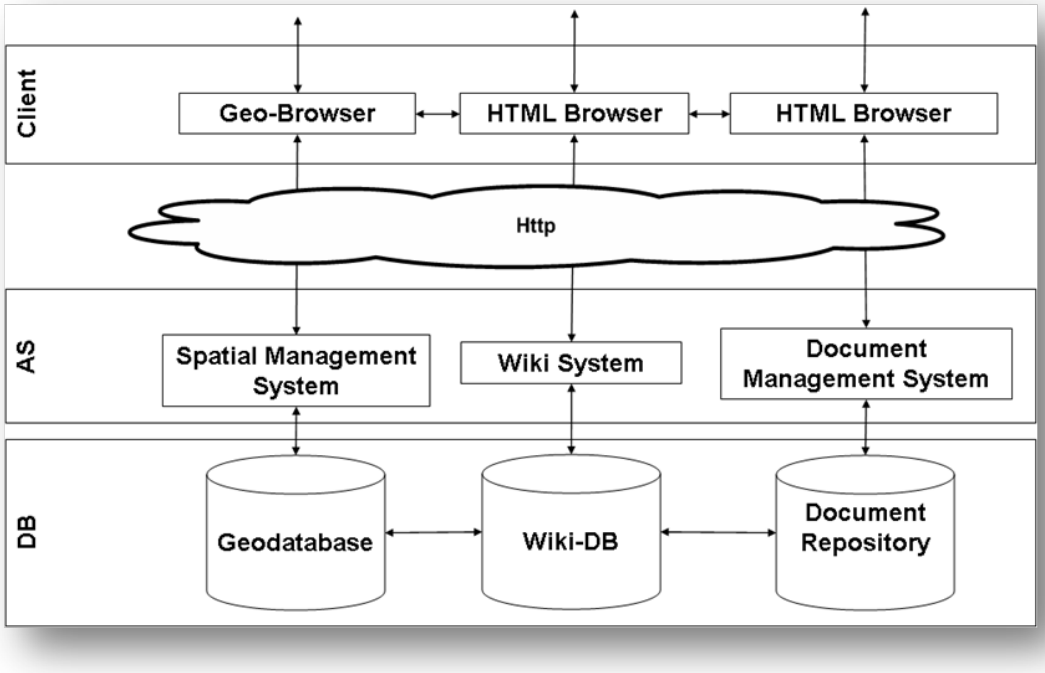

Figure 8: High-level architecture of the integration platform. The system integrates a geographic information system (left), a Wiki system (centre) and a document repository in order to support spatial and non-spatial information.

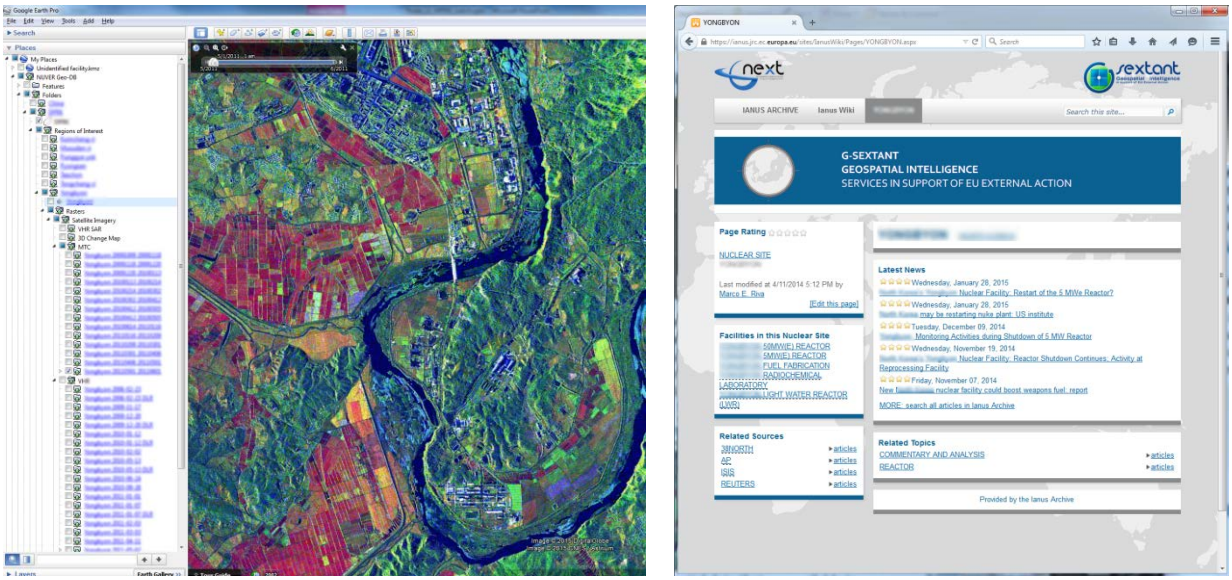

Figure 9: Left: Geo-browser (Google Earth) which allows loading and viewing all spatial data (images, vectors, results from processing) that are available in the local database for a given nuclear site. Right: HTML browser to view the non-spatial data for the same nuclear site. The snapshot shows the Open Source information that has been collected and stored on a regular basis.

3. Summary & Outlook

The work package related to monitoring of nuclear sites and activities was intended to develop tools to support the EO data analyst rather than producing ready-to-use products.

At the beginning of the project, the following user's requirements were expressed:

a) The degree of automation in the analysis and use of geospatial information should be increased.
b) Tools for automatic change detection in optical and radar imagery are needed.
c) Synergy effects should be used when combining the analysis of optical and radar satellite imagery.
d) Geospatial tools for improving the preparations of nuclear safeguards inspections would be helpful.

Regarding the request to create synergy effects between optical and radar satellite imagery, a SAR visualization tool was developed. This tool is able to visually connect pixels between radar and optical imagery. Thus, it allows for a better interpretation of SAR imagery.

Three tools for automatic change detection were developed: a SAR change detection tool using the Wishart distribution, a tool for SAR change detection named MIMOSA as well as a tool for object-based optical change detection. These image analysis tools fill the needs for such tools that were expressed by the user. Furthermore, they are able to be integrated into existing workflows. However, the tools require further software development to some extent in order to obtain a software tool to be used in an operative environment.

With respect to the request for geospatial tools supporting preparations of nuclear safeguards inspections, a GIS tool was developed. This software is based on the Google Earth Engine and allows visualizing EO data as well as the results from the image processing tools in a consistent, geo-referenced manner. Furthermore, it is able to integrate non-EO data using a wiki system.

While all tools developed proved to work properly, there is still room for improvements. In this context, the following next steps in the tools' development might be considered:

- Performance improvements for SAR visualization tool;
- Implementation of semi-automated change classification routine as an extension to the image processing software ENVI;

- Going from scientific tools to software in an operative environment;
- Training of users.

Acknowledgements

This paper was prepared as an account of work partly sponsored by European Commission under FP7- Space-2007-1/FP7-SPACE-2012-1 (GMES SECURITY).

References

[1] Niemeyer, I.: Challenges in Treaty Monitoring. In: *BICC brief 37*, 2008, 64-67

[2] Canty, M., Jasani, B., Lingenfelder, I., Nielsen, A.A., Niemeyer, I., Nussbaum, S., Schlittenhardt, J., Shamoni, M. & Skriver, H.: Treaty Monitoring. In: Jasani, B., Pesaresi, M.,Schneiderbauer, S. & Zeug, G. (Eds.): *Remote Sensing from Space. Supporting International Peace and Security*. Springer, Berlin, 2009, 167-188

[3] Dekker, R.J., Kuenzer, C., Lacroix, V., Lehner, M., Niemeyer, I., Nussbaum, S., Schoepfer, E., Sequeira, V. & Stringa, E.: Change Detection Tools. In: Jasani, B., Pesaresi, M., Schneiderbauer, S. & Zeug, G. (Eds.): *Remote Sensing from Space. Supporting International Peace and Security*. Springer, Berlin, 2009, 119-140

[4] Gonçalves J.G.M., Gutjahr, K.H., Listner, C., Loreaux, P., Marpu, P.R., Niemeyer, I., Patrono, A., Ussorio, A. & Wolfart, E: Integrated Analysis of Satellite Imagery for Treaty Monitoring - The LIMES Experience. In: *ESARDA Bulletin* 43, 2010, 40-56

[5] Qiun, G., Pinel-Puysségur, B., Nicolas, J.M. & Loreaux, P.: MIMOSA: An Automatic Change Detection Method for SAR Time Series. In: *IEEE Transactions on Geoscience and Remote Sensing* 52(9), 2014, 5349-5363

[6] Conradsen, K., Nielsen, A. A., Schou, J., and Skriver, H.: A test statistic in the complex Wishart distribution and its application to change detection in polarimetric SAR data. In: *IEEE Transactions on Geoscience and Remote Sensing* 41(1), 2013, 3-19

[7] Thonfeld, F., Nielsen, A. A., Skriver, H., Conradsen, K., and Canty, M. J.: Complex Wishart distribution-based change detection with polarimetric TerraSAR-X imagery. In: Fifth TerraSAR-X Science Team Meeting, DLR Oberpfaffenhofen, Germany, June 2013, 2013.

[8] Anfinsen, S., Doulgeris, A., and T. Eltoft, T.: Estimation of the equivalent number of looks in polarimetric synthetic aperture radar imagery. In: *IEEE Transactions on Geoscience and Remote Sensing*, 47(11), 2009, 3795–3809

[9] Listner, C. & Niemeyer, I.: Object-based Change Detection. In: *Photogrammetrie-Fernerkundung-Geoinformation*, PFG, E. Schweizerbart'sche Verlagsbuchhandlung, 2011, 2011, 233-245

[10] Canty, M. J. & Nielsen, A. A.: Automatic Radiometric Normalization of Multitemporal Satellite Imagery with the Iteratively Re-weighted MAD Transformation. In: *Remote Sensing of Environment, Elsevier*, 2008, 112, 1025-1036

[11] Nussbaum, S., Niemeyer, I. & Canty, M.: SEATH-a new tool for automated feature extraction in the context of object-based image analysis. In: Proceedings of the OBIA 2006 Conference - 1st International Conference on Object-based Image Analysis, 2006, 36, C42

[12] Gath, I. & Geva, A.: Unsupervised optimal fuzzy clustering. In: IEEE Transactions on Pattern Analysis and Machine Intelligence, ITPAMI, 1989, 11, 773 -780

[13] Douglas, D. & Peucker, T.: Algorithms for the reduction of the number of points required to represent a digitized line or its caricature. In: *Cartographica:* The International Journal for Geographic Information and Geovisualization, UT Press, 1973, 10, 112-122

[14] Cojazzi, G. G.M., van Der Goot, E., Verile, M., Wolfart, E., Rutan Fowler, M., Feldman, Y., Hammond, W., Schweighardt, J. & Ferguson, M.: Collection and Analysis of Open Source News for Information Awareness and Early Warning in Nuclear Safeguards". In: *ESARDA Bulletin* 50, 2013, 94-105

Mobile 3D Laser Scanning for Nuclear Safeguards

E. Wolfart, S. Ceriani, D. Puig, C. Sanchez, P. Taddei, V. Sequeira

Joint Research Centre, European Commission, Ispra, Italy

M. Murtezi, P. Turzak, A. Zein

DG ENER, European Commission, Luxembourg

L. Enkhjin, M. Ingegneri, S. Rocchi, Y. Yudin

International Atomic Energy Agency, Vienna, Austria

Abstract:

3D laser scanning is an established verification technology in nuclear safeguards, applied inter alia for Design Information/Basic Technical Characteristics Verification (DIV/BTC) and change monitoring in nuclear facilities. Current systems are based on high-accuracy, high-resolution 3D laser scanners which require one minute or more to acquire a single scan. Therefore, the scanners need to be immobile during data acquisition. In order to cover the complete scene, several scans are acquired in a so-called 'stop-and-go' mode, which are then registered into a single coordinate frame in an offline post-processing phase.

Recently, new 3D laser scanners with a significantly increased acquisition speed have emerged. They acquire 3D scans at a frame rate of 10Hz and more - at the cost of reduced accuracy and resolution – and thus enable the scanner to be mobile during acquisition, i.e. the data can be acquired while walking or driving. Mobile laser scanning can significantly increase the efficiency of existing safeguards applications for 3D laser scanning, i.e. DIV/BTC and change monitoring.

Furthermore, by registering each scan with a reference model (which can either be generated a priori or while scanning), it is possible to compute the current position and track the movement of the scanner. Hence, mobile laser scanning with real-time data processing provides indoor positioning capability to nuclear inspectors during their field work. It enables all observations and measurements to be connected with their respective location and time stamps and to retrieve location-based information as required.

The paper presents the Mobile Laser Scanning Platform (MLSP) developed at the JRC, which consists of a commercial mobile scanner, the processing unit and the proprietary software for real-time processing and visualization. The system will be illustrated using two test cases: a DIV/BTC scenario for the future Finnish underground repository (ONKALO) and indoor localization.

Keywords: 3D scanning, Design Information Verification, BTC Verification, change analysis, indoor localization, nuclear safeguards

1 Introduction

3D laser scanning is an established verification technology in nuclear safeguards and is approved by IAEA and EC for safeguards use. It has been applied inter alia for Design Information/Basic Technical Characteristics Verification (DIV/BTC) in several nuclear facilities throughout the world, both by IAEA and Euratom inspectors. [1], [2]

Current systems are based on high-accuracy, high-resolution 3D laser scanners which require one minute or more to acquire a single scan. Therefore, the scanners need to be immobile during data acquisition. In order to completely cover a given area of interest, several scans are acquired in a so-called 'stop-and-go' mode, which are then registered into a single coordinate frame in an offline post-

processing phase. The resulting 3D model is used to verify the correctness and completeness of the design drawings provided by the operator and it is stored as a reference for subsequent visits. On return, the inspector re-scans the area of interest and the data is analysed to verify that no undeclared modifications to the facility have occurred. Figure 1 illustrates the use of 3D laser scanning for detecting changes in a facility. The change map is calculated from the distances between 3D measurements acquired before and after the scene was changed.

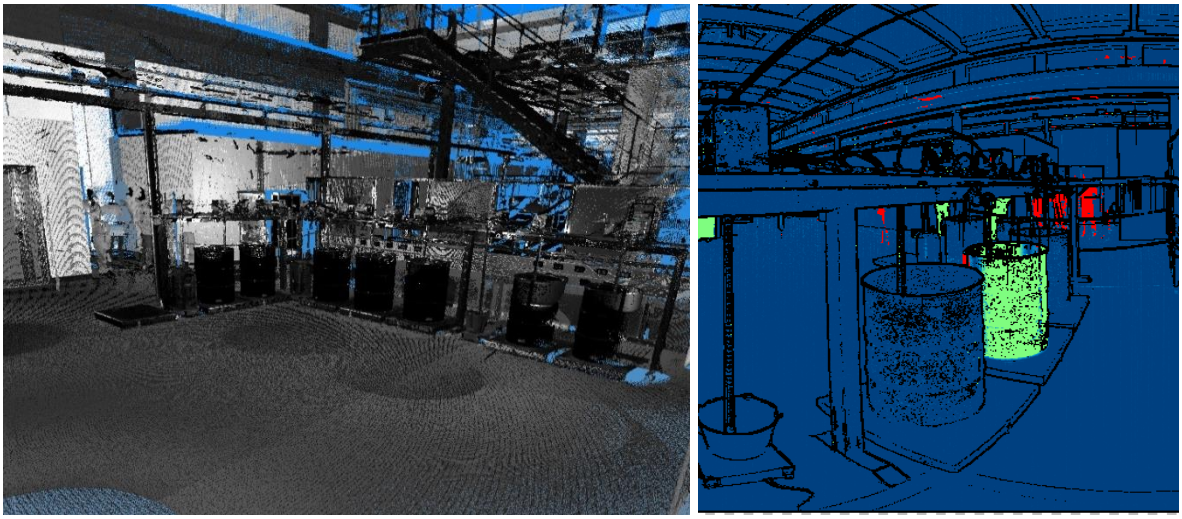

Figure 1: *Left*: snapshot of a 3D model of a (non-nuclear) facility; *Right*: change map generated by comparing the 3D model acquired before and after modifying the scene (Blue pixels correspond to unchanged objects; Green and red corresponds to changed objects).

Although 3D laser scanning provides detailed and accurate as-built information and change analysis, data acquisition and processing using stop-and-go scanning can be a considerable effort depending on the size and complexity of the facility. Recently, new 3D laser scanners with a drastically increased frame rate have emerged. They acquire 3D scans at 10Hz and more - at the cost of reduced accuracy and resolution – and therefore allow that the scanner is moved during acquisition, i.e. the data can be acquired while walking or driving.

JRC has developed a portable Mobile Laser Scanning Platform (MLSP), intended for real-time change monitoring inside nuclear facilities, in particular geological final repositories. It is also applicable for indoor localization which allows nuclear inspectors to associate all measurements and observations made during an inspection with the corresponding location inside the nuclear facility and thus facilitate subsequent analysis and future inspections. Section 2 describes the main MLSP components and section 3 outlines the core algorithms running on the system. Section 4 illustrates the applications of mobile laser scanning in nuclear safeguards; section 5 outlines future activities and section 6 draws conclusion.

2 Mobile Laser Scanning Platform

The Mobile Laser Scanning Platform (MLSP) is a portable sensor and processing system developed at the JRC. It is based on a mobile 3D laser scanner and provides real-time mapping, localization and change analysis in indoor, GPS-denied environments.

The main hardware components of the MLSP are (see Figure 2):

- A real-time laser range scanner. The current MLSP implementation uses the commercially available Velodyne HDL-32E, which acquires up to 15 frames per second.
- A processing unit which analyses the scanner data in real-time and generates a 3D map/model, localization information and change information.

- A tablet computer to control the system and view the processing results.

The hardware components can be mounted on different carrier systems according to the application need. Figure 3 shows the backpack-mounted MLSP (left) and the car-mounted MLSP (centre, right).

The analysis software which runs on the portable processing unit is the core of the MLSP system. It runs fully automatically in real-time and therefore needs to be highly efficient, reliable and accurate. Additionally, it is able to manage very large data sets, i.e. it is able to handle facilities and buildings that cover several thousands of square meters.

Processing results (tracks and change maps) are transferred to the portable device for visualization and interaction with the user.

Figure 2: Hardware components of MLSP system: 3D laser scanner, processing unit and tablet.

Figure 3: *Left*: backpack-mounted MLSP for scan-while-walk acquisition. *Centre, Right*: Car-mounted MLSP. The processing unit is situated inside the car.

3 Data Processing

The core of MLSP's data processing is the self-localisation within known environments, i.e. environments for which a 3D reference model has been acquired a-priori. The reference model is typically acquired with the stop-and-go scanning as described above. However, it can also be acquired with mobile scanning if the global accuracy is not essential (see section 4. 2). Since MLSP was developed for indoor use it relies solely on 3D measurements, in particular it does not require any GPS information. The process is divided in two components, which are briefly described in the remainder of this section: *Pose Recognition* and *Pose Tracking*. For a detailed description see [3].

3. 1 Pose Recognition

Pose recognition estimates the current user pose (position and orientation) within a given search space (i.e. the space covered by 3D reference model) when no prior knowledge of the current position is available, e.g. after system start-up.

Pose recognition runs in real-time and must be scalable to large environments. Therefore, a pre-processing stage is introduced that (1) reduces the search space of possible poses and (2) transforms the 3D reference model to a compact search tree that enables efficient searching:

- *Search Space Reduction*. Since we focus on ground motion (backpack or vehicle mounted sensor), the MLSP sensor is expected to be in a narrow space parallel to the *navigable floor* and we can reduce the search to the poses within this *navigable space*. Therefore, the navigable floor is computed using on a flooding-algorithm which detects the floor surface based on the surface normals (which are expected to be predominately vertical) and a ‘’reachable” condition (e.g. a table surface would not be detected as floor because it is not considered to be reachable from the floor surface). We also introduce physical constraints related to the specific mode of system operation (e.g. vertical and angular limits on the possible sensor pose).
- *Search Tree*. In order to enable efficient searching, we transform the 3D reference model into a compact descriptor space as follows: i) we randomly generate a set of poses in the known effective navigable space (computed as described above); ii) for each pose, we synthesize a depth image and extract a compact *descriptor* from the generated depth image: we split the range image in regular bins. For each bin, we estimate a median range value which is stacked to form a single descriptor (see Figure 1Figure 4); iii) we build a kd-tree which maps all generated descriptors to their corresponding pose.

Figure 4: Example of a synthesized depth image and the derived compact descriptor. The depth image is divided in twelve bins and the median depth value is calculated for each bin. The descriptor is then stored as a 12-dimensional vector.

At run-time, the system creates a compact descriptor for each depth image (i.e. 3D scan) in the same way as it is done when constructing the search tree. In order to resolve ambiguities, the pose recognition is based on a temporal series of descriptors and can be divided in an *initialization* and *update* phase as follows:

- During the *initialization, i.e.* when the pose recognition is started and no a priori information is available, the algorithm searches the descriptor space for descriptor/pose pairs matching the current descriptor thus returning a set possible poses of the sensor. Since the descriptors are

highly compacted and several positions might have similar geometries (e.g. offices of identical dimensions or positions in long corridors), we typically obtain several ambiguous candidate poses for the initial query.

- The algorithm reduces the set of candidate poses during the *update* phase: as the user navigates within the environment, the algorithm estimates the movement (using the odometer described below) and re-evaluates the likelihood for each initial candidate pose based on the query results at the new pose. The update stage is iterated until the candidate poses converge to a single location and the algorithm is able to disambiguate the current pose. At this point we consider the problem solved and the pose tracking component is started. Figure 5 shows an example of candidate poses after initialisation and after convergence.

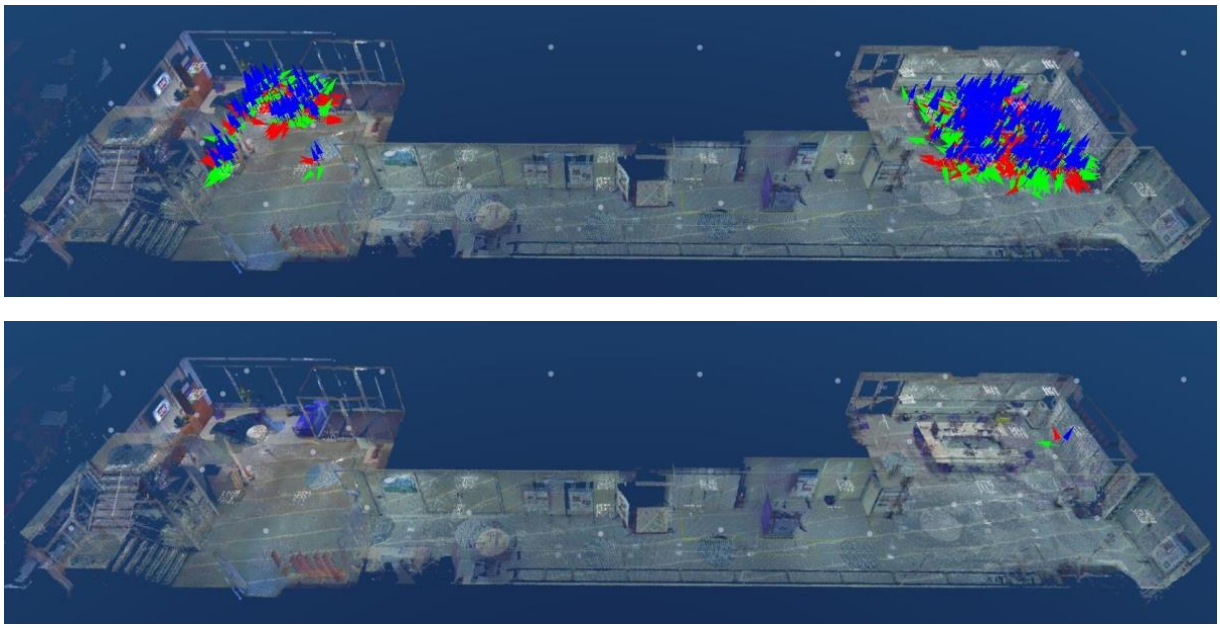

Figure 5: *Top*: Snapshot of pose recognition after initialization. The image shows several ambiguous candidate poses in the two areas that have similar geometries. *Bottom*: Snapshot of the pose recognition after convergence. The image shows that the candidate poses converge to the correct location (shown as the coordinate frame on the right side) as the user explores the environment for several meters.

3. 2 Pose Tracking

Pose tracking starts after the sensor pose has been identified by the pose recognition component. Since the sensor only moves small distances between two scans (i.e. within 0.1 sec), we have a good estimate of the pose of each new scan and it is possible to register the scan using the well-known Iterative Closest Point (ICP) algorithm [4]. Given an initial estimate of a scan pose, the basic ICP algorithm registers a scan with a 3D reference model as follows:

1. Select a sub-set of points from the new scan (control points).
2. For each control point, find the nearest neighbour in the 3D reference model (corresponding points).
3. Compute the transformation that minimises the distance between the control and corresponding points.
4. Update the scan pose using the computed transformation.
5. Iterate steps 1 to 4 until the pose of the scan converges.

The ICP registration accurately estimates the current scan pose (see Figure 6) and therefore the movement since the previous scan, which in turn allows estimating the pose of the next scan. In this

way, the ICP is repeatedly applied to each new scan to track the sensor pose as the user moves through the environment.

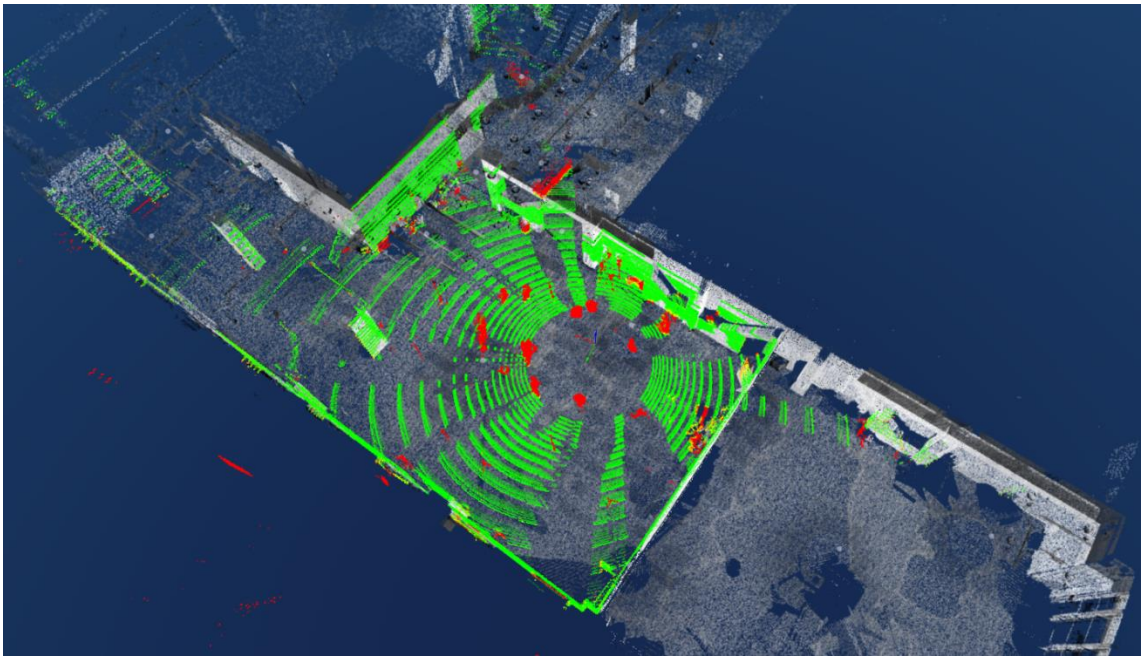

Figure 6: *The green and red points are a scan acquired with mobile scanner; the grey points are the 3D reference model. The current sensor pose is determined by registering the scan with the reference model. The trajectory is obtained by applying the registration repeatedly as the sensor moves through the environment.*

However, it is challenging to carry out the ICP registration in real-time. The most time consuming step is the nearest neighbour search that has to be carried out for each control point in each iteration. The remainder of this section describes the ICP extensions that were developed to allow real-time ICP processing, namely (1) the transformation of the 3D reference model into a data structure specifically designed for nearest neighbour searches, (2) a point selection and outlier removal strategy to ensure fast and accurate convergence.

3.2.1 Nearest Neighbour Search

In a pre-processing step, two different lists are computed from the 3D reference model: a compact list of points (together with their normals) and a dense grid of voxels. Each voxel can be either *full*, *empty* or *near*. *Full* voxels store an index to an associated point which is computed as the mean of the points inside the voxel. *Empty* cells store a null reference and *near* cells store an index to the nearest plane (see Figure 7, left image).

With this data structure, all nearest neighbour searches are pre-computed offline and stored inside the dense grid. At run time, given a query point in world coordinates, we estimate the nearest neighbour in the map by calculating the voxel that contains it. Then, if the cell state is *full* or *near*, we return the associated point. Otherwise, we notify that there are no neighbours.

3.2.2 Point Selection and Outlier Removal

For each control point, the nearest neighbour search returns the corresponding point in the reference model. However, outliers (mismatches between control and corresponding points which are, for example, due to objects that have been added or removed after the reference model was acquired) might introduce an error in the computed transformation. In order to allow an accurate and fast convergence of the ICP algorithm, outliers need to be detected and corresponding points need to be selected to properly represent the environment. Therefore, we modify the basic ICP as follows:

- In order to minimise the number of required control points, the selected points should represent all surface directions in 3D space. For example, if we would select only control points from the floor, the registration would not be able to properly lock the current scan in the direction of the walls. Therefore, we create three bins for the principle normal directions of the scan points and the points are classified according to their normals.
- Whereas the basic ICP uses a single set of (typically several hundred) control points, we select many sets, each containing only a small number of points (at minimum 3 points per set are required). The control points are selected from the bins that were pre-calculated as described above.
- For each set, we compute the transformation that minimises distance between control and corresponding points. All computed transformations are distributed around a well-defined central position. However, transformations computed from point sets containing outliers significantly differ from the central position.
- We compute the normal distribution of the transformations and remove the outlier transformations based on their distance to the mean value. This step is iteratively repeated until no transformations are discarded, or a minimum number of transformations is reached.

Figure 7 (right image) illustrates the process of the outlier removal. Notice how all independently computed transformations are distributed around a well-defined central position. Also notice that, after each iteration of outlier removal, the distributions quickly converge to the final estimated transformation, when considering all the correspondences marked as inliers.

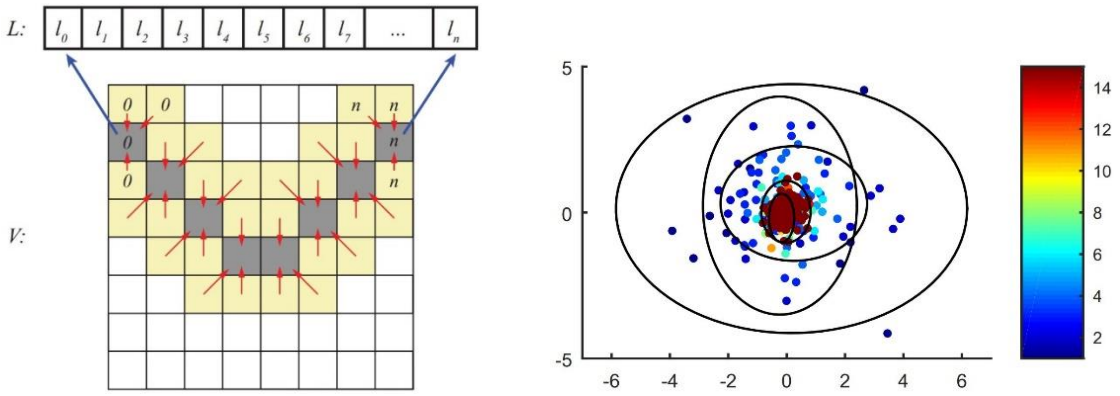

Figure 7: *Left:* Dense voxel structure where, for the sake of clarity, only the closest near voxels are shown. Full cells are displayed as grey boxes. Near cells are represented by yellow boxes with a red line connecting. Right: Example of a scan. *Right:* Outlier removal. Axes represent the main dominant dimensions of the detected transformations. Each point represents a candidate transformation coloured according to the iteration in which they have been marked as outliers (some outlier transformations too far from the centre have been omitted). Dark red points represent transformations marked as inliers. The ellipses represent the normal estimations at specific subsequent iterations.

3. 3 Odometer Integration

The odometer component tracks the movement based only on the sensor data, i.e. without the need of a pre-existing 3D reference model. It works on the same principle as the pose tracking described above, but instead of using the 3D reference model for the ICP registration, the current scan is registered with the previous scan thus generating an estimate of the local movement. Since no global reference model is available, the odometer accumulates drift over time. The odometer is used in two situations:

1. The pose recognition component uses the odometer to estimate the local movement during the update phase (see above).
2. If the user leaves the 3D reference model during the pose tracking (e.g. he might enter a room that has not been scanned during the acquisition of the reference model), the track is

estimated using the odometer output. The pose tracking automatically reverts to the 3D reference data when the user re-enters the reference model (see Figure 8).

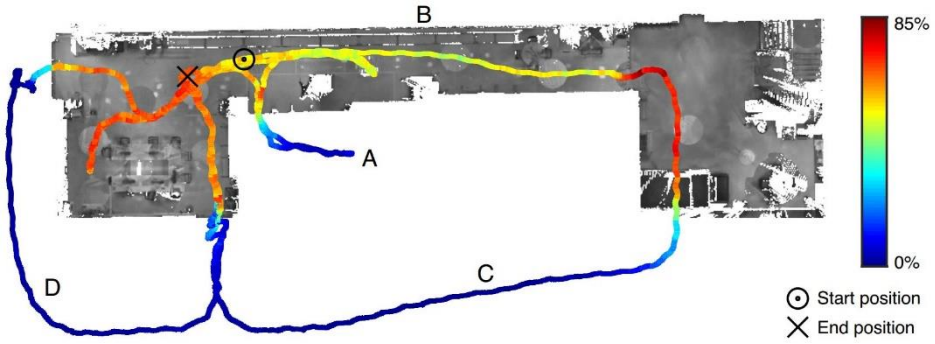

Figure 8: Results of the odometer integration during a sample walk-through inside a building where the user moves to a non-scanned room (A) without losing track of the position. Then, the user performs two loops outside the building (C and D). The trajectory is shaded according to the percentage of points used from the 3D reference model. The rest is taken from the odometer map.

4 Applications of Mobile Laser Scanning in Nuclear Safeguards

MLSP provides indoor localisation with unique accuracy and robustness under the condition that a 3D model of the environment is available. Additionally, it generates a new 3D model of the environment, which can be used for detecting changes with respect to the reference model in real-time: since the 3D scanner is accurately located at any time, an updated 3D model can be generated by simply merging the acquired 3D scans.

Therefore, MLSP is suitable for a series of applications, such as facility management and construction monitoring. In the field of nuclear safeguards, it can be used for position authentication and change monitoring during DIV/BTC verifications and as an enabling technology for location-based applications, for example during Complementary Access inspection. More details are provided below.

4. 1 DIV/BTC Verification

Stop-and-go laser scanning is an established verification technology in nuclear safeguards. It allows generating as-built 3D models of nuclear facilities with millimetre accuracy, which then can be compared i) to the design information provided by the operator for DIV/BTC verification or ii) to previously acquired 3D model for change monitoring.

However, stop-and-go data acquisition and the required off-line processing can be a considerable effort in large and complex facilities. In cases where millimetre accuracy is not required, mobile laser scanning is a complementary technology that significantly decreases acquisition effort and provides change information in real time.

The concept is illustrated using the DIV/BTC verification of the future Finnish underground repository in ONKALO. In November 2014, IAEA and DG ENER carried out a DIV/BTC verification at ONKALO using stop-and-go laser scanning. During one week, four teams of inspectors acquired over 900 scans covering more than 6km in total. In parallel, an additional team processed the data to generate an as-built 3D model. At the end, the drawings provided by the operator were verified by comparing them to the 3D model. Figure 9 illustrates the data acquisition and analysis carried out for the 2014 DIV at ONKALO.

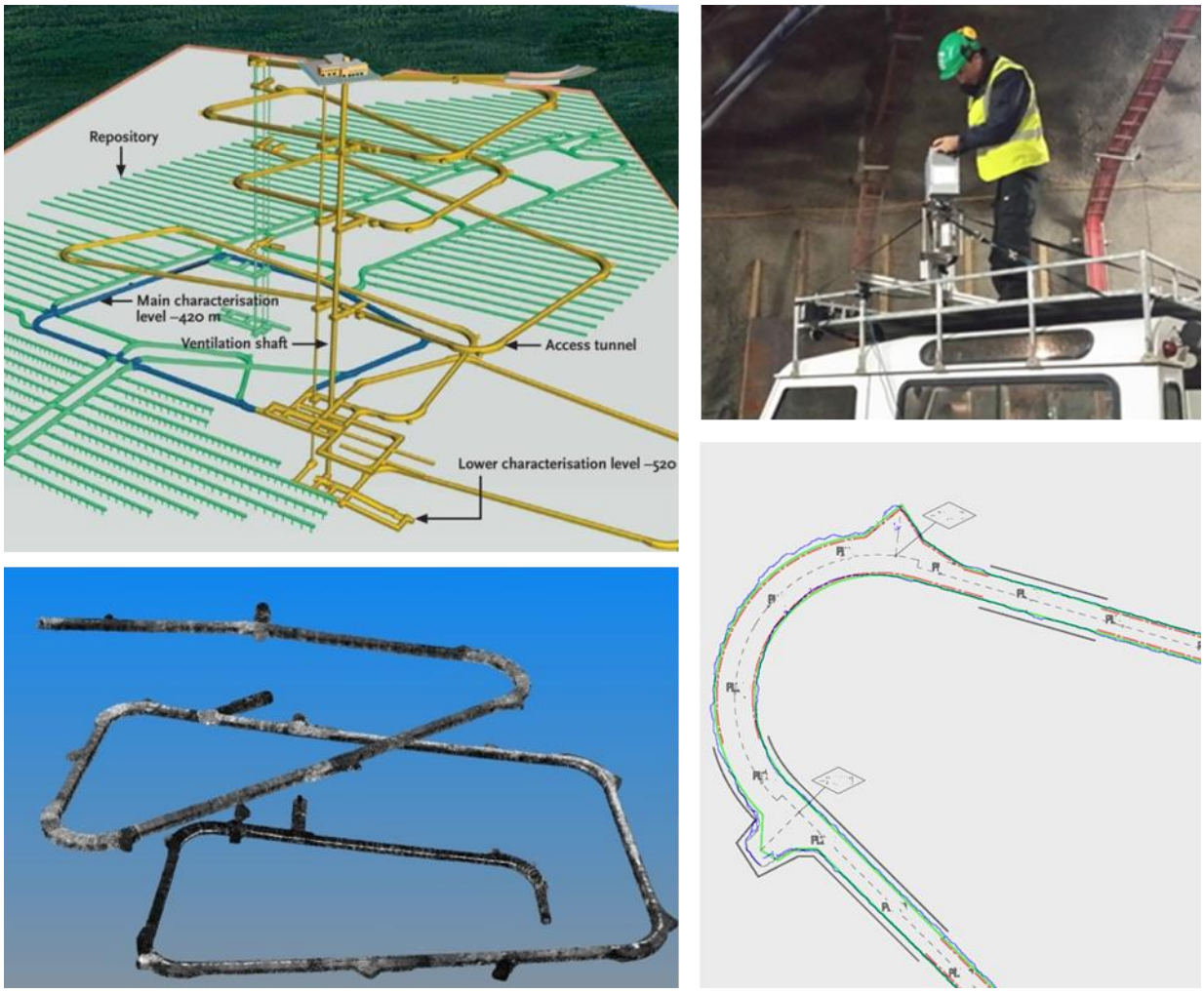

Figure 9: The top left image shows a schematic drawing of the ONKALO repository (yellow corresponds to excavations existing in 2014; green corresponds to deposition tunnels to be excavated in the future. Image courtesy of POSIVA). Data acquisition for the 2014 DIV at ONKALO was carried out in stop-and-go mode. Two scanners were mounted on a car roof (top right image) and two were mounted on a tripod. Over 900 scans were acquired in order to generate an as-built 3D model of the complete repository (the bottom left image shows a model of the first two km which was acquired during a technology demonstration in 2007). A cross section of the 3D model was generated and used to verify the drawings provided by the operator. The bottom right image is the zoom of a sample drawing; the blue line is a cross-section of the as-built laser data, which was used to verify the CAD drawing.

The next DIV at ONKALO is scheduled for late 2015. Although some excavations might take place in 2015, the major part of the repository will be the same as in 2014. It is planned to combine stop-and-go and mobile laser scanning as follows:

- The inspector visits the part of the tunnel that already existed in 2014 using the MLSP. The 3D model acquired in 2014 will be used as reference, which will allow to i) always have accurate knowledge of the current location and ii) have real-time information on possible changes with respect to 2014. Figure 10 illustrates the information provided to the inspector in real-time.[1]
- If the inspector identifies any significant changes or makes other relevant observations, he can add notes and comments, which will be location-tagged based on the MLSP information and stored for later reporting, analysis or inspections.

[1] See [8] for a video which replays the information shown to the user during a demonstration in November 2014. The stop-and-go data acquired during the demonstration in 2007 was used as 3D reference model. The changes that occurred in between (e.g. newly constructed firewalls; newly excavated side tunnels) are highlighted in red.

- In the areas excavated after November 2014 and in the areas where any significant changes are identified, the inspector acquires new 3D data using stop-and-go scanning, which will be integrated into the 3D model acquired in 2014 in order to obtain an updated as-built 3D model.
- New or updated drawings received from the operator will be verified against the updated as-built 3D model.
- The updated 3D model will be stored on site and serve as a reference for subsequent inspections.

The effort for the 2015 DIV will be considerably smaller than in 2014 while maintaining an accurate and up-to-date 3D model of the complete repository. If the procedure is repeated in subsequent inspections, it will enable the inspector to efficiently and effectively verify the correctness of the provided design information and to assure that no undeclared modifications to the facility occurred. It will also allow to navigate and authenticate the position in a facility which will become larger and more complex as the excavations advance.

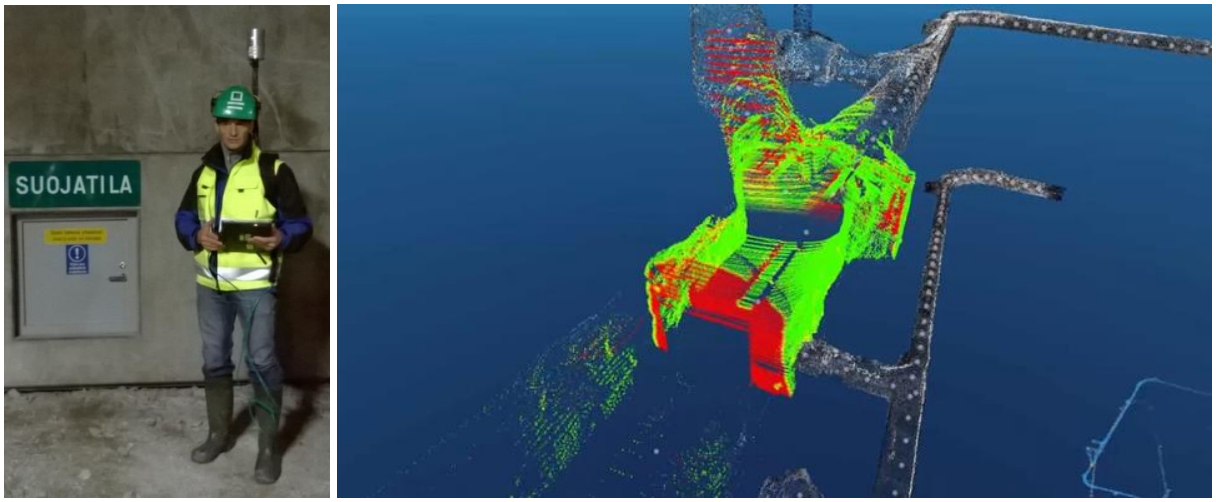

Figure 10: *Left:* MLSP demonstration in ONKALO in 2014. *Right:* Snapshot of the MLSP interface as it is provided to the user in real-time. The model acquired during the 2007 demonstration (which is used as reference) is shown in grey. The data acquired during the 2014 demonstration is color-coded as follows: green corresponds to objects that already existed in 2007 (i.e. the main tunnel excavation); red corresponds to changes (e.g. the fire door that was constructed after 2007).

4. 2 Indoor Localisation

Accurate indoor localisation of the inspector increases the efficiency and effectiveness of safeguards activities. It allows i) verifying the position and layout of a facility and ii) associating all observations and measurements made during the inspections with the respective location. Location-tagging the data acquired during the inspection greatly facilitates subsequent reporting, analysis and future inspections. For this reason, the IAEA tool kit of portable instruments, which is used to support complementary access activities, includes a GPS instrument. However, GPS measurements are not available indoors and therefore safeguards inspectors currently have no means to accurately localise themselves inside nuclear facilities.

As shown above, mobile laser scanning can be used for localization in indoor environments. Depending on the availability of a 3D reference model, it can be operated in two different modes:

1. *3D reference model available.* If a 3D reference model of the indoor environment is available, mobile laser scanning provides real-time localization with centimeter accuracy as described in section 3 . The reference model can be acquired with stop-and-go scanning. However, this might be a considerable effort, depending on the size and complexity of the environment. In

some cases (e.g. at ONKALO as described above), a 3D reference model has already been acquired for DIV purposes.

2. *3D reference model **not** available.* In cases where it is not practicable to acquire an accurate reference model prior to the inspection, the mobile laser scanner can be operated in an *Odometer* mode, i.e. the location is tracked (with reduced accuracy and robustness) using only the data acquired with the mobile scanner. After the inspection, the mobile 3D data can be re-processed using a SLAM (Simultaneous Localisation and Mapping) approach, which globally optimizes the generated track and generates a 3D model from the acquired data. Hence, inspector observations can be accurately located retrospectively and the 3D model can be used as reference for subsequent inspections. SLAM processing for the MLSP is currently under development. [5]

In 2014, the IAEA organised a technology workshop which aimed to evaluate the performance and suitability of currently available indoor navigation systems [5]. It defined the following use-cases:

- *Position Authentication*: “Inspector quickly verifies that he has been taken to the expected site location”.
- *Mapping*: “Inspector decides to perform an overall site survey; he walks or drives through the site so he may confirm / complete the IAEA knowledge of the site.”
- *Tracking and navigation*: “While surveying, the inspector continuously traces his itinerary through the site; he may also navigate toward a specified location.”
- *Geo-tagging/Location-based services*: “During the site survey, the inspector writes notes, draws sketches, records audio notes, takes pictures, takes samples, and makes various measurements. The inspector can also review on the map the actions conducted during the previous inspections.”

For the technology evaluation, IAEA defined a set of scenarios, which aimed to simulate different situations where the inspectors need to position themselves and navigate inside vast and complex sites. The evaluation was carried out inside and outside the IAEA HQ in Vienna. In total, eleven systems were tested, which can be grouped in two categories: i) systems using laser scanning, such as JRC’s MLSP and ii) systems based mainly on MEMS (Micro-electro-mechanical-systems) sensors including inertial measurement systems (IMU), magnetometers and compass. The JRC participated in the evaluation using an early version of the MLSP. Figure 11 shows the result of one of the scenarios.

In its final report, the IAEA concludes that “*laser-based sensors are the only solutions today that can offer near-perfect constant accuracy*”. Due to operational issues (i.e. the size of the system), IAEA does currently not envisage laser-based systems to be part of the standard inspector equipment, “*however they could become extremely valuable tools for specific missions*” [7].

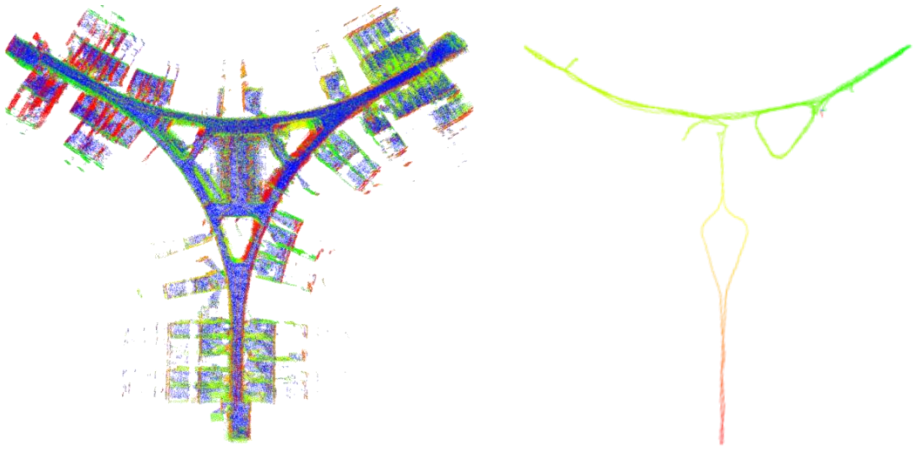

Figure 11: Results obtained with the MLSP for one of the scenarios of the IAEA technology evaluation workshop, in which the user walked through a corridor of the IAEA HQ. *Left:* top view of the 3D model created from the acquired 3D data. It covers the corridor and some of the offices (where the doors were open). *Right*: the track followed by the user as computed by MLSP.

4.2.1 Localisation Accuracy

In April 2015, JRC participated in an indoor localization competition in order to confront the MLSP accuracy to other state-of-the-art systems. The competition, organised annually by Microsoft, gathers teams from industry and academia to evaluate the performance of their respective localisation systems. The competition is carried out in two categories, involving infrastructure-based systems which require installation of equipment such as radio emitters in the environment and infrastructure-free systems which rely only on sensor readings. The JRC competed in the infrastructure-free category, where it came first, with a localisation error of 0.2 m, which also surpassed the best result in the infrastructure-based category, in which the winner had a localisation error of 0.31 m (see [7]).

The competition evaluated the measured 2D position of the user at pre-defined markers, i.e. the results were influenced by the accuracy with which the user positioned himself on the markers. The actual accuracy with which the MLSP sensor can be located in 3D space corresponds to the accuracy of the laser scanner, i.e. approximately 0.02 m.

5 Future Activities

IAEA and ENER plan to use the MLSP for future DIV/BTC verifications at the ONKALO underground repository in Finland as described above and it might be similarly be applied at other facilities.

JRC will further develop the system to make it more applicable for indoor localization during complementary access activities. Inter alia, JRC plans to i) implement a SLAM approach so that MLSP can be used without prior availability of a 3D reference model and ii) provide an interface to easily integrate with other in-field tools, location-based applications and HQ infrastructure.

Furthermore, MLSP will benefit from related technology advances: i) the miniaturization of 3D sensors will continue and therefore the overall size and weight of the system will reduce and ii) further developments in augmented and virtual reality technologies (such as Google Glass) will complement MLSP's accurate 3D positioning capability to provide enhanced infield inspection tools.

6 Conclusion

The paper describes the Mobile Laser Scanning Platform (MLSP), which was developed at the JRC for nuclear safeguards applications. MLSP is a portable system that combines a mobile 3D laser scanner with on-board processing for real-time localization, tracking and change analysis.

Mobile laser scanning can complement traditional stop-and-go laser scanning for DIV/BTC verification, thus significantly reducing the required acquisition and processing time. IAEA and ENER intend to use mobile laser scanning for future DIV/BTC verification at the Finnish underground repository to verify that no undeclared modifications to the facility have occurred.

Indoor localization is an enabling technology for many location-based applications and facilitates the storage, analysis and retrieval of observations and measurements made by an inspector, for example in complementary access scenarios. Mobile laser scanning provides an indoor localization accuracy which is currently not achievable with any other technology and therefore has the potential to significantly increase the inspector's efficiency and effectiveness during specific missions such as complementary access inspections. Future developments will further increase the applicability of 3D-based indoor localization for nuclear safeguards.

References

[1] E. Agboraw, S. Johnson, C. Creusot, S. Poirier, H. Saukkonen, B. Chesnay and V. Sequeira, "IAEA experience using the 3-Dimensional Laser Range Finder," in *IAEA Safeguards Symposium: Addressing Verification Challenges*, Vienna, 2006.

[2] P. Chare, Y. Lahogue, P. Schwalbach, A. Smejkal and B. Patel, "Safeguards By Design – As applied to the Sellafield Product and Residue Store (SPRS)," *ESARDA Bulletin (46),* pp. 72-78, 2011.

[3] C. Sanchez, P. Taddei, S. Ceriani, E. Wolfart and V. Sequeira, "Localization and Tracking in Known Large Environments using Portable Real-time 3D Sensors," *Computer Vision and Image Understanding,* Submitted.

[4] Y. Chen and G. Medoni, "Object modelling by registration of multiple range images," *Image Vision Computing 10 (3),* 1992.

[5] P. Taddei, C. Sanchez, S. Ceriani, E. Wolfart and V. Sequeira, "Pose Interpolation SLAM for Moving 3D Lidar Sensors," in *International Conference on Intelligent Robots and Systems*, Hamburg, 2015 (Submitted).

[6] IAEA, "User Requirements - Technology Evaluation Workshop of Core Components of an Autonomous Navigation and Positioning System for Safeguards (SG-UR-12711)," IAEA, Vienna, 2014.

[7] IAEA, "Report - Technology Evaluation Workshop - Autonomous Navigation and Positioning Systems - Results (SG-RP-13057)," IAEA, Vienna, 2014.

[8] Microsoft Research, "Microsoft Indoor Localization Competition - IPSN 2015," [Online]. Available: http://research.microsoft.com/en-us/events/indoorloccompetition2015/. [Accessed 30 04 2015].

[9] EC - JRC, "Demonstration of real-time change monitoring in tunnel environment.," [Online]. Available: http://npns.jrc.ec.europa.eu/Upload_NUSAF/Tunel-Walking.avi. [Accessed 04 05 2015].

Session 14

Combined Analytical Techniques

A user-friendly tool for easy and fast in-field Monte Carlo simulation of neutron collars

Paolo Peerani[1], Hamid Tagziria[1], Mario Vescovi[2], Paul de Baere[3], Peter Schwalbach[3], Stefano Vaccaro[3]

1) European Commission, Joint Research Centre (JRC), Institute for Transuranium Elements (ITU), Nuclear Security Unit, Via Enrico Fermi 2749, 21027 Ispra (VA), Italy
2) i-Science Srl, via Amedei 6, 20123 Milano, Italy
3) European Commission, DG Energy, Directorate of Nuclear Safeguards, Euroforum building, Luxembourg

E-mail: paolo.peerani@jrc.ec.europa.eu

Abstract:

Monte Carlo codes have found applications in nuclear safeguards as complementary tool in Non-Destructive Assay (NDA). Up to now, the use of Monte Carlo has been limited to specialised experts, due to the complexity of the modelling and to the skills required to properly use the code. In order to open the direct in-field use by nuclear inspectors, JRC and i-Science have developed XFUELBUILDER. This is a program that allows the inspector to prepare an MCNP-PTA input deck using a simple and user-friendly graphical interface, and then running the calculation simulating the measurements done with neutron coincidence collars.
This paper describes the functionalities of XFUELBUILDER and discusses the potential implications for its in-field use.

Keywords: neutron counting; Monte Carlo

1. Introduction

Monte Carlo codes are classical tools for computational simulation of particle and radiation transport in experimental physics [1]. They have found applications in nuclear safeguards as complementary tool in Non-Destructive Assay (NDA). Monte Carlo simulation has been extensively used for design optimisation of neutron counters [2, 3, 4, 5], for parametrical studies on the influence of different parameters on the detector response and, last but not least, to perform numerical calibration of counters in absence of suitable calibration samples.

JRC has developed MCNP-PTA [6], an extension of the classical Monte Carlo code from Los Alamos, specifically intended to simulate the response of neutron coincidence and multiplicity counters used in nuclear safeguards. The code adds to the standard model of neutron transport the possibility to reproduce the functionalities of the electronics used in neutron coincidence and multiplicity counting.

Models for a large variety of counters used by IAEA and Euratom have been developed and validated [6, 7, 8, 9, 10], providing an extremely satisfactory accuracy in the prediction of detector response, typically within few percent with respect to experimental data.

Up to now, the use of Monte Carlo has been limited to specialised experts, due to the complexity of the modelling and to the skills required to properly use the code. In order to open the direct in-field use by nuclear inspectors, JRC and i-Science have developed XFUELBUILDER. This is a program that allows the inspector to prepare an MCNP-PTA input deck using a simple and user-friendly graphical interface, and then running the calculation. This paper describes the functionalities of XFUELBUILDER and discusses the potential implications for its in-field use.

2. Main functionalities of XFUELBUILDER

XFUELBUILDER has already built-in the models of several neutron coincidence collars (JCC-71, 72 and 73), in thermal or fast configuration. The inspector can retrieve from a library the model of the fuel element (or build it if not already available) and introduce the operator's declaration. This is all he needs to do before launching the simulation that will provide the Totals and Reals count rates expected in the selected collar configuration.

When launching the application, the user has the possibility to select one of the main features allowed by the code that include the creation of new pin or assembly geometry, manage the library of existing pins/assemblies, the definition of measurement conditions, operator's declarations and Monte Carlo run parameters. Figure 1 shows the main entry screen.

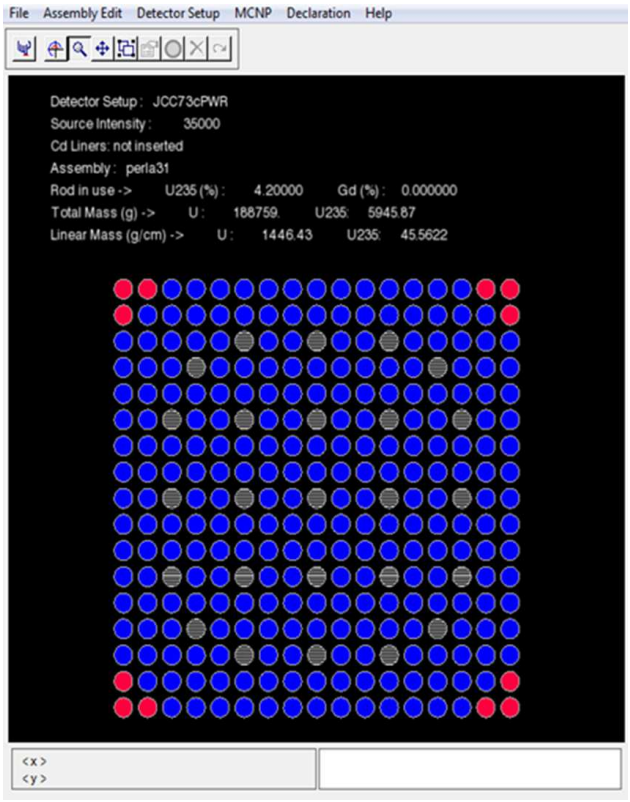

Figure 1: Screenshot of the main window of XFUELBUILDER

2.1. Build the fuel assembly geometry

To build new fuel assembly geometry, the user must first define the geometry of the pins and then the geometry of the lattice.

2.1.1. Pin geometry

To create a new pin the user must select the "Rod Edit" option in the task bar. A pin is defined by its radial dimensions (pellet, inner and outer clad diameters), the active length and the materials. For the clad composition the user can select from a drop-down menu the most common cladding materials (Zircalloy or stainless steel). Concerning fuel the current version of XFUELBUILDER is limited to uranium oxide, the only parameters to define is the nominal enrichment and eventually the gadolinium content if burnable poison rod.

XFUELBUILDER 2.0 allows axial heterogeneity of pins with multiple zones with different enrichments and/or poisoning. Any pin geometry can be saved with a “Rod Name” for use in different assembly geometries.

2.1.2. Lattice geometry

A fuel bundle is then built by assembling the pins in a lattice, using the “Assembly Edit” menu. The current version accepts only square lattices: then the lattice is determined simply by fixing the number of rows/columns and their pitch.

Once the empty lattice is defined, a simple graphical interface allows the user to fill the cells with the appropriate content: fuel pins (different fuel pins are allowed in the same assembly), poison rods, guide tubes or empty cells.

Any assembly geometry can be saved for future use.

2.2. Retrieve an assembly from a library

There are a limited number of PWR and BWR fuel assembly types used in European reactors. Therefore it is possible to pre-build the XFUELBUILDER library with the most common models. In this case, accounting for the large majority of cases, the inspector will not need to use the functionality for building the assembly, but he will have simply to retrieve from the library the assembly type of his interest.

2.3. Match the operator’s declaration

Once the nominal geometry of the assembly is defined, the uranium mass is fixed and determined by the fuel volume, the theoretical density of uranium oxide and the ideal stoichiometric uranium mass fraction in UO2. Then the U-235 mass is determined by the uranium mass and the nominal enrichment. As soon as an assembly is created or retrieved from the library, XFUELBUILDER computes and displays the nominal values of total uranium and U-235 masses (total in grams and linear in g/cm).

Then the inspector should provide the declared values of the actual element he wants to simulate. The code will rescale the nominal values in order to match the declared values. The reconciliation of the total uranium mass is done by adjusting the fuel density, whereas the U-235 mass is corrected using the declared enrichment (U-235/U mass).

2.4. Define the measurement parameters/conditions

Having completed the fuel assembly model, the detector and measurement conditions must be defined using the “Detector Setup” menu. The models of the most commonly used neutron collars are pre-built in XFUELBUILDER: the JCC-72 for BWR, the JCC-73 for PWR and the variable JCC-71 in PWR and BWR configuration. The detector can be selected from the menu.

Neutron collars can be operated in thermal or fast mode, which means without or with cadmium liners within the detector cavity. Also the thermal/fast mode configurations can be simply selected from the menu.

The next operational parameter to provide is the intensity of the AmLi source: this value can be either known from a calibration certificate or through cross-reference with a calibrated source. In case the intensity is not available it can be computed using XFUELBUILDER itself by the comparison of a simulation with empty fuel cavity with respect to a measurement with source and without fuel.

Finally, in case of axially heterogeneous elements, it becomes relevant to define the axial position of the detector. This can be done by activating the “Set 3D Collar Position” option, which allows moving the detector along the assembly length in a three-dimensional visualisation (figure 2).

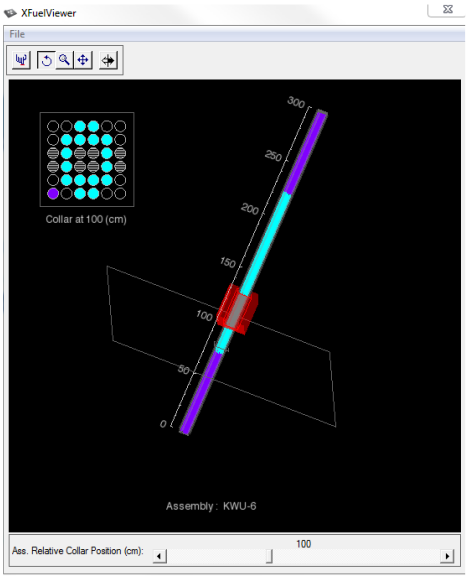

Figure 2: 3D panel for axial positioning of the collar

2.5. Run the Monte Carlo simulation

The user can finally launch the simulation by selecting the “Run MCNP” button. Monte Carlo run set-up parameters can be optionally adjusted: definition of the modality of termination of the simulation (by total number of neutrons or computing time or both), maximum number of simulated neutrons, maximum computing time, number of repetitions of PTA (Pulse Train Analyser).

XFUELBUILDER runs in sequence the MCNP module for neutron transport simulation, then the PTA module for the construction of the time distribution of pulses and simulation of the coincidence electronics (JSR-12) and at the end it prints the results: Simulated measurement time, Total neutron counting rate, coincidence rates (Reals and Accidentals) and associated statistical uncertainties.

3. Impact of simulation on in-field inspections

The use of XFUELBUILDER opens a possibility of changing the way verification are performed by replacing the classical method (measure the item, convert Reals to mass through the calibration law and compare measured versus declared mass) with a novel approach (measure the item, build a MC model from declaration, simulate the measurement, and compare measured versus expected count rate) that will eliminate the need of calibration [11].

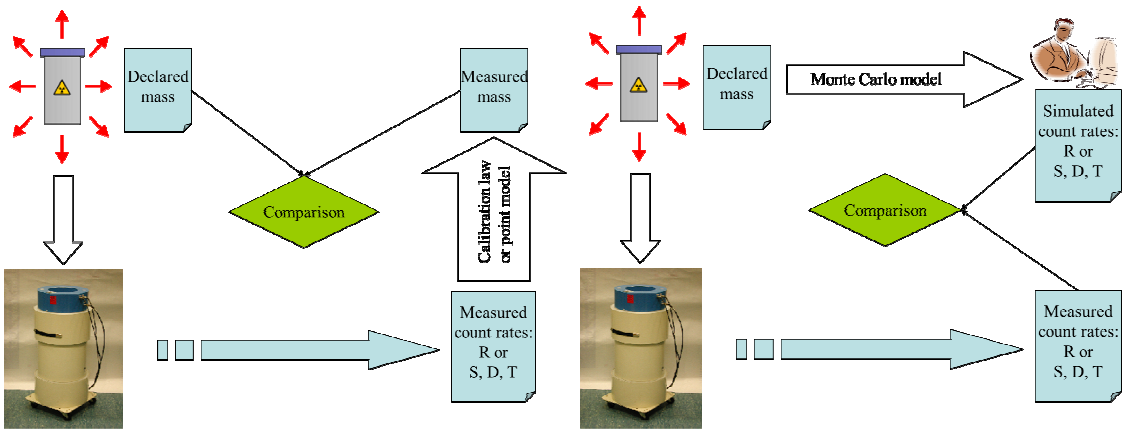

Figure 3: classical and new verification process [11]

4. Conclusions

XFUELBUILDER is a new approach to the use of Monte Carlo in NDA techniques for safeguards, allowing the in-field use by nuclear inspectors. Its user-friendly human-computer interface has been conceived in order to enable non-experts in nuclear physics to generate an input deck and run the Monte Carlo simulation on his laptop.

Using XFUELBUILDER, the inspector will be able to verify the operator's declarations by comparing the measurements of fresh fuel assemblies with neutron coincidence collars and the predictions from the Monte Carlo simulations. This will eliminate the need of specific calibrations or the use of corrective factors for the measurements of complex fuel elements containing burnable poisons and/or other radial/axial heterogeneities.

5. References

[1] J.F.Briemeister: "MCNP – A General Monte Carlo N-particle Transport Code", LA-13709-M, LosAlamos, 2000.

[2] M. Marin Ferrer, P. Peerani, M. Loman, L. Dechamp: "Design and performances of the Scrap Neutron Multiplicity Counter", Nucl. Instr. & Meth. in Phys. Res. A, vol. 574, (2007), 297-314.

[3] P. Peerani et al.: "Development of high-efficiency passive counters (HEPC) for the verification of large LEU samples", Nucl. Instr. & Meth. in Phys. Res. A, vol. 601, (2009), 326-332.

[4] A. Tomanin et al.: "Design of a liquid scintillator-based prototype neutron coincidence counter for Nuclear Safeguards", ESARDA BULLETIN, No. 49, June 2013, 4-12.

[5] P. Peerani, A.L. Weber: "Analysis of uncertainties affecting the Monte Carlo simulation of a neutron multiplicity counter", Radiation Measurements, vol. 47, (2012), 475-480.

[6] M. Looman, P. Peerani, H. Tagziria: "Monte Carlo simulation of neutron counters for safeguards applications", Nucl. Instr. & Meth. in Phys. Res. A, vol. 598, (2009), 542-550.

[7] H. Tagziria, P. Peerani, P. De Baere, P. Schwalbach: "Neutron coincidence counter for the verification of PuO2 cans", Nucl. Instr. & Meth. in Phys. Res. A, vol. 580, (2007), 377-379.

[8] H. Tagziria, J. Bagi, P. Peerani, A. Belian: "Calibration, characterisation and Monte Carlo modelling of a fast-UNCL", Nucl. Instr. & Meth. in Phys. Res. A, vol. 687, (2012), 82-91.

[9] P.Peerani, G.Bosler, I.Cherradi, P.Schwalbach: "Computational calibration of neutron collars for the verification of HEU fuel elements", Proceedings of the 45th INMM Annual Meeting, Orlando ,FL, 18–22 July 2004.

[10] P.Peerani, J.Tanaka: "Calibration of neutron collars for fresh fuel element verification", Proceedings of the 27th Annual Symposium on Safeguards and Nuclear Material Management, London, UK, 10–12 May 2003.

[11] P. Peerani, H. Tagziria, M. Looman: "Real-time simulation of neutron counters", Radiation Measurements, vol. 43, (2008), 1506-1510.

Non-destructive measurement of the plutonium content of high-active liquid waste

J. Zsigrai[1], A. Le Terrier[1], K. Casteleyn[1], G. Duhamel[2], A. Maddison[3], J.-G. Decaillon[2], A. Bosko[3]

[1]European Commission, Joint Research Centre, Institute for Transuranium Elements, Postfach 2340, 76125 Karlsruhe, Germany
[2]International Atomic Energy Agency, Safeguards Analytical Services, Tokyo Regional Office, Seibunkan Bldg. 9F, 1-5-9 Iidabashi, Tokyo 102-0072, Japan
[3]International Atomic Energy Agency, Safeguards Analytical Services, A-1400 Vienna, Austria

Abstract:

To verify that all Pu in a reprocessing plant is accounted for, IAEA inspectors need a method for measuring Pu in high-active liquid waste (HALW) remaining after reprocessing of spent fuel. Some of the Pu in HALW is attached to undissolved residues. However, constraints at the IAEA on-site laboratory do not allow use of common destructive methods to measure Pu in the residues. The non-destructive method presented here is based on X-ray fluorescence (XRF) measurement combined with stirring the particles. Tests with known amounts of Uranium in simulated HALW were done using a miniature stirrer installed into a modified sample changer. During these tests the hardware parameters have been optimized. Furthermore, it was shown that the XRF peaks of undissolved residues can be seen by stirring the synthetic HALW. The optimal stirrer speed has been determined and the shielding effect of the particles has been quantified. Hot tests with real HALW are planned to be done in the EURATOM on-site lab in La Hague, France, in co-operation with the French support programme. The planned implementation of the method at the IAEA laboratory will enable the verification of the total Pu content of HALW.

Keywords: Hybrid K-Edge, XRF, reprocessing, liquid waste, plutonium, residues,

1. Introduction

In this work a method for measuring the Pu concentration in high-active liquid waste (HALW) that contains particles is presented. HALW is what remains after reprocessing of spent fuel. It includes concentrated fission products, fines suspension and alkaline liquid waste [1].

IAEA inspectors need a robust method for timely measurement of Pu in HALW at reprocessing plants to prove that there is no significant amount of Pu in the HALW. This measurement in some specific material balance areas needs to be done before HALW is introduced to the vitrification process. The method routinely used by IAEA to measure Pu in homogeneous liquids at reprocessing plants, Hybrid K-Edge/K-XRF densitometry [2], cannot be directly applied because HALW is not homogeneous and a significant part of the Pu in the HALW is attached to undissolved particles. The methods applied by the operators of reprocessing plants to measure the Pu in HALW (such as dissolution in a pressurized vessel under high temperature) are complicated and practically cannot be implemented in the IAEA laboratory due to safety and other on-site constraints.

Therefore, in 2009 the IAEA launched a support programme request for developing a method compatible with on-site constraints and not requiring major new hardware or modification of the existing instrumentation. The French and European Commission's support programmes accepted the task.

Under this joint task the Institute for Transuranium Elements (ITU) is developing a method using the XRF branch of the Hybrid K-edge/K-XRF setup combined with homogenizing the HALW by a miniature stirrer. The method is being developed in ITU using simulated HALW. To be able to use the stirrer for HALW measurements in a hot cell, ITU designed a mechanical setup which does not interfere with the usual operation of the instruments in the hot cell. The method is planned to be tested in 2015 with real HALW in the EURATOM on-site laboratory in La Hague in co-operation with AREVA and the French support programme.

2. Method

The HALW sample is irradiated by a 150 kV X-ray tube. This produces X-ray fluorescence (XRF) of the elements, including U and Pu, present in the sample. The fluorescent X-rays emitted by the samples are recorded by a high-resolution gamma spectrometer. The intensity of the peaks in the XRF spectrum increases with the concentration of the elements emitting these XRF peaks in the observed sample volume. For homogeneous samples this represents the concentration of these elements in the entire sample.

HALW is not homogenous, because it contains particles which settle to the bottom of the sample jug. Therefore, they are not in the field of view of the XRF spectrometer. In this study the HALW is homogenized by a miniature stirrer during the XRF measurement, so that the XRF detector can "see" the particles,

The concentration of the Pu attached to the particles can be deduced from the difference between the measurement with stirrer on and stirrer off. The Pu concentration in the HALW is very low, both in the particles and in the supernatant (in the order of the mg/l). Furthermore, the XRF spectrum is "flooded" by high background radiation from the fission products in the HALW. Therefore, it might be difficult to evaluate the small Pu XRF peaks from the spectrum of real HALW and the uncertainties will be quite high. Nevertheless, it is expected that giving an upper limit on the Pu concentration in the HALW would be sufficient to show that there is no significant amount of Pu in the waste stream.

3. Instruments and materials

The X-Ray fluorescence branch of a hybrid K-edge/K-XRF densitometry (HKED) system available in ITU was used for method development. HKED systems are widely used around the world in reprocessing facilities to quantify the U and Pu content in reprocessing solutions. The particular setup used for the present studies is similar to the setups that are in use at the EURATOM on-site laboratory in La Hague, France and in the IAEA on-site laboratory in Rokkasho, Japan.

The main parts of the system are a 150 kV X-ray tube and two high-resolution gamma spectrometers (one for recording the transmitted X-ray spectrum and one for the X-ray fluorescence spectrum). The samples are introduced into the shielded measurement position by a sample changer, which accepts cylindrical sample jugs (the so called "COGEMA cruchons"). The detectors are controlled by Canberra Lynx electronics.

The XRF spectra were evaluated using the software "XRF" developed by R. Gunnink, based on detector response fitting.

A magnetic stirrer (12 × 12 × 5 mm) which fits inside the cavity of the sample changer was used (Variomag Mini produced by Thermo Scientific) to homogenize the material. As the stirrer has a height of 5 mm, the height of the sample cruchon had to be slightly reduced, in order that in can safely enter the tunnel of the HKED setup.

The system used for the studies in ITU is connected to a glove box which is not yet closed. Due to radiological safety reasons, no Pu measurements could be done at this box. Therefore, uranium was used to optimize the measurement setup and to develop the method. The results should apply by analogy to Pu, with minor modifications.

A synthetic waste solution containing the inactive isotopes of the elements which are present in real HALW, as well as particles composed of those elements, was used to simulate the samples expected in the waste of reprocessing plants. The synthetic HALW was donated to ITU by the Karlsruhe Institute of Technology, Institute for Nuclear Waste Disposal, Karlsruhe, Germany. Pure uranium solution was mixed to the synthetic waste in different proportions, to obtain different uranium and particle concentrations.

4. Results

4.1. Optimal sample position

In the "classical" HKED setup the sample position is a compromise between K-edge and XRF measurement. For the present application, however, the sample should be positioned in such a way, as to achieve the lowest possible detection limits for the XRF measurement. Therefore, the sample changer positions for which the count rate of the uranium XRF peaks is the highest in the HKED setup used in ITU were determined. These positions do not coincide with the positions of highest KED count rates.

4.2. Optimal stirrer bar and control unit

Five types of stirrer bars and two types of controllers were tested. The power of the default controller unit (7 W) was not sufficient to move the stirrer bars in the simulated HALW and all bars got stuck in the viscous medium of the undissolved residues. Therefore, a more powerful control unit (Telemodul 20C) was purchased, which is able of supplying up to 20 W power to the stirrer motor.

With the Telemodul 20C it was established that only one type of the available stirrer bars is able to stir the simulated HALW: the rounded cylindrical "Power Magnet" of 10 mm length and 6 mm diameter. All the other bars get stuck in the viscous medium and are unable to stir the simulated HALW, even at maximum power setting. Therefore, the cylindrical "Power Magnet" stirrer bar with dimensions 10 mm × 6 mm was selected for the further tests.

4.3. The effects of stirring

The experiments have shown that stirring has no effect on pure HNO_3 and clear U solutions. That is, the stirrer bar is below the field of view of the collimator and the detector does not "see" it.

In the synthetic HALW the XRF peaks of undissolved residues become visible in the spectrum when the stirrer is turned on. That is, the stirrer brings the particles into suspension, so that the detector can see them. This is illustrated in Figure 1.

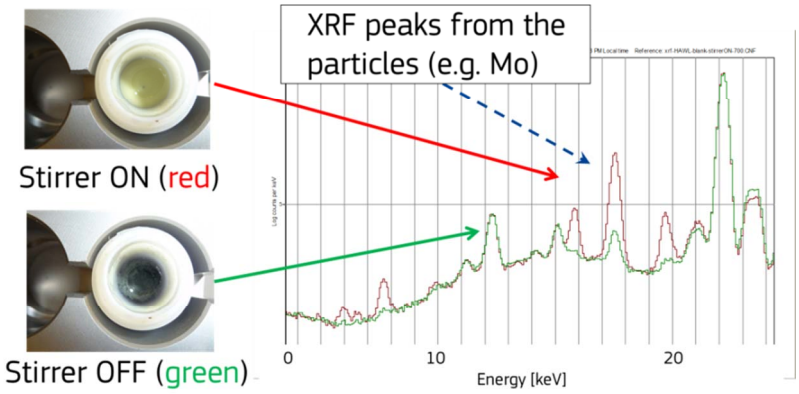

Figure 1. XRF spectra of simulated HALW. The XRF peaks from the un-dissolved residues are clearly higher for the spectrum with stirrer ON.

4.4. Optimal stirrer speed

The stirrer speed was varied from 0 to 1100 rpm and the height of several XRF peaks of the elements in the simulated HALW was recorded. It has been observed that turning the stirrer on has different effects on two groups of peaks: for one group the peak height increases, while for the other group the peak height decreases.

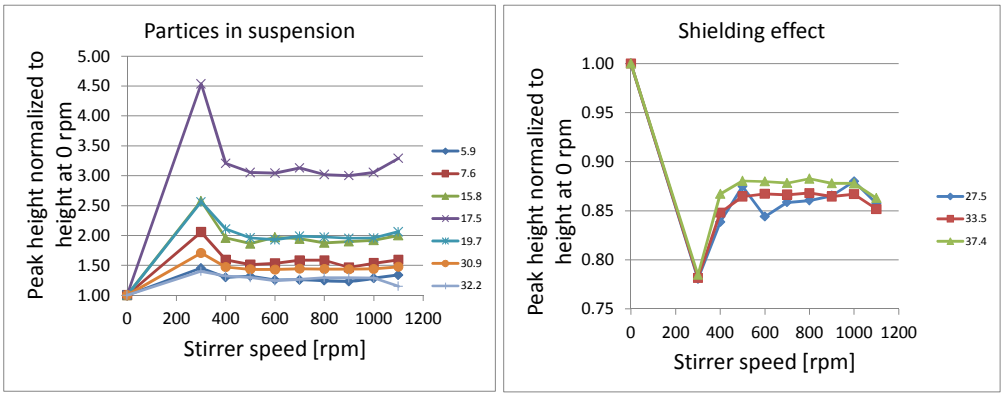

a) b)

Figure 2. The dependence of the peak height of several XRF peaks on the stirrer speed (The peak height is normalized to the height measured with stirrer off.) The numbers in the legend denote the energies of the XRF peaks in keV.

In Figure 2 we can see that for the first group the height of the XRF peaks of the elements present in the particles increases as soon as we turn on the stirrer at 300 rpm. As we further increase the stirrer speed the peak height drops. This is explained by the fact that when the stirrer rotates slowly the particles from the bottom of the sample jug rise slightly from the bottom coming into the view of the XRF collimator. However, the stirrer speed at this point is not enough to homogenize the suspension and the particles concentrate in the lower part of the jug in front of the collimator. As we increase the stirrer speed some particles rise higher and go to the volume which is above the collimator. As we see in Figure 2a) at 500 rpm the peak height reaches a plateau, which extends up to 1000 rpm. This means that when the stirrer speed is between 500 and 1000 rpm the particles are homogeneously distributed in the volume of the sample jug and small variations of the stirrer speed do not change the concentration of the particles in the view of the collimator. At 1100 rpm the stirrer bar starts to jump and to move chaotically causing some of the particles to fall to the lower part of the sample jug, increasing again the concentration of the particles in front of the collimator.

Figure 2b) shows an opposite effect. For the XRF peaks of the elements which are mainly present in the liquid phase (and possibly not present in the solid particles) there is a shielding effect from the particles. At low speeds there are many solid particles in front of the collimator so they shield the radiation coming from the elements present in the liquid phase. Between 500 and 1000 rpm there is a plateau of the height of the XRF peaks of the shielded elements corresponding to the constant concentration of particles in front of the collimator.

These measurements confirm that the optimal stirrer speed for the simulated HALW samples is at the middle of the plateau, that is, around 700 rpm.

4.5. Shielding effect of the particles

In order to estimate the shielding effect of the particles synthetic HALW was used. The original synthetic HALW ("mother solution") contained 11 g/l of particles. It was diluted and concentrated to obtain HALW solutions with 6 g/l and 19 g/l of particles. Then, known amounts of uranium solution were added to the synthetic HALW to achieve a U concentration of 30 g/l. Adding the U solution to the HALW caused dilution of the particles in the HALW giving final particle concentrations of 4, 8, and 14 g/l.

As in the synthetic HALW the particles did not contain any U, there was no increase of the intensity of the U XRF peaks from the particles when the stirrer was turned on. On the contrary, the intensity of the relevant XRF peaks of U decreased due to absorption by the particles. The decrease was 0.091 % for each g/l of particles. This means that for a typical particle concentration of ~10 g/l, the bias can go up to ~1 %

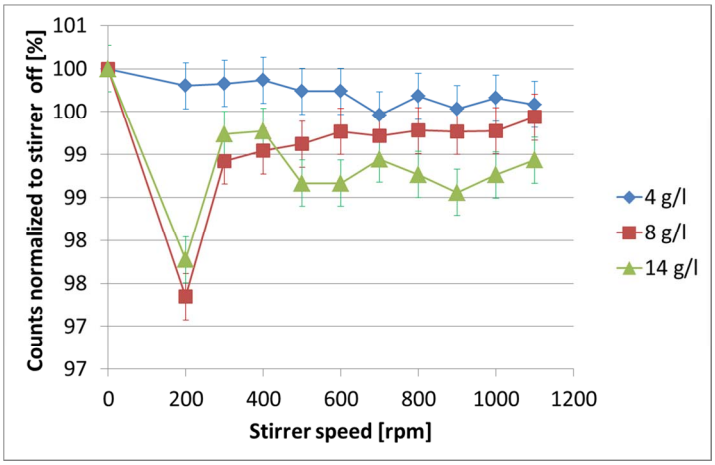

Figure 3. Counts of the U Kα1 peak in the synthetic HALW doped with U solution as a function of stirrer speed. The counts are given as the percentage of the counts with the stirrer off, for particle concentrations of 4, 8, and 14 g/l. The counts are unstable for low stirrer speeds because some of the particles are already in the view of the collimator while the solution is not yet homogenized. Above 500 rpm the particle distribution becomes homogeneous and it is clearly seen that the shielding effect is the highest for the highest particle concentration.

To measure the Pu content of HALW in the reprocessing plant, the XRF detector has to be calibrated with well characterized HALW, having well known particle concentration and well known Pu content in the particles and in the supernatant. Using this kind of well characterized HALW a bias-correction procedure can be implemented.

4.6. Confirming that pure HNO_3 can be used as reference for the background continuum

To evaluate the areas of the XRF peaks from the spectra, the "XRF" software needs a reference spectrum to be able to subtract the contribution of the background X-ray continuum. For pure U and Pu solutions without particles, the reference spectrum is the spectrum of a pure HNO_3 solution which has the same molarity as the solution with U and Pu. For HALW, however, the matrix is not pure HNO_3, but a solution with undissolved particles. Therefore, we investigated whether we should use this kind of matrix for obtaining the reference spectrum.

For this investigation we recorded at each stirrer speed also the spectrum of the "blank", that is, the spectrum of the synthetic HALW which had (roughly) the same particle concentration as the sample with U. Then we analysed each sample spectrum in two ways: using the spectrum of pure HNO_3 as reference and using the spectrum of the synthetic HALW as reference.

We calculated the difference between the two types of evaluations and obtained that it is -0.09 % on average. The difference is less than the combined statistical uncertainty of the peak areas (0.27 %). We noticed, however, that the result obtained with synthetic HALW as reference is always lower. Nevertheless, if we evaluate the calibration solutions in the same way using pure HNO_3 as reference, this small bias is expected to be automatically removed from the result for Pu concentration. Therefore, pure HNO_3 can be used for recording the XRF reference spectrum.

5. Conclusion

A method is being developed for measuring the Pu concentration in high-active liquid waste (HALW). The method should enable the safeguards inspectors to verify that no significant amounts of Pu are present in the liquid waste of reprocessing plants.

The method is based on using the XRF branch of the HKED instrument combined with stirring the particles by a miniature stirrer. Tests were done with a HKED instrument available in ITU. Various hardware parameters were optimized using synthetic (simulated) HALW mixed with uranium.

Tests with real HALW are planned to take place soon in a hot cell in the EURATOM on-site laboratory at the reprocessing facility in La Hague, France, in co-operation with the French support programme. For these tests real HALW will be used, characterized by the operator of the reprocessing plant. If the hot tests are successful the method can be implemented at the IAEA laboratory.

References

[1] K. Nakamura, N. Kanehira, T. Fukui, Y. Tanaka, M. Yoshioka, and T. Hamada, "Characteristics of Insoluble Residues in High Active Liquid Wastes at RRP," *Proceedings of the GLOBAL 2009 congress - The Nuclear Fuel Cycle: Sustainable Options and Industrial Perspectives*. France, p. 567, 2009.

[2] H. Ottmar and H. Eberle, "The hybrid K-edge/K-XRF densitometer: Principles-design-performance, Kernforschungszentrum Karlsruhe Report KFK4590," 1991.

Relative Actinide K-Shell Vacancy Production Rates in Hybrid K-Edge Densitometry

Robert D McElroy Jr, Steve L. Cleveland, Stephen Croft, George Spencer Mickum, and Andrew D. Nicholson
Oak Ridge National Laboratory
Oak Ridge, Tennessee 37831
E-mail: mcelroyrd@ornl.gov, clevelandsl@ornl.gov, crofts@ornl.gov, gsmickum@gmail.com, nicholsonad@ornl.gov

Abstract:

The Hybrid K-Edge Densitometer (HKED) is an active X-ray interrogation system combining K-Edge transmission densitometry (KED) and X-Ray Fluorescence (XRF) analysis for the determination of the actinide concentrations of dissolver solutions in the reprocessing of spent nuclear fuel. The hybrid analysis requires knowledge of the relative K-shell vacancy production rates in order to determine the concentration of minor actinides (i.e., Np, Pu, Am, and Cm) relative to the primary actinide (typically U for present commercial power reactors). The K-shell vacancy production rates vary with sample composition and energy distribution of the interrogating X-ray flux within the sample. Commercially available HKED analysis software currently employed for international safeguards applications includes a simple correction for the impact of U concentration on K-shell vacancy production rates and is suitable only for U:Pu concentration ratios around 100:1. In this paper we present a more complete representation of K-shell vacancy production rates for use in the HKED analysis, thereby extending the applicability of the hybrid analysis to a broader range of U:Pu concentration ratios (e.g., 1:1) as well as the inclusion of additional actinides (i.e., Np, Am, Cm). This approach incorporates the energy distribution of X-rays from the generator directly into the determination of the relative K-shell vacancy production rates, removing a potential source of bias (the impact of which has been found to be significantly greater than previously estimated) in the determination of the relative actinide concentrations.

Key words: hybrid K-edge densitometry; actinide K-shell photo-ionization; matrix correction

1. Introduction

The HKED measurement combines two separate measurement techniques, K-edge densitometry (KED) and relative X-ray fluorescence (XRF) analysis, to ultimately determine the concentration of both uranium and plutonium in dissolver solutions [1]. In its “hybrid” analysis mode, the KED transmission measurement provides the concentration value for the dominant actinide component of the solution (typically U) while the concentrations of minor actinide components (e.g. Pu, Np, Am) are determined relative to the U concentration by means of the XRF measurement. This combination of methods allows the HKED to provide both accurate and sensitive assay of the sample across a wide dynamic range of actinide concentrations within a sample.

Historically, the HKED system was used to examine a fairly narrow range of actinide sample compositions. Typically uranium was the dominant component of the solution while the other actinides might be present at near impurity levels constituting 1 to 2% or less of the total actinide content. The system and its associated software were optimized for these solutions characterized by U:Pu concentration ratios of 100:1. More recently efforts have been undertaken to extend the capability of the HKED technique to a broader mixture of actinide concentrations (e.g. U:Pu =1:1) and to include the capability for quantitative assay of actinides other than U and Pu [2, 3, 4, 5, 6]. To date these

efforts have largely focused on the multi-elemental KED analysis. The inclusion of multi-elemental capabilities into the Hybrid XRF analysis is a two part problem, the first is development of a proper spectrum fitting methodology for the XRF spectra that can yield accurate relative peak areas for the minor actinides in the presence of both the major elemental components and fission products, the second is the development of an accurate method for converting the observed peak areas to relative concentration values. This paper focuses on the later need.

2. Relative Peak Intensities to Relative Actinide Concentrations

The intensity of the characteristic X-rays emitted through the fluorescence reaction is proportional to the number of K-shell vacancies produced in each elemental component of the sample solution. The K-shell vacancy rates in each element are influenced by the presence of the other elements in the solution primarily through attenuation of the interrogating X-ray beam.
The traditional HKED Hybrid analysis [1, 7] was developed for use with aqueous dissolver solutions, where uranium is the dominant actinide, the uranium-to plutonium ratio is approximately 100 to 1, and other actinides (e.g., Am) can be treated as impurities. The relative U:Pu concentration is determined from a ratio of the uranium and plutonium $K_{\alpha 1}$ peaks [7] and a semi-empirically determined conversion coefficient, $R_{U/Pu}$. In this analysis the U:Pu concentration ratio is given by

$$U{:}Pu = \frac{A_U}{A_{Pu}} \cdot \frac{I_{UK\alpha 1}}{I_{PuK\alpha 1}} \cdot \frac{\varepsilon_{PuK\alpha 1}}{\varepsilon_{UK\alpha 1}} \cdot \frac{1}{R_{U/Pu}}, \quad (1)$$

where $R_{U/Pu}$ is related to a calibration parameter, $R^0_{U/Pu}$, adjusted for the attenuation due to the uranium in the sample

$$R_{U/Pu} = R^0_{U/Pu} \cdot e^{\alpha \cdot [U]}, \quad (2)$$

where

$$\alpha = 1.81079 \cdot 10^{-6} - 1.61582 \cdot 10^{-4} \cdot d_{vial} + 4.16665 \cdot 10^{-5} \cdot d^2_{vial}, \quad (3)$$

and
d_{vial} is the diameter of the sample vial in cm
$I_{UK\alpha 1}$ is the count rate in the uranium $K_{\alpha 1}$ peak
$I_{PuK\alpha 1}$ is the count rate in the plutonium $K_{\alpha 1}$ peak
A_U and A_{Pu} are the atomic weights of U and Pu respectively
$\varepsilon_{PuK\alpha 1}$ is the detection efficiency for the plutonium $K_{\alpha 1}$ X-ray
$\varepsilon_{UK\alpha 1}$ is the detection efficiency for the uranium $K_{\alpha 1}$ X-ray and
[U] is the uranium concentration within the sample in g/liter

For the most common type of HKED system and traditional U:Pu dissolver solutions (U: 100 to 300 g/U and U:Pu~100), $R^0_{U/Pu} \approx 1.5$.

In the traditional analysis the conversion factor, $R_{U/Pu}$, captures both the relative K-shell vacancy production rate and the attenuating impact of the matrix on the emitted fluorescence X-rays. The Eq.3 accurately reproduces the behavior of the conversion factor as a function of uranium density. References [1, 7] also detail a similar expression for the Am conversion factor, $R_{U/Am}$. However, this semi-empirical treatment has three drawbacks

1. The relationship is only valid for U:Pu ratios of approximately 100:1.
2. While in principle the method described in Ref. [1] can be extended to other elements, to date it has not yet been implemented in the common software packages.
3. The constant, R_0, must be determined through calibration with a variety of U-Pu solutions and is unique for each HKED instrument.

In developing the expressions in Eqs. 1 to 3 Ottmar et.al. appear to have followed a similar process to that described in the following sections, however, rather than working to provide a simplified algorithm set targeted towards limited elemental compositions, we seek to develop a robust solution applicable to an arbitrary mix of actinides.

3. Expanded Approach

The traditional method assumes an approximate U:Pu concentration ratio of 100:1 and that the other actinides will be present at even lower levels. For these solutions the impact of the minor actinides on the U:Pu ratio is small and is generally neglected. The more complex solutions will require that the attenuating effects on the interrogating X-ray spectrum and the fluoresced X-rays be addressed. Additionally, the fluorescence X-rays from the higher Z actinides can increase the emission rate of fluorescence X-rays from the lower Z actinides, also through the photoelectric effect. (For example, all of the K_{α} X-rays from Pu and Am have sufficient energy to eject a K-shell electron from U while only the $K_{\alpha 2}$, $K_{\alpha 4}$ and $K_{P2,3}$ lines from Np have sufficient energy.) This enhancement effect [8] of the low Z fluorescence rates increases with the relative concentration of the higher Z actinides. To further complicate matters, these effects vary as function of position within the sample vial.

With this in mind we expand Eq. 1 to highlight the various dependences of the U:Pu measurement

$$U{:}Pu = \frac{A_U}{A_{Pu}} \cdot \frac{I_{UK\alpha 1}}{I_{PuK\alpha 1}} \cdot \frac{\sum_i f_{PuKi} \cdot \varepsilon(E_{PuKi})}{\sum_i f_{UKi} \cdot \varepsilon(E_{UKi})} \cdot \frac{1}{\iiint (1 + F_{U:Pu}) \cdot \frac{\int_0^{E_0} \cdot\, g(E) \cdot \rho_{[U]} \cdot \mu_{U,PE}(E) \cdot dE}{\int_0^{E_0} g(E) \cdot \rho_{[Pu]} \cdot \mu_{Pu,PE}(E) \cdot dE} dxdydz}, \quad (4)$$

where $g(E)$ is the interrogating X-ray flux at the detectable interaction region of the sample vial,
$F_{U:Pu}$ is the relative uranium fluorescence rate due to the presence of higher Z actinides,
f_{UK_i} is the relative yield for the i[th] fluorescence X-ray (per K-shell vacancy) in uranium,
f_{PuK_i} is the relative yield for the i[th] fluorescence X-ray (per K-shell vacancy) in plutonium,
$\varepsilon(E_{UKi})$ is the detection efficiency of the i[th] fluorescence X-ray in uranium,
$\varepsilon(E_{PuKi})$ is the detection efficiency of the i[th] fluorescence X-ray in plutonium,
$[U]$ = the uranium concentration within the sample in g/cc,
$[Pu]$ = the plutonium concentration within the sample in g/cc,
$\mu_{U,PE}$ = the mass attenuation coefficient for photoelectric effect in uranium above the K-shell,
$\mu_{Pu,PE}$ = the mass attenuation coefficient for photoelectric effect in plutonium above the K-shell

In the expansion of Eq. 3 we have redefined the conversion factor, $R_{U/Pu}$, from the traditional analysis as

$$R_{U/Pu} = \iiint (1 + F_{U:Pu}) \cdot \frac{\int_0^{E_0} \cdot\, g(E) \cdot [U] \cdot \mu_{U,PE}(E) \cdot dE}{\int_0^{E_0} g(E) \cdot [Pu] \cdot \mu_{Pu,PE}(E) \cdot dE} dxdydz\,, \quad (5)$$

The function for the X-ray energy distribution, g(E) incorporates the properties of the X-ray source and attenuation from all sources between the X-ray tube and the point where the K-shell vacancy is created.

Extension of Eq. 4 for the other actinide components is fairly straight forward and will be addressed later in this paper. First, however, this rather complicated expression needs to be simplified for practical application. In order to accomplish this simplification we need to understand the spatial

distribution of the K-shell vacancies leading to the emission of a detectable fluorescence X-ray. Monte Carlo simulations using the MCNP6 code [9] were used to map the creation of K-shell vacancies that would ultimately lead to the emission of a detectable fluorescence X-ray. Fig. 1 shows the simulated distribution of events within the sample vial containing a nitric acid solution of 321 g U/L within the ORNL HKED system. For the ORNL system, we find that there is a fairly high degree of collimation on the interrogating X-ray beam. This allows us to approximate the spatial distribution of the K-shell production rates as a simple exponential attenuation function (e.g. $I_K = I_{K0} \cdot e^{-\mu\rho t}$). To correct for attenuation of the emitted fluorescence X-ray we need to determine the thickness of the material between the emission point and the edge of the sample vial (the attenuation path length) relative to the distance into the vial where the K-shell vacancy was produced.

The attenuating path length, d_F, for the emitted X-ray as a function of the interrogating path length, d_I, is given as:

$$d_F = \sqrt{d_{vial}^2/4 + d_I^2 - 2 \cdot d_I \cdot d_x}\,, \tag{6}$$

where θ is the angle between the XRF detector collimator and the axis of the interrogating beam and

$$d_x = \frac{(d_{vial}/2 - d_I) \cdot tan^2\theta + \sqrt{-\left((d_{vial}/2 - d_I) \cdot tan^2\theta\right)^2 + (1 + tan^2\theta) \cdot ((d_I \cdot tan\theta)^2 - d_{vial}^2/4}}{1 + tan^2\theta} \tag{7}$$

Based on the realization that the active portion of the sample vial is essentially a thin rectangular region in the center of the sample vial and for simplicity, we will assume that all K-shell vacancies are produced along the central axis of the interrogating X-ray beam. The expression simplifies to

$$R_{U/Pu} = \int_{d1}^{d2} (1 + F_{U:Pu}) \cdot \frac{\int_0^{E_0} \cdot\, g(E) \cdot [U] \cdot \mu_{U,PE}(E) \cdot dE}{\int_0^{E_0} g(E) \cdot [Pu] \cdot \mu_{Pu,PE}(E) \cdot dE}\, dy, \tag{8}$$

where d_1 and d_2 are the limits in y defined by the intersecting views of the XRF collimating aperture and the X-ray tube shielding aperture. The effective dimensions of the XRF collimator can be seen by re-examining the plot shown in Fig 1 after lowering the limit on the log intensity scale. Using this plot we determine that d_1=3.1 and d_2 = 11.0 mm for the ORNL system.

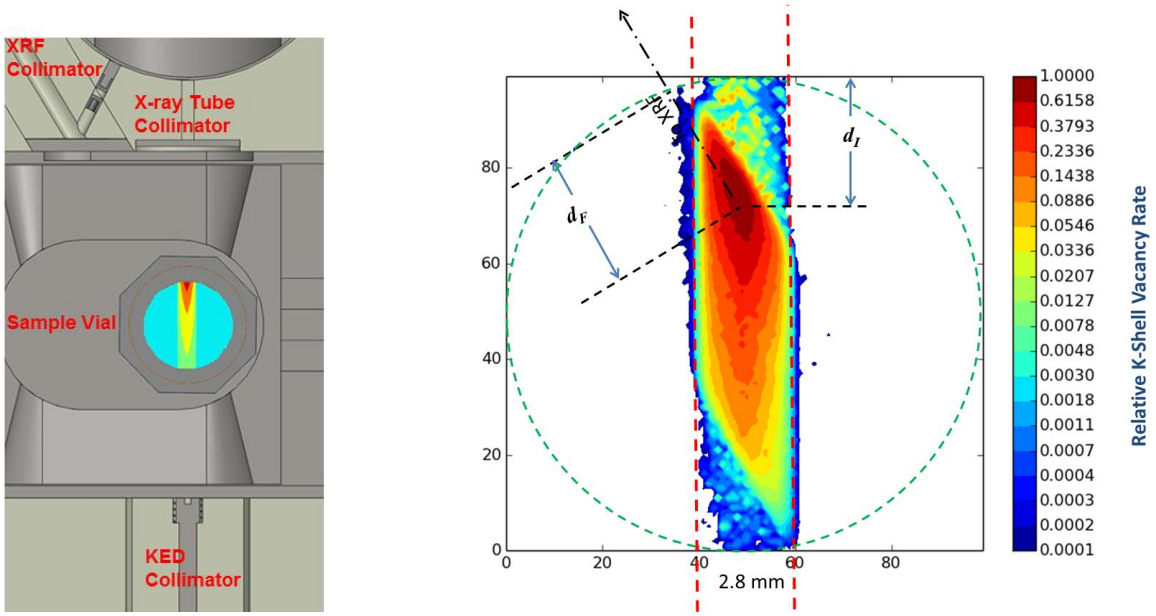

Fig.1. This figure, generated from MCNP6 simulations, shows the effective interaction region within a 250 U g/L in 3M nitric acid solution leading to detectable fluorescence X-rays (note the log scale). The circle represents the inner diameter of the sample vial. Even though interrogating X-ray beam has spread from 2 mm to 2.8 mm wide due to scattering at the tungsten aperture, K-shell vacancy production is essentially confined to a narrow region of the sample vial.

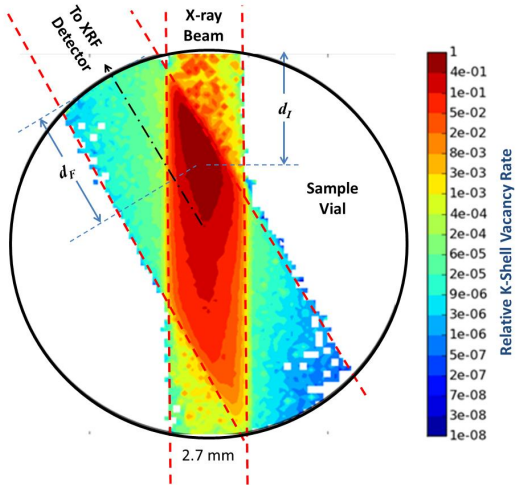

Fig.2. This figure presents the same data as presented in Fig.1. but with a much lower threshold (4 orders of magnitude lower) to highlight the interrogation region within the sample vial and more clearly illustrating the field of view of the XRF collimator. Note that the vacancies produced outside of the volume defined by the intersection of the collimator and the X-ray aperture do not contribute significantly to the observed count rates.

3.1 Representation of Interrogating X-ray Flux

Only a portion of interrogating X-ray beam creates K-shell vacancies resulting in detectable fluorescence X-rays. The interrogating X-ray flux reaching the detectable interaction volume is attenuated by the sample vial, any beam filters and the sample solution between the detectable interaction region and the X-ray source. The effective interrogating flux is given by

$$g(E) = e^{-\Sigma_{sample} \cdot d_I/2} \cdot e^{-\sum \rho_i \cdot \mu_i(E) \cdot t_i} \cdot g_X(E), \quad (9)$$

where $g_X(E)$ is the X-ray source term (from the X-ray tube),
d_I is the weighted path length of the interrogating X-ray beam through the sample leading to a detectable fluorescence X-ray,
ρ_i is the density of i[th] attenuator (e.g., Be window, Cd filter, vial wall) between the sample and X-ray source,
$\mu_i(E)$ is the mass attenuation coefficient of the i[th] attenuator between the sample and X-ray source,
t_i is the thickness i[th] attenuator between the sample and X-ray source, and

3.2. X-ray Source Term: $f_X(E)$

There are many representations of the X-ray source term described in the literature, however, we have chosen to use that of Shaltout [10] due to the completeness of their description. The interrogating X-ray source term is given by

$$g_X(E) = C \cdot \Omega \cdot I \cdot Z \cdot f_a(E) \cdot \left(\frac{E_0}{E} - 1\right)^x, \quad (10)$$

where

$$f_a(E) = \frac{\left(1 - e^{-2 \cdot \mu_W(E) \cdot \overline{\rho z} \cdot sin(\varphi)/sin(\epsilon)}\right)}{2 \cdot \mu_W(E) \cdot \overline{\rho z} \cdot sin(\varphi)/sin(\epsilon)},$$

$$\overline{\rho z} = \rho z_m \cdot \frac{(0.49269 - 1.0987 \cdot \eta + 0.78557 \cdot \eta^2)}{(0.70256 - 1.09865 \cdot \eta + 1.0046 \cdot \eta^2 + \ln(U_0))} \cdot ln(U_0),$$

$$\rho z_m = \frac{A}{Z} \cdot \left(0.787 \cdot 10^{-5} \cdot \sqrt{J} \cdot E_0^{\frac{3}{2}} + 0.735 \cdot 10^{-6} \cdot E_0^2\right),$$

$$\eta = E_0^m \cdot (0.1904 - 0.2236 \cdot ln(Z) + 0.1292 \cdot \ln(Z)^2 - 0.0149 \cdot \ln(Z)^3),$$

and

$U_0 = \frac{E_0}{E}$,
C is a constant,
I is the X-ray tube beam current,
Ω is the solid angle of the detector (or in our case the interaction region),
Z is the atomic number of the X-ray tube tungsten target (i.e., 74),
A is the atomic weight of the X-ray tube tungsten target (i.e., 183.84),
x is empirically determined to match the observed X-ray energy distribution and is ~0.92 for our system
$\mu_W(E)$ is the mass attenuation coefficient of tungsten,
E_0 is the X-ray tube endpoint energy,
$m = 0.1382 - 0.9211/\sqrt{Z}$ =0.03112,
$J = 0.135 \cdot Z$ = 9.99,

For our purposes we only require the shape, not the yield of the X-ray energy distribution. The relative K-shell production rates depend on the energy distribution of the interrogating X-ray source, specifically the distribution above the K-shell binding energies of the actinides. We have found that after the initial characterization of the X-ray source it is necessary to adjust the values of the end point energy, E_0, and the shape parameter, x, in Eq. 10 to obtain an accurate representation of the X-ray energy distribution. Because the X-ray generator output can vary even during a single HKED assay,

to obtain an accurate value for $R_{U/Pu}$ it is necessary to obtain values for E_0 and x for each measurement. While it is difficult to determine these parameters form the XRF spectra, it is fairly simple to extract these values from a fit to the KED transmission spectra.

3.3 Detection Efficiency

The detection efficiency term in Eq. 4 includes both the detector efficiency and the attenuation of the sample and vial on the emitted fluoresced X-rays on the attenuation of the fluoresced X-rays through the attenuator between the sample vial and High Purity Germanium detector (HPGe) detector and the intrinsic detection efficiency of the HPGE detector. The detection efficiencies for the U and Pu X-ray lines are given thus by,

$$\varepsilon(E_{ZKi}) = \varepsilon_{det}(E_{ZKi}) \cdot e^{-\Sigma_{sample}(E_{ZKi})\cdot\overline{d_F}} \cdot e^{-\sum \rho_i \cdot \mu_i(E_{ZKi})\cdot\tau_i}, \quad (11)$$

where $\mu_i(E)$ is the mass attenuation coefficient of the i[th] attenuator between the sample and detector,
τ_i is the thickness i[th] attenuator between the sample and detector,
$\varepsilon_{det}(E_{ZKi})$ is the HPGE detector efficiency for the i[th] K-shell X-ray of energy E_{ZKi} of element Z
$\Sigma_{sample}(E)$ is the macroscopic mass attenuation coefficient for the sample
$\overline{d_F}$ is the average distance the traveled though sample vial by the fluoresced X-rays assuming they originate along the axis of the interrogating X-ray beam.

3.4 High Z Enhancement Effect

To discuss the enhancement effect, we consider a solution containing only U and Pu. In this case the K_β X-rays from plutonium have sufficient energy to induce fluorescence of the uranium atoms. From Fig. 2 we can see that K-shell vacancy production from the interrogating beam is confined to a small region of the sample vial. The Pu X-rays inducing secondary fluorescence events will originate from this volume and will be emitted isotropically. The production rate of secondary U fluorescence events is proportional to the Pu K-shell vacancy production rate and the overall detection efficiency for the primary and secondary X-rays is the same so that the relative increase in the U X-rays is given simply as

$$F_{U:Pu} = \sum_i f_{\beta_i} \cdot \left(1 - e^{[U]\mu_{U,PE}(E_{\beta i})\cdot\overline{d_F}/2}\right), \quad (12)$$

where f_{β_i} is the relative yield for the i[th] K_β X-ray (per K-shell vacancy) from Pu and
E_{β_i} is the energy of the i[th] K_β X-ray from Pu.

4. Calculation of the Conversion Factors

The conversion factor $R_{U:Pu}$ is determined from a complex series of equations, the integration and summation will be carried out numerically rather than analytically. However, it is clear from this discussion that prior knowledge is required of the concentrations of the dominant actinides within the solutions. This information along with the values for E_0 and the shaping parameter x, will be provided from the KED transmission measurement performed in parallel with the XRF measurement.
To illustrate the importance of the expanded approach Fig. 3 plots the calculated values of $R_{U:Pu}$ for a typical HKED operating at 149.6 kV with a sample vial diameter of 1.418 cm for a range of U and Pu concentrations. For samples with U:Pu ratios of 100:1 the expanded approach and the traditional approach yield essentially the same values for concentrations above 100 g U/L. The observed values

for several measurements with U:Pu = 100:1 are also shown on the plot and agree well with the expected values. As the total concentration of actinides increases with the sample, the interrogating energy spectrum becomes harder resulting in less production of U K-shell vacancies relative to Pu. The magnitude of this effect can be seen in Fig 3. Use of the traditional algorithms for samples with U:Pu of 1:1 could result in over reporting of the Pu concentration by as much as 30% for typical samples.

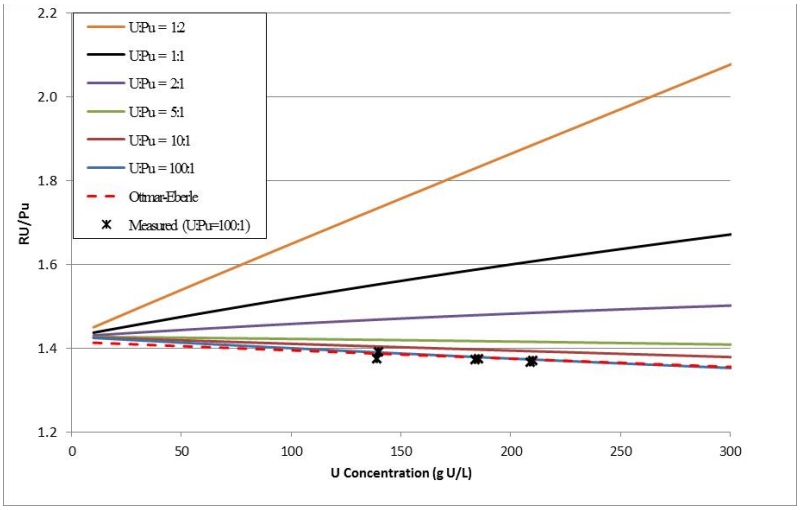

Fig. 3. Dependence of the conversion factor $R_{U/Pu}$ on the concentration of uranium and plutonium for a 14.2 mm diameter sample vial. Calculated values for a variety of U:Pu ratios are shown along with and measured ratios for several solutions with U:PU~100:1.The traditional conversion factor based on the expression from the work of Ottmar and Eberle Ref. [7] **is shown for comparison.**

When the HKED is operated in the Hybrid mode, the KED transmission measurement and the XRF measurement are performed simultaneously. The KED provides the concentration values for one or more dominant elements while the XRF provides relative count rates for each of the actinides present. The conversion factors $R_{U/Pu}$, $R_{U/Np}$, $R_{U/Am}$, and $R_{U/Cm}$ are calculated based on the KED results and the concentration values for Pu, Np Am and Cm are calculated from the measured XRF ratios.

As an example, Fig. 4 shows portions of the fitted KED and XRF spectra obtained from a sample with nominal concentration values of 100 g U/L and 7.5 g Pu/L. The fit to the KED spectrum provides a measured U:Pu ratio of 12.8 ± 0.3 but did not detect the Np clearly evident in the XRF spectrum. The hybrid analysis allows determination of the Np concentration, improved assay result for the Pu concentration and provides much lower detection levels for the Am and Cm concentration than is possible with only the KED measurement (Table 1). The observed minor actinides (Np and Cm) will have no impact on conversion factors.

The conversion factors ($R_{U/Pu}$, $R_{U/Am}$, $R_{U/Np}$, etc) are dependent on the actinide concentrations such that an iterative solution is necessary if only the XRF results are available. In use, it is expected that the KED transmission measurement will be used to determine the uranium and plutonium concentrations, and these results will provide the U:Pu ratio for use in determining the conversion factors for the minor actinide components of the solution.

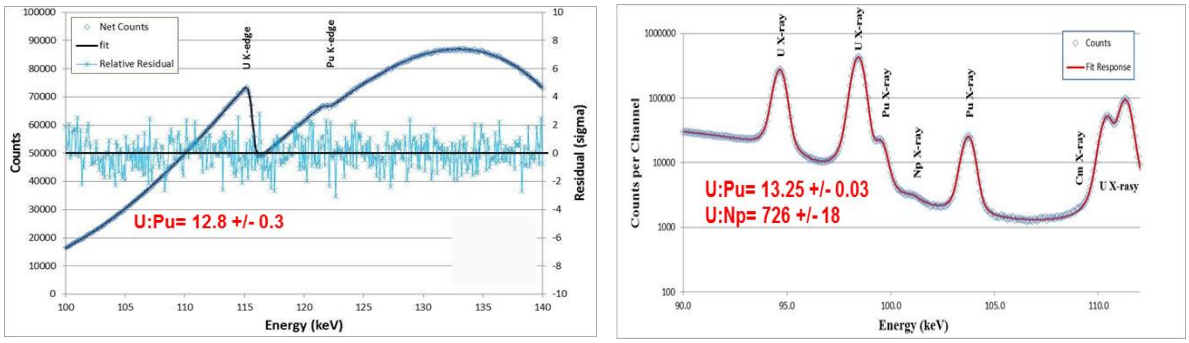

Fig. 4. KED (left) and XRF (right) spectra acquired from the assay of a sample containing nominally 100 g U/L and 7.5 g Pu/L. The fit to the KED spectrum provides the U and Pu concentrations as well as the X-ray generator parameters (E0 and x) for use in the analysis of the XRF spectrum.

Element	KED results (g/L)	HV End Point E_0 (kV)	Shape Parameter	$R_{U/Z}$ Calculated	U:Z Ratio Measured	Concentration (g/L)
U	100.60 ± 0.09	148.56	0.9018	--	--	--
Np	--	--	--	1.200	758.58	0.133 ± 0.008
Pu	7.81 ± 0.21	--	--	1.435	13.25	7.597 ± 0.022
Am	--	--	--	1.803	1031338	0.000 ± 0.003
Cm	--	--	--	2.587	16469	0.006 ± 0.003

Table 1. Hybrid analysis results for the 13:1 U:Pu sample (3000 s total assay time).

5. Conclusion

We have reexamined the calculation of the conversion factors $R_{U/Pu}$ and $R_{U/Am}$ developed by Ottmar and Eberle [1]. While the expressions they developed well addressed the traditional needs of the HKED analysis, changes in the nuclear fuel cycle and application of the HKED required extension of their work to accommodate a broader range of actinide mixtures and for potential use with non-aqueous reprocessing. We have developed a more robust and versatile algorithmic approach that will accommodate both the traditional 100:1 U:Pu mixtures as well as more challenging mixtures of high burn-up MOX materials and solutions with arbitrary relative U:Pu concentrations. The algorithms discussed here address the presence of additional actinides (e.g. Np, Am, Cm) and can be modified simply to determine the relevant conversion factors. The algorithms have been tested with only a handful of spectra covering a number of elemental combinations with nominal U:Pu ratios of 100:1, 10:1 and 1:1. Testing and evaluation is on-going and a follow-on report is planned.

The algorithm set developed for determination of the elemental conversion factors to convert relative count rates to quantitative concentration values provides several advantages over the traditional model. These advantages are summarized as:

Benefits of the enhanced approach

- Applicable to an arbitrary concentration ratios (i.e. not just U:Pu=100:1)
- Determination of conversion factors for arbitrary actinide combinations
- Corrects for high Z enhancement effect
- Corrects for variations in X-ray generator output
- Does not require calibration
  (while the traditional method required measurement of the calibration parameter, R_0)

6. References:

[1] H. Ottmar and H. Eberle, "The Hybrid K-Edge/K-XRF Densitometer: Principles – Design – Performance; Report KfK 4590," Karlsruhe, 1991.

[2] H. Zhu, M. Villani, J. Lamontagne, S. Croft, S. Gailey, H. Hassoubi, G. Landry, R. McElroy, R. Patel, S. Philips, P. Rouleau, R. Venkataraman and V. Yuschuk, "A New Software Application for Hybrid K-Edge Densitometry," in *Proceedings of the 50th Annual Meeting of the Institute of Nuclear Materials Management (INMM)*, Tucson, AZ, 2009.

[3] Canberra Industries, *Canberra Hybrid K-edge Densitometry (HKED) Software User's Manual, V1.0,* Meriden, CT, 2010.

[4] M. Collins and S. T. Hsue, "Nonlinear Fitting of Absorption Edges in K-Edge Densitometry Spectra," in *Institute of Nuclear Materials Management Annual Meeting, July 1997.*, 1997.

[5] M. L. Collins, "Validation of the KORINZU Four-Delta-Mu Method for KED Analysis of U-Pu MOX," in *Institute of Nuclear Materials Management Annual Meeting*, July 2014.

[6] R. D. McElroy, S. Croft, C. E. Romano and T. Guzzardo, "Hybrid K-Edge Densitometry Research at Oak Ridge National Laboratory," in *35th Annual Meeting ESARDA (European Safeguards Research and Development Association) Symposium on Safeguards and Nuclear Material Management*, Brugges, Belgium, 2013.

[7] H. Eberle and H. Ottmar, "Interner Berricht, Window-Based Calibration of the Hybrid K-Edge / XRF Spectrometer," Kernforschungscentrum Karlsrue, Karlsrue, Germany, 1993.

[8] R. Sitko and B. Zawisza, "Quantification in X-Ray Fluorescence Spectrometry," in *X-Ray Spectroscopy*, InTech,http://www.intechopen.com/books/x-ray-spectroscopy/quantification-in-x-ray-fluorescence-spectrometry, 2012, pp. 137 - 162.

[9] J. T. Goorley and et.al., "Initial MCNP6 Release Overview - MCNP6 version 1.0, LA-UR-13-22934," Los Alamos National Laboratory, Los Alamos, NM, 2013.

[10] A. A. Shaltout, "On the X-Ray Tube spectra, the dependence on the angular and electron energy of X-rays from the targets," *Eur. Phys. J. Appl. Phys.,* vol. 37, pp. 291-297, 2007.

Mass Attenuation Coefficient Data for Hybrid K-Edge Densitometry

Stephen Croft, Robert D McElroy Jr, and Andrew Nicholson

Oak Ridge National Laboratory,
Oak Ridge, Tennessee, USA
E-mail: crofts@ornl.gov, mcelroyrd@ornl.gov, nicholsonad@ornl.gov

Abstract:

In the domain of international nuclear safeguards measurement science, hybrid K-edge densitometry (HKED) is an example of a highly developed nondestructive assay method for the accurate and rapid quantification of actinides in nitric acid aqueous solutions. Experimental and theoretical work at Oak Ridge National Laboratory over recent years has focused on creating and demonstrating alternative algorithms so that the application space may be extended with confidence based on a first principles physics description of the photon spectra being analyzed.

This paper is concerned with one small part of this larger effort, concentrating particularly on how to describe the energy dependence of the actinide mass attenuation coefficients in the near K-absorption edges region as an example of data evaluation and applied uncertainty quantification. For many years the preferred reference data source has been the NIST XCOM database. The fundamental photoelectric cross-sections available in XCOM, although generally considered consistent with experiment, are actually based on theoretical calculations by Scofield [1]. As represented by XCOM the K-shell photoelectric cross-section has a perfectly sharp edge at the K-edge (although the calculated K-edge energy of Scofield is necessarily replaced by an experimental value) and in the near edge region falls (i.e. either immediately ahead of and/or after the K-edge), to a good approximation, according to a power-law energy dependence. The position and height of the step, and the energy dependence of the cross section are especially important in relation to modelling and fitting HKED spectra. An estimate of realistic associated uncertainties is also needed but it is difficult to obtain based on XCOM alone. Additionally, and most importantly, for full spectrum fitting, the K-shell absorption edge is not sharp but rather is broadened, owing to the natural line width (NLW) governed by finite lifetimes of the underlying quantum states.

To build a more realistic description and to establish associated confidence limits we use best available edge-energy data and natural line width values. We use the scatter between evaluations to estimate the uncertainty in the step height and the underlying energy dependence. We Lorentzian broaden the ideal saw-tooth behavior using an approximate analytical result as an alternative to full convolution, and add-in the underlying photo-absorption and incoherent scattering processes. In the case of uranium we make a comparison to the measurements of Materna et al who used a tunable X-ray source (with an energy spread comparable to the overall NLW) to map the near K-edge region [2].

We conclude that at the present time the uncertainty in the photoelectric step heights is far too large than required to enable an absolute HKED calibration to be made to the accuracy of current safeguards international target values. Furthermore, new and considerably improved measurements across the K-edge are needed to directly confirm the shape.

Keywords: K-shell photoelectric interaction; hybrid K-edge densitometry; data evaluation

1. Introduction

As commonly applied the Hybrid K-Edge Densitometer (HKED) is used to assay accountancy tank solutions with a U to Pu concentration of about 100 to 1. The U concentration is determined from the step change in transmission across the K-shell photoelectric absorption edge measured using high

resolution gamma ray spectroscopy by shining a filtered Bremsstrahlung beam through a vial of well-known dimensions containing a sample of solution. The Pu concentration is usually determined relative to the concentration from a simultaneous measurement of the induced x-ray fluorescence yield. In this paper we are concerned solely with the KED measurement. In principle the method is absolute, but is traditionally applied with calibration to empirically account for small potential biases. When the internal path length of the vial is 1-3 cm and the U concentration is 50-300 g/L the U concentration based on a 60-minute live-time assay may be expected to be accurate to 0.3% or better. KED is both a rapid and accurate analytical tool and, compared to exclusive use of destructive analysis, is cost effective, convenient, and saves both on shipment of radioactive materials and secondary waste generation. The KED method can also be applied to other elements. For the purposes of the present paper our focus is on the co-assay of the actinides Ac (Z=89) to Lr (Z=103) and how to describe the shape of the transmission spectrum from first principles. In particular we consider how to represent the K-shell photoelectric (PE) cross sections of the actinides.

Our discussion begins with one approach to interpreting a transmission measurement acquired with a white light source with a few to extracting the photoelectric cross section. Next we shall consider how to represent the PE cross section analytically. The heart of the paper is a brief review of the availability of the model parameters we need to compute the PE cross sections. We find that for the HKED application the present PE tables are in need of significant improvement.

2. Extraction of the K-shell Photoelectric Cross Section

The KED technique is essentially a cross section determination applied in reverse. It is useful to summarize the process we have in mind. For the present discussion we consider a KED style measurement based on interpreting a pair of measured transmission spectra assuming narrow beam geometry. One can write the recorded blank nitric acid reference energy dependent Bremsstrahlung spectrum as follows

$$Y_{ref} = \varepsilon i_{ref} \frac{I_{ref}}{I_o}$$

where I_{ref} is the transmitted beam intensity; I_o is the incident electron Bremsstrahlung beam intensity per unit electron beam current; i_{ref} is the electron beam current used to measure Y_{ref}; and ε is the efficiency of the detector system.

Similarly for a nitric acid actinide solution we may write

$$Y_{sol} = \varepsilon i_{sol} \frac{I_{sol}}{I_o}$$

I_{ref}/I_o and I_{sol}/I_o are the transmission factors of the sample vial and contents and the observed rates are proportional to the transmission factors because the detection efficiency of the system is controlled and the shape I_o is taken as fixed. It is assumed that corrections for rate loss and ambient background have been applied.

The transmission factors obey the Beer-Lambert-Bouguer law and so we may express the following ratio in terms of the so called optical thicknesses of the various attenuating materials as follows

$$T = \frac{Y_{sol}}{Y_{ref}} = \left[\frac{i_{sol}}{i_{ref}} exp\left[-\left(x_{vw,sol} - x_{vw,ref}\right)\right]\right] exp\left[-\left(x_{sol} - x_{ref}\right)\right] = aexp\left[-\left(x_{sol} - x_{ref}\right)\right]$$

where $x_{vw,sol}$ and $x_{vw,ref}$ are the combined optical thicknesses, expressed in multiples of mean free paths, of the vial walls (vw) of the solution and reference containers, respectively, and by design these are closely matched. x_{sol} and x_{ref} are the optical thicknesses of the contents.

Rearranging we have

$$ln\left(\frac{1}{Y_{sol}/Y_{ref}}\right) = x_{sol} - x_{ref} - \ln(a)$$

where $a \approx 3$ if the solution is measured using a current of (say) 15 mA and the less attenuating reference is measured using a current of 5 mA (to approximately match counting rates) and matched sample vials are used. Its value might be estimated more accurately than the nominal electron current setting by using a Gd-foil x-ray flux monitor.

In terms of basic photon interaction data we can write this expression as follows, assuming, for the purposes of illustration we have a known U solution

$$ln\left(\frac{1}{Y_{sol}/Y_{ref}}\right) = \left(\frac{\mu}{\rho}\right)_{U,K}\rho_U t_{sol} + \left\{\left[\left(\frac{\mu}{\rho}\right)_{U,tot-K}\rho_U t_{sol} + \left(\frac{\mu}{\rho}\right)_{mat}\rho_{mat} t_{sol} - \left(\frac{\mu}{\rho}\right)_{ref}\rho_{ref} t_{ref}\right] - \ln(a)\right\}$$

where ρ_U is the mass density of U in the solution; t_{sol} is the internal path length across the solution vial; $\left(\frac{\mu}{\rho}\right)_{U,K}$ is the mass attenuation coefficient (MAC) of U for the K-Shell PE process; $\left(\frac{\mu}{\rho}\right)_{U,tot-K}$ is the MAC of U for photon removal processes other than PE; $\left(\frac{\mu}{\rho}\right)_{mat}$ is the MAC of the solution 'matrix' and ρ_{mat} its mass density; and similarly for the reference (nitric acid blank).

The portion of the above equation in brackets $\left[\left(\frac{\mu}{\rho}\right)_{U,tot-K}\rho_U t_{sol} + \left(\frac{\mu}{\rho}\right)_{mat}\rho_{mat} t_{sol} - \left(\frac{\mu}{\rho}\right)_{ref}\rho_{ref} t_{ref}\right]$ represents the smooth difference of the sample of interested from the reference sample. Note the '*mat*' and '*ref*' terms partially cancel each other and we may scale the '*ref*' term without changing our basic approach – this is like using Y_{ref} raised to some power, Y_{ref}^{p}, as the fiducial. Collectively the four terms surrounded by the { } brackets represent a variation in energy that is both smooth and gradual. Over the narrow energy range in the vicinity of the K-edge we may approximate this contribution by a low order (e.g. quadratic) polynomial [3]. Using this approximation we arrive at our PE cross section measurement model

$$f(\Delta) = ln\left(\frac{1}{Y_{sol}/Y_{ref}}\right) \pm \sqrt{\left(\frac{\sigma_{C_{ref}}}{Y_{ref}}\right)^2 + \left(\frac{\sigma_{C_{sol}}}{Y_{sol}}\right)^2} \cong [b_0 + b_1\Delta + b_2\Delta^2] + \rho_U t_{sol}\left(10^{24}\frac{N_A}{A_U}\right) R * \sigma_K(\Delta)$$

where the energy parameter $\Delta = E - E_K$ is the distance to the K-edge, E_K; b_0, b_1 and b_2 are empirical fitting parameters; ρ_U is the U density in g/cm^3; t_{sol} is the path length through the solution in cm; $\sigma_K(\Delta)$ is the U K-shell microscopic PE cross section in units of barn per atom as a function of the energy parameter Δ; N_A is Avogadro's number, atoms per mole; A_U is the molar mass, $g.mol^{-1}$, of the U present in solution; and we have introduced the influence of the detector response function (resolution), R, which has the effect of resolution broadening (smearing) the true shape of the cross section via the convolution $R * \sigma_K$. The quadratic term is being used here to represent the smooth contribution to the function $f(\Delta)$ and the convolution term represents the additional jump created by the PE interaction. This is just one measurement approach to probing the K-edge region. The point spread function of the Low Energy Germanium planar energy dispersive spectrometers typically used in HKED instruments are well described by a tailed Gaussian with shape parameters which may be estimated by fitting narrow, isolated, gamma-ray peaks. We are now left with the question of how to represent $\sigma_K(\Delta)$, the K-shell PE cross section. A traditional approach used in KED analysis has been to treat the PE cross section as a sharp step and to use the projected step change across the edge as the measure of the actinide concentration.

The step change in MAC as one crosses the K-edge from below is related to the step change in the ideal underlying microscopic atomic K-shell PE cross section as follows

$$\left[\left(\frac{\mu}{\rho}\right)_{+} - \left(\frac{\mu}{\rho}\right)_{-}\right] = \frac{N_A x 10^{-24}}{A}[\tau_+ - \tau_-] = \frac{0.6022141\ 29}{A}[\tau_+ - \tau_-], cm^2 g^{-1}$$

where $N_A \approx (0.602214129 \pm 0.000000027)x10^{24}$ atoms per mole is Avogadro's number (the uncertainty being negligible for the present discussion), A is the molar mass of the target element is $g.mol^{-1}$, and the units of τ are $barn$ (1 *b* =10^{-24} cm^2). Since the cross section step is more fundamental than the MAC step, because the latter also requires the isotopic composition of the target element to be known so that A might be calculated, we elect to work in terms of the microscopic atomic cross section in what follows. A weakness of a number of studies and data evaluations that report MAC values is that the associated molar mass is not stated. Because we are dealing with various grades of, for example U and Pu, and are focused on accuracies at the 0.1% level, this alone can be a serious flaw.

3. Representing the K-shell Photo-Electric Cross Section

For a variety of mainly technical reasons, in the current generation of commonly used general purpose photon cross section databases, the K-shell PE cross section is represented as a sharp, power-law step. One of the challenges is that direct measurements of the photo-electric cross section are difficult, few in number, and subject to significant uncertainty within and between independent determinations. Direct methods detect the ejected photoelectrons or measure the intensity of the x-rays that follow the PE process. However, they still require some theoretical knowledge for data reduction, and close to the absorption edge the emergent photoelectrons are of low energy and easily perturbed so that direct methods are unsuitable. Consequently, experimental values are generally obtained by subtracting theoretical estimates of the Rayleigh and Compton scattering contributions from the observed values of the total interaction cross section. The total cross section is relatively easy to measure accurately, being a simple ratio measurement, although limited discrete photon source energies (radionuclide or pseudo-monochromatic beams), and sample uniformity (and thickness determination) can present challenges. Agreement with theoretical PE cross section values is generally within uncertainties and so theoretical PE values are generally used in compilations which side steps the issue of performing a complex evaluation of experimental data and also allows experimental gaps to be readily plugged in a self-consistent way [4]. Furthermore, in general purpose compilations near edge fine structure, the result of resonant behaviour with bound (Rydberg) states and the interaction of the outgoing electron wave function with the spatial pattern of electrons in the neighbourhood, is also disregarded. Uncertainties in the calculated PE cross sections for the actinides have been difficult to estimate and verify but accuracies of several percent in the vicinity of the absorption edges is typical of the guidance provided by data evaluators for many years [5].

It should be possible to accurately determine the magnitude of the K-edge jump from total cross section measurement data alone by fitting the regions below and above the edge and extrapolating to the edge energy – for example according to the approach we developed in the previous section. What do we mean by accurate? If each branch of the fit is based on multiple points, each individually determined to a few tenths of a percent, then the extrapolated values should be of comparable accuracy and the difference to similar accuracy (the upper branch being the more dominant). The role for calculation or data evaluation would then be to estimate the systematic (with Z) energy dependence of the PE cross sections.

If the natural line width is zero our model for the K-shell photoelectric cross section is

$$\tau(E) = 0, E < E_K$$
$$\tau(E) = C_\kappa \cdot \left(\frac{E_K}{E}\right)^n, E \geq E_K, n > 0$$

This form neglects chemical bonding and wave interference effects which could be present in the near edge region. We shall not consider these effects further, but we do want to address broadening of the edge due to the finite lifetime of the quantum states [6]. Thus, we refine our picture by considering the K-shell PE cross section to be more faithfully represented by a Lorentzian broadened sharp power-law step with a narrow natural line width (NLW) parameter Γ. On this basis the PE cross section requires four parameters to describe it: the energy of the edge, E_K; the ideal step height C_κ; the value of the power law parameter n, which governs the underlying energy dependence; and the NLW, Γ. If we use

'book values' for E_K and Γ then only two parameters need to be extracted from measurements or calculations to describe the K-shell PE cross section and these two parameters can become the focus of (photon cross section) data evaluation.

The convolution between a Lorentzian and the stepped power-law must be handled numerically. It is convenient however to also to have an algebraic approximation for rapid early iteration calculations. We shall now justify such an approximation based on the assumption that the ideal underlying PE cross section may be considered to be a sharp step over the narrow energy range where there is significant Lorentzian smearing. That is to say:

$$m \left| \frac{1}{C_\kappa} \cdot \frac{dC_\kappa \cdot \left(\frac{E_K}{E}\right)^n}{dE} \right|_{E_K} \cdot \Gamma \ll 1.$$

where m is a small positive number (of the order of a few). Then, in the vicinity of the K-absorption edge energy E_K, either below it or above it, the observed cross section will have the shape of a Lorentzian smeared rectangular step

$$C_\kappa \cdot \left(\frac{1}{2} + \frac{\tan^{-1}\left(\frac{E - E_K}{\Gamma/2}\right)}{\pi} \right) = \tau(E_K) \cdot S\left(\frac{E - E_K}{\Gamma/2}\right)$$

where

$$S\left(\frac{E-E_K}{\Gamma/2}\right) = \left(\frac{1}{2} + \frac{\tan^{-1}\left(\frac{E-E_K}{\Gamma/2}\right)}{\pi} \right).$$

In the far region above the edge, where $\left(\frac{E-E_K}{\Gamma/2}\right) \gg 0$, $S\left(\frac{E-E_K}{\Gamma/2}\right) \to 1$ and the observed cross section will take the unperturbed form $\tau(E)$.

Combining these two observations, made under the conditions stated, above the edge, we have the approximation for the observed cross section

$$\sigma_K(E) = \tau(E) \cdot S\left(\frac{E - E_K}{\Gamma/2}\right)$$

We recall that the mathematical operation of convolution preserves area and so the 'loss' of cross section above the edge results in an area matched redistribution below the edge. Additionally, guided by the ideal step result, this redistribution should be smooth and as symmetric as possible.

At a given energy above the edge if we approximate the observed cross section by $\tau \cdot S$ then we see that the corresponding value to be placed an equal distance below the edge is $\tau \cdot (1 - S)$. We can express this mathematically in a convenient way by writing the two functions in terms of the energy difference $\Delta = E - E_K$, so that

$$S\left(\frac{\Delta}{\Gamma/2}\right) = \left(\frac{1}{2} + \frac{\tan^{-1}\left(\frac{\Delta}{\Gamma/2}\right)}{\pi} \right)$$

which has the property $S(-|\Delta|)$=1- $S(|\Delta|)$.

Re-expressing the shape of the ideal non-Lorentzian broadened PE cross section can be done as follows

$$\tau(E) = P(\Delta) \approx C_\kappa \cdot \left(\frac{1}{1 + \Delta/E_K}\right)^n, \Delta \geq 0 \; and$$

$$\tau(E) = 0 \; otherwise$$

We note that $P(\Delta)$ is an odd function of Δ with physical meaning only for positive Δ that is for energies above the K-absorption edge. But mathematically we can reflect the trend below the edge by using $P(|\Delta|)$. We can now assemble all of the pieces of our approximate description to show how to conveniently represent the K-shell PE cross section in the following way

$$\sigma_K(E) \approx \; P(|\Delta|) \cdot \; S(\Delta) \; \forall \; \Delta$$

or explicitly

$$\sigma_K(E) \approx \; C_\kappa \cdot \left(1 + \frac{|E - E_K|}{E_K}\right)^{-n} \cdot \left(\frac{1}{2} + \frac{\tan^{-1}\left(\frac{E - E_K}{\Gamma/2}\right)}{\pi}\right)$$

where C_κ, is barns per atom, is the ideal underlying (non-Lorentzian broadened) cross section jump at the absorption edge in our simple physical picture, and $n > 0$ is a dimensionless number describing the energy dependence of the underlying ideal (non-Lorentzian broadened) cross section. One of the few published estimates of the cross section behaviour over the K-edge in the actinide region is that of Materna et al who used a quasi monochromatic beams selected by crystal diffraction from a LINAC derived white light source to map the energy dependence [2]. In general U is perhaps the best experimentally studied actinide. So it is perhaps the most favourable case for comparison. In the next section we shall review our state of knowledge regarding the model parameters.

4. Review of K-shell Photo-Electric Cross Section Parameters

We shall conclude with a review of C_κ and n values that can be used to describe the K-shell PE cross section and hence KED transmission spectra along the lines we have explained above.

Our focus on C_κ and n is because estimates for E_K and Γ are perhaps less contentious, although the situation is certainly not ideal. Deslattes et al [7] provide an extensive discussion and impressive tabulation of modern high accuracy evaluated experimental data and sophisticated relativistic many-body problem theoretical atomic calculations of x-ray energies for the K- and L-series transitions, edges and their estimated standard deviations for elements Z=10-100. For some high-Z elements small isotope dependent shifts are also included (^{239}Pu and ^{244}Pu being one relevant example). In these tables the absorption edge locations are associated with the energy needed to produce a single inner vacancy from an isolated ground state non-ionized atom with the photo-electron 'at rest at infinity'. For elements with atomic numbers 101 to 103 we extend Deslattes using the listing of Agarwal but with a linear adjustment of the energy difference with respect to Z=100 [6]. In passing we note that for the XCOM database (which stops at Z=100) the edge energies for the actinides are in good agreement with our adopted values with the exception of Z≥98 when a large deviation appears with XCOM being systematically high by about 1.07, 1.11 and 1.17 keV for Z=98, 99 and 100 respectively [5].

Papp, Campbell and Varga [9] discuss the significant challenges & complexity associated with the various experimental methods (usually on elemental solids), theoretical single-particle & many-body calculations (of free atoms), and data evaluation of generating x-ray and atomic energy level widths for a variety of pure and applied needs. The level width is the sum of radiative and non-radiative (Auger and Coster-Kronig) widths. Solid state and binding effects are often important – but we have no information about this. The energy distribution is usually described as a Lorentzian distribution, although deviation is expected when the so called dynamical relaxation (DR) is important this has to do with non-hole-hopping (static, the hole remains within the same orbital and so acts in monopole like way) and hole-hopping (dynamic, in which the holes fluctuates between orbitals and so acts in a dipole like way) relaxation [10]. DR can be relatively large (ie it is not just a within orbital perturbation, which additional introduces angular momentum quantum number dependence) and also alters the energy dependence from the Lorentzian shape – but again we have no information to go on. Updated values for the NLW's with extended coverage are available for Z=10 to 92 in Campbell and Papp [9]. Above Z=92 we extend the table by the procedure given in [4].

Although we have empirically extended the E_K and Γ data sources, and despite the fact that the 5f level electron filling sequence is anomalous, we feel justified in our approach because $E_K\ vs.Z$ is quite linear, the resulting $\Gamma\ vs.Z$ curve is reasonably linear, the K-jump is quite linear in $1/Z$, and $n\ vs.Z$ gives the impression of being monotonically decreasing and basically smooth as a function of atomic number. Table 1 summarizes the set of E_K and Γ values obtained.

Z	Element	E_K (keV)	Γ_K (eV)
89	Ac	106.759	84.4
90	Th	109.648	88.2
91	Pa	112.5984	92.1
92	U	115.5962	96.3
93	Np	118.6887	100.5
94	Pu	121.7902	104.4
95	Am	124.9861	108.2
96	Cm	128.2413	112
97	Bk	131.5556	115.7
98	Cf	134.9354	119.2
99	Es	138.3915	122.6
100	Fm	141.9304	125.8
101	Md	145.5	129
102	No	149.14	132
103	Lr	152.85	135

Table 1: A set of K-shell absorption edge energies and Lorentzian natural line widths for the actinides. Absorption energies up to Z=100 were taken from Ref. [8], while for Z>100, Ref. [7] was used. Lorentzian line widths up to Z=92 were taken from Ref. [9] and the rest were extended via the procedure described in the text.

The NIST XCOM database is one of the most widely used and influential sources of photon interaction data for the applied sciences [5,12,13]. In this compilation, the energy dependence of the PE cross section is represented by ideal simple sawtooth shapes based on the theoretical free static atom calculations of Scofield [1]. Uncertainties are not discussed in any detail. Scofield calculated and tabulated (on a reasonably coarse energy grid that steps across the absorption energies in an element dependent but unexplained way) for each of the individual sub-shells the photoelectric cross section to the continuum for photon energies from 1 to 1500 keV for isolated atoms with atomic number Z=1 to 101. In the calculations the electrons are treated relativistically and the ejected electron is assumed to be moving in the same (static atom) self-consistent effective screened Hartree-Slater central potential after absorption of the photon as the bound electron was beforehand. The Hartree-Slater potential approximates the effect of electron exchange that is not correct at the origin. A modification was used to cap the value of the potential in the outer regions. All contributing multipoles and retardation effects were included. Screening is least important for high-Z elements in the inner shells so for the actinides we expect the results to be relatively insensitive to the choice of potential. The Hartree-Fock model gives a more accurate charge density at the nucleus and so the Hartree-Fock wavefunctions *should* give more accurate results for high-energy photons and inner shells. For Z=1 to 54 Scofield provides some cross section scaling factors. However, comparison to data tends to favour the Hartree-Slater results without normalization [4]. Agreement with experimental data is within experimental uncertainty except for 10-30 keV for light elements. Because of the relatively large uncertainty in some of the experimental data Scofields cross sections are used as photoelectric reference data. In the 100 keV region for the actinides the K-shell cross section calculations of Scofield have a (computational) numerical accuracy of better than 0.1%. Because each shell is calculated separately we can represent the energy dependence of the two branches below and above the K-edge by 'other' and 'other+K' respectively. For the K-shell PE process the $1s_{1/2}$ state, which with the exception of hydrogen is populated by two electrons, is not degenerate and so we have a simple single. The K-shell binding energies calculated by Scofield are not, on the other hand, in fine agreement with direct measurement and we adjust the step change to our adopted edge values.

An older but valuable source of experimentally founded results is the work of McMaster et al [3]. Only the actinides Th, U and Pu are included. Data are given to four significant figures so the precision is better than the accuracy of the data. Note the energy dependence (n-value) is significantly steeper than for analysis based on the Scofield data.

The tabulation of Storm and Israel remains both detailed and easy to use [14]. The cross-section values are listed to 3 significant figures. In the region 6 keV to 200 keV it is stated that the results generally tend to be within 3% of both other calculations and measurements. We are concerned with the actinide region and of the comparisons made in Table VII (for the six elements Z=4, 13, 26, 50, 74, and 92) the data for uranium is of especial interest.

Z	Scofield [2]		McMaster [3]		Storm & Israel [14]		Veigele [15]		R&C [16]		Materna [2]	
	C_K	n	C_K	n	C_K	n	C_K	n	C_K	n	C_K	n
	barn		barn		barn		barn		barn		barn	
89	1545.0	2.520			1532	2.507	1711	2.719	1564	2.535		
90	1492.1	2.512	1513	2.596	1482	2.489	1497	2.556	1164	2.558		
91	1440.4	2.505			1431	2.459	1616	2.708	1350	2.523		
92	1390.2	2.495	1444	2.588	1381	2.428	1423	2.607	976	2.466	1479	2.736
93	1342.5	2.490			1338	2.395	1519	2.687				
94	1296.5	2.479	1349	2.589	1278	2.375	1301	2.51				
95	1251.3	2.466			1236	2.329						
96	1207.3	2.443			1194	2.28						
97	1166.2	2.419			1150	2.207						
98	1125.4	2.365			1109	2.094						
99	1085.0	2.285			1066	1.779						
100	1047.3	2.303			1033	1.346						
101	1009.9	2.215										

Table 2: Summary of main C_κ and n values discussed in the main text

An older but still valuable table of cross section is that of Veigele [15]. The work covers the energy range 0.1 keV to 1 MeV for elements H to Pu are based on some 153 sources of experimental total and photoelectric cross sections generated over the period 1920 to 1970. Calculated scattering cross sections were subtracted from total cross section data and the resulting photoelectric and measured photoelectric cross sections from 1 keV to 1 MeV were empirically evaluated by performing a least-squares fitting procedure. The theoretical scattering cross sections were then added to the resulting values to estimate the total cross sections over the range 0.1 keV to 1 MeV.

For our purposes the evaluation of Veigele provides a convenient source of experimentally based photoelectric cross sections as a function of energy, $\tau(E)$. In the vicinity of the K-edge the photoelectric cross section was represented by a power series in logarithmic space as if the behaviour were hydrogenic: $\ln(\tau) = \sum_{i=0}^{n} a_i(\ln(E))^i$, where $n = 3$ above and $n = 1$ below the K-absorption edge. In the atomic number (Z) direction low order (linear or quadratic) logarithmic series fitting was also used to complete the table. Uncertainties in the total cross section estimates were assigned to the recommended values of the cross sections based on the quantity of data, experimental errors and weights, the agreement of data among the different experiments, and the internal consistency of the compiled values. In the K-edge region of the actinide elements the relative uncertainties indicated are in the ±(5-10)% band. Original listings are given only to 3 significant figures. Veigele uses the following molar masses for U, Np, and Pu: 238.025, 245.697, and 241.946 g/mol. The conversion factors between MAC and cross sections appear to be identical between Veigele and Storm & Israel [14,15].

The compilation of Robouch and Cicerchia is potentially valuable and is experimentally based, but is also problematic [16]. MAC data are listed for Ac to U. In converting to cross section we take molar masses of 227, 232.0381, 231.0359, and 238.0289 respectively for these four elements. The

agreement with the other values reviewed is not very good. Closer inspection shows that the edge energies used by Robouch and Cicerchia are 106.9, 119.7, 115.9 and 121.6 keV (they quote the wavelength to three significant figures) whereas our adopted values are (rounding to four significant digits) 106.8, 109.6, 112.6 and 115.6 keV. The values for Ac and Th agree, but the Robouch and Cicerchia values for Pa and U seem to be those of U and Pu and not of Pa and U. So one is left to wonder if some mistake has been made. If we transform the step value to our standard energy grid we obtain values of 1568, 1166, 1452, and 1105 barn respectively, but whether this is a valid thing to do or not is uncertain.

The measurement of Materna et al for U is indicative of how future measurements might be conducted using modern methods to satisfy the data needs we have been discussing [2]. We have placed the step value onto our adopted energy grid. The accuracy is difficult to judge but can't be better than 1%, the approximate accuracy of the U-foil thickness determination. Materna et al also report their results as fit coefficients for the regions below the edge and above the edge (rather tan reporting the actual data points) and without covariance information on the parameters they can't be used to make meaningful uncertainty statements which is a pity. The n-value for the PE cross section shape function again is quite different to our estimate based on Scofield. Measurements of higher resolution across the edges of a wider range of targets would be desirable.

In Table VII of their Appendix, Storm and Israel tabulated values for U for three other estimates described as experimental values and reported without uncertainties to three significant figures [14]. For completeness we reproduce these here ascribed by author (see Storm and Israel for reference): Rakavy & Ron, 1369 b; McCrary et al, 1375 b; Perkin & Douglas, 1385 b. A summary of the other main results is given in Table 2.

5. Discussion

It is difficult to objectively estimate the accuracy of K-shell PE cross section data. If we take the view that the scatter between different respected compilations and selected measurements reviewed here is indicative of our state of knowledge then Table 2 is instructive. We see that more data covering the actinides is desirable – U, Np, Pu, Am and Cm are especially important to safeguards in dissolver solutions and Th could be a valuable inter-comparison standard. For U and Pu we see that an n-value of about 2.5 is supported but there is considerable uncertainty, of the order of 0.2. Concentrating on U, which is perhaps the most favourable case, and using all the data discussed, but excluding Robouch and Cicerchia for the reasons discussed, we have presented 8 values of the PE cross section steps, arranged on order these are: 1369, 1375, 1381, 1385, 1390.2, 1423, 1444, 1479 barn – a range of 110 b. The mean is 1406 b with a relative sample standard deviation of 2.8% and a relative standard error of 1%. A 1% uncertainty is about an order of magnitude larger than we need for HKED applications.

6. Conclusions

The behaviour of the K-shell photoelectric absorption cross section of the actinides is of scientific interest for a variety of both basic and applied reasons. The experimental database in the vicinity of the K-edge for the actinides is meagre and the uncertainties are wholly inadequate to permit HKED to be applied as an absolute method to meet current international target values [17]. New measurements with both fine energy resolution and high accuracy are needed in order to improve on this situation, and to enable testing the theoretical shape discussed in this paper. Experimental work using continuous Bremsstrahlung beams and the HKED instrument itself is complementary and requires actinide solutions of known concentrations at the 0.1% relative uncertainty level to be prepared. Solutions are uniform, but we caution that second order effects including scattering off the collimator and back scatter in the detector must be allowed for. A search for fine structure in the near-edge region, just above the edge, for foil and solutions would be especially interesting but the energy resolution of the HKED cannot address this. If the Lorentzian broadened edge model holds, the implication is the K-shell x-rays may be produced by photons with energies less than the binding energy by multiples of the natural line width. We have not seen this in a preliminary search.

7. References

[1] Scofield J.H., *Theoretical photoionization cross sections from 1 to 1500 keV*, Lawrence Livermore National Laboratory Report UCRL-51326, (1973).

[2] Materna Th., Jolie J., Mondelaers W., and Masschaele B. *Near K-edge measurement of the X-ray attenuation coefficient of heavy elements using a tunable X-ray source based on an electron LINAC*, Radiation Physics and Chemistry 59 (2000), p 449-457.

[3] McMaster W.H., Kerr Del Grande N., Mallett, J.H. and Hubbell J.H., *Compilation of x-ray cross sections,* Lawrence Radiation Laboratory, University of California, Livermore report UCRL-50174 (1969), Revision I, Sections I-IV.

[4] Hubbell J.H., *Review and history of photon cross section calculations,* Phys Med Biol 51 (2006), p R245-R262.

[5] Berger, M.J., Hubbell, J.H., Seltzer, S.M., Chang, J., Coursey, J.S., Sukumar, R., Zucker, D.S., and Olsen, K. (2010), *XCOM: Photon Cross Section Database* (version 1.5). Available: http://physics.nist.gov/xcom. National Institute of Standards and Technology, Gaithersburg, MD.

[6] Croft S., McElroy R.D., and Guzzardo T., *Representing the plutonium K-absorption edge in transmission measurements*, Proceeding of the 55th Annual Meeting of the Institute of Nuclear Materials Management, July 20-24 (2014), Atlanta, Georgia, USA.

[7] Deslattes R.D., Kessler Jr. E.G., Indelicato P., de Billy L., Lindroth E., and Anton J., *X-ray transition energies: new approach to comprehensive evaluation,* Rev Mod Phys 75 (2003), p 25-99.

[8] Agarwal B.K., *X-Ray Spectroscopy: An Introduction (Second Edition),* Springer-Verlag Berlin Heidelberg GmbH (1991). ISBN 978-3-540-50719-2.

[9] Papp T., Campbell J.L., and Varga D., *X-ray natural line widths and Coster-Kronig Transition Probabilities*, AIP Conference Proceedings 389 (1997) p 431-445.

[10] M Ohno and RE LaVilla, *Xenon L emission spectra and many-electron effects in core levels*, Phys Rev A45(199204713-4719.

[11] Campbell J.L. and Papp T., *Widths of the atomic K-N7 levels,* ADNDT 77(2001) p 1-56.

[12] Berger, M.J. and Hubbell, J.H., *XCOM: Photon Cross Sections on a Personal Computer*, NBSIR 87-3597, National Bureau of Standards (former name of NIST), Gaithersburg, MD (1987)

[13] Berger, M.J. and Hubbell, J.H., *NIST X-ray and Gamma-ray Attenuation Coefficients and Cross Sections Database*, NIST Standard Reference Database 8, Version 2.0, National Institute of Standards and Technology, Gaithersburg, MD (1990).

[14] Storm E. and Israel. H.I., *Photon cross sections from 1 keV to 100 MeV for elements Z=1 to Z=100*, Nuclear Data Tables A7 (1970), p 565-681.

[15] Veigele WM. J., *Photon cross sections from 0.1 keV to 1 MeV for elements Z=1 to Z=94,* Atomic Data Tables 5 (1973), p 51-111.

[16] Robouch B.V. and Cicerchia A., *X-ray mass absorption coefficients and absorption edges for the first 92 elements in the range 0.01 to 200 Å of wavelength i.e. 62 eV to 1.24 MeV of photon energy,* Comitato Nazionale Energia Nucleare (CNEN), Associazione Euratom-CNEN Sulla Fusione, Centro Di Frascati, Report 80.55 (December, 1980).

[17] Zhao K., Penkin M., Norman C., Balsley S., Mayer K., Peerani P., Pietri C., Tapodi S., Tsutaki Y.,

Boella M., Renha G. Jr., and Kuhn E., *International target values 2010 for measurement uncertainties in safeguarding nuclear materials,* International Atomic Energy Agency Department of Safeguards, Safeguards Technical Report STR-368, Vienna, Austria, (2010).

Validation of the new software for in-field uranium concentration and enrichment measurements by "COMPUCEA"

H. Schorlé[1], J. Zsigrai[1], M. Vargas-Zuniga[1], M. Toma[1], A. Berlizov[2]

[1]European Commission, Joint Research Centre, Institute for Transuranium Elements, Karlsruhe, Germany
[3]International Atomic Energy Agency, Vienna, Austria

Abstract:

COMPUCEA (Combined Procedure for Uranium Concentration and Enrichment Assay) is used to support physical inventory verifications (PIV) at uranium fuel production facilities by high-accuracy in-field uranium concentration and enrichment measurements. In order to improve the robustness of the COMPUCEA measurement procedure, new software was developed by the IAEA. The new software guides the user through the sample preparation process and provides a user-friendly interface for calibration, sample evaluation and quality control. Its development started in 2011 and since then it was constantly tested and refined to reach its current stage. In addition, some improvements of the analytical procedure were implemented in the new software. It was tested and validated by ITU to authorize its use for measurement campaigns at fuel fabrication plants and for analyses in ITU. The results calculated by the new software agree very well with results from the previous software and with results from Thermal Ionization Mass Spectrometry. As the new software makes it much easier to provide high-accuracy analytical results with COMPUCEA, it is planned to be used in field from 2015 onwards.

Keywords: U concentration, ^{235}U enrichment, in-field analysis, fuel-fabrication plants

1. Introduction

COMPUCEA (Combined Procedure for Uranium Concentration and Enrichment Assay) is a procedure for providing high-accuracy in-field uranium measurements to support physical inventory verifications at fuel production facilities. COMPUCEA was developed by the Institute for Transuranium Elements (ITU) [1], [2] and its present version is in routine use for EURATOM inspections in Europe since 2007 [3]–[5]. In 2011 it has been authorized by the International Atomic Energy Agency (IAEA) and it is used by the IAEA for PIV campaigns in Kazakhstan [6].

COMPUCEA determines the uranium concentration and ^{235}U enrichment in fuel pellets and powders. Prior to analysis the pellets or powders are dissolved in nitric acid, so the method is destructive. One aliquot of the solution is used to measure the uranium concentration based on X-ray transmission at the uranium L-absorption edge. Another aliquot is taken to determine the ^{235}U enrichment from the count rate of the 186 keV gamma peak of ^{235}U measured in a very well defined geometry by a $LaBr_3$ based gamma spectrometer. A third aliquot is used to determine the density of the solution, to be able to convert the results obtained in terms of U mass per unit volume of the solution (g/l) into results in terms of U mass per mass of the original pellet (weight %). The typical combined uncertainty of COMPUCEA is 0.20 % for U concentration and 0.30 for ^{235}U enrichment (given at the "1 sigma" confidence level of 67%) [4], [5], [7].

In 2011 the IAEA started the development of a new software package for performing COMPUCEA measurements and analyses [6]. It is based on the algorithms implemented in the well-established COMPUCEA software, developed in ITU, which has been in use since 2007. The aim was to improve the user friendliness of the interface, the traceability of the results, the fitting of the $LaBr_3$ spectrum and

the calculation of the uncertainties. Furthermore, a new module providing matrix correction for samples with gadolinium was added.

The new software, called CMPU hereafter, was tested and validated by ITU to authorize its use for measurement campaigns at fuel fabrication plants and for analyses in ITU. The objectives of the validation were the following:

- Check for bugs (and remove them)
- Test and fine tune the user interface
- Prove that the new software gives same (or better) results as the well-established software
- Validate correction for enrichment measurement for samples with Gd

The validation has shown that the results calculated by the new software agree very well with results from the previous software and with results from Thermal Ionization Mass Spectrometry. As the new software makes it much easier to provide high-accuracy analytical results with COMPUCEA, it is planned to be used in field from 2015 onwards.

2. Method of the validation

As the "old", well-established software has been already validated [4], [7], the performance of the new software was first checked by comparing its results to the results given by the old software. This was done by importing gamma and X-ray spectra to the new software. This kind of parallel evaluations by the two software codes was done for more than 60 samples, analysed during in-field and in-house campaigns.

In order to validate the matrix correction for samples which contain Gd, the ^{235}U enrichments calculated by the new software were compared to the results from Thermal Ionisation Mass spectrometry (TIMS).

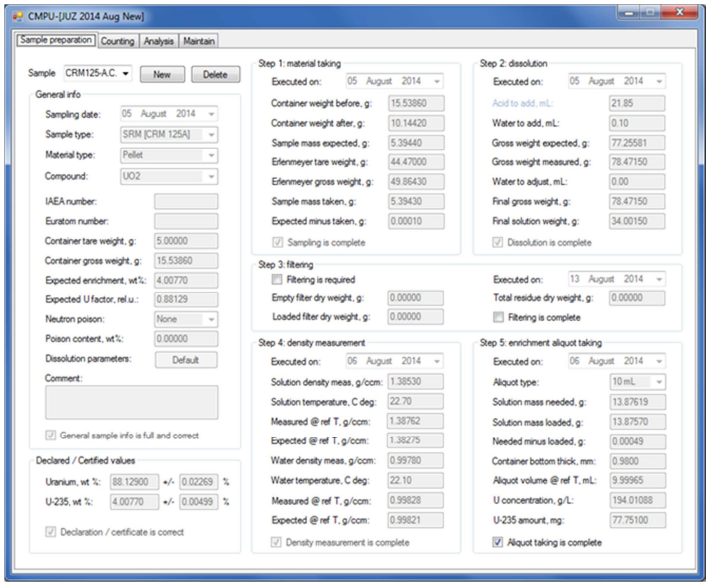

Figure 1. Default view of the new COMPUCEA software, showing the tab with details of sample preparation.

3. Results

3.1. User interface

With the old software 3 executables had to be used to carry out the analysis. A total of 5 excel sheets was used to keep track of the sample preparation, calibration and quality control and to calculate the results for U concentration and ^{235}U enrichment. An "analysis parameter file" had to be prepared for each campaign, containing the parameters used to carry out the analysis of the spectra. Finally, for

each sample a "sample information file" had to be made, containing the relevant information on sample preparation. The user had to select the correct files to introduce the data and to do the analysis.

Figure 1 presents the default view of the software, showing the details of sample preparation. The new software has a centralized, tabbed interface. It guides the user through the measurement and analysis process and by this it helps to avoid mistakes. All required settings can be adjusted from within the user interface. Extended testing with spectra from 4 measurements campaigns has proven the user-friendliness and robustness of the new interface.

3.2. U concentration

The U concentration was calculated by the new software from spectra already evaluated by the old software. Then the relative difference of U concentration calculated by the two software codes was determined. Figure 2 presents an example from an in-field campaign, where this difference was below 0.0024 % on average. For 3 other campaigns the difference was similar. This proves that the calculation of the U concentration is correctly implemented in CMPU.

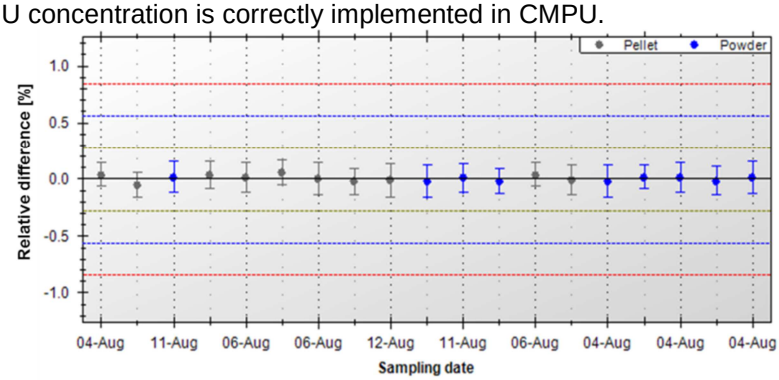

Figure 2. Example from an in-field-campaign, showing the differences of the U concentration calculated by the two software codes. The average difference is 0.0024%. The limits shown on the figure are the historical operator-inspector differences.

3.3. ^{235}U enrichment

Analogously to the U concentration, the ^{235}U enrichment was calculated by the two software codes. The differences for the same in-filed campaign as in Figure 2 are presented in Figure 3, showing an average of -0.091 %. For 3 other campaigns the difference was similar.

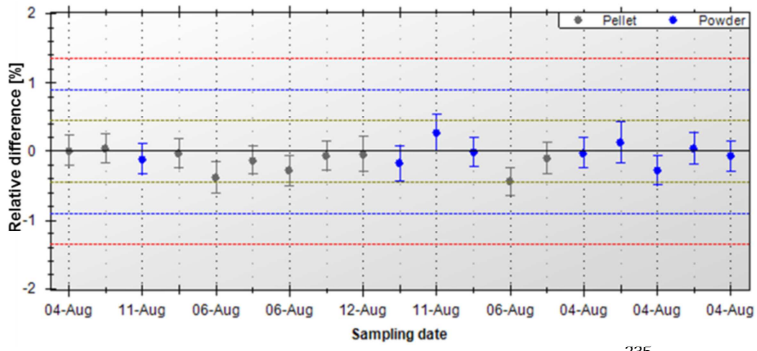

Figure 3. Example from an in-field-campaign, showing the differences of the ^{235}U enrichment calculated by the two software codes. The average difference is -0.091 %. The limits shown on the figure are the historical operator-inspector differences

If the sample contains neutron poison additives (e.g. Gd or Er) or impure materials with significant amount of heavy metals (e.g. dirty scraps), a matrix correction for the enrichment measurement is necessary because these additives and impurities affect the self-absorption of gamma rays in the sample. This correction is determined computationally using a custom Monte Carlo routine [6].

The algorithm models the transport of the 186 keV photons. The full energy events inside the detector are counted for two cases of sample material - with and without neutron poison content. The ratio of the two values gives the correction factor. An "effective Gd-content" is calculated by CMPU using the X-ray transmission measurement. This value or a user specified value for the Gd-content is used as input for the Monte-Carlo routine. For 0.05% relative accuracy, a typical computation time is about 10-15 min. The calculation is implemented as an independent process, thus it can be run simultaneously for several samples and with no interference with other functions of the CMPU software.

The performance of the matrix-correction algorithm was tested by comparing the ^{235}U enrichment obtained by CMPU to the ^{235}U enrichment from Thermal Ionisation Mass Spectrometry (TIMS). Figure 4 clearly shows that the enrichment results calculated by applying the matrix correction are closer to the TIMS values than the un-corrected results.

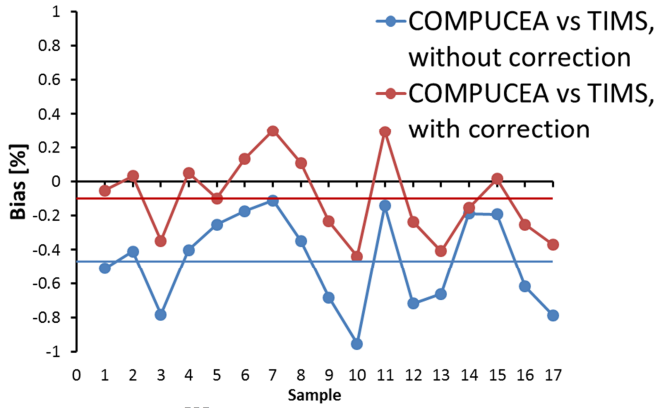

Figure 4. The differences between the ^{235}U enrichment calculated by CMPU and Thermal Ionisation Mass Spectrometry with and without applying matrix correction for samples containing neutron poison additives.

Therefore, the calculation of the ^{235}U enrichment in CMPU for samples without impurities is as good as in the old software, while for samples with impurities it is even better.

4. Conclusion

The required features of the new software for high-accuracy in-field uranium concentration and enrichment measurements by COMPUCEA were tested and validated in ITU. Some bugs were removed and the user interface was fine-tuned. The interface is more user-friendly than the previous one and it helps to avoid mistakes and improves traceability of the results. It was checked that the results given by the new software are consistent with the result from the well-established software. Furthermore, for samples with Gd the new software gives better results due to the implemented matrix correction algorithm.

As the validation has proven the good performance of the new software, it will be used for in-field campaigns in Europe from 2015 onwards.

References

[1] Matussek P, P. Laurent, W. Janssens, F. MacLean, and U. Blohm-Hieber, “Routine use and Recent Developments of the COMPUCEA Instrument (COMbined Product Uranium Concentration and Enrichment Assay),” in *Proceedings of the 19th ESARDA Annual Meeting, Montpellier*, 1997.

[2] H. Ottmar, S. Abousahl, N. Albert, P. Amador, H. Eberle, N. Erdmann, K. Lützenkirchen, G. Marissens, H. Schorlé, F. Lipcsei, and P. Schwalbach,

"COMPUCEA: A High-Perfoemance Analysis Procedure for Timely On-site Uranium Accountancy Verification in LEU Fuel Fabrication Plants," in *Procedings of the 48th INMM Annual Meeting, Tucson*, 2007.

[3] N. Erdmann, P. Amador, P. Arboré, H. Eberle, K. Lützenkirchen, H. Ottmar, H. Schorlé, and P. Van Belle, "COMPUCEA : A High-Performance Analysis Procedure for Timely On-site Uranium Accountancy Verification in LEU Fuel Fabrication Plants," *ESARDA Bull.*, no. 43, pp. 30–39, 2009.

[4] N. Erdmann, P. Amador, P. Arboré, H. Eberle, K. Lützenkirchen, H. Ottmar, H. Schorlé, P. van Belle, F. Lipcsei, P. Schwalbach, and R. Gunnink, "COMPUCEA 2nd generation performance evaluation," in *Proceedings of the 31st ESARDA Annual Meeting, Vilnius*, 2009.

[5] N. Erdmann, N. Albert, P. Amador, H. Eberle, H. Ottmar, P. van Belle, F. Lipcsei, P. Schwalbach, and S. Jung, "COMPUCEA 2nd generation performance evaluation," in *Proceedings of IAEA Safeguards Symposium, Vienna*, 2010.

[6] A. Berlizov, A. Schachinger, K. Roetsch, N. Erdmann, H. Schorlé, M. Vargas, J. Zsigrai, A. Kulko, M. Keselica, F. Caillou, V. Unsal, and A. Walczak-Typke, "Feedback from Operational Experience of On-Site Deployment of Bias Defect Analysis with COMPUCEA," *J. Radioanal. Nucl. Chem. Spec. Issue MARC X*, 2015.

[7] N. Erdmann, H. Ottmar, P. Amador, H. Eberle, and P. van Belle, "Validation of COMPUCEA 2nd Generation; JRC Technical Report JRC-ITU-TN-2008/37," 2008.

Session 15

Novel Technologies and Forensics

Nuclear Forensics Technologies in Japan

N. Shinohara, Y. Kimura, A. Okubo and H. Tomikawa

Japan Atomic Energy Agency
Tokai, Ibaraki 319-1195, Japan
E-mail: shinohara.nobuo@jaea.go.jp

Abstract:

Nuclear forensics is the analysis of intercepted illicit nuclear or radioactive material and any associated material to provide evidence for nuclear attribution by determining origin, history, transit routes and purpose involving such material. Nuclear forensics activity includes sampling of the illicit material, analysis of the samples and evaluation of the attribution by comparing the analysed data with database or numerical simulation. Because the nuclear forensics technologies specify the origin of the nuclear materials used in illegal dealings or nuclear terrorism, it becomes possible to identify and indict offenders, hence to enhance deterrent effect against such terrorism. Worldwide network on nuclear forensics can contributes to strengthen global nuclear security regime.

In the ESARDA Symposium 2015, the results of research and development of fundamental nuclear forensics technologies performed in Japan Atomic Energy Agency during the term of 2011-2013 were reported, namely (1) technique to analyse isotopic composition of nuclear material, (2) technique to identify the impurities contained in the material, (3) technique to determine the age of the purified material by measuring the isotopic ratio of daughter thorium to parent uranium, (4) technique to make image data by observing particle shapes with electron microscope, and (5) prototype nuclear forensics library for comparison of the analysed data with database in order to evaluate its evidence such as origin and history. Japan's capability on nuclear forensics and effective international cooperation are also mentioned for contribution to the international nuclear forensics community.

Keywords: nuclear forensics; impurity; isotopic composition; age determination; database

1. Introduction

International threat of nuclear terrorism is increasing according to IAEA report [1] and other security documents. Domestic technologies against illicit trafficking of nuclear material and radioactive substances must be established for criminal specification and prosecution for security and maintenance of public peace even in Japan. When illicit trafficking of nuclear material happens in a third-country in future, there is possibility that the nuclear material is suspected to be stolen in Japan because we have various nuclear facilities and multiplex nuclear materials. Japan's own technology for nuclear forensics (NF) should be retained in order to keep reliance of our nuclear activities.

Japan Atomic Energy Agency (JAEA) has engaged in research and development activities of NF for strengthening nuclear security in accordance with Japan's national statement at the Washington Nuclear Security Summit in 2010 [2]. The JAEA has developed analytical methods for measurement of isotopic abundance and impurity in nuclear material in order to identify its source and determine the point of its origin and routes of transit. Joint researches with the US national laboratories have been implemented in the fields of uranium age dating measurements, characterization of nuclear fuel for forensics purposes, and establishment of a proto-type national NF library. In this paper, capabilities of the NF technologies in Japan are presented for the purpose of sharing our experience with international NF community.

2. Development of nuclear forensics technologies

The JAEA has developed the fundamental technologies for NF from 2011 to 2013, namely (1) technique to analyse isotopic composition of nuclear material, (2) technique to identify the impurities contained in the material, (3) technique to determine the age of the purified material by measuring the isotopic ratio of daughter thorium to parent uranium, (4) technique to make image data by observing particle shapes with electron microscope, and (5) prototype nuclear forensics library for comparison of the analysed data with database in order to evaluate its evidence such as origin and history.

2.1. Isotopic composition of nuclear material

Isotopic abundances of nuclear material can be measured by means of Thermal Ionization Mass Spectrometry. A mass dependent bias observed in this analytical technique was previously corrected by measuring well characterized standards. Total evaporation (TE) is, however, an excellent analysis technique for the measurement of uranium isotopic ratios, where highly precise and accurate data can be obtained because the mass dependent bias is neglected. This TE technique has been demonstrated for isotope ratio measurements of uranium using well characterized Certified Reference Materials (CRMs) of U500 and U050 from New Brunswick Laboratory (NBL). The certified values and our results are shown in Table 1. It is concluded that the TE technique is applicable to the NF analysis of illicit nuclear materials. The TE technique has been applied to the analyses of several kinds of uranium (yellow cake, ammonium diuranate (ADU), UO_2, UO_3, U_3O_8) possessed in JAEA. The measured data was stored in database of our NF library.

Uranium Isotopic Standards	Atom Percent			
	^{234}U	^{235}U	^{236}U	^{238}U
NBL U500 Certified Value	0.5181±0.0008	49.696±0.050	0.0755±0.0003	49.711±0.050
Our Measured Value	0.5187±0.0001	49.703±0.004	0.0760±0.0001	49.703±0.007
NBL U050 Certified Value	0.0279±0.0001	5.010±0.005	0.0480±0.0002	94.915±0.005
Our Measured Value	0.0279±0.0001	5.011±0.001	0.0482±0.0001	94.913±0.001

Table 1: Isotopic abundances of uranium standards of CRM U500 and U050.

2.2. Impurities contained in nuclear material

Contents of impurity elements are quite different among the samples, because the points of their origins and routes of transit are varied. Information on the impurities of nuclear materials is useful for the purpose of NF investigation. Impurity analysis was then examined by ion exchange separation and mass spectrometry. Procedure for impurity analysis was accomplished by using extraction chromatography and inductively coupled plasma-mass spectrometry (ICP-MS) measurement. A result is shown in Table 2, where 53 elements can be analysed within one week by our method.

2.3. Age determination of uranium

The age of nuclear material is also essential information to identify the source of the material, especially for knowing the date when the material was produced or purified. The ^{234}U-^{230}Th chronometer is widely applied to NF, because the radioactive decay of ^{234}U provides a chronometer. The age *t* of the uranium can be calculated using equation (1):

$$t = \frac{1}{\lambda_{234U}-\lambda_{230Th}} * ln\left[1 + \frac{R(\lambda_{234U}-\lambda_{230Th})}{\lambda_{234U}}\right] \quad (1)$$

where *R* is measured $^{230}Th/^{234}U$ atom ratio and λ_x is the decay constant of isotope X.

Procedure for age determination of uranium by ion-exchange purification and mass spectrometry has been developed in JAEA. We conducted procedure exchange and inter-laboratory comparison exercise on uranium age dating between US national laboratories (LANL and LLNL) and JAEA, where

the same NBL standard materials of CRM U050 were independently analysed [3]. The analysis of age determination on the uranium oxide standard was performed and the time of its purification can be estimated as shown in Table 3.

Element	Minimum Limit of Determination by ICP-MS (μg/g of sample)	Element	Minimum Limit of Determination by ICP-MS (μg/g of sample)
Li	3	Sn	3
Be	1	Sb	1
Ca	500	Te	10
Sc	0.3	Cs	0.5
Ti	15	Ba	3
V	1	La	0.2
Cr	5	Ce	0.3
Mn	4	Pr	0.1
Fe	100	Nd	0.5
Co	1	Sm	1
Ni	3	Eu	0.2
Cu	2	Gd	0.4
Zn	15	Tb	0.2
Ga	2	Dy	0.3
Ge	10	Ho	0.1
As	4	Er	0.2
Se	100	Tm	0.2
Rb	1	Yb	0.2
Sr	1	Lu	0.2
Y	0.2	Hf	0.4
Nb	2	W	0.5
Mo	2	Re	0.5
Ru	1	Ir	0.2
Rh	0.5	Tl	1
Ag	1	Pb	2
Cd	3	Bi	1
In	0.5		

Table 2: Analysable elements and their limits of determination in impurity analysis.

Laboratory	Determine Model Age (years)
LANL	56.75 ± 0.99
LLNL	56.23 ± 0.43
JAEA	55.36 ± 0.60

Table 3: Results of age determination for the NBL standard material of CRM U050.

2.4. Particle analysis by electron microscope

Visual inspection of a sample can give useful information as an NF evidence. Scanning electron microscopy (SEM) displays an image or map of the sample. Figure 1 shows an example of particle image observed by SEM. Backscattered electrons carry information about average atomic number of the area and can detect spatially resolved phases of chemical composition. For the NF analysis, we have installed a transmission electron microscopy (TEM). The energetic electron beam of TEM transmits through an ultra-thin sample and can image extremely fine structure more than SEM in spite of tight restrictions on sample thickness. Transmitted electrons can undergo diffraction effects to determine crystal phases in the material.

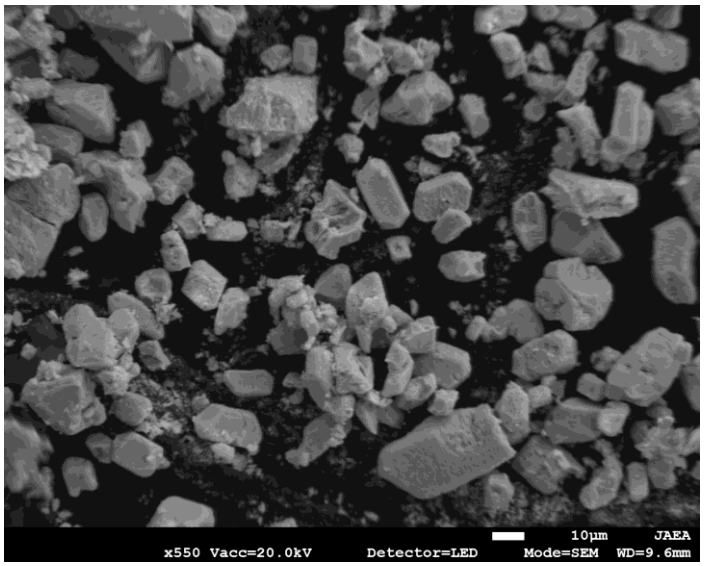

Fig. 1: Particle image of uranium (ADU) observed by SEM.

2.5. NF library

A prototype national nuclear forensics library (NNFL) was constructed based on the data related to nuclear materials and other radioactive materials. The data gathering on the nuclear materials possessed in JAEA has been continued. The JAEA participated in the first international table top exercise of NNFL "Galaxy Serpent," held by the International Technical Working Group (ITWG) as a part of our NNFL development project [4]. Figure 2 shows an isotope correlation plot in order to evaluate the seizure. The seized material strongly associated with the PWR-2 reactor as seen in this figure. The present prototype system will be transferred to the future national responsible authority as a real NNFL which will support the nuclear security activities in Japan.

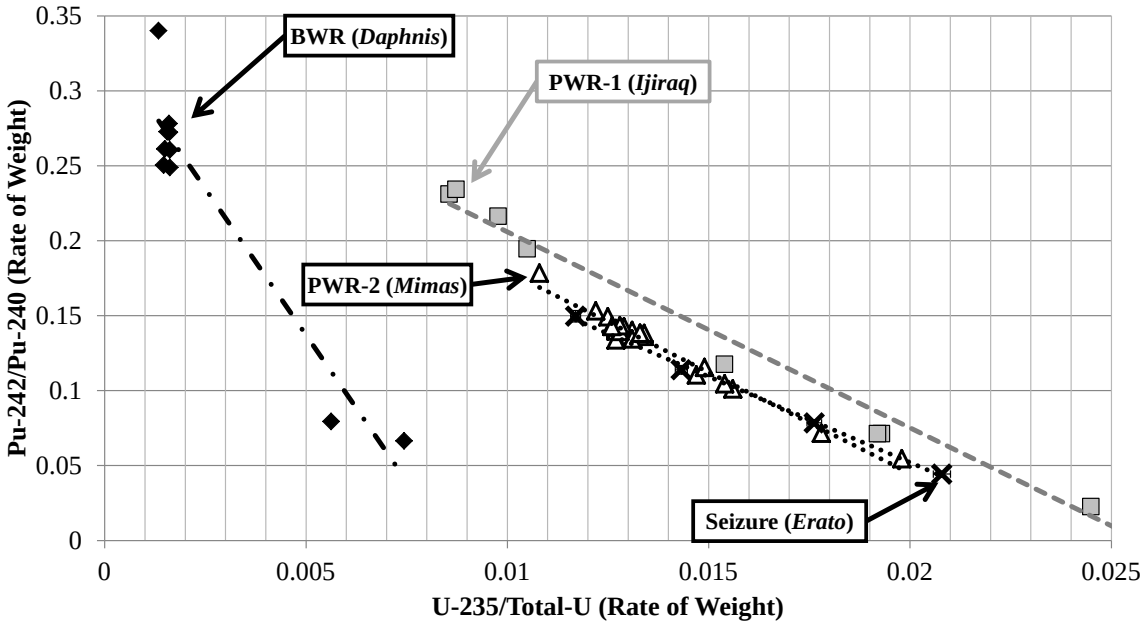

Fig. 2: Isotope correlation plot of $^{235}U/^{Total}U$ vs. $^{242}Pu/^{240}Pu$ for international table top exercise of NNFL "Galaxy Serpent." Daphnis, Ijiraq, Mimas and Erato are the nicknames of the exercise.

3. Recent activities to enhance the NF technologies at JAEA

Under the fundamental technologies of NF mentioned above, the JAEA has started a next project for enhancement of functionality of the NF technologies from 2014, which are (a) improvement of the library, (b) new technology of particle analysis by TEM, (c) database construction, (d) development of new age determination, and (e) further international cooperation.

3.1. Improvement of the NF library

In order to attribute the belonging of nuclear material to a datum from huge NF database by evaluating its analysed data, a multivariate analysis tool for seizure analysis is being developed together with image evaluation tool for microscope images. Knowledge accumulation system for such NF analysis is important for serial evaluation methodologies which deal with conditions for survey, data items, applied procedure, evaluation of results, and all performed records. According to the knowledge accumulation system, it is possible to carry out reliable and rapid attribution analysis which is independent of evaluator's ability.

3.2. JAEA database

A prototype system of NNFL deals with the data of nuclear and other radioactive materials that the JAEA has possessed in the past research activities. Basic data handling system for nuclear material database (NMDB) was already installed in our NNFL. Data compiling on the JAEA NMDB has been now continued. In the next step of the NNFL project, it is planned to develop a prototype of radioactive materials database (RMDB), which will contain the radioisotopes in medical and industrial usage and the radioactive waste produced in nuclear facilities. An integrated NNFL will consist of the combination of NMDB and RMDB complementally.

3.3. Particle analysis by TEM

Fine feature of nuclear material like crystal structure can be observed by using TEM. Such particle analysis is useful to obtain new NF signature, because fine structure of uranium oxide depends on its sintering temperature. For the purpose of particle analysis by TEM, observation method is now investigated by making very thin (less than 100 nm) specimen with focuses ion beam (FIB). Diffraction contrast image to observe crystal defect and damage, electron diffraction image to analyse crystal structure, and high-resolution transmission image to understand grain boundary become important evidences for NF. Electron energy-loss spectroscopy (EELS) installed in TEM is also available to analyse the elements and their bonding states.

3.4. New age determination

Age dating to elucidate the final purification date of uranium is important subject on NF analysis. The parent/daughter pair of ^{234}U-^{230}Th established in the field of geochemical science has been applied for nuclear forensics. If the uranium has not been fully separated or purified, the chronometer misleads incorrect information about the age. To avoid this systematic error, it is recommended to measure various parent/daughter ratios. The parent/daughter pair of ^{235}U-^{231}Pa is our next subject for age dating.

3.5. International cooperation

Exchange of the newest NF information through international cooperation is useful for each State, because the NF activity has a global side of criminal investigation. The JAEA implements joint researches with US and EC/JRC for forensics purposes. The Integrated Support Center for Nuclear Nonproliferation and Nuclear Security (ISCN) under the JAEA has been providing training courses to support domestic and international capacity building for regulators, mainly from Asian countries in

cooperation with the IAEA. The IAEA Regional Training Course on Introduction to Nuclear Forensics was hosted by the ISCN in May 2012 and received total 24 participants from ten Asian countries. The ISCN will promote International Training Course on Practical Introduction to Nuclear Forensics in February 2016.

4. Nuclear forensics capabilities in Japan

In view of the importance of nuclear security and international impetus to construction of NF regime, the pertinent agencies in Japan must cooperate with one another. It is necessary to organize Japan's own system for NF by establishing a national NF laboratory and collaborating with traditional forensics. We must "improve capabilities to search for, confiscate, and establish safe control over unlawfully held nuclear or other radioactive materials and substances or devices using them," as mentioned in the Statement of Principles committed to the participants in the Global Initiative to Combat Nuclear Terrorism (GICNT)

The NF laboratory consists of analytical and storage facilities for seizure materials and NNFL. The laboratory should have ability to secure the reliabilities of evidence analysis techniques, guarantee of quality to the results analysed as evidence, database and its comparison with evidence. Because the JAEA has developed the fundamental technologies for NF as mentioned above, it is possible for us to take charge of the analysis for nuclear materials as a work of NF laboratory. In the NF analysis of seizure and the database construction of NNFL, the judicial reliability of the data is required on the basis of standardization of the analytical scheme and inter-laboratory round-robin exercises. We should enhance our analytical skills for the sake of international progress of the nuclear security.

5. Conclusion

The JAEA has developed fundamental and reliable technologies for NF (Nuclear Forensics) and is now measuring actual uranium samples to make a NF database. A prototype system of NNFL (National Nuclear Forensics Library) is constructed on the basis of international cooperation. The pertinent agencies in Japan must cooperate with one another to organize Japan's own system for NF by establishing a national NF laboratory. The laboratory should have the reliabilities of evidence analysis techniques, guaranteed quality of the evidence, and database and its comparison with evidence. Another important subject of ours is domestic and international capacity building of nuclear security, especially for Asian countries, in cooperation with IAEA, GICNT and ITWG.

6. Acknowledgements

The authors would like to express our gratitude to Mr. N. Toda, Mr. Y. Funatake, Mr. O. Kataoka, and Mr. T. Matsumoto for their support and advice regarding this study. The work presented in this paper has been supported by the Ministry of Education, Culture, Sports, Science, and Technology (MEXT) of Japan

7. References

[1] International Atomic Energy Agency; IAEA Nuclear Security Series No.2, *Nuclear Forensics Support, Technical Guidance*; STI/PUB/1241; 2006.
[2] Nuclear Security Summit 2014; *National Progress Report Japan*; http://www.mofa.go.jp/dns/n_s_ne/page18e_000059.html; Hague; 2014.
[3] Steiner R, Kinman W.S, Williams R, Gaffney A, Schorzman K, Pointurier F, Hubert A, Magara M, Okubo A; *^{230}Th - ^{234}U Thorium Radiochronometry Method Comparison: A Tri-Lateral Round-Robin Exercise*; International Conference on Advances in Nuclear Forensics; IAEA; Vienna; IAEA-CN-218-54; 2014.
[4] Kimura Y, Shinohara N, Funatake Y; *Lessons Learned from the International Table Top Exercise of National Nuclear Forensics Library at JAEA*; Journal of Nuclear Material and Management; 42.4; 2014; p 4-11.

Gamma-spectrometric age-dating of uranium samples

András Kocsonya, Zsuzsanna Kovács, Cong Tam Nguyen, László Lakosi

Centre for Energy Research, Hungarian Academy of Sciences
Konkoly-Thege Miklós út 29-33., 1121 Budapest, Hungary
e-mail: andras.kocsonya@energia.mta.hu, laszlo.lakosi@energia.mta.hu

Abstract

For determining the origin of nuclear material out of regulatory control, information on the age of the material seems relevant. A novel method for uranium age dating was invented in 2001 in our laboratory at the Institute of Isotopes, one of the legal predecessors of our present institute, using high resolution gamma-spectrometry (HRGS) for determining the daughter/parent activity ratio $^{214}Bi/^{234}U$ by directly measuring the relevant gamma peaks. The method is non-destructive and does not require the use of reference materials of known ages. It works well for high-enriched and aged samples first of all. Applications extend to dating metal, oxide, powder, etc. seized and reference samples, reactor fuel rods and pellets, in the enrichment range of 4.4 to 90%. The least enriched uranium sample dated by HRGS was a 4.5% enriched oxide material, the age of which was determined as 29 ± 3 yr. The youngest sample was a 6.7 ± 0.7 yr old metallic U of 90.8% enrichment. In order to extend capabilities to low enriched uranium and improve sensitivity and accuracy of the method, a higher efficiency well-type HPGe detector was used and tested. The characteristics of the age dating measurements by this well-type detector and the first results are discussed.

Keywords: Nuclear forensics; non-destructive assay; low background HRGS; Bi-214/U-234 activity ratio; well-type detector

1. Introduction

For identifying the provenance of unknown material, the age of a sample has a unique significance in the nuclear forensic analysis. Although usually provide more sensitive analysis with lower detection limits, destructive (DA) methods (mass spectrometry, α-spectrometry) have certain drawbacks in such activities/applications, namely lack of promptness, sample preparation; need for preservation of evidence. They cannot be used e.g. for items which cannot be dismantled. Among other non-destructive assay (NDA) methods, high resolution gamma-spectrometry (HRGS) has long been routinely used for quantitative assay of U-bearing nuclear materials. No special sample preparation is necessary, whereas assay of some material as a whole is possible, without sampling (e. g. reactor fuel rods). Preservation of evidence can easily be ensured. This is essential for nuclear forensic application, where the material is evidence in jurisdiction. At the same time destructive methods preserve their traditional role, and combination of different analytical techniques increase the confidence in the results and can help to further narrow down the set of possible origins and intended uses of the investigated materials.

For categorization and characterization, including the determination of the origin of nuclear material out of regulatory control, information on the age of the material seems relevant. The daughter/parent ratio as a function of decay time is widely used for determining the age of radioactive samples. A new method for uranium age dating was developed using gamma-spectrometry based on the daughter/parent $^{214}Bi/^{234}U$ activity ratio by direct measurement [1, 2]. The method is non-destructive and does not require the use of reference materials of known ages. It was invented and first applied in

our laboratory at the Institute of Isotopes, one of the legal predecessors of our present institute, on the occasion of an inter-laboratory comparison (“Round Robin” Exercise) organized by the International Technical Working Group on Nuclear Forensics (ITWG) in 2001, where a 90% enriched oxide sample was assayed. Our age result obtained by HRGS was consistent with those of other labs measured by mass spectrometry.

2. Theoretical background

Uranium age-dating is based on the determination of the daughter/parent ratio of the radioactive decay chain of uranium. In course of enrichment process the elements of decay chain are removed from the sample, then the decay chain starts to build up again. Due to long half-life of ^{238}U and ^{235}U isotopes of uranium, the decay chain of these isotopes is not building up in measurable amount in human time scales. Since the half-life of ^{234}U is essentially shorter (2,455×10^5 years), this isotope may be a candidate for age dating. In natural uranium the ^{234}U/^{235}U ratio is roughly 1%. According to practical experiences, ^{234}U undergoes enrichment/depletion in parallel with ^{235}U, therefore the amount of ^{234}U in processed uranium remains roughly proportional to ^{235}U.

One has to consider that ^{234}U is the element of ^{238}U decay chain as well. Due to the long half-life of ^{238}U, the amount of ^{234}U from the decay of ^{238}U is lower by at least 3 orders of magnitudes than ^{234}U coming from the enrichment, in time-scales relevant in uranium age-dating.

Upon encountering unknown (e. g illicit) nuclear materials, ^{234}Th (24 d half-life) may be supposed to be practically in radioactive equilibrium with its parent ^{238}U in the occurring samples. Thus, determination of the daughter/parent ratio ^{230}Th/^{234}U is the first candidate for age dating of U samples. Indeed, the determination of this ratio is the basis of mass spectrometric U dating [3]. Considering gamma spectrometry, ^{234}U has well measurable gamma rays, whereas its daughter ^{230}Th does not have abundant gamma lines. Next member of the ^{234}U decay series is ^{226}Ra, with a significant gamma-line at 186,2 keV. However, this line strongly overlaps with the intense gamma-line of ^{235}U at 185.7 keV, therefore cannot be measured in trace amounts. ^{26}Ra decays to ^{214}Bi through three short-lived nuclides which have useful gamma lines, especially ^{214}Bi, whose 609.3 keV line can be appropriate to measure. The longest-lived daughter of ^{226}Ra is ^{222}Rn, with a half-life of 3.825 days. Thus, the time needed for secular equilibrium between ^{226}Ra and ^{214}Bi is about 2 weeks, so it can be assumed that the activities of ^{226}Ra and ^{214}Bi are equal at the time of the measurement. Due to characteristics of gamma-spectrometry, the 609.3 keV line of ^{214}Bi is the best candidate for age dating measurements. The signal/background ratio of ^{214}Pb lines are worse, while other gamma-lines of ^{214}Pb (1120.3 keV, 1764.5 keV) overlap with other lines in the spectra.

Hence, according to the kinetics of the radioactive decay series the activity ratio ^{214}Bi/^{234}U at time T after purification/enrichment of the material can be calculated with a good approximation as

$$\frac{A_{Bi\,214}}{A_{U\,234}} = \frac{A_{Ra\,226}}{A_{U\,234}} = \frac{1}{2}\lambda_{Th}\lambda_{Ra}T^2$$

where λ-s are the respective decay constants. Secular equilibrium is considered between ^{214}Bi and ^{226}Ra.

The activity ratio A_{Bi214}/A_{U234} can be described as

$$\frac{A_{Bi\,214}}{A_{U\,234}} = \frac{A_{Bi214}}{A_{U\,238}}\left(\frac{A_{U\,235}}{A_{U\,238}}\frac{A_{U\,234}}{A_{U235}}\right)^{-1}$$

Due to the characteristics of gamma-spectrometry these activity ratios can be measured easier: the representing gamma-lines are closer to each other in energy, thus due to the smaller correction factors for efficiency and self absorption the activity ratio can be measured more precisely. Practically the Bi214/U238 activity ratio is measured by a coaxial HPGe detector, while the uranium isotope ratios are measured by a planar one.

There are some limiting factors of the ^{214}Bi determination. Due to small amount of ^{214}Bi from ^{234}U decay, the gamma-spectrometric determination of this nuclide requires efficient detector and low background.

Since ^{238}U, as a terrestrial radionuclide occurs in the environment, its progeny including radon is always present in the laboratory background. The fluctuation of the natural background due to atmospheric ^{222}Rn, precursor of ^{214}Bi, has a substantial influence on the result. Even the reduction of radon level can also be considered to reduce the background.

In addition, a Compton background caused by high energy peaks of ^{234m}Pa (^{238}U daughter) is also present in the spectrum, hindering the evaluation of the 609 keV peak of ^{214}Bi (and of the U peaks, too).

Due to these limitations a lower limit on the ^{235}U abundance of the material exists that allows determining the age by gamma-spectrometry, depending on the amount and the age of the material, detector efficiency and background level.

3. Applications

In case of high enriched uranium samples the availability of this method was demonstrated by measurements in an iron chamber using a high purity germanium (HPGe) coaxial detector PIGC3520 with 30% relative efficiency. In case of low enriched uranium (LEU) samples, the lower amount of ^{234}U (and therefore of ^{214}Bi) is lower as well, so the corresponding activity is more difficult to measure and the uncertainty caused by the variation of the natural background becomes higher. Difficult-to-measure samples are the same as in case of mass spectrometry, i. e. low-enriched and/or “young” uranium.

The described age-dating method was tested on a set of uranium samples available in our laboratory.

The method was tested with 90 % and 36 % ^{235}U-containing samples of ages known as > 41y from records. The measured age of the sample 90% was 43 **±** 2y; that of the sample 36% was found 43 **±** 5y by relative efficiency calibration and 45**±** 4y by determining absolute detector efficiency.

Results of a certified reference material (CRM) of 10% ^{235}U content, measured in ITU, Karlsruhe and in our lab at the Institute of Isotopes, Budapest, agree well with each other and were consistent with certificate. The result of a CRM of 5 % enrichment was consistent with the certificate. Result of a LEU pellet of 4.4% ^{235}U content was confirmed by LA-ICP-MS.

Among practical applications, we assayed materials whose integrity is to be maintained, thus destructive methods were to be avoided. Such dismountable U-bearing materials like fuel assemblies used in research reactor or a fission ionization chamber containing ^{235}U above 90% abundance cannot even be analyzed by destructive methods at all. These objects may occur in illicit trafficking, too.

Research reactor fuel rods (type VVR-SM), enriched to 36%, of known ages as 39, 38, 21, and 6 y were dated as 45±4, 40±3, 29±4, and < 13 y, respectively. A 10% enriched EK-10 fuel rod of age either 39 or 47 y according to records was dated 47±4 y old.

Due to the Compton tail of high energy ^{234m}Pa lines (and some time those of ^{208}Tl peaks coming from the decay of ^{232}U being present in reprocessed material), the sensitivity of detecting the 609 keV ^{214}Bi

line decreases toward low enrichment. Using the 150 cm^3 coaxial detector, the least enriched uranium sample dated in our lab by HRGS was a 4.5% enriched oxide material, the age of which was determined as 29 ± 3 yr, whereas the youngest sample was a 6.7 ± 0.7 yr old metallic U of 91% enrichment.

Summarized age results [7] obtained in our lab, plotted against the measured activity ratios A_{Bi214}/A_{U234} are shown in Fig. 1 below.

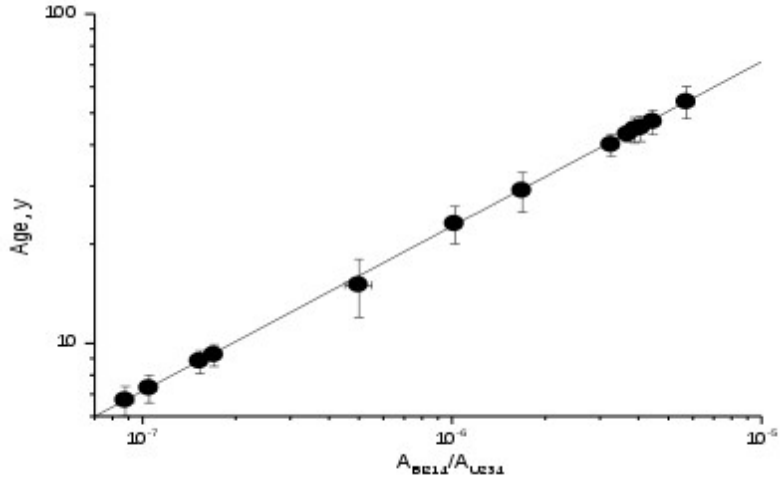

Fig. 1. U age determinations by gamma spectrometry at our laboratory so far

In course of the tests on various samples the limitations of the method became clear. The assessed detection limits of detection of age-dating as a function of enrichment are plotted in Fig. 2. This detection limits are calculated for a 150 cm^3 coaxial HPGe detector. The sensitivity and the range of applicability of the method can be improved by using a detector of higher efficiency, e.g. a bigger well-type Ge detector.

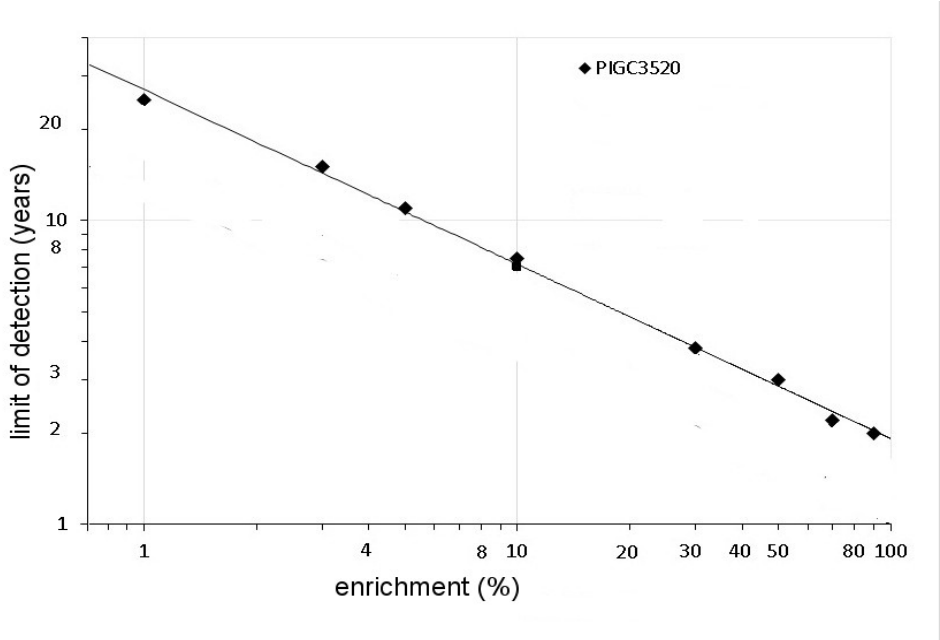

Fig. 2. Detection limit of age-dating vs. enrichment

4. Experiences by the well-type detector

Extension of the lower limits of both enrichment and age is, however, possible with the aid of a newly acquired large well-type HPGe detector (60% relative efficiency, 293 cm^3 active volume) used in low background. However, the high efficiency afforded by the high solid angle of the detector causes additional difficulties. Since ^{214}Bi shows a cascade-type gamma-decay, the true coincidence effect is rather significant using this detector. A direct method was developed for the measurement of the coincidence factor for the relevant lines (Fig. 3).

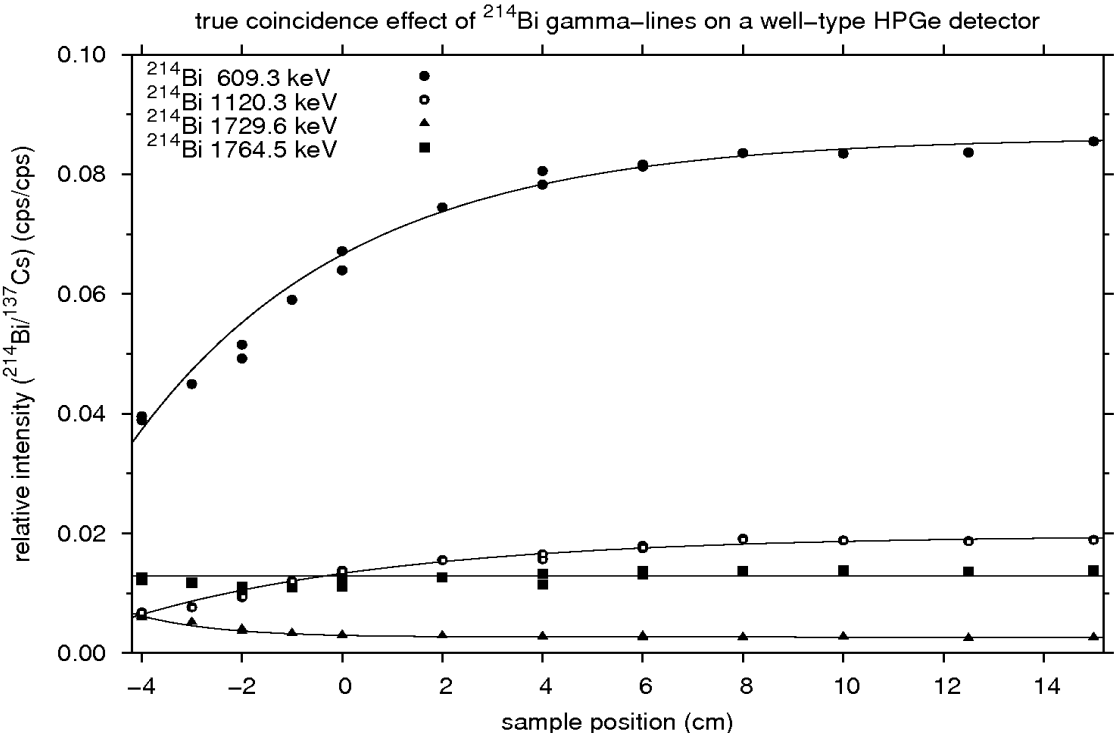

Fig. 3. Coincidence effect of ^{214}Bi gamma-lines

Since the age dating is based on the measurement of ^{214}Bi/^{234}U activity ratio, the evaluation is favourable using relative efficiency calibration by multi-line gamma emitters. It is an effective method in the case of lower efficiency detectors. By the well-type detector, this method is more complicated due to the changing of line intensities caused by the coincidence effect. Therefore the true-coincidence-effect is necessary to take into consideration for the calibration. The measured relative calibration curve of the detector measured is plotted in Fig. 4.

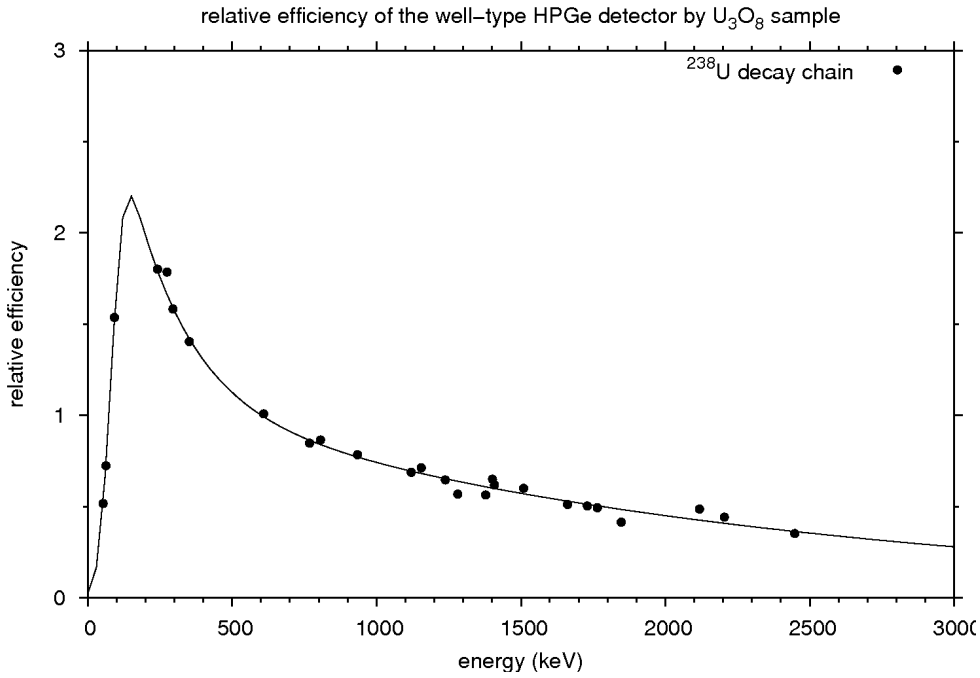

Fig 4: Relative efficiency of the detector

The relative efficiency (intrinsic) calibration can be determined from the same spectrum as the measured activity ratios [4 - 6]. At the same time, it accounts for the attenuation of different energy gamma rays in the absorbers and in the sample as well. The activity ratio can be obtained from the measured intensity ratio, the relative efficiencies taken at the corresponding energies, and from the values of the emission probabilities taken from literature. The relative efficiency calibration is applicable to samples of arbitrary shape and chemical form (e.g. fuel rods).

The radon in the air causes not only the increase of the background, but due to the varying of the radon level in the air causes the instability in time of the background to be subtracted. The radon level of the chamber was reduced by continuous nitrogen flow at ~ 1m^3/day flow rate. Due to this flow the reduction of the absolute value of the radon level was approximately 20% only, but its variation reduced from 30% to below 10%. This more stable background allows the reduction of detection limit. The continuous monitoring of radon level by an AlphaGuard radon monitor (based on an ionisation chamber) was tested also, which allows to take into consideration the radon background even if it is varying.

The size of samples is limited by the well-diameter of the detector. Taking into consideration the size of the plastic sample-holders, the maximum diameter is approximately 1 cm. Due to high efficiency of the detector the activity of samples is limited also to avoid long dead times. The total activity of samples should not be more than 1 kBq. In case of age-dating measurements of uranium samples, the intense lines of ^{235}U (143.8 keV, 185.7 keV) are reduced by a Pb shielding of 0.2 mm thickness.

In addition to the above discussed sample size limitations the optimal measurement geometry is not trivial. In the closest sample-detector geometry the sample is in the well of the detector. This geometry provides a rather good counting efficiency, but the coincidence effect is significant, and the continuous (Compton) background and the dead time are also increased. In order to test the effects of different sample-to-detector geometries, the same sample was positioned at various distances from the detector. The signal/background ratio was plotted as a function of sample-to-detector distance (Fig.: 3.). Zero distance means that the sample is positioned onto the upper surface of the detector capsule, while negative distances refer to the sample being in the well of the detector. The curve shows a significant maximum at zero distance. This was preferred at the measurements.

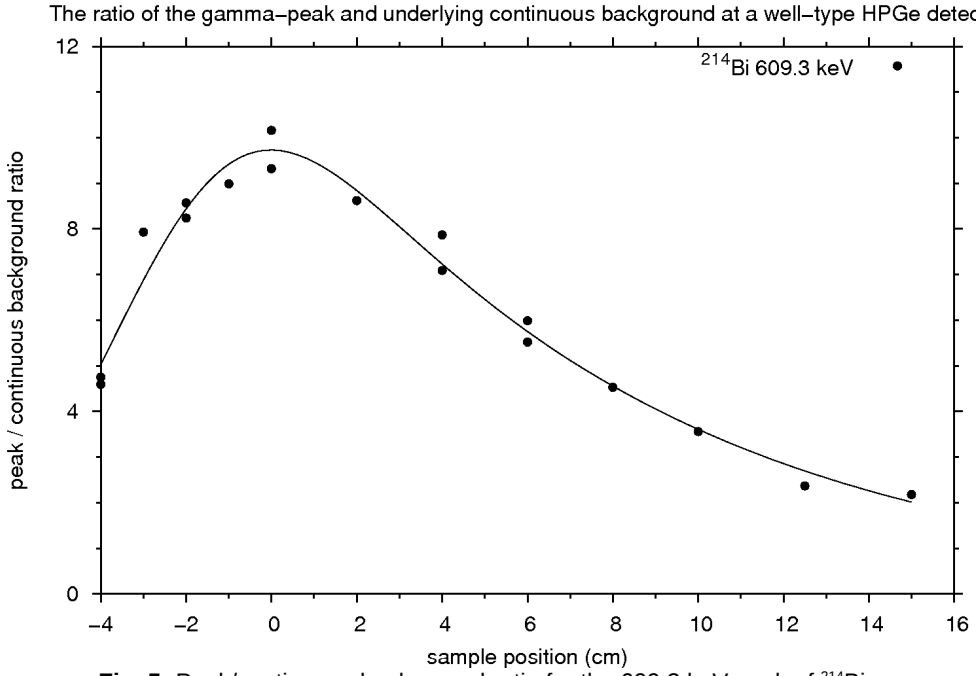

Fig. 5: Peak/continuous background ratio for the 609.3 keV peak of ^{214}Bi

Age-dating of LEU samples was tested on a sample of 10% nominal enrichment from a fuel rod of the training reactor of the Budapest University of Technology (BME). A piece of a fuel rod was available, which was already present at the start of operation of this reactor (1971). The rod was used for test purposes at the beginning of the operation, then it was cut to pieces for different analyses. A piece of ~1 g was measured (Fig 6). The 661.7 keV peak of ^{137}Cs is also visible in the spectra, since the fuel rod was irradiated for a short period.

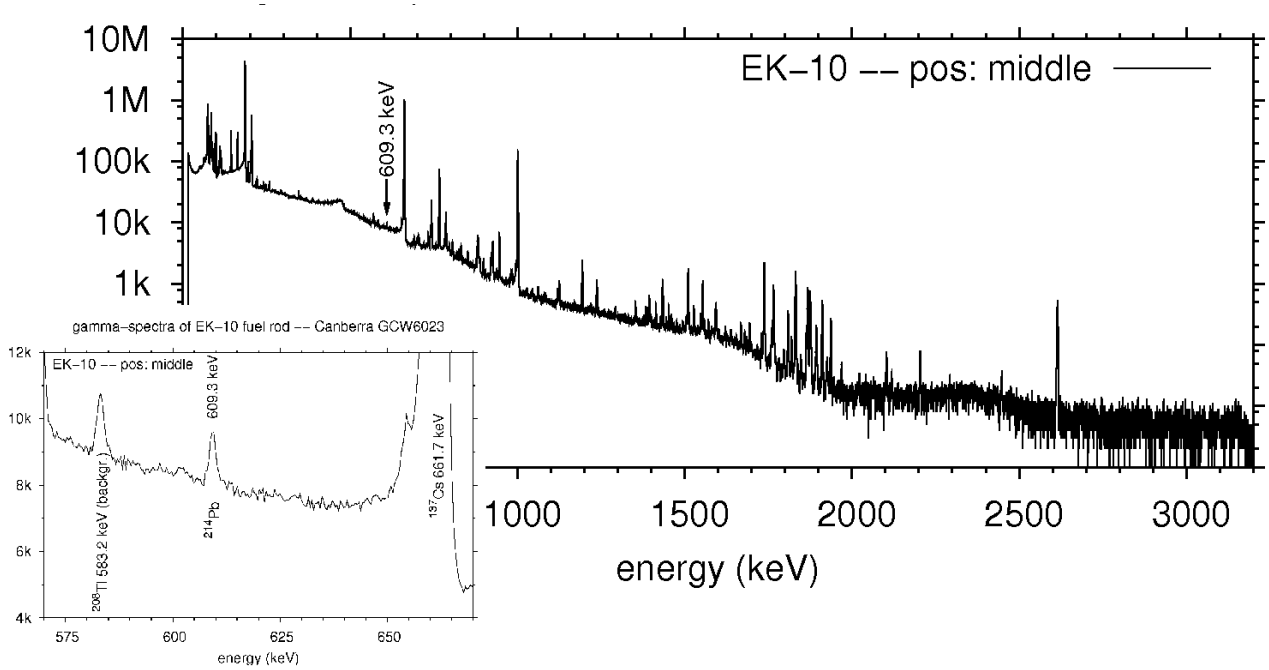

Fig. 6: Gamma-spectra of EK-10 fuel rod piece on the well-type HPGe detector

In order to check the correct accounting of the true-coincidence correction, the sample was measured at three positions, marked in Fig 7.

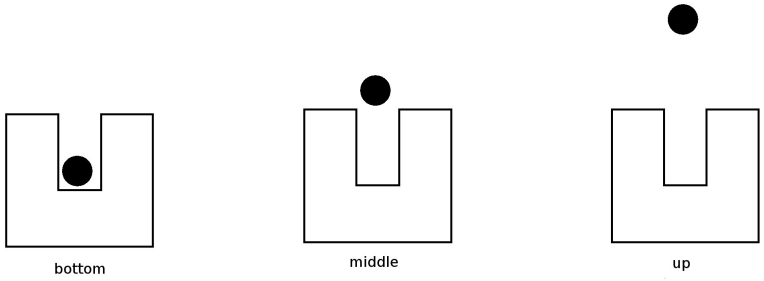

Fig. 7: Sample positions on the well-type detector

The results of measurement are listed in Table 1.

Table 1: Determined age of the EK-10 fuel rod measured at 3 sample positions

Sample position	Calculated age (year)	Limit of detection (year)
bottom	56 ± 5	24
middle	59 ± 7	22
up	62 ± 35	33

One can see that in the upper sample position the error is significantly higher than at the other two positions. At this position the signal intensity from the sample is rather small comparing to the radon background, therefore after the background subtraction the error is increased. The medium and upper measurement positions geometrically allow the increase of the sample size. However, the self-absorption of the sample limits the sample size to this 1-2 g range.
This result is reliable and does not contradict to the fact that the sample was present at the beginning of operation of the Training Reactor (age > 44 years in 2015).

5. Conclusions

A non-destructive gamma-spectrometric method for age-dating of uranium samples was developed and tested for various HEU and LEU samples. The method was extended to low enriched uranium (LEU) samples. The application of a well-type HPGe detector was developed and its specific properties and characteristics focusing on the true coincidence effect were tested. The method was successfully tested on a fuel rod piece of 10% enrichment.
Our future plan is to test the method of more LEU samples. A more efficient radon background reduction should allow lowering the detection limit. Taking into consideration the self-absorption would allow the increase of sample masses and the signal to background ratio, making available the method even for LEU and young samples.

6. Acknowledgement

This work was supported by the International Atomic Energy Agency in the frame of the Coordinated Research Project “Application of Nuclear Forensics in Illicit Trafficking of Nuclear and other Radioactive Material” [7] under contract No. 13839 - as well as by the Hungarian Atomic Energy Authority.

References

[1] Zsigrai J, Nguyen CT, Lakosi I, Bagi J; Non-destructive techniques for the assay of nuclear materials; Gamma-spectrometric uranium age dating, 9th ITWG Meeting, Cadarache, June 16-17, 2004

[2] Nguyen CT; Age dating of highly enriched uranium by gamma spectrometry, Nucl. Instr. Meth. B 229 (2005) 103-110.

[3] Wallenius M, Morgenstern A, Apostolidis C, Mayer K; Determination of the age of highly enriched

uranium, Anal. Bioanal. Chem. 374, (2002), 379-384.

[4] Nguyen CT, Zsigrai J; Gamma-spectrometric methods for age-dating of highly enriched uranium, Proc. 27th ESARDA Annual Meeting; London; 10-12 May 2005, CD-ROM: 012-zsigrai-050506

[5] Nguyen CT, Zsigrai J; Gamma-spectrometric uranium age-dating using intrinsic efficiency calibration, Nucl. Instr. Meth. B 243 (2006) 187-192.

[6] Dragnev TN; Intrinsic self-calibration of nondestructive gamma-ray spectrometric measurements, J. Radioanal. Chem. 36 (1977) 491-508;

Dragnev TN, Damjanov BP; Methods for precise absolute gamma-spectrometric measurements of uranium and plutonium isotopic ratios. Proc. IAEA Symp. Nuclear Safeguards Technology, Vienna, 1978, IAEA-Sm-231/130, Vol.I, 1979, p. 739-753.

[7] International Atomic Energy Agency: Lakosi L et al.; “Development of nuclear forensics methods and techniques for combating illicit trafficking of nuclear and other radioactive material”, Application of Nuclear Forensics in Combating Illicit Trafficking of Nuclear and Other Radioactive Material, IAEA-TECDOC-1730, Vienna, (2014) 25–47.

Standoff LIBS and Raman for security and safeguards applications

Divyesh Trivedi[1], Nick T Smith[1, 2], Owen Horsfall[1,2] , Chris Lennon[1,2] Lin Li[2], and David Whitehead[2],

[1]The National Nuclear Laboratory
5th Floor, Chadwick House
Warrington Road, Birchwood Science Park, Warrington WA3 5AE, UK
[2]The University of Manchester
Oxford Road, Manchester, UK
E-mail: divyesh.trivedi@nnl.co.uk

Abstract:

At a distance or standoff laser based techniques such as LIBS and standoff Raman are being investigated at the PHAROS laboratory, a collaboration between the UK NNL and the Manchester University. An extensive database of material characterisation information that is relevant to security and safeguards has been developed, especially using LIBs. This ranges from fuel furniture (ties, pneumonic springs, cladding materials etc) to graphite, waste grouting and building cladding cements etc. The ability to measure the composition of spent fuel gases in storage canisters has also been demonstrated. We have designed and built standoff Raman capable of identifying compounds from up 4 m (limited at present only by the length of the available containment box), to identify compounds relevant to nuclear site operations and to waste disposal studies. The results from these studies and the technical scope of future technical investigations will be discussed.

As these methods are both fast (seconds for analysis), stand-off and either non-destructive or minimally destructive (approx. 1-2um surface ablation), the tools being developed at the PHAROS laboratory will be of interest both to nuclear site operators and to those interested in independent safeguards and security inspection..

Keywords: LIBS, Raman, standoff technologies.

1. Introduction

At-a-distance or standoff analysis offers the capability to measure the composition of material at several metres distance, in real time and at detection limits that can provide useful. The development of high quality and spectrometers, optics and laser sources at lower costs over the last 10 years has meant that standoff technologies such as laser induced breakdown spectroscopy (LIBS) and standoff Raman are being developed and tested for multiple purposes. A few of these include real time characterisation of materials on production lines for quality control purposes [1,2] the detection of explosive residues and precursors for military and CBRN uses [3-5] and characterisation of materials on Mars during space exploration [6-8].

NNL and the University of Manchester has developed a collaboration that has established the PHAROS laboratory at the Photon Sciences Institute at the University of Manchester to develop standoff and also remote technologies including LIBS and Raman for application principally to the nuclear industry but also wider applications.

This paper will review the application of standoff technologies to security and safeguards and provide examples of work being undertaken by NNL/Manchester and by other workers to develop these technologies to deployable systems. As well as the measurement of spectra, key issues that affect the ability to use the technologies including data analysis methods are discussed.

2. Component of standoff systems

2.1. LIBS

LIBS has the merits of: (i) being a fast measurement technology (few seconds), (ii) sample preparation is not required, (ii) ablation only needs a microgram of material, (iii) being able to identify elements present in the <1ug of sample, and (iv) the LIBS system components are readily obtainable [9-10]. The basic principles of LIBS are that a high powered pulse laser (up to 100mJ) is focussed on a surface, into solution (rarely) or at a point in a gas, generating a high enough power density (up to a GW/cm^{-3}) to generate a microplasma spark, over nanosecond durations. Within a microsecond after the pulse the plasma has cooled sufficiently for ions to start recombining with stripped-off electrons and emit atomic emission spectral lines as electrons lose energy to regain stable atomic orbitals by emitting photons. After a couple of microseconds the atoms start to recombine to form molecules and in some cases molecular emission lines can also be measured.

No matter the specific logistics of deployment, the key components of standoff LIBS systems are: (i) a high powered pulsed laser generator, (ii) optics for laser focussing and signal collection, (iii) a gated system to allow synchronisation between pulse generation and (iv) spectral analysis of the return signal. A typical LIBS setup is shown in Figure 1. At the PHAROS Laboratory we are currently using a LIBSCAN 100 as supplied commercially by Applied Photonics Ltd, with modifications to house the equipment so that analysis can be undertaken with high precision in a controlled and safe working environment (Figure 2). In-house development of our own systems is on-going, to enable greater flexibility in developing bespoke equipment that is appropriate for a wide range of nuclear site applications.

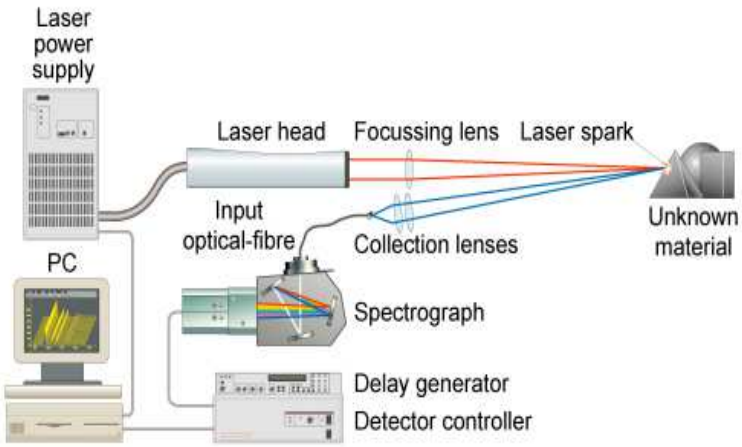

Figure 1: Typical LIBS apparatus.

Figure 2: LIBSCAN 100 at used at the PHAROS laboratory (image by APL Ltd)

2.2. Raman

Standoff Raman has the benefits of: (i) being non-destructive, (ii) identifying the compounds present in a sample (iii) the low powered laser can be sent through liquors to identify e.g. solids in material stored underwater, and (iv) has been tested to work at open path distances of up to 100m. Raman works by exciting and de-exciting vibrational and rotational energy states in compounds, resulting in a inelastic scattering of the incident laser photons. The spectra is obtained by measuring the compound specific wavelength shifts relative to the wavelength of the elastically scattered (Raleigh effect) incident laser photons.

Typical system components are shown in Figure 3 and the development and testing system put together at the PHAROS laboratory is shown in Figure 4.

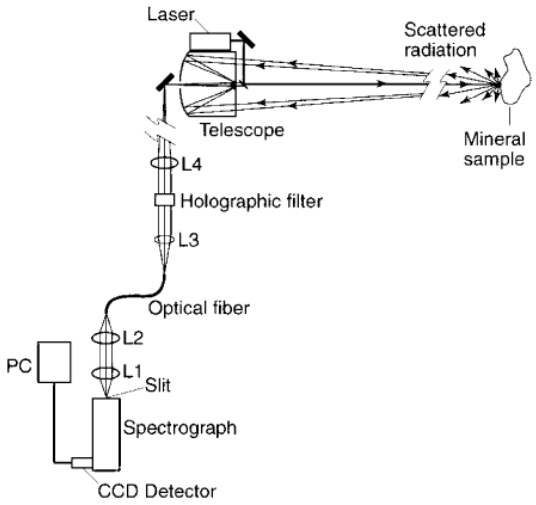

Figure 3: Typical standoff Raman apparatus.

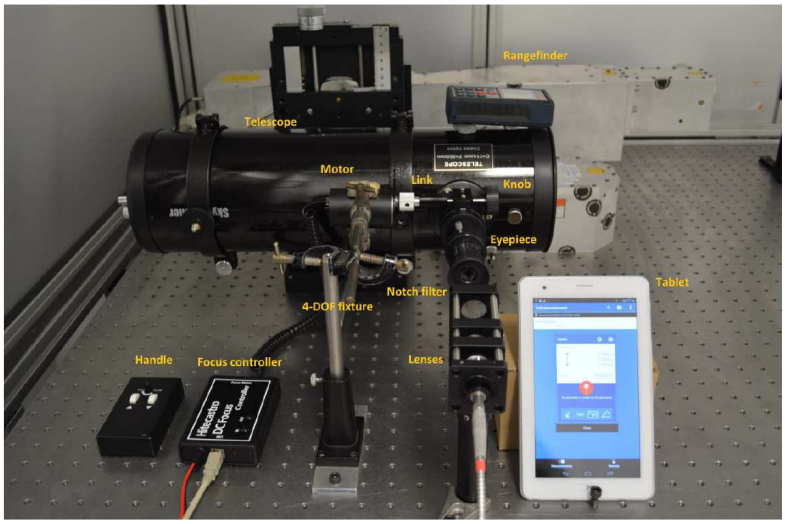

Figure 4: NNL's test purpose standoff Raman at the PHAROS laboratory.

3. Applications

3.1. LIBS analysis of structural materials

In a security and safeguards context, identifying the type or composition of e.g. a grout, concrete or other building material may not be a priority. However work undertaken by NNL in a nuclear decommissioning context is useful to discuss in this paper as it highlight how spectral data from samples can be treated to understand how significant differences in data can be detected.

In this context 5 samples disks roughly 1.5cm in diameter and 2mm thick of cement grout were produced by the University of Leeds, systematically covering a range of compositions of Ordinary Portland Cement/Blast Furnace Slag (OPC/BFS). The challenge was to determine of the composition of a grout could be measured by Standoff LIBS. For each disk 10 analysis were performed rastering over the sample, giving 50 analysis in total. Each analysis was obtained as the average spectra from 4 laser pulses, to even out the effect of laser energy fluctuations and surface heterogeneity. Each spectrum was converted to numerical values of peak intensity versus wavelength (in nm). The data was analyses by using the R statistical package [11-12].

Each of the 50 spectrum were normalised to the highest peak and centred. Principle component analysis (PCA) revealed that the key spectral peaks that systematically varied with compositional changes were for Si (504nm) and Ca (315nm) (Figure 5). Setting aside 10 spectra, 40 randomly selected spectra were used with partial least squares with discriminant analysis (PLS-DA) to produce a calibration line based upon the composition of the cement versus the measured Ca and Si line intensities (Figure 6). The composition of the reserved 10 samples was then predicted given the calibration curve. Analysis showed that compositions of each single measurement were predicted to within 10% given 95% confidence limits.

This suggests that, for these cements, LIBS can be used as a screening level tool to quickly determine the approximate composition of cements and identify samples or locations where compositions of interest need to be investigated. It also shows the uncertainty associated with identification; in this case a precision of 10% was obtained (for unreplicated or single data points) in blind predictions.

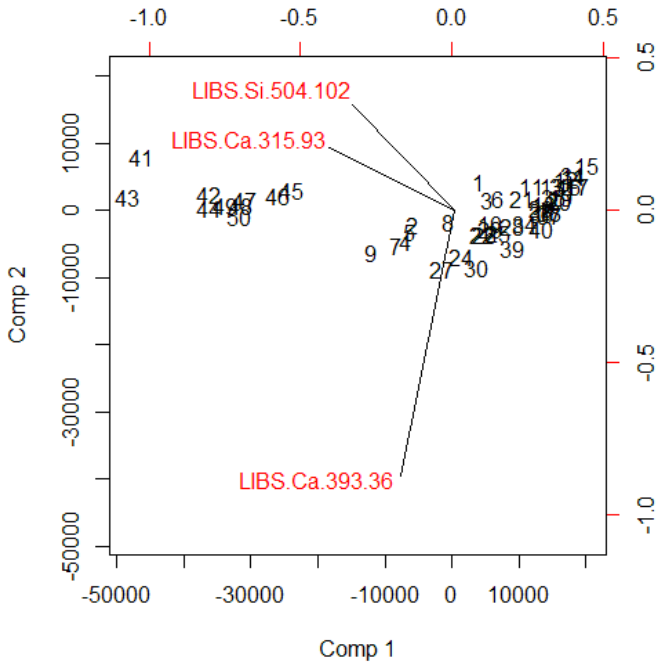

Figure 5: PCA loadings and scores for OPC/BFS sample .

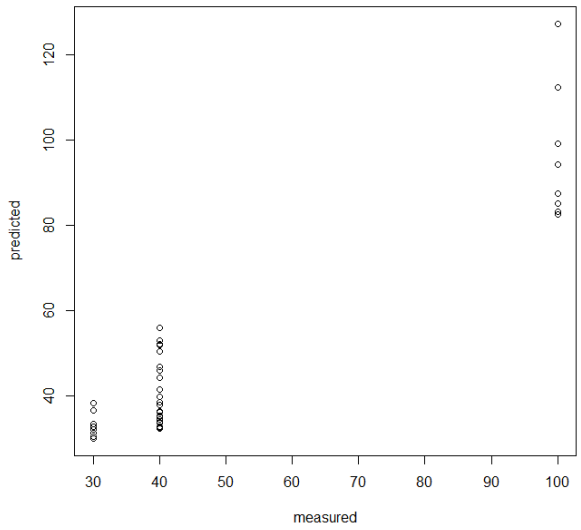

Figure 6: PLS-DA calibration for OPC/BFS samples .

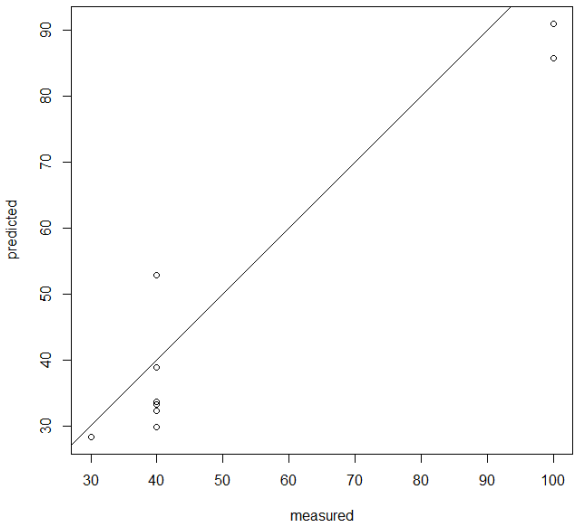

Figure 7: Predicted OPC content of 10 blind samples given the PLS-DA calibration.

3.2. LIBS analysis of steels

Different types of steel may be used for nuclear and non-nuclear applications. In a security and safeguards context, can a nuclear processing specific composition of steel be identified using standoff technologies? NNL and the University of Manchester have measured the LIBS spectra for a variety of steel materials as part of on-going studies. The spectra for a variety of metals and steel types used in the UK nuclear industry are shown (Figure 7). Studies concerning type SA508, 308L and other specific steels are on-going. The data to-date shows that the type of steel clearly produces unique spectra based upon the composition of the material, i.e. compositional differences can be detected. This is study is on-going; further work is required based upon systematic variations in steel compositions followed by PCA and PLS-DA analysis to produce calibration curves to numerically determine how well unique nuclear industry steel compositions can be identified. This type of statistical study will confirm: (i) if the steels can be readily distinguished; (ii) the confidence in the measurements and (iii) how many repeated measurements may be necessary for the desired level of confidence..

Wider than the nuclear industry, LIBS analysis of steels and metal alloys in general is widely used [12-12], particularly as a means of product quality control where bespoke and automated LIBS systems are installed on production lines [1-2].

Sample description	**Spectra**
Al_2O_3 and Al sheet	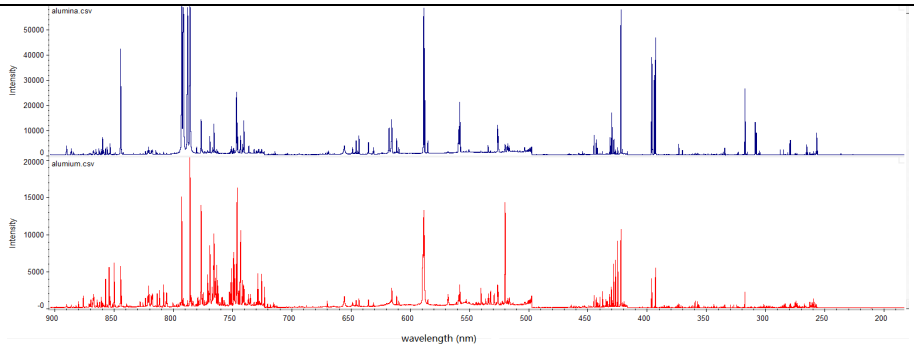

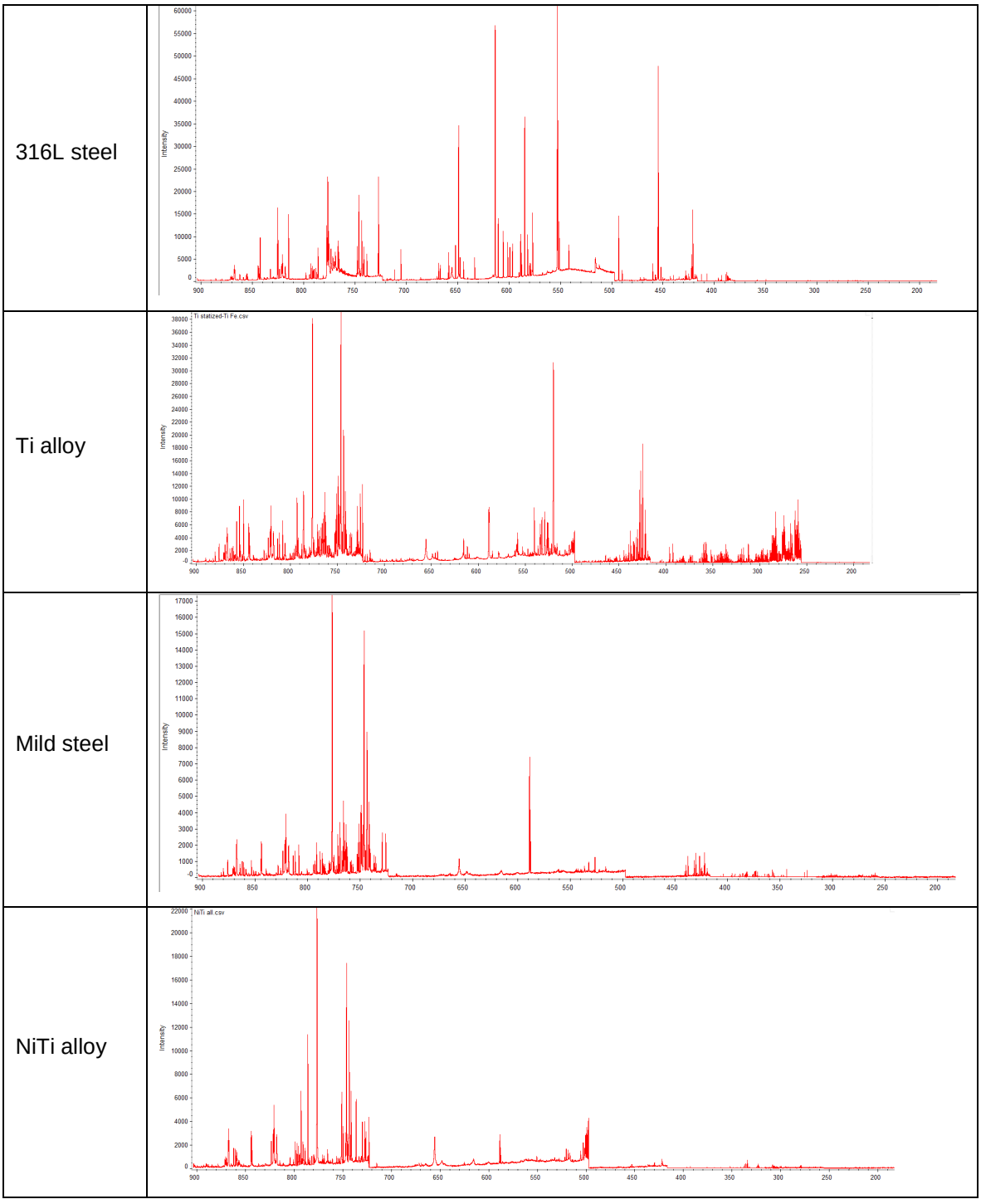

Figure 8: NNL LIBS spectra of various metals/steels used in the nuclear industry.

3.3. LIBS analysis of U and Pu isotopic ratios

One of the highest priority areas in safeguards work is to identify the isotopic ratio of materials. NNL has not begun work on LIBS and Raman analysis of nuclear materials to-date, but some work has been undertaken at CEA on uranium isotopic analysis [14] and in Los Alamos concerning Pu analysis[15]. The CEA studies showed that with sufficiently high resolution spectrometers, U-238 and U-235 can be measured. This was undertaken using the U(II) line at 424.437 nm. The lines for U-238

and U-235 were 0.025nm apart, which their spectrometer could pick up as each peak was approximately 0.012 nm wide, given an instrument resolution limit of 0.0055 nm.

The Los Alamos study utilised the Pu emission line at 594.522nm with a shift between Pu-239 and Pu-240 of 0.0067nm (Figure 9). The key difference in the CEA and Los Alamos experiments was the use of a longer wavelength peak and several microseconds longer delay between plasma formation to allow the Pu peak to increase in intensity and measure much smaller isotopic peak shifts.

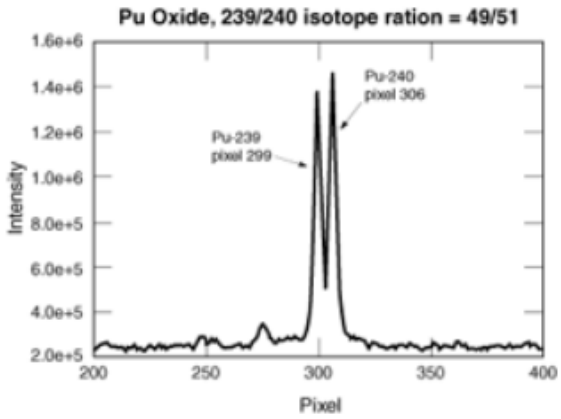

Figure 9: LIBS analysis of Pu-239 and Pu-240 isotopes at Los Alamos.

3.4. How can Raman be applied to safeguards studies?

To date, standoff Raman applications have focussed to a large extent on CBRN and military applications, particularly concerning detection of explosives, their residues and precursor chemicals[16]. NNL has so far investigated identifying algae and organic breakdown products through water in ponds and silos, and minerals that could be present in geological waste disposal environments, all measured at distances of up to 3m, limited only by the width of the facility. NNL routinely use desktop Raman for research studies concerning nuclear process chemistry [17]. Table 1 shows that many actinide species in solution are Raman active which means that Raman spectroscopy based tools have the potential to monitor process solutions for safeguards monitoring purposes.

Species	Raman signal (cm^{-1})
UO_2^{2+}	870
PuO_2^{2+}	833
NpO_2^{2+}	850
NpO_2^{+}	767

Table 1: Raman spectral lines for several actinide species [18].

As an example of such an application, the measurement of UO_2^{2+} and NO_3^- is reported as a means of PUREX process monitoring using remote Raman using fibre optic cables to carry the laser to a sample cell and to carry the return signal back to the spectrometer [19] (Figure 10).

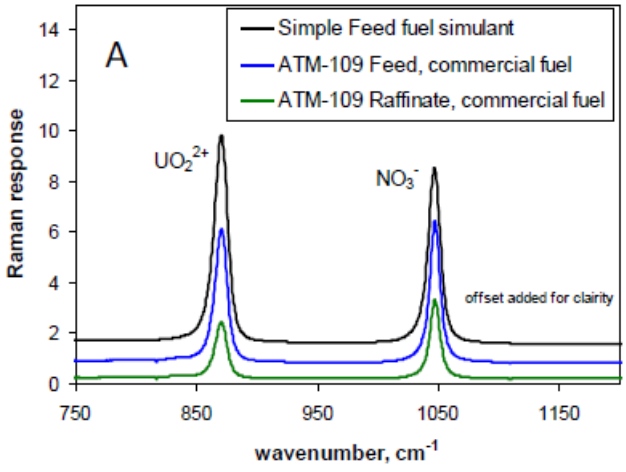

Figure 10: In-situ monitoring of PUREX using Remote Raman [19].

These observations suggest that in-line monitoring of actinides in solution using standoff and remotely operated ("remote") Raman has potential for independent verification of nuclear material accountancy, and could be an area for further development.

4. Conclusions

Standoff LIBS is already used for a wide variety of purposes and has potential as a means of readily identifying materials during site inspections as a verification tool. NNL is aiming to develop standoff LIBS into portable hand held devices that, for instance, security and safeguards inspectors could use to identify a material within minutes.

To date NNL has investigated the potential of the standoff LIBS for identifying unique nuclear-use construction materials and chemical processing vessels/pipework. Development work is required concerning direct measurement of nuclear material. Under laboratory conditions, recent investigations that have shown that the isotopic ratios of nuclear materials can be measured; this requires development into practical standoff measurement equipment.

Remote Raman is less well developed; benchtop Raman is a routinely used by NNL for investigations concerning process chemistry. The challenge is to turn this into equipment that could be used for in-line monitoring of actinides for nuclear material accountancy verification purposes.

5. Acknowledgements

The University of Manchester and NNL internal research funding are thanked for supporting the studies reported in this paper. The Royal Society is thanked for providing an Industrial Fellowship to Professor Nick Smith.

8. References

[1] Noll R; Sturm V; Aydin U; Eilers D; Gehlen C; Höhne H; Lamott A; Makowe J and .VrenegorJ. (2008). Laser-induced breakdown spectroscopy–from research to industry, new frontiers for process control, Spectrochim. Acta Part B 63 (2008) p1159–1166.

[2] Noll; R, Bette H; Brysch A, Kraushaar M; Mönch I; Peter L and Sturm V. Laser-induced breakdown spectrometry—applications for production control and quality assurance in the steel industry, Spectrochim. Acta Part B 56 (2001) 637–649.

[3] Gottfried J L; De Lucia F C; Munson C.A. and Miziolek AW. Laser-induced breakdown spectroscopy for detection of explosives residues: a review of recent advances, challenges and future prospects. Anal. Bioanal. Chem. v395 (2009). p283-300.

[4] Gottfried J L; De Lucia, F C; Munson C A and Miziolek A W. Double-pulse standoff laser-induced breakdown spectroscopy for versatile hazardous materials detection, Spectrochim. Acta Part B 62 (2007) 1405–1411.

[5] De Lucia F C; Gottfried J L; De Lucia, F C; Munson C A and Miziolek A W. Multivariate analysis of standoff laser-induced breakdown spectroscopy spectra for classification of explosive-containing residues Appl. Optic. 47. (2008). G112–G121.

[6] Fabre C; Maurice S; Cousin A; Wiens R, Forni O; Sautter V and Guillaume D. Onboard calibration igneous targets for the Mars Science Laboratory Curiosity rover and the Chemistry Camera laser induced breakdown spectroscopy instrument. Spectrochim. Acta Part B 66 (2011) 280–289.

[7] Wiens R C and Maurice S. The ChemCam Team, The ChemCam instrument suite on the Mars Science Laboratory rover curiosity: remote sensing by laser-induced plasmas, Space Sci. Rev. 170 (2012) p166–223.

[8] Lanza N. L. et. al. Evidence For Rock Surface Alteration With Chemcam From Curiosity's First 90 Sols. Paper number 1743 presented at the 44th Lunar and Planetary Science Conference, (2013).

[9] Singh J P and Thakur S N. Laser-induced breakdown spectroscopy, Elsevier, Amsterdam (2007).

[10] Radziemski L and Cremers D. A brief history of laser-induced breakdown spectroscopy: from the concept of atoms to LIBS 2012, Spectrochim. Acta Part B 87 (2013) 3–10.

[10] R Development Core Team. An Introduction to R. R Foundation for Statistical Computing, Vienna, Austria. ISBN 3-900051-12-7, URL http://www.R-project.org/ (2009).

[11] Mevik B H and Wehrens R. The pls Package: Principal Component and Partial Least Squares Regression in R. J of Statistical Software v18(2), (2007). p1-24.

[12] Werheit P; Fricke-Begemann C; Gesing M and Noll R. Fast single piece identification with a 3D scanning LIBS for aluminium cast and wrought alloys recycling, J. Anal. At. Spectrom. 26 (2011) p2166–2174.

[13] González A; Ruiz J; Cabalín L M and Laserna J. On-line laser induced breakdown spectroscopy determination of Mg coating thickness on electrolytically galvanized steel in motion, Appl. Spectrosc. 64 (2010) p1342–1349.

[14] Doucet F R; Lithgow G; Kosierb R; Boucharda P and Sabsabia M. (2011). Determination of isotope ratios using Laser-Induced Breakdown Spectroscopy in ambient air at atmospheric pressure for nuclear forensics. J. Anal. At. Spectrom. v26.(2011). p536-541.

[15] Smith, C.A; Martinez, M.A; Veirs, D.K; Cremers, D.A (2002). Pu-239/Pu-240 isotope ratios determined using high resolution emission spectroscopy in a laser-induced plasma. Spectrochimica Acta Part B: Atomic Spectroscopy, v57. (2002). p929-937

[16] Izake E I. Forensic and homeland security applications of modern portable Raman spectroscopy. Forensic Science International v202, (2010), p1–8

[17] Gregson C R; Goddard D T; Sarsfield M and Taylor R J. Combined electron microscopy and vibrational spectroscopy study of corroded Magnox sludge from a legacy spent nuclear fuel storage pond, Journal of Nuclear Materials 412, (2011) p145-156.
[18] Warburton J L. Spectroscopic methods of process monitoring for safeguards of used nuclear fuel separations. PhD Thesis, University of Nevada, Las Vegas. (2011)..

[19] Orton C; Fraga C; Douglas M; Christensen R; and Schwantes J. Monitoring Spent Nuclear Fuel Reprocessing Conditions Non-Destructively and in Near-Real-Time Using The Multi-Isotope Process (Mip) Monitor, Proceedings of the 2nd JAPAN-IAEA Workshop on Advanced Safeguards Technology for the Future Nuclear Fuel Cycle, Tokai-mura, Japan. (2009).

Determining the origins of Uranium Ore Concentrates using laboratory characterisation techniques

Jane Caborn, Colette Holmes, Jeremy Edwards

National Nuclear Laboratory
Preston Laboratory, Springfields,
Preston, Lancashire, PR4 0XJ, UK
E-mail: jane.a.caborn@nnl.co.uk, colette.g.holmes@nnl.co.uk, jeremy.edwards@nnl.co.uk

Abstract

IAEA's mandate for the application of safeguards has been in a process of modification in recent years. Verification of Comprehensive Safeguard Agreements (INFCIRC/153) has always been supported through the analytical measurement of uranium, plutonium and thorium content and associated isotopic compositions. With the advent of the Additional Protocol (INFCIRC/540) and adoption of Integrated Safeguards and the State Level Concept, increasingly comprehensive State declarations and additionally collected open source data now requires validation. As a result, in the field of nuclear materials there is now a greater emphasis on physical and chemical characterisation for both nuclear forensic and safeguard applications, in order to be able to differentiate between similar materials and potentially determine the origin. In particular, this requirement extends to Uranium Ore Concentrate (UOC) materials which are covered by increased reporting under INFCIRC/540 and are affected by recent IAEA Policy Papers concerning the application of the Starting Point of Safeguards.

The NNL have a number of UOC materials displaying different characteristics, which originate from different mines and milling facilities around the world. By measuring certain parameters of a sample of unknown origin, identification and characterisation is potentially possible by establishing a "fingerprint" for each nuclear material. This study involved analysing ten samples using a number of techniques with the aim of determining any differentiating characteristics (fingerprint) in the samples held by NNL, comparing these to any related data, and exploring their relevance to global nuclear forensic initiatives. The materials could potentially form the basis for commencing the population of a physical library of archive nuclear and non-nuclear materials of relevance to nuclear forensics and safeguards.

The analysis techniques included:

- *Inductively Coupled Plasma Mass Spectrometry (ICP-MS) for quantitative analysis of trace elemental impurities, total U and isotopic abundance;*
- *Gamma spectrometry for radioisotopic analysis;*
- *X-ray diffraction (XRD) for phase composition;*
- *Scanning Electron Microscopy/Energy Dispersive X-ray Analysis (SEM/EDX) for microanalysis and morphology.*

The samples have previously been analysed using some of the techniques by a number of laboratories allowing for inter-laboratory comparisons and the assessment of the identification of material using fingerprints.

Keywords: UOC; characterisation;

1. Introduction

Uranium ore concentrate (UOC), commonly known as yellow cake, refers to an intermediate product of the uranium nuclear fuel cycle. The UOC's are produced using a variety of metallurgical methods from the mining of uranium ores or recovered as a by-product of other mined products such as gold and copper. UOC's usually contain a high fraction of natural uranium (>65mass% uranium) in various chemical forms; ammonium urinate, sodium diuranate, uranyl hydroxide or in the oxide form. They are recovered by precipitating uranium post purification by solvent extraction or ion exchange.

The IAEA's Incident and Trafficking information system is a database of incidents concerning the illicit trafficking and other unauthorized activities and events involving nuclear and other radioactive material outside of regulatory control. Between 1995 and 2007, there were over 2000 confirmed incidents, of which 91 involved natural uranium. Although the number of incidents has decreased since the 1990's there is still a security and safeguarding requirement to effectively track the loss, theft, or diversion of purified natural uranium especially as there isn't a global "pit to conversion" tracking system. There has been a requirement to support the verification of Comprehensive Safeguards Agreements (INFCIRC/153) through the measurement of uranium, plutonium and thorium content and associated isotopic compositions. This has increased with the obligation to provide comprehensive State declarations and the validation of open source data since the advent of the Additional Protocol (INFCIRC/540) and adoption of Integrated Safeguards and the State Level Concept. As result, in the field of nuclear materials there is now a greater emphasis on physical and chemical characterisation for both nuclear forensic and safeguard applications, in order to be able to differentiate between similar materials and potentially determine the origin. In particular, this requirement extends to Uranium Ore Concentrate (UOC) materials which are covered by increased reporting under INFCIRC/540 and are affected by recent IAEA Policy Papers concerning the application of the Starting Point of Safeguards.

A number of characterisation techniques have been documented for the identification of the origin of unknown nuclear materials. Most common is the use of nuclear material fingerprints which are generated through the characterisation of metallic impurities which may be inherent (ore itself) or adherent (process/storage) with the IAEA listing them based on four groups (see Table 1).

Construction Material Elements	Nuclear Elements	Other elements	No interest
Al, Ni, Cr, Cu, Fe, Mg, Mo, Nb, Co, Si, Ti, V, W, Zn, Mn, Zr	B, Be, Cd, Ce, Gd, Hf, Li, Ta, Y	Ca, K, Na, P, Pb, Sn, Sr, Th, REE, Ba*, As*, Sb*	Rb, Cs, Ra, Sc, Ac, Tc, Re, Ru, Os, Rh, Ir, Pd, Pt, Ag, Au, Hg, Ga, In, Ge, Bi, Se, Te, Po

* only in yellowcake
REE – Rare Earth Elements
Table 1: Metallic Impurities of interest to IAEA (Ref. 1)

Metallic impurities are present in nuclear material samples at varying concentrations and potentially have the character of the accompanying elements. The levels will be significantly lower in the intermediate products (yellow cake). The composition of a number of Canadian samples was determined to identify the origin of UOC's and downstream uranium products leading to UF_6 production. The changes in trace element concentration during the conversion of UOC to UF_6 (Ref. 2) was reported by dissolving impure UOC in nitric acid to produce a uranyl nitrate solution. It was found that the trace element content of the UOC does not change but other elements are added during the process increasing the total elemental concentration. During solvent extraction most (>99.5%) of the trace elements follow the raffinate. The purified uranyl nitrate solution is then evaporated and thermally decomposed to remove the nitrogen, mechanically prepared and then reduced to produce UO_2, all of which have little effect on the trace element loading. Trace elements are added as recycled HF is used to dissolve the UO_2 producing UF_4 which is then dried and dehydrated again, only slightly effecting the trace element composition. The elemental concentration decreases during the conversion to UF_6 as non-volatile fluorides are produced which drop out as ash during the fluorination process. The uranium isotopic ratios were also determined throughout the conversion process and showed the $^{235}U/^{238}U$ isotopic ratio was constant and unaffected by mining methods, milling practises or chemical processes. However the $^{234}U/^{238}U$ ratios for the UOC materials did show significant differences with no significant differences in the ratios seen during the conversion process.

Széles *et al* (Ref. 3) carried out an assessment of the impurities present including the presence of rare earth elements along with measuring the isotopic composition of uranium and determining the morphology (surface roughness). Mayer and Wallenius (Ref. 4) stated that the metallic impurities can be used to identify coherences between samples or batches of material however the systematics behind the impurity patterns was not well understood. For example the concentrations of some impurities can vary dependant on the time the material is exposed to container materials or storage tanks. It was recommended that instead of using absolute impurity concentrations the ratios should be considered as a better indicator. Nesmeyanova and Alkhazashvili (Ref. 5) showed that the presence

of Fe, Mn, Cu, Ni, Co and V increase Uranium extraction, lowering the acidic concentration required for dissolution. The cations added and concentration may allow identification of the origin of the UOC material.

To distinguish between the samples of the same enrichment, Mayer and Wallenius (Ref. 4) determined the presence of minor abundant isotopes of uranium such as ^{234}U and ^{236}U. The presence of trace levels of ^{236}U indicated contamination with recycled uranium hence reprocessing activities and differences in the ^{234}U abundance reflected different enrichment processes.

Gamma Spectroscopy was used by Keegan *et al.,* (Ref. 9) for the initial categorisation of the UOC samples to provide information on the nature of the material. Fission and activation products (^{54}Mn, ^{60}Co, ^{106}Ru, ^{125}Sb, ^{137}Cs, ^{144}Ce, ^{152}Eu, ^{182}Ta and ^{226}Ra) were below the limit of detection with ^{226}Ra present at low levels which was residual from the incomplete removal during uranium ore milling.

NNL holds a number of UOC materials of which ten were identified as 'the same' materials (i.e. mine, conversion process and/or batch) as those analysed by nuclear forensic support laboratories. A number of analytical techniques were used to comprehensively characterise each of the materials to allow inter-laboratory comparisons to be made, assess the merits of each technique and determine a "fingerprint" of each UOC material enabling possible identification of the origin (country), mine and process.

2. Experimental

The NNL holds a number of UOC materials of which ten were selected for analysis using established National Nuclear Laboratory procedures (Table 2). These samples had previously been analysed by other nuclear forensic laboratories and have been stored under normal laboratory conditions at the NNL Preston Laboratory.

Reference	Country and Mine	Mine type	Deposit type
AKO/UOC 097009-645	Niger - Akouta	Underground	Sandstone
ENA/UOC 00915-S	Spain - ENUSA	Open	Pitchblende
KEY/UOC 001264-S	Canada - Key Lake	Open	Unconformity
NUF/UOC 000838-S	South Africa - NUFCOR	Open	Intrusive
PAT/UOC	USA (Shirley Basin or Lucky Mac)	Underground,open	Sandstone Roll Type
ROS/UOC 005160-S	Namibia - Rössing	Open	Intrusive
WEO/UOC 001295-S	Australia – Olympic Dam	By product/ underground	Hematite Breccia Complex
WEO/UOC 301105-S			
WISMUT UOC	Germany – mine unknown	mine unknown	mine unknown
WISMUT UOC/1			

Table 2: Details of UOC material held by NNL

For the initial categorisation each UOC material was visually inspected and photographs taken. This non-destructive technique provides a simple means of determining the different types of uranium but is subjective. To determine the phase composition of the materials X-Ray Diffraction (XRD) was used. A sample of approximately 100mg of each material was analysed using a PANalytical X'Pert³ Powder X-ray diffraction system to determine the long-range order of the structure. Again this is a screening tool which identifies the major and minor crystallographic phases.

To characterise the morphology of the materials and the elemental composition Environmental Scanning Electron Microscopy – Energy Dispersive X-ray (ESEM/EDX) was used. An aliquot of sample (10mg) was analysed using Environmental Scanning Electron Microscopy (FEI Quanta 200 FEG) using secondary electron imaging which provides topographical contrast at a range of magnifications on representative areas of each of the samples. The instrument was operated in vacuum mode enabling the observation of non-conductive specimens. Backscattered Electron Imaging was utilised in order to detect variations in the elemental composition of the materials. When imaging in this mode, portions of the sample containing high atomic weight species appear brighter than portions containing low atomic weight species. Energy dispersive X-ray (EDX) analysis (Oxford Inca 300 EDX system) was used to analyse the elemental compositions of the deposits.

To determine the elemental composition and uranium isotopic abundance approximately 1g of each UOC sample was taken in duplicate, dissolved in high purity concentrated nitric acid and refluxed for an hour at approximately 80°C. To digest any remaining insoluble material hydrofluoric acid was added and the samples were filtered through a 0.3µm membrane. All the residual material dissolved except for the two Wismut samples where one or two flecks of black material, possibly carbon were present. The residue was not measurable due to the small quantity. The samples were diluted 10 000 and 100 000 fold using ultra-pure water to decrease the nitric and hydrofluoric acid concentration and internal references added (Sc, In and Ir) to correct for instrumental drift and matrix effects. For the uranium isotopic composition the samples were diluted 50 million fold, with Ir added as the internal reference. All the samples were measured using a Perkin Elmer Elan 6100 with elemental results reported in ppm ($\mu g\ g^{-1}$).

3. Results

3.1. Visual Characterisation

The observations from the visual inspection results generally show that based on appearance the materials fall into two groups (Table 3). The first group of four samples from Niger Akouta, Spain ENUSA and Germany Wismut were all yellow in appearance. The UOC materials from Niger Akouta and Spain ENUSA are very similar in appearance; fine powders and bright in colour, whilst the two samples from Wismut were mustard yellow and present as a fine powder with larger particulate material possibly due to aggregation of the finer particulates.

Sample Reference	Description
Niger Akouta AKO/UOC 097009-645	Bright yellow, fine powder made up of particulates <1mm in size.
Spain ENUSA ENA/UOC 00915-S	Bright yellow, fine powder made up of particulates <1mm in size.
Canada Key Lake KEY/UOC 001264-S	Predominantly a dark grey powder with a small quantity (5%) of light grey powder present. Some fines present (<1mm) and the majority as larger particles (1-3mm) formed from compacted fines.
South Africa NUFCOR NUF/UOC 000838-S	Olive green powder. Majority of the sample (80%) comprises of larger particles (1-5mm) formed from compacted fines and the remainder as fines (<1mm).
US Pathfinder PAT/UOC	Olive green powder with khaki green (~10%) and pale yellow (1%) powder present. Mainly (80%) consists of larger particles (1 - 2mm) formed from compacted fines with the rest present as khaki green and yellow fines.
Namibia Rössing ROS/UOC 005160-S	The sample is an olive green, fine powder made up of particulates <1mm in size.
Australia Olympic Dam WEO/UOC 001295-S	Dark grey/black powder mainly present as fines (<1mm). Larger particles (1-7mm) formed from the compacted fines are also present accounting for 30% of the sample.
Australia Olympic Dam WEO/UOC 301105-S	A fine (<1mm), dark grey powder with a slight green tint with the presence (~2%) of mid-grey, larger particles (1 - 2mm) formed from compacted fines.
Germany Wismut WISMUT UOC	Mustard yellow powder. Larger particulates (1 - 3mm) formed from compacted fines account for ~70% of the material and the remainder as fines (<1mm).
Germany Wismut WISMUT UOC/1	

Table 3: Sample Descriptions following visual inspection of UOC materials

The remaining samples from Canada Key Lake, South Africa NUFCOR, US Pathfinder, Namibia Rössing and Australia Olympic Dam were either described as dark grey or olive green. As with the first group, the material is present as a fine powder for all, with the majority comprising of larger particulates formed from the fines.

3.2. Morphology characterisation using SEM

All the UOC samples consist of fine material, most less than 1µm in size, and agglomerates between 5 and 100µm. The SEM observations reflect the visual inspection findings with the samples falling into two groups (Table 4). The first group (Niger Akouta, Spain ENUSA and Germany Wismut) comprises of fines forming fused spheroidal clumps or platelets and irregular larger agglomerates. The remaining samples from Canada Key Lake, South Africa NUFCOR, US Pathfinder and Australia Olympic Dam are nodular with occasional larger platelet particles and larger agglomerates present. The Namibia Rössing material also contains fused platelet particles but with ultrafine nodular material and irregular agglomerates.

Sample Reference	Particle size (µm)	Morphology description
Niger Akouta AKO/UOC 097009-645	<1 (primary) 5-25 (agglomerates)	Fines forming fused spheroidal clumps (primary). Irregular with larger agglomerates more spheroidal (agglomerates).
Spain ENUSA ENA/UOC 00915-S	<1 (primary) 5-50 (agglomerates)	Fines forming fused spheroidal clumps (primary). Irregular with larger agglomerates more spheroidal (agglomerates).
Canada Key Lake KEY/UOC 001264-S	0.1-0.5 (primary) 1-25 (agglomerates)	Nodular with occasional larger (~2µm) platelet particles (primary). Irregular with larger agglomerates more spheroidal (agglomerates).
South Africa NUFCOR NUF/UOC 000838-S	0.05-0.5 (primary) 1-25 (agglomerates)	Nodular with occasional acicular particles (primary). Irregular with larger agglomerates more spheroidal (agglomerates).
US Pathfinder PAT/UOC	0.05-0.5 (primary) 10-100 (agglomerates)	Nodular with occasional larger irregular/fused particles (primary). Irregular (agglomerates).
Namibia Rössing ROS/UOC 005160-S	0.05-5 (primary) 5-25 (agglomerates)	Fused platelet particles (1-5µm) with ultrafine nodular material (primary). Irregular (agglomerates).
Australia Olympic Dam WEO/UOC 001295-S	0.1-0.5 (primary) 10-50 (agglomerates)	Nodular (primary). Spheroidal (agglomerates).
Australia Olympic Dam WEO/UOC 301105-S	0.1-1 (primary) 1-25 (agglomerates)	Nodular with some acicular or platelet particles (primary). Irregular (agglomerates).
Germany Wismut WISMUT UOC	0.1-2 (primary) 5-25 (agglomerates)	Acicular and platelet particles (1-2µm) with irregular fines (primary). Irregular (agglomerates).
Germany Wismut WISMUT UOC/1	0.1-10 (primary) 5-50 (agglomerates)	Predominantly platelet (1-10µm) with some acicular particles and irregular fines (primary). Irregular (agglomerates).

Table 4: Summary of SEM observations of UOC samples

3.3. Elemental Composition by XRD and EDX analysis

XRD and EDX analysis was carried out to determine the phase and elemental compostion of the UOC materials (Table 5). A limitation of both techniques is the small sample size used for the analysis. For the EDX analysis the identification of carbon is particularly difficult due to an overlap with a minor uranium peak.

As with the visual inspection, the XRD analysis seems to show two groups of UOC material. The first group (Niger Akouta, Spain ENUSA and Germany Wismut) all have a major phase of UO_3. Ammonia and sodium are present in the Spanish and Niger materials respectively indicating the materials are likely to be ammonium and sodium di-uranate. Significant quantities of sulphur were present in both German Wismut samples confirming the mustard yellow appearance. This group of samples appear to be yellow cake which was either precipitated under acidic conditions as ammonium diuranate or from alkaline solutions by addition of sodium hydroxide.

The remaining samples from Canada Key Lake, South Africa NUFCOR, US Pathfinder, Namibia Rössing and Australia Olympic Dam have U_3O_8 as the major phase. Four of the samples are pure with no other traces of any other uranium conpounds (originating from Canada, USA and Australia) whilst

the South African and Namibian materials contain other uranium compounds; UO_3 and UO_4 respectively, indicating the purification process was either incomplete or less effective.

EDX mapping was also used to assess the distribution of any impurity elements. These maps showed very even distributions of the impurities (down at the micron scale) and little to no segregation of the minor elements in the powder. All the samples showed major uranium and oxygen peaks. Some carbon may also be present but this cannot be determined with any certainty as the peak for carbon also coincides with a minor uranium peak. Again the samples follow the same trend with sulphur found in the first group (Niger Akouta, Spain ENUSA and Germany Wismut) confirming the XRD analysis and visual observations and is probably due to the use of H_2SO_4 and sulphate chemicals during processing. Sodium is identified in the Niger Akouta sample corroborating the XRD analysis and that the material is a sodium di-uranate. The two German Wismut samples contain traces of nitrogen, aluminium, sulphur, silicon and iron. In the Niger Rössing and Australia Olympic Dam samples no other elements were detected. Aluminium was detected in samples from Canada Key Lake, South Africa NUFCOR and US Pathfinder and traces of silicon and calcium identified in the Canadian and Australian samples respectively. The US Pathfinder sample has traces of sodium, aluminium, silicon, phosphorus, sulphur and iron.

Sample Reference	XRD analysis	EDX analysis	Compounds
Niger Akouta AKO/UOC 097009-645	$Na_2O(UO_3H_2O)x$ $UO_3NH_33H_2O$	Na, S	Sodium di-uranate, UO_3
Spain ENUSA ENA/UOC 00915-S	$U_2(NH_3)O_63H_2O$	S	Ammonium di-uranate, U_2O_3
Canada Key Lake KEY/UOC 001264-S	U_3O_8	Al, Si	U_3O_8 at different purities
South Africa NUFCOR NUF/UOC 000838-S	U_3O_8 $UO_3.8H_20$	Al	
US Pathfinder PAT/UOC	U_3O_8	Na, Al, Si, P, S, Fe	
Namibia Rössing ROS/UOC 005160-S	U_3O_8 $U_4O_{20}H_{16}$	None	
Australia Olympic Dam WEO/UOC 001295-S	U_3O_8	Trace Cu	U_3O_8
Australia Olympic Dam WEO/UOC 301105-S	U_3O_8	None	
Germany Wismut WISMUT UOC	$U_4H_{18}N_4O_{21}S_2$	N, Al, S, Si, Ca, Fe	Ammonium di-uranate Sulphur present
Germany Wismut WISMUT UOC/1	$U_4H_{18}N_4O_{21}S_2$	N, Al, Si, S, Fe	

Table 5: Chemical Composition Results Summary

3.4. Elemental Determination

The elemental compositions of the ten UOC materials were determined using ICP-MS. The percentage major and rare earth elements compared to the total elemental concentration was calculated to identify elements which could be used as markers to identify the origin of the materials. Normalised rare earth elemental patterns were produced for each material to establish a fingerprint and to allow comparisons to be made to the ITU and US laboratory data sets. The measured REE and Lanthanide concentrations were normalised to chondrite standard values (Ref. 10); an approach a number laboratories have followed based on general geochemistry practice (Ref. 8 and Ref. 9). The approach is taken to eliminate effects related to nuclear stability and allows REE and Lanthanide profiles to be compared. Internally and externally sourced data has been utilised to enable comparisons (Refs. 6 and 7).

The total elemental concentration for each UOC material was calculated and showed (Figure 1) the South African NUFCOR sample contains significantly higher levels, at least four fold, than the other nine samples.

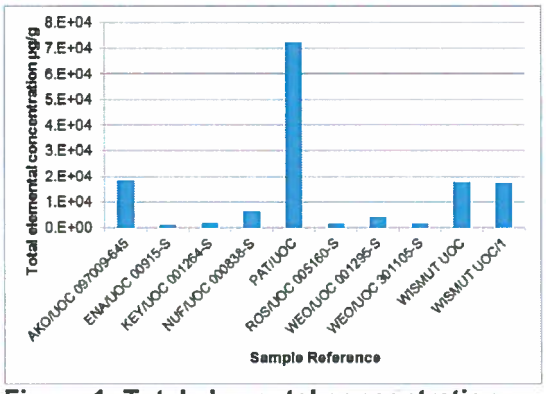

Figure 1: Total elemental concentration

3.4.1. Niger Akouta (AKO/UOC 097009-645)

Niger Akouta is an underground mine which processes magnesium uranate (75% U). The UOC material analysed contained a significant quantity of elemental impurities (18000 ppm) with sodium the main contributor confirming the EDX and XRD results (Figure 2). Mo and V were also present (7.57% and 1.80% respectively) which form volatile hexafluorides that are liable to contaminate uranium hexafluoride production at a later stage. Therefore this material is likely to be an intermediate product, possibly un-purified sodium di-uranate. The REE and lanthanides comprise of approximately 0.02% of the total elemental concentration with Y and Ce accounting for over 50%. The high Na content and presence of Mg are potential markers for the Niger Akouta material.

There is reasonable agreement between the NNL and US laboratories for all the elements except Ce (Figure 3). It is likely that the US and ITU laboratories have the same sample and the source is from the Arlit mine in Niger. Different mines may account for the differences in the elemental ratios observed.

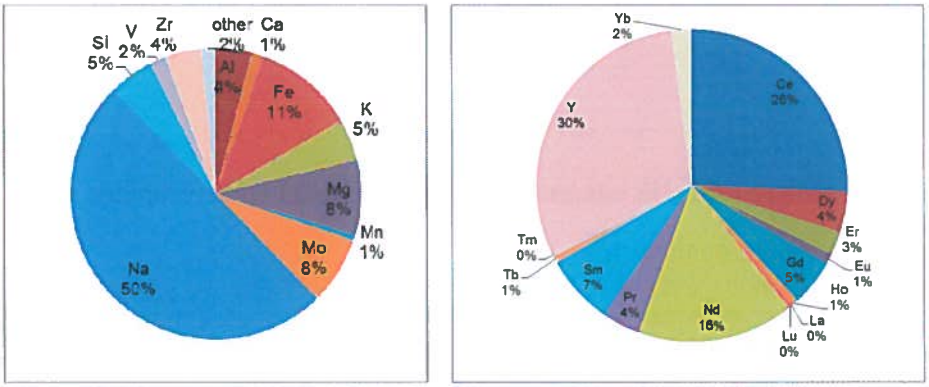

Figure 2: Major and Minor Elemental Composition Niger Akouta UOC material

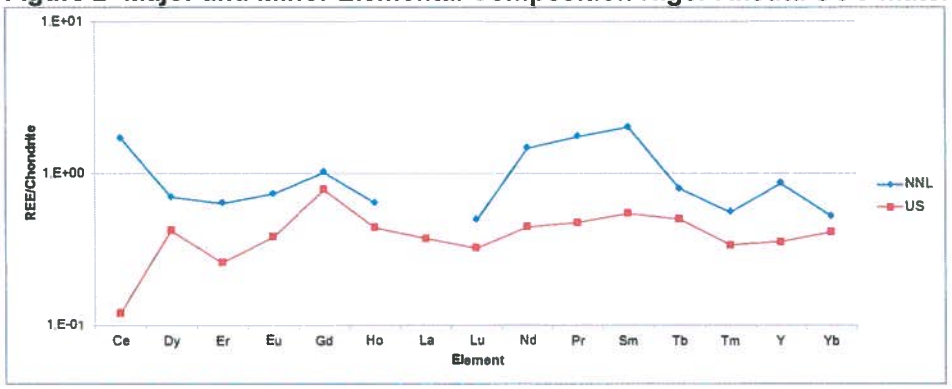

Figure 3: Comparison of NNL results with US laboratory for Niger Akouta UOC material

3.4.2. Spain ENUSA (ENA/UOC 00915-S)

The Spanish sample had the lowest total elemental content with the majority due to Al, Ca and Fe (Figure 4). The calcium impurities are likely to be present as a result of process chemistry and the aluminium and iron ore-related. This material also contains Mo and W, which are liable to contaminate the conversion process at a later stage. The REE and lanthanides account of less than 1% of the total elemental concentration with 41% due to Ce (Figure 5). Elevated aluminium and manganese concentrations could be considered as markers for this material.

Considering the differences in analytical measurement and preparation, the agreement is good between the NNL and US laboratories for all the elements indicating the materials are likely to be the same. The percentage deviation for all the elements except Tm is less than ± 20%.

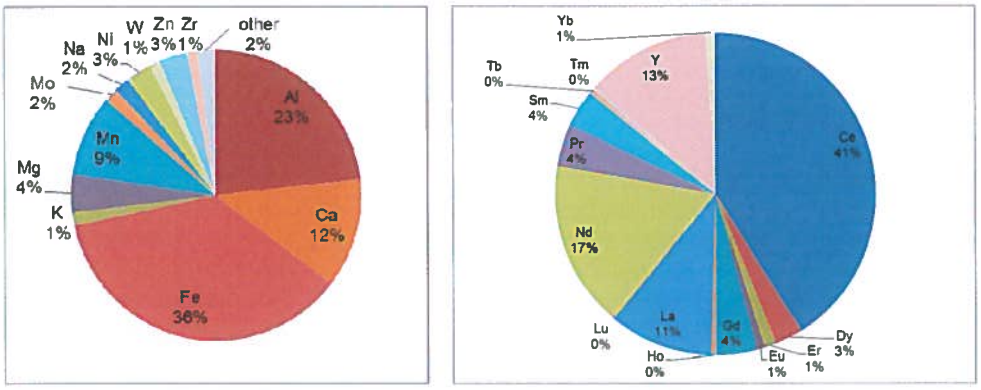

Figure 4: Major and Minor Elemental Composition for Spain ENUSA UOC material

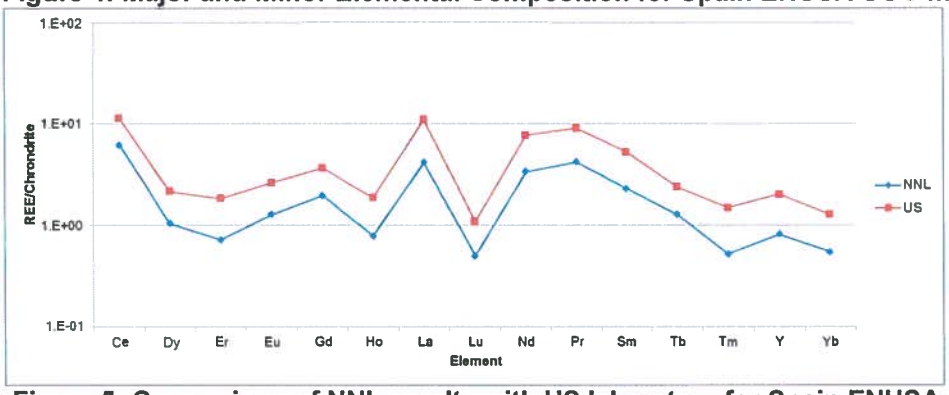

Figure 5: Comparison of NNL results with US laboratory for Spain ENUSA UOC material

3.4.3. Canadian Key Lake (KEY/UOC 001264-S)

Almost 81% of the total elemental composition is due to Mo, As, Si, Fe and Na with the presence of Al and Si confirming the EDX results (Figure 6). Mo, present in significant quantities, is a likely marker for the Key Lake samples. It is an element which is difficult to remove, however concentrations do alter during the process (Ref. 2) and along with W (often found in ores) they are detrimental to final use. The rare earth elements and lanthanides account for 0.32% of the total elemental concentration with Y accounting for over a third.

The agreement between the ITU and US laboratories is excellent with the results produced by NNL showing the same trend but a positive bias (Figure 7).

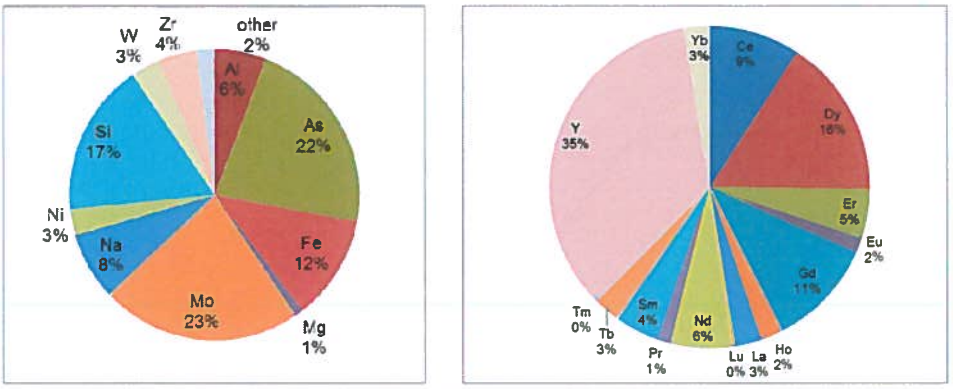

Figure 6: Major and Minor Elemental Composition for Canada Key Lake UOC material

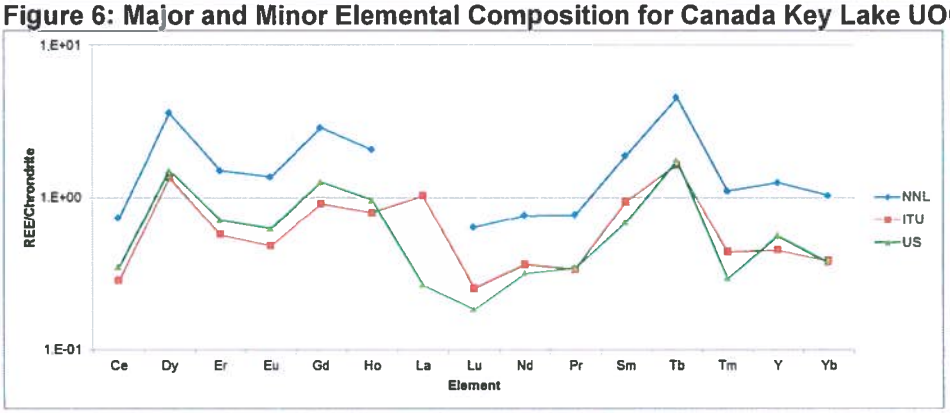

Figure 7: Comparison of NNL results with US laboratory for Canada Key Lake UOC material

3.4.4. South Africa NUFCOR (NUF/UOC 000838-S)

At NUFCOR ammonium di-uranate is calcined to form Uranium Ore Concentrates. The elemental content was approximately 6250 µg/g with Ca, Si, Mg and Fe accounting for almost 75% (Figure 8). Aluminium, detected also by EDX analysis, is present at 2.2% of the total elemental concentration. Th-232, which has similar chemical properties to uranium, is the most significant impurity (1.2% of total elemental concentration). The rare earth elements and lanthanides account for 0.34% of the total elemental concentration with Ce and Nd accounting for 65% (Figure 9). The elevated concentrations of Ca and P could be considered as markers.

NUFCOR own a number of mines in South Africa and the exact origin of this material was unknown. The NNL results agree well with those for Palabora, analysed by the US and ITU, following the same trend.

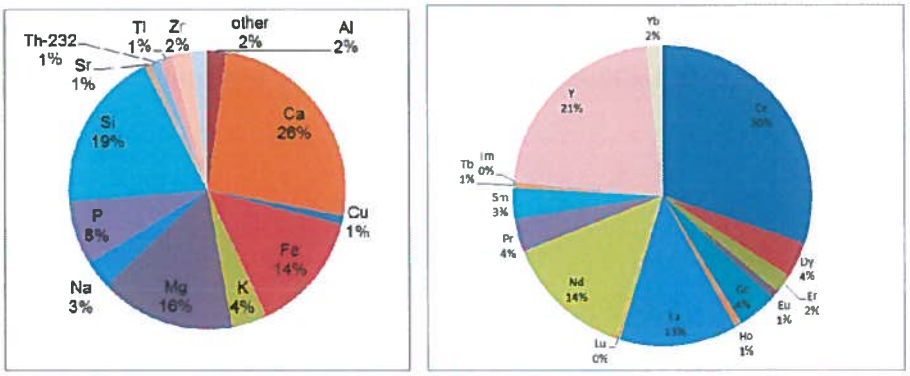

Figure 8: Major and Minor Elemental Composition for South Africa NUFCOR UOC material

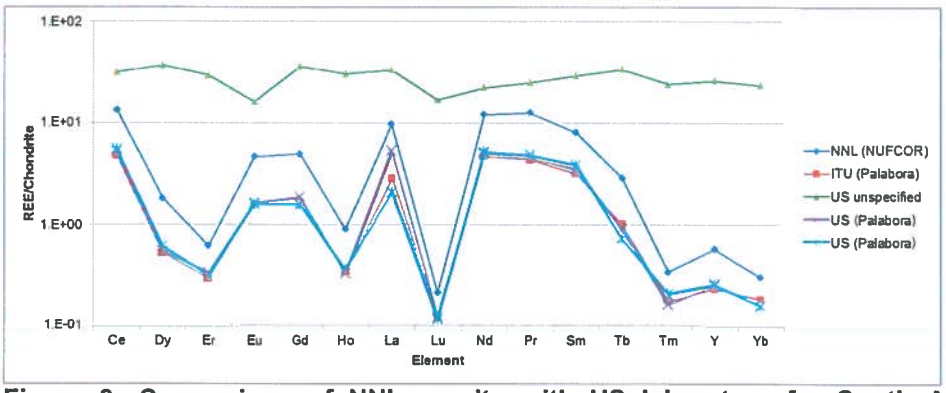

Figure 9: Comparison of NNL results with US laboratory for South Africa NUFCOR UOC material

3.4.5. US Pathfinder (PAT/UOC)

The exact origin of the NNL sample is unknown as Pathfinder owns a number of mines including Lucky Mac and Shirley Basin. This sample has the highest elemental concentration at over 72000µg/g with Fe accounting for over 50%, which has the potential to be used for identification for this material (Figure 10). The results obtained by ICP-MS confirm the EDX analysis with Na, Al, Si, P and Fe all present in significant quantities. The level of impurities present (Mo and V) is lower than previous samples at less than 1%. The REE and lanthanides concentration is also high (almost 300 µg/g) but similar in proportion to the other UOC material at 0.41% of the total elemental concentration.

The comparison data (Figure 11) clearly shows three distinct data sets which are in good agreement e.g. NNL and US Pathfinder, ITU and US Lucky Mac and ITU and US Shirley Basin. The Shirley Basin and Pathfinder results follow the same trend though there is a significant difference in the ratio factor. It is therefore possible that the US and NNL Pathfinder samples originate from the Lucky Mac mine but at a different time period.

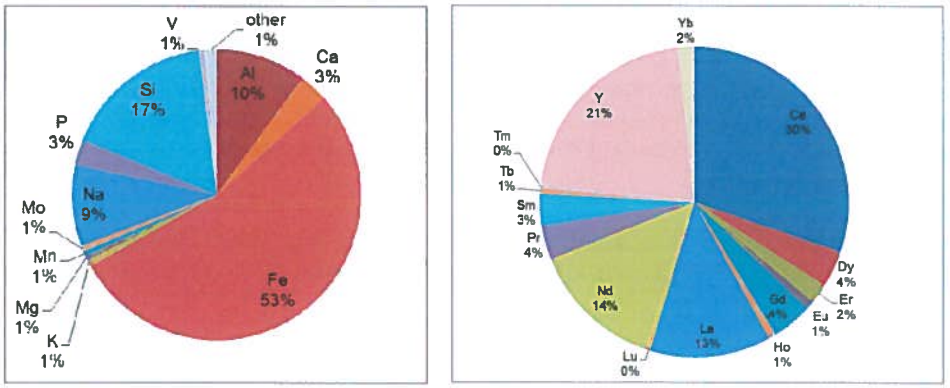

Figure 10: Major and Minor Elemental Composition for US Pathfinder UOC material

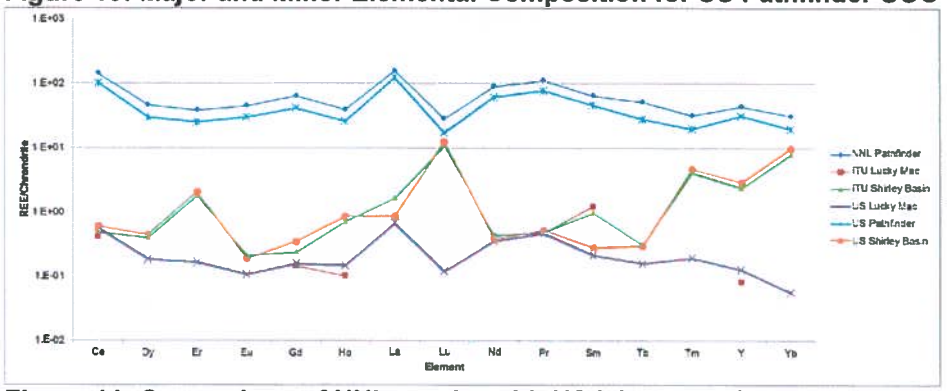

Figure 11: Comparison of NNL results with US laboratory for US Pathfinder UOC material

3.4.6. Namibia Rössing (ROS/UOC 005160-S)

The Namibia Rössing sample has a low elemental concentration (approximately 1500µg/g) reflecting the absence of elemental detection when analysed by EDX. The majority of the sample (68%) comprises of similar proportions of Si, Na and Mo (approximately 20%) which could be used as identification markers (
Figure **12**). The minor elements account for 0.05% of the total elemental inventory, with La dominant.

The ITU laboratories have confirmed the NNL sample is likely to be the same and the trends do agree with both reflecting the elevated La content. The US laboratory data shows a differing trend therefore likely that this material is not identical (Figure 13).

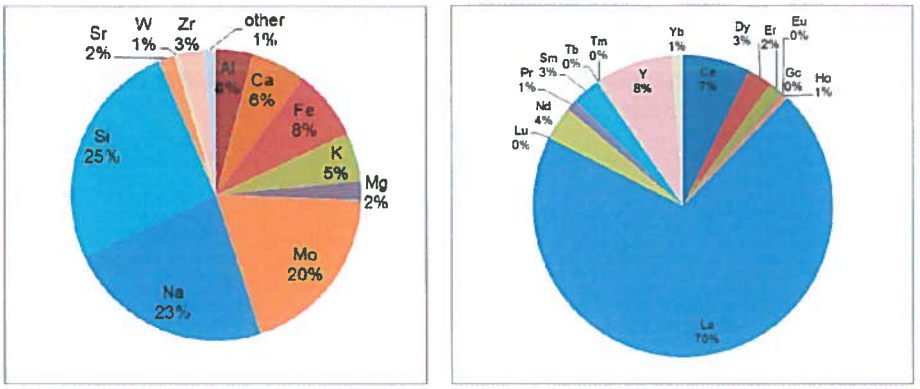

Figure 12: Major and Minor Elemental Composition for Namibia Rössing UOC material

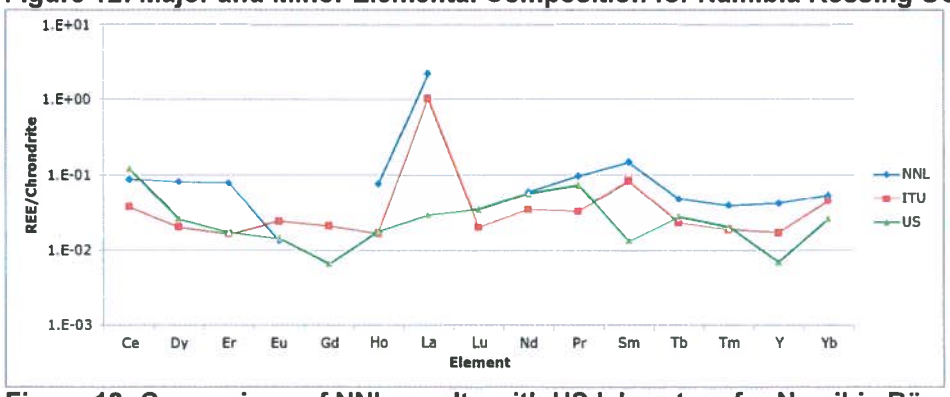

Figure 13: Comparison of NNL results with US laboratory for Namibia Rössing UOC material

3.4.7. Australia Olympic Dam (WEO/UOC 001295-S and WEO/UOC 301105-S)

NNL have two Australian Olympic Dam samples and it is likely from the sample references that they are from different time periods (circa. September 2001 and late 2002). The major elemental composition is quite different which accounts for the absence of elements detected by EDX; almost 4000 µg/g for WEO/UOC 001295-S and 1400 µg/g for WEO/UOC 301105-S. Copper is the dominant element (35%) in WEO/UOC 001295-S confirming the EDX analysis with the majority of the remaining concentration due to Zr, Si, Bi and Na. Copper is present in WEO/UOC 301105-S at a lower level with Na and Mo dominant. Mo and W impurities are present and can form volatile fluorides which are detrimental to uranium hexafluoride production. Bismuth is present in both samples and may provide a marker for the identification of samples from Olympic Dam (Figure 14).

Although the total elemental concentration for the major and minor elements is different the percentage of REE and lanthanides is the same accounting for 0.05% of the total inventory (WEO/UOC 001295-S only shown – Figure 15). Both samples have excellent agreement with La and Ce the most significant. There are differences between the NNL samples and those analysed by the US and ITU laboratories, especially for Ce, La, Nd and Y, however the same trend is followed (Figure 16).

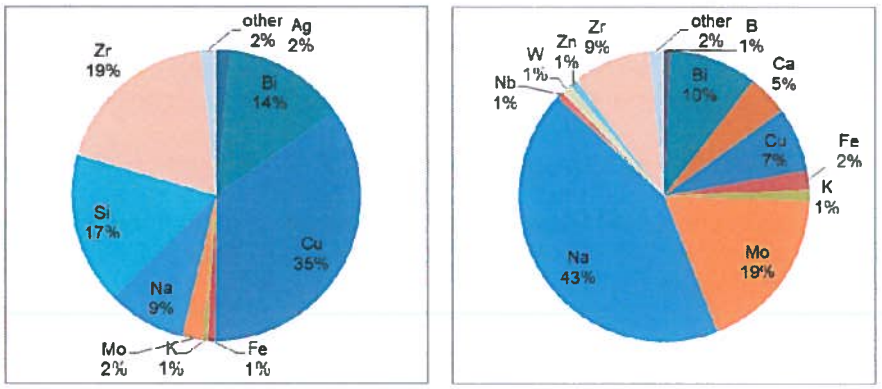

Figure 14: Major Elemental Composition for Australia Olympic Dam UOC Material (WEO/UOC 001295-S and WEO/UOC 301105-S)

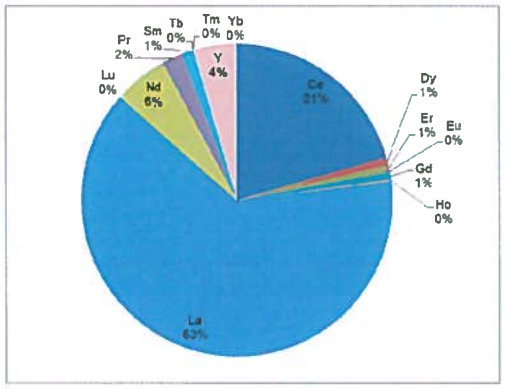

Figure 15: Minor Elemental Composition for Australia Olympic Dam UOC material

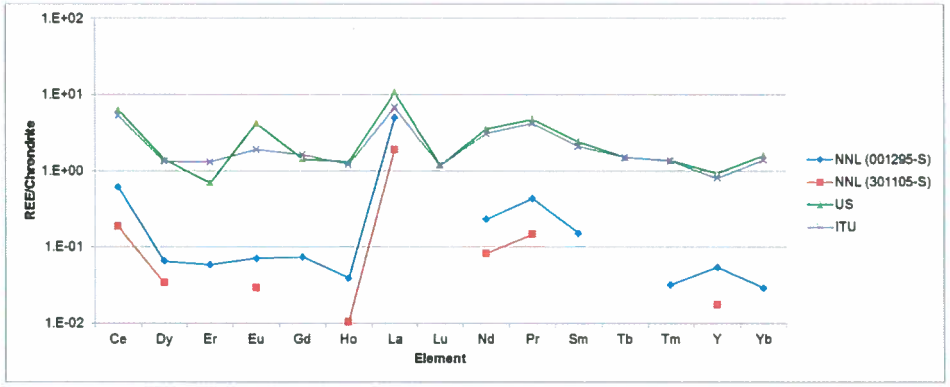

Figure 16: Comparison of NNL results with US laboratory for AN14/360 (Australia Olympic Dam)

3.4.8. German Wismut (WISMUT UOC and WISMUT UOC/1)

NNL holds two samples which are likely to be the same. The total elemental concentrations are in excellent agreement (17800 and 17500 µg/g) with Fe the most significant followed by K, Ca and Si both which were also detected by EDX (Figure 17). The minor elements make up 0.10% of the total elemental inventory with Ce and Y accounting for 44%. From the results it can be concluded that these samples are identical with potassium present in both samples which could be a marker.

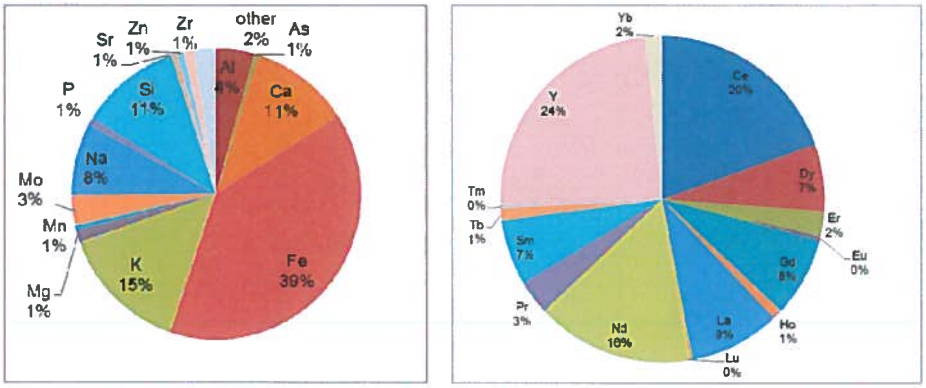

Figure 17: Major and Minor Elemental Composition for Germany WISMUT UOC material

3.5. UOC identification from REE and Lanthanide measurements

To ascertain if UOC materials have an individual fingerprint the normalised REE and Lanthanide patterns were compared (Figure 18). Apart from the two Wismut samples which are believed to be the same sample, the UOC materials can be distinguished from one another for most elements. The deconvolution of the normalised values for La and Lu is less obvious and therefore probably not the most reliable markers for fingerprinting. The elemental trend seen for the two Australian Olympic Dam samples is in good agreement but a difference in the magnitude of the normalised values confirm that the time points are likely to be different.

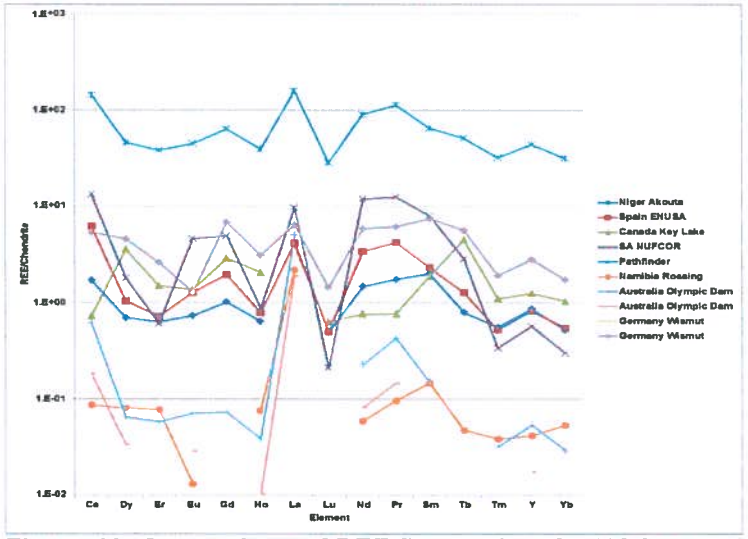

Figure 18: Comparison of REE fingerprints for UOC materials

3.6. Uranium isotopic Determination

Uranium isotopes were determined for the ten UOC materials however due to the lack of sensitivity of the NNL ICP-MS, changes in ^{234}U and ^{236}U were not detected with values of 0.006% and 0.001% achieved respectively (Table 6). The ratios for the German Wismut samples confirm the material is identical. Cross sample variation is observed which may provide additional fingerprinting information. As with the elemental fingerprints to further validate, analysis of material from the same mines and different time periods is required.

Sample Reference	total U	%U-235	%U-238
Niger Akouta, AKO/UOC 097009-645	72.7	0.712	99.281
Spain ENUSA ENA/UOC 00915-S	72.5	0.699	99.294
Canada Key Lake KEY/UOC 001264-S	83.5	0.708	99.285
South Africa NUFCOR NUF/UOC 000838-S	79.6	0.703	99.291
US Pathfinder PAT/UOC	68.1	0.702	99.291
Namibia Rössing ROS/UOC 005160-S	80.1	0.702	99.291
Australia Olympic Dam WEO/UOC 001295-S	83.9	0.704	99.290
Australia Olympic Dam WEO/UOC 301105-S	85.4	0.700	99.294
Germany Wismut WISMUT UOC	64.4	0.702	99.292
Germany Wismut WISMUT UOC/1	63.9	0.701	99.293

Table 6: Uranium Results for analysis of the UOC material

4. Discussion

The ability to verify the origin of uranium ore concentrates is critical for security and safeguarding of nuclear material. A number of analytical techniques have been used to characterise ten UOC materials to determine if they could be used to identify a sample and its provenance. Where analysis has been carried out by other laboratories there is generally good agreement between the results with the same elemental trends being observed.

The observations from the initial visual inspection were confirmed by the ESEM results which provided a less subjective analysis. The techniques reported that the samples fell into two distinct groups which were confirmed by the XRD phase composition data as being present as either diuranate or U_3O_8.

Characterisation by ICP-MS identified the major and minor elemental differences between the materials and allowed markers to be identified which may help ascertain the provenance of a sample. The data has enabled the mine for the South African and US materials to be identified using reference data from US and ITU laboratories. The Australian Olympic Dam samples were identified as having the same provenance but sampled at different time points which were clearly demonstrated in the differing major element compositions.

Fingerprints for each UOC material (elemental and uranium isotopic) have also been generated with clear differences and trends observed for the elements apart from Lu and La where the deconvolution of the normalised values for La and Lu is less pronounced. The fingerprints for the Australian samples reflected the differing sampling points; same elemental trend with differing magnitudes of normalised REE values indicating that trends may remain constant but the amount of REE present may fluctuate, maintaining the same overall composition, during the operational period of the mine.

5. Acknowledgements

The authors would like to acknowledge Sarah May, Walter Weaver, David Goddard, Jennifer Alcock and Keith Wright-Dawson for the analysis of the UOC materials. The authors would also like to thank NNL's IR&D program for supporting this program of work.

6. Legal matters

6.1. Privacy regulations and protection of personal data

I agree that ESARDA may print my name/contact data/photograph/article in the ESARDA Bulletin/Symposium proceedings or any other ESARDA publications and when necessary for any other purposes connected with ESARDA activities.

6.2. Copyright

The author agrees that submission of an article automatically authorises ESARDA to publish the work in whole or in part in all ESARDA publications – the bulletin, meeting proceedings, and on the website. The author declares that their work/article is original and not a violation or infringement of any existing copyright.

7. References

1. Aregbe, Y., Mayer, K., Balsley, S., Richter, S., 2009. Reading the information inherent to uranium materials. Symposium on Safeguards and Nuclear Material management, ISBN: 978-92-79-13054-0, LB-NA-24038-EN-Z p. Session 3 - 017 (1-12).
2. Button, P., Healey,G. 2013. Change in impurities observed during the refining and conversion processes. ESARDA Bulletin, 49, 57-65
3. Szeles, E., Varga, Z., Katona, R., Wallenius, M., Mayer, K., Nuclear forensics cooperation in the European Union: Results of the joint analysis of natural uranium samples of Hungarian origin. Presented at 33rd ESARDA Annual meeting, 16 - 20 May 2011,
4. Mayer, K., Wallenius, M. 2008. Nuclear Forensic Methods in Safeguards. ESARDA Bulletin 38, 44-49.
5. Nesmeyanova, G.M., Alkhazashvili, G.M., 1961. The effect of certain compounds on the oxidation of uranium in acid media. Atomnaya Energiya 10, 587-591.
6. IP20038.011/06/11/02 ITU data received from S Francis (Excel spreadsheet Springfields_Data_22MayMW)
7. IP20038.011/06/11/03 US data received from S Francis (Excel spreadsheet US_Springfields Results)
8. Varga, Z., Katona, R., Stfanka, Z., Wallenius, M., Mayer, K., Nicholl, A., 2010. Determiantion of rare-earth elements in uranium-bearing materials by inductively coupled plasma mass spectrometry. Talanta 80, 1744-1749.
9. Keegan, E., Kristo, M.J., Colella, M., Robel, M., Williams, R., Lindvall, R., Eppich, G., Roberts, S., Borg, L., Gaffney, A., Plaue, J., Wong, H., Davis, J., Loi, E., Reinhard, M., Hutcheon, I., 2014. Nuclear forensic analysis of an unknown uranium ore concentrate sample seized in a criminal investigation in Australia. Forensic Sci Int. 240, 111-21.
10. Andres, E.,Grevesse, N., 1989. Abundances of the elements: Meteoritic and solar. Geochimica et Cosmochimica Acta. 53, 197-214

A Safeguards Friendly Device for Monitoring Reactor Anti-Neutrinos

J Carroll, J Coleman, M Lockwood, C Metelko, M Murdoch*, Y Schnellbach, C Touramanis
Oliver Lodge Laboratory, Oxford Street, University of Liverpool, Liverpool, L69 7ZE
E-mail: mmurdoch@liverpool.ac.uk

Abstract:

Technology developed for the T2K particle physics experiment has been adapted to make a small footprint, reliable, segmented detector to characterise anti-neutrinos emitted by nuclear reactors. The device has been developed and demonstrated at the University of Liverpool and is currently undergoing field tests at the Wylfa Magnox Reactor on Anglesey, UK. It is situated in an ISO shipping container, above ground, ~60 m from the 1.5 GW_{th} reactor core. Based on the design of the T2K Near Detector, the device detects anti-neutrinos through the distinctive delayed coincidence signal of inverse beta decay interactions using plastic scintillator and Hammamatsu MPPCs.

Keywords: Anti-neutrino; remote monitoring; ISO-container; Novel Technologies

1. Introduction

The diversion of nuclear materials from peaceful use is of concern to the global community. Member States and the IAEA agree an array of safeguards measures to provide assurances that no diversion is taking place or that any diversion is detected in a timely manner. The methods applied at reactor site are numerous and comprehensive, including operator reports on fuel usage and reactor operations. The expected increase in the number of reactors worldwide will likely increase the cost and demands placed on the operators and regulatory agencies in applying safeguards. The application of reactor anti-neutrino monitoring technology could automate reporting in a non-intrusive manner whilst meeting the increasing demands and thus reduce costs for all parties.

The project presented here aims to provide a reliable, autonomous and safeguards friendly device for the monitoring of reactor anti-neutrino emissions. A version of such a device is currently deployed at Wylfa Power Station, Anglesey, UK through the aid of the Department of Energy and Climate Control (DECC) and the Office for Nuclear Regulation (ONR) in the UK. The detector was constructed and commissioned at the University of Liverpool, loaded into a 20' ISO shipping container, and shipped to Wylfa. The container is situated approximately 60 m from the reactor core outside the inner security barrier and requires only a standard 3-phase power supply for operation. The detector itself is roughly 1 ton in mass and utilizes technology from the T2K [1] particle physics experiment which is highly suitable for use on reactor sites being non-toxic, non-flammable and extremely robust. The T2K detector that formed the baseline design for this device withstood the magnitude 9 earthquake in Japan 2011 with minimal damage.

2. Reactor Anti-Neutrinos

Anti-neutrinos are, weakly interacting, sub-atomic, particles produced in the β-decay of nuclei. In operating nuclear reactors they are produced at a rate of roughly 10^{21}/s by the decays of fission daughter nuclei. Both the number of neutrinos produced and the average energy of the anti-neutrinos produced are dependent on the parent fission nuclei. At the these energies the inverse beta decay interaction, $\bar{\nu}_e + p \rightarrow e^+ + n$, is dominant. The detection of the positron, followed shortly by detection of a thermal neutron capture gives a distinctive delayed conicidence signal that identifies anti-neutrino interactions. The energy of the detected positron is linearly correlated with the energy of the anti-neutrino, allowing anti-neutrino spectroscopy measurements with a sensitive detector.

The detectors used in particle physics experiments are generally large (~1 kiloton) liquid scintillator devices using Photo-Multiplier Tube (PMT) readout. Liquid scintillator is generally highly-flammable and toxic while PMTs are expensive and fragile. Coupled with their large size, this makes traditional detectors unsuitable for reactor monitoring applications. Any ideal safeguards detector should be safe, robust, transportable and easy to operate. Failing to adhere to these ideal criteria creates an obstacle to use and wide scale deployment.

Smaller detectors must be of order 1 ton and constructed of suitably 'safe' materials to be placed in close proximity to a reactor whilst being cheap enough for wide scale deployment. Lawrence Livermore National Laboratory developed a prototype, liquid scintillator based, anti-neutrino detector of order 1 ton in size [2]. The detector was deployed at the San Onofre Nuclear Generating Station (SONGS) where reactor anti-neutrinos were used to observe both the reactor's operational state (on/off) and the fuel burn up during operations as shown in Figure 1. The fuel burn-up manifests as the decrease in anti-neutrino count rate as the fuel cycle progresses.

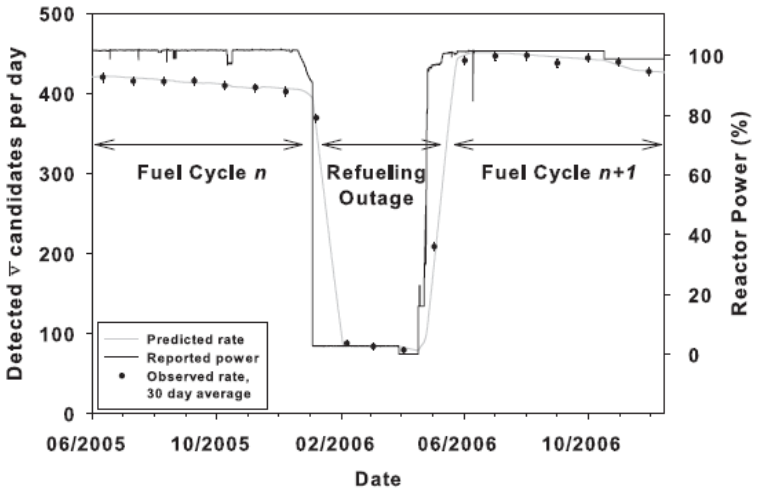

Figure 1: Anti-neutrino event rate in the SONGS1 detector showing fuel burn-up and refuelling period [2]

The observations made by the SONGS1 detector successfully showed the concept of a small scale reactor anti-neutrino monitoring device to be sound. However, the use of flammable liquid scintillator is not ideal for safeguards usage where the detector must be located close to the reactor core.

By utilizing the isotope dependance of both the anti-neutrino rate and energy, as shown in Figure 2., it is possible to measure the isotope content of the reactor core as well as its thermal power output over a given time period. As such, anti-neutrino detectors could provide material accounting, non-intrusively, during reactor operation. Due to the weakly interacting nature (i.e. low interaction cross-sections) of anti-neutrino particles, they pass through the containment vessels and other shielding, allowing direct, unshieldable, observation of the core. Therefore, a reliable, safe, device could be

beneficially deployed as an automated safeguards and accountancy measure, continuously providing detailed information about the reactor core

.

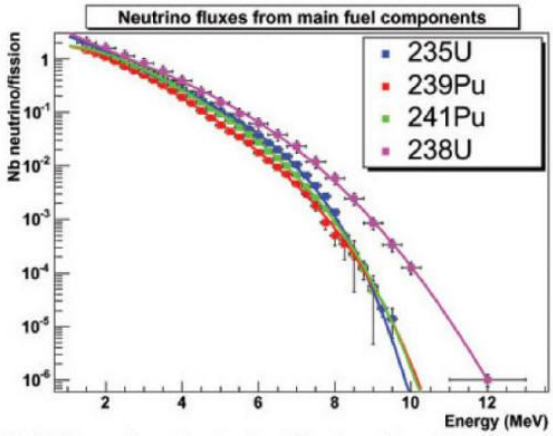

Figure 2: The anti-neutrino energy spectra per fission for the main fission reactor isotopes [3]. As fuel burn-up increases the number of anti-neutrinos emitted will decrease and the spectrum shift to lower energies.

3. The Liverpool Anti-neutrino Detector

3.1. Technology

The device deployed at Wylfa uses cutting edge neutrino detector technology from the T2K experiment's Electromagnetic Calorimeter designed to precisely measure the energy of electrons and positrons[1][4]. In contrast to traditional neutrino detectors the sensitive volume is formed of extruded plastic scintillator bars read out by silicon photo-multipliers, Hammamatsu Multi Pixel Photon Counters (MPPCs). The plastic scintillator is robust, non-toxic, non-flammable and cost effective. A wavelength shifting optical fiber is threaded through each bar to guide the light on to the MPPC readout. The MPPCs operate on low voltage and are incredibly resilient making them highly transportable and easy to operate in when compared to traditional PMTs. The active detector region is doped with gadolinium to allow the detection of thermal neutrons. The electronics readout system is based on the same Field Programmable Gate Array (FPGA) boards used in the T2K experiment with significant firmware adjustments for the detection of inverse beta decay interactions. An internal veto system is included in the design for the rejection of cosmic ray events and to allow effective operation at ground level.

The anti-neutrino detector contains roughly 1 ton of plastic scintillator as the neutrino interaction target and occupies a 1.7 m by 1.7 m footprint. The detector is surrounded by 75 mm of high density polyethylene neutron shielding to reduce background from the fast neutrons produced by the reactor. For ease of transport and deployment, the detector was loaded into a 20' ISO refrigerated shipping container. The shipping container was converted into a mobile laboratory such that all required resources for the operation of the detector were included within, including climate control and power supply. The self-contained unit proved simple to deploy on the reactor site with minimal overheads for the power station staff. The unit requires a 3-phase 420 V power socket, and preferably a data connection for remote operations of the device. Pictures of the full detector are shown in Figure 3.

Figure 3: Pictures of the completed anti-neutrino detector. Left: at Liverpool. Right: Installed into the shipping container

3.2. Anti-neutrino interactions in the detector

The plastic scintillator forms the active target region for anti-neutrino inverse-beta decay interactions. These interactions produce a positron and an epi-thermal neutron in the detector. The positron is detected immediately through the light emitted as it passes through the scintillator. The neutron does not create scintillation light as it travels through the detector and so will not be detected until sometime later when it captures on a nucleus. Gadolinium is used in the detector as a neutron capture agent due to its high thermal neutron capture cross-section and the release of an 8 MeV gamma ray cascade on capture. In the detector the neutron capture is observed through the Compton Scattering of the emitted gamma rays, creating a spatially diffuse energy deposit that is strongly correlated in time. Anti-neutrino interactions are then selected by looking for the distinctive signal of a positron followed by a neutron capture event within a given time window. The time elapsed between the positron and the neutron capture event follows an exponential decay pattern allowing the rejection of randomly coincidence events which display a flat timing distribution.

3.3. Detector commissioning and testing

A small scale prototype was built with removable gadolinium inserts to observe the difference between gadolinium and hydrogen neutron captures (hydrogen has a smaller capture cross section and gives a single 2.2 MeV gamma ray on neutron capture). Californium-252 was used as a neutron source. The source was enclosed in lead shielding to attenuate out its gamma ray emissions. Figure 4 shows the clear difference in neutron capture rates with and without gadolinium.

A full scale detector was subsequently constructed and tested using the same californium source with shielding. The full scale detector was also exposed to a colbalt-60 gamma ray source. Figure 5 shows the clear neutron-gamma discrimination of the detector.

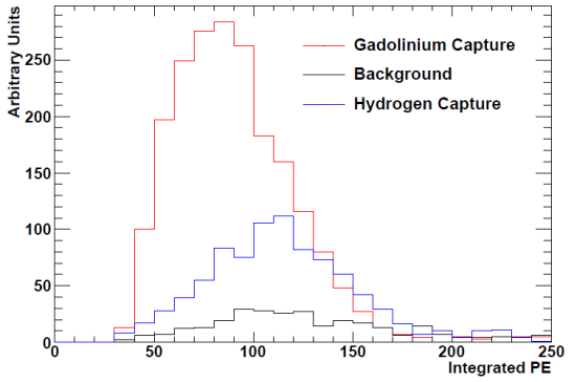

Figure 4: A histogram of integrated charge deposit for neutron capture events in a small prototype detector. The integrated area of the curves is proportional to the neutron capture rate

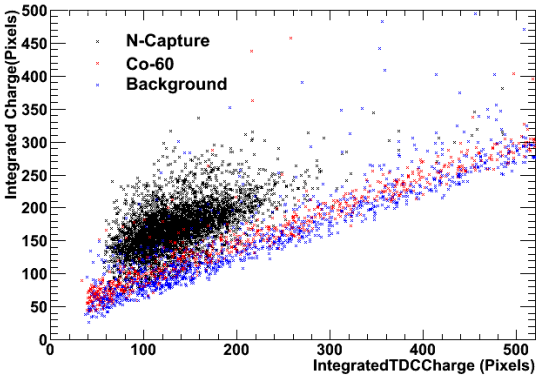

Figure 5: The neutron-gamma discrimination abilities for the full scale detector using Cf-252 and Co-60 sources. The x axis shows integrated charge for individual MPPC hits. The y axis shows total integrated charge.

In addition to the data taken with radio-active sources, several data runs were taken selecting cosmic ray muons for data performance check as well as a cross check for the energy scale calibrations. Muons passing through the detector deposit energy in accordance with the Bethe-Bloch formula. By comparing the observed charge deposit in the detector with the predicted energy deposit, an absolute energy scale calibration can be made. Energy scale calibrations from the radioactive Co-60 source and cosmic ray muons were found to be consistent. Figure 6 shows an event display of a cosmic ray track passing with a fit of its calculated path through the detector

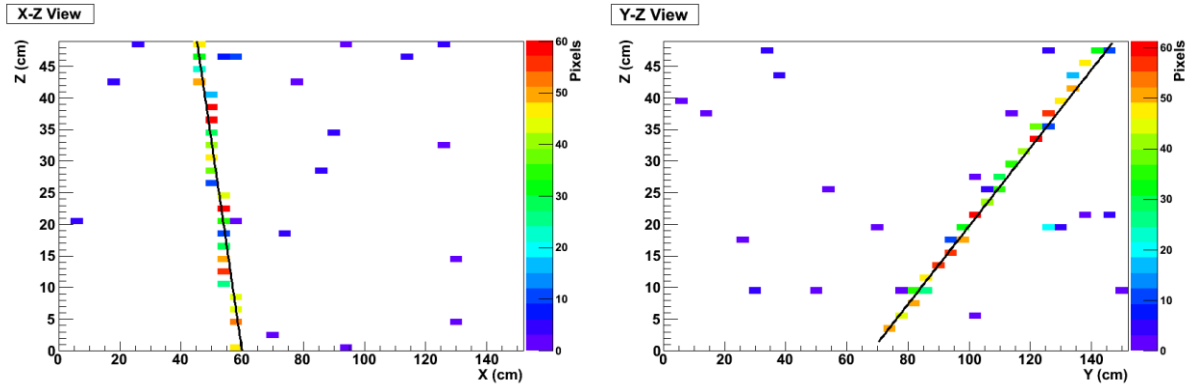

Figure 6: A cosmic ray track passing through the detector. Each plot shows a projection of the track on each face of the detector with each block representing a scintillator bar.

4. Field tests at Wylfa power station

4.1. Wylfa Power Station

The Wylfa site is located on the Isle of Anglesey, North Wales in the U.K. and houses two 1.6 GWth Magnox reactors which began generating in 1971. Reactor 2 was shut-down permanently in 2012. Reactor 1 continues operation under the novel inter reactor transfer (IRX) programme whereby partially irradiated fuel is transferred from reactor 2. Reactor 1 will be shut-down permanently at the end of 2015.

Magnox reactors are named for the magnesium-oxide cladding on the fuel assemblies. They use natural uranium fuel, carbon dioxide gas cooling and a graphite moderator. Due to the low burnup of

the natural uranium fuel, Magnox reactors were designed to be re-fuelled on load. In terms of the anti-neutrino field tests, this means that the effects of fuel burnup should be minimal as depleted fuel elements are replaced regularly. From a safeguards perspective, it is also interesting to note that the North Korean Yongbyon reactor was based on the Magnox design and that the re-fuelling on load makes the production of weapons grade plutonium simpler than in other reactor designs.

4.2. Deployment at Wylfa power station

The University of Liverpool detector has been deployed at Wylfa power station for testing since April 2014, shortly before the start of Wylfa's final power generating cycle. The container was transported via road from University of Liverpool to the Wylfa site. The flat-bed truck used for delivery, was an industry standard for transportation of cargo containers. It came with its own HIAB (lifting crane), hence reducing the requirements and burden on the power station for installation. Figure 7 shows the container being loaded on to the transport vehicle at the University of Liverpool. The detector was placed outside, between the reactor building and turbine halls at a distance of roughly 60 m from the reactor core. The detector is outside of internal security barriers, minimising the issues with site access and security clearance at the cost of being further from the reactor core. Figure 8 shows the container and project team on-site after successful deployment.

Figure 7: A picture of the shipping container being loaded on to the flat-bed truck at the University of Liverpool.

Figure 8: A picture of the University of Liverpool team and Wylfa power station staff after the successful deployment of container on the reactor site.

4.3. On-site test data and commissioning

On-site checks and commissioning runs were performed after deployment of the detector on-site. Through the analysis of cosmic ray events it was confirmed that no damage had occurred during transit. Minor calibrations were performed to adjust for the change in local environment. The detector then began collecting data before the reactor returned to service.

Further data was taken with a neutron source at the Wylfa site for the development of a neutron identification algorithm in the presence of realistic backgrounds. This data was combined with data from cosmic rays for comparison. A PID comparison plot is shown in Figure 9. The background data contains small clusters of energy deposit from high energy gamma rays and cosmic muons that clip the detectors edge, where the spatial size in the detector (x-axis) is roughly equal to the number of scintillator bars hit (y-axis). Cosmic rays that fully penetrate the detector are seen at a cluster length of 49 cm which is the height of the detector's active region. From the californium source data it can be seen that for neutrons there is no correlation between a cluster's size and the number of hits in the cluster. A series of cuts were developed from these PID plots to select Neutron capture candidate events. Candidate neutron capture events are selected at the rate of roughly 1 Hz as shown in Figure 10. By comparing data from reactor-off and reactor-on periods the neutron rate was observed to increase by roughly 15×10^3 during reactor operation at 1600 $MW_{th.}$

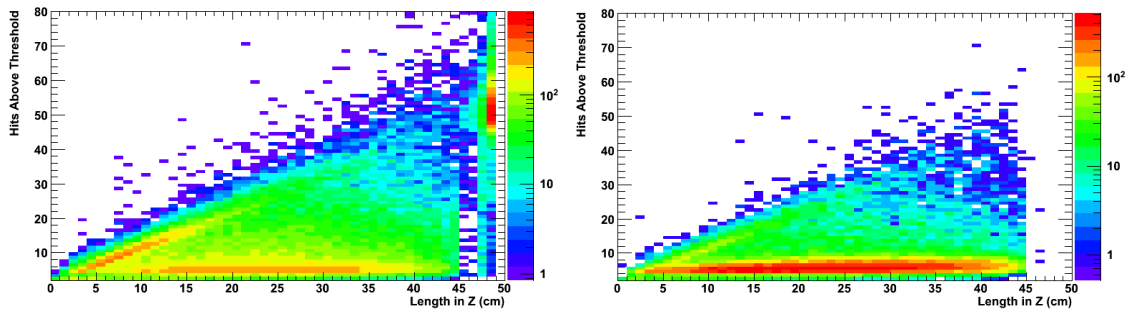

Figure 9: Neutron PID plots. Left: Data taken at Wylfa before reactor restart combined with cosmic ray data Right: Data taken with a Cf-252 neutron source.

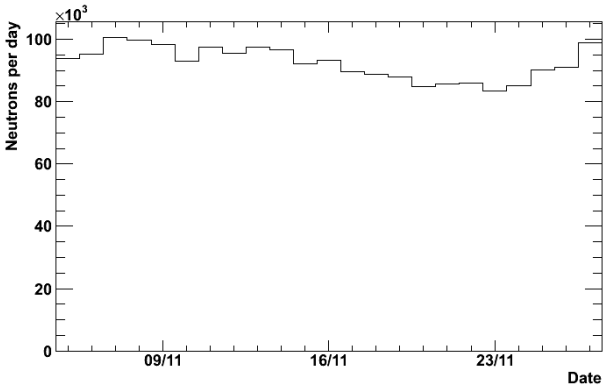

Figure 10: The number of neutron capture events selected per day over the period of 1 month.

4.4. Positron selection and fast neutron rejection

The neutron selection is used to select the delayed signal in an inverse beta decay event. A preliminary positron selection has been developed to identify the prompt signal component in the anti-neutrino events. The positron selection has been partially developed utilising electrons from high energy gamma ray interactions. Electrons (and positrons) leave a small clustered energy deposit in

the detector in the form of a particle track. The energy range of the positron track is dictated by the energy of the interacting anti-neutrino which informs energy range in which to search for the prompt signal. Data from the californium source was also used to develop methods for the rejection of fast neutron backgrounds which produce a correlated time signal similar to that of an anti-neutrino event. The time window for the delayed coincidence search is constrained by the electronics at 30 μs in the detector

4.5. Uncorrelated background suppression

Uncorrelated background events are when independent prompt and delayed events randomly occur within the time window of the delayed coincidence search. As the prompt and delayed signals are created independently they show a flat time-delay distribution rather than the exponential decay distribution from correlated events. The probability of such uncorrelated events occurring in the search window is continuously monitored in the data and thus their contributions to the anti-neutrino signal candidate events sample can be calculated and subtracted. Figure 11 shows the time delay distribution for anti-neutrino candidate events after subtraction of uncorrelated backgrounds. The data is fit with an exponential decay plus a constant. The constant is consistent with zero indicating that the majority of the uncorrelated background has been subtracted out.

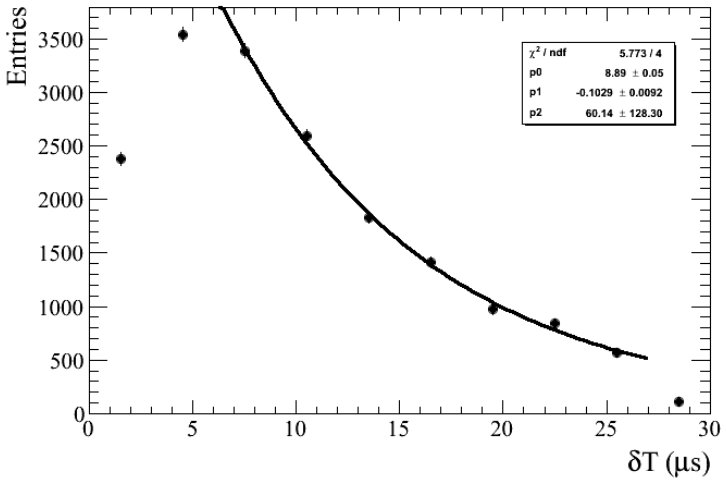

Figure 11: The time between delayed and prompt signals for candidate anti-neutrino events during reactor-on data taking after subtraction of uncorrelated backgrounds. Data is fit with an exponential function plus a constant (P2). Detector efficiency effects alter the timing distribution in the first two and the final bins which have been excluded from the fit.

5. Summary and Outlook

An anti-neutrino detector for safeguards purposes has been constructed and commissioned at the University of Liverpool based on the technology used for the T2K experiment. The detector design uses only safe, robust materials in order to be as safeguards friendly as possible. Commissioning data shows the detector to be highly effective at neutron-gamma ray discrimination due to the use of a gadolinium neutron absorber. Combined with the baseline design's ability to detect positrons, the anti-neutrino detector is well suited to the observation of inverse beta decay interactions. The detector has been deployed in and ISO container at the Wylfa power station reactor site in the UK for over one year. Analysis of the data and selection of anti-neutrino events is on-going and initial results have been presented here.

Acknowledgements

The authors acknowledge the support of the STFC, the Royal Society of Edinburgh and the Royal Society and are grateful for the support and contributions of the Particle Physics group and the mechanical workshop from the Physics Department at the University of Liverpool. The necessary

introductions for site access were facilitated through the Department of Energy and Climate Control (DECC) and the Office for Nuclear Regulation in response to approach from the UK Support Programme to the IAEA (UKSP). The UKSP is funded by DECC to provide technical support to the IAEA Department of Safeguards The authors are grateful for the on-going support and effort from the staff at Wylfa Power Station. The next phase of the project will see the University of Liverpool working with John Caunt Scientific Ltd.

References

[1] Abe, K, et al*; The T2K Experiment;* Nuclear Instruments and Methods A; **659**; 2013

[2] Bowden, NS, et al; *Reactor Monitoring and safeguards using antineutrino detectors;* J.Phys.Conf.Ser.*;* **136;** 2008

[3] Mueller, TA, et al; *Improved Predictions of Reactor Antineutrino Spectra*; Phys.Rev.C*;* 83:054615; 2011

[4] Allan, D, *et al*; *The electromagnetic calorimeter for the T2K near detector ND280;* JInst **8;** 10019; 2013

Session 16

Containment and Surveillance

EURATOM experiences on NGSS field implementation preparation

Juha Pekkarinen, Konrad Schoop, Jean-Michel Mazur, Carlo Demartini

European Commission, DG Energy, Directorate Nuclear Safeguards, Unit E1,
L-2920 Luxembourg
E-mail: Juha.Pekkarinen@ec.europa.eu

Keywords:

EURATOM, NGSS, Next Generation Surveillance System, test, implementation

Abstract:

This paper reports on the results of the EURATOM testing and evaluation programme of the Next Generation Surveillance System (NGSS).

EURATOM Safeguards has started replacing the aging DCM-14 based surveillance systems with NGSS since July 2014. Before beginning this replacing, an intensive testing and evaluation programme was carried out in close collaboration with the IAEA and Dr. Neumann, the system developer. The goal of this programme was to confirm the system's reliability and suitability for in-field use. Because the programme was started after hardware and security development had been completed, the focus was placed on the operating system features, performance, usability and NGSS compatibility with existing infrastructures.

The programme resulted in a series of important improvements to the system, making it more reliable, better performing, and more user-friendly. The programme also helped to determine the operational limits and optimal in-field system set-ups and configurations.

In parallel to the testing and evaluation campaign, an infrastructure was created to work with the NGSS. This included the development of software tools for installation and maintenance, evaluation of the system's performance, as well as analysing and archiving of data. In addition an inspectors' training programme and a documentation package including working papers and work instructions, was created.

Experiences drawn from the first installations in field, together with some further development needs, are presented in this paper.

1. Introduction

The European Commission's Directorate of Nuclear Safeguards (EURATOM) at the Directorate-General for Energy, is responsible for installing, operating, maintaining and reviewing about 600 safeguards cameras in the nuclear installations across the European Union. About 350 of these cameras are operated together with the IAEA Safeguards Department (IAEA).

Currently EURATOM is using two different surveillance technologies. In the Non-Nuclear Weapon States of the European Union (EU-NNWS), where EURATOM is present together with IAEA, the surveillance systems are based on the Digital Camera Module DCM-14 [1] technology. In the Nuclear Weapon States (EU-NWS) the EURATOM surveillance systems are based on FAST-NICE [2] technology.

Both of these currently used surveillance technologies will be reaching the end of their life in a few years time. The Next Generation Surveillance System (NGSS) [3] has been developed as a successor to these now outdated technologies. Initially, this development was driven by the IAEA and was financed by the German and US support programmes. Since 2012, EURATOM has contributed to the development of NGSS firmware and supporting software tools. EURATOM has also started its own project for further development of the NGSS components.

The reliability of installed safeguards equipment plays a very important role. Above all, reliable operation is needed in order to avoid complex and often very expensive re-verification measures in the case of loss of continuity of knowledge (CoK) of safeguarded nuclear material. Secondly, frequent maintenance of the equipment in the facilities is remarkably expensive. Furthermore, EURATOM has to optimise its limited installation and maintenance resources. Therefore, before releasing any equipment for safeguards use, EURATOM put much effort on testing. In many cases, the surveillance cameras are particularly difficult to access for maintenance. Consequently, it was imperative for the NGSS system to undergo an intensive testing and evaluation programme.

2. Scope of surveillance equipment upgrade

When planning safeguards instrumentation upgrades, it is very important to take into account every aspect affected by that work. In the case of surveillance equipment upgrades there are - besides the equipment itself - many other aspects like system set-up tools, re-use of existing infrastructures, data retrieval, data archival, data review, state-of-health monitoring, work instructions and training of technicians & inspectors to be taken in account.

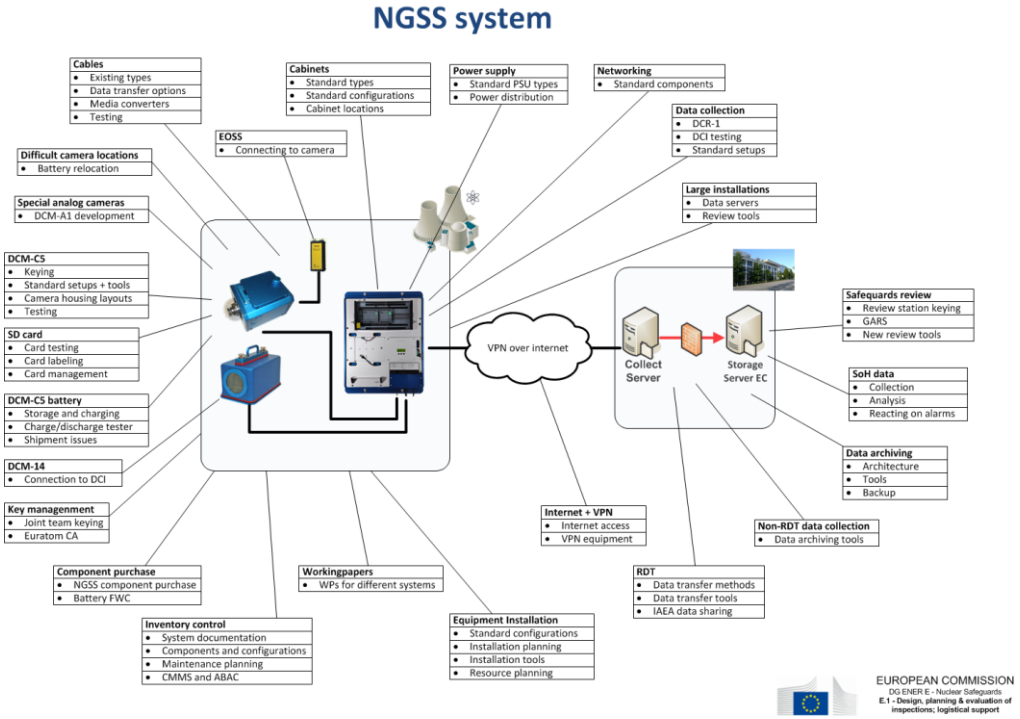

Picture 1. The scope of NGSS upgrade project

The fact that EURATOM is using two completely different surveillance technologies adds to the complexity of the upgrade planning. In the EU-NNWS, the video surveillance systems jointly used with IAEA are mainly applied in power reactors and storage facilities. With a few exceptions, the surveillance systems in these facilities are relatively small having only 1 to 6 cameras per system.

However, in the EU-NWS the surveillance needs are often much different. The surveillance systems are usually installed in large facilities and the number of installed camera per system can sometimes be higher than 30. This complexity places special requirements on the system's design.

EURATOM has observed, already in the early phases of the NGSS development, that the resulting products might not fully satisfy the technical requirements in the EU-NWS. Therefore, in 2012 EURATOM launched an open call for tender especially for digital multi-camera surveillance systems (DMSS) to be installed in the large facilities of the EU-NWS. The major award criteria of this tender were reasonable cost, reliability, modularity, and low maintenance need. Because of the high quality and the competitive price of NGSS compared to rival bidders, EURATOM awarded the DMSS contract to the developer of the NGSS system. The DMSS is foreseen to be an enhanced version of the NGSS with additional features such as analogue video input, image capturing in burst mode, enhanced front-end motion triggering and better system scalability. It is to be noted that the development of NGSS analogue video input was started under the German Support Programme already before the DMSS project.

3. NGSS test programme

EURATOM was not directly involved in the NGSS hardware development phase. Therefore, the test programme was developed after the point where the hardware development was already completed. The main objective of the testing was to prove NGSS equipment could be deployed for safeguards use by testing it in all circumstances and set-ups in which the equipment could be later used.

The focus of the test programme was on two key areas. The first area was the performance and reliability of individual NGSS components. In this context also the camera usability was assessed carefully in order to make sure it could be operated by the end users without difficulty and with minimal risk of entering incorrect settings by mistake.

The second key area of the testing was to simulate the use of the NGSS with all known cable infrastructures present in the nuclear facilities. This was particularly important because replacing the cabling in operating nuclear plants would be very time consuming and expensive. In some cases this might not be possible at all.

Besides the re-use of the cable infrastructures, EURATOM was also seeking possibilities to use the existing camera and recording enclosures for the NGSS installations. The goal of this was to reduce the materials cost and to optimise installation times.

EURATOM has collected the results of all tests performed in a NGSS test report. This report serves as a EURATOM guideline for the NGSS system design and provides recommendations on the NGSS installation.

3.1 Tests on NGSS components

3.1.1 DCM-C5 camera

EURATOM received the first DCM-C5 [4] camera units at the end of 2012. The first tests focused on the picture taking capacity and picture quality. The DCM-C5 features, besides normal single channel mode, a virtual 4-channel mode where 4 video channels can be recorded simultaneously from any selected area of the image sensor. Further, the camera can be equipped with either a normal varifocal lens or with a so-called fish-eye lens allowing viewing angles up to 185 degrees. All combinations of these features were covered in the tests.

Picture 2. DCM-C5 camera

Besides confirming the camera performance, the test on the picture taking capacity and picture quality helped to discover some software problems. The problems discovered were shared with IAEA and the system developer who delivered, within short times, firmware updates fixing the problems. During the evaluation period, from beginning of 2013 to end of 2014, altogether 8 camera firmware updates were released and tested.

A close cooperation with the IAEA resulted - besides the software bug fixing – in many valuable improvements to the camera. These included numerous improvements to the camera performance, reliability and cryptographic key management. A good example of such improvement is the changes made into the key management of the camera. These changes allow EURATOM and IAEA to install the cameras independently from the other organisation.

EURATOM also agreed with IAEA considerable improvements to the camera user menu structure. These modifications greatly improved the camera usability for the end users. Further, the joint testing with the IAEA resulted in a set of commonly agreed standard settings for the jointly used cameras.

Another area of interest with regards to the testing programme of the camera was the power autonomy. In the case of a mains power supply failure, the camera is powered from its emergency battery. The length of this power autonomy is an important parameter when setting up safeguards strategies or when planning maintenance of the surveillance system.

The tests done on the power autonomy delivered very positive results. Compared to the DCM-14 technology, the power autonomy of the NGSS camera is considerable higher. The firmware updates also resulted in an improved power management system of the camera. This improved the power autonomy even further.

EURATOM released the camera firmware for in-field use in July 2014. A large number of EURATOM and IAEA cameras have been operating since, without any significant problems. There are however ongoing investigations to improve some features of the camera. Both EURATOM and IAEA are willing to implement future improvements to the DCM-C5 in the form of firmware upgrades.

3.1.2 Digital Camera interface

Besides the camera, the second core component of the NGSS system is the Digital Camera Interface (DCI) [5]. The DCI polls data from the camera either over an Ethernet or over a RS-485 connection. Both connections types were intensively tested.

Picture 3. DCI together with DCR-1 user interface

The tests on the DCI began in early 2013. The first firmware versions limited the number of connected cameras per DCI to 4. Also, the download speed using the RS-485 protocol was not very satisfactory. Bearing in mind better scalability and cost optimisation of the systems, EURATOM was actively seeking, together with IAEA and the system developer, possibilities to improve the DCI performance.

In the course of the testing the system developer did indeed succeed to achieve several improvements on the DCI firmware. After 6 tested firmware releases, the DCI is now able to collect data from up to 32 cameras and the RS-485 download speed has improved by factor of four. Another important improvement in the firmware version released for in-field use is that information of connected cameras and downloaded data volume is displayed on an attached user interface.

3.2 Cable tests

As noted before, the new surveillance equipment to be installed must be able to work with the cable infrastructures already in place in the nuclear facilities. This means that both power transmission and data communication between the data collection point and the cameras must be backwards compatible.

EURATOM and IAEA have installed surveillance instrumentation in European nuclear sites since the 1980's. This is why many different cable types and cable layouts have been used in these installations. Even though the NGSS system has been designed to use the existing cable infrastructures, all different installation variations had to be taken in account and tested.

The experience from the DCM-14 technology has shown that the data communication over RS-485 protocol works reliably in an industrial environment. On the other hand, it is also known that some of the old cable types do not allow using an RS-485. In order to cover all existing, and also possible future, data transmission options, the following cable test plan was drafted.

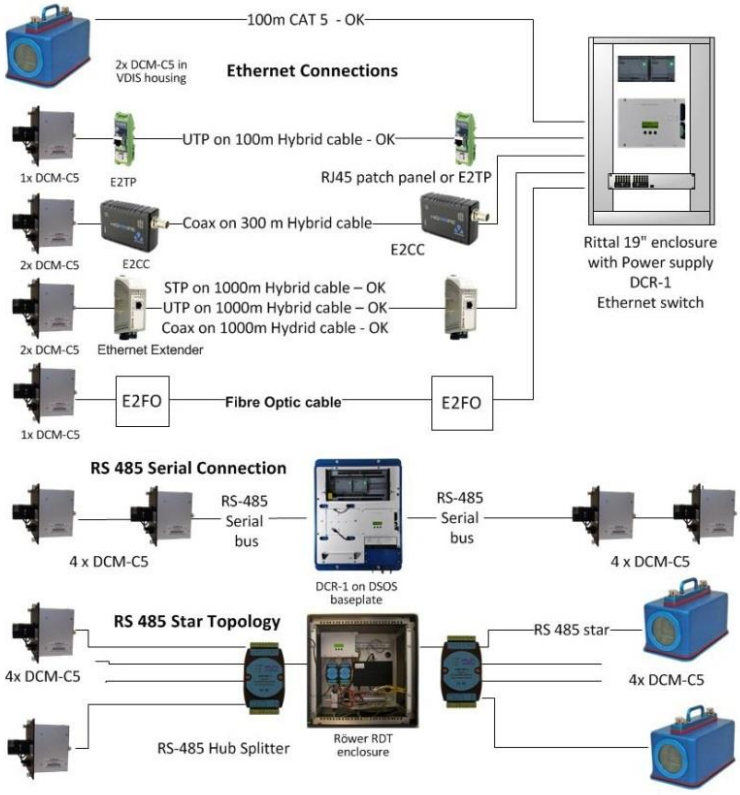

Picture 4. Extract of EURATOM cable test plan

The objective of the testing was to determine for each cable type and configuration, the maximum cable lengths on which the data transmission would still work reliably. The different cable types installed in the field are: shielded and unshielded twisted pairs in various dimensions; coaxial cables; and fibre optic cables.

One limiting factor on selecting the data transmission method is the cable topology. Due to the architectures of the surveillance systems used in the past, the existing cables are laid down from the recording unit to the cameras either in a star or in a daisy chain topology.

Due to its architecture, the Ethernet connections can be established over only a limited number of cable types and over a maximum cable length of 100 meters. Daisy chaining is not possible without additional switching devices. Therefore, some industrial Ethernet extenders were selected and tested in order to cover longer distances and to allow daisy chaining with the Ethernet protocol.

In turn, the RS-485 architecture does not support the star topology. Even though on some current DCM-14 systems the RS-485 transmission has been implemented in star topology, without fully respecting the bus structure, this would not work on the NGSS because of much higher data transfer rates. To overcome this problem and to avoid use of too many DCI units, EURATOM initiated the development of a simplified data retrieval interface. The result of this development was a Dual Comport Server (DCS). The DCS converts the traffic of two independent RS-485 buses to Ethernet.

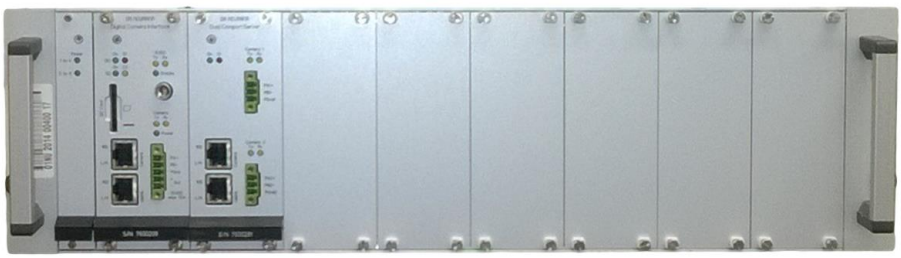

Picture 5. DCI (left) together with DCS in a DCI-B8 rack

One part of the testing programme was to study how interferences occurring in industrial environment affect the data transmission. Although it is very difficult to simulate industrial conditions in laboratory environment, the influence of electromagnetic interference was simulated by coiling the data transmission cables and introducing electromagnetic fields inside these coils. Such interference affected remarkably the data transmission over some cable types. This has been taken in account in the test results.

The conclusion of the cable testing was that the cameras can be connected using existing cables. In some cases the data link has to be established using special media converters. The most reliable data communication method is the RS-485 protocol.

4. Software tools

A prerequisite for the successful installation and operation of a surveillance system are adequate set-up, monitoring, remote data transfer (RDT) and safeguards review software tools. The following chapters give an overview on the tools developed during the course of the evaluation programme.

4.1 NGSS set-up tool

The NGSS system developer has provided a list of commands allowing the system set-up and status monitoring over a http protocol. In the beginning of the testing programme this was the only method to set-up the system. As this method was not practical, EURATOM designed and programmed a NGSS User Interface software tool for flexible system set-up, maintenance, manual system monitoring and manual data download.

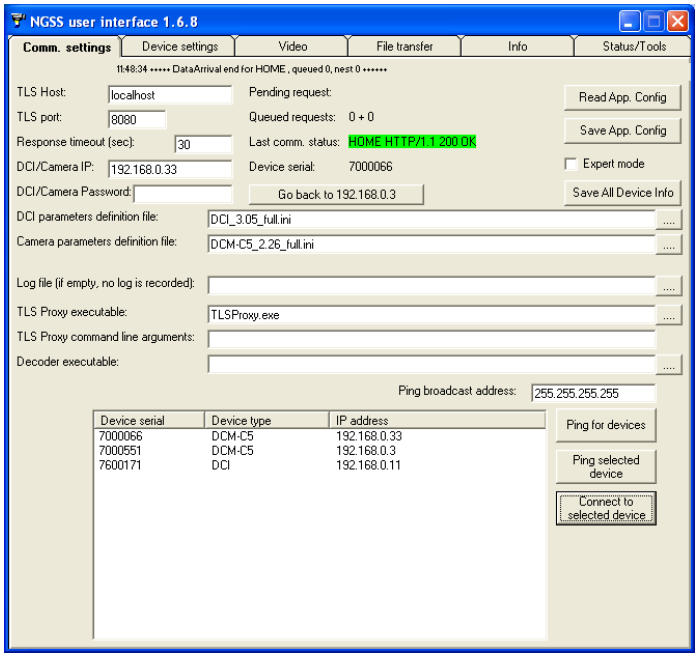

Picture 5. NGSS User Interface tool

4.2 Automatic data download and monitoring

The software modules for the data download over RDT and data archiving in headquarters have been developed by the NGSS developer and by the IAEA. EURATOM currently uses the modules from IAEA which have proven their reliability in production use. As part of the DMSS development the NGSS developer will provide EURATOM with new data download software.

EURATOM has also developed a state-of-health monitoring software for the systems connected over RDT. This Log File Parser can monitor both DCM-14 and NGSS systems and many other data acquisition systems. The tool alerts the EURATOM technicians if any predefined anomaly occurs on the connected systems.

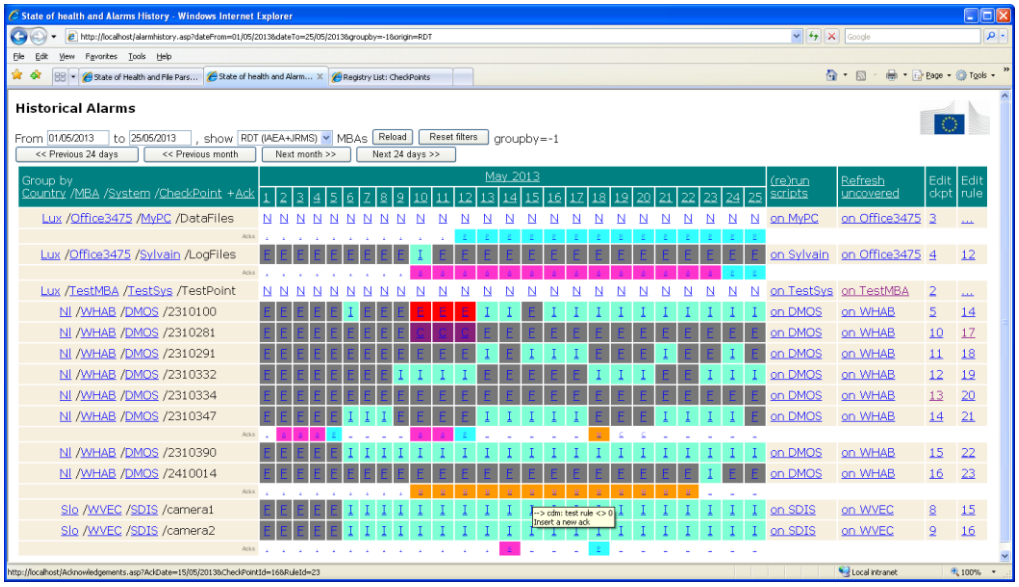

Picture 6. Log File Parser status of health monitoring tool

4.3 Review tools

Further, another essential tool for a surveillance system is the safeguards review software. The IAEA has developed software modules allowing NGSS to be reviewed on the General Advanced Review Software (GARS) review software platform. The tests and practical experiences have shown however that, because of its outdated structures and limited possibilities on modern computer processor technologies, the GARS is too slow and therefore not well suited for the NGSS review. EURATOM and IAEA have started a joint project to develop a new review tool. Also, the developer of the NGSS system is working on a review tool as part of the DMSS contract. EURATOM expects to receive the first versions of the DMSS review tool in the second half of 2015.

5. Work instructions

Written procedures are important tools for the quality assurance throughout the planning, installation and operation of all safeguards systems. EURATOM has written work instructions for both technicians and the inspectors. The technical work instructions cover all processes starting from the keying and set-up of the equipment through the lab testing, up to final installation of the equipment in the nuclear facilities. For the inspectors, the EURATOM surveillance team has prepared working papers for all different versions of the installed NGSS systems.

6. Training

Training is another essential element for new equipment. Since the beginning of the testing and evaluation programme, EURATOM has organised basic and expert training sessions for the technicians. These trainings cover introduction of individual system components, keying procedures, set-up, testing and installation.

The NGSS training for the EURATOM inspectors includes familiarisation with the system components and hands-on training on set-up and media exchange. The surveillance team has also produced a series of NGSS training videos targeted for the inspectors. On one hand preparation of these videos is an additional burden to the surveillance team, but on the other hand, the availability of such training videos is expected to reduce the need of traditional training sessions.

The fact that EURATOM has selected NGSS for both EU-NNWS and EU-NWS reduces the training effort remarkably. For the technicians, as well as for the inspectors, it is much easier to work on systems coming from the same manufacturer.

7. Experiences in the field

EURATOM started NGSS installations in July 2014. The first systems installed were single camera systems in nuclear power plants. For upgrading of DCM-14 based camera systems, EURATOM has purchased from the NGSS system developer modular components to be installed into the existing camera and recoding unit enclosures. This method helps to reduce the installation costs and shortens remarkably installation times. The modularity has also been found to improve the installation quality. The experiences from these installations have been very positive.

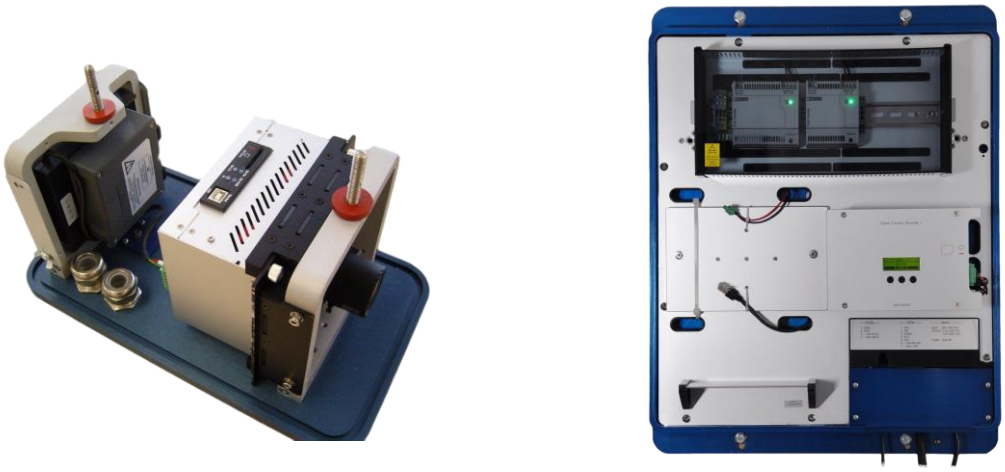

Picture 7. Modular single camera NGSS components in old enclosures

For example, in order to upgrade a DCM-14 based DSOS single camera system, the technician first removes the old components from the enclosures without the need to dismantle the whole system. Then he mounts the new NGSS components in the old enclosures using the existing mounting points. If the camera and recording unit are easy to access and the plant operator can provide mains power isolation when requested, the upgrade of such a system can be completed in just a few hours.

EURATOM installed the first NGSS multi camera system in March 2015. Thanks to the system's modularity, also these systems can be installed in the existing enclosures. In the case of old systems the diverse cable infrastructures and non-standard camera enclosures cause some additional effort but with careful planning, problems can be avoided and the systems can be upgraded in a reasonable time.

The first experiences from the multi-camera installations show that the Ethernet data transfer can be very challenging in the industrial environment. In order to avoid such problems the RS-485 communication protocol should primarily be used and if Ethernet transmission is unavoidable, the conditions where this will be applied should be known in advance in order to allow sufficient testing.

In the first multi-camera installation, EURATOM faced problems with the Ethernet transmission between the cameras and the DCI. These data transmission problems probably also caused some problems on the operation of the DCI itself. At the time of writing this paper, these issues are still under investigation.

In 2014, EURATOM installed 5 single camera NGSS systems. In 2015, the goal is to install a further 48 single camera and 4 multi camera systems.

8. Conclusions

EURATOM has spent almost two years on the NGSS testing and evaluation programme. These 2 years have resulted in numerous improvements to the NGSS system and qualified it for in-field use. The NGSS hardware and software have proven, through the tests and first in-field applications, to be of a very high quality and a reliable surveillance system.

The tests performed, helped to generate a list of recommendations which EURATOM uses as a guideline for further NGSS implementation design. The testing and evaluation programme also made it possible to create high quality work instructions and training material for both technicians and inspectors.

The modularity of NGSS has proven to be a great advantage for system installations and quality assurance. In addition the synergies from using components from only one manufacturer are notable.

The time spent on the testing and evaluation programme provided knowledge to design proper software tools for system set-up, data download, state-of-health monitoring, data archiving and safeguards review. Without these tools, the field implementation would have been very difficult.

EURATOM concludes that the testing and evaluation programme has been very well justified. The improvements made to the NGSS, have shown that the time selected for starting the in-field implementation has been well selected.

References

[1] B. Richter, G. Neumann, K.J. Gärtner, H. Meier, K. Schoop; *Digital Image Surveillance Systems Based on the Digital Camera Module DCM 14,* JOPAG/05.99-PRG-297; Task D.26/E920, Forschungszentrum Jülich GmbH, Jülich1999

[2] NiceVision alpha technology - User Manual based on version 5.83, NICE Systems Ltd, 2009

[3] M. Moeslinger, C. Liguori, G. Neumann, S. Lange, M. Stein, S. Pepper, B. Richter, K. Schoop; *The IAEA's XCAM Next Generation Surveillance System*, IAEA-CN-184/260, Proceedings of IAEA Symposium for International Safeguards, Vienna 2010

[4] G. Neumann, S. Lange; *Next Generation Surveillance System NGSS – DCM-C5, Instructions and Reference,* JOPAG/10.13-DOC-97, Forschungszentrum Jülich GmbH, Jülich, 2013 (not publicly available)

[5] G. Neumann, S. Lange; *Next Generation Surveillance System NGSS – Digital Camera Interface, Instructions and Reference,* JOPAG/08.11-DOC-, Forschungszentrum Jülich GmbH, Jülich, 2013 (not publicly available)

New Ultrasonic Optical Sealing Bolts for Dry Storage Containers

Francois Littmann, Marco Sironi
Institute for Institute for Transuranium Elements (ITU)
Nuclear Security Unit - Seals & Identification Techniques Laboratory (SILab)
Joint Research Centre, European Commission
E-mail: francois.littmann@jrc.ec.europa.eu

Peter Schwalbach, Lukasz Matloch
DG ENER – European Commission, Luxemburg

Bernie Wishard, Victor Kravtchenko,
International Atomic Energy Agency, Vienna

Abstract:

This paper presents a new seal for dry storage containers with nuclear material. Currently, sealing of dry storage casks containing spent fuel presents various challenges to safeguards inspectors. Continuity of knowledge needs to be reliably maintained over periods of time that can be decades. Seal replacements and verification , require significant Inspector efforts, radiological dose, and is continuing to grow. A decrease in Inspector effort is required and fail-safe redundancy is sought. These needs called for the development of a new compact sealing bolt covering these requirements. The Ultrasonic Optical Sealing Bolt (UOSB) is based on the JRC Candu Sealing System (JCSS), which is approved for safeguards use by IAEA and EURATOM safeguards. The new seal includes the same integrity element with the same identity element In addition, the UOSB integrates the additional element of a Fibre Optical Cable (FOC). This construction is in principal two seals-in-one allowing versatility.
After several design iterations, field trials and a positive Vulnerability Assessment, the UOSB design was finalized. The first UOSBs, combined with EOSS and Cobra seals, were installed on dry storage containers at the Ignalina nuclear power plant (Lithuania) in June 2014. IAEA gave a Category A label to the UOSB system later on October 2014.

Keywords: seal; cask; dry storage; optical fibre; Ignalina

1. Introduction

The Seals & Identification Laboratory (SILab) is part of the Joint Research Centre of the European Commission. As one of its main activities, SILab develops technologies and equipment based on ultrasonic techniques, suitable for sealing and identification of nuclear spent fuel assemblies in underwater storage ponds. Ultrasonic seals present, as main advantage, stability against time and radiation. Being purely static pieces of stainless steel they will last the lifetime of the stacking frames and remain stable as identity. There is an extensive literature explaining how the ultrasonic seals are designed and read [1].
The ultrasonic seals are currently used by both nuclear safeguards agencies, IAEA and Euratom in Europe, in France and Romania and outside Europe, in Canada and Pakistan.

2. Sealing dry storage casks

There is a need to have a simple and reliable sealing principle for dry storage casks of huge dimensions like Castor and Constor casks, sealed up to now with metallic seals with a cable passing through a drilled bolt. After a design review, a decision was taken to add to the ultrasonic sealing bolt a fiber optic passing through the main body of the seal. When the bolt is removed, the fibre is cut.
On top of simple installation and low vulnerability risk the seal has to fulfil the following minimum

requirements:

- To be used on the primary lid of a nuclear container for the replacing of one or more of its bolts, without any modification of the container body or of the lid;
- To be easily installed and removed, in any environmental condition;
- To include a fiber optic in the body of the seal that breaks at any attempt of tampering;
- To allow remote monitoring of the cask(s) looped by the fiber;
- To allow verification of the identity and integrity of the seal through an ultrasonic Inspection;
- To carry an identity which can be univocally coupled with the container;
- To have the possibility to identify a seal after removal (case of a broken seal);
- To be able to withstand harsh operating conditions;
- To maintain a proper answer to any check over a period of several years, as needed.

3. Ultrasonic Optical Seal Bolt design

Two possible designs were identified for the seal. The first design with a fiber optic passing through the seal and a design with connectors to allow the removal of the seal without replacing all the fiber loop. There are also two types of casks with different mechanical interfaces, one is called Castor with an Allen M36 structural bolt and the other is called Constor, with a threaded hole M36.

3.1. UOSB with connectors

This type is made for connection with an EOSS electronic seal, which explains why one connector is needed on each side of the UOSB. Internally, there is a short piece of optical fiber with two connectors, not visible on the design. This fiber is linked to the pin, which breaks when the seal is removed and cuts the fiber, then a real time alarm can be triggered by the electronic seal.

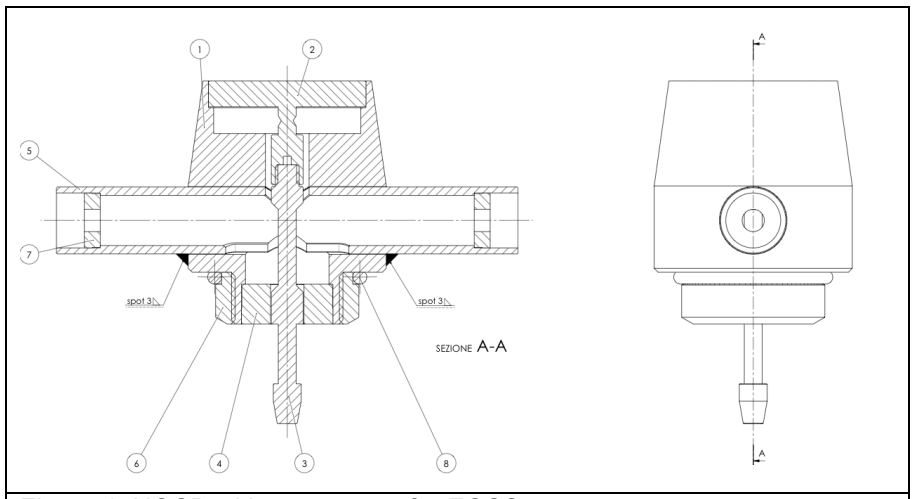

Figure 1: UOSB with connectors for EOSS

3.2. UOSB with the fiber passing through

This UOSB is much simpler because there is no need to add any connector. The seal has just two inclined holes drilled on each opposite sides of the seals, together with an associated hole inside the pin, where the fiber will pass through pushed by the inspector. This configuration could be used with a Cobra or any type of electronic seal with an optical fiber without connectors, like the new Active Optical Loop Seal (AOLS) developed by JRC.

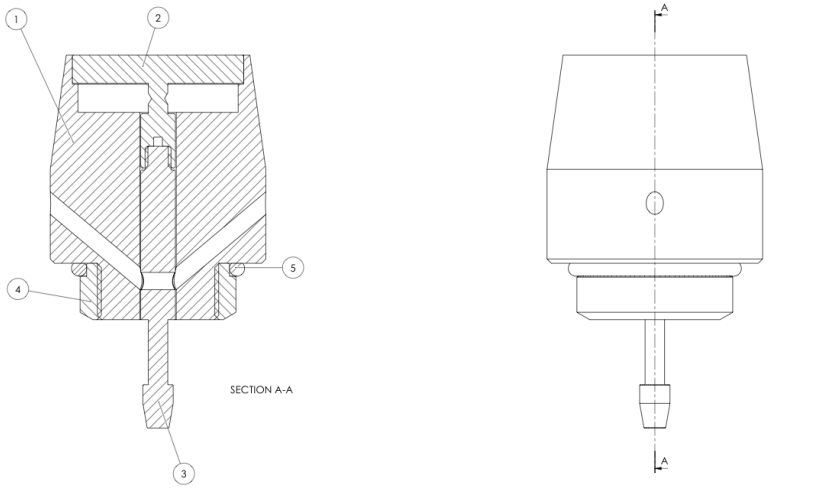

Figure 2: UOSB without connectors, for Cobra type of seal

4. Inserts design

Two possible designs were identified for the two different types of casks.

4.1. Inserts for Castor Casks

The lid of the Castor cask is bolted with several M36 Allen bolts, tightened with a specific high torque (figure 3 & 4). In order to seal the lid, one or two bolts are removed, one after the other and replaced with our own inserts. The insert Castor, is a standard Allen M36 bolt, drilled with a grip inside and resists to the same torque as the original one (figure 5).

Figure 3: Castor cask with standard Allen bolts

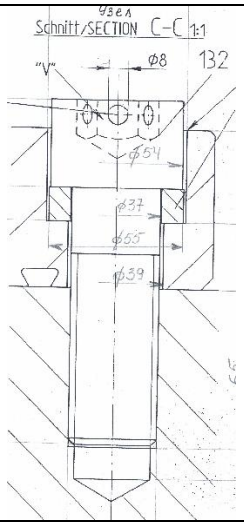

Figure 4: Standard Allen bolt

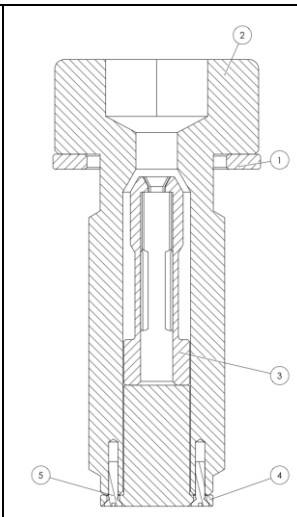

Figure 5: Modified Allen bolt insert

Figure 6: Exploded insert

4.2. Inserts for Constor Casks

The insert Constor, instead is based on a nut/counter nut assembly and is installed by the inspector.

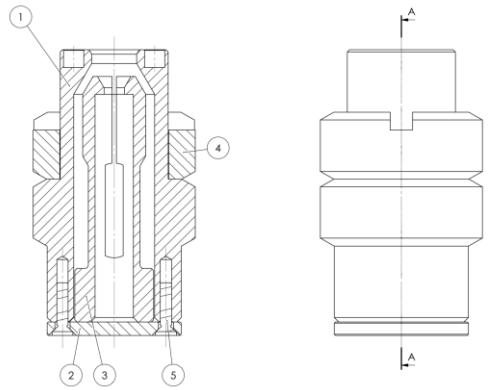

Figure 7: Insert for Constor casks

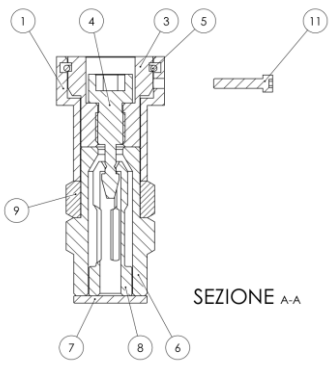

Figure 8: View of the insert with assembly tool

Figure 9: Exploded insert

The upper parts seen on figure 8 (ref. 1, 3, 4, 5 & 11) assembled the tool needed to put the insert at the right depth and to block the nut counter nut system. Just the lower parts (ref. 6, 7, 8 & 9) remain into the M36 threaded cavity.

5. Seals & Inserts

There are two different types of casks, Castor & Constor and two types of UOSBs, with connectors for the EOSS and without for the Cobra, so four different possible combinations.

Figure 10:
Castor / EOSS

Figure 11:
Constor / EOSS

Figure 11:
Castor / Cobra

Figure 12:
Constor / Cobra

6. Field trials

A first field trial was performed in June 2014 in Ignalina (Lituania), followed by a second one later in July. Several inserts and seals were installed by IAEA, Euratom and JRC technical experts on Constor and Castor casks and fibers were connected to EOSS and Cobra seals.

Figure 13: View of the dry storage casks

Figure 14: Seal installation

Figure 15: Ultrasonic reading of UOSB

7. Category A, ready for operational use

Following these successful two field trials and a positive Vulnerability Assessment, the IAEA decided to give a Category A label to the UOSB system, on the 2nd of October 2014. This very important recognition means that the UOSB seals developed by JRC are now ready for operational use in nuclear dry storage facilities. Euratom in charge of inspections within European countries acknowledged this category.
Within a few weeks from this recognition, the first set of 30 UOSB seals with and without connectors and 30 inserts for Castor and Constor casks were delivered.

Figure 16: 4 UOSBs & 2 inserts

Figure 17: Seals ready for shipment

8. Next steps

Inspectors from Euratom and IAEA will be trained in Ispra mid April on the installation of inserts & UOSBs, as well as reading ultrasonic signatures. Beginning of May, another batch of 62 UOSBs will be installed on Castors and Constors casks.

9. References

[1] *JRC CANDU Sealing Systems for Cernavoda (Romania) and Upcoming Developments M. Chiaramello, M. Sironi, F. Littmann, P. Schwalbach, V. Kravtchenko; ESARDA Bulletin n°44 June 2010.*

Activities towards Ceramic Seal Operational Readiness

Heidi Smartt, Juan Romero, Joyce Custer, Daniel Krementz*, Larry Harpring*, Michael Martinez-Rodriguez*

Sandia National Laboratories
Albuquerque, New Mexico, USA
E-mail: hasmart@sandia.gov, jarome@sandia.gov, jcuster@sandia.gov

Savannah River National Laboratory*
Aiken, South Carolina, USA
E-mail: daniel.krementz@srnl.doe.gov, larry.harpring@srnl.doe.gov, Michael.Martinez-Rodriguez@srnl.doe.gov

Abstract:

Containment/Surveillance (C/S) measures are critical to any verification regime in order to maintain Continuity of Knowledge (CoK). The Ceramic Seal project is research into the next generation technologies to advance C/S, in particular advancing security and improving efficiency. The Ceramic Seal is a small form factor loop seal with advanced tamper-indication including a frangible seal body, tamper planes, external coatings, and electronic monitoring of the seal body integrity. It improves efficiency through a self-securing wire and in-situ verification with a handheld reader.

Sandia National Laboratories and Savannah River National Laboratory have previously designed and are now fabricating the Ceramic Seal. Currently at the prototype stage, the Ceramic Seal will undergo a series of tests to determine operational readiness, and field tested in a representative verification trial in 2016. Design and development of seal readers are required for operation and testing and included in the current project scope. In this paper, we will describe the Ceramic Seal prototype, the design and development of a handheld standalone reader and an interface to a data management backbone, fabrication of the seals, and planned field testing.

Keywords: loop seal; tamper-indicating device; containment/surveillance; Continuity of Knowledge

1. Introduction

Containment/Surveillance (C/S) measures are critical to any verification regime in order to monitor declared activities, detect undeclared activities, verify the integrity of equipment or items, reduce inspector burden, and to maintain CoK between inspections [1]. Equipment used in C/S can include tags, seals, tamper indicating enclosures, optical surveillance, and radiation detectors, and this equipment currently exists at varying levels of technological sophistication and maturity. Some C/S equipment, such as the metal cup seal, has been fielded for 50 years. The legacy optical surveillance equipment, based on the DCM-14 camera module, is currently undergoing replacement. It is critical that C/S equipment evolve given the continuing advances in the threats posed by and the capabilities of potential adversaries as well as to take advantage of technology advances for continued efficiency and effectiveness gains for inspectors and to reduce burden on operators.

The U.S. National Nuclear Security Administration (NNSA) Office of Defense Nuclear Nonproliferation Research & Development funds the Ceramic Seal [2-7] effort underway at present to address the

Sandia National Laboratories is a multi-program laboratory managed and operated by Sandia Corporation, a wholly owned subsidiary of Lockheed Martin Corporation, for the U.S. Department of Energy's National Nuclear Security Administration under contract DE-AC04-94AL85000. SAND2015-3485C

technical containment requirements for securing access points (loop seals). Loop seals are common equipment used for C/S measures, as reflected by the tens of thousands of metal cup seals deployed globally, in addition to the Electronic Optical Sealing System (EOSS), the electronic Variable Coding Seal System (VACOSS), the passive Cobra seal, and the electronic/wireless Remotely Monitored Sealing Array (RMSA).

The Ceramic Seal has been in development by SNL and SRNL for more than three years and prototypes for operational testing are now in fabrication. The Ceramic Seal can provide an advanced and modernized alternative to the metal cup seal or other single use seals. The metal cup seal, although environmentally robust, inexpensive, and small in size, is operationally burdensome and its integrity is not able to be verified in-situ. The Ceramic Seal addresses issues with the metal cup seal and makes additional security advancements (tamper indication and unique identification) and efficiency improvements (in-situ verification and ease of application). Its innovation is the integration of these advanced capabilities in a small volume, including a self-securing wire feature; multiple levels of tamper indication via a frangible seal body, surface coatings, and active detection of state through low power electronics; electronic identification number verified in-situ through a contact reader, and physical identification via non-reproducible surface features.

2. Ceramic Seal Background

The most critical element of a seal applied in a treaty verification regime is its tamper-indicating features. A loop seal will employ a wire or fiber-optic cable (FOC) threaded through a monitored item's hasp or otherwise secured, and the wire or FOC will terminate within the seal body. In single use seals such as the Ceramic Seal and metal cup seal (versus multiple use seals in which the seal wire can be removed and reattached), confidence must be maintained that the wire is unable to be removed from the seal body once secured without detection and that the seal body has remained intact such that the seal body has not been opened and the wire removed/replaced. Tamper-indicating features on the seal body serve the role of providing this confidence. It is important to note that a vulnerability review (VR) team iteratively worked with the design team to evaluate and guide the tamper-indicating features of the seal.

The properties of the alumina (99.8% Al_2O_3) material used in the Ceramic Seal body meet the requirements of "frangibility" – that is, upon deformation it tends to break into fragments rather than retaining cohesion, yet the material is strong enough to withstand the operational environment. Frangibility is important so that a tamper attempt is prone to result in difficult-to-reassemble fragments.

The Ceramic Seal will be coated with spray coatings developed in partnership with Tetramer Technologies. These exterior fluorescent coatings act as a tamper indicating feature [8-10] as modification/tampering of the seal will be visible under UV illumination. The coatings are transparent to allow Laser Surface Authentication (LSA) for unique physical identification of the seal body.

The Ceramic Seal provides active tamper indication by monitoring both "tamper planes" embedded in the interior of the seal, as well as monitoring connectivity between the cap and base of the seal (to determine if the seal has been opened). The tamper planes are connected to the electronics and if disrupted, i.e., signals cannot pass, software within the electronics records a tamper attempt.

Seal firmware is programmed prior to deployment; however, the Ceramic Seal requires personality programming in-situ, meaning configuration must happen via the RS-232 serial communication vias located on the cap of the seal. Personality programming loads secret keys onto the seal, sets message creation interval, and sets absolute time. The electronics will not be powered until the seal cap and base is connected, so personality programming the seal must happen after it has been closed.

A seal reader (two variations are currently under development and described later in this paper), which will also have the secret keys, will be able to send an authenticated command to the seal (over the serial port), receive the requested message(s), and authenticate them using its copy of the secret key.

The capability of self-securing wire not only improves efficiency but touches upon security as well. The wire ends must securely terminate in the seal body in such a manner that they cannot be easily removed, and must do so in an efficient manner. In the Ceramic Seal design, the wire is routed through the monitored item and into the seal base, where it is secured by a tortuous path. The design team and SNL VR team iterated on several designs before choosing a final design.

The wire itself is important as well, and appropriate commercial candidates have been identified. The current seal prototype does not have the capability to monitor the integrity of the wire using the internal electronics; however, such a capability is anticipated in future research. There are instruments available to externally connect to the wire after deployment and subsequently during verification to determine if the wire has been tampered with.

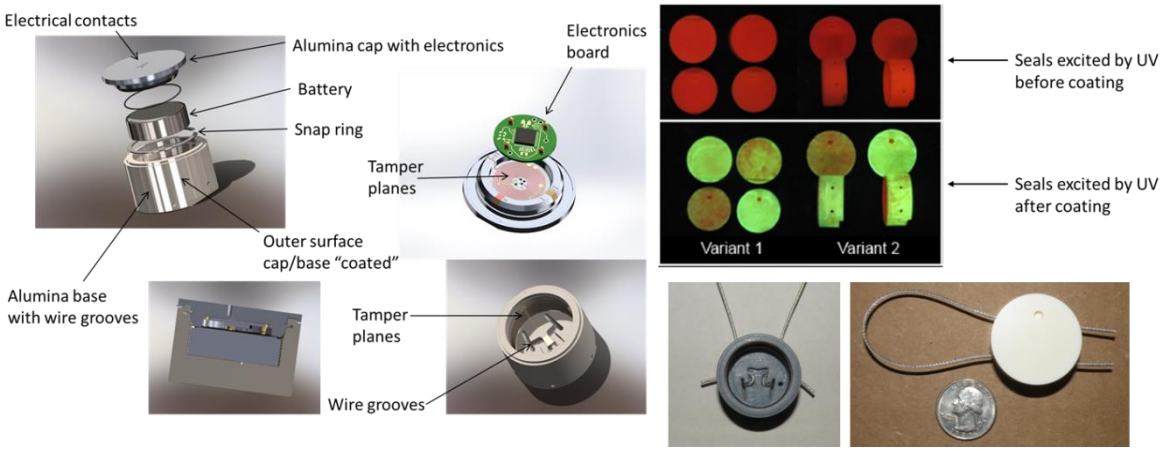

Figure 1: (Left) The Ceramic Seal design features. (Right) Ceramic Seals are shown on top uncoated, with alumina based sol gel doped with terbium coatings on the bottom. Excited by 254 nm UV. Images courtesy Tetramer Technologies.

The Ceramic Seal will operate as follows: the Ceramic Seal wire is looped around the item to be monitored and secured within self-securing grooves in the seal base. The battery is inserted into the seal base, and the seal cap is snapped onto the seal base, secured by a snap ring. Personality programming of the Ceramic seal is then performed, and once that is completed the seal is ready for use. Note: expected seal lifetime under stressed conditions is 12 years. It is expected that the seal would be periodically inspected physically and electronically. An inspector would attach a reader to download state-of-health (SOH) and events. Physical inspection (visual or instrumentation) would reveal deformations in structure or coatings.

3. Fabrication

As described above, the design of the Ceramic Seal is complete, and prototypes of various components of the seal have been fabricated and tested independently. The seal is now undergoing fabrication with the intent of testing complete prototypes in various scenarios. The fabrication has been an iterative optimization process. This section will describe some of the fabrication issues with the seal and our current progress.

The fabrication of the Ceramic Seal consists of the following steps:

- Fabricate ceramic caps and bases
- Brazing of metal pins into cap for electrical contact
- Application of exterior, tamper-indicating coatings
- Application of tamper planes onto seal cap
- Application of dielectric onto tamper planes
- Application of electrical patterning for circuit board onto dielectric layer

- Attachment of circuit board to cap
- Metallization of seal base interior for power contacts

The ceramic caps and bases are machined and fired by Astromet. Brazing of metal pins into pre-determined slots on the caps for the electrical contacts occurs at SNL. Brazing is a joining process whereby a filler metal is heated above 450ºC and distributed between two or more close-fitting parts by capillary action. The caps with brazed pins and bases are sent to SRNL for application of the exterior, tamper-indicating coatings and characterization using Laser Surface Authentication. (Figure 2).

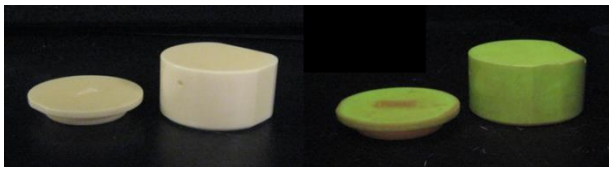

Figure 2: Tamper-indicating coatings illuminated with 254 nm UV in ambient light.

Tamper planes have been challenging due to the fine lines, narrow line spacing, and small size of the seal. The team originally pursued direct write technology for application of tamper planes as the parameters (line width and spacing) could be easily adjusted. However, direct write was ultimately unsuccessful due to the geometry of the seal and substrate porosity. The team instead pursued physical vapor deposition which is more suited for manufacturing, but requires deposition masks. These masks are fixed and thus the line width and features need to be known in advance. The team began by developing a laser cut mask at SNL, which is a simple and fast process. Unfortunately, the laser cut masks produced a melted slag on the pattern edges of the mask itself. This prevented uniform deposition of the metal onto the alumina cap, and was found to be unacceptable. The team next pursued a photoetch-processed mask made of Kovar created by Photo Stencil. The photoetch mask uses a chemical etching process and produced a much better result in terms of uniformity.

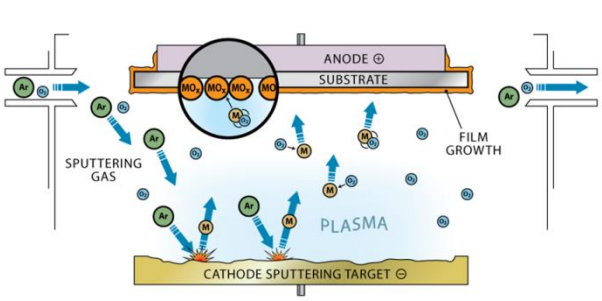

Figure 3: Physical vapor deposition process – requires physical mask to define pattern.

Figure 4: Photoetched Kovar masks. (Left and center) tamper planes use two separate spiral patterned masks. (Right) mask for circuit board electrical connections.

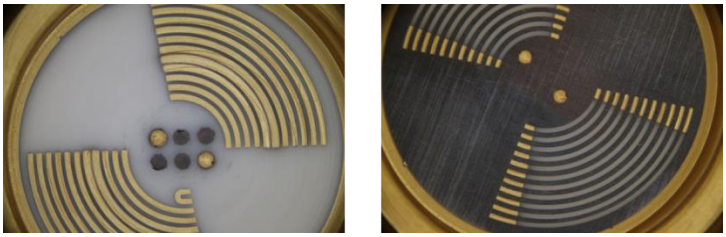

Figure 5: First and second half tamper planes.

Once the tamper planes are deposited, a dielectric coating is applied over the pattern. Next the patterning for the electrical connections is deposited while another photoetch mask is in place. The circuit board is attached to the cap and aligned to the proper electrical connections.

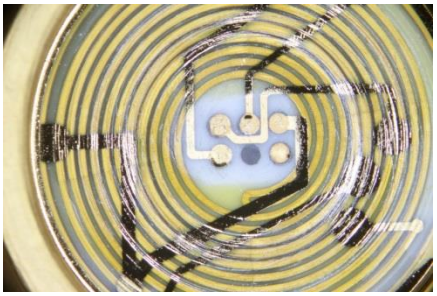

Figure 6: Electrical connection pattern.

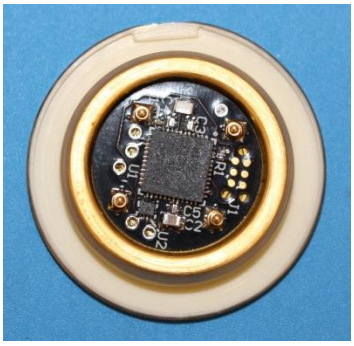

Figure 7: Completed seal cap with circuit board attached.

For the base, a fixture is used to prevent metallization of all except the interior section of the base. See Figure 8.

Figure 8: Seal base.

We have completed fabrication of a prototype and optimized the manufacturing process. We will continue to fabricate additional prototypes using this process.

4. Reader Development

The Ceramic Seal is read in-situ via a contact reader and the pins located on the seal cap. SRNL is developing a handheld, standalone reader and SNL is developing an interface to a data management system that is typically responsible for multiple devices.

The standalone reader, developed by SRNL, uses an Archer 2 handheld computer from Juniper Systems with a custom seal module. The Archer 2 is designed for industrial use, is shock-resistant, waterproof, has a high visibility screen for outdoor applications, and can operate up to 20 hours on one charge. Rather than modifying the rugged Archer 2 case, it was decided to design a separate seal module to connect to the Ceramic Seal electrical contacts. This module will communicate with the Archer 2 via USB. To use the seal reader, the seal would be slid into the seal module. The seal module is designed to automatically capture the seal and make electrical contact with the seal once the seal is fully inserted into the module. The module has internal electronics that alert the Archer 2 that a seal is connected. The Archer 2 then processes the data from the seal. If the state-of-health of the seal is “healthy” and no tamper attempts are registered, the seal module will indicate that the inspection is complete. If the seal is “unhealthy”, a tamper attempt is detected, or if there is an error in communicating with the module, the Archer 2 will direct the seal module to indicate to the inspector that further information is needed. The inspector will then activate the Archer 2 to determine the path forward based on the information processed by the reader. Once the seal interrogation is complete, a lever on the seal module is pushed to eject the seal from the module.

SRNL has completed a first generation reader (tested on a development board) and is currently implementing authentication and key management.

Figure 9: SRNL handheld standalone reader. (Left) Reader with seal (rapid prototype) inserted in module. (Right) Seal partially inserted in module.

The SNL-developed tablet interface reader is a Nexus 10 tablet with a USB to serial connection to the Ceramic Seal. Once physically connected to the seal, the tablet downloads state-of-health and event messages, and passes the received data via Wi-Fi to a data management system (DMS). The DMS may be responsible for multiple sensors/devices. SNL has completed a first generation reader with testing performed on a development board.

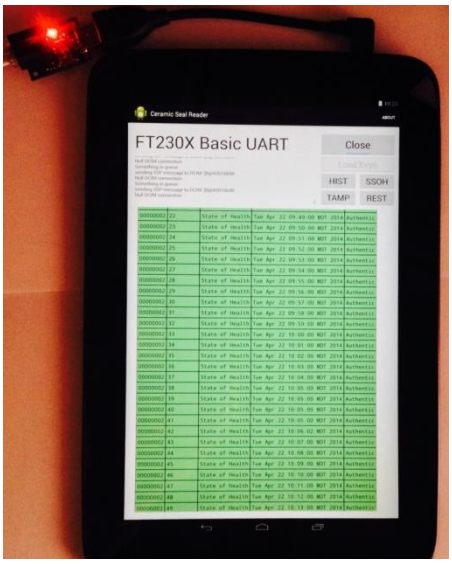

Figure 10: Tablet interface reader. Messages are passed to data management system.

5. Testing

Once a sufficient number of seals have been fabricated, they will be tested throughout 2015 and 2016 for operational readiness. In 2015, the Ceramic Seal will undergo functional and performance testing at SRNL, known as an “honest game assessment”. This assessment will be performed by independent personnel, where they will analyze functionality and user-friendliness, as well as estimating false positive and false negative errors.

The seal will also be attached to a variety of items in a bunker at SNL. Personnel will test ease of attachment to items, ease of personality programming of the seal, ability of seal to accurately record opening, ability of reader to make reliable contact with seal (under real-world conditions), receipt of

state-of-health and messages on the data management system, battery life, and other suitable tests. The seals will be physically inspected as well.

In 2016, seals will be deployed in a realistic field verification trial. Extensive testing will be performed, including tests performed previously in 2015, and also physical inspection with a coatings reader. It is expected that the tests in 2016 will be applied against a defined set of CONOPs, and the testing will integrate technologies from both SNL and SRNL.

6. Next Steps

The next steps in the project are to test both the SRNL-developed handheld standalone reader and the SNL-developed tablet interface reader with the complete Ceramic Seal prototype and make adjustments as necessary. The team will complete fabrication of multiple Ceramic Seal prototypes and begin both the honest game assessment at SRNL and the field testing at the SNL bunker. Recommendations will be developed for any improvements or modifications to the seals or readers.

7. Acknowledgements

We thank the Office of Defense Nuclear Nonproliferation Research and Development (DNN R&D) for funding this effort.

8. References

[1] Texas A&M Nuclear Safeguards Education Portal. Available: http://nsspi.tamu.edu/nsep/courses/containment-and-surveillance/introduction/what-is-cs-and-why-do-we-need-it-%28cont%29
[3] H.A. Smartt et al., “Intrinsically Tamper Indicating Ceramic Seal (ITICS),” in *Proc. Institute Nuclear Materials Management*, Palm Desert, CA, 2011.
[4] H.A. Smartt et al., “First Prototype of the Intrinsically Tamper Indicating Ceramic Seal,” in *Proc. Institute Nuclear Materials Management*, Orlando, FL, 2012.
[5] D. Krementz et al., “Development of a Ceramic Tamper Indicating Seal: SRNL Contributions,” SRNL, Aiken, SC, 2013.
[6] D. Krementz and M.J. Martinez-Rodriguez, “Ceramic Tamper Indicating Seal (Ceramic Seal) Final Report,” SRNL, Aiken, SC, 2013.
[7] H.A. Smartt et al., “Current Research on Containment Technologies for Verification Activities: Advanced Tools for Maintaining Continuity of Knowledge,” in *Proc. Symposium on International Safeguards: Linking Strategy, Implementation and People*, Vienna, Austria, 2014.
[8] A.E. Mendez-Torres et al., “Synthesis and Characterization of Smart Functional Coatings by Chemical Solution Deposition Methods,” in *Proc. Institute Nuclear Materials Management*, Palm Desert, CA, 2011.
[9] R.M. Krishna et al., “Characterization of Transparent Conducting Oxide Thin Films Deposited on Ceramic Substrates,” *Materials Letters*, vol. 65, no. 1, 2011.
[10] M. Shaughnessy et al., “Photoluminescence Measurement Characterization Report,” Tetramer Technologies, Pendleton, SC, 2013.

Enhanced Containment and Surveillance System: Active Container Tracking System (ACTS)

C. L. Britton, S. S. Frank, M. J. Kuhn, C. A. Pickett, B. J. Stinson, J. R. Younkin, R. Willems

Oak Ridge National Laboratory
Oak Ridge, TN 37831
E-mail: pickettca@ornl.gov

D. Krementz
Savannah River National Laboratory
Aiken, SC 29808-0001

Y. Y. Liu, B. Craig
Argonne National Laboratory
Lemont, IL 60439

E. Farquhar
Pacific Northwest National Laboratory
Richland, WA 99354

J. M. Shuler
DOE Packaging Certification Program
U. S. Department of Energy
Washington, DC

Abstract:

The Active Container Tracking System (ACTS) vision is to provide a secure container tag that can be used to optimize chain-of-custody monitoring for packaged nuclear materials as they are being stored, processed, and transported. ACTS is an active device that utilizes an almost-universal core platform that can be appropriately configured to provide the necessary data acquisition, data logging, and communications functions needed for 21st century material accountancy, monitoring, and tracking applications. The core design supports active monitoring of containment, movement and location and provides secure data transmission via selectable communication methods that can be utilized throughout the world. This core architecture enables appropriately designed modules to be easily interfaced to the basic system, thus providing an integration path for current and new technologies. The ACTS contains a built-in set of sensors but also supports an expansion bus for up to 6 additional communications, tracking, or sensing modules that may enhance monitoring and tracking of particular containers for specific applications. ACTS stores events in memory, communicates activity to Argonne's ARG-US TransPort tracking and information server, and provides options for data encryption and authentication. Although the core design philosophy will be container agnostic, the initial goal is to track and seal a 9980 packaging assembly. Partners for this system are Oak Ridge National laboratory (ORNL), Argonne National Laboratory (ANL), Savannah River National Laboratory, (SRNL), and commercialization partner The Aquila Group.

Keywords: tracking, authentication, sensing

1. Introduction

There is a continuing need for secure container tracking/reporting systems that can report location, intrusions, information on the status of contents, and any other anomalous data events. In addition, there is a need for long dwell time systems that require little or no battery maintenance. We present a new system under development that is designed to be a platform that can be configured for many applications in the area of asset tracking, and whose configuration provides support for almost any external device to be added to the system.

2. Architecture

The ACTS concept is being developed as a secure universal platform, compatible with ARG-US [1], for active monitoring of device containment and device position that can report and record status of user determined attributes via selectable communication methods. In order to achieve this, we have developed a general-purpose motherboard that contains captive sensors which will be used according to the application, and high-current communications or sensing platforms which are determined by the application, but are not currently an integral part of the ACTS platform.

The overall architecture and general use case is presented in Figure 1. The platform contains several built-in sensors in its core, but can be expanded through the use of a Serial Peripheral interface SPI bus for other type of communications, tracking, or sensing modules. This approach has several advantages, most notably expandability for future applications and flexibility to support only the functions dictated by the application. There are two main batteries in operation. One is sized for the basic motherboard and its sensors, and does not supply power to any of the external (application-required) peripherals. This allows the motherboard to act almost independently of the peripherals concerning power drain. The second battery is sized for the peripherals and their use case. The peripherals are expected to use the majority of the power in the module since they will typically be high-current communications and location electronics.

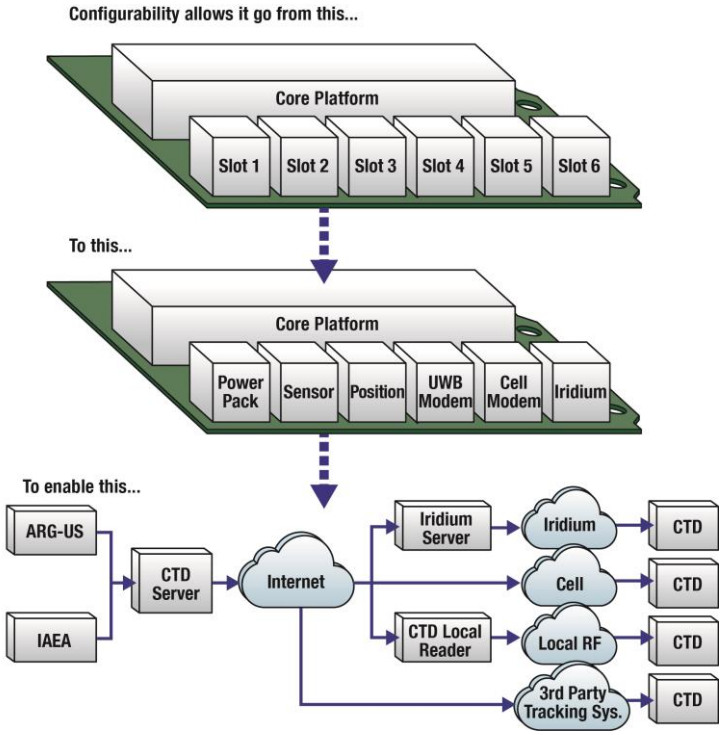

Figure 1. System architecture and use case.

The system block diagram is shown in Figure 2. The motherboard consists of a core microcontroller (Texas Instruments MSP430) and four sensor peripherals built in to the board which include an ambient light sensor, temperature and humidity measurement, barometric pressure, and an inertial

measurement/shock/magnetometer (IMU). The integrated peripherals are configured through an I2C bus interface by the MSP430. The IMU and light sensor are also connected as interrupts to the MSP430 allowing them to awaken the system by shock or ambient light change. In addition, there is a switch interface "farm" of connectors that allows the processor to read normally-open or normally-closed switches commonly used for intrusion detection. These are hardwired sensors that are plugged into the motherboard and are usually mounted on the box in which the motherboard is placed. A photograph of the system is shown in Fig. 3.

The SPI expansion bus uses the MSP430 in a master configuration with the expansion peripherals as slaves. Connectivity is provided by a 16-pin, 0.5-mm pitch ribbon connector that includes SPI signals

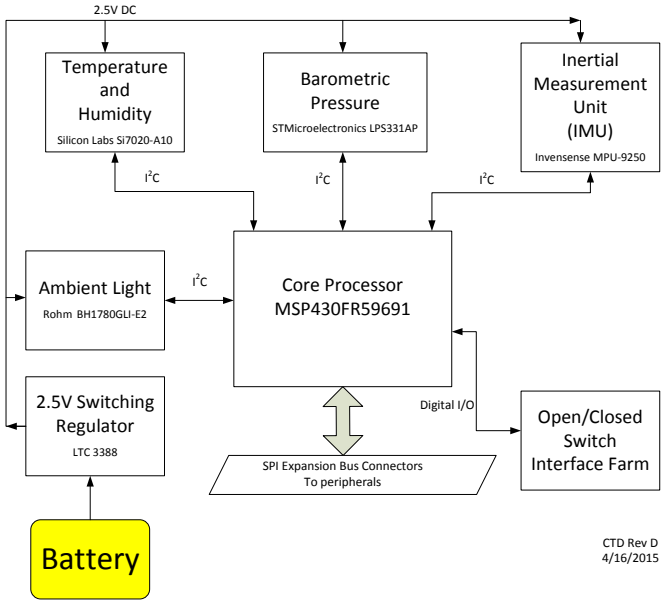

Figure 2. Motherboard block diagram.

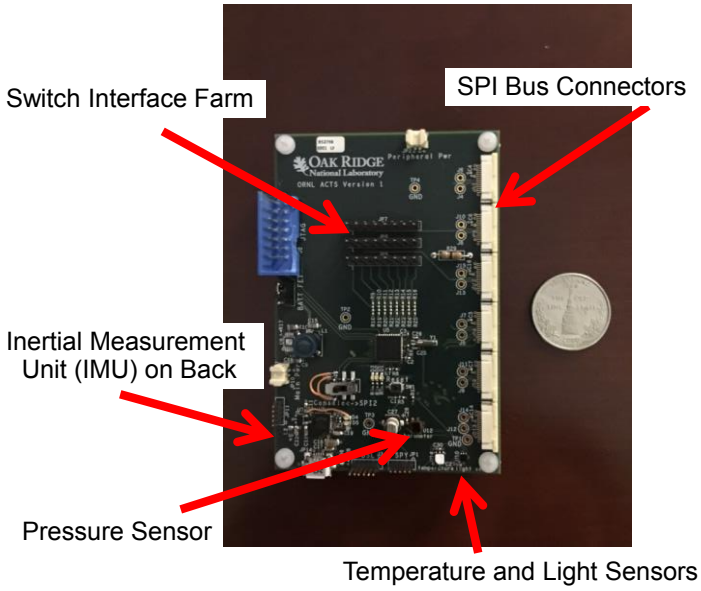

Figure 3. Motherboard photograph

plus the peripheral battery leads. We will be developing a standard interface architecture that can assist a user in connecting their non-SPI peripheral to the system. This will allow almost any peripheral to be able to use the ACTS architecture.

3. Requirements

Present system requirements cover the areas listed below.

Secure Communications – This system will be able to utilize modules on the SPI expansion bus which include GPS tracking, Iridium communications, GSM communications, and any other type of low- or high-power devices that can be added to the bus. There also is capability to provide AES encryption for communications.

Power – The system contains two different battery configurations. One is a long-term battery that is sized to power only the basic motherboard. This is presently a lithium thionyl chloride battery which can power the board for weeks or possibly up to months and is a C-sized cell. The second battery is intended to be sized to the specific application for the user's required board configuration, and operates only the peripherals on the SPI bus. This partitioning of battery usage allows the user to size the higher-power-drain peripheral battery for applications independent of the main controller battery.

Data Logging – Some data events will need to be stored until a clear communications channel is available. There is non-volatile storage set aside in the MSP430 for data logging. Events will be stored and delivered on a regular basis as communications channels allow. Also, state-of-health, system integrity, loss-of-power, and location will be logged.

Figure 5. Storage pad at URENCO USA.

Tamper Indicating Packaging – All pertinent electronics will be encapsulated into a tamper indicating enclosure that provides both passive and active features of tamper detection.

These requirements will allow potential applications such as tagging and tracking containers over a large area, such as those shown in Fig. 4. One or more appropriate communications links will be needed for this application, as well as data and event storage on board the tag.

4. Server Interface

Through one of its communications modules, the ACTS can reach the inter-web to transmit activity to the Argonne ARG-US TransPort tracking and information server, The Argonne ARG-US TransPort software has a web-based user interface (shown in Fig. 5) which incorporates Geographical Information System (GIS) elements with “trail-of-bread-crumbs” overlay as well as overview, summary, and tag event history tables, a current tag status pane and a tag sensor report generator. A database exists behind the user interface to archive the messages sent by ACTS. An ACTS message received by the ARG-US TransPort server is parsed and inserted automatically into the database. The message includes three fields, including the sensor values.

Figure 5. The Argonne ARG-US TransPort software has a web-based user interface incorporating Geographical Information System (GIS) elements as well as overview, summary, and tag event history tables, a current tag status pane and a tag sensor report generator.

5. Conclusion

We have presented a new system currently being developed for active container tracking. This system is configurable for a large number of secure asset-tracking applications, and contains electronic interfaces to enable handling a variety of digital and analog sensors or communications devices.

Reference

[1] http://www.anl.gov/technology/downloads/arg-us-rfid-system-managing-high-risk-materials

Enhancement of Safeguards Efficiency for Spent Fuel in Canada

Henry Gao, Karen Owen-Whitred

Canadian Nuclear Safety Commission

Ottawa, ON K1P 5S9, Canada

E-mail: henry.gao@cnsc-ccsn.gc.ca, Karen.Owen-Whitred@cnsc-ccsn.gc.ca

Abstract:

It has been recognized by the IAEA and CNSC that safeguarding spent fuel in Canada continues to be a resource challenge. While efficiencies have been increased through the implementation of Integrated Safeguards in Canada, further improvements are required in order to optimize the application of safeguards to spent fuel. There are currently over 2000 Dry Storage Containers (DSCs) containing discharged fuel bundles at Canadian spent fuel waste management facilities and more are added weekly. The current IAEA containment measure requires two types of seals to be applied to all DSCs in storage – metal seals and COBRA seals. The application and subsequent routine verification of these seals consume a large amount of IAEA resources which will continue to increase, making this approach unsustainable in the longer term.

In order to enhance safeguards efficiency for spent fuel in Canada, the CNSC has worked with the IAEA and facility operators to develop new approaches. This paper will discuss the development and implementation of these new approaches through trilateral cooperation between the IAEA, CNSC and facility operators, including: the establishment of laydown areas to allow IAEA inspectors to seal more DSCs per visit; and, the deployment of Laser Mapping for Containment Verification (LMCV) as a future replacement for metal seals on DSCs.

Keywords: efficiency; spent fuel; cooperation; laydown area; LMCV

1. Introduction

Canada is one of the States with a large nuclear programme and a full natural uranium fuel cycle, including mining, conversion, fuel fabrication, power reactor and spent fuel management. In Canada, the Canadian Nuclear Safety Commission (CNSC) is the federal agency mandated under the *Nuclear Safety and Control Act* with regulating the use of nuclear energy and materials to protect health, safety, security and the environment and to implement Canada's international commitments on the peaceful use of nuclear energy; and to disseminate objective scientific, technical and regulatory information to the public. In this capacity, the CNSC is the State System of Accounting for and Control of nuclear material in Canada.

As the State authority for safeguards, the CNSC collaborates with the International Atomic Energy Agency (IAEA) to implement and strengthen safeguards, develop safeguards concepts and approaches, improve and optimize safeguards measures and approaches, and support the research and development of safeguards equipment. Canada strongly supports the State-Level concept and has implemented a State-Level Integrated Safeguards Approach since first obtaining the broader safeguards conclusion in 2005. While efficiencies have been realized in Canada through the implementation of integrated safeguards, it has been recognized by the CNSC and the IAEA that further improvements are required in some areas, such as spent fuel. This paper will first describe spent fuel management in Canada, then discuss the challenge of safeguarding the spent fuel at multi-unit stations. It will then turn to the development of new approaches to optimize safeguards measures through trilateral cooperation between the IAEA, CNSC and facility operators, specifically: the establishment of laydown areas to allow IAEA inspectors to seal more Dry Storage Containers (DSCs) per visit; and, the deployment of Laser Mapping for Containment Verification (LMCV) as a potential future replacement for metal seals on DSCs.

2. Spent Fuel and its Storage in Canada

Canada's inventory of spent nuclear fuel comes mostly from the operation of nuclear power plants. Currently there are four power stations in operation in Canada, including three multi-unit and one single-unit CANDU nuclear generating stations: Bruce Nuclear Generating Station, Darlington Nuclear Generating Station (DNGS), Pickering Nuclear Generating Station (PNGS) and the single unit Point Lepreau Nuclear Generating Station (PLNGS), as listed in Table 1. DNGS, PNGS and the three waste management facilities belong to Ontario Power Generation (OPG).

Power Station	Associated waste management facility	Number of Units
Bruce Nuclear Generating Stations	Western Waste Management Facility (WWMF)	8 units
Darlington Nuclear Generating Station (DNGS)	Darlington Waste Management Facility (DWMF)	4 units
Pickering Nuclear Generating Station (PNGS)	Pickering Waste Management Facility (PWMF)	6 units
Point Lepreau Nuclear Generating Station (PLNGS)	Point Lepreau Nuclear Generating Station	1 unit
Gentilly- 2 Nuclear Generating Station (G2NGS)	Gentilly- 2 Nuclear Generating Station	1 unit; the reactor has been shut down since 2014.

Table 1: Canadian nuclear generating stations and associated waste management facilities.

It is estimated that about 5000 fuel bundles per power reactor are used and discharged to the storage pools each year based on normal reactor operation. Since the 1960s, Canada's nuclear power reactors have used over 2.5 million fuel bundles [1]. The remainder of the total used nuclear fuel – which accounts for approximately 2% of the total – comes from prototype reactors (used to test full-power reactor designs) and research reactors.

2.1 Wet storage

Spent nuclear fuel from the operation of nuclear power plants is kept onsite in the power station and in associated waste management facilities. This onsite storage is interim storage which consists of two phases: wet storage and dry storage. In the wet storage, the spent fuel bundles are stored for seven to ten years in storage bays (pools of water) within the power station, which provide cooling and shielding against radiation.

2.2 Dry storage

After seven to ten years in wet storage, the spent fuel will be transferred to medium term dry storage. There are three main types of dry storage units used in Canada:

- Concrete canisters;
- Modular Air-cooled Storage (MACSTOR) units; and
- Dry storage containers.

Concrete canisters, or silos, were developed in the 1970s by the Atomic Energy of Canada Limited (AECL) at Whiteshell Laboratories, to demonstrate that dry storage for spent reactor fuel was a feasible alternative to underwater storage. Silos are now used to store the spent fuel from PLNGS , as shown in Figure 1, as well as from the Canadian Nuclear Laboratories' prototype reactors, including those at Chalk River Laboratories, Whiteshell Laboratories, Gentilly-1 and Douglas Point. Each silo can hold between 325 and 600 bundles, and is built on reinforced concrete foundations.

The **MACSTOR** units, as shown in Figure 2, also developed by AECL, are similar to silos, but much larger. Each MACSTOR unit can store more than 10,000 bundles of spent fuel. MACSTOR units are currently installed at the Gentilly-2 Nuclear Generating Station.

Fig. 1: Concrete silos at the Point Lepreau Generating Station, left [1].

Fig. 2: MACSTOR units at the Gentilly-2 Nuclear Generating Station, right [1].

The **dry storage container** was developed by OPG and is made of reinforced concrete encased in interior and exterior shells made of carbon steel. The DSCs are currently used to store the spent nuclear

fuel from the Darlington, Pickering and Bruce nuclear power plants at their associated waste management facilities.

The DSC, as shown in Figure 3, is a rectangular cylindrical container made of a double carbon steel shell filled with reinforced concrete. Each container unit is designed to hold about 400 fuel bundles and weighs approximately 60 tonnes when empty and 70 tonnes when loaded [1]. The DSC stores irradiated fuel containing plutonium (Pu) and depleted uranium (DU) in CANDU fuel bundles. It is estimated that each DSC contains thousands of kilogram of DU and more than one significant quantity of Pu.

Fig. 3: OPG dry storage containers [1]

The DSC canister closure system consists of a lid, guide pins and a closure weld around the perimeter of the canister. The DSC lid is welded to the top flange of the DSC body by an automatic process.

3. Safeguards approach for DSC of spent fuel and its challenges

As described above, Canada's inventory of spent nuclear fuel comes mostly from the operation of nuclear power plants. As multi-unit power reactors are dominant in terms of spent fuel production, therefore, the CNSC focuses on the improvement of safeguarding the spent fuel from multi-unit reactors. Under the current State-level integrated safeguards approach, spent fuel is always under IAEA safeguards measures, both at the power station and associated waste management facility. Details of these measures include the following:

Power Station

- Twenty-four hour surveillance with the IAEA unattended monitoring system to monitor the bundle discharging from a reactor core;
- Spent fuel bundle counter to verify the discharged bundle transfer to wet storage;
- Surveillance of wet storage and physical inventory verification (PIV);

- Provision of facility's advance spent fuel transfer activities, including: operational plan, location, time, status of loading the DSC; update whenever the plans change;
- Near-real time inventory change reporting to the CNSC and IAEA; and
- Surveillance of spent fuel transfer and Unannounced Inspection (UI) (since March 1, 2007).

Waste Management Facility (WMF)

The DSC is transferred into the processing workshop at the WMF where the lid is welded to the top flange of the DSC body by an automatic process. The weld is a full ring of the DSC body upper plate. Safeguards measures of the spent fuel at WMF include:

- Provision of the facility's advance (annually, weekly) spent fuel transfer operational activities, including: operational plan, location, time, status of loading; update whenever the plans change;
- Near-real time inventory change reporting to the CNSC and IAEA, and PIV;
- Surveillance of the DSC processing in the workshop;
- A radiation profile as the signature of the spent fuel in the DSC; and
- Containment (i.e., seals) of the DSC with spent fuel in storage buildings.

Further, safeguards measures require that a radiation profiling must be taken and containment (sealing) must be applied before the DSC can be moved out of the processing workshop, which is under IAEA surveillance, for storage.

It can be seen that the current safeguards measures for spent fuel are sufficient at power plants and WMFs, with high confidence. However, challenges have also been recognized by the CNSC, the IAEA and facility operators. The first challenge comes from the limited space of the workshop which only holds up to about ten (e.g., nine at PWMF; eleven at DWMF) loaded DSCs for processing and limited IAEA resources. WMF operation requires that the DSC should be moved out of the workshop once the lid welding and painting are completed to free the space for receiving other DSCs. As a consequence, the IAEA inspector is required to travel frequently to the three WMFs to seal DSCs. Due to the fact that the number of DSCs that are ready to be sealed is small per each visit, this results in an insufficient use of IAEA resources.

The second challenge comes from the containment measure of the DSCs in storage. There are currently over 2000 DSCs containing discharged fuel bundles at WMFs and more are added weekly. The current IAEA containment measure requires two types of seals to be applied to all DSCs in storage – metal seals and optical fibre seals. The application and subsequent routine verification of these seals consume a large amount of IAEA resources, which will continue to increase, making this approach unsustainable in the longer term. As a result of these two challenges, the CNSC started consultations with the IAEA and facility operators to improve safeguards measures and approaches for spent fuel.

4. Improvement of safeguards efficiency at dry storage

Canada has a long history of collaborating with the IAEA on the development and implementation of safeguards measures. Existing mechanisms for discussing safeguards matters include the bi-annual Canada-Agency Safeguards Implementation Consultation (CASIC), Working Level Meetings (WLMs), trilateral meetings between the CNSC, IAEA and operators, and bilateral meetings between the CNSC and the IAEA or facility operators, in addition to routine communication via letter, email or by telephone. Depending on the nature and impact of the matter, the appropriate mechanism will be used to facilitate

the resolving of safeguards issues, improving safeguards measures, and developing new approaches. It can be seen from the following sections that all mechanisms have been used in the potential deployment of LMCV equipment while less tools in the establishment of the laydown areas at WMFs.

4.1 Laydown area

In order to resolve the inefficiency associated with sealing processed DSCs, the CNSC started discussion with the IAEA and Western WMF operators associated with Bruce Power in April 2010, followed by a bilateral WLM between the IAEA and the CNSC in May 2010.

The Western operator proposed to move partially processed DSCs to a “laydown area” in their storage building on an as-needed basis in the event of high DSC congestion in its processing workshop. The laydown area would be built with IAEA surveillance and allows the IAEA inspector to perform sealing and gamma profiling of more DSCs in each trip, thus avoiding a possible interruption in processing or transfer of DSCs and enhancing safeguards efficiency.

The laydown area approach was further discussed at an IAEA-CNSC-CANDU facilities trilateral meeting in 2012. Considering the benefit of the laydown area at WWMF that reduces DSC congestion in the processing area and allows more DSCs to be sealed at one time, both DWMF and PWMF expressed interest in establishing such a laydown area. The cost of the laydown area setting would be shared between the IAEA and Canadian facilities: the operator will provide support for installing the surveillance camera cable and the mounts in its storage building while the IAEA will supply the cable and the camera mounts, as well as install the cameras on the mounts and make the connections at the camera and surveillance cabinet ends. In collaborating with the IAEA and the CNSC, PWMF established its laydown area in October 2013 while DWMF will be establishing such an area in 2015.

4.2 LMCV – a longer term approach

As discussed in Section 3, applying and maintaining seals is identified as a challenge for the DSCs in dry storage buildings over the longer term. The CNSC raised this issue at CASIC in 2010 and consulted with the IAEA on the review of the application of Containment/Surveillance measures to material in DSCs at Canadian waste management facilities. In response to this consultation, the IAEA proposed the use of a LMCV on DSC welds as a potential replacement for the optical fibre and metal seals that are currently applied, as a longer term approach**.**

As shown in Figure 4, the LMCV system developed by JRC Italy, uses a laser triangulation technique to perform an accurate mapping of closure welds on containers of nuclear materials [2]. According to the IAEA proposed draft procedure [2], the application of LMCV is that once a container has been loaded with nuclear material, its lid closed and welded, a LMCV scan of the closure weld would be performed. The weld scan is used to derive a unique signature for a specific container, which remains valid as long as the weld has not been modified, i.e., the container has not been opened. For verification purposes, the same weld needs to be scanned by the LMCV equipment again. The reference and verification scans are then automatically compared by the LMCV software and the comparison result, “*Match*” or “*Match failed*”, is displayed on the LCD screen of the LMCV scanner. “*Match failed*” indicates significant differences between reference and verification scans and may indicate a tampering attempt. The detailed technical description will not be given here; instead, this paper will focus on the proposed application of LMCV at Canadian facilities.

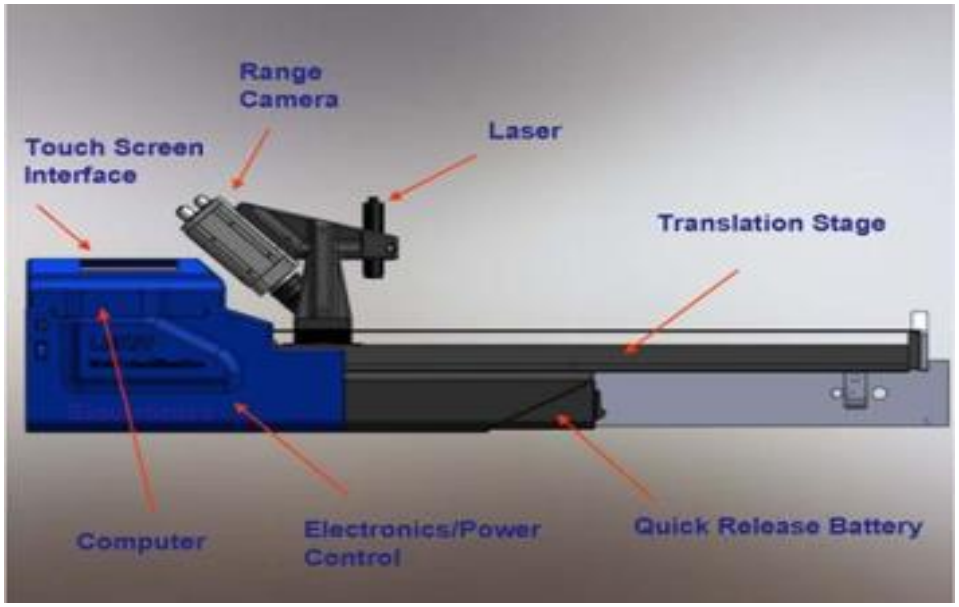

Fig. 4: the LMCV unit and its main components [2].

It was agreed by the CNSC and the IAEA that a field trial would be necessary to evaluate this technique. With agreement by all parties and support by PWMF operators, the first field trial was performed at PWMF in December 2010 attended by JRC and IAEA representatives. Further field trials were performed at PWMF, DWMF and WWMF during 2012 with support by these waste management facilities.

In addition to these field trials, extensive consultation has taken place between the CNSC, IAEA and facility operators on the LMCV since 2010. A few highlights are the following:

Facility feedback from the field trials was positive and the operators indicated that the equipment performed scans efficiently and that the equipment appeared easy to use. The IAEA has also indicated that the field trials at all three dry storages were successful.

In 2013, the IAEA informed during a trilateral meeting that the use of the LMCV was approved by the Agency in December 2012 and has been proposed as a replacement for one of the two components of the current dual containment approach for DSCs, namely, metal seal. The IAEA also proposed that the operators, under IAEA surveillance, could use the LMCV tool to take the initial reference signature. The potential joint use of the LMCV device with the operators or State authority was further discussed at CASIC in 2013. The Agency noted that the first LMCV equipment should be ready by 2014 and all parties agreed on implementation of the LMCV on a facility by facility basis. The IAEA proposal was discussed by the three waste management facility operators; recognizing the potential benefit, they welcome and support the application of the LMCV and are willing to learn and use the LMCV equipment to take the initial reference scan on the DSCs, as proposed by the IAEA.

It is expected that the application of LMCV will be implemented at WWMF in 2015. The CNSC is working closely with the IAEA and facility operators on the implementation of the LMCV and look forward to increasing safeguards efficiency with this new approach at the three waste management facilities. Further discussion between the CNSC, IAEA and facility operators will take place with the implementation of the LMCV, to share operators' operational experience, and optimize the application of LMCV at Canadian waste facilities.

5. Conclusion

In summary, this paper describes the management of spent fuel in Canada and discusses safeguards challenges for the spent fuel in dry storage and the improvement of safeguards efficiency. It can be concluded that (1) the establishment of laydown areas at two WMFs so far has enhanced safeguards efficiency; (2) extensive work has been done regarding the deployment of Laser Mapping for Containment Verification equipment as a future replacement for metal seals on DSCs; (3) collaboration between the CNSC, IAEA and facility operators is essential to develop new safeguards approaches, optimize safeguards measures and enhance safeguards efficiency. The CNSC will continue to collaborate with the IAEA and facility operators for the deployment of the LMCV tool at Canadian WMFs to improve safeguards measures and approaches for spent fuel, and to ensure safeguards is implemented sufficiently and effectively in Canada.

6. Acknowledgements

The authors would like to thank the IAEA inspectors and Western waste facility operators for useful discussions to finalize this paper.

7. References

[1] Radioactive waste, http://www.nuclearsafety.gc.ca/eng/waste/high-level-waste/index.cfm.

[2] IAEA proposed draft procedure of LMCV application – an internal document.

Development of structural materials identification approach based on iris recognition algorithms

Sednev D., Sharavina S.

National Research Tomsk Polytechnic University
Student, Department of Physical and Power Plants
634050, Russia, Tomsk, Lenin Avenue, 30
E-mail: sednev@tpu.ru, sharavina@tpu.ru

Abstract:

In order of ongoing joint R&D programme of TPU and "Mining and Chemical combine" on novel technologies, welds recognition system were proposed as improvement for account and control system. Spent nuclear fuel casks and containers with radioactive or nuclear materials were considered as possible objects for technology implementation. The objective of preliminary study was to find the most suitable characteristics for welds recognition system.

Authors decided to choose have chosen biometrical recognition systems as parental technology for current research due to the fact that mentioned technology can easily identify or recognize patterns of one kind or another samples. The paper observes and theoretically justifies possibilities of relevant algorithms implementation in order to increase accounting units identification accuracy and effectiveness with automated technique for casks welds identification task.

All major stages of iris recognition procedure were analyzed and transferred to weld recognition approach with the most appropriate technique: for the searching and selection of region of interest is linear Hough transform for detecting welds boundaries. Further to correct all uncertainties such as varying imaging distance, rotation of the camera, sample tilt the image registry method was chosen. Extraction template information and further encoding were performed by Log-Gabor filter, as this filter could make functional dependence between image intensity and position and convert this data into binary code for the later data comparison with application of weighted Euclidean distance technique.

Performed research could help to release described methods and algorithms in developing an open-source weld templates recognition system in the field of accounting and control of nuclear materials. In addition to that research contains proposed procedures and organizational issues for practical tests of intended technique.

Keywords: biometry, iris recognition, nuclear materials, casks

1. Introduction

Accounting and control system of nuclear materials, nuclear wastes and spent fuel requires implementation of safety measures through special organizational methods. One of the verification procedures is nuclear material localization during transporting and storage process. In order to maintain non-proliferation regime and prevent unauthorized access to nuclear materials, it is located in boxes, vaults, casks in material balance area. Identification of nuclear materials is essential part of accounting process in material balance area.

Both object recognition and matching are vital for all operation processes including displacing and transport. Both visual and automatic verification procedures are used in accounting process. Visual methods based on observations of identification marks while automatic verification use technical instruments for searching and matching marks. Decreasing of human factor influence is one of the

main advantages of automated system that makes these systems significantly robust. On the other hand those marks could be either forged, defected or falsified that in its turn causes incorrect signal.

2. Method selecting and substantiation

Identification means comparison of two samples – original stored in data base and identified one from input data – for decision making. Identifier could be either an assigned parameter or inherent one. For instance biometrical parameter is one of the most widespread examples of inherent properties used for identification. Biometry uses natural characteristics of human body when needed to recognize person identity. Nevertheless both types could represent statistical parameters which are the same in nature so this feature could be used in case of applying biometrical statistical algorithms not only for human marks identification. While identification samples have common visual data the result compared with original formula it could be assumed that there are the same or at least similar recognition and analysis approaches that do not pose restrictions on method choosing.

This paper explicates using algorithms based on iris identification adapted for casks weld identification in order to increase accuracy and efficiency. Choice of biometric technique is determined by a range of different factors. Pattern in iris recognition methods is similar to weld in appearance unlike to other identification methods. Both patterns have fiber-like areas needed for comparison.

Iris identification techniques are the leaders in biometric technique field. In comparison with fingerprint methods iris algorithms provides in 10 times more accuracy (1 from 1-2 bil. false iris matching as compared to 1 from 100 hund. fingerprints matching) [1].

As well eye cornea weld seam is naturally protected from harmful influence that leads to less noisy signal this fact is taken into account in identification algorithms development. Iris identification typically works with noncontact optical techniques which is the best choice for metal surface identification.

Identification process includes such steps as area of interest indention called Segmentation, process of Normalization so we can reduce noise or correct aberrations and feature Encoding and Matching.

Segmentation is used for the area forming, the latter matched with the original pattern. In order to that iris segmentation means locating iris boundaries and choosing certain area with defined sizes for the weld. Iris sector could be identified by two circles known as pupil and sclera boundaries. For the weld type of pattern or other non-circular areas it is reasonable to use simpler techniques of segmentation which do not require any types of data approximation. Moreover those criteria algorithms of non-circular segmentation are simplified with those types of noise like upper and lower lashes in iris method.

Wildes et al. proposed to use an automatic segmentation algorithm based on the circular Hough transform for coordinate center and pupil radius and iris sector locating [2]. In addition to that Hough transform can be used for line and free shape search parametrically at black and white image. Assuming we have some data points in an image which is probably the result of an edge detection process, or boundary points of a binary blob. We need to recognize the points that form a straight line. If we divide parameter space into a number of discrete accumulator cells we can collect “votes” in (a b) space from each data point in (x y) space. Peaks in (a b) space will mark the equations of lines of co-linear points in (x y) space. Thus we can find points of interest [3].

In this way preliminary image transformation into black and white and optimization of segmented area size including points of interest and background may produce output image data in digital form.

There was purposed Daugman’s Integro-differential Operator as alternative approach to iris and pupil circular area localization including upper and lower leads arches. The operator searches for the circular path where there is maximum change in pixel values, by varying the radius and center position of the circular contour [4]. The integro-differential can be seen as a variation of the Hough transform [5]. Since this operator is adapted for sector search technique it is not reasonable to use it in line search compared to Hough transform for line detection.

Matching of original and identified samples requires normalization step in case of different aberrations, such as mutual casks and equipment dislocation, tilt and rotation, distance shifts between inspected object and camera.

Efficiency of both Daugman and Wilde approaches for weld-like patterns was compared in respect of shifts, scaling and rotation aberrations reduction. Daugman method provides use of radial scaling either to correct contraction of the pupil or pupillary dilatation and image sizes relatively to original image. The Process includes Cartesian to polar coordinates transfer with respect to angle of rotation (1) [4].

$$\mathrm{I}\big(\mathrm{x}(\mathrm{r},\theta),\mathrm{y}(\mathrm{r},\theta)\big) \rightarrow \mathrm{I}(\mathrm{r},\theta),$$
$$\begin{cases}\mathrm{x}(\mathrm{r},\theta) = (1-\mathrm{r})\mathrm{x_p}(\theta) + \mathrm{r}\mathrm{x_i}(\theta)\\ \mathrm{y}(\mathrm{r},\theta) = (1-\mathrm{r})\mathrm{y_p}(\theta) + \mathrm{r}\mathrm{y_i}(\theta)\end{cases} \quad (1)$$

where I(x,y) is the iris region image, (x,y) are the original Cartesian coordinates, (r,θ) are the corresponding normalised polar coordinates, $\mathrm{x_p}$, $\mathrm{y_p}$ and $\mathrm{x_i}$, $\mathrm{y_i}$ are the coordinates of the pupil and iris boundaries along the θ direction.

Wilde's method uses image registration for normalization step both for rotation and scaling. This approach helps to transform disturbed image as original version with respect to scale and rotation parameters that is important within the work.

In order to normalize iris biometric patterns with use of image registration method we choose as normalized parameters: scaling factor *s* and a matrix representing rotation ϕ which includes cask and camera aberrations within three main axes that influence considerable on applied algorithms (2).

$$\begin{pmatrix}\mathrm{x}'\\ \mathrm{y}'\end{pmatrix} = \begin{pmatrix}\mathrm{x}\\ \mathrm{y}\end{pmatrix} - \mathrm{sR}(\phi)\begin{pmatrix}\mathrm{x}\\ \mathrm{y}\end{pmatrix}, \quad (2)$$

where s is scaling factor; $\mathrm{R}(\phi)$ is rotation matrix with angle of rotation ϕ.

Sample selection should include marking procedure in order to avoid unacceptable aberration. Mark provides a reference zero point relatively to which matching procedure will be performed. It is important to accurately place cask in front of a camera that makes coding and matching stages more successful. Those would be better to use supportive techniques and instruments to correct distance and angle of rotation for accurate normalization.

Characteristic point features contain graphic information that should be defined for further feature encoding. Those encode methods are based on integral transformation.

Only the significant features of the sample must be encoded so that comparisons between patterns can be made. Gabor filters are able to provide optimum conjoint representation of a signal in space and spatial frequency. A Gabor filter is constructed by modulating a sine/cosine wave with a Gaussian (3). It is able to provide the optimum conjoint localization in both space and frequency, since a sine wave is perfectly localized in frequency, but not localized in space [1].

$$\mathrm{Gabor}(\mathrm{x}',\mathrm{y}') = \mathrm{Gauss}(\mathrm{x}',\mathrm{y}') * \cos(2\pi\mathrm{f_0}\mathrm{x}' + \varphi), \quad (3)$$

where $\mathrm{f_0}$ is spatial frequency; φ is phase.

A Gabor filter modification is Log Gabor filter [6]. The Advantage of the Log Gabor filter is reduction of DC of Gabor filter for accurate pattern boundaries selection. This method is widely applied in different tasks and this is why it was chosen for this work.

The pattern that is generated in the feature encoding process will also need a corresponding matching metric, which gives a measure of similarity between two patterns. Metric measure methods like Hamming distance (4) and Euclidean distance (5) have widespread use but Euclidean Distance has benefits with weight counting.

$$d_{ij} = \sum_{k=1}^{p} |x_{ik} - x_{jk}|, \quad (4)$$

where d_{ij} – distance between i^{th} и j^{th} template; x_{ik} – i^{th} feature of the k^{th} area; x_{jk} – j^{th} feature of the k^{th} area.

$$D = \sum_{i=1}^{N} \frac{(f_i - f_i^{(k)})^2}{(\delta_i^{(k)})^2}, \quad (5)$$

where f_i – i^{th} feature of the unknown pattern; $f_i^{(k)}$ – i^{th} feature of the original pattern; $\delta_i^{(k)}$ is the standard aberration of the i^{th} feature in template k. The i^{th} unknown template is found to match template k, when D is a minimum at k.

The encoding process produces a bitwise template containing bits of information. Matching will be provided with finding similarity between two digital codes with respect to weight in order to get the information about templates identity.

3. Conclusion

The paper proposes biometric methods implementation to nuclear material cask welds identification. main stages for pattern identification and matching including algorithms and concluded appropriate ones for cask identification and analysis are described. The Work was realized in practice with development of cask identification program code.

4. References

[1] Mansfield T. // Biometrics Feasibility Study. – 2003. – V. 3. – No. 2. – P. 14–15.

[2] Wildes R. // Proceedings Of The IEEE. – 1997. – V. 85. – No. 9. – P. 1348–1263.

[3] Marr D. and Hildreth E. // Proceedings of the Royal Society (London B). – 1980. – P. 187–217.

[4] Daugman J. // IEEE Transactions On Circuits And Systems For Video Technology. – 2004. – Vol. 14. – No. 1. – P. 21-30.

[5] Masek L. // Bach. Report. The University of Western Australia. – 2003.

[6] Kermani A. and Hamker F. // Management, Computer Science and Informatics. - 2011. - S. 57-59

Session 17

Inhomogeneous Material Verification

Utilizing Delayed Gamma Rays for Fissionable Material Measurement in NDA

Douglas Chase Rodriguez, Jun Takamine, Mitsuo Koizumi, Michio Seya

Integrated Support Center for Nuclear Security and Nuclear Nonproliferation
Japan Atomic Energy Agency
2-4 Shirane Shirakata, Tokai-mura, Naka-gun, Ibaraki 319-1195, Japan
E-mail: rodriguez.douglaschase@jaea.go.jp, takamine.jun@jaea.go.jp, koizumi.mitsuo@jaea.go.jp, seya.michio@jaea.go.jp

Abstract:

Development of a non-destructive analysis system using a pulsed neutron source is under discussion by researchers of the JAEA, and JRC-ITU and JRC-IRMM. The system will utilize a combination of neutron resonance transmission analysis and differential die-away and both prompt and delayed gamma-ray (DG) spectroscopy (DGS) techniques. The DGS technique can establish fissionable material ratios to relatively high precision since each isotope has a unique fission yield that generates specific gamma-ray spectra with energy extending well above the 3-MeV limit of passive gamma-ray emissions. This system will be applied toward safeguards applications by effectively determining nuclear material (NM) compositions within MOX fuel samples and NM samples with high neutron or passive gamma-ray emissions (including the melted fuel generated in severe reactor accidents). Additionally, this system can be applied toward nuclear security by detecting the high-energy DGs that can more efficiently pass through shielding materials. This presentation describes the initial status of the DG portion of this system and how it will be used in conjunction with the other techniques to provide both high accuracy and high precision of the composition of the NM of interest.

Keywords: NDA; DGS; active; safeguards; security

1. Introduction

The Japan Atomic Energy Agency (JAEA) is developing multiple programs in order to improve state and international safeguards concepts and technologies. Included in these efforts are the technological aims of improving non-destructive analysis, detecting undeclared nuclear activity, and developing site-level safeguards-by-design. Particularly, there is increasing interest regarding how to effectively and efficiently determine the fissile and fissionable (FF) composition (FFC) of mixed nuclear materials (NM). Of significant interests are determining the Pu/U composition of purified NM (e.g. mixed-oxide (MOX) fuel and plutonium nitrate solutions) and of non-purified NM (e.g. spent fuel, vitrified waste, melted fuel from reactor accidents, and next-generation fuel cycle) materials. For each of these material forms, destructive analysis has been deemed inappropriate due to the difficulty of acquiring reasonable sample material.

To help fill this gap researchers of the JAEA and JRC (ITU, Ispra, and IRMM, Geel) are currently discussing the development of a non-destructive analysis (NDA) system and measurement campaign. The system will utilize a combination of neutron Differential Die-Away Analysis (DDA) [1], Neutron Resonance Transmission Analysis (NRTA) [2], Prompt Gamma-ray Analysis (PGA) [3], and Delayed Gamma-ray Spectroscopy (DGS) techniques [4]. Interrogation with an external neutron source enables each of these techniques to provide a unique and complementary perspective of establishing reasonable confidence and precision of the FFC of any given NM sample [5].

The important aspect of the DGS technique is that after a few microseconds the induced fission products generate specific delayed gamma-ray (DG) energy spectra that extend well above 3 MeV. This is especially important for those NM samples that have high passive gamma-ray emissions below

this energy. Since each of these fission products has a unique decay half-life, the energy spectrum changes over time but in a predictable manner since the isotopes decay in well-established chains. Ratios of FFC isotopes can be ascertained based on the relative fission yield (FY) contributions to the integrated fission yield of the measured NM.

Multiple presentations submitted will focus on various aspects of this new NDA project and the system being developed. This work describes initial studies from the JAEA regarding the DGS technique as an aspect of the overall project. Additionally, a description will be made of the necessary physics improvements required to enable this method to be more precise in determining the FFC.

2. Delayed Gamma-ray Spectroscopy

As mentioned above, the DGS technique has the potential to establish the fissile composition to high precision. The yield of fission products is unique to each fissile and fissionable isotope depending upon the energy of the fission-inducing neutron. Though many of the same fission products are produced between multiple isotopes, the relative proportions are different. The cross-section of the fissile isotopes are very similar above ~1-MeV, allowing the dominant isotope (e.g. ^{238}U for spent fuel) to overwhelm the signature. It then becomes important to measure differences from neutrons of energies below ~40-eV where the cross sections for the isotopes of interest are highly separated.

Mixed NM produces a unique combined FY dependent upon the relative quantity of each individual isotopic FF. As seen in Figure 1, the FY×σ contribution from equal amounts of ^{239}Pu, ^{241}Pu, and ^{235}U have drastically different shapes and proportions for the same thermal irradiation neutron flux. Ignoring the relative intensities that indicate the probability to fission, the integrated FY is seen to have an entirely different shape assuming there are equal amounts of these three isotopes contained in the same target. The integrated FY×σ is also different from a target containing twice as much ^{235}U as either Pu, indicating the capability for the DGS method to distinguish the unique ratio of the isotopes.

Much work has already been performed to develop systems and analytic methods to apply the DGS technique toward spent nuclear fuel [4,6,7] and NM detection [8]. Results of these indicate that the

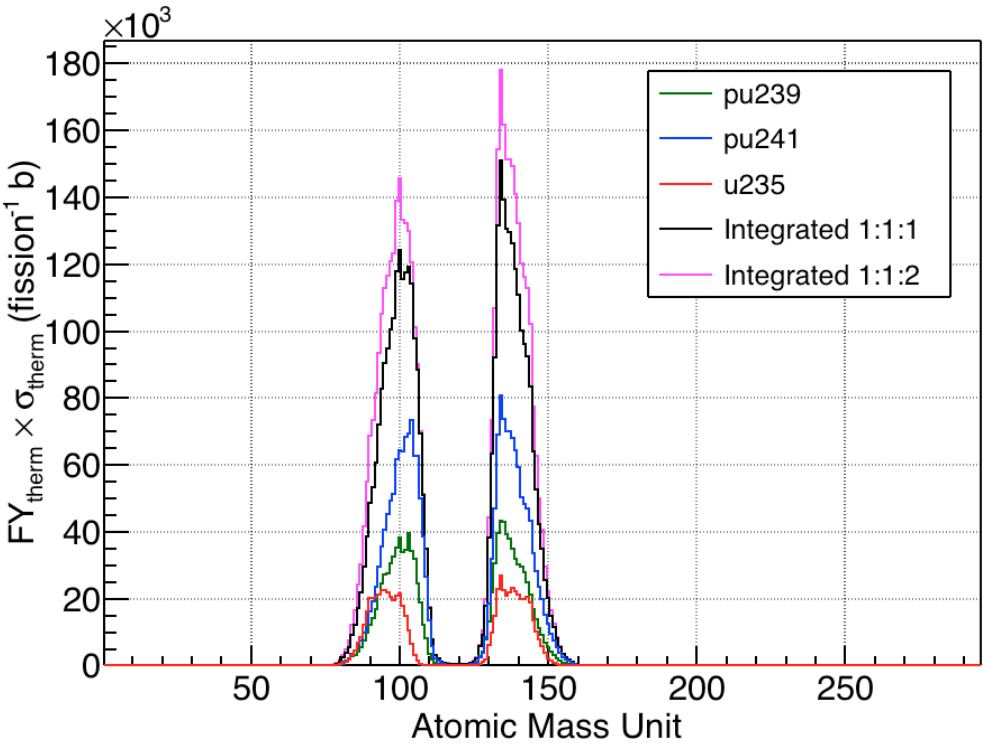

Figure 1: The thermal fission yield of ^{241}Pu, ^{239}Pu, and ^{235}U multiplied by the (n,fission) cross-section at a 25.3-meV irradiation neutron energy. Also shown are the FY×σ integrated values for a 1:1:1 and 1:1:2 ratio of the list-ordered isotopes.

DGS technique is quite effective for detection and has the potential to establish irradiation history rather well, however, there is still much uncertainty in the accuracy of quantifying the absolute values [9]. The primary problem for this arises in the relatively poor precision of the FY of the short- and medium-lived (e.g. less than ~20-minute half-lives) isotopes that tend to be ideal for establishing relative FFC (see Figure 2). This JAEA-JRC collaboration intends to improve these efforts by not only developing a uniform system capable of site-level application at the many mixed-NM facilities, but to also measure DG signatures of isotopic material to improve the precision of the important FY.

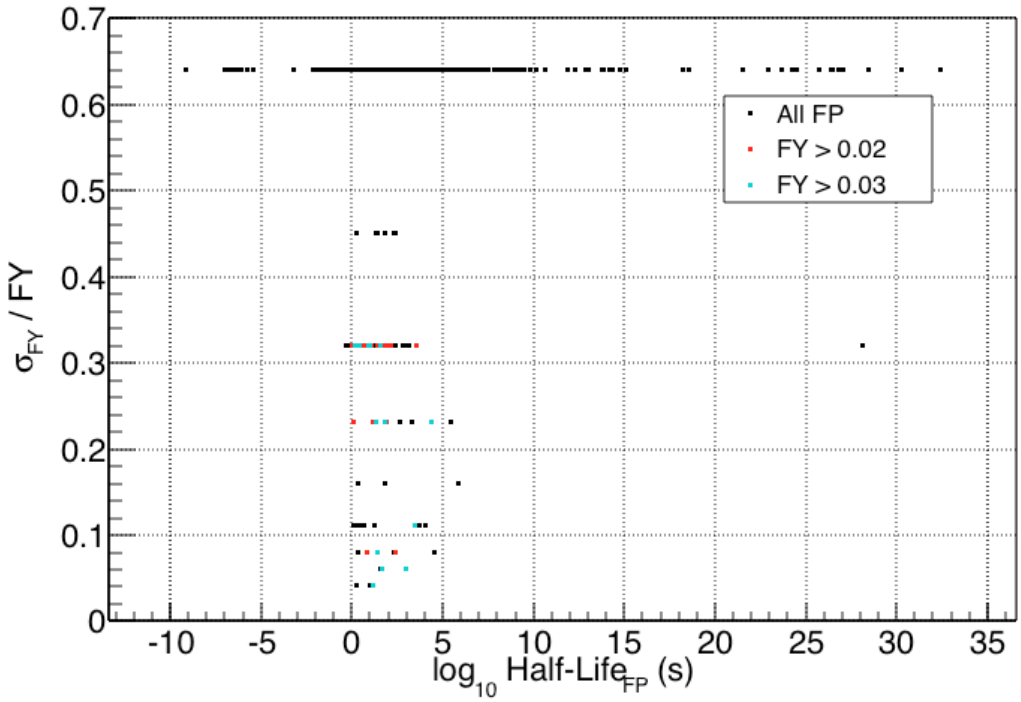

Figure 2: The relative yield error (σ_{FY}/FY) of ^{241}Pu fission products (FP) compared to their half-life. Note that most of the FPs have relative errors greater than 20%, including many high FY isotopes.

3. Multi-Technique NDA System

The active neutron-interrogation NDA system being developed by the JAEA, JRC-ITU, and JRC-IRMM is primarily intended to non-destructively assay multiple form factors of mixed NM. This system will consist of both neutron detection methods and gamma-ray detection methods to acquire as much detail of the fissile isotopic composition as possible. The intended targets will be from simple compounds (e.g. purified plutonium nitrate solution at a reprocessing facility) to highly active NM (e.g. spent nuclear fuel) that will require unique handling and system components. Each incorporated technique requires an external neutron source but provides complementary information based on the detection method for that technique. Table 1 describes different system elements that must be considered.

The DDA neutron technique can provide estimations of the bulk fissile content by correlating the number of fission-produced delayed neutrons to an effective-^{239}Pu mass [1]. The time frame for DDA is on the order of millisecond time windows requiring fast detectors. The PGA technique compliments DDA by covering the same time windows but observes gamma rays that can provide detail on which isotopes undergo (n,γ) reactions, including non-fissile materials [3]. NRTA is an auxiliary method that can provide a measure of isotopic composition observing suppressions of neutrons with energies that are more readily absorbed by the target material [2]. This technique requires a time-of-flight component but is the optimal method of determining irradiating-neutron energies. The DGS technique can provide isotopic fissile ratios by observing gamma rays from fission products that are proportionally unique to each induced isotopic fission yield [4].

	Ideal Source Energy	Ideal Source Flux	Source Collimation Required	Detector Rate Required	Detector Protection	Detector Collimation
DDA	Therm.	High	-	Mod.	Mod.	-
NRTA	Wide	High	High	High	Mod.	High
PGA	-	Mod.	Mod.	High	High	High
DGS	Therm.	High	High	High	High	High

Table 1: System considerations of potential mixed nuclear materials. Dashes are unimportant aspects.

The DGS technique of this system has the greatest potential to distinguish isotopic ratios and shielded NM, however it also requires the most development for NDA. Accordingly, much of the preliminary effort of this project will focus on improving the measurement capabilities of this technique. The DGS elements of the system will then be evaluated to determine the best way to incorporate it with the other techniques into an optimal system. Different elements will be required to optimize each technique as well as to address the large variety of environments and facilities in which this system can be used.

3.1. Neutron Irradiation

The required irradiation neutrons cover a wide range of energies, focusing on those below 40 eV. The DGS, PGA, and DDA techniques applied to the nuclear fuel cycle have mostly been studied using thermal energy (0.0253 eV) since there is a distinct separation in the neutron cross-sections for the various fissile isotopes with a minimum influence on the dominant ^{238}U. Alternatively, NRTA requires neutrons that cover the 0.1-eV and 40-eV range of energies in order to respond to the various neutron resonances.

However, there is no pure thermal or low-energy, broad-spectrum neutron source that can be easily transported to various facilities. This then necessitates the use of portable neutron sources of much higher energies: spontaneous-fission sources (e.g. ^{252}Cf Watt spectrum peaking at 2.2-MeV), deuterium-deuterium (DD) neutron generators (2.4-MeV), or deuterium-tritium (DT) neutron generators (14.1-MeV). Each of these must be moderated from the primary energy (or energy range) in order to be used effectively in this system.

Another aspect of these source neutrons is that they are produced with an isotropic distribution, necessitating a reflector to increase the neutron flux through the target, especially from low-emissive sources. To detect illicit trafficking of NM, isotopic composition measurement is not as important as observing fission or unique neutron resonance signatures. Studies will be performed to evaluate these cases since, as long as the desired signature is observed, a neutron focuser may not be necessary.

An element of the design is to establish which materials, as well as their thickness and shapes, are optimal for moderation and reflection of the irradiating neutrons. A difficulty arises due to the difference in requirements to moderate 14-MeV neutrons compared to moderate 2-MeV neutrons (e.g. neutron-multiplication will be less effective in a lower-energy source). As such studies will be performed with a modular design in mind: a moderator-reflector optimized for one primary source can be replaced with one optimized for a different primary source depending upon the facility requirements and capabilities.

Since improving the FY precision is one of the primary goals of this project, taking measurements at multiple facilities is also important, including neutron beam-lines from electron linear accelerators. These offer different capabilities based on the neutron source and possible target materials, but also require different methods of moderation. Studies will be performed to determine which elements of a modular system are important for these various sources.

3.2. System Detection Elements

Separate from improving the rate of neutron irradiation of the target is the requirement to detect the appropriate particle signatures. The DDA technique generally uses gamma-negligent detectors located near the target to minimize the diffusion time of the secondary neutrons [10]. Since only neutron counts (not energy) is used in this technique, the system constraint is primarily dependent upon fast detectors with low dead-times.

The NRTA technique uses a time-of-flight (TOF) configuration to measure the energy of the neutrons [2]. As such, not only is a fast neutron detector required, but also a collimating drift tube and a neutron filter to absorb neutrons below ~0.1 eV (for improved integration timing). These elements are not required for any of the other techniques and the filter will actually remove the important thermal neutrons optimal to fission the target for the DGS and DDA techniques. Allowing these components to be removed supports a modular system design.

Due to the nature of the high-energy neutron source, the gamma-ray detectors would need to be protected to prevent drastic degradation of their resolution (HPGe) [11,12] or to minimize signal interference (scintillator). However, as a compromise to enhanced protection, using detectors that can be replaced frequently to increase detection capability may be allowable. This aspect will be studied over the course of the design.

Additionally, the gamma-ray detectors will experience different rates of gamma rays for the PGA and DGS techniques over different time ranges. A preliminary model shows particles produced from 14-MeV neutrons can last for several milliseconds concurrently with the gamma rays from the target and surrounding materials (see Figure 3). A PGA detector must therefore 1) be extremely neutron resistant, 2) be able to distinguish the neutrons from gamma rays, 3) be able to handle input rates of ~10^5 s^{-1}, and 4) have the resolution to distinguish the multiple neutron-activation gamma rays.

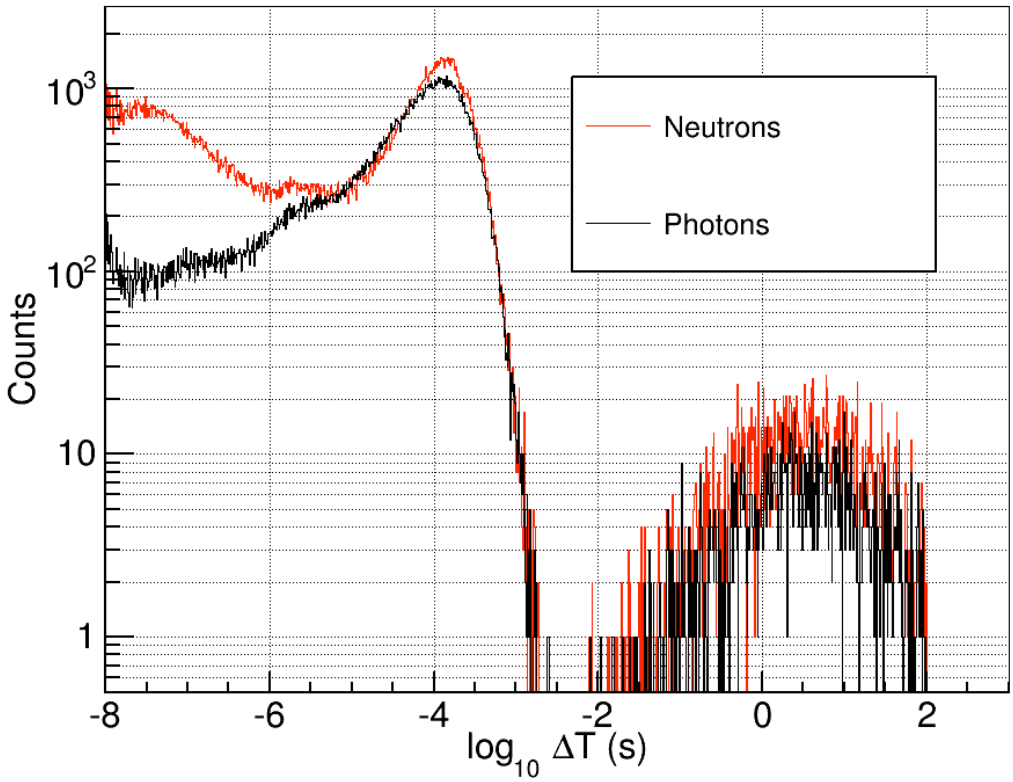

Figure 3: The time difference of a preliminary MCNP6 model distribution of particles passing through a detector after the generation of 14-MeV neutrons. In this model, the peaks around 100-μs are from neutron activation providing the DDA and PGA signatures. The gamma rays beyond 10-ms are the delayed signature from the fission products with overlapping delayed neutrons. The gap may be a potential problem in the MCNP6 model and will be analyzed.

The prominent DGS signature in this MCNP6 model, on the other hand, starts beyond 10 ms for a single primary neutron. Though the gap in the timing may indicate a problem in the MCNP6 modelling, it still represents a requirement for accurate timing control of the detector with minimal measurement lethargy. This can be performed using many different methods including shutters to block the neutrons from irradiating the target (i.e. thermal-neutron experimental reactors [13]), shuttling the target to a separate location (i.e. for beam-line experiments), shuttling the source to a separate location (i.e. for ^{252}Cf button sources), or precision time-analysis of the signal [7]. What is most practical may be different for each facility and will be studied over the course of the project design.

For the DGS, DDA, and PGA techniques, multiple detectors arrayed around the target can also improve the observed signature. Depending upon the facility, multiple detectors may not be feasible, so studies will be performed based on a single detector basis but additional models will be generated to study the systematic and statistical effects (including coincidence) of multiple detectors.

4. Summary

Researchers at the Japan Atomic Energy Agency and the European Joint Research Centers in Geel and Ispra are currently discussing the development of an active-interrogation, non-destructive analysis system and measurement campaign. This system will incorporate four different techniques (DGS, DDA, PGA, and NRTA) in order to quantify the fissile and fissionable content of multiple nuclear form factors from purified MOX fuel to high-activity spent nuclear fuel. As the DGS technique has the most restrictions of those being incorporated, primary efforts will be applied towards enabling this method, including optimizing the system's initial design and improving fission yield measurements.

5. Acknowledgements

This work is partially supported by the Ministry of Education, Culture, Sports, Science, and Technology (MEXT), Japan.

6. References

[1] Henzl, V. et al., *Determining the Pu Mass in LEU Spent Fuel Assemblies: Focus on Differential Die-Away Technique; Technical Report LA-UR-14-29124*; Los Alamos National Laboratory; 2014.

[2] Chichester, D.L. and Sterbentz, J.W., *Neutron Resonance Transmission Analysis (NRTA): Initial Studies of a Method for Assaying Plutonium in Spent Fuel*; 33rd ESARDA Annual Meeting; 2011.

[3] Choi, H.D. et al., *Database of Prompt Gamma Rays from Slow Neutron Capture for Elemental Analysis; STI/PUB/1263*; International Atomic Energy Agency; 2007.

[4] Campbell, L.W., Smith, L.E., and Misner, A.C., *High-Energy Delayed Gamma Spectroscopy for Spent Nuclear Fuel Assay; IEEE TNS 58*; 2011; pgs. 231-240.

[5] Bolind, A.M. and Seya, M., *A Review and Consideration of the State of the Art of the Nondestructive Assay of Spent Nuclear Fuel Assemblies of the NGSI from the Viewpoint of Obtaining Better Accuracy; JAEA Technical Report*; Capacity Building Cooperation Office, Integrated Support Center for Nuclear Nonproliferation and Nuclear Security, Japan Atomic Energy Agency, to be published.

[6] Campbell, L., Hunt, A., Ludewigt, B., and Mozin, V., *Delayed Gamma-Ray Spectroscopy for Spent Nuclear Fuel Assay; JNMM 40 (2)*; 2012; pg. 78.

[7] Campbell, L.W., *Fitting Methods for Delayed Gamma Spectroscopic Data; Technical Report PNNL-SA-99655*; Pacific Northwest National Laboratory; 2013.

[8] Rennhofer, H. et al., *Detection of SNM by delayed gamma rays from induced fission; NIM A 652*; 2011; pgs. 140-142.

[9] Campbell, L.W., *Preliminary Findings on the Calibration of Delayed Gamma Fuel Assay Methods and Integration with Neutron-Based Methods; Technical Report PNNL-22978*; Pacific Northwest National Laboratory; 2013.

[10] Henzl, V., *Evaluation of Differential Die-Away Technique Potential in Context of Non-Destructive Assay of Spent Nuclear Fuel; Technical Report LA-UR-14-29224*; Los Alamos National Laboratory; 2014.

[11] Borrel, V. et al., *Fast neutron-induced damage in INTEGRAL n-type HPGe detectors; NIM A 430 (2)*; 1999; pgs. 348-362.

[12] Van Siclen, C. DeW., *Phenomenological Model for Predicting the Energy Resolution of Neutron-Damaged Coaxial HPGe Detectors; IEEE TNS 59 (5)*; 2012; pgs. 2487-2493.

[13] Williford, R.S., *Temporal Gamma-Ray Spectrometry to Quantify Relative Fissile Material Content*; PhD Dissertation; Oregon State University; 2013.

7. Disclaimer

The work presented herein is preliminary and may change over the course of the project study.

R&D Status of Nondestructive Assay System Based on Nuclear Resonance Fluorescence

Toshiyuki Shizuma, Ryoichi Hajima, Takehito Hayakawa, Christopher T. Angell, and Michio Seya

Japan Atomic Energy Agency
Tokai, Ibaraki, Japan
E-mail: shizuma.toshiyuki@jaea.go.jp

Abstract:

Nondestructive assay (NDA) of nuclear materials is an important technology for nuclear security and safeguard applications. We have proposed an NDA system based on nuclear resonance fluorescence (NRF), which enables isotopic identification of materials in a nondestructive way. In the proposed detection system, an energy-tunable and mono-energetic photon source generated by Compton scattering of laser light (laser Compton scattering; LCS) with high-energy electrons is used. The NRF measurement can be more efficient by using such a mono-energetic photon beam. We have started the research and development program of LCS γ-ray NDA, which includes demonstration of LCS photon generation from an energy recovery linac (ERL), establishment of detection system, and benchmark of Monte Carlo simulation. The R&D status including recent results on the demonstrations of the LCS photon generation as well as the measurement principles will be reported.

Keywords: Nondestructive assay; Nuclear resonance fluorescence; laser Compton scattering

1. Introduction

Nondestructive assay (NDA) methods using a mono-energetic photon beam based on nuclear resonance fluorescence (NRF) can be used for assaying nuclear materials [1]. In the NRF-based NDA method (scattering method), isotope-specific analysis can be made by direct measurement of characteristic NRF signals emitted from the isotope of interest. An efficient NRF measurement is possible when we use a mono-energetic photon beam which can be generated by Compton scattering of laser photons with high energy electrons, *i.e*., laser Compton scattering (LCS) [1,2]. Transmission or self-interrogation technique is also useful for NDA of spent fuel. In the transmission method, nuclear resonance absorption is used to remove resonant photons from the incident beam. The selective isotope detection can be made by measuring the decrease of photon beam intensity at resonance energies [3]. This method can be improved by integrating the signal over multiple resonances in the energy region of a photon beam, termed the Integral Resonance Transmission (IRT) method [4].

Both the scattering and transmission methods need a mono-energetic photon beam. An intense mono-energetic LCS photon beam can be generated by combining two advanced technologies of the electron superconducting accelerator (energy recovery linac, ERL) and the laser enhancement cavity (or supercavity) to increase the collision density of both the electron and laser beams. In order to demonstrate the generation of a high-flux mono-energetic photon beam, we have constructed an LCS photon beam line at the Compact ERL (cERL) facility [5] at High Energy Accelerator Research Organization (KEK).

In this paper, we will show the R&D status of the LCS γ-ray NDA program which includes results of the demonstrations of the LCS photon generation as well as the measurement principle for the scattering and transmission methods.

2. R&D status of the NRF-based NDA

2.1. LCS photon generation based on the cERL

Major components of the cERL-LCS photon source, such as an electron superconducting linac (cERL) and laser enhancement cavity, have been developed in collaboration with KEK, JAEA, and several universities and institutes in Japan. The cERL consists of an electron gun, an injector linac, a main linac, and recirculation loop as shown in Fig. 1. Accelerated electrons collide with laser photons inside the enhancement cavity which is used to increase the density of the laser photons. The collision between the electrons and laser photons results in production of a LCS photon beam which is transported to the experimental hatch through the LCS beam line.

The commissioning of the injector linac started in April, 2013. We confirmed the generation of 5.5-MeV electron beam at the injector. The recirculation loop was constructed during a summer shutdown period in 2013. The commissioning of recirculation loop was done from December 2013 to March 2014. In the commissioning, an electron beam of 20 MeV was accelerated and then decelerated after recirculation. Further beam tuning was carried out from May 2014 for performance upgrade of the recirculating electron beam. From June to December 2014, a mode-locked fiber laser, a solid-state laser, an enhancement cavity, and a LCS beam line were installed. An experimental hatch and a measurement room were also constructed next to the accelerator room. During this period, tuning of the lasers and the enhancement cavity was carried out. From February 2015, the commissioning and tuning were restarted to increase the electron beam current and the demonstration experiment of the LCS photon generation has been carried out.

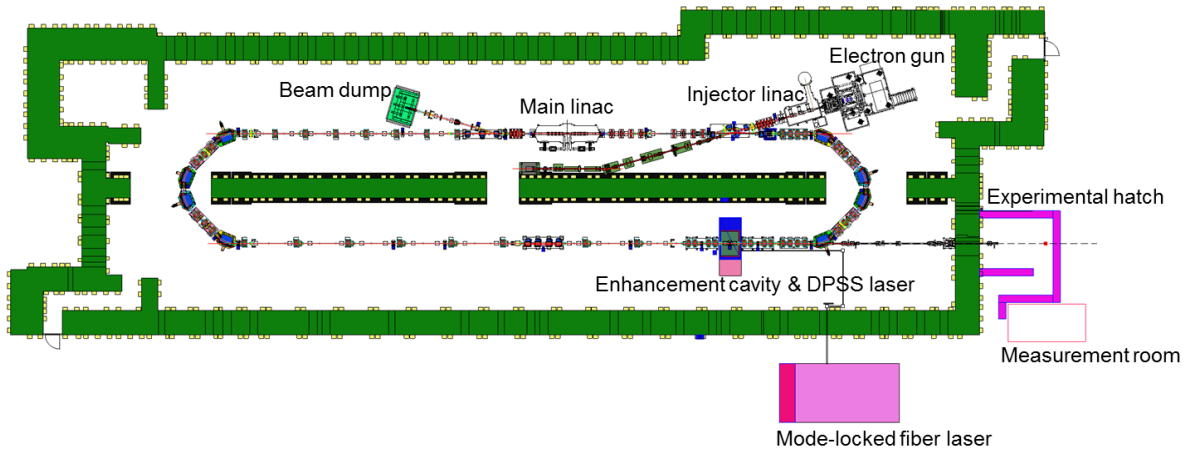

Figure 1; Schematic view of the Compact ERL and LCS beam line, and experimental hatch.

For demonstration of the LCS photon generation, an electron beam with bunch charge of 0.5 pC and length of 3 ps generated by the electron gun was accelerated up to 20 MeV at repetition rate of 162.5 MHz. The repetition rate of the electron beam pulse in the cERL is originally 1300 MHz, but it was modified to 162.5 MHz same as the laser repetition rate to enhance the signal to noise ratio of LCS photons by decreasing bremsstrahlung radiation backgrounds from accelerated electrons. The electron beam was transported to the collision point inside the enhancement cavity and was focused to spot size of 30 μm in root mean square (rms) and bunched to rms length of 2 ps at the collision point. After the collision with a laser beam, the electron beam was injected again to the main linac with deceleration RF phase before transferred to the beam dump.

We used two types of lasers, *i.e.*, a commercial diode-pumped solid-state (DPSS) laser (Time-Bandwidth Products AG, ARGOS) and a high-power mode-locked fiber laser developed at Kansai Photon Science Institute, JAEA [6]. The DPSS laser with the maximum average power of 45 W was installed on a movable optical bench together with the enhancement cavity for precise adjustment of the laser and electron beam position [7]. The laser beam power was enhanced up to 10.4 kW corresponding to the pulse energy of 64 μJ. On the other hand, the fiber laser with the maximum average power of 100 W was placed outside the accelerator room. Since the laser beam needed to be

transported approximately 20 m to the enhancement cavity, the position at the collision point became unstable. Therefore, we show the experimental data taken with the DPSS laser.

The electron beam collides with the laser beam inside the enhancement cavity at a crossing angle of 18 degrees. The maximum energy of the LCS photons is expected to be about 7 keV. Figure 2 shows an energy spectrum obtained by using the CAIN simulation code [8]. The total flux of the LCS photon beam is estimated to be 1.04×10^8 /sec with input parameters of the electron and laser beams listed in Table 1.

Electron beam	
Energy	20 MeV
Bunch charge	0.36 pC
Bunch length	2 ps (rms)
Spot size	30 μm (rms)
Emittance	0.4 mm mrad (rms)
Repetition rate	162.5 MHz
Laser	
Wave length	1064 nm
Pulse energy	64 μJ
Pulse length	5.65 (rms)
Spot size	30 μm (rms)
Collision angle	18 deg.
Repetition rate	162.5 MHz

Table 1: Parameters of the electron and laser beams at the collision point.

The LCS photon beam was transported to the experimental hatch through the LCS beam line in vacuum. Two beryllium foils with thickness of 250 and 300 μm was used at both the ends of the LCS beam line. The LCS photons were measured by a silicon drift detector (SDD) with effective area of 17 mm^2 in the experimental hatch. The LCS photons travelled 12 cm in the air from the end of the beryllium window to the SDD. The total distance between the collision point and the SDD was 16.6 m. We calculated an energy profile of the LCS photon beam at the SDD position with the Monte Carlo simulation code EGS5 [9]. The photon histories from the CAIN simulation were used as the input photon parameters in the EGS5 estimation. As a result of the EGS5 simulation, the flux, the peak energy, and the energy width of the LCS photons at the SDD position were obtained as 2940 /sec, 6.96 keV, and 32 eV in full width of half maximum (FWHM), respectively. The expected properties of the LCS photon beam are shown in Table 2.

Maximum energy	6.98 keV
Total flux	1.04×10^8 /sec
Flux at SDD	2.94×10^3 /sec
Peak energy, width at SDD	6.96 keV, 32 eV (FWHM)

Table 2: Expected properties of the cERL-LCS photon beam.

We measured an energy spectrum of the LCS photons by using the SDD placed in the experimental hatch as shown in Fig. 3. The count rate, peak energy, and energy width were obtained as 1200 cps, 6.96 keV, and 173 eV in FWHM, respectively. The photon flux is about 40 % of the expectation. The energy width of the SDD was measured to be 153 eV in FWHM for 5.9-keV X-rays from ^{55}Fe. Assuming quadratic nature for convolution of Gaussian width, the energy width of the LCS photon beam is estimated as 81 eV. The total photon flux at the collision point is also estimated with the aid of the EGS5 simulation to be 4.3×10^7 /sec at the average electron beam current of 57.7 μA. Further

upgrade and tuning of the cERL as well as the laser enhancement cavity are planned to increase the photon flux.

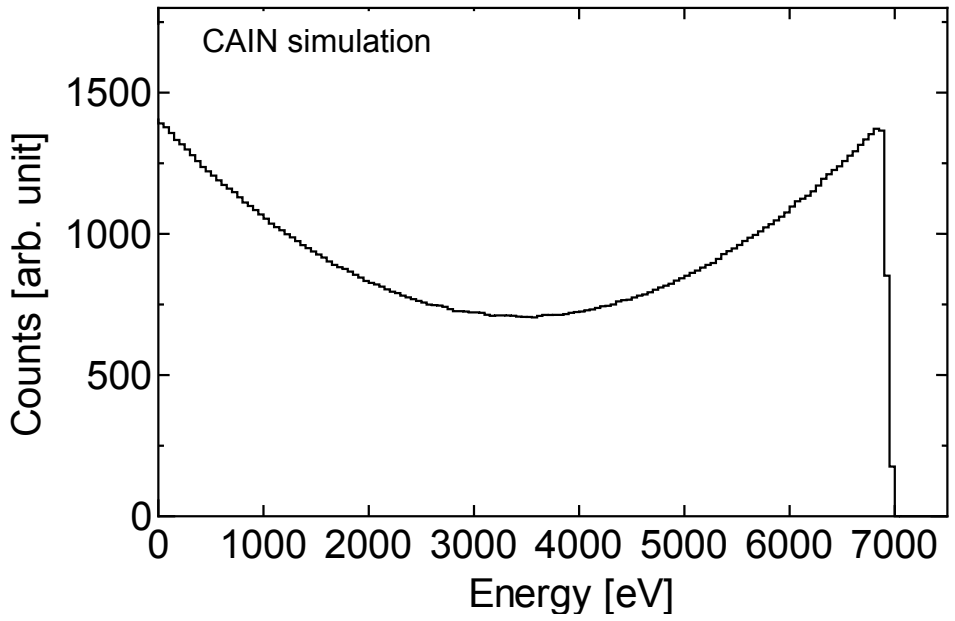

Figure 2; Energy spectrum of the LCS photons calculated by using the CAIN simulation code.

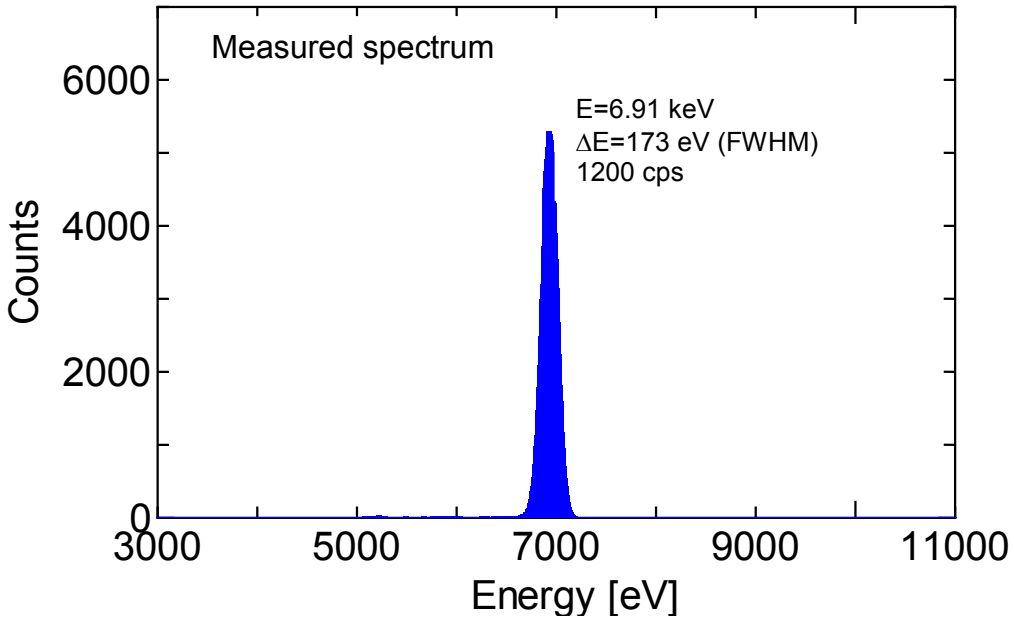

Figure 3; Energy spectrum of the LCS photons measured by a SDD detector which was placed 16.6 m from the collision point.

As an application of the ERL-based LCS photon beam, we have proposed an advanced hybrid K-edge/X-ray fluorescence densitometry (HKED) [10]. The HKED is a nondestructive assay technique used for the determination of U and Pu concentrations in solutions [11]. In the conventional HKED system, an X-ray tube is used to produce bremsstrahlung radiation as an incident photon source. The bremsstrahlung radiation is characteristic of strong photon intensity. However, the broad energy

distribution causes background counts due to inelastic photon scattering which affect the counting precision. From the Monte Carlo simulation study, we found that high precision HKED measurement is possible by using a mono-energetic photon source with the ERL and the enhancement cavity [10]. We have carried out a XRF test measurement with mono-energetic X-rays the cERL LCS photon beam. A stainless (SUS304) sheet with thickness of 100 μm was bombarded by the LCS photon beam. Emitted X-rays were measured by two low-energy HPGe detectors. As shown in Fig. 4, K_α and K_β X-rays of chromium which is one of the main compositions in SUS304 are clearly observed. Analysis of the data is in progress.

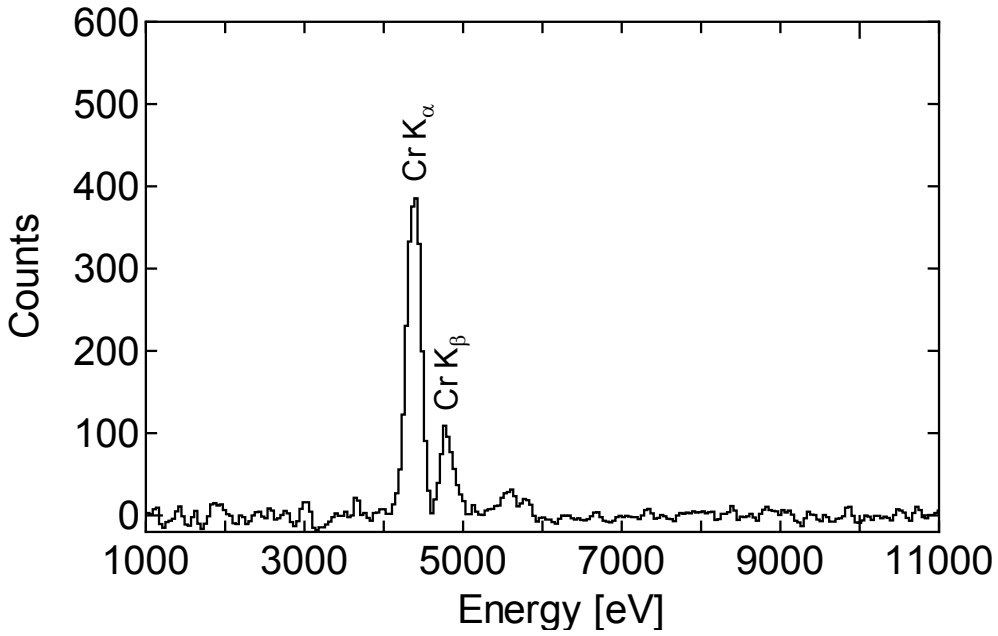

Figure 4; Energy spectrum of the emitted X-rays from a stainless (SUS304) target measured by two HPGe detectors placed at scattering angles of ±135 degrees.

2.2. NRF-based NDA measurement technique

NRF is a process of resonant excitation of nuclear levels by absorption of photons and subsequent de-excitation to lower-lying levels by photo-emission. It occurs if the energy of the incident photon is identical to the resonance energy of the nucleus. We have proposed two types of the NRF-based NDA, *i.e*., scattering and transmission methods. Schematic views of these NDA methods are shown in Figs. 5 and 6. In the scattering method, the amount of isotopes can be quantified by measuring the intensity of NRF γ-rays by using high resolution γ-ray detectors such as high-purity germanium (HPGe) detectors (see Fig. 5). In order to design an optimum NDA detection system and to evaluate its performance, we have developed a Geant4-based NRF simulation code, NRFGeant4 [12] and improved by adding several new functions including Doppler broadening, nuclear recoil, angular distribution, and so on [13]. The NRFGeant4 has been tested with experimental data as well as another NRF code, MCNP-X in collaboration with US-DOE.

For the scattering method, the performance of measurement system, such as statistical uncertainties, is affected by radiation background from spent fuel as well as background due to coherent scattering such as Rayleigh, nuclear Thomson, and Delbruck scattering. We investigated these effects and found that the radiation background can be reduced by using higher energy resonances at 3-5 MeV [14]. In addition, the contribution from the coherent scattering background can be eliminated by measuring the NRF transition to the first excited state instead of the transition to the ground state [14]. For actinide nuclei, the typical excitation energy of the first excited state is 10 to 50 keV and thus the transition energy to the first excited state is 10 to 50 keV lower than the coherent scattering peak which is almost identical to the energy profile of the incident photon beam. This type of measurement is only possible if

we use a mono-energetic photon beam with energy width less than 0.1% which can be achieved by our ERL-LCS technology.

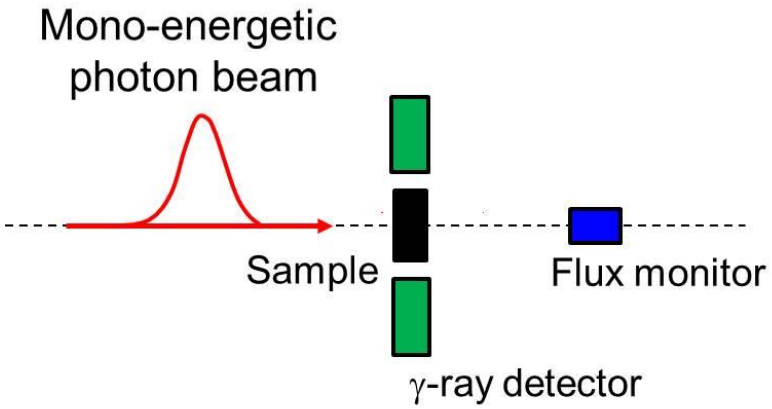

Figure 5; Schematic of the scattering measurement. NRF signals are measured by γ-ray detectors. The intensity of the NRF signal is proportional to the amount of material of interest.

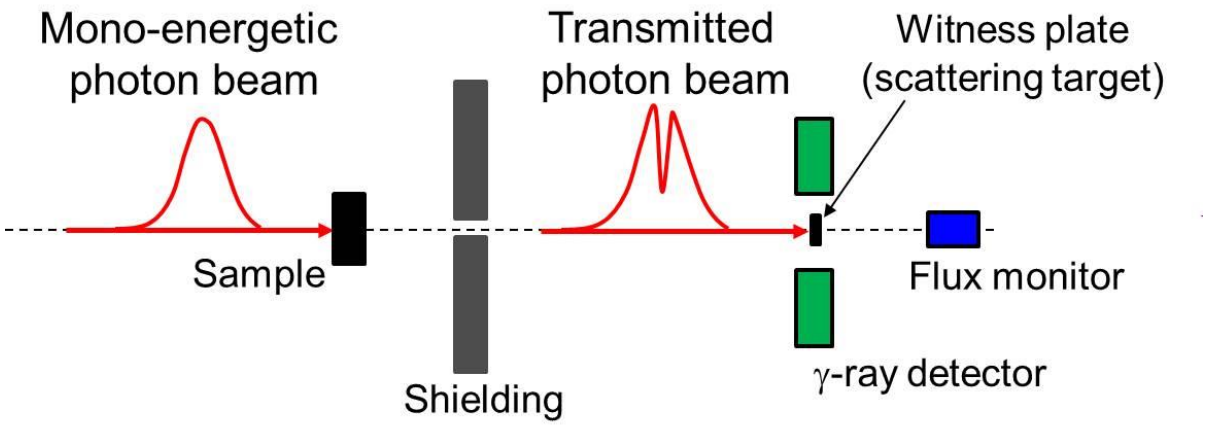

Figure 6; Schematic of the transmission measurement. The first sample resonantly removes photons. A decrease of the intensity of NRF signals from the scattering target is proportional to the amount of material of interest.

A transmission or a self-interrogation method uses nuclear resonance absorption which removes resonant photons from the incident beam. The selective absorption can be detected by measuring the scattered NRF signal in a second target placed after the sample. The second target is referred to as the witness plate, which consists of the isotope of interest. The self-interrogation measurement can be improved by integrating the signal over multiple resonances in the energy region of an incident photon beam which is termed the integral resonance transmission (IRT) method [4]. As shown in Fig. 6, the beam traverses the sample target where resonance states selectively absorb photons. The transmitted beam intersects with the scattering target in a shielded measurement location where the emitted NRF γ-rays are measured using γ-ray detectors. The total flux is measured to normalize for attenuation from non-resonant processes, particularly atomic scattering. The NRF γ-ray intensity drops proportionally to the amount of material of interest. We have carried out several measurements of the IRT method using ^{27}Al [15], ^{181}Ta, and ^{239}Pu [16] samples for practical NDA demonstration for spent or melted fuel. Nuclear resonant properties of ^{27}Al and ^{181}Ta are similar to those of ^{239}Pu. These measurements were made at the High Intensity γ-ray Source (HIγS) facility, Duke University. The scattered radiation from the witness target was measured using HPGe and LaBr detectors. Figure 7 is a NRF spectrum obtained for the Al target measurement for practical demonstration showing that a NRF transmission measurement is feasible through a TMI-2 container. Further analysis of the data sets is in progress.

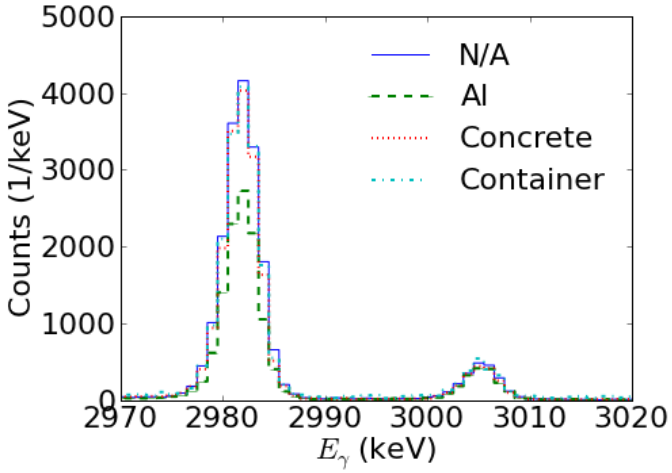

Figure 7; Energy spectra using an Al target for a simulant TMI-2 container. The spectra have been normalized for same flux on target, demonstrating resonant absorption of photons by the Al target.

3. Summary

We have proposed a nondestructive assay (NDA) system based on nuclear resonance fluorescence (NRF) for nuclear security and safeguard applications. The NRF-based NDA becomes more efficient if we use an intense mono-energetic photon beam. Such a photon beam can be generated by laser Compton scattering (LCS) together with advanced technology of an energy recovery linac (ERL) and a laser enhancement cavity. The research and development program of the LCS γ-ray NDA has been started. So far, the demonstration of the LCS photon generation from the Compact ERL has been carried out. We confirmed the generation of the LCS photon beam with intensity close to the expectation. Further upgrade of the cERL as well as the laser enhancement cavity are planned to increase the photon flux. We have also developed the measurement methods, scattering and transmission, of the NRF-based NDA which can be applied to spent or melted fuel.

Acknowledgements

We thank S. Kishimoto for lending a silicon drift detector. This work was supported by Ministry of Education, Culture, Sports, Science and Technology (MEXT), Japan.

References

[1] Hajima, R., et al.; J. Nucl. Sci. Technol.; 45; 441; 2008

[2] Pruet, J., et al.; J. Appl. Phys.; 99; 123102; 2006

[3] Walsh, W.J. et al.; Proc. of the Conference on Technologies for Homeland Security; 2009

[4] Angell, C.T., et al.; Proc. of INMM-53; 2012

[5] Sakanaka, S., et al.; Proc. of IPAC2013; 2159; 2013

[6] Mori, M., et al.; Proc. of CLEO-PR-2013 and OECC-2013; 2013

[7] Akagi, T., et al.; Proc. of IPAC2014; 2072; 2014

[8] Chen, P., et al.; Nucl. Instr. and Meth. in Phys. Res. A 355; 107; 1995

[9] Hirayama, H., et al.; SLAC-R-730; 2010

[10] Shizuma, T., et al.; Nucl. Instrum. Methods Phys. Res., Sect. A 654; 597/ 2011

[11] Ottmar, H. and Eberle, H.; Kernforschungszentrum Karlsruhe GmbH, Institut fur Kernphysik; Report 4590; February 1991

[12] Kikuzawa, T., et al.; Proc. AccApp'07; 1017; 2007

[13] Report of DOE-JAEA PAS-17; 2014

[14] Shizuma, T., et al.; Nucl. Instrum. Methods Phys. Res., Sect. A 737; 170; 2014

[15] Angell, C.T.; et al., Nucl. Instrum. Methods Phys. Res., Sect. B 347; 11; 2015

[16] Angell, C.T., et al., Proc. of the NPSNSN symposium; 2014

Technique of Neutron Resonance Transmission Analysis for Active Neutron NDA

H. Tsuchiya[1], M. Koizumi[1], F. Kitatani[1], M. Kureta[1], H. Harada[1], M. Seya[1], J. Heyse[2], S. Kopecky[2], W. Mondelaers[2], C. Paradela[2], P. Schillebeeckx[2]

[1]Japan Atomic Energy Agency (JAEA)
Tokai-mura, Naka-gun, Ibaraki 319-1195, Japan
E-mail: tsuchiya.harufumi@jaea.go.jp
[2] Joint Research Centre – Geel
Retieseweg 111, B - 2440 Geel, Belgium
E-mail: peter.schillebeeckx@ec.europa.eu

Abstract:
Neutron Resonance Transmission Analysis (NRTA) is a Non-Destructive Analysis (NDA) technique that relies on the use of resonance structures in neutron induced reaction cross sections. An active NDA system based on NRTA is under development to identify and quantify Special Nuclear Materials (SNM) and Minor Actinides (MA) in a wide variety of nuclear materials, including next generation fuel and highly radioactive materials. The development profits from the knowledge and experience gained in the development of Neutron Resonance Densitometry (NRD) as a NDA method to characterize particle-like debris from melted fuel. In this presentation, the basic principle of NRTA is explained. Results obtained for a NRD prototype device are used to estimate typical counting statistics uncertainties. In addition, the impact of the width of the pulsed charged particle beam on the experimental transmission is verified by measurements at the KURRI time-of-flight facility.

Keywords: neutron resonance transmission analysis; neutron time-of-flight

1. Introduction

Quantification of Special Nuclear Materials (SNM) (i.e. ^{235}U and Pu) is important for nuclear safeguards, nuclear non-proliferation and nuclear security. In addition, an accurate determination of the amount of Minor Actinides (MA) in next generation nuclear fuel material is important for nuclear transmutation applications. Hence, the development of a Non-Destructive Analysis (NDA) technique that is capable to quantify both SNM and MA in a wide variety of nuclear material is important for various nuclear technology applications.

A possible technique that can be applied for such a wide variety of materials is Neutron Resonance Transmission Analysis (NRTA) [1]. The potential of NRTA to quantify SNM in commercial fresh and spent fuel pins was tested experimentally at a pulsed reactor beam in Ref. [2] and a pulsed linear accelerator in Refs [3,4]. It was demonstrated that the areal densities of SNM determined by NRTA agreed within 4% with the reference values. Noguere et al. [5] applied NRTA to characterize a PbI_2 sample that was produced from a solution of radioactive waste originating from waste of a reprocessing facility.

Recently, NRTA was applied to determine the amount of ^{235}U and ^{238}U in an U_3O_8 reference sample that was enriched to 4.5 at% in ^{235}U [1]. The measurements were performed at the GELINA time-of-flight (TOF) facility of the Joint Research Centre (JRC) in Geel (BE) [6]. The difference between the experimentally determined areal densities of ^{235}U and ^{238}U and the

reference values was less than 1%. This agreement is remarkable since the attenuation of the neutron beam due to the presence of matrix material was about 99% [1]. These measurements were part of a collaboration between the Japan Atomic Energy Agency (JAEA) and JRC. The objective of this collaboration was to develop a NDA method, referred to as Neutron Resonance Densitometry (NRD), for the determination of the amount of SNM in particle-like debris generated in a severe nuclear accident [7,8,9]. The method strongly relies on NRTA to quantify the amount of SNM in the melted fuel. Within this project systematic effects that have a strong impact on the accuracy of the results, such as the variety in shape and size of the particle like debris samples [10], irregular shapes of samples [11] and the presence of neutron absorbing impurities [1], were investigated. The results obtained within this collaboration suggest that NRTA is a suitable technique to determine with a high accuracy the areal density of SNM in fresh and spent fuel and debris of melted fuel.

For further feasibility studies with the objective to develop an industrial system, we plan to develop a prototype NRTA facility using a DT pulsed neutron generator. This facility is part of a large NDA system which combines different neutron active interrogation techniques. More details about this system will be given in the contribution of Kureta et al. [12] at this symposium. The neutron intensity of a typical DT generator is about 2 to 5 orders of magnitude lower compared to the intensity of a neutron source produced by a pulsed linear electron accelerator (LINAC) like GELINA [6]. This difference in intensity can be compensated by reducing the flight path distance. However, a decrease in flight path length will affect the time-of-flight resolution. In addition, the pulse width of a DT generator, which is mostly ≥ 1μs, is substantially longer than the one of a pulsed LINAC, which is mostly ≤ 0.1 μs. In this contribution, a compact NRTA system based on a DT generator is presented and the impact of the width of the beam pulses is verified.

2. Neutron Resonance Transmission Analysis

2.1. Basic of NRTA

NRTA uses a pulsed white neutron source as a diagnostic beam. Since SNM and MA possess one or more strong resonances in the low energy region (see Figure 1), neutrons in the thermal and epithermal energy region are preferred to quantify SNM and MA. The quantity of interest for NRTA is the transmission, i.e. the probability that a neutron passes the sample without interaction. This transmission is experimentally determined from the ratio of a sample-in and sample-out measurement. To study the resonance structures the transmission is measured as a function of neutron energy. The neutron energy is obtained by the time-of-flight (TOF) technique. The TOF is measured by the time difference between a start signal and a stop signal, provided by the pulsed beam and neutron detector, respectively.

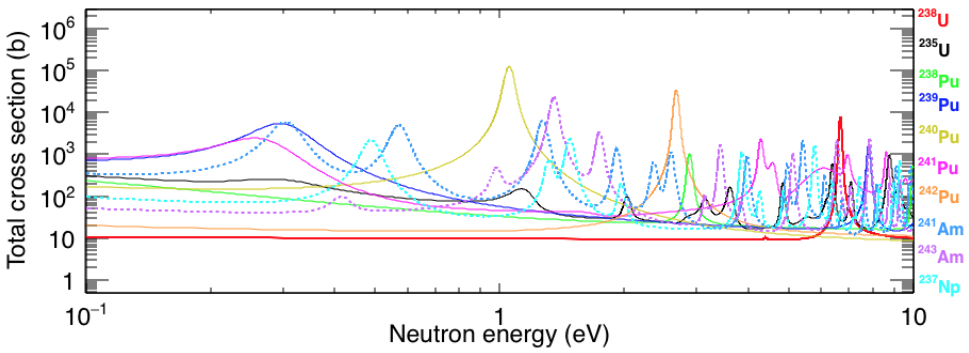

Figure 1: Total cross section of individual isotopes of SNMs (solid lines) and MAs (dashed ones). The cross section data are based on ENDF/B VII.1.

The characteristic dips in the experimental transmission as a function of TOF are due to resonance structures in neutron-induced reaction cross sections. These dips can be used to derive the areal number density of the nuclides present in the sample by a fit to the experimental data. In an ideal transmission experiment, i.e. with a homogeneous sample, measurements in a good transmission geometry and neglecting broadening due to the TOF-response, the theoretical estimate T of the transmission is:

$$T = \exp(-\sum n_k \cdot \sigma_{tot,k}),$$

where $\sigma_{tot,k}$ is total cross section and n_k is the number of atoms per unit area (or areal number density) of nuclide k. Hence knowing the total cross sections the areal densities can be derived. The total cross sections and corresponding resonance parameters are available from the major evaluated nuclear data libraries such as ENDF/B, JENDL and JEFF. The total cross sections are derived from transmission measurements which are the most accurate cross section measurements. Since NRTA is based on the same procedures it can be considered as one of the most accurate NDA techniques to quantify the areal density of SNM and MA.

2.2 NRTA for new NDA

Figure 2 shows a conceptual design of a NRTA system as part of the NDA system presented by Kureta et al. [11]. The pulsed neutron source is a commercially available GENIE 35 neutron generator produced by SODERN. Its minimum pulse width is 10 μs and the repetition rate can be varied with a maximum of 5 kHz. Its average total neutron emission rate is between 10^8 and 10^9 s^{-1} for a repetition rate of 100 Hz and 1 kHz, respectively. The generator is surrounded by neutron moderating material to slow down the 14 MeV neutrons, emitted from the neutron generator, to the thermal and epithermal energy region. The neutrons scattered from the moderator are collimated into a flight path through an evacuated beam tube. The neutron beam traverses the sample which is placed half-way between the neutron production target and the neutron detector. Neutrons traversing the sample without any interaction are detected by a neutron detector. The latter will be based on a scintillator material containing ^{6}Li coupled to a photomultiplier (PMT). The time of flight of the detected neutron is obtained from the time difference between the stop signal derived from the neutron detector and the start pulse from the pulsed neutron generator. From a measurement with and without sample in the beam, the experimental transmission is derived as a function of time-of-flight. This transmission can be used to quantify SNM and MA in the sample.

The objective is the development of a compact NDA system to be used as a prototype for an industrial system used for routine applications. Therefore, the flight path length of the NRTA facility will be ≤ 10 m. The short flight path length together with the 10 μs pulse width has a strong impact on the TOF resolution. The impact is discussed in section 3.2.

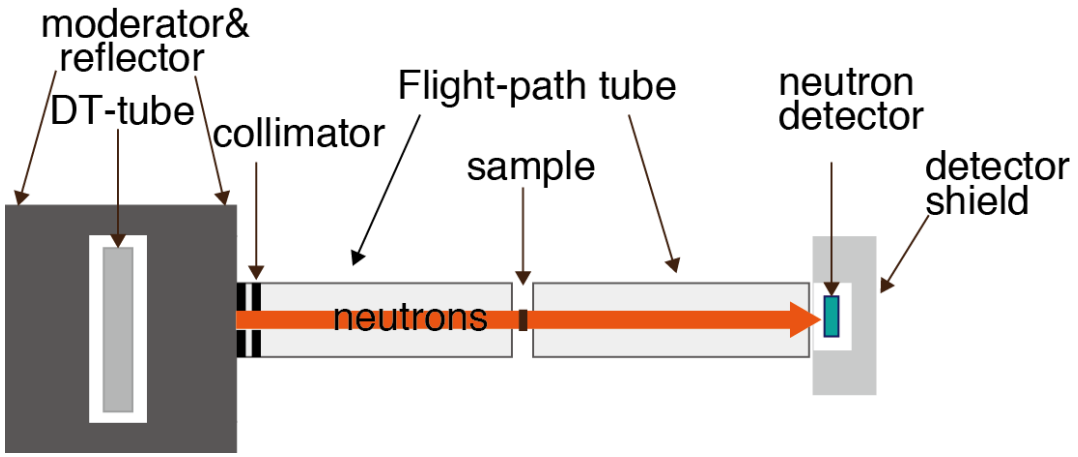

Figure 2: Schematic design of a NRTA facility

3. Feasibility study of NRTA with a short flight path

3. 1. Achievable statistical uncertainty on SNM quantification

Kitatani et al. [13] studied the performance of a NRTA system for the characterization of debris of melted fuel considering a facility with a 5 m flight path. They considered a sample using the composition of a typical spent fuel pin from a light water reactor and added 10 wt% of ^{nat}B and 10 wt% of ^{56}Fe as matrix material. They estimated the uncertainty on the areal number density of ^{235,238}U and the main Pu isotopes due to counting statistics for a neutron intensity between 10^8 and 10^{11} s^{-1}. From the results in Table 2 in Kitatani et al. [13], one can conclude that for a 24 h measurement the uncertainty ranges from 0.19% (0.06%) to 18% (5.3%) for a neutron emission rate of 10^8 s^{-1} (10^9 s^{-1}). Given the assumptions made by Kitatani et al [13], similar uncertainties can be expected for the system described in section 2.2.

3. 2. Pulse width effect on a TOF spectrum

One of the main drawbacks for NRTA applications of the DT generator, as described in section 2.2, is the 10 μs pulse width. To study the impact of such a pulse width, experiments have been carried out at the electron LINAC of the Kyoto University Research Reactor Institute (KURRI). Detailed information on the KURRI-LINAC is available from Ref. [14] and references therein. It offers a pulsed white neutron source covering a region from thermal energy up to a few MeV.

TOF transmission spectra were taken using a pulsed electron beam with a varying width of 0.1, 1, 2 and 4 μs. The transmission sample was a 0.15-mm thick ^{nat}U metallic foil with an effective area of 4 cm x 2 cm. To estimate the background a 0.02-cm thick In and 0.025-cm thick Ag filter were placed in the beam. A 1-cm thick Pb filter was used to reduce the background due to both the γ-ray flash and 2.2 MeV γ-rays from the neutron moderation process. The sample and the filters were located half-way between the neutron source and the neutron detector. The neutrons transmitted through the sample and the filters were detected by a Li-glass scintillation detector (GS-20; 95% enriched in ^{6}Li). The Li-glass scintillator has a volume of $10\times10\times1$ cm^3. The detector was installed 7.3 m away from the neutron source.

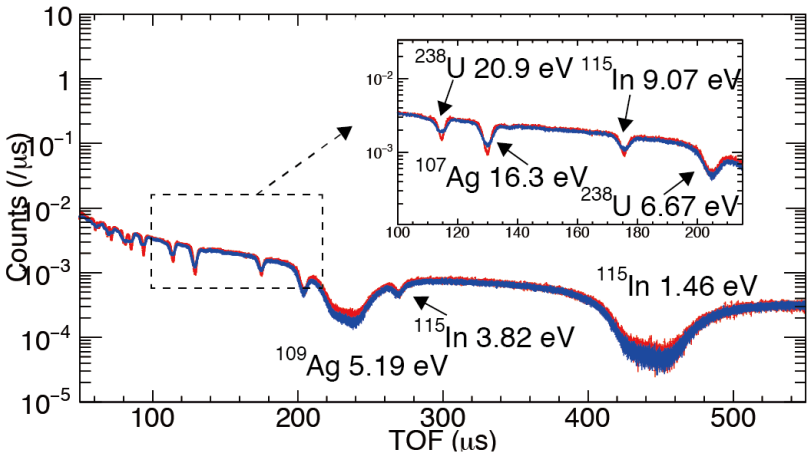

Figure 3: Comparison of TOF spectra with a neutron pulse width of 1 μs (red) and 4 μs (blue). Horizontal and vertical axes show TOF in μs and counts per μs TOF respectively. The counts were normalized by total neutron counts detected in each experiment by a BF_3 monitor located at the measurement hall.

Figure 3 compares the TOF spectra with a pulse width of 1 μs (red) and 4 μs (blue). Resonance dips due to the presence of the U sample and filters can be observed in the two spectra. The saturated dips around 450 μs and 240 μs in TOF were caused by the In and Ag black resonance filters, respectively.

For a TOF > 180 μs, i.e. neutron energies < 8 eV, no clear differences between the spectra taken with a different pulse width are observed. For TOF < 180 μs the influence of the increasing pulse width is obvious. To quantify the impact of the pulse width the transmission dips were fitted using the sum of a Gaussian distribution and a linear function. The parameters of the analytical expression were adjusted in a fit to the experimental data. The results of this fit, i.e. the amplitude (dip) and width (FWHM), are summarized in Table 1. The results in Table 1 are the values of the dips (D) and width (W) relative to those obtained from the measurements with a 0.1-μs pulse width. Evidently the observed width increases and the dip decreases with increasing pulse width and the effect is more pronounced at higher energies.

	^{238}U (6.67 eV)		^{115}In (9.07 eV)		^{107}Ag (16.3 eV)		^{238}U (20.9 eV)	
Pulse	W	D	W	D	W	D	W	D
1 μs	0.99±0.01	0.95±0.07	1.07±0.02	0.93±0.05	1.04±0.01	0.96±0.05	1.06±0.02	0.84±0.03
2 μs	1.00±0.01	0.77±0.05	1.11±0.02	0.77±0.04	1.09±0.01	0.83±0.04	1.16±0.02	0.69±0.03
4 μs	1.10±0.02	0.83±0.05	1.50±0.03	0.72±0.03	1.46±0.01	0.71±0.03	1.82±0.03	0.57±0.02

Table 1: The width (W) and depth (D) of the observed resonance profiles for the resonances at 6.67 eV, 9.07 eV, 16.3 eV and 20.9 eV. The values for a pulse width of 1 μs, 2 μs and 4 μs are given relative to those for a pulse width of 0.1 μs.

4. Summary

To determine the amount of SNM and MA in a variety of nuclear materials, including those from the next generation fuel cycles such as fuel from nuclear transmutation, a new NDA system will be developed that includes a compact NRTA facility. Expected uncertainties due to counting statistics were estimated based on a system with a 5 m flight path length. In addition, the influence of the width of the pulsed charged particle beam was studied using TOF-spectra obtained from measurements with a width of 0.1 μs, 1 μs, 2 μs and 4 μs. These

results can be used to verify the performance of a compact NRTA facility using a DT neutron generator.

5. Acknowledgements

J. Hori and T. Sano kindly supported the experiments at KURRI.

References

[1] Schillebeeckx P., Becker B., Harada H. and Kopecky S., "Neutron Resonance Spectroscopy for the Characterisation of Materials and Object", Report EUR 26848 EN.

[2] Priesmeyer H.G. and Harz U., Atom-kernenergie **25**; 109-113, 1975.

[3] C.D. Bowman, R.A. Schrack, J.W. Behrens and R.G. Johnson, "Neutron resonance transmission analysis of reactor spent fuel assemblies", Neut. Radiography, 503-511, 1983.

[4] J.W. Behrens, R.G. Johnson and R.A. Schrack, "Neutron resonance transmission analysis of reactor fuel samples", Nuclear technology 67 162-168, 1984.

[5] Noguere G., Cserpak F., Ingelbrecht C., Plompen A.J.M., Quetel C.R. and Schillebeeckx P., Nucl. Instr. Meth. **A575,** 476-488, 2007.

[6] Mondelaers W. and Schillebeeckx P., "GELINA, A neutron time-of-flight facility for high-resolution neutron data measurements", Notiziario Neutroni e Luce di Sincrotrone, 11(2), 19 – 25, 2006.

[7] K. Koizumi, F. Kitatani, H. Harada, J. Takamine, M. Kureta, M. Seya, H. Tsuchiya and H. Iimura, "Proposal of Neutron Resonance Densitometry for Particle Like Debris of Melted Fuel using NRTA and NRCA", Proc. of INMM 53, 2012.

[8] Harada H., Kitatani F., Koizumi M., Tsuchiya H., Takamine J., Kureta M., Iimura H., Seya M., Becker B., Kopecky S. and Schillebeeckx P., Proc. of ESARDA35, 2013.

[9] Schillebeeckx P., Abousahl S., Becker B., Borella A., Harada H., Kauwenberghs K., Kitatani F., Koizumi M., Kopecky S., Moens A., Sibbens G. and Tsuchiya H., ESARDA Bulletin 50, 9 – 17, 2013.

[10] Becker B., Kopecky S., Harada H. and Schillebeeckx P., "Measurement of the direct particle transport through stochastic media using neutron resonance transmission analysis", Eur. Phys. J. Plus 129, 58 – 59, 2014.

[11] Harada H., Kimura A., Kitatani F., Koizumi M., Tsuchiya H., Becker B., Kopecky S. and Schillebeeckx P., "Generalized analysis method for neutron resonance transmission analysis", J. Nucl. Sci. Techn., 52, 837 – 843, 2015.

[12] Kureta M. et al., contribution to this ESARDA Symposium.

[13] F. Kitatani, H. Harada, J. Takamine, M. Kureta and M. Seya, "Uncertainty assessment of neutron resonance transmission analysis using the linear absorption model", J. Nucl. Sci. Technol., 51, 1107-1113, 2014.

[14] T. Kubota, N. Abe, J. Hori and T. Takahashi, "Generation of low-energy electron beam using KURRI-LINAC", Proc. of Linear Accelerator Conference LINAC2010, 67-69, 2010.

Techniques of Neutron Resonance Capture Analysis and Prompt Gamma-ray Analysis for Active Neutron NDA

Mitsuo KOIZUMI[1], Harufumi Tsuchiya[1], Fumito Kitatani[1], Masatoshi Kureta[1], Michio Seya[1], Hideo Harada[2], Jan Heyse[2], Stefan Kopecky[2], Willy Mondelaers[2], Carlos Paradela[2], Peter Schillebeeckx[2]

[1]Japan Atomic Energy Agency (JAEA)
Tokai-mura, Naka-gun, Ibaraki 319-1195, Japan
E-mail: koizumi.mitsuo@jaea.go.jp

[2]EC-JRC-IRMM
Unit D.4. Standards for Nuclear Safety, Security and Safeguards
Retieseweg 111, B-2440 Geel, Belgium
E-mail: peter.schillebeeckx@ec.europa.eu

Abstract:

Active non-destructive assay (NDA) techniques utilizes elementary particles (such as photons and neutrons) to induce nuclear reactions in sample objects. Materials in an object are deduced from measured particles coming out of them. Techniques of neutron resonance capture analysis (NRCA) and/or prompt gamma-ray analysis (PGA) are methods of measurement of neutron induced gamma rays from sample objects. These techniques are useful to identify elements (interacting nuclides) in an object without opening it. That would be potentially useful to investigate some suspicious objects relevant to CBRN (Chemical, Biological, Radiological and Nuclear) materials as well as explosives. In this paper, we review NRCA and PGA for identification of materials in objects.

Keywords: Non-destructive assay (NDA); neutron resonance capture analysis (NRCA); prompt gamma-ray analysis (PGA); neutron resonance densitometry (NRD)

1. Introduction

Active non-destructive assay (NDA) techniques utilizes elementary particles (such as photons and neutrons) to induce nuclear reactions in sample objects. Materials in an object are deduced from measured particles coming out of them. As an active NDA, some of the authors have developed a method called neutron resonance densitometry (NRD) [1-6] for quantification of special nuclear materials (SNMs) in particle like debris with a pulsed neutron beam in a collaboration between the JAEA and the JRC-IRMM. This method is a combination of neutron resonance transmission analysis (NRTA) [7-9], and neutron resonance capture analysis (NRCA) [7-9] or prompt gamma-ray analysis (PGA).

In NRTA, neutron transmission is measured as a function of neutron energy with a time-of-flight (TOF) technique. Characteristic neutron absorption dips of Pu and U isotopes are observed at the neutron energy range of 1-50 eV [10, 11], which is achievable with a short-flight-path TOF system. Strong gamma-ray radiation from debris samples does not interfere in measurements. Instead, containing materials may absorb neutrons and distort NRTA spectra. Those containments, however, could not be identified because they do not resonantly absorb neutrons in the energy range of the spectra. Thus, techniques of NRCA/PGA were introduced to identify containing isotopes in the samples from gamma ray emission induced by neutron capture reactions.

In this paper, we review the methods and techniques on NRCA and PGA showing some experimental results obtained in a collaboration of the JAEA and JRC-IRMM [1-6]. These techniques are useful to identify elements in an object without opening it. An idea of investigation method with NRCA/PGA for suspicious objects relevant to CBRN (Chemical, Biological, Radiological and Nuclear) materials and explosives is mentioned.

2. Techniques of NRCA and PGA

2.1 General description

Observation of capture/prompt gamma-ray is complicated as Fig. 1 shows. A certain portion of the incident neutrons passes through the materials without any reaction. The other portion of them causes nuclear reactions: elastic/inelastic scattering, fission, capture, and the other nuclear reactions. Gamma rays emitted in nuclear reactions are called prompt gamma rays. The nuclear reactions are caused by the incident neutrons as well as by the secondary neutrons coming after scattering and the other nuclear reactions. Such secondary neutrons increase with the thickness of the materials [7-9].

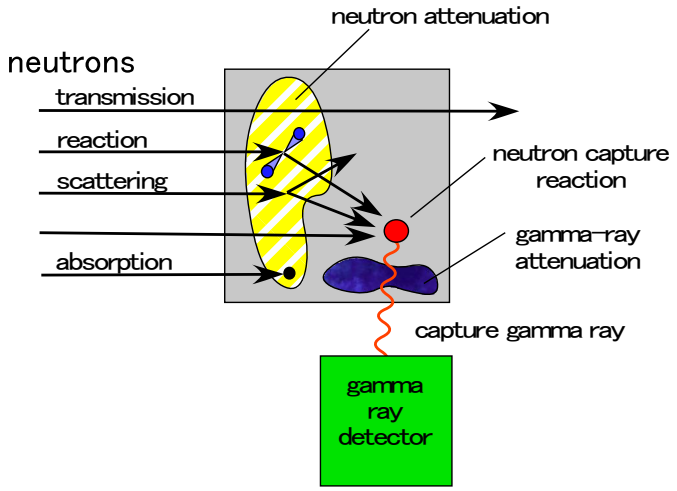

Figure 1: A conceptual view of prompt gamma-ray measurement.

Capture gamma rays from a nuclide is characterized by their energies and intensities, which are determined by its nuclear structure. In PGA measurement, a high energy resolution detector, such as a Ge detector, is used to obtain a gamma-ray energy spectrum. The energies of the observed peaks are clues for identification and quantification of the interacting nuclei.

The strength of gamma rays also depends on neutron capture gamma interaction cross section, which varies as the neutron kinetic energy. The resonance structures of cross section differ for each nuclide. Therefore, a TOF technique can be applied to measure the nuclear interaction profiles of materials from the resonance structure, and to determine the composing nuclides. In NRCA experiments, pulsed neutrons produced at a neutron source travel in a flight path to reach an experimental apparatus as schematically shown in Fig. 1, where capture gamma rays are measured with a fast response detector, such as a C_6D_6 liquid scintillator, to make a TOF spectrum. The kinetic energy of a neutron is deduced from the flight length and the flight time, i.e., the time difference between the pulsed neutron production and the gamma-ray detections.

The energies and intensities of capture gamma rays and neutron capture gamma reaction cross sections are found in tables for each nuclide, e.g. Ref. [12] and [13], respectively.

Simultaneous measurement of gamma-ray energy and detection time enables us to combine PGA and NRCA, TOF-PGA [14]. The resolving power can be improved by a multiple-dimension spectrum obtained by the event-by-event analysis of simultaneously recorded gamma-ray energies and a detection time, i.e., TOF.

A characteristic capture gamma-ray emission yield $Y_{k,\gamma}(E_n)$ of a nuclide k is expressed as a sum of the yield of primary and secondary neutrons, $Y_{k,\gamma}(E_n)$ and $Y'_{k,\gamma}(E_n)$, respectively [7-9]. The secondary component is due to a capture reaction after at least one neutron scattering event, and neutron-emission reactions.

$$Y_{k,\gamma}(E_n, \boldsymbol{r}) = Y_{k,\gamma}(E_n, \boldsymbol{r}) + Y'_{k,\gamma}(E_n, \boldsymbol{r}),$$

where E_n is an energy of neutrons. The primary capture gamma-ray emission yield $Y_\gamma(E_n, \boldsymbol{r})$ at the position ***r*** is given by:

$$Y_{k,\gamma}(E_n, \boldsymbol{r}) = \phi_n(\boldsymbol{r}) I_\gamma \cdot \rho_k(\boldsymbol{r}) \cdot \bar{\sigma}_{k,\gamma}(E_n),$$

where I_γ is the emission probability of the gamma-ray γ, $\rho_k(\boldsymbol{r})$ the density of a nuclide *k*, and $\bar{\sigma}_{k,\gamma}(E_n)$ Doppler broadened capture cross section, and $\phi_n(\boldsymbol{r})$ the neutron flux at the position ***r***.

The total gamma-ray detection efficiency is also an important factor in experiments: that is determined by the solid angle, gamma-ray attenuation in the sample materials, and the efficiency of the detector. Figure 2 shows attenuation coefficients μ of photons in elements [15]. The incident photon intensity I_o with an energy *E* is attenuated in a material following the exponential law: $I(E) = I_0(E)\exp[-(\mu(E)/\rho)t]$, where *t* and *ρ are* the thickness *and* density *of* a layer of the material. Because the attenuation coefficients decreases with the photon energy, gamma-rays are easily penetrates materials in comparison with low energy gamma rays and x-rays. At the photon energy around 1.5 MeV, the attenuation coefficients become approximately 0.05 cm^2/g. The thicknesses of some materials are given in Table 1. For example, a 4-cm Pb plate attenuates the intensity of 1.5-MeV gamma ray to be 1/10.

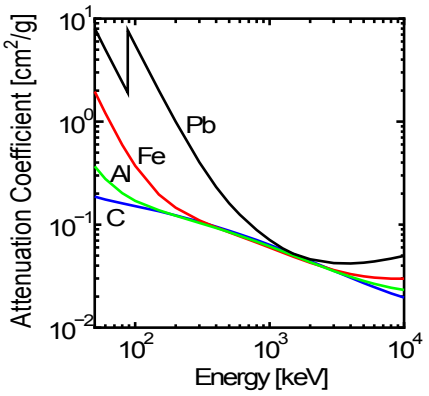

Figure 2: Attenuation coefficients of photons in materials.

material	density [g/cm^3]	Thickness of 0.05 cm^2/g
carbon	2.26	8.8 cm
Al	2.70	7.4 cm
Fe	7.87	2.5 cm
Pb	11.34	1.8 cm

Table1: Densities of various materials.

2.2 Measurement of a thin uniform samples

For a parallel uniform neutron beam penetrating a homogeneous sample material, the primary capture gamma-ray emission yield $Y_\gamma(E_n)$ is given by:

$$Y_{k,\gamma}(E_n) = \phi_0 I_\gamma \left(1 - e^{-\sum_j n_j \cdot \bar{\sigma}_{j,tot}(E_n)}\right) \frac{n_k \cdot \bar{\sigma}_{k,\gamma}(E_n)}{\sum_j n_j \cdot \bar{\sigma}_{j,tot}(E_n)},$$

where $\bar{\sigma}_{j,tot}(E_n)$ the Doppler broadened total cross section of nuclides *j*. In case of very thin samples and/or small total cross sections, the capture gamma emission is approximated to a proportional function to the capture cross section $\bar{\sigma}_{k,\gamma}(E_n)$ and the areal density $\mathrm{n}_k = \rho_k \cdot \mathrm{t}$, where *t* is the thickness of the sample. For relatively thick samples, secondary neutrons contribute to the yield $Y_{k,\gamma}(E_n)$ and complicate the analysis [7, 8]. If the gamma-ray attenuation effect in the sample is negligible small, the experimentally observed gamma-ray yield can be described by $Y_{exp,k,\gamma}(E_n) = A\,(1 - \exp(-B \cdot \mathrm{n}_k))$. Once the relation of the curve is determined, the areal density of a sample can be deduced from a measured gamma-ray yield.

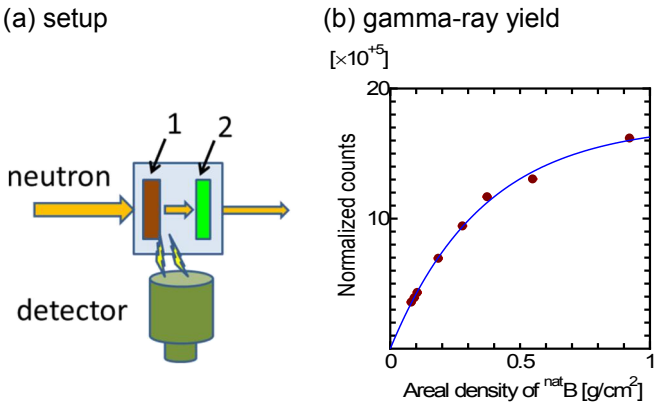

Figure 3: (a) Schematic drawing of the experimental setup of a black box measurement. (b) A gamma-ray yield.

A black box experiment was carried out with an apparatus placed in an experimental hall at the 13-m flight path of GELINA, a pulsed neutron TOF facility of JRC-IRMM [16]. Figure 3 (a) shows a schematic drawing of the experimental setup. An $LaBr_3$ scintillation detector was introduced for the gamma-ray measurements, because of its better energy resolution and fast decay time [17]. An about 10-cm cubic aluminum box was prepared as a black box, in which eight sample plates can be stored. Gamma-ray yields induced by $^{10}B(n, \alpha\gamma)$ reaction were measured. Thin aluminum containers are used to store B_4C powder. The 478-keV gamma-ray peaks from ^{10}B were clearly observed. Figure 3(b) shows the result of the measurements. The peak yields were normalized with the counts of a neutron flux monitor. The abscissa is the total areal density of ^{nat}B in the black box. The data points are fitted with a function of $Y_{exp,\gamma}(x) = A\,(1 - \exp(-B \cdot \mathrm{x}))$. The areal density of ^{nat}B of an unknown B_4C sample plates, thus, can be deduced with the curve.

A demonstration experiment with the black box was performed in a workshop on neutron resonance densitometry (NRD) [18]. Some participants secretly chose sample plates to make a black box; the available choices were Fe, Ni, Cr, B, Gd, and Hf. The box was then sealed and brought to the measurement position. Figure 4 (a) and (b) are the spectra obtained. Identification of Ni, Hf, and Gd samples were successfully done, proving the ability of elemental identification in unknown objects.

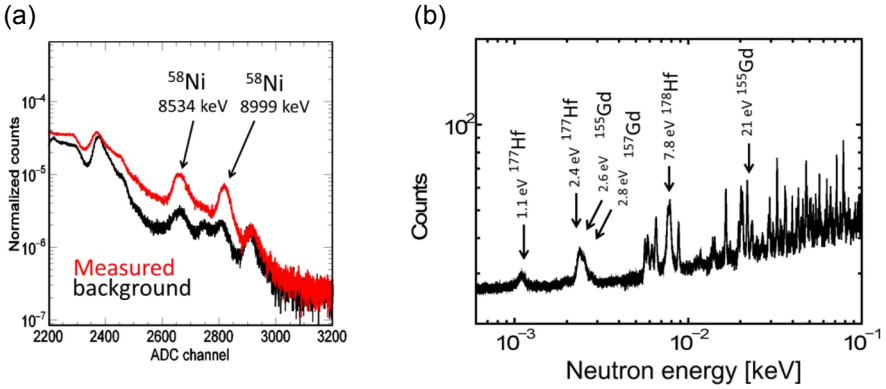

Figure 4: (a) A gamma-ray spectrum. (b) A TOF spectrum. Identification of some peaks is given in the spectra.

Quantification of nuclides in a complex sample is, however, difficult. Figure 5(a) shows an experimentally determined function of the 478-keV gamma-ray yields to the areal density of ^{nat}B; the curve is the same as that of Fig. 3(b). From a gamma-ray count, for example, we can deduce the areal density as shown by the red pint in Fig 5(a). However, the value is the lower limit because unknown attenuation materials can be in front of the boron sample as shown in Fig. 3(a). To determine the upper limit, transmission measurement should be coupled.

Figure 5(b) shows calculated transmission spectra of a spent fuel sample plus boron with different areal density: 0 cm, 1 cm, and 2 cm. The isotopic composition is taken from a UO_2 fuel (3.9 wt% ^{235}U) after a burn-up of 40 GWd/Mt [19]. In the spectra, resonant boron absorption does not appear.

Analyzing the existing dips, we can determine the areal densities of Uranium and Plutonium isotopes. Transmission of a sample containing only those isotopes can be reproduced as given by the black line of Fig. 5(b). The additional attenuation effect due to ^{10}B and the other matrix material is calculated by the comparison of the calculated and the measured spectra. The maximum limit of the areal density of boron is deduced from the base line decrease by an assumption that the additional attenuation effect is only due to boron. The upper limit of the areal density is in this way calculated: the green dashed line in Fig. 5(a) show the upper limit obtained.

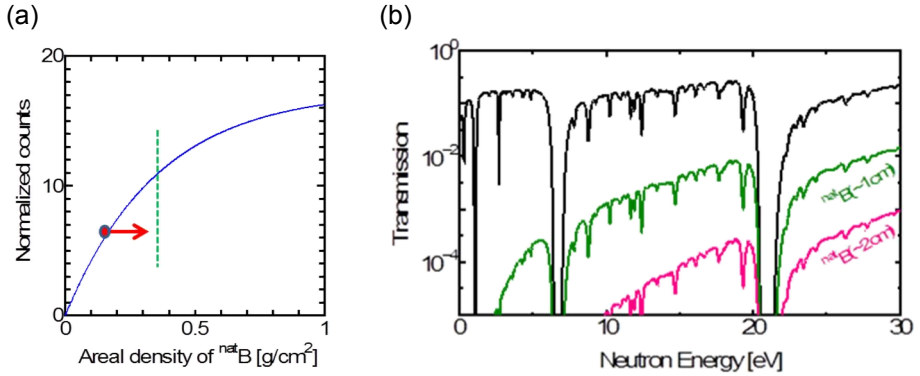

Figure 5: (a) Experimentally determined relation between ^{nat}B areal density and 478-keV gamma-ray counts. (b) Calculated transmission spectra of a 1-cm-thick spent fuel sample plus boron plate with different thicknesses.

3. Nuclear Security Applications of NRCA/PGA

Detection of CBRN materials and explosives are one of the topics of security guard. X-ray inspection stems are installed in any airport. Conventional X-ray techniques are useful for investigation of shapes of the contained objects quickly. The contrast of the images depends on the elements mass attenuation coefficients as shown in Fig. 2. However, the techniques could not distinguish nearby elements because of their similar attenuation coefficients. Element specific techniques must be introduced to inspect the objects. Accordingly, it is desirable to introduce an NDA technique to investigate the materials in a suspicious object.

Neutron interrogation techniques are, therefore, worth to be applied. As discussed above, a neutron penetrates materials, cause nuclear characteristic reaction, and then induce gamma-ray emissions. Figure 6 is a conceptual drawing of an inspection system of a doubtful object. A collimated neutron beam is installed. Prompt gamma rays and transmission neutrons are measured separately. The collimator of the gamma-ray detector eliminates the inspecting position. Figure 7 schematically shows positional dependence of elementally characteristic gamma-ray yields. Since incident neutron beam comes from the left side of the plot, the neutron attenuation effect causes the reduction of the gamma-ray yields. The gamma rays from ^{14}N are due to the explosive materials. Generally, most commercial products do not contain little nitrogen, and only explosive materials and fertilizers do. Although the spatial resolution of this method is low, combining other imaging techniques, the details of the unknown object would be revealed.

One disadvantage of this method is the strong nuclear-depend sensitivity. In case of boron, only 1-cm plates reduce the neutron flux 1/10 -1/100 at the neutron energy below 30 eV as shown in Fig. 5(b), while the main attenuation effect is due to ^{10}B, of which abundance is 19.9%. Oppositely, some material is rather transparent to neutrons.

When neutron attenuation is too large to investigate unknown objects, fast neutron beam would be useful to penetrate and probe the objects. It also opens the other reaction channels such as (n, n'γ), (n, p γ), etc. [20]. While this method may reduce the signal intensity, background reduction techniques with TOF and/or multiple gamma-ray coincidence techniques [14] would improve the elemental identification ability.

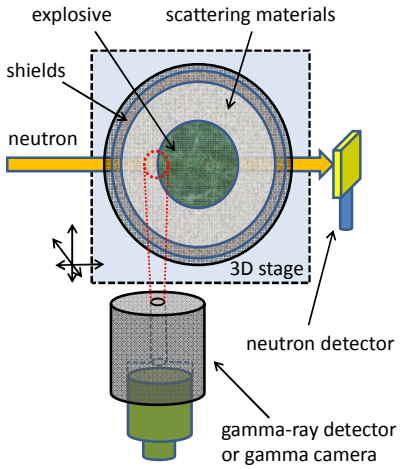

Figure 6: A conceptual drawing of an inspection system. Scattering materials can be shrapnel (metal fragments) of a bomb, radioactivity, or nuclear materials (NMs) of a dirty bomb.

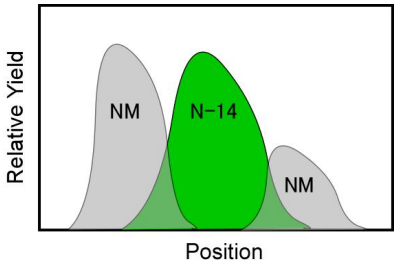

Figure 7: Relative gamma-ray yield for each nuclide. The abscissa is the gamma-ray detector position of Fig. 6.

4. Summary

In this reports, we reviewed the techniques of NRCA/PGA showing some experimental results obtained in a collaboration of the JAEA and JRC-IRMM. These techniques are useful to identify elements in an object without opening it. That would be potentially useful to investigate some suspicious objects relevant to CBRN materials as well as explosives. A new program of active neutron NDA techniques [21] will start for nuclear security and non-proliferation under the collaboration between the JAEA and JRC. Methods of NRCA/PGA are considered as one category of the techniques to be considered in the project.

5. Acknowledgements

The part of this research and development was supported by the Japanese government (MEXT: Ministry of Education, Culture, Sports, Science and Technology).

References

[1] M. Koizumi, F. Kitatani, H. Harada, J. Takamine, M. Kureta, M. Seya, H. Tsuchiya, H. Iimura, *“Proposal of Neutron Resonance Densitometry for Particle Like Debris of Melted Fuel using NRTA and NRCA”, Proc. of INMM* 53, 2012.

[2] P. Schillebeeckx, S. Abousahl, B. Becker, A. Borella, F. Emiliani, H. Harada, K. Kauwenberghs, F. Kitatani, M. Koizumi, S. Kopecky, A. Moens, M. Moxon, G. Sibbens, H. Tsuchiya, “Development of Neutron Resonance Densitometry at the GELINA TOF Facility”, ESARDA Bulletin 50, 2013, 9-17

[3] B. Becker, H. Harada, K. Kauwenberghs, F. Kitatani, M. Koizumi, S. Kopecky, A. Moens, P. Schillebeeckx, G. Sibbens, H. Tsuchiya, *“Particle Size inhomogeneity Effect on Neutron Resonance Densitometry”, ESARDA Bulletin* 50, 2013, 2-8.

[4] F. Kitatani, H. Harada, J. Takamine, M. Kureta, M. Seya, *“Uncertainty assessment of neutron resonance transmission analysis using the linear absorption model”, J. Nucl. Sci. Technol.*, 51, 2014, 1107-1113

[5] H. Harada, A. Kimura, F. Kitatani, M. Koizumi, H. Tsuchiya, B. Becker, S. Kopecky, P. Schillebeeckx, *“Generalized analysis method for neutron resonance transmission analysis”, J. Nucl. Sci. Technol.* 52, 2015, 837–843.

[6] P. Schillebeeckx, B. Becker, H. Harada and S. Kopecky, *"Neutron Resonance Spectgroscopy for the Characterization of Materials and Objects", JRC Science And Policy Report in 2014.*

[7] H. Postma and P. Schillebeeckx, *"Neutron Resonance Capture and Transmission Analysis", Encyclopedia of Analytical Chemistr*y (John Wiley \& Sons Ltd), 2009, 1-22.

[8] P. Schillebeeckx,A. Borella, F. Emiliani, G. Gorini, W. Kockelmann, S. Kopecky, C. Lampoudis, M. Moxon, E. Perelli Cippo, H. Postma, N.J. Rhodes, E.M. Schooneveld and C. Van Beveren, *"Neutron resonance spectroscopy for the characterization of materials and objects", Proc. of The 2nd International Workshop on Fast Neutron Detectors and Applications (FNDA2011)* C03009.

[9] P. Schillebeeckx, B. Becker, Y. Danon, K. Guber, H. Harada, J. Heyse, A.R. Junghans, S. Kopecky, C. Massimi, M. Moxon, N. Otuka, I. Sirakov and K. Volev, *"Determination of Resonance Parameters and their Covariances from Neutron Induced Reaction Cross Section Data", Nucl. Data Sheets* 113, 2012, 3054-3100.

[10] C.D. Bowman, R.A. Schrack, J.W. Behrens, and R.G. Johnson, *"Neutron Resonance Transmission Analysis of Reactor Spent Fuel Assemblies," in Neutron Radiography,* Barton, J. P. and von der Hardt, P., eds., ECSC, EEC, EAEC, Brussels, Belgium and Luxembourg, 1983, 503-511.

[11] J.W. Behrens, R.G. Johnson and R.A. Schrack, *Nuclear Technology,* 67, 1984, 162-168.

[12] J.K. Tuli, and B.Pritychenko, BNL, National Nuclear Data Center, http://www.nndc.bnl.gov/capgam/.

[13] Nuclear Data Center, Japan Atomic Energy Agency, http://wwwndc.jaea.go.jp/jendl/jendl.html.

[14] Y. Toh, M. Ebihara, A. Kimura, S. Nakamura, H. Harada, K.Y. Hara, M. Koizumi, F. Kitatani, and K. Furutaka, *"Synergistic Effect of Combining Two Nondestructive Analytical Methods for Multielemental Analysis", Anal. Chem.* 86, 2014, 12030–12036.

[15] J. H. Hubbell and S. M. Seltzer, *"Tables of X-Ray Mass Attenuation Coefficients and Mass Energy-Absorption Coefficients from 1 keV to 20 MeV for Elements Z = 1 to 92 and 48 Additional Substances of Dosimetric Interest", NISTIR* 5632, (http://www.nist.gov/pml/data/xraycoef/, Online: May 1996).

[16] W. Mondelaers and P. Schillebeeckx, *"GELINA, a neutron time-of-flight facility for high-resolution neutron data measurements", Notiziario Neutroni e Luce di Sincrotrone,* 11, 2006, 19-25.

[17] R. Nicolini, F. Camerar, N. Blasi, S. Brambilla, R. Bassini, C. Boiano, A. Bracco, F.C.L. Crespi, O. Wieland, G. Benzoni, S. Leoni, B. Million, D. Montanari, A. Zalite, *Nucl. Instru. Meth. in Phys. Reseach* 582, 2007, 554-561.

[18] Workshop on Neutron Resonance Densitometry (NRD), (4-5 March 2015, Geel Belgium) (https://www.jaea.go.jp/04/iscn/activity/2015-03-04/index.html).

[19] Y. Ando and H.Takano, *"Estimation of LWR Spent Fuel Composition*", JAERI-Research 99-004, 1999.

[20] G. Vourvopoulos and P.C. Womble, *Pulsed fast/thermal neutron analysis: a technique for explosives detection*, Talanta, 54, 2001, 449-468.

[21] M. Kureta, M. Koizumi, A. Ohzu, K. Furutaka, M. Seya, H. Harada, S. Abousahl, J. Heyse, S. Kopecky, W. Mondelaers, B. Pedersen, and P. Schillebeeckx, *Introduction of JAEA-JRC Collaboration on Development Active Neutron NDA Techniques, Proc. of ESARDA 37*, 2015.

Characterization of special nuclear material by neutron resonance spectroscopy

C. Paradela[1], G. Alaerts[1], B. Becker[1], J. Heyse[1], S. Kopecky[1], W. Mondelaers[1], P. Schillebeeckx[1] and R. Wynants[1]

H. Harada[2], F. Kitatani[2], M. Koizumi[2], M. Seya[2] and H. Tsuchiya[2]

[1]European Commission, Joint Research Centre, Geel site
Unit D.4. Standards for Nuclear Safety, Security and Safeguards,
Retieseweg 111, B- 2440 Geel, Belgium
E-mail: carlos.paradela@ec.europa.eu

[2]Japan Atomic Energy Agency (JAEA)
Tokai-mura, Naka-gun, Ibaraki 319-1195, Japan

Abstract:

Neutrons can be used as a tool to study materials and objects. Cross sections of neutron induced reactions show characteristic resonance structures which can be used as fingerprints to determine the elemental and isotopic composition of materials and objects. They are the basis of two analytical methods which have been developed at the European Commission's Joint Research Centre in Geel (BE): Neutron Resonance Capture Analysis (NRCA) and Neutron Resonance Transmission Analysis (NRTA). The first technique is based on the detection of gamma rays emitted during a neutron capture reaction in the sample being studied; the latter determines the fraction of neutrons transmitted through a sample positioned in a neutron beam. They rely on well-established methodologies in neutron resonance spectroscopy.

It has been shown that NRCA is a useful technique to determine the composition of archaeological objects. In contributions to a previous ESARDA symposium in Bruges the use of NRTA to characterize particle-like debris of melted fuel that is formed in severe nuclear accidents has been presented. However, the discussion was primarily based on theoretical studies. In this contribution the performance of NRTA as a non-destructive method to determine the amount of fissile material is discussed based on measurements carried out at the time-of-flight facility GELINA using reference materials containing uranium and plutonium. The results of these experiments demonstrate that the relative amount of special nuclear material in particle like debris can be derived absolutely without the need of calibration materials with an uncertainty less than 2%, even in the presence of strong neutron absorbing matrix materials.

Keywords: non-destructive assay; time-of-flight; resonance analysis; melted fuel; severe accidents; nuclear safeguards; transmission; neutron resonance transmission analysis; GELINA

1. Introduction

Neutron Resonance Transmission Analysis (NRTA) and Neutron Resonance Capture Analysis (NRCA are based on the presence of resonance structures in the cross sections of neutron induced reactions [1]. Since resonances are observed at energies which are specific for each nuclide, they can be used as fingerprints to determine the elemental and isotopic composition. Both NRCA and NRTA are non-destructive methods, which determine the bulk elemental composition, do not require any sample preparation and result in a negligible residual activation. They are applicable to almost all medium-weight and heavy elements.

At the previous ESARDA Symposium Neutron Resonance Densitometry (NRD) has been introduced as a non-destructive analysis (NDA) method to characterize particle-like debris of melted fuel resulting from severe accident, such as happened in the Fukushima-Daiichi nuclear power plants [2,3]. NRD relies on a combination of NRTA and NRCA. In this contribution, we focus on the principles of NRTA and on the progress that has been made to apply NRTA as an absolute method to determine the amount of fissile and fertile materials in debris of melted fuel. The use of NRCA combined with Prompt Gamma-ray Analysis (PGA) for the characterization of melted fuel debris is discussed in another contribution to this symposium [4].

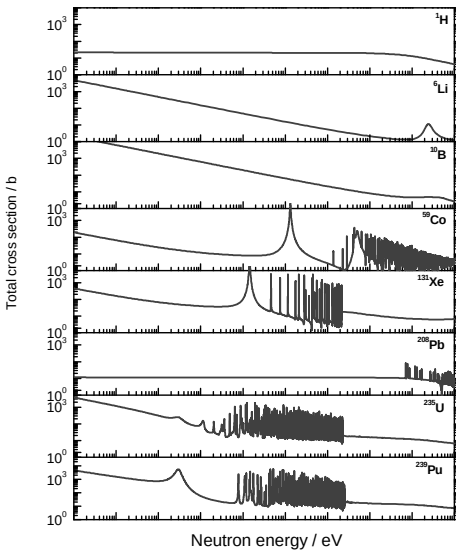

Figure 1: Total cross section as a function of neutron energy for neutron induced reactions in ^{1}H, ^{6}Li, ^{10}B, ^{60}Co, ^{131}Xe, ^{208}Pb, ^{235}U and ^{239}Pu.

2. Basic principles of NRTA

NRTA is a NDA method based on the time-of-flight (TOF) measurement technique. It relies on well-established principles and methods for nuclear cross section measurement, which have been reviewed in Ref. [5]. NRTA is based on the analysis of characteristic dips in a transmission spectrum that can be obtained from a measurement of the attenuation of the neutron beam by a sample. These dips are observed at TOF values corresponding to resonance energies in the total cross sections which are shown in Fig.1.

2.1. Time-of-flight measurements

An accurate knowledge of the energy of the neutron inducing a reaction in the sample is required to make use of the resonance structures in neutron induced reaction cross sections for material analysis. For a quantitative analysis covering a wide range of elements, TOF measurements at an accelerator-based pulsed white neutron source are preferred [1].

Experimentally, the time-of-flight t_m is derived from the difference between a stop (T_s) and a start signal (T_0). The start signal is produced by the pulsed charged particle beam. The stop signal in a transmission experiment (NRTA) is provided by the neutron detector. The time-of-flight t that a neutron needs to travel a distance L can be related to the velocity v of the neutron at the moment it leaves the neutron producing target and enters the detector [1,5]:

$$v = \frac{L}{t} = \frac{L}{t_m - (t_t + t_d)}, \qquad (1)$$

where t_t is the time the neutron spends in the neutron producing target and t_d the time it spends in the neutron detector. For low-energies, the non-relativistic expression suffices to relate the neutron energy E to the time t and distance L by:

$$E = \frac{1}{2}m\left(\frac{L}{t}\right)^2 = \frac{1}{2}m\left(\frac{L}{t_m - (t_t + t_d)}\right)^2, \qquad (2)$$

where m is the rest mass of the neutron.

For the analysis of TOF data the response function of the TOF-spectrometer is required. The response function $R(t_m,E)$ expresses the probability that a neutron with energy E produces a measured TOF t_m. This response is a convolution of different components due to the parameters L, t_m, t_t and t_d in Eq. 2. The distance L can be determined by metric measurements with an uncertainty smaller than 1 mm. The contribution due to the TOF depends on the broadening of T_0,T_s, t_t and t_d. In case of a moderated neutron beam, the broadening in time is dominated by the neutron transport in the target-moderator assembly, i.e. the component t_t. This component is mostly represented by introducing an equivalent distance L_t which is in first approximation independent of the neutron energy [1,5]. In case of transmission measurements the transport time in the detector is also represented by an equivalent distance L_d [1,5].

In first approximation the energy resolution ΔE can be described by the broadening due to the time-of-flight (Δt) and distance (ΔL):

$$\frac{\Delta E}{E} = \frac{2}{L}\sqrt{(v\Delta T_0)^2 + (v\Delta T_s)^2 + \Delta L_t^2 + \Delta L_d^2}, \qquad (3)$$

where the broadening due to the parameters L, T_0, T_s, t_t and t_d are denoted by ΔL, ΔT_0, ΔT_s, ΔL_t and ΔL_d, respectively. Eq. 3 shows that the broadening decreases with increasing distance. Since the neutron beam intensity decreases quadratically with increasing distance a compromise between resolution and intensity has to be made.

2.2. Transmission experiment

In a NRTA experiment the observed quantity is the fraction of the neutron beam traversing the sample without any interaction. For a parallel neutron beam which is perpendicular to a slab of material, this fraction or transmission T is given by:

$$T(E) = e^{-\sum_k n_k \bar{\sigma}_{tot,k}(E)}, \quad (4)$$

where $\bar{\sigma}_{tot,k}$ is the Doppler broadened total cross section and n_k is the number of atoms per unit area (or areal number density) for nuclide k. Hence, knowing the cross sections, one can derive the areal number density from the transmission.

Experimentally the transmission T_{exp} is obtained from the ratio of the counts of a sample-in measurement C_{in} and a sample-out measurement C_{out}, after subtraction of the background contributions B_{in} and B_{out}, respectively:

$$T_{exp} = \frac{C_{in} - B_{in}}{C_{out} - B_{out}}. \quad (5)$$

The spectra in Eq. 5 are corrected for losses due to the dead time of the detector and electronics chain. All spectra are normalized to the same intensity of the neutron beam and TOF bin width. The background is determined by an analytical expression applying the black resonance technique. A detailed discussion on the background determination can be found in Ref. [5].

Eq. 5 shows that the experimental transmission is independent of both the detector efficiency and incoming neutron flux. Therefore, a transmission measurement is an absolute measurement which does not require additional calibration experiments using representative samples or any reference to a standard cross section. In addition, the experimental observable T_{exp} (Eq. 5) is a direct measure of the theoretical transmission (Eq. 4) if the measurements are performed in a good transmission geometry, which implies that:

- the sample is perpendicular with respect to a parallel incoming neutron beam;
- all neutrons that are detected have passed through the sample;
- neutrons scattered by the sample are not detected.

The conditions of an ideal or good transmission geometry can be achieved by a proper collimation of the neutron beam at the sample and detector position. However, it also requires a homogeneous sample.

2.4. Data analysis

The areal number densities $n_{1,...,p}$ of the nuclides present in the sample can be derived by a least squares fit, that is by minimizing the expression:

$$\chi^2(n_{1,..,p}) = (T_{exp} - T_M)^T \, V_{T_{exp}}^{-1} \, (T_{exp} - T_M), \quad (6)$$

where T_M is a model describing the experimental observable. The theoretical estimate T_M is the result of a folding to account for the response function of the TOF spectrometer:

$$T_M(t_m) = \frac{\int R(t_m, E)\, e^{-\sum_{k=1}^{p} n_k \bar{\sigma}_{tot,k}(E)} \, dE}{\int R(t_m, E)\, dE}. \quad (7)$$

The theoretical model depends on resonance parameters and experimental parameters. The resonance parameters are used to parameterize the cross sections by the R-matrix theory. The experimental parameters include e.g. the detector and sample characteristics including sample temperature and the areal number densities $n_{1,...,p}$ of the nuclides present in the sample.

The least squares fit can be performed by a resonance shape analysis (RSA) code, such as REFIT [6]. This code, which has been developed to parameterize cross section data in terms of resonance parameters, is based on the Reich-Moore approximation [7] of the R-Matrix formalism [8]. It accounts for various experimental effects such as Doppler broadening and the response of the TOF spectrometer and detectors. Examples of the use of REFIT for NRTA are given in Refs. [1,9,10,11,12].

3. Challenges to characterize particle-like debris of melted fuel

Neutron Resonance Densitometry (NRD) has been proposed as a method to quantify special

nuclear material (SNM) in particle-like debris of melted fuel formed in severe nuclear reactor accidents [2,3]. The quantification of the fissile material is based on NRTA. The potential of NRTA as a NDA method for the characterization of fresh and spent fuel has already been demonstrated by Priesmeyer and Harz [13] and Behrens et al. [14]. Noguere et al. [11] applied NRTA to characterize a PbI_2 sample that was produced from a solution of radioactive waste originating from waste of a reprocessing facility.

The samples analysed in Refs. [11,13,14] were homogeneous samples with a regular shape. The analysis of particle like debris samples of melted fuel is far more complex and challenging due to their characteristics, in particular:

1. the diversity in shape and size of particle like debris samples;
2. the presence of neutron absorbing impurities (e.g. ^{10}B);
3. the overlapping of resonances;
4. the sample temperature;
5. the radioactivity of the sample.

To study and solve these problems the Japan Atomic Energy Agency (JAEA) and the Joint Research Centre of the European Commission (JRC) started a collaboration in 2012. The progress made on points 1-3 within this collaboration is summarized in this paper. This progress strongly relies on theoretical studies which were validated by experiments at GELINA. A detailed description of this facility is given in Ref. [15].

Studies for a better understanding of the impact of the sample temperature and radioactivity of the sample are part of a next collaborative effort that is also discussed in a contribution to this workshop [16].

4. Results of the JAEA/JRC collaboration

4.1. Diversity in shape and size of particle like debris samples

Analytical expressions for homogeneous samples with irregular shapes have been proposed by Harada et al. [17]. A main difficulty for an unbiased analysis of transmission data of particle like debris samples is to account for their heterogeneous character. For such samples Eq. 7 is not valid. Algorithms that can be applied to characterize heterogeneous samples, have been extensively studied by Becker et al. [18,19].

In Ref. [18] several numerical benchmarks were produced by creating stochastic geometries using Monte Carlo methods. The transmission through these geometries was then calculated assuming that the particle consisted of a mixture of uranium and plutonium oxide. Six different analytical models were applied when adjusting the areal density. Using the model proposed by Kopecky et al. [20] or the LP model of Ref. [21] the quality of the fit significantly improved compared to the assumption of a homogeneous sample.

To validate the analytical models experimentally, transmission measurements were performed on a sample consisting of a mixture of tungsten and powder sample. The measurements were performed at a 25 m transmission station of GELINA. Details on this measurement station are given in Ref. [22].

The results of the measurements on the mixed powder sample reveal that by applying the LP model bias effects due to the variety in shape and size of the samples can be reduced to less than 2% [19]. Supposing a homogeneous model, i.e. neglecting the particle size distribution, the areal density was underestimated by 15%.

4.2. Presence of strong neutron absorbing matrix material

It is expected that the analysis of the amount of SNM in the melted fuel debris samples will be complicated due to the presence of water, boron, concrete, structural materials and in particular boron. Some of them are important neutron absorbers and their content is not well established. Therefore, the transmission will be strongly influenced by the attenuation of the neutron beam by the presence of these elements as illustrated in Fig. 2.

Unfortunately, light elements such as ^{10}B do not have resonances in the low energy region. To account for the contribution of such strong absorbing matrix material a method has been proposed and validated in Ref. [1]. The influence of these materials can be taken into account by lumping their contribution to the transmission introducing a single cross section of a dummy element X. The energy dependence of this cross section is expressed as:

$$n_X \sigma_{tot} = a_X + \frac{b_X}{v}. \qquad (8)$$

with a_X and b_X parameters which can be adjusted in a fit to the experimental data.

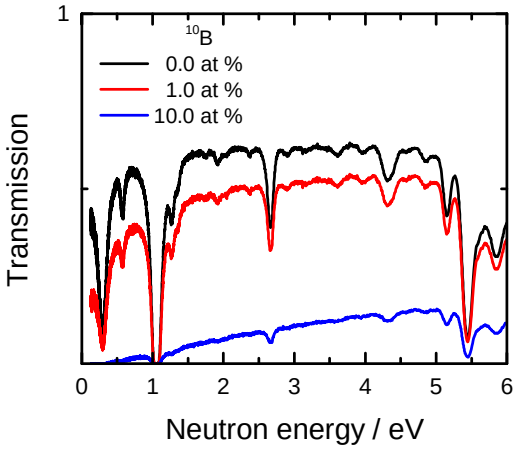

Figure 2: Transmission through a 2.5 cm thick sample with a composition similar to that of spent fuel and with different amounts of ^{10}B (0, 0.1, 1 and 10 at %).

This procedure was validated by transmission measurements using a U_3O_8 reference sample with reference CBNM446 [23]. The sample was enriched to 4.515 at% in ^{235}U. The areal density of ^{235}U and ^{238}U and corresponding ^{235}U/^{238}U ratio was determined by an analysis of transmission data obtained at a 25 m station of GELINA.

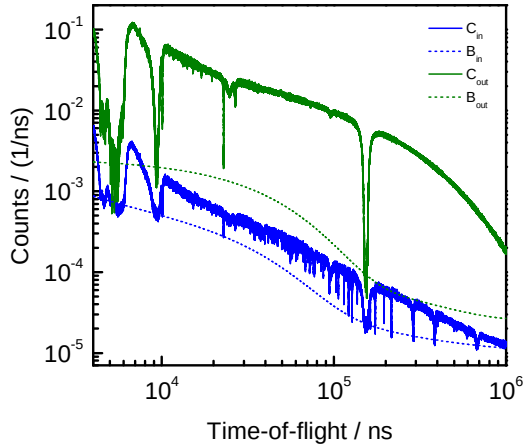

Figure 3: TOF-spectra measured at GELINA of the reference sample (C_{in}) and of an aluminum dummy sample (C_{out}).

The sample contains a substantial amount of EPOXY that led to a strong attenuation of the incident neutron beam, i.e. to an extreme low transmission baseline of about 0.0085. Figure 3 shows the strong attenuation due to the EPOXY matrix. Obviously it is not an ideal sample to determine the amount of ^{235}U and ^{238}U by NRTA. On the other hand, it is ideal to validate the procedure to account for the presence of matrix material that cannot be identified and quantified by neutron resonance analysis.

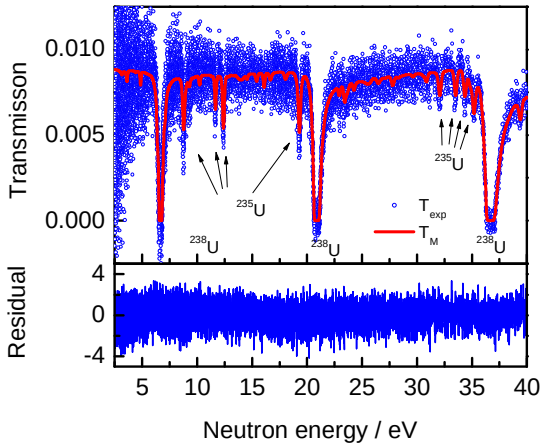

Figure 4: Experimental transmission (top) through the reference sample CBNM466 together with the result of the resonance analysis with REFIT (red curve). The fit residual is shown at bottom.

The transmission in Fig. 4, derived from the data in Fig. 3, reveals that transmission dips due to ^{235}U and ^{238}U resonances can be clearly resolved and analysed.

The areal densities of ^{235}U and ^{238}U resulting from a least squares fit with REFIT to this transmission are reported in Table 1. In the fit the parameters a_X and b_X, which account for the matrix material, were also adjusted. The results in Table 1 reveal that the NRTA results are in agreement with the reference values within the quoted uncertainties. The resulting isotopic ratio ^{235}U/^{238}U = 0.0475±0.0008 is in very good agreement with the certified value 0.04729 ± 0.000003. The quoted uncertainties are only due to counting statistics.

	U_3O_8 Reference samples EC NRM 171	
	Declaration	NRTA
^{235}U	(5.0326±0.0080) 10^{-4} at/b	(5.06±0.09) 10^{-4} at/b
^{238}U	(1.0628±0.0015) 10^{-2} at/b	(1.06±0.01) 10^{-2} at/b

Table 1: Areal densities of ^{235}U and ^{238}U resulting from the fit to the experimental transmission, compared to the reference values.

4.3. Overlapping of resonance dips

A final industrial NRTA system will be based on a relatively short flight path (≤ 10m), which limits the resolution of the TOF-spectrometer. Therefore, the analysis of the experimental transmission will be complicated due to overlapping resonance dips resulting from elements with a high level density in the low

energy region, i.e. uranium, plutonium, minor actinides and fission products.

To verify the performance of NRTA under such conditions, a demonstration experiment was organized at the 10 m transmission station of GELINA. This demonstration experiment was organized as part of a Workshop on Neutron Resonance Densitometry that was organized at the JRC Geel site in the framework of the JAEA/JRC collaboration.

Figure 5: Photo of the sample changer and detector of the 10 m transmission station at GELINA.

The samples are placed in an automatic sample changer, which is positioned at 7.7 m from the target. This sample changer can also be used to mount background filters. Neutrons passing through the sample and filters are detected by a Li-glass scintillator, placed at 11 m distance from the neutron producing target. The detector is a 6.35 mm x 76 mm x 76 mm Li-glass scintillator, which is enriched to 95 % in ^{6}Li and directly viewed by one photomultiplier tube. To minimize the background from neighbouring beam lines, the detector was placed inside a shielding structure composed of lead and borated polyethylene. A photo of the sample changer and detector is shown in Fig. 5.

Mostly measurements are performed with the accelerator operated at 800 Hz and either a ^{10}B or 4 mm thick Cd overlap filter is used to eliminate slow neutrons from the previous burst. The use of ^{10}B filters reduces significantly the beam intensity at low neutron energies. Therefore a Cd filter is used to study the energy region between 1 eV and 60 eV. For energies above 60 eV, however, it is better to use a ^{10}B filter due to the presence of strong cadmium resonances. Therefore, the transmission station is equipped with a double overlap filter which can be exchanged to cover the whole energy range of interest. Moreover, measurements with a low operating frequency (50 Hz) can be carried out to investigate materials in the thermal regions.

During the Workshop on Neutron Resonance Densitometry a "blind" experiment was carried out. Three participants (from DOE, IAEA and DG-ENER respectively) were asked to assemble a test sample. To do this an inventory of 18 different samples in the form of metallic discs was available. Because the use of radioactive fuel components was not feasible due to radioprotection, different samples of medium-weight elements (Cu, Co, Mn, Nb and Rh) and heavy elements (W and Au) with different thicknesses were made available. These elements were chosen based on their characteristic resonances in the eV range in order to mimic the resonance structure of the fuel components. In addition, one of the cobalt samples was drilled to artificially reproduce the effect of inhomogeneities present in the melted fuel debris. Finally, two strong neutron absorbing B_4C samples where also made available.

To perform these measurements a special aluminum sample box has been designed that could contain up to 8 samples. The selected samples were placed in the box, which was completely closed and sealed by the DG-ENER representative.

After a 14-hours transmission measurement the transmission data were analysed by using the AGS data analysis [24] and REFIT resonance analysis codes [6], together with the up-to-date total cross sections in the nuclear data libraries. The resonance analysis method consists on partial fits on the most significant resonances of the transmission spectrum. The final composition of the sample was obtained following an iterative procedure that determines the areal density of each component. The results of the analysis were presented during the workshop and compared to the expected composition, which was kept hidden in a sealed envelope. The results obtained by NRTA were compatible to the nominal sample composition within 2% for all the components.

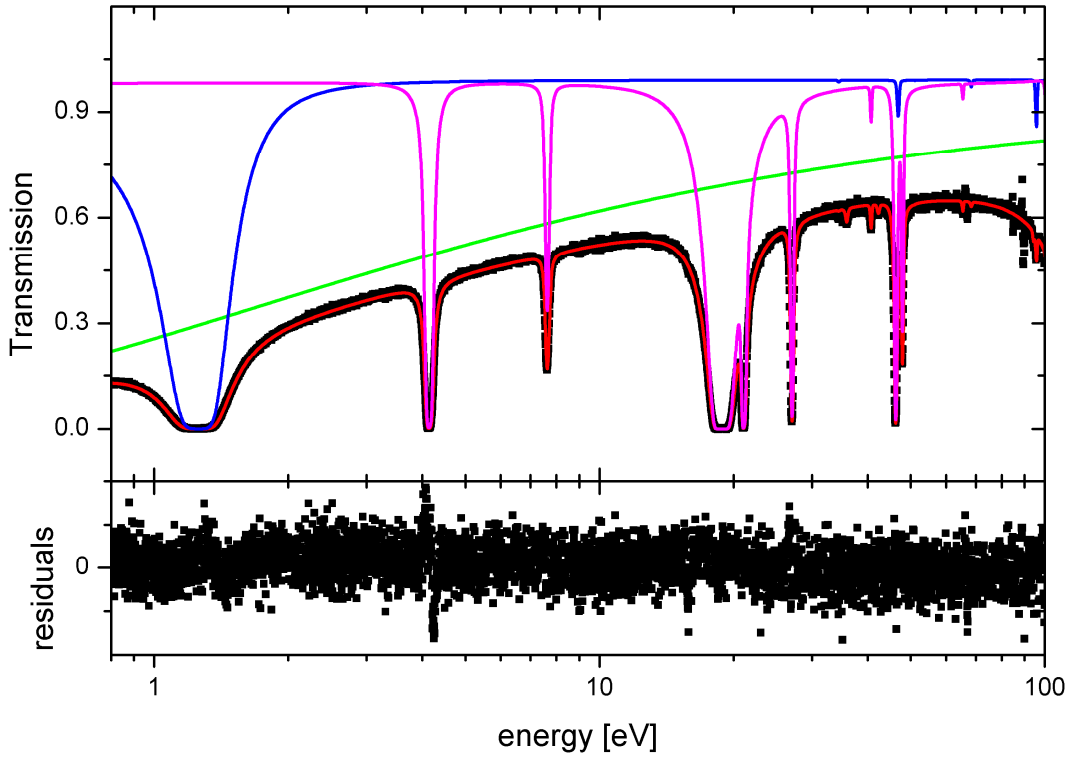

Figure 6: REFIT result for the "blind" measurement performed during the Workshop on Neutron Resonance Densitometry. The red curve shows the total fit; the green curve accounts for the B_4C presence in the sample and the resonance structure in this energy range is due to the rhodium (blue) and tungsten (magenta) contributions.

5. Summary and conclusions

A method, referred to as Neutron Resonance Transmission Analysis (NRTA), has been described. The method, which relies on the appearance of resonance structures in neutron induced reaction total cross section, has been applied for the characterization of melted fuel that is formed after a severe nuclear accident. The basic principles have been explained and special challenges related to measurements of particle-like debris have been presented.

The experimental programme developed at JRC Geel to validate the NRTA capabilities has been described and the main results concerning the resonance analysis in the presence of multiple isotopic contributions and of strongly absorbent matrix materials have been shown. This R&D programme, which is part of a collaboration between JAEA and JRC, strongly relies on measurements at the time-of-flight facility GELINA.

6. Acknowledgements

This work is part of a collaboration between the Japan Atomic Energy Agency (JAEA) and Joint Research Centre (JRC) in the field of nuclear materials safeguards research and development.

7. References

[1] Schillebeeckx P., Becker B., Harada H., Kopecky S., *Neutron Resonance Spectroscopy for the Characterisation of Materials and Objects*, Report EUR 26848 EN.

[2] Harada H., Kitatani F., Koizumi M., Tsuchiya H., Takamine J., Kureta M., Iimura H., Seya M., Becker B., Kopecky S., Schillebeeckx P., Proc. of ESARDA35 (2013).

[3] Schillebeeckx P., Abousahl S., Becker B., Borella A., Harada H., Kauwenberghs K., Kitatani F., Koizumi M., Kopecky S., Moens A., Sibbens G. and Tsuchiya H., ESARDA Bulletin 50, 9 – 17 (2013)

[4] Koizumi M. et al., contribution to this ESARDA Symposium.

[5] Schillebeeckx P., Becker B., Danon Y., Guber K., Harada H., Heyse J., Junghans A.R., Kopecky S., Massimi C., Moxon M.C., Otuka N., Sirakov I., Volev K., Nuclear Data Sheets **113**, 3054-3100, 2012.

[6] Moxon M.C., Brisland J.B., AEAInTec-0630, AEA Technology, October, 1991.

[7] Reich C.W., Moore M.S., Phys. Rev. **111,** 929-933, 1958.

[8] Lane A.M. and Thomas R.G., R-matrix theory of nuclear reactions, Rev. Mod. Phys. 30, 257 – 353 (1958).

[9] Schillebeeckx P., Borella A., Drohe J.C., Eykens R., Kopecky S., Massimi C., Mihailescu L.C., Moens A., Moxon M., Wynants R., Nucl. Instr. Meth. **A613**, 378-385, 2010.

[10] Schillebeeckx P., Borella A., Emiliani F., Gorini G., Kockelmann W., Kopecky S., Lampoudis C., Moxon M., Perelli Cippo E., Postma H., Rhodes N.J., Schooneveld E.M., Van Beveren C., *JINST* **7,** C03009, 2012.

[11] Noguere G., Cserpak F., Ingelbrecht C., Plompen A.J.M., Quetel C.R., Schillebeeckx P., Nucl. Instr. Meth. **A575,** 476-488, 2007.

[12] Tsuchiya H., Harada H., Koizumi M., Kitatani F., Takamine J., Kureta M., Iimura H., Kimura A., Becker B., Kopecky S., Kauwenberghs K., Mondelaers W. and Schillebeeckx P. *Impact of systematic effects on results of neutron transmission analysis*. Nucl. Instr. Meth. Phys. Res. A 767, 364 – 371 (2014)

[13] Priesmeyer H.G., Harz U., Atomkern-energie **25**; 109-113, 1975.

[14] Behrens J.W., Johnson R.G., Schrack R.A., *Nuclear Technology* **67**, 162-168, 1984.

[15] Mondelaers W. and Schillebeeckx P., GELINA, *A neutron time-of-flight facility for high-resolution neutron data measurements*, Notiziario Neutroni e Luce di Sincrotrone, 11(2), 19 – 25 (2006).

[16] Kureta M. et al., contribution to this ESARDA Symposium.

[17] Harada H., Kimura A., Kitatani F., Koizumi M., Tsuchiya H., Becker B., Kopecky S. and Schillebeeckx P., *Generalized analysis method for neutron resonance transmission analysis*, J. Nucl. Sci. Techn., 52, 837 – 843 (2015).

[18] Becker B., Kopecky S., Harada H. and Schillebeeckx P., *Measurement of the direct particle transport through stochastic media using neutron resonance transmission analysis*, Eur. Phys. J. Plus 129, 58 – 59 (2014)

[19] Becker B., Harada H., Kauwenberghs K., Kitatani F., Koizumi M., Kopecky S., Moens A., Schillebeeckx P., Sibbens G., Tsuchiya H. ESARDA Bulletin 50, 2-8 (2013)

[20] Kopecky S., Siegler P. and Moens A., *Low energy transmission measurements of ^{240,242}Pu at GELINA and their impact on the capture width*, Proc. Int. Conf. Nuclear Data for Science and Techn., Nice, France, April, 2007, pp. 623 – 626

[21] Levermore C.D., Pomraning G.C., Sanzo D.L., Wong J., *Linear transport theory in a random medium*, J. Math. Phys. 27, 2526 – 2536 (1986).

[22] Lampoudis C., Kopecky S., Bouland O., Gunsing F., Noguere G., Plompen A. J. M., Sage C., Schillebeeckx P. and Wynants R., *Neutron transmission and capture cross section measurements for ^{241}Am at the GELINA facility*, Eur. Phys. J. Plus 128, 86 – 105 (2013)

[23] De Bievre P., Eschbach H.L., Lesser R., Meyer H., Van Audenhove J. and Carpenter B.S. Joint Research Centre Report COM 4153 (1985).

[24] Becker B., Bastian C., Emiliani, F., Gunsing, F., Heyse J., Kauwenberghs K., Kopecky S., Lampoudis C., Massimi C., Otuka N., Schillebeeckx P., and Sirakov I., JINST 7-11 (2012) P11002 .

Session 18

Destructive Analysis Measurements

Semi-Automatic Separation Unit for Actinides at JRC-ITU and IAEA

Razvan Buda, Steven De Vry Balsley*, Lorenza Emblico, Andreas Schachinger*, Evelyn Zuleger

Institute for Transuranium Elements
Joint Research Centre, European Commission
Karlsruhe, Germany
* International Atomic Energy Agency | IAEA Laboratories,
Seibersdorf, Austria
E-mail: razvan.buda@ec.europa.eu

Abstract:

High accuracy is required for analysis of nuclear safeguards and forensic samples. The best precision can be obtained by use of the Isotope Dilution Mass Spectrometry method. Separation of actinides is performed on chromatographic columns as sample preparation step for mass spectrometry measurements. The chromatographic separation is a time consuming process which, if performed manually, necessitates the constant presence of an operator.
A semi - Automatic Separation Unit (ASU) was developed by JRC-ITU in collaboration with the IAEA as an alternative to manual separations under the EC support task to the IEA EC A-1391. It is already in use in the JRC-ITU and in cold testing for the LSS, La Hague and at SAL, IAEA. A fourth unit will be produced for the OSL Sellafield.
The main features of ASU are its modular construction for simple replacement of components, minimum need for operator intervention, a light structure from materials resistant to acid environment and a remote control function over a LabView based software. A detailed report of the experience with ASU in JRC-ITU laboratories is presented.

Keywords: actinide separation, semi-automated unit

1. Introduction

Proper safeguarding of nuclear material depends on precise analyses of samples taken in key points of processes at nuclear facilities. One of the most accurate methods for analyses of nuclear samples is the Isotope Dilution Mass Spectrometry (IDMS) [1]. The technique uses mass spectrometers like the Thermal Ionisation Mass Spectrometry (TIMS) to determine the content of plutonium and uranium in various matrixes with uncertainties below 0.28% expressed as relative combined standard uncertainty as requested by the International Target Values (ITV) of the ESARDA working group [2].

The samples need several specific treatments before the measurement by TIMS can be performed. One of the steps is the chemical separation of plutonium and uranium in fractions from other trivalent actinides and/or fission products using chromatographic columns. This step is necessary for removing the isotopes that could bias the results by isobaric interferences like $^{241}Am/^{241}Pu$ or $^{238}Pu/^{238}U$ and at the same time removing the high radiation doses from the samples. The radiation doses released by samples taken from the input tanks at reprocessing plants are particularly high due to the highly energetic gamma radiation of the fission products. Even after dilution to reach the Pu and U concentration levels typically used for mass spectrometric analyses (ppm levels) the doses of such an input sample can reach 300 – 400 µSv/h/mL. The separations are performed simultaneously on several samples, grouped in one "*run*"; it usually takes around ninety minutes to complete a run. Even though the operations are carried out in glove boxes shielded with lead glass screens, the radiation doses are elevated especially for the hands of the operators. One possibility to reduce the radiation dose intake by the operators and at the same time increase efficiency of work is replacing the manual work by an automated or semi-automated device.

A semi-Automated Separation Unit (ASU) was developed by the Joint Research Centre, Institute for Transuranium Elements (JRC-ITU) in collaboration with the International Atomic Energy Agency (IAEA) in an attempt to tackle the challenges indicated above. The current

paper describes the criteria used in the design and the main features of the ASU.

2. Materials and design

After the past experience of JRC-ITU with more elaborated commercial automated systems it became clear that a right balance had to be found for a system which could fulfil the purposes without being too complicated and sensitive to the harsh environment of the glove boxes. Due to the inevitable extensive use of HNO_3 in the chemical preparation of the samples for MS analyses the environment is rather corrosive in the glove boxes. The space is a further limitation in the glove boxes. Thus, the following criteria were considered when drafting the outlines for the automatic separation unit. It had to be robust, easy to use, resistant to acidic environment and within a relatively low budget.

The concept was made such as to reduce as much as possible the number of parts that have to be introduced in the glove box. Plexiglas and Teflon were found as the most suitable materials for the construction of the unit body that is introduced in the glove box. The power transmission is ensured through commercially available parts which are made out of aluminium. The design was made modular such that all critical parts can be easily replaced at a turn of a few screws. This allows shortening the downtime intervals to perform reparations when necessary.

One further factor that was considered in the design was the high costs of radioactive liquid waste produced during the process. Therefore, the volumes of solutions introduced in the glove box are strictly those which are used in the separation. A syringe pump is used to transfer liquid in the glove box. The software reduces the amount of liquid introduced in the glove box by priming the external ducts and the syringe and dispensing these “dead” volumes to a container outside the glove box. The diameters of the tubes were also chosen such as to have the minimum amount of “dead” volumes inside the glove boxes.

The production of the system consisted of two parts: the hardware design and construction and the writing of the software. The two parts are described below.

2.1. Hardware

The parts of the system are:

2.1.1. The X/Y axis mobile unit

The unit was designed and constructed in JRC-ITU mechanical workshop using Plexiglas and Teflon for the waste collection tray as shown in Fig. 1. Two stepper motors enable the X and Y axis movement by means of toothed drive belt axes (produced by Festo [3]). At the extremities of the axes there are proximity switch sensors, which prevent the motion beyond the axes termination points.

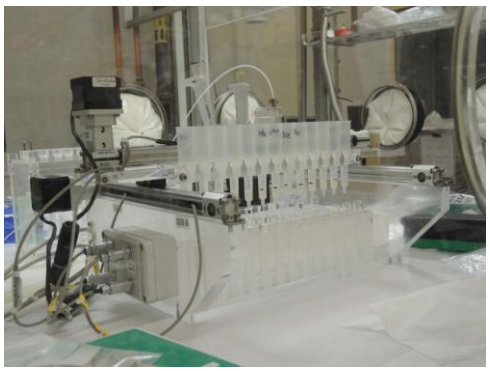

Figure 1: The separation unit inside the glove box. The two stepper motors for the axis movement can be seen on the left side, together with the electrical connections. The dispenser head is moving on top of the columns to dispense the reagents

A waste tray is located between two collection racks. The racks are manually fed with the containers used for the collection of the separated U and Pu fractions. The amount of samples that can be processed simultaneously varies between 12 and 20, depending on the laboratory convenience i.e. the setup of the samples flow, which is mostly imposed by the capacity of the type of mass spectrometer used. A further column is used as a "waste funnel" while the system is filling the line with a new

eluant. The liquid waste is gravimetrically drained to a collection container.

2.1.2. The glove box adapter

The interface between the inside and outside of the glove box is shown in Fig. 2. The control cables for the stepper motors and for the proximity switch sensors as well as the tube used to transfer the reagents from the pump to the dispenser head are fed through using this system.

Figure 2: The glove box adapter

2.1.3. Liquid dispenser system

A Duratec PSD/3 [4] mini syringe pump equipped with a Hamilton eight ports valve and connected to a computer by means of a serial cable provides for the liquid transfer to the main unit in the glove box. The valve has ceramic coating to avoid corrosion. The syringe is also produced by Hamilton and has a volume of 1.25 mL.
The syringe pump picks up the required reagents from side reservoirs and dispenses the pre-set volumes on the columns during the separation. A PTFE tube is used for the dispensing of reagents. The PSD/3 mini dispenser is configurable and different tubes sizes, valves and syringes can be used if necessary.

2.1.4. Motion controllers

National Instruments [4] electronic components are used for the motion control. They consist of a PCI board 7334 installed in the computer and of a motion control interface *UMI 7774* equipped with stepper motor and limit switch controllers. A dedicated power supply is required for the UMI and the connection between the UMI and the PCI board inside the PC requires specific National Instruments cables. The UMI is fixed preferably under the glove box.

2.1.5. Computer

A computer is required to manage the ASU. The computer casing shall be large enough to accommodate a *PCI 7334* [5] board and a serial port for the pump connection.

2.2. Software

The control software was written with the LabView System Design Software [5]. The control computer does not need the installation of LabView program; merely the executable is sufficient for the operation of the system. Currently the computer runs using Windows 7 Professional and the control software was developed by IAEA.

The software enables the configuration of the hardware parameters, e.g. the tubes' lengths and diameters, the position of the racks relative to the "home" position, or the reagents associated to the different valve ports. These steps are necessary when setting up the system or after changing components and resetting is necessary. The software can be used in a manual modus to command the movement of the X and Y axes to predefined positions.

Apart from the hardware setup, the software controls the separation. Different programs like plutonium-uranium either independent or cumulated or rinsing of tubes are saved in the library. The operation of the different programs is described in Chapter 3. Further programs can be easily created and saved.

3. Operating the ASU

ASU is a semi-automatic setup thus, prior to starting the chemical separations ran by the software the following preliminary operations need to be carried out by the analyst manually:
- reagents preparation and filling of the bottles. The type of reagents and the required volumes depend on the type of separation (e.g. Pu, U only or U and Pu together) and on the number of samples to be separated.
- priming the lines between the reagent bottles and the pump. The control software on the computer has a specific function for this task.
- collecting vials must be placed in the racks to collect the separated Pu and/or U fractions. Two collection racks are provided, one in the front to collect Pu fractions and one in the back to collect the U fractions. The waste tray lies between the two collection racks.
- the columns need to be brought in the dedicated positions
- with the columns rack positioned over the waste tray the samples are loaded on the columns.
- while the samples flow through the columns, the software can be set up for the separation, by specifying the number of columns and the required separation sequence. The chosen program can be started by pressing the start button on the interface when the entire volume of the samples has passed through the chromatographic columns.

The separation consists of several consecutive rinsing sequences. The software dispenses predefined volumes of liquid in the chromatographic columns depending on the chosen separation sequence. For the collection of the different fractions, the columns are positioned over the respective racks by the controlling program.

The resin is placed manually into the columns so it is reasonable to assume that the time needed for the same volume of liquid to flow gravimetrically varies strongly from column to column. The software allows for this time to be defined by the operator. It is usually set two minutes longer than the values empirically assessed for the “slowest” column of the series. It is possible to check the progress of the operations on the computer. If needed, the program offers the possibility for the separation to be paused, stopped or shortened by skipping waiting times.

When the separation sequence is started by the operator, the tube from the pump to the dispenser head is filled with the first reagent and then the dispenser moves along the X axis to dispense the required amount of reagent on each column. When it is time to dispense the second reagent, the line is primed automatically by the program with the new eluant.

The most common used programs are Pu or U separation individually or both from the same sample. They are described bellow.

3.1. Plutonium separation

- dispensing of 3 X 2 mL of 6M HNO3 on each column containing the samples with the column rack located over the waste tray; the dispensing of a new liquid fraction will only be performed after the complete dripping of the previous one
- dispensing of 250 µL of Pu eluant (“pre-strip”)
- after the dripping of 250 µL is completed the racks are moved over the pots prepared for the collection of Pu and 800 µL of Pu eluant is dispensed. The Pu fraction is such collected.

3.2. Plutonium and uranium separation

The same sequence as previously described at point 3.1. with the subsequent steps:

- dispensing of 3 X 2 mL of Pu eluant on each column with the column rack located over the waste tray
- dispensing of 250 µL of U eluant (“pre-strip”)
- after the dripping of 250 µL is completed the racks are moved over the pots prepared for the collection of U and 1 mL of U eluant is dispensed on each column. The U fraction is such collected.

3.3. Uranium separation

Although not very common this type of separation can also be performed. The program follows the same sequence as described at point 3.2., but without collecting the Pu fraction.

4. Experience

The first ASU became operational in 2014 in the laboratories of JRC-ITU. It has been used since for routine separations. The first separations were performed on well characterised reference materials. These trials were used for the validation of the proper functioning of the system by comparing the results with those from analyses for samples that were prepared manually.

The unit runs smoothly and silently and once started does not need the intervention or supervision of any operator. The motion of the

mobile parts is at low speed and the power of the step motors is limited so that no hazards are induced by e.g. damaging of glove box parts. The status of the separation is constantly updated and displayed for the operator on the computer screen.

After the demonstration of ASU's capabilities a new unit was produced for the Euratom on-site laboratory run by JRC-ITU in La Hague. The unit is specifically designed to meet the requirements of this site. For this, the maximum amount of samples that can be processed simultaneously is fourteen. The unit has been cold tested in JRC-ITU and is on the process of implementation in La Hague. A further unit will be produced for the Euratom on-site laboratory at Sellafield. For this site, the racks are designed to accommodate a maximum of twenty samples simultaneously.

A further unit was built in Seibersdorf, Austria by the IAEA. Due to logistic constrictions in commissioning the new dedicated glove boxes the ASU could not be yet tested for hot operations. However, it has undergone successfully the cold testing.

5. Conclusions

ASU is a compact, robust and reliable system. It is produced and operates economically and does not pose any hazards to the operators or the operating environment. It reduces considerably the radiation doses received by the analysts. Furthermore, it facilitates the management of the workload to be optimised in order to increase the effective use of manpower in time. This is a significant aspect especially for the on-site laboratories where the manpower is a limiting factor.

One of the critical point in the separation process is the time required for the liquid to flow through the chromatographic column. Particularly when changing the positions of the racks, it is essential to ensure that all the liquid has drained from the top of the resin. The current software uses pre-defined delay intervals for the dispensing of the following sequence. The delays have to be chosen using a very conservative approach to ensure an unproblematic progress of the operations. The total duration of a separation run can therefore be very long. It is foreseen to overcome this problem by implementing an ultra-sonic fill height sensor on the dispensing nozzle. The sensor can provide the actual status of the liquid level in the columns. This information can be processed by the software to shorten unnecessary waiting times automatically. A prototype of this technique is already in the test phase in the laboratories of IAEA. The preliminary results look very promising.

6. Acknowledgements

The authors would like to acknowledge the contribution of Mrs. L. Duinslaeger and Dr. K. Casteleyn who initiated the project, Dr. E. Hrnecek and A. Mavroeidis for preparing the initial version of the system. Furthermore, the authors are very thankful for the support received from the design office, the mechanical and the electrical workshop of JRC-ITU and all those who have reviewed this paper and contributed to its completion.

7. References

[1] E. Zuleger, K. Mayer, L. Duinslaeger, K. Casteleyn. Evaluation of Uncertainties for Pu and U Measurements Achieved in the On-Site Laboratory by Thermal Ionisation Mass Spectrometry during Two Years of Operation, Symposium of International Safeguards, IAEA-SM-367/5/03, Vienna 2001
[2] International Atomic Energy Agency; International Target Values 2010 for Measurement Uncertainties in Safeguarding Nuclear Materials – IAEA/STR – 368; Vienna November 2010
[3] www.festo.com
[4] www.duratec.com
[5] www.ni.com

Implementation of Large-Geometry SIMS for Safeguards: 4 years later

Laure Sangély, Jane Poths, Herbert Siegmund, Thippatai Tanpraphan, Olivier Bildstein, Matvey Aleshin, Axel Schwanhäusser

International Atomic Energy Agency, Vienna International Centre,
A-1400 Vienna, Austria
E-mail: Laure.Sangely@iaea.org, J.Poths@iaea.org

Abstract:

Four years after its installation and validation for the purpose of uranium particle analysis of Environmental Samples, the IAEA's Large Geometry Secondary Ion Mass Spectrometer (LG-SIMS) is regarded as a prominent asset within the Safeguards toolbox. Its improved performance has achieved the goal of precise and accurate minor uranium isotopic results (234U and 236U) on a routine basis. In addition to its excellent performance for destructive isotopic analysis, LG-SIMS advances the state of the art for uranium particle detection and isotopic pre-characterisation capability. This particle screening capability is critical with respect to characterising the entirety of the uranium isotopic signatures captured by Environmental Sampling. Over the past years, a balance has been struck between stability and high performance to allow the operation of LG-SIMS in a production mode. The target of 100 samples analysed per year was reached in 2013 and 2014, with an average instrument availability of >90%. Considerable effort was put into the characterisation and the prevention of instrumental memory effects. Efficient measures were demonstrated and adopted, although a slight reduction of the intrinsic quality of data was observed. A better fixation of particles during sample preparation was identified as an area for future method improvement. An improved scheme for mass bias and detector dead-time corrections would be a further step towards an overall reduction of measurement uncertainties. However, this development is conditional upon the availability of an ad hoc range of certified reference materials (CRMs) in the form of particles of diverse and well-characterized size and chemical composition. Further improvement of data quality would require the development of software tools for real-time, automated optimization of analytical parameters.

Keywords: Environmental Samples; particle analysis; Secondary Ion Mass Spectrometry; minor uranium isotopes

1. Introduction

Shortly after very promising tests were reported by Ranebo et al. in 2009 [1], the Safeguards Analytical Services (SGAS) at the IAEA purchased a Large Geometry Secondary Ion Mass Spectrometer (LG-SIMS instrument, model CAMECA IMS 1280) in replacement of its old conventional instrument (CAMECA IMS 4f). Since then, this instrument has been dedicated to a single application: the detection and the individual analysis for uranium isotopes of the micrometre-sized particles that are collected by Environmental Sampling. This paper provides an overview of the 4 year experience of SGAS with LG-SIMS operation. The initial approach for implementation is presented and put in perspective with the current status of LG-SIMS operation at SGAS. The lessons learnt over the successive development phases, the remaining challenges and ways for future improvement are also discussed.

2. Development of the LG-SIMS project at SGAS

2.1. Goals

The primary goal for SGAS's LG-SIMS instrument was to establish an independent, in-house source for the verification results that are evaluated by the Department of Safeguards in the process of drawing conclusions regarding the completeness of declarations. As part of the initial requirements for LG-SIMS, an emphasis was put on the determination of precise and accurate minor isotopes (234U and 236U) and on the ability to confidently detect and measure the particles revealing the maximum and minimum U-235 enrichment captured by the sample, regardless of the size and frequency of the particles bearing the signature. The expectation is throughput of 100 samples analysed a year with a target response time of 60 and 30 days for routine and high priority samples, respectively.

2.2. Approach

In 2009, most of the 17 LG-SIMS instruments already-installed worldwide were research instruments, each of them performing multiple types of measurements (mainly stable and radiogenic isotopic measurements) on diverse, well-characterized matrices (mainly minerals in the form of polished sections). The overlap between the analytical protocols in use and Safeguards needs was fairly limited. An original approach was followed to develop and validate an analytical method with an emphasis on robustness, reliability, and timeliness with respect to the project schedule. Figure 1 provides a brief overview of the overall process in use at SGAS for particle analysis using LG-SIMS. The transfer of particles from the samples (usually cotton swipes) to the analysis mounts (typically glassy carbon planchets) is based on a fast and straightforward aerosol impaction technique. First, the planchet is screened using an instrument-supplied piece of software (named APM for Automated Particle Measurement) to generate an exhaustive map of the uranium particles deposited on the planchet and an estimate of their respective isotopic abundances [2; 3].

Despite their low precision, screening isotopic results provide valuable insights to the analyst into a range of particles that are critical in terms of Safeguards information and are targeted by subsequent destructive micro-beam analysis for precise and accurate determination of uranium isotopes (so-called microprobe analysis). Analytical conditions are detailed in [4]. In addition to common certified reference materials, the validation plan emphasized the use of a large set of real inspection samples. Moreover, considerable effort was put into the development of a comprehensive uncertainty budget that was designed such as to accommodate the extreme variability of sample and particle characteristics rather than to minimize the general level of final uncertainty. Details of uncertainty calculation are given in [4].

2.3. Milestones

The milestones of the LG-SIMS project between 2009 and 2014 are summarized in table 1. The commissioning of the LG-SIMS was made in two steps. After the factory acceptance tests, the LG-SIMS instrument was operated at the manufacturer's facilities (CAMECA, in Genneviliers, France) during 10 months until a purpose-built building was commissioned (the clean lab extension of the IAEA's laboratories in Seibersdorf). During the period of internal validation (August 2010 to July 2011), inspection samples were processed in parallel using both IAEA's instruments (4f and LG-SIMS). Following its installation in Seibersdorf in April 2011 and the on-site acceptance tests, the LG-SIMS was revalidated so that it was fully operational when the 4f was shut-down on schedule in August 2011. External validation by our customer at the Department of Safeguards was mainly based on comparisons of LG-SIMS with FT-TIMS (Fission Tracks-Thermo-Ionization Mass Spectrometry) results acquired in parallel on sub-samples from identical source [5]. In addition, the participation of SGAS in the NUSIMEP VII proficiency test (organized by the IRMM, Institute for Reference Materials and Measurements, in September 2011) confirmed that the method developed was fit-for-purpose in terms of accuracy, precision, and uncertainty budget [4; 6].

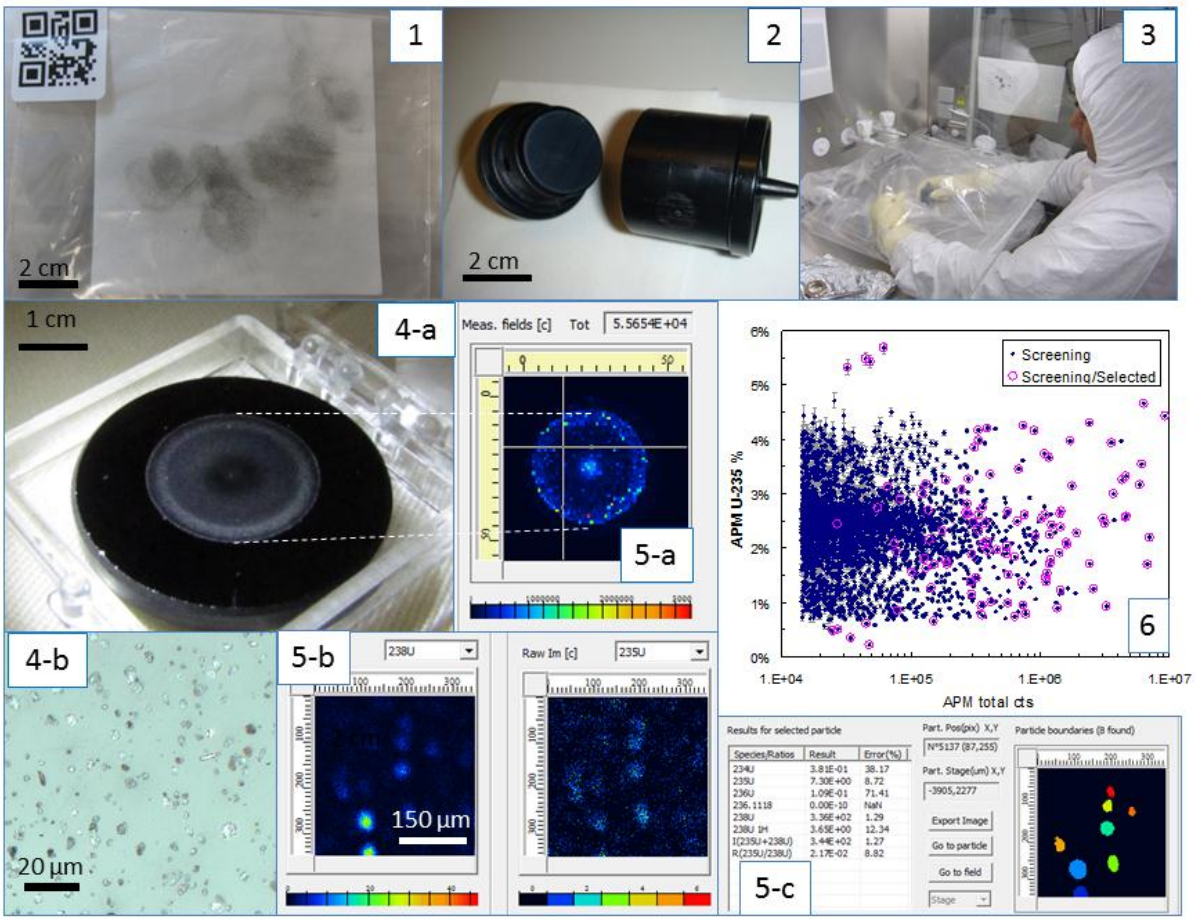

Figure 1: Sample preparation and screening operations preparatory to microprobe analysis (1) Typical environmental sample (here a cotton swipe), (2) Vacuum impactor head for sample preparation, (3) Particle transfer from swipe to analysis mount via vacuum impaction, (4-a) Particles deposited on an analysis mount (commonly a glassy carbon planchet), (4-b) Same as 4-a, observed under light microscope, (5-a) Uranium distribution over a 2.5 cm diameter carbon planchet as revealed by APM screening. The map consists of approximately 2400 fields of view of 350 µm ×350 µm each. The colour scale corresponds to the total uranium counts integrated over each field and over time (here 20s per field), (5-b) Distribution of U-238 and U-235 isotopes over a single field of view of 350 µm ×350 µm (location on planchet displayed by the cross on 5-a). The colour scale corresponds to the total number of counts integrated per pixel for each isotope over time (here 20 s). The “hot spots” correspond to occurrences of uranium-bearing particles. The apparent size of particles reflects the lateral resolution of scanning ion image under APM screening conditions and is approximately 25 µm, (5-c) Outcome of APM algorithm for processing the images displayed in 5-b. Here 8 clusters of pixels were recognized as particles and characterized in terms of isotopic composition. The values displayed in the table correspond to the dark blue particle at the bottom of the field of view, (6) APM screening data obtained over the whole planchet and displayed as U-235 enrichment vs total uranium counts. A range of particles is selected for micro-beam analysis (pink circles) such as to characterize the full U-235 enrichment range. Error bars correspond to the counting statistics (one sigma).

Date	Number of samples analysed			Turn-over (days)	Method validation and R&D effort	Comments
	ES	Blank	Test			
2010	47	26	102	n.a.	Factory acceptance tests (June) Initial validation study	Operated at the manufacturer's (as of July) Analyses duplicated using the IAEA's conventional SIMS (IMS4f)
2011	59	54	73	n.a.	On-site acceptance tests Re-validation study	Commissioning of the purpose-built facilities (clean lab extension at the IAEA's laboratories, March) Reinstallation of the LG-SIMS (April-June) Shutdown of the IAEA's conventional SIMS (August)
2012	68	62	76	31 days	Study of memory effects	
2013	103	101	3	28 days		
2014	101	77	6	28 days		

Table 1: Milestones of the LG-SIMS project

3. Lessons learnt along the way

3.1. Early compliance with initial requirement

The initial goals set by the Department of Safeguards regarding measurement precision and accuracy were met during the early stage of LG-SIMS validation thanks to its excellent level of performance. On a routine basis, U-235 and U-234 are reported with typical final uncertainty of 1-2% and 2-6% relative, respectively, for small particles in the LEU range (U-236 detection limit being between 10-15 ppm). In the most favourable cases, final uncertainties as low as 0.35% and 1% relative can be reported for U-235 and U-234, respectively (and U-236 detection limit around 5 ppm).

LG-SIMS analysis and the related uncertainty budget proved robust over a large range in particle size and analytical parameters. Figure 2 shows the outcome of a series of U-235 measurements performed on 98 individual particles of Certified Reference Material (CRM) IRMM 9060-01-B chosen to cover our usual working range in terms of particle size and analytical conditions. The range in total U counts yielded during microprobe analysis (almost 3 orders of magnitude) reflects much of the variability in particle size that is encountered in inspection samples. Individual measurements appeared statistically consistent with the certified value within final uncertainties, ranging between 0.4% and 7% relative.

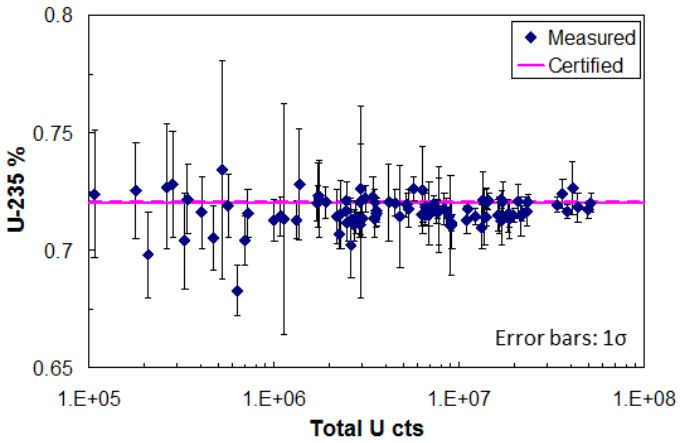

Figure 2: Test on measurement and uncertainty robustness using a series of 98 particles of CRM 9060-01-B chosen selected as to reflect the variability in particle size and analytical conditions encountered when analysing inspection samples.

Agreement between the measured and certified values was met with a coverage factor of less than one for 74 particles (out of 98 analysed), less than two for 95 particles, and less than three for one particle. This highlights the fact that final U-235 uncertainties exactly reflect our level of confidence in each individual measurement. Note the presence, when considering the entire population of particles, of a systematic bias of approximately -0.5% relative in average. This reflects a particle size effect that cannot be corrected for in our current calibration scheme but is conservatively accounted for in the final uncertainty.

The IAEA's LG-SIMS instrument was intended to be operated under optimized instrumental conditions by multiple staff, 24 hours a day and 6 days a week, with minimum downtime. A quality chart approach underpins this operation mode and allows evidence of LG-SIMS hardware and lab environment stability over extended period of time. The routine quality checks include: i) daily series of measurements made on a calibration plus an internal quality control CRM (NBS U010 and IRMM 9073-1-B, respectively), ii) calibration of the magnetic field (twice a day) with continuous regulation using NRM control, iii) centering of the spot image relative to the optical axis at the entrance of the analyser before each analysis. Tuning sessions are usually triggered by planned maintenance services (every 3 months in average). On those occasions, an inter-calibration of the electron multiplier is performed. Figure 3 shows the results obtained on the CRM use as internal quality control (yellow cake IRMM 9073-1-B) over a period of 1.5 years. As a further quality measure, other CRMs with U-235 enrichment between 0.5% and 93% are periodically measured.

Experience has shown that tuning for stability rather than maximum sensitivity is a necessary compromise for consistent, high quality data and at high sample throughput. Operation at maximum sensitivity level causes drifts in tuning and detector gains and results in higher overall uncertainties. A throughput of 100 samples analysed a year (50 to 300 reported particles each) could be achieved in 2013 and 2014 (Table 1). Unplanned downtime was less than 10% with routine quarterly maintenance.

LG-SIMS is now regarded as an established technique for particle analysis, however, due to the extreme variability of particle characteristics, both within and between samples, it is not routine. To address the fact that analyst judgement influences both particle detection and destructive analysis, SGAS has been exploring the effect of measurement parameters on the instrument performance in terms of inter alia particle detection sensitivity and accuracy of microprobe data. For instance, Figure 4 illustrates the dependence of screening sensitivity upon the parameters selected by the analyst for the purpose of generating screening data through a built-in routine for image processing. When the parameters are selected such as to sharpen the discrimination between particles and background (and thus reduce the "noise" caused by erroneous particle detection), a compromise is made, overlooking small particles. In the present case, this would have resulted in the non-detection of 2 of the 3 particles depicting the weakest signature (here outliers with U-235 above 5% U-235).

3.2. Coming across unexpected successes and challenges

3.2.1. Insights from LG-SIMS screening data into minor isotopic signatures

As described in [4], one of the important yet unanticipated advantages of using LG-SIMS for particle analysis of Environmental Samples results from the intrinsic quality of screening data generated for uranium minor isotopes (U-234 and U-236). Unlike the other methods in use for particle screening that exclusively provide information on U-235 distribution, LG-SIMS has a potential to estimate the tri-dimensional distribution of U-235, U-236 and U-234 of a fraction of the particles detected. As a result, LG-SIMS screening offers a much higher probability for detecting and selecting for subsequent microprobe analysis, weak and rare minor isotopic signatures. Since screening datasets can range up to 30000 particles, we find it necessary to use statistics-based software tools to assist the analyst in selecting particles for destructive analysis, to ensure all significant minor isotopic variations are captured [4].

Figure 5 shows two different samples for which screening results were used to select particles for microprobe analysis using U-234 and U-236 screening data, respectively. In both cases, the various minor isotopic signatures found in screening data could be confirmed and quantified by microprobe measurements.

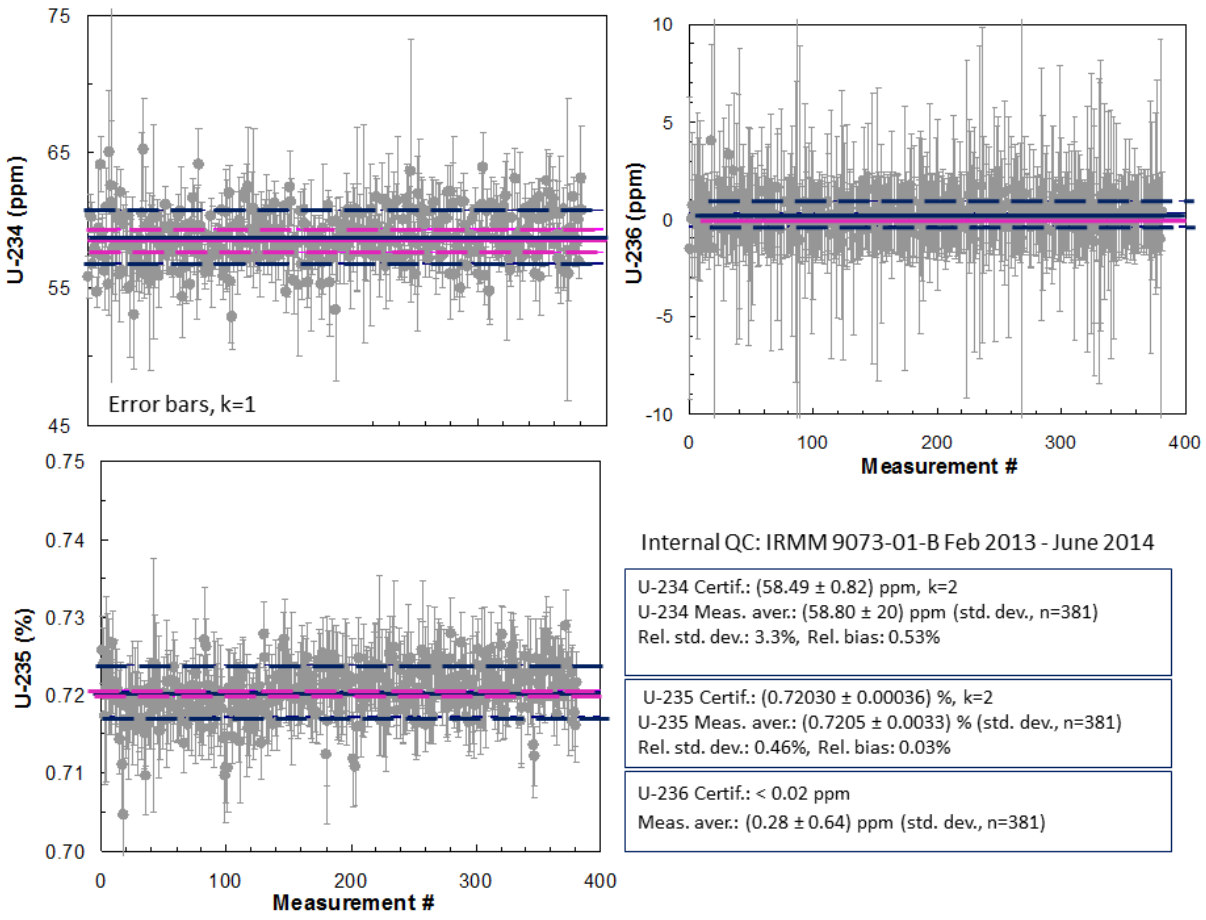

Figure 3: Long-term reproducibility of U-234, U-235, and U-236 measurements performed on individual particles of CRM IRMM 9073-01-B (yellow cake) as daily quality control

3.2.2. Memory effects dependant on the nature of the non-uranium particles present in samples

As part of the validation plan, experiments were carried out in order to explore instrumental memory effects during particle analysis. One of the unexpected finding was the strong dependence of memory effect upon the nature of the uncharacterized fraction of particles that are collected and deposited on the planchets together with uranium particles (the so called matrix). An experiment using different types of blanks could be designed after an increased uranium background was inadvertently generated by sputtering a large amount of uranium, while a massive uranium sample was used for tuning the instrument (Table 2). It appeared that APM screening was more affected for blanks loaded with a matrix consisting of silica particles than for matrix-free blanks. A microscopy study of blanks with matrix revealed a phenomenon of particle displacement and/or loss during the screening. It was interpreted as the result of particle charging under instrumental conditions (positive high voltage and progressive implantation of positive charges at the sample surface). The fraction of charged particles that are not tightly bound to the sample surface is prone to travel back and forth between instrument and planchet surfaces. The increase in uranium background may be explained by the potential for those projectiles to erode the uranium coating in the instrument and to transport traces of uranium back to the sample.

A preconditioning treatment was developed in order to minimize the potential of samples to collect uranium material originating from the instrument. A pulsed nitrogen-stream is applied to the planchet surface such as to blow off the loose particles that are prone to leave the surface due to uncontrolled electrostatic phenomena under measuring conditions. The efficiency of this preconditioning is demonstrated by the difference of uranium background observed during the screening of untreated and treated blanks (Table 2). These results emphasize the need for performing “matrix-matched” blanks in order to assess the risk for memory effect during screening.

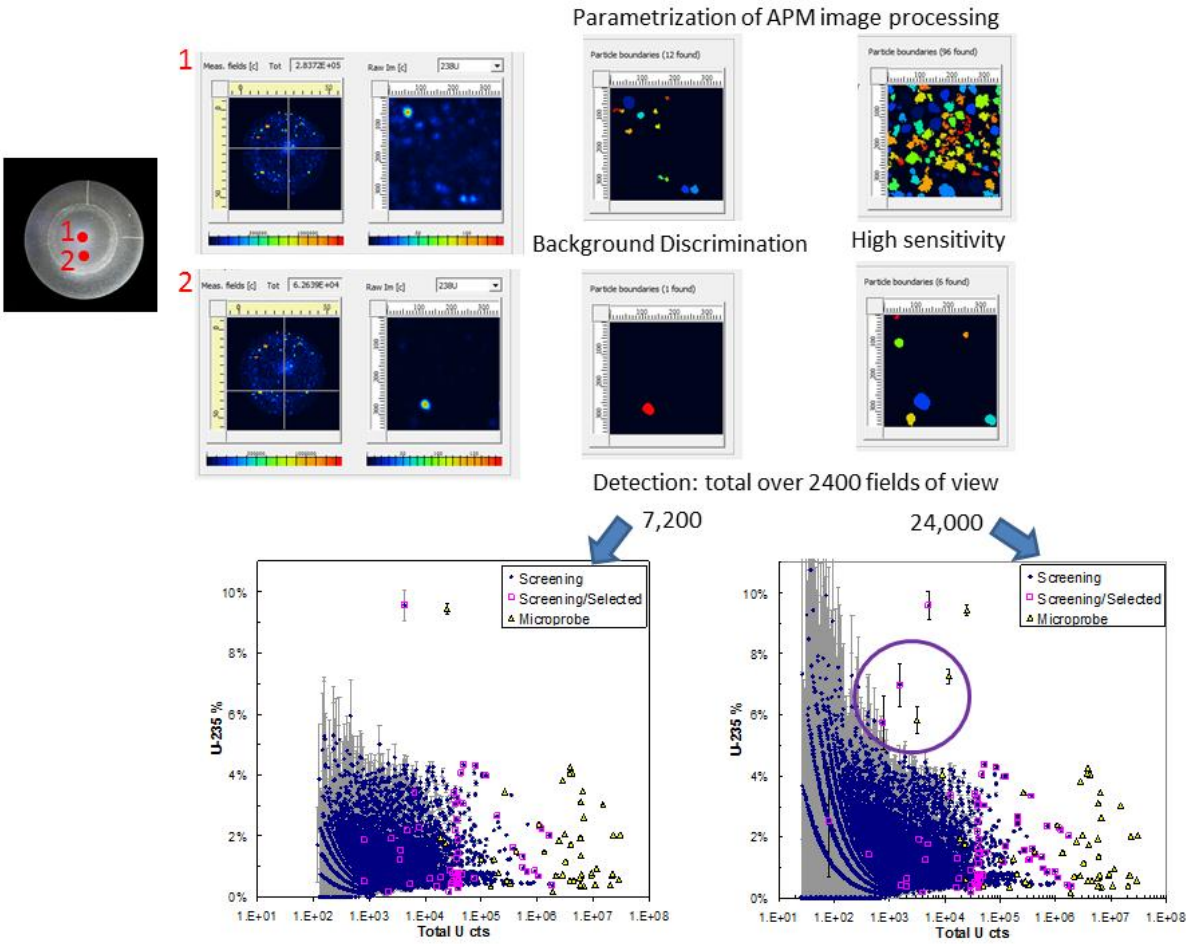

Figure 4: Dependence of particle screening sensitivity upon the parametrization of the instrument-supplied routine for image processing

Consequently, it was conservatively decided to use untreated blanks loaded with silica particles and to systematically precondition samples. Although our long-term blank record indicates that memory effects have been efficiently prevented, this method has drawbacks that are discussed below. Further measures consisted in limiting the quantity of uranium at the surface of planchets (no massive samples were allowed in the instrument from then on). Following this experiment, the increased uranium background could be mitigated by a thorough cleaning of all instrument parts facing the ionization area (Table 2).

4. Future areas of improvement

4.1. Sample preparation: prevention of memory effects without altering the size distribution of uranium particles

Further experiments were carried out in order to investigate the impact of sample preconditioning on the quality of data. Figure 6 illustrates the differences in microprobe results that can be observed between two different planchets prepared from a same sample, one being preconditioned while the other is not. For each planchet, more than 40 of the biggest particles detected by screening were selected for microprobe analysis. The total uranium counts yielded during microprobe data can be regarded as an indication for particle size. Those results suggest that the untreated planchet contained significantly larger particles than the preconditioned one. This is likely due to the fragmentation and/or the loss of the coarser fraction of particles during the step of preconditioning. Under these circumstances, the ability of LG-SIMS to detect and resolve rare isotopic signatures might be hampered.

Date (2013)	Blank with silica matrix	Pre-conditioning	Total U cts per field (×10^3), (350×350 µm, 18 s, 350nA)		Comment
			Min	Max	
2nd April	Yes	No	2	8	
3rd April (Tuning)					A mm sized U-ore mineral was sputtered for one hour at very high sputtering rate (2-3 orders of magnitude higher than for particle analysis)
8th April	Yes	No	40	2000	
9th April	No	n.a.	5	70	
10th April	Yes	Yes	8	200	
12th April					Cleaning of the analysis chamber and immersion lens
17th April	Yes	No	10	30	

Table 2: Investigation of instrumental memory effect using different types of blanks

For this reason, one clear way of data improvement would be to develop a method to strengthen the adhesion of particles onto the sample surface without altering the size distribution of uranium particles. Testing is underway to determine if reducing the nitrogen pressure for preconditioning the sample provides a better balance between reduction of memory effect and preserving a better particle size distribution. An alternative approach would be to selectively remove the non-uranium particles that are prone to charge under instrumental conditions before the introduction of samples into the instrument.

4.2. From the percent to the permil uncertainty: a significant challenge

Our current state of the practice for uranium particles of 1 micron or larger generates a final uncertainty for U-235 abundance of around 0.4% for an ideal run. The terms dominating the final uncertainty for U-235 are related to the correction for mass bias, detector intercalibration and a larger dead-time correction. Reducing the final uncertainty from 0.4% to 0.1% would require a considerable effort that would need to be weighed against the benefit for safeguards interpretation. Effort would have to be invested in, among other things, correcting the signal for deadtime on a pixel-by-pixel basis instead of the current spatially integrated basis, better protocols for detector intercalibration and a thoroughly understanding of the influence of particle size and composition on the mass bias correction. An immediate challenge in this effort is the scarcity of adequate CRMs, in the form of uranium particles of diverse and well-characterised sizes, densities and chemical compositions that cover the characteristics of typical safeguards environmental samples.

In order to improve the reproducibility of isotopic measurements performed in multicollection mode to an uncertainty of 0.1%, effort also would be required to understand the phenomenon of short-term drift of the electron multiplier detectors. Recent experiments within the IAEA NWAL discovered a complex but systematic pattern in the drift of detector gain when the detectors are exposed to a secondary ion beam in the 10^5 cps range (Hedberg et al., in preparation). A preliminary study indicated that the optimization of the electron multiplier gain on a particle-by-particle basis substantially improved the reproducibility of individual U-235 measurements for a series of large CRM particles. This method improvement could be validated and applied to future analyses requiring the highest precision for Safeguards purposes.

For smaller particles, the uncertainty budgets for U-235, U-234, and U-236 abundances are dominated by the counting statistics. Therefore, improvement for these particles must await future method developments aimed at enhancing efficiency of uranium ionization and transfer into the mass spectrometer.

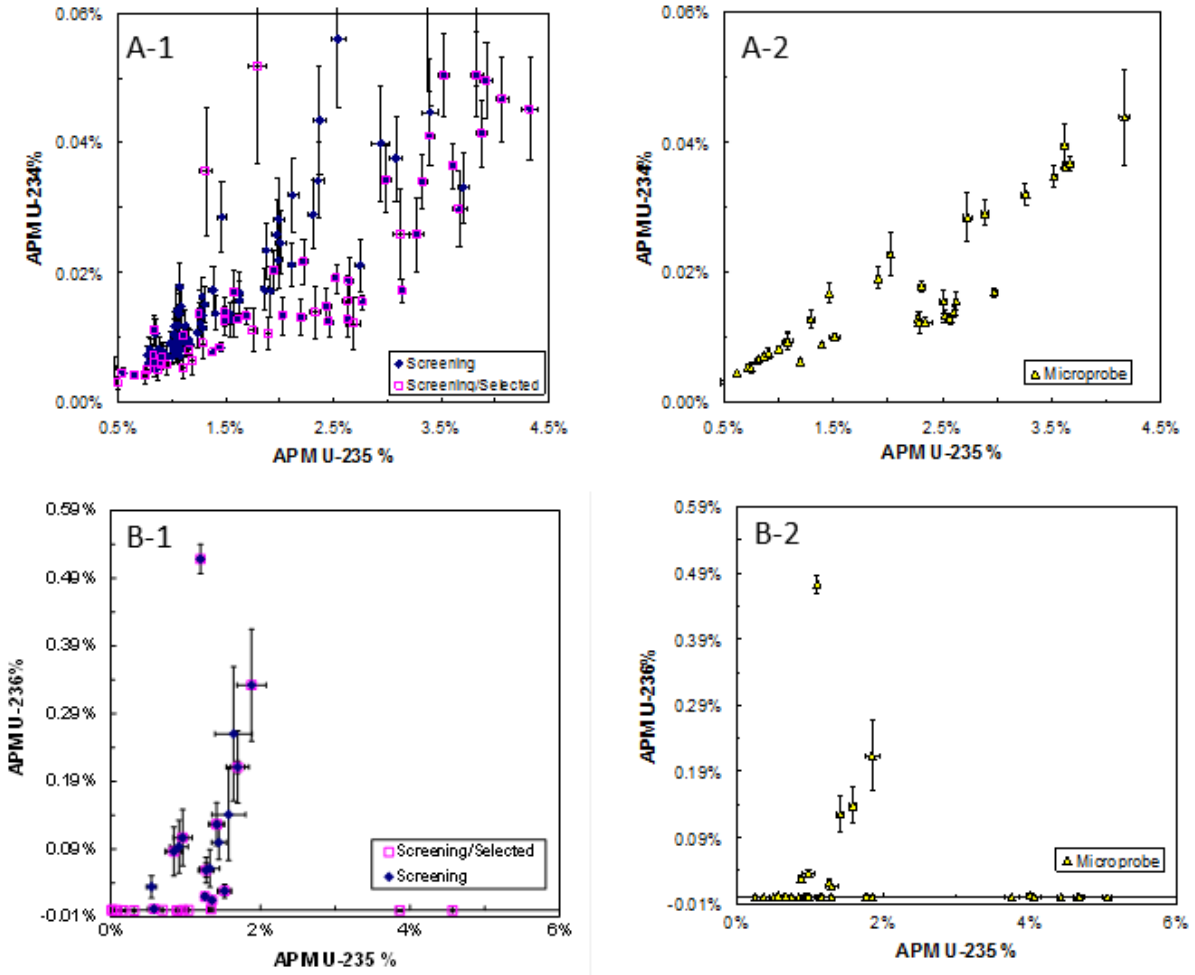

Figure 5: Minor isotopic signatures as depicted by screening and microprobe analysis results. In A-1: closed diamonds correspond to particles with more than 20 total screening U-234 counts and open circles correspond to the particles that were selected for subsequent microprobe analysis. In B-1: closed diamonds correspond to the particles having 2 sigma significant screening U-236 and more than 20 total U-235 counts and open square correspond to the particles that were selected for subsequent microprobe analysis. A-2 and B-2 show the outcome of microprobe analysis for both samples.

4.3. Development of an automated system for optimizing the analytical conditions during screening and microprobe analysis

As mentioned above, in the current version of the LG-SIMS data acquisition software, the analyst must manually optimize a number of parameters for an APM screening acquisition or microprobe analysis. Since those parameters are then fixed over the course of the acquisition, they must be chosen as a compromise between particle load and other characteristics varying across the 2400 fields examined during an APM run. This compromise necessarily leads to low sensitivity in some fields or deadtime issues and other artefacts in more heavily loaded parts of the planchet. For microprobe analyses, use of automation to efficiently analyse a series of particles in unattended mode results in a reduction in quality of the final particle data due to the large variability and unpredictability of particle response under microprobe erosion. SGAS has carried out a proof of principle investigation and demonstrated that automation of the probe beam intensity and associated focus parameters is feasible. Under these circumstances, SGAS has proposed the development of new acquisition modules for a real-time, automated optimization of analytical parameters over the course of screening or microprobe analysis. The expected gain would be the assurance that every particle in a sample could be targeted under analytical conditions that would minimize the level of final uncertainty. As a result a larger number of useful results could potentially be derived from each sample with no increase in response time.

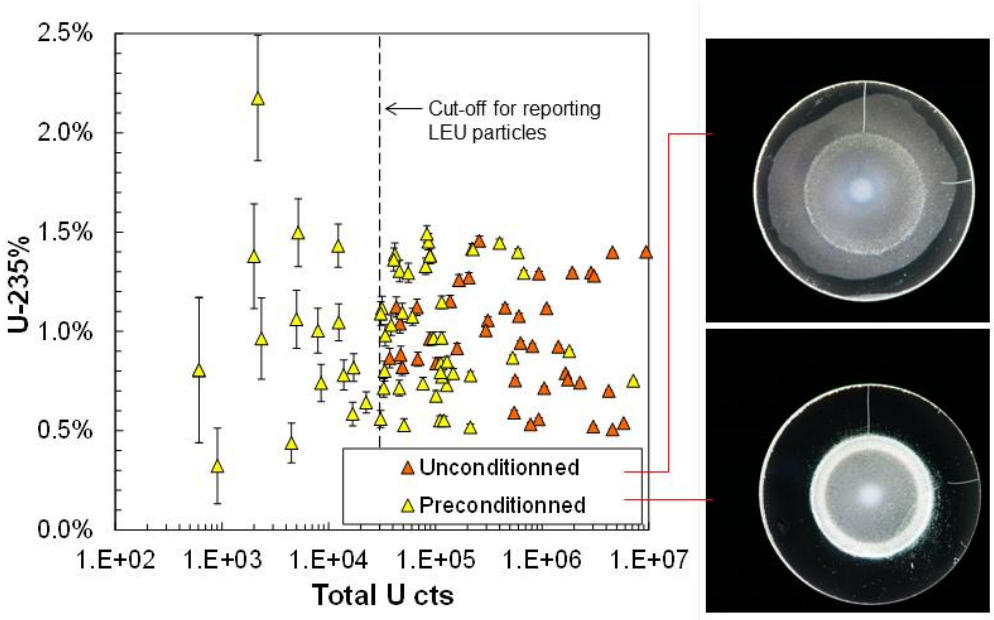

Figure 6: Comparison between unconditioned and preconditioned samples in term of particle size distribution

5. Conclusions

The LG-SIMS analysis of uranium particles at the IAEA has entered a phase of stable operation producing high quality data. Due to the variable nature of the particles between and within samples, some challenges have been overcome to produce data that are highly sensitive and accurate, in addition to being robust. Other areas for improvement over the longer term have been identified. However, progress for several of these areas is contingent upon the availability of a wider range of certified reference materials in the form of particles than is currently available.

6. Acknowledgments

We gratefully acknowledge the Government of Japan for providing the funding for the LG-SIMS instrument and the purpose-built building as well as all the other Member States that contributed to fund the IAEA's ECAS project (Enhancing the Capability of Safeguards Analytical Services). In addition, we warmly thank our colleagues who participate in the IAEA's Network of Laboratories (NWAL) for their continued and valuable cooperation.

7. References

[1] Ranebo Y., Hedberg P.M.L., Whitehouse M.J., Ingeneri K.and Littman S.; *Improved isotopic SIMS measurements of uranium particles for nuclear safeguard purposes*; *J. Anal. At. Spectrom*.; 24; 2009; 277-287

[2] Hedberg P.M.L., Peres P., Cliff J. B. ,Rabemananjara F., Littmann S., Thiele H., Vincent C. and Albert N.; *Improved particle location and isotopic screening measurements of sub-micron sized particles by Secondary Ion Mass Spectrometry; J. Anal. At. Spectrom*.; 26; 2011; 406–413

[3] Peres, P., Hedberg, P. M. L., Walton, S., Montgomery, N., Cliff, J. B., Rabemananjara, F. and Schuhmacher, M.; *Nuclear safeguards applications using LG-SIMS with automated screening capabilities; Surf. Interface Anal*.; 45; 2013; 561–565

[4] Poths J. , Sangely L., Bildstein O., Schwanhaeusser A., Tanpraphan T., Siegmund H., Balsley S.; *Application of LG-SIMS to uranium particles analysis for IAEA Safeguards;.* INMM 55th Annual Meeting Proceedings; Atlanta (USA); 2014

[5] Poths J., Sangely L., Bildstein O., Kitao T., Schwanhaeusser A., Hosoya M., Tanpraphan T.; *Improved uranium particle analysis using large-geometry SIMS;* 33rd ESARDA Annual Meeting Proceedings; Budapest (Hungary); 2011

[6] Truyens J, Stefaniak EA, Aregbe Y., *NUSIMEP-7: uranium isotope amount ratios in uranium particles*; *J Environ Radioact.;* 125; 2013; 50-55

Validation of a Cameca 1280 High-Resolution SIMS instrument for Analysis of Nuclear Safeguards Environmental Swipes

A Simons, N Montgomery, T Nicholls, A Pidduck, S Crooks & J Collins

Nuclear and Analytical Science, AWE, Aldermaston, Reading, RG7 4PR, UK
E-mail: allan.pidduck@awe.co.uk

Abstract:

We describe the validation of a Cameca IMS 1280HR large-geometry secondary ion mass spectrometry (SIMS) instrument, newly-installed at AWE, for the search, location and isotopic ratio measurement of uranium particles derived from environmental cotton swipe samples. The work involved measurement of five selected samples: (1) A uranium particle isotopic standard sample, to establish the instrument mass bias for uranium isotopes, as well as to assemble quality control data over an initial six month period of operation; (2) A blank carbon planchet, to check that measurable cross-contamination was absent; (3) A well-characterised sample prepared from a field swipe, providing a measurement difficulty representative of challenging samples; (4) A uranium isotopic standard comprising sub-micrometer-sized particles, to test particle isotopic measurement precision, accuracy and detection sensitivity, and (5) A second selected swipe sample previously measured using standard geometry SIMS and found to give a characteristic isotopic distribution.

Sample preparation development work was also undertaken to examine methodologies for the removal of any loosely-adhered particles from substrates prior to SIMS, in order to minimise risks of particle cross-contamination.

The qualitative and quantitative results obtained demonstrate that the validation was completed successfully, and that the capability is suitable for the analysis of environmental swipe samples.

Keywords: SIMS; uranium; particle analysis; isotopic analysis; nuclear safeguards;

1. Introduction

A large geometry (LG) Cameca 1280HR secondary ion mass spectrometry (SIMS) instrument has been installed at AWE and was successfully commissioned in April 2014. This paper documents SIMS analysis results obtained in order to validate the performance of this instrument for the detection and isotopic measurement of uranium particles from environmental cotton swipe samples. AWE is an accredited member of the International Atomic Energy Agency (IAEA) Network of Analytical Laboratories (NWAL) for performing isotopic analysis of uranium-containing particles from environmental swipe samples using two different techniques: fission track thermal ionisation mass spectrometry (FT-TIMS), and secondary ion mass spectrometry (SIMS). This work supports the IAEA Department of Safeguards in their mission to assure the absence of undeclared nuclear activities by the analysis of cotton swipe samples collected by inspectors from nuclear facilities worldwide [1].

The overall criterion adopted for validation of the Cameca 1280HR has been to demonstrate data of equivalent or better quality to that obtained previously from standard-geometry (SG) SIMS measurements of the samples selected. This work closely follows the methodology previously used for the validation of a Cameca 4f SG SIMS instrument for this application [2] in 2012.

1.1. Need for SIMS high-mass-resolution

In SIMS, a focussed high-energy O_2^+ primary ion beam is used to sputter and ionise surface layers. The ions formed are extracted by an electric field, mass analysed and collected, permitting measurements of isotope ratios as the sample material is eroded. For uranium, the ionisation efficiency under typical conditions is of the order of 1% which gives sufficient sensitivity for isotope ratio measurements of particles down into the micrometre diameter size range [3].

The specificity of the SIMS uranium particle searching step is particularly dependent on the mass resolving power of the spectrometer. This is because uranium elemental ions must be distinguished from molecular ions with the same nominal mass formed during the SIMS process. These mass interferences can be prevalent in field samples which can contain particles from many different chemical species. SG SIMS permits only near-unit-mass resolution over the uranium mass range without loss of ion transmission. Isobaric interferences can then result in false positive detection of candidate particles other than uranium, and/or in the reporting of perturbed isotope ratios, in particular elevated uranium minor isotope levels. Lead-containing compounds are the most common source of such mass interferences, although barium and bismuth compounds can also be problematic. A mass resolution of about 0.1 atomic mass unit (amu) is sufficient to negate mass interferences from most inorganic atomic combinations (a notable exception being actinide hydrides) in the uranium mass range. In M/ΔM terminology, where ΔM is the peak-width (usually quoted at 10% peak height) at mass M, a mass spectrometer resolution of ≥2,400 is needed. Use of a scaled-up double-focussing mass spectrometer geometry can successfully achieve this without loss of instrument transmission and hence sensitivity [3]. Further, the larger instrument geometry gives sufficient space for inclusion of a multi-detector array enabling parallel collection of signals from the uranium isotopes (instead of mass-peak-switching) and hence superior sensitivity.

To emphasise this point, Figure 1 shows a high-resolution mass spectrum from an area of a conductive carbon substrate loaded with a deposited mixture of NBS U010 reference uranium particles and SRM2586 NIST dust. SRM 2586 contains many transition metals, which can form polyatomic ions, giving rise to multiple interference peaks occurring slightly below the uranium isotopes. Uranium isotope positions are marked by the vertical black lines in Figure 1. Relative intensity measurements fixed at these positions give the correct NBS U010 isotopic ratios, despite the presence of major levels of extraneous material. This clearly would not have been the case if measurement had been made under unit mass resolution conditions using a SG SIMS (uranium minor isotope ratios would have been grossly perturbed and even the major isotopic ratio would have been biased).

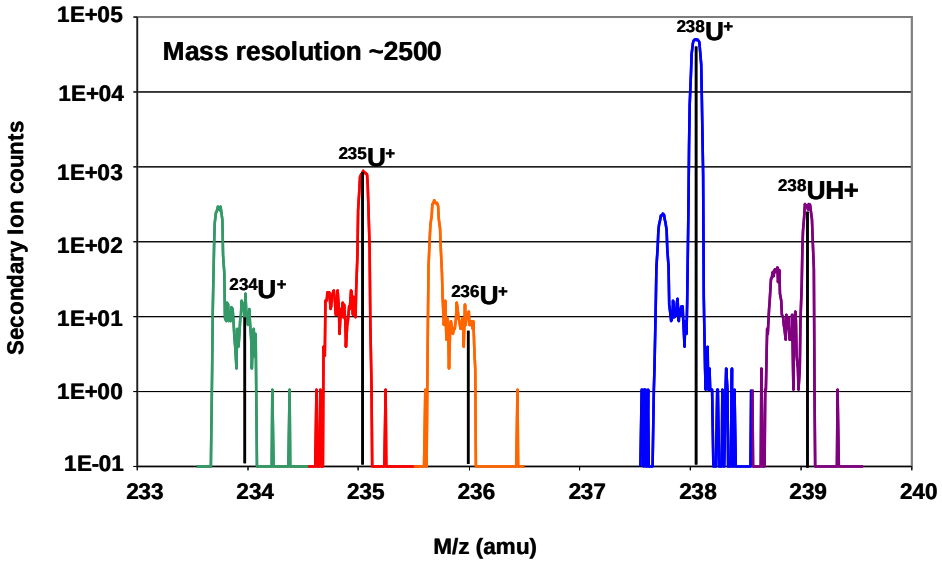

Figure 1: Cameca 1280 limited-range mass spectrum from a mixed uranium particle (NBS U010) – standard dust (NIST 2856) specimen.

2. Experimental

2.1. SIMS instrument

The LG-SIMS instrument installed at AWE is Cameca IMS 1280HR number 25 (Figure 2). The instrument was delivered in November 2013 and site acceptance tests were successfully completed in April 2014. Before delivery, the laboratory was refurbished to provide an environment that fully met Cameca specifications for thermal, acoustic and electromagnetic stability. A housing external to the laboratory was constructed to hold the electrical, compressed air and chilled water services. A nearby room has also been converted to allow remote operation of the instrument.

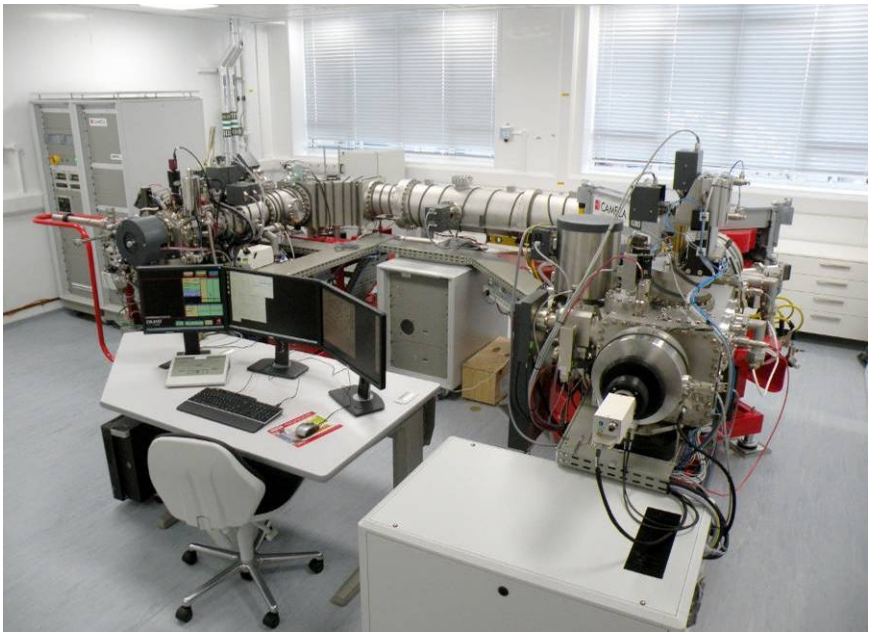

Figure 2: Cameca 1280HR-25 after installation

2.2. SIMS measurement conditions

The instrument is first operated in ion imaging mode for uranium particle searching, and then in ion microprobe mode for individual particle assessment. A 15keV O_2^+ primary ion beam was used with a secondary ion extraction potential of 8keV, corresponding to a net ion impact energy of 7keV. The beam is focussed to spot size of typically less than10µm. The instrument secondary ion optics are set-up under near-full ion transmission conditions so as to give the highest possible sensitivity. Using an exit slit width of 500µm a mass resolution, M/ΔM of approximately 2,400 is obtained. Electron multiplier (EM) detectors capable of single ion counting are used, and the options of using either a single EM detector (mono-collector) or an array of up to five parallel EM detectors (multi-collector) are available. Tables 1 and 2 summarise the instrument conditions used.

Parameter	Ion Imaging (Particle Search)	Ion Microprobe (Individual Particle Assessment)
Primary beam species	O_2^+	
Primary beam ion energy	15keV	
Secondary voltage	8kV	
Mass resolution	~2,400	
Primary beam current	~10nA	~10pA
Primary beam spot size	Focussed spot (<10µm)	
Raster size	250µm	6 to 15µm

Table 1: Typical 1280HR-25 SIMS instrument operating conditions

Mass/Charge Ratio (m/z) / (Isotope)	Ion Imaging (Particle Search)	Ion Microprobe (Individual Particle Assessment)
233 (Background)	-	2
234 / (^{234}U)	80	6
235 / (^{235}U)	80	4
236 / (^{236}U)	80	8
238 / (^{238}U)	80	2
239 (^{238}U+^{1}H)	80	4
Detector Type	Multi-collector (parallel)	Mono-collector (serial)

Table 2: Typical detector dwell times (seconds) used during analysis

2.2.1. Uranium particle searching

The aim of particle searching is to achieve a high sensitivity for the detection of any uranium present whilst consuming the minimum particle volume during sputtering, thus allowing subsequent more detailed microprobe measurements. Use of the multicollector detector gives the most efficient conditions for this.

A short pre-sputter period was applied to each SIMS analysis field before image collection to remove surface contamination. Uranium particle searching and location was carried out by raster-scanning the focussed primary ion beam over 250µm areas whilst using the multicollector detector to simultaneously collect ion images corresponding to $^{234}U^+$, $^{235}U^+$, $^{236}U^+$, $^{238}U^+$ and $^{238}UH^+$ signals.

The Cameca Automated Particle Measurement (APM) software [4] steps the sample automatically under the beam so as to cover relatively large areas of the planchet during extended (for example overnight) operation. The APM software then processes the ion images, to identify uranium-containing particles, determine their locations and estimate the $^{235}U/^{238}U$ isotopic ratio for each particle. Minor isotopic ratios can also be estimated, albeit with very low precision due to the relatively weak signals. Figure 3 shows example ion images and the uranium particle map derived from them.

The main validation criterion applied is a statistical cut-off to ensure that ion counts are adequate to allow major isotopic measurement with acceptable precision. The criterion used is that the relative standard deviation (RSD) contributed by ion counting statistics be less than 10%. For $^{235}U/^{238}U$ ratios of a few % or below this effectively amounts to a ^{235}U minimum signal level of about 100 counts.

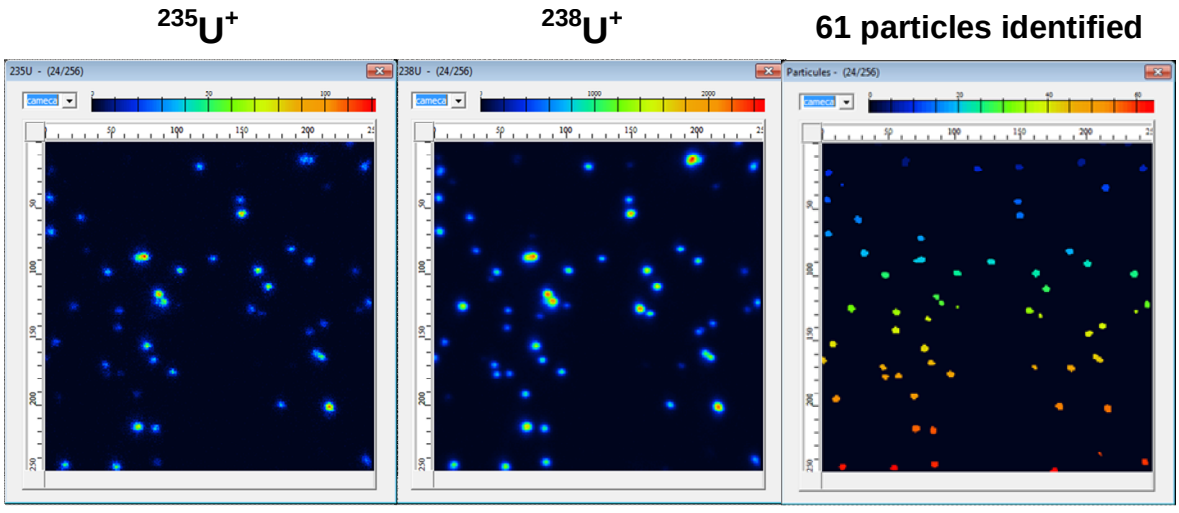

Figure 3: APM software output showing $^{235}U^+$ and $^{238}U^+$ ion images from a single 250µm field, and the derived map of identified U particles

2.2.2. Ion microprobe analysis

The aim of microprobe analysis is to obtain the highest quality measurements of uranium major and minor isotopic ratios possible within the constraint of individual particle size (and hence available sputtering time and total cumulative ion counts). Particles of most interest are selected for microprobe examination from the $^{235}U/^{238}U$ isotopic ratio distribution detected by APM. For this work mono-collector detection was used, with magnetic field switching to cycle between the uranium isotope mass peaks. Data from typically 40-60 cycles were collected per measurement. This allows isotope ratio measurement with high precision and accuracy, and permits minor isotope ratios to be reliably determined. A fine-scale raster is used, and the particle may be completely consumed during analysis.

Parameters adjusted in response to particle size, and hence signal strength, are primary ion beam current and raster area. As the particle erodes, signals may initially increase slowly before decaying more rapidly as the particle is consumed. All microprobe data collected is individually inspected to ensure that only good quality results are reported. Factors considered are (a) signal levels, which for the most intense isotope should ideally be in the range 1×10^4 to 2×10^5 counts per second, (b) total cumulative ion counts, and (c) changes in the isotope ratio or signal level, such as a rapid decay or spurious events, during sputtering.

As-measured ratios are corrected for the instrument mass bias (see section 3.1) and reported uncertainties are calculated by combining uncertainties of the as-measured ratio and mass bias. The $^{236}U/^{238}U$ ratio is calculated after subtracting the cycle-to-cycle ^{235}UH isobaric interference from the as-measured signal at m/z=236 (^{236}U + ^{235}UH). The ^{235}UH signal is calculated from the $^{235}UH/^{235}U$ ratio, which is assumed to be equal to the observed ^{238}UH (m/z=239) /^{238}U signal ratio.

2.3. Sample details

Five different samples were measured, selected so as to allow basic instrument calibration, measurement stability and sensitivity to be evaluated, as well as to represent the range of measurement challenges typically encountered in this application:

2.3.1. NBS U010

The U010 particle isotopic reference material was used to determine the instrument mass bias (MB) factor (where MB is defined as measured / certified isotope ratio). Repeat MB measurements over an extended period of operation provide a test of instrument stability and sensitivity. Particles on this sample were relatively large (typically 1µm or greater), easily found, and were analysed solely in ion microprobe mode.

2.3.2. NU7-064

A NUSIMEP7 particle isotopic standard pre-prepared by the Institute for Reference Materials and Measurements (IRMM), Geel, Belgium, by the vapour phase pyrolysis of UF_6 [5]. The sample was very heavily loaded with uranium particles. The analytical challenges in this case arise from the very small particle size (below 500nm diameter) and the presence of two particle isotopic ratios, providing direct tests of both the sensitivity and accuracy of uranium major and minor isotopic ratio measurements.

2.3.3. Sample D

This was selected as an example field swipe, previously identified as challenging in respect of particle size and reliable uranium minor isotope ratio measurement using SG SIMS [6]. Different areas of the planchet, which was fairly heavily loaded with uranium particles, have been used for previous characterisations using a Cameca IMS 1270 LG-SIMS instrument located at the Ion Microprobe Facility in the School of Geosciences at Edinburgh University, and a Cameca 4f SG-SIMS instrument at QinetiQ (Malvern) and later relocated to AWE. The results expected from this sample were therefore felt to have been well-established. The planchet had additionally been examined by scanning electron microscopy (SEM) with energy-dispersive X-ray fluorescence (EDX) microanalysis [6]. As common for field swipes, uranium particles were shown to be only a small minority (ca. 1%) of the total number of particles present, with a consequential high risk of SIMS isobaric mass interferences.

2.3.4. Sample S

Sample S was from a field swipe recently measured by SIMS using a Cameca 4f instrument at AWE. This was selected for Cameca 1280HR analysis on the basis of a characteristic distribution of major isotope ratios found in the presence of mass interferences.

2.3.5. IMS-BLANK1

A blank planchet stored in the instrument during the validation measurement series.

2.4. Sample preparation

The particle samples were prepared onto carbon planchets to provide flat conductive substrates for SIMS analysis. The field samples derived from environmental cotton swipes had been prepared using vacuum impactor deposition.

Steps were taken to minimise the potential for particle cross-contamination within the SIMS instrument. This work followed two approaches:

(1) Control of the coverage level of deposited particles to avoid build up of multiple layers, with assessment by optical microscopy prior to loading into the SIMS

(2) Integration of a simple means for the removal of loosely-adhered particles (by application of air-pulses after deposition) into the vacuum impactor deposition method.

Figure 4 highlights the optical microscopy methodology, comparing an approximately 500 µm field-of-view area of a deliberately heavily-loaded test planchet before and after air-pulsing. The circular rings are centred on particles evidently removed by this step.

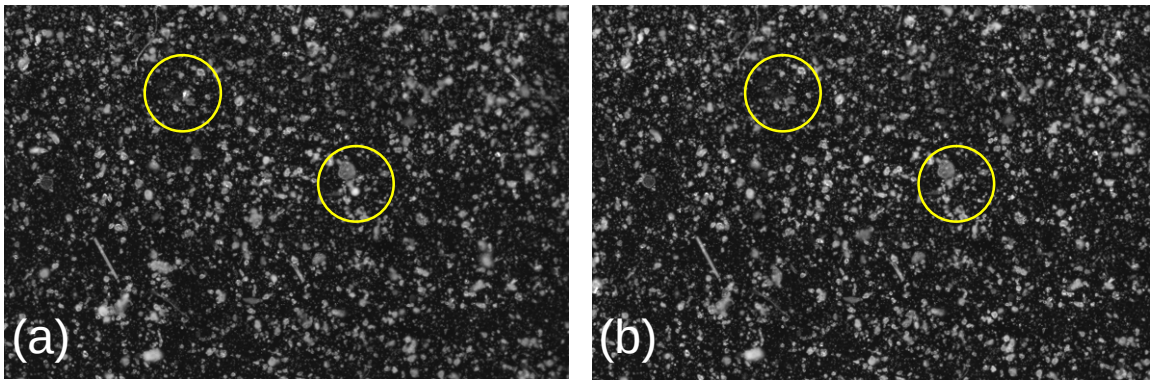

Figure 4: Comparison optical micrographs from a test planchet (a) before and (b) after air-pulsing.

SEM images of example uranium particles from some of the samples measured are shown in Figure 5.

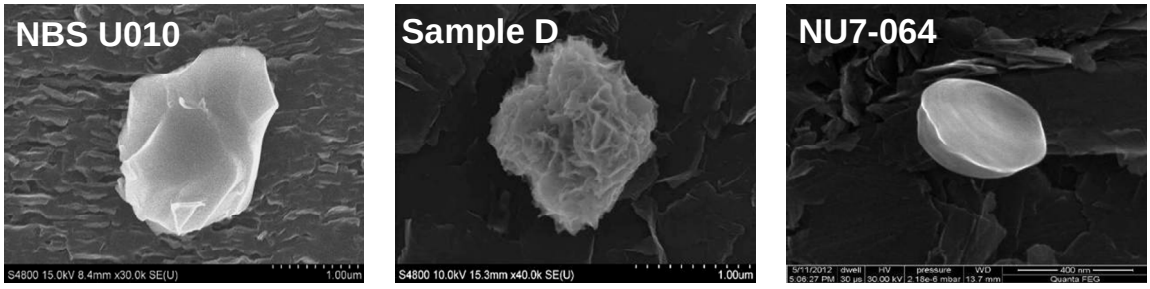

Figure 5: Example SEM images of uranium particles.

3. Results

3.1. NBSU010: Mass bias factor (MB) measurements

Microprobe measurements of $^{235}U/^{238}U$ ion signal ratios from a NBSU010 uranium particle standard were used to determine the instrument MB factor. Measurements made from 95 randomly-selected particles over a 6 month period are shown in Figure 6.

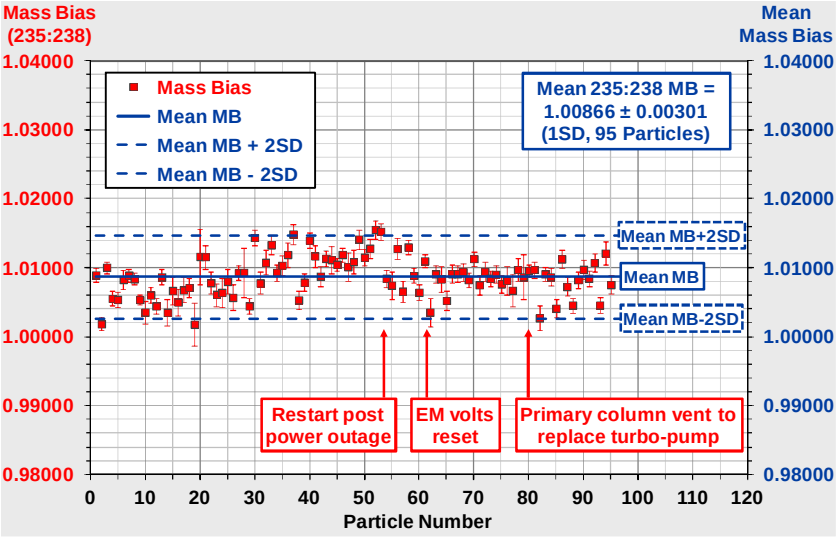

Figure 6: Mass bias derived from NBSU010 microprobe measurements.

The mean mass bias was 1.00866 (solid blue line) which corresponds to a bias of 0.289% per mass unit over the uranium isotopic range. The standard deviation (SD) was 0.0030 (0.30% relative SD). Error bars plotted in Figure 6 are standard error (SE) values derived from cycle-to-cycle variation of the ratios during each individual particle measurement. Only one data point was excluded, on the basis of a narrow spike seen in the ratio during mass cycling. It is clear that particle-to-particle and measurement-to-measurement effects dominate the variation, rather than cycle-to-cycle effects. This is unsurprising as the data includes measurements from 3 operators using a realistic range of set-up and measurement conditions with particles selected from the full planchet area. The period also included one instrument restart following a power outage, one adjustment to the EM detector operating voltage, and an extended shutdown for replacement of a failed turbomolecular pump.

Assuming that the same overall measurement variation could be expected from unknown particles, this result would be consistent with measurement of an unknown $^{235}U/^{238}U$ isotopic ratio with a combined relative uncertainty of about 0.85% (~2SD or 95% confidence level).

Cumulative results also provide quality control (QC) data from which long term instrument behaviour can be monitored. Visual inspection suggests a possible change in mass bias near run 54 which correlates with the instrument restart after power outage. The first half of data points exhibits a possible trend for mass bias to increase (by about 1% over the period) as would be consistent with slow detector aging during usage. However no such trend is evident in the second half of data points.

3.2. NBSU010: Minor isotope measurements

Averaged minor isotope ratio measurements obtained during the above series of NBSU010 measurements, after mass bias correction, are compared with certified ratio values [7] in Table 3.

Isotope	m/z 233 / ^{238}U	^{234}U / ^{238}U	^{236}U / ^{238}U
Certified ratio	-	0.0000547	0.0000688
Measured ratio	0.00000004	0.0000543	0.0000696
2 SD	0.00000008	0.0000022	0.0000027

Table 3: Averaged NBSU010 minor isotope ratios after mass bias correction

Agreement with the certified values is very good, deviations from reference values being -0.6% and +1.2% for $^{234}U/^{238}U$ and $^{236}U/^{238}U$ respectively, well within the measured relative standard deviations of ±2% in both cases. Signals measured at m/z 233 are recorded as a background indicator (there being no ^{233}U in NBSU010). All measured $233/^{238}U$ ratios were at or below 0.2ppm, with an average value of 0.04ppm, as consistent with the typical level of detector dark noise.

3.3. NU7-064: NUSIMEP7 dual U ratio standard

A grid of 25x25, 250µm diameter fields examined by APM yielded 5,342 valid particles. The distribution of $^{235}U/^{238}U$ particle isotopic ratios is shown in Figure 7. This is dominated by two clear peaks centred close to the certified NUSIMEP7 $^{235}U/^{238}U$ ratios of 0.00907 and 0.03415. A small number of particles with intermediate ratios were located. These are a probable result of the extremely high particle loading of the NU7-064 planchet, resulting in some particles which are too closely spaced to be spatially resolved in the ion images. The number of such occurrences is many times less than observed in previous 4f SIMS results, which correlates with the smaller diameter primary ion beam spot achieved using the 1280HR instrument.

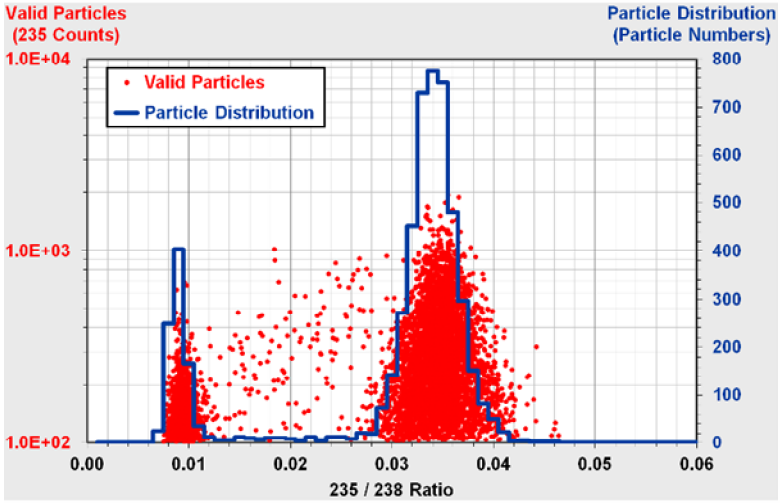

Figure 7: APM results from sample NU7-064. Left axis: Particle 235U signal versus as-measured $^{235}U/^{238}U$ ratio. Right axis: Particle $^{235}U/^{238}U$ histogram.

A few particles from each of the two enrichment populations were selected for measurement by ion microprobe. Tables 4 and 5 compare the measured and certified [8] major and minor isotope ratios respectively. Good agreement is apparent in all cases.

Isotope	Enrichment 1	Enrichment 2
Certified $^{235}U/^{238}U$ ratio	0.0090726 ± 0.0000045	0.034148 ± 0.000017
Particles measured	4	7
Average measured ratio	0.009056	0.03395
SD	0.000034	0.00020
Deviation (Meas-Cert (%))	-0.19%	-0.59%
RSD (%)	0.38%	0.58%

Table 4: Averaged NU7-064 $^{235}U/^{238}U$ ratio after mass bias correction

Isotope ratio	$^{234}U/^{238}U$		$^{236}U/^{238}U$	
$^{235}U/^{238}U$ ratio	0.0090726	0.034148	0.0090726	0.034148
Particles measured	4	7	4	7
Mean measured ratio	7.475E-05	3.443E-04	8.34E-06	1.055E-04
RSD (%)	4.5%	2.3%	3.6%	4.5%
Certified ratio	7.437E-05	3.451E-04	8.02E-06	1.033E-04
Deviation (Meas-Cert (%))	0.51%	-2.3%	4.0%	2.1%

Table 5: Averaged NU7-064 minor isotope ratios after mass bias correction

3.4 Sample D: Well characterised field swipe

A grid of 25x25, 250µm diameter fields were examined by APM. 3,387 candidate uranium particles were found of which 724 passed the validation criteria. The distribution of uranium particle enrichments measured is shown in two formats in Figure 8. Ion microprobe isotope ratio measurements were made on 35 particles, selected so as to sample over the observed enrichment range, and the results are shown in Figure 9.

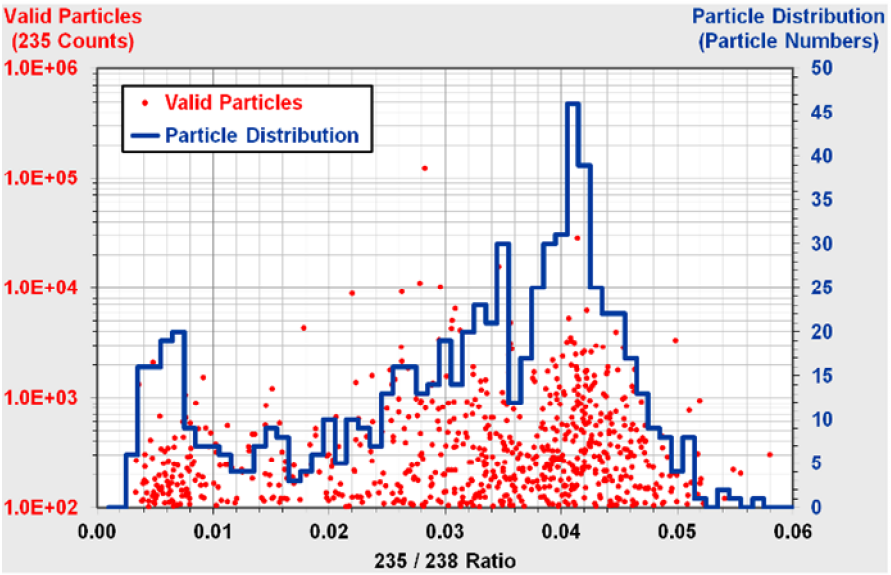

Figure 8: APM results from sample D. Left axis: Particle 235U signal versus as-measured $^{235}U/^{238}U$ ratio. Right axis: Particle $^{235}U/^{238}U$ histogram.

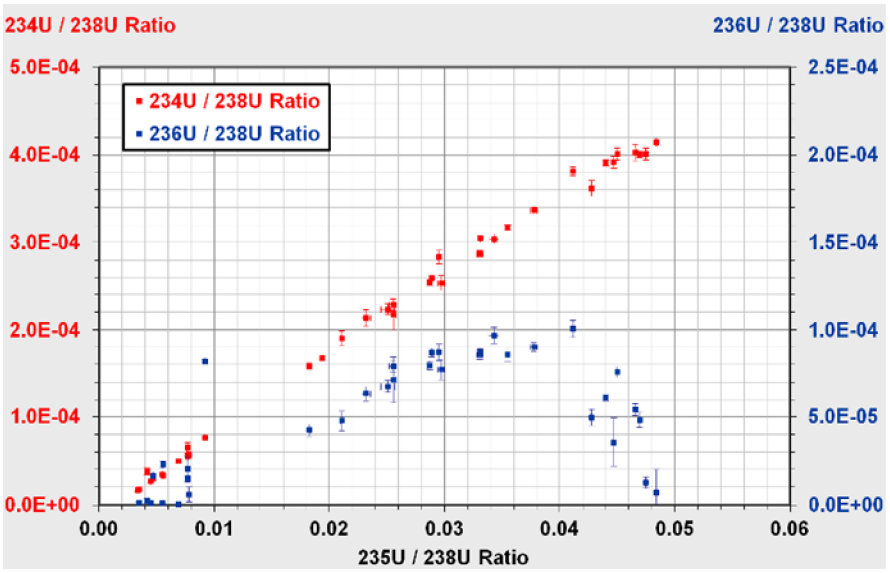

Figure 9: Ion microprobe results from Swipe D. Left axis: $^{234}U/^{238}U$ ratio versus $^{235}U/^{238}U$ ratio. Right axis: $^{236}U/^{238}U$ ratio versus $^{235}U/^{238}U$ ratio. Error bars shown are combined standard errors.

The distribution of $^{235}U/^{238}U$ ratios in Figure 8 shows maxima near 0.007 and 0.041. This is in good agreement with that obtained previously using a 4f SIMS [2,6] as are the number densities of uranium particles detected. The trends of $^{234}U/^{238}U$ and $^{236}U/^{238}U$ minor isotope ratios in Figure 9 are also the same as measured previously using 4f and 1270 SIMS instruments [6].

3.5. Sample S: Swipe sample recently characterised on 4f SIMS instrument

A total of 765, 250µm diameter fields, were examined by APM. 2,010 candidate uranium particles were found of which 599 passed the validation criteria. The distribution of uranium particle $^{235}U/^{238}U$ isotopic ratios obtained is shown in Figure 10.

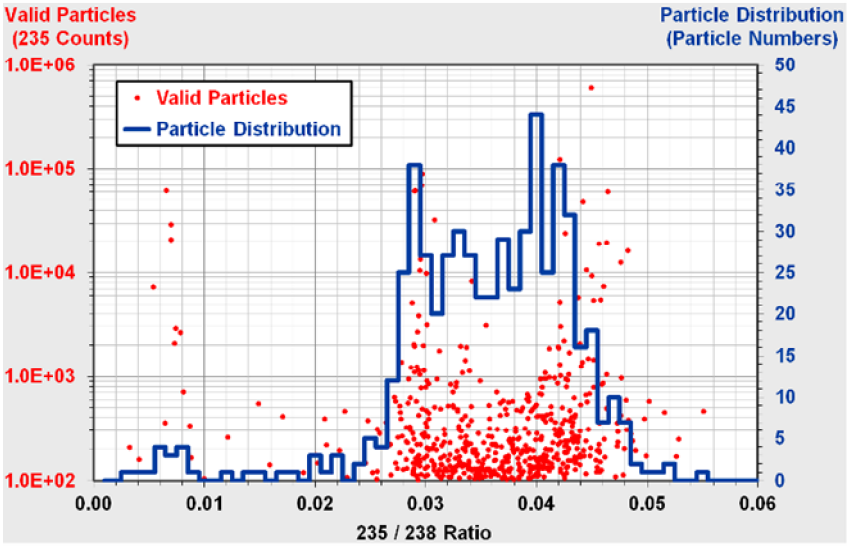

Figure 10: APM results from sample S. Left axis: Particle 235U signal versus as-measured $^{235}U/^{238}U$ ratio. Right axis: Particle $^{235}U/^{238}U$ histogram.

Previous 4f SIMS results [2,6] showed 3 well-defined populations associated with $^{235}U/^{238}U$ ratios of about 0.007, 0.03 and 0.045. The same distribution characteristics are clearly seen in Figure 10. 4f ion microprobe results showed consistent measurements of particles having $^{235}U/^{238}U$ ratios of 0.029 and 0.045. 1280HR microprobe results are shown in Figure 11 and clearly reproduce this behaviour. Also measured are a depleted particle and a cluster of particles near 0.007, the approximate natural uranium (NU) isotopic abundance.

4f SIMS minor isotope ratio values showed (where measurable) a linear dependence of $^{234}U/^{238}U$ on $^{235}U/^{238}U$ ratio, as would be expected for enrichment from NU feedstock, and this trend is also clear in Figure 11. In the 4f results, $^{236}U/^{238}U$ ratios measured for the enriched populations were all in the range 85-120ppm, and the 1280HR results in Figure 11 are very similar. Overall, the 1280HR-25 results show good agreement with the 4f measurements.

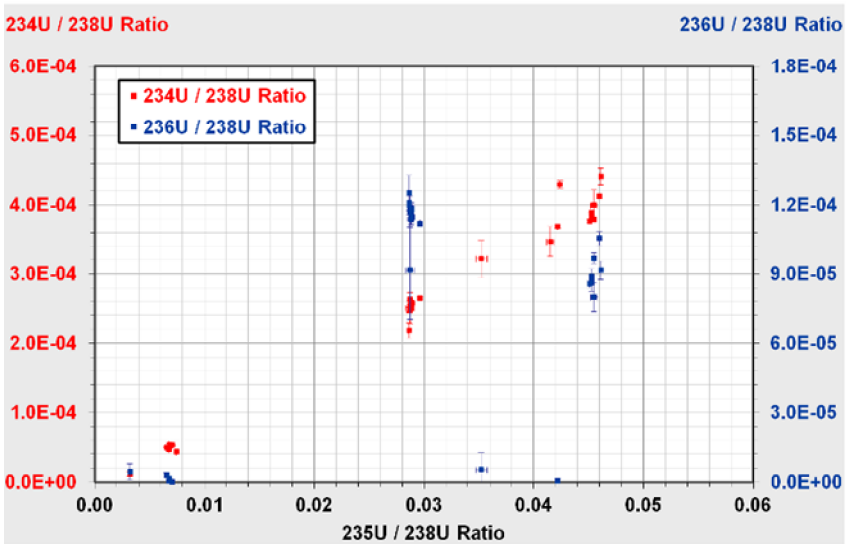

Figure 11: Ion microprobe results from sample S. Left axis: $^{234}U/^{238}U$ ratio versus $^{235}U/^{238}U$ ratio. Right axis: $^{236}U/^{238}U$ ratio versus $^{235}U/^{238}U$ ratio. Error bars shown are combined standard errors.

3.6 Sample IMS1-BLANK: Blank planchet

A grid of 48x43, 250µm diameter fields were examined by APM under the same conditions as used for all other samples. No uranium particles were detected.

4. Conclusions

Measurements of NBSU010 uranium isotopic reference particles were used to determine the mass bias factor of the 1280HR-25 SIMS instrument. Measurements made over a 6 month period were used to establish quality control information. These showed variations of the $^{235}U/^{238}U$ ratio within 0.3% relative SD. Good agreement between measured and certified minor isotope ratios (in the 50-70 ppm range) was found.

Measurements were also made of a NUSIMEP7 standard planchet having two certified uranium particle isotopic populations. APM search results showed a clear separation of the two major isotope ratios present. The proportion of particles measured with intermediate values was significantly lower than previously observed using a 4f SIMS instrument. This is probably due to the smaller diameter primary ion beam spot achieved with the 1280HR instrument, which allows better spatial resolution of closely neighbouring particles with different enrichments. There was good agreement of both major and minor isotope ratios measured by ion microprobe with the certified values (which spanned the range 8-350ppm). Measurement of the lowest $^{236}U/^{238}U$ ratio of 8ppm with acceptable agreement was particularly encouraging given the additional SIMS uncertainty resulting from the ^{235}UH hydride correction and the very small (ca. 500nm diameter) uranium particle size present on this sample.

The results from particle isotopic standards are compared in Table 6 and show that consistently better measurement precision and accuracy is achieved using the 1280HR instrument.

Reference sample	Measurand	Certified value	4f results [2]		1280HR results	
			Dev (%)	RSD (%)	Dev (%)	RSD (%)
NBSU010	$^{235}U/^{238}U$ MB	N/A	+2.09	0.95	+0.866	0.30
	$^{234}U/^{238}U$	5.47×10^{-5}	-0.2	8.7	-0.6	2.0
	$^{236}U/^{238}U$	6.88×10^{-5}	+4.0	8.2	+1.2	2.0
NUSIMEP NU7-064 Enrichment 1	$^{235}U/^{238}U$	9.073×10^{-3}	+0.23	2.8	-0.19	0.38
	$^{234}U/^{238}U$	7.44×10^{-5}	-2.8	10.7	+0.51	4.5
	$^{236}U/^{238}U$	8.0×10^{-6}	+19.1	28.5	+4.0	3.6
NUSIMEP NU7-064 Enrichment 2	$^{235}U/^{238}U$	3.4148×10^{-2}	-0.40	0.58	-0.59	0.58
	$^{234}U/^{238}U$	3.45×10^{-4}	-2.9	6.4	-2.3	2.3
	$^{236}U/^{238}U$	1.03×10^{-4}	+3.4	5.3	+2.1	4.5

Table 6: Comparison of 4f SIMS and 1280HR SIMS ion microprobe measurements (after mass bias correction) from reference particles

As a cross-contamination check, a blank (new) carbon planchet was stored in the instrument during validation. APM SIMS searching detected no uranium particles.

A field swipe sample, D, previously well-characterised by SIMS and SEM techniques, was measured to verify that previous results could be replicated. As is common with field swipe samples, uranium particles were only a small fraction of the total particles present. Consequently, there is a risk that uranium isotope measurements might be affected by mass interferences. Hence this sample provides a good test of the instrument performance with field swipe samples. The number density of uranium particles detected during the searching step using the 1280HR SIMS with APM software was similar to that detected previously using the 4f SIMS, and the major isotope ratio distributions obtained using the two instruments showed the same form. The minor isotope ratios measured by ion microprobe showed the same quantitative trends with ^{235}U enrichment in both cases.

Sample S provided a second comparison of a previously measured sample. The results again demonstrated a good correspondence in the number densities and $^{235}U/^{238}U$ ratio distributions of uranium particles detected using a 1280HR instrument with those detected using a 4f SIMS

instrument. Ion microprobe measurements from selected particles were also in good agreement between the two instruments.

The conclusion from this work is that the Cameca 1280HR-25 instrument at AWE provides at least equivalent performance in terms of uranium particle detection and location, as well as improved isotope ratio measurement precision and accuracy, in comparison with that achieved previously using a 4f SIMS instrument, and hence that validation of this instrument for analysis of environmental swipe samples has been successfully completed.

5. Acknowledgements

This work was part-funded by the UK Department of Energy and Climate Change through the UK Safeguards Technical Support Programme in support of IAEA Safeguards.

6. References

[1] IAEA Department of Safeguards report STR-348 (revision 1), *"Environmental sampling for Safeguards"* November 2011.

[2] Simons A J, Pidduck A J, Montgomery N J and Cairns J W , *"Revalidation of Cameca 4f SIMS Instrument for the Isotopic Analysis of Uranium Particles Extracted from Environmental Swipe Samples"*, Report SRDP-R312, UK Department of Energy and Climate Change, October 2012.

[3] Ranebo Y, Hedberg P M L, Whitehouse M J, Ingeneri K and Littmann S, *"Improved isotopic SIMS measurements of uranium particles for nuclear safeguards purposes",* J. Analytical Atomic Spectrometry 24, 277-287, 2009.

[4] Peres P, Hedberg P M L, Walton S, Montgomery N, Cliff J B, Rabemananjara F and Schuhmacher M, *"Nuclear safeguards applications using LG-SIMS with automated screening capabilities"*, Surface and Interface Analysis, wileyonlinelibrary.com DOI 10.1002/sia.5015, 2012

[5] Kips R, Leenaers A, Tamborini G, Betti M, Van den Berghe S, Wellum R and Taylor P D P, *"Characterisation of uranium particles produced by hydrolysis of UF_6 using SEM and SIMS"*, Microsc. Microanal. 13, 156–164, 2007.

[6] Pidduck A J, Houlton M R and Williams G M, *"A Comparison of Standard SIMS, Large-Geometry SIMS and SEM-EDX Analysis of Selected Environmental Swipe Samples"*, Report SRDP-R308, UK Department of Energy and Climate Change, October 2011

[7] Uriano G A, *"National Bureau of Standards Certificate, Standard Reference Material U-010"*, Office of Standard Reference Materials, Washington D.C., USA, 6 April 1981

[8] Truyens J and Aregbe Y,*"NUSIMEP-7 Uranium Isotope Amount Ratios in Uranium Particles"*, IRMM, Geel, Belgium, 29 September 2011

Precise and Accurate U Isotope Analysis using 1E13 Ohm Resistor Amplifiers on a Thermo Scientific ™ TRITON Plus™ MC-TIMS

Anne Trinquier[1], Helene Isnard[2], Michel Aubert[2], Peter Komander[1]

[1]Thermo Fisher Scientific
Hanna-Kunath-Str. 11, 28199 Bremen, Germany
[2]CEA Saclay (DEN/DPC/SEARS/LANIE)
91191 Gif-sur-Yvette cedex, France
E-mail: anne.trinquier @thermofisher.com

Abstract:

This study presents analytical advances in multi-collector thermal ionization mass spectrometry (MC-TIMS) that allow for improved uranium isotope ratio analysis, and introduces the newly designed 1E13 Ohm resistor current amplifiers. Accurate and precise uranium isotopic analysis is challenging because of the extreme range of the relative abundances of the U isotopes, peak tailing effects onto the minor isotopes and the requirement for certified isotopic reference materials. This study focuses on the conventional analysis at constant ion beam intensity of U isotope ratios down to the 1E-5 range on microgram-size sample loads. The samples were certified reference standards run in multiple static multicollection mode, combining 1E11 Ohm amplifiers for the major U ion beams with a 1E13 Ohm amplifier on the ^{236}U ion beam and a 1E12 Ohm amplifier or a secondary electron multiplier on the ^{234}U ion beam. Repeatability for static multicollection analysis of the NBS-U010 certified standard using a SEM and a 1E13 Ohm amplifier were compared. Repeatability for ion beams ≥ 60 kcps is twice as good with a 1E13 Ohm amplifier (RSD = 0.27%, k = 2.13, 90% confidence level) as with a secondary electron multiplier (RSD = 0.49%, k = 2.13, 90% confidence level), reflecting the superior stability of high-ohmic current amplifiers. External reproducibility for static multicollection analysis of the IRMM-187 certified standard was assessed. ^{234}U and ^{236}U ion beams were amplified by 1E13 Ohm resistor current amplifiers and peak tailing from the major isotopes was corrected using an off-line correction, based on the repeated estimates of peak tailing effects at masses ^{234}U and ^{236}U from other campaigns of analyses and the in-run analysis of the peak tailing at mass 237.05. This study shows that Faraday cups using high gain amplifiers provide precise (down to the subpermil range) and accurate analyses (down to the permil range) for uranium isotopic ratios in the 1E-5 range, with ion beams down to the 10 kcps range.

Keywords: 1E13 Ohm amplifiers; uranium; peak tailing; repeatability; accuracy

1. Introduction

The determination of uranium isotope ratios is required at various stages in the nuclear power fuel cycle, in nuclear safeguards, nuclear forensics and environmental monitoring. Thermal ionization mass spectrometry is the technique of choice for precise and accurate measurements of uranium isotope ratios. Due to the large range of uranium isotope ratios, different types of detection systems are typically used for detection of major and minor isotopes. The objective of this study was to investigate the potential of 1E13 Ohm resistor amplifiers for uranium isotope ratio measurements involving minor isotopes. The analyses originally focused on investigating and comparing the repeatability of isotope ratio determination, for ion beams in the 10 kcps range measured in a Faraday cup connected to a 1E13 Ohm resistor amplifier (for convenience, this detection system is thereafter referred as FC-1E13) and a Secondary Electron Multiplier (SEM) detector. In a second step, measurement accuracy was improved by a peak tailing correction scheme. There are different strategies to correct for peak-tailing. One such strategy, which involves measuring half-masses of the minor isotopes during the analysis and performing a cycle-by-cycle subtraction to the minor isotopes, is expected to be the most accurate, and is used in the Modified Total Evaporation routine developed

by NBL, IAEA-SGAS, ITE and IRMM[1]. In this study, the aim was to design an analytical protocol with one line of analysis only, resulting in half-masses of the minor isotopes not being measured. Instead, the approach was taken to apply an off-line peak tailing correction. The certified standards NBL CRM U010 and IRMM-187 analyzed in this study are characterized by similar ^{236}U relative abundances (Table 1).

	$n(^{234}U)/n(^{238}U)$	$n(^{235}U)/n(^{238}U)$	$n(^{236}U)/n(^{238}U)$
NBL CRM U010	0.000054484 (77)	0.010140 (10)	0.000069242 (57)
IRMM-187	0.00038700 (16)	0.047325 (14)	0.000071965 (39)

Table 1: Certified reference materials used in this study[1].

2. 1E13 Ohm resistor current amplifiers

The 1E13 Ohm resistor current amplifiers have been developed to improve the Johnson noise to signal ratio at low ion beam intensity (<50 fA) with respect to 1E11 Ohm and 1E12 Ohm resistor current amplifiers. The gain calibration of 1E13 Ohm resistor current amplifiers was performed using a neodymium reference standard[2]. Typical external reproducibility on the gains of 1E13 Ohm resistor current amplifiers over a year was less than or equal to 100 ppm (RSD, k=2, 95% confidence level).

3. Conventional analysis combining Faraday Cup and SEM detection

3.1. Ion beam setting and detection systems

SEM equipped with an energy filter	Faraday cup - 1E11 Ohm amplifier	Faraday cup – 1E13 Ohm amplifier	Faraday cup – 1E11 Ohm amplifier
^{234}U	^{235}U	^{236}U	^{238}U

Table 2: Detector configuration.

3.2. NBL CRM U010 analytical protocol

The certified standard NBL CRM U010 was measured on 5 different loads of 4 µg U each. The standard was scanned for interferences on the SEM detector. No interferences were found. Uranium isotope ratios were measured in multiple collection static mode for total integration times ranging from 900 to 1680 s. The signal was kept stable over the analysis with an average ^{236}U ion beam intensity between 10 and 30 fA, corresponding to ion beam signals between 100 and 300 mV on 1E13 Ohms resistor current amplifier, or 1 to 3 mV on 1E11 Ohm resistor current amplifier. This is also equivalent to 62 to 187 kcps detected on a SEM.

The SEM yield was assessed by the sequential analysis of a stable ion beam of Re on a Faraday Cup and on the SEM. The uncertainty associated with the SEM-Faraday cup inter-calibration, expressed as the standard error of the mean of 9 yield replicates, was propagated into the reported overall uncertainty u_y of the $^{234}U/^{238}U$ ratio (Table 4).

3.3. Results

The results are reported in Tables 3 to 5. 2RSE corresponds to the relative standard error, RD represents the relative deviation to certified ratios, and U_c represents the combined uncertainty comprising the absolute uncertainty associated to the analyses (2RSE) and the deviation (RD) to certified ratios. It can be noted that the relative deviation (RD) from the measured $n(^{235}U)/n(^{238}U)$ ratios to the certified $n(^{235}U)/n(^{238}U)$ ratio (Table 3) is less than the uncertainty on the certified $n(^{235}U)/n(^{238}U)$

ratio (0.1%, k=2, Table 1). Consequently, the n(^{234}U)/n(^{238}U), n(^{235}U)/n(^{238}U), and n(^{236}U)/n(^{238}U) ratios were not corrected for instrumental mass bias.

Analysis	I ^{236}U (fA)	^{235}U/^{238}U	2RSE %	RD (%)	U_c (%)
U010#1	30	0.010137	0.003	-0.028	0.028
U010#2	10	0.010136	0.002	-0.042	0.042
U010#3	12	0.010135	0.003	-0.050	0.050
U010#4	24	0.010136	0.003	-0.038	0.038
U010#5	26	0.010138	0.003	-0.021	0.021
Mean		0.010136			
RSD % (k=2.13)		0.025			

Table 3: ^{235}U/^{238}U ratios for NBL CRM UO10 using the Conventional protocol.

Analysis	I ^{236}U (fA)	^{234}U/^{238}U	2RSE (%)	u_y % (k=2)	RD (%)	U_c (%)
U010#1	30	0.0000555	0.02	0.28	1.91	1.93
U010#2	10	0.0000552	0.02	0.38	1.28	1.34
U010#3	12	0.0000553	0.03	0.38	1.47	1.52
U010#4	24	0.0000553	0.02	0.38	1.52	1.57
U010#5	26	0.0000553	0.02	0.28	1.42	1.45
Mean		0.000055				
RSD % (k=2.13)		0.491				

Table 4: ^{234}U/^{238}U ratios for NBL CRM UO10 using the Conventional protocol.

Analysis	I ^{236}U (fA)	^{236}U/^{238}U	2RSE %	RD (%)	U_c (%)
U010#1	30	0.0000713	0.03	2.95	2.95
U010#2	10	0.0000712	0.06	2.81	2.82
U010#3	12	0.0000712	0.06	2.77	2.77
U010#4	24	0.0000713	0.04	3.02	3.02
U010#5	26	0.0000714	0.03	3.08	3.08
Mean		0.000071			
RSD % (k=2.13)		0.272			

Table 5: ^{236}U/^{238}U ratios for NBL CRM UO10 using the Conventional protocol.

No peak tailing correction was performed on the minor isotopes, resulting in a significant deviation in the % range to certified values (Tables 4 and 5). Due to peak tailing variability over the course of an analysis and from run to run, peak tailing significantly contributes to analytical precision and repeatability.
As expected, for ^{234}U and ^{236}U, the combined uncertainty U_c is dominated by the deviation to certified values, thus calling for a peak tailing correction protocol.

Equivalent ion beams of ^{234}U measured on the SEM and ^{236}U measured with FC-1E13 show similar repeatability. For ion beam intensities > 30 fA and integration times > 1000 s, SEM and FC-1E13 provide similar analytical uncertainty (Tables 4 and 5). For ion beam intensities < 10 fA, the analytical uncertainty on the SEM is twice as good as on FC-1E13. However, for all ion beams investigated in

this study (>10 fA), the repeatability (RSD, k=2.13, 90% confidence level) was twice as good with FC-1E13 as with the SEM, thus validating high stability of the 1E13 Ohm resistor current amplifiers.

As expected, both accuracy and repeatability on minor isotopes would improve by applying a peak tailing correction, as exemplified in section 4.

4. Conventional analysis on Faraday cups with off-line peak-tailing correction

4.1. Ion beam setting and detection systems

Faraday cup -$10^{12}\Omega$ amplifier	Faraday cup -$10^{11}\Omega$ amplifier	Faraday cup -$10^{13}\Omega$ amplifier	Faraday cup -$10^{11}\Omega$ amplifier
^{234}U	^{235}U	^{236}U	^{238}U

Table 6: Detector configuration.

4.2. IRMM 187 analytical protocol

The certified standard IRMM-187 was measured on 4 different loads of 5.5 µg each. Uranium isotope ratios were measured in multiple collection static mode for total integration times ranging from 1380 to 1920s. The signal was kept stable over the course of the analysis with an average ^{236}U intensity between 29 and 33 fA, corresponding to between 290 and 330 mV on 1E13 Ohm resistor current amplifier, or 2.9 to 3.3 mV on 1E11 Ohm resistor current amplifier, also equivalent to 181-206 kcps on a SEM detector.

4.3. Peak tailing assessment and correction study

A protocol to correct for peak tailing on minor isotopes was designed, using the following approach. Peak tailing at mass 237.05 was measured simultaneously with U masses. Independently, the ratios $A_{236}/A_{237.05}$ and $A_{234}/A_{237.05}$ where A_{236} is the peak tailing at mass ^{236}U, A_{234} is the peak tailing at mass ^{234}U and $A_{237.05}$ is the peak tailing at mass 237.05 were assessed during several campaigns of analysis of IRMM-187 by MTE. In these campaigns, mass 237.05 and half-masses for the minor isotopes were measured, over the course of a multiple collection peak-jumping routine. The corresponding reproducibility was 23 % for $A_{234}/A_{237.05}$ and 26 % for $A_{236}/A_{237.05}$ (RSD, k = 2, 95% confidence level).

4.4. Results

The results are reported in Tables 7 to 10. It can be noted that the mean of the relative deviations (RD) from the measured $n(^{235}U)/n(^{238}U)$ ratios to the certified $n(^{235}U)/n(^{238}U)$ ratio (Table 7) is less than the uncertainty on the certified $n(^{235}U)/n(^{238}U)$ ratio (0.030%, k=2, Table 1). Consequently, the $n(^{234}U)/n(^{238}U)$, $n(^{235}U)/n(^{238}U)$, and $n(^{236}U)/n(^{238}U)$ ratios were not corrected for instrumental mass bias.

For IRMM-187, $A_{236}/A_{237.05}$ = 0.321 (73) and $A_{234}/A_{237.05}$ = 0.174 (45) (k=2, 95% confidence level). These ratios determined by MTE and $A_{237.05}$ measured simultaneously with U masses provide an estimate of A_{234} and A_{236} for the present study (Table 8). The reported uncertainty u_A on A_{236} and A_{234} combines the analytical uncertainty on $A_{237.05}$ and the propagated uncertainty of $A_{236}/A_{237.05}$ and $A_{234}/A_{237.05}$ ratios (Table 8). In turn, the reported uncertainty u on the minor isotope ratios combines the analytical uncertainty and the propagated peak tailing correction uncertainty (Tables 9 and 10). Though the combined uncertainty Uc (combining 2RSE and RD) is dominated by the relative deviation (RD), the obtained minor ratios corrected for peak tailing are accurate within the permil range, which represents one order of magnitude improvement compared to analyses without peak tailing correction, as demonstrated in section 3.

Analysis	I ^{236}U (fA)	^{235}U/^{238}U	2RSE (%)	RD (%)	U_c (%)
IRMM 187#1	33	4.7348E-02	0.008	0.050	0.050
IRMM 187#2	30	4.7320E-02	0.003	-0.010	0.010
IRMM 187#3	29	4.7346E-02	0.002	0.045	0.045
IRMM 187#4	29	4.7332E-02	0.004	0.016	0.016
Mean		4.734E-02			
RSD % (k=2.35)		0.065			

Table 7: ^{235}U/^{238}U ratios for IRMM-187 using the Conventional protocol.

Analysis	$A_{237.05}$	2RSE (%)	A_{236}	u_A (%) (k=2)	A_{234}	u_A (%) (k=2)
IRMM-187#1	5.55E-06	0.81	1.78E-06	7.31	9.66E-07	4.49
IRMM-187#2	6.00E-06	0.65	1.93E-06	7.31	1.04E-06	4.49
IRMM-187#3	5.19E-06	0.96	1.67E-06	7.31	9.05E-07	4.49
IRMM-187#4	5.41E-06	0.69	1.74E-06	7.31	9.41E-07	4.49

Table 8: Peak tailing on masses 237.05, ^{236}U and ^{234}U.

Analysis	I ^{236}U (fA)	^{234}U/^{238}U	2RSE (%)	^{234}U/^{238}U $_{corrected}$	u % (k=2)	RD (%)	U_c (%)
IRMM 187#1	33	3.884E-04	0.013	3.8747E-04	0.017	0.120	0.121
IRMM 187#2	30	3.882E-04	0.009	3.8720E-04	0.015	0.052	0.054
IRMM 187#3	29	3.884E-04	0.009	3.8745E-04	0.014	0.117	0.118
IRMM 187#4	29	3.882E-04	0.008	3.8729E-04	0.014	0.076	0.077
Mean		3.883E-04		3.874E-04			
RSD % (k=2.35)		0.057		0.078			

Table 9: ^{234}U/^{238}U ratios for IRMM-187 using the Conventional protocol and peak tailing correction.

Analysis	I ^{236}U (fA)	^{236}U/^{238}U	2RSE (%)	^{236}U/^{238}U $_{corrected}$	u % (k=2)	RD (%)	U_c (%)
IRMM 187#1	33	7.4105E-05	0.025	7.2321E-05	0.182	0.494	0.527
IRMM 187#2	30	7.4151E-05	0.023	7.2223E-05	0.197	0.359	0.409
IRMM 187#3	29	7.3917E-05	0.025	7.2248E-05	0.171	0.393	0.428
IRMM 187#4	29	7.3980E-05	0.021	7.2242E-05	0.177	0.385	0.424
Mean		7.404E-05		7.226E-05			
RSD % (k=2.35)		0.344		0.139			

Table 10: ^{236}U/^{238}U ratios for IRMM-187 using the Conventional protocol and peak tailing correction.

The repeatability degrades marginally by 0.021% on the ^{234}U/^{238}U ratios corrected for peak tailing (RSD, k=2.35, 90% confidence level) but the accuracy improves by 0.25% (Table 9). The propagated uncertainty from the off-line peak tailing correction is significant and dominates the uncertainty u on the n(^{236}U)/n(^{238}U) ratios (Table 10). However, the repeatability and accuracy improve by a factor of 2.5 on the ^{236}U/^{238}U ratios corrected for peak tailing (RSD, k=2.35, 90% confidence level).

It should be noted that this off-line correction scheme must be considered with some caution. The ca 25% uncertainty (RSD, k=2) on $A_{236}/A_{237.05}$ and $A_{234}/A_{237.05}$ ratios on the certified standard IRMM-187 reflects variability with analytical conditions. Some added variability would result from mismatch in matrices and isotopic compositions. As such, this approach is sample-dependent and $A_{236}/A_{237.05}$ and

$A_{234}/A_{237.05}$ ratios determined on a certified standard cannot readily be applied to unknown samples. For users performing uranium isotope ratio determinations on a body of samples with identical, or near-identical, sample matrices and highly similar isotope ratios, application of this procedure using a generic or "standard" sample holds potential for a simplified, yet robust method of enhancing overall precision in uranium isotopic ratio analysis by TIMS.

5. Conclusion

This study demonstrates the potential of Faraday cups using 1E13 Ohm current amplifiers for precise and accurate analysis of uranium isotopic ratios in the 1E-5 range, down to ion beams in the 10 kcps range. Using 1E13 Ohm current amplifiers, accuracy and repeatability are not limited by ion counting statistics but are primarily governed by sample running conditions and data processing, such as peak tailing corrections, calling for a rigorous assessment of the validity of selected peak tailing correction schemes and associated uncertainties.

6. Acknowledgements

The authors would like to acknowledge Charles Douthitt, Peter Huelstede, Hartmut Bars, Richard Heming, Johannes Schwieters and Heinz Lerche for constructive comments and technical support.

7. References

[1] Richter S, Kuehn H, Aregbe Y, Hedberg M, Horta-Domenech J, Mayer K, Zuleger E, Buerger S, Boulyga S, Koepf A, Poths J and Mathew K; *Improvements in routine uranium isotope ratio measurements using the modified total evaporation method for multi-collector thermal ionization mass spectrometry; J. Anal. At. Spectrom.;* 25; 2011; p 550-564.

[2] Trinquier A; *Gain Calibration Protocol for 1E13 Ohm Resistor Current Amplifiers using the Certified Neodymium Standard JNdi-1 on the TRITON Plus;* Thermo Fisher Scientific technical note*;* TN30285.

Session 19

Geological Repositories

CIGEO : The French Industrial Project of Deep Geological Repository Developed by Andra - Future Safeguards Considerations

Florence Poidevin[a], Pascal Leverd[b]

[a]IRSN (Institut de Radioprotection et de Sûreté Nucléaire)
Fontenay-Aux-Roses, France
[b]ANDRA (Agence Nationale pour la gestion des Déchets Radioactifs)
Châtenay-Malabry, France

Abstract:

This paper will start by an overview of ANDRA, the French public body in charge of waste management, and IRSN, the French public body in charge of the scientific assessment of nuclear and radiation risks.
The future French deep geological repository for High Level Waste and Intermediate Level Waste (Long Lived), called Cigéo, will be described.
Finally this paper will focus on safeguards consideration for Cigéo, in a Safegards by Design prospect.

Keywords: repository; safeguards; France; ANDRA; IRSN

1. ANDRA

Andra is a publicly owned industrial and commercial body, set up by the French radioactive waste management and research Act of 1991. It is responsible for identifying, implementing and guaranteeing safe management solutions for all French radioactive waste, in order to protect present and future generations from the risks inherent in such substances.
Andra is independent of the producers of radioactive waste.

Figure 1: ANDRA's sites

90% (in volume) of the radioactive waste produced every year is disposed of in existing repositories in France (VLLW & L/ILW-SL). Andra is currently looking into solutions for dealing with other types of waste. In the meantime, the waste is in interim storage in specific facilities.

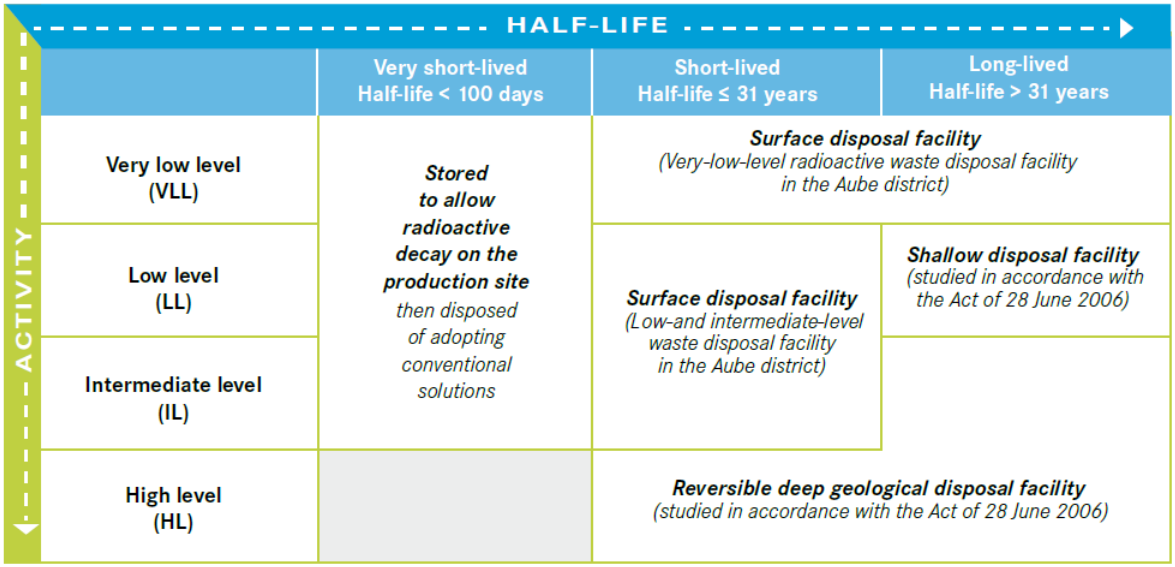

Figure 2 : the French waste classification

Andra is responsible for the study and the design of Cigéo, the future industrial deep geological repository devoted to the French high and intermediate level waste. It will also be the future operator of the repository.

Andra's website is www.andra.fr/international.

2. IRSN

IRSN is a publicly owned industrial and commercial body, in charge of the scientific assessment of nuclear and radiation risks.
It is the French technical expert for safeguards, safety, security and radioprotection.

The SACI department is the technical support of the French Authorities for International Safeguards and CWC Implementation. Its four main activities consist in advising the French Authorities (CTE) and assisting the operators, producing national declarations, escorting international inspections, assessing documentation. As a result, SACI will be involved in the discussion about Cigéo's future safeguards.

SACI's website is http://non-proliferation.irsn.fr.

3. Technical description of CIGEO

In 2006, the French Parliament opted for deep reversible disposal as the solution for the long-term management of HLW and ILW-LL radioactive waste. Cigéo will be the French deep geological repository project for this waste.
The license application of Cigéo is currently being prepared and the first operations should start in 2025.

The inventory of Cigéo covers conditioned waste originating from the activities and the dismantling of 50 years of operations of the French nuclear installations licensed to date. In agreement to French policy, irradiated fuel is being reprocessed. As a result, the license application of Cigéo will not include the disposal of fuel assemblies.

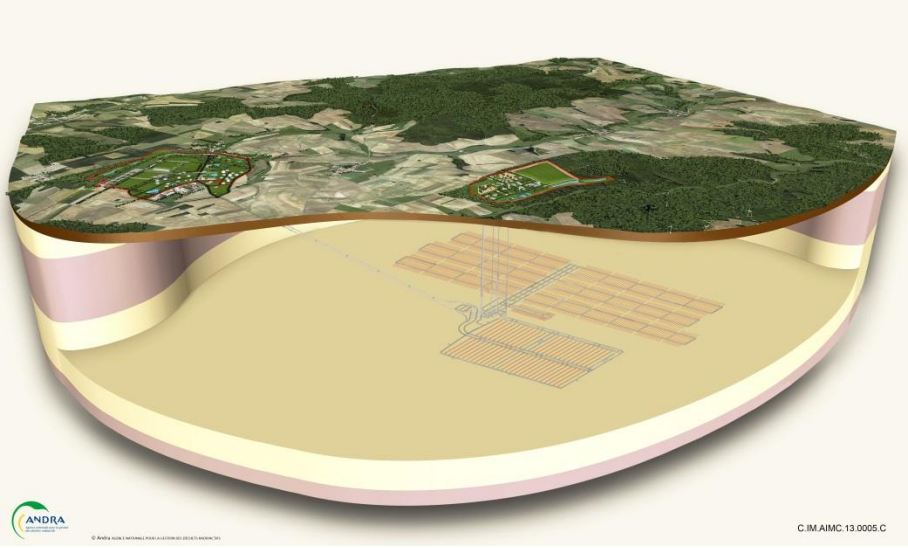

Figure 3 : the planned lay-out of the deep geological disposal facility

4. Safeguards considerations

Some of the waste disposed of in Cigéo contains nuclear material (U, Pu…) which will be entirely placed under Euratom safeguards (design information verification, control of accounting reports, inspections…).
Safeguards have been integrated as an early stage in the industrial project according to safeguards by design approach:

- Participation to international working groups : ESARDA (IRSN) & ASTOR (Andra & IRSN) ;
- First official contact with Euratom in 2014 in order to launch a regular technical exchange process.

The idea is to identify potential difficulties and introduce specific control needs as soon as possible in the project.
The technical important specificities to take into account are :

- The mass of nuclear material in the packages are declared to Andra by waste producers ;
- The conditioned waste disposed of are equivalent to safeguards-terminated material ;
- Cigéo does not extract any nuclear material from the waste ;
- Once a waste package has been emplaced in the underground disposal facility, it cannot be retrieved without being detected ;
- The exact location and movement of all waste packages are permanently known ;

Information on the inventory disposed of is kept with no duration limit (at least several centuries).

Safeguards instrumentation to the final disposal facility in Finland

Olli Okko, Timo Ansaranta, Elina Martikka, Mikael Moring

Radiation and Nuclear Safety Authority
Laippatie 4, 00880 Helsinki, Finland
E-mail: firstname.lastname@stuk.fi

Abstract:

In the disposal process, the spent fuel assemblies will be encapsulated in the disposal canister which will be the new item for accountancy and control. The spent fuel will not be available for re-verification and thus the containment and surveillance (C/S) measures will be essential to confirm the integrity of the disposal canisters during the storage, transfer to underground repository and to final emplacement position. The non-verifiability and non-accessibility of the disposed fuel create a challenge in creating and preserving reliable knowledge about the nuclear material and its location over centuries.

The national safeguards system has been effective from the beginning of the site investigation and the excavation phase in order to enable continuous design information verification and assurance on the absence of undeclared safeguards relevant activities and to facilitate possible future safeguards activities by the IAEA and the European Commission. The instrumentation of the facility is currently at a crucial moment, while all these needs are to be incorporated in the national licensing and further development of the disposal facility.

Keywords: final disposal of spent fuel, containment and surveillance, continuity of knowledge

1. Introduction

The direct disposal of spent nuclear fuel became an option already in the early 1980's and geological investigations to locate a suitable site for a deep repository begun in several countries. The safeguards concerns were addressed and the main issues were raised to be agreed upon with international consensus. The spent fuel assemblies will be encapsulated in welded disposal canisters which will be the new subject for accountancy and control. The spent fuel will not be available for re-verification and thus the containment and surveillance (C/S) measures will be essential, to confirm the integrity of the disposal canisters during storage and transfer to the underground repository, as well as to verify that they remain there until the drifts are closed and the repository is closed [1]. The continuity of knowledge must not be lost after the canisters have been disposed of in the geological formation because the repository shall not be reopened due to failure of safeguards. Therefore, robust and reliable C/S is required to confirm continuously that no nuclear material is retrieved from the underground premises. The up-to-date techniques to verify the nuclear material content to be disposed of and to confirm the integrity of the canisters during the transfer also in the underground were addressed by Fritzell et al. [2]. This paper focuses on the C/S techniques to safeguard spent nuclear fuel during the disposal process.

2. Review of the licence application for the disposal facility

The Finnish operator Posiva submitted an application to construct the final disposal facility at Olkiluoto to the Finnish government at the end of 2012. In addition to this, the applicant submitted to the Finnish regulator, STUK, a plan for arranging the nuclear materials safeguards which are necessary to prevent the proliferation of nuclear weapons, among other documents required in the national legislation. The safeguards plan describes the means and methods that will be applied by the future operator to fulfil the safeguards requirements laid down in the national legislation that includes also the international safeguards requirements. The current issues are the provision of design information, annual activity

plan and site declaration. A preliminary description of the applicant's internal control and reporting system for the nuclear materials is also included in the safeguards plan. According to the plan, the spent fuel will be under the operator's continuous surveillance during the encapsulation and disposal processes when the facility is constructed and commissioned, approximately by 2022. The whole application was reviewed by STUK during 2012 – 2015 and the plan for safeguards arrangements was separately approved by STUK. A similar procedure was used for the preliminary plan for security arrangements, preliminary safety assessment report and all other documents required by the national nuclear energy legislation. The licensing body is the Ministry for Employment and the Economy that will asses all the stakeholder's and public opinions, and will process the licence conditions accordingly.

In order to facilitate international safeguards the design information questionnaire documents are prepared separately for the encapsulation plant and the geological repository. The preliminary versions were reviewed in advance by the European Commission (EC) and the International Atomic Energy Agency (IAEA). After a few consultative negotiations between IAEA, EC, STUK and Posiva in 2013 and 2014, the need for safeguards instruments for the encapsulation process were specified according to the current integrated safeguards approach [3], and a requirement document was prepared by the EC and IAEA and submitted to STUK and the operator. The spent fuel shall be verified at the current location at the power plants and kept under IAEA/EC C/S through the whole encapsulation process [4]. The adaption of the surveillance methods requires some additional rooms and spaces that the operator will incorporate in the facility design updates. The needs were indicated to the operator during the review process. In case of changes in the detailed plans of the plant, the safeguards plan will also be reviewed and updated if necessary in the "Safeguards-by-Design" (SbD) process that is expected to continue during the planning and construction of the encapsulation facility.

The C/S equipment to be introduced in the geological repository can be adjusted later with the progress of facility construction and development, but the same SbD process shall be carried out for the whole disposal facility during its whole lifetime. The shape and volume of the accessible part of the repository will evolve during its lifetime, thus safeguards instrumentation will be adjusted continuously during the disposal process. The tunnels will be designed only for the intended use, thus equipment, e.g. portal monitors may need some additional spaces. Thus, the communication between the inspectorates and the operator will be essential during the development and in particular the excavation work, in case any additional spaces are needed for the instruments, e.g. for portal monitors.

2. New challenges for the C/S system

The need to know the exact location of the spent fuel canister in the repository is not considered relevant in the generic safeguards approaches for geological repositories as the fuel becomes inaccessible in the geological medium. Therefore, the safeguards conclusions can be based solely on the effective containment and surveillance measures in stead of traditional item counting and re-verification [5]. In the generic safeguards approach [6] the access points to the repository shall be safeguarded for transfers of nuclear material. The continuity of knowledge is extremely important to provide credible assurance about inventories and to avoid any re-verification in the repository. In the current integrated safeguards approach [7] highly reliable redundant C/S systems are suggested to be applied during the transfer to the repository, but no C/S is considered in the repository itself. Remote data transmission should be used to give immediate responses on possible equipment failure.

The assurance of the integrity of the disposal canister during the transfers in the repository is essential for safety, security and safeguards. Fritzell et al. [2] suggested that the emplacement vehicle could be equipped with positioning and radiation monitoring systems to detect any replacement activities as the circumstances in the Swedish and Finnish repositories are suitable for this kind of devices. As the first prototype vehicle is constructed, the planning of the installation of the IAEA/EC C/S equipment on the vehicle should be a rather straightforward procedure before the operations start. In the safeguards plan, the operator has indicated that the spent fuel movements will be recorded and documented to assure the safe transfer of the disposal canisters to their final position. It is important to have also international confidence in the integrity of the disposed canisters to avoid all possible confrontations and discussions about unsafeguarded transfers of spent fuel in the underground.

3. Possible joint use of equipment

For safety reasons, the operator must have an environmental, and in particular a radiation monitoring programme in the facility, thus the movement of radioactive materials is followed by radiation detectors trough the encapsulation and disposal process. It is essential to have security measures applied on the fuel transfers also in the underground. Therefore both understanding the tunnel systems and having surveillance and navigation systems in place are necessary. All these data contribute to confidence building measures for safety, security and safeguards. However, the need to have independent or authenticated records to be used by the IAEA, has shown to be one of the obstacles for the efficient use of original data collected by the stakeholders, e.g., operator's staff, contracted companies, science community etc.. In particular as the positioning of the sensors and also scheduling of maintenance breaks are decided by the operator, there is a reason for the IAEA and the EC to have their own C/S devices in place when considered necessary. However, the interaction between the parties and also 3 S's is to be encouraged to support the state findings and consequent safeguards conclusions.

4. Continuity of knowledge

During the underground construction of the geological repository, the main focus in safeguards is on the generation of credible safeguards-relevant documents on the underground premises and geoscientific monitoring records during the over 100-year long disposal project [8]. The documentation of the planned and, in particular, the excavated, and later back-filled rock volumes is intended to generate the design information declarations to be verified as safeguards measures during the operational time of the repository. The current integrated safeguards approaches [3 and 7] indicate that the DIV/PIV inspection will take place once a year, most likely also the C/S will be analysed on an annual base and safeguards conclusions will be drawn accordingly for the encapsulation plant and for the geological repository. After the closure of the repository these documents will also serve as assurance for non-diversion and as inventory maps providing the Continuity of Knowledge, CoK, for future generations. The repository site may be inspected as long as there is societal control over the land-use. The methods in archiving these data will evolve during the years to come. Therefore, the information and data need to be maintained over centuries with appropriate methods.

5. Summary

The generic concepts to safeguard spent fuel in a geological repository were developed 25 years ago when it became obvious that several countries were aiming at geological disposal of spent nuclear fuel. After that, the safeguards approaches have been slightly modified, e.g. owing to the introduction of the Additional Protocol, but the main principles are still valid. Most important is that during the disposal process continuous IAEA/EC surveillance is in place to confirm that no diversion of nuclear material occurs. As long as there is societal control over the disposal site, other IAEA safeguards measures can be reduced to a minimum according to the state-level approach.

The safe and secure disposal of spent nuclear fuel is a societal prerequisite for the use of nuclear power. In Finland, the operating company Posiva has submitted the construction licence application for the planned final disposal facility. A plan to conduct safeguards arrangements, including nuclear material accountancy and control, at the future facility is included in the application. The practical requirements for IAEA/EC safeguards instrumentation at the encapsulation plant, e.g. spaces requirements, cabling, office rooms are specified and will be fitted in the design and construction of the new building. The design and installation of the safeguards equipment will be carried out during the design, construction and operation of the whole disposal facility.

Up-to-date technology will be used in the safeguards of the disposal process. The material flow to the underground has to be controlled with reliable dual containment and surveillance techniques. It is recommended that existing C/S methods are to be applied to the canisters, all the way to the final disposal position, to confirm the integrity of the disposal canister. The conclusions about non-diversion as well as records about the location and the nuclear content of disposed canisters shall be maintained under institutional control for as long as possible.

6. References

[1] Fattah, A., Khlebnikov N.; *International safeguards aspects of spent-fuel disposal in permanent geological repositories,* IAEA Bulletin 1/1990, pp. 16 – 20.

[2] Fritzell A, Honkamaa T, Karhu P, Okko O, Håkansson A, Dahlin G.; *C/S in Final Disposal Processes –Swedish and Finnish Perspectives.* ESARDA Bulletin 38, 2008, pp. 10-16.

[3] International Atomic Energy Agency; *Model Integrated Safeguards Approach for a Spent Fuel Encapsulation Plant*. IAEA-SG-PR-1305, 2010, 9 p.

[4] Park, W.S., Coyne, J., Ingegneri, M., Enkhjin, L., Chew, L.S., Plenteda, R., Sprinkle, J., Yudin, Y. Ciuculescu, C., Baird, K., Koutsoyannopoulos, C., Murtezi, M., Schwalbach, P., Vaccaro, S., Pekkarinen, J., Thomas, M., Zein, A., Honkamaa, T., Hämäläinen, M., Martikka, E., Moring, M., Okko, O.; *Safeguards by Design at the Encapsulation Plant in Finland*, IAEA Safeguards Symposium 2014.

[5] Stein, G., Weh, R., Randl, R., Gerstler R.; *Final Disposal of Spent Fuel. Safeguards Aspects.* ESARDA Bulletin 12, 1987, pp. 6 – 10.

[6] International Atomic Energy Agency; *Safeguards for the Final Disposal of Spent Fuel in Geological Repositories*. IAEA, STR-312, 1998. 5 Volumes.

[7] International Atomic Energy Agency;. *Model Integrated Safeguards Approach for a Geological Repository.* IAEA-SG-PR-1306, 2010, 16 p.

[8] International Atomic Energy Agency; *Monitoring of Geological Repositories for High Level Radioactive Waste*. IAEA-TECDOC-1208, 2001, 25 p.

Modelling Seismic-Signal Propagation at a Salt Dome for Safeguards Monitoring

Jürgen Altmann
Experimentelle Physik III, Technische Universität Dortmund,
44221 Dortmund, Germany

Abstract:

The potential of seismic detection for detecting undeclared activities in/near an underground repository is an area of high interest for the German Support Programme to the IAEA. An experimental and theoretical focus is on salt since this is the best-investigated potential repository medium in Germany. After measurements of seismic and acoustic signals from various mining activities in a salt dome 2010 - 2012 the follow-on project is dealing with modelling of the propagation of seismic signals from relevant sources to potential sensor positions.

Model structures resembling a part of the salt dome and meshes covering it were constructed using the Trelis/Cubit program, by "sweeping" a two-dimensional cross section through the third dimension. For the seismic parameters of the various strata typical values were used; attenuation was modelled by quality factors constant with frequency. The three-dimensional propagation was computed by the program SpecFEM3D. Computation was done on the LiDO computer cluster of TU Dortmund. The source was put close to the potential repository. To simulate blasts a seismic-moment step function was used, picking and other sources were modelled by force impulses. Seismic signals were gained at many positions, underground and at the surface. For repetitive sources the single-pulse signals were superposed with appropriate delays. By fitting model amplitudes to measured ones preliminary assessments of source strengths can be done.

Keywords: final repository, salt, seismic monitoring, seismic modelling

1. Introduction

Without reprocessing spent nuclear fuel contains plutonium, thus such material should remain under IAEA safeguards even after emplacement in an underground final repository. This presents a new challenge for monitoring; geophysical techniques and methods have been proposed for this task. During operation, the creation of undeclared cavities needs to be detected, and those parts of the mine already filled with refuse have to be kept under surveillance for undeclared re-opening. After the emplacement phase, when drifts and shafts will have been closed, and the above-ground parts of the final repository will have been cleared for other uses, the IAEA needs the capability of long-term monitoring for covert access to the mine.

One potential technique is seismic sensing. Mining and other underground operations produce vibration directly as well as via acoustic noise. Seismic excitation propagates through the ambient medium and can thus be used to detect activities at a distance. The main question with seismic monitoring is whether signals from undeclared activities can be separated from signals from other sources and from background noise. In the operational phase of the repository most noise stems from the normal activity (mining, transport, filling, etc.), and sensors can be deployed at many sites in the mine. After closure, no sensors and cables can remain in the mine; in this phase sensors need to be located at some distance, but still underground in order to reduce seismic background, produced by traffic, industry, agriculture and weather at the surface.

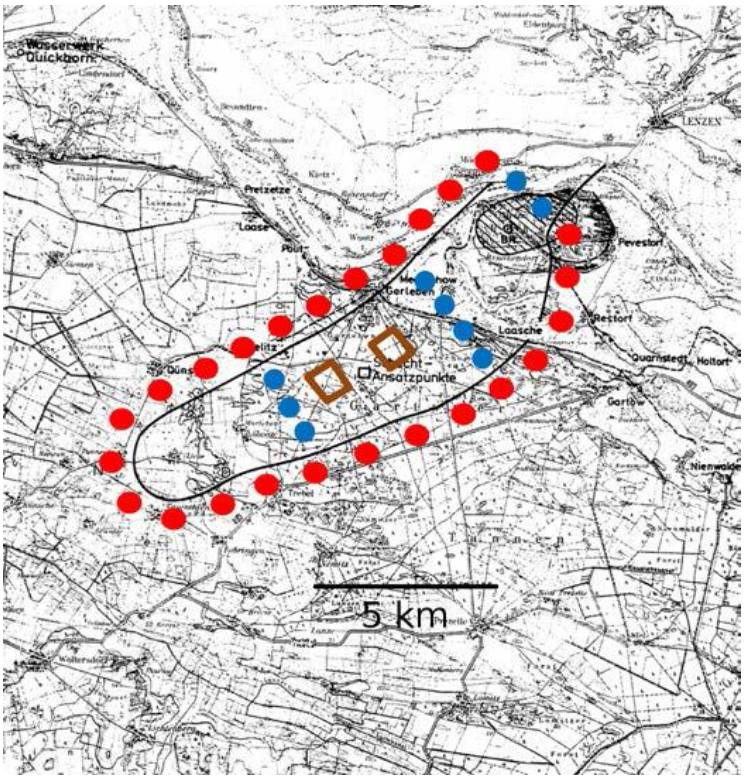

Figure 1: Notional possibilities for placement of seismic sensors after a possible emplacement phase in Gorleben, avoiding the planned repository volume at around 900 m depth (brown quadrangles) in the salt-dome centre. Blue: in the salt dome, red: surrounding it. Additional positions could be underground hundreds of metres above the repository, and at the surface. (Based on BfS map)

The German Support Programme to the IAEA has since many years taken an interest in seismic monitoring for final-repository safeguards. One potential repository site in Germany is the Gorleben salt dome (Figure 1); it was explored for its usability since 1986 under contract to the Federal Office for Radiation Protection (BfS). Following the new German Site Selection Act (Standortauswahlgesetz) of 2013, exploration has been stopped, but in the new search for an optimum repository medium and site, Gorleben remains an option.

Should this site be selected, the repository would be built at around 900 m depth in the centre of the salt dome (Figure 2). To detect undeclared activities in the vicinity, mainly new excavation, a monitoring system would use a sensor “fence” around the repository (Figure 1), with sensors and cables at safe distances from the backfilled and sealed shafts and tunnels. While sensors at the surface could contribute, they would suffer from relatively strong background noise from natural as well as artificial sources. For higher detection sensitivity most sensors would be deployed under-ground, at several hundred metres depth, laterally around the repository, outside and inside of the salt dome. In addition, underground positions above the repository could be used.

In order to gain information on the properties of seismic signals from mining activities, a dedicated measurement project had been carried out 2010-2012 at Gorleben, tasked by the German Support Programme to the IAEA [1, 2]. Many sources were measured with seismic and acoustic sensors deployed at various positions in the exploratory mine and at the surface. However, underground positions outside of the mine or even outside of the salt dome, as they would be used for seismic monitoring, could not be covered.

To find out the actual strengths and other properties of the signals from mining activities at such positions, measurements are needed, but these require expensive drilling that could be done only at very few test sites. As a prior step, a modelling project was done, again tasked by the German Support Programme to the IAEA.

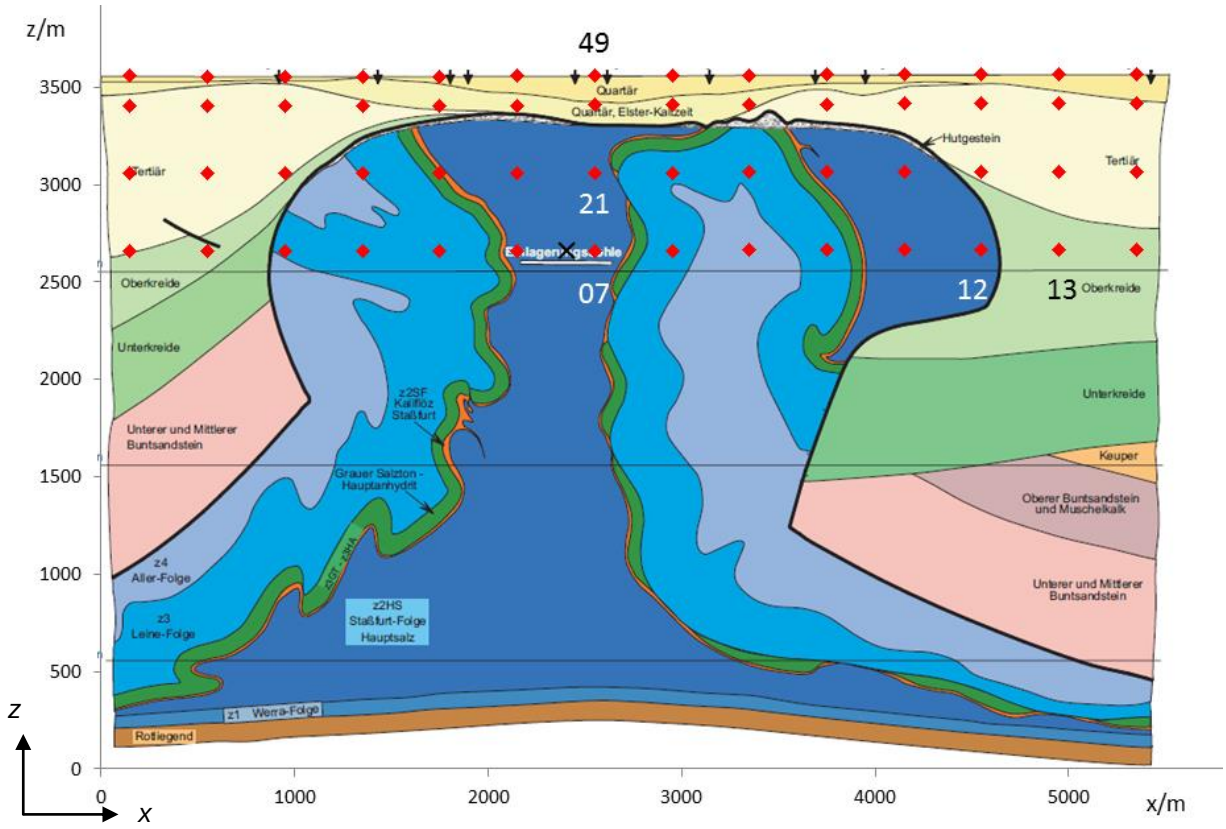

Figure 2: Simplified geological cross section in NW-SE direction through the salt dome. A possible repository level at about 930 m depth is indicated. The *x* and *z* axes of the chosen co-ordinate system are shown, the *y* axis points into the section plane. The section measures 5.52 km in the *x* and 3.57 km in the *z* direction, respectively. *x* is roughly south-east. In the model runs the source was put at 900 m depth (**X**). Red dots denote the sensor Positions 1 to 56 that lie in the centre plane at *y* = -500 m, corresponding sets of 56 sensors each are located in the planes at y = -900 m, -700 m, -300 m and -100 m. 32 additional positions at *y* = -600 m and -400 m, in *x* and *z* closer to the source, shift the total to 312. (Based on Figure 36 in [8])

2. Modelling programs

Since August 2012 a modelling project has been done, the final report is due at the end of June 2015. Because the salt dome and its surroundings have a complicated structure, numerical computations are needed. For this the spectral-finite-element code called SPECFEM was used, it has been developed for numerical simulation of seismic-wave propagation in heterogeneous and anisotropic media [e.g. 3, 4]. This open-source program [5] is widely used in the seismological community. It is very efficient, with boundary conditions included. Attenuation can be incorporated by quality factors constant with frequency.

After a two- or three-dimensional structure was set up e.g. in AutoCAD, it was transferred as an ACIS file to the commercial program Trelis (formerly CUBIT) [6] which was then used to produce a mesh of quadrilaterals or hexahedra, respectively, assign seismic properties to the partial volumes and combine those belonging to the same geological stratum to blocks. Several programs, part of the SpecFEM2D or SpecFEM3D packages, then separated the geometry into parts, one for each processing node to be used, and built the respective data-base files of mesh nodes and the associated seismic properties.

While two-dimensional propagation was run on a single Linux PC with a 4-core CPU, three-dimensional computations were done on mostly 340, sometimes 256 or fewer processors of the LiDO computing cluster of Technische Universität Dortmund [8]. The processing time depended on the number of mesh elements and the modelling duration, of course. Running the model for 2 seconds on 340 processors for 100,000 time steps of 0.02 ms required around 1 hour in case of about 420,000

elements (intended mesh-element size 40 m) and around 40 hours (close to the limit of 48 h with such a number of processors) with 5.5 million elements (intended size 15 m) (see also Table 1 below).

3. Model structures, meshing

For realistic simulations of seismic propagation, in principle knowledge of the full three-dimensional structure of the underground would be needed, at a resolution comparable to the size of the mesh elements, on the order of 10 m. However, this information was not available throughout the salt dome – the data that were provided by the Bundesanstalt für Geowissenschaften und Rohstoffe (BGR, Hannover) comprise several horizontal and vertical planes only [see e.g. 9]. As a consequence it was decided to proceed from the simplified geological cross section of the salt dome and its surroundings shown in Figure 2, and extend it along the salt-dome axis (*y*) direction. The cross section was converted to an AutoCAD file describing the boundaries of the 16 media involved. Because the z2SF stratum (red/orange) is too thin and partly curled, it had to be removed to allow meshing with acceptable, that is not too small, elements. For the same reason some narrow valleys of the salt-dome cap (Hutgestein, grey) had to be flattened somewhat. A tedious process was needed to remove very small gaps and lateral protrusions caused by non-coinciding vertices of adjacent regions.

A first three-dimensional structure was built by joining the 15 remaining media of the cleaned cross section to four: base rock, salt, adjoining rock and overlying rock. This was then swept orthogonally, in the -*y* direction, by 1.0 km (Figure 3). A better approximation to reality was to keep the 15 media and sweep the full structure along the same orthogonal vector of the same length. This kept the different structures in the salt as well as in the adjoining rock that – even though the differences in wave speeds and densities are small – give rise to reflection. But this structure shows identical *x*-*z* cross sections at all *y* co-ordinates, and the media boundary surfaces are flat in *y* direction. As a consequence, specular reflection could occur over relatively large media-boundary areas.

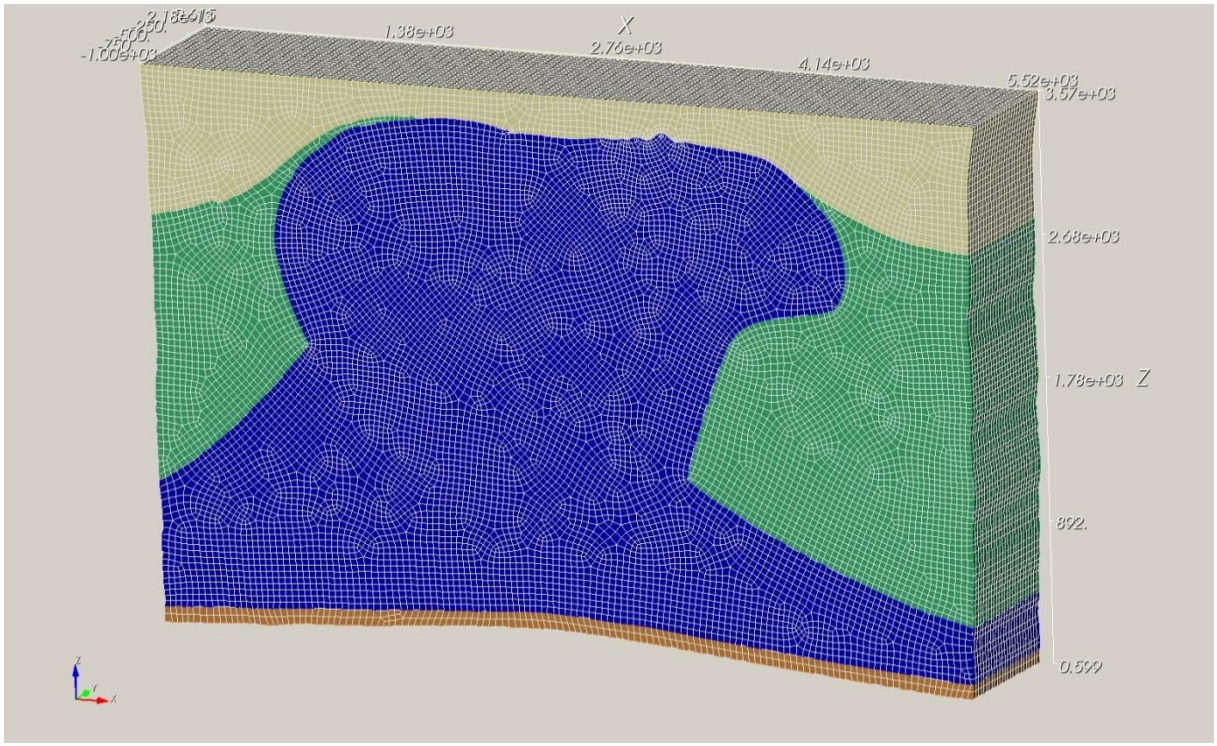

Figure 3: Three-dimensional underground model where the strata of Figure 2 have been united to form four partial blocks and the result has been swept in -*y* direction by 1.0 km, here with a mesh of 40 m intended element size.

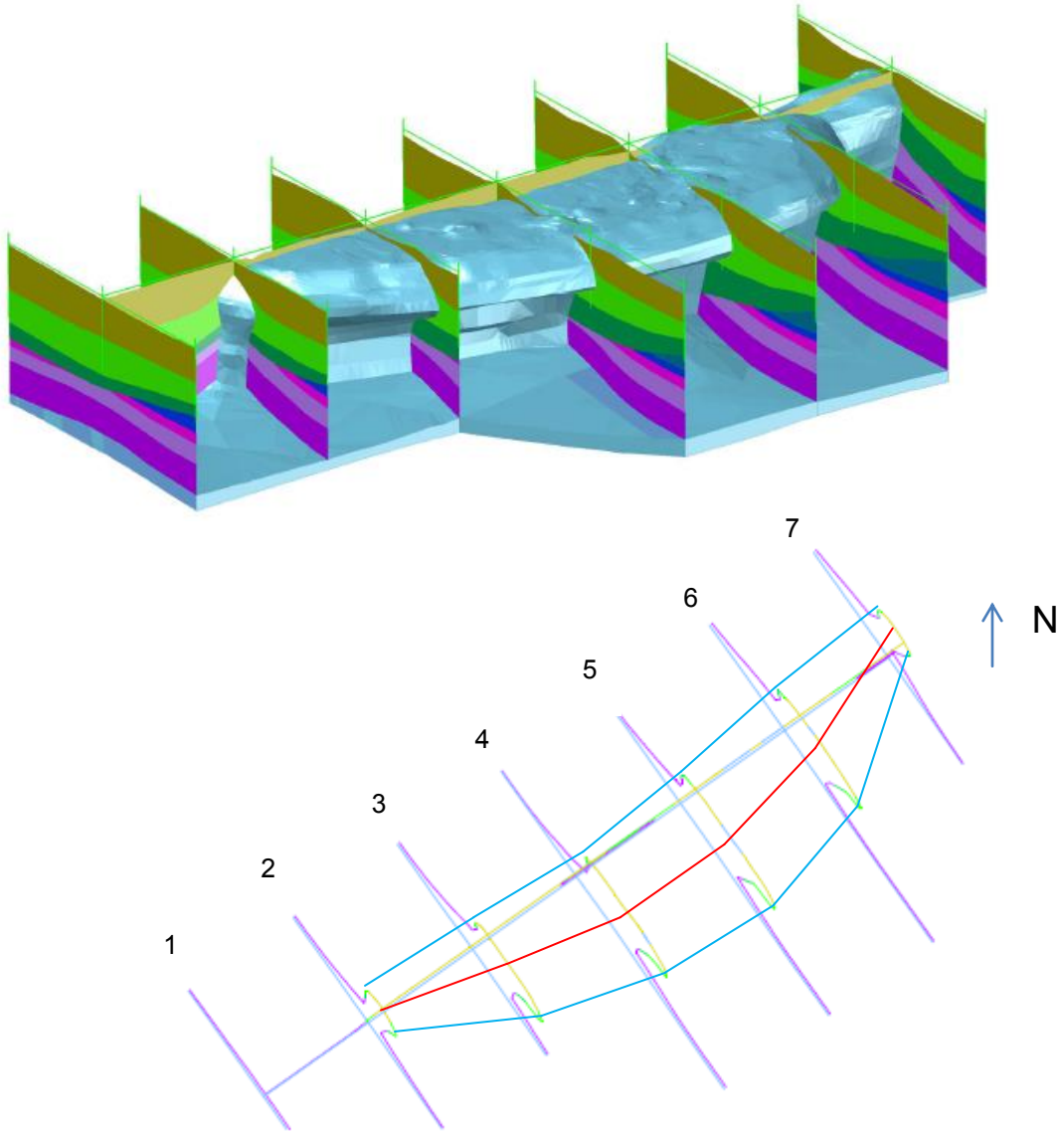

Figure 4: Salt-dome hull and adjoining layers.
Top: View of the salt-dome hull, looking roughly north, and the outer layers in various sections.
Bottom: Vertical sections through the outer salt-dome surface, seen nearly from vertically above. The cross section of Figure 2 is close to Section 5, the exploratory mine is between Sections 4 and 5. The extent of the salt-dome bulge is marked, the red line connects the respective centre points.
(Produced from BGR data)

To achieve curved boundary surfaces that better represent the actual salt-dome shape, it was intended to “sweep” the two-dimensional cross section through the third (*y*) dimension, while “morphing” it according to the actual variations of the salt dome along its axis. For this purpose, data describing the salt-dome hull and the layer boundaries outside of it in seven sections, provided by the BGR, were used (Figure 4). The respective extent of the salt-dome bulge as well as the depth of the salt-dome top were determined. The centre points were to be used for shifting the two-dimensional cross section in the *x* and *z* directions. Unfortunately, neither morphing nor the simpler change of scale in sweeping from one section to the next succeeded. Thus finally the two-dimensional cross section was put at Section 5 and swept to Section 2 along a three-dimensional spline through the centre points of sections 2 to 6, without scaling. To limit the number of mesh elements, the resulting structure of 9 km length was cut at 1 km from Section 5 (Figure 5).

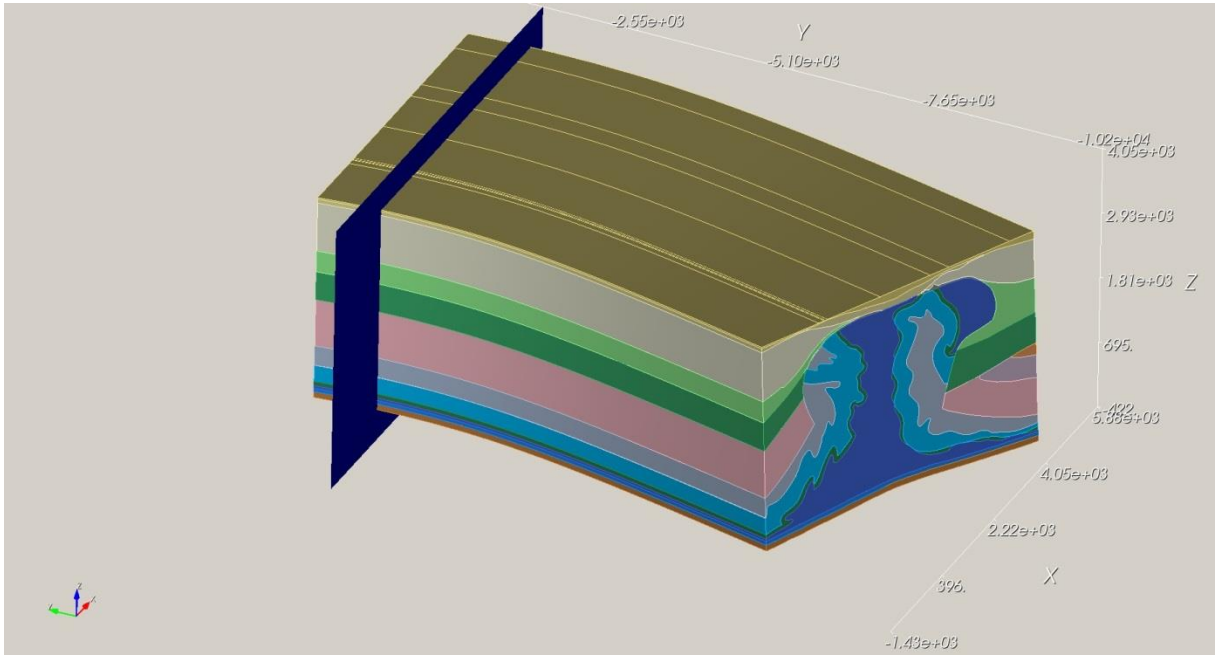

Figure 5: Result of sweeping the 15-media cross section of Figure 2 (with the modifications) along the three-dimensional spline. The structure was then cut at *y* = -1000 m and only the part left of the cut plane retained.

Meshing by the Trelis program was done first in two dimensions, applied to the media surfaces at Section 5. This was then extended towards the respective surfaces on the opposing margin of the model. One has to define an intended mesh-element size; the program then adapts the shape and size of the mesh elements so that the elements fit to the media boundaries. Table 1 shows the resulting number of elements if the intended size is varied between 40 and 10 m, for the three structures: 4- and 15-media models, swept along an orthogonal vector, and 15-media model, swept along the spline. It is evident that the actual element size varies significantly as the mesh accommodates the shapes of the various media boundaries. Similarly the distances between the so-called Gauss-Lobatto-Legendre (GLL) points (there are 5^3 GLL points in each mesh element), where the various properties are to be computed,[5] vary markedly.

Intended mesh-element size / m	**40**	**20**	**15**	**10**
No. elements with 4 media, vector sweep	0.320E6	2.39E6	5.50E6	16.5E6
No. elements with 15 media, vector sweep	0.415E6	2.40E6	5.49E6	18.2E6
No. elements with 15 media, spline sweep	0.419E6	2.39E6	5.47E6	18.4E6
Minimum element size / m, 15 media, vector sweep	2.1	2.1	2.1	2.6
Maximum element size / m, 15 media, vector sweep	84.3	52.4	38.1	30.1
Min. GLL point distance / m, 15 media, vector sweep	0.36	0.36	0.36	0.45
Max. GLL point distance / m, 15 media, vector sweep	27.6	17.2	12.5	9.8
Approximate run time per s / h	0.4	6	19	100

Table 1: Properties of the meshes for the three models with various intended element sizes: numbers of mesh elements (hexahedra), minimum and maximum element sizes, minimum and maximum distance between the Gauss-Lobatto-Legendre (GLL) points in the elements (the latter two for the 15-media orthogonal-vector sweep, the others are very similar), and approximate run time per second of model time using 340 processors with 0.02 ms time step.

After a mesh was built its quality was assessed, using the distribution of characteristics such as the skew and aspect ratio. For an acceptable mesh, the former should be below 0.8, and the latter above 0.2 for (nearly) all mesh elements [5]. This was fulfilled strictly for 15 m intended size and below, but for 20 m and 40 m the share of elements with worse characteristics was very low.

The last row of Table 1 gives the approximate run time for 1 second of model time using 340 processors and a 0.02 ms time step. Because about 2 s of model time are needed mostly, 10 m

intended size with around 200 hours computation time, far above the maximum of 48 h with a few hundred processors, is excluded. But 15 m fits, so this intended size was used mostly.

The time step was chosen as 0.02 ms for most runs. This is about half the threshold acceptable using a stability criterion. As source time functions for a force pulse a quasi-Dirac function was used, and an explosion was modelled by a quasi-Heaviside function for the seismic moment. The SpecFEM3D program simulates the former by a Gaussian function for the time derivative of the force; the half duration of a triangle function similar to the Gaussian is 1.63 * 5 times the time step, that is mostly 0.163 ms. The latter is approximated by the error function, the integral of a Gauss function similar to a triangle function of half duration 5 times the time step, mostly 0.10 ms. This short excitation causes spurious higher-frequency contributions in the seismic signals that were filtered out by convolution with a Gaussian function of the much longer half duration of mostly 10 ms, equivalent to 500 time steps. This number was found necessary for sufficient suppression of the higher frequencies. A doubled time step, still allowed under stability considerations, would lead to worse separation of individual arrivals.

Constant-quality attenuation is implemented in SpecFEM3D by normally three standard linear solids. The highest characteristic frequency is derived from the longest propagation time between neighbouring GLL points. This was 32 Hz with 15 m intended mesh-element size, whereas the source time function convolved with 10 ms half duration has a spectrum to above 100 Hz. Whether this mismatch produces errors in the attenuation needs to be investigated. It will be attempted to modify the meshing in order to reduce the maximum element size and GLL-point distance.

Because the seismic excitation is computed at all points for every time step, recording it at many positions does not increase the computation time, only the memory and disk space for the result files. Thus 56 sensors were put in five *x*-*z* planes each, at *y* = -500 m (the plane of the source), -900 m, -700 m, -300 m and -100 m, as shown in Figure 2. In addition to these 280 sensors, 32 more were placed at y = -600m and -400 m, relatively close to the source also in the *x* and *z* co-ordinates.

4. Results – two-dimensional propagation

For testing and better visualisation a few model runs were done in two dimensions with the program SpecFEM2D, just using the modified cross section. Here the geometric expansion in a homogeneous volume reduces the seismic amplitude with distance r in proportion to $r^{-0.5}$ whereas in three dimensions it is with r^{-1}. Figure 6 shows snapshots of wave propagation every 0.1 s after an explosion was ignited at the usual source position. The same parameters were used for the 15 media as in the three-dimensional case (Table 3), only here in addition to shear attenuation some bulk attenuation was included, with $Q_\kappa = 2\ Q_\mu$ for all media.

In Figure 6 the grey values indicate the P-wave velocities, the red colour in the wave fronts is linked to the ground velocity. Various effects can be seen, most relevant are reflection and transmission at the salt-dome boundaries with strong velocity contrast and at the free surface, but they occur also between different salt layers with a small velocity difference. Also visible is conversion from P to S waves and vice versa. Pictures such as these can be used to assign wave arrivals at a certain sensor position to the respective propagation paths.

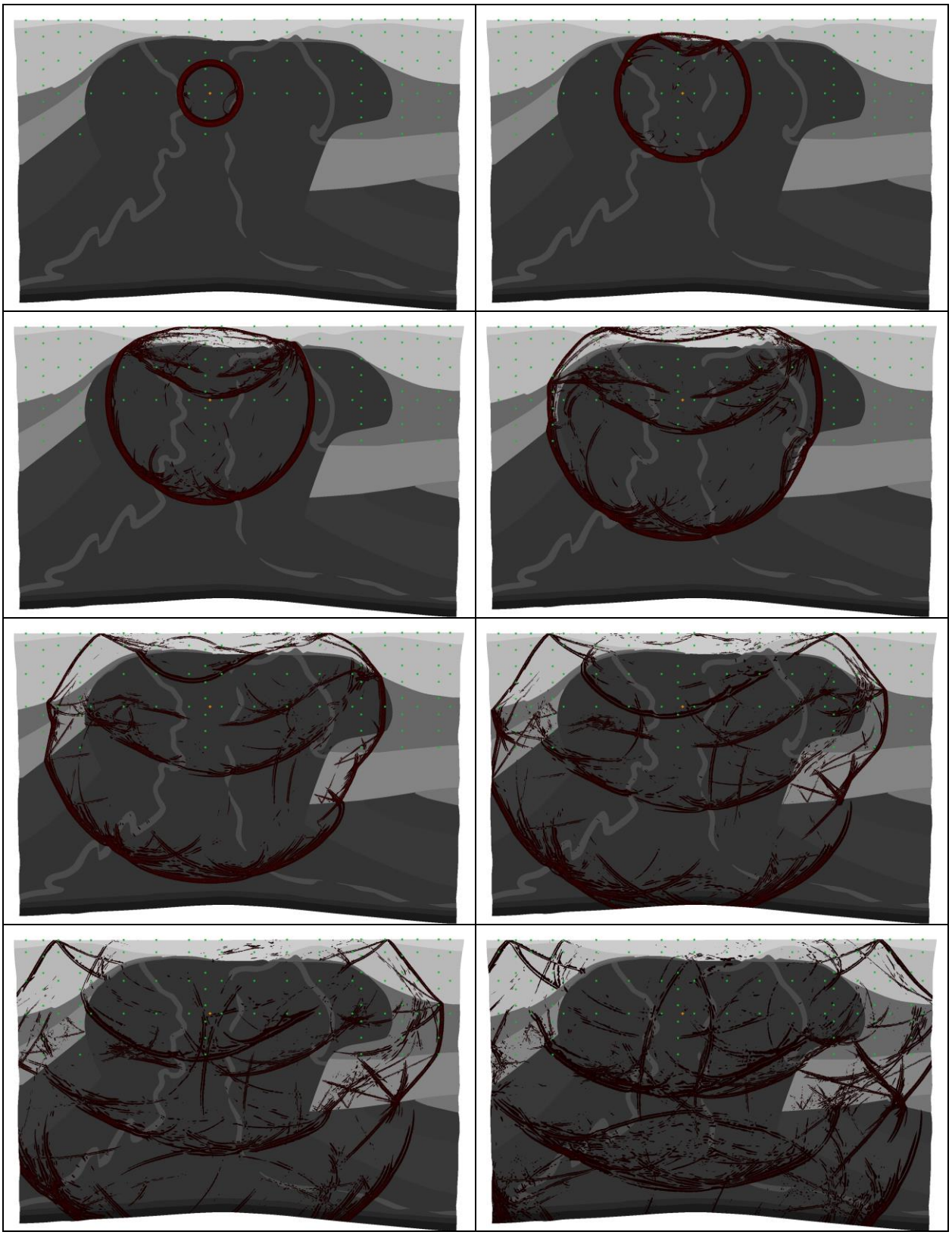

Figure 6: Snapshots of wave propagation every 0.1 s from an explosion (yellow dot) at 900 m depth, from 0.1 s to 0.8 s. Shown is the absolute magnitude of the seismic velocity, indicated by red colour, with some logarithmic distortion to make smaller values better visible. The grey value follows the P-wave velocity, from 1750 m/s at the surface to 4850 m/s in the base rock at about 3,300 m depth. The green dots denote sensor positions.

No.	Medium	ρ /(kg/m^3)	v_P /(m/s)	v_S /(m/s)	Q_κ	Q_μ
1	Rotliegendes	2,650	4,850	2,800	9,999	125
2	Surrounding rock	2,400	3,500	1,850	9,999	50
3	Overlying rock	2,000	1,750	1,000	9,999	20
4	Salt	2,200	4,400	2,600	9,999	50

Table 2: Seismic properties of the underground model of four different media as shown in Figure 3. Given are the density ρ, the P-wave velocity v_P, the S-wave velocity v_S, the bulk quality Q_κ (9,999 means no bulk attenuation) and the shear quality Q_μ.

No.	Medium	ρ /(kg/m^3)	v_P /(m/s)	v_S /(m/s)	Q_κ	Q_μ
1	z4	2,200	4,400	2,700	9,999	125
2	Oberer Bundsandstein/ Muschelkalk	2,600	4,350	2,500	9,999	50
3	Hutgestein	2,550	3,750	2,200	9,999	125
4	z3GT/HA	2,200	4,000	2,650	9,999	125
5	Unterkreide	2,350	3,000	1,400	9,999	50
6	z3	2,200	4,400	2,700	9,999	125
7	Tertiär	2,100	2,100	1,200	9,999	20
8	z2HS	2,200	4,400	2,600	9,999	125
9	Oberkreide	2,400	3,500	1,850	9,999	50
10	Keuper	2,500	3,300	1,700	9,999	50
11	Unterer/Mittlerer Buntsandstein	2,650	4,300	2,500	9,999	50
12	Rotliegendes	2,650	4,850	2,800	9,999	125
13	z1	2,200	4,600	2,650	9,999	125
14	Quartär Elster	2,000	1,750	1,000	9,999	20
15	Quartär	2,000	1,750	1,000	9,999	20

Table 3: Seismic properties in the 15-media model. For the media see Figure 2. Given are the density ρ, the P-wave velocity v_P, the S-wave velocity v_S, the bulk quality Q_κ and the shear quality Q_μ. In order to have only shear attenuation, the Q_κ values were set to fictitious 9,999.

5. Results – three-dimensional propagation

The results given here are still somewhat preliminary. The final findings will be presented in detail in a JOPAG report.

5.1 Single and repetitive signals

Two types of repetitive signals were modelled: a sequence of blast shots and picking. The four-media model was used here, with 40 m intended mesh-element size and a time step of 0.05 ms. In the convolution a Gaussian function with an equivalent half duration of 5.0 ms was used. Many single-pulse signals were superposed with time delays and in numbers similar to the ones observed in the measurements. As examples the signals at Sensors 7 and 13 (at the source depth of 900 m, 144 m and 2544 m, respectively, from the source in *x* direction), and at Sensors 21 and 49 (near-vertically above the source at 500 m depth and the surface, respectively, the *x* co-ordinate of both is 144 m higher than the one of the source) are shown.

Blast shots: When a tunnel was to be extended by five more metres, usually about 11 shots were done with 0.25 s spacing, igniting groups of charges in the different drill holes. The shots were modelled by a spherically symmetric point source, that is the seismic-moment tensor had equal values in the three main-diagonal elements and zero in the other components. The value was chosen as 1 Nm. Figure 7 shows the single-shot signals at the left and the 11 superposed ones with 0.25 s spacing at the right. Since an explosion excites nearly exclusively P waves, for the sensors lying in horizontal direction from the source the *x* component of ground velocity is shown, for the ones near vertically above the source the *z* component is presented. The *z* component at Sensors 7 and 13 as well as the *x* component at Sensors 21 and 49 are very small. The *y* component is essentially zero for sensors in

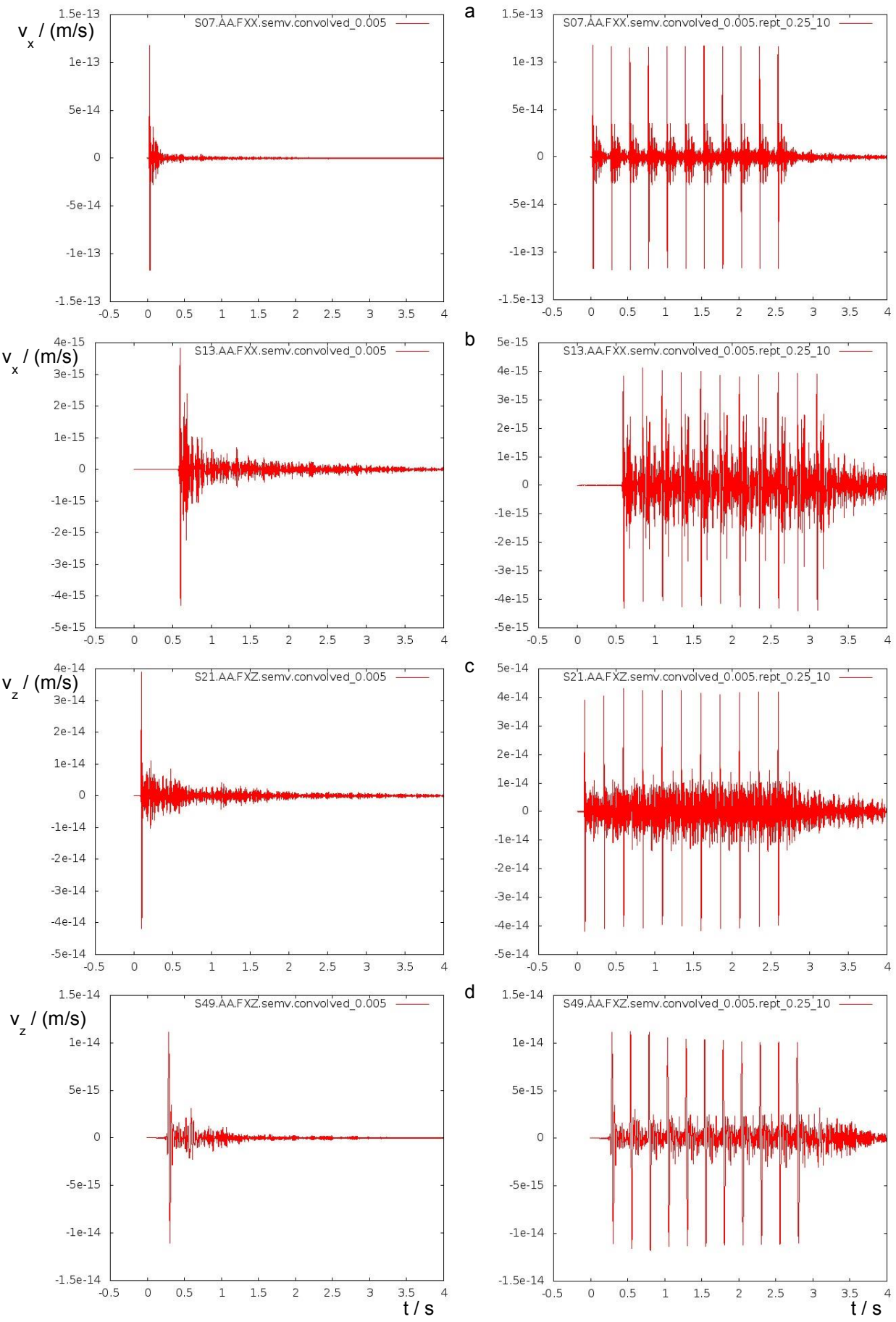
a
b
c
d
v_x / (m/s)
v_z / (m/s)
t / s
S07.AA.FXX.semv.convolved_0.005
S07.AA.FXX.semv.convolved_0.005.rept_0.25_10
S13.AA.FXX.semv.convolved_0.005
S13.AA.FXX.semv.convolved_0.005.rept_0.25_10
S21.AA.FXZ.semv.convolved_0.005
S21.AA.FXZ.semv.convolved_0.005.rept_0.25_10
S49.AA.FXZ.semv.convolved_0.005
S49.AA.FXZ.semv.convolved_0.005.rept_0.25_10

Figure 7: (Previous page) Model signals (ground velocity) at various sensor positions from a single explosion (left) and an 11-shot blast with 0.25 s spacing (right) in the main salt at 900 m depth.
a) *x* component at Sensor 7 (900 m depth, 144 m from the source in *x* direction);
b) *x* component at Sensor 13 (900 m depth, 2544 m from the source in *x* direction, just outside the salt);
c) *z* component at Sensor 21 (500 m depth, *x* co-ordinate 144 m higher than the source);
d) *z* component at Sensor 49 (at the surface, *x* co-ordinate 144 m higher than the source).

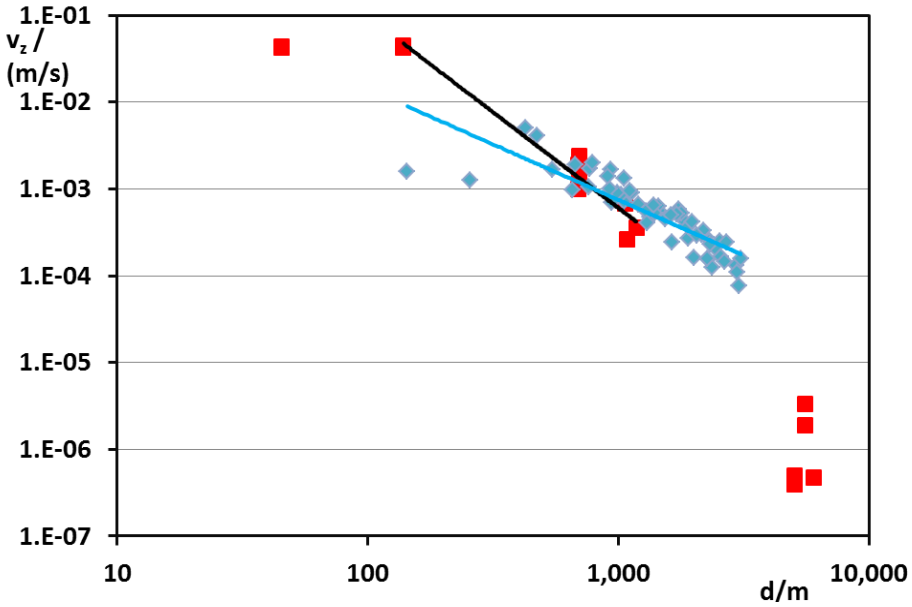

Figure 8: Peak-to-peak value of vertical seismic velocity versus distance. Red squares: measured from blast shots at 840 m depth; blue diamonds: model computation from an 11-shot blast at 900 m depth, multiplied by $6 \cdot 10^{10}$ to fit to the measured data at several 100 m distance. Measured values and trend as in [1]: Fig. 67; distances excluded from trend: 44 m (the sensor is in the seismic shadow of a drift), 5-6 km (much lower recording bandwidth). Power-law exponents are -2.2 for the measured data and -1.3 for the model ones.

the *y* = -500 m plane of the source, but it gets significant in the other planes where the P wave has a slant projection in the *x*-*y* plane. At many positions the duration of the one-shot signals is shorter than the repetition period, thus not much mutual overlap exists and the superposed signals look similar to simple repetitions, with similar amplitudes and spectra.

To compare the absolute amplitudes with the measured ones, Figure 8 shows the peak-to-peak values of seismic velocity of the model signals at all 56 sensor positions shown in Figure 2 (the *y* = -500 m plane of the source) versus geometric distance, in double-logarithmic scale. The best-fit power-law trend line has an exponent of -1.3. In order to fit the model values to the measured ones at several 100 m distance, the former had to be multiplied by $6 \cdot 10^{10}$. This means that – with the chosen moment-step equivalent-triangle half duration of 0.25 ms and the convolution half duration of 5.0 ms – the seismic moment is around 10^{11} Nm. Whether this is the correct order of magnitude for a momentary release of the mechanical energy of several kilograms of explosive, that is several megajoules, needs to be investigated.

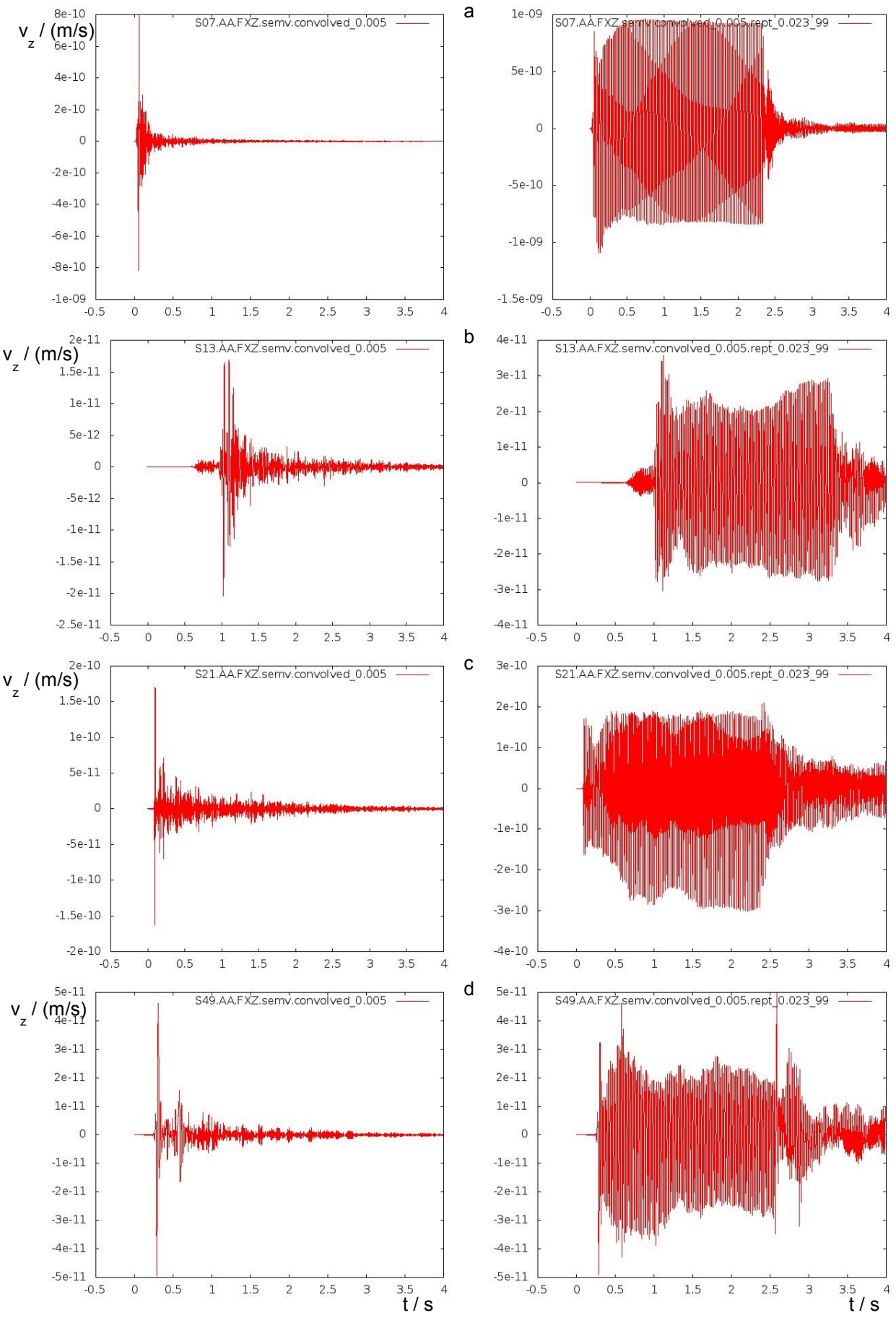
a
b
c
d
S07.AA.FXZ.semv.convolved_0.005
S07.AA.FXZ.semv.convolved_0.005.rept_0.023_99
S13.AA.FXZ.semv.convolved_0.005
S13.AA.FXZ.semv.convolved_0.005.rept_0.023_99
S21.AA.FXZ.semv.convolved_0.005
S21.AA.FXZ.semv.convolved_0.005.rept_0.023_99
S49.AA.FXZ.semv.convolved_0.005
S49.AA.FXZ.semv.convolved_0.005.rept_0.023_99
v_z / (m/s)
t / s

Figure 9: (Previous page) Model signals (ground velocity) at various sensor positions from a single force pulse in -*z* direction (left) and a sequence of 100 such picking blows with 23 ms spacing (right) in the main salt at 900 m depth.
a) *z* component at Sensor 7 (900 m depth, 144 m from the source in *x* direction);
b) *z* component at Sensor 13 (900 m depth, 2544 m from the source in *x* direction, just outside the salt);
c) *z* component at Sensor 21 (500 m depth, *x* co-ordinate 144 m higher than the source);
d) *z* component at Sensor 49 (at the surface, *x* co-ordinate 144 m higher than the source);

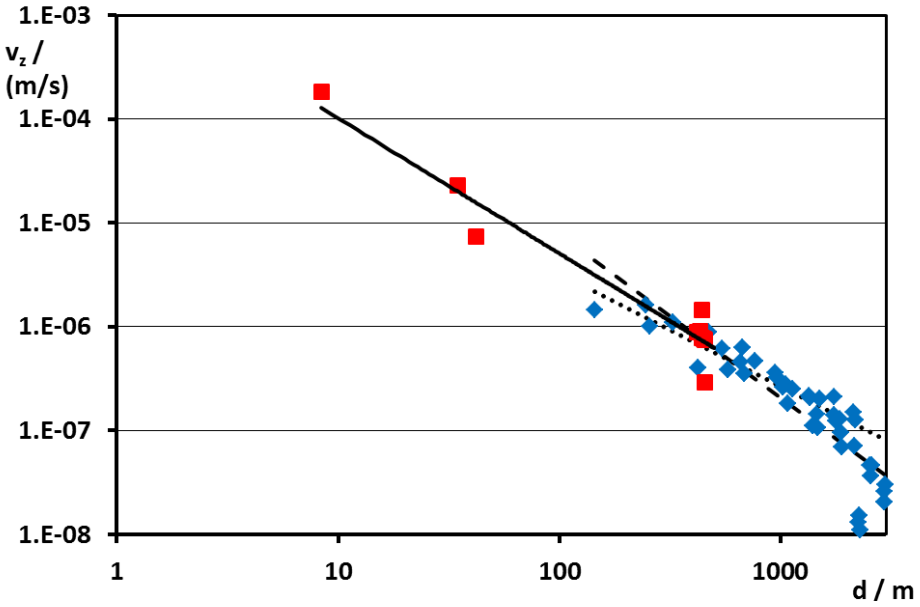

Figure 10: Measured peak-to-peak values for picking (red squares) with power-law trend line (solid), and model results from 100 blows with 23 ms spacing, multiplied by 700 (blue diamonds). Power-law exponents are -1.3 for the measured data and -1.6 for the model data using all positions (dashed) and -1.1 for the positions in the salt dome only (dotted).

Picking: The hand-held electrohydraulic pick hammer is used for a few seconds at a time. To model a single chisel blow a Gaussian force pulse of 1 N with equivalent half duration of 0.163 ms, applied in the -*z* direction, was assumed. The measurements had shown that the repetition frequency of the pick-hammer chisel is 44 Hz. Thus 100 single-pulse signals were superposed with 23 ms spacing. Here the single-signal duration is shorter than the repetition period, thus considerable overlap and significant variation of the envelope shape results. Figure 9 shows the single signals at the selected sensor positions at the left, and the superposed ones at the right. Because the force was vertical, the *z* component is shown for all four sensors; it has to be noted that in the horizontal direction (to Sensors 7 and 13) the main excitation travels as an S (transversal) wave whereas in the (near-)vertical direction (to Sensors 21 and 49) the seismic motion is mainly vertical, that is in the form of a P (longitudinal) wave. The *x* and *y* components are markedly smaller. Because the next single-blow signal is added to the preceding one when the latter still has significant amplitude, the superposed signal was found to be stronger than the single one by up to a factor 3.

Figure 10 shows the peak-to-peak values of vertical ground velocity from the model (all 5*14 sensors at the source depth in the planes at *y* = -900 m, -700 m, -500 m, -300 m and -100 m) and from the measurements versus geometric distance, again in double-logarithmic scale. Depending on whether the positions outside of the salt dome are included or not, the power-law trend line has an exponent of -1.6 or -1.1, the exponent for the measured data is -1.3. To fit the model values to the measured ones at several 100 m distance, the former had to be multiplied by $7 \cdot 10^2$, corresponding to an integrated model force of around 700 N with the source half duration of 0.163 ms and the convolution one of 5.0 ms. Whether this is plausible for a picking chisel releasing about 25 J energy needs to be investigated.

5.2 Comparison of the three underground models

Runs using a force pulse in –z direction were done with the three model structures produced from the two-dimensional cross section: the four-media, orthogonal-vector sweep, the 15-media orthogonal vector sweep, and the 15-media spline sweep.

Figure 11 and Figure 12 show the vertical component of ground velocity for several sensors at the depth of the source, 900 m, in the *y* = -500 m plane of the source. Proceeding from the closest Sensor 7 at 144 m from the source to the farthest Sensor 14 at the model margin one can follow the dominant S-wave excitation as it arrives with increasing delay. The expected arrival times from the partial distances and corresponding S-wave speeds are marked “S” in the salt and “SS” after transmission to the adjoining rock, they fit very well.

Figure 13 presents the vertical ground velocity at the sensors near-vertically above the source, from 500 m depth via 150 m depth to the surface. Due to the vertical excitation here the P wave is dominant; its expected arrivals are marked “P”, and “PP” after transmission to the overlying rock.

The major difference between the three structures is that at some sensors at the source depth the four-media arrivals are somewhat later. This can be understood because the S-wave speed in the united salt body is the one of the main salt z2HS whereas in the 15-media model the wave additionally propagates through layers z2GT/HA, z3 and z4 with slightly higher S-wave velocities. But the general appearance and amplitudes are similar for all three models. Concerning the 15-media structures, the differences between the orthogonal-vector sweep and the spline sweep are relatively small.
Similar behaviour was observed at the other sensor positions analysed.

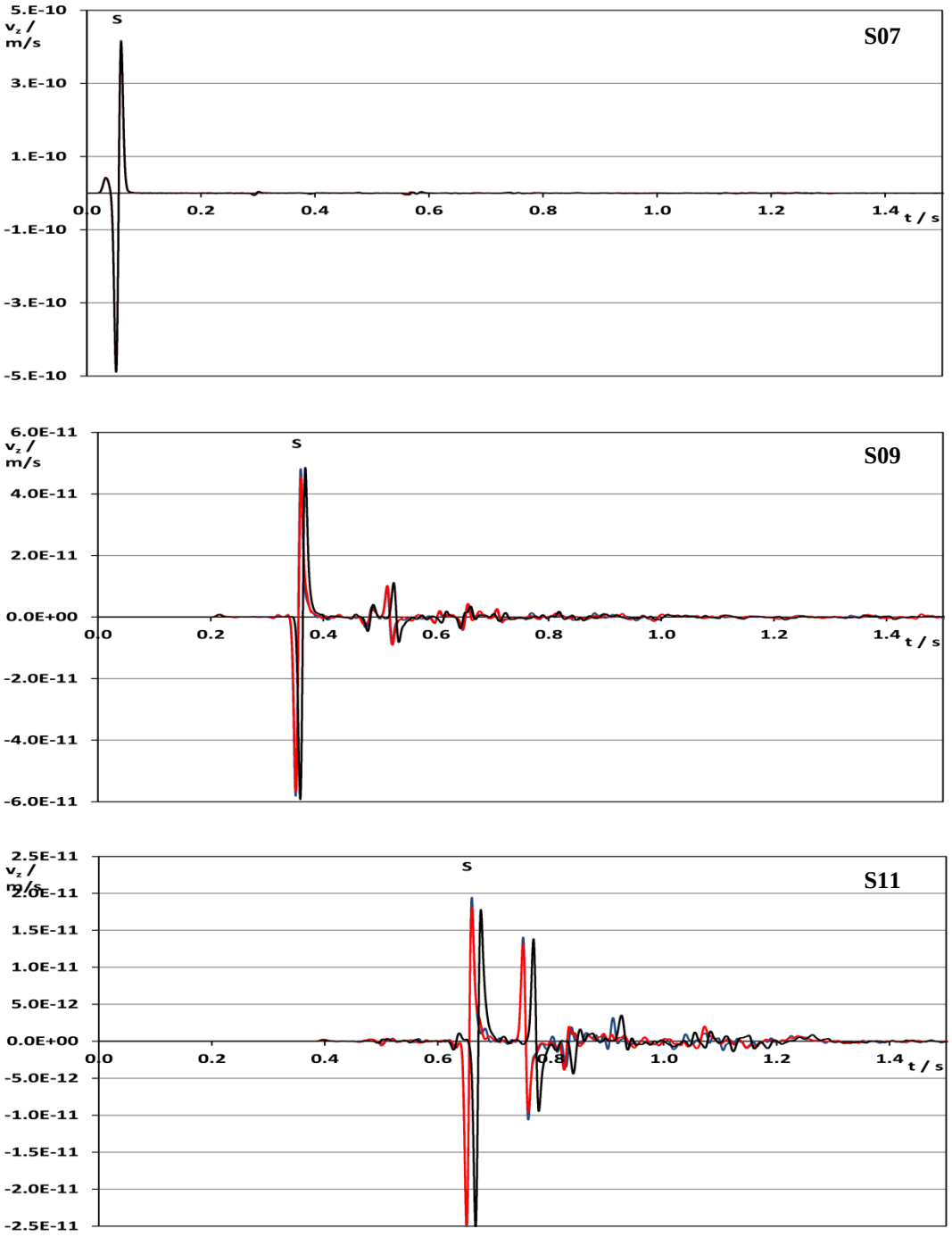

Figure 11 Vertical component of ground velocity at various *x* co-ordinates in the source plane (*y* = -500 m) at the source depth (900 m) after a force pulse in -*z* (down) direction. Sensors and source distances in *x* direction, from the top: 7, 144 m; 9, 944 m; 11, 1744 m. Black: 4 media, orthogonal sweep; blue: 15 media, orthogonal sweep; red: 15 media, spline sweep. The S-wave arrivals are marked.

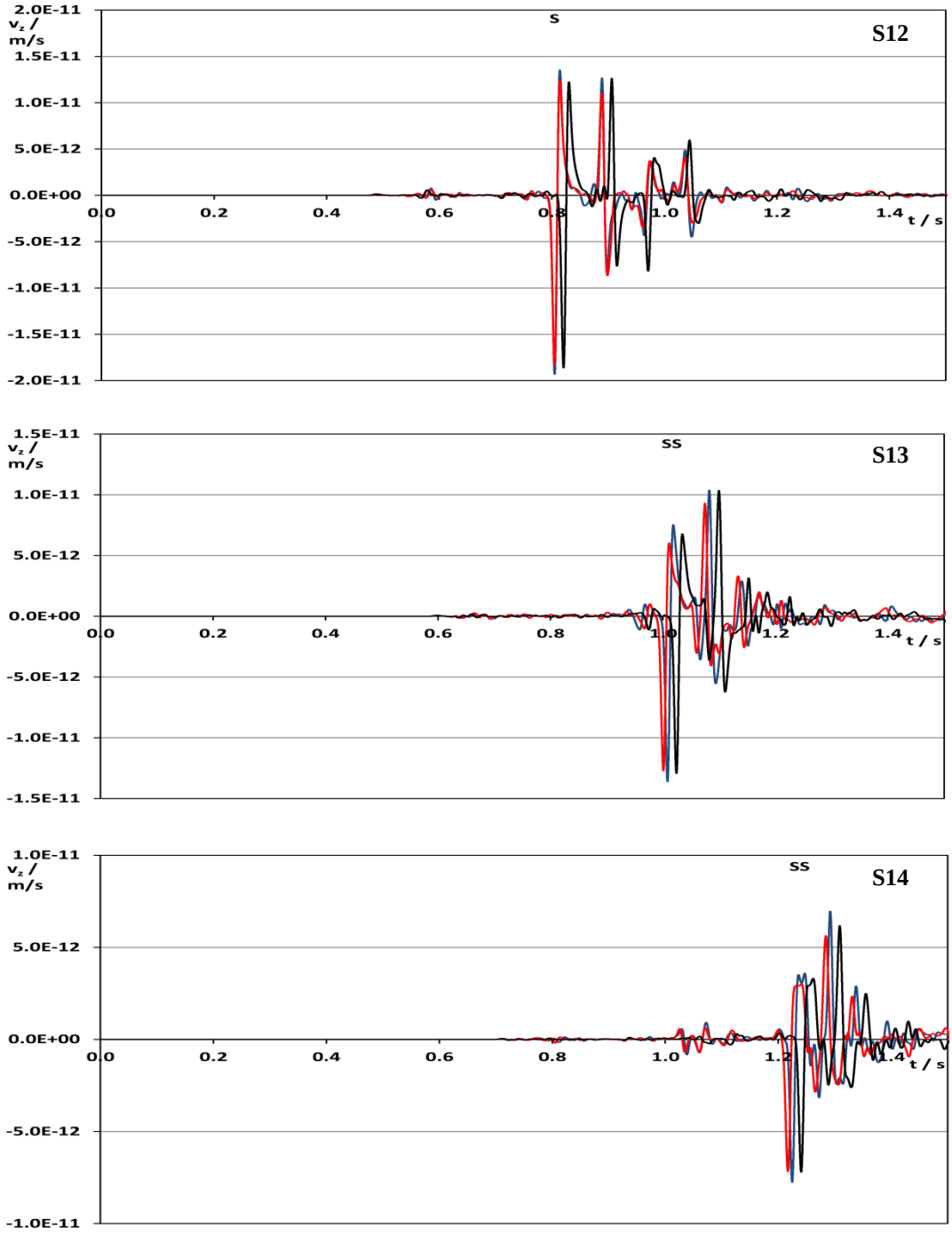

Figure 12 Vertical component of ground velocity at various *x* co-ordinates in the source plane (*y* = -500 m) at the source depth (900 m) after a force pulse in -*z* (down) direction. Sensors and source distances in *x* direction, from the top: 12, 2144 m; 13, 2544 m; 14, 2944 m. Black: 4 media, orthogonal sweep; blue: 15 media, orthogonal sweep; red: 15 media, spline sweep. The S- and SS-wave arrivals are marked.

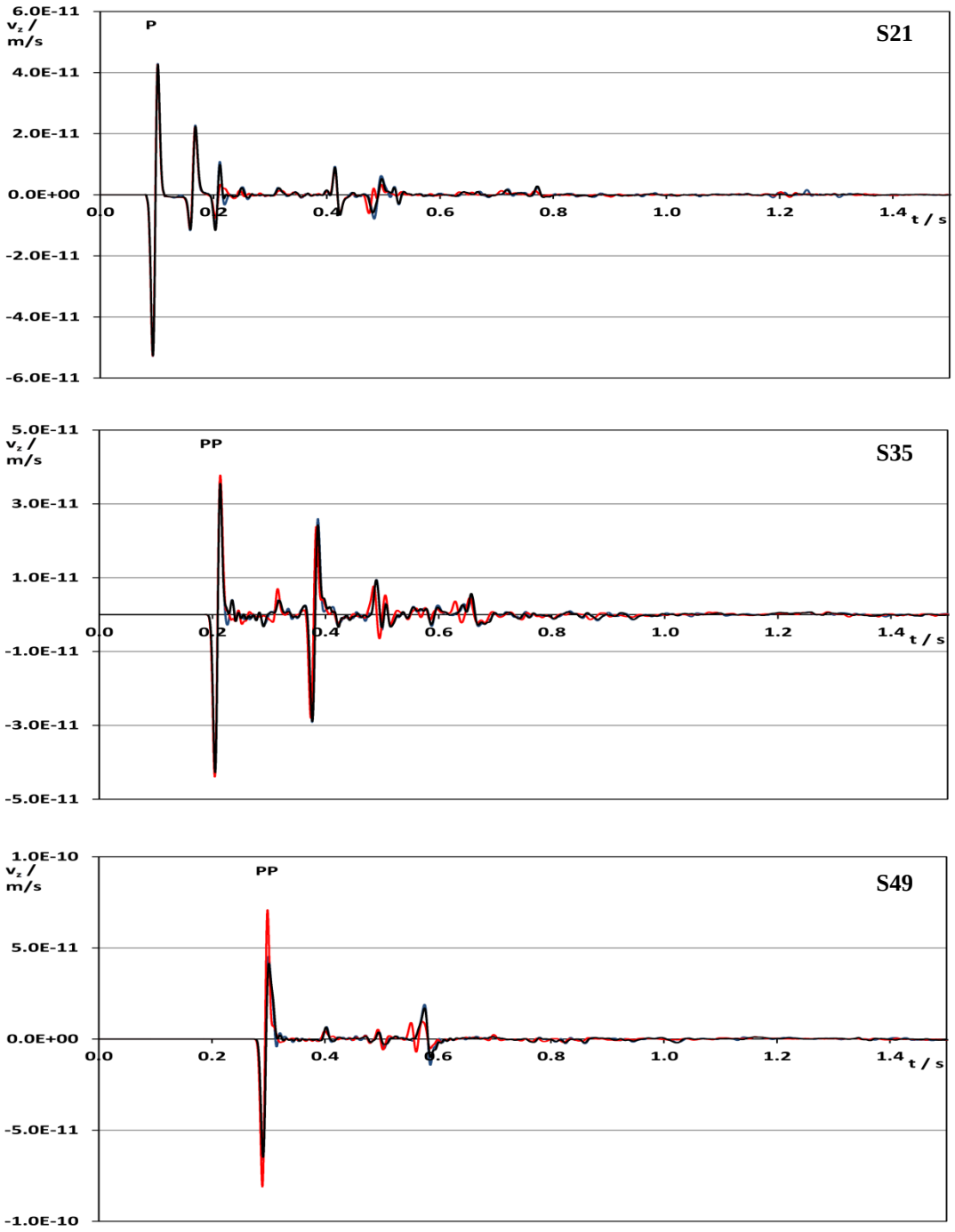

Figure 13 Vertical component of ground velocity at various *x* co-ordinates in the source plane (*y* = -500 m), near-vertically above the source (at depth 900 m) after a force pulse in -*z* (down) direction. Sensors and source depths, from the top: 21, 500 m; 35, 150 m; 49, 0 m. Black: 4 media, orthogonal sweep; blue: 15 media, orthogonal sweep; red: 15 media, spline sweep. The P- and PP-wave arrivals are marked.

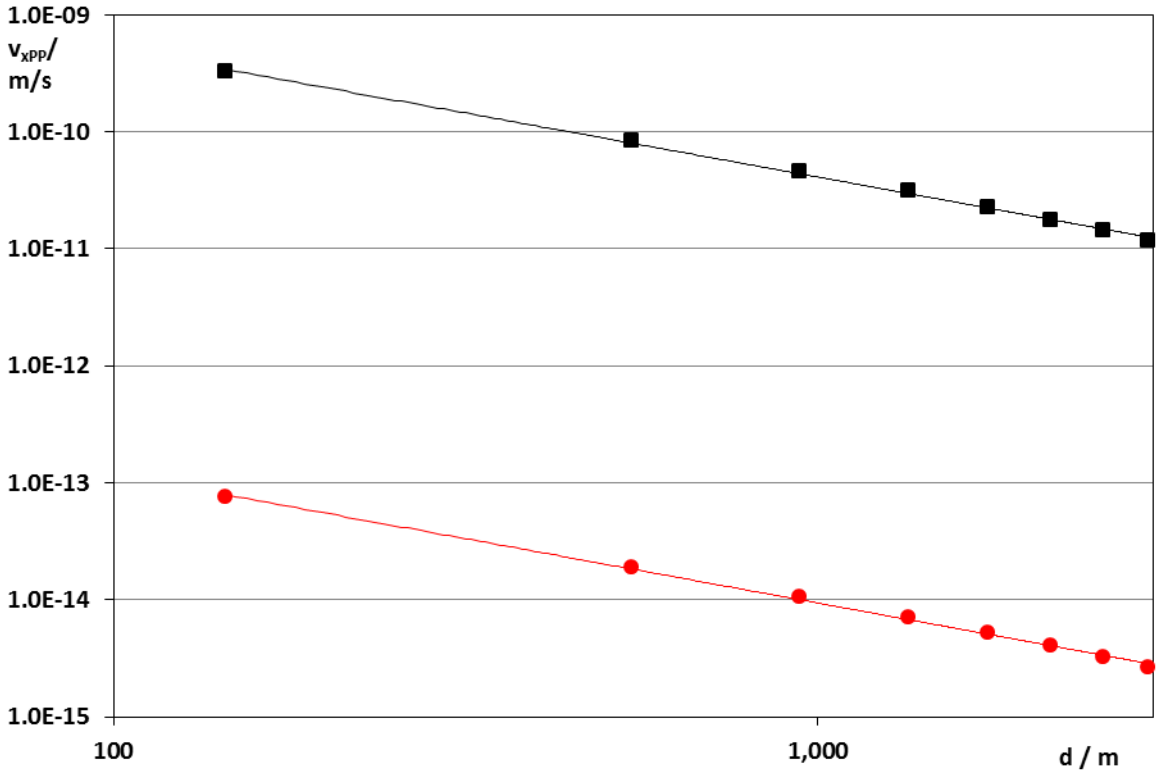

Figure 14 Peak-to-peak value of the *x* component of seismic velocity versus distance along the horizontal line from the source in *x* direction (Sensors 7 to 14). Signals were computed with the 15-media structure, spline sweep, with 0.02 ms time step, and then convolved with a Gauss function of 10 ms half duration. Black: force of 1 N in *x* direction, red: explosion with 1 Nm seismic moment. Power-law trend lines are indicated, their exponent (slope in double-logarithmic scale) is -1.1 for both sets.

5.3 Additional observations

Assignment of events: Many signals contain several smaller events. They come about by reflection and transmission at media boundaries. When the wave does not impinge orthogonally, continuity conditions effect conversion from P to S waves and vice versa. In case of a second boundary – for instance the salt-dome top and the surface – various waves with mixed histories can occur, for example PPP, PPS, PSP etc. If the partial path lengths in the different media are known well, the expected arrival times can be found precisely, allowing unique assignment at least for the simpler events, but for some mixed histories the arrival times are too similar for differentiation.

Comparison of excitation by directed force and by explosion: In test runs of an explosion and a horizontal force pulse – for propagation in *x* direction both produce mainly P waves – the *x* components of seismic velocity at the corresponding Sensors 7 to 14 were very similar, except for much lower amplitudes in the case of the explosion. Figure 14 shows the peak-to-peak values, determined as the difference between the maximum and the minimum values over the full time for each signal; these extreme values occur at the respective main events. The ratio between the values from the force pulse of 1 N and an explosion of 1 Nm seismic moment (half durations by convolution in both cases 10 ms) has a mean of 4400. Also this issue needs some further investigation.

Transmission from salt to surrounding media: Whereas reflection and transmission at a media boundary are normally very complex, in case of orthogonal incidence of a plane wave on a plane boundary the respective coefficients can be described simply in terms of the impedances $Z_i = v_i \rho_i$, where v_i is the relevant (P- or S-)wave speed and ρ_i, is the density in medium *i*. The reflection and transmission coefficients are

$$R = \frac{Z_2 - Z_1}{Z_2 + Z_1}, \qquad T = \frac{2Z_1}{Z_2 + Z_1}.$$

For monitoring a final repository in a salt dome most sensors would be positioned outside of the salt (Figure 1). Thus the transmission from the salt to the adjoining and overlying layers is relevant. For a rough check of this transmission results from the 15-media orthogonal-vector sweep were used. The signal strength at a position just inside the salt was compared with the one at the neighbouring position just outside it, corrected for distance r assuming an r^{-1} dependence. For P waves propagating in x direction the peak-to-peak values of the x components of ground velocity at Sensors 12 and 13 are used, for vertical propagation this concerns the z components at Sensors 21 and 35. The resulting ratios of peak-to-peak velocities are compared with the expected transmission ratios in Table 4, the impedances were gained by multiplying the P-wave speed and density entries of the respective media in Table 3. There is good agreement, the fact that the incidence is not exactly perpendicular and that the wave fronts and boundaries are curved does not seem to produce a strong deviation. This means that sensors outside of the salt dome should have generally similar detection capabilities as ones inside the salt dome. Only when attenuation becomes stronger, such as with the low quality values in the overlying sediment at higher frequencies, detectability is expected to deteriorate.

Sensor	Medium	Z / kg/(m^2 s)	R	T	v_{PP} ratio	Distance-corrected
S12	z2HS	5.72E6				
S13	Oberkreide	4.44E6	-0.071	1.071	0.81	0.96
S21	z2HS	5.72E6				
S35	Quartär/Elster	2.00E6	-0.469	1.469	0.83	1.50

Table 4: Impedances Z for P waves at sensors on both sides of a media boundary, ensuing (amplitude) reflection (R) and transmission (T) coefficients, and ratio of the peak-to-peak velocities v_{PP} in x (S12, S13) and z (S21, S35) directions, respectively, plus this ratio corrected for source-sensor distance.

6. Conclusion and Outlook

Lacking full three-dimensional data of the salt dome and its surroundings, considerable effort was spent to achieve a model structure that resembles the reality to some extent, from a simplified two-dimensional section. The three structures investigated showed some differences in the seismic signals, but these seem small enough to not be relevant from the perspective of monitoring and detecting activities where the exact time of arrival or small-scale events are of little importance. But since the 15-media spline-sweep model is closer to reality, it should be used in future investigations, as long as additional methods of improving the fidelity of the model, such as scaling and morphing while sweeping, are not available.

One should keep in mind that the complex inner structure of the salt dome, with for example inner boundaries intersecting the axis direction, is not represented in the model. Also, broken-up and mixed layers at the salt-dome margins could give rise to multiple scattering, reducing the transmission from salt to the surrounding rock.

A few issues remain to be investigated. This concerns above all the question of absolute amplitudes, since it is the ratio of signal to background that defines detectability in the simplest scheme. Some calibration was possible by comparison with measured data, but this needs to be looked at further, for example with respect to the frequency content. The frequency range in the model is a few hundred hertz whereas the measurements contain frequencies up to a few kilohertz.

While the final quantitative evaluation of signal strength versus background noise for relevant activities still needs to be done, it seems that, given the relatively strong transmission through the salt-dome boundaries, the outlook for the utility of seismic monitoring for safeguarding an underground final repository in salt is generally good.

Acknowledgements

I want to thank the Bundesanstalt für Geowissenschaften und Rohstoffe (BGR, Hannover) for providing figures and for allowing the use of their data of the salt-dome surroundings, and the firm bicad (Hannover) for actually providing them, including reactions to several requests. Thanks go to

Wolfgang Friederich who heads the Chair of Geophysics, Ruhr-Universität Bochum, and to Andreas Schuck of GGL Geophysik und Geotechnik Leipzig, for valuable advice. I am grateful to Marcel Paffrath, student at the Chair of Geophysics, Ruhr-Universität Bochum, for his work in producing three-dimensional structures from the two-dimensional section. Further I thank Lasse Lambrecht, PhD student at the Chair of Geophysics, for tips in case of program problems. Particular thanks go to the LiDO team at Technische Universität Dortmund; these colleagues gave invaluable advice on the use of the computer cluster, including providing scripts.

This work was funded under task JNT C1611 of the German Support Programme to the IAEA.

References

[1] Altmann, J., Kühnicke, H.; *Acoustic and Seismic Measurements for the Detection of Undeclared Activities at Geological Repositories – Results from the Gorleben Exploratory Mine*, JOPAG/11.13-PRG-404; Joint Programme on the Technical Development and Further Improvement of IAEA Safeguards between the Government of the Federal Republic of Germany and the International Atomic Energy Agency, Nov. 2013.

[2] Altmann, J.; *Seismic Monitoring of an Underground Repository in Salt – Results of the Measurements at the Gorleben Exploratory Mine*; *ESARDA Bulletin* no. 50, 61-78, Dec. 2013.

[3] Komatitsch, D., Vilotte, J.P.; *The spectral-element method: an efficient tool to simulate the seismic response of two-dimensional and three-dimensional geological structures*; *Bull. Seismol. Soc. Am.* 88 (2), 368-392, 1998.

[4] Komatitsch. D., Tromp, J.; *Introduction to the spectral-element method for three-dimensional seismic wave propagation*; *Geophys. J. Int.*, 139, 806-822, 1999.

[5] Computational Infrastructure for Geodynamics (CIG), Princeton University (USA), CNRS and University of Marseille (France), ETH Zürich (Switzerland); *SPECFEM 3D Cartesian User Manual*, Version 2.1; Sept. 30, 2013, via https://geodynamics.org/cig/software/specfem3d (20 Jan. 2014).

[6] csimsoft; *Trelis — Advanced Meshing Software*; http://www.csimsoft.com/ (29 April 2015).

[7] O. Bornemann et al.; *Standortbeschreibung Gorleben Teil 3 – Ergebnisse der über- und untertägigen Erkundung des Salinars*; Geologisches Jahrbuch C73; Hannover/Stuttgart: BGR/Schweizerbart, 2008 (English version via http://www.bgr.bund.de/DE/Themen/Endlagerung/Aktuelles/2011_04_20_aktuelles_gorleben_engl_Part1bis3.html (29 April 2015)).

[8] *LiDO – Der Linux-HPC-Cluster an der Technischen Universität Dortmund*; http://www.itmc.tu-dortmund.de/dienste/hochleistungsrechnen/lido.html (29 April 2015).

[9] Bundesanstalt für Geowissenschaften und Rohstoffe (BGR); *Erkundung des Salzstockes Gorleben*; http://www.bgr.bund.de/DE/Themen/Endlagerung/Projekte/Endlagerstandorte/laufend/Erkundung_Salzstock_Gorleben.html?nn=1550704 (29 April 2015).

Application of safeguards in the geological disposal of spent nuclear fuel: safeguards data requirements and contribution to very long lasting records and knowledge retention

Mentor Murtezi[1], Christos Koutsoyannopoulos[1], Peter Schwalbach[1], Ali Zein[1], Wolfgang Kahnmeyer[1], Valenti Canadell Bofarull[1], Peter Turzak[1], Andreas Smejkal[1], Vitor Sequeira[2], Erik Wolfart[2]

[1]European Commission – Directorate-General for Energy
Direction E – Nuclear Safeguards, L-2530 Luxembourg
E-mail: Mentor.Murtezi@ec.europa.eu

[2]Institute for the Protection and Security of the Citizen
Joint Research Centre, European Commission
Via E. Fermi, Ispra 21027 (VA) Italy

Abstract:

One distinctive feature of the geological disposal process for spent nuclear fuel is its timescale. Any of the proposed safeguards-related measures and solutions must adhere to this very long time perspective. The applicable safeguards-related infrastructure may be upgraded and even completely exchanged along with the technological progress and changes in the disposal project advancement as decades will go by. However, there is one element that from the very beginning should withstand the test of time, spanning over the entire timescale of the final disposal projects; this is the data and knowledge retention system.

The EC and the IAEA safeguards services have the unique possibility and responsibility of acquiring, processing and storing the safeguards-relevant data according to the provisions of the applicable safeguards obligations. Furthermore, also information related to the development of safeguards approaches and evaluation methods needs to be maintained. The related knowledge retention arrangements have an important role not only in safeguards but can also contribute to the wider scope of knowledge retention contributing to the information-based decision making in the future.

In this paper, based on considerations on the necessary safeguards equipment infrastructure and the proposed safeguards measures, we describe the necessary data feeds from the operators of the geological disposal systems, as well as the data to be collected by the safeguards inspectorates themselves. We discuss the plausible arrangements for accessing the relevant data and the very long lasting records and knowledge keeping as well as their multi-purpose safeguards and knowledge-retention use.

Keywords: geological disposal; spent fuel; safeguards data needs; knowledge retention

1. Introduction

The geological disposal (GD) of spent nuclear fuel (SF) is becoming reality in Europe; the first two GD systems are to become operational within a decade. The first is scheduled to be launched in 2022 in Finland, the second one should be commissioned a few years later in Sweden. The GD projects in Finland and Sweden are implemented with "safeguards in mind". This safeguards-by-design (SBD) approach facilitates the application of safeguards and integration of its systems with the physical system components but also with the safety and security arrangements. SBD is aiming at effective and

efficient verification of the SF to be encapsulated and deposited and 100% assurance of continuity of knowledge (CoK) between the encapsulation and the deposition of the SF.

EURATOM Safeguards has valuable past experience with preparations of a conditioning facility, as intensive discussions were held and agreements made during the preparation and construction phase of the German pilot conditioning facility. The principles and concepts developed then [1], [2] are mainly still applicable. The plant did not become operational following a political decision but also Germany will come back to this question in time.

For a number of decades the EU safeguards inspectorate is putting a lot of effort in assuring a tight control of the nuclear material within the nuclear fuel cycle. The GD concept adds additional stages to this cycle: encapsulation of spent fuel and its transfer to the underground location and emplacement in its defined position. The overall goal of the EU's nuclear safeguards system is stated in chapter VII of the Euratom Treaty. Obligations on operators of nuclear installations are outlined in the Commission Regulation (Euratom) No 302/2005. The major goal of safeguards measures is to know and verify who, where, what and how much of nuclear material is used for what purpose and to verify if the reality on-site is correctly reflected in the operators' declarations. All civil nuclear material in the European Union is subject to Euratom safeguards and must be strictly accounted for. The accountancy declarations are verified via on-site inspection activities, aided by remote monitoring techniques. All these activities are currently routinely implemented. The addition of the GD as a new very long lasting stage in the nuclear fuel cycle is calling for rethinking and possibly revision of our data requirements.

When launched, a GD system will operate continuously over decades. More than a century can pass from the day of disposal of the first canister with SF to the moment when the underground repository will reach its capacity. During all this time, the necessary safeguards related information must be collected, classified, and archived. The information provided by the GD system operators must satisfy the legal safeguards requirements and be sufficient to satisfy the data requirements of the implemented safeguards approach. As it is very difficult to define a safeguards approach that would last for a century, the collection of data should take into account evolution in approaches. For example, currently available verification techniques may not need very detailed records characterising the spent fuel to be placed underground, however, future development of new measurement techniques and possible changes in safeguards approach may require more detailed records on the SNF to be disposed of. Thus future requirements need to be considered now as far as feasible.

The timescale of the GD process and non-excludable possibility of retrieval of the previously deposited SF requires adequate measures and techniques for data transfers, data management and archiving of the collected records. The information to be collected should be classified according to its relevance and purpose. The directly safeguards-related dataset should be a subset of a broader knowledge-retention oriented dataset. The latter dataset can act as a repository from which data, originally not directly intended for safeguards purposes, could be retrieved and re-analysed.

2. Safeguards approach to geological disposal system: safeguards infrastructure and data needs

The GD system has two main components: the encapsulation plant (EP) and the geological repository (GR). Each of these components will have its safeguards infrastructure and, being separate material balance areas (MBA), will have separate sets of nuclear accountancy and operating records, as well as tailor-made, facility-specific, continuity of knowledge arrangements.

2.1. The encapsulation plant: safeguards infrastructure and facility and process specific flexible approach for final verification of SF

Responding to the need of establishing the appropriate safeguards approach and its implementation measures and techniques and following the safeguards-by-design concept, the EC and the IAEA jointly proposed in 2014 to the operator the Equipment Infrastructure Requirements Specification for the Spent Fuel EP in Finland. The Finnish GD system, as the first one to be launched after the blockage of the German development, is treated as a model for a modern baseline safeguards approach for GD of SF [3].

The possible safeguards measures have been identified with the aim to have the least possible impact on the spent nuclear fuel geological disposal process, while allowing each safeguards authority to effectively fulfil their mandate and draw independent conclusions. The technical measures have been specified wide enough to cover the expected scope of the final safeguards approach, also allowing for a degree of flexibility for possible future changes in safeguards strategies.

One of the key points in the elaboration of the safeguards approach for GD of SNF was the definition of the location in the process where the final verification measurement of SF will be made. The two following options have been examined:

- The flexible option: Verification at the SF shipping facility (= the nuclear power plant (NPP) interim spent fuel storage), while keeping re-verification capabilities at the EP;
- The EP option: Final verification only at the SF receiving facility (= the EP).

The at-EP option would pose strict time constraints on the availability of reliable and approved equipment, which is still under development, and also on verification and approval actions. Instruments would have to be highly automated and rely on Remote Data Transmission (RDT), leaving very small margins for dealing with anomalous situations. On these grounds, (mainly anomaly resolution concerns leading to the need for immediate remedial actions in case of equipment failures and RDT interruptions), a flexible verification option is proposed locating the final verification of the SF assemblies at the interim stores of the NPPs while preserving the measurement capability at the EP.
The chosen verification option is based on approved and tested equipment and procedures, leaving the possibility to move the verification to the EP at a later stage, when adequate SF measurement devices will be available.

Compared to the scenario with final verification at the EP, the chosen flexible option poses stricter continuity of knowledge (CoK) requirements. The flexibility of this option is based on preserving the full capability for performing the final verification of the SF to be encapsulated in the EP. This would act as a back-up scenario in case of loss of CoK between the interim store of the NPP and the EP.

The proposed equipment infrastructure for the EP has been designed to ensure complete verification possibility at the EP and to assure CoK inside the EP: from the arrival of the transport casks containing SF assemblies through to encapsulation of the SF assemblies and transfer of the loaded and welded disposal canisters to the underground disposal.

The high throughput of the EP and its operational timescale require efficient unattended material flow monitoring (visual and radiation-based), identity reading, fingerprinting and verification measurements' data transfer. The proposed equipment infrastructure requirements assume upgradability and adaptability of the planned system components. The space reserved for the safeguards equipment in the EP assumes the possibility of adding in the future novel equipment, such as an unattended gamma emission tomography device (see e.g. [4] and references therein)..

2.2. Geological repository: black box margins and assurance of retention

In the proposed safeguards approach the geological repository (GR) is seen as a "black box". This means that all the nuclear material deposited underground must be accounted for and characterised, enabling its future re-verification in the event of retrieval at least until the final back-filling stage. However, the disposed SF will not be subject to any re-verification as long as it is staying in the black box. According to the currently adopted safeguards model, the black-box GR as a whole will neither be monitored internally nor externally for safeguards purposes (e.g. using seismic, acoustic or thermal sensing techniques). Following evolution of safeguards needs, mandates ad approaches the black box monitoring can be introduced in the future. Following the current safeguards model, portal radiation monitoring, possibly complemented by surveillance, will be applied to all penetrations leading to the disposal area. Periodical reviews of the technical characteristics of the GR (including underground) will be conducted. This containment-like black-box option is in agreement with the rationale of the GR concept and its wider context of safeguards, safety and security (the so-called 3S approach).

A very important decision to be taken in respect to black box boundaries is exactly where to put these boundaries. One option is to treat the entire underground as a black box, i.e. as soon as a DC disappears from the surface it is already considered as transferred to the black box. Alternatively, the

black box boundaries could be limited to the underground disposal level itself. In the second case the material flow monitoring would have to be designed in a way allowing to follow the disposal canisters down to their disposal area hundreds of meters underground.

By defining the black-box boundaries at the surface:

- It would be easier to install and operate the required safeguards infrastructure (no equipment underground)
- The necessary safeguards infrastructure would cost less (less cables, less equipment, less maintenance, less inspection effort)

On the other hand, having such a large black box would mean that:

- Arrival of the DC to the deposition level could not be traced and confirmed independently
- An undeclared activity warning would be delayed: SF could potentially be kept between the deposition depth and the surface

Limiting the black box to the disposal level and treating the overlaying rock masses as a confinement (with almost 450 meters thickness in case of the Finnish GD) would enable:

- Tighter control on a smaller black box confirming transfers of the DCs to the disposal level
- Earlier warning in case of undeclared activities

On the downside, narrowing the black box would make safeguards more costly and would require inspectors' presence underground (which might be necessary anyway for the basic technical characteristic verification).

Currently, the two options for black box boundaries are being analysed comparing the necessary safeguards equipment infrastructure and the assurance levels provided.

3. Discussion on data needs and knowledge retention

The above described model safeguards approach, based on the currently available SF verification and CoK assuring techniques, requires extensive data feeds from the operator of a GD system. Any safeguards approach formulated for a particular GD systems will have to evolve along with the advancement of the consecutive GD process stages (preparation, operation, partial and final backfilling and also, with non-excludable retrieval events). Taking into account that more sophisticated and data-hungry measurement techniques may, and certainly will, appear, the safeguards inspectorates should have access to the most detailed and accurate information on the SF to be disposed of. Apart from the routine information on the initial enrichment and burn-up values, the irradiation and cooling history of each SF assembly should be made available to the inspectorates. Moreover, whenever possible, detailed information characterising the SF design and even particular fuel rods should also be provided (data such as nodal burn-up, number and location of removed fuel rods, number and location of partial length fuel rods, burn up at a pin level etc).

Part of the information on the SFA to be encapsulated can be obtained from the currently used inventory change reports (ICR) submitted by the operator. Some other characteristic details of the SFA can be obtained from the basic technical characteristics of the NPP. It will be necessary to merge the two data sources and create a comprehensive and detailed database. Other data are part of operating and accounting records which currently are not submitted to the inspectorates but kept available to the inspectorates by the NPP operators.

All the above described data would have to be made available to the inspectorates in advance, so that they could be analysed in preparation for the final verification of the SNF using the agreed non-destructive analysis technique. To avoid delaying the encapsulation and disposal process, it is also very important to agree on the declaration acceptance criteria. As the operator will be submitting very detailed information, it should be made clear which parameters will be primarily used for confirmation of the operator's declaration. The set of these parameters may vary depending on the agreed non-destructive analysis technique to be used as a final verification tool. As these may evolve significantly over the long period of operation, a wider dataset will be envisaged by the safeguards authorities. This needs to be specified in thorough discussions with the concerned operators. It is clear that if only such information will be provided as currently required under Euratom Regulation 302/2005, it will be

insufficient to fully exploit the capability of even the currently envisaged NDA techniques. Novel data needs introduced by the launch of the GD processes could be regulated via revision of the applicable legal acts and by creation of adequate legal arrangements such as Particular Safeguards Provisions under Commission Regulation (Euratom) No 302/2005 and could be reflected in the related Facility Attachments.

Another very important set of data is required for the underground GR. The inspectorates' must have access to very detailed design characteristics of the underground GR in order to be able to understand and control the black box. Safeguards services must be sure that the GR is built as designed. For future reference it is also very important to understand the 3D layout of the GR enabling precise localisation of the disposed spent fuel.

To be sure that the black box meets safeguards requirements (such as the indicated disposal depth and area) it must be very precisely characterised spatially. This characterisation and its periodic updating will allow for understanding its state and evolution. Currently the best available and fit for purpose technique is the 3D Laser scanning. It acts as a general independent verification technique for built as designed and declared confirmation, providing in addition an independent orientation for inspectors.

The above described data needs and verification techniques are primarily safeguards-related. Their main goal is to help the safeguards inspectorates, Euratom and IAEA, in fulfilling their mandates. However, the collected data and experience have also a broader scope and can be used in the overall context of knowledge retention. The safeguards-related data is actually a subset of this wider databank. The preservation of detailed records and general knowledge will be more certain if they are shared and kept in redundant databanks. The safeguards inspectorates have a unique position on the international arena, as organisations designated for and capable of processing and keeping sensitive information for a very long time. In relation to the extremely long operational time of the GD systems, current record keeping solutions may not be sufficient. Actually any of the currently proposed or envisaged data retention techniques and measures will not be sufficient facing the GD timescale. Therefore, it seems that before revising the current data retention and record management solutions, we should define our role in knowledge retention and decide on knowledge transfer and handover approach.

References

[1] Laupe W.D., and Richter B.; *Possible Safeguards Measures for the Pilot Conditioning Facility.* JOPAG/05.89-PRG-179, 1989.

[2] Leitner E., Rudolf K. and Weh, R.; *Advanced Techniques in Safeguarding the Gorleben Pilot Conditioning Facility for Spent Fuel*. Proc. 17th ESARDA Symposium, ESARDA 28, 1995 pp. 261-264.

[3] Ingegneri M., Baird K., Park W.-S., Coyne J. M., Enkhjin L., Chew L.S., Plenteda R., Sprinkle J., Yudin Y., Ciuculescu C., Koutsoyannopoulos C., Murtezi M., Schwalbach P., Vaccaro S., Pekkarinen J., Thomas M., Zein A., Honkamaa T., Hämäläinen M., Martikka E., Moring M. and Okko O.; Saf*eguards by Design at the Encapsulation Plant in Finland.* IAEA Symposium 2014, Vienna.

[4] White T, Jacobsson Svärd S., Smith E., Mozin V., Jansson P., Davour A., Grape S., Trellue H., Deshmukh N., Wittman R., Honkamaa T., Vaccaro S and Ely J.: *Passive Tomography for Spent Fuel Verification: Analysis Framework and Instrument Design Study.* This conference.

Session 20

Tomography for Spent Fuel Verification

Monte Carlo simulations of a Universal Gamma-Ray Emission Tomography Device

Peter Jansson [1], Peter Andersson [1], Timothy White [2], Vladimir Mozin [3]

[1] Uppsala University, Sweden
[2] Pacific Northwest National Laboratory, USA
[3] Lawrence Livermore National Laboratory, USA

***Abstract*:**

A design of a universal gamma-ray emission tomography (UGET) device has been defined within the IAEA MSSP project JNT1955 in order to evaluate partial defect detection capabilities when using tomography on used nuclear fuel assemblies. The design is intended to allow for fuel assembly verification using single photon emission tomography on a broad range of fuel assembly types and fuel parameters.

In this paper, results from a set of Monte Carlo radiation transport simulations for the UGET design are presented. In these simulations, two cases are studied, each of them with a PWR fuel, in one case the complete fuel assembly and in the other with 11 missing rods. The characteristic features of the design are presented including expected performance requirements on the gamma-ray collimator and detector system, supported by the simulation results. In addition, the agreement between the two simulation tools used, Geant4 and MCNP, indicate that any of the two can give satisfactory accuracy for this purpose.

Keywords: nuclear fuel assemblies; partial defect verification; gamma-ray emission tomography; Monte Carlo

1. The IAEA MSSP project 1955: UGET

The IAEA has identified a need to re-assess the viability of using gamma emission tomography (GET) for verification of used nuclear fuel to be transferred to difficult-to-access storage. The joint task JNT A 1955, “Unattended Gamma Emission Tomography (UGET) for Partial Defect Detection”, has been set up within the support programmes of Sweden, USA, Finland and the European Commission. In the first phase of the project, the purpose is to provide an assessment of the viability of the technique for safeguards applications. Two verification objectives have been defined [1]; 1) pin counting for routine verification of item integrity and 2) quantitative determination of pin-by-pin properties such as burnup and cooling time for detection of anomalies.

For the first objective, no operator-provided information is assumed to be known to the inspecting party and verification should be fully independent. For the second objective, operator-declared information may be used to detect anomalies in comparisons between measured data and operator-declared data. However, it is not completely required since by using results from the tomographic technique (i.e. pin-by-pin isotopic concentrations of studied isotopes), anomalies may also be detected in inter-comparisons between pins in the population itself. E.g., by using an assumption of similar cooling time between pins, the pin-by-pin burnup distribution may deduced from tomographic measurements of two isotopes [2].

2. Tomography system design

Informed by prior work [3,4,5] and a simulation study of the capability of an existing tomography system to detect missing pins, a preliminary design of a universal gamma-emission tomography (GET) has been developed. Design considerations included energy and spatial resolution as well as the ability to manage total count rate for short cooling time scenarios while maintaining adequate photopeak count rates for isotopes of interest across scenarios. In order to estimate pin-to-pin burnup variations, it will be necessary to separate the gamma response from different isotopes, primarily ^{137}Cs (662keV) and ^{154}Eu (5 lines between 723 and 1264keV). In addition, for very short cooling times, it would be desirable to separate the response of ^{134}Cs (605 and 796keV) from the ^{137}Cs lines. These objectives drive the system design toward high energy resolution scintillators as the detection material; $LaBr_3$(Ce) was chosen for both its speed and energy resolution.

In order to manage count rates for shorter cooling times and to achieve the spatial resolution necessary to image pins in the center of an assembly, a collimator with long, narrow, open slits was designed for imaging. This collimator closely resemble that in [6], although for the present case the thickness of the collimator depth can be less. To achieve high count rates for lower-activity fuel (long cooling times), the collimator had to be opened up slightly. In order to manage the count rate for higher-activity fuel, a provision to include lead filtration in the collimator was included.

To collect tomography data, the imaging head consisting of the collimator and scintillator is to be used in a translate-rotate geometry in which projection data is collected by translating the detector along a linear track, and angular data is collected by rotating the head with respect to the fuel assembly. In this geometry, there is a trade-off between the number of detectors in the head and the number of steps required to collect a projection. This trade-off is further complicated by the detector photopeak efficiency (a function of scintillator size) and total data collection time. While it might seem that many small detectors would be the appropriate design choice, calculations demonstrated that scintillators on the order of 38-50 mm diameter provided an optimal count rate and imaging time. This results in a head with 6-10 detectors, depending on the overall field of view of the system.

A drawing of the proposed geometry of a single detector head is shown in figure 1 and a table of design parameters are shown in table 1. Additional shielding is included in the

design to protect the detectors in the high radiation fields and to manage count rates. In a full system, the head would sit on a rotating platform in a “donut” that would surround the fuel assembly at some vertical offset from the bottom of the assembly. Multiple heads could be included on the ring to decrease total data-collection time. For simulation purposes, only a single head is included.

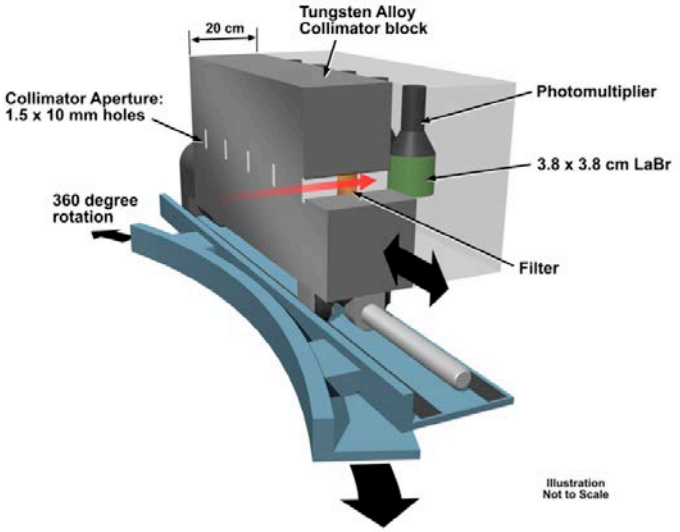

Figure 1: Drawing of the proposed UGET design.

Object and Scanner Parameters		
Maximum object diameter	375	mm
Scanner radius (object center to collimator face)	225	mm
Scintillator Parameters (Right Circular Cylinder)		
Diameter	38.1	mm
Height	38.1	mm
Collimator Parameters		
Material: Triamet-S18 (95% W, 3.5% Ni, 1.5% Cu)	18.0	g/cm^3
Length	20.0	cm
Width	1.5	mm
Height	10.0	mm
Detector Head and Scan Parameters		
Number of detectors	8	
Collimator pitch	46.0	mm
Inter-scintillator gap	4.0	mm
Number of steps per projection for 2 mm sampling	23	
Number of angles	128	

Table 1: Parameters of the proposed UGET design.

3. Results from Monte Carlo simulations

Two Monte Carlo frameworks were used in this work: MCNP [7] and Geant4 [8]. The design of the UGET device was modelled in both frameworks but the Geant4 model was used in this work to validate the MCNP model. In Geant4, no techniques for variance reduction were used which limited the amount of cases to that could be simulated in the available time frame. Therefore, only a few selected cases for a PWR 17x17 fuel assembly were simulated, as summarized by table 2.

Case #	Lateral positions of the device [mm]	Pattern of removed rods
1	-23	None (complete assembly)
2	-23, -21, -19, …, 17, 19, 21 (one projection)	[-7,0], [-4,-4], [-4,3], [-4,8], [0,-8], [0,5], [1,-1], [2,2], [4,-2], [5,6], [8,-3]

Table 2: Summary of selected cases for simulation of a PWR 17x17 fuel assembly. In all cases, two source energies (661657 and 1274436 eV) and two rotations of the device (0 and 45 degrees) were used.

3.1 MCNP simulations

Two sets of MCNP simulations have been performed. First, a using model to specifically compare case 1 (with a complete fuel assembly) presented in this paper. Second, using a model capable of calculating all combinations of device positions (lateral positions and rotations) and source energies in a reasonable time to specifically compare case 2 (with missing pins). The second model, described in more detail in [9], is using a virtual geometry setup with a simultaneous calculation in all possible lateral positions at each rotation. The first model is described below.

In the second MCNP model, MCNPX 2.5.0 has been used to model the 1274 keV gamma transport in case 1 of table 2. The MCNPX cell geometry used for the simulations is shown in figure 2 below. It includes the fuel assembly with fuel rods and guide tubes, contained in a steel cylinder and a collimator with eight slits to the detector locations corresponding to the UGET design, as shown in figures 2 and 4. It can be noted, that the physical detectors have not been modelled. Instead, the photon current integrated over the detector end surface is estimated using the F1:P tally of MCNPX. Variance reduction has been introduced by truncation of the axial source distribution and the angular emission distribution, where the axial emission is limited to 42.5 mm height and the angular emission is limited to a 5° cone centred on phi. 10^{10} photons were started from the fuel rod in each simulation.

In each calculation, the contribution of each rod to each of the eight detector positions has been investigated. Figure 3 shows the accumulated contribution of each rod in the two cases (i.e. the summed contribution of each rod to all detector positions.)

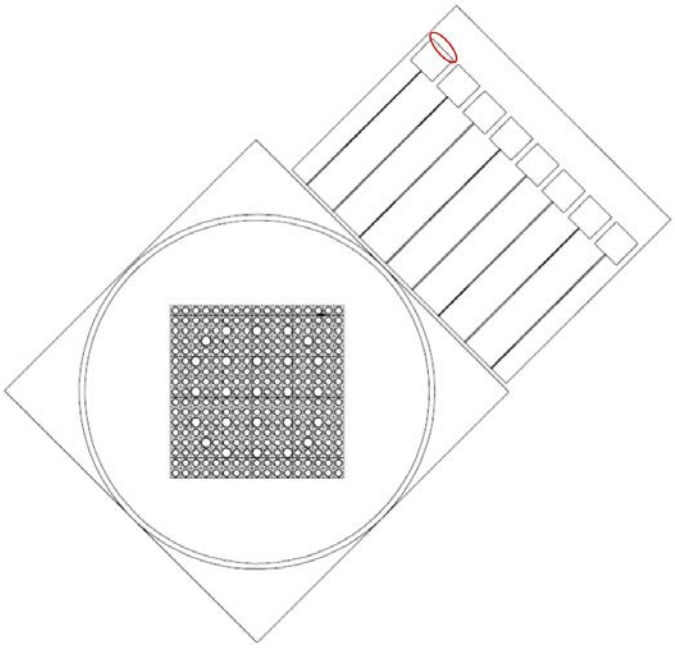

Figure 2: MCNPX geometry used the 45° rotation (and -23 mm lateral position) in case 1. Black lines representing cell borders. The red marking at the back of the detector space shows an example of a surface used for photon current tally in MCNPX (i.e. the F1 tally).

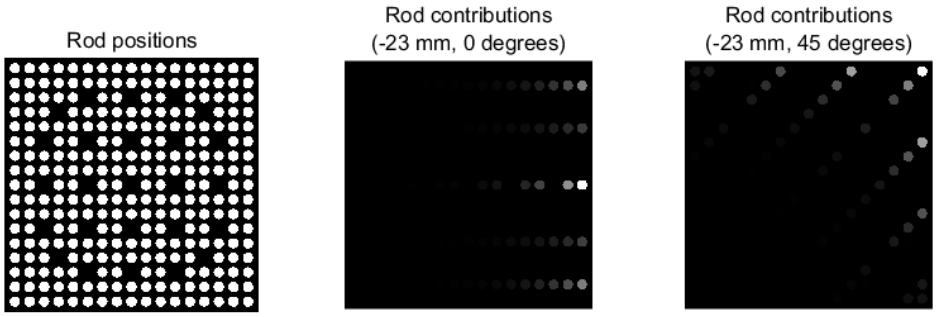

Figure 3: Left: The investigated rod positions. Centre: The contribution of each rod to all detector positions in the 0° rotation of case 1. Right: The corresponding contributions in the 45° rotation of case 1.

3.2 Geant4 simulations

Geant4 simulations of the UGET design were performed in order to validate the MCNP models. A screen dump of the Geant4 model of the UGET design is displayed in figure 4. The coordinate system used, that defines the lateral position and the rotation of the device, is also shown in figure 4. The reference physics list FTFP_BERT was used in Geant4, implying that all standard electromagnetic interactions were modelled.

For each case, the spectrum of energy depositions in the eight detectors of the collimator head was calculated for each pin in the fuel assembly. I.e. the response in each detector to gamma rays emitted isotropic and homogenous in a 42.5 mm high cylinder in each fuel pin, centred in front of the collimator opening. Due to large attenuation of gamma rays originating from fuel pins on the opposite side of the assembly, as seen from the detectors, the contribution to the response for these pins is relatively small. Figures 5 and 6 shows the response per fuel pin for case 1.

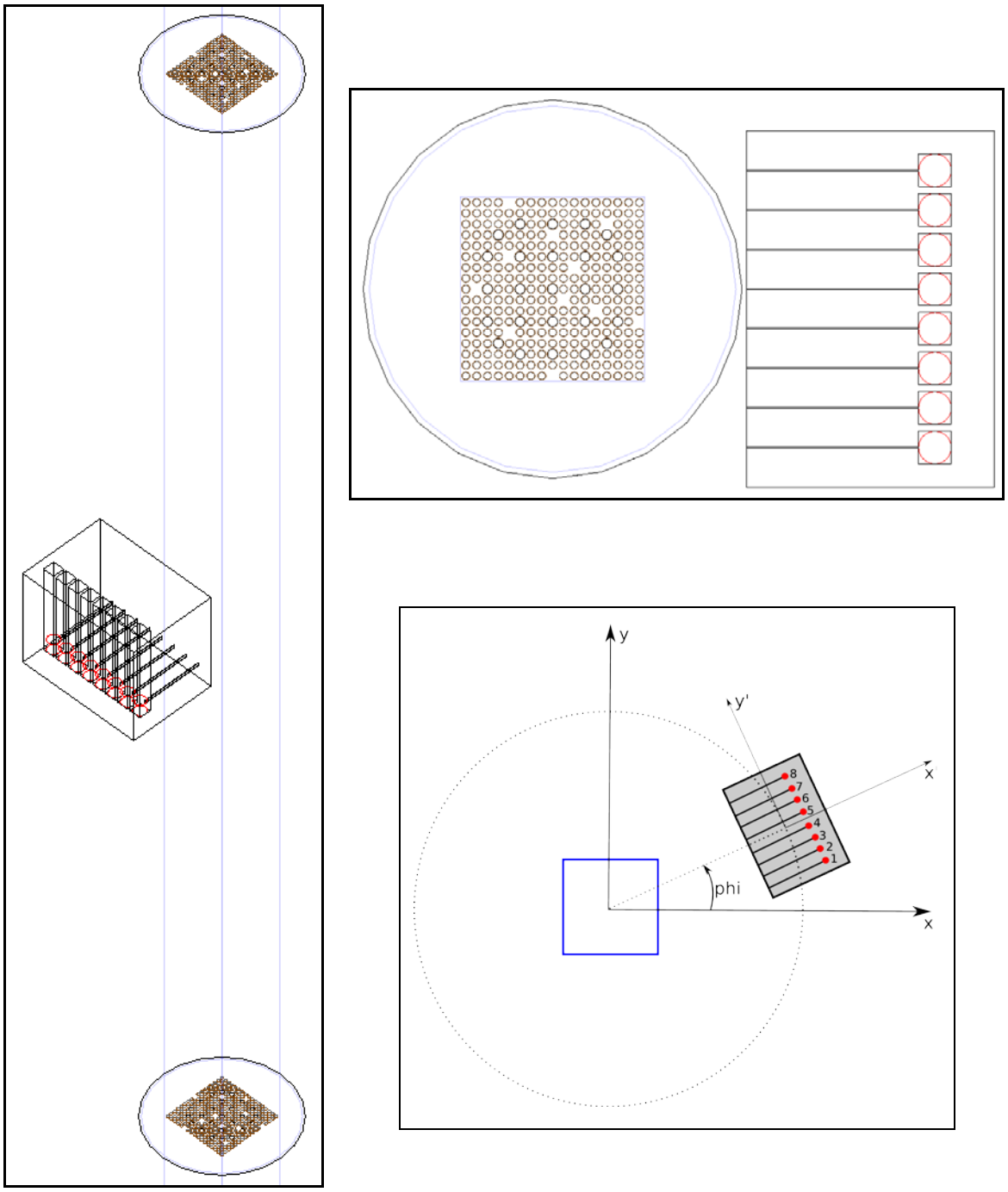

Figure 4: Schematics showing the Geant4 model of the UGET device (left and upper right). The upper right image indicates a view from above for case 2 with 0° rotation and -23 mm lateral position (i.e. with detector number 5 pointing towards the central rod in the assembly). The bottom right part illustrates the used coordinate system that defines the lateral position and rotation of the device relative to a fuel assembly indicated by the blue square in the centre. The rotation is given by angle phi. The lateral position is given by the y' position of the collimator head, i.e. the distance between the centre of the head and the x' axis.

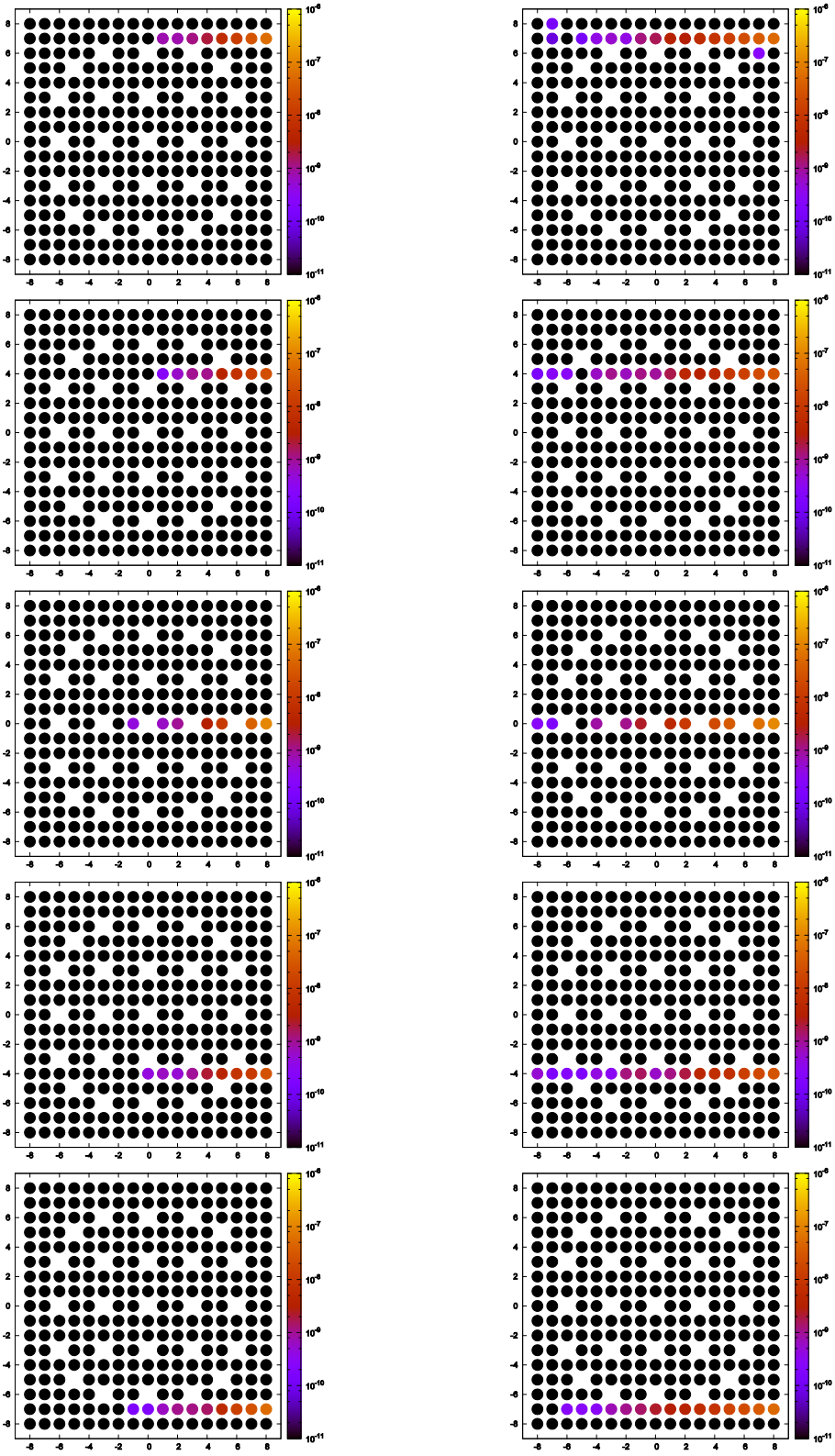

Figure 5: The number of counts in the full energy peak, per emitted source photon for the energies 662 keV (left column) and 1274 keV (right column), for detector numbers 3 (bottom) through 7 (top) in the 0° rotation of case 1.

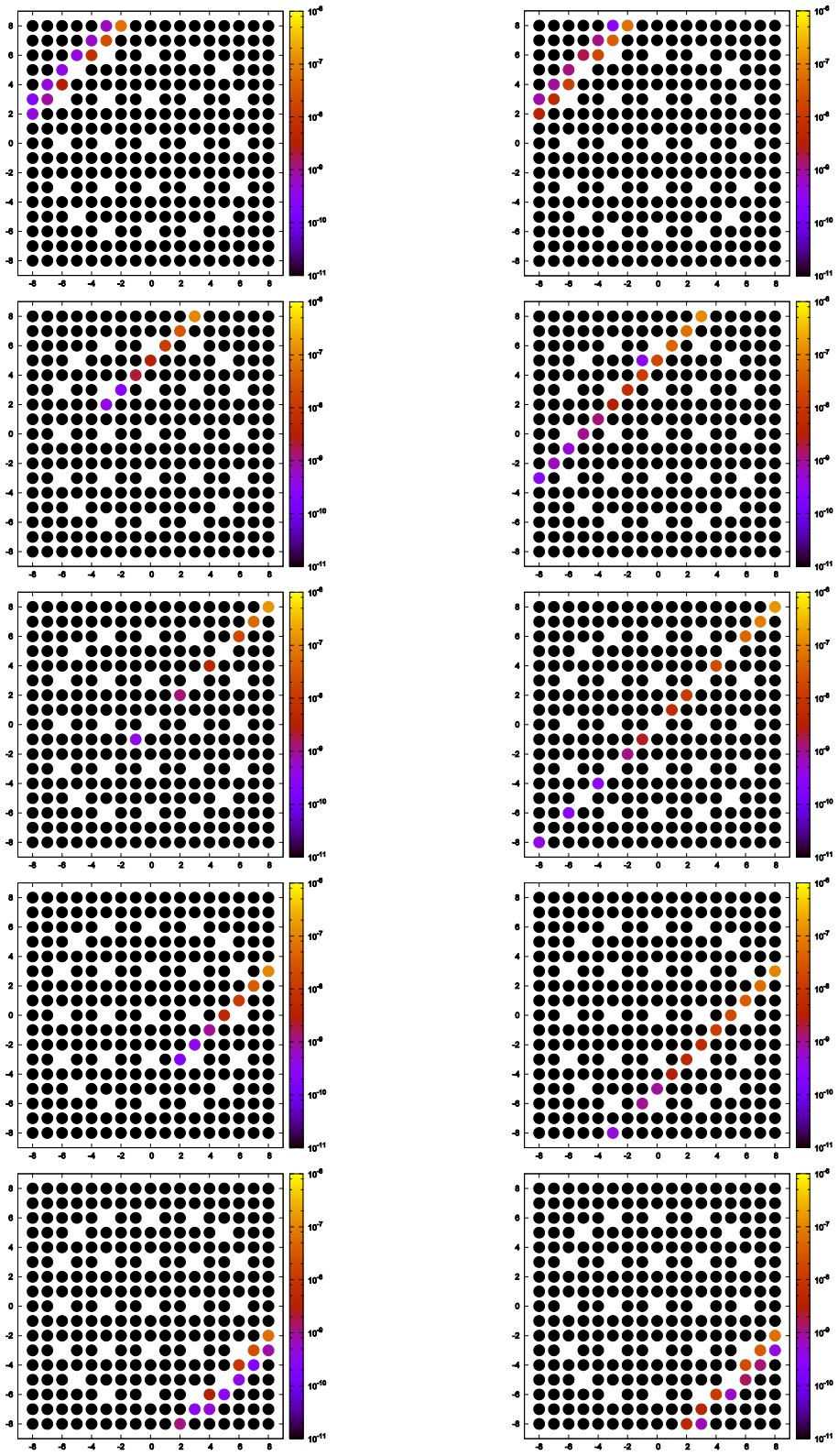

Figure 6: The number of counts in the full energy peak, per emitted source photon for the energies 662 keV (left column) and 1274 keV (right column), for detector numbers 3 (bottom) through 7 (top) in the 45° rotation of case 1.

4. Comparison between simulation results

Variations of case 1 were used to compare calculated contributions to the full energy detector response for each fuel pin. Variations of case 2 were used to compare calculated projections.

4.1 Comparison of pin contributions, case 1

The results of the Geant4 and the MCNP modelling of case 1, with a complete 17x17 PWR fuel assembly, were used to compare calculated full energy response for each fuel pin. The results are shown in figure 7. The MCNP and Geant4 models are clearly linearly dependent on each other, indicating that either of the two models can be used to predict the contribution to the detector count, per fuel pin.

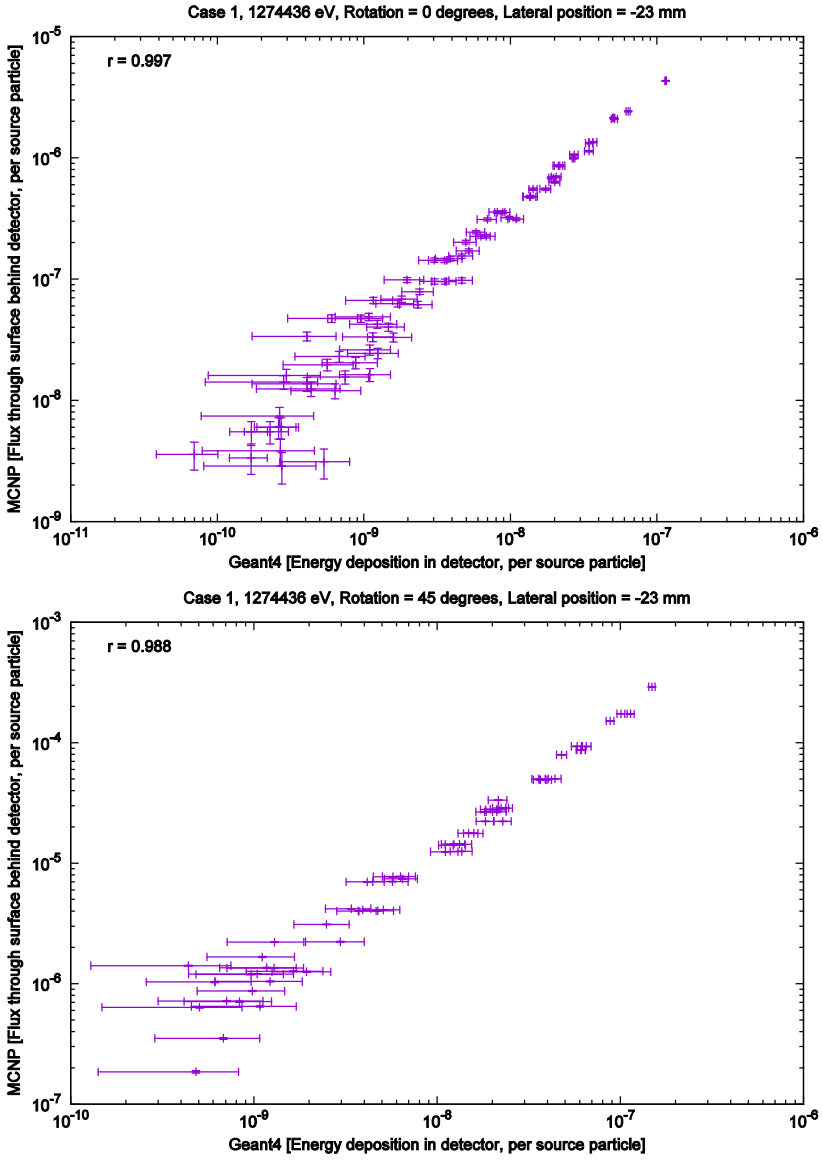

Figure 7: Comparison between Geant4 and MCNP calculations of the 1274 keV source in case 1. Top part shows the 0° rotation and the bottom part shows the 45° rotation. About 10^{12} source particles were emitted in each Geant4 run. The correlation coefficient when for a linear model is indicated by the parameter r.

4.2 Comparison of calculated projections

The results of the Geant4 and the MCNP modelling of case 2, with a 17x17 PWR fuel assembly with 11 missing pins, were used to compare calculated projections. Figure 8 shows this comparison, specifically with a 1274 keV source distributed homogenously over the rods in the fuel assembly.

Due to high computational demands for the Geant4 model, the variation due to statistics in the calculated projections, as seen in figure 8, is relatively large compared to the projection calculated with MCNP. The correspondence between the projections from the two models is expected to be improved as the calculations progress.

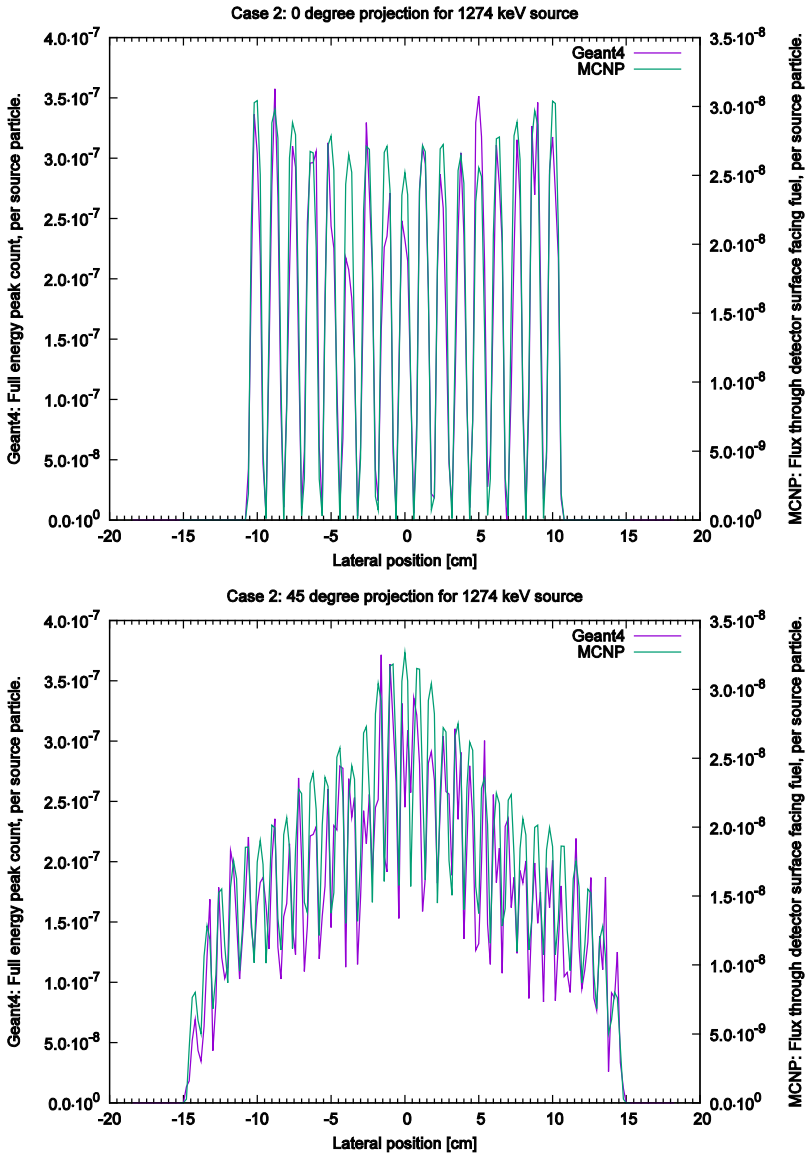

Figure 8: The projections for 0° (top) and 45° (bottom) rotation using a 1274 keV source distributed homogenously over the fuel rods, calculated with the MCNP and Geant4 models.

5. Conclusions

Figures 5 and 6 demonstrate the effect of different attenuation for 662 and 1274 keV gamma-rays, respectively. About an order of magnitude less full energy counts are expected in the Cs-137 peak at 662 keV compared to Eu-154 peak at 1274 keV for a central rod in the PWR 17x17 fuel assembly (assuming the nuclide activities are equal).

Comparing the pin-by-pin detector responses, in case 1, the results indicate that the Geant4 and MCNP models are linearly dependent which implies that either of the two models can be used to predict detector responses.

Comparing the calculated projections, in case 2, is more difficult due to low statistics in the Geant4 modelling. However, the general shape of the projections from MCNP and Geant4 seem to agree relatively well. The results from case 1 indicate that the shape of the calculated projection in Geant4 might converge to the projection calculated in MCNP.

In conclusion, the Geant4 and MCNP calculations are comparable for the cases simulated in this paper, thereby increasing confidence in the models used in the UGET project to establish the design of a universal gamma-ray emission tomography device as presented in [10].

6. Acknowledgements

The participation by Uppsala University in the UGET project is funded by the Swedish Radiation Safety Authority (SSM). The computations performed by Uppsala University were partially performed on resources provided by Swedish National Infrastructure for Computing (SNIC) through Uppsala Multidisciplinary Center for Advanced Computational Science (UPPMAX) under projects p2013091, snic2013-1-296, snic2014-1-203 and snic2014-1-392.

7. References

[1] Unattended Gamma Emission Tomography (UGET) Phase I, JNT A 1955, Joint Work Plan, Developed by the GET Working Group in the UGET project. 2013.

[2] S. Jacobsson Svärd et.al. ”Gamma-ray Emission Tomography for Partial Defect Verification: Response Modeling Methodology and Benchmarking”. 2015 ESARDA Symposium, Manchester, UK, May 2015.

[3] F. Levai, et.al., “Feasibility of Gamma Emission Tomography for Partial Defect Verification of Spent LWR Fuel Assemblies,” Finnish Radiation and Nuclear Safety Authority, STUK-TYO-TR 189, November 2002.

[4] T. Honkamaa, et.al., “Progress Report on JNT 1510 Measurements on VVER Fuel Assemblies,” presentation at IAEA JNT 1995 project meeting, May 2014.

[5] S. Jacobsson Svärd, A. Håkansson, A. Bäcklin, O. Osifo, C. Willman, P. Jansson, “Non-destructive Experimental Determination of the Pin-power Distribution in Nuclear Fuel Assemblies”, Nuclear Technology, 151 (1), 2005.

[6] T. A. White, et.al. “Gamma-ray Emission Tomography for Spent Fuel Assay: Modeling and Performance Evaluation Methods,” proceedings of the INMM-2014 annual meeting, 2014

[7] D. B. Pelowitz, editor. MCNPX USER’S MANUAL Version 2.5.0. 2005.

[8] S. Agostinelli, et.al., G4 Collaboration, “Geant4 - a simulation toolkit”, Nuclear Instruments and Methods in Physics Research Section A: Accelerators, Spectrometers, Detectors and Associated Equipment, Volume 506, Issue 3, 1 July 2003, Pages 250-303, ISSN 0168-9002, http://dx.doi.org/10.1016/S0168-9002(03)01368-8.

[9] V. Mozin, et.al. ”Gamma-ray Emission Tomography for Partial Defect Verification: Response Modeling Methodology and Benchmarking”. 2015 ESARDA Symposium, Manchester, UK, May 2015.

[10] T. A. White, et.al. “Passive Tomography for Spent Fuel Verification: Analysis Framework and Instrument Design Study”. 2015 ESARDA Symposium, Manchester, UK, May 2015.

Passive Tomography for Spent Fuel Verification: Analysis Framework and Instrument Design Study

Timothy A. White[1], Staffan Jacobsson Svärd[2], L. Eric Smith[1], Vladimir Mozin[3], Peter Jansson[2], Anna Davour[2], Sophie Grape[2], Holly Trellue[4], Nikhil Deshmukh[1], Richard S. Wittman[1], Tapani Honkamaa[5], Stefano Vaccaro[6], James Ely[7]

[1]Pacific Northwest National Laboratory, Richland, WA, USA
[2]Uppsala University, Uppsala, Sweden
[3]Lawrence Livermore National Laboratory, Livermore, CA, USA
[4]Los Alamos National Laboratory, Los Alamos, NM, USA
[5]STUK – Radiation and Nuclear Safety Authority, Helsinki, Finland
[6]European Atomic Energy Community
[7]International Atomic Energy Agency
E-mail: timothy.white@pnnl.gov

Abstract:

The potential for gamma emission tomography (GET) to detect partial defects within a spent nuclear fuel assembly is being assessed through a collaboration of Support Programs to the International Atomic Energy Agency (IAEA). In the first phase of this study, two safeguards verification objectives have been identified. The first is the independent determination of the number of active pins that are present in the assembly, in the absence of a priori information. The second objective is to provide quantitative measures of pin-by-pin properties, e.g. activity of key isotopes or pin attributes such as cooling time and relative burnup, for the detection of anomalies and/or verification of operator-declared data. The efficacy of GET to meet these two verification objectives will be evaluated across a range of fuel types, burnups, and cooling times, and with a target interrogation time of less than 60 minutes.

The evaluation of GET viability for safeguards applications is founded on a modelling and analysis framework applied to existing and emerging GET instrument designs. Monte Carlo models of different fuel types are used to produce simulated tomographer responses to large populations of "virtual" fuel assemblies. Instrument response data are processed by a variety of tomographic-reconstruction and image-processing methods, and scoring metrics specific to each of the verification objectives are defined and used to evaluate the performance of the methods. This paper will provide a description of the analysis framework and evaluation metrics, example performance-prediction results, and describe the design of a "universal" GET instrument intended to support the full range of verification scenarios envisioned by the IAEA.

Keywords: spent nuclear fuel assemblies, partial defect verification, gamma-ray emission tomography

1. Introduction

Spent fuel verification measurements are central to the International Atomic Energy Agency's (IAEA) safeguards approaches at facilities handling and storing irradiated fuel. Generally speaking, IAEA safeguards approaches call for verification of spent fuel using a partial defect or 'best-available' method, for fuels that are being transferred to difficult-to-access storage and that have a design allowing disassembly [1-2]. At present, IAEA's authorized instruments for partial defect detection have limitations in terms of independence, defect sensitivity, and implementation flexibility. The IAEA has documented the need for new fuel verification tools as Capabilities 5.5 and 5.7 in the Department of Safeguards Long-Term R&D plan [3].

Passive gamma-ray emission tomography is attractive for addressing partial defect detection and verifying the "completeness" of the fuel assembly because it has the potential to directly image the spatial distribution of the active fuel material in the fuel pins and the relative locations of the pins in the assembly structure, without the need for any operator-declared information. The gamma-ray signatures, particularly in younger fuels, can be strongly correlated to irradiation parameters such as final (integral) burnup and cooling time, thereby achieving more specificity than other methods. Further, tomography has the potential to directly image the interior of the assembly, at multiple axial locations along the assembly length so that pin-level assay (as opposed to volume-integrating assay) can be achieved. Finally, gamma tomography is viable in both wet and dry measurement environments, and in either unattended or attended modes, characteristics that afford significant operational flexibility.

A substantial body of knowledge has been assembled, both through modelling and measurements, regarding the viability of gamma-ray tomography. An overview of these techniques is discussed in section 2. While the prior emission tomography work has been informative and encouraging, a number of technical and viability questions need to be addressed in the context of IAEA's evolving fuel verification needs. Addressing these questions is the primary motivation for the viability study described in this paper, a study performed under the auspices of several Support Programs to the IAEA: United States, Sweden, Finland and the European Commission. Feasibility is quantified relative to the ability to perform specific verification objectives, described in the following sections. Expected performance of existing tomography capabilities will be used as a benchmark for design of a "universal" gamma-emission tomographer capable of examination of a wider variety of fuel types, burnups, and cooling times.

In this paper, we review the verification objectives and implementation scenarios defined by the IAEA, describe the modeling and analysis framework, provide example performance-prediction results for an existing fuel tomographer developed at the request of the IAEA, and describe the design of a "universal" GET design intended to support the full range of use cases envisioned by the IAEA.

2. Verification Objectives and Implementation Scenarios

Verification objectives and representative implementation scenarios were defined in order to focus the scope of the viability study and ensure that the study's results are immediately relevant to IAEA's decisions about viability. The guiding parameters for the study, as defined by the IAEA and the GET study team, are summarized below.

Verification Objective 1: Independent pin counting for routine verification of item integrity
In this case, verification of the spent fuel assembly integrity is performed in a manner completely independent of operator-declared information (e.g., fuel assembly type, initial enrichment, burnup, and cooling time). The assembly is treated as an unknown sample and emitted gamma rays at one or more energies are used to directly calculate the spatial distribution of the emitting material. This spatial distribution is then used to determine the geometric pattern of the pins (e.g., sparse and rectangular for BWR, dense and hexagonal for VVER) and to count the number of pins composing that array. Two types of partial defects are considered: 1) diverted pins that are not replaced with any material, leaving an empty water or air channel, and 2) diverted pins that are substituted with depleted uranium oxide pins. Pins are removed/substituted in various locations of the simulated assemblies to provide insight into the impact of partial-defect location. The evaluation metrics for Objective 1 should recognize the inherent tradeoffs between the probability of detection (*PD*) and false alarm rate (*FAR*).

Verification Objective 2: Quantitative pin-by-pin burnup determination
Gamma emission tomography may also be used to quantify the burnup of each pin in an assembly. Characterizing the magnitudes and gradient of pin-by-pin burnup could help reveal, for example, diversion scenarios where one or a few pins are replaced between reactor cycles. Such pin-level burnup data could also be useful for indirect calculation of fissile material content (e.g., total Pu) at the head end of reprocessing facilities, particularly where direct measurement of fissile material may not be viable by conventional means. Verification of the contents of atypical items, for example canisters containing fuel pins extracted from other assemblies or unirradiated dummy fuel assemblies used by the operator for legitimate purposes, are other potential uses of a tomography device. For this

verification objective, operator-declared information could be incorporated (e.g., fuel assembly type and geometry in order to correct for self-attenuation), but it should not be required.

The implementation scenarios to be considered, for all three major fuel types (i.e., BWR, PWR and VVER), are summarized below.

Implementation Scenario	Cooling time (years)	Deployment constraints	Target Measurement Time (minutes)
Routine verification of old fuel being transferred to a geologic repository	40	Attended or unattended; dry or water	30
Routine verification of fuel being transferred to dry storage	5	Attended or unattended; water	30
Random verification of in-pool inventory	1	Attended; water	30
Anomaly resolution of specific assemblies	1 to 40	Attended; water	60

Table 1 Description of scenarios to be considered in this study.

3. Modeling and Analysis Framework

The GET viability study described in this paper is based entirely on simulated instrument responses. An overview of the modeling and analysis approach is given in Figure 1. Note that the approach allows for the simultaneous evaluation of candidate approaches in each step, which will support comparative evaluations of different instrument designs, analysis algorithms, and performance metrics under the different verification objectives discussed above. A more complete description of each step in the framework is given in [4]. Benchmarking with relevant field data is used to build confidence in the accuracy of the results and ultimately, the study's findings (see [5-7]).

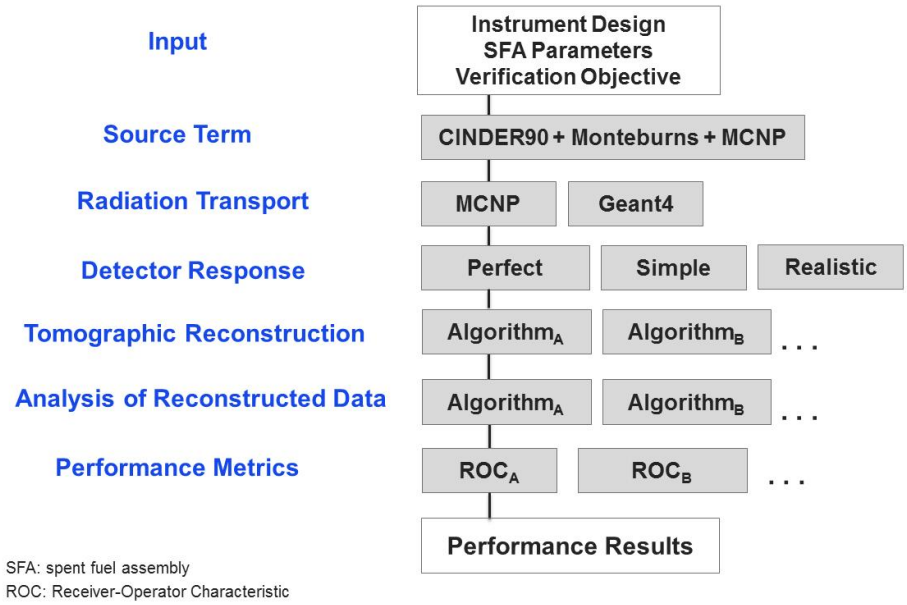

Figure 1 Flow chart illustrating the analysis framework that is used in the GET feasibility studies.

A novel and particularly important aspect of the GET modelling and analysis framework depicted in Figure 1 is the concept of the single-pin sinogram. The single-pin sinogram is the detector response for a virtual assembly in which all of the pins are inert (they attenuate but do not emit radiation) except for one pin. The summation of the set of single-pin sinograms in the assembly is equivalent to the

sinogram from the full assembly. This single-pin sinogram modelling approach allows the characteristics of each emitting pin to be varied, while the attenuation characteristics of the surrounding pins are unchanged. The net result is that a large population of simulated spent fuel assemblies (SFAs), each with a distinctive and inhomogeneous pin-to-pin burnup, can be created from a single transport calculation. The large populations of virtual fuel assemblies then allow concepts from statistical decision theory, in particular the receiver-operating characteristic (ROC) curve, to be used to measure task performance. Note that a virtual assembly in which a pin has been substituted with a depleted uranium oxide pin can be simulated by omitting that pin when creating the assembly from the single-pin sinograms, but simulation of a missing pin requires that the pin be missing in the initial photon-transport used to calculate the sinograms.

It is recognized that task performance will be significantly impacted by the fidelity of the reconstruction algorithm. For instance, attenuation correction may impact the ability to detect the absence of inner pins in the assembly. The flexibility of the framework allows testing different reconstruction and analysis approaches on the same ensemble of simulated data and quantitative performance comparisons to be made on changes of any of the steps in the process. Both verification objectives can be tested in this framework. More discussion on reconstruction algorithms and data analysis can be found in [8].

4. Performance Prediction: Example Results

The modelling and analysis framework described above can be used to analyse many combinations of tomographer design, and reconstruction and analysis algorithms. A current tomographer, developed under direction of the IAEA and currently undergoing modification by the Finnish Support Program, provides a convenient and relevant system design for illustrating the value of the evaluation framework. The “Passive Gamma Emission Tomographer” (PGET) is a portable instrument for underwater fuel measurements, designed primarily for the verification of longer-cooled (i.e., >5 years cooling) fuels. The availability of measured data from PGET campaigns on BWR and VVER fuels in Finland has proven invaluable to the benchmarking of the modelling methods, and for comparison of image-reconstruction and analysis results from both simulated and measured PGET data. The PGET design and field-trial results are more fully described in [9-10].

The example case study presented here considers two burnup and cooling time combinations for PWR fuels: 10 GWd/MTU and 40 years; 20 GWd/MTU and 5 years. Cooling times shorter than ~5 years for even modest-burnup assemblies will produce count rates in the PGET instrument that would paralyze the pulse processing electronics—such fuels are not considered here.

Gamma emission from 40-year-old fuel is dominated by activity from ^{137}Cs while the activity at 5 years is a combination of ^{137}Cs, ^{154}Eu and ^{134}Cs. Single-pin sinogram data were calculated for the two former isotopes independently and a model of the solid-state CdTe detectors was used to develop a detector response function to convert sinogram data to counts in the detector. For this system, the energy-dependent detector-response data is divided into three bins: 400-700 keV, 700-1100 keV, and greater than 1100 keV, consistent with the field settings of the PGET instrument. For the longer-cooled fuel, only Cs contributes significantly to the lowest energy bin, and only that isotopic response is used in subsequent image reconstruction and performance analysis. For the shorter cooling time, the low energy bin includes significant downscatter from the Eu lines—therefore only the middle bin is used for performance. Both approaches are consistent with how the PGET has been applied in field trials. A sinogram and an example of a reconstructed image from the middle energy bin, 700-1100 keV, for a simulated PWR fuel assembly with burnup of 20 GWd/MTu and cooling time of 5 years is shown in Figure 2.

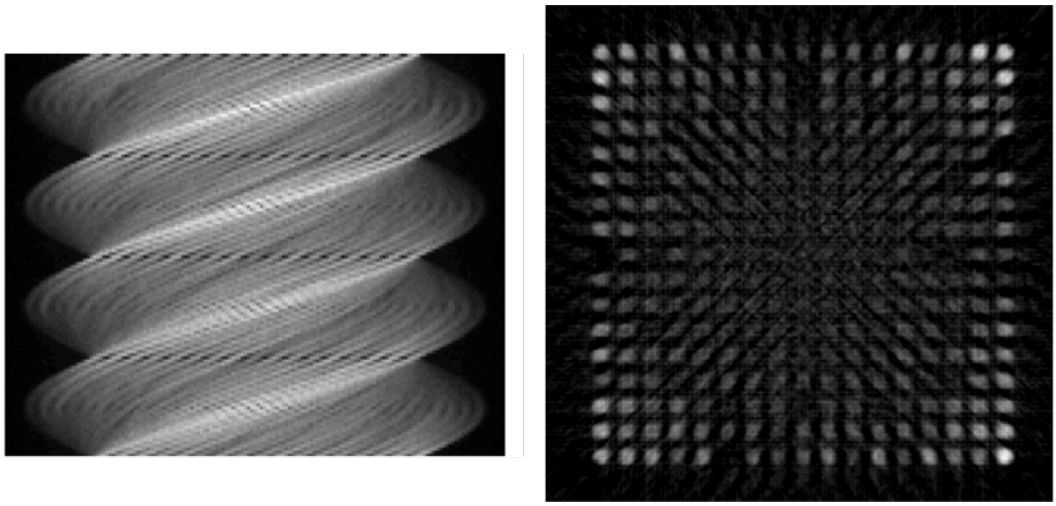

Figure 2. Sinogram and reconstructed image for the PGET instrument assaying a PWR assembly (20 GWd/MTU, 5 years cooling), using simulated data from the 700-1100 keV energy window. There are 11 missing pins scattered through the assembly.

In the example case shown in Figure 2, photon transport from a 17x17 PWR assembly with 11 missing pins was simulated to create 253 single-pin sinograms. The single-pin sinogram data were scaled independently and used to create a simulated fuel bundle with pin-to-pin variations in burnup. For this study, we assumed a uniform pin-to-pin variation of ±20%, a number at the extreme end of likely burnup variations even for BWR fuels (less variation is expected for PWR fuels), but within bounds indicated by discussions with operators. Note that any other patterns of burnup variation are possible by proper scaling of the single-pin sinograms as discussed earlier. The data were reconstructed on a regular pixel grid and the aggregated intensity of multiple pixels in a "neighbourhood" centred on each pin location was calculated. These aggregated pin-region intensity values are referred to as the "pin scores." This process was repeated for each simulated fuel assembly, approximately 10,000 for each fuel type (PWR and BWR). This produces a large population of virtual fuel assemblies that have the same average burnup, but different pin-to-pin variations and statistical noise realizations. (For more discussion, see [4].)

The pin-score summary for 100 PWR assemblies are shown in Figure 3. In this plot, the pins are indexed by their distance from the centre of the assembly (abscissa) and the score is plotted on the ordinate. Pins that are present in the assembly are shown in green, and pins that are missing are shown in red (the scores for water channels are shown in blue). It is clear that the scores for missing pins near the periphery of the assembly (right side of the plot) are well-separated from scores of pins that are present, and that toward the centre of the assembly the distribution of scores of missing and present pins overlap.

The ability to distinguish present from missing pins – the probability of detection – as a function of the misclassification of pin – the false-alarm rate – can be quantified by the receiver-operator characteristic (ROC) curve as shown in Figure 4. ROC analysis is used in many fields; an example from imaging sciences relevant to this work can be found in [11]. For this simulated PWR assembly population (average burnup of 20 GWd/MTU and 5 years cooling) and the device simulated and the reconstruction methods used here, missing pins can be detected with high probability and a low false alarm rate. Some acceptance of false alarms (~1%) must be made in order to achieve high detection rates greater than 90% for missing pins in the center of the assembly. Important to note is that these performance-prediction curves in Figure 4 should be considered to be upper bounds on realistic PGET performance, since real-world instrumentation and processing effects (e.g., pixel to pixel variations in detector sensitivity) that can degrade image quality have not been included in the simulations.

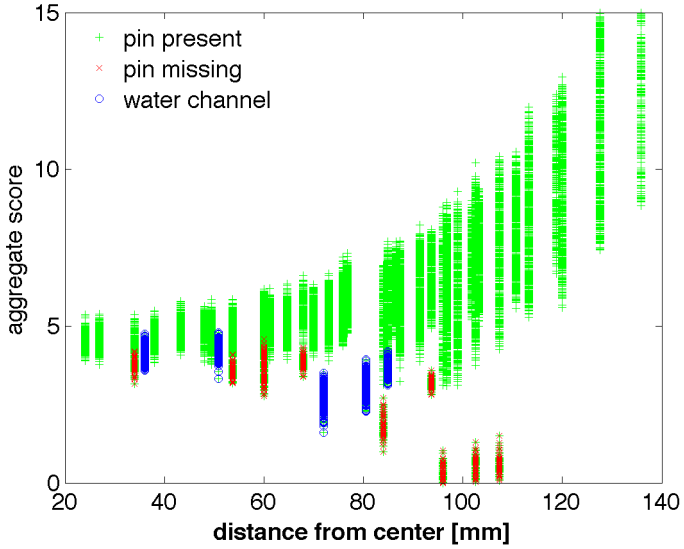

Figure 3 Pin scores from an ensemble of 100 assemblies for a simulation of PWR with a burnup of 20 GWd/MTU and a cooling time of 5 years. These data represent variation in inhomogeneous burnup and counting statistics from the data in Figure 2.

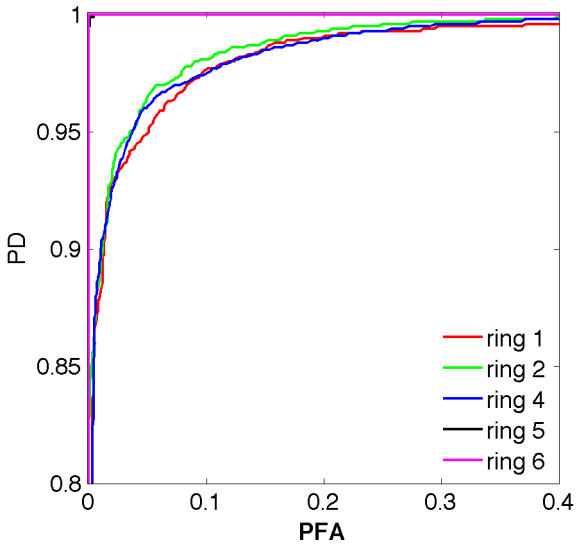

Figure 4 ROC curves as a function of pin location in the assembly for the study described in Figure 3. The scoring is aggregated into “rings” of pins. Ring 1 is composed of the 8 pins that form a square closest to the centre of the assembly, Ring 2 is formed from the pins in the next square region, and the rest of the rings are aggregated similarly. Scores from the water channels are not included in the ROC analysis. Rings 6-8 have identical performance; only Ring 6 is shown.

5. Design of a “Universal” Tomographer for Safeguards

Examination of prior tomographic applications to spent nuclear fuel is informative for the development of a “universal” tomographer design for safeguards that can cover both verification objectives and all expected implementation scenarios. Two prior and/or ongoing projects are highlighted here because in many ways they represent the extremes of the design space.

The first design is the PGET instrument described earlier. This portable, underwater device was designed to assay relatively long-cooled fuels (>5 years) where the intensity of emissions, and the proportion of those emissions that are at energies greater than 1500 keV, are relatively low. PGET was specifically designed to deliver on Objective 1 (pin counting) but not necessarily Objective 2 (pin-

by-pin burnup quantification) Each PGET detector head has a dense array of CdTe detectors with very limited spectroscopic capability (i.e., broad ROIs) and relatively "light" collimation. The detector array collects projection data, and rotates through 360-degrees to collect a full sinogram. (Two detector heads are used in order to provide more inter-detector collimation.) This approach can offer rapid data collection in a rotate-only geometry. This system has been field-tested and has shown promise for detecting missing pins with various fuel types and characteristics [10].

The second example design was a tomographer built by Uppsala University in Sweden for the purpose of validating the burnup codes of reactor operators. This large, underwater device was designed to measure commercial BWR fuel shortly after removal from the reactor (few weeks) where the total emission intensity is high and the proportion of high-energy emissions is high compared to longer-cooled fuels [7]. Because individual isotopes were to be assayed, spectroscopic detectors (i.e., BGO scintillators) were required. This system used a sparsely populated detector array with very heavy collimation. The detector head required a translation step to adequately sample the projection data as well as rotate to collect complete sinogram data. This system was developed for and demonstrated on BWR fuel at a nuclear power plant in Sweden [12].

These two approaches can be considered bounding cases for the detector-head design of a universal GET for safeguards. In one case, there are sufficient detector pixels in the detector head to sample a single projection and thus the only motion necessary to collect sinogram data is rotation of the detector head around the fuel assembly. Addition of the second detector head enables both reduced sampling time and finer sampling along a projection (because the detector arrays are offset by half of the detector pitch relative to each other). This approach is possible in part because the detector elements (2mm wide by 5mm tall by 10mm deep CdTe crystals) are small enough to allow the fine pitch. Some problems with this geometry are (1) the potential for crosstalk between collimator openings (septal penetration), which reduces the fidelity of the line integrals and thus the resolution of the reconstruction, and (2) the low full-energy detection efficiency of these small detectors, which implies that spectroscopic peak analysis with background subtraction would result in low counting rates and thus discriminated (binned) counting is used instead, which introduces some level of scattered gamma rays in the recorded data.

The other approach is to have a sparser detector array (larger pixel pitch) and fewer total pixels in a detector array. The detector must be translated laterally in order to "fill in the gaps" between the widely spaced pixels. This design is required if the detector (scintillator) is larger than the pixel pitch, and has the advantage of not being a susceptible to septal penetration as a finer-pitch design (this may be an especially important feature for scenarios is which higher energy photons must be detected). Furthermore, since the detector (scintillator) is larger, it allows for efficient full-energy detection and thus spectroscopic peak analysis with background subtraction applied in order to efficiently select the radiation of interest for the analysis. This is the design to be adopted in the present work.

In general, the design parameter space reduces to spatial resolution (Can individual pins be distinguished?), energy resolution (How well can isotopic lines be distinguished?), and collection efficiency (Are total count rates manageable? Is there sufficient collection of key emission lines to ensure reasonable total assay times?). The collimator parameters (bore length, width and height) are the principle determinants of the spatial resolution and collection efficiency, and also define the data-collection geometry (number of samples per projection and angular sampling)[1]. Energy resolution and to a lesser extent the collection efficiency, are coupled through the choice of detector material. Total data-collection time will depend on each of these parameters, as well as other engineering and cost considerations (e.g., acquisition time could be decreased by the use of multiple detector assemblies, increasing cost and mechanical complexity).

Informed by prior work and simulations of the existing tomography instrument, it was determined that a collimator with a length-to-width aspect ratio of between 100:1.5 and 300:1 will be sufficient to meet spatial-resolution requirements for all three fuel types considered in this study. In order to meet Verification Objective 2 and identify gamma-ray signatures from specific isotopes, it will be necessary to have a detector with a spectroscopy capability, see ref. [13]. For calculating pin-wise burnup values,

[1] Only parallel-beam CT geometries are considered in this work. Other data-collection geometries may be considered after a performance baseline has been established for benchmarking performance and cost.

it will be necessary to resolve emission lines from key isotopes, primarily ^{137}Cs (662 keV) and ^{154}Eu (5 principal lines between 723 and 1264 keV). In addition, for very short cooling times, it would be desirable to separate the response of ^{134}Cs (605 and 796 keV) from the ^{137}Cs lines. These objectives drive the system design toward high energy resolution scintillators as the detection material. A comparison of detector responses to simulated projection data for a single pixel for both NaI(Tl) and $LaBr_3$(Ce) are shown in Figure 5. Lanthanum bromide was chosen as the scintillator for both its speed and energy resolution. On-going work [14], outside of the scope for the UGET project, will provide information about potential neutron activation interference with the peak evaluation capability of the $LaBr_3$(Ce) detector.

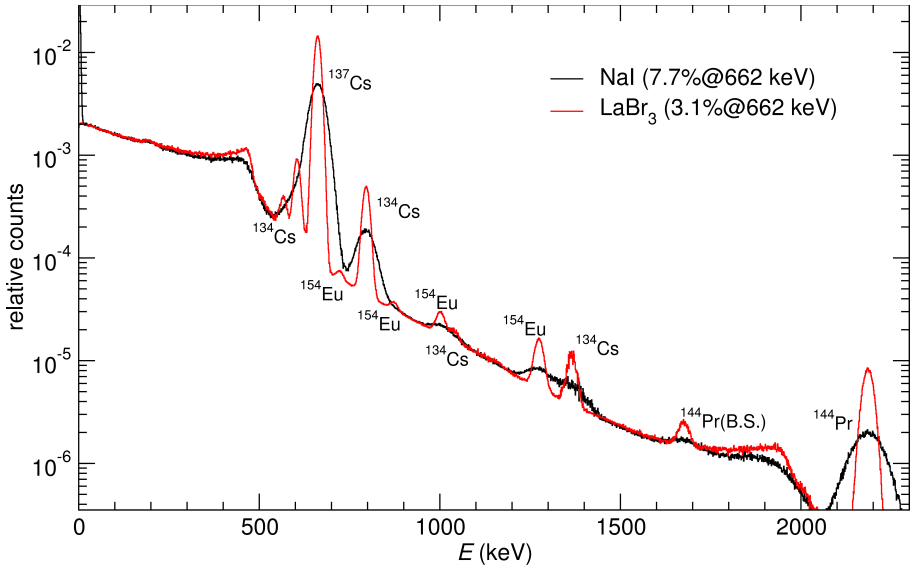

Figure 5 Detector response functions for NaI and $LaBr_3$ for simulated projection data.

Once the spatial resolution has been set by the collimator field of view, and the energy resolution requirement defined by the detector material, the design challenge reduces to striking a balance between managing count rates across all implementation scenarios while ensuring sufficient imaging efficiency for challenging cases:

- *High-count rate*: For high burnup, short cooling time fuels, the total count rate at the detector needs to be less than ~10^6 counts/second in order to prevent excessive pileup in scintillators (e.g., $LaBr_3$(Ce)). An example scenario for this case would be PWR, 40GWd/MTU, 1-year cooling time.
- *Sufficient efficiency*: For medium-length cooling times (5-10 years), the system design must be efficient to the 1274keV line from ^{154}Eu (for PWR), and for longer cooling times, efficient to the 662keV line from ^{137}Cs.

To achieve this balance, the detector-head design strategy is to choose a collimator geometry that is consistent with spatial-resolution requirement and efficient for the longer-cooling time, lower activity fuel, and use in-collimator filtration to address the higher count rates at short cooling times. Detector-head design is explored for two parallel-bore and one diverging-bore collimator, see Figure 6., assuming a 5.08 cm diameter right circular cylinder (RCC) $LaBr_3$ scintillator. This plot shows that a collimator with bores having dimensions 1.5 mm wide by 10 mm tall by 200 mm long is sufficient to keep the count rate below 10^6 cps for the shortest cooling times. Note that the total count rate would be reduced if a less efficient (smaller) detector was used, thereby increasing the integration time needed to achieve sufficient counts rates in the photopeak but allowing more detector elements to fit in the detector head (decreasing the pixel pitch). This poses an interesting optimization study investigating the tradeoff between the number of pixels in the detector and the total collection time for a projection, a function of the efficiency and the number of steps. This tradeoff is summarized in Figures 7 and 8.

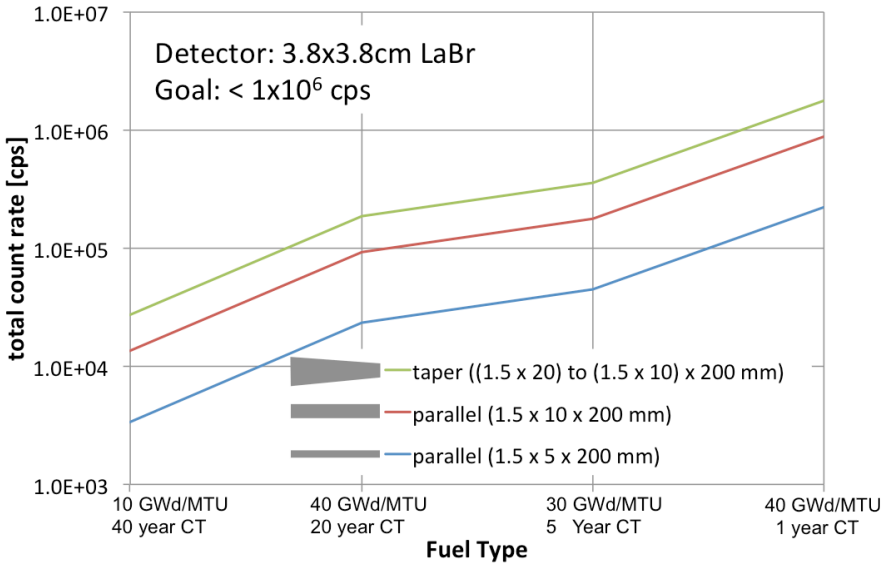

Figure 6 Total count rate for simulated PWR fuel as a function of the collimator bore size assuming a 5.08 cm diameter $LaBr_3$ scintillator for three different collimator designs.

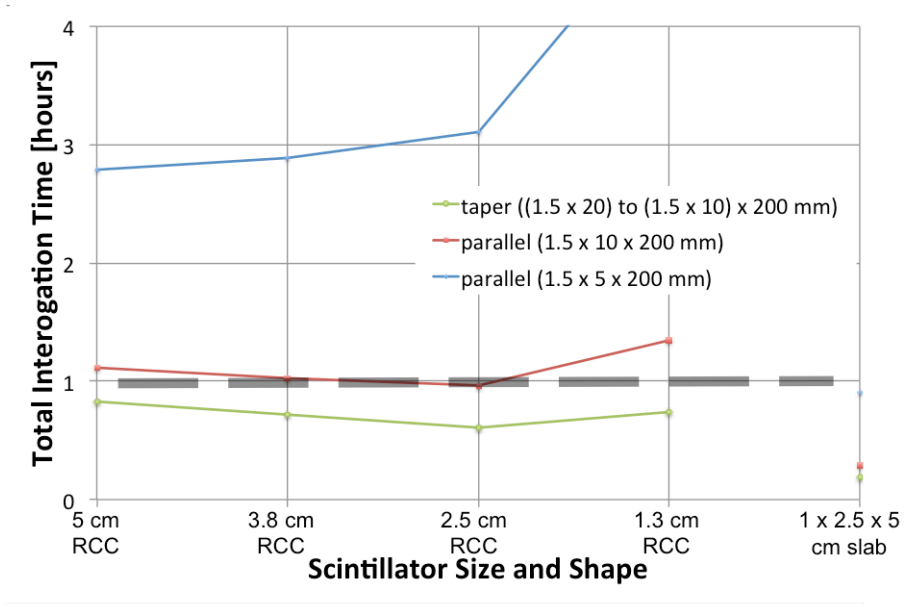

Figure 7 Peak count rate as a function of collimator and scintillator size. The efficiency of larger detectors allows shorter integration times, but requires more steps per projection. These data simulate a PWR assembly with a 20GWd/MTU burnup and 5 year cooling time.

The optimization of scintillator size with respect to total data-collection time is driven mainly by the scintillator efficiency. The knee in the efficiency curve for a right-circular cylinder (RCC) $LaBr_3(Ce)$ scintillator is in the neighbourhood of a diameter of 2.5-5.1cm. Smaller detectors allow fewer steps to collect a projection, but result in longer total integration times with respect to larger detectors that take require more steps per projection. An alternative to the RCC is a slab detector that is thick in the direction parallel to the collimator bore and narrow in the transverse direction. This allows a higher packing fraction (higher pixel pitch), fewer steps, and shorter overall data-collection time. However, this design would drive up cost considerably – these are custom detector geometries and the required number of detectors is higher – for a decrease in imaging time of only a factor of 4.

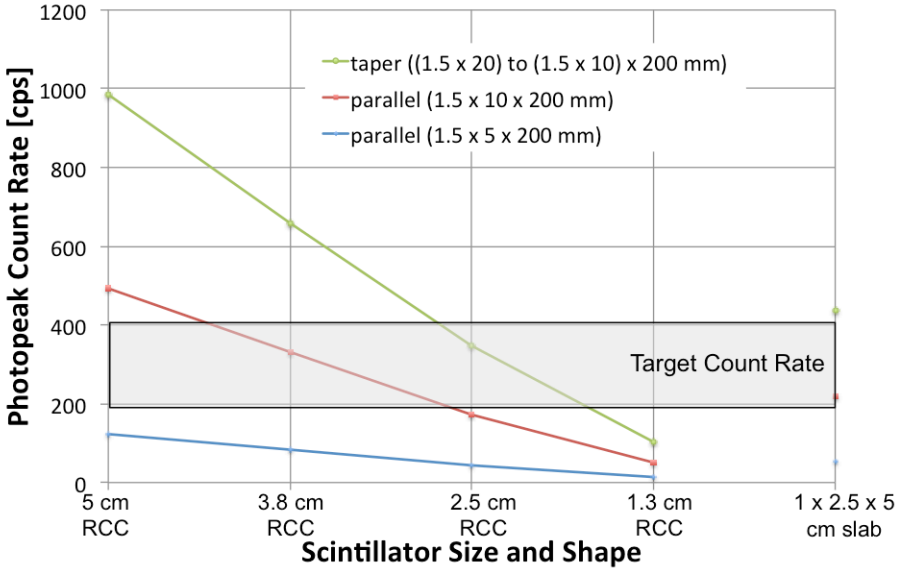

Figure 8 Total data collection time as a function of collimator and scintillator size. This demonstrates the trade-off between integration time and number of steps in a translate-rotate geometry. These data simulate a PWR assembly with a 20GWd/MTU burnup and 5 year cooling time.

These considerations drive toward a detector design with 8, 3.8cm diameter scintillators behind a collimator with dimensions 1.5mm wide by 10mm tall by 200mm long. While only a single detector head is required for full data collection, multiple heads will speed up the total collection time. To collect projection data, each head would have to scan laterally. This could be done in discrete steps, or the motion could be continuous and the data collected in list mode (and sorted out later). A drawing of a single detector head and a schematic drawing of the multi-head assembly demonstrating the translate-rotate scanning protocol are shown in Figure 9.

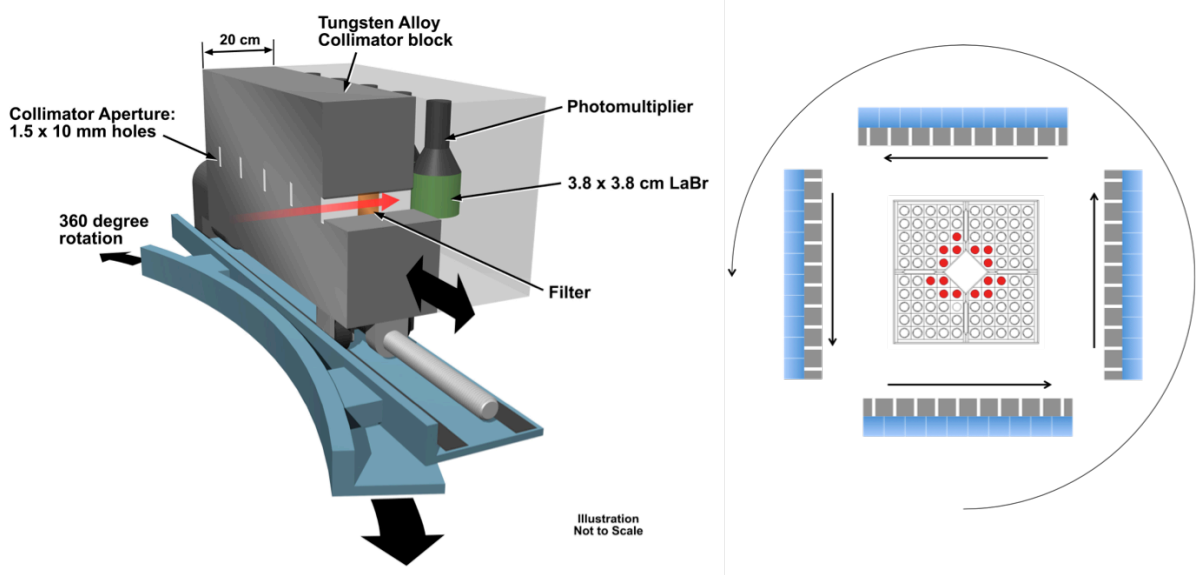

Figure 9 Diagram of a single detector head of a “universal” GET design for safeguards applications. In the proposed system design, four heads would be arranged around the object to minimize data-collection time, as shown in a top-view diagram on the right. To collect tomographic data with the sparse detector array, a translate-rotate geometry will be necessary.

6. Summary and Next Steps

A modeling and analysis framework has been developed to examine the feasibility of gamma-ray tomography instruments for safeguards verification of spent nuclear fuel. The framework is an end-to-end evaluation process consisting of: detailed modeling of different tomographer designs; conversion of MCNP-generated transport data to energy-dependent flux sinograms; compilation of pin-wise flux sinograms into full fuel assembly with missing or substituted pins; calculation of the corresponding detector response sinogram for each virtual assembly; and energy-windowing analysis on the detector response sinograms. The generated sinograms may then be used in various analyses for each virtual assembly. For example, for Verification Objective 1, one may consider image reconstruction using filtered back projection or algebraic methods, pin scoring based on pin-region grey level or image analysis [15], and application of ROC-curve analysis to the pin-scoring histogram data. For Verification Objective 2 on the other hand, reconstructions using detailed algebraic models to extract quantitative pin-wise data may be required along with other quantitative measures of the capability to reconstruct the original simulated distribution.

Using the modeling and analysis framework, experience gained from prior work utilizing tomography for spent-fuel interrogation, and the commercial availability of key hardware components, a “universal” GET design for safeguards applications has been defined. Such an instrument could be used for assaying high-burnup fuel with cooling times as short as 1 year, but also has sufficient collection efficiency to achieve reasonable assay times for lower-burnup fuels with long cooling times (e.g., 40 years). This tomographer would support not only the detection of missing pins, but also the quantitative determination of pin-wise burnup.

Continuing work will progressively improve the fidelity of the radiation transport and other analysis steps in ways that can support realistic performance predictions. For example, in the image reconstruction and analysis steps presented here, only very simple reconstruction methods and image-processing tools have been exercised. In the near future, the GET team will explore alternative reconstruction approaches that incorporate different flavors of attenuation correction and models of the imaging geometry, as well as different approaches to analysis of the reconstructed pin activities, see e.g. refs. [8] and [15]. These candidate analysis modules can be “dropped in” to the modular analysis framework and exercised to generate comparative ROC curves. Once the modeling and analysis framework is extended to address both verification objectives, the team will complete the systematic walk through each of the implementation scenarios and fuel types prescribed for the study.

7. Acknowledgements

Funding for this work has been provided by the U.S. Support Program to the IAEA and the National Nuclear Security Administration’s Office of Nonproliferation and International Security (NA-24) and the Next Generation Safeguards Initiative. The participation by Uppsala University is funded by the Swedish Radiation Safety Authority (SSM) under contracts SSM2014-94 and SSM2015-99. The authors would also like to thank the IAEA’s James Ely and Alain Lebrun for their guidance of the GET viability study.

8. References

1. International Atomic Energy Agency, *Integrated Safeguards for Spent Fuel Transfers to Dry Storage*, SG-OP-GRNL-PL-0019, IAEA, 2006.

2. International Atomic Energy Agency, *Model Integrated Safeguards Approach for a Spent Fuel Encapsulation Plant*, SG-PR-1305, IAEA, 2010.

3. International Atomic Energy Agency, *IAEA Department of Safeguards Long-Term R&D Plan, 2012-2023,* STR-375, IAEA, 2013.

4. T. White, et al., *Gamma-Ray Emission Tomography for Spent Fuel Assay: Modeling and Performance Evaluation Methods*, proceedings of the INMM 55th Annual Meeting, Atlanta, USA, 2014.

5. V. Mozin, et al. *Gamma-ray Transport Calculations for Gamma Emission Tomography of Spent Nuclear Fuel in the Context of the UGET Project*, proceedings of the INMM 55th Annual Meeting, Atlanta, USA, 2014

6. V. Mozin, et al., *Gamma-ray Emission Tomography for Partial Defect Verification: Response Modeling Methodology and Benchmarking*, 2015 ESARDA Symposium, Manchester, UK, May 2015.

7. P. Jansson, et al., *Monte Carlo simulations of a Universal Gamma-Ray Emission Tomography Device*, 2015 ESARDA Symposium, Manchester, UK, May 2015.

8. S. Jacobsson Svärd et al., "*Applicability of a set of tomographic reconstruction algorithms for quantitative SPECT on irradiated nuclear fuel assemblies*", Nuclear Instruments and Methods in Physics Research A, 783, 2015.

9. F. Levai, et al., "Feasibility of Gamma Emission Tomography for Partial Defect Verification of Spent LWR Fuel Assemblies," Finnish Radiation and Nuclear Safety Authority, STUK-TYO-TR 189, November 2002.

10. T. Honkamaa, *Arranging Spent Fuel Verification Campaign in NPPs – Experiences in Finland*, Proceedings of the INMM 55th Annual Meeting, 2014.

11. H. H. Barrett and K. J. Myers, *Foundations of Image Science*, Wiley Series in Pure and Applied Optics, 2004.

12. S. J. Svärd, et al., *Non-destructive Experimental Determination of the Pin-power Distribution in Nuclear Fuel Assemblies*, Nuclear Technology, 151 (1), 2005.

13. S. J. Svärd, et al., *Tomographic determination of spent fuel assembly pin-wise burnup and cooling time for detection of anomalies*, 2015 ESARDA Symposium, Manchester, UK, May 2015.

14. K. Ianakeiv, et al., *Underwater Testing of Detectors and Electronics Hardware for Spent Fuel Measurements*, 2015 ESARDA Symposium, Manchester, UK, May 2015.

15. A. Davour et.al, "*Image analysis methods for partial defect detection using tomographic images on nuclear fuel assemblies*", 2015 ESARDA Symposium, Manchester, UK, May 2015.

Tomographic determination of spent fuel assembly pin-wise burnup and cooling time for detection of anomalies

Staffan Jacobsson Svärd[1], Peter Andersson[1], Anna Davour[1], Sophie Grape[1], Scott Holcombe[2], Peter Jansson[1]

[1]Uppsala University, Uppsala, Sweden
[2]Institutt for Energiteknikk, Halden, Norway

***Abstract**:*

The IAEA has initiated Member States' Support Program project JNT A 1955 to assess the partial defect detection capabilities of gamma emission tomography (GET) for spent nuclear fuel assembly verification. The GET technique is based on measurements of the gamma-ray flux distribution around a spent fuel assembly using dedicated, tomographic equipment and subsequent reconstruction of the internal source distribution using tomographic algorithms applied on the recorded data. One of the verification objectives identified for the project is the quantitative measurement of pin-by-pin properties, e.g. burnup and/or cooling time, for the detection of anomalies and/or verification of operator-declared data. For this objective, reconstruction algorithms that return quantitative, isotopic pin-by-pin data are applied.

Previously, GET measurements performed on commercial nuclear fuel assemblies in Sweden have proven capable of determining the relative pin-by-pin power distribution with high precision in BWR fuel with short cooling time, based on the measured distribution of the gamma-ray emitting fission product ^{140}Ba/La in the fuel. In the current project, the capabilities of GET to determine additional pin-wise fuel parameters in additional fuel types are being assessed. The evaluations are based on Monte Carlo simulations of the emission of gamma-rays from the fuel and their detection in a tomographic measurement device.

This paper describes the algorithms used for reconstructing quantitative pin-wise data and the results that are anticipated with this technique. It is argued that detailed modelling of the gamma-ray attenuation through the highly inhomogeneous mix of strongly-attenuating fuel rods and less-attenuating surrounding water (wet storage) or air (dry storage) is required to yield high precision in the reconstructed data. The burnup distribution assessment would be based on the recording of 662-keV gamma radiation from ^{137}Cs, whereas the assessment of both burnup and cooling time simultaneously requires the GET measurement and pin-wise reconstruction of at least two isotopes, which puts constraints on the measurement equipment used.

Keywords: Nuclear fuel assemblies; Partial defect verification; Gamma emission tomography; Burnup; Cooling time

1. Introduction

Verification of spent nuclear fuel assemblies is an important constituent of the IAEA's measures at fuel handling and storage facilities, and recently, a general request has been posed for verification using a partial-defect method for spent fuel having designs that allow disassembly before these are transferred to "difficult to access" storage [1],[2]. One promising candidate method for such verification is gamma-ray emission tomography (GET), for which both experimental and simulation studies have indicated that even removal or replacement of individual fuel rods from an assembly may be detected.

GET on spent nuclear fuel assemblies is performed in two steps; (1) the gamma-ray flux emitted from an assembly at one axial level is recorded in a large number of positions (typically 1,000 to 10,000) using well shielded and collimated detectors, and (2) the internal gamma-ray source distribution at the

measured axial level is reconstructed using tomographic algorithms. As a result, a qualitative cross-sectional image of the internal source distribution and/or quantitative pin-wise source contents of the fuel may be obtained. The method is attractive in that it yields pin-wise information without requiring the fuel assembly to be dismantled.

The previous work on tomography includes the design, fabrication and field-testing of a portable, underwater device within the IAEA JNT1510 project [3],[4]. Additional experience has been gained on equipment design, tomographic reconstruction techniques and analysis methods in Swedish projects, including the construction of a laboratory mockup and a heavy, stationary type of underwater tomograph, which was used in measurements at a commercial BWR reactor [5],[6]. In addition, a collaborative Swedish-Norwegian project has resulted in an operational tomography device for measuring power, burnup and fission gas distributions in research reactor fuel at the OECD Halden reactor [7].

In order to bring together previous experiences and assess the viability of GET for verification of used nuclear fuel to be transferred to difficult-to-access storage, the joint task JNT A 1955, ”Unattended Gamma Emission Tomography (UGET) for Partial Defect Detection", has been set up within the support programmes of Sweden, USA, Finland and the European Commission. In the first phase of the project, the purpose is to provide an assessment of the viability of the technique for safeguards applications. Two verification objectives have been defined; 1) pin counting for routine verification of item integrity and 2) quantitative determination of pin-by-pin properties such as burnup and cooling time for detection of anomalies. For the first objective, no operator-provided information is assumed to be known to the inspecting party and verification should be fully independent. For the second objective, operator-declared information may be used. In the latter case, the anomaly detection may either be based on comparisons between operator-declared pin-wise BU and CT and measured values of these properties, or more independently by inter-comparing measured pin-by-pin contents of studied isotopes.

This paper accounts for the current status of the work performed on verification objective 2.

2. **Verifying spent fuel parameters**

As a result of a fuel assembly’s irradiation history in a reactor core, the isotopic inventory of the fuel changes, and during the time period after irradiation, further changes occur due to isotopic decay. One way of keeping track of the isotopic inventory is to save information on the fuel’s initial enrichment and its detailed irradiation history. However, most often the history is summarized in two parameters; burnup (BU) and cooling time (CT), the former giving a measure of the total number of fissions that have occurred in the fuel during irradiation, and the latter describing the time period that has passed since final discharge from the reactor core.

Both BU and CT of spent fuel can be measured and compared to operator declarations, thus enabling a verification of the fuel properties and a confirmation that the irradiation corresponds to a civil fuel cycle. As described below, spectroscopic measurements of the gamma radiation field around a nuclear fuel assembly may be performed (*gamma scanning*) to assess the content of gamma-ray emitters in the fuel, and estimations of BU and CT can be inferred based on these data [8], [9]. This type of measurement is typically performed on a complete assembly, and accordingly, gamma scanning may be used in safeguards for item verification, where the item is an assembly.

When employing emission tomography, isotopic contents, and thus also BU and CT, may be obtained on the individual fuel pin level, potentially enabling the capability to detect anomalies not only in terms of presence of fuel pins but also in terms of pin-wise fuel properties.

2.1. Gamma-ray spectroscopy to determine burnup and cooling time

Gamma spectroscopy is an established method for non-destructive assay of irradiated nuclear fuel. The availability of different characteristic gamma rays for measurement depends on the emitting isotope’s production modes (fission, neutron absorption and/or nuclear decay) and half-lives, and the gamma ray’s branching ratio and energy. In particular, the latter has to be high enough to escape the assembly. Some of the most commonly measured gamma rays for fuel with CT ≥ 1 year are ^{137}Cs

($T_{½}$ = 30.1 years), ^{134}Cs ($T_{½}$ = 2.1 years) and ^{154}Eu ($T_{½}$ = 8.6 years). Examples of experimentally recorded gamma-ray spectra from PWR fuel assemblies with CTs ranging from 5 to 28 years are presented in Figure 1, identifying the strongest characteristic peaks from these isotopes.

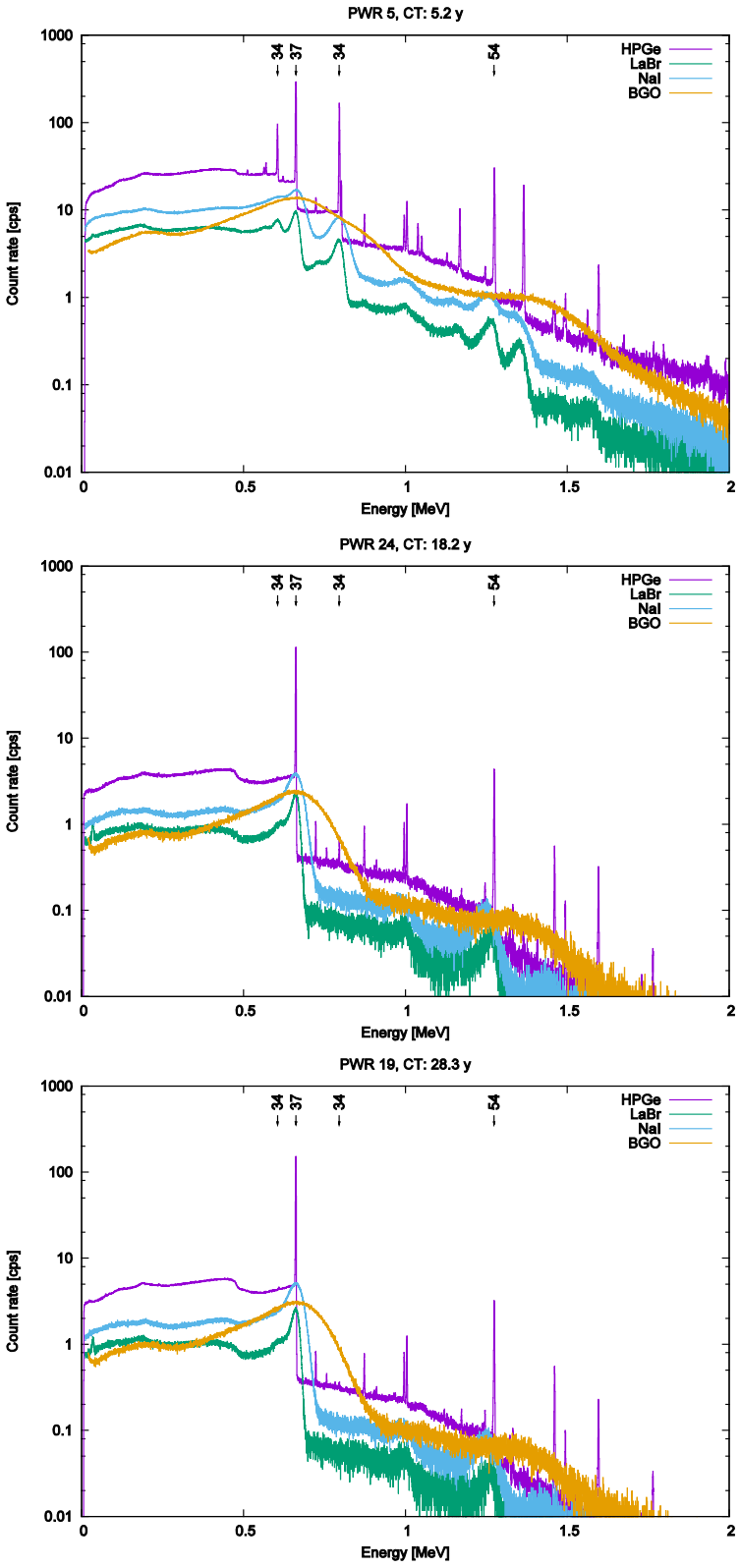

Figure 1: Measured gamma-ray spectra (logarithmic scales) from three PWR fuel assemblies with CT ranging from 5 to 28 years. The spectra were recorded using a 44% efficiency HPGe, a cylindrical 25.4 x 50.8 mm LaBr, a cylindrical 50.8 x 50.8 mm NaI and a rectangular 20 x 30 x 50 mm BGO detector. Peak positions for Cs-134 (605 and 796 keV), Cs-137 (662 keV) and Eu-154 (1274 keV) are marked 34, 37 and 54, respectively. Data from [10].

It has long been established that the produced amount of ^{137}Cs in the fuel is nearly proportional to its BU and so is the ratio of the production of ^{134}Cs and ^{137}Cs, see e.g. ref [11]. Accordingly, the BU of the fuel may be assessed by measuring the gamma radiation emitted in the decay of these isotopes. In addition, the measurement of this intensity ratio is approximately independent of, e.g., detection efficiency. However, directly using these proportionalities requires knowledge of the CT of the used fuel. On the other hand, reference [9] shows that BU can be determined independently of CT using gamma-scanning measurements of the intensities[1] from two isotopes, see equation (1).

$$BU = exp\left[\frac{ln\left(\left(\frac{k_2}{I_2}\right)^{\lambda_1}\cdot\left(\frac{I_1}{k_1}\right)^{\lambda_2}\right)}{\lambda_2\kappa_1-\lambda_1\kappa_2}\right] \tag{1}$$

where:

I_1 and I_2 are two measured intensities of, e.g., ^{137}Cs and either of ^{134}Cs or ^{154}Eu.

k_i and κ_i are fitting parameters for a calibration curve on the form $I = k{\cdot}BU^{\kappa}{\cdot}e^{-\lambda\cdot CT}$ for each isotope i. (For ^{137}Cs, ^{134}Cs and ^{154}Eu, κ_i are about 1.0, 2.0 and 1.6, respectively, see ref [9].)

λ_i is the decay constant of isotope i.

Neglecting uncertainties in the calibration curves and correlations between the two measured intensities, the relative uncertainty of BU can be written as in equation (2).

$$\frac{\Delta BU}{BU} = \frac{1}{|\lambda_2\kappa_1-\lambda_1\kappa_2|}\cdot\sqrt{\lambda_2^2\left(\frac{\Delta I_1}{I_1}\right)^2+\lambda_1^2\left(\frac{\Delta I_2}{I_2}\right)^2} \tag{2}$$

Reference [9] also elaborates on how CT can be determined, independently of BU, using measured intensities of, e.g., ^{137}Cs and either of ^{134}Cs or ^{154}Eu. In this case, equation (3) is used.

$$CT = \frac{ln\left\{\left(\frac{k_2}{I_2}\right)^{\kappa_1}\cdot\left(\frac{I_1}{k_1}\right)^{\kappa_2}\right\}}{\lambda_2\kappa_1-\lambda_1\kappa_2} \tag{3}$$

Assuming again independent intensity measurements and neglecting calibration uncertainties, we can write the uncertainty of CT as in equation (4).

$$\Delta\mathrm{CT} = \frac{\sqrt{(\kappa_2\Delta I_1/I_1)^2+(\kappa_1\Delta I_2/I_2)^2}}{|\lambda_2\kappa_1-\lambda_1\kappa_2|} \tag{4}$$

For fuel assemblies with long cooling time, ^{137}Cs with its long half-life of 30 years is most widely used for passive gamma measurements. Provided that all fuel rods have the same CT, the distribution of ^{137}Cs in the fuel gives a direct measure of the BU distribution. For younger fuel assemblies, with CT up to about 10 years, ^{134}Cs is still available for assay (having a half-life of 2.1 years), enabling the independent assessment of both BU and CT in combination with ^{137}Cs. The half-life of ^{154}Eu (being 8.6 years) enables similar assay using ^{154}Eu and ^{137}Cs for yet some decades.

2.2. Tomographic assessment of pin-level burnup and cooling time

The discussion in section 2.1, regarding the ability to estimate BU and/or CT from peaks available in the energy spectrum, is directly transferrable to an evaluation of a tomographic measurement, where the gamma-ray intensity is measured in a large number of positions and the activity distribution is reconstructed using tomographic algorithms. For tomographic evaluation, there are thus two possibilities, depending on the number of gamma peaks available in the measured energy spectrum:

[1] Analogously, activity contents of two isotopes may be used, which may be measured by means of tomography. Exchanging intensities with activities in equations (1)-(4) only affects the calibration constants k_i.

1. In cases where peaks of two different isotopes are available in the spectrum, e.g. from ^{137}Cs and ^{154}Eu, a tomographic reconstruction of pin-by-pin activities of these two isotopes may be performed. Subsequently, equations (1) and (3) can be used to estimate the BU and CT pin by pin with a precision governed by how accurately the tomographic technique can assess the isotopic contents of individual pins, in combination with equations (2) and (4).
2. In cases where only the ^{137}Cs peak is analysable in the energy spectrum, i.e. for long-cooled fuel, the relative pin-by-pin BU distribution can be estimated with a precision of the same order of magnitude as that by which the tomographic technique can assess the pin-by-pin ^{137}Cs content. However, one should note that this analysis builds on an implicit assumption that all fuel rods in the assembly have the same cooling time.

In both cases, the direct analysis of the pin-wise contents of measured isotopes is also useful to identify anomalies, because large deviations in pin contents are generally not expected under normal irradiation conditions.

3. **Tomographic algorithms for deducing quantitative pin-by-pin data**

Once data on the gamma-ray flux distribution around a fuel assembly has been recorded, a variety of algorithms may be applied to reconstruct the assembly's internal source distribution. The applicability of some algorithms for quantitative measurements on nuclear fuel assemblies has been discussed in ref. [12], covering two general classes of reconstructions: analytic and algebraic. Analytic reconstructions, e.g., filtered backprojection, require no a priori information about the object and assume an idealized imaging geometry. These algorithms may be well suited for Verification Objective 1, in which little or no information about the fuel assembly is provided by the operator. As a result, qualitative images of the internal source distribution are produced, which may be analysed further to additionally give rough estimates of the quantitative pin-wise source contents.

The other class, model-based or algebraic reconstructions, allows more information about the imaging system and object to be incorporated. In particular, gamma-ray attenuation through the highly inhomogeneous mix of strongly attenuating fuel rods and less attenuating surrounding water (in case of wet measurement conditions) or air (in the case of dry conditions) affects the recorded intensities significantly. Furthermore, the finite width of the collimator slits attached to each detector element and the transmission of gamma rays through the corners of even the strongest attenuating collimator material will cause large deviations from an idealised measurement geometry. As shown in [12], taking the detailed attenuation conditions and measurement geometry into account in algebraic reconstructions allows for conclusive quantitative pin-wise data to be obtained. Such algorithms are thus well suited to address Verification Objective 2, and they are further elaborated upon below.

3.1. The algebraic approach

In this approach, the sought-after activity distribution is represented by the activities in N picture elements (pixels) in an axial cross-section of the fuel assembly. Using this representation, the gamma-ray intensity I_m measured in each detector position m can be mathematically defined as a sum of the contribution from the activity A_n in each pixel. The whole set of measured data points then form an equation system:

$$\begin{aligned} I_1 &= \omega_{11}A_1 + \omega_{12}A_2 + \ldots + \omega_{1N}A_N \\ I_2 &= \omega_{21}A_1 + \omega_{22}A_2 + \ldots + \omega_{2N}A_N \\ &\vdots \\ I_M &= \omega_{M1}A_1 + \omega_{M2}A_2 + \ldots + \omega_{MN}A_N \end{aligned} \qquad \text{or equivalently} \quad \bar{I} = \overline{\overline{W}} \bullet \bar{A} \tag{5}$$

where ω_{mn} is the probability that gamma radiation emitted from pixel n will be detected in detector position m. ω_{mn} are here called *contribution coefficients,* and the performance of the reconstruction, to a large degree, depends on the accuracy of these values, which form what is also called the *system matrix*, $\overline{\overline{W}}$. The system matrix is generally obtained by means of calculations, in which various levels of detail may be introduced. This is further discussed in section 3.2 below.

Accordingly, after calculating the contribution coefficients and measuring the gamma-ray intensities, the source distribution can be reconstructed by solving the equation system (5). In this work, an iterative solution technique called ASIRT (Additive Simultaneous Iterative Reconstruction Technique) has been applied to solve the system for $\overline{A}$, which updates the activities from one iterative step, k, to the next according to Eq. (6).

$$A_n^{k+1} = A_n^k + \frac{1}{\sum_{m=1}^{M} \omega_{mn}} \sum_{m=1}^{M} \frac{\left(I_m - \sum_{n=1}^{N} \omega_{mn} A_n^k \right) \omega_{mn}}{\sum_{n=1}^{N} \omega_{mn}} \tag{6}$$

ASIRT is considered to be appropriate for the purpose considered here, but several other solution techniques may also be used [13]. However, the application of a relevant system matrix is considered to be more important to the quality of the reconstruction than the solution technique selected.

3.2. Calculating the system matrix

The calculations of the contribution coefficients ω_{mn} in eq. (5) can be performed with various levels of complexity, ranging from idealised instrument response functions, which neither consider the finite width of the collimator slits nor take gamma-ray attenuation into account, to very complex models that include detailed properties of the instrument and object as well as all physics processes that influence the recorded intensities. The more accurate model that is used, the more accurate reconstructions can be expected, and consequently, detailed models can be expected to return more accurate estimations of pin-wise isotopic contents and thus of BU and CT according to equations (1)-(4).

In this work, the instrument response function is modelled in detail, including not only the finite width and height of the collimator slits but also gamma-ray transmission through the corners of the collimator material adjacent to the slits. Furthermore, the transport of gamma rays through the fuel matrix is considered in detail. (See the most detailed models applied in ref. [12].) An example of the intrinsic instrument response function is presented in Figure 2, for the device design suggested in the framework of this project, JNT A 1955, see ref. [14]. This device design comprises a tungsten-alloy collimator, where the slits attached to each detector element have a length of 200 mm, a height of 10 mm and a width of 1.5 mm.

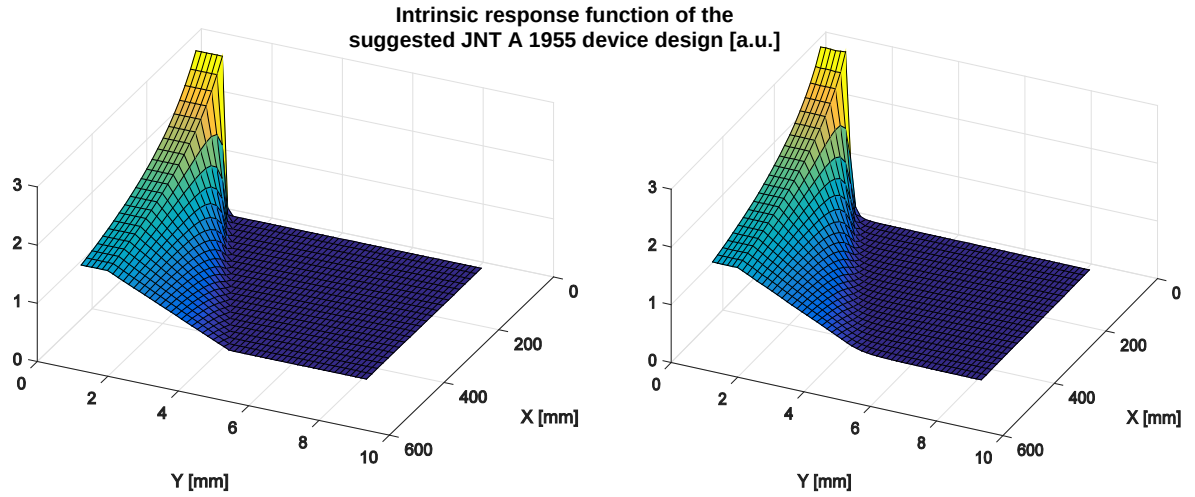

Figure 2: The intrinsic response function of the device design suggested in the JNT A 1955 project [14] for 1274 keV gamma-rays (^{154}Eu) emitted at various distances x from one collimator slit opening and distances y from the slit axis. The response is presented in relative units on the z axis. The plateau at small y for each x value corresponds to the region directly in front of the slit, while the sensitivity decrease for larger y values when entering the penumbra and finally the umbra regions. **Left:** The response when only taking geometric effects into account. **Right:** The response when considering also gamma-ray transmission through the collimator material, showing that in the order of 15% of the radiation reaching the detectors has passed the collimator material.

As shown in Figure 2, gamma-ray transmission through corners of the collimator material adjacent to the slits will contribute notably to the gamma-ray intensity that reaches the detector. In total, in the order of 15% of the 1274 keV signal (^{154}Eu) can be expected to come from radiation that has passed the collimator material in the suggested JNT A 1955 device design. Consequently, to reach the percent-level accuracy in measured pin-wise isotopic contents, these contributions should be taken into account, which is possible using algebraic reconstruction methods modelling the setup.

With respect to the gamma-ray transport through the fuel matrix, one should note that only full-energy transport of mono-energetic gamma rays is considered in this work, and elastic scattering is also neglected. To justify these assumptions, measuring equipment that is conforming to these assumptions must be used, i.e. having spectroscopic capabilities so that a full-energy peak can be selected and analysed. The devices employed in refs. [5] and [7] fulfil these criteria, as well as the device design suggested in the framework of this project, see ref. [14].

For a more detailed description of the methods to calculate the system matrix, we refer to [12]. Examples of their application on tomographic data are presented below.

4. **Viability study of tomography for assessing pin-by-pin fuel properties in BWR fuel**

As described in section 1, the purpose of these investigations is to study the performance of GET for Verification Objective 2: quantitative determination of pin-by-pin properties such as burnup and cooling time for detection of anomalies, for which operator-declared information may be used. In this section, the application of quantitative algebraic reconstruction methods on experimental and simulated data from BWR fuel is demonstrated.

4.1. Using a priori information to calculate the system matrix

One piece of a priori information, which is particularly useful for accurately calculating the system matrix in eq. (2), is the nominal geometry of the fuel. However, nuclear fuel assemblies are exposed to harsh conditions in the reactor core, and geometric changes often occur during irradiation, such as assembly bow, torsion and/or single-pin displacements. Accordingly, we propose that image analysis methods are applied to basic reconstructed images before detailed reconstruction of pin-wise properties are performed, see ref. [15]. As demonstrated in [15], image analysis allows the position of the assembly in the measurement device to be deduced and possible dislocations of individual fuel rods to be detected and corrected for. One should note that all analyses are performed using the same measured data set, and accordingly such a procedure requires no additional measurements to be performed.

Once the current fuel geometry is established, one can model the gamma-ray transport through the fuel in detail. One can also make use of the a priori knowledge to assign pixels only to regions in the fuel that may contain gamma-ray emitting materials. (If a full-energy gamma peak from a solid fission product is analysed, and the fuel is intact, only the fuel rods may contain the measured activity.) This assignment is equivalent to forcing the background in the image to be zero, which is justified if the background in measured data is negligible, a prerequisite that is considered valid for the devices in refs. [5] and [7] as well as for the planned JNT A 1955 device [14]. However, in cases where the background is found to be significant, pixels may also be assigned to regions outside the fuel rods.

In this work, a pixel pattern with five pixels covering each fuel pin has been used, as illustrated in Figure 3 for in a SVEA-96 BWR assembly. Pixels are only assigned to regions that contain fuel, and no pixels cover both active and non-active materials, which would adversely affect the quality of the reconstructions. Furthermore, the selection of one central and four peripheral pixels per pin has proven useful in making the reconstructions less sensitive to possible dislocations of individual fuel rods as compared to defining only one pixel per pin.

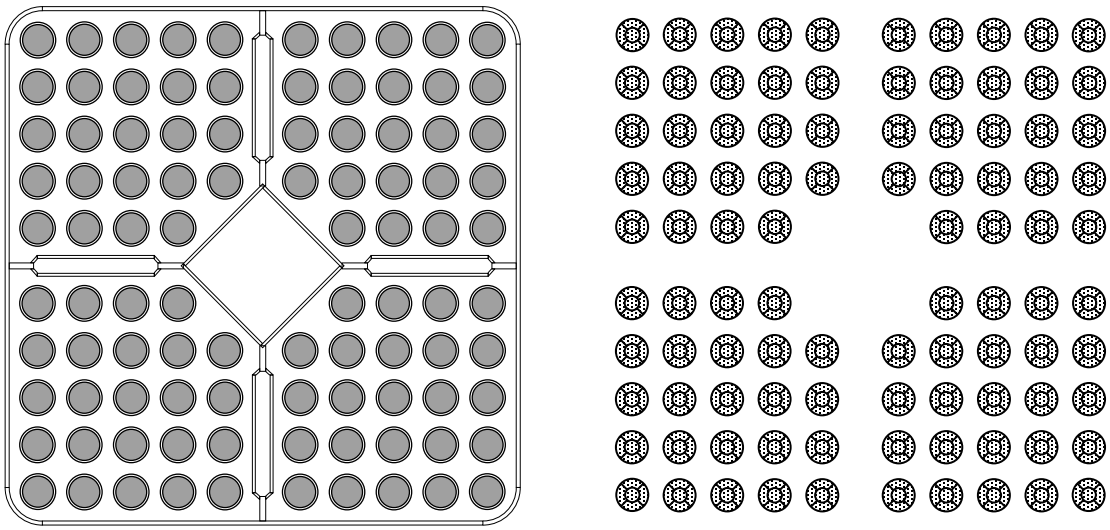

Figure 3: For fuel assemblies with well-known geometry, one may use a priori information to improve the algebraic reconstructions, enabling the measurement of highly accurate, quantitative pin-by-pin data. **Left:** The nominal geometry of a SVEA-96 BWR assembly. Knowing the fuel geometry, the gamma ray attenuation in the fuel can be taken into account in detail when calculating the system matrix, by introducing exact estimates of the gamma-ray travel distances through different materials in the fuel. **Right:** The pixel pattern can be adapted to fit the regions containing gamma-ray emitting materials, thus avoiding pixels that cover both active and non-active materials, which would adversely affect the quality of the reconstructions. Here, each of the 96 fuel rods in the SVEA-96 assembly is covered by 5 pixels and no pixels are assigned to other regions in the assembly.

4.2. Measurement geometry under study

The demonstrations of the performance of algebraic tomographic reconstruction algorithms for deducing quantitative pin-by-pin isotopic contents presented below are based on the measurement geometry of the PLUTO device, used in [5], which is schematically presented in Figure 4.

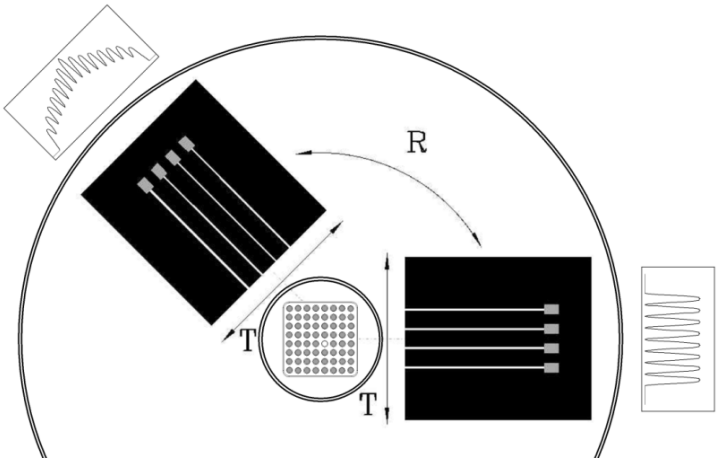

Figure 4: The geometry of the PLUTO measurement device used in the experiments in ref. [5], here schematically illustrated from above with a BWR 8x8 fuel assembly in the centre of the device. Four BGO detectors in a heavy tungsten-alloy collimator could be rotated (R) and translated (T) to record gamma-ray intensities in various positions relative to the measured assembly.

Section 4.3.1 describes the results of analyses of experimental data from a 4-week-cooled SVEA-96 BWR assembly, as presented in [5], collected on the 1596 keV gamma radiation from ^{140}Ba/La in 10 200 data points, covering 120 angular and 85 lateral positions relative to the assembly. In order to assess the possibilities to analyse pin-wise BU and CT based on equations (1)-(4), section 4.3.2 additionally describes the results of analyses of simulated data for the 662 keV radiation from ^{137}Cs in the same measurement geometry.

4.3. Results

4.3.1. Analysis of experimental ^{140}Ba/La data

The experimental data from ref. [5] have been analysed in tomographic reconstructions, both in terms of quadratic-pixel-based image reconstructions of the ^{140}Ba distribution and in terms of pin-wise source-content reconstructions. One should note that the actual distribution of ^{140}Ba was not known, but the reactor operator's core simulator provided calculations of the pin-wise ^{140}Ba content with a stated precision of 4% (1 σ), which could be used for comparison of relative pin-wise data. According to the core simulator data, the pin-wise ^{140}Ba contents varied significantly; between -27% and +20% from the average content. The results of the tomographic reconstructions are presented in Figure 5.

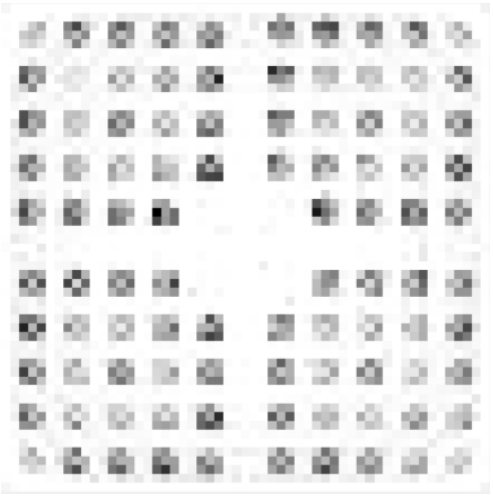

-9.1%	-1.9%	1.1%	-1.5%	-0.1%	-1.1%	0.7%	0.8%	-1.1%	-8.3%
-0.3%	-5.0%	-0.3%	3.9%	1.9%	1.9%	1.3%	2.7%	1.0%	1.0%
1.3%	1.7%	2.1%	0.6%	0.6%	-1.8%	0.2%	0.4%	1.1%	2.7%
0.7%	-1.7%	-4.3%	-2.2%	0.7%	-3.9%	-0.4%	1.0%	2.4%	2.9%
2.0%	1.4%	-2.2%	-2.6%			-3.5%	2.6%	3.7%	2.9%
-1.2%	1.2%	-0.5%	-0.5%			-5.6%	-2.7%	1.4%	0.2%
2.2%	0.2%	1.0%	-1.5%	-1.8%	-1.4%	-3.0%	-5.7%	0.0%	2.2%
0.7%	-0.9%	3.8%	-3.2%	1.5%	-4.2%	-2.1%	-1.3%	-1.9%	-0.3%
0.2%	1.9%	3.3%	1.1%	4.3%	3.6%	2.8%	0.6%	0.7%	-2.7%
-6.8%	2.9%	5.0%	6.5%	3.8%	2.0%	3.1%	1.1%	-3.8%	-12.3%

Figure 5: Results obtained in tomographic reconstructions of experimental ^{140}Ba/La data from a SVEA-96 fuel assembly measured in the PLUTO device. (Data from [5].) **Left:** A grey-scale 55x55-pixel image of the ^{140}Ba distribution in the assembly cross section, obtained in a tomographic image reconstruction. This image has been used for deducing the assembly's position in the device and identifying possible dislocations of individual fuel pins; see ref. [15]. **Right:** The pin-wise agreement between the relative pin-by-pin contents of ^{140}Ba from the operator's core simulator and those obtained in an algebraic reconstruction, where the instrument response and gamma-ray transport through the fuel matrix were taken into account when calculating the system matrix. According to the operator's core simulator, the pin-wise contents of ^{140}Ba ranged between -27% and +20% from average, and the agreement between calculated and measured relative pin-wise contents was 3.1% (1 σ).

As accounted for in Figure 5, the relative pin-wise contents of ^{140}Ba obtained in the algebraic pin-activity reconstruction exhibited an agreement with the data from the operator's core simulator of 3.1% (1 σ), which was well within the claimed accuracy of the core simulator of 4% (1 σ). However, no benchmarking data on the actual rod-by-rod content of ^{140}Ba at higher precision was available, and accordingly, the precision obtained in the tomographic measurements is unknown, albeit the high level of agreement indicates a high level of precision in the tomographic data, demonstrating that relative pin-wise isotopic contents may be measured with high precision for this fuel type.

In conclusion, the tomographic experimental data from ref. [5] show that high-precision relative pin-by-pin isotopic contents may be obtained by means of algebraic reconstructions, where the system matrix is modelled with a high level of detail with respect to the instrument response function and the gamma-ray transmission through the fuel matrix. The results in Figure 5 were based on data collected serially, which required 10 hours of measurements in the PLUTO device. With the JNT A 1955 device design [14], comprising 32 detector elements collecting data in parallel, a similar data set may be collected in about 20 minutes.

4.3.2. Analysis of simulated ^{137}Cs data

In order to further investigate the performance of the algebraic reconstruction methods for tomographic measurement of pin-wise fuel properties, simulations have recently been performed also for 662 keV gamma rays from ^{137}Cs [12]. The simulations were performed using the Monte Carlo simulation code MCNP, modelling a SVEA-96 fuel assembly in the PLUTO equipment and a similar measurement

scheme as for the experimental data presented above. These simulations provide a means to investigate whether the lower gamma-ray energy of ^{137}Cs may be used with similar precision as that of ^{140}Ba, which was experimentally demonstrated above. As described in section 2, the pin-wise isotopic contents of ^{137}Cs can provide a means to assess pin-wise BU, and, in combination with measured ^{134}Cs and/or ^{154}Eu contents also pin-wise CT.

To facilitate the analysis, all rods were simulated with equal ^{137}Cs content. The results of the tomographic reconstructions are presented in Figure 6.

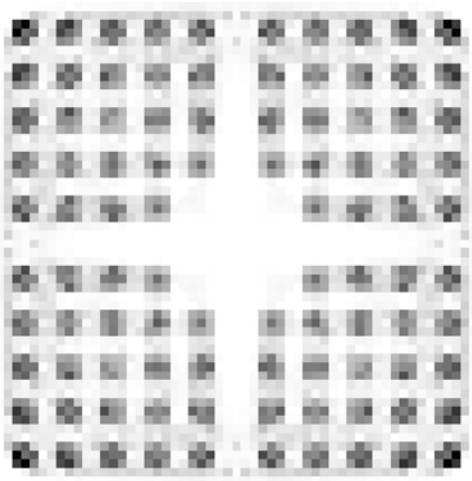

0.995	0.996	1.004	0.995	0.992	0.990	0.993	1.006	0.997	0.994
0.998	1.016	0.994	0.998	1.004	1.004	0.999	0.993	1.016	0.996
1.007	0.994	0.986	1.001	1.017	1.017	1.004	0.986	0.994	1.004
0.993	1.000	1.004	0.987	1.005	1.005	0.989	1.003	0.998	0.995
0.990	1.004	1.018	1.003			1.004	1.017	1.003	0.992
0.992	1.004	1.018	1.005			1.005	1.018	1.005	0.990
0.994	0.998	1.001	0.986	1.003	1.003	0.983	1.002	1.000	0.992
1.004	0.994	0.986	1.005	1.018	1.018	1.002	0.985	0.994	1.007
0.996	1.016	0.994	1.000	1.004	1.004	0.998	0.994	1.016	0.998
0.995	0.998	1.007	0.993	0.990	0.992	0.995	1.005	0.996	0.996

Figure 6: Results obtained in tomographic reconstructions of simulated ^{137}Cs data from a SVEA-96 fuel assembly in the PLUTO device. (Data from [12].) All rods were assigned equal ^{137}Cs contents in the simulations. **Left:** A grey-scale 55x55-pixel image of the ^{137}Cs distribution in the assembly cross section obtained in a tomographic image reconstruction. **Right:** Relative pin-by-pin contents of ^{137}Cs obtained in an algebraic reconstruction, where the instrument response and gamma-ray transport through the fuel matrix have been taken into account when calculating the system matrix. The precision obtained was 0.87% (1 σ), indicating that relative pin-by-pin ^{137}Cs contents may be measured at the 1% level for this fuel type.

According to the results in Figure 6, the tomographic technique comprising a PLUTO-like design and an algebraic reconstruction methodology involving detailed modelling can produce relative pin-by-pin contents of ^{137}Cs with a precision at or even below 1% (1 σ). However, one should note that the precision obtained for each individual fuel rod depends on rod position in the assembly; the precision is higher for peripheral rods than for central fuel rods depending on the amount of gamma rays escaping the fuel from the different regions. For the 36 peripheral fuel rods, the precision was about 0.5% (1 σ), while for the innermost 32 rods, the precision was about 1.1% (1 σ) and the 28 rods in between were reconstructed with a precision of 0.7% (1 σ). Extrapolating this to fuel types with more fuel rods in larger and denser configurations, even larger uncertainties must be expected, which will be subject for further studies.

The level of precision that was demonstrated in the simulations and that was indicated in the measurements corresponds well to the precision of measured gamma-ray intensities previously reported in gamma scanning of complete fuel assemblies, see ref. [16], which could be used to deduce assembly burnup and cooling time with a precision in the order of 2%. Accordingly, similar precision may be expected for individual fuel rods in tomographic measurements on SVEA-96 assemblies, provided that data of the above quality can be recorded. The obtainable precision for larger and/or denser assembly geometries like PWR or VVER fuel has so far not been investigated.

5. **Discussion and outlook**

5.1. Applicable detector types for tomographic assessment of pin-wise fuel properties

The HPGe detector is currently the best available detector type for high-resolution spectroscopic measurements, and it would allow for several well-resolved gamma-ray peaks to be used in

tomographic measurement and evaluation. However, the detector size, measurement time constraints and practicalities, such as the need for cooling of this detector type, limit its applicability in a tomographic inspection device. Other semiconductor detectors of relevance are CdTe and CdZnTe, of which the latter has been used in refs. [3] and [4]. However, the analysis of full-energy peaks for deduction of pin-wise isotopic contents requires detectors with relatively high full-energy detection efficiencies - a constraint which excludes these detectors for this application.

In the current project (JNT A 1955), scintillator detectors have been considered to be the best choice due to their ruggedness, reliability and high full-energy detection efficiency, including in relatively small crystals. In particular, the latter property enables the analysis of full-energy peaks, which is required for deducing information on BU and CT according to section 2. Furthermore, the instrument may contain multiple scintillator detectors, each connected to an individual collimator slit, in a relatively small total collimator volume, which is important to limit the required time for measurement. However, as compared to HPGe, the use of scintillator detectors will increase the uncertainty in determined peak intensities because the larger peak width, making subtraction of background under the peak less accurate. For the same reason, one may expect higher resolution scintillators (such as LaBr) to perform better in the determination of BU and CT than lower resolution alternatives (such as NaI and BGO).

Here, the data from [10], with gamma-ray spectra displayed in Figure 1, has been used to draw the following conclusions on the applicability of NaI, BGO and LaBr detectors:

- LaBr: Its energy resolution of about 3% is high enough to resolve the most dominant gamma peaks in the energy spectrum, even for relatively short-cooled fuel (demonstrated in Figure 1 for a PWR assembly with a CT of 5 years). Accordingly, it may be used to determine the pin-by-pin BU and CT independently in tomographic measurements by studying a combination of either ^{134}Cs and ^{137}Cs, or ^{154}Eu and ^{137}Cs.
- NaI: At relatively short cooling times (see the spectrum for CT=5 years in Figure 1), the interference of the^{134}Cs peak with the ^{137}Cs peak makes the applicability of NaI doubtful. At longer cooling times (for the measured PWR assemblies with a CT of 18 and 25 years, respectively), it can be readily used to resolve the ^{137}Cs peak, and it is also applicable for measuring the count rate in the ^{154}Eu peak, albeit this peak may become too weak to be practically useful after a few decades cooling time. Accordingly, NaI may be useful for assessing pin-wise BU and CT in tomographic measurements of fuel cooled for a decade or two, until ^{154}Eu is no longer available.
- BGO: For long-cooled fuel, BGO detectors can also be used to evaluate the intensity of the dominant ^{137}Cs peak. According to the spectra presented in Figure 1, they are applicable for cooling times at 18 years and beyond. However, these data do not support its use for measuring the ^{154}Eu peak, hindering assay of both BU and CT using BGO detectors.

In conclusion, all scintillation detectors mentioned above may be used to measure the intensity in the ^{137}Cs peak for long-cooled fuel (demonstrated in Figure 1 for PWR assemblies with CT of 18 and 25 years, respectively). According to the discussion in section 2.2, the pin-wise ^{137}Cs content would give a direct measure of the pin-wise BU under the assumption of equal CT. For measurements on short-cooled fuel (CT ≤ 5 years), LaBr is most likely required, and it may resolve multiple peaks in the gamma-ray spectrum for short- as well as medium-cooled fuel, enabling the determination pin-wise contents of several isotopes and thus both BU and CT according to equations (1)-(4). For fuel cooled longer than a few decades, count rate limitations will most likely limit the measurements to ^{137}Cs.

5.2. Results obtained until date and further studies

The applicability of detailed algebraic tomographic reconstruction algorithms for assessing relative pin-wise isotopic contents in BWR fuel with accuracy in the order of a few percent has been demonstrated using experimental ^{140}Ba/La data as well as using simulated ^{137}Cs data, indicating that even the 1% level is achievable for this fuel type. One may note that these studies are based on the PLUTO device design [5], whereas a somewhat different design is planned for within the JNT A 1955 project [14]. Still, these device designs also involve several similarities, such as the use of scintillator detectors and spectroscopic peak evaluation, making the demonstrations above relevant also for JNT A 1955.

However, the studies presented here have been limited to BWR fuel, and the actual performance of the JNT A 1955 tomographic instrument for measuring pin-wise fuel properties will depend on several factors, such as fuel dimensions and cooling times, assessment time constraints, detailed instrument design, detector dimensions, etc. Accordingly, additional studies are currently underway in order to assess more specifically the JNT A 1955 device's performance for a range of fuel with different properties and for various levels of statistics, corresponding to variations in the assessment time. In particular, the possibilities for tomographic assessment of the most central fuel rods in larger fuel arrays, such as PWR, will be covered.

6. **Acknowledgements**

This work was supported by the Swedish Radiation Safety Authority (SSM), under contract SSM2014-94, respectively from the Swedish Research Council (VR) under grant number 80588801. The efforts are carried out as part of the IAEA support program project JNT A 1955, and the authors are grateful for the leadership by Eric Smith, Nick Mascarenhas and James Ely (IAEA) and the collaborative efforts by the whole project team, mentioning in particular the U.S. participants Tim White (PNNL), Eric Smith (PNNL) and Vladimir Mozin (LLNL).

7. **References**

[1] International Atomic Energy Agency: "*Integrated Safeguards for Spent Fuel Transfers to Dry Storage*", SG-OP-GRNL-PL-0019, IAEA, 2006.
[2] International Atomic Energy Agency: "*Model Integrated Safeguards Approach for a Spent Fuel Encapsulation Plant*", SG-PR-1305, IAEA, 2010.
[3] F. Levai, et al., "*Feasibility of Gamma Emission Tomography for Partial Defect Verification of Spent LWR Fuel Assemblies*", STUK-TYO-TR 189, 2002.
[4] T. Honkamaa, et al., "*Progress Report on JNT 1510 Measurements on VVER Fuel Assemblies*", presentation at IAEA JNT 1995 project meeting, May 2014.
[5] S. Jacobsson Svärd, et.al., "*Non-destructive Experimental Determination of the Pin-power Distribution in Nuclear Fuel Assemblies*", Nuclear Technology, 151 (1), 2005.
[6] S. Jacobsson Svärd, et.al., "*Tomography for partial-defect verification - experiences from measurements using different devices*", ESARDA Bulletin, 33, 2006.
[7] S. Holcombe, "*Gamma Spectroscopy and Gamma Emission Tomography for Fuel Performance Characterization of Irradiated Nuclear Fuel Assemblies*", Digital Comprehensive Summaries of Uppsala Dissertations from the Faculty of Science and Technology; 1201, Acta Universitatis Upsaliensis, Uppsala, 2014.
[8] International Atomic Energy Agency: "*Guidebook on Non-destructive Examination of Water Reactor Fuel*", STI/DOC/010/322, 1991.
[9] P. Jansson, "*Studies of Nuclear Fuel by Means of Nuclear Spectroscopic Methods*", Comprehensive Summaries of Uppsala Dissertations from the Faculty of Science and Technology; 714, Acta Universitatis Upsaliensis, Uppsala, 2002.
[10] P. Jansson et.al., "*Experimental Comparison between High Purity Germanium and Scintillator Detectors for Determining Burnup, Cooling Time and Decay Heat of Used Nuclear Fuel*", Proc. From the 40th annual Waste Management (WM) Conference, Phoenix, AZ, USA, March 2014.
[11] Los Alamos National Laboratory: "*Passive Nondestructive Assay of Nuclear Materials (PANDA)*", Report LA-UR-90-732, 1991.
[12] S. Jacobsson Svärd et al., "*Applicability of a set of tomographic reconstruction algorithms for quantitative SPECT on irradiated nuclear fuel assemblies*", Nuclear Instruments and Methods in Physics Research A, 783, 2015.
[13] C. Niculae and T. Craciunesco, "*On the Reconstruction of the Fission Products Distribution in Nuclear Fuel Rods*", International Journal of Energy Research, 20, 1996.
[14] T. White et.al. "*Passive Tomography for Spent Fuel Verification: Analysis Framework and Instrument Design Study*", 2015 ESARDA Symposium, Manchester, UK, May 2015.
[15] A. Davour et.al., "*Image analysis methods for partial defect detection using tomographic images on nuclear fuel assemblies*", 2015 ESARDA Symposium, Manchester, UK, May 2015.
[16] O. Osifo, et.al., "*Verification and determination of the decay heat in spent PWR fuel by means of gamma scanning*", Nuclear Science and Engineering, 160(1), 2008.

Session 21

Non-Proliferation and Arms Control

Systems Approach to Arms Control Verification

Keir Allen[1], Mona Dreicer[2], Cliff Chen[2], Irmgard Niemeyer[3], Clemens Listner[3], Gotthard Stein[4]

[1] Atomic Weapons Establishment, Aldermaston, UK
[2] Lawrence Livermore National Laboratory, Livermore, USA
[3] Forschungszentrum Jülich, Jülich, Germany
[4] Consultant, Bonn, Germany

Abstract:

Using the decades of experience of developing concepts and technologies for verifying bilateral and multilateral arms control agreements, a broad conceptual systems approach is being developed that takes into account varying levels of information and risk. The IAEA has already demonstrated the applicability of a systems approach by implementing safeguards at the State level, with acquisition path analysis as the key element. In order to test whether such an approach could also be implemented for arms control verification, an exercise was conducted in November 2014 at the JRC ITU Ispra. Based on the scenario of a hypothetical treaty between two model nuclear weapons states aimed at capping their nuclear arsenals at existing levels, the goal of this exercise was to explore how to use acquisition path analysis in an arms control context. Our contribution will present the scenario, objectives and results of this exercise, and attempt to define future workshops aimed at further developing verification measures that will deter or detect treaty violations.

Keywords: arms control verification; systems approach

1. Introduction

The reduction or elimination of nuclear arms is not likely to occur absent a lower perceived need for nuclear weapons and high confidence that commitments are being honoured. Over more than 50 years of IAEA verification has taught us that achieving confidence requires a coherent and comprehensive picture of the State's compliance with its obligations.

The traditional IAEA verification approach was based solely on the type and quantity of nuclear materials present in a state, without regard to other factors that correlate with proliferation risk. The State-Level Concept (SLC) was recently proposed as a way to increase the efficiency and effectiveness of safeguards. The SLC consists of the development of state-level safeguards approaches (SLAs) to identify areas of higher proliferation risk and the collection and evaluation of multi-source information, including safeguards information, to optimize future safeguards activities. By piecing together a broad range of information encompassing declared, undeclared, international technical monitoring data, information from national technical means, open source, state-level, and international trade controls, it may be possible to provide state-level confidence that commitments are being upheld. It takes into account broader State-specific factors, potentially allowing greater focus on areas of higher risk of non-compliance. This approach could be extended to all types of treaty verification, including nuclear arms control and disarmament. So, in addition to verifying compliance for a particular treaty or agreement, such as the Nuclear Non-proliferation Treaty, it could be used to identify areas where effective verification could provide the greatest confidence that a State is complying with its commitments, and therefore help inform the most fruitful avenues for future arms reductions or disarmament efforts.

2. State-level analytical approach in development of future arms reductions initiatives

The IAEA SLC methodology consists of three processes which help to develop SLAs (for more details see Cooley 2011):

1. Identification of plausible acquisition paths.
2. Specification and prioritization of State-specific technical objectives (TO).
3. Identification of safeguards measures to address the technical objectives.

Listner et al. (2012, 2013, 214) demonstrated how acquisition path analysis can be carried out using a formal methodology which is yet compatible with the principles defined by Cooley (2011). The acquisition path analysis method uses a three-step approach: First, the potential acquisition network is modelled based on the IAEA's physical model and experts' evaluations. Second, using this model all plausible acquisition paths are extracted automatically. Third, the State's and the inspectorate's options are assessed strategically. Moreover, Listner et al. (2015) proposed and evaluated also two possibilities for determining technical objectives.

Applied to verifying arms control reductions, the development of a SLA could include the following three steps:

1. Modelling of a cheating network and identifying cheating pathways. This is a purely technical assessment of attractiveness including technical difficulty, timing and costs;
2. Determination of technical objectives, including identifying limits for detection probabilities for each area of a potential cheating network. It is assumed that requirements for high confidence verification result in the need for high detection probabilities for areas of highest risk; and
3. Identification of the technical and administrative measures that would provide the required detection probabilities. This would be expanded beyond classical inspections and could include all types of measures related to the field of interest (e.g. information barrier approaches could be useful).

When an existing treaty or agreement is in effect, the legal commitments set out the context under which non-compliant behaviour needs to be detected by the monitoring regime. Ultimately, pathways identified in this context should be developed to better understand how to verify compliance with a specific set of treaty objectives and commitments. However, the methodology could be applied to a full range of assumed conditions, and therefore allow for a more general analysis. Following this approach, cheating pathways (CP) could be mapped out to produce a state-specific inter-connecting network of nodes and processes/flows for nuclear materials and weapons – beginning with more generic models to protect sensitive information. The “relative attractiveness” or usefulness in a particular nuclear weapons program CP could then be considered. It is recognized that expert judgment will be required where no data is available.

To achieve a state-level approach for arms control or disarmament, the methodology will need to take into account materials, weapons and the links between the two. Being that the IAEA SLC has been designed for implementation in Non-Nuclear Weapons States (NNWS) for verifying peaceful uses of nuclear materials, it may not be much of a stretch to expand to verification of nuclear *material* cycles to states possessing nuclear weapons. However, significant work will be needed to expand the model to *nuclear weapons*, because national security requirements and Nuclear Non-Proliferation Treaty (NPT) Articles 1 and 2 commitments will impede the ability to provide many details. To-date, considerations regarding verification of nuclear materials and nuclear weapons disarmament verification have usually been addressed separately but the importance of these linkages have been recently presented (NTI 2014).

3. Applying the material pathway analysis to nuclear weapons-possessing states

For the purposes of developing the methodology, we will consider the verification of nuclear materials in a state possessing nuclear weapons that is subject to international commitments. It is assumed that an international inspectorate exists. It is important to remember that non-compliant behaviour is defined as the violation of commitments so the legal situation or the assumptions must be taken into account. Two examples that we considered are:

- Nuclear Weapons State (NWS) within NPT and Voluntary Offer Agreement (VOA). A State having signed a VOA must not use the facilities under this agreement to produce material that will be used in a weapon.
- State outside NPT and INFCIRC/66 in-force. A State outside the NPT but with facility or item-specific commitments (INFCIRC/66 type agreements) must not use these facilities or items for military purposes.

Possible non-compliant behaviour (edge types), in addition to clandestine processing, misuse of existing facilities, undeclared import and diversion from existing facilities considered for NNWS would be included to account for the possible additional commitments beyond the NPT and IAEA safeguards. Depending on the commitments, clandestine processing (i.e. production in undeclared facilities) would not be part of the model because without a comprehensive agreement like in INFCIRC/153, states producing fissionable material in undeclared facilities would not be violating a commitment.

In states possessing nuclear weapons, two additional edge types could be considered: diversion from the military fuel cycle and military processing. These are illustrated in Figure 1.

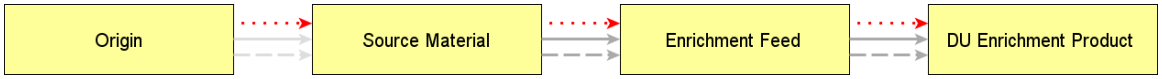

Figure 1: Example for a Cheating Path. Grey arrows represent misuse and diversion in the civil nuclear fuel cycle. Additional edge types consider the military fuel cycle: Diversion from the military fuel cycle is represented by the red arrow from “origin“ to “source material“ and military processing is represented by all the remaining red arrows).

So, depending on the type of commitment, these processes could be carried out by the state without violating international law (e.g. in a INFCIRC/66 case but not if a multilateral treaty was in-force). When an activity is allowed, it would be represented in the model but the detection probability would be set at 0% because an allowed activity will not need to be monitored.

The methodology could be applied to three example scenarios:

1. A state with a complete military fuel cycle without safeguards but with the civilian facilities under safeguards. This could be under INFCIRC/66 or a VOA. In this case, where a military fuel cycle is allowed, the military pathways will remain the most attractive pathway for producing materials for weapons and therefore it is assumed that there will be no need for misuse or diversion from the declared civil fuel cycle. The risk of sanctions, if non-compliant behaviour (such as pursuing a pathway that using civil installations under international surveillance) is detected would also deter misuse and possibly eliminate the need for an inspection effort at this pathway.

2. A case where some gaps in military fuel cycle exist, where those gaps would be represented by missing diversion edges or reduced processing attractiveness values in the acquisition path model. Effective verification, possibly including increased monitoring, could deter non-compliant behaviour so that if State finds these pathways attractive, appropriate monitoring measures in particular facilities would increase the risk to the State of detection, should they attempt to exploit the pathway. If the risk (and costs) of detection are high, the State should be deterred from non-compliant actions.

3. Military facilities & materials put under fissile material control regime. If military facilities and materials are put under a multilateral treaty, these installations may be under the same restrictions as civil facilities under the NPT. Therefore there could be increased attractiveness to use these facilities for the production materials for nuclear weapons. To deter the use of these paths in violation of the commitments, the model would recommend a significant increased monitoring/inspection effort. The ability to verify a baseline declaration and knowledge of past production will be a key factor.

4. Applying the nuclear weapons pathway analysis to weapons-possessing states

To-date, consideration of monitoring and verification of weapons or weapons components has been in the context of specific treaties or during negotiations of possible new regimes. In applying a state-level methodology to weapons, and developing the appropriate CPs, it will be important to consider the strategic objectives of a state. The CPs could be different if the objective is to expand the size of the national stockpile or to increase the degree of technical sophistication of their stockpile. Some potential cheating pathways include warheads or weapons that were not included in baseline declarations, diversion of materials or components from dismantlement, and undeclared production of warheads. Ways to link monitored nuclear material and facilities with warhead production & dismantlement will need to be considered to achieve confidence that new production is not occurring.

NTI (2014) has worked to advance methods to verify material and warhead baseline declarations in states possessing nuclear weapons. The confidence in these declarations will be key to modelling an effective monitoring/verification regime that could detect clandestine activities.

One option to begin modelling the weapons complex would be to use IAEA Physical Models and indicators and modify them as appropriate. There will also be a need to consider weaponization indicators, to take into account possible reconstruction of existing warhead designs without use of development/testing facilities as well as acquisition of a weapon or development of more sophisticated weapons. A challenge to the successful modelling of the weapons complex arises from the fact that many of the processes, actions and infrastructure that might constitute an indicator of non-compliance in a proliferant state may exist or take place as a matter of course in a weapons state.

5. Workshops

A workshop held at the European Joint Research Center in Ispra, in conjunction with the 2014 Fall Meeting of the ESARDA Verification Methods and Technologies (VTM) Working Group (WG), began to explore this systems concept by studying the possible parallels with the IAEA's State Level Approach (SLA), currently used to develop effective safeguards for nuclear materials.

An exercise scenario was presented to the working group that bridged the gap between safeguarding of materials and NEW START style verification of nuclear weapon delivery systems. Under this scenario, a treaty was signed by two states that required each state to cap the total number of warheads in its nuclear arsenal and to cap the number warheads it deployed to no more than 500. Each state maintained a full nuclear weapons enterprise from material production and weapons design, through manufacture and deployment on multiple delivery systems. Members of the VTM WG were asked to consider the potential pathways one of the states could take to cheat on its treaty commitments, and discuss the possible application of acquisition pathway analysis and a state level approach for identifying verification requirements for the treaty. Figure 2, below, illustrates a simple example pathway (highlighted in red) that could be taken by the state.

The workshop resulted in a number of lessons that will require further consideration as the application of systematic level analysis to arms control verification is refined. They are introduced below:

6. Verification Objectives

Verification objectives need to be specifically identified for arms control treaties, in order for the systems approach to be applied correctly. The IAEA has a well defined "significant quantity" concept around which an APA can be organized; safeguards measures are designed to be capable of detecting the diversion of one significant quantity of material within four weeks of diversion.

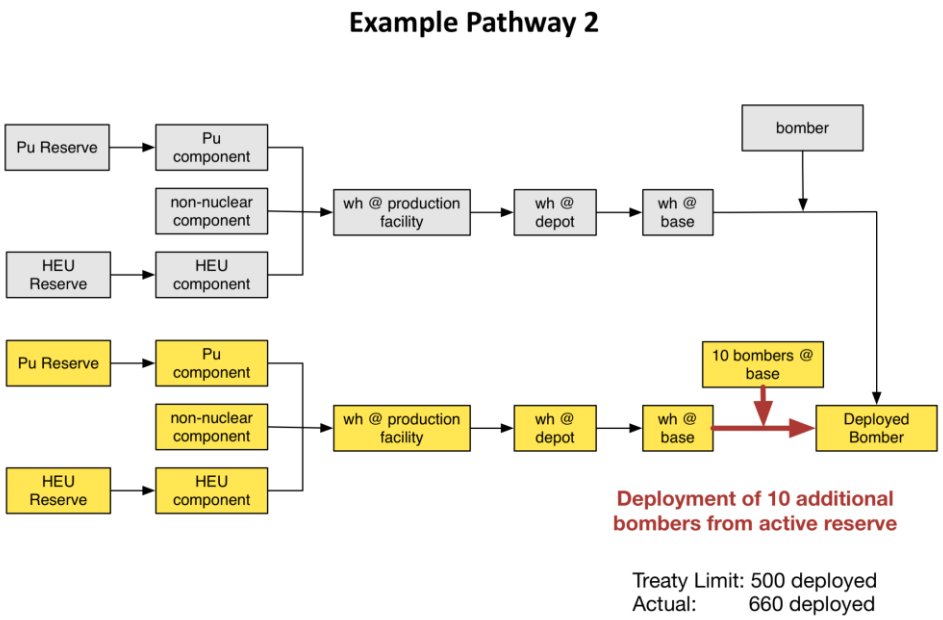

Figure 2: An example pathway used during the workshop, visualising the weapons enterprise as a linear flow from weapons useable material to deployed weapons. Declared facilities are coloured yellow, undeclared facilities are coloured grey. In this example, the pathway exploited is to deploy additional warheads from the total declared stockpile onto reserved aeroplanes, increasing the total number of deployed warheads from 500 to 660, significantly breeching treaty limits. Neither the declared reserve aeroplanes, nor the declared reserved warheads, would breech the treaty so long as they remain in reserve. More complex pathways exist which may involve combinations of declared and undeclared materials, components, weapons, facilities, process, stockpiles and delivery vehicles.

In contrast, verification objectives are not yet defined for future warhead treaties and may well be treaty dependent. For example, under the exercise scenario, the definition of a significant quantity of weapons as agreed by the states might be tolerant of small discrepancies since each state is allowed to deploy 500 weapons and small fluctuations around this limit may not pose threat to either state. Small fluctuations may not threaten strategic security or stability and so may not be strategically significant. Nevertheless, the discovery of even one extra deployed weapon might be indicative of larger scale cheating that could threaten the security of one or the other state. Overall perceptions of what constitutes a threat may well differ between treaty parties. It may be useful to separately consider a significant quantity for detection purposes and a strategically significant quantity for stability considerations and the purpose of identifying detections timeliness requirements. Lastly, it might be that a suitable definition of a significant quantity during treaties where large numbers of warheads remain deployed is not suitable when deployed numbers are considerably reduced. It is therefore important to develop a mechanism for achieving consensus on these verification objectives.

It is also important to define a significant quantity of the controlled item in such a way that declarations made about it in relation to the treaty can be verified effectively. Because of the secrecy surrounding weapons systems, verifying that an item declared to be a weapon is a weapon (and that it is in the declared status of deployment) could be challenging. Therefore definitions of category of weapon by deployment status (e.g. deployed or non-deployed, in reserve, inactive, disassembled, or weapon component) should be framed in a verifiable way, which also allows items that are declared as none of those categories to be verified as ‘none of the above’. Significant detail concerning the activities of the nuclear enterprise and locations of declared weapons may need to be shared, and updates exchanged regularly, to facilitate verification of deployment status.

To be effective, any verification system must be capable of detecting the diversion (or clandestine production and deployment) of the significant quantity (of weapons) in a timescale that ensures that the strategic security of treaty signatories or the security of the wider international community is not undermined by the actions of a state that cheats.

An extension of the Acquisition Path Analysis approach to monitoring weapons as well as materials could include additional terms. See Table 1 for a suggested extension.

Graph Theory	Route Planning	Acquisition Path Analysis	Weapons Verification
Node	Location	Material form	Weapon status/form
Edge	Street	Process / path segment	Deployment process/path segment
Path	Route	Acquisition Path	Deployment Path
Edge Weight	Distance	Attractiveness	Attractiveness

Table 1: An example extension of the acquisition path model to include nuclear weapon verification by deployment status

7. Measures of Attractiveness

The working group discussed suitable measures of attractiveness for identifying the cheating pathways most likely to be exploited under this scenario. Comparison was made with the proliferation resistance metrics defined in the Evaluation Methodology for Proliferation Resistance &Physical Protection of Generation IV Nuclear Energy Systems (2011). Broadly, the metrics were considered to be suitable. The metrics are titled below as per the Gen IV definitions for simplicity and are accompanied by a summary of the discussion of each:

- *Proliferation Technical Difficulty* – Since weapons states already maintain the full weapons enterprise, the ability to deploy existing weapons, build additional weapons or modify stockpiles is not considered to be beyond the state's capability. Furthermore, such actions could be masked to a large extent by allowed processes. Nevertheless, some pathways may require mobilisation and coordination of greater resources than other pathways (e.g. deployment of reserve warheads onto reserve bombers may be accomplished more simply than building a clandestine stockpile of new weapons and secretly loading them onto a submarine). *Proliferation Difficulty* and *Detection Probability* were discussed in terms of the stealth required to successfully exploit a CP.
- *Proliferation Cost* – The cost of certain pathways relative to others is evident (see example in previous bullet point). Nevertheless, capital and operational costs of pathways may already be accounted for in national budgets. Only pathways requiring significant capital investment may be deemed less attractive to a state wishing to cheat. Overall, cost may not be a primary factor in the decision to exploit a CP.
- *Proliferation Time* – The minimum time required to deploy a strategically significant quantity of additional weapons. The significance of the proliferation time is closely tied to the strategic goals of the state. For example, a short proliferation time allowing the deployment of large numbers of weapons very quickly might be considered strategically advantageous in some situations by a cheating state. Equally, a long proliferation time associated with a very stealthy build up of a clandestine stockpile might be considered attractive in other circumstances. Since both routes could be attractive, each should be appropriately weighted in a state level model.
- *Fissile Material Type* – Not discussed in great detail since stockpiles of material were declared under the treaty.
- *Detection Probability* – With no standard set of verification measures assumed to have been agreed or allowed under this treaty, cumulative detection probabilities cannot be determined in advance. This reflects well the situation for future nuclear warhead arms control verification where no specific verification technologies or methods have been agreed. However, Acquisition Path Analysis can be used to identify where specific verification measures might be of most benefit. Design requirements for technologies can then be stipulated based upon the identified verification requirement. This systems level analysis can therefore help identify technology requirements for future treaties. Weapons or weapons components require

sufficiently robust monitoring to ensure that their location remains known to the inspectorate to a high level of confidence, thus ensuring that they are not deployed in breach of treaty commitments. High confidence might also be required in ensuring that only declared items can interact with declared delivery systems. Detection probabilities for undeclared items at declared deployment sites must therefore be sufficiently high. Linked to this, the detection times in such instances should also be very rapid.

- *Detection Resource Efficiency* – The efficiency in the use of staffing, equipment, and funding to apply verification measures across different parts of the weapons enterprise. There may be points in the nuclear weapons enterprise where the ability to verify declarations with high confidence would be particularly beneficial. In the case of the exercise scenario, the monitoring to ensure delivery systems only carried the declared number of warheads was identified to be important. Nonetheless, the verification focal point could shift depending upon the aims and objectives of the treaty.

8. System Level Analysis Benefits

A systematic or state level analysis is likely already performed by states (such as US and Russia) that have extensive experience in arms control agreements. In the context of bilateral arms control agreements, Weapons States have a basic understanding of a nuclear weapons complex, in particular the competing needs for effective verification, protection of national security information, and upholding NPT Article VI commitments. In this case, the system level analysis can help identify specific verification requirements based upon a state's own strategic concerns. It can help identify useful ways of framing and defining verifiable objects and timescales and identify the types of technologies needed to provide monitoring capabilities in specific locations. While a formal approach may add value to a Weapons State's analysis, its primary benefit may be the common framework it can provide to states without the capacity for or experience with analysing arms control verification regimes. In this case, the state level approach can promote understanding about the strategic and technical challenges associated with arms control verification.

9. Further considerations

The development of a state-level approach to modelling material CPs is more advanced than for weapons, but work can be done to further expand the models and make the linkages between material and weapons cycles. As mentioned earlier, a challenge to the successful modelling of the weapons complex arises from the fact that many of the processes, actions and infrastructure that might constitute an indicator of non-compliance in a proliferant state many exist or take place as a matter of course in a weapons state. True indicators of non-compliance with agreements may therefore be much more subtle in nuclear weapons states, requiring detailed information of the level of expected activity in the state with regards to the weapons enterprise. Verification methods need to be fine tuned such that allowed activities do not mask cheating. Furthermore, non-compliant actions with potentially significant consequences could take place of very short time scales, and so detection times must be commensurately short. Therefore the level of intrusiveness required to effectively monitor allowed activities may be considerably greater than for current or historical agreements. All of these factors can be incorporated into suitable systems level models to improve the links between materials and weapons.

The challenges associated with the protection of national security and non-proliferation information must be taken into account as a realistic physical model is developed that incorporates further intrusiveness. Existing ideas for managing access for routine and challenge inspections or new ideas will need to be considered. Verification that declared items are situated in their declared location may prove to be a relatively traditional matter of accounting, assuming suitable managed access procedures can be developed. In contrast, verifying the absence of undeclared items, either in declared facilities or undeclared facilities, could be perceived to be an onerous task. Nevertheless, as suggested by the results of the workshop, early priorities in this area could focus of ensuring undeclared items cannot successfully be mated with delivery systems and there are parallels following this approach to verifying the absence of warheads on delivery systems as accomplished under NEW START at present.

Systems level analysis, including acquisition path analysis can therefore provide clear verification objectives for site visits based upon information already provided by the inspected state. Clear verification objectives may enable managed access procedures to be defined that met those objectives whilst protecting sensitive information.

Any advancement in arms reductions and disarmament is likely to proceed in a step-by-step way. Bilateral agreements are likely to provide the steps that will pave the way for more multilateral implementation. For example, future US/Russia disarmament treaties limiting warhead numbers may build the infrastructure for facility monitoring and inspection activities, and transparency and confidence-building measures amongst the de-facto nuclear weapons states may provide capital for more intrusive monitoring activities. Such a state-level methodology could help inform the direction of future negotiations, present day technology R&D, and assessment of possible effective verification regimes.

References

J.N. Cooley. Progress in Evolving the State-level Concept". In: Seventh INMM/ESARDA Joint Workshop Future Directions for Nuclear Safeguards and Verification, 2011.

Listner, C.; Canty, M.; Rezniczek, A.; Stein, G. & Niemeyer, I.
A Concept for Handling Acquisition Path Analysis in the Framework of IAEA's State-level Approach. Proceedings of the INMM Annual Meeting, 2012.

Listner, C.; Canty, M.; Rezniczek, A.; Stein, G. & Niemeyer, I.
Approaching acquisition path analysis formally - a comparison between AP and non-AP States. Proceedings of the 35rd ESARDA Annual Meeting, 2013.

Listner, C.; Canty, M.; Rezniczek, A.; Stein, G. & Niemeyer, I.
Evolution of Safeguards - What can formal Acquisition Path Analysis contribute?
Proceedings of the INMM Annual Meeting, 2014.

Listner, C.; Niemeyer, I.; C.; Canty, M.; Stein, G. & Rezniczek, A.
Formalizing Acquisition Path Analysis for the IAEA's State-Level Concept
Proceedings of the ESARDA Symposium, 2015

Nuclear Threat Initiative (NTI)
Innovating Verification: New Tools & New Actors to Reduce Nuclear Risks. Verifying Baseline Declarations of Nuclear Warheads and Materials, 2014.

The Proliferation Resistance and Physical Protection Evaluation Methodology Working Group of the Generation IV International Forum, ‘Evaluation Methodology for the Proliferation Resistance and Physical Protection of Generation IV Nuclear Energy Systems’ revision 6, Sept 2011, ref: GIF/PRPPWG/2011/003, https://www.gen-4.org/gif/upload/docs/application/pdf/2013-09/gif_prppem_rev6_final.pdf , accessed 12/05/2015

Neutron multiplicity counting for warhead authentication: Bias reduction and quantification

Malte Göttsche[1], Gerald Kirchner[1]

[1]University of Hamburg
Centre for Science and Peace Research
Beim Schlump 83, 20144 Hamburg, Germany
E-mail: malte.goettsche@physik.uni-hamburg.de

Abstract:

Neutron multiplicity counting is useful in warhead or warhead component authentication to determine if an item declared to be a warhead fulfils an attribute related to its fissile mass. The inspector will not know the configuration of the warhead or component, in particular the exact fissile material geometry and the configuration of potential material between the plutonium and detector. Assay bias for highly multiplicative samples has been studied only to a limited extent; corrections to the point model are based on empirical data valid for only a small range of geometries. We systematically study the bias and propose physics-based corrections for spherical shell geometries using MCNPX-PoliMi simulations. As a result, the bias compared to the point model equations can be significantly reduced, but an uncertainty remains which must be quantified.

Keywords: disarmament, verification, neutron multiplicity counting, point model

1. Disarmament Verification

As part of verified fissile warhead and warhead component inventory declarations and the verification of warhead dismantlement, three elements will most likely be key to a sound verification regime. First, warheads and warhead components must be uniquely identified so that warheads and components in stock are not counted twice. Second, warheads and components must be authenticated. Authentication in this context is the process during an on-site inspection by which it is assessed by measurements whether a specific item is a nuclear warhead (or component). Third, a robust Continuity of Knowledge could be defined as providing means to effectively demonstrate over a certain time or process, e.g. during warhead dismantlement, the unchanged identity of the treaty-accountable item and its integrity (i.e. that no undeclared changes to the item occurred).

Due to the classified nature of the items under investigation, direct measurements for authentication purposes will most likely not be possible as they would reveal information that is considered sensitive for nonproliferation, national security and possibly other reasons. The use of information barriers could overcome this problem. An information barrier takes classified measurements but converts the results to an unclassified output (such as a binary yes/no signal) while protecting the sensitive data from the inspector's view.

In the attribute approach, the inspecting and host parties agree on a set of attributes that the items would be checked against and on an analysis algorithm. This set should be defined in a way that it allows for an assessment whether a declared warhead (component) is genuine. One of the attributes that could be considered is related to its fissile mass. This attribute could perhaps be assessed by neutron multiplicity measurements using He-3 detectors.

A high reliability of attribute measurement techniques is required as inspectors cannot review and analyze detailed measurement results, if they are in doubt for whatever reasons. In contrast to other

situations where radioactive samples are characterized, the knowledge that exists prior to the measurements, for example the sample's geometry, may be inadequate. Many measurement techniques require certain information on a sample to function accurately. Inspectors must understand how large deviations between real and measured values (bias) become as the properties of the item and intervening materials vary in plausible manners. Besides the configuration of the fissile material itself, bias may be the result of the potential presence of materials between warhead component and detector. In the case of fully assembled warheads, materials such as a conventional explosive surround the fissile component. Furthermore, most nuclear warheads and warhead components are stored in containers for safety reasons [1, p. 33].

In this paper, the major source of neutron multiplicity counting bias with relevance to warhead authentication is discussed which occurs for samples with high masses and neutron multiplication. Furthermore, it is investigated how this bias depends on the sample configuration in order to assess the reliability of neutron multiplicity counting when the configuration remains unknown.

2. Bias for highly multiplicative plutonium samples

Neutron multiplicity counting assesses the plutonium mass by counting the neutrons that are detected within a defined gate length after a neutron trigger. The measured quantities are the Singles, Doubles and Triples rates S, D and T. The theory behind neutron multiplicity counting that allows the deduction of the fissile mass, the neutron multiplication and the quantification of (α, n) reactions from S, D and T is based on a derivation by Böhnel [2]. It inter alia makes the assumption that the amount of induced fission started by the neutrons from a spontaneous fission is constant regardless of where an original spontaneous fission event occurred (“point model”). While this assumption is unproblematic for gram quantities of plutonium metal, it becomes a major source of bias with increasing sample size.

Indeed, leakage of neutrons from a spontaneous fission and secondary neutrons from induced fission depends on the position of the initial spontaneous fission event [3]. For spherical configurations, this dependence can be expressed by the function $M(r)$, where M is the multiplication, i.e. the total number of leaked neutrons per spontaneous fission neutron, and r is the position of the spontaneous fission event.

There has been some success in applying empirical correction factors that depend on the measured multiplication: Krick et al. [3] determined separate S, D and T corrections based on MCNPX simulations of plutonium cylinders to obtain the correct masses. These corrections remain, however, geometry-dependent [3].

Croft et al. [4] proposed another model coupled with the desired physical understanding: In the equations required to deduce the fissile mass, the multiplication $\langle M^n \rangle$ appears up to the fifth order $(\mathrm{n} = 5)$ [5]. According to the “point model”, assuming constant multiplication at all spontaneous fission locations, $\langle M^n \rangle = \langle \mathrm{M} \rangle^{\mathrm{n}}$. Therefore, Croft et al. propose correction factors [4]

$$\mathrm{g_n} = \frac{\langle \mathrm{M^n} \rangle}{\langle \mathrm{M} \rangle^{\mathrm{n}}}, \qquad \mathrm{n} = 2 \ldots 5$$

to correct for falsely using $\langle M \rangle^n$. The g_n are calculated from

$$\langle \mathrm{M^n} \rangle = \frac{1}{\mathrm{V}} \int \mathrm{M^n}(\vec{\mathrm{r}}) \mathrm{dV}$$

The corrected equations are then [4]

$$S = F \cdot \epsilon \cdot \langle M \rangle \cdot \nu_{sf1}(1+\alpha)$$

$$D = \frac{F \cdot \epsilon^2 \cdot f_d \cdot \langle M^2 \rangle}{2}[\nu_{sf2} \cdot g_2 + (g_3 \cdot \langle M \rangle - g_2)\frac{\nu_{sf1} \cdot \nu_{i2}}{\nu_{i1}-1}(1+\alpha)]$$

$$T = \frac{F \cdot \epsilon^3 \cdot f_t \cdot \langle M^3 \rangle}{6}[\nu_{sf3} g_3 + (g_4 \cdot \langle M \rangle - g_3)(1+\alpha)\frac{\nu_{sf1} \cdot \nu_{i3}}{\nu_{i1}-1} +$$

$$3(g_4 \cdot \langle M \rangle - g_3)\frac{\nu_{sf2} \cdot \nu_{i2}}{\nu_{i1}-1} + 3(g_5 \cdot \langle M^2 \rangle - 2g_4 \cdot \langle M \rangle + g_3)(1+\alpha)\frac{\nu_{sf1} \cdot \nu_{i2}^2}{(\nu_{i1}-1)^2}]$$

where ν_{sfn} are the factorial moments of the spontaneous fission multiplicity distribution, ν_{in} are the factorial moments of the induced fission multiplicity distribution, F is the spontaneous fission rate from which the fissile mass m can be deduced if the isotopic composition is known, ϵ is the detection efficiency, α is the ratio of (α, n) to spontaneous fission reactions, f_d and f_t are the Doubles and Triples gate fractions. We have solved these equations for $\langle M \rangle$, α and m.

3. Simulations

It has been shown that this approach indeed removes the bias [6]. This requires, however, full knowledge of the sample configuration in order to obtain $M^n(\vec{r})$ and the g_n from Monte Carlo simulations. In the following, parameter studies are presented with the aim of showing how the g_n can be estimated when the sample configuration is not fully known.

MCNPX-PoliMi simulations [7] have been performed with plutonium metal samples (94% Pu-239 and 6% Pu-240, $\rho = 19.8\ {}^{\mathrm{g}}/_{\mathrm{cm}^3}$) in spherical geometries, defined by their outer radius $\mathrm{r_{out}}$ and in the case of hollow spheres their inner radius $\mathrm{r_{in}}$. A series of solid spheres and four series of hollow spheres ($\mathrm{r_{in}} = 1.0\ \mathrm{cm}, 2.0\ \mathrm{cm}, 3.5\ \mathrm{cm},\ 5.0\ \mathrm{cm}$) were simulated with a variety of masses and accordingly $\mathrm{r_{out}}$. In the individual series, the thickness $\mathrm{d} = \mathrm{r_{out}} - \mathrm{r_{in}}$ was increased up to 2.9 cm.

<u>$g_n$estimate based on thickness</u>

The simulations show a strong dependence of the correction factors on the thickness d. Figure 1 shows $g_2(d)$ for the configurations with different $\mathrm{r_{in}}$. The slopes of g_3, g_4 and g_5 are similar, as can be seen from Figures 4, 5 and 6 in the Appendix. Most importantly, the figures show that the dependence of the g_n on r_{in} is rather limited; the curves of all hollow spheres are very similar.

Based on these results, the g_n can be approximated as a function of d if it is known whether the configuration is best resembled by a solid or hollow sphere, but without necessarily knowing r_{in} or r_{out}. When for example choosing our results for $r_{in} = 2.0\ cm$ as reference curves to determine the g_n, the deviations of the plutonium mass obtained with the corrected analysis from the true values can be expected to be small for hollow spheres with different r_{in} but constant d.

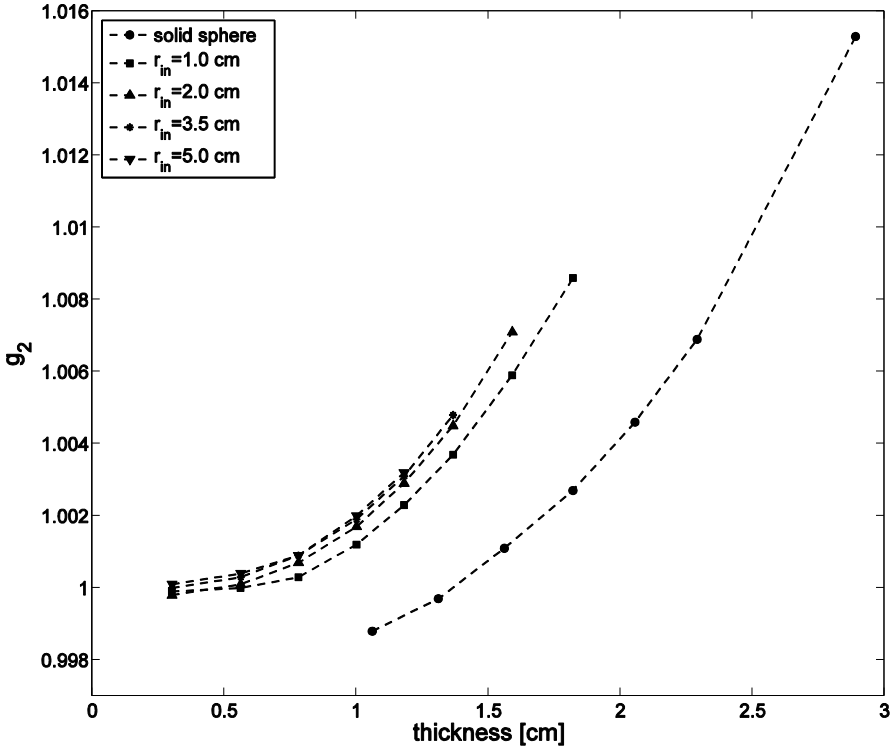

Figure 1: g_2 as a function of thickness

$g_n$estimate based on multiplication

If d is not available, an estimate of the g_n can also be obtained as a function of the average multiplication, a direct output of the analysed multiplicity counting results. From Figure 2 and also Figures 7, 8 and 9 in the Appendix, it can be seen that the slopes of $g_n(< M >)$ are steeper for smaller $\mathrm{r_{in}}$. Depending on the available information on the sample configuration, we suggest to choose a reference curve and an empirical fit function. Double exponential functions are suited to sufficiently represent the data. Assuming a hollow sphere, a reasonable choice for a reference curve could for example be the $r_{in} = 2.0\ cm$ data. In general, the magnitudes of the differences between the curves of the different r_{in} are larger for $g_n(< M >)$ than for $g_n(d)$. As a result, the possible deviations of the g_n estimated from $g_n(< M >)$ are generally larger compared to $g_n(d)$.

$g_n$estimate based on fissile mass

It has been proposed to estimate the g_n as a function of fissile mass for solid sphere and cylinder configurations [4]. Figure 3 shows g_2 of the solid and hollow sphere configurations. The results for g_3, g_4 and g_5 are shown in Figures 10, 11 and 12 in the Appendix. Determining the g_n from a reference function of the fissile mass introduces large uncertainties, as their values strongly depend on the actual configuration. Thus, a reliable reference function cannot be given without additional information such as the radius or the multiplication.

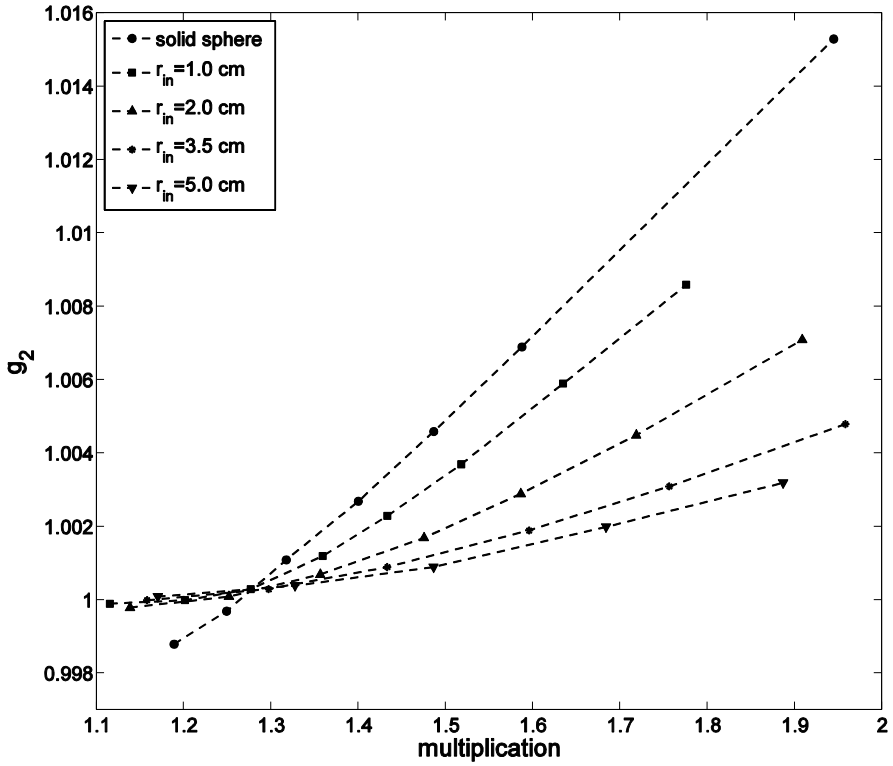

Figure 2: g_2 as a function of multiplication

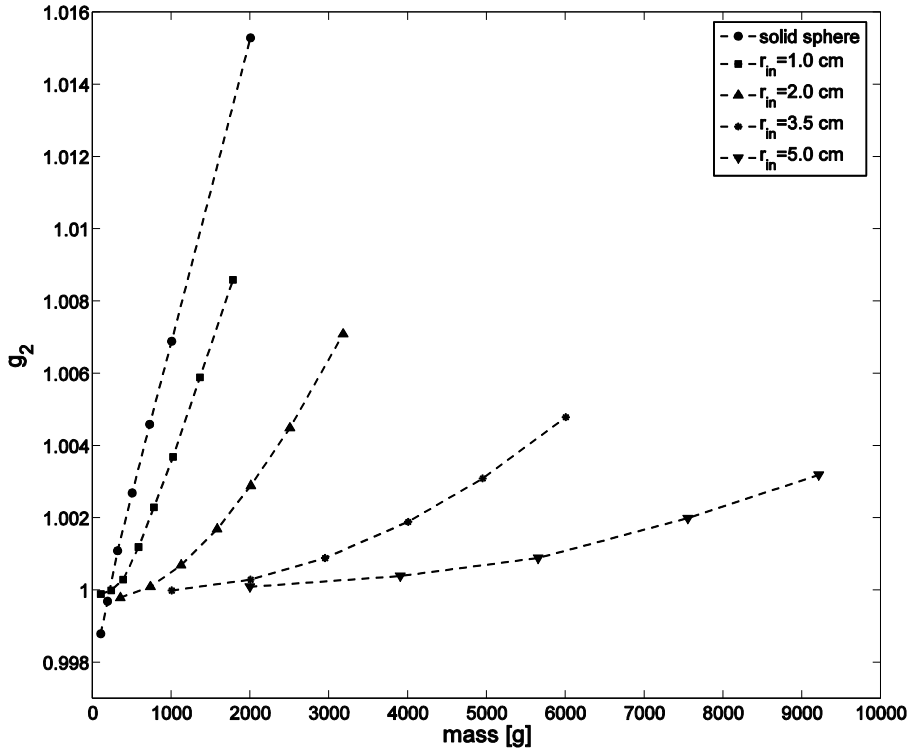

Figure 3: g_2 as a function of fissile mass

Influence of isotopic composition

Results of simulations with different plutonium isotopic compositions are shown in Table 1. The g_n increase slightly with Pu-239 content. Compared to the influence of geometries, the effect of the isotopic composition is small. Knowledge of the isotopic composition is helpful to estimate the g_n, but g_n estimates without considering the isotopic composition can remain fairly accurate.

Pu-239	Pu-240	g_2	g_3	g_4	g_5
0.70	0.30	1.0040	1.0118	1.0233	1.0383
0.85	0.15	1.0045	1.0133	1.0263	1.0433
0.97	0.03	1.0049	1.0146	1.0288	1.0474

Table 1: g_2 of a hollow sphere configuration (inner radius 3.5 cm, outer radius 4.9 cm) and different isotopic compositions

	Reflected solid sphere $r_{out} = 2.3\ cm$	Reflected hollow sphere $r_{in} = 3.5\ cn, r_{out} = 4.9\ cm$
g_2	1.0059	1.0033
g_3	1.0187	1.0098
g_4	1.0385	1.0193
g_5	1.0656	1.0319

Table 2: g_n for reflected configurations

Influence of neutron reflection

In order to study the influence of neutron reflection, simulations have been performed for two plutonium configurations (a solid sphere, $r_{out} = 2.3\ cm$ and a hollow sphere, $r_{in} = 3.5\ cn, r_{out} = 4.9\ cm$) surrounded by a 3 cm thick layer of polyethylene ($\rho = 0.955\ {}^{g}/_{cm^3}$). The results for the g_n are shown in Table 2. Compared to the unreflected configurations, they are somewhat smaller. Accordingly, information of reflection is helpful to determine the g_n with high accuracy.

4. Conclusion

Without detailed knowledge of the sample configuration, the g_n must be estimated. For hollow spheres, they can be approximated with high accuracy when the thickness d is known. A less accurate estimate is obtained when only the multiplication is known. Reflection decreases the g_n. As the available information on the sample configuration will be limited in the case of warhead authentication, uncertainties in the mass assessments remain due to the uncertainties of the g_n. The more information is available, the more reliable will the assessment be. In any case, according to which information is given, the remaining uncertainties should be quantified to understand the reliability of the technique.

5. Acknowledgements

The authors would like to thank Götz Neuneck and Caren Hagner for their contributions and the German Foundation for Peace Research for funding this research project.

6. References

[1] Nuclear Threat Initiative; *Innovating Verification: New Tools & New Actors to Reduce Nuclear Risks, Verifying Baseline Declarations of Nuclear Warheads and Materials*; Washington D.C.; 2014.

[2] Böhnel K; *The Effect of Neutron Multiplication on the Quantitative Determination of Spontaneously Fissioning Isotopes by Neutron Correlation Analysis*; Nuclear Science and Engineering 90; 1985; p 75-82.

[3] Krick M, Geist W, Mayo D; *A Weighted Point Model for the Thermal Neutron Multiplicity Assay of High-Mass Plutonium Samples, LA-14157*; Los Alamos National Laboratory; Los Alamos; 2005.

[4] Croft S, Alvarez E, Chard P, McElroy R, Philips S; *An Alternative Perspective on the Weighted Point Model for Passive Neutron Multiplicity Counting*; 48th INMM Annual Meeting; Tucson; 8-12 July 2007.

[5] Ensslin N, Harker W, Krick M, Langner D, Pickrell M, Stewart J; *Application Guide to Neutron Multiplicity Counting, LA-13422-M*; Los Alamos National Laboratory; Los Alamos; 1998.

[6] Göttsche M, Kirchner K; *Neutron Multiplicity Counting for Future Verification Missions, Bias When the Sample Configuration Remains Unknown*; 2014 IAEA Safeguards Symposium; Vienna; 20-24 October 2014.

[7] Pozzi S, Clarke S, Walsh W, Miller E, Dolan J, Flaska M, Wieger B, Enqvist A, Padovani E, Mattingly J, Chichester D, Peerani P; *MCNPX-PoliMi for Nuclear Nonproliferation Applications*; Nuclear Instruments and Methods A 694; 2012; p 119-125.

Appendix

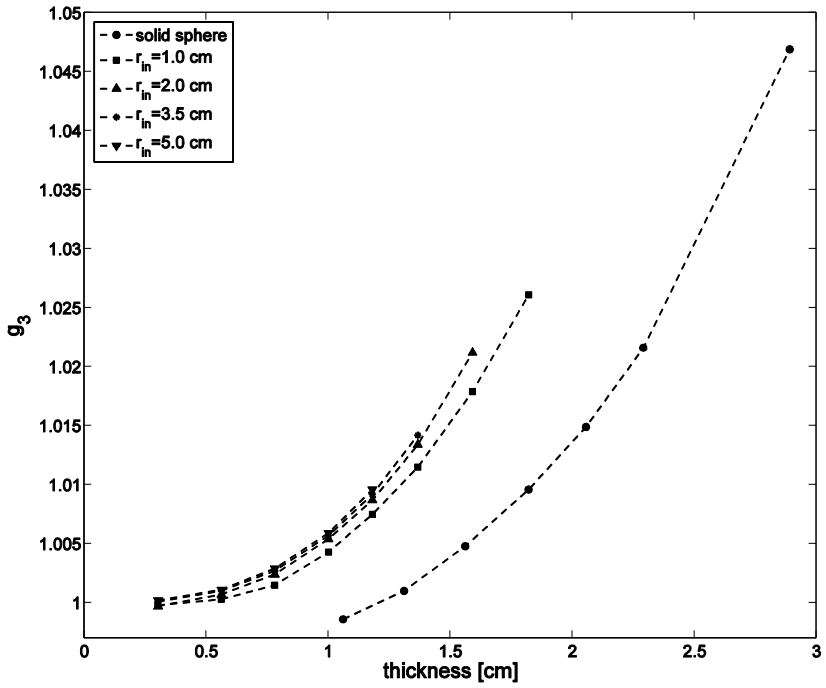

Figure 4: g_3 as a function of thickness

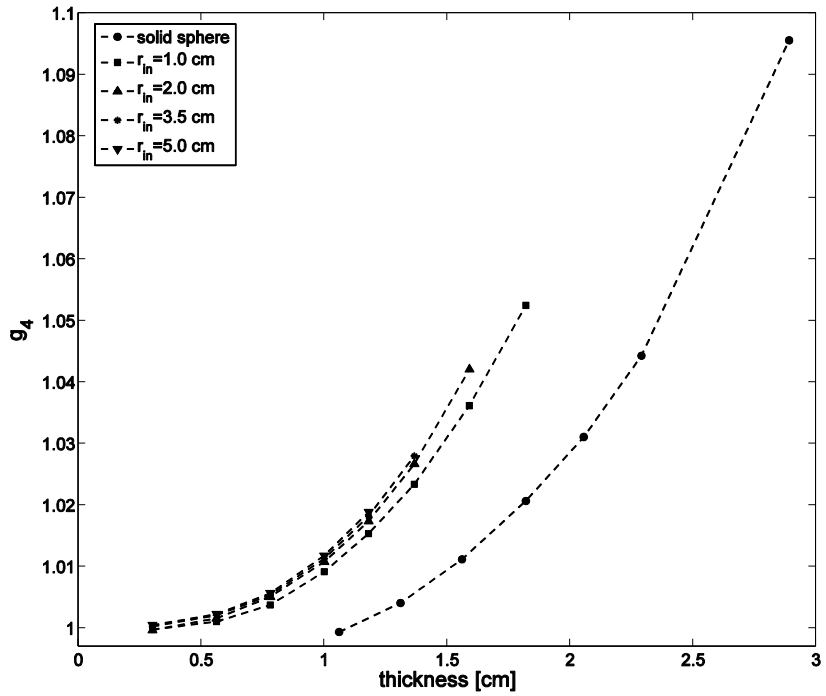

Figure 5: g_4 as a function of thickness

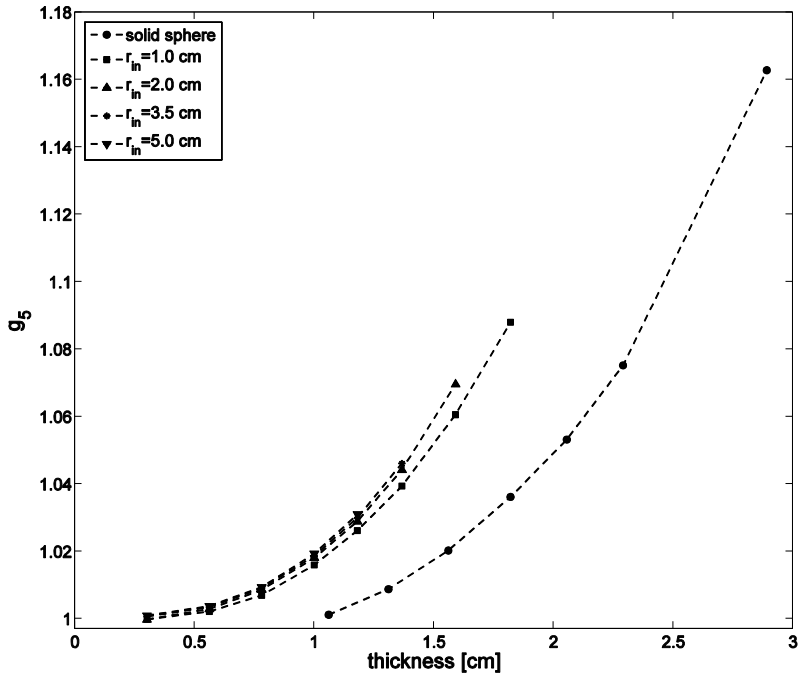

Figure 6: g_5 as a function of thickness

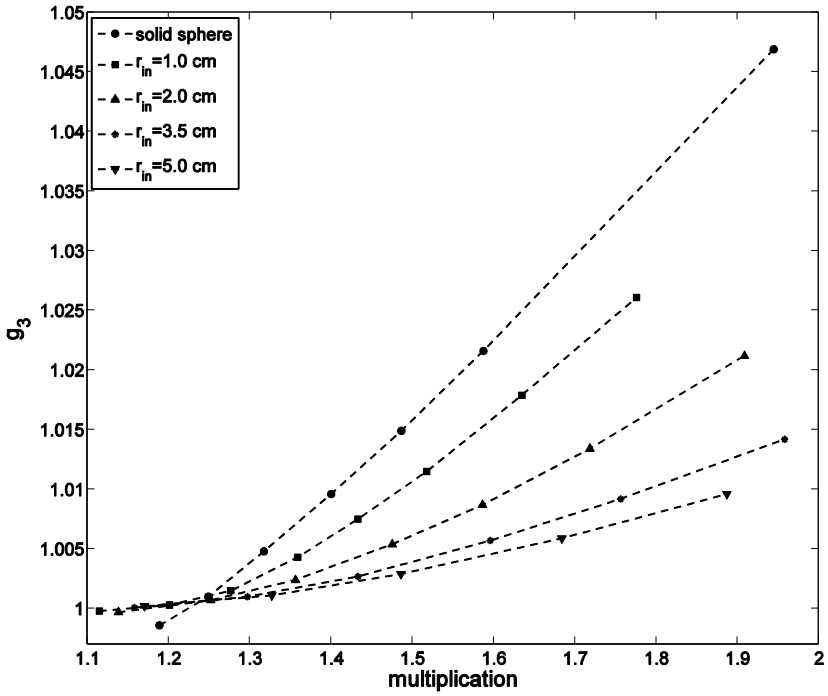

Figure 7: g_3 as a function of multiplication

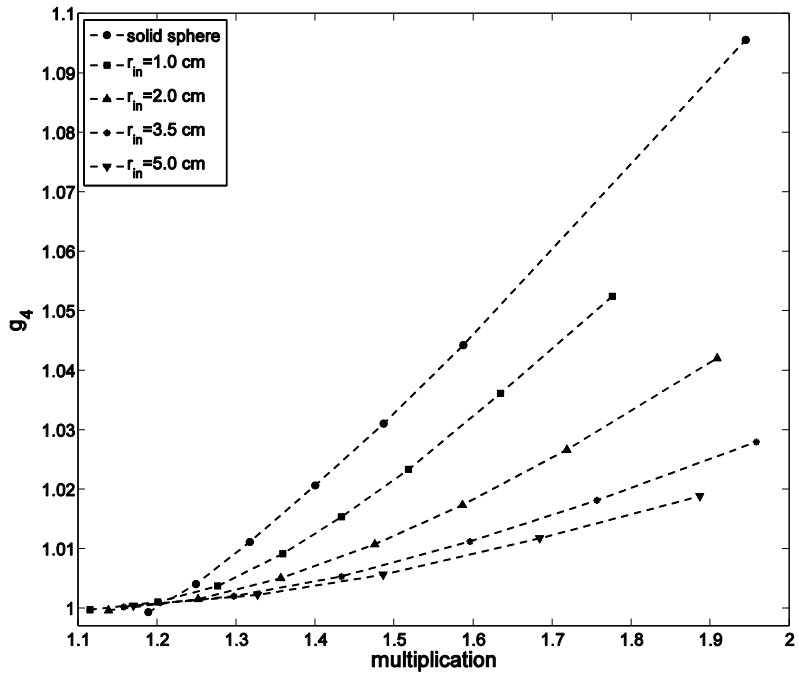

Figure 8: g_4 as a function of multiplication

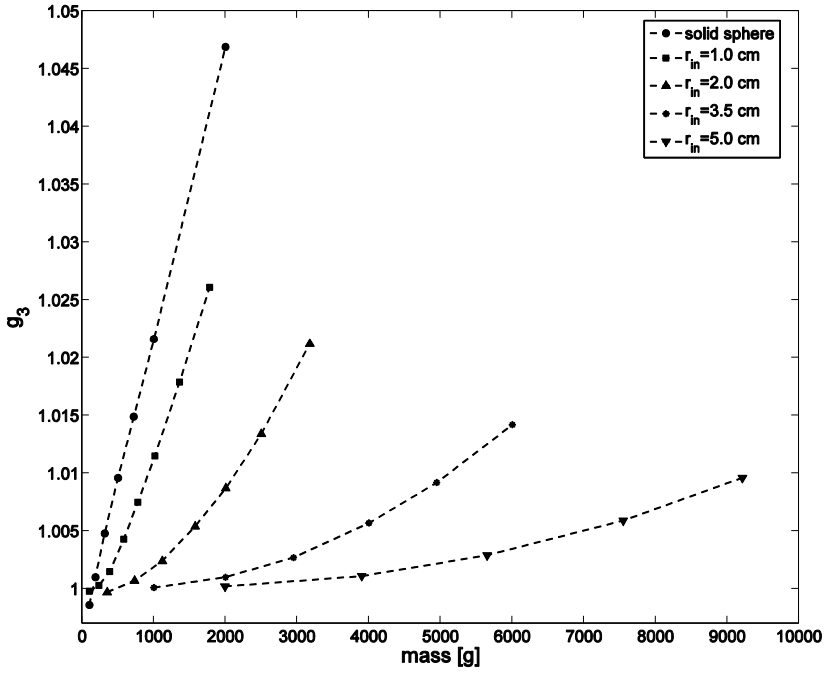

Figure 9: g_5 as a function of multiplication

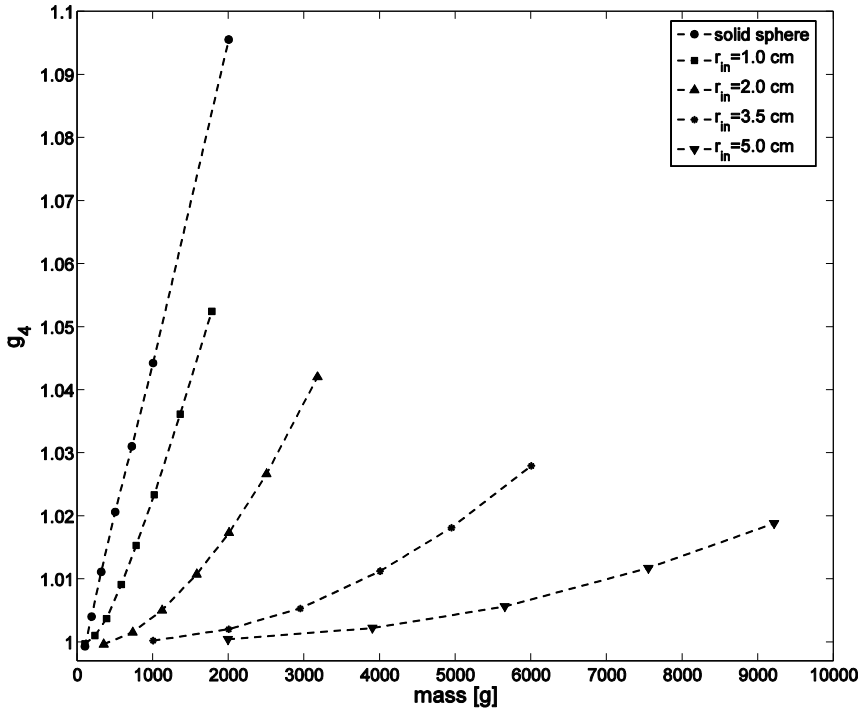

Figure 10: g_3 as a function of fissile mass

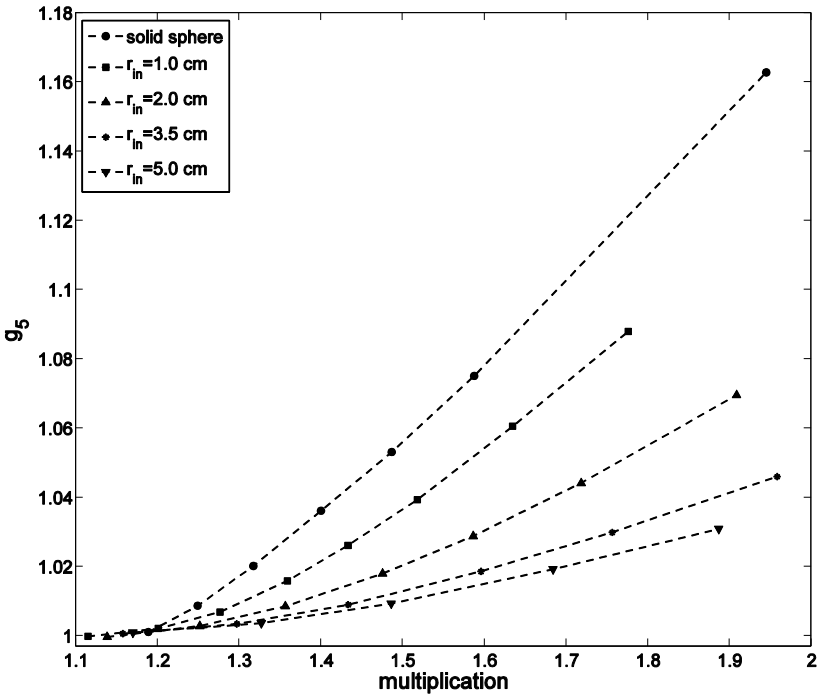

Figure 11: g_4 as a function of fissile mass

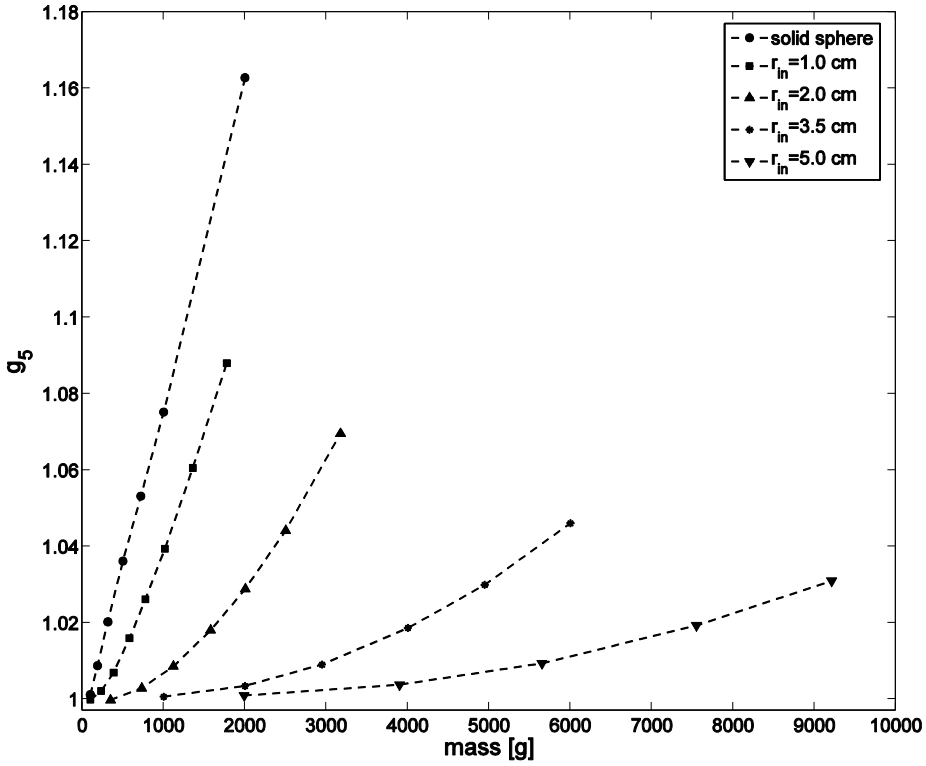

Figure 12: g_5 as a function of fissile mass

Disposition of Certain U.S. Exports of High Enriched Uranium

Santiago Aguilar, Danielle Emche, Brian Horn,

U.S. Nuclear Regulatory Commission
Washington, D.C.
Santiago.Aguilar@nrc.gov, Danielle.Emche@nrc.gov, Brian.Horn@nrc.gov,

Abstract:

In 2012, the United States (U.S.) Congress, under provisions of the American Medical Isotopes Production Act, required the Chairman of the U.S. Nuclear Regulatory Commission (U.S. NRC) to submit a report detailing the current disposition of previous U.S. exports of highly enriched uranium (HEU) used as fuel or targets in a nuclear research or test reactor (RTR). In January 2014, the U.S. NRC submitted the requested report to Congress. In the preparation of the report, U.S. NRC staff reviewed nearly 1,700 HEU export transactions, 1,400 HEU import transactions, and compared the information to nearly 800 export licenses and license amendments. The report found that the bulk of the U.S. HEU exports and imports, approximately 95 and 80 percent respectively, occurred prior to 1990. The U.S. HEU exports peaked in the late 1960s and have since declined dramatically due to the shutdown of many foreign HEU-fueled RTR facilities and programs. The U.S. exported approximately 22,600 kilograms (kg) of HEU, of which 7,700 kg was imported back to the United States.

The United States continues the effort to reduce and eliminate the use of HEU for use in RTRs and medical isotope production. Although the U.S. exported HEU to 35 countries, 20 countries still possess some U.S. HEU as RTR fuel or target material. Some of the outcomes from the 2010, 2012, and 2014 Nuclear Security Summits were statements on behalf of various countries, endorsing or committing to the minimization of HEU and potential replacement of HEU use in the future production of medical isotopes.

Keywords: Highly Enriched Uranium; Export; Minimization; Safeguards; Security

Introduction

Acknowledging the comprehensive international framework and global partnerships that ensure nuclear material safeguards and security, there is likewise a high degree of United States (U.S.) domestic interest to identify and minimize risks associated with highly enriched uranium (HEU). In accordance with U.S. domestic legislation requirements,[1] the U.S. Nuclear Regulatory Commission (U.S. NRC) developed a report that assessed the current disposition of U.S. exported HEU, defined as uranium enriched to 20 percent or more in the isotope uranium-235. In January 2014, the Chairman of the U.S. NRC submitted the, "Report to Congress on the Current Disposition of Highly Enriched Uranium Exports Used as Fuel or Targets in Nuclear Research or Test Reactors." For all previous U.S. exports of HEU used as fuel or targets in a research or test reactor (RTR), the U.S. NRC reported to Congress on:

- the current location of the HEU;
- whether the HEU has been irradiated;
- whether the HEU has been used for the purpose stated in their export license;
- whether they have been used for an alternative purpose and, if so, whether such alternative purpose has been explicitly approved by the Commission;
- the year of export, and re-importation, if applicable;
- the current physical and chemical forms of the HEU; and
- whether the HEU has been stored in a manner which adequately protects against theft and unauthorized access.

The U.S. NRC developed the report by examining information dating from 1950 through 2012. Data sources analyzed included export license records (over 800); reports by and technical discussions with staff from the National Nuclear Security Administration's (NNSA's) Global Threat Reduction Initiative (GTRI); records for tracking movements of nuclear materials from and to facilities within the United States known as the Nuclear Materials Management and Safeguards System (NMMSS) database (over 1,700 export transactions and 1,400 transactions involving imports and receipts); and U.S. interagency bilateral physical protection visit report information. The report also built upon information that the U.S. NRC presented to Congress in a January 1993 report on the disposition of previous HEU exports.[2] Additionally, the U.S. NRC staff consulted with the U.S. Department of Energy (DOE), U.S. Department of State (DOS), and other relevant agencies.

The report recognizes the significant duration of U.S. experience with exporting HEU and the changes that have occurred over the last 60 years. In order to accurately capture the complexity associated with the current disposition of U.S. exported HEU, the report provides an overview of the historical and legislative evolution of the U.S. experience with exporting HEU, and distinguishes particular policy and technological developments that have contributed to the current disposition of U.S. exported HEU.

Summary of Report Findings

The U.S. Government reviewed all of the available data and contacted the foreign governments relevant to the U.S. HEU that was exported since 1957, which totaled 22,600 kilograms (kg). This equates to approximately 896 significant quantities, as defined by the International Atomic Energy Agency (IAEA). The U.S. NRC was able to identify the disposition or location of 93 percent of this previously exported HEU. This was a major accomplishment, considering the challenges that many historical records predate electronic recordkeeping (increasing the likelihood that records were incomplete); the agreements under which the United States exports HEU do not require the receiving country to report to the United States on the ultimate disposition of the HEU; and, there are inherent accounting uncertainties associated with HEU RTR fuel cycle and medical isotope processing operations.

Of the 22,600 kg of previously exported HEU, the U.S. NRC determined that 7,700 kg was imported back to the United States, and 6,100 kg currently resides in 20 countries. Of the remaining 8,800 kg, information indicates that more than 4,300 kg of the U.S. HEU was eliminated by down-blending to LEU; approximately 500 kg of HEU was eliminated in highly-dilute processing waste; and at least 2,400 kg of HEU was burned up through irradiation in RTRs. There is a remaining seven percent, or 1,600 kg, of HEU that was not precisely reconciled by existing records. This percentage will continue to decrease as the United States continues to work with foreign governments to reconcile information and import material back to the United States.

U.S. History of Exports of Highly Enriched Uranium

The United States has always recognized and continues to recognize the importance for preserving the security interests associated with nuclear materials in order to ensure the peaceful uses of nuclear energy. During the U.S. NRC's work developing the report, it was useful to examine and assess the policy and historical factors that contributed to the creation of the U.S. and international nuclear materials export regime. Through a review of the U.S. history and experience with exporting HEU, the U.S. NRC was able to further contextualize its data findings, and identify enhancements that have developed over the years related to the U.S. and international nuclear export regime, and which contribute to the current disposition of U.S. exported HEU.

The origin of the U.S. experience with exporting HEU began with President Dwight D. Eisenhower's "Atoms for Peace" speech, given to the United Nations General Assembly on December 8, 1953. Following this speech, Congress amended the Atomic Energy Act of 1946 by replacing it with the Atomic Energy Act of 1954 (AEA) to establish the legal framework for developing the U.S. civilian nuclear industry, promoting cooperation with other countries in the peaceful uses of nuclear energy, and ensuring appropriate controls to protect public health, safety, and U.S. common defense and security. In tandem with the "Atoms for Peace" speech, the U.S. Government recognized the need for establishing an effective, independent safeguards verification system administered by an autonomous international organization of broad membership and strong collective purpose. The

U.S. Government strongly promoted the development and implementation of IAEA's safeguards verification.

U.S. Agreements and Requirements for Exports

Starting in the 1950s, the United States established peaceful nuclear cooperation agreements, under Section 123 of the AEA, which became known as "123 Agreements," with countries and organizations. These Agreements are a cornerstone of and precondition for U.S. export of nuclear materials. Presently, the United States maintains bilateral 123 Agreements with 20 individual countries, the European Atomic Energy Community (EURATOM),[3] the IAEA,[4] and Taiwan.[5] The scope and content of 123 Agreements have evolved significantly since the 1950s, reflecting the progression of the international nuclear nonproliferation regime and its key policy instruments – IAEA safeguards agreements and the Treaty on the Non-Proliferation of Nuclear Weapons (NPT). Additionally, 123 Agreements evolved to reflect technological advancements in the nuclear field, and U.S. statutory requirements, such as the Nuclear Non-Proliferation Act of 1978 (NNPA).

Certain fundamental U.S. principles set forth in the 123 Agreements have not changed over the last 60 years. The United States continues to obtain guarantees from the governing bodies of the cooperating nations and organizations stipulating that safeguards will be maintained, no material or equipment supplied by the United States under the agreements will be used for nuclear weapons or for research on or development of nuclear weapons or for any other military purpose, the appropriate physical protection measures will be maintained, and the United States will have certain prior consent rights (for example if the material or equipment supplied under an agreement may be transferred to a third party that had not been provided for in the agreement).

Up until the 1970s, most of the 123 Agreements in force with countries interested in building and operating RTRs provided for the lease of HEU with explicit provisions for the return of the spent nuclear fuel to the United States. Following ratification of the NPT, the United States began relying on the IAEA to implement safeguards, and the United States stopped applying bilateral safeguards. From 1964 – 1988, the United States also began to operate under a policy known as the "Off-Site Fuels Policy," and no longer required returns of spent fuel but continued to accept, store and process it for certain countries and in certain cases. During the 1990s, the Off-Site Fuels Policy and associated programs evolved into the present-day NNSA/GTRI managed Foreign Research Reactor Spent Nuclear Fuel Acceptance Program, which is discussed further in this paper.

The U.S. requirements and process for the licensing of HEU exports have evolved significantly since the 1950s. Initially, all aspects of the U.S. reactor research, development, and demonstration programs, and associated international cooperation agreements were promoted, executed, and administered by the U.S. Atomic Energy Commission (AEC). In 1975, the responsibility for nuclear material export licensing was transferred to the U.S. NRC, as a result of the Energy Reorganization Act of 1974. The U.S. NRC licenses exports of nuclear material and equipment pursuant to the criteria set forth in the 1954 AEA, as amended. The existing U.S. NRC regulations in Title 10 of the Code of Federal Regulations, Part 110, set forth the criteria for licensing exports of nuclear materials and equipment as prescribed by the AEA.[6]

U.S. NRC licensing criteria address the issues of nuclear non-proliferation, physical protection, and HEU minimization. Overall, it must be determined on a case-by-case basis that an approval of proposed exports of nuclear material or equipment will not be adverse to the common defense and security of the United States. In conducting nuclear material export licensing reviews, the U.S. NRC must seek the judgment of interested U.S. Government executive branch agencies (i.e., the U.S. Departments of Commerce, Energy, and Defense, as coordinated by DOS) as to whether approving a proposed export would be consistent with U.S. statutory and foreign policy requirements. The U.S. NRC cannot issue an export license if the Executive Branch recommends denying the license; however, if the Executive Branch recommends approval and the U.S. NRC disagrees, the license application must be referred to the President of the United States for action, which is subject to Congressional review. To date, every HEU export license issued by the AEC and the U.S. NRC has satisfied U.S. domestic law, internal AEC/NRC export licensing regulations, 123 Agreements, Project and Supply Agreements, the NPT as applicable, and IAEA agreements and protocols.

Significant Recent Policy Developments

In recent years, the global community, including the U.S. Government, led by the National Security staff, DOE, and DOS, has intensified efforts and achieved significant successes to minimize the use of HEU for fuel or targets in RTRs. In this context and consistent with the provisions of U.S. domestic law concerning medical isotopes production,[7] the U.S. Government continues to engage with foreign governments through DOE's GTRI Reduced Enrichment for Research and Test Reactors (RERTR) and associated programs to convert existing facilities to LEU fuel and targets, prioritize returns of HEU to the United States, and reconcile record discrepancies. Concurrently, the GTRI/RERTR program is involved in converting existing U.S. research reactors to LEU fuel and targets to minimize all HEU in civilian use. The U.S. NRC strongly supports and recognizes the sensitive nature of these ongoing efforts.

The importance of continuing these efforts is highlighted by the international commitments that have been made as a result of the Nuclear Security Summits (NSS). In April 2010, President Obama hosted the first NSS in Washington, D.C. and met with 47 heads of state to discuss actions to increase security for nuclear materials and prevent acts of nuclear terrorism and trafficking. The summit reinforced the principle that all states are responsible for ensuring the best security of their materials, for seeking assistance if necessary, and for providing assistance if asked. It promoted the international treaties that address nuclear security and nuclear terrorism and led countries to commit to specific national actions to advance global security. One of the key items included in the Joint Communique issued by the Summit is that world leaders, "Recognize that highly enriched uranium and separated plutonium require special precautions and agree to promote measures to secure, account for, and consolidate these materials, as appropriate; and encourage the conversion of reactors from highly enriched to low enriched uranium fuel and minimization of use of highly enriched uranium, where technically and economically feasible."[8]

At the 2012 Seoul NSS, Belgium, France, the Netherlands, and the United States issued a, "Joint Statement on Minimization of HEU and the Reliable Supply of Medical Radioisotopes." That statement reaffirmed commitments on the part of those four countries to support conversion of European production industries to non-HEU based processes by 2015, subject to the regulatory approvals to reach a sustainable medical isotope production for the benefit of patients in need of vital medical isotope diagnostic treatments in Europe, the United States, and elsewhere. It was also agreed at the 2012 Summit that in the longer term, the use of HEU will be completely eliminated for production of medical isotopes.

The most recent Nuclear Security Summit was held in 2014 at The Hague. In the significant final joint communique that was issued, participants affirmed the shared goal to, "…encourage States to minimize their stocks of HEU (…). Similarly, we will continue to encourage and support efforts to use non-HEU technologies for the production of radioisotopes (…)."[9] Commitments resulting from the 2010, 2012, and 2014 NSS underscore the importance for ensuring safety and security of HEU, with the goal of minimizing or eliminating its use.

Detailed Analysis of the Disposition of U.S. Exported HEU

Since 1957, the United States exported HEU for use as fuel or targets in RTRs to a total of 35 countries either directly (to 32 countries) or indirectly (to an additional three countries) as a result of re-transfers between those countries in Table 1, on the following page. Approximately 6,100 kg of U.S. supplied HEU presently remains in 20 countries, with 95 percent of that material located in Europe and Canada. Many of the 20 countries have converted their RTRs from HEU to low enriched uranium (LEU) fuel or have committed to doing so in the future. The remaining 15 countries no longer possess any U.S. supplied HEU for these purposes and have either converted facilities to LEU or have shut down the facilities that required HEU. Approximately 7,700 kg of HEU has been returned to the United States primarily as irradiated fuel.

Table 1: Disposition of U.S. HEU Used as Fuel or Targets in a Nuclear Research or Test Reactor

Countries that received HEU (Direct exports from the U.S.)		Countries that no longer possess U.S. HEU for these purposes[10]	Countries with less than 1 kg of U.S. HEU for these purposes[10]	Countries with 1 kg or more of U.S. HEU for these purposes[10]
Argentina	Netherlands	Austria	Australia	Argentina
Australia	Pakistan	Chile	Brazil	Belgium
Austria	Philippines	Colombia	Jamaica	Canada
Belgium	Portugal	Denmark	South Africa	France
Brazil	Republic of Korea	Greece	Turkey	Germany
Canada	Romania	Mexico		Indonesia
Colombia	Slovenia	Philippines		Iran
Denmark	South Africa	Portugal		Israel
France	Spain	Republic of Korea		Italy
Germany	Sweden	Romania		Japan
Greece	Switzerland	Slovenia		Netherlands
Indonesia	Taiwan	Spain		Norway
Iran	Thailand	Sweden		Pakistan
Israel	Turkey	Taiwan		Switzerland
Italy	United Kingdom	Thailand		United Kingdom
Japan				
Mexico				

As shown in Figures 1 and 2 below, the bulk of U.S. HEU exports occurred in the 1960s and 70s, with the peak occurring in the late 1960s. The dramatic decline of U.S. HEU exports is attributed to the shutdown of many foreign HEU-fueled RTR facilities and programs, additional export controls imposed under the NNPA in 1978, and the establishment of DOE's GTRI/RERTR program to convert such facilities to LEU. Overall, the bulk of the U.S. HEU exports and imports (approximately 95 and 80 percent respectively) occurring prior to 1990, as displayed in Figures 1 and 2. Although there is no current requirement for U.S.-origin HEU to be returned to the United States, in August 1982, the U.S. NRC issued a "Statement of Policy on the Use of HEU in Research Reactors" (47 Fed. Reg. 37,007), expressing support for the RERTR program to convert facilities to LEU. The U.S. NRC also stated that it would perform more rigorous reviews related to U.S. supplied material used in foreign RTRs, with the intent of eliminating inventories of U.S. supplied HEU to the maximum degree possible. Furthermore, AEA Section 134 was amended in 1992 to add more stringent criteria for licensing U.S. exports of HEU to be used as fuel or targets in RTRs. In addition, NNSA/GTRI continues to work with foreign governments to return additional amounts of fresh and irradiated U.S. HEU to the United States.

Figures comparing U.S. HEU Used as Fuel or Targets in a Nuclear Research or Test Reactor

Figure 1: Exports 1957 - 2012

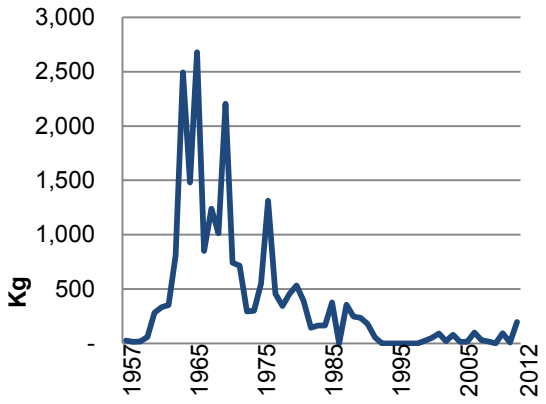

Figure 2: Imports 1957 - 2012

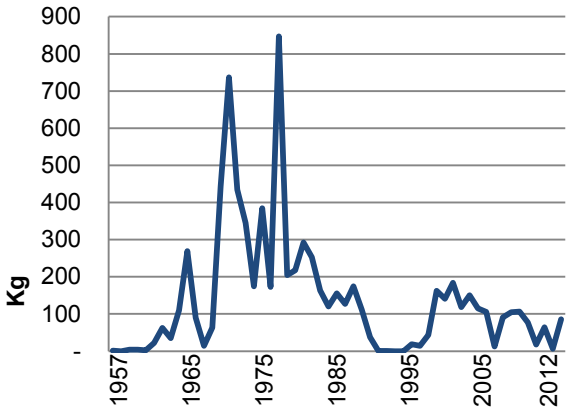

In 2005, additional criteria were added to AEA Section 134 for licensing exports of HEU to certain countries[11] for medical isotope production. Under these provisions, the U.S. NRC is required to review the adequacy of physical protection requirements that are applicable to the transportation and storage of the HEU for medical isotope production or control of residual material after irradiation and extraction of medical isotopes. If the U.S. NRC determines that additional physical protection requirements are necessary (including a limit on the quantity of HEU that may be contained in a single shipment), the U.S. NRC shall impose such requirements as licensing conditions or through other appropriate means. Presently, the United States continues to export HEU for use as RTR fuel or targets to a limited number of facilities in Canada and Europe.[12] The primary purpose of these HEU exports is to support medical isotope production.

Reconciling the Current Disposition of U.S. Exports of HEU

The U.S. Government continues to work with certain partners to reconcile inventory records. These reconciliations are not facility specific, but at a State level. The U.S. NRC does not believe that adding new inventory reconciliation or other requirements to U.S. 123 Agreements or other international instruments would be an acceptable change to the status quo in the national interests of other countries.

U.S. law has instead required the U.S. Government to obtain nonproliferation, peaceful use, and safeguards assurances from foreign government authorities on a case-by-case basis as a pre-condition for authorizing the export of any special nuclear materials, including HEU to foreign RTRs for use as fuel or targets. The U.S. Government has relied on these assurances among other factors in determining that the foreign recipient and the responsible government oversight authority will implement and maintain the controls to ensure that the nuclear materials are appropriately used, controlled and safeguarded. Additionally, the U.S. Government and the global community rely on the IAEA to conduct independent safeguards audits and inspections to verify that the records for and physical inventories of nuclear materials, whether supplied by the United States or another country, are consistent and provide no evidence of diversion.

HEU Irradiation Status and Current Physical and Chemical Forms

Approximately 60 percent of the U.S.-origin HEU remaining in foreign countries is irradiated and 40 percent is un-irradiated. Most of the irradiated material is in the form of irradiated RTR fuel, targets, and medical isotope production residues. The un-irradiated U.S. HEU at foreign facilities exists primarily in the form of fabricated RTR fuel and medical targets, but some of the un-irradiated HEU is in the form of metal, compounds, scrap, and waste.

Uses Stated in Export License, Alternative Uses, U.S. NRC-Approved Alternative Uses

In most cases, U.S. supplied HEU was used for its stated uses as described in relevant U.S. export licenses. For the most part, U.S. export licenses have anticipated the need for transfers among certain countries and typically identified approved intermediate facilities (fuel and/or target fabrication facilities) and ultimate foreign consignees (RTRs and target processing facilities). In a number of instances, and to the extent that some countries subsequently transferred and/or received U.S. supplied HEU between themselves and other countries, they were required to obtain additional approval (prior consent) from the U.S. Government to do so. Requests for prior consent are processed as “subsequent arrangements” by NNSA in accordance with Section 131 of the AEA as amended. In a limited number of cases, based on international agreements and requirements for HEU exports in effect at that time, no additional U.S. approval was required. The U.S. NRC identified 13 requests to use U.S. supplied HEU for purposes other than what was originally authorized, as noted in Table 2 on the following page.

Table 2: Requests to Use U.S.-Supplied HEU for Purposes Other than Originally Authorized[13]

Country	Original use	New use
Japan	KUHFR	KUR
	KUHFR	KUR
	KUHFR	KUR
	JMTR	JRR-4
	KUHFR	KUR
	KUHFR	KUR
	KUHFR	KUR
	KUHFR	samples
	YAYOI	Down blend
Argentina	RA-3 &RA-6	Down blend
South Africa	SAFARI	Storage
Canada	Chalk River	Dounreay

Total U.S. HEU 112.5 kg

KUHFR - Kyoto University high Flux research Reactor; KUR - Kyoto University Reactor;
JMTR - Japan Material Test Reactor; JRR-4 - Japan Research Reactor #4;
YAYOI - Research Reactor located in Japan; RA-3 - Argentina Research Reactor #3;
RA-6 = Argentina Research Reactor #6; SAFARI - South African Research Reactor;
Chalk River - Canadian nuclear site; Dounreay - United Kingdom nuclear site; Down blend - HEU into LEU

Adequate Protection against Theft and Unauthorized Access

Consistent with the current U.S. NRC export licensing criteria, physical protection measures at foreign facilities are assessed against recommendations in IAEA publication Information Circular (INFCIRC/225).[14] To determine the adequacy of physical protection measures for high-risk nuclear materials at foreign facilities, the U.S. NRC primarily relies upon bilateral physical protection information exchange and assessment visits to the foreign country.[15] These visits are conducted by a U.S. interagency team and involve exchanges of technical physical protection information as well as site-level security assessments. When appropriate, a determination is made on a country-wide basis as to whether the measures employed at a facility provide protection comparable to the INFCIRC/225 guidelines.[16]

Returned U.S.-origin HEU is stored and processed at a small number of DOE facilities as well as at U.S. NRC licensed facilities. Most of the material returned to the U.S. has been irradiated HEU fuel, but has also included un-irradiated HEU – in addition to HEU that was down-blended to LEU. The physical protection measures at these U.S. facilities are maintained, as appropriate, in accordance with either DOE or NRC requirements and they provide adequate protection of the HEU against unauthorized access and theft.

U.S. NRC has neither any evidence to suggest nor any reason to believe that any U.S. exported HEU has been stolen or diverted from a foreign facility. The U.S. NRC is confident of this assessment, based on the effectiveness of the aforementioned physical protection measures at foreign facilities to which U.S. materials have been licensed and exported. International safeguards containment, surveillance, and verification measures, and IAEA inspections provide further confidence that no U.S. HEU has been stolen or diverted. All recipient countries have provided nonproliferation and physical protection assurances and peaceful use guarantees as a precondition of supply, as required by U.S. law. Furthermore, HEU that has been transferred and/or retransferred to foreign countries has not been reported as missing or unaccounted for, nor has any country has

ever notified the U.S. Government that they lost or did not receive U.S. supplied HEU or that they relinquished control over the material.

As reaffirmed by heads of state participating in the 2010 and 2012 NSS, recipient countries are responsible for maintaining safety and ensuring the adequacy of physical protection measures for nuclear materials they receive from the United States and other countries. As part of the U.S. export licensing process, the responsible foreign government authority in the recipient country must confirm on a case-by-case basis that a facility is authorized to receive and possess the material and agree to maintain protection at least comparable to the recommendations in the current version of INFCIRC/225. The U.S. Government must receive these and other written assurances, including commitments to convert to LEU fuel or targets from the receiving country as part of the U.S. NRC export licensing process.

Documentation and Data Gaps

There are gaps and uncertainties in the historical records available to the U.S. NRC staff. The following reasons explain why the U.S. NRC was unable to fully document the status and location of all HEU exported by the United States:

- HEU transfers between countries.
- Material losses and waste
- HEU consumption in reactors
- HEU down-blending
- Co-mingling of U.S. and non-U.S. HEU
- Co-mingling of RTR and non-RTR HEU
- National classification information laws

Observations and Conclusions

The U.S. Government continues to work with its foreign partners to reconcile historical records for the disposition of the past U.S. HEU exports and to maintain an appropriate level of awareness regarding the disposition of the current and future U.S. HEU exports.

The United States continues to be a leader in the effort to reduce and eliminate the use of HEU for use in RTRs and medical isotope production. Some of the outcomes of the 2010, 2012, and 2014 Nuclear Security Summits were statements endorsing the minimization of HEU and possible replacement of HEU use in future production of medical isotopes. The United States recognizes that the peaceful use of nuclear technology can only occur when it is pursued and fostered in a way that does not compromise global security.

Acknowledgements

This paper reflects contents of the “Report to Congress on the Current Disposition of Highly Enriched Uranium Exports Used as Fuel or Targets in Nuclear Research or Test Reactors,” (January, 2014).

The authors of this paper would like to acknowledge additional individuals who reviewed and contributed to the information discussed in this paper:

Janice Owens, Janice.Owens@nrc.gov
Gary Langlie, Gary.Langlie@nrc.gov
Jenny Weil, Jenny.Weil@nrc.gov
Oleg Bukharin, Oleg.Bukharin@nrc.gov
Maureen Conley, Maureen.Conley@nrc.gov
Michelle Albert, Michelle.Albert@nrc.gov

Legal matters

Privacy regulations and protection of personal data

I agree that ESARDA may print my name/contact data/photograph/article in the ESARDA Bulletin/Symposium proceedings or any other ESARDA publications and when necessary for any other purposes connected with ESARDA activities.

Copyright

The author agrees that submission of an article automatically authorizes ESARDA to publish the work/article in whole or in part in all ESARDA publications – the bulletin, meeting proceedings, and on the website.

The author declares that their work/article is original and not a violation or infringement of any existing copyright.

Endnotes and References

[1] The National Defense Authorization Act for Fiscal Year 2013 (NDAA 2013), Title XXXI, Subtitle F, American Medical Isotopes Production Act of 2012, Section 3175, required the "Report on Disposition of Exports," by the Chairman of the NRC, to be delivered to the U.S. Congress within one year after President Obama signed the NDAA 2013 into law on January 2, 2013.
[2] The NRC 1993 report was pursuant to section 903(b) of the Energy Policy Act of 1992.
[3] The current U.S.-EURATOM 123 Agreement entered into force in March 1996 and meets the Nuclear Non-Proliferation Act of 1978. The agreement encompasses U.S. peaceful nuclear cooperation with all 28 EURATOM members. It is in force through April 2026, with an option for rolling five-year extensions.
[4] The current U.S.-IAEA 123 Agreement entered into force June 2014 and meets the Nuclear Non-Proliferation Act of 1978. It enables the U.S to supply power reactor fuel through the IAEA to Member States, under long-term Project and Supply Agreements, and remains in force until June 2054.
[5] This agreement is administered on a non-government basis by the American Institute in Taiwan.
[6] DOE has authority under section 54d. and 111b of the AEA to export up to 500 grams of HEU.
[7] NDAA 2013, Title XXXI, Subtitle F, American Medical Isotopes Production Act of 2012, Section 3175.
[8] "Communiqué of the Washington Nuclear Security Summit," (The White House, Office of the Press Secretary, Washington, DC, April 13, 2010).
[9] "The Hague Nuclear Security Summit Communiqué," (The Hague, March 25, 2014).
[10] Three countries – Chile, Jamaica, and Norway – received U.S. HEU from other countries, not directly exported from the United States.
[11] Those countries include Belgium, Canada, France, Germany, and the Netherlands.
[12] In 2013, the appropriate HEU export licenses were amended to add RTRs in Poland and the Czech Republic as temporary intermediate consignees to receive and irradiate medical isotope targets. These reactors may receive HEU targets, containing gram-quantities of HEU each, for irradiation. Following irradiation, the targets are promptly shipped away to isotope production facilities in other countries.
[13] The NRC did not locate records indicating whether these 13 requests for alternative uses were approved by the U.S. Government or whether the HEU was used for the requested alternative use.
[14] Revision 4, June 1999, ''The Physical Protection of Nuclear Material and Nuclear Facilities''
[15] High-risk materials include Category II and Category I quantities of nuclear materials. For HEU, these correspond to the material quantities containing greater than or equal to 1 kg but less than 5 kg uranium-235 (Category II HEU), and greater than or equal to 5 kg uranium-235 (Category I HEU). For material irradiated to greater than 100 r/h at 1 m, the material category is reduced by one.
[16] Country-wide determinations are usually made for lower risk, Category III or less materials (less than 1 kg uranium-235); and for nuclear sites, which have not received a U.S. Government assessment team visit, but which are located in countries where such visits have occurred. In all cases, a country-wide determination involves consideration of available public and non-public sources.

Addressing Proliferation Concerns within the Existing NRC Regulatory Framework

Thomas Grice, Brian Smith, and Brooke Smith

U.S. Nuclear Regulatory Commission
Washington, DC 20555-0001

Abstract:

Interested persons may petition the U.S. Nuclear Regulatory Commission (NRC) to issue, amend or rescind any regulation in accordance with 10 CFR § 2.206. As part of the established practice of reviewing requests for rulemaking, the NRC staff will evaluate the petition for rulemaking and any comments it received and will either consider the petition for rulemaking in the NRC's rulemaking process or deny the petition for rulemaking. On November 10, 2010, the American Physical Society (APS) submitted such a petition for rulemaking to the NRC requesting the NRC amend 10 CFR Part 70, "Domestic Licensing of Special Nuclear Material," to require each applicant for an enrichment or reprocessing (ENR) facility license in the United States to include an assessment of the proliferation risks as part of the application for an NRC license. The staff considered the petition, public comments, information related to the current threat environment, and the existing NRC licensing framework for ENR facilities and on October 25, 2012 recommended NRC denial of the petition for rulemaking to the NRC Commissioners. On May 22, 2013, the NRC Commissioners approved the staff's recommendations to deny the APS petition for rulemaking and the final decision was published in the Federal Register on June 6, 2013. This paper provides an overview of the APS petition, a summary of the NRC staff evaluation of the APS petition, overview of how NRC's existing comprehensive regulations for licensing, oversight and security of nuclear facilities protect classified information, nuclear materials and technology, and why a specific assessment of the proliferation risk by a license applicant is not warranted.

Keywords: Nonproliferation; Security; Safeguards; Regulations

1. Background

Nuclear proliferation refers to the spread of nuclear weapons and associated technology, information, materials and expertise. Nuclear nonproliferation refers to efforts to control or prevent the spread of nuclear weapons and the means to make them. Nuclear nonproliferation efforts are focused on controlling three aspects:

1) Physical access to special nuclear materials (SNM)[1] (e.g., uranium and plutonium),
2) Physical access to specialized or sensitive nuclear related equipment, i.e., Nuclear Supplier's Group (NSG) Trigger List items, and
3) Access to sensitive nuclear related information, like design specifications or operating parameters.

Although there are many possible acquisition pathways for a potential nuclear proliferator, uranium enrichment and the extraction of plutonium through reprocessing spent fuel or irradiated targets are the two primary paths for producing the nuclear material necessary for a nuclear weapon.

[1] For the purposes of this paper, the term special nuclear material can be considered interchangeable with special fissionable material, which is defined in the IAEA statute.

Nonproliferation is a crucial policy and technical focus of the U.S. Government and the international community. The NRC works closely with its U.S. interagency partners and supports U.S. nonproliferation policy by ensuring NRC-licensed facilities are constructed and operated safely and securely, international safeguards obligations are met, and that nuclear materials and classified information are properly protected. This is achieved through licensing nuclear facilities, licensing exports of nuclear materials and nuclear related equipment, and oversight of the NRC's licensees' implementation of NRC regulations (e.g., material control and accounting, physical protection, IAEA safeguards, personnel security, information protection, and export controls) and voluntary commitments incorporated into a facility's license.

On November 10, 2010, the NRC received a Petition for Rulemaking filed by Dr. Francis Slakey, Ph.D., on behalf of the American Physical Society requesting the NRC revise its regulations to require that each applicant for an enrichment or reprocessing facility license provide an assessment of the proliferation risks associated with the construction and operation of the proposed facility and assigned it Docket No. PRM-70-9. The NRC published a notice of receipt of the petition and request for public comment in the Federal Register (FR) on December 23, 2010 (75 FR 246). In accordance with established NRC practices, NRC staff evaluated the petition for rulemaking and corresponding comments, reviewed the NRC's role within the overall U.S. nonproliferation program, and the adequacy of the requirements found in existing NRC regulations to meet these nonproliferation objectives and commitments. On October 25, 2012, the NRC issued SECY-12-0145, "Denial of Petition For Rulemaking (PRM-70-9) – American Physical Society," which detailed staff's analysis and recommendation to the NRC Commissioners to deny the petition for rulemaking. Upon review of staff's completed analysis, the Commission voted to deny the petition for rulemaking in agreement with staff's conclusion that the NRC's comprehensive regulatory framework appropriately assesses proliferation risks and concerns associated with the licensing of an enrichment or reprocessing facility in the United States. This framework includes:

1) Licensing and regulatory requirements;
2) Oversight and enforcement; and
3) Active interagency cooperation.

This position was subsequently published in the June 6, 2013, Federal Register notice "Nuclear Proliferation Assessment in Licensing Process for Enrichment or Reprocessing Facilities; Petition for Rulemaking; denial," (78 FR 33,995; June 6, 2013).

2. Existing NRC Regulations

Nonproliferation is addressed in several areas of the Title 10 of the Code of Federal Regulations (10 CFR). Licensees must demonstrate satisfactory programs, plans and procedures to comply with these requirements as part of the licensing process. In reviewing a license application, renewal application, or license amendment for a fuel cycle facility, the staff must determine whether there is reasonable assurance that the facility can and will be operated in a manner that will not be inimical to the common defense and security, and will adequately protect the health and safety of workers, the public, and the environment. Nonproliferation issues are addressed through three distinctive, yet inter-related licensing mechanisms within existing NRC regulation. These are:

1) Limiting the availability of special nuclear material (SNM) by controlling the creation of and access to SNM, with specific consideration for uranium enrichment facilities;
2) Control of proliferation sensitive technologies, both information and equipment, through physical protection, information protection, counterintelligence programs and export controls; and
3) Participation in international activities to control nuclear materials, technology, facilities and equipment.

While each area possesses unique attributes, the three areas are woven together through the NRC licensing process to provide a "defense-in-depth" approach to help prevent the proliferation of nuclear weapons through the control of SNM, nuclear facilities, equipment and/or proliferation sensitive technologies.

In addition to the domestic requirements set forth to obtain a NRC license, 10 CFR also includes specific regulations to implement the requirements established by treaties between the United States and the IAEA. These specific requirements to allow the application of IAEA safeguards in accordance with the U.S.-IAEA Safeguards Agreement and establish reporting requirements for licensees related to the U.S. Additional Protocol are codified in 10 CFR Part 75. If a particular NRC licensed facility is selected by the IAEA for the application of safeguards, the commitments negotiated in the facility attachment are incorporated into the facilities license.

3. Physical Access to Special Nuclear Materials

Several areas of the NRC regulations address nonproliferation through the minimization of the use of highly enriched uranium (HEU) and plutonium, the consideration of theft or diversion of SNM, and the detection of the production of unauthorized enriched uranium. These include 10 CFR Part 70, *Domestic Licensing of Special Nuclear Material*; 10 CFR Part 73, *Physical Protection of Plants and Materials*; and 10 CFR Part 74, *Material Control and Accounting of Special Nuclear Material*.

Regulations under 10 CFR Part 70 are the foundation for the issuance of licenses to receive title to own, acquire, deliver, receive, possess, use, and transfer special nuclear material. While focused on the licensing process (i.e., content of applications, license modification and renewal) and safety (radiological health and safety, environmental protection, and accident analysis), the regulations also recognize that requirements should differ based on the type and amount of material possessed by licensees. For licensees possessing small quantities of SNM, 10 CFR 70.20a contains basic requirements that require general licensees to provide for the physical protection of such material against theft or sabotage. For licensees with larger, more significant quantities of SNM, 10 CFR Part 70 refers to 10 CFR Parts 73 and 74 for additional requirements related to physical protection and material control and accounting requirements.

Regulations under 10 CFR Part 73 prescribe the requirements for the establishment and maintenance of a physical protection system to protect SNM at fixed sites and in transit, and to protect plants where SNM is used. At Category I facilities, these regulations include requirements to protect against radiological sabotage and to prevent the theft and diversion of SNM through the establishment of physical protection requirements for facilities and materials including armed protective force personnel, physical barriers, access controls, intrusion detection and surveillance systems, criminal background checks, portal monitors and response procedures. For example, 10 CFR 73.67 and 73.71 include physical protection requirements for SNM of moderate and low strategic significance and reporting requirements for safeguards events. In addition, 10 CFR 73.73 and 73.74 include requirements for advance notice and protection of export and import shipments of specified materials. Further, Appendix B to 10 CFR Part 73 contains the Criteria for Security Personnel (training) for these types of facilities and Appendix C to 10 CFR Part 73 includes detailed requirements for a safeguards contingency plan.

Regulations under 10 CFR Part 74 include requirements for the control and accounting of SNM at facilities and for documenting the transfer of SNM. For example, general performance objectives in 10 CFR 74.31, 74.41, and 74.51 address material control and accounting (MC&A) requirements for various levels of strategic significance. To meet these objectives, licensees must have a Fundamental Nuclear Material Control Plan that includes measures to ensure proper control of and accounting for the SNM possessed by the licensee. These MC&A programs are designed to track and account for SNM using accepted accounting practices, ensure the presence of SNM through physical inventory and inventory reconciliation programs, and maintain accurate values for SNM at the facility through measurement and measurement control programs. Through this combination of measures, licensees provide further assurance that SNM is properly controlled and maintained. These activities also provide a significant deterrent to potential theft or diversion scenarios through their ability to identify potential losses, and aid in or conduct investigations into SNM losses. Additionally, 10 CFR 74.33 requires licensees authorized to possess equipment capable of enriching uranium or operating a uranium enrichment facility, and producing, or possessing a specified amount of SNM, to have an MC&A system that will protect against and detect unauthorized production of enriched uranium or enrichment to levels beyond 10 percent. Finally, 10 CFR 74.11 includes requirements for licensees that possess specified quantities to report loss, theft or attempted theft or unauthorized production of SNM to the NRC. By requiring capabilities to measure, control, detect, and report the loss, theft or

attempted theft or unauthorized production of SNM, a licensee's compliance with 10 CFR 74 supports the overall objectives of the U.S. nonproliferation program.

4. Access to Sensitive Nuclear Related Technology, Information and Equipment

Controls of proliferation sensitive technology, information and equipment are addressed in a similar manner. The NRC regulations relevant to controlling access to sensitive nuclear related equipment include: 10 CFR Part 25, *Access Authorization*; 10 CFR Part 95, *Facility Security Clearance and Safeguarding of National Security Information and Restricted Data*; 10 CFR Part 110, *Export and Import of Nuclear Equipment and Material*.

In addition to these NRC regulations, NRC licensees are also subject to the requirements established in 10 CFR Part 810, *Assistance to Foreign Atomic Energy Activities*, which implements section 57 b.(2) of the Atomic Energy Act of 1954 and regulates civil nuclear trade to ensure that nuclear technologies and assistance exported from the United States will be used for peaceful purposes.

Regulations under 10 CFR Part 25 establish the requirements and procedures for granting, reinstating, extending, transferring, and terminating access authorizations of licensee personnel, licensee contractors or agents, and other persons who may require access to classified information. Included in these requirements is submission of the following information:

1) A completed Questionnaire for National Security Positions (SF-86, Parts 1 and 2)
   The SF-86 is the standard questionnaire used to obtain relevant information for a clearance investigation
2) Two standard fingerprint cards (FD-258)
3) Security Acknowledgment (NRC Form 176)
   The Security Acknowledgment form documents an individuals is knowledgeable and understands the controls over access, handling, and dissemination of, classified information; and
4) Other related forms where specified in accompanying instructions.

This information is used by the Office of Personnel Management to determine whether an individual should be granted the requested U.S. Government security clearance. NRC licensees and licensee contractors may be granted a "Q" access authorization or "L" access authorization, depending upon the level and category of classified information to be accessed. These access authorization requirements address an employee's suitability, trustworthiness and reliability before and during the time an employee or contractor works at the facility. Additionally, periodic reviews of an individual's background and trustworthiness continue during the individual's employment. An important aspect of this program is informing the employees of their continuing responsibilities with respect to protection of classified information upon termination of their employment.

Similar to the controls established in 10 CFR Part 73 for physical access to SNM, 10 CFR Part 95 establishes requirements for access to and the physical protection of classified information, including classified documents, materials and equipment. 10 CFR 95.25 and 95.27, respectively, establish the requirements for licensees to maintain appropriate protection of National Security Information and Restricted Data while in storage and in use. These requirements address all of the areas routinely associated with a classified information protection program.

It should also be recognized that NRC enrichment licensees and their contractors that possess classified material have voluntarily committed to adhere to additional information security measures not addressed in 10 CFR Part 95. These voluntary security enhancements are set forth in Nuclear Energy Institute (NEI) 08-11, "Information Security Program Guidelines for Protection of Classified Material at Uranium Enrichment Facilities," and NEI 13-04, "Counterintelligence Program for Uranium Enrichment Facilities" published by the NEI. These documents provide guidance for the protection of classified information, equipment, and technology and recommend the development and implementation of several programs and additional requirements. The measures are contained in each licensee's security plan, which is an integral component of their license and specifically approved by the NRC as part of the issuance of a facility security clearance prior to facility operation. This allows these requirements to be used as the basis for enforcement action if a licensee violates

the terms of the plan. The Information Security (INFOSEC) additional measure program requirements include:

1) Operations Security (OPSEC) Program
2) Telecommunications Electronic Materials Protected from Emanating Spurious Transmissions (TEMPEST) program
3) Technical Surveillance Countermeasures (TSCM) Program
4) Counterintelligence (CI) Program
5) Information Technology (IT) Security requirements for classified networks
6) Classified Item Control and Inventory (CICI) requirements
7) Defensive Counterintelligence Program

In addition to these requirements, the NRC regulates the export and import of nuclear related materials and equipment under 10 CFR Part 110. Included in the appendices to Part 110 are illustrative lists of regulated equipment specific to various enrichment technologies and reprocessing plants. 10 CFR Part 110, “Export and Import of Nuclear Equipment and Material,” includes requirements for controlling the export and import of nuclear materials and equipment by NRC or Agreement State licensees. Export license reviews address proliferation concerns by requiring the U.S. Government to obtain assurances from the recipient foreign government that, among other things, include: 1) IAEA safeguards will be applied as required by Article III (2) of the Treaty on the Nonproliferation of Nuclear Weapons; 2) adequate physical security measures will be maintained; and 3) the material being exported will not be transferred to another country without prior U.S. Government approval. These export applications are reviewed by multiple offices within the NRC and also by other U.S. Government agencies (i.e., U.S. Departments of State, Defense, Commerce, Energy, and Homeland Security) to assess security concerns and proliferation risks. 10 CFR 110.27 authorizes, by general license, the import of nuclear material if the U.S. consignee is authorized to receive and possess the material under the relevant NRC or Agreement State regulations. By controlling the export and import of nuclear materials and equipment, these requirements address proliferation risks and concerns. The additional voluntarily adopted security practices further enhance the protection of sensitive nuclear related technology, information and equipment.

5. Control of Classified Data Systems

Based on past experience and anticipated activity, any NRC licensee that owns or operates a uranium enrichment facility will need to possess a classified information data system. The National Industrial Security Program (NISP), established by Executive Order (E.O.) 12829 for the protection of classified information classified under Executive Order 12958, as amended, or its successor or predecessor orders, and the Atomic Energy Act of 1954, as amended, requires that classified information can only be processed on secure information technology (IT) systems or networks that have been accredited by certain agencies of the Federal government. This includes both the NRC and the U.S. Department of Energy (DOE). The NISP Operating Manual (NISTPOM) is set forth in Department of Defense (DoD) 5220.22-M, and requires that for a specific classified IT system a Federal government agency must agree to serve as the Designated Approval Authority (DAA). The DAA is responsible for inspecting the classified IT system to determine that it is installed and capable of operating in accordance with all applicable security requirements. After the DAA makes a favorable determination, an accreditation statement is issued that authorizes the system to be operated.

As the licensing authority for commercial uranium enrichment facilities in the United States, the NRC is responsible for enforcing any violations of the licenses issued to these facilities, including any security violations. Therefore, in order to avoid the appearance of a conflict of interest, NRC entered into a Memorandum of Understanding (MOU) with DOE to allow DOE to act as the DAA for NRC licensed uranium enrichment facilities. All classified cyber security plans and their corresponding computer systems will be assessed in accordance with this agreement between the NRC and the DOE. As such, DOE conducts site audits, with NRC presence, and reports the results to the NRC and the inspected NRC licensee. Based upon the results of these inspections, the NRC will authorize operation of the computer systems following approval and accreditation by the DAA. Each enrichment facility license includes a requirement for an accredited information technology (IT) plan in their Standard Practice Procedures Plan (SPPP). This IT plan is updated as the DAA requirements change and the licensee must obtain NRC approval of any substantive changes to the plan.

6. NRC Oversight Activities

Each of the preceding areas mentioned are not only licensed by the NRC, but also routinely inspected by the NRC and subject to the NRC Enforcement Program. Inspections are performed to verify a licensee's compliance with all applicable regulations, and all commitments contained in the licensee's plans and procedures which have been incorporated into the operating license. Any deficiencies that are identified are evaluated using a graded approach based upon actual consequences, potential consequences, potential for impacting the NRC's ability to perform its regulatory function, and any willful aspects of the violation. All cited violations require licensees to provide the NRC with a written response with details of the proposed corrective actions to correct the issue and prevent recurrence. Significant violations may result in civil penalties or the issuance of orders by the NRC. In addition to regular inspection oversight, each licensee's performance is monitored on a routine basis. If a licensee's performance warrants, the NRC may take such actions and increase oversight through special inspections, augmented inspections or increasing the frequency of routine core inspections. Through this oversight and enforcement process, the NRC ensures licensees are maintaining the proper controls to operate the licensed facilities in a safe and secure manner.

7. Licensee Performance of a Proliferation Assessment

In addition to evaluating the adequacy of NRC's regulatory framework, NRC staff also considered the potential benefit of licensees conducting proliferation assessments for their facilities. Staff concluded a commercial entity would not have access to the necessary intelligence resources, capabilities, and information essential to compiling a meaningful nuclear proliferation assessment.

The task of assessing proliferation risks is best performed by the Federal Government. Other Federal agencies, including the Department of State, the Department of Energy, the Department of Defense, and the Department of Commerce along with the NRC, have primary responsibility for implementing national nonproliferation policies and goals and conducting proliferation assessments of sensitive technologies, including nuclear technologies. Staff in these agencies have access to the necessary classified information and are better informed concerning the motives and intent of potential proliferators. This information is closely held and would not be available to an NRC licensee or applicant for use in their evaluation. An assessment based solely on information available to a commercial entity would be of little value to the NRC in assessing the proliferation risks associated with licensing a particular facility.

8. Conclusion

The mission of the NRC is to license and regulate the Nation's civilian use of byproduct, source, and special nuclear materials to ensure the adequate protection of public health and safety, promote the common defense and security, and protect the environment. One of the NRC's primary concerns is to ensure that the facilities it regulates that manufacture or use enriched uranium and plutonium do so safely and securely. The NRC's regulations on physical security, information security, material control and accounting, IAEA safeguards, cyber security, and export control create a tapestry of protection for the material and technology at NRC-regulated fuel cycle facilities. These regulations, which focus on preventing, deterring, and detecting the theft or diversion of radioactive materials and classified technologies, ensure proliferation considerations are taken into account during the licensing and oversight activities of the NRC. Consistent with its statutory authority under the Atomic Energy Act (AEA) of 1954, as amended, the Commission will not issue a license for an ENR facility if it determines that such a facility would constitute an unreasonable risk to the health and safety of the public or would be inimical to the common defense and security.

Session 22

Nuclear Material Accountancy

THE USE OF MEASUREMENT UNCERTAINTY IN NUCLEAR MATERIALS ACCOUNTANCY AND VERIFICATION

O. Alique; S. Vaccaro; J. Svedkauskaite

Nuclear Safeguards Directorate E, DG Energy, European Commission,
L-2920 Luxembourg, Luxembourg

Abstract:

EURATOM nuclear safeguards are based on the nuclear operators' accounting for and declaring of the amounts of nuclear materials in their possession, as well as on the European Commission verifying the correctness and completeness of such declarations by means of conformity assessment practices. Both the accountancy and the verification processes comprise the measurements of amounts and characteristics of nuclear materials. The uncertainties associated to these measurements play an important role in the reliability of the results of nuclear material accountancy and verification.

The document "JCGM 100:2008 Evaluation of measurement data – Guide to the expression of uncertainty in measurement" - issued by the highest international instances in metrology, standardisation, accreditation, physics and chemistry - describes a universal, internally consistent and transferable method for the evaluation and expression of uncertainty in measurements.

This paper discusses different processes of nuclear materials accountancy and verification where measurement uncertainty plays a significant role. It also suggests the way measurement uncertainty could be used to enhance the reliability of the results of the nuclear materials accountancy and verification processes.

Keywords: measurement uncertainty, conformity assessment, verification

1. Euratom Nuclear Safeguards operating principle

The holders of nuclear materials in the European Union are subject to Euratom nuclear safeguards. The obligations for nuclear operators derived from nuclear safeguards include the implementation of a Nuclear Material Accountancy and Control (NMAC) system and the declaration of nuclear materials flows (monthly) and stocks (yearly). The European Commission verifies consequently the correctness and completeness of the declarations produced for nuclear materials flows and stocks by means of inspections. In a nutshell, Euratom nuclear safeguards are based on three sequential processes:

1. Accountancy and control of nuclear materials, performed by nuclear operators;
2. Declaration to the European Commission of flows and inventories of nuclear materials, performed by nuclear operators; and
3. Verification of the correctness and completeness of these declarations by the European Commission.

Measurements and measurement uncertainties play a crucial role in the first and third processes. The role of measurement uncertainty and the way it is estimated and reported has been discussed on several occasions without reaching a clear agreement amongst the nuclear safeguards community. A deeper analysis can assist safeguards practitioners to understand the role of measurement uncertainty.

2. International standardisation of measurement uncertainties and application to Nuclear Safeguards

The metrology community has discussed for long in its attempt to find a harmonised way of reporting uncertainty. In 1977, recognizing the lack of international consensus on the expression of uncertainty in measurement, the world's highest authority in metrology, the 'Comité International des Poids et Mesures' (CIPM), requested the 'Bureau International des Poids et Mesures' (BIPM) to address the problem in conjunction with the national standards laboratories and to make a recommendation.

The BIPM prepared a detailed questionnaire covering the issues involved and distributed it to 32 national metrology laboratories known to have an interest in the subject (and, for information, to five international organizations). The BIPM then convened a meeting for the purpose of arriving at a uniform and generally acceptable procedure for the specification of uncertainty; it was attended by experts from 11 national standards laboratories. This Working Group on the Statement of Uncertainties developed Recommendation INC-1 (1980), Expression of Experimental Uncertainties [1]. The CIPM approved the Recommendation in 1981 and reaffirmed it in 1986.

The task of developing a detailed guide based on the Working Group Recommendation (which is a brief outline rather than a detailed prescription) was referred by the CIPM to the International Organization for Standardization (ISO), since ISO could better reflect the needs arising from the broad interests of industry and commerce.

In 1995, the JCGM (Joint Committee for Guides in Metrology) formed by the highest instances in chemistry, physics, metrology and standardisation, issued the first version of the Guide to the Expression of Uncertainty in Measurement (GUM). In 2008, a second version of the GUM [2] was published. Together with its supplements, this is the most recent international standard in the matter globally accepted.

It is important to note that not every actor of the nuclear safeguards community has incorporated to their practices the use of measurement uncertainties calculated according to the GUM Guide [2]:

- **Laboratories** providing measurement results to the nuclear inspectorates and nuclear operators laboratories provide uncertainties calculated according to the GUM Guide [2].
- Measurements performed at **nuclear facilitie**s by plant staff do not always carry uncertainties calculated according to the GUM Guide [2]. Frequent examples are mass and volume measurements performed in the operations areas.
- Traditionally **nuclear inspectorates** have been using the classical statistical model of error for uncertainty calculation and for measurement data evaluation. The harmonized standard method for estimation and use of measurement uncertainty is not used by nuclear inspectorates 30 years after the first issue of this international standard.

3. Accountancy and control of nuclear materials

Nuclear operators account for and control all nuclear materials inside the Material Balance Areas (MBA) for which they are responsible. This process includes accounting for every amount of nuclear material entering or leaving the MBA and taking an inventory of the nuclear material held in the MBA once per year. When the nuclear material is in loose form, at any stage of the processes which take place in the MBA, measurements will play an important role in the accountancy process.

In this case the legislation in force, specifically Article 7 of the Commission Regulation (Euratom) 302/2005 of 8 February 2005, on the application of Euratom safeguards [3], obliges the measurement system used for accountancy purposes to be conform or equivalent in quality to the latest international standards. This legal requirement is often interpreted as the uncertainties of the nuclear operators' measurements to be equal or less than those expressed in the International Target Values (ITV) [4] issued by the IAEA (International Atomic Energy Agency). However, the ITVs are not standards with requirements on the quality of measurement systems. They are reference values to be used by every actor in nuclear safeguards in order to evaluate their measurement performance when validating their measurement methods or assessing their fitness for purpose.

There exist international standards that contain requirements about the quality of measurement systems. The most widely recognised standards are:

- ISO 17025:2005. General requirements for the competence of testing and calibration laboratories [5]
- ISO 10012:2003. Measurement management systems -- Requirements for measurement processes and measuring equipment.[6]

Both standards require that measurement methods are validated, and that measurement results are metrologically traceable. This condition requires the measurement results to be traceable to a unit of the International System of Units by an unbroken chain of calibrations, each one contributing to the final uncertainty of the result. It is therefore implicit as a requirement that every measurement performed with nuclear materials accountancy purposes must be reported together with its associated uncertainty.

Other than the quality of the measurement systems, the European Commission imposes to nuclear operators the obligation of keeping operating records. Regulation 302/2005 [3] stipulates in its article 8 that:

> "For each material balance area, the operating records shall include, where appropriate:
> […]
> (c) the data, including derived estimates of random and systematic errors, obtained from the calibration of tanks and instruments as well as from sampling and analysis;
> (d) the data resulting from quality control measures applied to the nuclear material accountancy system, including derived estimates of random and systematic errors;"

The expression *'estimates of random and systematic errors'* must be understood here as the combined standard uncertainty as defined in the GUM [2]. It is important to note that no requirement exists for accompanying the declarations performed by the nuclear operators about nuclear materials with the associated uncertainties that these data hold, when they are originated by measurements.

The same applies for the requirement of stating estimations of random and systematic errors as stated in Annex I of the above mentioned Regulation 302/205 [3], with the purpose of declaring the Basic Technical Characteristics of the installation. This declaration must respond to a typical uncertainty obtained, so it must be interpreted as the maximum acceptable uncertainty for the nuclear operator.

The different measurements performed in nuclear materials accountancy can be grouped in two categories with respect to the uncertainty calculations required:

1. **Measurements performed in analytical laboratories**, which are in most of the cases metrologically traceable. These measurements are designed to obtain low uncertainties. Typically individual uncertainties are calculated for every measurement result, according to the GUM guide [2]. Titrations, mass spectrometry or calorimetry are good examples of this type of measurements.
2. **Measurements performed on industrial plants**. These measurements can be grouped as:
    a. Nuclear measurements. These measurements are designed to provide fast results without generating any waste and not destroying the sample analysed. The uncertainties obtained are normally bigger than those obtained in analytical laboratories. Often the full metrological traceability of these measurements is not ensured.
    b. Mass and volume measurements. When mass and volume measurements are performed in an industrial environment, an overall uncertainty associated with the instrument can be attributed to every measurement performed by that instrument, avoiding the necessity to perform uncertainty calculations for every measurement performed. This practice is only acceptable when three conditions are fulfilled:
        i. The overall uncertainty for the measurement instrument is recalculated after calibration;
        ii. Appropriate quality control is applied to the measurement device to ensure that last calibration is still valid;

iii. The environmental conditions influencing the measurement are monitored and acceptance limits have been set-up in advance.

It happens more often than expected that mass and volume measurements in industrial plants are not metrologically traceable, The most common reasons for this are the use of inappropriate standards for calibration or the incorrect uncertainty calculations.

Another important aspect of nuclear materials accountancy and control where measurement uncertainty plays an important role is the Material Balance Evaluation (MBE). MBE performed by nuclear operators consists in evaluating the difference between the results obtained in the accountancy books and the physical reality. This difference is named MUF (Material Unaccounted For). In installations that handle and measure materials in loose form (liquid, gas or powder), the MUF figure stemming from a physical inventory taking will be different to zero. The potential causes of MUF are:

- Clerical mistakes
- Hidden inventories non accounted for
- Hidden loses non accounted for
- Legitimate measurement errors.

From these potential causes, only the last one is acceptable. In order to assess whether the MUF can be justified by legitimate measurement errors, it is compared with the parameter σ_{MUF}. σ_{MUF} is the result of properly propagating all the uncertainties associated to the measurements that could explain the difference between accountancy books and physical reality. In order to perform a reliable assessment of MUF, the uncertainties propagated into σ_{MUF} must all be comparable and realistic. The method described in the GUM [2] provides uncertainty values that take into account all relevant factors and are comparable, transferrable and auditable. Moreover, the combined standard uncertainty provided according to the GUM [2] has the mathematical form of a standard deviation. This allows for statistical testing of MUF considering this parameter as a normally distributed variable.

4. Verification of the correctness and completeness of these declarations by the European Commission

The European Commission verifies the correctness and completeness of nuclear materials declarations provided by nuclear operators, following a series of conformity assessments. They are grouped according to their objectives in three groups:

1. *First layer assessments*. This first group of conformity assessment activities serves as preparation for the physical verification of the nuclear materials declarations. They include the periodical verification of the Basic Technical Characteristics of the nuclear installations and the assessment of the correspondence between the nuclear materials declarations, accountancy records and operational records kept by nuclear operators. Further, the correctness in format and consistency of declarations provided to the European Commission is also checked. Finally, the quality of the measurement systems of the nuclear operators is evaluated.
   One basic activity performed to evaluate the quality of the nuclear operators' measurement systems is the performance of independent measurements and comparison of the results obtained by the nuclear operators and the inspectorate. This assessment is performed according to the definition of metrological compatibility from the International Vocabulary of Metrology (VIM) [7]:

   "Metrological compatibility of measurement results is a property of a set of measurement results for a specified measurand, such that the absolute value of the difference of any pair of measured quantity values from two different measurement results is smaller than some chosen multiple of the standard measurement uncertainty of that difference.
   Metrological compatibility of measurement results replaces the traditional concept of 'staying within the error', as it represents the criterion for deciding whether two measurement results refer to the same measurand or not. If in a set of measurements of a measurand, thought to be constant, a measurement result is not compatible with

the others, either the measurement was not correct (e.g. its measurement uncertainty was assessed as being too small) or the measured quantity changed between measurements.
Correlation between the measurements influences metrological compatibility of measurement results. If the measurements are completely uncorrelated, the standard measurement uncertainty of their difference is equal to the root mean square sum of their standard measurement uncertainties, while it is lower for positive covariance or higher for negative covariance."

Hence, for fully independent measurements between the nuclear operator and nuclear inspector, the assessment on the compatibility is done according to the following formula:

$$\left|R_{op} - R_{ins}\right| \leq k \cdot \sqrt{u_{op}^2 + u_{ins}^2}$$

Where:
R_{op} is the measured value obtained by the nuclear operator,
R_{ins} is the measured value obtained by the inspectorate,
u_{op} is the combined standard uncertainty of the nuclear operator result,
u_{ins} is the combined standard uncertainty of the inspectorate result.
k is a constant to be chosen in function of the risk of false alarm. Typically, in nuclear safeguards assessments k equals three, which corresponds to a false alarm rate of 0.135 %

2. *Physical verification of nuclear materials*. This group includes physical verification techniques as identification, item counting, qualitative testing, quantitative testing, as well as verification of the results of containment and surveillance techniques.

Quantitative testing of nuclear materials with the purposes of physical verification implies the conformity assessment of a declaration with the support of a measurement result. This conformity assessment activity is different to the assessment of the nuclear operators' measurement system in different aspects:

- The first difference originates from the property of nuclear material declarations not holding an associated uncertainty, contrary to measurement results provided by nuclear operators as operating records. Therefore, the conformity assessment for nuclear materials declarations cannot be supported in the concept of metrological compatibility.
- Another difference lies in the fact that nuclear materials declarations can refer to an item, or a batch of items, or a bulk amount of nuclear materials, so to support the conformity assessment in a measurement result often a sampling process takes place. Therefore, occasionally the sampling uncertainty will have a crucial importance in the conformity assessment of nuclear materials declarations.
- Another difference comes from declarations that could originate from estimations, calculations, or measurements not performed directly on the referred item or batch, but on the material while being in previous phases of the industrial process.
- Finally, there is a difference in the fact that often the inspectorate uses measurement techniques of lower accuracy than the techniques used by nuclear operators to produce their declarations, which influences strongly the conformity assessment process.

Therefore, for quantitative testing of nuclear materials with the purpose of physical verification, it is necessary to set a decision rule[1] to document the judgement of conformity based on a measured value and its uncertainty. There is extensive literature on how to set decision rules when the conformity assessment is based on the measurement of a property of the item to assess, and the conformity is conditioned by tolerance limits in the form of intervals or thresholds. The decision rules are set in function of the risk that can be assumed of judging an item as conform when this is not the case and the risk of rejecting a conforming item.

[1] From JGCM 106:2012 [8]
"Decision rule":
documented rule that describes how measurement uncertainty will be accounted for with regard to accepting or rejecting an item, given a specified requirement and the result of a measurement.

Unfortunately, there is limited literature that refers to the use of measurement uncertainty for the assessment of nuclear materials declarations. There is a generally applied decision rule used in nuclear safeguards based on the measurement uncertainty obtained by the inspectorate. Acceptance is granted to the declaration if:

$$|D - R_{ins}| \leq k \cdot u_{ins}$$

Where:
D is the declared value for the assessed property of an item or batch of nuclear materials,
R_{ins} is the measured value by the nuclear inspectorate for the same property of the item/batch
u_{ins} is the combined standard uncertainty of the inspectorate result
k is a constant.

Typically, in nuclear safeguards assessments k has been assigned a fixed value equal to three. However, the risk that the inspectorate and the nuclear operator can assume of accepting a non-conform declaration or rejecting a conform declaration is not always the same. It depends on the type and amount of nuclear material measured, on the measurement method used, on the uncertainty obtained, on the possibilities to repeat the measurement and the cost of it, etc…

This is why, documented decision rules with clear risk assessments shall be performed by the inspectorates instead of using a fixed value for the constant *k*.

A practical application can be explained with two examples. In cases a and b the declaration by the nuclear operator refers to an item and it is based on indirect measurements, i.e. the measurement of the amounts and characteristics of the nuclear material contained in the item has not been performed on the item, but in previous stages of the industrial process having the considered item as a product. In both cases, the inspectorate will perform direct measurements on the considered item to assess the conformity of the nuclear operator's declaration:

a. The nuclear operator declares the mass of uranium contained in a fresh fuel element prepared for shipment in a fuel fabrication plant. In this case, the operator will declare the mass of uranium contained based on the measurements performed during the fabrication process, whereas the inspectorate performs a non-destructive measurement, by Active Neutron Coincidence Collar, directly on the fuel element with uncertainties going up to 11% of the measured value.
b. The nuclear operator declares the mass of plutonium oxide contained in cans produced in a reprocessing plant. The operator declares a mass value based on analysis performed during the chemical reprocessing process and weighing, while the inspectorate performs a non-destructive assay, by a combination of gamma spectroscopy and passive neutron coincidence counting, with uncertainties going up to 2%. Complementary to this, the nuclear inspectorate is branched to the weighing device of the nuclear operator, obtaining the weighing results and assesses the nuclear operator's measurement system quality by means of destructive assay.

The cases a and b are totally different from the safeguards risk point of view regarding the amount and type of material, the cost of a second measurement or the consequences regarding nuclear safeguards of a non-conform result. That is why the value of k should be used to adjust the risk assumed by the inspectorate of declaring conform a non-conform declaration and the risk assumed by the nuclear operator of getting non-conformity over a conform declaration.

3. *Material Balance Evaluation*. This is a group of activities that have the objective of gaining additional assurance on the correctness and completeness of the nuclear material declarations. The accountancy and physical verification processes are strongly based on measurements, therefore they are strongly influenced by measurement uncertainty. By assessing the declared MUF by nuclear operators, the nuclear inspectorate mitigates the risk

of the nuclear safeguards conclusions drawn being erroneous due to inaccuracies in measurements.

In order to assess the declared MUF by the nuclear operators, the inspectorate has to obtain a figure for $\sigma_{MUF.}$ This can be properly done only by propagating the measurement uncertainties over the material balance period to evaluate. This information is not known to the inspectorate, and a recurrent practice is to estimate a figure for σ_{MUF} from other data as uncertainties declared in the BTC (Basic Technical Characteristics) or using the ITVs (International Target Values). An alternative technique used is to estimate the measurement uncertainties from the statistical analysis of paired measurement results and induction of uncertainty values from a set of estimators. Any of the above mentioned techniques draw an overestimation of the σ_{MUF} value, hence decreasing the added value of this assessment. We strongly argue that it would be more reasonable to audit and validate all the components of the σ_{MUF} value performed by the nuclear operator and then use it in the consequent tests, which is why a realistic and auditable way of estimating uncertainties becomes very important for the benefit of nuclear safeguards conclusions.

Another important assessment that takes place in the phase of Material Balance Evaluation is the assessment of shipper-receiver differences. When a shipper MBA declares a different value for the transferred nuclear material than the receiver MBA, the inspectorate must assess whether this difference is due only to legitimate measurement errors. To do that, the inspectorate will again support its decision in the definition of metrological compatibility of measurements, by applying the following formula:

$$|R_{sh} - R_{re}| \leq k \cdot \sqrt{u_{sh}^2 + u_{re}^2}$$

Where,

R_{sh} is the measured value obtained by the nuclear operator shipping the nuclear material,
R_{re} is the measured value obtained by the nuclear operator receiving the nuclear material,
u_{sh} is the combined standard uncertainty of the result obtained by the nuclear operator shipping the nuclear material,
u_{re} is the combined standard uncertainty of the result obtained by the nuclear operator receiving the nuclear material.
k is a constant to be chosen in function of the risk of false alarm. Typically, in nuclear safeguards assessments k equals three.

Again the use of the constant k shall be optimised by the inspectorate as a function of the risks assumed by the nuclear operators and the inspectorate.

Conclusions

- Measurement uncertainties are an essential element in the nuclear material accountancy and control processes.

- The use of measurement uncertainties calculated according to the GUM Guide should be extended to all safeguards actors.

- Measurement uncertainties are involved in a number of conformity assessments leading to drawing nuclear safeguards conclusion, so they play a very important role in nuclear safeguards.

- Since these conformity assessments are based in the comparison of measurement results and the respective uncertainties, it is crucial for the reliability of the assessments to ensure the metrological traceability of the measurements and the compatibility of the measurement uncertainty calculations. The use of the most widely accepted methodology to estimate

measurement uncertainties by nuclear operators and inspectorates becomes crucial to the reliability of the nuclear safeguards system.

- In order to optimize the use of measurement results and their associated uncertainties in nuclear safeguards, the inspectorates shall introduce the concept of risk in their decision rules for conformity assessment.

All the proposed improvements in the nuclear safeguards practices come at a cost. The benefit and cost of improvements needs to be assessed beforehand, however, some of the requirements for measurement systems have already been implemented in several disciplines running from nuclear safety to industrial products trade showing an important rate of return. It is calculated that for an industrialized country, measurements performed according to agreed metrology practices cost around 3% of GDP, returning around 9% of the GDP.

References

[1] KAARLS, R. (1981), *BIPM Proc.-Verb. Com. Int. Poids et Mesures* **49**, A1-A12 (in French); Giacomo, P. (1981), *Metrologia* **17**, 73 -74 (in English).

[2] JCGM 100:2008 GUM 1995 with minor corrections. Evaluation of measurement data — Guide to the expression of uncertainty in measurement. Joint Committee for Guides in Metrology, 2008.

[3] Commission Regulation (Euratom) 302/2005 of 8 February 2005 on the application of Euratom safeguards. Official Journal of the European Union 28/02/2005, L 54/1 - L 54/70.

[4] STR-368. International Target Values 2010 for Measurement Uncertainties in Safeguarding Nuclear Materials. IAEA. Vienna, November 2010.

[5] ISO 17025:2005. General requirements for the competence of testing and calibration laboratories

[6] ISO 10012:2003. Measurement management systems -- Requirements for measurement processes and measuring equipment.

[7] JCGM 200:2012. International vocabulary of metrology – Basic and general concepts and associated terms (VIM). 3rd edition. 2008 version with minor corrections. Joint Committee for Guides in Metrology. 2012

[8] JGCM 106:2012 Evaluation of measurement data – The role of measurement uncertainty in conformity assessment. Joint Committee for Guides in Metrology. 2012

Nuclear material management system PATI

Tommi Henttonen, Jukka Sorjonen

Fortum Power and Heat Oy
Keilaniementie 1
FI-02150 Espoo, Finland
E-mail: tommi.henttonen@fortum.com, jukka.sorjonen@fortum.com

Abstract:

Licence holder of a nuclear power plant is responsible for his nuclear material management system as a part of the state system of accounting for and control of nuclear material (SSAC).

Fortum has developed a software tool to manage nuclear material in power plant environment. Tool includes nuclear material accountancy and reporting features as the heart and optional features for planning and management of nuclear material.

Keywords: reporting; nuclear; material; accountancy;

1. Introduction

Fortum Power and Heat Oy has operated Loviisa nuclear power plant as Licence holder since 1977 and is responsible for the nuclear material management system (NMMS) as a part of the Finnish state system of accounting for and control of nuclear material (SSAC).

The NMMS system is described in Nuclear Material Handbook as a part of power plants management systems. Handbook (Figure 1) describes nuclear material management as well as management of export controlled items in detailed level and acts as a guide for personnel dealing with nuclear material.

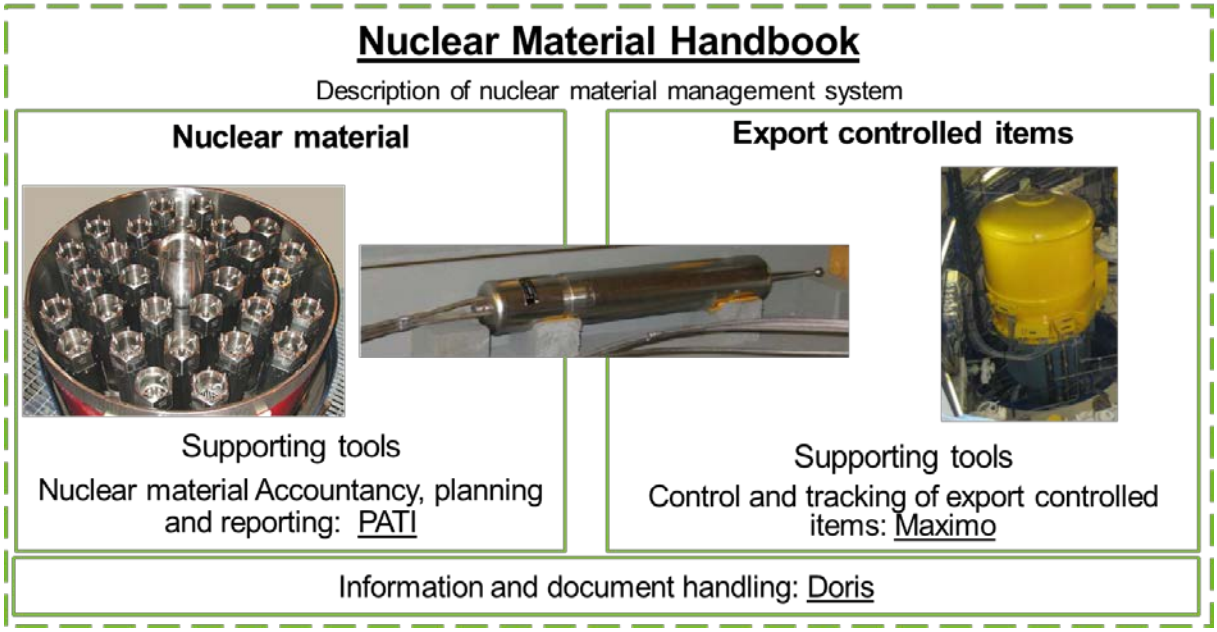

Figure 1: Nuclear Material Handbook.

Fortum uses software tool called PATI [1] for nuclear material management in Loviisa nuclear power plant to meet the requirements set by SSAC. This article describes the tool and its benefits for the plant Operator.

2. PATI Users and Use Cases

PATI is used as a daily tool for managing tasks like nuclear material reception, planning of fuel transfers, planning for reloads, planning the use of spent fuel storage capacity and accountancy reporting to Authorities. Management of these tasks concerns many users at power plant. These users and their tasks may be following:

- Nuclear Material Responsible Person: Authority reporting
- Reactor Engineer: Management of fuel stores, planning of transfers, reloads and reporting
- Reactor Physicist: Information for planning of reactor reloads
- Fuel Procurement: Fresh fuel stock
- Fuel Manufacturing Surveillance: Fuel information for reactor reload license
- Fuel examinations: Fuel history, fuel damage information

Concise and valid data is needed to meet user requirements in a format that is easy to use and maintain. Fortum uses PATI to meet the need by main functions like:

- Centralized storage for fuel life time data
- Import and operation license information of fuel assemblies
- Usage and movement history of fuel assemblies
- Mass changes of fissile Uranium and Plutonium isotopes during plant operating cycles
- Graphical maps of internal rod burn-up of fuel assemblies after any given plant cycle
- Graphical maps of fuel assembly locations on any given date
- Residual thermal power of fuel assemblies at any given date
- Planning of reactor reloading and transfer operations
- Generation of instructions for the fuel handling machine (FHM) operators
- Generation of fuel movement files for the FHM automation system.
- Authority reporting (PIL, ICR, MBR)

Figure 2 shows general life cycle of a fuel assembly as nuclear material at power plant.

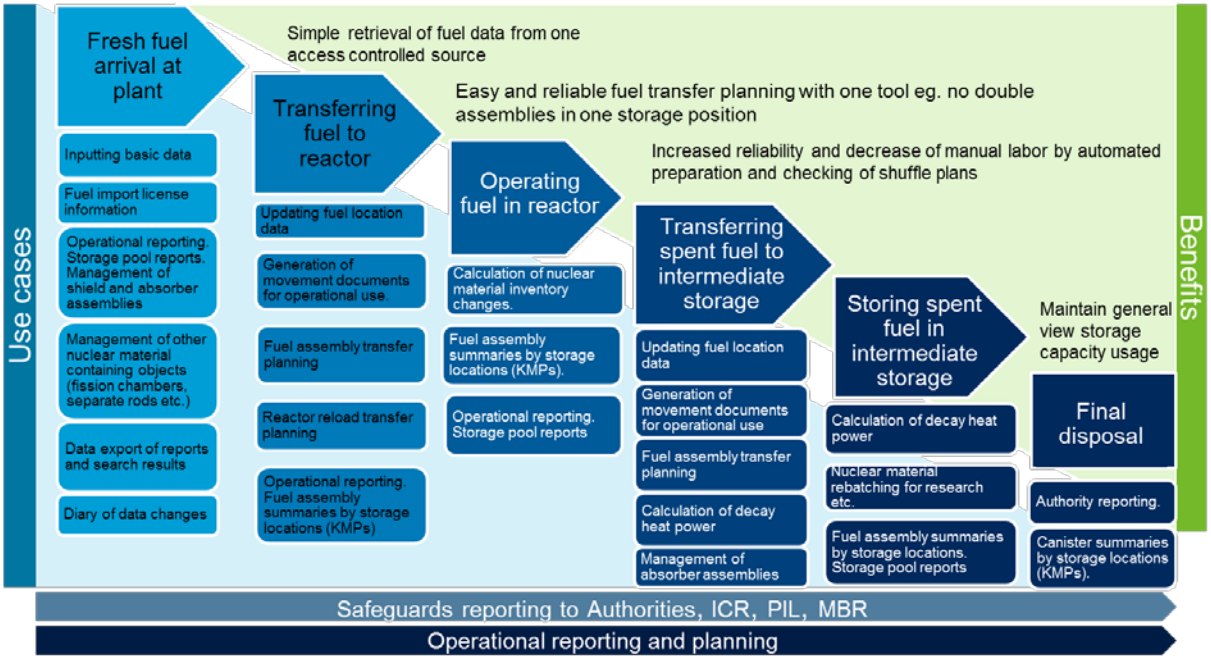

Figure 2: PATI Use cases and benefits.

3. PATI User experience

PATI user interface is based on menus (Figure 3). The underlying database structure is not directly visible to the user, thus the use does not require special IT skills.

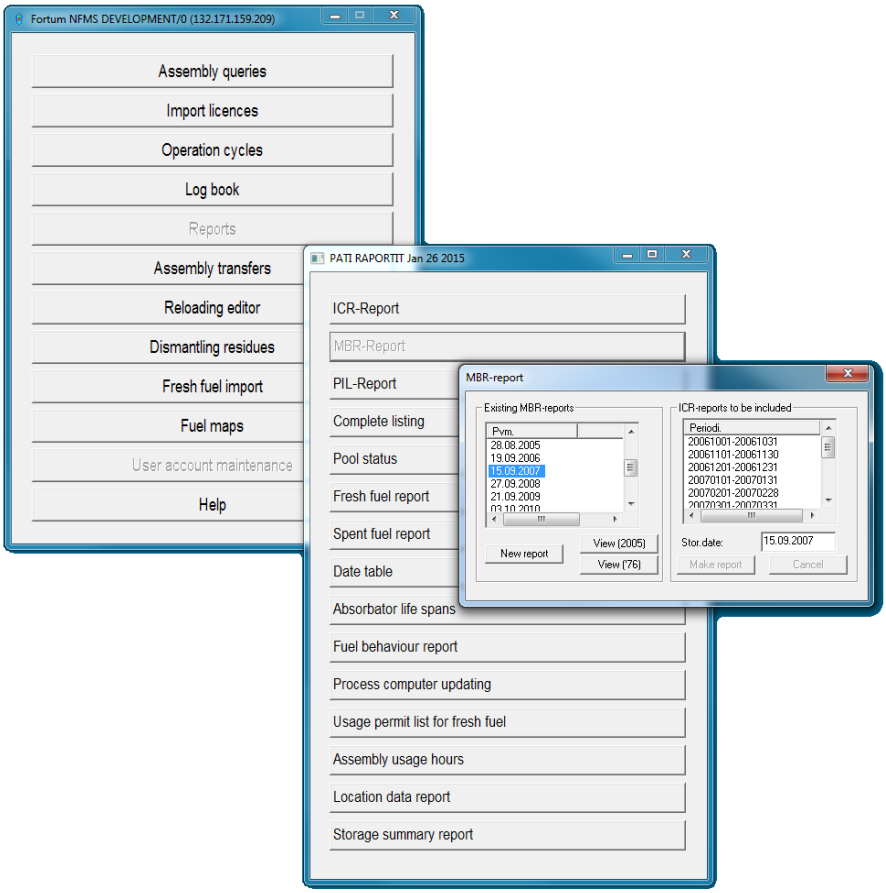

Figure 3: User interface

Figure 3 presents steps to generate a Mass Balance Report (MBR) with four selections. User selects "*Reports*" in main menu, "*MBR-report*" in the next dialog and this opens MBR generation dialog. Here user shall select Inventory Change Reports (ICR) that he wants to be included on the MBR and finalises the process by pressing "*Make report*" button. Now MBR report is generated, saved in PATI database and shown to the User for sending to the Authority.

Same philosophy is used in all other tasks with PATI. The data to PATI is imported using file transfer dialogues that minimise the need for handwork. This enables the User to import data from fuel supplier systems or his own existing tools like core management systems to PATI.

All data stored in PATI can be searched for using query dialogue. Figure 4 shows example of query dialogue. Query results are shown to User in separate text file for software independent post processing. Background of Figure 4 shows PATI graphics capabilities to generate maps of fuel storage locations.

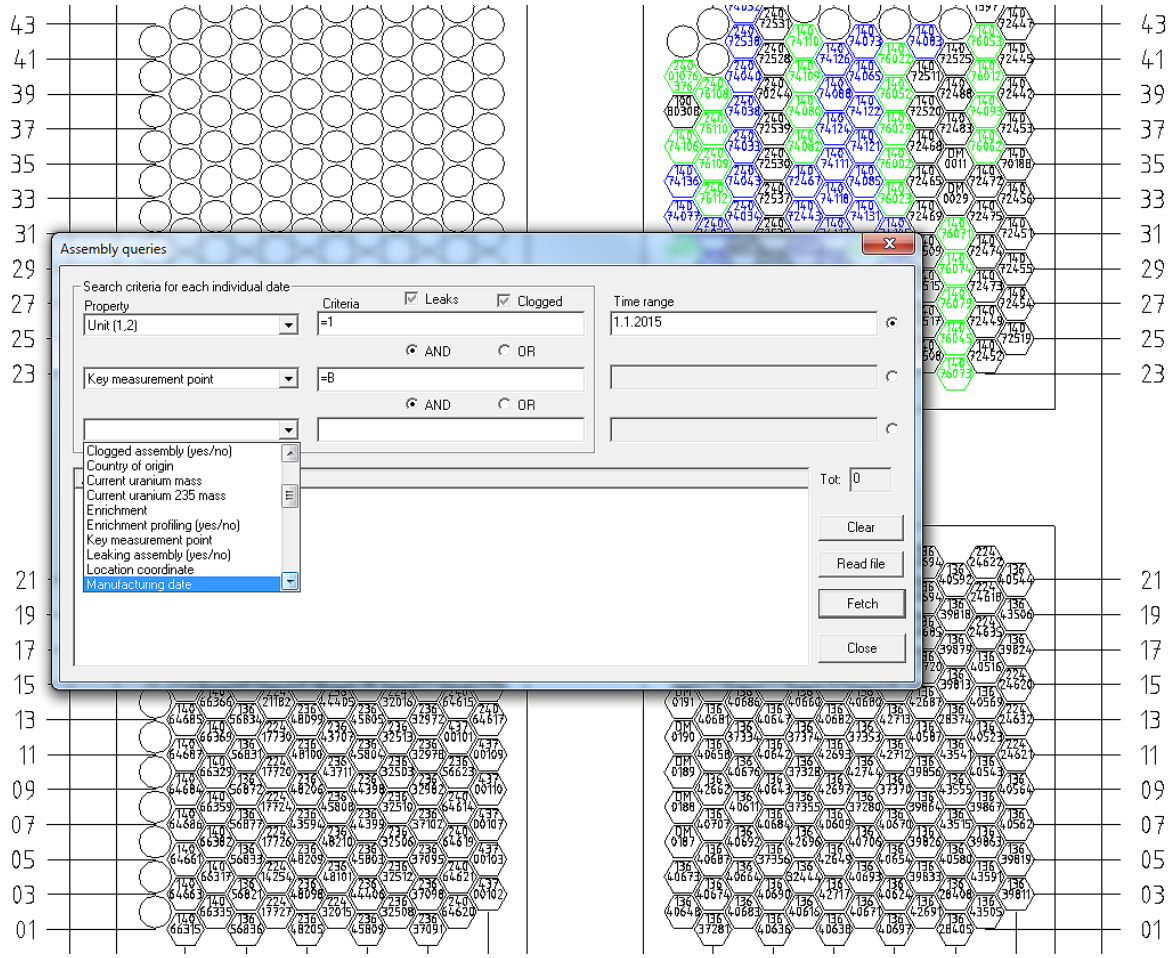

Figure 4: Fuel storage location maps and assembly queries

4. Conclusions

Fortum Power and Heat Oy has developed and uses PATI Nuclear material management system at its own Loviisa nuclear power plant to meet the challenges of nuclear material management, accountancy an reporting.

We have found PATI tool very practical to support every day work of different Users dealing with nuclear fuel. Fortum is interested to share our experiences and software tools to nuclear material management community.

5. References

[1] Fortum, *Nuclear IT systems*, http://www.fortum.com/en/products-and-services/powersolutions/psnuclear/it/, 2015

Implementing a Model for a Computerised Nuclear Materials Accounting System.

Richard Last, Jasper Kirkman

Sellafield Ltd

Abstract:

The Computerised Nuclear Materials Accountancy System (CNMAS) project is a project to replace various nuclear materials accountancy and tracking systems used on the Sellafield Site with a single, up to date system. During the design phase of the project, the project team developed a business model. This was then implemented using an agile software development methodology (scrum) in a pilot, during which a system was developed to account for Uranium Oxide (UO3) being produced from Magnox Reprocessing Operations, its storage on site and its despatch off site. This paper documents the model as originally conceived, the way the model was implemented in the pilot area, and learning from experience in the pilot area. The model uses a system where the user enters records, which are filed. Once filed records cannot be changed, but they can be withdrawn or superseded by later versions. The records are used to calculate a view of the plants stock, and relevant accountancy reports. Correcting data proved difficult, and the authors are aware that this has been the case in other accounting systems. This is because of the bitemporal nature of the records, which all have both an event date (when the event being recorded happened) and a system date (when the event became known to the system). The paper will highlight the approach now being taken to corrections in the light of the pilot experience. The paper will also highlight the advantages of using an agile development methodology.

Keywords: Accountancy; System; Bitemporal; Agile

1. Introduction

The Computerised Nuclear Materials Accountancy System (CNMAS) project is a project to replace various nuclear materials accountancy and tracking systems used on the Sellafield site with a single, up to date system. The system is being developed using an agile methodology.

During the design phase of the project, the project team developed a business model. This was then implemented in a pilot, which covered the production of UO_3 arising from Magnox Reprocessing operations, its storage on site and despatch off site.

The purpose of this paper is to document:

- The model as originally conceived
- The way the model was implemented in the pilot area
- Learning from the pilot about the model and about the agile methodology used to implement the system.

2. The System Model

Figure 1 illustrates the business model used. It consists of five main areas. This section of the paper gives a brief description of these areas.

Records Management. The purpose of this part of the model is to receive inputs to the system. These include records of what the user says has actually happened on plant, as well as records of what other systems say has happened.

Figure 1 - The CNMAS Model

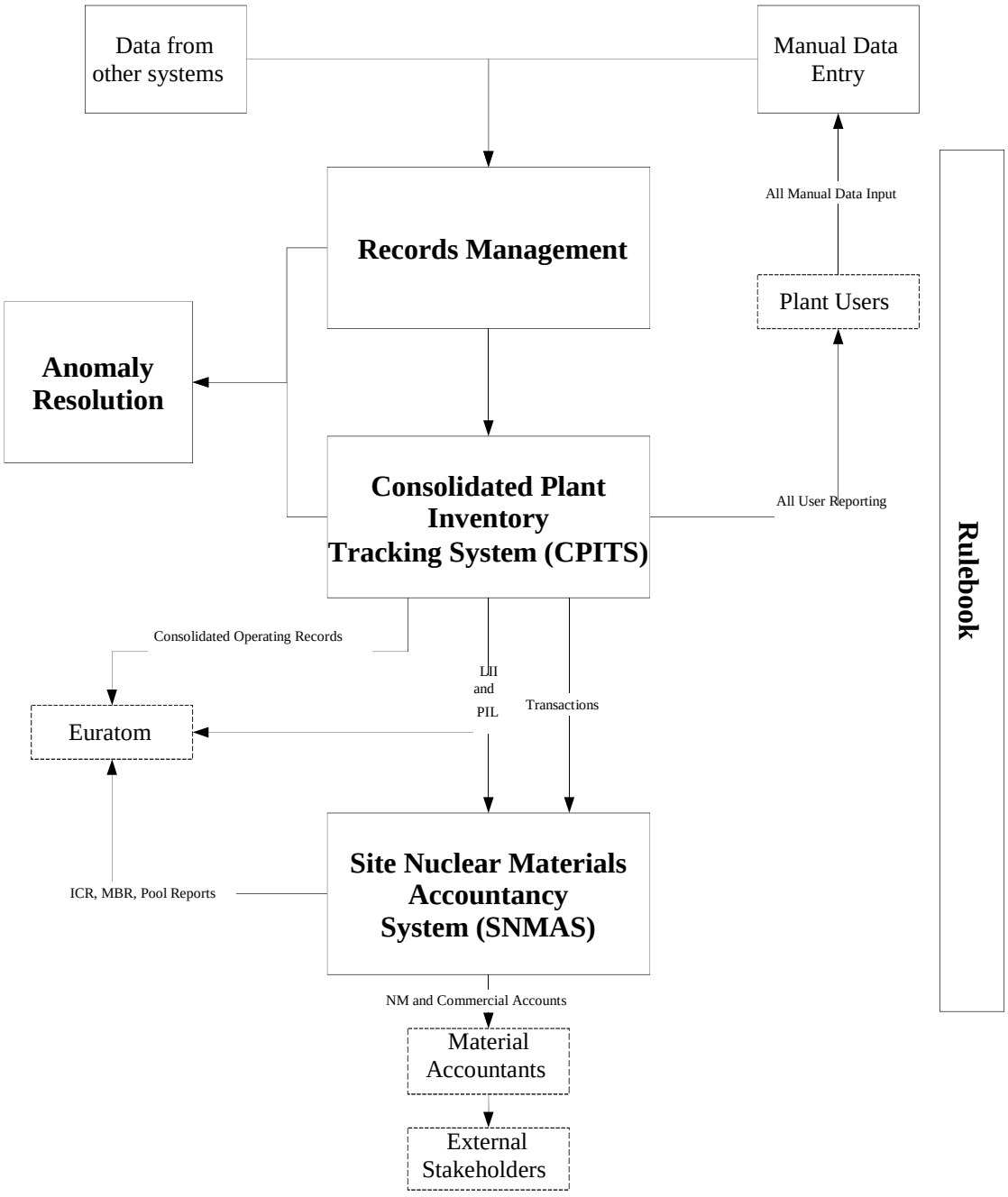

- All data should be provided to the system as “records”.
- The records provided to the system cannot be amended. Any corrections must be made by providing further records to withdraw, supplement or replace the originals, and withdrawn or replaced records must be available for inspection.
- The record storage should be sufficiently robust so that the records can be used for evidential purposes if required.
- Data should be captured once and only once.
- Data should be subject to Quality Assurance(QA) checks by a person independent of the person who captured it.
- The system needs to be simple and robust so that it minimises the chance of operator error.

- Where appropriate, to avoid manual re-entry of data, records should be received from other systems. These records will be subject to automated QA checks. Manual checks may also be required if the QA methods used by the system providing the data are not deemed to be sufficient.

Consolidated Plant Inventory Tracking System (CPITS). The purpose of this part of the model is to take the (often plant specific) records, translate them into discrete instructions and use them to update the model of what material is where.

- This part of the system should be the definitive statement of the properties of nuclear material items and where they are.
- To avoid duplication, this part of the system must hold all relevant data on items, not just nuclear data.
- This part of the system will produce the List of Inventory Items and Physical Inventory Listings required for Euratom reporting.
- This part of the system will produce the Consolidated Operating Records.

Site Nuclear Materials Accountancy System (SNMAS). The purpose of this part of the model is to receive data from CPITS and use it to provide material accounts and statutory reports to Euratom.

- A few accountancy transactions do not arise from changes to the physical items on plant. In these unusual cases, data will still be entered into records management but will bypass CPITS.

Rulebook. This is the part of the system that knows about what sort of thing can be where. As far as possible, running of the system should be based on the rulebook rather than on hard coded rules.

- Appropriate users should have the ability to update the rulebook by entering records into the records management system.
- The rulebook will include a location hierarchy, splitting the site into Material Balance Areas (MBAs), Works Accountancy Areas, Locations and Sub-locations. It will also know about off site locations and MBAs. It will distinguish between “stock” locations where all material must be held in discrete items, and “process” locations where discrete items do not exist.
- The rulebook will include details of what type of items exist, what the properties of the items can and should be, and how items can be containerised.
- The rulebook will include flow information about which types of items can exist in which locations and can move between which locations.
- The rulebook will include details about user roles, so that we can ensure that users can only enter or QA data where they are suitably qualified, experienced and authorised to do so.

Anomalies and performance management. As the system develops, it will be important to track information on anomalies and performance and make this information available to the right people. Examples might include:

- Advising senior staff where “warnings” issued by the system have been acknowledged but not acted on.
- Producing performance statistics on the number of errors being corrected and length of time taken to enter data.
- Alerting staff to data inconsistencies arising and being resolved. (An example of a data inconsistency would be the case where a user asserts in an operating record that an item has moved from B to C when the system thinks the item is in A. This may be because the item is indeed in A, and the system should warn the user of that possibility. However it may also be because another user has failed to record a movement from A to B. The records management system should not prevent a user entering a record asserting something to be true, but must highlight such inconsistencies and allow for them to be resolved before updating CPITS.)

3. The Pilot Plant

The Pilot area plant was a UO3 drumming plant at the end of a spent fuel reprocessing facility. Figure 2 illustrates the normal flow of material in the plant. Essentially, the plant works as follows:

Figure 2 - Pilot Area

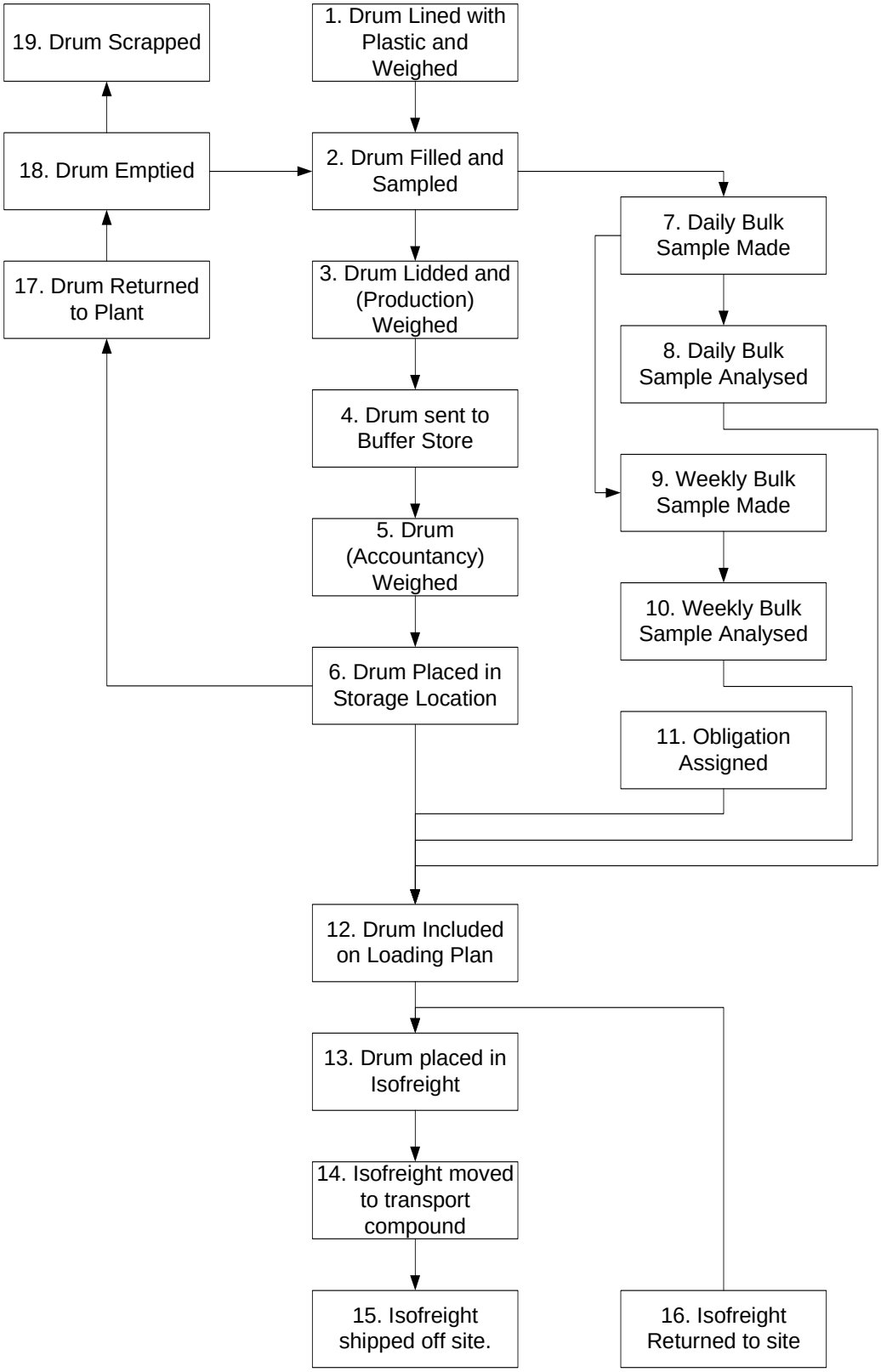

Empty drums are lined with plastic and a tare mass taken (1), filled with UO3 (2) and lidded (3). During filling they are placed on a load cell which provides an indication of their gross mass after filling (3). Due to the conditions it operates in, this gross mass is considered to be indicative rather than accurate. The full drums are moved to a buffer store (4), accurately weighed (5), and placed in a

storage grid location (6). During filling a sample is taken from the material entering the drum (2). The samples are aggregated into a daily bulk sample (7) which is analysed to find the % of 235U in U (8). They are then further aggregated into a weekly bulk sample (9) which is analysed to find the % of U in UO3 (10). The materials accountants assign the drums an obligation code (11), based on the obligation codes of the material entering the reprocessing plant. When the store's supervisor is content that the drums are in a good condition, that the data on the drums is accurate, that the U and 235U analytical results have been received, and that the obligation has been set, he will prepare a loading plan (12), identifying a set of drums to be despatched off site to the long term store. The loading plan is executed, and the drums are placed into a container (13). The container is moved to a transport area (14), and then shipped off site to the long term store (15). Occasionally, drums have to be sent back from the buffer store to the plant (17). This might be because there are quality issues associated with the drums, or because material is needed to prime the plant when operations are commencing after a shut-down. The drums are emptied back into the production plant (18). In theory, the drums can be reused once the contents have been emptied into the plant, but in practice they are often scrapped (19).

4. Scope of the Pilot Implementation

Material tracking in the pilot plant was performed using an old computer system. The computer system passed data to the site's main accountancy system. While the set-up was very advanced at the time it was installed in the early 1990's, there were a number of reasons why it was no longer considered fit for purpose. The scope of the pilot implementation was to replace the existing system, and to do it in a way that was consistent with the overall model.

It was agreed that the pilot implementation should cover all required aspects of Records Management and CPITs (although it was known that the requirements for this plant were simpler than for some other plants that need to be dealt with later in the programme).

A conscious decision was made to limit the amount of SNMAS included in the pilot. The drumming plant and the buffer store are in separate MBAs. The MBA containing the drumming plant contains other areas of the reprocessing plant. The proposed system could not, therefore, account for all material in that MBA. It would have to send data to the existing materials accountancy system. Because of this, the decision was made that SNMAS should simply collate a list of transactions, and that, for the pilot, all these transactions would be transferred to the existing system to produce the necessary reports. Transferring the reporting to the new system would be done later in the project.

The pilot implementation included the minimum required rule book. Data was necessary on the location hierarchy and material types. However, as there are, at this stage, very few material types and locations, and the plant functionality is stable, the decision was made not to include the functionality to enable the user to update the rulebook in the pilot.

The pilot implementation did not include any anomaly and performance management tools.

5. Implementation – Manual Data Entry Process.

A number of plant specific data capture screens were designed to capture information on drum location and properties.

For all manual data entry screens affecting the properties or location of the item, a QA system was implemented. On entering the data, the user must save the data for QA. A different user then confirms (or rejects) the data on a separate screen. The data can also be saved as draft in case the original user realises that the data set is suspect or incomplete during data entry.

For all screens, checks were built in to assist the user by trapping obvious errors. Three types of obvious errors are looked for:

- Data outside expected ranges (e.g. gross mass outside norms).
- Impossible dates (e.g. dates in the future, process steps in wrong order)
- Data conflicting with other records (e.g. item identity already used).

The error trapping built into data entry screens results in warnings and errors.

- Warnings indicate that the data is unusual but might be correct. The person undertaking QA is asked to provide a specific comment to acknowledge the warning. An example of a warning might be an unusually low gross mass. This could indicate a data error (e.g. a decimal point in the wrong place) but might be genuine (e.g. drumming off the final material at the end of a production run.)
- Errors indicate that data is clearly incorrect. The user is not allowed to accept the data.
- In this implementation, the restriction was added that any errors are assumed to be in the record being entered. This simplification is discussed further in section 11.

A system to allow users to withdraw the most recent record was put in place. This system fell short of the final requirements but was sufficient to allow the project to proceed to the first release. Again, for more discussion on this, see section 11.

Security protocols were built into the system to ensure that only appropriate user groups could see and use data entry screens.

One data entry screen (Create Loading Plan) does not actually change the status of a drum or its properties. It simply prepares the system for the next step. It was agreed that this step would not need independent QA.

Manual data entry is provided to allow the users to link the drums to analytical data through the Laboratory Serial Number (LSN) uniquely assigned to each set of analysis. However, the analytical data itself is provided automatically from a Laboratory Information Management System (LIMS). The data provided from the LIMS is considered to be a record. It is subjected to automated QA checks. If these succeed (no warnings or errors) the data is allowed into the system. If these fail, the data is held pending manual QA. If the reason for the failure is a warning, the operations support or quality control groups may accept the results, providing the warning has been acknowledged.

6. Implementation – Routine Reporting.

All routine reports are generated from data in the CPITS area of the system. The reports only reflect data that has been through QA. Draft data and data pending QA is not included in CPITS.

7. Implementation – Material Accounts and Inventory Change Reports

In the initial deployment, the CPITS part of the system provides data for the SNMAS part of the system which then uses the data to create a transaction. However, very limited functionality associated with the SNMAS system is included. Instead, data will be transferred to the existing Nuclear Materials Accountancy System (NMAS) which will be used to provide accounting functionality and produce Inventory Change Reports.

8. Learning about the Model – General Points

The model was generally shown to be robust.

The need for separation between different parts of the model was highlighted. Rework was caused as the model was developed when insufficient separation was identified.

Ensuring appropriate data security caused some issues. This was because it was not considered right at the start of the project. Although the project had only been going a few months when data security was added, there was already a significant amount of rework required. Other projects should consider data security right at the start of product development.

9. Learning about the Model – Corrections.

The biggest issue which slowed the project down was the failure to appreciate the complexity caused by bitemporal data.

All records received into the database have two time stamps, the “event date” timestamp indicates when the thing referred to in the record actually happened, while the “system date” time stamp indicates when the record became known to the system. These two timestamps have an effect on both data input and output.

The effect on data input is that, when considering if the data being presented is consistent, the system must consider the event date not the system date. When telling the system that item x moved from B to C at time t, the system needs to consider whether the item was at B at time t, not whether it is there now.

To complicate this, data may be entered in the wrong order. This is particularly likely if the data is being entered from two different sources. A simple example of this is shown with the application of analytical results to the system. The UO3 drums are placed into the drum store as soon as possible after production. At that point, we have to report on the mass of UO3 leaving the production area and being placed in the store. However, the chemical analysis of the UO3 to determine its assay will not have been completed. Later, when the analytical results become available we have to correct the movement report with a more accurate figure.

Data input is further complicated by corrections. As a general principle, while the users are expected to ensure data is as correct as possible when it is originally entered, and the system should facilitate this, human performance is fallible. The system has to assume that if there is any possibility of entering data which is in error, then sooner or later it will happen and corrections will be required. Where a series of corrections are input, it may be the case that none of the corrections are valid on their own, but the series is fine.

For data output, the system needs to consider that the user may ask three similar but very different questions.

- The question operations will normally ask is “What is the state of the system now?”
- As part of historic investigations, we may need to ask “What do I now believe the state of the system was at time t?”.
- When trying to get data to line up for purposes such as QA, we may need to ask “At time t1, what did I believe the state of the system was at time t0?” This is a particularly important question when making sure that data held in different systems is aligned, as it avoids the need to suspend data entry in one system while a related system is being updated.

The project concluded that the considerable problems raised by bitemporal data were too difficult to fix in the timeframe allowed for release 1. As a fall back, QA constraints were imposed to ensure that the differences between system and event date could not result in the system getting into an invalid state. The biggest consequence of this is that the correction mechanism used is a “roll back” mechanism where only the most recent item can be rolled back and hence corrected. While this was better than the system being replaced (which had no method for the user to make corrections) it was clearly going to be unsatisfactory in the long term leaving the need to address this issue in later releases.

10. Changes Being Made To The Model To Cover Corrections

In the light of the pilot experience the way the final system works has been changed significantly.

In the pilot, data was received into the system in the form of records. However, in common with most traditional system design, the records are used once to update a database which is then considered to be the source of truth on what items are where, etc.

In the revised design, “event sourcing” is used. The records provided to the system are considered to be the source of truth. These are played into an object model which is used to answer the user’s questions about what is there. If the user wants to know what was there at a given time, using the

records that were available at a different time, the system replays the relevant records through the system. This is proving a much better way to answer the bitemporal questions and report on the effects of corrections or late data.

11. Learning About The Agile Process

We had spent longer than we should have done trying to initiate this project using a traditional waterfall technique. The problem with that approach is that it requires a complete, clear and tightly defined and designed end product prior to the commencement of work. On a site as complex as Sellafield, and for a large material tracking system, it would be very difficult to achieve this. It would then be very difficult to get the customers to be able to understand the design documents in sufficient detail to confirm that the system is the one they need. Even if you succeeded in doing that, the operations in the plant are changing, and an accurate design for a system now would need to be modified by the time the system is built.

To avoid this problem, the project has used an agile methodology. The particular methodology selected was scrum. In this methodology, the problem is divided up into large chunks known as “epics” to get an idea of the amount of work involved. As work proceeds, these epics are further broken down into small “stories”. Work is divided into short “sprints” of one to four weeks (we have been using two week sprints). Stories are refined prior to the start of the sprint to ensure that the developers have sufficient understanding of them. They are then designed, constructed, tested and accepted during the sprint. The work is done in close co-operation with the customer.

The project has found that this has been an extremely effective way of making sure that the product is what the customer needs.

The main difficulty the project has experienced with this methodology is confusion when reporting back into an engineering environment where, for very good reasons, the waterfall approach is far more common.

It is also vital to keep the real customer involved with the process. How well the system meets the customer’s needs depends very largely on getting the right level of involvement.

Scope creep is a potential problem. The customer can easily ask questions along the lines of “can you just add a bit on to enable the system to …?” To prevent this from happening, the customer and project team have to have a very clear idea of the objective and scope of the project, and the product owner has to challenge if additional work does not seem to contribute to meeting the objective. It is also worth noting that this is a problem in “waterfall” projects as well. However, in waterfall projects, it tends not to be changing scope because the customer sees the possibilities, but rather the customer asking for things at the start of the project to be done “just in case” or in a way that will not be efficient. As a result, waterfall projects can end up with very good functionality which is rarely if ever used, and inefficient functionality which is in frequent use.

12. Conclusion

Evaluation at the end of the pilot phase confirmed that the basic model in use by the project appeared to be sound.

The need to consider data security right at the start of work of this type was highlighted.

The issues arising from the bitemporal problem were highlighted and an alternative approach is now being used.

The advantages of using an agile development method were highlighted.

Potential Causes of Inventory Differences at Bulk Handling Facilities and the Importance of Inventory Difference Action Levels

Alan Homer, Brendan O'Hagan

Nuclear Materials Accountancy & Safeguards Department
Sellafield Limited, Seascale
Cumbria, CA20 1PG, United Kingdom
E-mail: alan.homer@sellafieldsites.com

Abstract:

Accountancy for nuclear material can be split into two fundamental categories. Firstly, where possible, accountancy should be in terms of items which are objects that can be transferred as discrete packages and their contents are fixed at the time of their creation. All items must remain accounted for at all times and a single missing item is considered significant. Secondly, where nuclear material is unconstrained, for example in a reprocessing plant where it can change form, there is an uncertainty that relates to the amount of material present in any location. Cumulatively, these uncertainties can be summed and provide a context for any estimate of material in a process. Any apparent loss or gain between what has been physically measured within a facility during its physical inventory take and what is reported within its nuclear material accounts is known as an inventory difference. The cumulative measurement uncertainties can be used to set an action level for the inventory difference so that if an inventory difference is observed outside of such action levels, the difference is classified as significant and an investigation to find the root cause(s) is required. The purpose of this paper is to explore the potential causes of inventory difference and to provide a framework within which an inventory difference investigation can be carried out.

Keywords: inventory difference; action levels; uncertainty; measurement; investigation

1. Introduction

Accountancy for nuclear material falls into two fundamental categories. Firstly, where possible, accountancy is in terms of 'items'. Items are objects that can be transferred as discrete packages. Their contents are fixed at the time the discrete package or item is created. Generally, items are recognised in terms of being containers that can be counted, for example a uranium drum, a plutonium can or a transport flask. The safeguards criteria for areas where the nuclear material contents are only in the form of items is uncomplicated. Items are counted into and out of the area and all items must be accounted for. A single missing item is considered significant.

Where nuclear material is unconstrained, for example as part of a process within a reprocessing facility, then there is an uncertainty in any measure that relates to the amount of nuclear material present. Cumulatively these uncertainties can be summed and can provide a context for any estimate of material in the process. In summary, the aim is to know how much nuclear material is present by measurement and the level of confidence in that measurement by analysis of the uncertainty so as to demonstrate that the area is in control and to detect losses or diversion of nuclear material.

The difference between what is physically measured within a facility at a physical inventory take (PIT) and the amount of nuclear material declared within its nuclear material

accountancy system is known as the inventory difference (ID). The uncertainty of measurement defines what is known as the inventory difference action level (IDAL).

2. The Basic Units

For the remainder of this discussion, everything will be viewed in terms of quantity and proportion:

- Quantity is usually either volume or mass, however it can be the result of a more complicated indirect measurement system e.g. mass is equal to volume multiplied by density in plutonium nitrate (PuN) liquor transfers.
- Proportion is the concentration of a particular accountable nuclear material contained within an amount of some other substance e.g. the amount of plutonium in plutonium dioxide (PuO_2) powder.

Whether the nuclear material in question is an inventory item or the amount of nuclear material being transferred into or out of an area (a transaction), the nuclear material quantity is calculated in the same way, nuclear material is equal to quantity multiplied by proportion. For example, if a uranium trioxide (UO_3) drum contains 800 kg of UO_3, and its uranium assay is 88% (a proportion of 0.88), then 88% of the material in the drum is uranium, 704 kg.

3. What is Inventory Difference?

A minimum of once per calendar year (and at intervals of not greater than 14 months), each material balance area (MBA) will shutdown normal operations, move their nuclear material into an area where it can be measured and verified, and perform a PIT. During the period since the previous PIT, the nuclear material accountants will have maintained a book account (BA) where

Book **A**ccount = **O**pening Physical **I**nventory + **R**eceipts – **S**hipments (Eq. 1)

where the opening physical inventory (OI) is the amount of nuclear material in the MBA at the time of the previous PIT, and receipts (R) and shipments (S) are the amounts of nuclear material moved into and out of the MBA since the previous PIT. The results of the PIT are then compared with the book account. Theoretically these values should be identical, however in practice they usually differ producing an ID where:

$$\begin{aligned} ID &= PIT_{now} - BA \\ &= PIT_{now} - (OI + R - S) \end{aligned} \quad \text{(Eq. 2)}$$

and PIT_{now} is the amount of nuclear material measured at the current PIT. If there was no uncertainty involved with this process i.e. all measurements were exact, then the ID should be zero because everything would add up as expected. Although an observed ID will commonly occur due to the fact that it is not possible to measure all material exactly, the root cause of an ID can be due to many factors, some of which are examined later in this paper.

4. What is an Inventory Difference Action Level and why do we need it?

As nothing can be measured exactly, there are uncertainties associated with each measurement of inventory, receipts and shipments. These uncertainties can then be combined to calculate the total uncertainty on the ID (using Eq. 2). If the measured ID falls within the bounds given by the overall measurement uncertainty, then the statistical data supports a theory that the apparent difference is due to measurement uncertainty rather than a true difference. The IDAL is the maximum acceptable ID based on measurement uncertainty. If the ID is outside of these bounds then the difference must be investigated.

It is important that all measurement uncertainties for inventory, receipts and shipments are technically justified. This means that the uncertainties are underpinned with calibration data or reviewed technical papers justifying the parameters used. International Target Values (ITVs) [1] are primarily used as targets but can be used as a starting point for estimating uncertainties. The IDAL is required to ensure the plant is in control and, in the event of loss of control, to initiate the start of an investigation to determine the cause.

5. Who Needs an Inventory Difference Action Level?

Process facilities have nuclear material that is unconstrained (i.e. not confined to discrete containers) as the material is in a constant state of flux between holding vessels, with the material often undergoing a change in form. The measurement uncertainty then accumulates with each measurement which makes up the receipts, shipments and inventories. This can lead to an ID and hence an IDAL is required in these facilities.

Storage facilities do not need an IDAL since the material is constrained in containers such as drums and cans. There is however a need to count the containers to ensure none are missing. Exact knowledge of the number of containers does not imply exact knowledge of their contents. When the containers are put into the storage facility, the amount of material in each container is recorded in the inventory. Each container will have its own uncertainty which leads to a global uncertainty for the store. Take for example a PuO_2 storage can which consists of an inner can, a polyethylene bag and an outer can. The amount of nuclear material in the can is the gross mass minus the tare masses of the two cans and the bag making up the overall package. If the polyethylene bag mass was systematically being reported incorrectly, then the amount of nuclear material claimed to be in the store would be incorrect even though it can be confirmed that what went into the store is still in the store.

The storage area would not register an ID because the item count and the product can gross masses would be correct, but the supplying MBA would show a consistent ID as the shipments would be systematically biased. This type of problem is difficult to identify and the exact nature of the problem may only become truly apparent if the store and its contents are re-measured.

6. Causes of Inventory Difference

This work categorizes the main reasons why an ID may occur into six areas, shown diagrammatically in figure 1. It is not sufficient to identify a single cause without considering all contributory factors. Figure 2 shows that there are significant links that should be considered and it is worth noting that many of them lead back to the "personnel" category. These interconnections and the finer detail are discussed throughout the remainder of this paper. If learning from experience (LFE) is to have any meaning then it is important that all linking parts are examined.

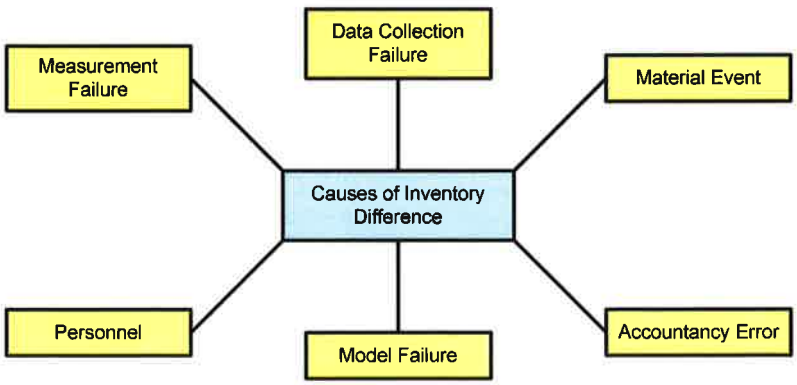

Figure 1: A diagram illustrating the main reasons why an inventory difference may arise.

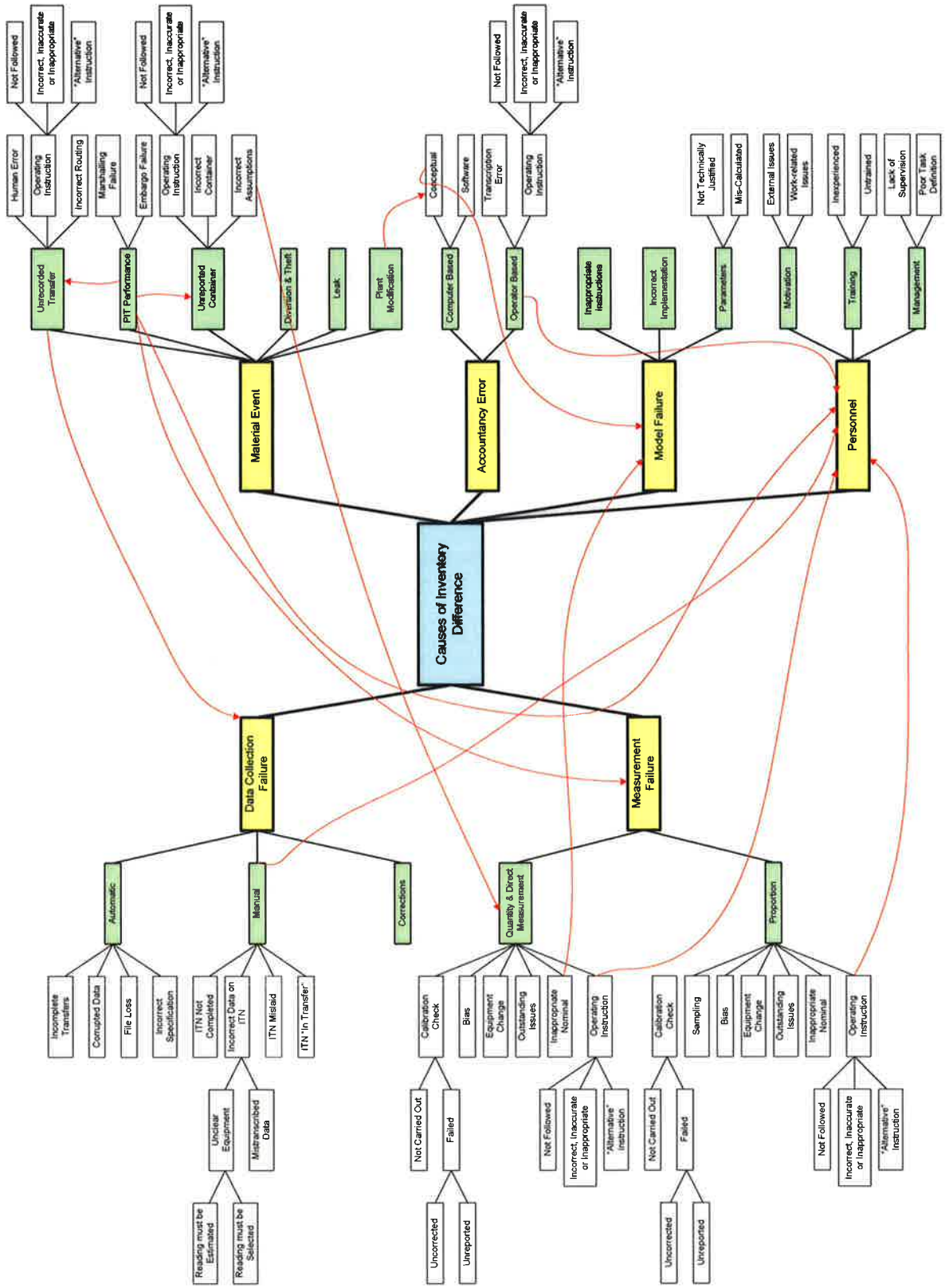

Figure 2: A diagram to illustrate potential causes of inventory difference and some of their various inter-dependencies.

When a potentially true ID is identified (i.e. an ID outside of the bounds of a calculated IDAL) an investigation must take place to explain what has happened within the associated material balance period (the period between two consecutive PITs). At Sellafield, the following framework for an investigation has been developed. The first phase of any ID investigation focuses on three main areas:

- Has there been a nuclear material event?
- Has there been a data collection failure?
- Has there been a failure of the nuclear materials accountancy model.

These questions will be considered in more detail in sections 6.1 – 6.3. If any of the questions are answered in the affirmative then they should be addressed immediately, the ID recalculated and if the issue is not resolved, the investigation should move into a second phase which is discussed in more detail in sections 6.4 – 6.6.

The second phase of the investigation focuses on whether or not there been a measurement failure, an accountancy error or if there are any personnel issues with people involved. Generally, the most common cause of an ID is measurement failure as particularly for flows, small errors can accumulate over a long campaign into very substantial amounts. It should also be remembered that, although measurement failures can also be associated with inventory measurements, these would apply to both opening and closing inventories and therefore the error would be associated with the difference between opening and closing values. Given that, under most circumstances, the facility should be minimising its inventory, the status of a facility at PIT is usually fairly constant and this difference is not usually that large.

6.1. Nuclear Material Event

Of all of the potential causes of ID, a nuclear material event is the most crucial. The underlying premise of a nuclear material event is that nuclear material is not where it is expected to be.

6.1.1. Diversion and Theft

From a safeguards perspective the worst scenario is that nuclear material has been diverted or stolen. Good practice therefore informs that any investigation should start from a position of no diversion or theft has occurred. It is essential to inform the Security Department as soon as there is thought to be an apparent breach of IDAL. This approach allows the Security Department to perform any preliminary investigations they see necessary, feedback their findings to provide assurance to the Nuclear Material Custodian / Controller and through them to other stakeholders.

6.1.2. Nuclear Material Leak

The Nuclear Material Custodian / Controller should arrange for those with direct oversight of the various areas within an MBA to perform a visual check of plant areas. Where a direct visual check is not possible, assurance should be sought through indirect measures such as sump checks, neutron monitor alarms etc. looking for any unusual readings or behaviours.

6.1.3. PIT Performance

When a PIT is performed, best practice informs that all movements should be embargoed in an area. In practice however, movements are often still required between a PIT and physical inventory verification (PIV). All such moves should be recorded and provided to the safeguards inspectorates. Failure to correctly record moves or lack of communication between the facility, the Nuclear Material Custodian / Controller and the Nuclear Materials Accountancy and Safeguards (NMAS) department can easily lead to nuclear material being

mislaid or double counted, its location being recorded incorrectly and general confusion surrounding nuclear material control.

6.1.4. Unrecorded Transfer and/or Unreported Container

An unrecorded transfer would tend to be caused by a procedural breakdown when a nuclear material move takes place with no paperwork generated, paperwork going astray, or a failure in an automated transfer system. An unreported container could be described similarly but in actuality would include finds[1] of nuclear material. The nuclear material status of a facility is recorded on a list of inventory items (LII) and the Nuclear Material Custodian / Controller must ensure that there is a direct correlation between the LII and the facilities physical layout. For example, it can be easy to overlook a sweepings container in a glovebox if it is normally present and empty. Similarly, the assumption that a hopper is empty is open to challenge if no physical assessment has been made and / or the location is unverifiable.

6.1.5. Facility Modification

Nuclear materials accountancy is based on a shared model with the actual facility. The Nuclear Material Custodian / Controller is responsible for the control of nuclear material in their area and therefore must inform the NMAS department of any modifications to the facility. There is also a regulatory obligation to inform the safeguards inspectorates in a timely manner to ensure they can verify such modifications. If there is disconnect between the facility model and the nuclear materials accountancy system then transfers could be lost and storage locations missed.

6.2. Data Collection Failure

The premise of data collection failure is that the nuclear material is where it should be but there has been a process failure in collecting the data.

6.2.1. Manual Failure

Data is often recorded on some type of form and failure to complete an appropriate form is not necessarily easy to detect. Such failures may only be identified through a check within the facility for missing or extra inventory items against the LII. Mislaid or in-transfer forms are easier to identify as most forms for nuclear materials accountancy purposes have a sequence number which can be checked. The latter should become clear to the NMAS department when performing a check of paperwork received. At this time the NMAS department should also perform a quality check of the data received to identify transcription errors e.g. wrong decimal places recorded or figures incorrectly transposed.

6.2.2. Automatic Failure

The initial testing and commissioning of automatic data transfer should be sufficient to give confidence in a systems performance, however, if a facility suffers an unexpected outage it is possible for errors to occur. Data may be lost or incorrect shutdown and restart procedures can give rise to file corruption or loss. Care must always be taken in the event of a power failure or unplanned shutdown to ensure that there is no effect on data transfer.

[1] A "find" is unforeseen nuclear material which is found in a material balance area.

6.2.3. Corrections

All corrections made to nuclear materials accountancy paperwork should be countersigned and be fully traceable. Similarly, where changes are made in the nuclear materials accountancy system, they should be logged, with an explanation to allow traceability in the event of an investigation.

6.3. Model Failure

The premise of a model failure is that measurements have been made correctly and the nuclear material is correctly located, but the interpretation of that data is inappropriate in some way. The Nuclear Material Custodian / Controller should commence an investigation utilizing both facility technical support and NMAS department as early as possible within the investigation. Such an investigation will effectively undertake a qualitative check on the nuclear materials accountancy model.

6.3.1. Inappropriate Assumptions

When a measurement is made there are usually some associated assumptions. For example, it is a reasonable assumption that the surface of a liquid is flat in a large vessel though not when estimating a level of a receptacle with a narrow diameter. Similarly, a container holding powders is unlikely to have a level surface where material has recently been dispensed. Also, powders in a vessel typically compact when left to settle, therefore the density will be different at the top and bottom causing sampling issues. The nuclear materials accountancy model must reflect physical reality as accurately as possible.

6.3.2. Incorrect Implementation

Generally, testing of software or spreadsheets which manipulate data should have been sufficiently detailed to ensure that the process exactly replicates manual calculation. It is possible, nonetheless, to generate incorrect data, especially if the implementer of the system and the user do not share a common set of assumptions. Equally important here is a review of the IDAL calculation itself because failure to capture all relevant details or incorrect estimations of associated uncertainties (both random and systematic) can lead to an ID uncertainty that is artificially small or large and consequently an IDAL that is simply unattainable or unrealistic.

6.3.3. Model Parameters

Where data manipulation takes place that involves the use of parameters then these parameters should be supported by a technical justification. Any that do not have an associated technical justification should be flagged for consideration.

6.4. Measurement Failure

The premise of measurement failure is that the nuclear material is where it should be but there has been an error in measuring the quantity or proportion of the material. Before investigating each and every measurement it is worthwhile assessing the probability of contribution to an ID that can be assigned to any particular flow or inventory location. By producing a list of all flows and inventory locations, a simple rule to prioritise areas of interest could be to assign the observed ID to each flow and inventory location and ask the question, what would it take to generate an ID of that magnitude from that specific flow or inventory point and what are the implications?

Such analysis should identify the most probable areas where measurement failure could produce or impact on ID and therefore provide some focus for the investigation. This does not

mean that smaller effects should be ignored – where identified they should still be corrected, but the most appropriate areas of concern should be targeted first.

6.4.1. Quantity and Direct Measurement

In general the first thought with quantity measures should be to analyse the routine verification activities of the measurement system. With weighing systems this should be relatively straightforward, with traceable evidence that the system has been recently calibrated and routine checks between calibrations have been performed to ensure the system is working as expected. With large vessels, and in general volumetric calibration, it may be extremely difficult to recalibrate after initial commissioning. The best option may be an inter-tank transfer comparison with other tanks in the processing stream.

Additional issues may occur where non-destructive analysis (NDA) equipment shares a joint function with safety and nuclear materials accountancy. Measurements generated for safety reasons can be deliberately biased to incorporate a 'worst-case' scenario for criticality purposes. Where such readings are used for nuclear materials accountancy without reference to a 'best estimate', these biases can accumulate. For example, PCM packets with an absolute plutonium content of less than half a gram should generate a zero accountancy value but the measurement system may typically record accountable quantities for safety purposes. It does not take many packets over a material balance campaign to generate a 1 kg ID.

6.4.2. Proportion

Where analysis for assay, concentration, or density takes place then it is important to confirm that no changes in the measurement process or equipment have occurred as these can affect both ID and IDAL. Where possible some repeat analysis for large bulk samples is useful confirmation as is the use of alternative procedures to ensure consistency and lack of bias.

6.5. Accountancy Errors

6.5.1. Computer-Based Errors

Computer based errors fall broadly into two areas, the first being conceptual issues. If there has been a plant modification, or change to a measurement process, does the accountancy system reflect physical reality? If not, there is a fundamental failure of the accountancy model and these changes can propagate errors throughout the accountancy system which could potentially result in material being unaccounted for, double counted or in the case where incorrect parameters are set in the underlying nuclear materials accountancy system code, incorrect data.

The second issue relates to the actual software itself which computes the nuclear material accountancy records. Where software is upgraded or operating systems are changed, robust testing of the accountancy system is required to ensure there are no bugs in the system. This is especially important when dealing with legacy accountancy systems which may have limited technical support and the expertise is not available to support transfer of the systems.

6.5.2. Operator-Based Errors

Ideally all nuclear materials accountancy systems would utilize automatic data capture and an operator or nuclear materials accountant would be responsible for peer-review and data verification. In many cases, especially with older plants, manual data entry by both plant operators and nuclear materials accountants is still required. An obvious error trap with manual data entry is transcription errors which can be difficult to recognise and correct. Therefore, a robust peer-checking process is essential.

The importance of clear, robust operating instructions must also be considered. Where operating instructions are not followed, are incomplete, inaccurate, inappropriate or there are multiple instructions for the same task, mistakes are likely to occur. Such issues also result in a lack of transparency, consistency and accuracy which is necessary for good nuclear materials accountancy.

6.6. Personnel

People work within systems and if those systems are properly constructed, supervised and appropriate training and understanding are given, then mistakes are less likely to happen. However, there always remains the 'human factor' meaning errors cannot be totally eliminated. To mitigate the propagation of repeatable errors it is good practice to undertake regular debriefs and post job reviews to ensure any LFE is captured.

A key personnel issue worth considering in an investigation is motivational issues. Are the individuals involved focussed on the task at hand? Has enough time been allocated to the operators for completing the PIT and the nuclear materials accountants for producing the relevant reports to the required quality? Secondly, are the individuals involved with the PIT, suitably qualified and experienced (SQEP'd). Mistakes can happen with both inexperienced and experienced personnel and it is key that all people involved with nuclear materials accountancy are aware of and maintain an awareness of their responsibilities and the impact that their actions may have. Finally, from a management perspective adequate supervision must be ensured to drive a high standard of plant condition at the time of the PIT, accountancy data is kept up to date and people involved have clear task definition.

7. Conclusions

The conclusions of this paper are as follows:

- In item accountancy areas of a facility, an IDAL is not required. A single missing item is considered significant, and an investigation required.
- In process areas of a facility, where material is changing form and measurements are being made, an IDAL is required. All measurements have an uncertainty and it is the cumulative sum of these uncertainties for all receipts into an area, shipments out of an area and for inventory measurements at a physical inventory take which determine the IDAL.
- An IDAL will change from one material balance period to the next as it depends on plant throughput and the amount of inventory change between successive physical inventory takes.
- If an ID falls outside of the bounds of a technically justified IDAL then an investigation should be performed.
- There are many potential causes of ID and this paper categorizes them into six key areas:

    1. Material Event
    2. Data Collection Failure
    3. Accountancy Error
    4. Measurement Failure
    5. Model Failure
    6. Personnel Issues

- Many causes of ID are interlinked and identifying the root causes of an ID is a complex task which must be fully examined. If a potential contributing cause to an ID

is identified early in an investigation, it should still be completed in its entirety to ensure all contributing factors are captured.

8. Privacy regulations and protection of personal data

The author agrees that submission of this work automatically authorises ESARDA to publish the work in whole or in part in all ESARDA publications – the bulletin, meeting proceedings, and on the website.

The author declares that this work is original and not a violation or infringement of any existing copyright.

9. References

[1] International Atomic Energy Agency, *International Target Values 2010 for Measurement Uncertainties in Safeguarding Nuclear Materials*, STR-368, Vienna, November 2010.

Closing Plenary

ESARDA Symposium 2015 / 37th Annual Meeting, 18-21 May, Manchester, UK

Closing Plenary

Irmgard Niemeyer

ESARDA Vice President

Ladies and Gentlemen, dear colleagues, good afternoon and welcome to the closing session of the 37th ESARDA Annual Meeting in Manchester.

The closing session of an event like this always offers an excellent opportunity to review the past days, to sort the many impressions and achievements, and probably also to realize what you may have missed. So I will try to give a brief overview of some Symposium highlights, noting that this summary may be subjective and to some extend different from what you have experienced.

Summary

Most of us this gathered already on Monday in course of the traditional working group (WG) and committee meetings before the official start of the ESARDA Symposium. Six WGs hold meetings with 20 to 30 participants each, covering organisational issues, the review of joint projects, such as the International WG on Gamma Spectroscopy Techniques (NDA WG), inter-laboratory comparison programs for quality control (DA WG), and presentations on a variety of topics, such as antineutrino detection (NA/NT WG) as well as satellite imagery and geoinformation technologies (VTM WG). The details of the meetings will be available soon via ESARDA's information repository of CIRCABC.

Approximately 30 participants attended the open meeting "Building Capability in Safeguards R&D – A Role for Universities" on Monday. The objectives of this event were 1) to provide some basic safeguards background for those new to ESARDA and the safeguards world, especially those from the UK nuclear research community, 2) to demonstrate university research projects that have developed to include support for the safeguards regime and 3) to describe training opportunities and existing networks for increasing safeguards awareness and understanding amongst university researchers and young nuclear professionals more generally (specifically the ESARDA and wider Europe Young Generation Networks). During the discussions, it turned out that there is a continuing demand for and benefits of short courses to increase safeguards awareness and basic understanding, also to help researchers to identify possible safeguards applications for otherwise non-safeguards projects. Though this demand for providing safeguards education, taught courses specific to safeguards remain limited, including because of the 'niche' nature of the subject. The participants identified means for more systematic higher-level safeguards engagement with the UK University nuclear research community.

Also the Steering Committee (SC) discussed, among other topics, the importance of safeguards education and training. The chair of the TKM WG, Sophie Grape from Uppsala

University, presented a strategy paper entitled “Building a strategy for ESARDA – Education, Training and Knowledge Management”. The SC acknowledged this initiative, next to the ESARDA Young Generation initiative, in order to increase the awareness of nuclear safeguards by making educational and research material available. However, the success of this strategy requires support from all ESARDA WGs, and I call on all ESARDA WG members to contribute to the initiative. The strategy paper presented will also be available in the symposium proceedings.

Moreover, SC was pleased to approve an application for membership from the Nuclear Research and Consultancy Group, NRG, the only provider of nuclear services in the Netherlands. Sandia National Laboratories (SNL), the first US National lab joining ESARDA activities in the very early 80’s, applied for associated membership, and the SC approved this application, too. Hence, the number of ESARDA parties and associated members is constantly increasing.

In the evening, just before the reception, the INMM International Safeguards Division (ISD) met. This event attracted about 35 participants and included presentations on the quantification of detection probabilities, the forthcoming joint INMM/ESARDA Workshop: “Building International Capacity” and general background on the NPT Review Conferences.

On Tuesday, the ESARDA president Jim Tushingham opened the ESARDA Symposium officially. The opening plenary included four invited speakers providing keynotes.

First, Mr. Sallit, Deputy Chief Nuclear Inspector and Programme at the Office of Nuclear Regulation (ONR), introduced the safeguards obligations of the UK in fulfilment of the related treaties and safeguards agreements. As part of the Cross ONR Programme, safeguards tasks of ONR are to provide the UK Government with informed independent assessment of safeguards application and compliance in the UK, to meet the international and domestic safeguards-related reporting obligations, and to provide advice and support to the Department of Energy & Climate Change (DECC) and other Government Departments on safeguards implementation in the UK, the effectiveness of regulation and associated policy development.

The second keynote was given by Prof. Sucha, Director General of the EC Joint Research Centres (JRC). He emphasised the importance of the many contributions of the JRC for nuclear non-proliferation, safeguards and security by referring, inter alia, to the 15 years anniversary of the on-site laboratories at the reprocessing plants located at Sellafield (UK) and La Hague (France), the development of verification technologies based on 3D laser scanning for Design Information/Basic Technical Characteristics Verification (DIV/BTC), and the provision of certified reference materials. Prof. Sucha recognized as one of the largest challenges that too much knowledge would be available and therefore called for further efforts on knowledge management, for example by means of a new knowledge centre on energy under the JRC as focal point.

Third, Ms. Renis addressed the Symposium on behalf of IAEA DDG Mr. Vajoranta. In her keynote, she reported, inter alia, on the implementation of measures under the Framework for Cooperation and the Joint Plan of Action on Iran's nuclear programme, noting also the implications of the additional verification efforts on personnel and budget. She provided an

update on the safeguards implementation at the State level and the plans of the IAEA to update the existing State-level safeguards approaches (SLAs) under Integrated Safeguards and to develop SLAs for other States in future. With reference to the data on safeguards activities listed in the Safeguards Implementation Report (SIR) 2014, Ms. Renis noted the challenge of doing more with less. She stated that enhancing the effectiveness and improving the efficiency of IAEA safeguards could only be achieved by improving the productivity of processes, including 1) optimization of internal processes, 2) enhanced cooperation by Member States and 3) better use of modern technologies.

In the fourth keynote, Dr. Szymanski, Director EC ENER E, described developments within Euratom since the last ESARDA Annual Meeting with regard to 1) strengthening of communication with stakeholders, 2) completing the integrated management system, 3) improving effectiveness and efficiency of Euratom safeguards, and 4) improving relations with the IAEA. He also gave an update on the technical developments for the in-field inspection activities, including, inter alia, the progress on remote data transmission and equipment (DCVD, EOSS sealing interface for operators, NDA equipment in fuel fabrication). Dr. Szymanski recognized the important role of ESARDA in the development of new approaches, innovations and technological advances, noting that Euratom strongly relies on the support provided by ESARDA.

All speakers emphasized the challenges of the today's changing (nuclear) world given the shrinking financial resources and called for technical and scientific innovations and to work even more closely together.

The Symposium continued with the technical plenary with contributions from the INMM President Mr. Satkowiak, Mr. Abousahl (EC DG JRC) on the nuclear safeguards and security activities under Euratom research and training programme, Ms. Mathews (IAEA) on recent developments in IAEA safeguards guidance and outreach, Mr. Seya (JAEA) on the JAEA-ISCN's NDA development programs, and Mr. Johnson (ONR) on the experience implementing the UK Additional Protocol. The papers of the technical plenary will be published soon via the ESARDA website.

On Tuesday afternoon, the technical sessions started. 119 Papers were presented in 23 sessions, including one poster session, and covered a large variety of topics:

- Implementation of Safeguards
- Safeguards Concepts
- Export Control
- International Collaboration
- Training and Knowledge Management
- Nuclear Material Accountancy
- Geological Repositories
- Containment and Surveillance

- Integrated Measurement and Monitoring
- Spent Fuel Verification
- Inhomogeneous Material Verification
- Neutron Measurements
- Gamma Measurements
- Uncertainties in NDA Measurements
- He-3 Alternatives for Neutron Detection
- Destructive Analysis (Quality Control, Measurements)
- Combined Analytical Techniques
- Novel Technologies and Forensics
- Geospatial Information
- Non-Proliferation and Arms Control

All papers presented at the 37th ESARDA Annual Meeting will be made available via the ESARDA website, while a selection of "best papers" will also be published in the ESARDA Bulletin. In this context, I should like to point out, that the Editorial Committee would appreciate if more volunteers could assist with the peer review of these papers.

Acknowledgements

The closing session is also the place to say "Thank you" you to all people being involved in the Symposium.

My first and sincere thanks go to Jim Tushingham, our ESARDA president and Chair of the ESARDA Symposium. Jim, my congratulations for successfully preparing, organising and holding the 37th ESARDA Annual Meeting in Manchester. While the City of Manchester alone was worth a visit, the organisational settings of the Symposium, including also the reception at the Midland Hotel, the Symposium dinner at Tatton Park, and the evening tours to the Cold War Nuclear Bunker at Hackgreen were outstanding.

I am grateful to the National Nuclear Laboratory (NNL) for hosting the Symposium and the ESARDA Event Management Team from Marick Communications for their professional support.

Moreover, I would like to thank Filippo Sevini, our ESARDA secretary for his efforts, not only in the context of this Symposium. Filippo, please pass my thanks also to Andrea de Luca for his support with regard to ESARDA website, EasyChair and others.

I should also like to thank our sponsors for their financial support, specifically the exhibition sponsors Baltic Scientific Instruments, Canberra, Hybrid Instruments, Kromek, Nu Instruments, and Thermo Fisher Scientific, the coffee sponsors Sellafield Ltd and Urenco, as well as the technical sponsors EC, JRC ITU and NNL.

I wish to thank the members of the Symposium Committee for their time and efforts to review almost 130 abstracts and to structure the programme of this symposium. On a related note, I also thank JRC ITU Ispra for hosting the 1.5 days Symposium Committee meeting in January.

Last but not least, I would like to extend my thanks to all of you, the 218 participants of the 37th ESARDA Annual Meeting, representing 73 institutions. We have had 22 participants from 10 universities, 36 participants from 17 institutions from outside Europe. Thank you very much for your interest, time and contributions.

Outlook

Lastly, this final session also offers a chance to announce future ESARDA meetings.

True to the motto "After the Game is before the Game", the organisation of the 2017 event has already started. I am pleased to announce that the ESARDA Symposium 2017 will be held in Germany and hosted by Forschungszentrum Jülich and is likely to take place in the vicinity of the research centre, with date and venue still to be decided.

The next ESARDA Annual Meeting will take place in Luxembourg in May 2016 as internal meeting of all ESARDA WGs. Before, many of the WGs meet in Oct/Nov 2015 at JRC ITU Ispra.

However, there are some possibilities to continue your ESARDA activities already tomorrow. You may attend the meeting of the IS WG or the joint meeting of the NDA and DA WGs. The WG Meetings are open to all interested participants. Moreover, Urenco has generously offered a site visit to their uranium enrichment facility at Capenhurst tomorrow.

Finally, I wanted to point again to the 8th INMM/ESARDA Joint Workshop 2015, entitled "Building International Capacity. The workshop will be held from October 4 to 7, 2015, at the Jackson Lake Lodge just inside the Grand Teton National Park near Jackson Hole, Wyoming.

During four concurrent working group sessions, a total of 12 topics related to non-proliferation and nuclear security, arms control, international safeguards, and education and training will be discussed. Information about registration and the venue can be found at the workshop's website at http://www.inmm.org/8th_INMM_ESARDA_Workshop.htm.

Ladies and Gentlemen, now I have the honour to officially close the 37th ESARDA Annual Meeting. On behalf of the Symposium Programme Committee, I thank you all for your participation and for making this symposium a success. I hope you will take numerous impressions, new contacts and new ideas home with you. I wish you a very pleasant remaining stay in the city of Manchester and a safe travel home.

Thank you very much.

European Commission
EUR 27342 – Joint Research Centre – Institute for Transuranium Elements

Title: **ESARDA 37th Annual Meeting Proceedings**

Author(s): Filippo Sevini

Luxembourg: Publications Office of the European Union

2015 – 1045 pp. – 21.0 x 29.7 cm

EUR – Scientific and Technical Research series – ISSN 1831-9424 (online)

ISBN 978-92-79-49495-6 (PDF)

doi: 10.2789/099293

LC-NA-27342-EN-N

JRC Mission

As the Commission's in-house science service, the Joint Research Centre's mission is to provide EU policies with independent, evidence-based scientific and technical support throughout the whole policy cycle.

Working in close cooperation with policy Directorates-General, the JRC addresses key societal challenges while stimulating innovation through developing new methods, tools and standards, and sharing its know-how with the Member States, the scientific community and international partners.

Serving society
Stimulating innovation
Supporting legislation

doi: 10.2789/099293

ISBN 978-92-79-49495-6

Publications Office